

Full Texts & Abstracts of SERES'18

Editors

Servet TURAN, Alpagut KARA, Mutlu BAŞKAYA

seres'18

**IV. INTERNATIONAL CERAMIC, GLASS, PORCELAIN,
ENAMEL, GLAZE AND PIGMENT CONGRESS**

**October 10-12, 2018
Anadolu University
Eskisehir Technical University
Eskisehir / Turkey**



Turkish Ceramic
Society



ANADOLU UNIVERSITY



ESKİŞEHİR TECHNICAL UNIVERSITY

INDEX

INVITATION.....	1
-----------------	---

COMMITTEES.....	2
-----------------	---

FULL TEXT OF INVITED SPEAKERS

CURRENT BATTERY TECHNOLOGIES FOR ELECTRIFICATION.....	6
---	---

RECENT NEW APPLICATIONS OF HBN.....	15
-------------------------------------	----

PHOSPHORESCENT GLASS.....	24
---------------------------	----

THE DEVELOPMENT OF DECORATION IN TURKISH ÇİNİ ART.....	52
--	----

FULL TEXT OF ORAL PRESENTATIONS

3D DISPERSION OF $\text{La}_2\text{Al}_{0.5}\text{Li}_{0.5}\text{O}_4$ AND LiAlO_2 in Al CONTAINING $\text{Li}_7\text{La}_3\text{Zr}_2\text{O}_{12}$ SOLID ELECTROLYTES.....	64
---	----

LITHIUM ION CONDUCTING GLASS CERAMIC MEMBRANES FOR DUAL ELECTROLYTE LITHIUM AIR BATTERY APPLICATIONS.....	70
---	----

SHAPING OF SILICON NITRIDE CERAMICS VIA DIRECT COAGULATION CASTING.....	75
---	----

INVESTIGATION OF WEAR RESISTANCE OF THE PORCELAIN TILE BODIES BY SOLID PARTICLE IMPINGEMENT USING ALUMINA PARTICLES.....	81
--	----

BENEFITS AND EFFECTS OF THE SUITABLE GLAZE SELECTION FOR CERAMIC DIGITAL EFFECTS.....	89
---	----

RHEOLOGICAL BEHAVIOR OF BORON WASTE CONTAINING PORCELAIN TILE SLURRIES.....	95
---	----

EFFECT OF LEATHER WASTE ADDITION ON THE PROPERTIES OF CERAMIC WALL TILES.....	102
---	-----

PHASE AND ORIENTATION MAPPING OF CERAMIC COMPOSITES BY APPLICATION OF PRECESSION ELECTRON DIFFRACTION IN TEM.....	108
---	-----

THE STRUCTURAL MODIFICATION OF QUARTZ ACCORDING TO FIRING TEMPERATURE AND ATMOSPHERE.....	113
---	-----

MINERALOGICAL INVESTIGATION OF NEPHELINE SYENITE AND ITS USAGE IN CERAMIC PRODUCTION.....	126
---	-----

PRODUCTION OF MAGNESIUM DIBORIDE POWDER BY SELF PROPAGATING HIGH TEMPERATURE SYNTHESIS.....	134
---	-----

LIGHTWEIGHT BULLETPROOF VESTS: HOT-PRESSED BORON CARBIDE FOR BALLISTIC PURPOSES.....	140
USING of VARIOUS AMORPHOUS SILICATES in MANUFACTURING of LIGHTWEIGHT SANITARYWARE PRODUCTS.....	147
IMPROVING THE PROPERTIES OF Al_2O_3 -TiC CUTTING TOOLS BY USING GAS PRESSURE SINTERING TECHNIQUE.....	154
EFFECT OF DIFFERENT SINTERING SPEEDS ON GRAIN SIZE OF ZIRCONIA CERAMICS.....	160
PRELIMINARY STUDIES ON THE ENRICHMENT OF THE CORUNDUM (RUBY).....	166
DISSOLUTION BEHAVIOR OF SILVER ION DOPED HYDROXYAPATITE COATING ON METAL IMPLANT IN BLOOD PLASMA.....	175
MODIFICATION OF PECHINI METHOD FOR OBTAINING $(Yb_2O_3)_{0.2}(Y_2O_3)_{0.2}(ZrO_2)_{0.6}$ SOLID ELECTROLYTE.....	185
CHARACTERIZATION OF COMMERCIAL CLAYS USED IN CERAMIC SANITARY WARE SECTOR.....	191
BEHAVIOR OF COBALT SPINEL PIGMENT IN TRANSPARENT GLAZE.....	201
THE EFFECT OF ZIRCON SILICATE PIGMENT ON AMORPHOUS PHASE OF TRANSPARENT GLAZE.....	208
AN INVESTIGATION OF RAW MATERIAL EFFECTS ON NANO SiC BASED FOAM GLASS PRODUCTION.....	214
MARBLE LOOK QUARTZ SURFACES WITH CRISTOBALITE.....	222
EFFECT OF TiO_2 AND B_2O_3 ADDITION ON CRYSTALLIZATION BEHAVIOR OF K_2O - MgO - Fe_2O_3 - Al_2O_3 - SiO_2 -F SYSTEM GLASS-CERAMICS.....	230
SYNTHESES OF AlN NANOPOWDER.....	237
FABRICATION AND CHARACTERIZATION OF Al_2O_3 - Cr_2O_3 CERAMICS BY USING 5 VOL. % Cr_3C_2 AS PRECURSOR.....	248
AN EXPERIMENTAL STUDY ON LIGHTWEIGHT GEOPOLYMER SYNTHESIS.....	254
ASSESSMENT OF MECHANICAL PROPERTIES IN PORTLAND CEMENT BY OPTICAL MICROSCOPY AND NUMERICAL COLOR ANALYSIS.....	258
MECHANICAL AND PHYSICAL PROPERTIES OF CARBON BLACK BLENDED CONCRETE.....	265
MECHANICAL AND FREEZE-THAW RESISTANCE PROPERTIES OF C30 CLASS CONCRETE: THE EFFECT OF FINELY MILLED WIRE AND RUBBER OBTAINED FROM WASTE TIRE.....	272

THE EFFECT OF WATER/CEMENT RATIO ON THE COMPRESSIVE STRENGTH OF THE CEMENT MORTARS PRODUCED BY POLYCARBOXYLATE BASED PLASTICIZING CHEMICAL ADMIXTURE.....	291
AN INVESTIGATION ON THE PRODUCTION POTENTIAL OF GEOPOLYMER MORTAR WITH TUNÇBİLEK FLY ASH.....	295
INVESTIGATION OF HYDRATION PROPERTIES OF SLAG-BLENDED CEMENTS.....	301
THE ROLE OF CHEMICAL ADMIXTURES IN READY MIXED CONCRETE MIXTURES.....	312
INVESTIGATION OF THE PROPERTIES OF POROUS STAINLESS STEELS COATED WITH BOEHMITIC ALUMINA VIA DIP COATING METHOD.....	319
SYNTHESIS AND OPTICAL PROPERTIES OF EU ³⁺ -DOPED NATURAL FLUORAPATITE.....	322
PRODUCTION OF LUMINESCENT Eu ³⁺ -DOPED MONTICELLITE BASED CERAMICS OBTAINED FROM BORON DERIVATIVE WASTE.....	330
INVESTIGATION OF THE LI-FREE ENAMEL FRIT EFFECTS ON SURFACE CHARACTERISTICS OF VITREOUS ENAMEL COATINGS.....	337
DEVELOPMENT OF NEW GENERATION ELECTROSTATIC ENAMEL POWDERS FOR WATER STEAM CLEANABLE FUNCTIONAL COOKING DEVICES.....	344
ENHANCED THERMAL CONDUCTIVITY PERFORMANCE OF BORON-DOPED REFRACTORY PARTICLE COATINGS ON VITREOUS ENAMEL COOKWARES AND INVESTIGATION OF ITS POTENTIAL APPLICATION ON MEAT COOKING AS A NOVEL METHODS.....	349
INFLUENCE OF TABULAR ALUMINA ADDITION ON THE PROPERTIES OF SELF-FLOWING MAGNESIA BASED CASTABLE REFRACTORIES.....	355
SYNTHESIS AND CHARACTERIZATION OF MICRONIZED CoAl ₂ O ₄ SPINEL CRYSTALS AS CERAMIC PIGMENTS BASED ON INK-JET PRINTING.....	359
FULL LAPPATO GLAZE.....	366
IMPROVEMENT OF MECHANICAL PROPERTIES OF TRANSPARENT POTTERY GLAZES BY USING BASALT.....	371

FULL TEXT OF POSTER PRESENTATIONS

THE EFFECTS OF BLAST FURNACE SLAG ON THERMAL PROPERTIES OF CERAMIC SANITARYWARE BODIES.....	377
THE INVESTIGATION OF BUILDING MATERIAL PRODUCTION CONDITIONS AND ITS PROPERTIES BY USING BLAST FURNACE SLAG AND MAGNESITE WASTE.....	384
PRE-TREATMENT TO ESTIMATE THE GLAZE COMPOSITIONS IN CERAMIC GLAZE	

APPLICATIONS USING ARTIFICIAL NEURAL NETWORKS.....	390
THE EFFECT OF STRONTIUM ADDITIVE ON THE BIOACTIVITY PROPERTIES OF BIOACTIVE GLASS.....	400
THE EFFECT OF ZnO ADDITION ON THE PROCESSING OF CERAMIC TILES FROM WASTE GLASS AND FLY ASH.....	406
CHARACTERIZATION AND INVESTIGATION OF CORROSION PREVENTION PERFORMANCE OF METAL INDUSTRIAL COATINGS CONTAINING DIFFERENT TYPES OF RESIN.....	413
THE INVESTIGATION OF THE EFFECTS OF GLAZE COMPONENTS CHANGES TO CERAMIC DIGITAL INK PERFORMANCE ON FLOOR TILE MAT GLAZES.....	419
GLASS-CERAMIC COATED STAINLESS STEEL AS SOLID OXIDE FUEL CELL SEALANT.....	425
ENGOGLAZE DEVELOPMENT FOR THE PRODUCTION OF GLAZED PORCELAIN TILES.....	431
EFFECT OF COMPOSITION ON FLY ASH GEOPOLYMERS.....	438
EVALUATION OF PHOSPHORESCENT PIGMENTS PREPARED BY SOL-GEL METHOD ON EARTHENWARE SURFACES.....	444
PRODUCTION AND CHARACTERISATION OF AL ₂ O ₃ /SI CERAMIC-METAL COMPOSITE ARMORS.....	451
ABSTRACT OF KEYNOTE & INVITED SPEAKERS.....	459
ABSTRACT OF ORAL PRESENTATIONS.....	519
ABSTRACT OF POSTER PRESENTATIONS.....	591
ARTISTIC INVITED SPEAKERS	
THE SODEISHA JOURNEY.....	631
STOP MOTION USING CLAY.....	639
IN MEMORY OF HAMİYE ÇOLAKOĞLU.....	647
IN MEMORY OF İBRAHİM BODUR.....	652
IN MEMORY OF SADİ DİREN.....	653
BLACK POTTERY FIRING SINCE PREHISTORIC TIMES TO THE PRESENT.....	654
ARTISTIC APPROACH WITH ZISHA CLAY IN YIXING.....	655

CULTURAL INTERACTION BETWEEN EAST-WEST AND ITS REFLECTIONS ON CERAMICS.....	656
HERITAGE / CONTEMPORARY CERAMIC ART.....	663
COLOUR IN GLASS ART.....	664
“MULTIPLE MODERNISMS”:A PERSPECTIVE ON CONTEMPORARY ASIAN GLOBALISM.....	665
ESKİŞEHİR INTERNATIONAL TERRA COTTA SYMPOSIUM EXEMPLAR: CITY, PUBLIC SPACE AND CERAMIC SCULPTURES.....	668
ARTISTIC ORAL & POSTER PRESENTATIONS	676

SERES'2018 Brings Ceramic People Together in Eskisehir

With the assistance of Anadolu University, Turkish Ceramic Society (TSD) organizes **SERES'18 "IV. International Ceramic, Glass, Porcelain Enamel, Glaze and Pigment Congress"** which aims to bring academicians, artists, designers in the fields of ceramic, glass, porcelain enamel, glaze, pigment and cement, and people of regarded industries together, supplying them suitable arena for sharing knowledge and experiences and for determining possible future collaborations with its wide range of coverage. SERES'18 will be held on the **10 - 12 October 2018** in Anadolu University, Yunusemre Campus Congress Centre and in Eskisehir Technical University, Iki Eylul Campus Eskişehir/Turkey.

As you know, congresses are not only the activities anymore where scientists gather together and foster the recent advances in art, science and industry but they have also become the organizations where the culture and values of their location are appreciated. Accordingly, a rich social program waits for you so that you can enjoy the unique artistic and cultural features of Eskişehir.

On behalf of the organizing committee, it is my pleasure for me to invite you to participate in this exciting meeting.

I look forward to seeing you in October in Eskişehir.

Best Regards,

On behalf of Organising Committee

Prof. Dr. Alpagut KARA (Chairman)

COMMITTEES

Honorary Presidents

Erdem ÇENESİZ (Chairman of Turkish Ceramic Federation)
Şafak Ertan Çomaklı (Rector), Anadolu University
Tuncay Döğeroğlu (Rector), Eskişehir Technical University

Organizing Committee

Alpagut KARA (TSD Chairman of the Board of Directors)
Tolun VURAL (TSD Vice Chairman of the Board of Directors)
Servet TURAN (TSD Vice Chairman of the Board of Directors)
Mutlu BAŞKAYA (TSD Vice Chairman of the Board of Directors)
Ayhan ÇAVUŞOĞLU (TSD Board Member)
Fatma BATUKAN BELGE (TSD Board Member)
İlhan MARASALI (TSD Board Member)
Sedat ALKOY (TSD Board Member)
Taner KAVAS (TSD Board Member)
Ertuğrul ULUDAĞ (TSD Board Member)

Scientific Committee

Alphabetically ordered by first name

A. Murat AVCI (ENTEKNO Materials)
Abdullah ÖZTÜRK (ODTÜ, Turkey)
Abdüllatif DURGUN (Afyon Kocatepe University, Turkey)
Ahmet ÇAPOĞLU (Gebze Technical University, Turkey)
Ahmet TURAN (Yalova University, Turkey)
Ali Osman KURT (Sakarya University, Turkey)
Alpagut KARA (Eskişehir Technical University, Turkey)
Arca İYİEL (ŞİŞECAM, Turkey)
Aydın DOĞAN (Eskişehir Technical University, Turkey)
Aygül YEPREM (Yıldız Technical University, Turkey)
Ayşe KALEMTAŞ (Bursa Technical University, Turkey)
Azade YELTEN-YILMAZ (Istanbul University, Turkey)
Bekir KARASU (Eskişehir Technical University, Turkey)
Bora DERİN (Istanbul Technical University, Turkey)
Bora MAVİŞ (Hacettepe University, Turkey)
Burcu Apak GÜLSEVER (Istanbul Technical University, Turkey)
Caner DURUCAN (Middle East Technical University, Turkey)
Cemal AKSEL (Anadolu University, Turkey)
Cengiz KAYA (Sabancı University, Turkey)
Davut UZUN (Tübitak MAM)
Deniz UZUNSOY (Bursa Technical University, Turkey)
Derya MARAŞLIOĞLU (ETİ MADEN, Turkey)
Dušan GALUSEK (Alexander Dubček University of Trenčín)
Duygu AĞAOĞULLARI (Istanbul Technical University, Turkey)
Duygu GÜLDİREN (Türkiye Sise ve Cam Fabrikaları A.Ş., Turkey)
Ebru MENŞUR ALKOY (Gebze Technical University, Turkey)

- Eda TAŞÇI (Dumlupınar University, Turkey)
 Eliseo MONFORT (ITC, Spain)
 Emel CENGİZ (Afyon Kocatepe University, Turkey)
 Emel ÖZEL (Eskişehir Technical University, Turkey)
 Emine TEKİN (TÜBİTAK-MAM)
 Emrah ÜNALAN (Middle East Technical University, Turkey)
 Ender SUVACI (Eskişehir Technical University, Turkey)
 Enrique Sánchez VILCHES (ITC, Spain)
 Ertuğrul ULUDAĞ (Eczacıbaşı, Turkey)
 Evren ARIÖZ (Eskişehir Technical University, Turkey)
 Fatih AKKURT (BOREN, Turkey)
 Fatma BATUKAN BELGE (Mimar Sinan University, Turkey)
 Ferhat TOCAN (PiroMET Inc.)
 Figen KAYA (Yıldız Technical University, Turkey)
 Filiz Şahin (Istanbul Technical University, Turkey)
 Gökçe DARA (ROKETSAN, Turkey)
 Gökhan Kürşat DEMİR (Eti Seydişehir Aluminum Inc.)
 Gül YAGLIOĞLU (Ankara University, Turkey)
 Hakan SESİĞÜR (Türkiye Sise ve Cam Fabrikaları A.S., Turkey)
 Hasan GÖÇMEZ (Dumlupınar University, Turkey)
 Hatem AKBULUT (Sakarya University, Turkey)
 Hüseyin Özkan TOPLAN (Sakarya University, Turkey)
 Hüseyin YILMAZ (Gebze Technical University, Turkey)
 İlhan MARASALI (Hacettepe University, Turkey)
 İskender IŞIK (Kütahya Dumlupınar University, Turkey)
 Kadir KILINÇ (Kırklareli University, Turkey)
 Kadri AYDINOL (Middle East Technical University, Turkey)
 Kagan KAYACI (Kale Seramik, Turkey)
 Keriman PEKKAN (Dumlupınar University, Turkey)
 Lucian PINTILIE (National Institute of Materials Physics, Romania)
 Lütü ÖVEÇOĞLU (İTÜ, Turkey)
 Maksude CERİT (NUROL Technology, Turkey)
 Melike SUCU (ÇİMSA ArGe)
 Merve Akdemir KUTLUĞ (Şişecam Türkiye Sise ve Cam Fabrikaları A.S., Turkey)
 Metin ÖZGÜL (Afyon Kocatepe University)
 Mine TAYKURT DADAY (Adana Science and Technology University, Turkey)
 Mustafa URGEN (Istanbul Technical University, Turkey)
 Mustafa YILDIIM (Middle East Technical University, Turkey)
 Mutlu BAŞKAYA (Hacettepe University, Turkey)
 Nil TOPLAN (Sakarya University, Turkey)
 Nuran AY (Eskişehir Technical University, Turkey)
 Nurcan ÇALIŞ AÇIKBAŞ (Bilecik Şeyh Edebali University, Turkey)
 Onuralp YÜCEL (Istanbul Technical University, Turkey)
 Ömer ARIÖZ (Hasan Kalyoncu University, Turkey)
 Özkan KURUKAVAK (KÜMAŞ, Turkey)
 Pervin DAĞ (Ceramic Research Centre, Turkey)
 Ramis Mustafa ÖKSÜZOĞLU (Eskişehir Technical University, Turkey)
 Rattikorn YIMNIRUN (Vidyasirimedhi Institute of Science and Technology, VISTEC), Thailand.
 Recep ARTİR (Marmara University, Turkey)
 Recep KURTULUŞ (Afyon Kocatepe University, Turkey)
 Rezan DEMİR CAKAN (Gebze Technical University, Turkey)
 Richard BOWMAN (Principal at Intertile Research Pty Ltd, Australia)
 Sedat AKKURT (Izmir Institute of Technology, Turkey)
 Sedat ALKOY (Gebze Technical University, Turkey)
 Serdar ÖZGEN (Istanbul Technical University, Turkey)

Servet TURAN (Eskişehir Technical University, Turkey)
Shaowei ZHANG (Exeter University, Turkey)
Suat YILMAZ (Istanbul University, Turkey)
Süleyman TEKELİ (Gazi University, Turkey)
Şaban PATAT (Erciyes University, Turkey)
Şenol YILMAZ (Sakarya University, Turkey)
Şerafettin EROĞLU (İstanbul University, Turkey)
Şevket EROL (Kümaş Magnesite Inc, Turkey.)
Taner KAVAS (Afyon Kocatepe University, Turkey)
Tayfun UYGUNOĞLU (Afyon Kocatepe University, Turkey)
Tuba C. YILDIZ (Turkish-German University)
Tuğhan DELİBAŞ (ÇİMSA Ar-Ge, Turkey)
Yahya Kemal TÜR (Gebze Technical University, Turkey)
Yalçın ELERMAN (Ankara University, Turkey)
Ziya ARSLANOĞLU (Konya Krom-Magnesite Inc. , Turkey)

TSF: Turkish Ceramic Federation
TSD: Turkish Ceramic Society

seres'18

IV. INTERNATIONAL CERAMIC GLASS PORCELAIN
ENAMEL GLAZE AND PIGMENT CONGRESS
October 10-12, 2018, Eskişehir, Turkey

Full Text of INVITED SPEAKERS

INVITED SPEAKERS

CURRENT BATTERY TECHNOLOGIES FOR ELECTRIFICATION

Muhsin MAZMAN

MUTLU AKÜ SAN.ve TİC. A.Ş. Tepeören Mah. Eski Ankara Asfaltı Cad. No:210 Tuzla

İstanbul/TÜRKİYE

ABSTRACT

Key-words: Hybrid/Electric Vehicle, Battery, Li ion, Battery Market

We are living in a revolutionary decade in automotive industry through electrification. The future has been creating by this time. Hybrid/Electric Vehicle technology holds much promise for reducing petroleum demand in transportation which is mandatory through Europe legislations for CO₂ emission reduction. This potential is highly dependent to the improvements on energy storage systems. This paper gives the market trends in electrification and battery technologies. Our target is to define the challenges in the market for researchers to work on it.

1. INTRODUCTION

Although electrical vehicle systems are one of the first research areas in automotive technology which discovered by Davenport in 1835, this technology was neglected after the commercial success of Ford Model T with serial production technics in affordable price. The electric car studies were in silence for decades and wake up again during petroleum crisis. This crisis has two pillars; the first is oil price and the second is environmental problems which caused by oil usage. The rate of fossil fuel combustion products (CO_x, NO_x, SO_x) begun to increase in atmosphere. Therefore, the EU countries announce new legislations for automotive to decrease these gases (Figure 1). This legislation put target as 95 gr/km CO₂ in 2020 for Europe.

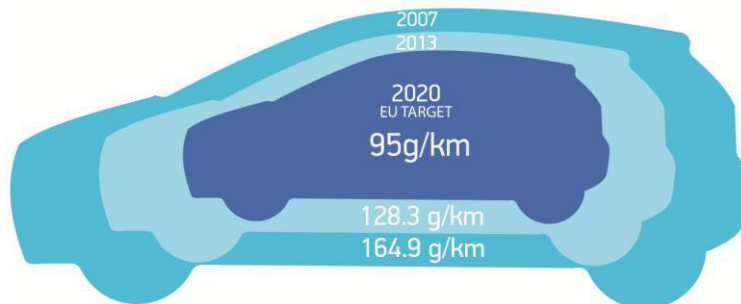


Figure 1. European Legislation Target for Automotive [1]

The target (95 gr/km) is to reach an average CO₂ emission which calculated by covers all the filo. Many countries who has activities in Europe followed this legislation by different targets to decreasing the CO₂ in their countries and continue the business in Europe (Figure 2.).

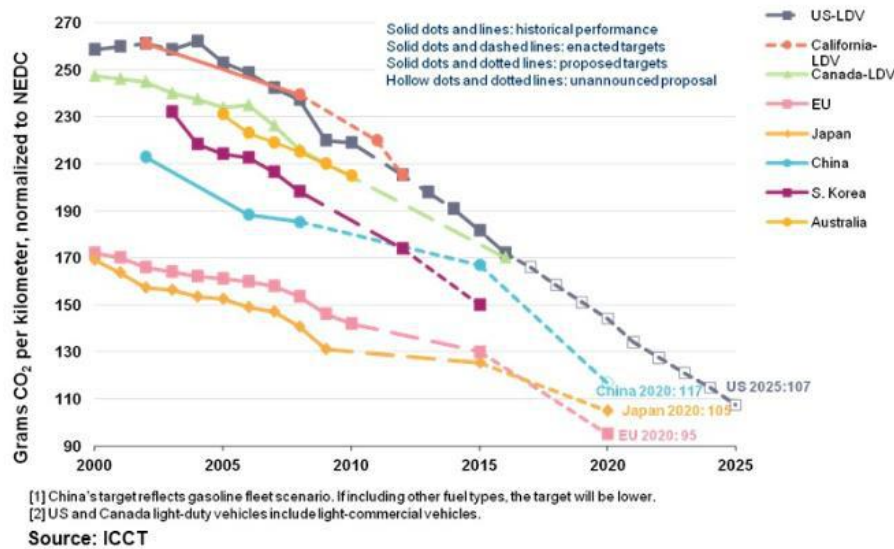


Figure 2. The target of CO₂ in different countries [2]

In 2018, October, EU announced new targets by decreasing the target CO₂ emission as 45% in 2030 [3]. The target was 75 gr/km for 2030. It is changed as 45 gr/km for 2030.

This target can't be realized without higher electrification in all the filo.

2. GLOBAL AUTOMOTIVE MARKET

Total automotive production was 97,3 Million on the world in 2017. The biggest 20 companies produced 83 Million (87 %) of the total production. 93% of the total production was produced in 20 countries. China is the leader in manufacturing by 29.8 % of the world production. Turkey manufactured 1.695.731 vehicles in 2017. Turkish ranking is 14th on the world and 6th in Europe. This amount is 1,74% of the world production (Table 1)[4].

On the other hand, at the same year (2017) 1.007.368 electric/hybrid vehicles produced on the world (Table 2)[4]. This is 1% of the World vehicle production. Although this is looking as small percentage in the total market, the electrified vehicles increase their market share in high rates. The growing rate of the electrified vehicles are around 50% at the last 5 years -between 2013 and 2017-. 5 years ago less than 500 000 cars were on the road and the last year this numbers pass the 3 million (Figure 3).

Table 1. World Automotive Production [4]

Rank	Country	Cars	Commercial vehicles	Total
	Total	73.456.531	23.846.003	97.302.534
1	China	24.806.687	4.208.747	29015434
2	USA	3.033.216	8.156.769	11189985
3	Japan	8.347.836	1.345.910	9693746
4	Germany	5.645.581	0	5645581
5	India	3.952.550	830.346	4782896
6	S. Korea	3.735.399	379.514	4114913
7	Mexico	1.900.029	2.168.386	4068415
8	Spain	2.291.492	556.843	2848335
9	Brazil	2.269.468	430.204	2699672
10	France	1.748.000	479	2227000
11	Canada	749.458	1.450.331	2199789
12	Thailand	818.44	1.170.383	1988823
13	UK	1.671.166	78.219	1749385
14	Turkey	1.142.906	552.825	1695731
15	Russia	1.348.029	203.264	1551293
16	Iran	1.418.550	96.846	1515396
17	Czech Rp.	1.413.881	6.112	1419993
18	Indonesia	982.356	234.259	1216615
19	Italy	742.642	399.568	1142210
20	Slovakia	1.001.520	0	1001520

Table 2. Electric Vehicle Sales in 2017

PI	WORLD	YTD
1	BYD	109.485
2	BAIC	103.199
3	Tesla	103.122
4	BMW	97.057
5	Chevrolet	54.308
6	Nissan	51.962
7	Toyota	50.883
8	Roewe	44.661
9	Volkswagen	43.115
10	ZhiDou	42.484
11	Renault	40.598
12	Zotye	36.862
13	Chery	36.444
14	JMC	29.951
15	Changan	29.822
16	Mercedes	29.800
17	JAC	28.659
18	Mitsubishi	26.634
19	Geely	24.866
20	Hyundai	23.456
	TOTAL	1.007.368

Although global electric car stock is expanding rapidly, crossing the 3 million vehicle threshold in 2017, this is still 0,21% of the total vehicles which is 1 billion 400 million on the world [5].

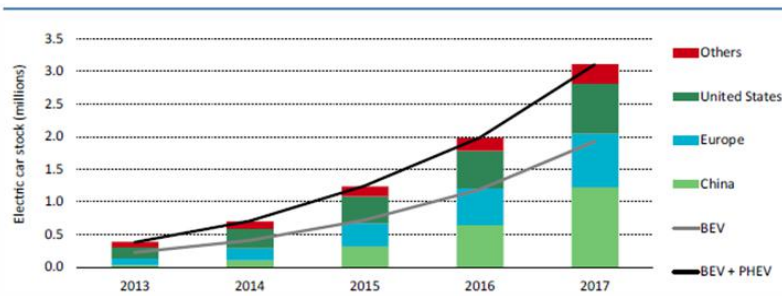


Figure 3. Evolution of the global electric car stock, 2013-17 [5]

All the figures and the market forecast show that, the electrification is a fact on the near future. The electrification studies go on two ways; the first is electric/hybrid vehicles and the second is autonomous vehicles. Both branches are highly dependent to battery technologies to go further.

3. BATTERY MARKET OVERVIEW

Total battery market reach to 500 GWh/year in 2017. The *Compound Annual Growth Rate (CAGR)* is 26 % in li ion for the last 7 years. Even this impressive growing rate in li ion, the lead acid battery still dominated the market (Figure 4) [6].

The main player is lead acid in this capacity with roughly 400 GWh market penetration. The second and important player is li ion with more than 100 GWh market share. Lead acid battery is dominated the 80% of the capacity.

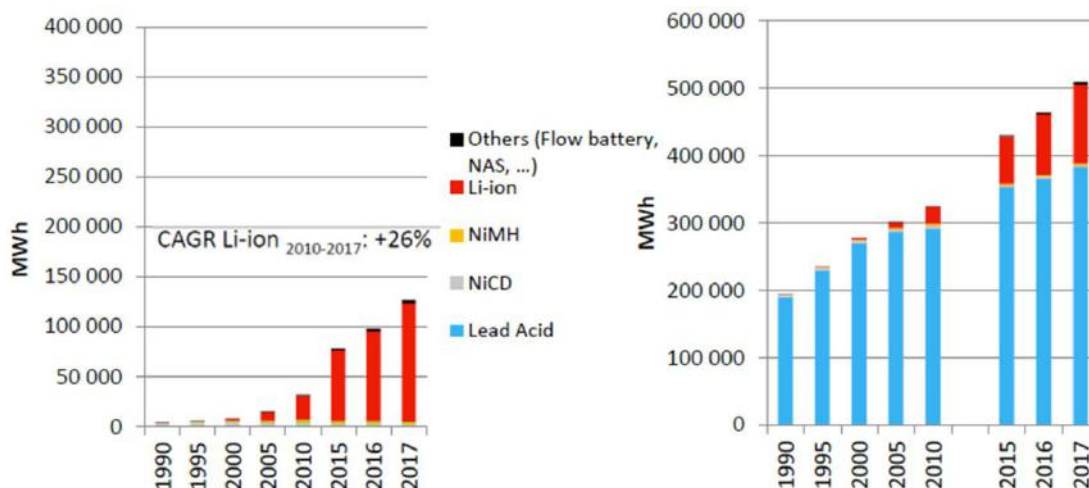


Figure 4. The global battery market growth in MWh, 1990-2017 [6]

On the other hand, Lead acid still covers the 63% of the market by 47 Billion US \$. But also, li ion reach to roughly 30 billion US \$. The main applications are automotive, industrial and portable usage for the energy storage (Figure 5).

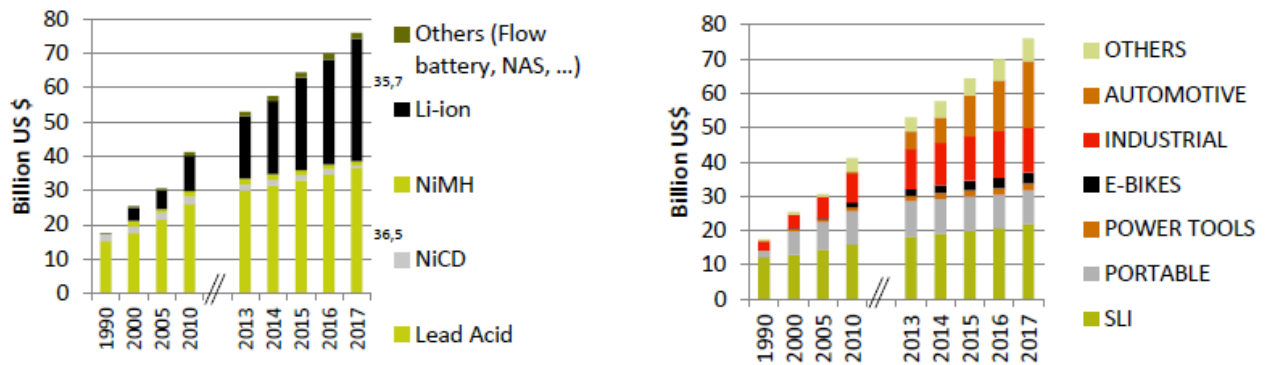


Figure 5. The global battery market growth in US \$, 1990-2017 [6]

The lead acid can't supply the requirements in higher voltages. So above 48 V all the electrified systems need li ion battery. Lead acid battery will continue as a SLI battery in micro, mild, full hybrid and battery electric vehicles. But in higher voltages the main energy supplier will be the li ion.

3.1. Li ion Cost Trend

Bloomberg new energy finance reported that, the cost of li ion battery has been decreasing year by year. The cost was 162 \$/kWh in 2017 for the Korean suppliers and their aim is 74 \$/kWh in 2030 [7]. The low price can supply by giga factories which have higher volumes in production to decreasing the cost. Even though the estimations show low prices the market cost is higher than 150 \$/kWh (Figure 6).

Also, this low price is under the government subsidy. On the other hand, the low price is increasing the production, this causing to higher raw materials demand. The higher demand is causing to increase the raw material cost. This paradox is creating press on the price.

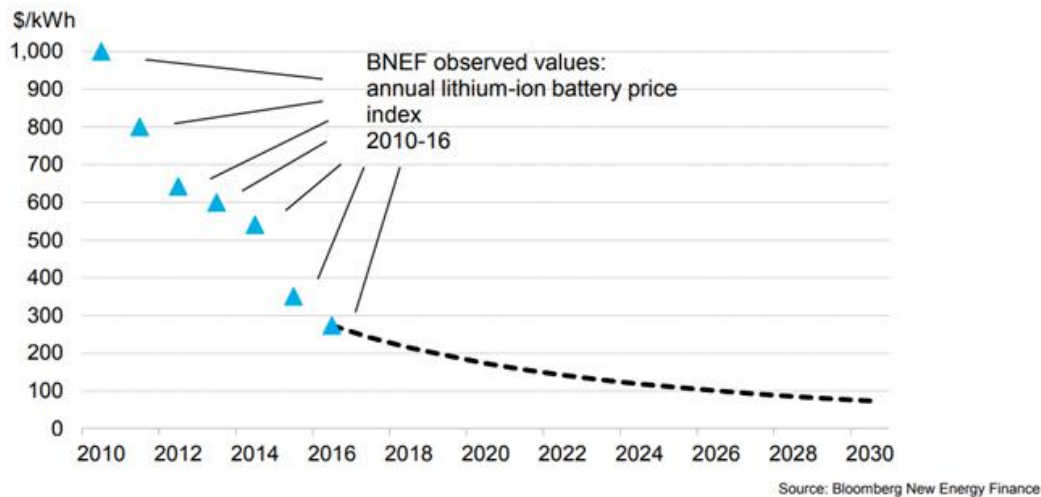


Figure 6. Li-ion cell based cost trend forecast in US \$, 2010-2030 [7]

3.2. Cell Production and Raw Materials

The li ion cell production is mostly located in Far East (China, Korea and Japan). The market leader is China. On the other hand, most of the lithium mining is in South America. Bolivia has the highest lithium mine reserve on the world. But the highest production is in Chili. Also, Australia and Argentina are big player in lithium ore market(Figure7).

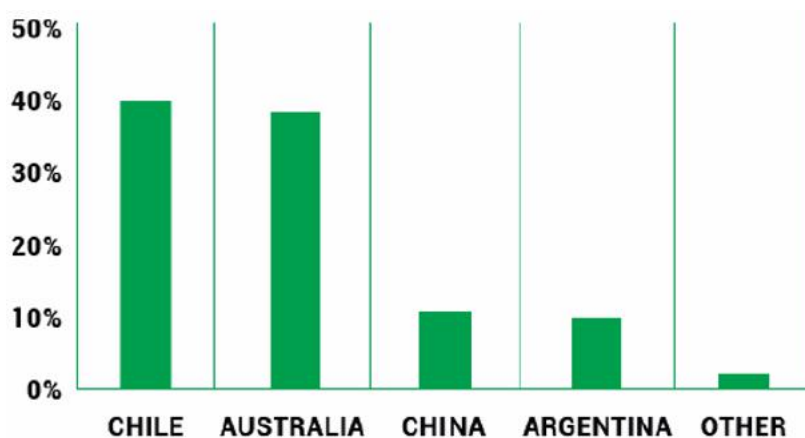


Figure 7. Lithium ore production on the world [8]

The lithium ore is base for the lithium ion batteries. But the active materials which produced from the ore are crucial on the technology. The batteries include anode, cathode, electrolyte and separator.

Lithium ion batteries mostly includes Graphite as anode. But also, the composites with silisium and tin are under development for commercial applications. The Titanate also is using as high rating performance anode in lithium ion batteries. China is producing the 95% of the graphite on the world.

But Japan is still main supplier in battery grade graphite. On the other hand, also the electrolyte and cathode production mostly dominated by China (Figure 8).

The cathode includes cobalt in $\text{LiNi}_x\text{Mn}_y\text{Co}_z\text{O}_2$ composition. This is one of the most widely using chemical composition in lithium ion batteries. Cobalt is crucial for this technology and half of the cobalt is producing in Congo.

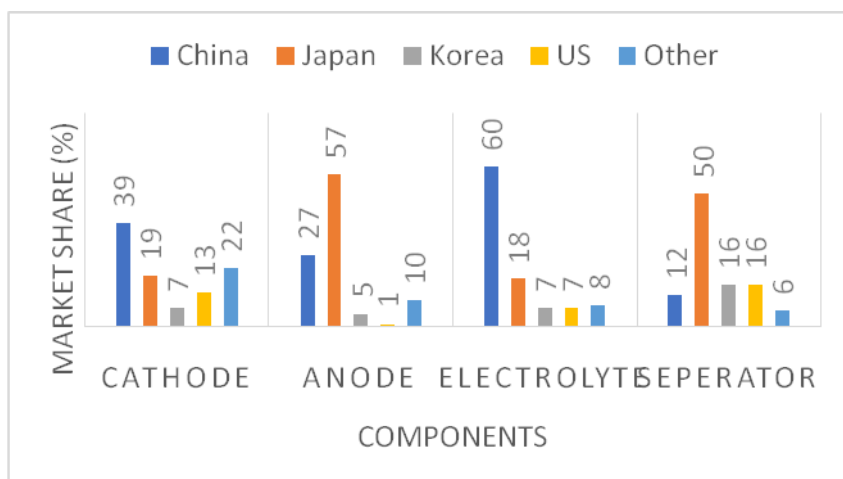


Figure 8. Market share by countries for Li-ion cell sub material production [8]

The parameter shows that all the supply chain (raw materials, cell production, market etc.) are in Far East. This make the far east is so competitive.

Lithium ion cell production will be continuing to increase in far east at the near future because of their competitive position. Euro region (include Turkey), US and other part of the world will be focus on battery pack development and production. Also, beyond lithium ion technologies will be developed in these countries.

3.3. Beyond Lithium Ion

Though the li ion is the common technology in the market for electric and hybrid vehicles, the technology still has many difficulties in the market. The main problems of the EV which caused by the battery are distance, safety, fast charge, recycle and cost. The future studies have been focusing on solid state electrolyte batteries, metal-air and Li-S [9]. These technologies aren't ready for commercial application yet. But many researchers and companies are working on them to develop a commercial grade product. Alternative chemistries like li-S and li-air are mostly in laboratory scale and need more effort to pass the technological barriers.

Li ion improvement studies have been focusing on solid state electrolyte. Solid state electrolyte battery is a li-ion battery. The main difference between the current li ion technology is the electrolyte. This one is special ceramic separator which is ionically conductive but electronically non-conductive.

Automotive companies have many programs to developing solid electrolyte for li ion batteries. Because the technology promises many advantages, like; thermal stability(safety), long life, low self-discharge rate, high energy and power density, fast charge/discharge. Especially the safety and fast charge are the most challenging issues for the automotive companies. Although this impressive advantage the technology has many challenges which restrict this advantage. These challenges are; limited ionic conductivity of the electrode and electrolyte materials, limited electrical conductivity of the electrode materials, interface reactions and the resistance at the interface. Also, manufacturing methods for mass scale production is still a barrier for the technology.

4. CONCLUSION

The electric vehicle has small share (1%) in world yearly automotive production. But this technology is increasing the market share in double each year. The main challenges in the technology is the li ion battery. Because this technology has safety problems, low energy density (means low distance) and high cost. The studies are focusing on alternative chemistries and improvement of li-ion by using solid electrolyte. All the alternatives still in laboratory scale and needs more effort to be commercial. Even though, this challenges in li ion the technology is the main commercial solution in the market and most of the companies are developing solution with this technology.

The main challenges are still distance, safety and cost in li-ion. Also, the fast charge capability is the other big barrier in front of the mass scale commercialization. Solid state batteries are the main focusing area to increase this capability.

The beyond li-ion technologies like li-S and metal-air are in the laboratory scale. The expectations is showing that, the fuel cells also have potential as alternative in electrification.

5. ACKNOWLEDGMENTS

We gratefully acknowledge the support provided by TUBITAK Project no: 3170398

6. REFERENCES

1. <https://www.smmmt.co.uk/2014/03/uk-passes-eu-new-car-co2-emissions-landmark/>
2. <https://www.acea.be/industry-topics/tag/category/co2-from-cars-and-vans>
3. <https://www.reuters.com/article/us-eu-auto-emissions/eu-lawmakers-set-to-back-45-percent-cut-target-for-co2-from-cars-and-vans-by-2030-idUSKCN1LN1SJ>
4. <http://www.oica.net/production-statistics/>
5. <https://www.iea.org/gevo2018/>
6. Pillot Christophe, Avicenne Energy, “The rechargeable battery market and main trends”, AABC, 29 Jan.2018, Mainz, Germany
7. <https://data.bloomberglp.com/bnef/sites/14/2017/07/BNEF-Lithium-ion-battery-costs-and-market.pdf>
8. <https://webstore.iea.org/world-energy-outlook-2018>

INVITED SPEAKERS

RECENT NEW APPLICATIONS OF HBN

N.Ay¹, G.M.Ay² and Y. Göncü³

¹Eskişehir Teknik Üniversitesi, ²Eskişehir Osmangazi Üniversitesi, ³BORTEK Inc.Eskişehir

ABSTRACT

Boron nitride (BN) is a synthetic material that can be synthesized in different crystalline structures such as hexagonal or cubic. Based on crystalline structures, BN shows different physical and chemical properties. Balmain first synthesized BN in 1842; it took until the 1940s before it gained limited economic significance. Looking at past industrial trends, BN was not used till 1990s because of the high production cost. Hexagonal boron nitride (hBN) has been used in various industries more than the other polymorphs. Depending on its structural characteristics, hBN is a good solid lubricant that is chemically inert and is a very good electrical insulator with high thermal conductivity and good thermal shock resistance. This very versatile material has been utilized in a number of applications (metallization, the metal industry, space industry, cosmetics, the automotive industry, high- temperature furnaces, thermal management, etc.). Recently, hBN nanomaterials (nanoparticles, nanotubes, nanosheets etc.) has attracted attention due to its unique properties in nuclear technology, marine antifouling paint, biological and medical applications, biomarkers and biosensors technologies, and drug delivery systems, implant coating, oral care products as they have no toxic and cytotoxic effect on cells and are biocompatible.

Keywords: Hexagonal boron nitride, Applications, Nanomaterials, Biocompatible

HISTORY

BN was first synthesized by heating boronoxide with NaCN by English chemist W.H.Balmain in 1842 [1]. R. Wöhler characterized boron nitride which produced by the interaction of ammonia with trihalogenboron in 1850. The fundamentals studies of boron and nitrogen compounds have been carried out since 1935, but BN did not gain economic significance till 1940. In 1951, Pease defined the hBN structure. R.H.Wentorf synthesized cubic boron nitride (cBN) starting from hBN in 1957 at General Electric Research Laboratory and named it BOROZAN. Later US Carborundum and Union Carbide achieved to produce cBN at the industrial size and shaped it [2]. Due to high production cost, BN was not used for a long period and after the 1990s it has been utilized in many industries and applications. Through intensive research, hBN nanomaterials were developed as fullerenes/ nanocages and nanotubes in the 1990s, nanosheets and other morphologies, e.g. nanomeshes, nanoparticles, nanowires, nanoribbon, and nanoporous in the 2000s [3]. Qingsongite, the natural analog of cBN was discovered in the rocks rich in chromium in the southern Tibet at the Earth's upper continental crust in 2009 [4].

The crystal structures observed in polymorphs of BN are cubic, wurtzite, hexagonal, and rhombohedral (Fig1). Other varieties of BN are amorphous BN (aBN) and turbostratic BN (tBN) with hexagonal basal planes stacked in a random sequence and randomly rotated about the c axis. In addition, theoretical calculations predict the existence of a rocksalt phase (rsBN) under very high pressures (>800 GPa) but the experimental demonstration is still lacking. Structural and physical properties of various BN polymorphs are given in Table 1 [5].

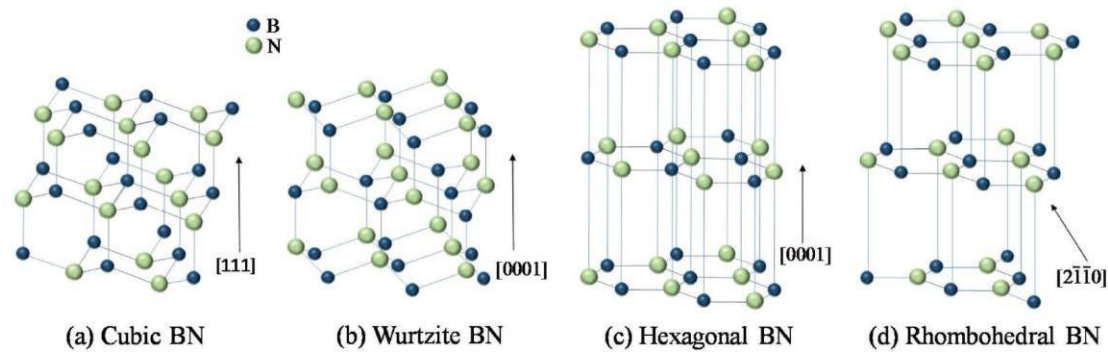


Fig. 1. The crystal structures observed in polymorphs of BN [5].

Table 1. Literature data on structural and physical properties of various BN polymorphs.

Material	c-BN	h-BN	w-BN	r-BN	rs-BN
Structure	zinc blende	hexagonal	wurtzite	rhombohedral	rocksalt
Space group	$F\bar{4}3m$	$P6_3/mmc$	$P6_3mc$	$R\bar{3}m$	$Fm\bar{3}m$
Lattice parameter [Å]	$a = 3.6169^{[21]}$	$a = 2.5043$ $c = 6.6562^{[22]}$	$a = 2.5494$ $c = 4.2229^{[21]}$	$a = 2.5042$ $c = 9.99^{[22]}$	$a = 3.482^{[49]}$
Density [g cm^{-3}]	$3.4847^{[21]}$	$2.2^{[23]}$	$3.4674^{[21]}$	$2.26^{[45]}$	$3.903^{[49]}$
Standard molar volume [$\text{cm}^3 \text{mol}^{-1}$]	$7.1183^{[24]}$	$10.892^{[24]}$	$7.145^{[24]}$	$10.904^{[24]}$	
Bandgap [eV]	Experimental indirect $6.4^{[25,26]}$ $6.2^{[27]}$	Experimental direct $5.971^{[15]}$ Experimental indirect $5.955^{[16]}$	Calculated indirect $6.86^{[17]}$	Calculated indirect $3.9\text{--}4.8^{[29,30]}$	Calculated indirect $\approx 2^{[49,50]}$
Thermal conductivity [$\text{W cm}^{-1} \text{K}^{-1}$]	$\approx 13^{[31]}$	2.35 in-plane 2.3×10^{-2} out-of-plane ^[32]			
Thermal expansion [10^{-6}K^{-1}] at room temperature	$1.15^{[47]}$	-2.72 in-plane 37.7 out-of-plane ^[46]	2.3 in-plane 2.7 out-of-plane ^[48]		
Hardness on the Mohs scale	$9.5^{[33]}$	$1.5^{[33]}$			
Surface hardness [kg mm^{-2}]	$4500^{[33]}$		$3400^{[33]}$		
Bulk modulus [GPa]	$369\text{--}400^{[34-40]}$	$36.5^{[33]}$	$390^{[34]}$ $375^{[42]}$	$\approx 33^{[44,45]}$	$398^{[49]}$

APPLICATION

Depending on its structural characteristics, hBN can be used as a lubricant, protective coating, insulator, cosmetic agent, paint additive, material for crucibles, electrically insulating and thermally conductive fillers, microwave-transparent shields, high-temperature bearings, etc [6]. Hexagonal boron nitride powder is a soft, white, lubricious powder with unique characteristic that makes it an attractive, performance-enhancing alternative to graphite, molybdenum disulfide and other inorganic solid lubricants. The coefficient of friction (COF) value of hBN is lower than graphite and MoS₂ and it keeps this property up to 900°C (Fig 2) [7]. BORONMAX oil additive was produced with hBN by utilizing its low COF value [8]. Tribological tests were conducted to determine COF and wear rate values of BORONMAX by O.N.Çelik. Samples were tested in dry condition and in oil. Friction and wear tests were performed using a CSM ball-on-disc tribometer. WC 6% Co balls with a diameter of 3mm were used as a counterpart. Discs made of AISI 4140 steel were austenitized at 860°C for 1 h, oil quenched, and subsequently, tempered at 300°C for 20 min. Surface profiles of discs were measured using a Mitutoyo SJ-400 profilometer (Mitutoyo Corp., Japan) before and after the wear tests. Wear-test settings were established in accordance with the DIN 50324 standard. Tests were conducted at 20°C and at a relative humidity of 32%. Wear tests were performed in a 50mL oil tank, and the substrate surface was flooded with lubricant at least 5mm above the sliding surface. The ball-on-disc sliding

speed was 2.5 cm/s, and the diameter of the wear track was 6 mm. The chosen normal load in all of the wear tests was 10 N. The calculated Hertzian contact stress was 2.93 GPa. The measurement results of the friction coefficient of engine oil and BORONMAX were 0.111 and 0.095 respectively (Fig. 3). The friction coefficient of BORONMAX was decreased by 14.4% with respect to engine oil. When the surface profiles of the samples in dry, oil and BORONMAX were examined, it was found that the smallest surface profile was formed by BORONMAX. The wear rate with BORONMAX was reduced by 60% compared to engine oil (Fig 4).

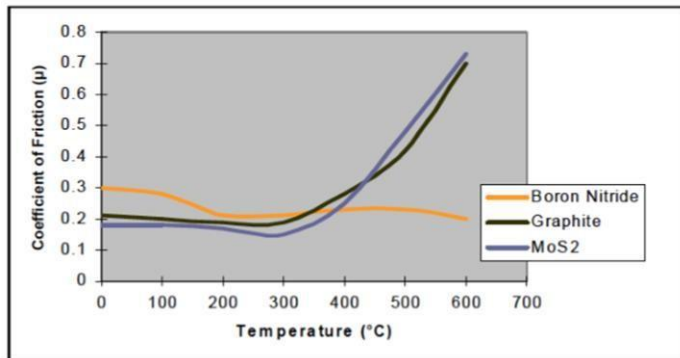


Fig 2. COF values comparison [7].

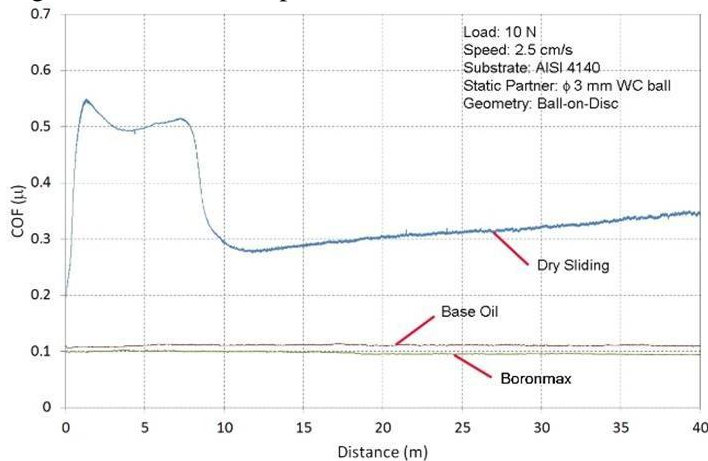


Fig 3. COF values in different media.

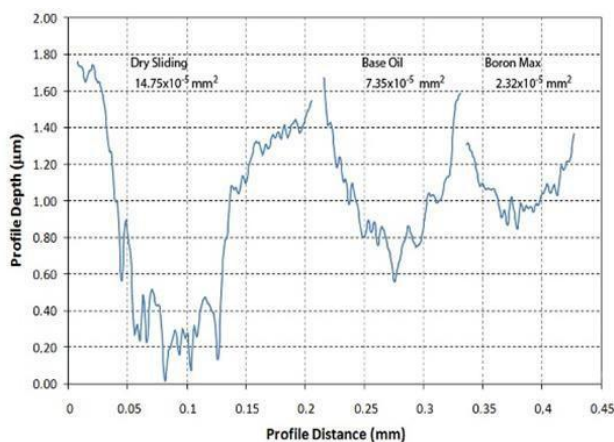


Fig 4. Wear profiles comparison.

The high chemical and thermal stability combined with the non-wetting property make hBN a useful crucible and structural material in metallurgical applications [9]. Because of its non-wetting properties on melted metals and glass, smooth metal surfaces are obtained with painting the dies with hBN [10]. It is used in various products in the metallurgy industry (crucibles, break rings for horizontal continuous castings, pipes, and nozzles for handling liquid metals, etc.) due to high-temperature refractoriness of hBN [11]. hBN is reported to function in cosmetics as a slip modifier, that enables other substances to flow more easily and smoothly, without reacting chemically. The data reported (2013) that boron nitride is used in 643 cosmetic formulations [12].

RECENT STUDIES

Yaras et al. reported that hexagonal boron nitride nanosheets (BNNS) were prepared using methods include direct sonication (aq-BNNS) and sonication after pretreatment with Hummers method (Hum-BNNS) in an aqueous medium. The aq-BNNS and Hum-BNNS were utilized to coat the surface of cellulosic tent fabric using an airbrush spray with 0.3mm nozzle at 3.0 atm of nitrogen pressure (Fig 5). As seen from Fig 6, the water contact angles (WCA)s were found to be 118.2° and 108.2° for fabrics coated with Hum-BNNS and coated with aq-BNNS, respectively, but cannot be measured for uncoated fabric due to instant penetration of the water through the fabric surface. The results showed that the hydrophobic surfaces were obtained by coating with BNNS, but the uncoated cellulosic fabric is hydrophilic [13].

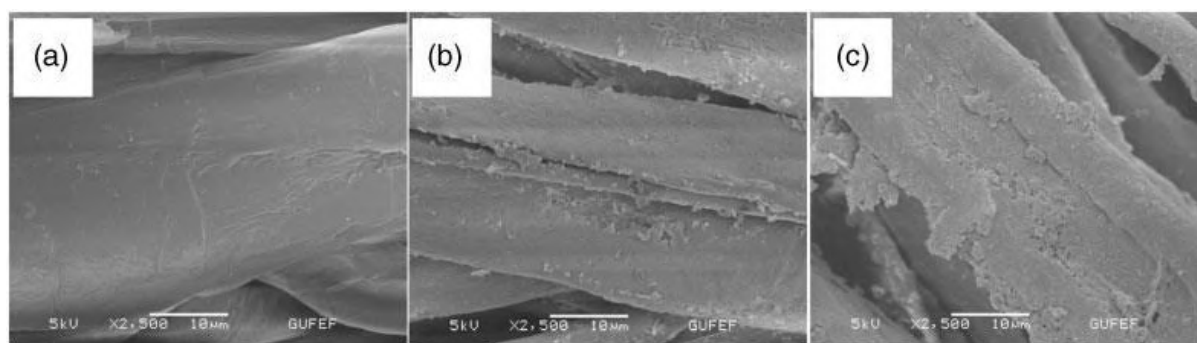


Fig 5. SEM images of uncoated cellulosic fabric (a), Hum-BNNS coated fabric (b), and aq-BNNS coated fabric (c) [13].

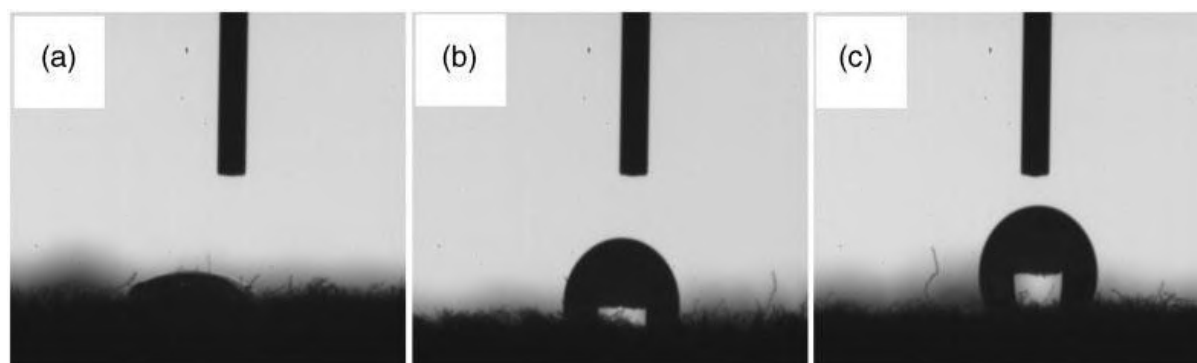


Fig 6. The water contact angles of uncoated cellulosic fabric (a), aq-BNNS coated fabric (b), and Hum-BNNS coated fabric (c) [13].

Fire-resistant wood coatings have been sought much research field. Liu et al. investigated the use of binder-free exfoliated hBN nanosheets in fire-resistant wood coatings. The average sizes of the hBN nanosheets are in the range of 50–300 nm. Fire-resistant property of the hBN nanosheet coatings was performed using a firelighter employing a wood substrate in which half of the portion is coated with

BN nanosheets. The fire-resistance experiment is depicted in Fig 7. Fig 7a shows the wood substrate in which white portion is coated with hBN nanosheets, exhibits an opaque white color, and can be easily differentiated with the uncoated portion that possesses the yellowish tint color of the pristine wood substrate. The experiment is carried out for the same time frame and the hBN coated portions endured the fire and remained intact after 60 seconds. Fig 7f shows the wood substrate after fire experiment was carried out for 1 min with (left) and without hBN nanosheet coating (right). It can be clearly seen that the hBN-coated portions of the wood substrate remained intact after exposing to fire. The anisotropic thermal conductivity and low thermal diffusivity and effusivity of hBN make it an excellent wood protection coating [14].

In Fischnaller et al's studies, the great potential of hBN, as a new SPE-material, on the enrichment, preconcentration, and desalting of a tryptic digest of model proteins is demonstrated. A special attention was dedicated to the efficient enrichment of hydrophilic phosphopeptides. Two elution protocols were developed for the enrichment of peptides compatible for subsequent MALDI-MS and ESI-MS analysis. In addition, the recoveries of 5 peptides and 3 phosphopeptides with a wide range of pI values utilizing hBN materials with different surface areas were investigated. It was found that 84–106% recovery rate could be achieved using hBN materials. The results were compared with those obtained using graphite and silica C18 under the same elution conditions, and lower recoveries were obtained. In addition, hBN was found to have a capability of protein depletion, which is requisite for the peptide profiling [15].

Fischnaller et al's 2016 study describes the development of a fast, simple, efficient and validated dispersive SPE method utilizing hBN for the determination of BPA and its derivatives (BPF, BPZ, BADGE, and BADGE.2H₂O). The developed method permits trace analysis of bisphenols without evaporation and reconstitution. The method showed good recovery rates ranging from 80% to 110% [16].

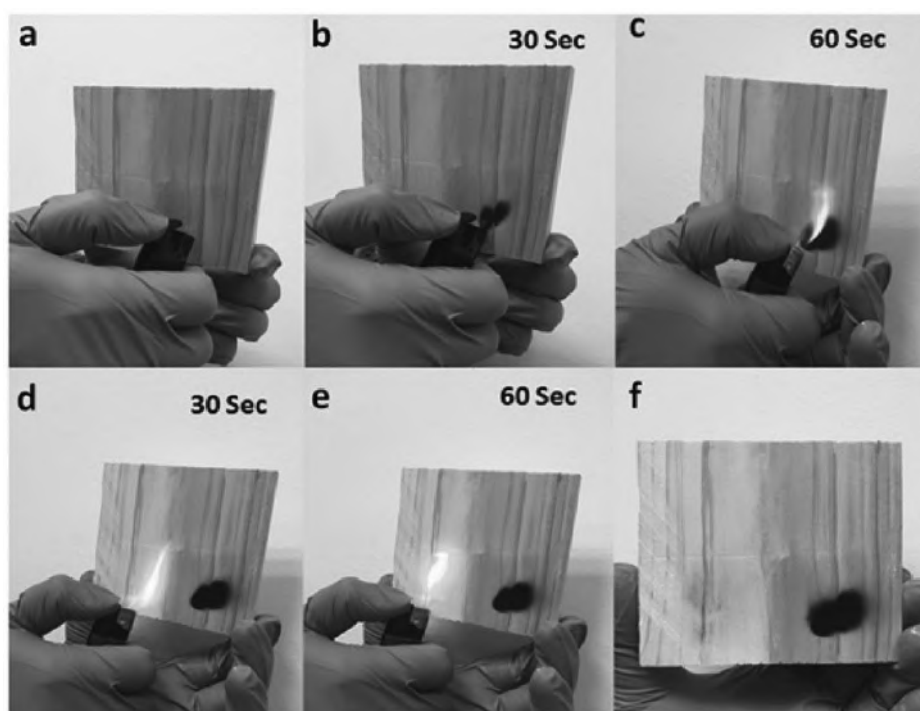


Fig 7. a–f) The fire-resistant property of BN-coated wood substrates. a) The coated and uncoated surface of the wood substrate. b,c) The carbonization of pristine uncoated wood substrate surface exposed to fire after 30 and 60 s. d,e) The fire resistance of hBN nanosheet coating on exposure to fire following the same time. f) The aftermath of the fire-resistant experiments[14].

Mercury (Hg^{2+}) is a well-known contamination owing to its high toxicity at low concentration, as well as its bioaccumulative effect in human body. A T-rich ssDNA probe (P2) was designed for the detection of Hg^{2+} . In the absence of Hg^{2+} , P2 was adsorbed onto the BNNS and therefore the fluorescence was quenched. Upon the addition of Hg^{2+} , an intramolecular double helical structure was formed via the strong affinity of T- Hg^{2+} -T, which weakened the adsorption of P2 onto BNNS and thereby recovered the fluorescence. To evaluate the selectivity of this proposed biosensor, several metal cations such as Ba^{2+} , Ca^{2+} , Co^{2+} , Mg^{2+} , Cu^{2+} , Ni^{2+} , Pb^{2+} , Mn^{2+} , Zn^{2+} , and Fe^{3+} (12.5-fold concentrations of Hg^{2+}) were employed. The selectivity of the BNNS-based Hg^{2+} biosensor (the concentration of Hg^{2+} and all other ions is 4 μM and 50 mM, respectively). This strategy is versatile and quick fluorescence sensing of DNA and extensive DNA related analytes such as metal cations and small molecules and it might be available for the practical application in the future [17].

Dopamine (DA) is one of the most significant catecholamines, that is very important for brain functions. Extreme abnormalities of DA concentration levels may lead to symptoms of diseases such as Parkinson's, Alzheimer's, and schizophrenia. In this study, Polyimide (PI) and polyimide-boron nitride (PI-BN) composites as dopamine- selective membrane were synthesized. Dopamine selectivity behavior of prepared membranes was examined by differential pulse voltammetry (DPV). Using this process it was possible to obtain a good dopamine selective electrode with wide linear ranges, easy preparation, selectivity, reusability, and very high R-value. Based on these excellent characteristics, PI-5%BN composite electrode provides a new strategy for the development of dopamine sensor [18].

Nitrite is widely present in the human environment and is the most common nitrogen-containing compound in nature. Because of its special nature, nitrite is widely used in industry and construction. Nitrite is also allowed in a limited amount in hair dyes and meat products. However, excessive intake of nitrite is harmful to humans and animals, because nitrite can interact with amines and undergo conversion into carcinogenic N-nitrosamines. The highly sensitive detection of nitrite requires expensive and complicated instrumentation, highly trained technicians, and time-consuming extraction steps. The developed electrochemical sensor for nitrite assays displayed superior analytical performance, such as good selectivity, excellent reproducibility, a wide linear range (0.09 to 9853.45 μM) and a low limit of detection (0.03 μM). The recovery experiment shows that the proposed method is promising for the determination and monitoring of nitrite in water and food samples [19].

The demand for fresh water and clean air will increase all over the world owing to population growth and industrial development. Li et al. investigated the activated BN with the high efficient absorption for numerous pollutants in water and air. The activated BN has been exhibited an excellent adsorption performance for metal ions and organic pollutant in water, as well as volatile organic species in air. The excellent reusability of activated BN has also been confirmed. All the features render the activated BN a promising material suitable for environmental remediation [20].

Rafiee et al. revealed that hBN concrete composite (including both gravel and cement) was tested for separation of bitumen crude oil mixture diluted with water. They used Canadian bitumen heavy crude oil diluted with naphtha (1:4) and mixed 100 mL of the mixture with 400 mL of water before applying the filtration. It was found that h- BN concrete composite effectively filters the crude oil from water and the filtered water becomes clear [21].

hBN/BNNS reinforced cementitious composites was produced and was tested for mechanical properties. The results showed that the BNNSs enhanced mechanical properties of Portland cement [22].

The coatings for prevention of biofouling that contaminate the environment due to the compounds in the formulation of paints was investigated. Copper-based paints have been the leader in the antifouling paint market. In recent decades, it has been clear that copper has negative environmental effects. It has been considered that copper is toxic for the marine organisms and harmful for some fishes. Some Baltic countries like Sweden and Denmark banned to use antifouling paint which includes copper oxide. The development of new generation copper-free paint that has antifouling properties for the sustainable environment solves this problem. The research is patent pending by European Patent Office

(EP3044266 A2) and Turkish Patent Institute (2013/10673). The research results promise better performance compared with seasonal or one-year life cycle paint [23,24].

Ciofani et al. investigated the interaction of BNNTs with the first living cells. Living cells are human neuroblastoma cell line (SH-SY5Y)s. These results showed a very good cell viability up to a concentration of 5.0 µg/ml of PEI coated BNNTs in the cell culture medium [25].

Lahiri et al propose boron nitride nanotube (BNNT) reinforced hydroxyapatite (HA) as a novel composite material for orthopedic implant applications. Osteoblast proliferation and cell viability show no adverse effect of BNNT addition. HA–BNNT composite is, thus, envisioned as a potential material for stronger orthopedic implants [26].

Human dermal fibroblasts (HDFs) and adenocarcinoma human alveolar basal epithelial cells (A549) internalized the modified and unmodified BNNTs, and BNNTs were found to not cause significant viability change and DNA damage. The results indicated that the unmodified BNNTs, h-BNNTs, and m-BNNTs had no negative effects on the viability of HDFs, whereas BNNTs and h-BNNTs were highly cytotoxic on A549 cells at high concentrations (100–200 µg/mL). BNNTs are multi-walled, randomly oriented, have an outer diameter of 10–30 nm and a wall thickness of 5 nm. The length of BNNT used in this study was not pointed out [27].

Rasel et al. shows, BNNP (100–250 nm) is assessed as a promising biomaterial for medical applications. The toxicity of BNNP was evaluated by assessing the cells behaviors both biologically (MTT assay, ROS detection etc.) and physically (atomic force microscopy). The TEM images showed that BNNP's are successfully internalized by the cells. A significant amount of nanoparticles were observed to be taken in by osteoblast cells. The effect of nanoparticle uptake on the mechanical stiffness of cells was also studied. It was observed that despite significant BNNP uptake, there was no change in the cell stiffness. This signifies cells still maintained their structural integrity [28].

Atila et al. investigated serum boron levels using ICP-MS after implantation of different ratios of nano-hBN–HA composites in rat femurs. They demonstrated that neither short-term nor long-term implantation of hBN–HA composite resulted in statistically increased serum boron levels in experimental groups compared to the healthy group. The study showed that hBN–HA is a promising material as an implant [29].

Kıvanç et al investigated the effect of the antimicrobial and antibiofilm activities of hBN nanoparticles against *Streptococcus mutans* 3.3, *Staphylococcus pasteurii* M3, *Candida* sp. M25 and *S. mutans* ATTC 25175. Minimum Inhibitory Concentration (MIC) of hBN nanoparticles were determined against *Streptococcus mutans* 3.3, *Staphylococcus pasteurii* M3, *Candida* sp. M25 growth. In addition, the cytotoxic effects of hBN nanoparticles on human normal skin fibroblast (CCD-1094Sk, ATCC® CRL 2120™) and Madin Darby Canine Kidney (MDCK) cells by using various toxicological endpoints were evaluated. Surprisingly, hBN nanoparticles showed a high antibiofilm activity on preformed biofilm, which inhibited biofilm growth of *S. mutans* 3.3, *S. mutans* ATTC 25175 and *Candida* sp.M25. hBN nanoparticles inhibit bacterial growth and do not kill bacteria at used concentration. hBN nanoparticles show high antibiofilm activity on preformed biofilm, which inhibited biofilm growth of *S. mutans* 3.3, *S. mutans* ATTC 25175 and *Candida* sp.M25. These results show that hBN nanoparticles may be an option to control oral biofilms. In cell viability tests, the cells were exposed to 0.025–0.4 mg/ml concentrations of hBN nano particle suspension. The results indicate that there is no cytotoxic effect on CRL 2120 and MDCK cells at the concentration range of 0.025–0.1 mg/mL [30].

ACKNOWLEDGEMENT

Authors would like to thank Dr. Osman Nuri ÇELİK for his help in tribology tests of Boron Nitride.

References

1. Rudolph S. Materials Review: Boron Nitride. American Ceramic Society Bulletin 2002;81:31–4.
2. Wentorf RH. Cubic Form of Boron Nitride. The Journal of Chemical Physics 1957;26:956–956.
3. Jiang X-F, Weng Q, Wang X-B, Li X, Zhang J, Golberg D, et al. Recent Progress on Fabrications and Applications of Boron Nitride Nanomaterials: A Review. Journal of Materials Science & Technology 2015;31:589–98.
4. Dobrzhinetskaya LF, Wirth R, Yang J, Green HW, Hutcheon ID, Weber PK, et al. Qingsongite, natural cubic boron nitride: The first boron mineral from the Earth's mantle. American Mineralogist 2014;99:764–72.
5. Izyumskaya N, Demchenko DO, Das S, Özgür Ü, Avrutin V, Morkoç H. Recent Development of Boron Nitride towards Electronic Applications. Advanced Electronic Materials 2017;3:1600485.
6. Jansen M. High Performance Non-Oxide Ceramics II. Berlin, Heidelberg: Springer-Verlag Berlin Heidelberg: Springer e-books; 2002.
7. Idealube Boron Nitride Platelet Powders Product Datasheet [Internet]. [cited 2018 Oct 6];Available from: <https://www.bn.saint-gobain.com/sites/imdf.bn.com/files/idealube-bn-platelets-powders-nsf-ds.pdf>
8. BORONMAX Bor Bileşikli Yağ Katkısı [Internet]. [cited 2018 Oct 6];Available from: <http://boronmax.com/>
9. Lipp A, Schwetz KA, Hunold K. Hexagonal boron nitride: Fabrication, properties and applications. Journal of the European Ceramic Society 1989;5:3–9.
10. Ay N, Göncü Y. Ergimiş Alüminyumun BORTEK 11 Üzerindeki Islatma Davranışı. 2009. page 381–6.
11. Eichler J, Lesniak C. Boron nitride (BN) and BN composites for high-temperature applications. Journal of the European Ceramic Society 2008;28:1105–9.
12. Fiume MM, Bergfeld WF, Belsito DV, Hill RA, Klaassen CD, Liebler DC, et al. Safety Assessment of Boron Nitride as Used in Cosmetics. Int. J. Toxicol. 2015;34:53S–60S.
13. Yaras A, Er E, Çelikkan H, Disli A, Alicilar A. Cellulosic tent fabric coated with boron nitride nanosheets. Journal of Industrial Textiles 2016;45:1689–700.
14. Liu J, Kuttu RG, Zheng Q, Eswariah V, Sreejith S, Liu Z. Hexagonal Boron Nitride Nanosheets as High-Performance Binder-Free Fire-Resistant Wood Coatings. Small 2017;13:1602456.
15. Fischnaller M, Köck R, Bakry R, Bonn GK. Enrichment and desalting of tryptic protein digests and the protein depletion using boron nitride. Anal. Chim. Acta 2014;823:40–50.
16. Fischnaller M, Bakry R, Bonn GK. A simple method for the enrichment of bisphenols using boron nitride. Food Chem 2016;194:149–55.

17. Zhan Y, Yan J, Wu M, Guo L, Lin Z, Qiu B, et al. Boron nitride nanosheets as a platform for fluorescence sensing. *Talanta* 2017;174:365–71.
18. Aksoy B, Paşahan A, Güngör Ö, Köytepe S, Seçkin T. A novel electrochemical biosensor based on polyimide-boron nitride composite membranes. *International Journal of Polymeric Materials and Polymeric Biomaterials* 2017;66:203–12.
19. Zhang Y, Xia Z, Li Q, Gui G, Zhao G, Luo S, et al. Copper/hexagonal Boron Nitride Nanosheet Composite as an Electrochemical Sensor for Nitrite Determination. *International Journal of Electrochemical Science* 2018;5995–6004.
20. Li J, Xiao X, Xu X, Lin J, Huang Y, Xue Y, et al. Activated boron nitride as an effective adsorbent for metal ions and organic pollutants. *Scientific Reports* 2013;3:3208.
21. Rafiee MA, Narayanan TN, Hashim DP, Sakhavand N, Shahsavari R, Vajtai R, et al. Hexagonal Boron Nitride and Graphite Oxide Reinforced Multifunctional Porous Cement Composites. *Advanced Functional Materials* 2013;23:5624–30.
22. Wang W, Chen SJ, Basquiroto de Souza F, Wu B, Duan WH. Exfoliation and dispersion of boron nitride nanosheets to enhance ordinary Portland cement paste. *Nanoscale* 2018;10:1004– 14.
23. Karabay ZA, Göncü Y, Fidan G, Ay N. THE EFFECT OF NANOMATERIALS IN ANTIFOULING PAINTS. In: 7th International Paint, Paint Raw Materials, Construction Chemicals, Adhesives and Raw Materials, Laboratory and Production Equipments Exhibition and Congress Proceeding Book. Istanbul: 2018.
24. KARABAY ZA, FİDAN G, KALAFATLAR H, Göncü Y, Ay N. Environmentally friendly new generation copper-free antifouling paints. *Industrial Paint, Powder Coating, Surface Treatment Chemicals, Paint applications and Coating Technologies* 2017;28–38.
25. Ciofani G, Raffa V, Menciasci A, Dario P. Preparation of boron nitride nanotubes aqueous dispersions for biological applications. *J Nanosci Nanotechnol* 2008;8:6223–31.
26. Lahiri D, Singh V, Benaduce AP, Seal S, Kos L, Agarwal A. Boron nitride nanotube reinforced hydroxyapatite composite: Mechanical and tribological performance and in-vitro biocompatibility to osteoblasts. *Journal of the Mechanical Behavior of Biomedical Materials* 2011;4:44–56.
27. Emanet M, Şen Ö, Çobandede Z, Çulha M. Interaction of carbohydrate modified boron nitride nanotubes with living cells. *Colloids Surf B Biointerfaces* 2015;134:440–6.
28. Rasel MAI, Li T, Nguyen TD, Singh S, Zhou Y, Xiao Y, et al. Biophysical response of living cells to boron nitride nanoparticles: uptake mechanism and bio-mechanical characterization. *J Nanopart Res* 2015;17:441.
29. Atila A, Halici Z, Cadirci E, Karakus E, Palabiyik SS, Ay N, et al. Study of the boron levels in serum after implantation of different ratios nano-hexagonal boron nitride-hydroxy apatite in rat femurs. *Mater Sci Eng C Mater Biol Appl* 2016;58:1082–9.
30. Kivanç M, Barutca B, Koparal AT, Göncü Y, Bostancı SH, Ay N. Effects of hexagonal boron nitride nanoparticles on antimicrobial and antibiofilm activities, cell viability. *Materials Science and Engineering: C* 2018;91:115–24.

INVITED SPEAKERS**PHOSPHORESCENT GLASS**

Ali Ozan Yanar, Hakan Arda, Bekir Karasu

Eskişehir Technical University, Department of Materials Science and Engineering,
Eskişehir/TÜRKİYE

ABSTRACT

Phosphorus is the light-emitting ability, sometimes after taking light from an anode source. In the scientific world, new materials characterized as phosphorescent with the resistance to heat, atmospheric effects and chemicals have recently been developed. Such a new generation has been extensively researched as long-lasting phosphors due to a growing market for rare earth-enriched alkaline earth silicates and aluminates used in glasses, ceramic glazes, resins, brick and tile coatings. In this study, detailed information was given about luminescence, phosphorescence, phosphors, their synthesis, preparation, properties and applications. Additionally, knowledge about phosphorescent glass are presented.

Keywords: Phosphor, Phosphorescence, Pigment, Glass, Properties, Application.

1. INTRODUCTION AND A BRIEF HISTORY OF PHOSPHORESCENT MATERIALS

Before knowing what phosphorus was, it is better known that its glowing properties have been reported in ancient writings. The oldest known written observations were made in China, dating back to 1000 BC, regarding fireflies and glow-worms. In 1602, Vincenzo Casciarolo discovered the phosphor glowing "Bolognian Stones" just outside of Bologna that was the first scientific study on photoluminescence.

Phosphorus was first isolated in 1669 by German physician Hennig Brand who was an alchemist attempting to change metals into gold when he isolated phosphor. To make a toy to glow in the dark, toymakers use phosphor energized by normal light and that has a very long glowing time. Zinc sulphide and strontium aluminate are among the two most commonly used phosphors [1].

The decent scientific researches on phosphors also have a long history going more than 100 years back. A prototype of ZnS-type phosphors, an important class of phosphors for television tubes, was first prepared by Théodore Sidot, a young French chemist, in 1866 rather accidentally. It seems that this was marked the beginning of scientific research and synthesis of phosphors. From the late 19th century to the early 20th century, Lenard et al. in Germany performed active and extensive research on phosphors, and achieved impressive results. They prepared various kinds of phosphors based on alkaline earth chalcogenides (sulphides and selenides) and zinc sulphide, and investigated the luminescence properties [2].

By the definition photo luminescent objects emitting visible light when light, visible or UV, is shined upon them. Two broad categories are phosphorescence (glow-in-the-dark) and fluorescence. Photo luminescent materials such as the phosphor coating found on fluorescent tubes, fluorescent minerals, and phosphorescent tooth brushes contain many solid atoms. As a result, these materials have valence and conduction energy bands that are separated by an energy gap. Photo luminescent solids also contain many impurity atoms which result in the formation of a band of energy levels found inside the energy gap of the solid material. As a brief review, the animation represents an energy band diagram for the phosphor coating found in a typical “white” fluorescent lamp that emits visible light [3].

The minerals are luminescence-enhanced products with improved results of interaction of foreign materials called activators; under various conditions. It returns the light it receives from daylight or from any lighting device. In some sectors, when it participates in production, it continues its function within the product.

In Türkiye the production of phosphorescent pigments with different emission colours has been made at small scale by Fosfortek Co. which was originally established in 2011 as a university base research and development firm. Phosphorescence (or radiation) is the phenomenon of an excitation of an insulator (usually ultraviolet) [4]. This delayed light emission is a process in which charge carriers (e- or gaps) formed by excitation are trapped in certain fault zones and recurred by the decay of salinity [4-5]. Excitation is similar to fluorescence and phosphorescence radiation as it occurs by absorbing (absorbing) the photons [6]. Fluorescence is the phenomenon of visible light emission when a material is stimulated by an externally applied source. A fluorescent lamp, tube and cathode light tube (CLT) systems, which allow the electric current to start, each emit fluorescence light [7].

2. LUMINESCENCE AND ITS PROPERTIES

Luminescence is an emission of [light](#) by a substance not resulting from heat; it is thus a form of cold-body [radiation](#). It can be caused by [chemical reactions](#), [electrical energy](#), subatomic motions or [stress on a crystal](#), which all are ultimately caused by [spontaneous emission](#). This distinguishes luminescence from [incandescence](#), which is light emitted by a substance as a result of heating. Historically, [radioactivity](#) was thought as a form of "radio-luminescence", although it is today considered to be separated since it involves more than electromagnetic radiation [8-9].



Figure 1. [Luminol](#) and Hemoglobin. Luminol glows in an alkali solution when added Hemoglobin and H_2O_2 [10].

3. WHAT IS THE PHOTOLUMINESCENCE?

This is the emission of light induced by the light absorption. Two types of emissions are generally accepted: Fluorescence in the form of fluorescence at about one hundred nanoseconds; and phosphorescence, which lasts longer.

Figure 2 shows the basic properties of the molecular photoluminescence as discussed by Turro (1991). The ground state is denoted by S_0 , the first excited singlet state, S_1 and the first triplet state, the schematic potential energy curves for T_1 , the corresponding vibrational energy levels. Transitions between the states of the same spin multiphase are allowed and take place rapidly; Between different multisite situations are banned and usually appear relatively slowly. Absorption (ABS) fills the vibration levels at S_1 and S_2 . In denser phases, they usually relax within several picoseconds until the lowest vibration level of S_1 with vibrational relaxation (VR) and internal conversion (IC). At this point, the relative proportions of intersystem crossing (ISC), internal conversion (IC) and fluorescence (FL) determine fluorescence and triplet quantum yields. If the ISC comes to the scene, the vibrational relaxation will give the lowest level of vibration, usually at room temperature, from the inverse ISC to S_0 , or at low temperatures causing phosphorescence.

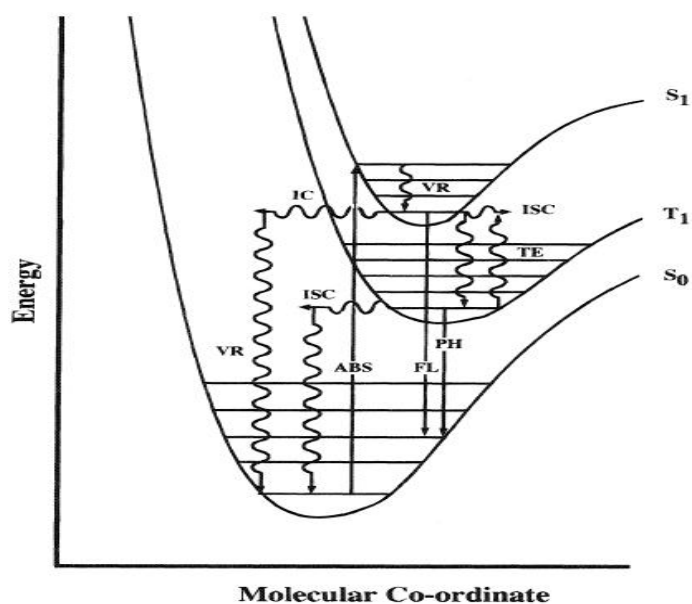


Figure 2. Processes in molecular photoluminescence [11].

Fig. 3 indicates the relative positions of the absorption and emission bands. It can be seen that degradation of the excitation energy leads to a Stokes shift, for instance, the fluorescence is emitted at lower energy than excitation and the fluorescence is performed at lower energy than the fluorescence. Reprocessing of S_1 may cause T_1 delayed thermal excitation (TE) or triple-tertiary annihilation, may give rise to weak but long-lived "delayed fluorescence". Organic photo luminescent materials are discussed by Krasovitskii and Bolotin (1988).

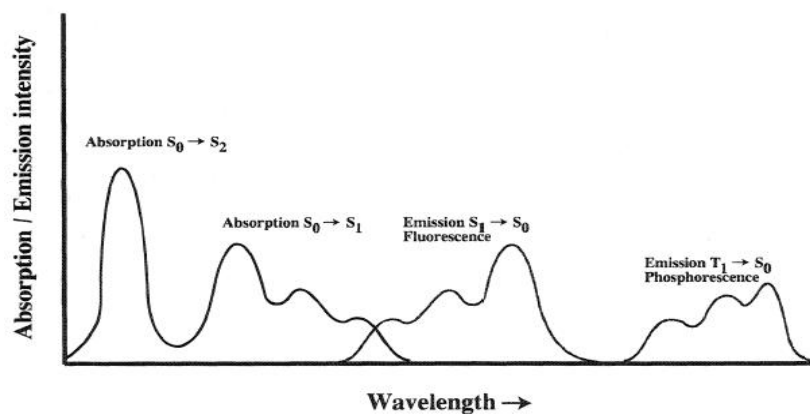


Figure 3. Typical absorption and emission spectra [11].

4. PHOSPHOR PREPERATION

The following methods are essentially the preparation procedures used by the writer W. Lehmann to make the phosphors described. Many points probably are trivial to the professional phosphor chemist but they are certainly not so to the novice or to anyone preparing phosphors only once in a while.

Almost all good inorganic phosphors consist of a crystalline "host material" in which small amounts of certain impurities, the "activators" are dissolved. The activators are primarily responsible for the

luminescence. Other impurities, the “co-activators,” are necessary in some (not in all) cases to dissolve the activator impurities into the host crystal. Co-activators do not, or only to a very minor degree, participate in the luminescence process. Both activators and (if necessary) co-activators are diffused into the host crystal at elevated temperatures, during the sintering. Even the final host material frequently is formed only during the firing by solid-state reactions between several starting materials. The firing temperature often is little below the melting temperature of the host material. If that is impractical because of excessively high-melting temperatures of the host material, the crystallization is facilitated at lower temperatures by addition of a “flux” (frequently a halide) to the raw mix before firing [12].

4.1. Starting Materials

Commercially available high-purity grade chemicals (e.g., analytical reagent grade, luminescent grade) are adequate to prepare most of the phosphors. Only sulphide-type phosphors are exceptions because they are sensitive to undesired impurities, sometimes down to the parts per million range. Sufficiently pure ZnS and CdS are available not to require additional purification for the preparation of ZnS-type phosphors. However, the chemicals needed to prepare CaS-type phosphors are not normally available in the required purity.

The chemicals mentioned in the individual recipes are those that usually are the most readily available. They can frequently be exchanged with others. For instance, CaCO_3 can frequently be replaced by CaO , CaO_2 , $\text{Ca}(\text{NO}_3)_2$, or $\text{Ca}(\text{OH})_2$. Similarly, MnCO_3 can be replaced by MnO_2 , MnO , MnS , MnSO_4 , $\text{Mn}(\text{C}_2\text{H}_3\text{O}_2)_2$, and so on. What counts are only the necessary amounts of the particular chemical elements measured in moles, and that the used compounds decompose readily during the firing of the phosphor to provide the necessary building blocks to the final material [12].

4.2. Amounts

The recipes were given in whole molar units to make them as clear as possible. Whenever such large amounts of phosphors are not needed or wanted, all amounts can be reduced by constant factors as long as the molar ratios between the individual components in the recipe are maintained. However, it is impractical to reduce the amounts to less than about 1 or 2 g of the final phosphor. The materials become poorly reproducible with such very small amounts.

The weightings of the starting materials are not very critical. Phosphor properties vary relatively little only with a variation of the starting material ratios. Roughly, the amounts of the chemicals involved in the formation of the host materials need to be weighed only within $\pm 1\%$ of the mentioned proportions, sometimes even within still wider tolerances. The smaller amounts of the activating chemicals involved are even less critical. Variations of $\pm 10\%$ of the mentioned activator concentrations normally have little effect on the performance of the final phosphor [12].

4.3. Mixing

It is extremely important that the starting materials are mixed well before firing to ensure that a good phosphor is prepared successfully. Some of the best methods are; slurring, wet ball-milling, dry ball-milling, mortaring respectively.

4.4. Containers

The best container material for the preparation of most phosphors is clear quartz (silica). Only some materials (the alkali elements, in particular) react too badly with quartz at firing temperatures and are better fired in other types of containers. Pure alumina serves fairly well in these cases.

Phosphor raw mixes not containing volatile (at firing conditions) constituents are best fired in open boats so that the charge is fully exposed to the desired atmosphere surrounding the material. Raw mixes not containing volatile constituents (e.g., halides) are better fired in loosely covered containers permitting some contact with the surrounding atmosphere but still keeping at least some of the volatile part in the container. Capped silica tubes are widely used in the laboratory; they consist of two tubes each closed at one end and both loosely fitting into each other. Loosely covered crucibles are appropriate wherever alumina is the container material.

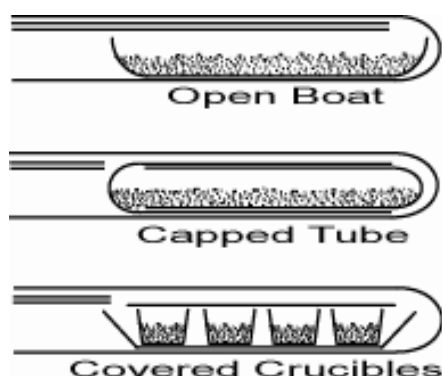


Figure 4. Schematic illustration of different containers during phosphor firing [12].

All these containers are placed near the closed ends of bigger firing tubes made of silica. Some typical arrangements are exhibited in Fig. 4.

4.5. Furnace

Phosphor firing requires an electrically heated furnace permitting temperatures between about 500 °C and at least 1200 °C, better up to about 1400 °C. Any desired temperature should be maintained during firing by means of an automatic temperature controller to within ± 20 °C or better. A simple on-off control is acceptable [12].

4.6. Firing Atmospheres

The various phosphors are fired in different atmospheres depending on the materials and the desired reactions. Oxygen-dominated phosphors (oxides, silicates, phosphates, etc.) may be fired in oxidizing (air, O_2), inert (N_2 , Ar), or reducing atmospheres (CO, forming gas, H_2NH_3). Sulfurization of sulphide phosphors may be achieved by firing either in H_2S or in an inert gas loaded with CS_2 . Many of these gases are interchangeable. It makes no difference, for instance, whether a phosphor is fired in N_2 or in Ar. Some arrangements used to handle the various gases in the firing tubes are given in Fig. 5, assuming the phosphor containers are both open boats.

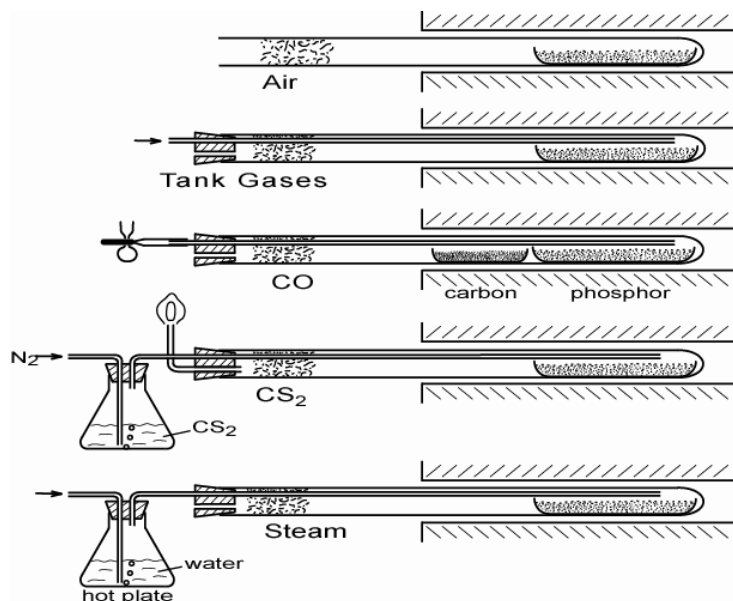


Figure 5. Presentation of different containers employed during phosphor firing [12].

4.7. Treatments after Firing

Fired phosphors often (not always) are slightly sintered cakes that have to be powderized to obtain the desired fine powder. This powderizing usually is possible by gentle grinding or milling. All hard milling must be avoided because it is likely to damage the phosphor. Phosphors coming out the furnace as badly sintered lumps indicate that something is wrong; most likely the firing temperature was too high.

Some phosphors require special washings after firing, usually to remove one or the other undesired residues (e.g., halides). Phosphors of recipes not mention here a washing is not needed.

All phosphors should finally be screened to remove undesired big particles. A 200-mesh stainless steel sieve is adequate for most general purposes but some special applications may require finer screens. Some phosphors are free flowing and easily screened. Others tend to lump and are not screenable with any reasonable effort. Such materials can easily be made free flowing by addition of small amounts (roughly 1/10 % by weight) of some additives like very fine SiO_2 , Al_2O_3 , Sb_2O_3 , etc. Unfortunately, there is no general rule to pick the best additive; to find one remains up to the ingenuity

of the experimenter. Phosphors that stubbornly refuse to become free flowing with any additive can still be wet screened in a suspension in water, methanol, etc. However, this still requires subsequent drying, of course.

All phosphors that are not immediately used up for some application should be stored in closed and labelled containers. Closed containers obviously are necessary for any phosphor that is not completely stable in room air, but they are a good practice also for all others. Remember that good phosphors are precious materials [12].

5. A SAMPLE OF PHOSPHATES USED IN PHOSPHOR PREPERATION

$\text{Zn}_3(\text{PO}_4)_2: \text{Mn}^{2+}$

5.1. Structure: Monoclinic

5.2. Composition

Ingredient	Mole	% By weight (g)
ZnO	99	81
MnCO ₃	1	1.15
H ₃ PO ₄ solution	62 (of P)	47.6 ccm

5.3. Preparation

A thin slurry is made of ZnO + MnCO₃ in water or methanol and stirring must be applied for uniformity as much as possible. Then, while stirring (slurry heats up) H₃PO₄ solution is slowly added. Ball-mill the slurry is ball-milled for about 1 hour, followed by drying in air and Powderized when drying is ended [14].

1. Firing in open quartz boats, air, ~500 °C, 1 h followed by powderizing.
2. Firing in open quartz boats, air, 900 °C, 1 h, then powderizing.
3. Firing in open quartz boats, air, 950 °C, 2 h.

5.4. Optical Properties

Emission colour: Light red

Emission peak: 1.94 eV

Emission width (FWHM): 0.25 eV

Excitation efficiency by UV: – (4.88 eV), – (3.40 eV)

Excitation efficiency by e-beam: ~7–8 %

Decay: Near–exponential decay, 30 msec to 1/10

5.5. Spectra

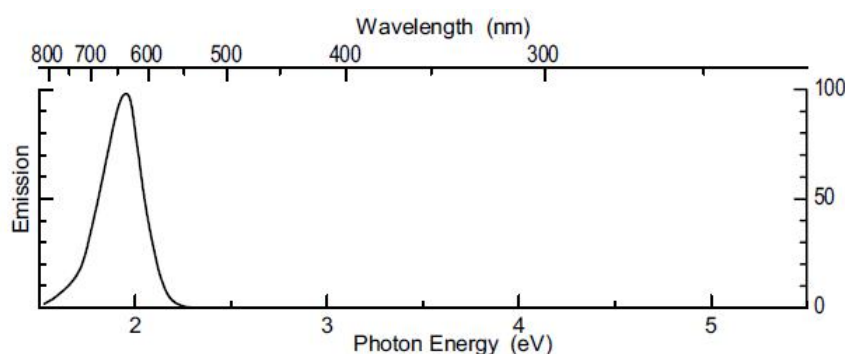


Figure 6. Emission spectra of $\text{Zn}_3(\text{PO}_4)_2: \text{Mn}^{2+}$ [13].

Remarks:

1. This is strictly a catholuminescent phosphor. It cannot be sensitized to respond to 4.88 or 3.40 eV UV.

2. This phosphor has been used as the red component in early colour TV picture tubes [13].

In addition to these, Fig. 7(a) illustrates the emission spectrum and the excitation spectrum of the $\beta\text{-Zn}_3(\text{PO}_4)_2: \text{Mn}^{2+}$ and $\beta\text{-Zn}_3(\text{PO}_4)_2: \text{Mn}^{2+}, \text{Pr}^{3+}$. As stated in the figure, the emission peak at 620 nm is attributed to the ${}^4\text{T}_{1g} \rightarrow {}^6\text{A}_{1g}$ transition of Mn^{2+} ions in octahedral coordination. The excitation spectrum monitored at 620 nm consists of several bands at 385, 411.96, 453 and 477 nm, ascribing to the transition from the ground state ${}^6\text{A}_{1g}$ to the excited states of ${}^4\text{T}_{2g}$, (${}^4\text{E}_g \rightarrow {}^4\text{A}_{1g}$), ${}^4\text{T}_{2g}$ and ${}^4\text{T}_{1g}$ energy levels, respectively [14]. One broad band dominates the wavelength range from 200 to 250 nm when monitored via the emission at 620 nm. It is assigned to the charge transfer state (CTS) of $\text{Mn}^{2+}\text{-O}^{2-}$ [15] rather than the host absorption because the edge of the host absorption band for $\beta\text{-Zn}_3(\text{PO}_4)_2$ is situated at 180 nm [16].

Mn^{2+} ion can exhibit a broad emission band covering the colour from green to red owing to the d-d transition, with lower intensity derived from the 3d-3d forbidden transitions of Mn^{2+} [17]. Therefore, the emission of Mn^{2+} ion is generally excited by energy transfer from the sensitizer or the host [18]. As a promising sensitizer for Mn^{2+} ion, Pr^{3+} can be used to improve the emission intensity of Mn^{2+} in many hosts [19]. The emission spectrum of $\text{Zn}_3(\text{PO}_4)_2: \text{Pr}^{3+}$ is displayed in Fig. 2(b). The emission spectrum monitored at 323 nm consists of several bands peaking at 441, 460 and 485 nm, and so on. The emission peaks of 441 and 460 nm are attributed to the ${}^1\text{I}_6 \rightarrow {}^3\text{H}_4$ and ${}^3\text{P}_J \rightarrow {}^3\text{H}_4$ transition of $\text{Pr}^{3+} 4f^2$, respectively. The emission intensity of Pr^{3+} decreases with co-doping Mn^{2+} in samples while the emission intensity of Mn^{2+} increases with co-doping Pr^{3+} . From Fig. 2(b), it was found that there is some overlap between the emission spectrum of the $\text{Zn}_3(\text{PO}_4)_2: \text{Pr}^{3+}$ and the excitation spectrum of the $\beta\text{-Zn}_3(\text{PO}_4)_2: \text{Mn}^{2+}$. The emission bands of ${}^1\text{I}_6 \rightarrow {}^3\text{H}_4$ and ${}^3\text{P}_J \rightarrow {}^3\text{H}_4$ (around 441 and 460 nm) transitions in $\text{Zn}_3(\text{PO}_4)_2: \text{Pr}^{3+}$ are close to the excitation bands corresponding to ${}^6\text{A}_{1g} \rightarrow {}^4\text{T}_{2g}$ and ${}^6\text{A}_{1g} \rightarrow {}^4\text{T}_{1g}$ (around 450 and 470 nm) transition in $\beta\text{-Zn}_3(\text{PO}_4)_2: \text{Mn}^{2+}$. According to the Dexter's theory, the mechanism of energy transfer basically requires a spectral overlap between the donor emission and the acceptor

excitation [20]. Apparently, there exists the efficient energy transfer from Pr^{3+} to Mn^{2+} in these phosphors. Based on the emission intensity of Pr^{3+} in only Pr^{3+} doped and Pr^{3+} , Mn^{2+} co-doped samples shown in Fig. 7(b), the energy transfer efficiency from the sensitizer Pr^{3+} to the activator Mn^{2+} was calculated as η_T of 0.06 using the following equation [21]: $\eta_T = 1 - I_S/I_{S0}$, where η_T is the energy transfer efficiency and I_{S0} and I_S are the luminescence intensity of a sensitizer in the absence and presence of an activator, respectively.

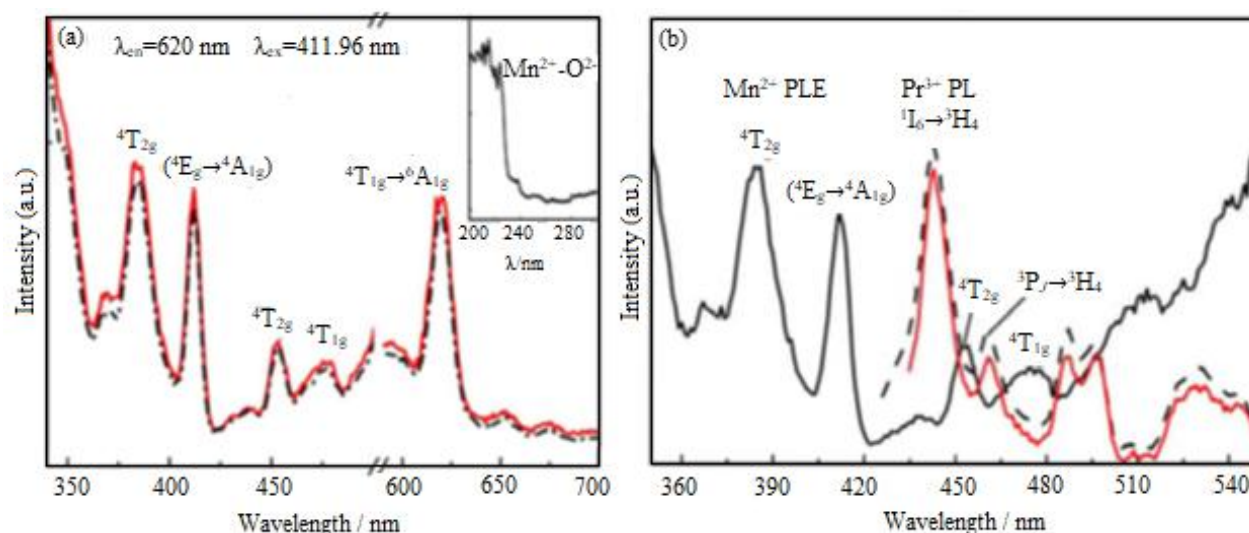


Figure 7. Excitation and emission spectrum of $\beta\text{-Zn}_3(\text{PO}_4)_2: \text{Mn}^{2+}$ (black dotted curve) and $\beta\text{-Zn}_3(\text{PO}_4)_2: \text{Mn}^{2+}, \text{Pr}^{3+}$ (red solid curve) (a) and the excitation spectrum of $\beta\text{-Zn}_3(\text{PO}_4)_2: \text{Mn}^{2+}$ (black solid curve) and the emission spectrum of $\text{Zn}_3(\text{PO}_4)_2: \text{Pr}^{3+}$ (black dotted curve) and $\beta\text{-Zn}_3(\text{PO}_4)_2: \text{Mn}^{2+}, \text{Pr}^{3+}$ (red solid curve) (b) [22].

6. WHAT ARE THE PHOSPHORESCENT PIGMENTS?

Phosphorescence is a specific type of photoluminescence related to fluorescence. Materials which are phosphorescent do not immediately re-emit the radiation they absorb. The slower time scales of the re-emission are associated with forbidden energy state transition. After absorbing visible sun light and UV-A 365 nm light, it can glow for more than 12 hours in the dark. In general pigments with a bigger particle size have longer afterglow properties than the smaller ones. Therefore, pigments with a particle size of 1–2 μm (phosphorescent sands) can glow for more than 12–15 hours [23].

6.1. Synthesis and Experimental Studies of Bluish-Green and Yellowish-Green Phosphorescence Pigments

Bluish-green and yellowish-green phosphorescent pigments were synthesized according to the flowchart given in Figure 8.

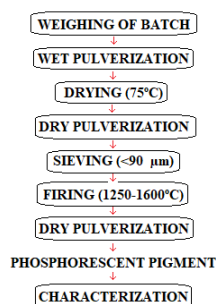


Figure 8. Flowchart for the generation of bluish-green and yellowish-green phosphorescent pigments [24].

In line with the recipes determined in the light of research in literature; first, mixed batches were prepared using SrCO_3 , CaCO_3 , BaCO_3 , H_3AlO_3 , SiO_2 , Eu_2O_3 , Dy_2O_3 and H_3BO_3 raw materials. To that end, firstly mole ratios of raw materials in the compound were calculated. Later, mole weights were addressed. Final quantities of each raw material to be used prior to wet pulverization were determined. Accordingly, the necessary raw material amounts for 20 gr powder mix were calculated. Tables 1–2 give the mole intervals of raw materials used for each recipe.

Table 1. Bluish-green pigment recipe	
Raw material	Quantity (mole)
H_3AlO_3	9-14
H_3BO_3	0,5-1,2
Eu_2O_3	0,001-0,02
Dy_2O_3	0,01-0,08
SrCO_3	2-4

Table 2. Yellowish-green pigment recipe	
Raw material	Quantity (mole)
Al_2O_3	0,23-0,48
H_3BO_3	0,01-0,06
Eu_2O_3	0,001-0,003
Dy_2O_3	0,002-0,006
SrCO_3	0,024-0,46

6.2. The Production and the Use of Bluish–Green and Yellowish–Green Phosphorescent Pigments in Wall Tile and Vetrosa Applications

Many inorganic phosphors with superior properties consist of a crystalline “main material” containing minute amounts of specific impurities and soluble “activators” [4, 12]. Basically, activators are responsible for the formation of the luminescence mechanism. Other impurities, that is auxiliary activators, are in some cases necessary for releasing the activators contained in the main crystal. Both activators and when necessary, auxiliary activators are incorporated in the structure of the crystal at high temperatures during firing. Firing temperature is usually a little below the melting temperature of the material. However, if crystallization is difficult due to excessively high melting points of main crystal, crystallization may be facilitated by bringing down the melting temperature by addition of various solvents to the initial phosphor recipe [24].

$\text{ZnS}:\text{Cu}$ has been known since with the beginning of 20th century as a long-term green light emitting material; however, the glow it provides in applications and the continuity of such glow is limited. The

visible phosphorus effect cannot be maintained more than a few hours and the phosphorescent glow is lost easily. Therefore, to maintain glow, sometimes radioactive elements (e.g. ^{1147}Pm 1H) are added to $\text{ZnS}:\text{Cu}$ phosphorus based pigments allowing phosphorus to emit the energy emitted by the radioactive substance. However, the procedure of processing and disposal of radioactive elements is very difficult leading to many problems. Consequently, the use of such a pigments is also limited [25]. Phosphors in the strontium aluminates system activated with europium (Eu) and dysprosium (Dy) draw great interest due to many superior properties they own. When compared to the classical sulphur phosphors, they are superior because of their high radiation intensity, colour purity, long emission duration, chemical stability and because they are reliable and have no radiation [12, 26]. SrAl_2O_4 , $\text{SrAl}_{12}\text{O}_{19}$, $\text{Sr}_2\text{Al}_6\text{O}_{11}$ and $\text{Sr}_4\text{Al}_{14}\text{O}_{25}$ phases are four well known main crystals in the $\text{SrO}-\text{Al}_2\text{O}_3$ system [26].

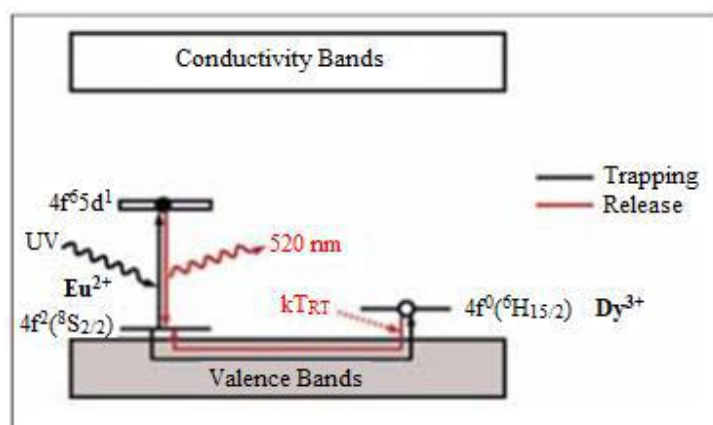


Figure 9. Phosphorescence mechanism proposed by Matsuzawa, et. al. for $\text{SrAl}_2\text{O}_4:\text{Eu}^{2+}$ system [12].

Different mechanisms have been proposed for auxiliary additive incorporated $\text{SrAl}_2\text{O}_4:\text{Eu}^{2+}$ and $\text{Ca}-\text{Al}_2\text{O}_4:\text{Eu}^{2+}$ systems. One of these is the mechanisms developed by Matsuzawa, et. al. for the $\text{SrAl}_2\text{O}_4:\text{Eu}^{2+}$ system which relies on the photoconductivity function of powder samples in the $\text{SrAl}_2\text{O}_4:\text{Eu}^{2+}$ system. This phenomenon indicates that UV radiation leads to hole type photoconductivity, therefore indicating the existence of hole trapping (Fig. 9) [12].

7. PHOSPHORESCENT GLASS BEADS

Phosphorescent glass beads have properties of phosphorescence and retro-reflectivity.

7.1. Benefits

- Phosphorescence property and retro-reflectivity provides high visibility.
- Excellent waterproof property that other phosphorescent products do not have.

7.2. Applications

- Additives for special paints: High visibility, optical ornamental effect, paints for outside and water base paints for specific road marking or ornament

- Point decoration for ornament: Sparkling effect
- Others

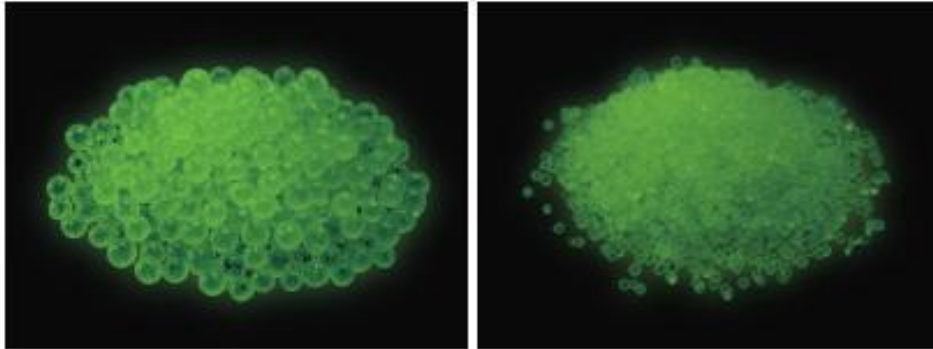


Figure 10. Phosphorescent glass beads [27].

7.3. Large Glass Beads Specifications

Phosphorescent glass beads consist of glass beads coated with phosphorescent pigments and transparent waterproof resin. Transparent waterproof resin completely covers low water resistant of phosphorescent pigments. This structure enables high waterproof property (Japanese Patent Application No.2008-05527).

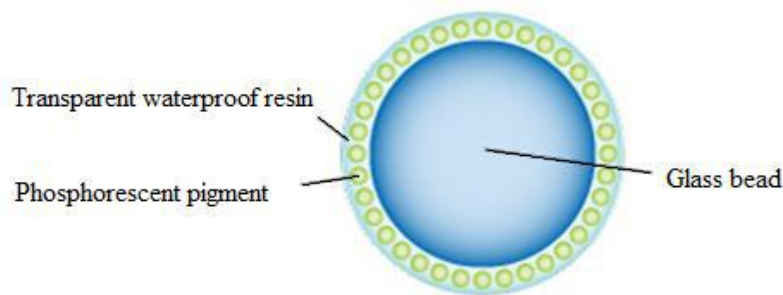


Figure 11. Phosphorescent pigment on glass bead [27].

Table 3. Evaluation data of water resistivity and chemical resistivity [27]

Water Resistivity	Dipping Test		No change after 4 months
Chemical Resistivity	Dipping Test	95 % Ethyl alcohol	No change for 2 days
		2 % NaOH	No change for 2 days
		0.4 % HCl	No change for 2 days

7.4. Phosphorescence property

Table 4. Phosphorescence properties from Luminova Technical Data (Nemoto & Co, Ltd.) [27]

Excitation Wave Length	200 – 450 nm
Emission Wave Length	520 nm
Afterglow Extinction * 1	> 1,000 min.
Excitation Time * 2	~20min.
Light Fastness * 3	> 1,000 hours

1. Time to decrease the afterglow to 0.32 mcd/m^2 when excited with D65 light at 200 lux.
2. Time required for saturation with D65 light at 200 lux.
3. Time to drop the initial afterglow brightness by 20 % after irradiation with 300W high

7.4.1. Evaluation data of phosphorescence property

- Measurement of phosphorescent brightness (JIS Z9107)
- Brightness measurement after 200 lux light emission for 20 minutes

Table 5. Brightness meter (Topcon Co. BM-5A) Angle 2 degrees, Distance 1. Light source Colour testing D65 Fluorescent lamp (Toshiba Lightec) [27]

Time	5 min.	10 min.	20 min.	30 min.
Phosphorescent Glass Beads + Epoxy paint	25.9	12.6	5.93	1.46
Phosphorescent Glass Beads + Emulsio paint	25.9	12.9	5.82	1.57

7.5. Retro-reflectivity



Figure 12. Phosphorescent glass beads have retro-reflectivity enabling high visibility and ornamental effect. Retro-reflection model of glass beads [27].

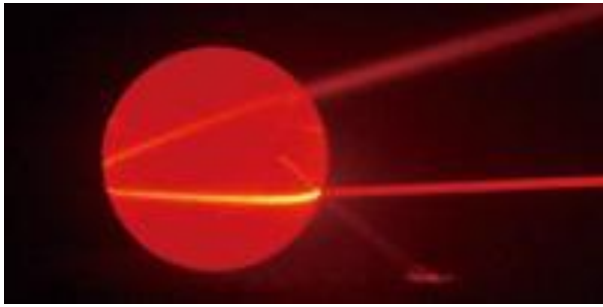


Figure 13. Retro-reflection model of glass beads using laser beam [27].

7.5.1. Evaluation data of retro-reflectivity measured by Mirolux7

Table 6. Evaluation data of retro-reflectivity measured by Mirolux7 [27]

	Reflectivity unit mcd / (m ² ·lx)
Phosphorescent Glass Beads + Epoxy paint	162
Phosphorescent Glass Beads + Emulsion paint	129

7.6. Particle size

- Appropriate size range of glass beads product can be selected for phosphorescent pigments and transparent resin coating.
- Minimum particle size range 0.4-0.6 mm

8. PHOSPHOR IN GLASS (PIG)

Reducing energy consumption and promoting low-carbon green growth has become a global problem, resulting in an increased attention to light-emitting diodes (LEDs) due to low power consumption and high efficiency, leading to a more economical usage of electrical energy. In the past, LEDs have been used as information display elements due to their rapid response and long life. Today, however, the employment of LEDs is expanding. They are now backlit and used as headlamps for LCD TVs and automobiles. Even the next generation of lighting products, fluorescent lamps and other products are expected to take its place.

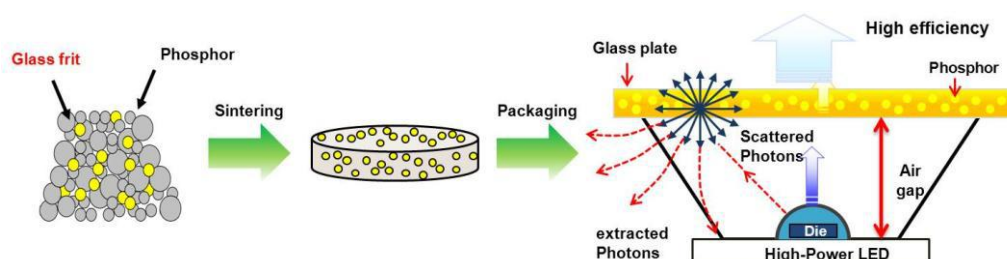


Figure 14. Schema of phosphor in glass [28].

Glass capsules appear to be better candidates than epoxy resins or silicones, which are intact and have high thermal and chemical stability. Phosphor-glass (PIG) type capsular is produced by blending phosphorus and glass frit. There are requirements for this LED encapsular, a thermal expansion coefficient for glass and phosphorus and PIG cracks [28].

8.1. Development of PIG System

The light extraction efficiency in the LED package can be increased by matching the refractive index between phosphorus and encapsulant to the minimum reduction of the scattering effect. In addition, the light efficiency of LED packaging can be increased by optimizing the pore properties of the glass plate and the interface properties between glass and phosphor.

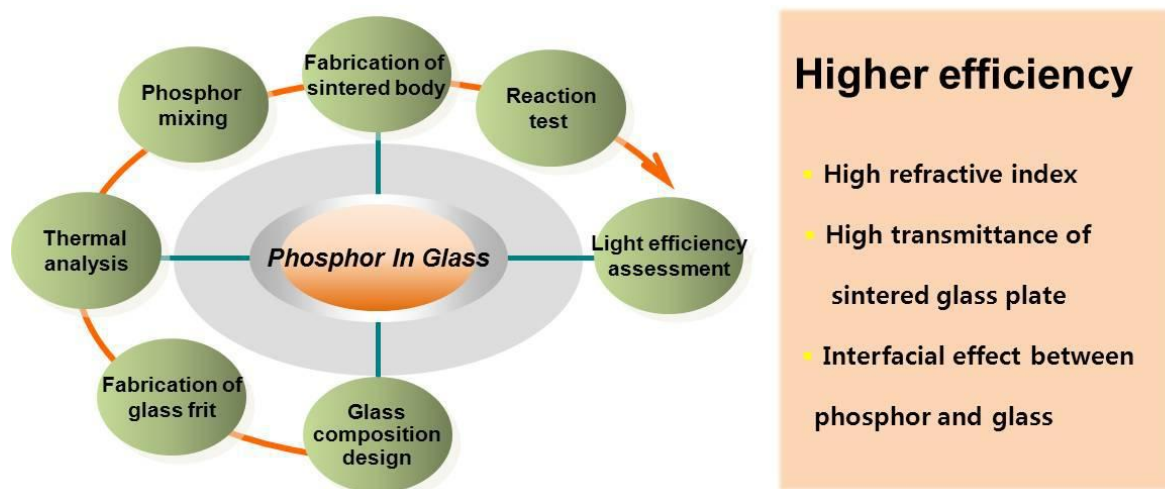


Figure 15. Development of phosphor system in glass [28].

9. LONG-LASTING PHOSPHORESCENT GLASS

- Long-lasting phosphorous glass stores light energy and continues to burn in the dark.
- Store light energy with transparent glass.
- The glass shines in more than a few hours.
- A completely new type of luminescent material that applies rare earth, terbium.

9.1. Mechanism of Long-Lasting Phosphorescent Glass

Long phosphorescent glass interior, electrons move due to light energy. Electrons are temporarily stored, called trapping. If we go back gradually to the original position, we come to the result that we have in the long run.

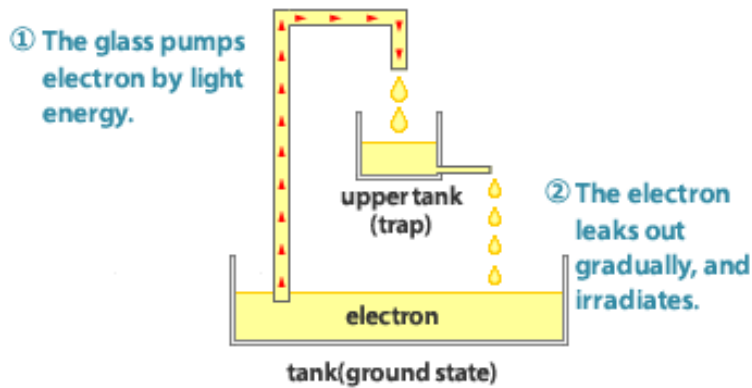


Figure 16. Mechanism of long-lasting phosphorescent glass [29].

9.2. Necessary Light for Storing Lights

- Sunlight
- Fluorescent light (for general lights, black light, antiseptic lamp)
- The light source contains ultraviolet rays

Furthermore;

- When temperature of long-lasting phosphorescent glass is high, luminescence gets dark. Thus, emitting times gets shorten.
- When the glass stores light, it turns yellow. But, as it irradiates, the colour gets pale along with emitting.

9.3. Green Long-Lasting Phosphorescent Glass

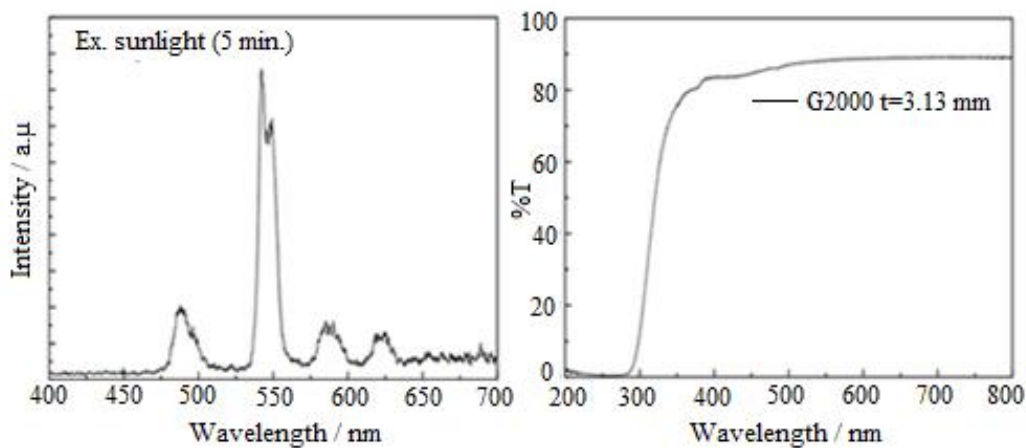


Figure 17. Irradiation and transmittance spectrums of green long-lasting phosphorescent glass [29].

9.4. Red Long–Lasting Phosphorescent Glass

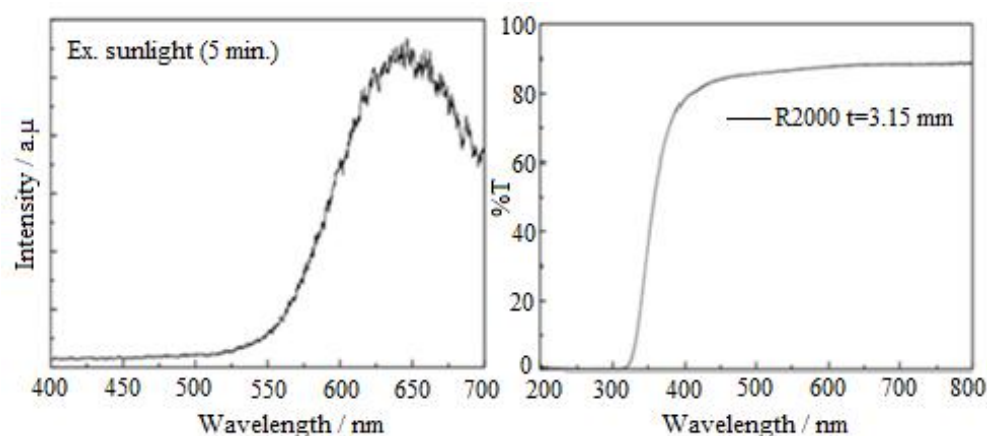


Figure 18. Irradiation and transmittance spectrums of red long-lasting phosphorescent glass [29].

10. PHOSPHORESCENCE PIGMENT APPLICATIONS IN GLASSES

Phosphorescent pigments can be used in traffic safety signs, traffic control gloves, vehicle reflection plates, reflection flags, highway signs, tires, shoes, raincoats, telephone keypads, watches, stairwells, emergency exit signs, fire extinguisher tube surfaces, toys, etc. They find their application area in ceramic and glass applications [5].

In recent years, strontium aluminate servers such as $\text{Sr}_4\text{Al}_{14}\text{O}_{25}:\text{Eu}^{2+}, \text{Dy}^{3+}$ and $\text{SrAl}_2\text{O}_4:\text{Eu}^{2+}, \text{Dy}^{3+}$ have been extensively studied due to their advantages such as high quantum efficiency, long term phosphorescence and high stability [30–81].

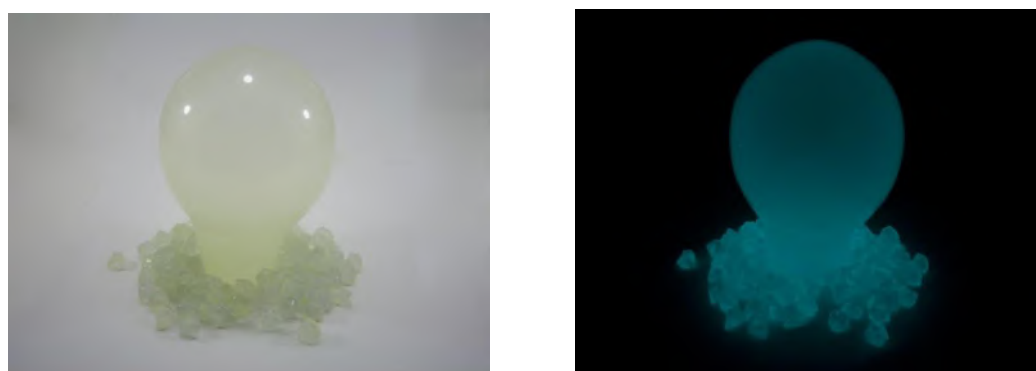


Figure 19. Glass object with bluish-green pigment-epoxy resin mixture [42, 44, 47, 57].

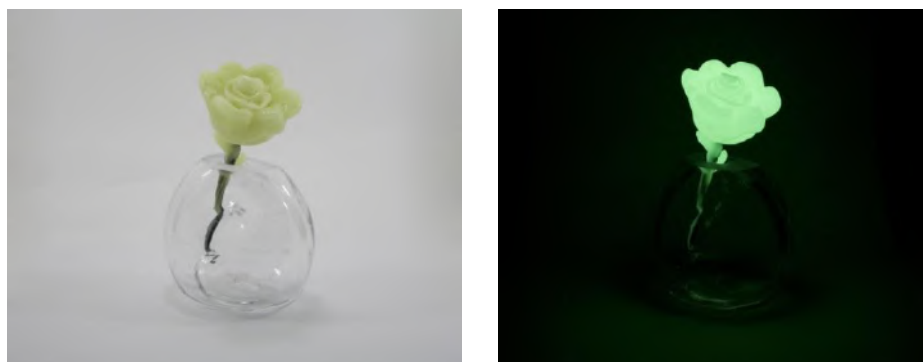


Figure 20. Rose figure with yellowish–green phosphorescence pigment–epoxy resin mixture [42, 44, 47, 57].

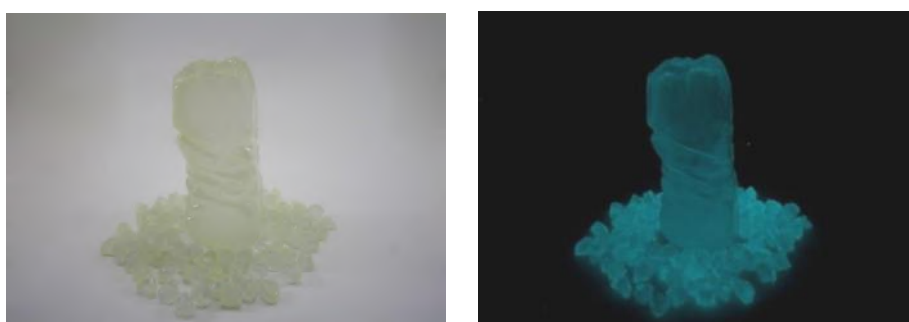


Figure 21. Glass object with blueish–green phosphorescence pigment–epoxy resin mixture [42, 44, 47, 57].



Figure 22. Glass object with yellowish–green phosphorescence pigment–epoxy resin mixture [42, 44, 47, 57].

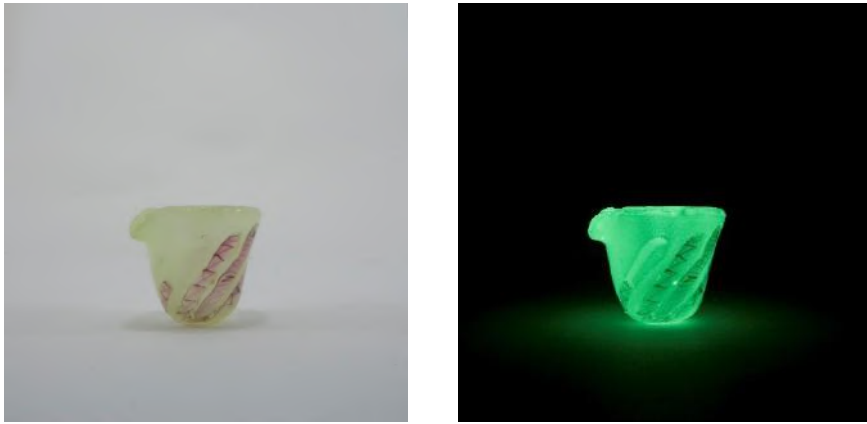


Figure 23. Glass object with yellowish–green phosphorescence pigment–epoxy resin mixture [42, 44, 47, 57].



Figure 24. Glass objects into which yellowish–green pigments were applied [42, 44, 47, 57].

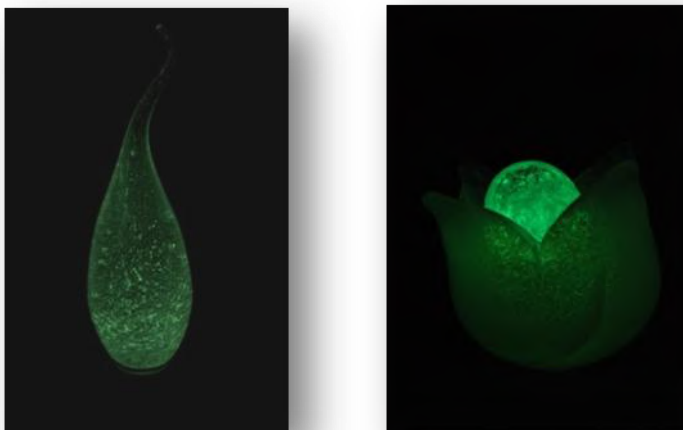


Figure 25. Glass objects into which yellowish–green pigments were applied [42, 44, 47, 57].

The application of the phosphorescence pigment–resin mixture on glass objects and flat glass was carried out after a certain period of time (~ 10 min) in order to reduce the fluidity of the mixture. Particularly when working on objects with vertical surfaces, the resin must have gained some rigidity

to cover the surface without flowing through the glass surface. Applications were performed by direct spill (Figs. 19–23). Figs. 24–25 illustrate some applications of phosphorescent pigment in and on art glasses [42, 44, 47, 57].



Figure 26. Flat glass with yellowish–green phosphorescence pigment–epoxy resin mixture and decor application [42, 44, 47, 57].

In the decoration works performed on the flat glass, the sandblasting tape (adhesive foil) was cut first and the desired pattern was formed. Then, the sandblasting tapes with single–sided adhesion property are glued onto the flat glass, and the regions forming the pattern are exposed so that the desired surface can be obtained by abrading the glass surface by sanding. After the sanding, the reduced regions were filled with a mixture of phosphorus–based pigment–epoxy resin and left at room temperature for hardening. After the mixture is completely frozen, decorative and functional glasses with glare characteristics are obtained by lifting the band on the glass (Fig. 26). When decorations were applied on glass objects with a mixture of phosphorescent pigment and epoxy resin, which has a luminous property in the dark, rich visual effects were obtained by the transparent property of the glass [42, 44, 47, 57].

Violet–blue color emitting long–lasting phosphorescent pigments in the $\text{CaAl}_2\text{O}_4\text{:Eu}^{2+}$, Dy^{3+} , Nd^{3+} systems and yellowish–green giving long–lasting phosphorescent pigments in the $\text{SrAl}_2\text{O}_4\text{:Eu}^{2+}$, Dy^{3+} , Y^{3+} system have been successfully synthesized and produced. In the $\text{CaAl}_2\text{O}_4\text{:Eu}^{2+}$, Dy^{3+} , Nd^{3+} systems the trivalent rare–earth ion, Dy^{3+} co–doping would effectively enhance the persistent luminescence intensity considering the phosphor with Nd^{3+} ions. By using violet–blue and yellowish–green luminescence given phosphorescent pigments an artistic three layered glass fountain with an attractive appearance and some other nice looking objects were successfully achieved (Fig. 27) [48, 51].

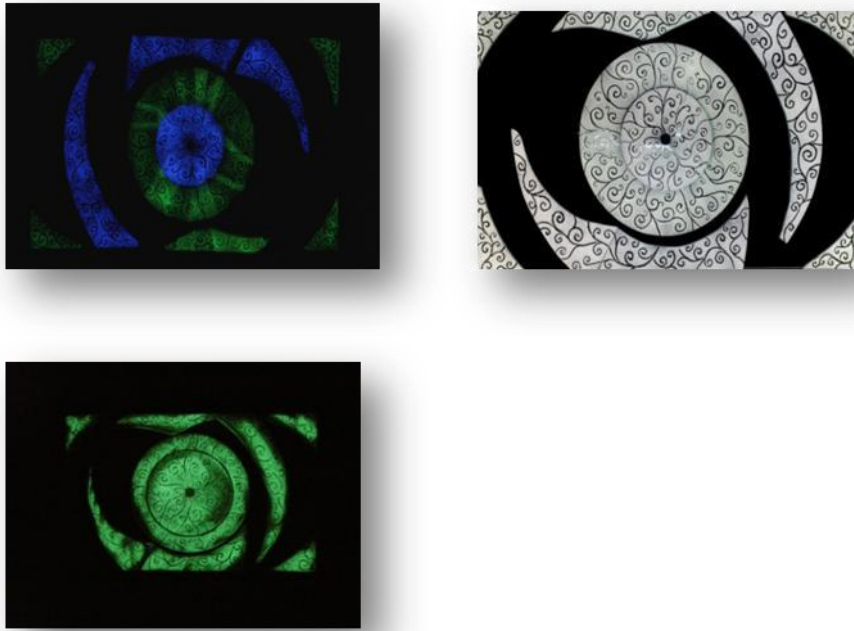


Figure 27. Glass fountain with phosphorescent decoration undergone fusion process in an electrically heated furnace and its appearances in the dark [48, 51].

REFERENCES

- [1] Bellis, M., The science behind glow in the dark. updated at 'thoughtco.com' on April 16, 2017.
- [2] Yen, W. M., Shionoya, S. and Yamamoto, H., Phosphor Handbook, Second Edition, 4–5, 2006.
- [3] <https://web.phys.ksu.edu/vqm/tutorials/phosphorescence/index.html> (Access Date: 03.06.2018).
- [4] Matsuzawa, T., Aoki, Y., Takeuchi, N., Murayama, Y., Rare Earths, 29, 79, 1996.
- [5] Murazaki, Y., Ichinomiya, A. K., Tomaki, H., Oishi, T., A blue green super long persistence phosphor and 1st applications, Fourth International Display Workshops, IDW'97 Advance Program, November Tokyo, Japan, 1997.
- [6] Katsumata, T., Nabae, T., Sasajima, K., Komura, S., Morikawa, T., J. Electrochem. Soc., 144, 243–245, 1997.
- [7] Karasu, B., Kısacık, Y., Kaya, G., Uçar, T., Toplutepe, N. Ö., Sarımsı–yeşil renkli fosforlu pigmentlerin üretiminde süreç parametrelerinin iyileştirilmesi, III. Uluslararası Katılımlı Seramik, Cam, Emaye, Sır ve Boya Semineri (SERES 2005) Bildiriler Kitabı, Eskişehir, 767–771, 2005.
- [8] [ÜberFluoreszenz und Phosphoreszenz, I., Abhandlung](#) (On fluorescence and phosphorescence, first paper), Annalen der Physik, 34: 446–463, from page 447, 2015.

- [9] Valeur, B. and Berberan-Santos, J. M. N., A brief history of fluorescence and phosphorescence before the emergence of quantum theory. *Chem. Educ.*, 88 (6), pp 731–738, 2011.
- [10] Author: Everyone's idle from Berlin, Germany, Description: Luminol and Hemoglobin: Luminol glows in an alkali solution when you add hemoglobin and H_2O_2 , Source: "<https://www.flickr.com/photos/mgdtgd/140282001/>" taken on May 4, 2006.
- [11] Douglas, P., Photoluminescence, published article at [A-to-Z Guide to Thermodynamics, Heat & Mass Transfer, and Fluids Engineering](#), 2 February, 2011.
- [12] Yen, W. M. and Weber, M. J., Inorganic phosphors: Compositions, preparation and optical properties, The CRC Press Laser and Optical Science and Technology Series, p 9, 2004.
- [13] Sarver, J. S., Katnack, F. L., and Hummel, F. A., Phase equilibria and manganese activated fluorescence in the system $\text{Zn}_3(\text{PO}_4)_2\text{--Mg}^3(\text{PO}_4)_2$, *J. Electrochem. Soc.*, 106, 960, 1959.
- [14] Wang, J., Su, Q., Wang, S. B., A novel red long lasting phosphorescent (LLP) material $\beta\text{-Zn}_3(\text{PO}_4)_2\text{:Mn}^{2+}, \text{Sm}^{3+}$. *Mater. Res. Bull.*, 40: 590, 2005.
- [15] Lin, J., Sanger, D. U., Mennig, M., Barner, K., Sol-gel deposition and characterization of Mn^{2+} -doped silicate phosphor films. *Thin Solid Films*, 360: 39, 2000.
- [16] Berkowitz, J. K., Olsen, J. A., Investigation of luminescent materials under ultraviolet excitation energies from 5 to 25 eV. *J. Lumin.*, 50: 111, 1991.
- [17] Shi, L., Huang, Y. L., Seo, H. J., Emission red shift and unusual band narrowing of Mn^{2+} in NaCaPO_4 phosphor. *J. Phys. Chem. A*, 114: 6927, 2010.
- [18] Furusho, H., Holsa, J., Laamanen, T., Lastusaari, M., Niittykoski, J., Okajima, Y., Yamamoto, A., Probing lattice defects in $\text{Sr}_2\text{MgSi}_2\text{O}_7\text{:Eu}^{2+}, \text{Dy}^{3+}$. *J. Lumin.*, 128: 881, 2008.
- [19] Wan, M. H., Wang, Y. H., Wang, X. S., Zhao, H., Hu, Z. F., The properties of a novel green long afterglow phosphor $\text{Zn}_2\text{GeO}_4\text{:Mn}^{2+}, \text{Pr}^{3+}$, *Opt. Mater.*, 36: 650, 2014.
- [20] Dexter, D. L., A theory of sensitized luminescence in solids. *J. Chem. Phys.*, 21: 836, 1953.
- [21] Paulose, P. L., Jose, G., Thomas, V., Unnikrishnan, N. V., Warriar, M. K. R., Sensitized fluorescence of $\text{Ce}^{3+}/\text{Mn}^{2+}$ system in phosphate glass, *J. Phys. Chem. Solids*, 64: 841, 2003.
- [22] Ting, X., Hongxu, G., Junying, Z., Odetola, C., Yuneng, H., Heng, L., et al. Phosphorescence properties and energy transfer of red long-lasting phosphorescent (LLP) material $\beta\text{-Zn}_3(\text{PO}_4)_2\text{:Mn}^{2+}, \text{Pr}^{3+}$, *Science Direct*, 33 (10), 1056, 2015.
- [23] <http://www.luminochem.com/pigments-for-industrial-applications/phosphorescent-pigment-production> (Access Date: 08.07.2018).
- [24] Kaya, S. Y., Karasu, B., The production and use of bluish-green and yellowish-green phosphorescent pigments in wall tile and vetroso applications, *Seramik Türkiye Magazin*, No: 35, 128–134, January 2011.
- [25] Clabau, F., Rocquefelte, X., Jobic, S., Deniard, P., Whangbo, M.-H., Garcia, A., and Le Mercier, T., Mechanism of phosphorescence appropriate for the long-lasting phosphors Eu^{2+} -doped SrAl_2O_4 with codopants Dy^{3+} and B^{3+} , *Chem. Mater.*, (17) 3904–3912, 2005.

- [26] Bem, D.Y., Luyt, A. S. and Dejene, F. B., Structural, luminescent and thermal properties of blue SrAl_2O_4 : Eu^{2+} , Dy^{3+} phosphor filled low-density polyethylene composites, *Physica B* 404, 4504–4508, 2009.
- [27] <http://www.pqj.co.jp/en/product/21.html> (Access date: 05.08.2018).
- [28] http://iml.inha.ac.kr/sub/menu3_4.html (Access date: 12.07.2018).
- [29] <http://www.sumita-opt.co.jp/en/products/optical/luminous-glass.html> (Access date: 12.07.2018).
- [30] Yuan, Z., Changa, C., Maoa, D. and Ying, W., Effect of composition on the luminescent properties of $\text{Sr}_4\text{Al}_{14}\text{O}_{25}$: Eu^{2+} , Dy^{3+} phosphors, *Journal of Alloys and Compounds*, 377, 268–271, 2004.
- [31] Karasu, B., Özkara, Ö., Cam ve seramik sanayiinde kullanılan fosfor esaslı malzemeler, *Metalürji, TMMOB Metalürji Mühendisleri Odası*, Vol. 23, 121, 28–32, 1999.
- [32] Karasu, B., Kaya, G., Özkara, Ö., Tuğla ve çatı kiremitlerinin fosfor ışıdamalı sırlarla kaplanması, II. Uluslararası Eskişehir Pişmiş Toprak Sempozyumu Bildiriler Kitabı, 108–113, 2002.
- [33] Karasu, B., Kaya, G. ve Özkara, Ö., Fosfor esaslı boyaların çeşitli seramik sırlarında kullanımı, *Anadolu Üniversitesi, Araştırma Fonu Yüksek Lisans Proje Son Raporu*, 2002.
- [34] Karasu, B. ve Kaya, G., Flüoresans özellikli sır kompozisyonlarının geliştirilmesi, TÜBİTAK Seramik Araştırma Merkezi (SAM), P/2001–03, Proje Son Raporu, 2002.
- [35] Karasu, B., Kaya, G., Kısacık, Y., Uzun ışıma süreli fosforesans özelliğe sahip SrAl_2O_4 : Eu^{+2} , Dy^{+3} sisteminde pigment üretimi, III. Uluslararası Katılımlı Seramik, Cam, Emaye, Sır ve Boya Semineri (SERES 2005) Bildiriler Kitabı, Eskişehir, 750–756, 2005.
- [36] Karasu, B., Kaya, G., Kibici, A., Uzun ışıldama süresine sahip mavi ve mavimsi–mor renkli fosforesans tozların üretimi, 6. Uluslararası Katılımlı Seramik Kongresi Bildiriler Kitabı, Sakarya, Türk Seramik Derneği, 272–276, 2006.
- [37] Kaya, Y. S., Karasu, B., Karacaoğlu E., General review of application of phosphorescence pigments in ceramic industry, the Proceedings of SERES'09 I. International, Ceramic, Glass, Porcelain Enamel, Glaze and Pigment Congress, Eskişehir, 608–616, 2009.
- [38] Yeşilay, S., Karasu, B. ve Karacaoğlu, E., SrAl_2O_4 : Eu^{+2} , Dy^{+3} Sisteminde mavimsi–yeşil ve sarımsı–yeşil fosforların üretimi ve karakterizasyonu, III. Lüminensans Dozimetri Kongresi Bildiri Özetleri Kitapçığı, Bodrum, 15, 2009.
- [39] Kaya, Yesilay, S., Karasu, B., Kaya, G., Karacaoğlu, E., Influences of Eu^{3+} and Dy^{3+} contents on the properties of long afterglow strontium aluminate phosphors, *Advances in Science and Technology*, Vol. 62, 88–94, 2010.
- [40] Kaya, Yesilay, S., Karasu, B., Kaya, G., Karacaoğlu, E., Effects of firing temperature and time on the luminescence of phosphors in strontium aluminate system co-doped by Eu_2O_3 and Dy_2O_3 and prepared by solid state reaction processing, *Advances in Science and Technology*, Vol. 62, 82–87, 2010.

- [41] Karasu, B., Kaya, Yesilay, S., Karacaoğlu, E., Çakı, M., Özel, E., Kaya, G., Fosforesans özelliğe sahip mavimsi-yeşil, sarımsı-yeşil pigmentlerin üretimi ve III. pişirim (dekor pişirimi) duvar karosu sırlarında ve vetroza uygulamalarında kullanımı, TÜBİTAK 1001 Bilimsel ve Teknolojik Araştırma Projelerini Destekleme Programı, 108M464, Proje Son Raporu, 2010.
- [42] Kaya, Yeşilay, S., Karasu, B. ve Karacaoğlu, E., Camlarda fosforesans pigment uygulamaları, **Camgeran 2010 Uluslararası Katılımlı Uygulamalı Cam Sempozyumu Bildiri Kitabı**, Eskişehir, 41–44, 2010.
- [43] Kaya, Yesilay, S., Karasu, B., Karacaoğlu, E., The effects of boron oxide content on the phosphorescence mechanism of strontium aluminate phosphors, Proceeding of the 15th International Metallurgy and Materials Congress, İstanbul, 2140–2146, 2010.
- [44] Kaya, Y. S., Production of inorganic phosphorescent pigments and their usage in glass and glaze systems, Anadolu University, Graduate School of Sciences, Ceramic Engineering Program, PhD Thesis, 2011 (in Turkish).
- [45] Karacaoğlu, E., Kaya, Yesilay, S., Karasu, B., Kaya, G., The synthesis of violet emitting long afterglow calcium aluminate phosphors and their luminescence properties, Abstract Book of ECerS XII, XII. Conference and Exhibition of the European Ceramic Society, Stockholm, Sweden, 2011.
- [46] Unal, A., Karasu, B., Kaya, Yesilay, S., Synthesis and characterization of blue long afterglow strontium silicate phosphors and luminescence properties, Abstract Book of ECerS XII, XII. Conference and Exhibition of the European Ceramic Society, Stockholm, Sweden, 2011.
- [47] Karasu, B., Inorganic phosphorescent pigments in glass applications, Abstract Book of SERES'11 II. International, Ceramic, Glass, Porcelain Enamel, Glaze and Pigment Congress, Eskişehir, 2011.
- [48] El Kazazz, H., Karacaoğlu, E., Karasu, B. and Agatekin, M., Production of violet–blue emitting phosphors via solid state reaction and their uses in outdoor glass fountain, Journal of American Science, 7 (12), 998–1004, 2011.
- [49] Kaya, Yeşilay, S., Karasu, B., Process parameters determination of phosphorescent pigment added, frit-based wall tiles vetrosa decorations, Ceramics International, Vol. 38, Issue 4, 2757–2766, May 2012.
- [50] Kaya, Yeşilay, S. and Karasu, B., Glass and ceramics with phosphorescent ability, Ceramics Technical, No: 34, 94–99, May 2012.
- [51] El Kazazz, H., Karacaoğlu, E., Karasu, B. and Agatekin, M., Production of Pr_6O_{11} -doped SrAl_2O_4 : Eu^{2+} , Dy^{3+} , Y^{3+} yellowish–green phosphors and their usage in artistic glasses, Anadolu University, Journal of Science and Technology A, Applied Sciences and Engineering, Vol. 13, No: 2, 81–87, 2012.

- [52] Karacaoglu E., Karasu, B., Investigations on luminescence characteristics and influence of co-doping different rare earth ions of bright white long-afterglow phosphorescent pigments, IntertechPira's 10th Annual Phosphor Global Summit, Arizona, USA, March 2012.
- [53] Karacaoğlu, E., Karasu, B., General review on the persistent luminescence phosphors in Türkiye and the world, Abstract Book of Paint İstanbul Fair and Congress, p. 93, 2012.
- [54] Karasu, B., Türkiyede fosforesans pigmentlerin gelişimi, VIII. Uluslararası Katılımlı Seramik Kongresi, Afyonkarahisar, Kasım 2012.
- [55] Karacaoglu, E. and Karasu, B., The effects of re-firing process under oxidizing atmosphere and temperatures on the properties of strontium aluminate phosphors, Mater. Research Bull., 48, 10, 3702–3706, 2013.
- [56] **Karasu, B.**, Geleneksel seramiklerde kullanım potansiyeline sahip inorganik esaslı fosfor ışıldamalı pigmentler, VII. Uluslararası Eskişehir Pısmış Toprak Sempozyumu Bildiriler Kitabı, Eskişehir, 305–321, 2013.
- [57] **Karasu, B.**, Inorganic phosphorescent pigments for the usage on the surfaces of ceramics, Glasses and Metals, Abstract Book of International Conference on Traditional and Advanced Ceramics 2013 (ICTA2013) in conjunction with ASEAN Ceramics 2013, Bangkok, Thailand, p. 23, 2013.
- [58] Karasu, B., Kırmızı ve tonlarında fosfor ışıldama yeteneğine sahip inorganik pigmentlerin geliştirilmesi, pilot çapta üretimi, seramik, cam ve metal sektörlerinde değerlendirilmesi, T.C. Bilim, Sanayi ve Teknoloji Bakanlığı, Sanayi Araştırma ve Geliştirme Genel Müdürlüğü, San-Tez Projesi, 00857.STZ.2011–1, Proje Son Raporu, 2013.
- [59] Karasu, B., Beyaz ışıldamalı inorganik esaslı fosforesans pigmentlerin üretimi, seramik ve camlarda kullanımı, KOSGEB Araştırma–Geliştirme, İnovasyon ve Endüstriyel Uygulama Destek Programı Projesi, Proje Son Raporu, 2013.
- [60] **Karasu, B., Aksoy, T., Yastı, Yalçın, Ş.**, Kırmızı fosfor ışıldaması sergileyen farklı sistem pigmentlerinin kullanım performanslarının artırılması, VIII. Uluslararası Eskişehir Pısmış Toprak Sempozyumu, 141–152, 2014.
- [61] Karasu, B., Aksoy, T., Kırmızı fosforesans ışıldama sergileyen pigmentler (I), ESO Dergi, Eskişehir Sanayi Odası (ESO), Yıl 3, Sayı 6, 82–86, 2014.
- [62] Karasu, B., Aksoy, T., Kırmızı fosforesans ışıldama sergileyen pigmentler (II), ESO Dergi, Eskişehir Sanayi Odası (ESO), Yıl 3, Sayı 8, 94–97, 2014.
- [63] Karacaoglu, E., Karasu, B., Ozturk, E., Investigations on luminescence characteristics and influence of doping and co-doping different rare earth ions of white phosphorescence materials having different luminescent centers, Periodical of Advances in Science and Technology, 13th International Ceramics Congress–Part D, Vol. 90, 133–40, 2014.

- [64] Karasu, B., Aksoy, T., Yastı Yalçın, Ş., Çeşitli oksit esaslı sistemlerde kırmızı fosfor ışıllığa sahip uzun ışıldama süreli inorganik pigmentlerin geliştirilmesi, Anadolu Üniversitesi, Yayın ve Araştırma Teşvik Projesi, 1306F209, Proje Son Raporu, 2014.
- [65] Karacaoğlu, E. and Karasu, B., The effects of different activators and sintering atmosphere on the luminescence properties of akermanite type phosphors, Indian Journal of Chemistry Section A (IJCA), Vol 54A, 1394–1401, 2015.
- [66] Karasu, B., Yeşilay, S., Karacaoğlu, E., Çakır, A., Beyaz fosforesans ışıldama sergileyen pigmentler, Seramik Türkiye Bilim Teknik ve Endüstri Dergisi, Seramik Federasyonu, Eylül–Aralık Sayısı, 112–121, 2015.
- [67] Pekkan, K., Gün, Y., Taşçı, E., Karasu B., Mavimsi–yeşil ve sarımsı–yeşil fosforesans pigmentlerin çini sırında değerlendirilmesi, IX. Uluslararası Eskişehir Pişmiş Toprak Sempozyumu Bildiriler Kitabı, 249–259, 2015.
- [68] Karasu, B., Beyaz yayımlı fosfor ışıldarların ışıma şiddet ve sürelerinin artırılması, Anadolu Üniversitesi, Yayın ve Araştırma Teşvik Projesi, 1404F153, Proje Son Raporu, 2015.
- [69] Karasu, B., Stronsiyum alüminat (SrAl_2O_4) sisteminde, karanlıkta sarımsı–yeşil renkte uzun süreli ışıldama özelliğine sahip fosforesans pigmentler, Ulusal Patent Numarası: TR 2011 05883 B, 2015.
- [70] Karasu, B., Stronsiyum alüminat ($\text{Sr}_4\text{Al}_{14}\text{O}_{25}$) sisteminde, karanlıkta mavimsi–yeşil renkte uzun süreli ışıldama özelliğine sahip fosforesans pigmentler, Ulusal Patent Numarası: TR 2011 05879 B, 2015.
- [71] Karasu, B., Kalsiyum alüminat (CaAl_2O_4) sisteminde, karanlıkta mor (eflatun)/mor–mavi renkte uzun süreli ışıldama özelliğine sahip fosforesans pigmentler, Ulusal Patent Numarası: TR 2011 05980 B, 2015.
- [72] Karasu, B., Düşük sıcaklıkta ergiyen, fosforesans pigmentlerle de kullanılabilirlik özelliğine sahip şeffaf vetroza friti, Ulusal Patent Numarası: TR 2011 05981 B, 2015.
- [73] Pekkan, K., Gün, Y., Taşçı, E., Karasu, B., Effects of the physical properties of phosphorescent glazes on luminescence, Proceeding Book of the X. International Eskişehir Terracotta Symposium, 633–639, 2016.
- [74] Özer, M. S., Karasu, B., Yeprem, A., Synthesis of $\text{SrAl}_2\text{O}_4:\text{Eu}^{2+}$, Dy^{3+} phosphorescent pigments via combustion assisted sol–gel method, Abstract Book of International Conference on Traditional and Advanced Ceramics 2017 (ICTA2017) in conjunction with ASEAN Ceramics 2017, Bangkok, Thailand, 2017.
- [75] Gün, Y., Taşçı, E., Pekkan, K., Karasu, B., Farklı ticari fritlerin değişen sıcaklık aralıklarında fosforesans ışıma etkisi, Uluslararası Hakemli Mühendislik ve Fen Bilimleri Dergisi, Sayı: 10, 42–58, 2017.

- [76] Pekkan, K., Gün, Y., Kaymak, K., Taşçı, E., Karasu, B., Farklı renk veren fosfor ışııl pigmentler açısından düşük sıcaklık sır bileşimlerinin belirlenip çini bünyelerde uygulanması, Şişe Cam Teknik Bülten, Eylül 2017.
- [77] Karasu B., Özer, M. S., Sarımsı yeşil fosfor ışııl pigmentin sol jel yöntemiyle sentezi, üretimi, karakterizasyonu ve katı hal metoduyla elde edilen pigmentle karşılaştırılması, Anadolu Üniversitesi, Yayın ve Araştırma Teşvik Projesi, 1605F341, Proje Son Raporu, 2017.
- [78] Pekkan, K., Taşçı, E., Gün, Y., Kaymak, K., Acer, O., Karasu B., Fosforesans pigmentler için çini sıırı geliştirilmesi, üretimi ve ilgili bünyeler üzerine uygulanması, TÜBİTAK 3001 Projesi, 114M135, Proje Son Raporu, 2017.
- [79] Karasu, B., Özer, M. S., Çakı, M., Gür, M. E., Evaluation of phosphorescent pigments prepared by dry mixing conventional method on schamot surfaces, Proceedings of IV. International Ceramic, Glass, Porcelain Enamel, Glaze and Pigment Congress (SERES'18), Eskişehir, 10–12 October 2018.
- [80] Karasu, B., Özer, M. S., Çakı, M., Gülmez, B., Evaluation of phosphorescent pigments prepared by sol–gel method on earthenware surfaces, Proceedings of VI. International Ceramic, Glass, Porcelain Enamel, Glaze and Pigment Congress (SERES'18), Eskişehir, 10–12 October 2018.
- [81] Karasu, B., Özer, M. S., Çakı, M., Gür, M. E., Kuru Karıştırmalı Geleneksel Yöntemle Hazırlanmış Fosforışııl Pigmentlerin Kırmızı Çamur Yüzeyinde Değerlendirilmesi, XII. Ulusal Eskişehir Pişmiş Toprak Sempozyumu Bildiriler Kitabı, Eylül 2018.

INVITED SPEAKERS

THE DEVELOPMENT OF DECORATION IN TURKISH ÇİNİ ART

İskender Işık¹, Remzi Gören², Gökhan Akca³

¹ Kütahya Dumlupınar University, Engineering Faculty, Department of Metallurgy and Material
Science Engineering, Kütahya/Türkiye

² Kütahya Dumlupınar University, Fine Art Faculty, Department of Ceramic and Glass,
Kütahya/Türkiye

Famous traveller Evliya Çelebi mentioned Çini in his book "Seyahatname", reporting about the beauty and unicity of the Çini articles manufactured by local Kütahya artists in 17th century. Historically the ceramic manufacturers have been producing work in Kütahya since the Phrygian period and continued with çini-ceramic works made with red paste material in the last half of the 14th century. In the late half of the 16th century, Iznik çini art reached its brightest period. In the years after however, Iznik manufacturers were severely damaged since they lost the support of the palace and the production of Çini almost ceased to stand.

Initially, Kütahya çinis were produced to meet the needs of the local people and with a more modest quality level compared to the Iznik çinis that were produced. As a result of this situation, the designs of the motifs were arranged and formed with more density. The Çini products were filled with dense motifs and patterns to hide the mistakes and dull background color. In this way; they aimed to mask the quality deficiencies that occur in the çini bisques, the glazes and the colors with intensive pattern designs. The need for intensive pattern designs is one of the most basic features that reflect the characteristic structure of Kütahya çinis. The solution, which emerged as a necessity, was to enrich the motif and pattern designs and increase the aesthetic qualities.

One of the most important problems that the çini producers are facing is; the motifs and designs that directly affect the sale of Çinis are not rich and sufficient in quality and quantity. Therefore, the production of Çinis that are decorated with similar motifs and designs threaten the domestic and foreign markets. Re-interpretation of Çini motifs and patterns went from a contemporary perspective without straying away from the original; it is important to save the Kütahya Çini art which has been going on for hundreds of years from repetition and copies, and to determine a new route in its original line. For these reasons, there is a need for real artists who have internalized the characteristics of Kütahya Çini art.

Turkish Çini Art

Çini is a kind of ornamentation art, mostly a mixture of architectural ornaments, daily use items or objects for decoration purposes. They are shaped objects from mud which is usually kaolin, quartz, clay and feldspar mixed with a certain amount of water. These products are fired in high-grade ovens, also called bisque firing. Then the patterns prepared by traditional methods are applied with the help of a brush on the bisques with some raw materials and colorized oxides. In order to protect these designs and make the surface smoother, the diluted raw material mixtures are ground in much finer grain sizes and then applied on the first fired decorative body. After, they are fired for the second time. This firing is also called glaze firing. The patterns between the bisque and the glaze can be preserved for hundreds of years.

It is acknowledged by the art history specialists that Çini is an art unique to the Turks. Turks first manufactured Çini in Central Asia. The oven residues and çini fragments that were found in excavations in Kashan, Turfan, Aşkar and Koça areas in Central Asian territories indicated that there was such type of pottery art which the Turks consider as traditional artifacts from before the 8th century. The city of Kashan in Central Asia, which is thought to be the Çini production center of the period, created the "Kaşı" used in the architecture until the 18th century and the other used products (such as plates, vases, bowls, etc.) were named "Evani", standing for pots and pans.

The fact that the word 'çin' means the word 'China' in Turkish, was changed by the Ottomans to 'Çini', adding an 'i' just to separate the differences in the pottery manufactured by each country's potters. Yet, due to the good reputation of the porcelain imported from China starting from the 18th century, the word Çini was preferred instead of Kaşı for commercial reasons. Çini was first properly used in Turkish literature and scriptures in 1958 by Prof. Dr. Hakkı İzzet.

Çini art was moved to Anatolia by the Seljuks and reached its peak in the centers of Bursa, Istanbul, İznik and Kütahya during the Ottoman period. In the following periods, Kütahya became one of the two most important çini centers in Anatolia together with Iznik. Since the manufacturers of Iznik were under the protection of the Ottoman Palace, they had the highest level of possibilities both in the bisque firing and design of the çini.

Decoration in Çini Art

As a general acceptance; all products obtained by kneading and shaping of non-organic raw materials with water in certain proportions are called ceramics. When evaluated in this aspect, the Çini is actually a kind of ceramic. However, the distinctive feature of Çini products is the decorations made

under the glaze with brush. Decor; it can also be considered as an in other words of the pattern integrity created with unit motifs. These decors can be preserved for hundreds of years by being confined between the structure and the glaze (Fig. 1). From the moment it was made, it is the main reason why Çini is considered as a branch of art as it is able to carry its social values, social-cultural structure, beliefs and aesthetic perspective beyond centuries.



Figure 1. Çini plate decorations by çini artist Hamza Üstünkaya
(Photographer: Gökhan AKCA, 07 August 2017, Kütahya/ Turkey)

Turkish society is a society that has managed to maintain its existence in different states and different flags in almost every stage of human history. The continuity in history has brought with it the opportunity to establish a rich culture and civilization. Since the first finds of the Pazırık Kurgan, the Turks have depicted scenes, beliefs, social value judgments and imaginary worlds reflecting their daily lives by symbolizing the beauty perception of their periods and produced different works of art throughout the history.

It was the material culture data of the Turks, which documented the historical past of Turkish societies dating back centuries. The earliest of these finds are mine, stone and ceramic-çini. The inscriptions, miniatures, embroideries, pieces of cloth, Çinis, which are in the center of the Uighurs called Karahoço, are among the important examples of Turkish culture and art [1].

Although the first information in the historical sources of the Turks is found in Chinese and Arabian sources, the oldest artifacts found to have belonged to the Turks date back to 2500-3000 BC. These artifacts include stone, metal, ceramics, Çini, pieces of fabric, rock paintings, sculptures, as well as numerous artifacts made by the Turkish states that have managed to survive without interruption throughout history (Fig. 2, 3 and 4).



Figure 2. Man in Golden Dress (B.C. 5th century Saka Turks, found in Kazakhstan's Esik Kurgan)

References: <https://insanveevren.wordpress.com> Date of access: 28 September 2018



Figure 3. Tomb of Hodja Ahmet Yesevi

(It was built by Timur in Turkestan between 1389 and 1405)

(Photographer: Gökhan AKCA, 10 October 2017, Türkistan/Kazakistan)

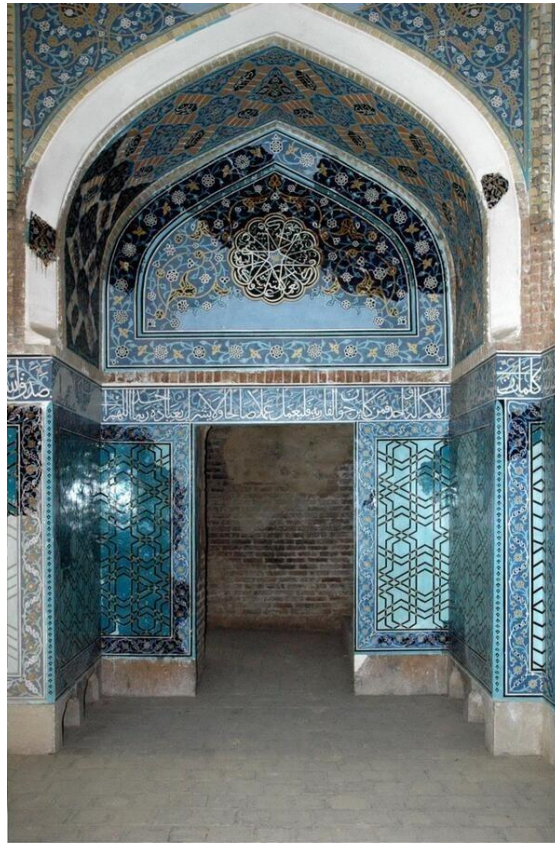


Figure 4. The Gök Mescid / Çini Door

(It was built in Tabriz in 870 (1465-66) by Cihan Shah, the ruler of Karakoyunlu)

References:: <https://www.tasnimnews.com> Date of access: 28 September 2018.

Turks, who generally have a nomadic lifestyle, used the figures of human figures in the decoration of works of art, the wild animals and natural phenomena they frequently encountered in their daily lives, especially in the death and burial ceremonies (Fig. 5). On the other hand, after the acceptance of Islam by the Turks, the use of the human figure, which was frequently seen in Turkish artworks, left the place of Islamic art in herbal and geometric motifs and patterns. As it is understood from this point, similar processes in other societies, such as life style, beliefs and aesthetic perception of Turkish society, are the determinants of the design of motifs and patterns which are the main elements of the works of Turkish societies.



Figure 5. Uighur Period, Sculpture and Wall Freski Samples

References: <https://tarihvearkeoloji.blogspot.com>, Date of access: 25 October 2018

Although the art of Turkish art has spread to a very wide area from its birth to the present, it has largely preserved its cultural and artistic characteristics [2]. In their journey from Central Asia to Anatolia, the Turks carried along with the elements of the cultures and civilizations of the other nations in the Central Asian basin, as well as their accumulations, which were synthesized by the effects of Islam. Without losing its national identity, Turks, who bring together the values they have received from different cultures and their social characteristics in harmonious designs, have a rich cultural heritage in this sense.

For thousands of years, Turkish culture has succeeded in expressing its emotions, thoughts, beliefs, tastes and desires with an aesthetic perception on a universal level. The most basic issues that determine the design of motifs and patterns are the social moral rules, lifestyle, tastes, desires and wishes that the designer has affected as a result of cultural accumulation. The starting point of these designs is sometimes natural phenomena such as natural phenomena, animals, flowers, trees and other plants, and sometimes they are the geometric lines used as the means of expression of abstract concepts. However, the designs of the motifs and patterns designed by the Turks are in any case equipped with a meaning load (Fig. 6, 7 and 8).



Figure 6. Tree of Life Motif

(Represents the bond connecting the life of the worldly and the hereafter)

References: Çini Artist Hamza Üstünkaya, 08 November 2010, Kütahya/Turkey



Figure 7. Tulip Motif

(Tulip Motif represents the unity of God in İslamic mystical thought)

References: Çini Artist Hamza Üstünkaya, 07 February 2013, Kütahya/Turkey



Figure 8. Carnation Motif

(Carnation Motif represents spring, nature awakening, renewal.)

References: Çini Artist Hamza Üstünkaya, 19 July 2009, Kütahya/Turkey

Traditional Kütahya Ware (Also Known as Çini)

Çini is the symbol of Kütahya and at the same time introduces to the whole world an important art branch as well as the livelihood of Kütahya. The ceramic manufacturers have been producing work in Kütahya since the Phrygian period and continued with Çini-ceramic works made with red paste material in the last half of the 14th century. The motifs and colors of the Çini in Kütahya made during this period were similar to the Iznik çini. In these first examples, cobalt blue, manganese purple, turquoise and black colors were mainly used. The colors that were used had darker tones than the ones used in the Iznik works yet the features were similar to the Anatolian Seljuk Çini ornaments. The transition from red Çini and ceramics to blue-white manufacturing began in Kütahya at the same time as Iznik in the middle of 15th century. Instead of red bisque, a new style was created with white, hard bisque bearing porcelain-like blue-white Çini and ceramics.

In the late half of the 16th century, Iznik Çini art reached its brightest period, with work that was developed with vivid and radiant colors. When the characteristic features of Iznik çini art are examined, one can see that the quality structure of the work, which is called “Sclera” (white part of the eye), give off a more homogeneous and clear white background. With this technique, the motifs and patterns have a much more striking and brighter appearance. With this in mind, to show the quality of the white background, the motifs and patterns were made with more plainness. In the years after

however, Iznik manufacturers were severely damaged after the loss of support from the Palace (at the end of WW1) and the production of Çini almost ceased to stand.

Evliya Çelebi, who is a famous traveller from Kütahya, mentioned Çini in his book "Seyahatname", reporting about the beauty and unicity of the Çini products manufactured by local Kütahya artists in 17th century. In the 18th century when the art of Iznik was completely lost, Kütahya ateliers gained momentum with the withdrawal of Iznik and developed a brand new style of art as a result of free brush use and more modern approaches [3].

Since Kütahya Çini manufacturers did not receive great support as the Iznik did in any period of history, the manufacturers in this region followed a more humble line. Initially, Kütahya Çinis were produced to meet the needs of the local people and with a more modest quality level compared to the Iznik Çinis that were produced. As a result of this situation, the motif designs were arranged and formed with more density. The Çini products were filled with dense motifs and patterns to hide the mistakes and dull background color. In this way; they aimed to mask the quality deficiencies that occur in the Çini bisques, the glazes and the colors with intensive pattern designs. The need for intensive pattern designs is one of the most basic features that reflect the characteristic structure of Kütahya çinis. The Solution, which emerged as a necessity, was to enrich the motif and pattern designs and increase the aesthetic qualities.

These tiny pieces of Çinis made of hard white clay are put under the glaze technique, then made into small sized elegant works such as cups, bowls, pitchers and plates etc. These items all carry a different local artistic character from each classical style with light brush strokes. They are decorated with small flowers, plant motifs, leaves, vines, raindrops and medallions with light blue, navy blue, red, yellow, purple, green, and lilac colors. Besides these, lifelike birds, fish and local outfit designs were widely used. However, in the second part of the 18th century, the quality of Kütahya's Çini had deteriorated in terms of color, motif and shape. This dreadful period lasted a long time. In 1905, the governor, Fuat Pasha, had the government building decorated with Çinis. Then later wrote in a report to the center saying; "Three centuries ago in Kütahya, there were more than three hundred Çini manufacturers. In 1795, the number of manufactured Çini ateliers had fallen. Towards 1902, Hafız Emin and Hacı Minasyon's ateliers had closed down. During the Second World War, Çini manufacturing in Kütahya was revived once again in response to the need and continues its development today [4].

Kütahya is the only city in Turkey that has earned importance in statistics today with its commercial and artistic contribution to Çini culture, aesthetic line, continuous developing production, technology and globalizing world markets since the beginning of production start in the 13th century. Despite this, it cannot be denied that negative factors such as commercial expectations and inadequate academic

training have led to a great decrease in the art of Çini and its industry. The characteristics of the Çini products that started to rise from the 16th century have fallen due to the 19th century national and sectoral negativities. The Çini sector, which has gained a momentum with the Republican era, has now become more intense and has achieved a significant success level in the area of quality and standard as the concomitant result of increasing research-development and product-development studies.

However, in order to meet the anticipation of globalized domestic and foreign markets, handiwork shifted to technology-intensive production as it is a lot quicker. The inability to fully hold the academic balance of the traditional master apprenticeship has resulted in a decrease in quality in design as well as aesthetics. The quality and standards that are captured in the production of Çini structure are unfortunately not current for Çini motifs and patterns production due to the lack of trained artists and masters. In today's Çini motifs and designs, it is not possible to talk about innovation when we compare them to the motifs and designs in the sixteenth and seventeenth centuries as there is no extreme change in design. Due to commercial concerns and lack of academic publications and research, the Çini sector has not gone beyond the repetition of old motifs and patterns.

Conclusions & Recommendations

One of the most important problems that the Çini producers are facing is; the motifs and designs that directly affect the sale of Çinis are not rich and sufficient in quality and quantity. Therefore, the production of Çinis that are decorated with similar motifs and designs threaten the domestic and foreign markets.

Re-interpretation of Çini motifs and patterns went from a contemporary perspective without straying away from the original; it is important to save the Kütahya Çini art which has been going on for hundreds of years from repetition and copies, and to determine a new route in its original line. The most important feature that distinguishes Çini products from other ceramic products is the decorations applied under the glaze. The term of decor can also be referred to as pattern integrity created with unit motifs.

Çini art is one of the oldest art branches of Turkish history. It has been continuously produced until the present day because it can survive for years and can deliver its social values to future generations. Çini artifacts have also been used frequently in religious buildings and state-owned public buildings, because they make it more aesthetically valuable.

Çini Art lived its most spectacular days in the Ottoman Empire during the 15th and 16th centuries. İznik and Kütahya stand out as the two most important Çini production centers in this period. At the end of World War I, Iznik Çini production, which lost its support of the palace, has losed its importance in the following years. This situation has brought Kütahya Chineseism to an even more important position. Today, the most important and even the only representative of the Turkish Çini Art, Kütahya Çini sector is experiencing a blockage due to repetition and copying in motif and pattern design despite the increasing technical possibilities. For this reason, it is necessary to reinterpret today's Turkish society with the contemporary aesthetic point of view in accordance with the original of the Çinis and patterns. Çini art, which has been carried on with the master apprentice relationship for hundreds of years, needs to be transferred to the younger generations with traditional and academic methods especially in terms of motif and pattern design.

References

1. Faruk Şahin, 1989, “Türk Çini Sanatı Süslemeciliği”, Anadolu Üniversitesi Kütahya M.Y.O. Yayınları, Page :13, Kütahya/Türkiye.
2. İskender Işık, Gökhan Akca and Uğur Kut, 2016, “İpek Yolu Medeniyetlerinde Çini Sanatı”, VI. Avrasya Sosyal Bilimler Forumu, Oral Presentation, Bişkek/Kırgızistan
3. <http://www.kutahya.bel.tr/sanat.asp>, Date of access: 28 September 2018
4. Eren Sarı, 2016, “Türk Çini Sanatı”, Net Medya Yayıncılık, First Edition, Antalya/ Türkiye

seres'18

IV. INTERNATIONAL CERAMIC GLASS PORCELAIN
ENAMEL GLAZE AND PIGMENT CONGRESS
October 10-12, 2018, Eskişehir, Turkey

**Full Text of
ORAL
PRESENTATIONS**

LITHIUM ION BATTERIES POTENTIAL IN TURKEY

3D DISPERSION OF $\text{La}_2\text{Al}_{0.5}\text{Li}_{0.5}\text{O}_4$ AND LiAlO_2 in Al CONTAINING $\text{Li}_7\text{La}_3\text{Zr}_2\text{O}_{12}$ SOLID ELECTROLYTES

K. Burak Dermenci¹, Sinem Başkut¹, Piotr Bobrowski², Marek Faryna², Servet Turan¹

¹ Eskişehir Technical University, Dept. of Material Science and Engineering, 26555, Eskişehir, Turkey

² Institute of Metallurgy and Materials Science of the Polish Academy of Sciences, Krakow, Poland

Keywords: $\text{Li}_7\text{La}_3\text{Zr}_2\text{O}_{12}$, Solid electrolytes, Li-ion batteries, FIB-EBSD

ABSTRACT

Solid electrolyte containing all solid state Li-ion batteries are considered as a potential solution for the safety issues of high-energy density batteries. However, solid electrolytes in all solid-state batteries show low ionic conductivity. Cubic $\text{Li}_7\text{La}_3\text{Zr}_2\text{O}_{12}$ (LLZO) is a new composition that shows nearly liquid electrolyte ionic conductivities. One of the main challenges for LLZO as Li-bearing materials is the lack of information obtained from 3D structures about porosity and secondary phase distribution. In this conceptual study, 25 mole % Al containing LLZO was synthesized by using solid-state reaction method with 2-step calcination at 900 and 980 °C followed by sintering at 1050 °C for 24 hours. According to XRD results, tetragonal-cubic LLZO mixture was formed along with phases of LiAlO_2 and $\text{La}_2\text{Al}_{0.5}\text{Li}_{0.5}\text{O}_4$. Microstructural investigations of grain and grain boundary phases were evaluated in 3-D by using FIB-SEM techniques. Quantitative analysis was conducted by using both EDS and FIB-SEM software. EDS results emphasize nearly stoichiometric ratio of LLZO and grain boundary phases. 3D models generated by FIB-SEM showed that 87.7 vol. % LLZO; 7.3 vol. % $\text{La}_2\text{Al}_{0.5}\text{Li}_{0.5}\text{O}_4$ which was believed to be melted and flowed through porosities during sintering; 5 vol. % LiAlO_2 which remained in a solid form during synthesis and pores.

INTRODUCTION

Li-ion batteries are considered as a next generation energy storage devices. Especially for energy applications such as EV's, organic liquid electrolytes are highly explosive and flammable which cause safety problems for long-term usage. Because of that, electrolytes' stability would be crucial parameter in high energy density Li-ion batteries. In order to overcome such problems, a lot of solid electrolytes are studied [1-3].

Among them, garnet type $\text{Li}_7\text{La}_3\text{Zr}_2\text{O}_{12}$ (LLZO) solid electrolytes show excellent electrochemical stability window, explosion and flame resistant properties. They are also known as non-toxic [2]. There are two polymorphs of LLZO reported so far. The room temperature stable phase of tetragonal LLZO shows quite low ionic conductivity. However, high temperature stable phase of cubic LLZO shows nearly comparable ionic conductivity with liquid electrolytes [3].

It's also reported that doping with stabilizers such as Y [4], Ta [5], Al [6-15], Hf [16,17] Ga [5,18], Te [14], Si [15], Nd, Ca and Nb [19] during synthesis reduce the cubic stabilization temperature. More work has been done related on Al since it's a common substance found in nature.

There has been a growing need for explaining sintering behavior during synthesis. X-ray and neutron diffraction techniques are widely used to understand and explain the formation mechanism during synthesis. Up-to-date knowledge in case of Al reveals that, low-melting point intermediate phases will be formed and help sintering behavior of LLZO [9,10]. However, for better understanding

on cubic phase LLZO stabilization mechanism, quantitative results obtained from diffraction techniques should be visually supported by electron microscopy techniques. In this study, elemental and phase analysis by using SEM-EDS and FIB-SEM on the polished surface of 25 mole % Al containing LLZO pellets sintered at 1050 °C for 24 hours is discussed. 3D microstructural analysis, the dispersion of porosities and impurity phases as well as LLZO phase is also evaluated by using FIB-SEM.

EXPERIMENTAL

25 mole % Al containing LLZO was synthesized via solid-state reaction method. Firstly, Li_2CO_3 (Merck) was dried at 200 °C, whereas La_2O_3 (Sigma-Aldrich) and ZrO_2 (Inframat) were dried at 900 °C before mixing to get rid of the hydroxides and humidity. Al_2O_3 (Ceralox) was used as Al source to stabilize the cubic phase. Stoichiometric amounts of powders were mixed in agate mortar grinder (Retsch RM200). 15 % of excess Li as Li_2CO_3 was added in order to compensate Li losses during the calcination. Powders were calcined at 900 and re-calcined at 980 °C for 12 hours in a muffle furnace (Nabertherm). Between each calcination step, powders were reground. After that, 2 g of calcined powders were isostatically pressed into pellet (16 mm diameter) at 290 MPa. Then, as-prepared pellet were sintered at 1050 °C for 24 h within a powder bed containing calcined powders. Alumina crucible was used for all heat treatments. 2 °C min⁻¹ heating rate was set in order to minimize unexpected Li losses during heat treatments. The pellet were ground using 2-propanol as coolant and their crystal structures were determined by using Rigaku MiniFlex 600 X-ray diffractometer (XRD) with a scan speed of 1°/min and step size of 0.02° by using $\text{Cu K}\alpha$.

For SEM investigations, samples were polished by using both mechanical polisher (STRUERS, Tegra pol-25) and cross section polisher (CP, Jeol, SM 09010). During mechanical polishing, water-free solutions (AKASEL – DiaDoubo Water Free Diamond Suspensions) were used to avoid contacting of water to the LLZO. Then, samples were polished at 2.5 kV accelerating voltage for 16 hours in the CP.

Imaging and chemical analysis studies were carried out in a field emission gun-scanning electron microscope (ZEISS-SUPRA 50 VP) attached with an energy dispersive X-ray spectrometer (EDS-OXFORD Instruments). 3D-BSE reconstructions were performed in a FIB-SEM (FEI Company, Quanta 3D FEG) system. During the slice and view application, operating parameters of the electron beam were set to 5 kV accelerating voltage and 4 nA beam current. Also, the materials were milled by using Ga^+ ions at 30 kV accelerating voltage and 3 nA beam current conditions. Milling was carried out 20 µm deep into the material by 75 BSE images with 200 nm thickness.

RESULTS & DISCUSSION

The XRD pattern of 25 mole % Al containing LLZO pellet sintered at 1050 °C for 24 hour is shown in Figure 1.

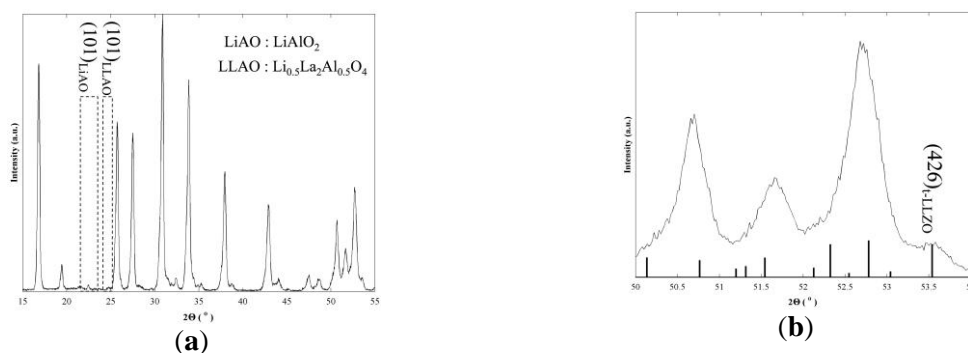


Figure 1. XRD patterns of as-synthesized LLZO sample. (a) Whole pattern; (b) Pattern between 2 θ= 50-54° showing (426) plane of tetragonal LLZO.

As it can be obtained from the Figure 1 (a) that all of the peaks can be indexed as cubic LLZO (PDF Card No: 01-080-9103), tetragonal LLZO (PDF No: 01-080-6141), LiAlO_2 (PDF Card No: 00-038-1464) and $\text{La}_2\text{Al}_{0.5}\text{Li}_{0.5}\text{O}_4$ (PDF Card No: 01-084-1470). Besides, the small peak at $2\theta=53.5^\circ$ is (426) plane of tetragonal LLZO in Figure 1 (b) which proved the presence of tetragonal LLZO. Moreover, the background between $2\theta=50-54^\circ$ in Figure 1 (b) formed due to the tetragonal and cubic peak overlays. The pattern showed bold belonged to tetragonal LLZO structure. Sintering at 1050°C for 24 hours resulted in tetragonal and cubic phase LLZO, LiAlO_2 and $\text{La}_2\text{Al}_{0.5}\text{Li}_{0.5}\text{O}_4$ in the structure. The latest studies concerning calculation of LLZO and impurity phases by in-situ neutron diffraction technique emphasizes that $\text{La}_2\text{Al}_{0.5}\text{Li}_{0.5}\text{O}_4$ and small amount of LiAlO_2 are the most likely intermediate phases at sintering temperatures around 1000°C . The same study also implies that tetragonal phase tends to remain during transition. In all, findings given above are in accordance with the previous studies [20].

The microstructure investigations of surface morphology were carried out by using both Secondary Electron (SE) and Backscatter Electron (BSE) Mode. Surface morphology of polished samples and phase contrast is presented in Figure 2.

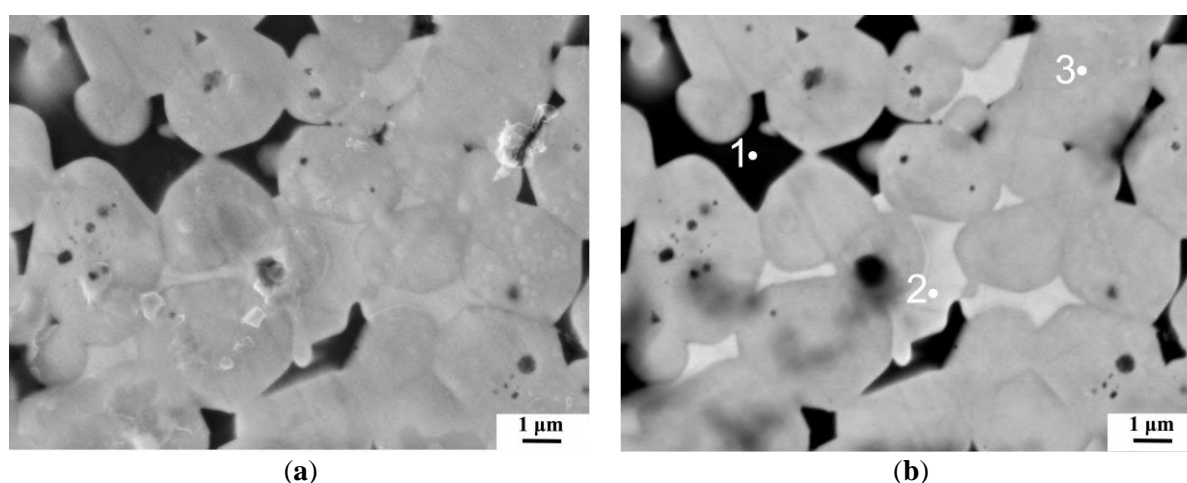


Figure 2. XRD patterns of as-synthesized LLZO sample. (a) Whole pattern; (b) Pattern between $2\theta = 50-54^\circ$ showing (426) plane of tetragonal LLZO.

Images in Figure 2 (a) showed that grains with a diameter of 2-3 μm were partially surrounded by secondary phase. Since the shape of secondary phase is the shape of intergranular voids, it can be referred that sintering temperature exceeded its melting point and flowed through the intergranular voids. There were also submicron porosities within the grains microstructure. Table 1 showed the quantitative elemental analysis results obtained by EDX point analysis from Points 1-3 in Figure 2 (b).

Table 1. Quantitative elemental analysis from SEM-EDX on different points

Point	La (at. %)	Al (at. %)	Zr (at. %)	O (at. %)
1	0.0	30.3	0.0	69.7
2	26.6	6.9	0.0	66.5
3	15.8	0.3	11.8	72.1

The point EDS analysis in dark regions (denoted as 1) showed only Al and O that was the sign of LiAlO_2 found in Figure 1. The brighter regions (denoted as 2) were La-rich regions. Zr was not detected which was the clue of $\text{La}_2\text{Al}_{0.5}\text{Li}_{0.5}\text{O}_4$ phase. $\text{La}_2\text{Al}_{0.5}\text{Li}_{0.5}\text{O}_4$ melted and partially filled grain boundaries at sintering temperature. It can be inferred from the Point 3 that La and Zr ratio was precisely conformed LLZO stoichiometry. But, the content of Al was lower than what it was expected. The Al diffusion through LLZO grains was not completed. There were also Al-rich phases such as $\text{La}_2\text{Al}_{0.5}\text{Li}_{0.5}\text{O}_4$ and LiAlO_2 around the grains. However, dispersion of LiAlO_2 was not as same as

$\text{La}_2\text{Al}_{0.5}\text{Li}_{0.5}\text{O}_4$. Since it remained its solid form at sintering temperatures, LiAlO_2 phase were deposited within intergranular voids.

Since SE and BSE images only gives information about surface morphology, there's a need of proving the hypothesis in 3-D. For more accurate evaluation of findings above, it's important to show what's behind the surface. A series of slices were excavated from the surface of polished LLZO. By combining all slices, 3-D models of three different regions stated in Figure 2 (b) were built and given in Figure 3.

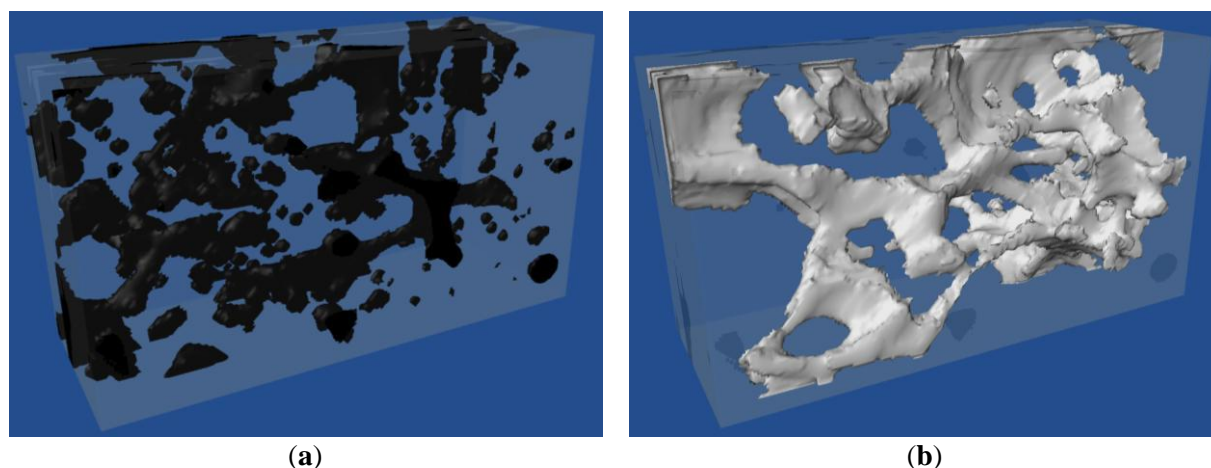


Figure 3. 3-D models obtained from excavated region for the (a) Point 1; (b) Point 2

3-D model of excavated volume was presented in Figure 3. Region denoted as 1 in Figure 2 (b) was shown in Figure 3 (a). In this model, dark region consist LiAlO_2 . Since porosities act as electron sinks and appeared dark in BSE mode, residual porosities were also located in the given model. The contrast difference does not allow discriminating each other. It can also be inferred from the Figure 3 (a) that discrete LiAlO_2 grains were on the triple junction of LLZO grains. There were LiAlO_2 grain growth and LiAlO_2 - LiAlO_2 grain boundaries which is the sign of solid state reaction at sintering temperatures. A thermodynamic study based on Li_2O - Al_2O_3 system emphasizes that LiAlO_2 compounds melt at 1775 °C which is relatively high comparing with sintering conditions [21]. So, LiAlO_2 phase will be formed in solid state. Thus, current study correlates with the literature.

3D model formed by $\text{La}_2\text{Al}_{0.5}\text{Li}_{0.5}\text{O}_4$ denoted as 2 in Figure 2 (b) were seen in Figure 3 (b). Unlike Figure 3 (a), all white regions are strongly interconnected. No sign of discrete grain boundaries were presented. According to the morphology in Figure 3 (b), $\text{La}_2\text{Al}_{0.5}\text{Li}_{0.5}\text{O}_4$ melted during sintering; flowed through and filled grain boundary voids partially. Furthermore, the grey colored remaining phase in both Figure 3 (a) and (b) was tetragonal and cubic LLZO phases denoted as 3 in Figure 2 (b).

Quantitative analysis was done by analyzing the volume of darker and white obtained in Figure 2 and 3. Results were presented in Table 2.

Table 2. Quantitative data analysis from 3D-FIB Slices

Region ¹	Volume (vol. %)
1	5.0
2	7.3
3	87.7

¹Region numbers are the same as in Figure 1.

It can be obtained from the Table 2 that volumes in percentage from different regions show that 87.7 % of total volume is LLZO and only 5.0 % and 7.3 % of total volume contain pores, LiAlO_2 and $\text{La}_2\text{Al}_{0.5}\text{Li}_{0.5}\text{O}_4$ respectively. These results are parallel with XRD patterns in Figure 1 (a).

CONCLUSIONS

To summarize the findings above, 25 mole % Al containing LLZO is synthesized via solid state reaction method with 2-step calcination and sintering at 1050 °C for 24 hour. According to XRD results, a mixture of tetragonal and cubic LLZO is formed with impurities of LiAlO_2 and $\text{La}_2\text{Al}_{0.5}\text{Li}_{0.5}\text{O}_4$. SE and BSE images in combination with quantitative EDS analysis show that, because of relatively low atomic weight, LiAlO_2 appears dark along with porosities and it's hard to discriminate them in BSE mode. Besides, white regions are $\text{La}_2\text{Al}_{0.5}\text{Li}_{0.5}\text{O}_4$. 3-D models formed by slicing with FIB visualize high LLZO ratio of 87.7 vol. % with a very low $\text{La}_2\text{Al}_{0.5}\text{Li}_{0.5}\text{O}_4$, LiAlO_2 and pore volumes of 7.3 % and 5.0 % , respectively. Another outcome of this study is that LiAlO_2 was in a solid state whereas $\text{La}_2\text{Al}_{0.5}\text{Li}_{0.5}\text{O}_4$ was in liquid form during the sintering.

REFERENCES

1. Bachman, J.C.; Muy, S.; Grimaud, A.; Chang, H.H.; Pour, N.; Lux, S.F.; Paschos, O.; Maglia, F.; Lupart, S.; Lamp, P., *et al.*, Inorganic solid-state electrolytes for lithium batteries: Mechanisms and properties governing ion conduction. *Chemical Reviews* 2016, *116*, 140-162.
2. Knauth, P., Inorganic solid li ion conductors: An overview. *Solid State Ionics* 2009, *180*, 911-916.
3. Thangadurai, V.; Narayanan, S.; Pinzaru, D., Garnet-type solid-state fast li ion conductors for li batteries: Critical review. *Chem Soc Rev* 2014, *43*, 4714-4727.
4. Murugan, R.; Ramakumar, S.; Janani, N., High conductive Yttrium doped $\text{Li}_7\text{La}_3\text{Zr}_2\text{O}_{12}$ cubic lithium garnet. *Electrochem Commun* 2011, *13*, 1373-1375.
5. Allen, J.L.; Wolfenstine, J.; Rangasamy, E.; Sakamoto, J., Effect of substitution (Ta, Al, Ga) on the conductivity of $\text{Li}_7\text{La}_3\text{Zr}_2\text{O}_{12}$. *Journal of Power Sources* 2012, *206*, 315-319.
6. Ahn, J.H.; Park, S.Y.; Lee, J.M.; Park, Y.; Lee, J.H., Local impedance spectroscopic and microstructural analyses of Al-in-diffused $\text{Li}_7\text{La}_3\text{Zr}_2\text{O}_{12}$. *Journal of Power Sources* 2014, *254*, 287-292.
7. Dermenci, K.B.; Cekic, E.; Turan, S., Al stabilized $\text{Li}_7\text{La}_3\text{Zr}_2\text{O}_{12}$ solid electrolytes for all-solid state li-ion batteries. *Int J Hydrogen Energ* 2016, *41*, 9860-9867.
8. Jin, Y.; McGinn, P., Al-doped $\text{Li}_7\text{La}_3\text{Zr}_2\text{O}_{12}$ synthesized by a polymerized complex method. *Journal of Power Sources* 2011, *196*, 8683-8687.
9. Langer, F.; Glenneberg, J.; Bardenhagen, I.; Kun, R., Synthesis of single phase cubic Al-substituted $\text{Li}_7\text{La}_3\text{Zr}_2\text{O}_{12}$ by solid state lithiation of mixed hydroxides. *J Alloy Compd* 2015, *645*, 64-69.
10. Raskovalov, A.A.; Ilina, E.A.; Antonov, B.D. Structure and transport properties of $\text{Li}_7\text{La}_3\text{Zr}_{2-0.75x}\text{Al}_x\text{O}_{12}$ superionic solid electrolytes. *Journal of Power Sources* 2013, *238*, 48-52.
11. Rettenwander, D.; Blaha, P.; Laskowski, R.; Schwarz, K.; Bottke, P.; Wilkening, M.; Geiger, C.A.; Amthauer, G., Dft study of the role of Al^{3+} in the fast ion-conductor $\text{Li}_{7-3x}\text{Al}_{x+3}\text{La}_3\text{Zr}_2\text{O}_{12}$ garnet. *Chemistry of Materials* 2014, *26*, 2617-2623.
12. Rosenkiewitz, N.; Schuhmacher, J.; Bockmeyer, M.; Deubener, J., Nitrogen-free sol-gel synthesis of al-substituted cubic garnet $\text{Li}_7\text{La}_3\text{Zr}_2\text{O}_{12}$ (LLZO). *Journal of Power Sources* 2015, *278*, 104-108.
13. Takano, R.; Tadanaga, K.; Hayashi, A.; Tatsumisago, M., Low temperature synthesis of Al-doped $\text{Li}_7\text{La}_3\text{Zr}_2\text{O}_{12}$ solid electrolyte by a sol-gel process. *Solid State Ionics* 2014, *255*, 104-107.
14. Wang, D.W.; Zhong, G.M.; Dolotko, O.; Li, Y.X.; McDonald, M.J.; Mi, J.X.; Fu, R.Q.; Yang, Y., The synergistic effects of al and te on the structure and Li^+ -mobility of garnet-type solid electrolytes. *Journal of Materials Chemistry A* 2014, *2*, 20271-20279.

15. Kumazaki, S.; Iriyama, Y.; Kim, K.H.; Murugan, R.; Tanabe, K.; Yamamoto, K.; Hirayama, T.; Ogumi, Z., High lithium ion conductive $\text{Li}_7\text{La}_3\text{Zr}_2\text{O}_{12}$ by inclusion of both Al and Si. *Electrochem Commun* 2011, 13, 509-512.
16. Awaka, J.; Kijima, N.; Hayakawa, H.; Akimoto, J., Synthesis and structure analysis of tetragonal $\text{Li}_7\text{La}_3\text{Zr}_2\text{O}_{12}$ with the garnet-related type structure. *J Solid State Chem* 2009, 182, 2046-2052.
17. Zaiß, T.; Ortner, M.; Murugan, R.; Weppner, W., Fast ionic conduction in cubic Hafnium garnet $\text{Li}_7\text{La}_3\text{Hf}_2\text{O}_{12}$. *Ionics* 2010, 16, 855-858.
18. Rettenwander, D.; Geiger, C.A.; Tribus, M.; Tropper, P.; Amthauer, G., A synthesis and crystal chemical study of the fast ion conductor $\text{Li}_{7-3x}\text{Ga}_x\text{La}_3\text{Zr}_2\text{O}_{12}$ with $x=0.08$ to 0.84 . *Inorganic chemistry* 2014, 53, 6264-6269.
19. Hanc, E.; Zajac, W.; Molenda, J., Synthesis procedure and effect of Nd, Ca and Nb doping on structure and electrical conductivity of $\text{Li}_7\text{La}_3\text{Zr}_2\text{O}_{12}$ garnets. *Solid State Ionics* 2014, 262, 617-621.
20. Chen, Y.; Rangasamy, E.; dela Cruz, C.R.; Liang, C.D.; An, K., A study of suppressed formation of low-conductivity phases in doped $\text{Li}_7\text{La}_3\text{Zr}_2\text{O}_{12}$ garnets by in situ neutron diffraction. *Journal of Materials Chemistry A* 2015, 3, 22868-22876.
21. Kulkarni, N.S.; Besmann, T.M.; Spear, K.E., Thermodynamic optimization of lithia-alumina. *J Am Ceram Soc* 2008, 91, 4074-4083.

BATTERIES AND SUPERCAPACITORS

LITHIUM ION CONDUCTING GLASS CERAMIC MEMBRANES FOR DUAL ELECTROLYTE LITHIUM AIR BATTERY APPLICATIONS

Mine Kırkbınar*, Abdulkadir Kızılaslan, Hatem Akbulut, Tugrul Cetinkaya*

Sakarya University, Engineering Faculty, Department of Metallurgical & Materials Engineering,
Esentepe Campus, 54187, Sakarya, Turkey

1. INTRODUCTION

Lithium-air batteries are considered to be next generation energy storage systems with theoretical energy density of ≈ 12000 Wh/kg, approximately equal to energy density of gasoline. Current Li-air battery systems compose of lithium metal and porous carbon based materials as anode and cathode respectively. Shuttle of Li^+ ions between anode and cathode realized by aqueous and aprotic(non-aqueous) liquied electrolytes. Corrosion of Li anode in contact with aqueous electrolyte requires to utilize a dense and highly ionic conductive membrane to protect lithium anode without preventing lithium ion transport[1].

Among various glass-ceramic membranes, oxide based solid electrolytes are promising candidates to be utilized in Li-air batteries due to their better characteristics over other systems, e.g. higher oxidation and reduction stability [2]. $\text{Li}_{1+x}\text{Al}_x\text{Ti}_{2-x}(\text{PO}_4)_3$ systems are widely utilized in Li-air battery systems as membranes which combine electrochemical stability with high ionic conductivities on the order of 10^{-4} S/cm [3–5].

This study covers the synthesis of $\text{Li}_{1.3}\text{Al}_{0.3}\text{Ti}_{1.7}(\text{PO}_4)_3$ solid electrolytes with sol-gel route. Phase and morphology of synthesized membrane powders were carried out with XRD and FESEM respectively. Thermal analysis were conducted by DSC-TG analysis. Besides, cylindrical shaped pellets were produced by cold-pressing LATP powders at different pressures and subsequent heat treatment were applied to investigate the pressure-sintering temperature-pellet thickness relation.

2. EXPERIMENTAL METHODS

Synthesis of LATP carried out with sol-gel method. Initially titanium isopropoxide dissolved in citric acid and water mixture for 4h at 80°C . In another beaker, lithium acetate and ammonium dihydrogen phosphate dissolved. Then, first mixture poured into lithium acetate-ammonium dihydrogen phosphate solution at room temperature. Aluminum isopropoxide were then added to mixture. Ethylene glycol were then added to whole mixture under magnetic stirring. Ammonium hydroxide were added to

adjust the pH of the mixture into neutral. After magnetic stirring for about 6h at 80°C, the mixture converted into gel form. The gel dried at 150 °C for 5h. After drying, the gel subjected to a two-step heat treatment where the gel initially converted into glass form and subsequent heat treatment converted the glass into crystalline form.

Thermal analysis of the powders were carried out with NETZSCH STA under nitrogen medium. Phase analysis was conducted by X-ray diffraction between 10-50°. Pellet were produced from 100 mg LATP powders by cold pressing under different pressures. Morphology and elemental analysis of the LATP carried out at FESEM Quanta FEI450.

3.RESULTS and DISCUSSION

Figure 1 shows the DSC-TG analysis result of LATP synthesis. Strong exothermic peak observed at the onset of 800 °C stands for the crystallization of LATP structure from glass. Another endothermic peak at about 200 °C were observed which is due to the decomposition of ammonium dihydrogen phosphate[6]. TG analysis revealed the weight loss at about 150 °C which is due to the pyrolysis of ethylene glycol and citric acid to emancipate CO₂ and H₂O [7].

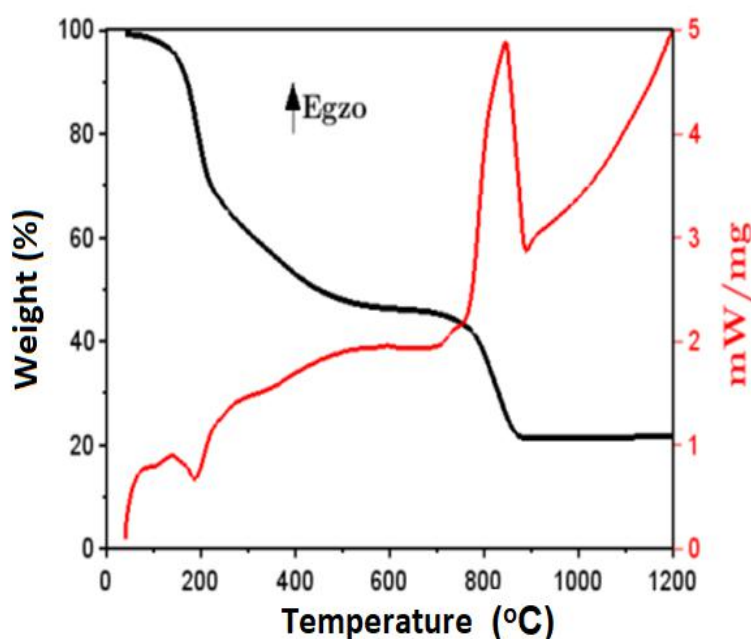


Fig. 1. DSC-TG analysis of LATP under N₂ medium.

XRD analysis were performed to reveal phase analysis of LATP and to detect impurity phases emerged up on heating up to 1000 °C. Powders heat treated at 800 °C were found to contain less impurity AlPO₄ phase which is the main impurity phase in these systems[8]. Amount of impurity phase were increased with increasing temperature.

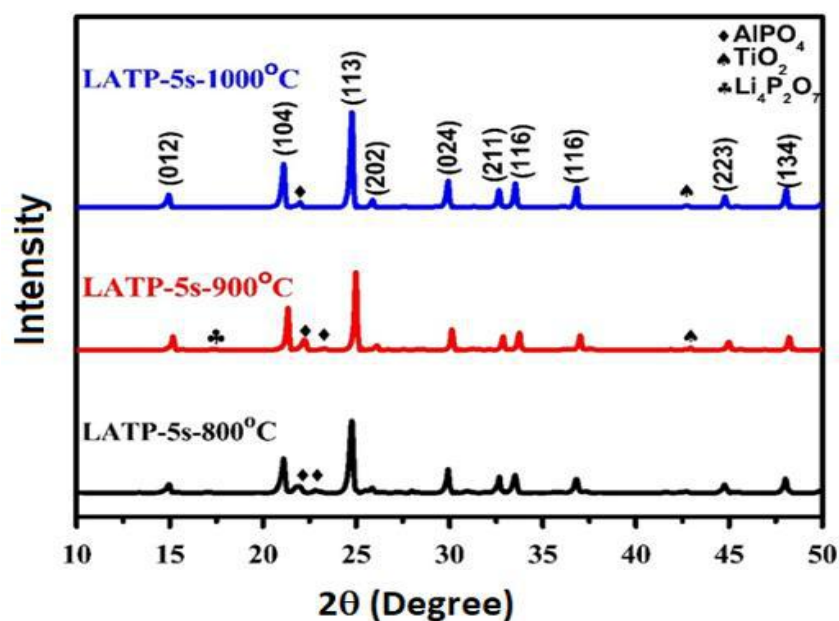


Fig. 2. XRD patterns of LATP powders crystallized at 800, 900 and 1000 °C for 5h.

Morphology of LATP pellets sintered at 800, 900 and 1000 °C were shown in Figure 3. Pellets sintered at 1000 °C have microcracks which impede ionic conductivity and deteriorate mechanical stability of pellets.

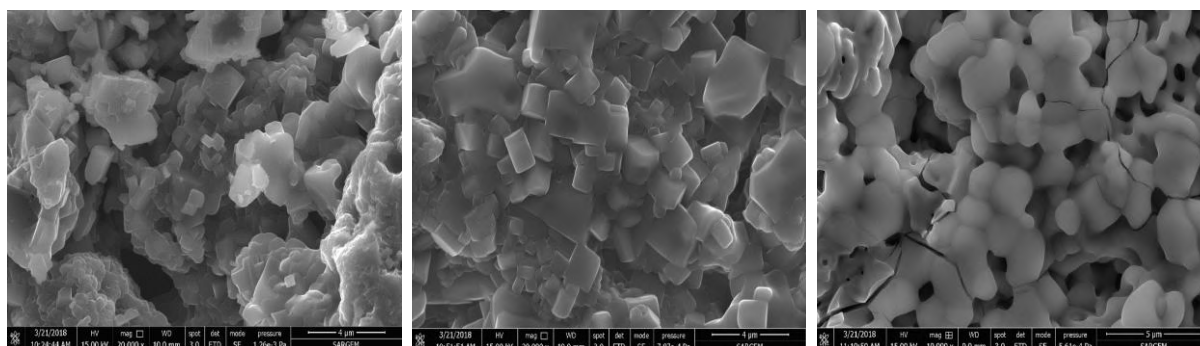


Fig. 3. SEM images of LATP pellet membranes sintered at 800, 900 and 1000 °C.

EDS analysis given in figure x shows that the amount of Al dramatically increased at 1000 °C due to the formation of AlPO_4 phase. At 900 °C the amount of Al is more than the stoichiometry of $\text{Li}_{1.3}\text{Al}_{0.3}\text{Ti}_{1.7}(\text{PO}_4)_3$ which is consistent with XRD analysis where the amount of impurity phase were found to be increased.

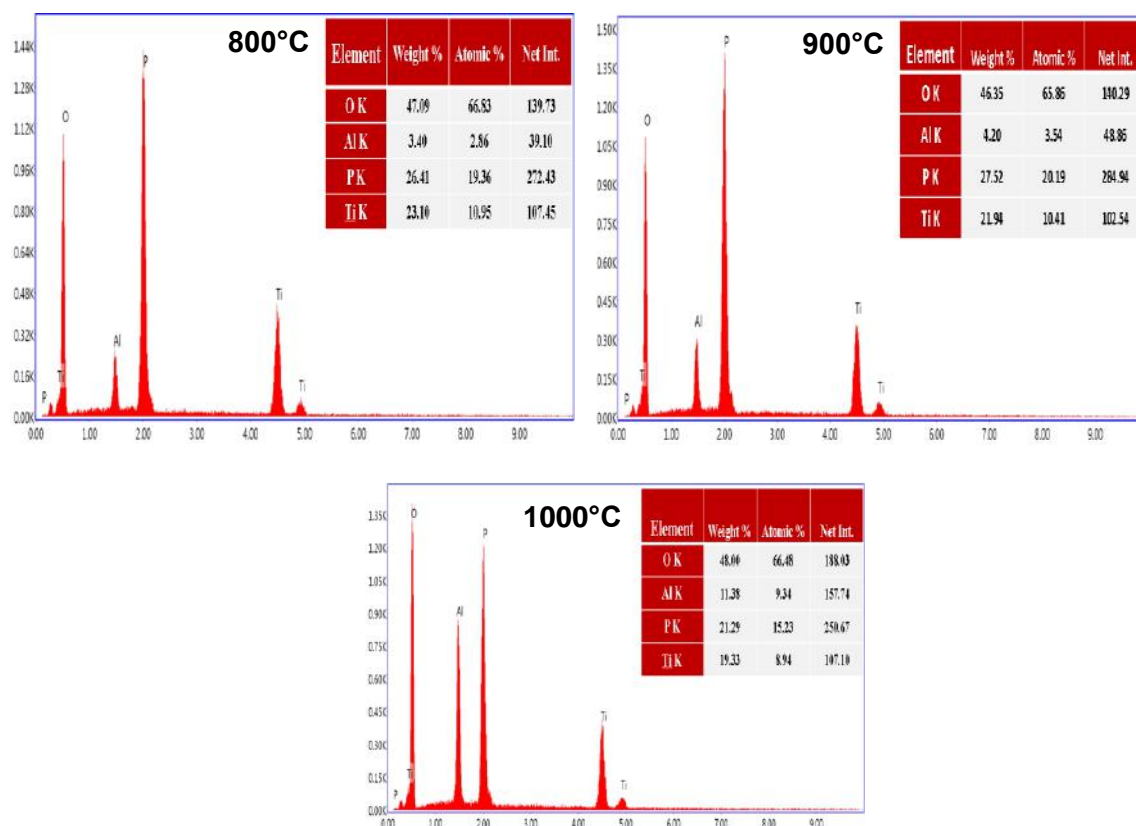


Fig. 4. EDS Analyses of LATP pellets sintered at 800(a),900(b) and 1000 °C(c).

LATP pellets in cylindrical form were produced by cold pressing at different pressures. Sintering were then carried out at 800, 900 and 1000 °C to impart mechanical strength through reducing porosities within pellets. Table 1 shows the pressure-sintering temperature and pellet thickness relation. Pellets as thin as 130 μm were obtained after sintering at 1000 °C. Synthesized LATP were shown in figure 5 in powder and pellet forms.

Table 1. Effect of pressures and temperatures on the thickness of LATP membrane.

Temperature Pressure	800 °C	900 °C	1000 °C
300 MPA	215,3 μm	249,0 μm	176,4 μm
400 MPA	193,7 μm	231,5 μm	156,9 μm
500 MPA	191,6 μm	186,7 μm	130,8 μm



Fig. 5. Synthesized LATP powders (left) and pellet form (right) after pressing and sintering.

ACKNOWLEDGEMENTS

This work is supported by the Scientific and Technological Research Council of Turkey (TUBITAK) under the contract number 315M461. The authors thank the TUBITAK MAG workers for their financial support.

REFERENCES

- [1] P. Tan, W. Kong, Z. Shao, M. Liu, M. Ni, Advances in modeling and simulation of Li–air batteries, *Prog. Energy Combust. Sci.* (2017).
- [2] A. Manthiram, X. Yu, S. Wang, Lithium battery chemistries enabled by solid-state electrolytes, *Nat. Rev. Mater.* (2017).
- [3] H. Bai, J. Hu, X. Li, Y. Duan, F. Shao, T. Kozawa, et al., Influence of LiBO₂ addition on the microstructure and lithium-ion conductivity of Li_{1+x}Al_xTi_{2-x}(PO₄)₃ (x = 0.3) ceramic electrolyte, *Ceram. Int.* 44 (2018) 6558–6563.
- [4] L. Hallopeau, D. Bregiroux, G. Rousse, D. Portehault, P. Stevens, G. Toussaint, et al., Microwave-assisted reactive sintering and lithium ion conductivity of Li_{1.3}Al_{0.3}Ti_{1.7}(PO₄)₃ solid electrolyte, *J. Power Sources.* 378 (2018) 48–52.
- [5] X.M. Wu, X.H. Li, Y.H. Zhang, M.F. Xu, Z.Q. He, Synthesis of Li_{1.3}Al_{0.3}Ti_{1.7}(PO₄)₃ by sol–gel technique, *Mater. Lett.* (2004).
- [6] R. Ramaraghavulu, S. Buddhudu, Analysis of structural, thermal and dielectric properties of LiTi₂(PO₄)₃ ceramic powders, *Ceram. Int.* 37 (2011) 3651–3656.
- [7] Y. Yoon, J. Kim, C. Park, D. Shin, The relationship of structural and electrochemical properties of NASICON structure Li_{1.3}Al_{0.3}Ti_{1.7}(PO₄)₃ electrolytes by a sol-gel method, *J. Ceram. Process. Res.* (2013).
- [8] M. Kotobuki, M. Koishi, Preparation of Li_{1.5}Al_{0.5}Ti_{1.5}(PO₄)₃ solid electrolyte via a sol–gel route using various Al sources, *Ceram. Int.* (2013).

ADVANCED CERAMICS

SHAPING OF SILICON NITRIDE CERAMICS VIA DIRECT COAGULATION CASTING

Hande Marulcuoğlu¹, Ferhat Kara¹¹Eskişehir Technical University, Faculty of Engineering, Department of Material Science and Engineering, 26480, Eskişehir, Turkey**Keywords:** Si₃N₄, Direct coagulation casting method, Mechanical properties, Microstructure

ABSTRACT

Direct coagulation casting via dispersant reaction in silicon nitride suspension was studied. High solid concentration and low viscosity silicon nitride suspensions were prepared using TMAH (Tetramethylammonium hydroxide) as a dispersant. GDA (Glycerol diacetate) was used to destabilise the Si₃N₄ slurries. The effect of solid loading and GDA concentration on the viscosity of slurries, green and sintered bodies were investigated. Silicon nitride parts were fabricated defect-free with 50 vol% solid loading, 0.4 wt% TMAH and 2 vol% GDA. The bulk density of sintered silicon nitride parts was almost 3,22±0,01 gr/cm³, four point bending strength of 600±170 MPa, fracture toughness of 6.75±0.05 MPa.m^{1/2} and Vickers hardness of 13.5±0.2 by gas pressure sintering.

1. INTRODUCTION

Silicon Nitride (Si₃N₄) based ceramics have developed into a well-established material for several structural applications, at both ambient and elevated temperatures, due to its high mechanical properties, good thermal shock resistance, high corrosion resistance, hardness and wear resistance [1]. These beneficial properties arise from dense microstructures containing interlocking β-Si₃N₄ [2]. Due to these properties, this materials has been used in such applications as aerospace and automobile industries, cutting, electronic substrates, gas turbine and engineering components [1]. Also, Si₃N₄ ceramics have been shown to be biocompatible so they have been used as implant materials [3].

Complex-shaped silicon nitride ceramic parts have conventionally been made using injection molding, slip casting, extrusion and pressing methods. Nevertheless, these methods have problems associated with production of molds, interactions with the mold materials, cracking during their green forming stages, binder removal, and long production time [4]. Therefore, slurry based methods such as direct coagulation casting and gel casting have been developed as alternative shaping processes. With these methods, complex shaped parts can be easily produced with the requirement of no or minimal machining processes.

Direct coagulation casting (DCC) is a new shaping method for ceramic green bodies [5]. Direct coagulation casting relies on coagulation of a stable colloidal suspension by using a suitable additive in the suspension which leads to its destabilisation. The ceramic powder suspension is coagulated by either change the pH toward the isoelectric point (IEP) of the suspension or increase the electrolyte concentration in the suspension [6]. In this way, the suspension is gelled to a rigid structure that take the shape of the mould with any complexity. This method has been produced homogenous microstructures with high green density. DCC is especially suitable for fabricating complex shaped components with large and small cross sections in the same part. Large and complex silicon nitride parts have been successfully shaped using the DCC technique [7].

The aim of this study, concentrated and low viscosity Si₃N₄ slurries, stabilised with TMAH is destabilised by using glycerol diacetate. Glycerol diacetate reacts with TMAH to reduce pH. After

shaping of silicon nitride ceramic parts using these slurries, drying and sintering behaviour of shaped parts, their microstructure and mechanical properties is reported.

2. EXPERIMENTAL PROCEDURE

2.1. Materials and Method

A commercially available silicon nitride powder was used. Alumina powder and yttrium oxide powder were used as sintered additives. TMAH (concentration of %10) and GDA (Glycerol diacetate) were used as dispersant and coagulant agent, respectively. Deionized water was used in preparing the suspension.

Figure 1 is shown the flowchart of the direct coagulation casting process. The suspensions were prepared by mixing silicon nitride powder, sintering additives, deionized water, dispersant and ball milling for 3 days using silicon nitride grinding media. The suspensions took approximately 25-30 min. in vacuuming to dispose of air bubbles. Then, different amounts of glycerol diacetate as a coagulating agent was used. The suspension was filled into the nonporous mold and at 60°C. The suspension is gelled to a rigid structure that takes the shape of the mould and then demoulded. The parts dried at 60°C for 24 hours and GPS method was used to sintering at 1950°C for 2 hours.

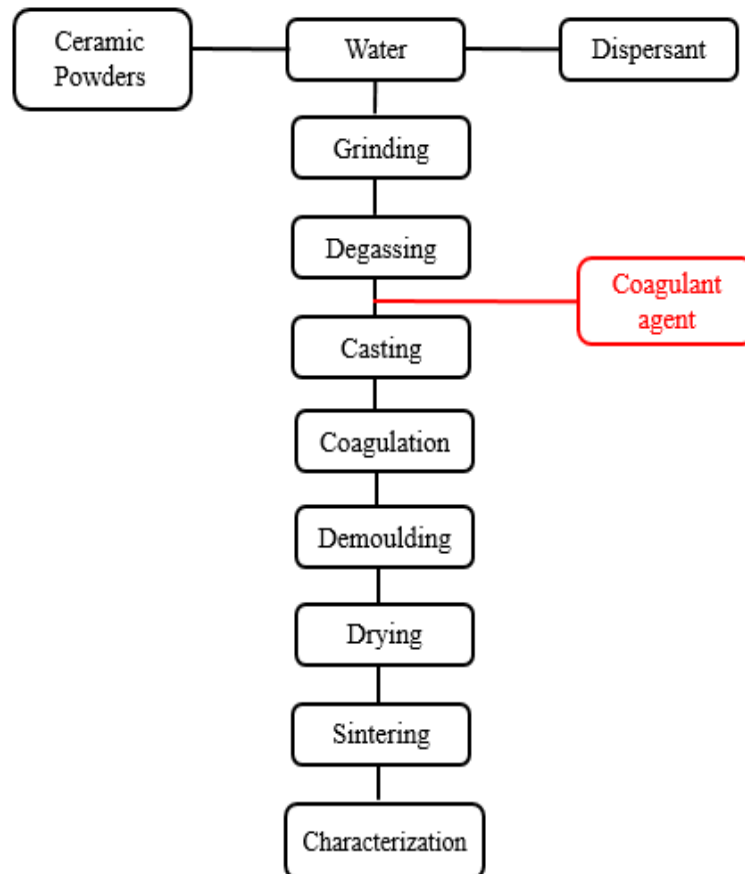


Figure.1. Flowchart of the direct coagulation casting process

2.2. Characterization

Particle size distribution of used powders was measured by Malvern MasterSize Analyzer 2000. The rheological properties of suspensions were measured using a rheometer (AntonPaar MCR 102) at 25°C. After shaping, green densities of rectangular parts were calculated by measuring dimensions and

weights. The densities of the sintered ceramic parts were determined using the Archimedes technique. The mechanical properties of the sintered samples were measured by using four point bending method (Instron, MDS666C). The fracture surface and polish surface of sintered parts microstructures were imaged using scanning electron microscopy (Zeiss EVO-50, Germany).

3. RESULTS AND DISCUSSION

Tetramethylammonium hydroxide is a widely used dispersant for the electrostatic stabilization of silicon nitride suspensions. The pH of prepared suspensions are approximately 11 with TMAH as dispersant. The effect of different solid concentrations on the viscosity of silicon nitride suspensions with 0.4 wt% TMAH is shown in Figure 2. It was observed that the viscosity of suspension increased due to the solid loadings. The viscosity of suspension at 50 vol% and 52 vol% solid loading are 1 Pa.s and 1.45 Pa.s at 10 s^{-1} , respectively. The suspension with a suitable fluidity for casting above 52 vol% solids concentrations could not be prepared. In order to prevent high viscosity and to facilitate the casting of the ceramic suspension into the mold, 50 vol% solid loading were chosen in the experimental studies.

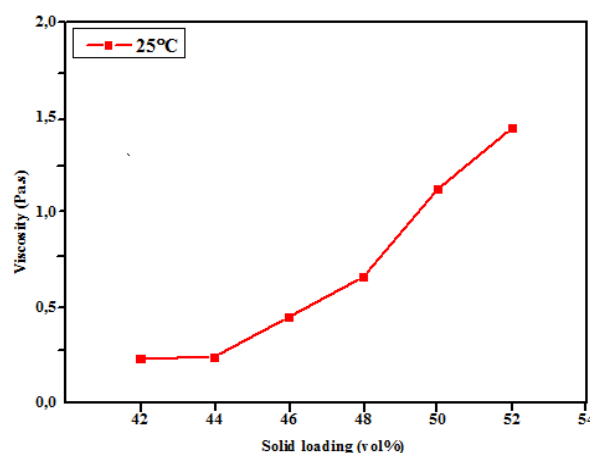


Figure.2. Effect of solid loading on the viscosity of silicon nitride suspension at the shear rate 10 s^{-1} .

Glycerol diacetate (GDA) is used as a coagulation agent for shaping by direct coagulation casting. It has been commonly used in practical applications for the pH regulator in systems. GDA is hydrolyzable ester and produce acetic acid in the alkaline region. Depending on the reaction between the TMAH and the acetic acid formed from the hydrolysis of the GDA in the suspension. Tetramethylammonium hydroxide is gradually consumed and dispersant concentration is reduced in the suspension. The silicon nitride particle surface loads are reduced and the system is formed by coagulation in the system [8].

Figure 3 shows the effect of concentration of glycerol diacetate on the viscosity of silicon nitride suspensions. The viscosity of the suspension was increased depending on the amount of GDA. The slurry's viscosity at 2 vol% and 2.5 vol% glycerol diacetate are 2.30 Pa.s and 6 Pa.s at 10 s^{-1} , respectively. With the use of 2.5 volume percent GDA, the viscosity was increased due to quickly Coagulation and Casting was difficult. Therefore, silicon nitride suspension with glycerol diacetate of 2 vol% is prepared for experiments.

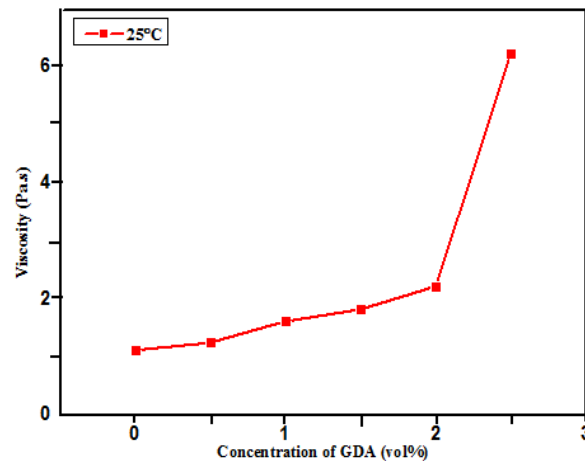


Figure.3. Effect of concentration of glyserol diacetate on the viscosity of 50 vol% silicon nitride suspensions at shear rate of 10 s^{-1}

Figure 4(A) shows green complex parts shaped by direct coagulation casting. The parts are fabricated smooth surface and defect-free such as bubble. Figure 4(B) shows the micrograph of green parts. Silicon nitride green bodies are observed in homogeneous microstructure due to the good stabilization of suspensions. Moreover, increasing solid concentration can lead to decrease in the gaps between particles in the suspension and the density increases. Figure 5(A) shows microstructures of polished surface, 5(B) fracture surface and 5(C) β - Si_3N_4 grains in a pore of sintered silicon nitride parts. When the microstructure of polished surfaces of sintered samples is examined, it is observed that β - Si_3N_4 elongated grains with a high ratio of length-diameter were formed. At the same time, the exist of pores are observed in samples. When the fracture surfaces of the samples are examined, it was observed that the intercrystalline and transcrystalline fracture mechanisms.

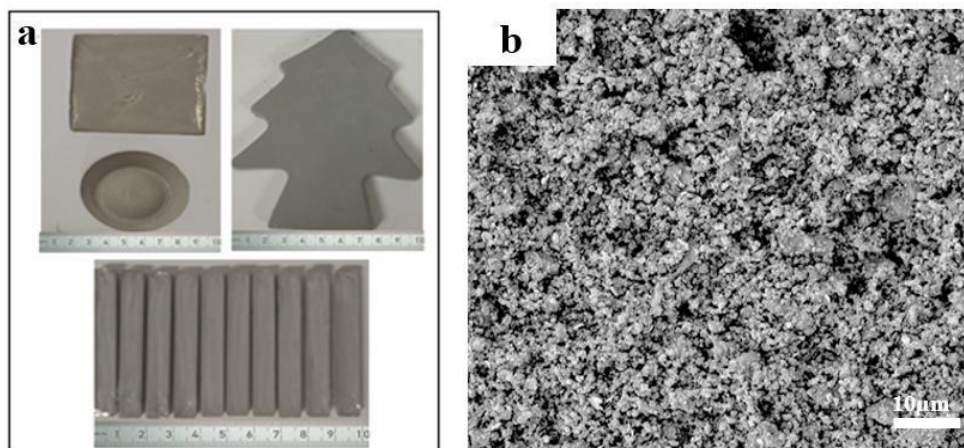


Figure 4. (A) green complex ceramic parts and (B) microstructure of green parts

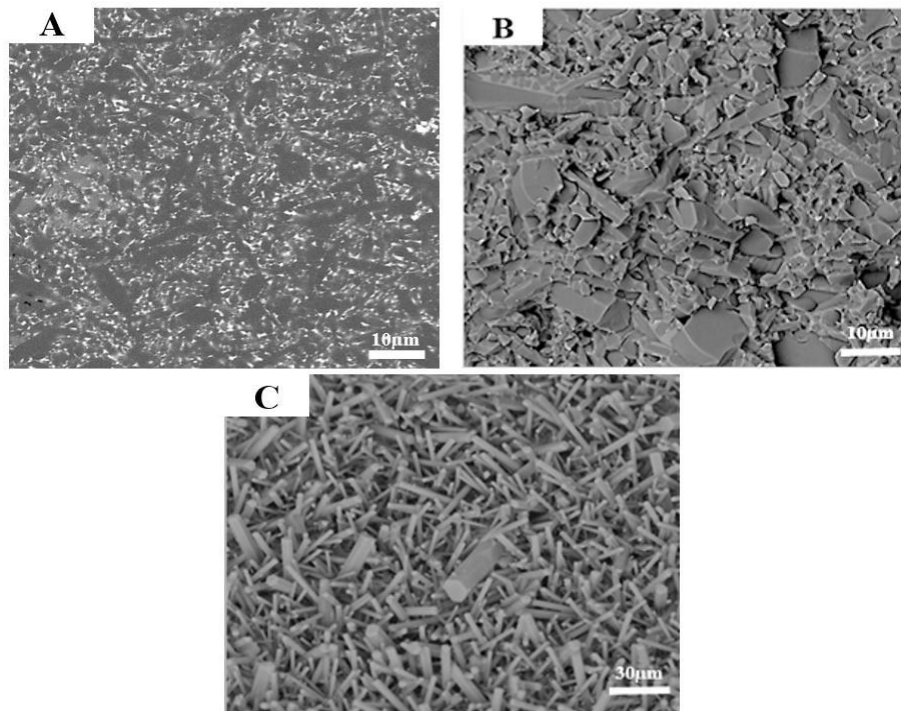


Figure 5. Microstructure of A) Polished surface, B) Fracture surface, C) β - Si_3N_4 grains in a pore

The complex shaped Si_3N_4 ceramic parts prepared by DCC method shows good mechanical properties. Besides, The average bulk density, flexural strength, fracture toughness and Vickers hardness of gas pressure sintered samples are determined as $3.22 \pm 0.01 \text{ gr/cm}^3$, $600 \pm 170 \text{ MPa}$, $6.75 \pm 0.05 \text{ MPa.m}^{1/2}$ and $13.5 \pm 0.2 \text{ GPa}$ respectively. The deviation were high because of defects in the microstructure such as bubbles. To decrease the deviation, the cold isostatic press was used.

4. CONCLUSION

Silicon nitride based ceramic parts were successfully shaped by direct coagulation casting method. Low viscosity suspensions were fabricated by solid concentration of 50 vol% and adding 0.4 wt% TMAH. The suspension was coagulated by Glycerol diacetate of 2 vol% at 60°C . Silicon nitride suspension was destabilized by reaction between TMAH and acetic acid which is occur after hydrolysis of GDA. Sintered bodies obtained bulk density $3.22 \pm 0.01 \text{ gr/cm}^3$, flexural strength $600 \pm 170 \text{ MPa}$, Vickers hardness $13.5 \pm 0.2 \text{ GPa}$, indenter fracture toughness $6.75 \pm 0.05 \text{ MPa.m}^{1/2}$. Complex shaped ceramic parts are fabricated by DCC method with no defect during demoulding. The new coagulation method is a recommended process for the production of near net shaped ceramics.

REFERENCES

- [1] Bernal, H.M. ve Matovic, B., Mechanical properties of silicon nitride-based ceramics and its use in structural applications at high temperatures. *Materials Science and Engineering*, 2010, 527, 1314-1339.
- [2] Trice, W.R. and Halloran, J. W. Mode I Fracture Toughness of a Small-Grained Silicon Nitride : Orientation, Temperature, and Crack Length Effects. *J. Am. Ceram. Soc.*, 1999, 82, 2633–40.
- [3] Rahaman, M. And Xiao, W., Silicon nitride bioceramics in healthcare. *International Journal of Applied Ceramic Technology*, 2018 15, 861-872.
- [4] He, G. ve Hirschfeld, A.D., "Processing of silicon nitride ceramics from concentrated aqueous suspensions by robocasting. 2000, 2000-2055.
- [5] Li, W., Zhang, H., Jin, Y., Gu, M., Rapid coagulation of silicon carbide slurry via direct coagulation casting. *Ceramics International*, 2004, 30, 411-416.
- [6] Sigmund, W.M., Bell, N.S., Bergström, L., Novel powder-processing methods for advanced ceramics. *J. Am. Ceram. Soc.*, 2000, 83 (7), 1557–1574.

- [7] Si, W., Graule, T.J., Baader, F. H. and Gauckler, L.J., Direct coagulation casting of silicon carbide components. *J. Am. Ceram. Soc.*, 1999, 82 (5), 1129–1136.
- [8] Gan, K., Xu, J., Zhang, X., Huo, W., Yang, M., Qu, Y. ve Yang, J., Direct coagulation casting of silicon nitride suspension via a dispersant reaction method. *Ceram. Int.*, 2016, 42, 4347-4353.

CERAMIC TILE

INVESTIGATION OF WEAR RESISTANCE OF THE PORCELAIN TILE BODIES BY SOLID PARTICLE IMPINGEMENT USING ALUMINA PARTICLES

Tuna Aydın¹, Osman Bican¹, Recep Gümrük²

¹Kirikkale University, Engineering Faculty, Metallurgy and Material Engineering Department, Kirikkale, Turkey

²Karadeniz Technical University, Mechanical Engineering Department, Trabzon, Turkey

Abstract

Wear resistance is of great importance for many industries in drilling processes and for minerals. The particles seen in these industries may cause erosion. These particles may have various sizes, shapes and hardness. These particles may also impact the surface at various angles and speeds. Wear resistance is also important for ceramic tile industry because these materials, which are also used in building facades, must withstand all kinds of weather conditions. In this study, the wear resistance of the porcelain tile bodies was investigated by solid particle impingement using alumina particles. The effects of technological, mechanical and microstructural properties on wear resistance were also investigated. It was determined that the technological, mechanical and microstructural properties were improved with the addition of spodumene. The improvement of technological, mechanical and microstructure properties also reduced wear rates.

Keywords: wear resistance, solid particle impingement, porcelain, abrasive wear

1. Introduction

Porcelain tiles contain quartz, feldspar and mullite which are crystalline phases. Porcelain tiles also contain vitreous phase. The amount of glassy phase is between 40-80 wt. %. Mullite crystals are between 8-10 wt.% depending on sintering processes [1-4]. Porcelain stoneware tiles are used as covering materials in floor, internal walls and exterior walls. Different properties are required for these applications, especially mechanical properties [1-4]. The mechanical properties of porcelain tiles are related to their microstructure [5]. Due to the close-to-zero open porosity, porcelain tiles show less than 0.5% water absorption; however, they show noticeable closed porosity [3, 5, 6]. Closed porosity may be higher than 10% [5, 7]. The firing temperature reaches up to 1230°C for 40-60 min. The sintering process results in a decrease in the total porosity [5]. The total porosity is the sum of the open porosity located at the surface and the closed porosity trapped in the bulk material. This shows a dependence of the mechanical characteristics and service behaviour on the closed porosity [5, 8]. As mentioned before, different properties are required depending on the type of the applications. For exterior wall applications, mechanical properties such as strength, hardness, wear resistant are essential. Environmental conditions will significantly affect porcelain tiles. Mostly, extreme weather conditions are observed in deserts. The most characteristic properties of desert climate are sand storms and hurricanes. Both of them are composed of high-speed sand particles. When sand particles hit the surface of exterior wall material, they result in surface erosion [9]. High-speed sand particles in a desert are an important factor, because they can cause a decrease in the reliability of the exterior wall materials. Porcelain tiles can be used in exterior sides of buildings due to their aesthetic appearance and many important features such as mechanical strength and wear resistance [10]. Although there are many studies on porcelain tiles in the literature, there is not enough study about extreme conditions such as high-speed sand particles.

In this study, the relationship among properties of technological, mechanical, microstructural and wear resistance of porcelain tiles with the addition of spodumene ($\text{Li}_2\text{O} \cdot \text{Al}_2\text{O}_3 \cdot 4\text{SiO}_2$) under solid particle impingement was investigated.

2. Experimental studies

Standard porcelain tile bodies are composed of clay, kaolin, quartz and feldspar. The granules were shaped using uniaxial press in a $50 \text{ mm} \times 100 \text{ mm}$ die at 450 kg/cm^2 . After shaping, samples were dried at 110°C . Sintering was carried out in a laboratory kiln (Carbolite CWF 12/13) at 1210°C for 60 min. The technological properties of samples, such as water absorption, porosity, firing shrinkage were determined at Ceramic process laboratory in Kirikkale University. Chemical analyses of raw materials, analyses of phase, microstructure, bending strength and elastic modulus were investigated at Ceramic Research Centre in Anadolu University. The chemical compositions of the raw materials were analysed using an XRF (Rigaku, ZSX Primus XRF). Phase analyses from fired samples were conducted using X-ray diffraction (XRD) (Rigaku Rint 2200) (with $\text{CuK}\alpha$ radiation) at 40 kV and 30 mA. Test was performed from $2\theta = 5^\circ$ to 55° , at a scanning speed of $2^\circ/\text{min}$. The scanning electron microscope was used to determine microstructural properties (SEM, Zeiss EVO 50EP). Archimedes method and Helium pycnometer (Quantachrome Model MVP-1 Multipycnometer) were used to determine the bulk density and the total porosity. The ultrasonic test method was used to determine the elastic module. The technique used in the ultrasonic test method is the time-delay of propagation between transmitted and received ultrasonic waves. The velocity of ultrasonic waves can be measured from the thickness of the samples and the time-delay. The longitudinal transmission time and the shear wave transmission time was measured from the fired porcelain tiles using Olympus Panametrics Model 5800 Computer Controlled Pulsar/Receiver. The longitudinal and shear wave's transmission time was measured with contact ultrasonic transducers operating on a pulse-echo mode. The transducer centre's frequencies were 5 MHz for longitudinal waves, and 2.25 MHz for shear waves. The digital oscilloscope was used to measure transmission time (Tektronix TDS 1012 Two Channel Digital Storage Oscilloscope). The wear resistance measurements of porcelain tiles were carried out by particle/sand erosion testing method using alumina sand (particle diameter: $50\mu\text{m}$, impact angle: 90° , velocity: 74 m.s^{-1} and flow rate: 2.5 gr. min^{-1}). The solid particle erosion test system is shown in Fig. 1. The system contains three main sections. An air compressor (with a pressure capacity of 40 bar) and a reservoir tank for pressurized air is the first section. A pressure conditioning tank and dust feeding system (alumina particles) is the second section. In this section, the air is adjusted to the predetermined pressure values to obtain the required speeds for the alumina particles. In the final section, there is a test cabinet that includes a linear moving platform operated by a motor. The test system can provide different impact angles and nozzle distances. The test system was used to determine the wear performance of porcelain tile bodies according to ASTM G76-13 standard.

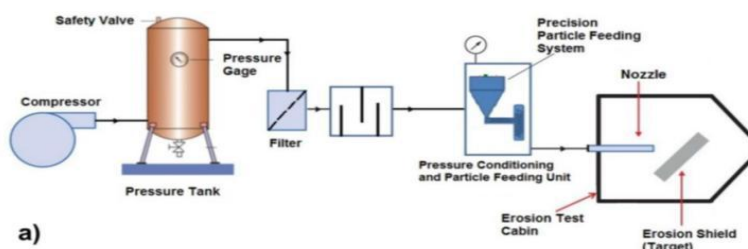


Fig. 1. Solid particle erosion test system [11]

3. Result and Discussion

3.1. Chemical composition and phase analyses

Chemical compositions of the raw materials are shown in Table 1. Std body is composed of kaolin 1, kaolin 2, Na feldspar, quartz, clay 1, clay 2 and clay 3. D1, D2 and D3 bodies contain kaolin 1, kaolin 2, Na feldspar, quartz, clay 1, clay 2, clay 3 and spodumene. In this study, spodumene was used instead of Na-feldspar at a rate of 1%, 2% and 4% in D1, D2 and D3 bodies. D4 body is composed of kaolin 1, clay2, sodium feldspar and spodumene. D4 body contains spodumene at a rate of 1% wt.

instead of sodium feldspar. D5 body contains kaolin 1, clay 1, clay2, sodium feldspar and spodumene. D5 body contains spodumene in ratio of 1% wt. instead of sodium feldspar. Quartz was not used in D4 and D5 bodies.

Table 1. Chemical compositions of raw materials

	Lol.	SiO ₂	Al ₂ O ₃	Fe ₂ O ₃	TiO ₂	CaO	MgO	Na ₂ O	K ₂ O	Li ₂ O
Kaolin 1	10.0	65.00	23.0	0.5	0.50	0.20	0.15	0.20	0.30	-
Na Feldspar	0.50	71.10	17.40	0.05	0.24	0.60	0.10	9.36	0.34	-
Quartz	0.43	97.64	0.73	0.18	0.03	0.10	0.01	0.01	0.47	-
Clay 1	10.0	59.00	26.0	1.20	1.50	0.60	0.10	0.10	2.00	-
Clay 2	8.5	59.00	25.0	1.00	1.50	0.60	0.70	0.60	2.70	-
Clay 3	7.5	65.00	21.5	2.50	1.30	-	-	0.10	2.00	-
Kaolin 2	0.51	78.78	13.34	0.02	0.16	4.78	0.01	2.1	0.04	-
Spodumene	0.36	65.2	25.12	0.15	0.05	0.21	0.1	0.34	0.57	7.5

Phase analyses of the samples are shown in Fig. 2. Quantitative Phase Analyses (QPA) of the samples are also given in Table 2. QPA was obtained using MAUD software programme. As can be seen in Fig. 1, Quartz and mullite crystals and glassy phase were determined for standard body. The mullite and quartz phases together with glassy phase were also observed in the investigated bodies. As can be seen in Table 3, the amount of mullite crystal increased with the addition of spodumene in D4 and D5 bodies. However, the amount of quartz crystal decreased with the addition of spodumene in D1, D2 and D3 bodies. Spodumene ($\text{Li}_2\text{O} \cdot \text{Al}_2\text{O}_3 \cdot 4\text{SiO}_2$) is highly effective fluxing agent and is a source of Li_2O . Alkali and alkaline earth oxides are defined as glass network modifiers. They cause the formation of non-bridging oxygen sites. All alkali and alkaline earth oxides is responsible for decrease in the viscosity approximately in the order $\text{MgO} < \text{CaO} < \text{SrO} < \text{BaO} < \text{K}_2\text{O} < \text{Na}_2\text{O} < \text{Li}_2\text{O}$ [12]. The addition of spodumene instead of Na feldspar results in a decrease in liquid phase viscosity and also causes further dissolution of quartz and albite. As seen in Table 2, the decrease in the viscosity of the liquid phase contributed to the growth and the increase in the amount of mullite crystals [8].

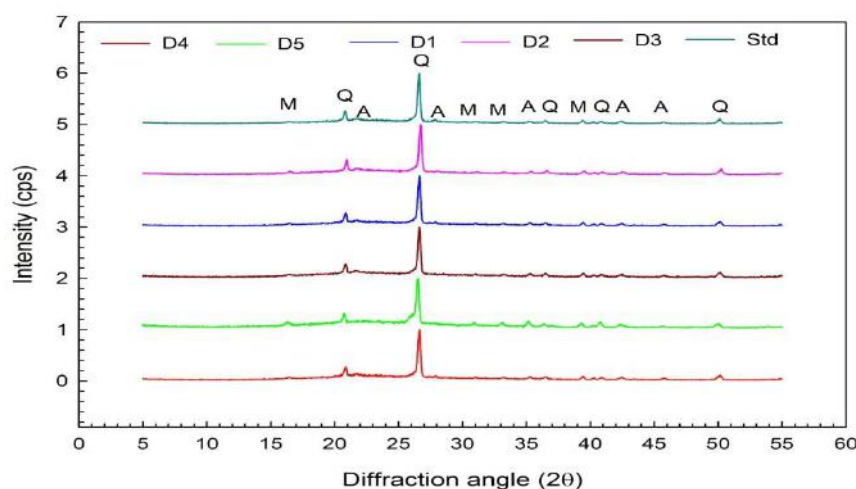


Fig. 2. XRD analyses of the samples, M: mullite, Q: Quartz and A: Albite

Table 2. Quantitative phase analyses of the samples

	Mullite	Albite	Quartz	Glassy
--	---------	--------	--------	--------

	(%)	(%)	(%)	Phase (%)
STD	5.40 ± 0.18	1.36 ± 0.17	17.23 ± 0.25	76.01 ± 0.93
D1	5.1 ± 0.22	0.82 ± 0.18	14.70 ± 0.29	79.38 ± 1.35
D2	4.01 ± 0.25	0.28 ± 0.19	14.72 ± 0.34	80.99 ± 1.67
D3	5.62 ± 0.22	0.021 ± 0.25	14.35 ± 0.25	79.98 ± 1.4
D4	8.39 ± 0.56	4.72 ± 0.52	14.25 ± 0.76	72.64 ± 1.3
D5	10.12 ± 0.19	0.018 ± 0.22	12.06 ± 0.13	77.80 ± 1.21

3.2. Technological properties

Technological properties of the samples are given in Table 3. Bulk density and bending strength increased with the addition of spodumene. As mentioned before, the addition of spodumene decreases viscosity. Most importantly, the decrease in the viscosity of liquid phase results in an increase in densification rate. The decrease in viscosity accelerates densification rate [8]. As seen in Table 3, the acceleration of the densification rate resulted in denser bodies than the STD body. Total porosity and water absorption decreased with the addition of spodumene. As can be seen in Table 3, as the amount of mullite increased, bending strength also increased. There are three main theories explaining the strength of porcelains. These are mullite hypothesis, the matrix reinforcement and the dispersion-strengthening hypothesis. According to mullite hypothesis, the strength of a porcelain body is directly related to the interlocking of fine mullite needles [8]. As seen in Fig. 4 and Fig. 5, these fine mullite needles contributed to obtain higher bending strength.

Table 3. Technological properties of the samples

	Water absorption (%)	Bulk Density (g/cm ³)	Porosity	Bending strength (N/mm ²)
			Total porosity (%) (P _T)	
STD	0.15	2.36	5.88	52
D1	0.03	2.38	3.59	55
D2	0.01	2.37	4.39	67
D3	0.01	2.37	4.16	67
D4	0,001	2.41	2.80	69
D5	0,002	2.40	3.01	69

3.3. Solid particle erosion test and mechanical properties

Solid particle erosion test method was performed according to ASTM G 76-04 [13]. The graph showing the wear loss and time relationship obtained from the solid particle erosion test is shown in Fig. 3. Hardness, wear rate and elastic modulus of the samples are also given in Table 4. When this graph is examined, it is seen that the highest loss of volume occurs at D3. Among the ceramic materials subjected to the test, the highest wear resistance was obtained from the D5 code sample. This can be explained based on the microstructure and mechanical properties of the materials [14]. In other words, it was determined that the samples were composed of crystalline phases such as mullite, albite, quartz and glassy phase. As seen in Table 2, the samples with the highest amount of mullite crystal phase were determined as D5 and D4, respectively. The elastic modulus of these samples is higher than the other samples. The increases in the amount of mullite and increases in elastic modulus along with the decrease in the number of the pores also increased the abrasion resistance of D4 and D5 samples [14]. Hardness is also a critical property in wear and abrasion applications. One of the characteristics of ceramic materials is that they have good hardness. Wear rate is very low in very hard material.

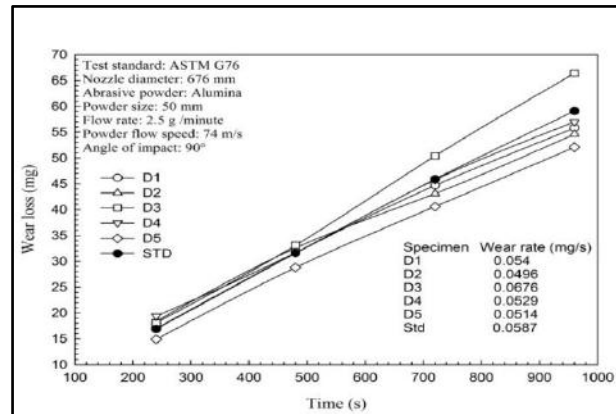


Fig. 3. The graph of the solid particle erosion test

Table 4. Hardness, wear rate and elastic modulus of the samples

	STD	D1	D2	D3	D4	D5
Hardness	534.41	783.56	653.26	738.48	524.15	637.11
Elastic modulus	57	55	67	71	78	75
Wear rate	0.0587	0.0540	0.0496	0.0676	0.0529	0.0514
Bending strength	52	55	67	67	69	69

3.4. Microstructural analysis

SEM micrographs of the samples are shown in Fig. 4, Fig. 5 and Fig. 6. SEM micrograph of Fig. 4 is given in Fig. 4. Microstructure includes mullite and quartz crystals embedded in the glassy phase. Pores are also seen in microstructure in intense amounts.

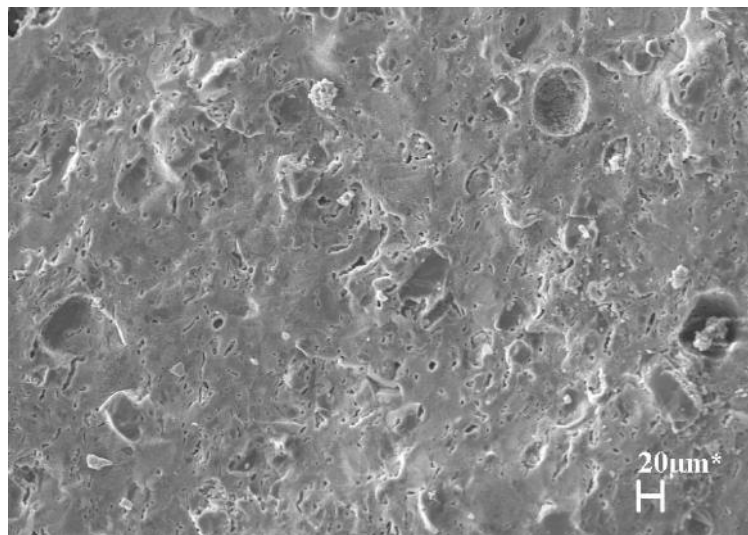


Fig. 4. SEM micrograph of STD body

Fig. 5 and Fig. 6 show the microstructure images of D4 and D5 bodies, respectively. As seen in Fig. 4 and Fig. 5, there are mullite and quartz crystals embedded in the glassy phase. The cuboidal crystals defined as Primary Mullite (PM) are developed from clay agglomerate relicts [8, 15, 16]. The elongated needle-shaped crystals defined as Secondary Mullite (SM) is the result of the growth of Primary Mullite crystals. Secondary Mullite crystals grow in feldspar, clay and kaolin-rich regions. Both cuboidal and needles mullite crystals are common in D4 and D5 bodies. As seen in Table 3 and Table 4, the bending strength in porcelain tile is directly related with Secondary Mullite crystals. The

mullite hypothesis clearly explains this relationship [8, 15, 17]. As mentioned before, the strength of a porcelain body is directly related to the interlocking of fine mullite needles. These interlocking of fine mullite needles also results in a decrease in the wear rate of D4 and D5 bodies because mullite have a low friction coefficient and good wear resistance under the common attack of wear and corrosion [18].

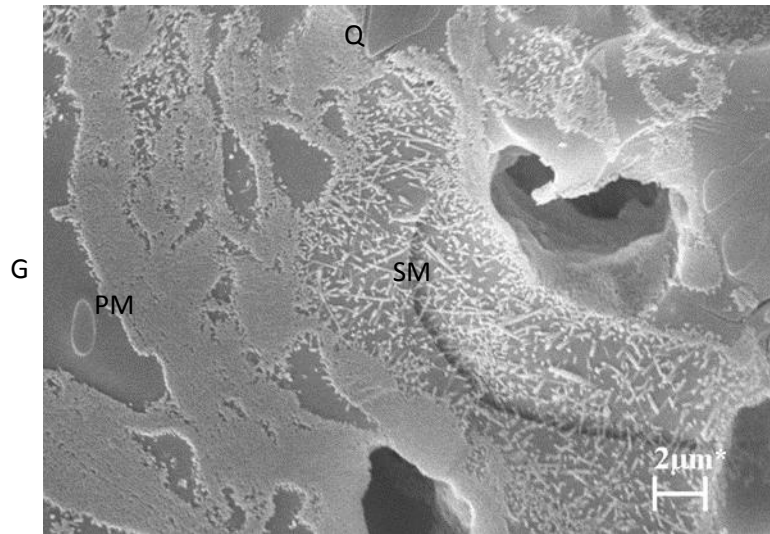


Fig. 5. SEM micrograph of D4 body; M: mullite, Q: quartz, PM: primary mullite, SM: secondary mullite, G: glassy phase.

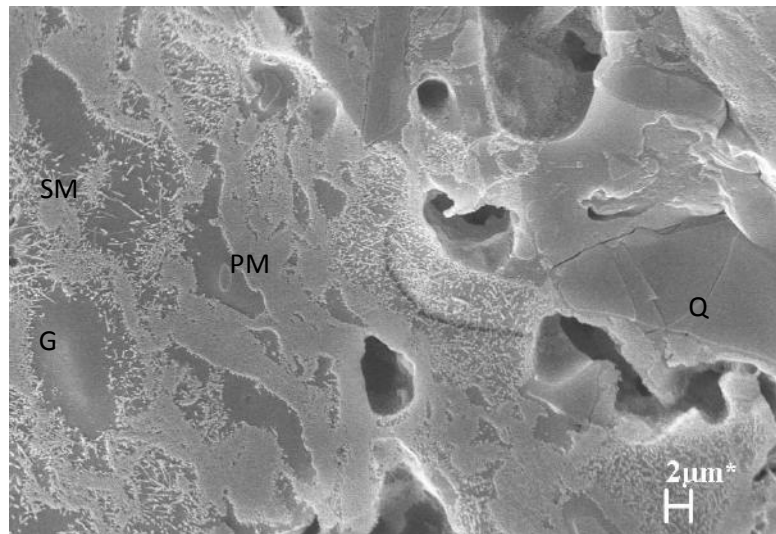


Fig. 6. SEM micrograph of D5 body; M: mullite, Q: quartz, PM: primary mullite, SM: secondary mullite, G: glassy phase.

4. Conclusion

In this study, it was determined that the technological, mechanical and microstructural properties were improved with the addition of spodumene. Densification rate increased with the addition of spodumene. The increase in densification rate resulted in a decrease in water absorption and total porosity. The increase in densification rate also provided denser bodies. In other words, the bulk density increased. The increase in the bulk density contributes to obtain higher elastic modulus. The elongated needle-shaped crystals defined as Secondary Mullite contributed to increase the bending strength. The higher elastic modulus and higher bending strength contributed to decrease in the wear rate of the samples.

References

- [1] Gültekin E. E., Topateş G., Kurama S.: The effects of sintering temperature on phase and pore evolution in porcelain tiles. *Ceramics International* 43, 11511–11515 (2017)
- [2] Bernasconi A., Diella V., Pagani A., Pavese A., Francescon F., Young K., Stuart J., Tunncliffe L.: The role of firing temperature, firing time and quartz grain size on phase-formation, thermal dilatation and water absorption in sanitary-ware vitreous bodies. *J. Eur. Ceram. Soc.* 31 (8), 1353–1360 (2011)
- [3] Sanchez E., Ibanez M.J., Garcia-Ten J., Quereda M.F., Hutchings I.M., Xu Y.M.: Porcelain tile microstructure: implications for polished tile properties. *J. Eur. Ceram. Soc.* 26, 2533–2540 (2006)
- [4] Leonelli C., Bondioli F., Veronesi P., Romagnoli M., Manfredini T., Pellacani G.C., Cannillo V.: Enhancing the mechanical properties of porcelain stoneware tiles: a microstructural approach. *J. Eur. Ceram. Soc.* 21, 785–793 (2001)
- [5] Rambaldi E., Pabst W., Gregorová E., Prete F., Bignozzi M. C.: Elastic properties of porous porcelain stoneware tiles. *Ceramics International* 43, 6919–6924 (2017)
- [6] Cavalcante P.M.T., Dondi M., Ercolani G., Guarini G., Melandri C., Raimondo M., Rocha e Almendra E.: The influence of microstructure on the performance of white porcelain stoneware. *Ceram. Int.* 30, 953–963 (2004)
- [7] Romero M., Pérez J. M.: Relation between the microstructure and technological properties of porcelain stoneware. A review, *Materiales de Construcción*. (2015). <http://dx.doi.org/10.3989/mc.2015.05915>
- [8] Aydın T.: Investigation of stain resistance of porcelain tiles doped by spodumene. (Ph.D. thesis), Anadolu University, Eskişehir, Turkey, 2012.
- [9] Hamza A.H.A., Abdelgawad N. M.K., Arafa B. A.: Effect of desert environmental conditions on the flashover voltage of insulators. *En. Conver. and Manag.* 43, 2437–2442 (2002)
- [10] Tucci A., Esposito L., Malmusi L., Rambaldi E.: New body mixes for porcelain stoneware tiles with improved mechanical characteristics. *J. Eur. Ceram. Soc.* 27, 1875–1881 (2007)
- [11] Acar D., Meriç D., Budur A. İ., Gümrük R., Sofuoğlu H., Gedikli H., Cora Ö. N.: Experimental investigations on particle erosion behavior of AA 6061 alloy. 9th Ankara International Aerospace Conference, AIAC-2017-147, 20-22 September 2017 - METU, Ankara TURKEY
- [12] Fluegel A.: Glass viscosity calculation based on a global statistical modelling approach. *Glass Technol.:Eur. J. Glass Sci. Technol. A*, 48 (1), 13–30 (2007)
- [13] ASTM G76-04, Standard Test Method for Conducting Erosion Tests by Solid Particle Impingement Using Gas Jets1
- [14] https://www.metalurji.org.tr/dergi/dergi127/der127_39.pdf
- [15] Pérez J.M., Romero M.: Microstructure and technological properties of porcelain stoneware tiles moulded at different pressures and thicknesses, d at different pressures and thicknesses. *Ceram. Int.* 40, 1365-1377 (2014)
- [16] Aydın T., Kara A.: Effects of Alumina on Porcelain Insulators. *Journal of The Australian Ceramic Society* Volume 52[1], 83 – 88 (2016)
- [17] Leonelli C., Bondioli F., Veronesi P., Romagnoli M., Manfredini T., Pellacani G. C., Cannillo V.: Enhancing the mechanical properties of porcelain stoneware tiles: a microstructural approach. *J. Eur. Ceram. Soc.* 21 785-793 (2001)

- [18] Lia S., Zhao X., An Y., Denga W., Hou G., Haoa E., Zhou H., Chen J.: Effect of deposition temperature on the mechanical, corrosive and tribological properties of mullite coatings. *Ceram. Int.* 44, 6719–6729 (2018)

CERAMIC TILE

BENEFITS AND EFFECTS OF THE SUITABLE GLAZE SELECTION FOR CERAMIC DIGITAL EFFECTS

Tufan Aşık^{1,2}, Bünyamin Öztürk¹, Alev Aşık¹, A. Hakan Aktaş²

¹ Gizemfrit A.Ş R&D Center Ceramic Division

² Süleyman Demirel University, Graduate School of Natural and Applied Science
Isparta

ABSTRACT

Ceramic Digital Effect inks provides us to apply traditional ceramic effects from the Ceramic Digital Printing Machines. Innovation of print heads on last years, we can apply many ceramic traditional effects from the inkjet machines. On digital ceramic- digital effect inks application, it is very important to use the correct printing technology for the suitable ink as well as to use the suitable glazes. This study showed us that using with correct glaze formulation with suitable frits. We can get the same effect using with lower amount of digital inks. In this study contains comparison of usual factory glaze on floor tile mat production and suitable effect glaze xrf analyses, color gamut and physical properties (gloss values, color coordinates L-a-b), and what will be the total benefits of the users of Digital Effects inks with suitable glazes

Key words: Ceramic, Digital Printing, inkjet, ceramic digital effects, reactive effect glazes

1.INTRODUCTION

Few years ago, the only way to decorate ceramic tile was screen printing. Many tile producers were looking for the tile production process which will give freedom of design ability, lower cost for decoration pigments and long production runs. [3]

After the digital printing machines have started to work, factories became able to work with more design options and lower production cost. In few years digital printing usage reached %98 of the entire ceramic production. Many digital machines and printheads brands started to produce digital machines to ceramic industry. Many pigment and glaze suppliers have started to produce ceramic inkjet inks which can perform according to machine and factory conditions. Ceramic digital production also reduced the wastes and gave a chance to factories to produce tiles according to customer's demands, elimination of printing media and shorter product development time. Ceramic inks got a huge importance for factories and OEMs day by day.

Ceramic inks usually have 3 components which are solids, vehicle, additives. Solids can be pigments, raw materials or frits. Inks solid content usually %40 by weight. Vehicles are liquids and these liquids used to apply the solids on the ceramic surface. Glycols, esters and oil have been used as vehicle. Additives usually determines the ink rheological behavior. The main ink parameters are chemical compatibility, density, viscosity, surface tension, particle size and stability. [4][1]

Usually factories are using CMYK sequence. On ceramic field on this CMYK sequences refers to Blue, Brown, Yellow, Black inks. According to factories customers demand's and production conditions, factories are adding extra pink, beige green, ochre and etc color bars to in order to satisfy the customers and getting more color gamut and color range.

On last decade after the factories saw that the digital products on the market started to repeat. Therefore, in order to make the difference on tile design, ink and glaze manufacturers developed different types of ceramic effects. Together with these ceramic digital effects, tiles gained the more spectacular views. There are many types of digital effects and day by day numbers of digital effects are increasing. Nowadays the most popular effect is Reactive effect. Reactive effect is also calling Sinking effect. After reactive effect the other effect inks also became popular. [3] These are mat effect, glossy effect, white effect, carving effect (it is also called deep ink) and metallic effects.

These effects inks are special inks therefore they need special applications. [3] Normally ceramic industry is working with printheads which can be apply 12pl to 26 pl drop size on the ceramic green tile surface. Some of digital effects can be apply with these printheads but some of them can not apply. Therefore, printhead OEM s developed new type of printheads which can be apply 40-120 pl. With these printheads the ceramic effects can appear much more better and factories have started to design spectacular tiles. [3]

Many times, in order to get good effect and good colors on the final tile, factories use a lot of ink quantity. It makes the tiles costlier and decreases the margin of company. Due to high cost of inks and special effects, the suitable printhead and the glaze is getting more importance. Specially on this study the focus point was getting with suitable glaze mat glazed porcelain glaze for reactive ceramic ink and increasing the color gamut of the glaze

2. MATERIALS AND METHODS

2.1 Preparation of Glazes/Tiles

For this study many ceramic glazes have been prepared. Using with ceramic glaze raw materials like clay, kaolin, Sodium feldspar, Potassium feldspar, quartz, barium carbonate, dolomite, wollastonite, alumina oxide, Zirconium silicate, Zinc oxide, nepheline syenite, calcite and frits.

The glazes have been prepared in Ceramic jars with 500 grs of Alumina balls and balanced 200 grs of each glaze. The glazes residue are 1-2% (45 micron or 325 mesh sieves residue over sieve) . After glazes have been applied to tiles using airless method using a spray gun according to 600 gr /sm² and 1,600 gr/lit density. The prepared tiles printed with same image in order to see difference on tonality. Firing conditions are 1200 °C and 60 mins on Sacmi Kilns. After seeing the tonality, the color profiles have been prepared with i1profiler profiling program. The colors drop volume 12pl and the reactive effect drop volume is also 12 pl.

2.1 Seger Analyse of Suitable Glaze Formulas

STANDARD				GR11				GR13				GR15			
Basic Oxide	Amfoter	Acid Oxide		Basic Oxide	Amfoter	Acid Oxide		Basic Oxide	Amfoter	Acid Oxide		Basic Oxide	Amfoter	Acid Oxide	
-	-	1,565	SiO ₂	-	-	2,220	SiO ₂	-	-	2,19	SiO ₂	-	-	1,734	SiO ₂
-	0,374	-	Al ₂ O ₃	-	0,484	-	Al ₂ O ₃	-	0,519	-	Al ₂ O ₃	-	0,274	-	Al ₂ O ₃
0,011	-	-	K ₂ O	0,079	-	-	K ₂ O	0,088	-	-	K ₂ O	0,041	-	-	K ₂ O
0,043	-	-	Na ₂ O	0,084	-	-	Na ₂ O	0,097	-	-	Na ₂ O	0,037	-	-	Na ₂ O
0,695	-	-	CaO	0,593	-	-	CaO	0,390	-	-	CaO	0,676	-	-	CaO
0,126	-	-	MgO	0,023	-	-	MgO	0,095	-	-	MgO	0,100	-	-	MgO
-	-	0,055	B ₂ O ₃	-	-	0,018	B ₂ O ₃	-	-	0,021	B ₂ O ₃	-	-	0,012	B ₂ O ₃
-	-	0,155	ZrO ₂	-	-	0,142	ZrO ₂	-	-	0,154	ZrO ₂	-	-	0,218	ZrO ₂
0,126	-	-	ZnO	0,175	-	-	ZnO	0,203	-	-	ZnO	0,116	-	-	ZnO
0	-	-	Li ₂ O	0,000	-	-	Li ₂ O	0,000	-	-	Li ₂ O	0,000	-	-	Li ₂ O
-	-	0,003	TiO ₂	-	-	0,009	TiO ₂	-	-	0,004	TiO ₂	-	-	0,007	TiO ₂
0	-	-	BaO	0,046	-	-	BaO	0,128	-	-	BaO	0,031	-	-	BaO

Table-1: Seger analyses of suitable glaze formulations

Amongst 15 different formulation and approaches 3 formulas were suitable and have better reactive ink development. On these formulation, the different types of frit also checked. The standart glaze is normal production glaze for glazed porcelain tiles. Fritt 1 is opaque mat frit for glazed porcelain technology and frit 2 is Ba-Zn Mat frit for glazed porcelain conditions.

3. RESULTS AND DISCUSSIONS

It is also very much important that to get similar glaze to standard glaze in terms of thermal coefficient values, heating behaviors. Therefore Xrf, Heat Microscope and dilatometric values, color values and color gamut have been checked for glazes.

The most suitable glaze for reactive effect was Glaze 15

3.1 Color Coordinates

	BLUE	BROWN	YELLOW	BLACK	BEIGE	PINK	BASE
	L-a-b						
GR-STD	46.26	46.98	89.44	29.63	82.89	73,04	91.97
	6.63	26.8	-5.52	2.73	2.7	22,47	-0.75
	-34.01	29.46	31.08	5.04	30.11	6.2	2.23
GR-15	45.94	42.65	87.77	23.96	81.6	69.62	92.76
	6.66	28.66	-3.65	2.14	5.16	26.43	-0.84
	-34.4	31.02	38.74	5.63	35.61	7.79	2.87

Table-2 : Color coordinates %100 batches printed on Digital printer , values after firing and measured with i1 Profiler

After the measurements on Glaze 15 color developments are better than standard glaze color development. Glaze 15 is more whiter glaze than standard glaze.

3.2 Heat Microscope

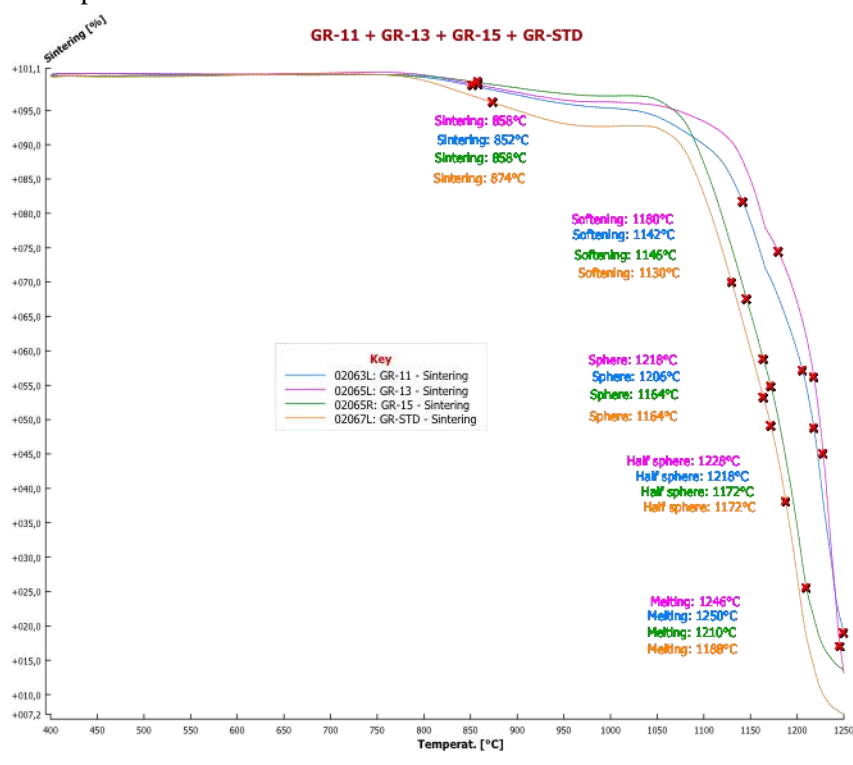


Fig-1: Heat Microscope results

Glaze 15 has very close heating microscope result to standard glaze. These values show us both glazes can perform on same factory conditions. Glaze11 and Glaze 13 have more harder glazes comparing with Glaze 15.

3.3 Dilatometric Analyses

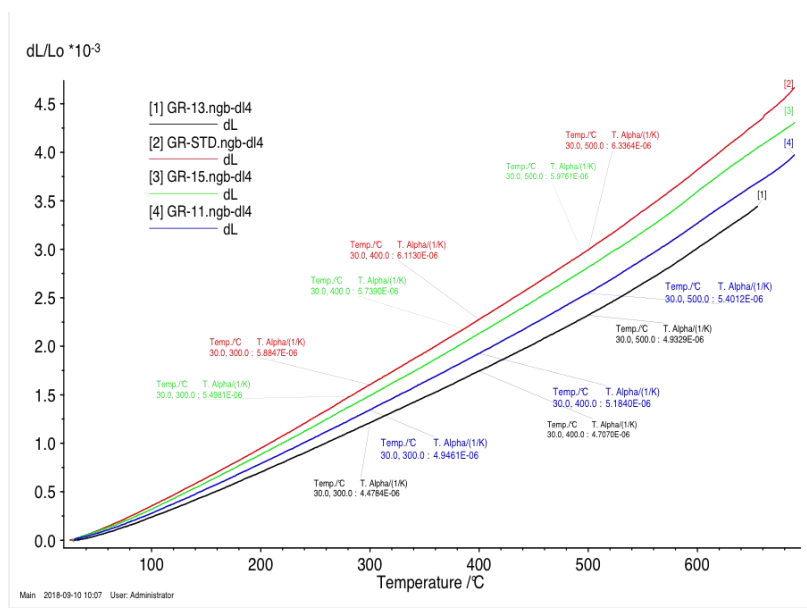


Fig-2 : Dilatometric result of Glazes

Glaze 15 has similar dilatometric results with standard glaze which means it can be use on similar conditions like standard glaze.

3.3 XRF Analyses

	STD	GR11	GR13	GR15
SiO ₂	43,79%	50,52%	47,44%	46,93%
CaO	18,82%	11,35%	7,37%	15,11%
Al ₂ O ₃	18,21%	17,80%	16,83%	12,41%
ZrO ₂	9,14%	6,66%	6,59%	11,91%
ZnO	4,79%	5,11%	5,12%	3,67%
MgO	2,14%	0,25%	2,48%	2,45%
Na ₂ O	1,07%	1,95%	2,05%	2,02%
B ₂ O ₃	0,89%	0,26%	1,13%	2,45%
K ₂ O	0,42%	2,58%	2,62%	1,66%
P ₂ O ₅	0,29%	0,29	0,29%	0,31%
Fe ₂ O ₃	0,21%	0,26	0,21%	0,20%
TiO	0,10%	0,079	0%	0,05%
BaO		2,77	7,72%	2,04%

Table-3 : Xrf Analyses of Glaze

As informed before the best reactive effect glaze was Glaze 15. This xrf analyses showed us that decreasing Al₂O₃ is increasing reactive effect, increasing ZrO₂ is increasing reactive effect, on similar level of ZrO₂ and Al₂O₃, CaO level is getting importance. On this situation CaO decreases reactive effect is increasing. This analyses is also showed that the good reactive effect can be obtain when the CaO, Al₂O and ZrO₂ on closer levels like Glaze 15.

3.3 Profile, Print and Gamut Comparison

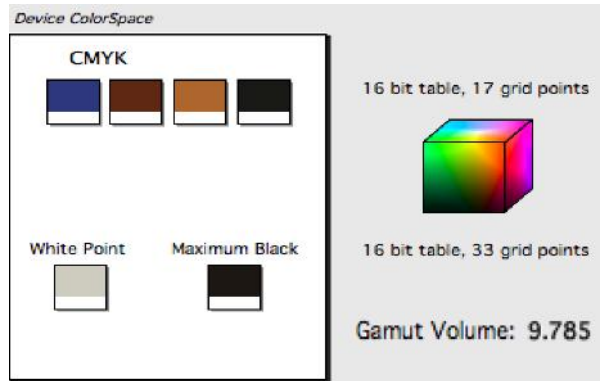


Fig-3 Gamut Volume of Standard Glaze

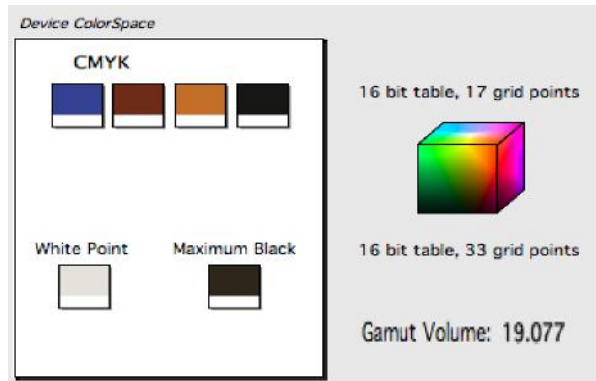


Fig-4 Gamut Volume of Glaze15

The CMYK profiles have been prepared with Blue-Brown-Beige-Black sequence with 150 ink limit (the color limited due to getting more color gamut) on i1 profile maker. After the creating icc profiles for both glaze, gamut volume calculated with ColorThink Pro 3.0.3 program and gamut volume doubled with glaze 15.

According to this result, ink consumption decreases significantly and the same reactive effect can be obtained half of reactive ink consumption.

3.4. Cost Calculation of Glazes

According to glaze cost calculation Glaze 11 has %20, glaze 13 has %15 and glaze 15 has %25 more cost than the standard glaze.

3.5. Ink Consumption

	STD (gr/sm ²)	GR15 (gr/sm ²)
BLUE	3.3	1.5
BROWN	2.8	1.5
BEIGE	3.9	2.5
BLACK	0.9	0.4
REACTIVE	7.5	2.5
TOTAL	18.4	8.4

Table-4 : Ink Consumption for same product made with Standard glaze and Glaze 15

Total ink consumption decreased %54.34 reactive ink consumption decreased %66.

3.5. Final Cost Calculation of product

The final product cost decreased %16 only in this product. When we analyze the all product of the companies it is clear that the benefit of companies will be increase significantly

4.CONCLUSSIONS

Using with suitable glazes, (even glaze cost is higher) the color gamut can increase %100, ink consumption can decrease %54, reactive effect ink consumption can decrease %66. The final product cost decrease. Using suitable glaze also help to avoid ceramic faults which can be appear on high ink consumption, it helps drying time of inks, due to lower consumption of ink the voltages on printhead decrease and it brings more life for printheads. The bigger gamut provides the designers to work with more colors and makes easy to be adjusting colors on designs. The decreasing ink consumption of effect inks gives more ability to designers to use this special effect more freely and to develop more spectacular tiles.

References

1. Hansen T, Ceramic ink , https://digitalfire.com/4sight/glossary/glossary_ceramic_ink.html
2. Montorsia M, Mugonia C, Passalacqua A, Annovic A, Maranic F, Fossac L, Capitanid R, Manfredinib T. Improvement of color quality and reduction of defects in the ink jet-printing technology for ceramic tiles production: A Design of Experiments study Ceramics International 42 (2016) 1459–1469
3. Xaar Ceramic Guide. <https://www.xaar.com/media/1310/xaar-ceramic-guide.pdf>
4. Solona V. Inkjet printing technology for ceramic tile decoration. Qualicer 14

CERAMIC TILE

RHEOLOGICAL BEHAVIOR OF BORON WASTE CONTAINING PORCELAIN TILE SLURRIES

Emirhan Karadağlı^{1,2*}, Buğra Çiçek^{1,2}, Fatma Duman³

¹Koç University Akkim Boron Based Materials and High Technology Chemicals Research and
Application Center, Rumelifeneri Yolu, 34450 Sarıyer/Istanbul/Turkey

²Department of Metallurgy and Materials Science Engineering, Yıldız Technical University,
Esenler/Istanbul/Turkey

³Eczacıbaşı Building Products Company, Bilecik/Turkey

Abstract

Utilization of process and mining wastes in the production of various traditional ceramic products such as tiles, bricks, frits and concrete has recently become contemporary based on the benefits on both industrial and environmental issues. Rheology of ceramic materials is mainly controlled by the amount metal oxides present in their composition. Considering the varying amounts and types of metal oxides existing in waste compositions, the addition of wastes accompanies modifications to be made on the initial composition. In this study, rheological properties of boron waste containing porcelain tile compositions were investigated, implementation of boron wastes into the compositions were formulated and rheological effects of oxides in the content of boron wastes and different types of deflocculants were explained. Used boron wastes mainly included B₂O₃ (14-31%), CaO (25-52%) and MgO (up to 9%), hence the effects of these particular oxides on the rheology were investigated in detail. Development of waste-containing porcelain compositions were carried out in respect with the Seger formulations of the initial standard composition. The study presented has cleared the problems may be faced with the rheology of a boron waste containing porcelain slurry and submitted a different look on the effects of waste utilization on rheology in ceramic production.

Keywords: Porcelain tile, boron waste, rheology, viscosity

1. Introduction

Porcelain is a hard, fine-grained, dense and usually translucent and white ceramic material that essentially contains kaolin, quartz, and a feldspathic rock and is fired at temperatures higher than 1180 °C [1]. Owing to its both physical and chemical properties, porcelain is considered suitable for several unrelated areas such as decoration, construction, biomedical, electronics. For the porcelain tiles, they are used for both constructional and architectural purposes where durability and visuality are of major significance.

In 2016, total of 13,056 million m² of ceramic tiles were manufactured globally and Turkey has a 2.5% share in this production[2]. This massive production is mainly consists of 3 groups of tiles which are floor, wall and porcelain. Sintering or firing is the most energy-intensive stage of ceramic tile production which takes place at elevated temperatures[3,4]. Different kinds of fluxes, glass-formers and additives are employed in the sintering stage in order to decrease sintering temperature to achieve cost-efficient firing systems.

B₂O₃ is an effective glass-former present in the structure of boron mining and enrichment wastes in high amounts (16-31%) together with CaO (25-52%) and MgO (up to 9%). Addition of boron wastes into the porcelain tile composition allows B₂O₃ to enter the system as a fluxing agent to decrease the sintering temperature of the tile. Although, it causes total amounts of alkali and

alkaline earth oxides to change in the porcelain composition. Rheology of a ceramic slurry is controlled by the total amounts and ratios of metal oxides present in the composition, so each addition into the composition should be done respecting the Seger formulations of the initial composition. Because rheological properties such as viscosity and thixotropy are of major importance in the production and in the quality of the final product.

In this paper, rheological behaviour of boron waste containing porcelain tile slurries were investigated, composition modifications to stabilize the rheology were explained.

2. Materials and Methods

In this study, six different boron wastes, coded as A1, A2, A3, A4, A5 and A6, were used. Four of these wastes (A1, A2, A3 and A4) were provided by the mine extracting facilities of Eti Mine and the remaining two (A5 and A6) were provided by borate enrichment facilities of Eti Mine. The chemical compositions of the wastes and the standard porcelain tile, coded as PT-STD, were obtained by X-ray fluorescence (XRF) spectroscopy, given in Table 1. and Table 2. respectively.

Table 1. Chemical compositions of the boron-rich mining and enrichment wastes

Oxides (wt%)	A1	A2	A3	A4	A5	A6
SiO ₂	10.25	19.81	16.98	17.13	0.39	1.28
Al ₂ O ₃	0.34	0.72	0.57	0.31	0.11	0.63
Fe ₂ O ₃	0.19	0.33	0.24	0.31	0.13	0.13
B ₂ O ₃	20.41	18.41	21.20	16.37	29.52	31.11
CaO	34.18	25.34	23.31	31.28	52.75	33.41
MgO	3.70	8.96	8.82	7.32	0.80	0.60
K ₂ O	0.04	0.13	0.12	0.17	0	0.03
Na ₂ O	0.17	0.57	1.34	0	0.81	0.90
P ₂ O ₅	0	0.04	0.01	0.03	0.01	0.01
SnO ₂	0	0	0	0	0	0.338
Cr ₂ O ₃	0	0	0	0	0	0.03
BaO	0	0.23	0	0	0	0
*L.O.I.	30.17	24.11	24.97	25.43	14.68	30.74

*Loss on Ignition

Table 2. Chemical composition of the standard porcelain tile

Oxides	(Wt%)
L.O.I.*	7,37
SiO ₂	67,11
Al ₂ O ₃	18,03
Fe ₂ O ₃	0,41
B ₂ O ₃	0,00
TiO ₂	0,41
CaO	2,48
MgO	0,88
Na ₂ O	2,36
K ₂ O	1,44
P ₂ O ₅	0,05
Total	% 100

*L.O.I. Loss on Ignition

Depending on the obtained chemical composition of PT-STD, it was seen that the structure included high amounts of SiO_2 and Al_2O_3 but lower amounts of CaO and MgO . Concerning the high CaO and MgO present in the boron waste structures, additions in big amounts may create obstacles in the means of rheology, so the additions were kept in small amounts (up to 10%).

Firstly, all the raw materials were dried in a drying oven (Nüve FN 400) for 24 h 100 °C, then dried solid mixtures of 500 g were poured into a milling cap along with water and deflocculant. Then, the slurry was ball milled (Ceramic Instruments Rapid Mills-Moduler System SD Series) using alumina balls to yield a particle size of 45 μm . The density of the slurry was obtained by a pycnometer (TQC VF2097) and was compared with the standard value for ceramic tiles (1648-1782 g/l). Then a rheological study was applied on the acquired slurry to obtain the amount of deflocculant needed to provide the optimum viscosity and thixotrophy characteristics. The optimum viscosity and thixotrophy of a slurry is the minimum reachable values for those properties. The amount of the added deflocculant varies due to different amounts of oxides in the composition but the optimum (minimum reachable) value is controlled by the ratios between the oxide groups, in other words “Segeer” formulations. Because the fluidity of a slurry is highly relevant with average specific gravity, so if the ratios can be kept constant as they kept in this study, rheology of the modified compositions will not differentiate from each other. Differences between the added deflocculant amount is only caused by the changing amounts of the raw materials, so the rheological study was carried out both to understand the effects of certain oxides on rheology and to find out the exact deflocculant amount needed to reach the desired viscosity and thixotrophy values for every composition

After each consecutive addition of deflocculants (0.1, 0.2 mg depending on the difference between the measured and desired viscosity values), added deflocculant was dispersed homogenously at 700 rpm for 3 min using a mixer (IKA RW 20 Digital).

After each mixing step, the viscosity was measured using a rotational viscometer (Brookfield Dial Reading). This process continued until a viscosity within the range of 4.5-6.0 Poise was achieved. The optimum amount of deflocculant for every composition was calculated according to Eq. 1. The flow chart of porcelain tile experimental procedures are given in Fig.2.

$$\frac{\text{Total Added Deflocculant Amount}}{\text{Total Solid Amount}} \times 100 = \text{Optimum Deflocculant Amount \%} \quad (\text{Eq. 1})$$

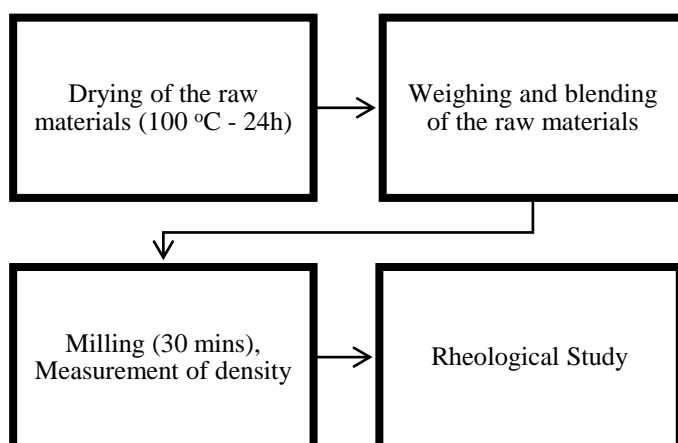


Fig. 2. Flow chart of the experimental procedure applied to the PT bodies.

3. Results and Discussion

3.1. Formation of new compositions

The “Seeger” tables are globally used as a composition standardisation method in ceramics industry. Forming of the Seger tables, or formulations, was accomplished by calculating the oxide ratios $\text{SiO}_2/\text{Al}_2\text{O}_3$, $\text{Na}_2\text{O}/\text{K}_2\text{O}$ and MgO/CaO as well as the total amount of alkiline earth metals and total amount of R_2O_3 .

Development of boron waste containing porcelain tile compositions were transferred into practise respecting the Seger formulations of the PT-STD[5]. Seger tables of the prepared compositions were given in Table 3. along with PT-STD's. As can be seen, both oxide ratios and total alkiline amount were achieved to be similar to same with those of PT-STD composition. In order to acquire that, all of the calcite (source of CaO) present in the PT-STD was removed from the compositions. As mentioned before, employed boron wastes are rich in CaO, so they became the only source of CaO instead of calcite.

Table 4. Seger formulations for the waste-containing PT compositions in comparison with that of PT-STD

	SiO₂/Al₂	Na₂O/K₂	MgO/Ca	B₂O	Total Alkaline	Total R₂O₃
PT STD	6,327	2,489	0,495	0,00	0,12	1,29
PT1-A6	6,326	2,497	0,547	0,03	0,11	1,29
PT2-A6	6,325	2,505	0,610	0,08	0,11	1,29
PT3-A6	6,322	2,446	1,252	0,12	0,11	1,29
PT4-A6	6,316	2,461	0,803	0,16	0,11	1,28
PT5-A6	6,320	2,369	0,682	0,19	0,11	1,27
PT1-A5	6,327	2,526	0,507	0,13	0,12	1,62
PT2-A5	6,311	2,511	0,283	0,21	0,15	1,33
PT3-A5	6,255	2,533	1,562	0,06	0,12	1,29
PT1-A1	6,377	2,496	0,620	0,14	0,12	1,57
PT1-A2	6,547	2,572	0,509	0,18	0,11	1,63
PT1-A3	6,500	2,600	0,540	0,21	0,11	1,67
PT1-A4	6,450	2,471	0,531	0,12	0,11	1,61

3.2. Effects of certain oxides on porcelain slurry rheology

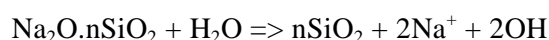
During the rheological study, it was determined that the increase in the amount of BW addition, increased both viscosity and thixotrophy of the compositions respectively. This change in viscosity and thixotrophy was the result of flocculation mechanism. Regarding the amount of BW used, CaO content of the compositions were also affected. Ca^{2+} is the most effective flocculating cation in all soil-based materials, meaning compositions including high amounts of Ca^{2+} cation are tend to flocculate. In this case, it can easily be said that, increasing amounts of BW addition caused an high Ca^{2+} concentration in the slurry, which resulted as flocculation and further, increase in viscosity[6].

Similar to Ca^{2+} , Mg^{2+} is also a strong flocculating cation. Likewise, addition of BW increased the Mg^{+2} concentration in the slurry and this resulted as an increase in viscosity and thixotrophy.

3.3. Effects of used deflocculant type and amount on porcelain slurry rheology

The term "deflocculant" stands for a compound which, when added to scattered particles in suspension, provides a reduction in apparent viscosity. Deflocculants avert flocculation by increasing zeta potential and therefore the opposite magnetic forces between particles. Different types of deflocculants act in various mechanisms such as shifting pH, substituting flocculant cations with alkilines, adding a protective colloid and increasing the negative electrical charges on agrillaceous particles. Deflocculants can be used as a mixture if more than one mechanism is needed to prevent flocculation[7].

Sodium silicate is the main deflocculant used for the preparation of porcelain slurries. The ratio of SiO_2 to Na_2O can vary from 3.75:1 to 1:1 and is available in liquid or solid form. Sodium silicate increases the pH of the suspension, owing to hydrolisis, whereas the silicon separates out in the form of colloidal silica which also performs a role as protective colloid, according to the following reaction.



Liquid sodium silicate including 24.7% SiO_2 was firstly used to fluidify the BW-containing slurries. But the deflocculation mechanism ensured by sodium silicate was not adequate to provide enough fluidity to the BW-containing slurries. Concentration of flocculating cations were too high for the sodium silicate to act as an effective fluidifier. Therefore, a more complete and effective deflocculant defined as polyacrylate sodium salt was introduced to achieve the desired rheological characteristics. Polyacrylates reduce interactive forces between particles, attaching themselves to those areas of the particles whose charge is responsible for the formation of three-dimensional structures, another mechanism of flocculation. Polyacrylates act more strongly than polyphosphates and polysilicates in reducing thixotrophy and yield point, and, like them, are strong absorber of of polyvalent ions. Main reason for the introduction of sodium polyacrylate salt is to replace strong flocculating cations (Ca^{2+} and Mg^{2+}) with poor flocculating cation Na^+ .

Viscosity-added deflocculant diagram of PT-STD composition is given in Fig. 3. As can be seen, approximately 1.4-1.7 ml sodium silicate is enough to deflocculate the standard porcelain slurry.

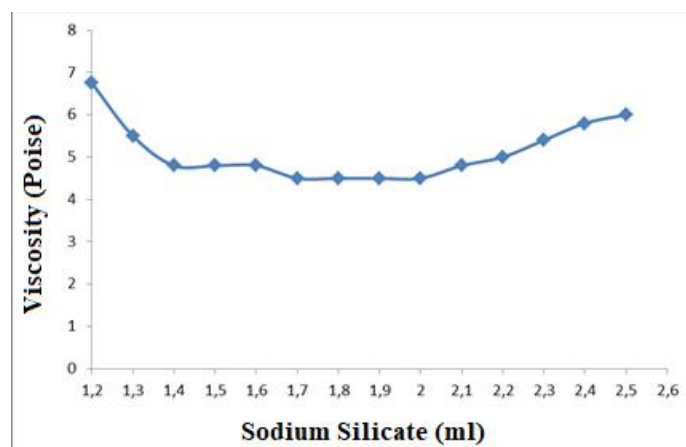


Fig. 3. Viscosity-added deflocculant diagrams of PT-STD composition

In Fig. 4 and Fig.5, viscosity-added deflocculant diagrams of the BW containing compositions were given. As can be seen, polyacrylate sodium salt and sodium silicate were used together in PT2-A6, PT3-A6, PT4-A6 and PT5-A6. The reason for the employment of two different deflocculants is to surpass the negative effects of excess Ca^{2+} cations joining into slurry by A6 waste (CaO content 52.75%). As mentioned, mix of two or more deflocculants can support each other by providing different mechanisms to prevent flocculation.

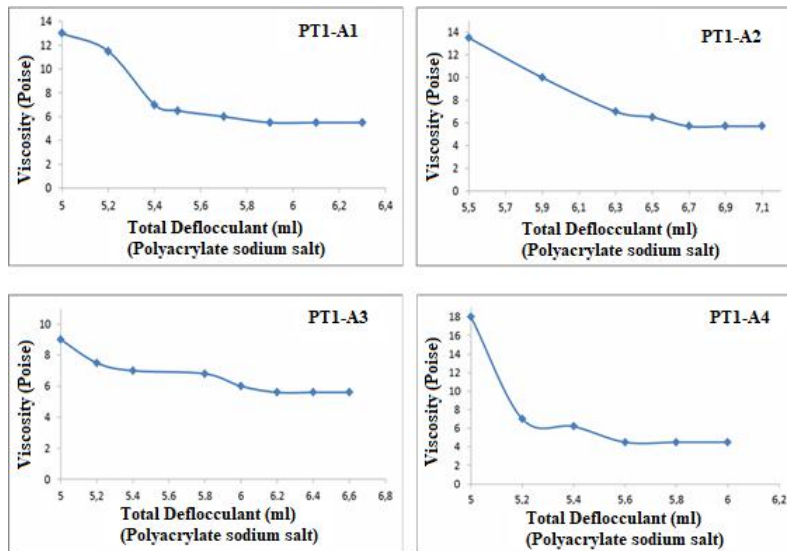


Fig. 4. Viscosity-added deflocculant diagrams of porcelain compositions including boron-mining wastes (A1-A2-A3-A4).

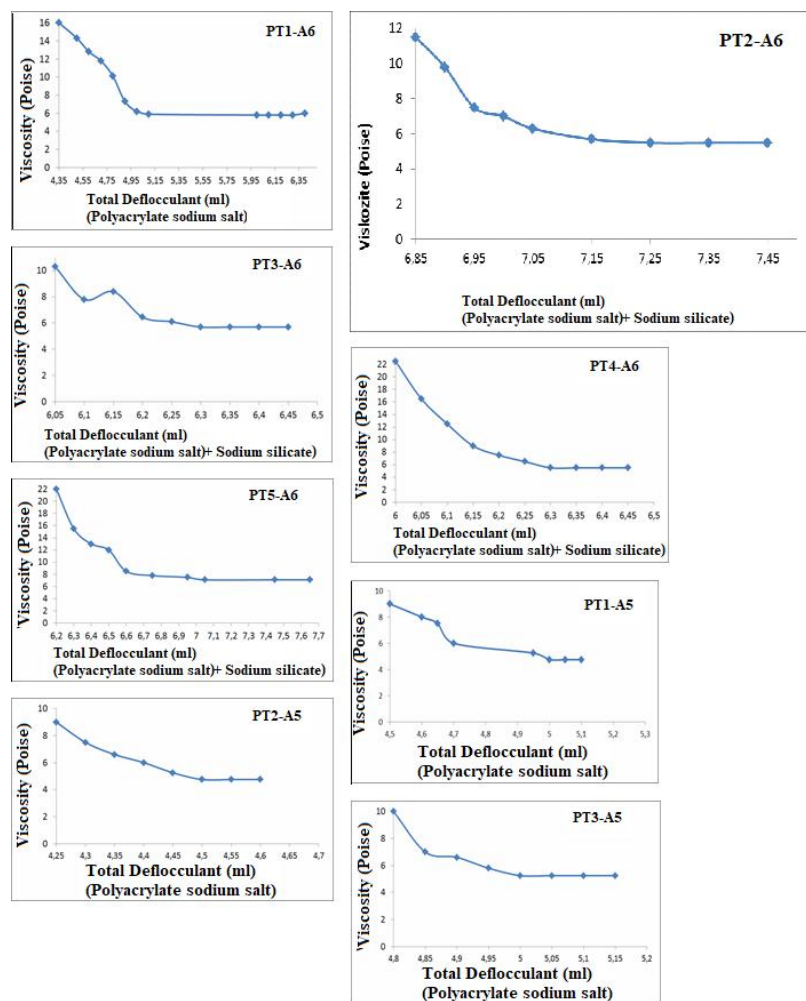


Fig. 5. Viscosity-added deflocculant diagrams of porcelain compositions including boron-enrichment wastes (A5-A6).

4. Conclusion

Rheological behaviour of BW-containing porcelain tile slurries were determined and main outcomes can be counted as; i) strong flocculating cations such as Ca^{2+} and Mg^{2+} are the main obstacles limiting the amount of BW addition into compositions, ii) typical deflocculants such as sodium silicate and other polyphosphate or polysilicates are not efficient enough to prevent flocculation in BW-containing porcelian slurries, iii) more complete and efficient deflocculants like polyacrylate sodium salt can be used as an active fluidifier and if it is still not effective, combination of different deflocculants can be used to set rheological properties.

It was also determined that, rheological properties of a porcelain slurry can be controlled via using both Seger tables and different deflocculant types.

References

1. T. Hansen, Porcelain. https://digitalfire.com/4sight/glossary/glossary_porcelain.html (accessed November 11, 2018).
2. World production and consumption of ceramic tiles, 2017, 5th Edition.
3. I. Allegretta, G. Eramo, D. Pinto, A. Hein, The effect of mineralogy, microstructure and firing temperature on the effective thermal conductivity of traditional hot processing ceramics. *Appl. Clay Sci.*, (2017), 135, 260–270.
4. H.W. Hennicke, A. Hesse, Traditional Ceramics, *Concise Encycl. Adv. Ceram. Mater.*, (1991), 488–494.
5. B. Cicek, E. Karadagli, F. Duman, Valorisation of boron mining wastes in the production of wall and floor tiles. *Constr. Build. Mater.*, (2018), 179.
6. T. Hansen, Viscosity. https://digitalfire.com/4sight/glossary/glossary_viscosity.html (accessed November 11, 2018).
7. T. Hansen, Deflocculants: A Detailed Overview. https://digitalfire.com/4sight/education/deflocculants_a_detailed_overview_324.html (accessed November 11, 2018).

CERAMIC TILE

EFFECT OF LEATHER WASTE ADDITION ON THE PROPERTIES OF CERAMIC WALL TILES

Sena Teber¹, Eylem Kılıç¹, Müge Tarhan², Baran Tarhan²

¹ Uşak University, Faculty of Engineering, Material Science and Nanotechnology Engineering

Department, 64100 Usak/Turkey

² Uşak University, Faculty of Arts, Ceramic Department, 64100 Usak/Turkey

ABSTRACT

In this study, some preliminary laboratory investigations were performed in order to investigate possible utilization of leather industry waste to increase porosity and provide lower thermal conductivity values without significant decrease of mechanical properties in ceramic wall tiles. For this aim leather industry waste derived from buffing process of chromium tanned leather was incorporated into ceramic tablets in various concentrations such as 1%, 3%, 5%, 7%, and 10%. The effect of addition of leather waste on the properties of the resultant ceramic tablets were presented in comparison to the leather waste-free ceramic tablets. All tests specimens prepared under industrial conditions and fired at industrial roller kiln. Porosity, water absorption properties were examined according to 10545-3 standard, and breaking strength was examined according to 10545-4 standard. Incorporation of tanning wastes into ceramic matrices resulted in increase in porosity and decrease in thermal conductivity and mechanical properties as expected. Results obtained from this study revealed that homogeneous dispersion of leather waste in ceramic matrix should be improved to provide good thermal conductivity values without significant decrease of mechanical properties.

Key words: leather waste, ceramic tile, porosity, heat transfer property

1. INTRODUCTION

The leather production industry generates large amount of solid tanned waste throughout tanning process, which converts raw skins and hides into leather. Among the tanned solid wastes, shavings and buffing dust from chromium-tanned leather, constitute an important part and pose environmental problems throughout their disposal. Although the characteristic of this waste depends on the process and the employed techniques, it is basically composed of protein, chrome oxide, ash, traces of chemical substances and water [1].

Management of leather solid wastes is difficult, and actual practice of its disposal includes its incineration and land codisposal. In the literature attempts have been made by researchers for finding alternative uses of these wastes, and numerous studies reported alternative processes to recycle and utilize them in different matrices [2]. Use of leather waste in production of building materials, to provide porosity and lower thermal conductivity was also reported [3].

Ceramic technology can be considered as another option for rendering tannery wastes, as it enables destruction of organic matter and immobilize heavy metals in a stable matrix [4]. However, literature survey reveals that studies are limited and there are several researches reporting use of tannery sludge for clay products [5] and use of chromium rich ash obtained by incineration of leather waste, in ceramic pigment [6, 7]. Therefore, in this study an attempt has been made to investigate possible

utilization of leather industry waste, to increase porosity and provide lower thermal conductivity values without significant decrease of mechanical properties in ceramic tiles. For this aim leather industry waste was incorporated into ceramic tablets in various concentrations and the impact was investigated in terms of thermal conductivity, mechanical properties and water absorption properties of ceramic tiles.

2. EXPERIMENTAL STUDIES

Leather waste derived from buffing process of chromium tanned leather was collected from a leather factory. Wall tile granule and other materials used in composition of ceramic tile were provided from Usak Seramik Usak/Turkey.

2.1. Preparation of ceramic tiles

All tests specimens prepared under industrial conditions and fired at industrial roller kiln. For the experimental studies leather waste was incorporated into ceramic tablets in various ratios such as, 1%, 3%, 5%, 7%, and 10%, and the tile masses were pressed using a uniaxial press in a 55 mm×110 mm die at 300 kg/cm² pressure and then dried at 110 °C. Finally fired at industrial roller kiln at 1125°C for 37 minutes (Fig. 1).

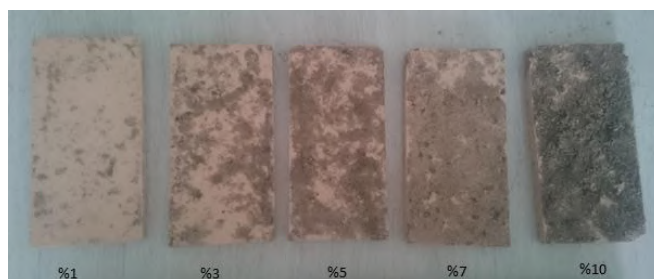


Fig. 1. Fired ceramic tiles with different concentrations of leather waste

The effect of addition of leather waste on the properties of the resultant ceramic tablets were presented in comparison to the leather waste-free ceramic tablets. Porosity, water absorption properties were examined according to 10545-3 standard, and breaking strength was examined according to 10545-4 standard. Heat transfer coefficient was measured with QTM (Quick Thermal Conductivity Meter)-500.

3. RESULTS AND DISCUSSION

The effect of leather waste incorporation into ceramic tile composition, on dry strength and fired strength test results were given in Fig. 2 and Fig. 3 respectively. Mechanical properties of standard ceramic tiles without any waste addition were also presented.

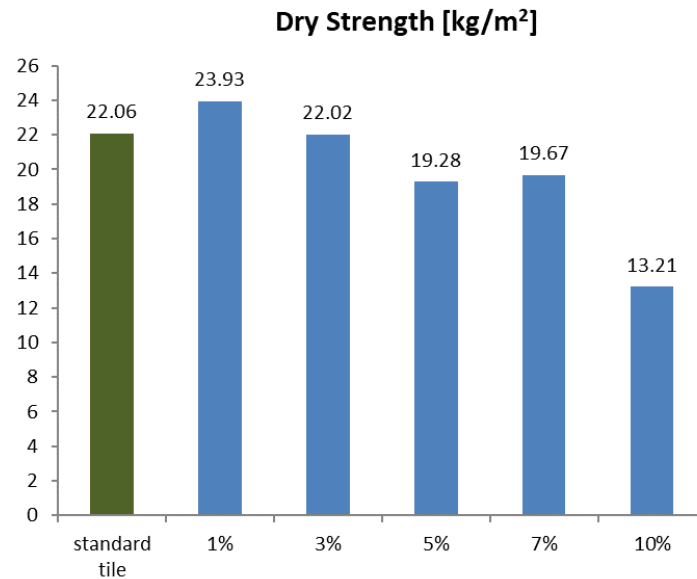


Fig. 2. Effect of leather waste addition concentration on dry strength of samples

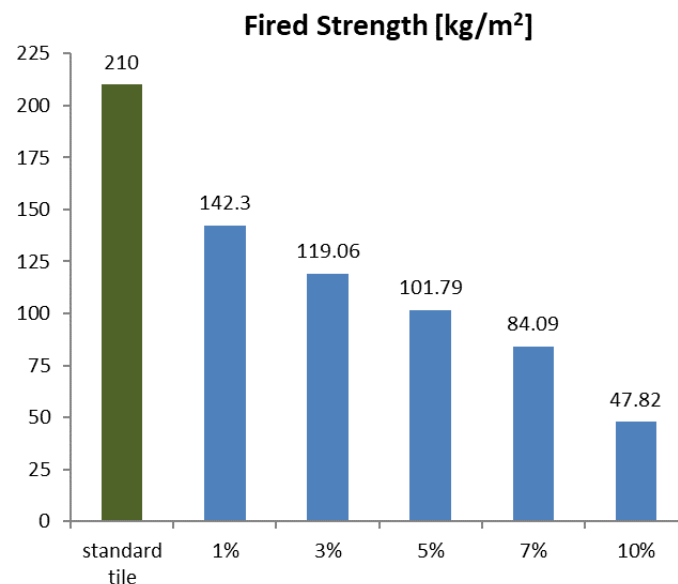


Fig. 3. Effect of leather waste addition on fired strength of samples

The results showed that introduction of buffing dust waste from chrome tanned leather into ceramic tiles decreased mechanical performance of final material with increasing waste addition ratios. Even with a 1% addition ratio fired strength value was reduced by nearly 30%, and reached maximum reduction at 10% addition ratio by 78%.

The effect of leather waste incorporation on water absorption properties of ceramic tiles were given in Fig. 4. As expected and in line with previously published papers, increasing concentrations of leather waste addition enhanced water absorption of ceramic tile samples, and provided the highest value with a 60% increase at 10% of leather waste addition in comparison to ceramic tile without any waste addition.

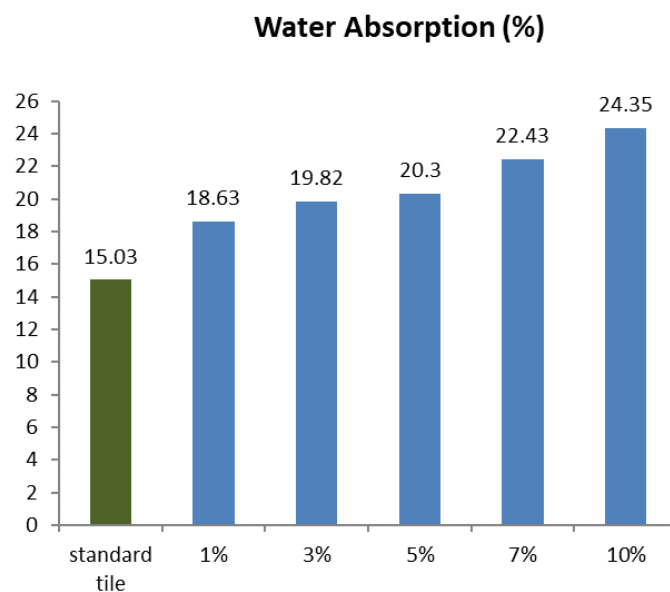


Fig. 4. Water absorption values of samples versus leather waste concentration

Figures 5 and 6 show the mean values of the physical testing of apparent porosity and bulk density of the ceramic tile compositions.

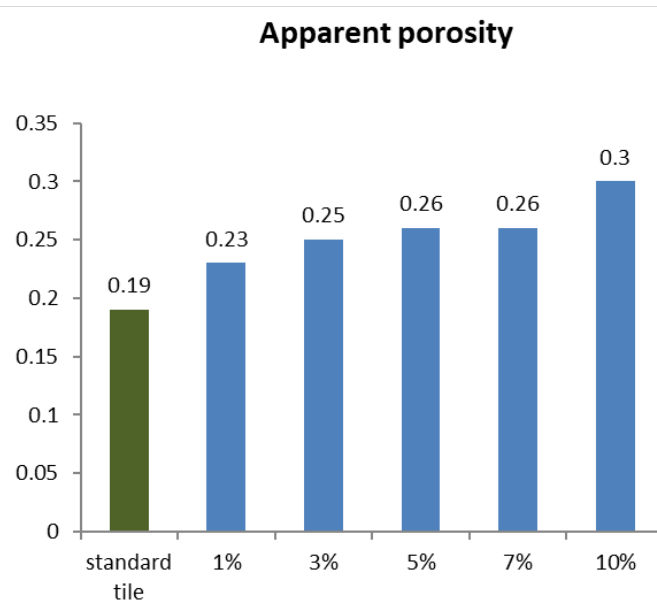


Fig. 5. Mean values of apparent porosity

Apparent porosity was increased with increasing leather addition concentrations and reached highest with a nearly 60% increase at ceramic samples with 10% leather waste. Analyses of bulk density showed that values are decreased with increasing percentage of leather waste.

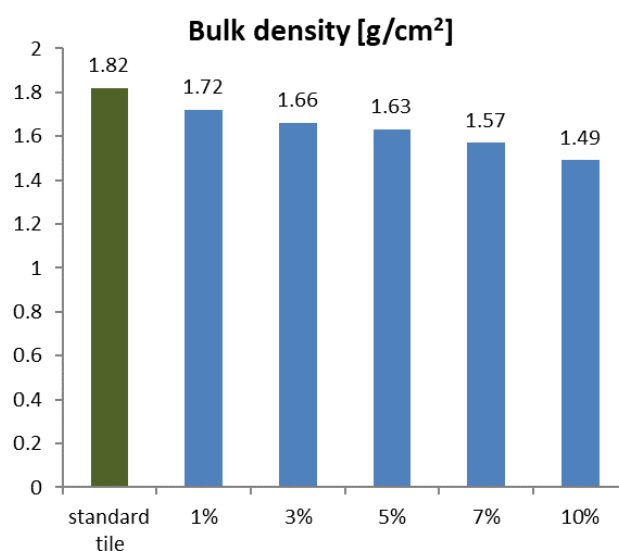


Fig. 6. Mean values of bulk density

Results obtained from heat transfer coefficient measurement tests were presented in Fig. 7. Heat transfer coefficient values of ceramic samples were decreased by increasing leather addition concentration, especially significant decrease was observed at samples with 7% and higher leather waste content.

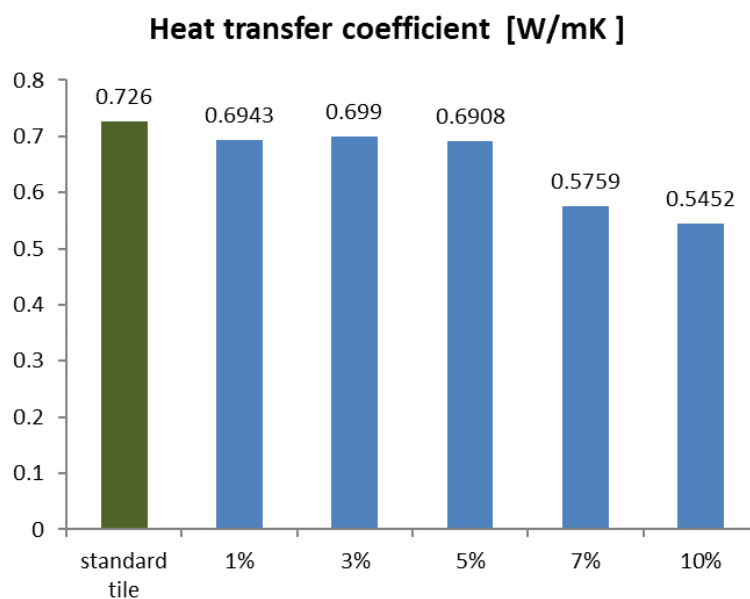


Fig. 7. Effect of leather waste addition on heat transfer coefficient of samples

4. CONCLUSION

In this study preliminary experiments were carried out to investigate the possibility of incorporating leather waste in ceramic tiles and to evaluate its effect on properties of final material. Addition of leather waste into ceramic wall tiles improved porosity, heat insulation performance of ceramic tiles.

Considering the results obtained from this study incorporation of leather waste at 1% ratio in the production of ceramic tiles can be a potential use for this types of waste, as it provides comparable results to standard values in terms of fired strength and water absorption values. However, increasing concentrations of waste resulted in significant decrease of mechanical properties especially at fired strength of tiles.

5. ACKNOWLEDGEMENTS

Financial support provided by The Scientific and Technological Research Council of Turkey (TUBITAK) under the Research Projects Fellowship Programme for Undergraduate Students, 2209-A, is acknowledged.

6. REFERENCES

1. Ozgunay, H., Colak, S., Mutlu, M.M., Akyuz, F., Characterization of leather industry wastes. Polish Journal of Environmental Studies, 2007, 16 (6), 867-873.
2. Senthil, R., Hemalatha, T., Manikandan, R., Das, B.N., Sastry, T.P., Leather boards from buffing dust: A novel perspective. Clean technologies and environmental policy, 2015, 17, 571–576.
3. Karaçakı, E., Deri sanayi katı atıklarının tuğla üretiminde kullanılabilirliği üzerinde araştırmalar, Ege Üniversitesi Fen Bilimleri Enstitüsü, 2004, İzmir.
4. Pelino, M., Recycling of zinc-hydrometallurgy wastes in glass and glass ceramic materials, waste manage, 2000, 20, 561–568.
5. Basegio, T., Berutti, F., Bernardes, A., Bergmann, C.P., Environmental and technical aspects of the utilisation of tannery sludge as a raw material for clay products, Journal of the European Ceramic Society, 2002, 5. 22, 2251–2259.
6. Lazau, R.I., Pacurariu, C., Becherescu, D., Ianos, R., Ceramic pigments with chromium content from leather wastes, Journal of the European Ceramic Society, 2007, 27, 1899–1903.
7. Ömür Ş., Tokatlıgil D., Karacasu Deri Fabrikalarında Ortaya Çıkan Kromlu Atıksuların Seramik Çözelti Boyası Olarak Kullanılması, Uluslararası Deri Mühendisleri Sempozyumu, 29 Nisan-01 Mayıs 2009, İzmir, Türkiye.

TEXTURED & EPITAXIAL PIEZOELECTRICS / FERROELECTRICS

PHASE AND ORIENTATION MAPPING OF CERAMIC COMPOSITES BY APPLICATION OF PRECESSION ELECTRON DIFFRACTION IN TEM

Umut SAVACI¹, Servet TURAN¹

¹. Eskişehir Technical University, Department of Materials Science and Engineering, Eskişehir, Turkey.

Keywords: Precession electron diffraction, Transmission electron microscope, Ceramic composites, Orientation mapping

Abstract

Structure-property relationship has great importance in materials science. The microstructural features e.g. present phases and their distributions and crystal orientations have an impact on the material properties. For characterization of structural features stated above, electron backscatter technique (EBSD) is widely used by scanning electron microscopes (SEM); however, due to the resolution limits of this method, transmission electron microscope (TEM) based advanced methods like precession electron diffraction (PED) method had been developed for phase and orientation mapping at high resolution. In this study, phase and orientation mapping were carried out for the characterization of orientation relationships between in-situ formed and matrix phases as well as phase identifications of various ceramic composites such as β SiAlON-cBN, SiC-hBN, and B_4C -TiB₂ were characterized. Samples were prepared by various pressure assisted sintering methods like spark plasma sintering and hot pressing. In order to reveal answer of the question of “Is there any orientation relation present in the ceramic composites?” PED method was utilized and obtained results will be given and discussed. Phase and orientation maps were obtained by scanning a nano sized probe over an area with a certain precession angle.

1. Introduction

Structure and property relationship is an important constituent of the materials tetrahedron since it directly affects the performance of material. Therefore, microstructural characterization become a very important step to understand link between structure and property. Properties of the materials can be modified with different production methods. For example, pressure assisted sintering methods and pressureless sintering methods resulted with different microstructures that can affect the material properties. Pressure assisted methods resulted with texturing of the grains with preferred orientation that might change material properties such as toughness, electrical and thermal conductivity. Because of the significant effects of microstructural features on the bulk properties as stated above, characterization of these features has become very important. In the literature, there are several different methods for the characterization of orientation relations within microstructure. For example, x-ray diffraction can be used; however, this method only provides information about the average of the sample and cannot be used for the local orientation characterizations. For the characterization of local orientation information of a specific area within the microstructure, SEM-EBSD technique can be used. SEM-EBSD method can provide orientation information up to a certain resolution limit that is 50-100 nm, depending on the material and accelerating voltage [1]. But it is a well-known fact that, microstructural features below 100 nm has also great influence on the material properties. For the characterization of these features TEM based methods should be used and the only method allows users to scan a custom region of interest over TEM sample is the precession electron diffraction method with very high resolution (down to 1 nm). Here TEM-PED method was used for the characterization of orientation relations between present phases in SiC-hBN,

β SiAlON-cBN and B_4C -TiB₂ ceramic composites as well as phase identification in B_4C -TiB₂ via automated orientation mapping.

2. Materials and Methods

In this study, β SiAlON-cBN ceramic composite sample was produced by the mixing of starting powders (Si_3N_4 , Al_2O_3 , AlN, Y_2O_3 and cBN) by using planetary ball mill within alcohol media. The dried and sieved powder mixture was sintered with SPS at 1650°C for 3 minutes under 50 MPa pressure.

Characterizations of the microstructures were conducted by using scanning electron microscope (SEM) and transmission electron microscope (TEM). SEM studies were conducted by using Zeiss Supra 50VP field emission SEM attached equipped with energy dispersive X-ray (EDX) at 15keV accelerating voltage. SEM samples were prepared by using conventional mechanical polishing method with diamond solutions and polishing discs. Imaging of the samples were done by using either backscattered electron (BSD) or in-lens detectors. TEM samples were prepared by conventional TEM sample preparation as well as focused ion beam (FIB) methods and prepared samples were characterized by using JEOL™ JEM 2100F field emission transmission electron microscope (TEM) was used. The TEM was operated at 200 keV accelerating voltage and it is equipped with Fischione 3000 STEM high angle annular dark field (HAADF) detector and Gatan™ bright field (BF) detector, as well as JEOL™ JED2300T energy dispersive X-ray spectrometer (EDX) and Gatan™ GIF Tridiem electron energy loss spectrometer (EELS). Precession electron diffraction unit from NanoMEGAS™ with Digistar P1000 scan generator and ASTAR V2 software package was retrofitted to this microscope

3. Results and discussion

3.1. β SiAlON-cBN Ceramic Composites

The SiAlON ceramics, which are formed by the substitution of Si and N with Al and O within Si_3N_4 crystal structure, is an important engineering ceramic thanks to its great mechanical properties and they used in numerous applications such as ball bearings and cutting tools. In order to improve the wear performance of the SiAlON ceramics, incorporation of various secondary phases such as cBN, SiC and TiC were tried in the literature [2-4]. cBN is one of the promising additive for SiAlON because it was reported that it improves both hardness and fracture toughness of the SiAlON matrix. In the literature there are several different studies about sintering and mechanical properties of β SiAlON/cBN composites and according to these studies cBN phase transformation into hBN phase occurs during sintering. Even though there are several studies about this composite system none of these studies [3, 5, 6] were focused on the characterization of possible orientation relations between cBN and hBN phases that might occur during SPS. In the literature, it is reported that hBN particles can be textured during pressure assisted sintering methods like SPS or HP [7, 8]. In this part of this work, orientation characterization between cBN and hBN phases to search for the question of “*Is there any orientation relation between cBN and hBN?*” were conducted for the first time by using TEM methods.

SEM-BSE images given in Figure 1 showed that there is a ~200-500 nm thick transformation layer around cBN particles. For the detailed analyses of the transformation layer FIB prepared sample was characterized with TEM methods. TEM images given in Figure 1 showed that morphology of the grains within transformation layer have both conventional plate-like and irregular/random morphology depending on the position within transformation layer. This morphology change can be explained by the volume expansion occur during cBN to hBN transformation [5]. At the beginning of the transformation, hBN particles can grow freely due to lack of any constrain; however, as transformation continues with the volume expansion within a limited space particles grow with an irregular morphology. STEM-HAADF image also showed that sintering additive phase is present around the particles in transformation layer. In order to investigate the possible orientation relations between cBN and hBN particles, orientation maps were obtained by using TEM-PED method. According to orientation maps, it was found that there was no specific orientation relation between phases. One reason for this behavior is the overlapping of both phases at the intersection and these particles were indexed as cBN, even though both phases were present. Other reason could be the transformation

mechanism, which is solution and precipitation from the liquid phase around cBN particles [3]. Presence of liquid phase might prevent the effect of cBN orientation.

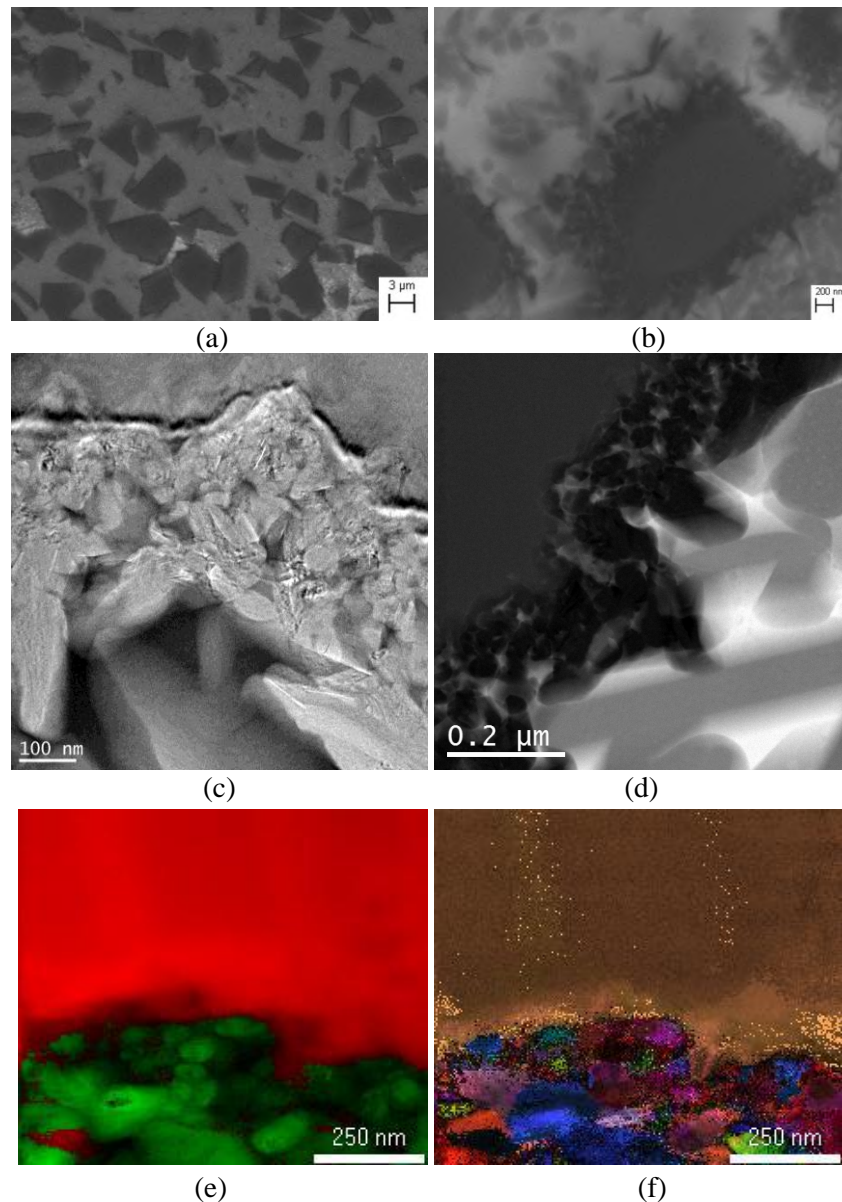


Figure 1. (a, b) SEM-BSE images, (c) TEM and (d) STEM-HAADF images, (e) phase map (green:hBN, red:cBN) and (f) orientation map of β SiAlON/cBN.

3.2. SiC-hBN and B_4C - TiB_2 Ceramic Composites

Silicon carbide (SiC) is an important high temperature ceramic material thanks to its properties like high elastic modulus, high chemical and thermal stability and high strength at elevated temperatures. Due to its great mechanical properties, it is hard to obtain complex geometries by machining. In order to improve the machinability of this type of ceramics, addition of secondary phase to obtain ceramic composite structure is used and hexagonal boron nitride (hBN) is a possible candidate due to its high temperature stability and machinability properties. It is reported that hBN addition, improve the machinability of SiAlON and Si_3N_4 ceramics [9]. One of the major problem to obtain SiC-hBN composite is the difficulty to obtain homogeneous distribution of secondary phase by conventional mixing methods. Homogeneous distribution of the secondary phase particles can be obtained with in-situ hBN synthesise approach during sintering. In this study, SiC-hBN composite was obtained with in-situ formation of hBN particles and details of the sample production is given in

materials and methods section. In the literature, there are several different composites produced with in-situ formation method and in these studies, it is reported that in-situ formed particles may have special orientation relation with the host structure. [10, 11]. In order to characterize the orientation relations between SiC and hBN particles, novel TEM-PED method was successfully used for the first time. The results of this study will be published and can be accessible from Z. Yilmaz, U. Savaci, S. Turan, N. Ay "Synthesis and properties of SiC- hBN composites" article.

Boron carbide (B_4C) is an important ceramic material due to its extreme hardness and chemical properties [12]. Extreme hardness of this material comes with a disadvantage during densification. Due to the very high bond strength between atoms it is hard to densify with pressureless sintering methods. To obtain high density bulk products, sintering additives like TiB_2 is added to B_4C [13, 14]. Even though the sintering additives improve the densification during pressureless sintering, the sintering temperatures are about $2250^\circ C$. In order to decrease the sintering temperatures, pressure assisted sintering methods like SPS and HP are used [15, 16] for the densification of B_4C containing ceramics. Here B_4C - TiB_2 ceramic composites produced with R-SPS and HP methods will be characterized to understand orientation relations between phases and phase identification of the present phases, respectively, by using TEM-PED method. The results of this study will be published and can be accessible from U. Savaci, S. Failla, D. Sciti, S.Turan "Microstructural characterization of solid solution formed during hot pressing of B_4C - TiB_2 composites doped with WC" article.

4. Conclusions

In this study, TEM-PED method was conducted successfully for the characterization of the orientation relations between present phases as well as phase identification of SiC-hBN, B_4C - TiB_2 and β SiAlON-cBN ceramic composites. According to the TEM-PED analyses there are several different conclusions can be made;

- (i) Orientation relations between cBN and hBN transformation layer was conducted in β SiAlON/cBN composite sample. However, it was found that there was no specific orientation relations between phases, possibly caused by growth of hBN particles from liquid phase with the solution and precipitation mechanism. Overlapped grains within the transformation layer significantly decrease the reliability of the results, which is a disadvantage of TEM-PED method.
- (ii) In the SiC-hBN and R-SPS'ed B_4C - TiB_2 composites, orientation relations between in-situ formed phases were successfully identified by using TEM-PED method. In addition to these studies, phase identification and phase analysis of the solid solution formed during hot pressing were successfully carried out

This study showed that orientation and phase mapping of the ceramic composites can be conducted with high resolution for the orientation relation and phase identification analyses by using TEM-PED method.

Acknowledgements

The authors would like to acknowledge the financial support from the Scientific Research Project Commission of Anadolu University (grant no:1504F168) and The Scientific and Technological Research Council of Turkey (TUBITAK) Directorate of Science Fellowships and Grant Programmes (BİDEB) 2211 National Ph.D scholarship programme. The authors would also like to acknowledge Dr. Zuhail YILMAZ, Dr. Ufuk AKKAŞOĞLU and Dr. Simone FAILLA for providing samples and Dr. Meltem SEZEN for the FIB sample preparations.

References

1. Abbasi, M., et al., *Application of Transmitted Kikuchi Diffraction in Studying Nano-oxide and Ultrafine Metallic Grains*. ACS Nano, 2015. 9(11): p. 10991-11002.
2. Lenčič, Z. and M. Havari, *SiAlON/SiC Micro-Nano-Composites*, in *Engineering Ceramics '96: Higher Reliability through Processing*, G.N. Babini, M. Havari, and P. Šajgalík, Editors. 1997, Springer Netherlands: Dordrecht. p. 179-187.

3. Garrett, J.C., I. Sigalas, and M. Herrmann, *TEM investigation of the interface formation in cubic boron nitride containing α -SiAlON composites*. *Ceramics International*, 2014. **40**(10): p. 16169-16175.
4. Maglica, A., et al., *Preparation and properties of B-SiAlON/ZrN nano-composites from ZrO₂-coated Si₃N₄ powder*. *Processing and Application of Ceramics*, 2007. **1**(1-2): p. 49-55.
5. Garrett, J.C., et al., *cBN reinforced Y- α -SiAlON composites*. *Journal of the European Ceramic Society*, 2013. **33**(11): p. 2191-2198.
6. Ye, F., et al., *Spark plasma sintering of cBN/ β -SiAlON composites*. *Materials Science and Engineering: A*, 2010. **527**(18-19): p. 4723-4726.
7. Yuan, S., et al., *How to Increase the h-BN Crystallinity of Microfilms and Self-Standing Nanosheets: A Review of the Different Strategies Using the PDCs Route*. *Crystals*, 2016. **6**(5).
8. Xue, J.-X., et al., *Pressure-induced preferential grain growth, texture development and anisotropic properties of hot pressed hexagonal boron nitride ceramics*. *Scripta Materialia*, 2011. **65**(11): p. 966-969.
9. Shuba, R. and I.W. Chen, *Machinable α -SiAlON/BN Composites*. 2006.
10. Wang, X., et al., *Orientation relationship in WC-Co composite nanoparticles synthesized by in situ reactions*. *Nanotechnology*, 2015. **26**(14): p. 145705.
11. Wang, H., et al., *In situ fabrication and microstructure of Al₂O₃ particles reinforced aluminum matrix composites*. *Materials Science and Engineering: A*, 2010. **527**(12): p. 2881-2885.
12. Gunjishima, I., T. Akashi, and T. Goto, *Characterization of Directionally Solidified B₄C-TiB₂ and B₄C-SiC Eutectic Composites Prepared by Floating-Zone Method*. *Materials Transactions, JIM*, 2002. **43**(4): p. 712-720.
13. Sigl, L.S., *Processing and mechanical properties of boron carbide sintered with TiC*. *Journal of the European Ceramic Society*, 1998. **18**(11): p. 1521-1529.
14. Sahin, F.C., et al., *Spark plasma sintering of B₄C-SiC composites*. *Solid State Sciences*, 2012. **14**(11-12): p. 1660-1663.
15. Ji, W., et al., *Sintering boron carbide ceramics without grain growth by plastic deformation as the dominant densification mechanism*. *Scientific Reports*, 2015. **5**: p. 15827.
16. Yamada, S., et al., *High strength B₄C-TiB₂ composites fabricated by reaction hot-pressing*. *Journal of the European Ceramic Society*, 2003. **23**(7): p. 1123-1130.

CERAMIC RAW MATERIALS

THE STRUCTURAL MODIFICATION OF QUARTZ ACCORDING TO FIRING TEMPERATURE AND ATMOSPHERE

Dilek ŞEN¹, Hanife KADIOĞLU¹, Enver TARIM¹, Harun TAŞDEMİR¹, Kemal KARADAL¹,
Veli UZ²

¹Kütahya Porcelain, Research & Development Department, Kütahya

²Kütahya Dumlupınar University, Metallurgy and Material Engineering, Kütahya

Abstract

Quartz has different polymorphic forms troubling with shrinkage and expansion behavior in ceramic products. In this study was investigated polymorphic transition of quartz according to sintering in different ceramic furnace having different atmosphere and temperature. Phase transition of quartz samples were determined by X-Ray diffraction and Rietveld method. It has been determined based on the crystal structure of quartz samples and the oxides it contains that they are effective in the development of the cristobalite phase. Highest cristobalite phase ratio was determined as a result of firing the transparent quartz sample at a temperature of 1340°C. It was found out that the accordance of the quartz used to the kiln conditions should be decided based on phase analyses after firing.

Keywords: Porcelain, Quartz, Polymorph, Firing

1. Introduction

Quartz which is one of the main raw materials of ceramic materials may cause deformations on polymorph transformation products according to the heat regime in kilns depending on the particle size and crystal structure. Hence, the accordance of quartz used with the firing regime should be controlled [1,2]. Quartz has a trigonal crystal balancing is attained by Li^{+1} and Na^{+1} cations [3]. The polymorphs of quartz are beta-quartz, tridymite and cristobalite. Quartz slowly transforms to tridymite and cristobalite when heated [4-7]. However, cation addition or the presence of cation in the structure may speed up these transformations. While Ca, Mg, Fe and Ba are effective in cristobalite formation [8-10], alkali ions are effective in tridymite formation [11-14]. However, the Al^{+3} and Ti^{+4} cations are not effective in these transformations. Indeed, Al^{+3} has a tendency to prevent or slow down these quartz transformations [15,16]. Therefore, the presence of these cations and their ratios during quartz formation has significant impacts on quartz transformations and their stability. In this study, the changes in the crystal structures of 4 different quartz minerals upon firing at different temperatures in kilns along with the quartz transformations that took place were determined in addition to examining the crystal lattice parameters.

2. Materials and Method

The 3 quartz samples used in the studies were selected from among those used in ceramic products and one quartz samples was selected as single crystal transparent quartz. Quartz samples were fired in facility kilns at reductive atmosphere in 980°C biscuit kilns and in 1340°C glaze kilns at an oxidative atmosphere in 1000°C and 1080°C biscuit kilns and in 1260°C and 1120°C glaze kilns. The chemical analyses of the quartz samples were carried out in Spectro X-Lab Pro 2000 XRF device. Mineralogical and phase analyses were carried out using the Rigaku Miniflex Brand XRD device located at the Kütahya Dumlupınar University Metallurgy and Material Engineering department. Rigaku X-ray Diffractometer model Rint 2000 device was used for the phase analyses of the samples. Phase analyses were carried out under conditions of 30 kV and 15mA (Cu-K α , $\lambda=1,541 \text{ \AA}$, 2θ 5-70°, 2°/min.). MDI Jade6.00 software was used for phase determination and MAUD 2.80 crystal analysis software was used for crystal calculations.

3. Results

3.1. Chemical Analyses

The oxide ratios of the quartz samples used have been given in Table 1. It was determined that the Al₂O₃ content of Quartz B and Quartz C samples was 5.20 % and 4.58 % respectively.

Table 1. Chemical analyses result of the Quartz samples

Oxides	Ratio at weight (%)			
	Quartz A	Quartz B	Quartz C	Quartz D
Na ₂ O	0,08	0,09	0,08	0,08
K ₂ O	0,14	0,54	0,30	0,01
Al ₂ O ₃	0,10	5,20	4,58	0,10
SiO ₂	99,19	91,31	92,42	98,51
CaO	0,08	0,05	0,13	0,63
TiO ₂	0,01	0,65	0,08	0,01
Fe ₂ O ₃	0,14	0,40	0,14	0,05
MgO	0,05	0,05	0,05	0,10
LOI	0,20	1,69	2,06	0,42

3.2. Mineralogical Analyses

X-Ray diffraction parameters of raw quartz samples have been given in Figure 1. It was determined based on the mineralogical analyses of the Quartz samples that quartz A (Figure 1A) and quartz D (Figure 1D) samples contain quartz. Other quartz B (Figure 1B) and quartz C (Figure 1C) samples include a small amount of kaolinite together with quartz.

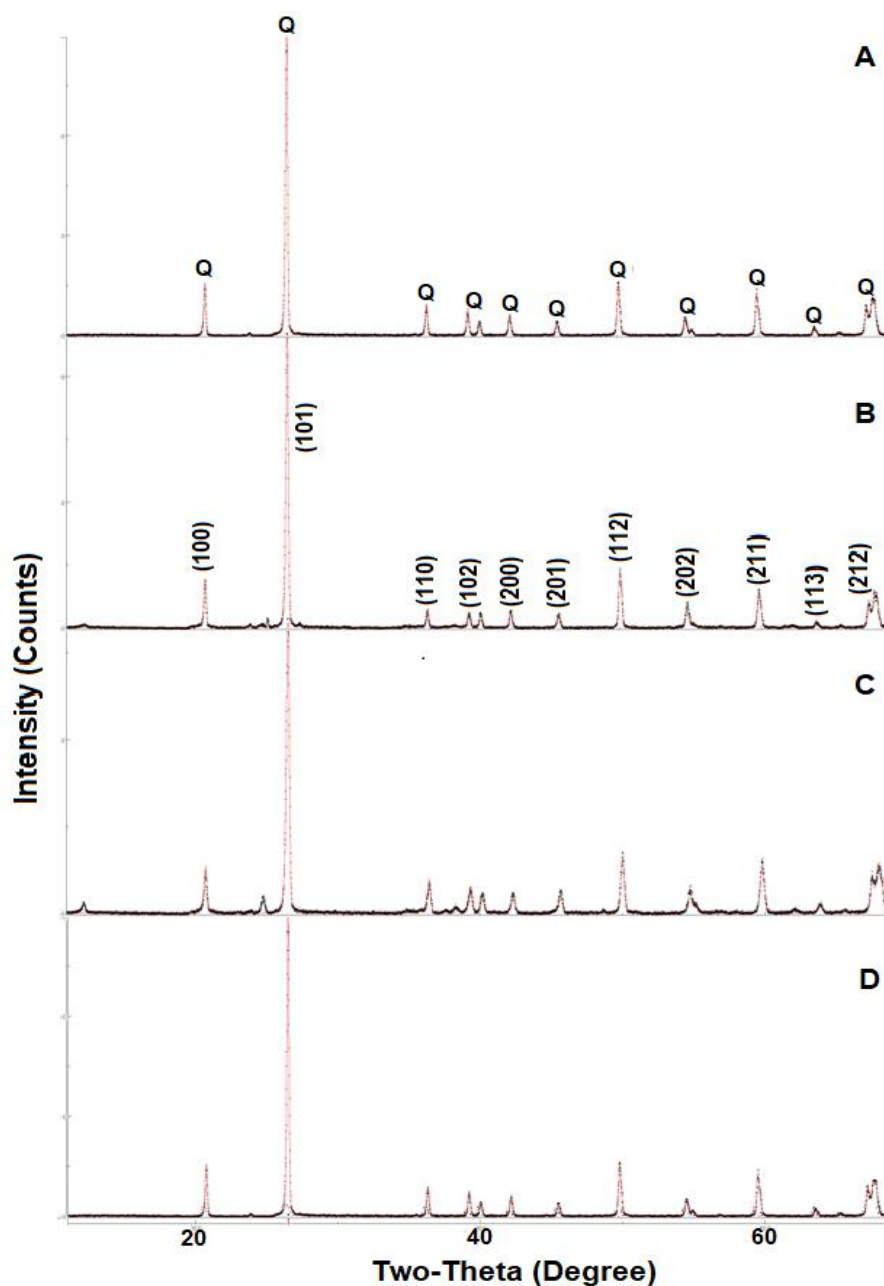


Figure 1. X-Ray diffraction patterns of raw quartz samples.

3.3. Phase analyses after firing

The X-Ray diffraction patterns indicating the phase analyses of quartz samples after firing at 980°C temperature in a biscuit kiln under reductive atmosphere have been given in Figure 2. It was determined following firing in biscuit kiln that all quartz samples have only quartz. The coding used for the Quartz samples have been given as quartz A (Figure 2A), quartz B (Figure 2B), quartz C (Figure 2C) and quartz D (Figure 2D).

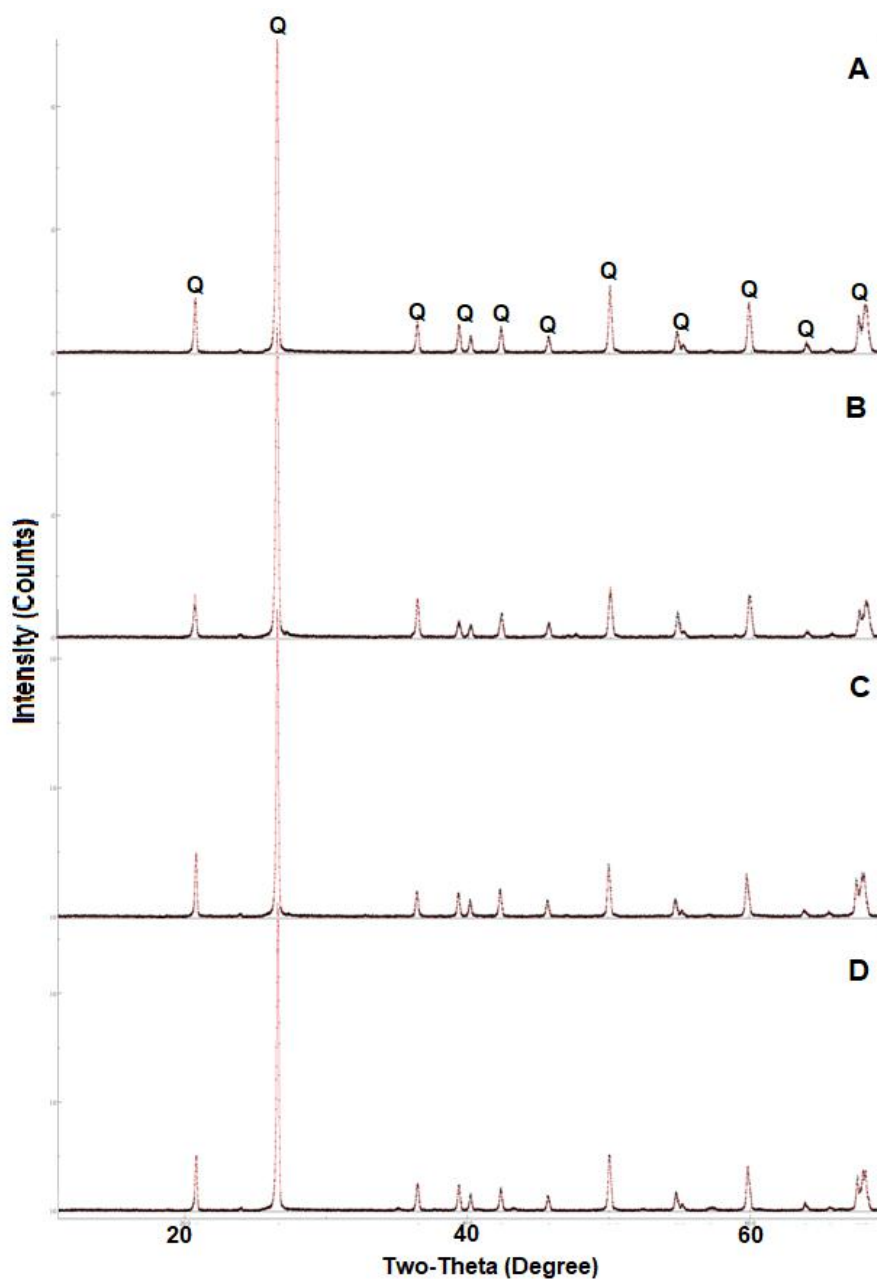


Figure 2. X-ray diffraction patterns of quartz samples fired in biscuit kiln (980°C)

It was determined after firing the Quartz samples in a glaze kiln at 1340°C under a reductive atmosphere that the cristobalite phase developed. While the peak indicating the (101) plane of cristobalite was observed clearly for the cristobalite that developed in the quartz A (Figure 3A) and quartz B (Figure 3B) samples after firing, the peaks indicating the (111) and (102) planes were not observed as clearly. It was determined in both quartz samples that cristobalite developed on the (101) plane. It was found out in other quartz C (Figure 3C) and quartz D (Figure 3D) samples that the peaks indicating the (100) plane of quartz decreased and that the peak indicating the (101) plane of the developing cristobalite increased in intensity and that the other (111) and (102) plane peaks were also distinctive. The cristobalite that forms during firing remains stable since rapid cooling takes place in glaze ovens. The reason for this shift is the change in the lattice parameters or the impacts of stress that develops in the crystal structure.

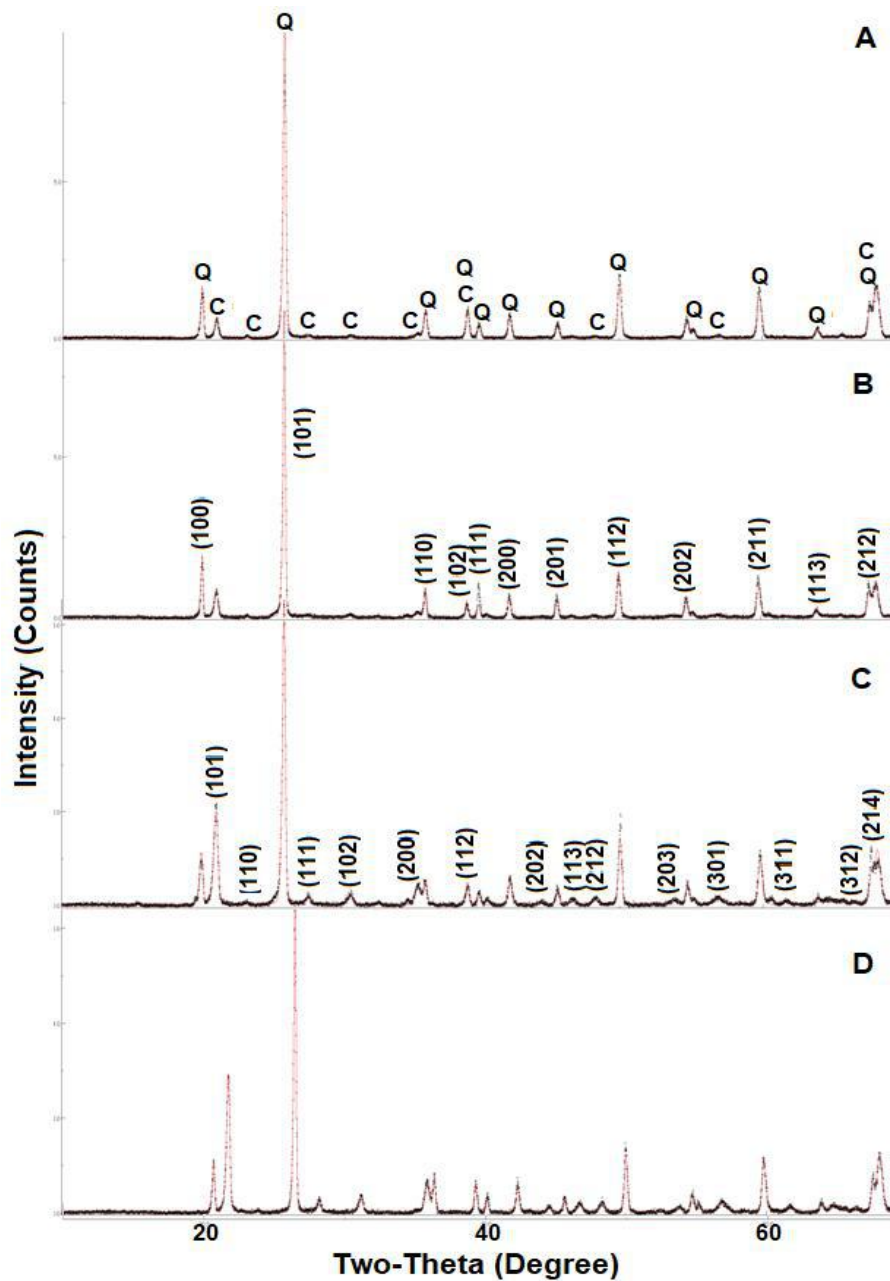


Figure 3. X-ray diffraction patterns of quartz samples fired in glaze kiln (1340°C)

Small amount of cristobalite formation was determined in quartz samples fired in biscuit kiln at 1000°C under oxidative atmosphere and in glaze kiln at 1260°C excluding the Quartz A (Figure 4A) sample. While the peaks of cristobalite that is formed in the Quartz B (Figure 4B) sample are not very distinct, the peaks indicating the (101) plane of cristobalite became more distinct in quartz C (Figure 4C) and quartz D (Figure 4D) samples.

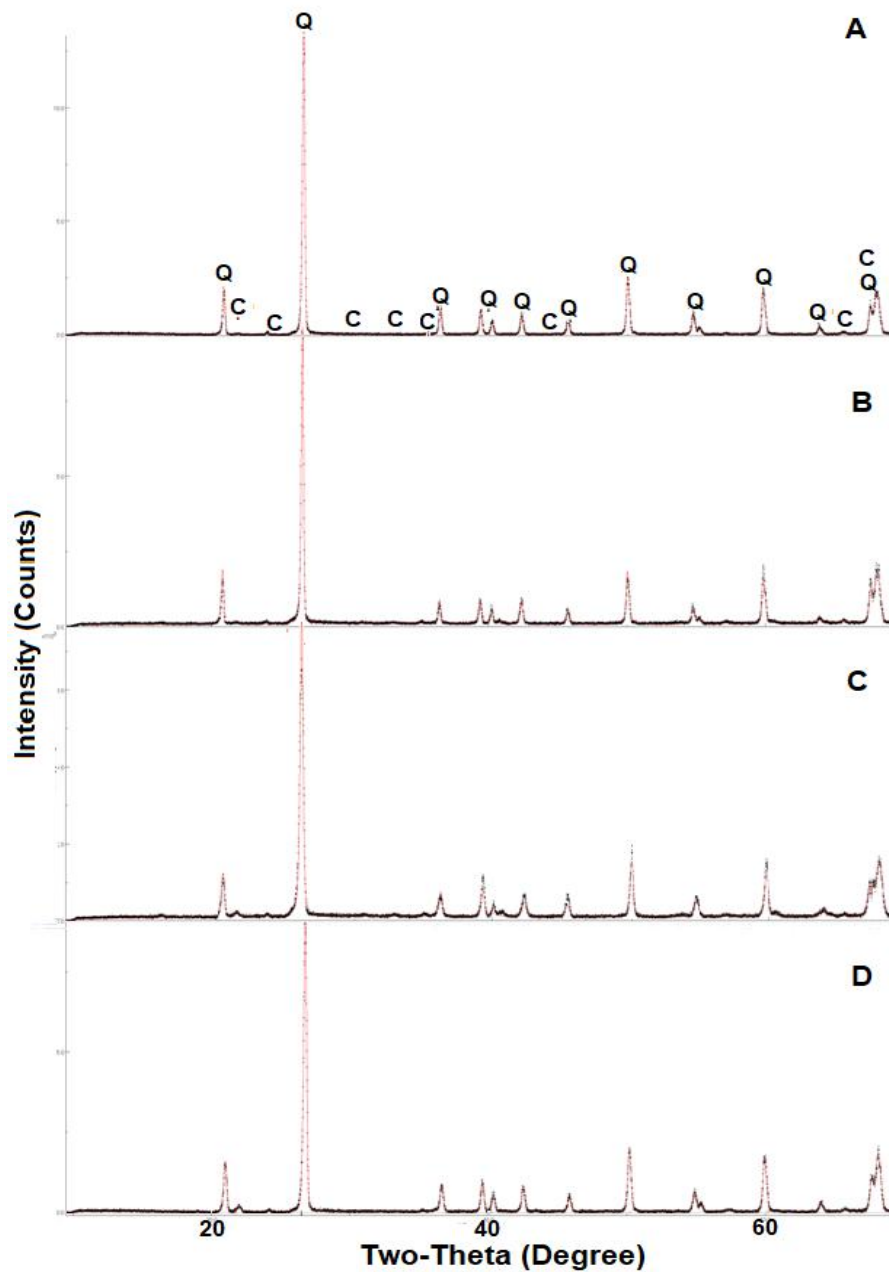


Figure 4. X-ray diffraction parameters of quartz samples fired in biscuit (1000°C) and glaze (1260°C) kilns

No cristobalite formation was observed in the samples fired at 1080°C in biscuit kiln under oxidative atmosphere and at 1120°C in the glaze kiln (Figure 5). It was determined that the peak indicating the (101) plane for the quartz B sample shifted to the right.

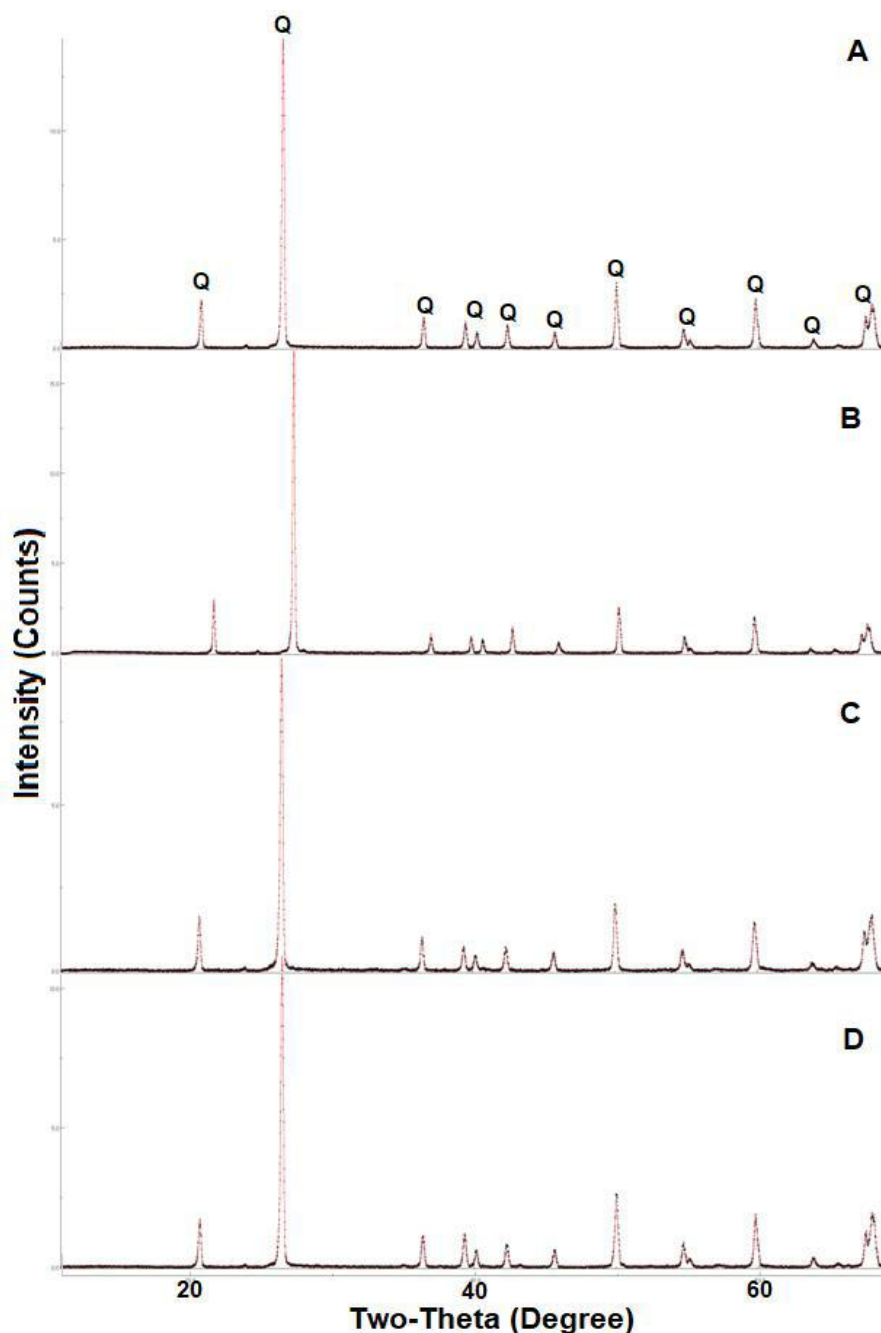


Figure 5. X-ray diffraction patterns of quartz samples fired in biscuit (1080°C) and glaze (1120°C) kilns

3.4. Rietveld analysis of the Phases

Mineralogical and phase analyses of the raw and fired samples were carried out via MAUD Crystal software based on the Rietveld method. The phase ratios calculated for the raw and fired quartz samples have been given in Table 2. No phase formation was observed in addition to the quartz following the firing of quartz samples in biscuit kiln at 980°C under reductive atmosphere and in biscuit kiln at 1000°C and 1080°C under oxidative atmosphere and in glaze kilns at 1120°C.

However, cristobalite phase formation was observed in the samples fired in glaze kiln at 1340°C in reductive atmosphere and in glaze kilns at 1260°C under oxidative atmosphere. The rapid cooling applied in glaze kilns in order to ensure that the surface is bright plays a role in the cristobalite to remain stable. The highest cristobalite ratio after firing in a glaze kiln at 1340°C under reductive atmosphere was about 37 % in quartz D sample. Whereas the lowest cristobalite ratio was about 8 % in quartz A sample. Less cristobalite formation was observed in samples fired in biscuit kiln at 1000°C under oxidative atmosphere and in glaze kilns at 1260°C in comparison with the samples fired in glaze kilns at 1340°C under reductive atmosphere. While cristobalite formation is not observed in the quartz A sample fired in biscuit kiln at 1000°C under oxidative atmosphere, highest cristobalite formation was 3 % in the quartz D sample.

Table 2. Phase analyses of Quartz samples

Samples	Phases	Firing Atmosphere				
		Reductive			Oxidative	
		Raw	980°C	1340°C	1000°C 1260°C	1080°C 1120°C
Quartz A	Quartz	100	100	92.22	100	100
	Cristobalite	-	-	7.78	-	-
Quartz B	Quartz	100	100	90.00	99.57	100
	Cristobalite	-	-	10.00	0.43	-
Quartz C	Quartz	85	100	71.04	98.64	100
	Kaolinite	15	-	-	-	-
	Cristobalite	-	-	28.96	1.36	-
Quartz D	Quartz	100	100	63.40	96.97	100
	Cristobalite	-	-	36.60	3.03	-

The lattice parameters calculated for raw and fired Quartz samples have been given in Table 3. Minor increases were observed in the lattice parameters of Quartz A, Quartz C and Quartz D samples after firing. No decrease was observed in the lattice parameters for the Quartz B sample fired in biscuit kiln at 980°C under oxidative atmosphere and in glaze kiln at 1340°C along with the samples fired in biscuit kiln at 1080°C and in glaze kiln at 1120°C. The a-axis and c-axis lattice parameters of quartz

samples fired in biscuit kiln at 1000°C under oxidative atmosphere and in glaze kiln at 1260°C were higher in comparison with the samples fired in other kilns.

The a-axis and c-axis parameters of Quartz A sample fired in glaze kiln at 1340°C under reductive atmosphere increased by about 0.13 % after firing whereas the a-axis of the Quartz C samples fired in biscuit kiln at 1000°C under oxidative atmosphere and in glaze kiln at 1260°C increased by 0.16 % and the c-axis increased by 0.13 %. It was observed upon comparing the lattice parameters of the cristobalite phase that forms after firing for the samples fired in reductive glaze kiln at 1340°C with those fired in glaze kiln at 1260°C that the a-axis increased for the Quartz B sample while the c-axis decreased. The contrary was true for the other Quartz C and Quartz D samples with a-axis decreasing while the c-axis increased.

Table 3. Crystal lattice parameters of the quartz samples

Samples	Phases	LatticeValues	Raw	Firing Atmosphere			
				Reductive		Oxidative	
				980°C	1340°C	1000°C	1080°C
					C	1260°C	1120°C
Quartz A	Quartz	a-axis, Å	4.919	4.922	4.926	4.925	4.923
		Changing Ratio, %	-	0.06	0.14	0.12	0.08
		c-axis, Å	5.411	5.415	5.418	5.418	5.416
		Changing Ratio, %	-	0.07	0.13	0.13	0.09
	Cristobalite	a-axis, Å	-	-	5.005	-	-
		c-axis, Å	-	-	6.984	-	-
Quartz B	Quartz	a-axis, Å	4.924	4.927	4.924	4.919	4.919
		Changing Ratio, %	-	0.06	0	-0.10	-0.10
		c-axis, Å	5.415	5.419	5.419	5.413	5.413
		Changing Ratio, %	-	0.07	0.07	0.04	0.04
	Cristobalite	a-axis, Å	-	-	4.988	4.996	-
		c-axis, Å	-	-	7.044	6.989	-
Quartz C	Quartz	a-axis, Å	4.921	4.922	4.922	4.929	4.926
		Changing Ratio, %	-	0.02	0.02	0.16	0.10
		c-axis, Å	5.415	5.415	5.415	5.422	5.416
		Changing Ratio, %	-	0	0	0.13	0.02
	Cristobalite	a-axis, Å	-	-	4.999	4.974	-
		c-axis, Å	-	-	6.979	7.101	-
Quartz D	Quartz	a-axis, Å	4.918	4.921	4.924	4.927	4.924
		Changing Ratio, %	-	0.06	0.12	0.18	0.12

	c-axis, Å	5.409	5.414	5.414	5.418	5.416
	Changing Ratio, %	-	0.09	0.09	0.17	0.13
	a-axis, Å	-	-	4.997	4.961	-
Cristobalit	c-axis, Å	-	-	6.968	7.133	-
e						

According to the acquired results;

- While no cristobalite phase formation was observed in samples fired in biscuit kiln at 980°C under reductive atmosphere and in biscuit kilns at 1000°C and 1080°C under oxidative atmosphere, and in glaze kilns at 1120°C; cristobalite phase formation was observed in samples fired in glaze kiln at 1340°C under reductive atmosphere and in glaze kilns at 1260°C under oxidative atmosphere.
- Cristobalite formation in samples fired in glaze kiln at 1340°C under reductive atmosphere was much higher in comparison with those for the samples fired in glaze kiln at 1260°C under oxidative atmosphere.
- Based on the crystal structure, the highest cristobalite ratios were 37% for the transparent quartz crystal in the reductive environment at 1340°C and 3% in oxidative environment at 1260°C.
- The lattice parameters of the Quartz B samples decreased after firing at temperatures of 980°C, 1080°C, 1120°C and 1340°C.
- Changes were determined in the lattice parameters of quartz samples after firing.
- The lattice parameters of quartz samples fired at 1000°C and 1260°C under oxidative atmosphere were higher as a-axis and c-axis in comparison with samples fired in other kilns.
- The highest lattice parameter was obtained as a-axis and c-axis parameters of Quartz A sample fired in glaze kiln at 1340°C under reductive atmosphere which increased by about 0.13 % after firing whereas the a-axis of the Quartz C samples fired in biscuit kiln at 1000°C under oxidative atmosphere and in glaze kiln at 1260°C increased by 0.16 % and the c-axis increased by 0.13 %.
- While for the a-axis from among the lattice parameters of cristobalite increased for the Quartz B sample in samples fired at 1340°C under reductive atmosphere in comparison with samples fired at 1260°C under oxidative atmosphere, the c-axis values decreased. Contrary to these results, the a-axis decreased and the c-axis increased for the Quartz C and Quartz D samples.
- It was determined that the crystal structure of quartz and the oxides other than silicon it contains are effective in cristobalite formation after firing and that accordingly it is important

for reducing errors in production to fire the quartz samples in the operating kiln prior to using them in ceramic production and to carry out phase analyses for the fired samples.

References

1. M. Dapiaggi, L. Pagliari, A. Pavese, L. Sciascia, M. Merli, F. Francescon, The formation of silica high temperature polymorphs from quartz: Influence of grain size and mineralising agents, *European Ceramic Society* 35 (2015) 4547-4555
2. E. I. Suzdaltsev, The Sintering Process of Quartz Ceramics, *Refract. and Ind. Ceram.*, 44-4, 2003, 236-241
3. Sistemati mineraloji,
4. M. Nabil, K.R. Mahmoud, A.E. Shaer, H.A. Nayber, Preparation of crystalline silica (quartz, cristobalite, and tridymite) and amorphous silica powder (one step), *Physics and Chemistry of Solids* 121 (2018) 22–26
5. M.F. Zawrah, E.M.A. Hamzawy, Effect of cristobalite formation on sinterability, microstructure and properties of glass/ceramic composites, *Ceramics Int.* 28 (2002) 123-130
6. C. Tang, J. Zhu, Z. Li, R. Zhu, Q. Zhou, J. Wei, H. He, Q. Tao, Surface chemistry and reactivity of SiO₂ polymorphs: A comparative study on quartz and cristobalite, *Applied Surface Science* 355 (2015) 1161-1167
7. L.G. Baikova, R.I. Mamalimov, T.I. Pesina, A.E. Chmel, A.I. Shcherbakov, Structural Transformations During Heat-Treatment of Quartz Ceramic, *Glass and Ceramics*, Vol. 70, No 7-8, 2013, 303-305
8. L. Pagliari, M. Dapiaggi, A. Pavese, F. Francescon, A kinetic study of the quartz–cristobalite phase transition, *European Ceramic Society* 33 (2013) 3403-3410
9. I.M. Abdulagatov, S.N. Emirov, T.A. Tsomaeva, K.A. Gairbekov, S.Y. Askerov, N.A. Magomedova, Thermal conductivity of fused quartz and quartz ceramic at high temperatures and high pressures, *Physics and Chemistry of Solids* 61 (2000) 779-787
10. M.J. Jackson, B. Mills, Dissolution of quartz in vitrified ceramic materials, *Mater. Sci.* 32 (1997) 5295-5304
11. O.A. Alharbi, D.Y. Zaki, E.M.A. Hamzawy, Effect of TiO₂, LiF and Cr₂O₃ in the Crystallization of Cristobalite and Tridymite in Sintered Glass-Ceramics, *Silicon* (2012) 4:281–287
12. A. Nukui, O.W. Flörke, Three tridymite structural modifications and cristobalite intergrown in one crystal, *American Mineralogist*, Vol. 72, 167-169, 1987
13. W. Pabst, E. Gregorova, J. Kutzendörfer, Elastic anomalies in tridymite- and cristobalite-based silica materials, *Ceramics Int.* 40 (2014) 4207-4211

14. G.R. Fischer, R.R. Wusirika, J.E. Geiger, The crystal lattice thermal expansion of an oxynitride glass-ceramic material of high-quartz structure, *Materials Science* 20 (1985) 4117-4122
15. I. Allegretta, G. Eramo, D. Pinto, V. Kilikoglou, Strength of kaolinite-based ceramics: Comparison between limestone- and quartz-tempered bodies, *Applied Clay Science* 116-117 (2015) 220-230
16. J.J. Liang, Q.H. Lin, X. Zhang, T. Jin, Y.Z. Zhou, X.F. Sun, B.G. Choi, I.S. Kim, J.H. Do, C.Y. Jo, Effects of Alumina on Cristobalite Crystallization and Properties of Silica-Based Ceramic Cores, *Materials Science & Technology* 33 (2017) 204-209

CERAMIC RAW MATERIALS

MINERALOGICAL INVESTIGATION OF NEPHELINE SYENITE AND ITS USAGE IN CERAMIC PRODUCTION

Veli Uz¹, Nihal Derin Coşkun^{2*}

¹Dumlupınar University, Faculty of Engineering, Metallurgy and Materials Engineering Department,
Kütahya/Turkey

²Ordu University, Faculty of Fine Arts, Ceramic and Glass Department, Ordu/Turkey

ABSTRACT

Feldspar, one of the basic raw materials of the ceramics industry, causes microstructural changes that affect the firing and final product properties of the ceramic product due to their high K_2O and Na_2O ratios. For this reason, feldspars have an important place for providing of desired properties of ceramic products. However, the increasing population of the world and the accompanying production demand are causing these raw materials to be consumed. The demand for alternative raw material resources for solution of this problem is increasing day by day. Mineralogical and thermal examination of nepheline syenites with high K_2O and Na_2O ratios obtained as a result of the enrichment was carried out. The samples whose product characteristics were determined and the feldspars used in ceramics were compared and their usability as an alternative raw material was investigated.

1. Introduction

Feldspars which provide glassy phase formation during the firing stage in addition to improving the physical properties of the ceramic product have an important place in the ceramic sector [1]. However, the search for alternative raw materials continues since the quality and amount of clean feldspar reserves decrease every day [2]. There are two main minerals as the nepheline group. The main mineral of this group is Nepheline ($Na_3(Na,K)[Al_4Si_4O_{16}]$) and the other is kalsilite ($(K)[AlSiO_4]$). Replacement of potassium with sodium results in an increase in crystal lattice parameters as well as both a and c-axes. Nepheline generally puts forth intermediate growths with potassium feldspar in general and rarely with plagioclase. Nephelines with no iron content can be used as an alternative raw material to feldspar due to their high aluminum content [3-4]. Nephelines are used directly in the glass industry and the production of plate glass, television tube, bulb glass blocks and glass wool due to their high alkaline oxide content. Nephelines are also used in ceramic industry, paint industry as well as aluminum, cement and alkaline material production. They are used in the construction sector for obtaining roof material [5]. Nepheline syenites increase alkaline level inside the glassy phase by decreasing the firing temperature when used in sanitary ware, electricity porcelain and glazed tile [6]. Firing is an important stage in ceramic production. It should be carried out in a controller manner due

both to the consumed energy amount as well as for the shaping of the final product in production. Many studies are carried out for the methods applied at this stage. Reducing firing time is among the primary methods [7]. The firing process for sanitary ware products that takes up to about 10-13 hours in our day varied between ~30-35 hours during the 1970's [8]. These studies have brought about further studies on kiln technology as well as the raw materials used thereby increasing the search for alternative raw materials [9-10]. The fact that the change in Na_2O and K_2O ratios has an impact on the viscosity of the liquid phase that forms during firing is among the primary reasons for this [11]. Nepheline syenites with a total $\text{Na}_2\text{O}+\text{K}_2\text{O}$ ratio of ~%14 contain more alkaline than feldspars with ~%9-12 and lead the way for use as an alternative feldspar source [12-13] The purpose of this study was to carry out analyses for nephelines as a feldspar alternative with high sodium and potassium and to examine their potential to be used in ceramic products.

2. Materials and Method

The nepheline samples used in the study were acquired from B&S Investment Inc. Company at the Kırşehir region. Rigaku, ZSX Primus brand device was used for the chemical analyses of the nepheline samples. Mineralogical and phase analyses were carried out using the Rigaku Miniflex Brand XRD device at the Kütahya Dumlupınar University Department of Metallurgy and Material Engineering laboratories. MDI Jade 6.00 software was used for phase determination during which crystal calculations were carried out via MAUD 2.80 crystal analysis software. The thermal behaviors of the samples were determined using the MISURA ODHT HSM 1600/80 brand optical dilatometer device at the Eskişehir Technical University, Materials Science and Engineering Department laboratories.

3. Results

3.1. Chemical analysis

The chemical analysis results for nepheline samples have been given in Table 1. The naming of nephelines has been given based on the high ratios of their sodium and potassium oxide content. Sodium nepheline contains 9.6% Na_2O whereas nepheline contains 4.4 % Na_2O . The high ratio of K_2O in potassium nepheline was determined as 10.5 % and K_2O in sodium nepheline was determined as 6.3 %. CaO content in the case of sodium nepheline was 1.11 % whereas CaO content in potassium nepheline was determined as a very low amount of 0.15 %.

Table 1. Chemical analysis of nepheline samples

Oxides	Sodium	Potassium
	Nepheline	Nepheline
SiO₂	58,43	62,70
Al₂O₃	23,48	21,05
Fe₂O₃	0,22	0,10
TiO₂	0,01	0,03
CaO	1,11	0,15
MgO	0,04	0,07
Na₂O	9,58	4,40
K₂O	6,25	10,45
Loss of Ignition	0,75	0,70

The Seger values calculated according to the chemical analyses have been given in Table 2. According to the Seger values, while the Na₂O value in sodium nepheline was 0.64, the K₂O value in potassium nepheline was determined as 0.6. The low SiO₂ content separates nepheline syenites from feldspars. SiO₂ values in Seger values are lower in comparison with albite and orthoclase [7]. While for the Albite mineral 1Na₂O·1Al₂O₃·6SiO₂ Seger values are 1-1-6 it was determined for sodium nepheline that these values are 1(Na₂O+K₂O)·0.95Al₂O₃·4SiO₂, and for potassium nepheline as 1(Na₂O+K₂O)·1.11Al₂O₃·5.6SiO₂.

Table 2. Seger values for Nepheline syenite samples

Sample	Acidics				Amphoters		Basics	
	Na ₂ O	K ₂ O	CaO	MgO	Al ₂ O ₃	Fe ₂ O ₃	SiO ₂	TiO ₂
Sodium Nepheline	0.639	0.275	0.082	0.004	0.952	0.006	4.027	0.00052
Potassium Nepheline	0.380	0.596	0.014	0.009	1.106	0.003	5.601	0.00201

3.2. Mineralogical analysis

X-Ray diffraction patterns for Nepheline syenite samples have been given in Figure 1. It was determined that both the sodium nepheline samples and potassium nepheline samples contain albite, orthoclase, and two different nephelines that have Al_{3.84}K_{0.57}Na_{3.24}O₁₆Si_{4.16} and Al₄K_{0.78}Na₃O₁₈Si₂ compositions (Fig 1).

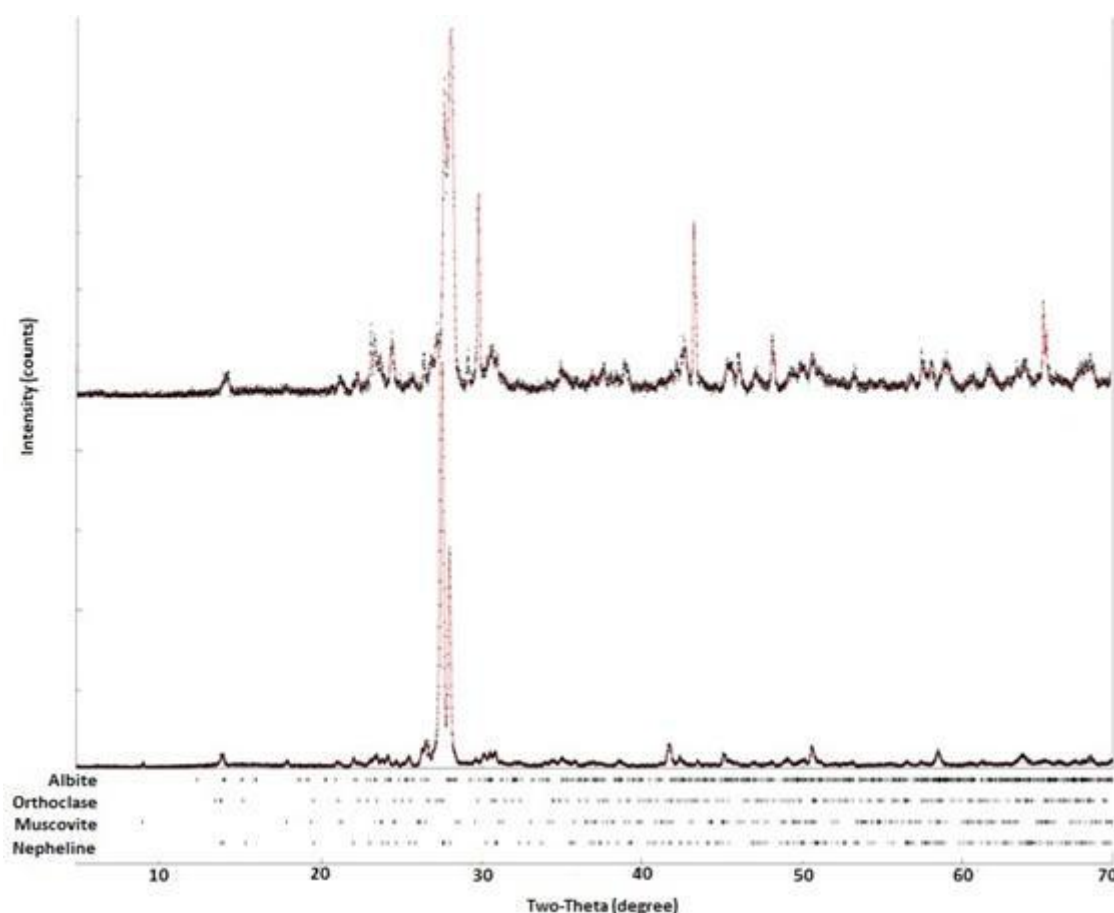


Figure 1. X-Ray Diffraction Patterns of Nepheline syenite samples

The mineral ratios calculated using the X-ray analysis results have been given in Table 3. It was determined for the Sodium nepheline samples ($\text{Al}_{3.84}\text{K}_{0.57}\text{Na}_{3.24}\text{O}_{16}\text{Si}_{4.16}$) mineral at a ratio of %78 potassium, ($\text{Al}_4\text{K}_{0.78}\text{Na}_3\text{O}_{18}\text{Si}_2$) mineral at a ratio of %55. In addition, sodium nepheline contains %0,68 of albite whereas potassium nepheline contains %17,34 orthoclase.

Table 3. Mineral ratios of Nepheline syenite samples

Minerals	Potassium Nepheline	Sodium Nepheline
Nepheline (Na,K) (AlSi_3O_8)	78.07	54.99
Muscovite, $\text{KAl}_2(\text{AlSi}_3\text{O}_{10})(\text{OH})_2$	5.77	26.98
Orthoclase $\text{K}_2\text{OAl}_2\text{O}_36\text{SiO}_2$	8.68	17.34
Albite $\text{Na}_2\text{OAl}_2\text{O}_36\text{SiO}_2$	7.48	0.68

The crystal structure appearance of the Nepheline ($\text{Al}_{3.84}\text{K}_{0.57}\text{Na}_{3.24}\text{O}_{16}\text{Si}_{4.16}$) mineral in nepheline syenite samples and the crystal structure based on XRD analysis results have been given in Figures 2A and 2B respectively.

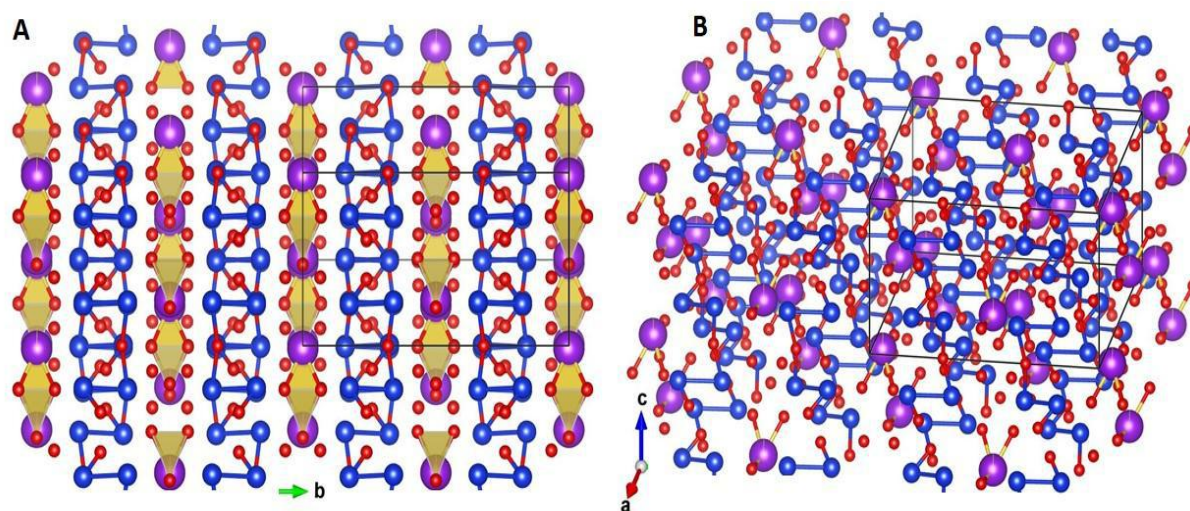


Figure 2. Crystal structure images of the minerals in Nepheline syenite samples

3.3. Thermal analysis

The optical dilatometer analysis carried out for determining thermal behaviors has been given in Figure 3. The optical dilatometer curves of albite and orthoclase minerals have been drawn together with the optical dilatometer curves of the nepheline syenite samples in order to compare the melting behavior of Nepheline syenite samples. It was determined that the shrinkage behavior of the Sodium nepheline sample took place at lower temperatures in comparison with the others. It was observed that the temperature at which Sodium nepheline started to shrink was 1100°C and that particle-particle interaction started thereby leading to the bonding of the particles at a temperature that is 100°C lower in comparison with the albite mineral [6-7]. This sintering onset temperature difference will be advantageous with regard to energy consumption during production. It was determined that the shrinkage onset temperature of the Potassium nepheline sample was 800°C followed by a second shrinkage at 1230°C after a short amount of shrinkage leading to the onset of melting after 1380°C. Whereas the shrinkage onset temperature for the orthoclase mineral was determined as 1200°C. However, shrinkage slows down at around 1380°C. Potassium nepheline shrinks at a lower temperature in comparison with the orthoclase mineral and has a higher shrinkage ratio in comparison with orthoclase. While it was determined that potassium nepheline will be advantageous in sintering in comparison with orthoclase.

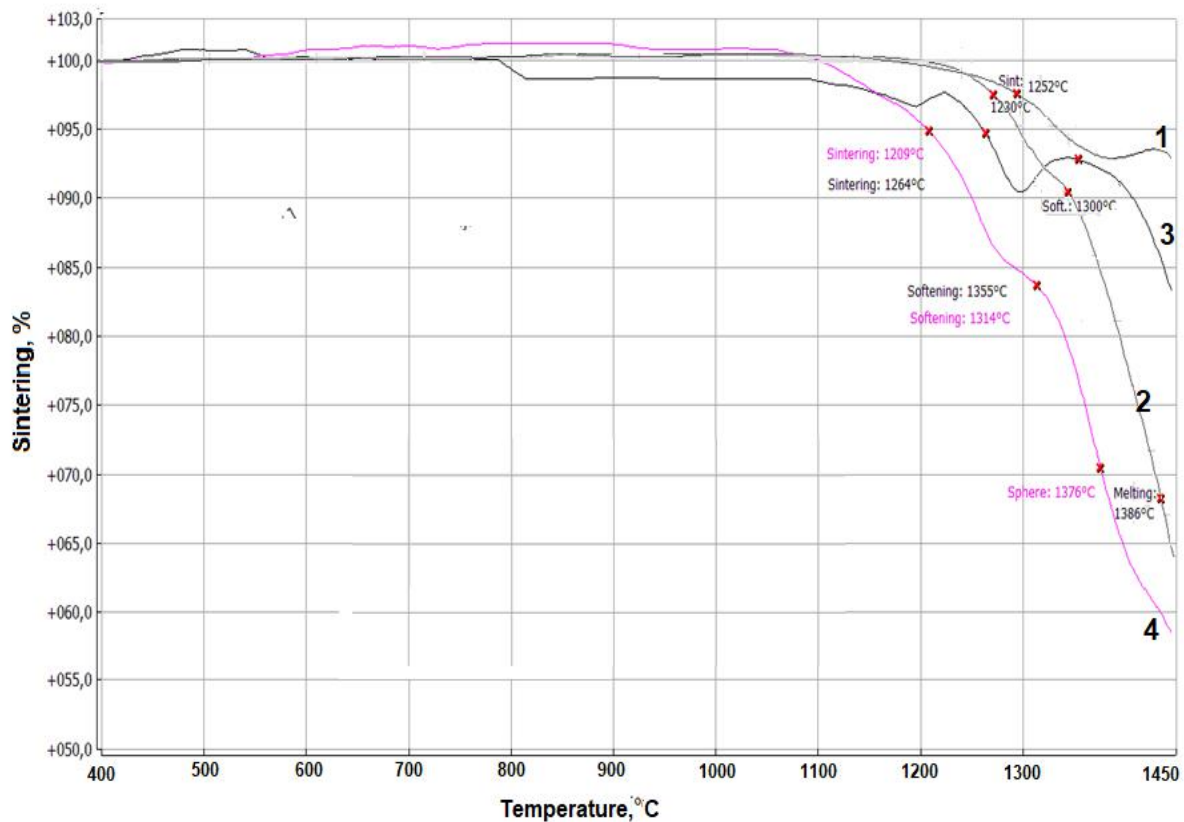


Figure 3. Optical dilatometer results of Nepheline syenite samples

The critical temperature values determined by taking the first derivative of the dilatometer curve in optical dilatometer analysis have been given in Table 5. Whereas the sintering point temperature which is the point with the highest time-dependent shrinkage was 1230°C for the albite mineral, it was determined as 1209°C for sodium nepheline.

Table 5. Critical temperature points for the Nepheline syenite samples

	Orthoclase	Albite	K- Nepheline	Na- Nepheline
	1	2	3	4
Sintering Point, °C	1252	1230	1264	1209
Softing Point, °C	-	1300	1355	1314
Sphere Point, °C	-	-	-	1376
Melting Point, °C	-	1386	-	-

According to the obtained results;

- ✓ While the alkaline ratio ($\text{Na}_2\text{O}+\text{K}_2\text{O}$) of Sodium nepheline syenite was about 16 %, alkaline total was determined as 15 % in potassium nepheline samples. High sodium and potassium oxide

content of nepheline syenites is an indication that it can be used as a fluxing agent in ceramic products.

- ✓ It was determined that nepheline syenites may be used in ceramic recipes as both alkaline and aluminum oxide source due to lower SiO_2 and higher Al_2O_3 content in comparison with feldspars.
- ✓ It was determined that both nepheline syenite samples may be advantageous in firing colors as well due to the fact that the coloring pigment oxide ratio is below 0.22 % for both samples.
- ✓ It was determined that Sodium nepheline syenite may be more advantageous in comparison with albite mineral since it starts shrinking due to particle-particle interaction at a temperature that is 100°C lower.
- ✓ It was determined that Nepheline syenites contain minerals such as albite, orthoclase, different formulas nepheline as $(\text{Al}_{3.84}\text{K}_{0.57}\text{Na}_{3.24}\text{O}_{16}\text{Si}_{4.16})$ and $(\text{Al}_4\text{K}_{0.78}\text{Na}_3\text{O}_{18}\text{Si}_2)$.
- ✓ It was determined that Sodium nepheline syenites contain % 26,98 muscovite, % 0,68 albite and % 17,34 orthoclase.
- ✓ Potassium nepheline syenites contain % 5,77 muscovite, % 7,48 albite and % 8,68 orthoclase.
- ✓ It was determined that Sodium nepheline has a shrinkage onset temperature of 1100°C and that potassium nepheline syenite has a primary shrinkage temperature of 800°C, secondary shrinkage temperature of 1230°C and melting temperature of 1380°C.
- ✓ It was determined that Potassium nepheline syenite starts shrinking at a lower temperature in comparison with the orthoclase mineral and that it has a higher shrinkage ratio.
- ✓ It was observed after determining which nepheline syenite can be used according to the firing temperatures and firing regimes of ceramic products and carrying out studies for determining the ratios at which they can be used in recipes that nepheline syenites are more advantageous in comparison with feldspars.

References

1. Esposito L., Salemb A., Tuccia A., Gualtieri A., and Jazayeri S.H., The use of nepheline-syenite in a body mix for porcelain stoneware tiles. *Ceramics International*, 2005, 31, 233–240.
2. Tchakounte Bakop T., Tene Fongang R.T., Melo U.C., Kamseu E., Miselli P., Leonelli C., Sintering behaviors of two porcelainized stoneware compositions using pegmatite and nepheline syenite minerals. *J. Therm. Anal. Calorim.*, 2013, 114:113–123.
3. Coyle R.T., Shelby J.E., Vitko J., Lind M.A., Shoemaker A.F., Properties of a solar alumina-borosilicate sheet glass. *J. Non-Cryst. Solids*, 1980, 38–39, 133–238.

4. Karakaya M.Ç., Karakaya N., Systematic mineralogy. Selçuk University Faculty of Engineering-Architecture, 2007, Konya.
5. Haner S. and Demir M., Nepheline Syenite: A Review. *Journal of Geological Engineering*, 2018, 42, 107-120.
6. Matteucci F. Dondi M., Guarini: Effect of Soda-Lime Glass on Sintering and Technological Properties of Porcelain Stoneware Tiles. *Ceramics International*, 2006, Volume 28 number 8 2002 pp 873-880 by Elsevier Science limited access online march 3.
7. Durgut E., The production of appropriate raw materials for ceramic sector from Kırşehir Region nepheline syenite. Çanakkale Onsekiz Mart University, Graduate School of Natural and Applied Sciences, Mining Engineering Department, Master Thesis, 2018.
8. Bhattacharya, A., Optimization of firing parameters for ceramic wares by thermal analysis., *Journal of Thermal Analysis*, 1997, 49, 1365–1371.
9. Manfredini, T., Pennisi, L., Recent innovations in fast firing process, *Science of White ware*. The American Ceramic Society, Westerville, A.B.D., 1995, 213-223.
10. Heckroodt, R. O., Raw material selection in the quest for productivity., *Interceram*, 1990, 39, 16–17.
11. Salem, A., Jazayeri, S.H., Rastelli, E. and Timellini, G., Dilatometric Study of Shrinkage during Process for Porcelain Stoneware Body in Presence of Nepheline Syenite. *Journal of Materials Processing Technology*, 2009, 29, 124-126.
12. Klein, G., Application of feldspar raw materials in the silicate ceramics industry. *Interceram*., 2001, 50 (1-2), pp. 8-11.
13. Kumbasar I. and Akyol A., *Mineraloji*. İTÜ Publications, 1993, İstanbul.

DEVELOPMENT IN CERAMIC POWDER SYNTHESIS AND BORON BASED CERAMICS

Production of Magnesium Diboride Powder by Self Propagating High Temperature Synthesis

Şükrü Kaya¹, Murat Alkan¹

¹ Department of Metallurgical and Materials Engineering, Dokuz Eylül University,
Tınaztepe Campus, İzmir/Turkey

Even if MgB₂ is known comparatively for long time, its high T_c superconductivity was discovered recently. [Akimitsu], [Nagamatsu]. There are many production method to produce MgB₂ Powder. Some of these are: Synthesis of MgB₂ from elemental boron and magnesium by Autogenous Pressure Method (Mackinnon, 2014), batch process for the conversion of plasma synthesized boron powder into MgB₂ powder and Mg diffusion method (D. K. Finnemore and J. V. Marzik 2015), [J. M. Hur, K. Togano, A.\(2009\)](#) .

The main aim of this study is to determine of producibility of MgB₂ powders by Self-Propagating High Temperature Synthesis method which is a simple and low cost method. In this study, unlikely other SHS studies we tried to produce MgB₂ powder from relatively low-cost raw materials such as Mg and B₂O₃ rather than high purity elemental starting materials. This is also unique side of our study to achieve lower production cost.

EXPERIMENTAL STUDIES

Before beginning SHS experiments, some theoretical calculations were made to predict amount of required raw material, released energy and adiabatic temperature of SHS reactions by using HSC Chemistry 6.1 software.

After thermochemical calculations, the stoichiometric amount of B₂O₃ and Mg were used to produce MgB₂ product due to equation 1. B₂O₃ powders have a purity of 92.65 wt.% were brought from Ref-San AŞ. Mg powders have different particle size (0-75 µm, 75-150 µm 150-250 µm) were brought from Magnezyum ve Metal Tozları AŞ.



Mg and B₂O₃ powders were weighted (100 g) by using assay balance and mixed 15 minutes by using a mechanical mixer. SHS reactions were realized in a copper crucible. The crucible has an inner diameter of 60 mm and height of 200mm. SHS reactions were initiated by passing electricity throughout a resistance wire. A power supply of 7.5 kVA was used and reactions were initiated with 20V and 50A. The products were discharged from the crucible after cooling.

DTA analysis was carried out to find out the temperature of exothermic reactions. The characterizations of the products were realized by XRD techniques.

EXPERIMENTAL RESULTS AND DISCUSSIONS

In SHS method, reaction enthalpy is an important point to illustrate whether there is enough energy to reaction occur or not. Adequate heat should be occur to sustain reaction through the mixture. The specific heat value should be between 2250 J/g and 4500 J/g. The specific heat is calculated from dividing of the reaction enthalpy to total molecular weight of the products. If the specific heat is less than 2250 J/g, reaction doesn't propagate. And if this value excess 4500 J/g mixture could explode. After switch on power supplier, exothermic reaction began by resistance wire. After beginning of reaction, it became self-sustaining and self-propagating.

One of the most important features of a combustion process is the highest temperature of the combustion products that can be achieved called adiabatic temperature. The adiabatic temperature value (T_{ad}) which is an important indicator, determines if a reaction is a self-propagating or not. For a self-propagating reaction, the adiabatic temperature value should be higher than 1800 K (Z.A. Munir, U.A. Tamburini Mater. Sci. Rep., 3 (1989), pp. 277-365)

Due to the thermochemical calculations, the production reaction (Eq.1) has an adiabatic temperature of 2850, 65 K and specific heat of 3745 J/g.

DTA results was given in Fig.1 indicates that SHS reactions were realized after 633, 50°C. Also, with increasing in particle size, as illustrated Fig.2 and Fig.3 the initiation temperature is increased from 633,5°C to 666,15°C.

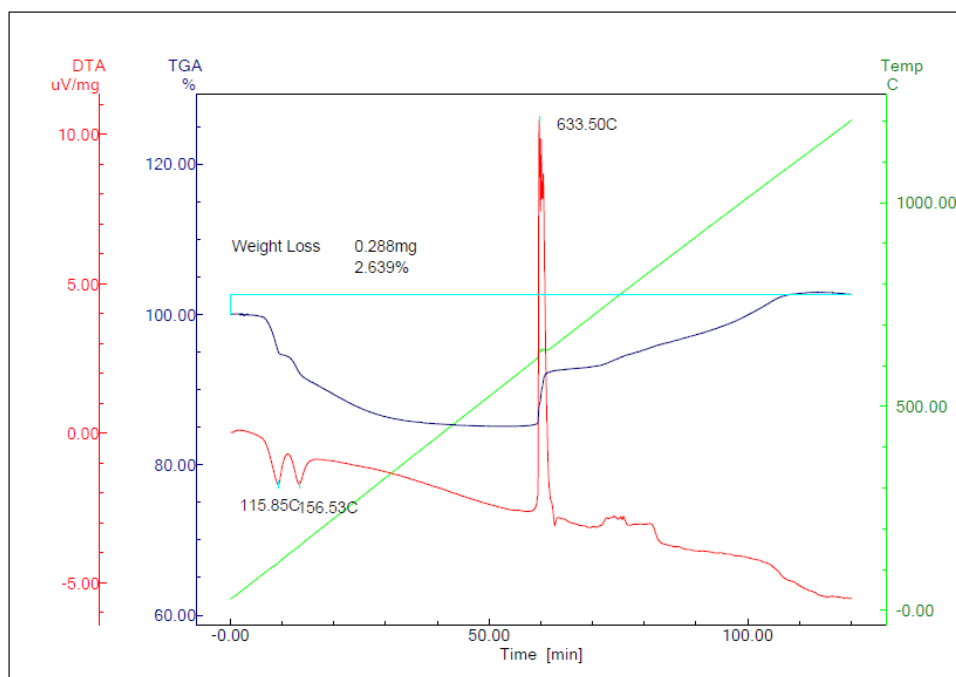


Figure 1. DTA result of SHS reaction of the mixture where 0-75 µm Mg and B₂O₃ were used

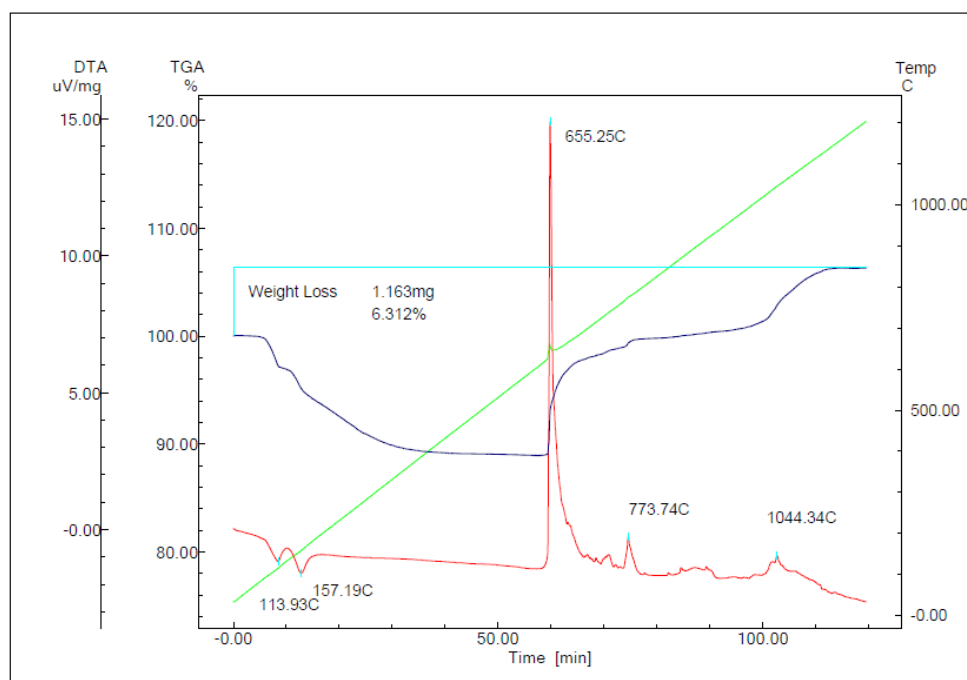


Figure 2. DTA result of SHS reaction of the mixture where 75-150 µm Mg and B₂O₃ were used

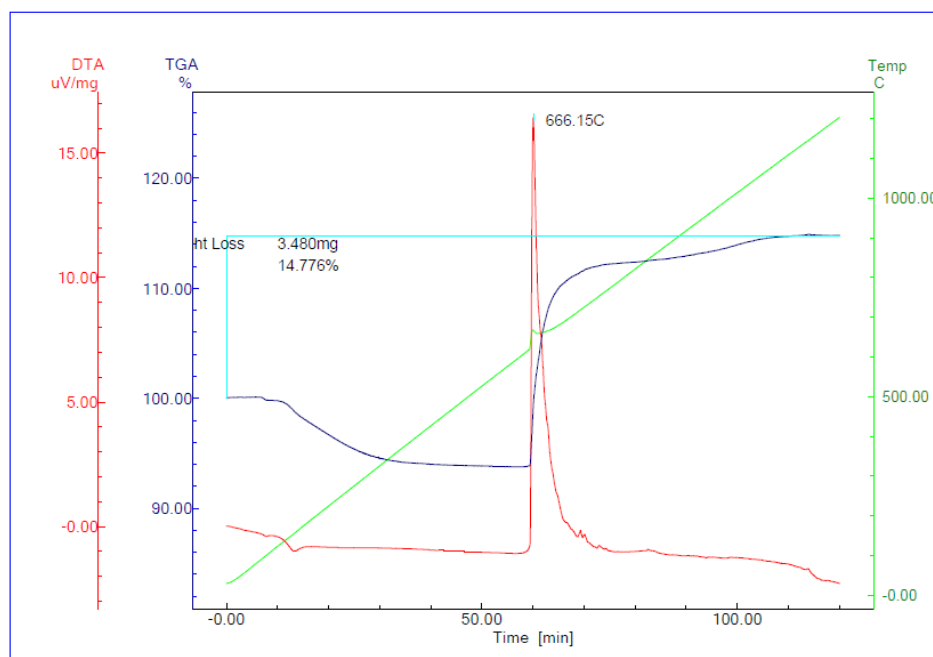


Figure 3. DTA result of SHS reaction of the mixture where 150-250 μm Mg and B_2O_3 were used

XRD results was given in Fig.4. indicates that the main SHS products were MgO and $\text{Mg}_3\text{B}_2\text{O}_6$. There are also some unreacted Mg and B_2O_3 phases were detected in XRD results. The XRD results of commercial MgB_2 powders was given in Fig.5. To determine whether MgB_2 powders were produced or not by SHS reactions, SHS products were leached by using HCl acid solutions.

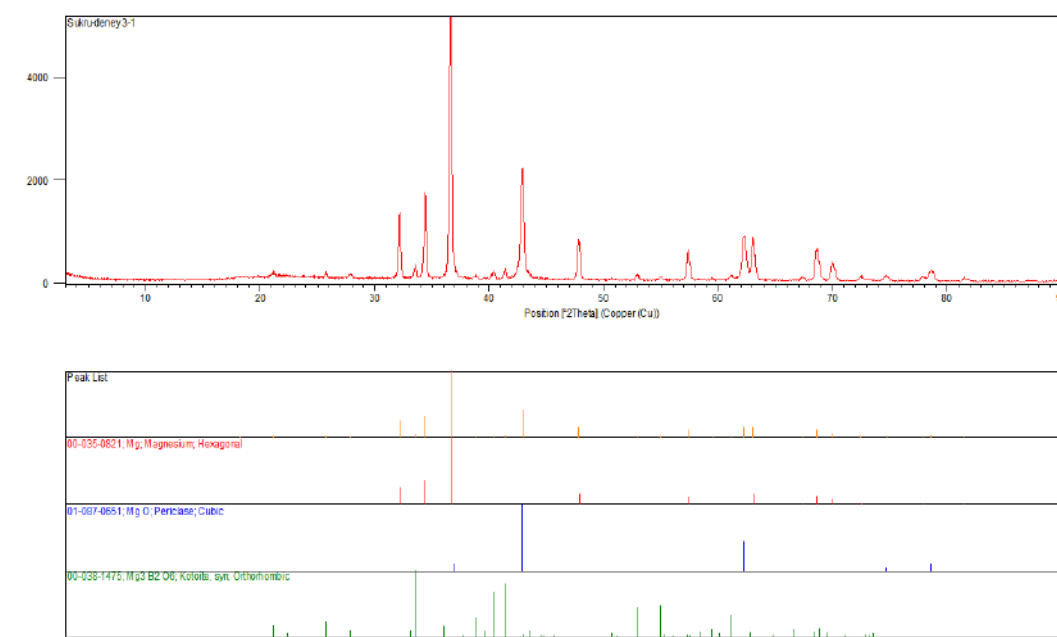


Fig.4. SHS products obtained from 0-75 μm Mg and B_2O_3 powder mixture

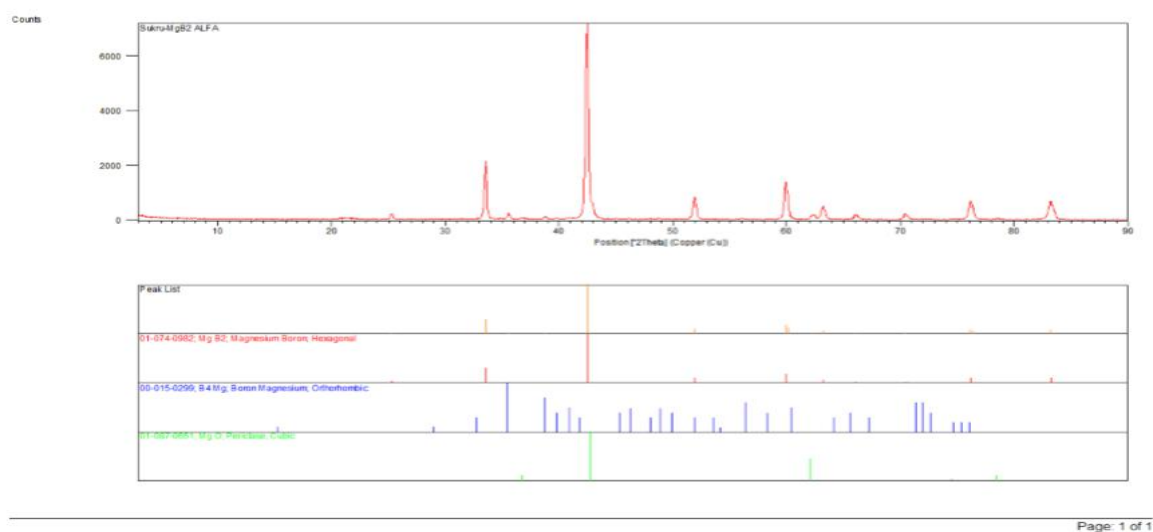


Figure 5. Commercial MgB_2 XRD patterns

XRD results of leached SHS products was given in Fig.6 there were a few amount of MgB_2 and MgB_4 phases detected in XRD results. The total dissolution of MgO and MgO containing by-product were not obtained. Due to the dissolution of MgB_2 by HCl acid solutions (Hao Zhu1, 2010), the using of acidic solutions are not suitable for MgB_2 containing products.

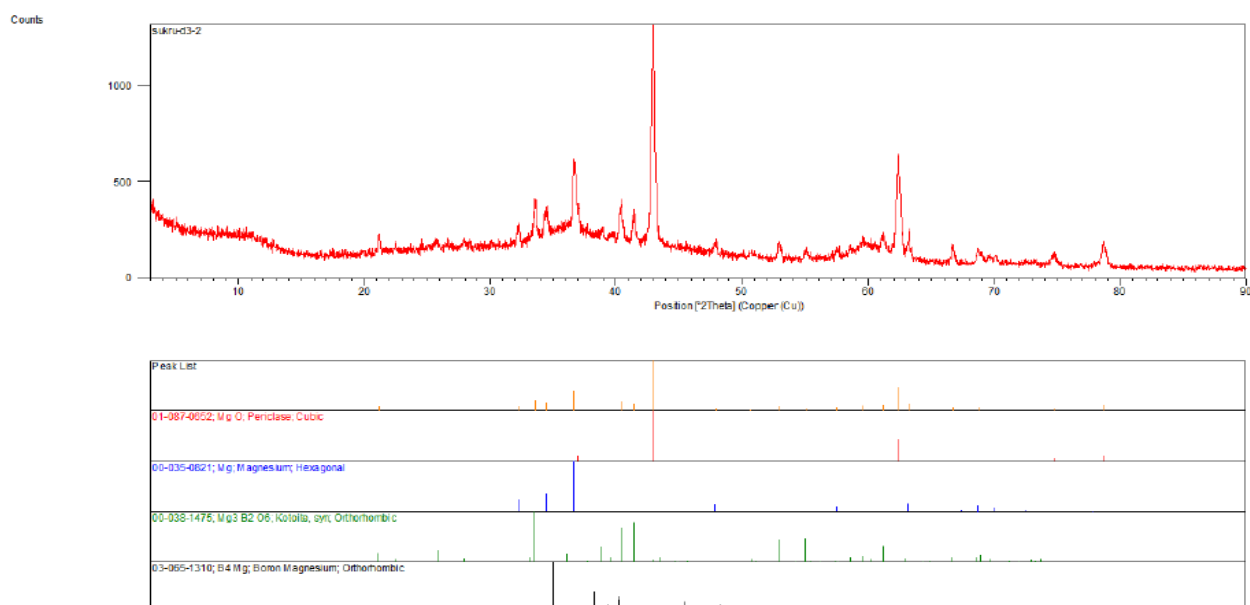


Fig.6. XRD patterns of leached SHS products obtained from 0-75 μm Mg and B_2O_3 powder mixture

CONCLUSION

In this study, production of MgB_2 powders were tried starting from a mixture of B_2O_3 and Mg containing raw materials. Leaching process was studied to purify of SHS products from MgO-containing byproducts.

Acid could trigger the decomposition of MgB_2 but in contrast to acid, alkali blocks the decomposition. Due to acid could accelerate the decomposition reactions, strong acids couldn't be used. Briefly, MgB_2 powder's degradation is limited in water. This study clearly indicates that HCl and other strong acids are not suitable for leaching and selective removal process.

In further studies, SHS reactions will be carried out under inert atmosphere. Also, some additives such as KClO_3 and NaClO_3 will be used to reach a completed SHS reactions. SHS reactions will be studied by using metallic Al powders and Al-Mg mixed powders followed by leaching with alkaline solutions.

References

- Bouquet F, Fisher R A, Phillips N E, Hinks D G and Jorgensen J D 2001 Phys. Rev. Lett. 87 047001
- Tu J J, Carr G L, Perebeinos V, Homes C C, Strongin M, Allen P B, Kang W N, Choi E-M, Kim H-J and Lee S-I 2001 Phys. Rev. Lett. 87 277001
- Qing-rong Feng^{1*}, Chinping Chen¹, Jun Xu^{1, 2}, Ling-wen Kong¹, Xiu Chen¹, Yong-zhong Wang¹, and Zheng-xiang Gao¹ (2015) *Study on the formation of MgB_2 phase*. [Online]. Available at: <https://arxiv.org/ftp/cond-mat/papers/0309/0309615.pdf> (Accessed: 8th october 2018).
- Ian D. R. Mackinnon (2014) 'Synthesis of MgB_2 at Low Temperature and Autogenous Pressure', *Materials*, (), pp. .
- T. A. Prikhna, Ya. M. Savchuk, (2014) 'SYNTHESIS AND SINTERING OF MgB_2 UNDER HIGH PRESSURE', *Indian Journal of Pure & Applied Physics*, 4(), pp. 461-467.
- ~~D K Finnemore and J V Marzik (2015) 'Synthesis of nanoscale magnesium diboride powder', *ICMC*, 4(), pp.~~
- [D K Finnemore and J V Marzik \(2015\) 'Synthesis of nanoscale magnesium diboride powder', *IOP Conf. Series: Materials Science and Engineering* 102 \(2015\), \(\), pp. .](#)
- [Hao Zhu, Shumao Wang, Zhinian Li, Xiaopeng Liu, Lijun Jiang \(2010\) 'Degradation Behavior of \$\text{MgB}_2\$ Powders in Different Medium Environment', *Materials Science Forum*, \(\), pp. .](#)
- [J. M. Hur, K. Togano, A. Matsumoto, H. Kumakura H. Wada, K. Kimura \(2009\) 'Fabrication of high performance \$\text{MgB}_2\$ wires by an internal Mg diffusion process', , \(\), pp. 3-4.](#)

LEAD-FREE, TEXTURED & EPITAXIAL PIEZOELECTRICS / FERROELECTRICS & OTHER ELECTROCERAMICS

LIGHTWEIGHT BULLETPROOF VESTS: HOT-PRESSED BORON CARBIDE FOR BALLISTIC PURPOSES

İrem Duru ¹, Savaş Özkaya ², Mert Akıncı ³, Burcu Ertuğ ⁴

^{1,2,3} Department of Mechanical Engineering, Nişantaşı University, Maslak Mahallesi Söğütözü Sk. No:20/Y Maslak 1453 Neotech Campus, Sarıyer, 34398 Istanbul, Turkey.

⁴ Department of Mechatronics Engineering, Nişantaşı University, Maslak Mahallesi Söğütözü Sk. No:20/Y Maslak 1453 Neotech Campus, Sarıyer, 34398 Istanbul, Turkey.

Abstract

The military, police and government special forces commonly use lightweight bulletproof vests. From 2018 to 2021, US Army will replace a new modular scalable vest particularly while deployed, instead of the ones used today. Fully loaded with its ballistic plates, the weight of the vest is about 11 kg. Marine Corps is also in a race with US Army to make the load lighter for the personnel. Carbide ceramics such as boron carbide (B_4C), silicon carbide (SiC), tungsten carbide (WC) are common armour ceramics. High hardness, modulus of elasticity and relative density are the necessary characteristics for the ballistic efficiency. Fully dense B_4C can only be produced by Hot-pressing technique, by using fine starting powders and the addition of sintering additives. Sintering temperatures above $2470^\circ C$ is also required to obtain full density B_4C . Ballistic tests indicate that the areal density of B_4C ceramics is the lowest among other armour ceramics. In addition to low density and excellent mechanical properties, B_4C provides weight reduction of 20% in comparison to SiC . However, the cost of B_4C tile is four times higher than SiC . As a result, the production parameters have got a deep effect on the microstructure and mechanical properties of B_4C based bulletproof vests. In order to improve the ballistic efficiencies of B_4C armour ceramics, it is more than necessary to fully understand the relationship between the microstructure and the mechanical properties. In the present study, recent hot-pressing studies related to B_4C armour ceramics and corresponding characterization results will be introduced.

Key words: Hot pressing, boron carbide, ballistic, armor.

1. INTRODUCTION

NIJ Standard-0101.06 indicates that the armors can withstand different levels of energy between Type I and Type IV against 22 long rifle and 38 ACP armor piercing rifle rounds [1].

In general, Level IV ballistic armors are used against large and high velocity bullets as in the military. These armors are made up of some types of ceramic and can stop rounds fired by rifles and submachine guns [2].

When a bullet hits the body, only a small area is exposed to high energy in a very fast manner. Bullet proof vests are used to absorb this high energy only the small area and to disperse it over a larger area of the body during a longer time. Even still causing injury, the body is damaged much less instead of bullets penetrating the internal organs. That is the reason why bullet proof vests are utilized [3].

In terms of hardness, boron carbide (B_4C) is after diamond and cubic boron nitride and is known to be one of the hardest materials. However, sintering aids must be added into boron carbide to reach full density during sintering due to the low sinterability. Typical characteristics of boron carbide are low

density, high compressive strength and elastic modulus, low thermal conductivity and most important of all, extreme hardness[4].

Table 1 shows some of the main properties of boron carbide. As the main applications, boron carbide is used as abrasives, in polishing and lapping, in nozzles, for slurry pumping, grit blasting, and water jet cutters due to the wear and abrasion resistance as well as an absorbent material for neutron radiation purposes in nuclear power plants. Body armor, application combines hardness, compressive strength, high elastic modulus and low specific density properties [4].

Table 1 Physical and mechanical properties of hot-pressed boron carbide [4]

Property	Value range
Density (g cm^{-3})	2.45-2.52
Apparent porosity (%)	< 3
Compressive strength (MPa)	1400-3400
Hardness, Knoop (kg. mm^{-2})	2800-3500
Hardness, Vickers (kg. mm^{-2})	3200
Shear strength (MPa)	210-380
Tensile modulus (GPa)	440-470

Recently, the usage of armors has become more military personnel. These which are inserted into ballistic vests, thus they provide 50% reduction in weight. Furthermore, they are able to indicate a protection greater than previous products, or equal protection at the worst case. These armors can be produced in order to fit to the body in a better way, which then increases the performance and life saving chance [5].

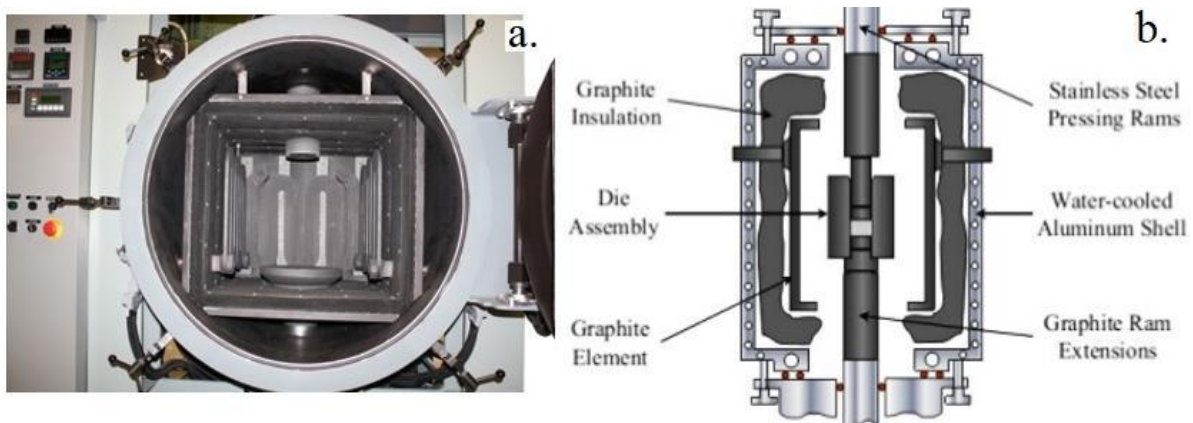


Figure 1 a. Hot zone of a hot press [6], b. Image of a hot press furnace [7].

The lightweight bulletproof vests are often used by the military, police and government special forces. Till 2021, US Army will have changed the previous vests with their newly developed ones. Fully loaded with its ballistic plates, this new vests will be quite lightweight. Marine Corps are also working on to make the load lighter for the personnel [8].

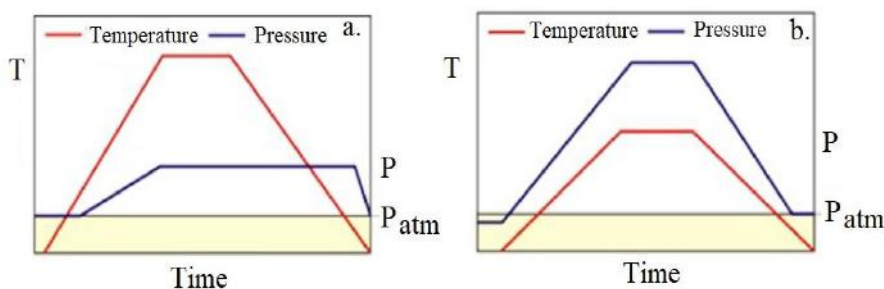


Figure 2 a. and b. Sintering procedure examples for hot-pressing [9].

Hot-pressing is the only method to produce the most dense B_4C with the usage of fine starting powders and also sintering additives as shown in Fig.1. Very high sintering temperatures are also required. Sintering temperatures and times in some hot-pressing examples are shown in Fig.2. According to the ballistic performance tests, boron carbide gives the best result in comparison to other armour ceramics. Despite the weight reduction provided by B_4C in comparison to SiC , the cost is four times higher for boron carbide than SiC . The hot-pressing parameters affect the mechanical properties of bulletproof vests made of B_4C greatly [4].

The relationship between the microstructure and the mechanical properties is quite important for the ballistic efficiencies of B_4C armour ceramics. In the present study, recent hot-pressing studies related to B_4C armour ceramics and corresponding characterization results will be introduced.

2.HOT PRESSING AND CHARACTERIZATION OF BORON CARBIDE

One of the very recent studies on hot pressed boron carbide, the microstructure of samples sintered by hot pressing (HP) has been observed to be very homogeneous and has a relative density of about 91%. In this study, using another method, Spark Plasma Sintering (SPS), a high relative density over 94% has been determined. Zhang et al. tested the mechanical properties after SPS sintering and have found that these are superior to those sintered by HP due to the heterogeneous microstructures [10].

After hot pressing under a pressure of 100 MPa at a low temperature of 1800°C, high hardness, fracture toughness and flexure strength have been determined with the grain sizes between 70 nm and 1.6 μm . Before hot pressing, high-energy ball milling has been used to prepare ultrafine particle sizes in the range of a few nanometres and a few hundred nanometres. No sintering aid has been used during the sintering process. Transgranular and intergranular fracture modes have been observed together as a result of the co-existence of small and large grains, which in turn has increased the fracture toughness to 4.41 $MPa \cdot m^{1/2}$. The relative density, Vickers hardness and flexure strength values have been measured to be 99.5%, 41.3 GPa and 564 MPa, respectively [11].

Alexander et al. used graphene nano-platelets (GNP) as reinforcement for B_4C based composites, which has improved the density of the composite acting as the sintering aid. 2 vol% of GNP has increased hardness and elastic modulus. The indentation and single edge notch bend (SENB) methods have showed the fracture toughness has reached up to 5.41 $MPa \cdot m^{1/2}$ and 4.52 $MPa \cdot m^{1/2}$ with 10 vol% of GNP [12].

An application of the pressures in the range of 30-110 MPa indicated that the plastic deformation is the predominant densification mechanism under high pressure. Since the grain growth is easy with reduced pores, grain size has increased with increasing pressure, also with increasing soaking time. Inversely, Vickers hardness and fracture toughness have increased with grain refinement. By applying a pressure of 100 MPa during hot pressing, relative density, grain size, Vickers hardness and fracture toughness values have been measured to be 99.73%, 1.96 μm , 37.85 GPa and 3.94 $MPa \cdot m^{1/2}$, respectively [13].

A ceramic particulate composite consisting of Al_2O_3 with 15 vol% SiC and 15 vol% B_4C has been produced at 1650°C with full density. This composite has showed a strength, Vickers hardness and fracture toughness of 880 MPa, 21 GPa and $4.5 \text{ MPa m}^{1/2}$, respectively. Resulting from the thermal expansion mismatch of Al_2O_3 matrix and SiC/ B_4C reinforcement, some microcracks have formed at the grain boundaries [14].

Recently, Kovalcikova and co-workers have produced B_4C based composites using 4-10 wt% of graphene platelets as sintering aids. Hot pressing has been carried out at 2100°C , resulting in a bending strength of 398 MPa and a fracture toughness of $5.89 \text{ MPa m}^{1/2}$. The crack deflection, crack branching and crack bridging have been proposed as the main toughening mechanisms as the reason for high fracture toughness obtained [15].

Kumar et al. used 0.001 Pa vacuum atmosphere to produce hot pressed boron carbides samples at a sintering temperature of $1700\text{-}1900^\circ\text{C}$ under the pressures of 30-50 MPa. An addition of MoSi_2 powder of 10 and 30 wt% has resulted in MoSi_2 and B_4C reaction to form SiC, MoB_2 and Mo_2B_5 . Highly dense B_4C and 30 wt% MoSi_2 samples have indicated that the hardness, elastic modulus and fracture toughness values to be 35.1 GPa, 555 GPa and $4.8 \text{ MPa m}^{1/2}$, respectively [16].

3. RECENT BALLISTIC PERFORMANCE TESTS

A recent study has carried out the simulation of a simplified ballistic impact in order to evaluate the ballistic performance of B_4C tiles with an addition of molybdenum disilicide powder in the range of 10 and 30 wt%. Hard steel armor piercing (AP) projectile of 12.7mm caliber has been used in the standard depth of penetration (DOP) test where the projectile velocities have been taken as 700-825m/s [17].

B_4C has also been used as the reinforcement in Al 6061-based metal matrix composites in the range of 5-20 wt%. Transgranular fracture in B_4C reinforcement particles has been detected in these composites after mechanical testing. Hardness, transverse rupture strength and tensile strength have increased with B_4C reinforcement whereas the impact toughness has decreased. Following the mechanical tests, a ballistic test with a $7.62 \text{ mm} \times 51 \text{ mm}$ M80 projectile for Type III has been made in which the ballistic resistance has been evaluated by analyzing the hole surface in the armor composite. As a result, a petal failure mechanism has been detected with a ductile behaviour. standard depth of penetration (DOP) has been low since the samples have absorbed the impact energy of the bullet [18].

Savio and co-workers very recently, have examined the failure mechanism of 7.62 mm AP projectile which has impacted the boron carbide tiles. This has been carried out by the post-ballistic study of projectiles. These researchers have concluded that the failure of the projectile has originated from two locations; initially, the target interaction front of the projectile and secondly, a location near the tail end of the projectile. These two failures have resulted from the harsh deformation at the interaction front in the first case; and from the stress wave generated micro-cracks in the latter. The tile thickness and projectile velocity (600-820 m/s) factors have also been observed for the failure mechanism [19].

A novel composite ballistic armor system developed by Garcia-Avila and co-workers has been produced in multi-layer structure; with a strike face of boron carbide, a kinetic energy absorber interlayer made up of metal foam and the backplates made of Aluminum 7075 or Kevlar™ panels, which can be seen in Fig.3. This newly developed system has had a total armor thickness of about 25 mm. Applying U.S. National Institute of Justice (NIJ) standard 0101.06, a ballistic test has been carried out against $7.62 \times 51 \text{ mm}$ M80 and $7.62 \times 63 \text{ mm}$ M2 armor piercing projectiles. It has been showed that 60-70% of the total kinetic energy of the projectiles has been absorbed by the composite metal foams which have acted as the interlayer. During the ballistic test, this armor system has stopped the projectiles. Standard depth of penetration (DOP) and backplate deformation have been low [20].

Another armor system has been developed to consist of two layers; boron carbide layer and Kevlar 49 fiber composite layer. An analysis of a projectile penetration in composite armor has been made by the simulation of penetration process. The type of projectile impacts to armor has been simulated and it has been showed that with oblique impact type, the ballistic limit velocity of armor has increased. Normal and oblique impacts of projectile have been compared for the particular armor system [21].

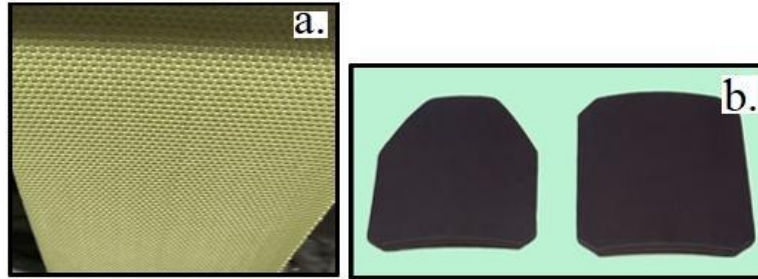


Figure 3 a. Bulletproof Kevlar 49 Aramid fiber fabric [22], b. Boron carbide armor plates [23].

Orphal has recently used flash X-rays to examine the penetration into the boron carbide. Also, by using the penetrator-target interaction, the speed of penetration into the target and consumption rate of penetrator were determined [24].

Hogan has explored the impact fragmentation of boron carbide and has found that different fragmentation mechanisms take place in the targets. Using Scanning Electron Microscope (SEM), the cracks parallel and perpendicular to the impact direction have been detected. He has concluded that by controlling the fragment size and shape of the boron carbide targets, next-generation advanced ceramics for personal protection can be designed [25].

4.CONCLUSION

1. Highly dense B_4C compacts had a relative density of 99.5-99.7%.
2. Vickers hardness, flexure strength and elastic modulus of the samples were 35-41 GPa, 564 MPa and 555 GPa, respectively. Fracture toughness values were 4.4-4.8 $Mpa \cdot m^{1/2}$.
3. The simulations of penetration process were done. From the views of the penetrator-target interaction, the relevant data were determined. Experimental data and simulation results were compared.
4. Due to impact failure of boron carbide targets, different fragmentation mechanisms were observed.
5. It was concluded that by controlling the fragment size and shape in boron carbide targets, the design of next-generation advanced ceramics for personal protection can be made possible.

REFERENCES

- [1] Ballistic Resistance of Body Armor NIJ Standard-0101.06, Prepared for: National Institute of Justice Office of Science and Technology Washington, DC, July 2008.
- [2] <https://www.safeguardclothing.com/articles/protection-types-breakdown/>
- [3] <https://www.emsworld.com/article/12244254/body-armor-injuries-expect-the-unexpected>
- [4] Everitt P. and Doggett I., Ceramic Carbides: The Tough Guys of the Materials World, Goodfellow Ceramic and Glass Division c/o Goodfellow Corporation, Coraopolis, Pa.

- [5] Opportunities in Protection Materials Science and Technology for Future Army Applications, Chapter: Appendix E: Processing Techniques and Available Classes of Armor Ceramics The National Academies of Sciences, Engineering, and Medicine, 2018.
- [6] <http://thefurnacesource.com/portfolio-item/50-ton-vacuum-hot-press-2/>
- [7] Behera S.K., Solid State Lecture notes, Department of Ceramic Engineering, NIT Rourkela.
- [8] <https://www.bodyarmornews.com/marine-corps-awards-contract-for-lighter-weight-body-armor-to-better-fit-all-marines/>
- [9] Prof. Jakob Kübarsepp, Technology of full density powder materials and products, Institute of Materials Engineering, Tallinn University of Technology.
- [10] Zhang X., Zhang Z., Wen R., Wang G., Zhang X., Mu J., Che H., Wang W., Comparisons of the densification, microstructure and mechanical properties of boron carbide sintered by hot pressing and spark plasma sintering. *Ceramics International*, 2018, 44, 2615-2619.
- [11] Zhang X., Zhang Z., Nie B., Chen H., Wang G., Mu J., Zhang X., Che H., Wang W., Ultrafine-grained boron carbide ceramics fabricated via ultrafast sintering assisted by high-energy ball milling. *Ceramics International*, 2018, 44, 7291-7295.
- [12] Alexander R., Murthy T.S.R.Ch., Ravikanth K.V., Prakash J., Mahata T., Bakshi S.R., Krishnan M., Dasgupta K., Effect of graphene nano-platelet reinforcement on the mechanical properties of hot pressed boron carbide based composite. *Ceramics International*, 2018, 44, 9830-9838.
- [13] Zhang X., Gao H., Zhang Z., Wen R., Wang G., Mu J., Che H., Zhang X., Effects of pressure on densification behaviour, microstructures and mechanical properties of boron carbide ceramics fabricated by hot pressing. *Ceramics International*, 2017, 43, 6345-6352.
- [14] Neuman E.W., Hilmas G.E., Fahrenholtz W.G., A high strength alumina-silicon carbide-boron carbide triplex ceramic. *Ceramics International*, 2017, 43, 7958-7962.
- [15] Kovalčíková A., Sedlák R., Rutkowski P., Dusza J., Mechanical properties of boron carbide-graphene platelet composites. *Ceramics International*, 2016, 42, 2094-2098.
- [16] Kumar S., Sairam K., Sonber J.K., Murthy T.S.R.Ch., Reddy V., Nageswara Rao G.V.S., Rao T.S., Hot-pressing of MoSi_2 reinforced B_4C composites. *Ceramics International*, 2014, 40, 16099-16105.
- [17] Savio S.G., Madhu V., Effect of tile thickness and projectile velocity on the ballistic performance of boron carbide against 12.7 mm AP. *Procedia Engineering*, 2017, 173, 286-292.
- [18] Karakoç H., Karabulut Ş., Çıtak R., Study on mechanical and ballistic performances of boron carbide reinforced Al 6061 aluminum alloy produced by powder metallurgy. *Composites Part B: Engineering*, 2018, 148, 68-80.
- [19] Savio S.G., Senthil P., Singh V., Ghoshal P., Madhu V., Gogia A.K., An experimental study on the projectile defeat mechanism of hard steel projectile against boron carbide tiles. *International Journal of Impact Engineering*, 2015, 86, 157-166.
- [20] Garcia-Avila M., Portanova M., Rabiei A., Ballistic performance of composite metal foams. *Composite Structures*, 2015, 125, 202-211.

[21] Shokrieh M.M., Javadpour G.H., Penetration analysis of a projectile in ceramic composite armor. *Composite Structures*, 2008, 82, 269-276.

[22] <https://www.globalsources.com/si/AS/Yixing-T-Carbon/6008850596340/Homepage.htm>

[23] <http://www.bulletproofindia.com/BULLET%20PROOF%20HARD%20ARMOR%20PLATE.htm>

[24] Orphal D.L., Franzen R.R., Charters A.C., Menna T.L., Piekutowski A.J., Penetration of confined boron carbide targets by tungsten long rods at impact velocities from 1.5 to 5.0 km/s. *International Journal of Impact Engineering*, 1997, 19, 15-29.

[25] Hogan J.D., Farbaniec L., Mallick D., Domnich V., Kuwelkar K., Sano T., McCauley J.W., Ramesh K.T., Fragmentation of an advanced ceramic under ballistic impact: Mechanisms and microstructure. *International Journal of Impact Engineering*, 2017, 102, 47-54.

SANITARYWARE

USING of VARIOUS AMORPHOUS SILICATES in MANUFACTURING of LIGHTWEIGHT SANITARYWARE PRODUCTS

B. İdil Özcan¹, Sevil Yücel², H. Aygül Yeprem¹

¹ Yildiz Technical University, Faculty of Chemistry- Metallurgy, Department of Metallurgical and
Materials Engineering, Davutpaşa Campus, 34220/İstanbul/Turkey

²Yildiz Technical University, Faculty of Chemistry- Metallurgy, Department of Bioengineering,
Davutpaşa Campus, 34220/İstanbul/Turkey

ABSTRACT

In this study, instead of quartz, lightweight amorphous silicate and lightweight amorphous calcium silicate materials used for preparation of sanitary ware products and it is aimed to develop a product which have desired properties in the view of design. In the case of sanitaryware products, it is desirable that the product is lightweight and having thinner wall thickness and durable. In the experimental study, Fine Fire Clay (FFC) slurry mostly preferred in sanitaryware products was used with the addition of amorphous silicates with different ratios. The mixing process was carried out with the addition of silicate and calcium silicate in the ratio of 4% and 6% in solid FFC mixture. The casting process of the slurries carried out and the wall thickness of the samples were measured. The samples were sintered at 1250 °C for a certain time. The samples were subjected to water absorption tests and wall thicknesses and weights of samples measured. From the point of change in wall thickness (45%), change in weight (33.60%) and the water absorption (8.67%) the sample which contains %6 amorphous silicate showed the best results. It is observed that amorphous silicates are more successful than amorphous calcium silicates in sanitaryware products.

Keywords: Amorphous Silica, FFC, Sanitaryware, Calcium Silica.

1. INTRODUCTION

It's a known fact that ceramic sanitaryware products are important materials in our daily life. Production of these products in larger sizes with desired dimensions is an issue that manufacturers face. [1, 2] The shrinkage and deformation of large sized sanitaryware products have some risks during the production stage. There are studies related to reducing these risks for the production, sanitaryware products without faults. [3, 4]

In general, sanitary wares are produced by mixing inorganic raw materials such as clay, quartz, kaolin and feldspar into a fluid slurry by mixing with a certain amount of water and then shaping the slurry by suitable methods and sintering it at a temperature of 1200-1250 °C. In the design of the sanitary ware ceramic products, it is desired that the product is light in weight, the wall thickness is thin and the strength is high. These properties are provided by the proportions of the raw materials that contained in the ceramics.

Some amorphous silicas produced by the sol-gel method are high porosity (%85-99.8), low density (as low as 0,003 g/cm³) materials [5, 6]. These are materials with unusual properties such as high specific surface area (up to 1200 m²g⁻¹), very low thermal conductivity (0.01 W/m.K), dielectric constant (1.1) and refractive index (1-1.05) [7]. Due to these properties, amorphous silicas have various uses.

Monolithic amorphous silicas are used as Cherenkov detectors due to their optical properties such as low refractive index and transparency. Thanks to their high porosity and low density properties, they are used as catalyst, sensor and adsorbent [8]. It is also possible to use them as thermal and sound insulation materials [9, 10].

Clays are hydrated aluminum silicates which are generally containing the base metals such as iron, alkali and alkaline earth metals. They have very fine grain size and they acquire plastic properties with the addition of water [11]. Kaolin is usually comprise of the result of feldspar degradation. They include other clay minerals such as iron, feldspar and quartz, at varying rates [12]. Because it has a larger particle size than other ceramic raw materials and it has less cation exchange capacity due to its purity and therefore the plasticity value of kaolin is lower than the other ceramic raw materials. Because of these properties, kaolin acts as a skeleton in ceramic structures and keeps the raw materials together [12]. Feldspars are non-plastic raw materials. Although the feldspars are in the class of non-plastic raw materials, when they reach a certain sintering temperature in the mud, they clump up the mud and become slag [13]. Quartz constitutes 25% of the known part of the earth crust (The chemical formula of quartz is SiO_2). It increases the pore volume and the amount of water absorption in sintered clay and reduces the ability of binding of the mud [14].

Three different bodies which are vitreous china, fire clay and fine fire clay bodies are popular for production of sanitaryware products [15]. In the sanitary ware products, large sized products are cast with slurries containing high clay content, which is known as FCC [16]. Approximately, a characteristic FCC slurry consists of; 3% Feldspar, 18% Quartz, 15% Clay, 20% Kaolin and finally 31% Fireclay [12]. Sanitaryware manufacturers in Turkey are known to use the fireclays in the range of 30-35% in FCC slurries. Fireclay gives resistance to the sanitaryware products and minimizes deformation behavior [16].

This study was carried out to alleviate the sanitaryware products and to decrease the wall thicknesses. It is based on to improve the design of the sanitaryware products. For this purpose, FCC slurries containing 4% and 6% amorphous light silica and 6% amorphous light calcium silica were prepared. After casting and sintering, water absorption, wall thickness and weight analysis were performed.

2. EXPERIMENTAL STUDY

2.1 Raw Materials

The raw materials used in the experiments were supplied through Duravit A.Ş. These raw materials are clay, kaolin, quartz, potassium feldspar and wollastonite respectively. The manufacturers of the raw materials was given in Table 1. Amorphous silica and amorphous calcium silica were produced at the Lipid and Composite Laboratories of the Department of Bioengineering, Yıldız Technical University.

Table 1. Raw materials and their manufacturers

Raw Materials	Manufacturer
Fireclay	Kaolin AD
Quartz	Matel A.Ş.
K-Feldspar	-
Wollastonite	Matel A.Ş.
K-2 Kaolin	Kaolin AD
MASK6 Clay	Matel A.Ş.

2.2 Preparation of FCC Slurries

The raw materials were mixed with water and sodium silicate at a certain ratio according to the FFC slurry prescriptions, and the slurry was obtained. Slurries coded as Reference, N1, N2, N3. Table 2 shows the amount of amorphous silica and amorphous calcium silica contained in these slurries.

Table 2. Amounts of amorphous silica and amorphous calcium silica in slurries (%)

Raw Materials	Reference	N1	N2	N3
Amorphous Silica (%)	-	4	6	-
Amorphous Calcium Silica (%)	-	-	-	6

In Table 3 the amounts of water and sodium silicate used during the preparation of the slurry were given and compared with TSE EN 997+A1 standards. As can be seen from this table, the amounts of water and sodium silicate used increased as the ratio of amorphous silica in slurry increased.

Table 3. Amounts of water and sodium silicate in slurry (%)

	Reference	N1	N2	N3	Standard
Amount of water (% wt.)	34,5	45	52	62,05	35
Amount of Sodium Silicate (% wt.)	0,24	0,26	0,29	0,29	0,15-0,25

2.3 Characterization of Silicas

BET analysis of amorphous silica and amorphous calcium silicate raw materials were performed. The surface area, pore size, micropore volume, mesopore volume and single point total pore volume of the amorphous silicas were analyzed using a Specific Surface Area and Pore Size Distribution Analyzer (Micromeritics, TriStar II 3020) at 77 K. The Brunauer-Emmett-Teller (BET) method was used to estimate the specific surface area of amorphous silica and amorphous calcium silica. Pore size and pore volume was calculated using Barrett-Joyner-Halenda (BJH) method. The tapping density was evaluated as described by Temel et al. [6]

2.4 Rheology of Slurries

The density, thixotropy and viscosity of the prepared slurries were measured based on TSE EN 997+A1 standards. Density is the weight of the slurry in a 1 liter container. The amount of sodium silicate and the raw material types forming the slurry are two important factors that determine density of the slurry. Determination of the solid /liquid ratio in the slurry and the compliance with the standards are ensured by measuring density of the slurry. The universal torsion viscometer Gallenkamp is one of the most used instruments in the ceramic field for rapid measures of suspensions viscosity and thixotropy. Manually operated. During the test the disk was rotated by 360°C and then released, the braking effect of the sample on the outer part of the cylinder was used to measure viscosity. The thixotropy was value is determined making a second measurement after 5 minutes (in which the sample remained in a static condition), and was calculated the difference respect to the first measure.

2.5 Sintering and Drying Processes

The samples were air dried for 24 hours. Then, samples sintered at 1250 °C. These processes were performed according to TSE EN 997+A1 standards. Sintering regime was given below:

From 40 °C to 800 °C, 160°C / hour temperature increase,
From 800 °C to 1250°C, 180°C/hour temperature increase,
Soaking 30 minutes at 1250 °C,
From 1250°C to 40 °C uncontrolled cooling.

2.6 Water Absorption Test

Water absorption tests were carried out according to TSE EN 997+A1 standards. According to these standards, first, the dry weights (G_1) of the samples were measured. Then, the samples were boiled in distilled water for 2 hours. After the boiling process finished, the samples were left in the water for 20 hours. After the process completed, the surface of the samples were dried and their weights (G_2) measured again.

$$\text{Water adsorption\%} = \frac{(G_2 - G_1)}{(G_1)} \times 100$$

2.7 Wall Thickness and Weight Analysis

Wall thickness and weight analysis were carried out according to TSE EN 997+A1 standards. For the wall thickness analysis, the samples were first poured into a mold by the slip casting method. After casting process, the samples were hold in the mold for 1 hour. The samples were removed from the mold and then the wall thicknesses were measured. After drying and sintering processes, the wall thicknesses were measured again and compared with each other. For the weight analysis, the samples wet, dry and sintered weights were measured and compared with each other.

3. EXPERIMENTAL RESULTS

Table 4 shows the relative rheological properties of slurries. As can be seen from Table 4 the slurries are in accordance with the TSE EN 997+A1 standard except the sample containing amorphous calcium silicate (N3).

Properties	Reference	N1	N2	N3	Standard
Density (g/L)	1784	1785	1786	1237,9	1785-1795
Thixotropy ($^{\circ}$)	92	91	90	31	80-110
Viscosity (s)	24	28	32	No flow	24-30

Table 4. Rheologic properties of slurries

The properties of amorphous silica and amorphous calcium silica used in the experiments were given in Table 5. As can be seen here, amorphous silicas attract less water, with greater surface area and density than the amorphous calcium silica.

Table 5. Properties of Amorphous Silica and Amorphous Calcium Silica

Properties	Amorphous Silica	Amorphous calcium silica
Bulk density (g/cm ³)	0,187	0,182
Tap density (Tap) (g/cm ³)	0,249	0,243
Surface area (m ² /g)	242	80
Water adsorption (%)	20	40

The wet, dry and sintered weights of the samples were given in Table 6. It was observed that the weight of the samples, obtained by the addition of amorphous silica and amorphous calcium silica, decreases compared with reference sample.. Increasing the amount of amorphous silica added resulted in a further reduction of sample weights.

Table 6. Wet, dry and sintered weights of samples

Weight (g)	Reference	N1	N2	N3
Wet	270,40	203,00	178,30	232,50
Dry	248,00	181,30	158,20	211,20
Sintered	206,70	158,10	137,10	165,30

According to Table 7, it was observed that the weight change (20%) by calcium amorphous silica addition in sintered sample was less than the weight change (33,6%) by amorphous silica addition. From here, it can be said that amorphous silicas are more successful in alleviating the product than amorphous calcium silicas.

Table 7. Changes of weight (%) according to reference sample after drying and sintering

Change in weight (%)	N1	N2	N3
Wet	24,90	34,00	14,00
Dry	26,80	36,20	14,80
Sintered	23,50	33,60	20,00

The wet, dry and sintered wall thicknesses of the samples were given in Table 8. As amorphous silica ratio in sample increased, a slightly decrease in the wall thicknesses were observed. Calcium amorphous silica reduced the wall thickness of the material to a lesser extent than the amorphous silica. According to these results, it was decided that amorphous calcium silica should not be used in later experiments.

Wall Thickness (mm)	Reference	N1	N2	N3
Wet	11,00	7,00	6,85	9,00
Dry	10,6	6,52	6,33	8,13
Sintered	10,00	6,00	5,50	6,50

Table 8. Wet, dry, and sintered wall thicknesses of samples

Water absorption test results were given in Table 9. Test results show that as the amount of amorphous silica used increased, the product absorbed less water. According to these results, The N2 sample (6% amorphous silica) showed the best results in terms of water absorption.

Table 9. Water absorption test results

	Reference	N1	N2
Water absorption (%)	9,86	9,26	8,67

4. GENERAL EVALUATION AND DISCUSSION

In conclusion, as the amount of amorphous silica and amorphous calcium silica were increased, weights and wall thicknesses of the samples were decreased. Amorphous silica was found to be more successful in sanitary ware products than amorphous calcium silica. The main reason of this situation is moisture absorption capacity of amorphous calcium silica is higher than amorphous silica. Calcium amorphous silica was observed to exhibit undesirable behavior, such as cracking in the ceramic body during sintering, due to the moisture absorption capacity. For this reason, it is recommended that future studies will be continued with amorphous silicates. With the increasing ratio of amorphous silica in slurries, less water absorption ratio was observed in the sintered samples.

References:

1. Golder T., The development of high performance sanitaryware bodies to improve manufacturing productivity and yield. Cfi/Ber DKG. 2007, **84**(1-2), 60-63.
2. Mikhalev V. V., et al.: Effect of the physical properties of slip on the molding of commercial grade sanitaryware. Glass and ceram.,2007, **64**(3-4), 129-131.
3. Waters B., Balancing firmness with packing in pressure casting sanitaryware. Cfi/Berg, DKG, 2005, **82**(3), 32-36.
4. Golder T., Sanitaryware reformulation- why bother? Cfi/Ber. DKG, 2010, **87**(3), 29-32.
5. Temel T. M., Karakuzu B., Yücel S., Aerogel: Superior features, types and developing application fields. Türkchem, 2016, 52-66.
6. Temel T. M., Karakuzu B., Terzioğlu P., Yucel S., Elalmış Y., The effect of process variables on the properties of nanoporous silica aerogels: an approach to prepare silica aerogels from biosilica. JSST, 84, 2017, 51–59.
7. Dorcheh A. S., Abbasi M. H., Silica aerogel; synthesis, properties and characterization. Journal of Materials Processing Technology, 2008, 199:10-26.
8. Ülker Z., Preparation and characterization of silica aerogel polymer composites, Yüksek Lisans Tezi, Koç Üniversitesi Fen Bilimleri ve Mühendislik Enstitüsü, 2011, (İstanbul).
9. Tang Q., Wang T., Preparation of silica aerogel from rice hull ash by supercritical carbon dioxide drying. Journal of Supercritical Fluids, 2005, 35: 91-94.

10. Yücel S. , Influence of gel aging time on the properties of various silica aerogels synthesized from water glass. Materials Science Forum, 2016, Vol. 866, pp. 176-180
11. Gökbek M. Seramik döküm çamurlarının hazırlanması, Yüksek Lisans Tezi, Dokuz Eylül Üniversitesi Güzel Sanatlar Enstitüsü, 2014, (İzmir).
12. Bayraktar I. , Ersayın S. , Gülsoy Ö. Y. , Ekmekçi Z. , Can M. , Temel., Seramik ve Cam Hammaddelerimizdeki (Feldspat, Kuvars ve Kaolin) Kalite Sorunları ve Çözüm Önerileri. 1999.
13. Sümer, G. ve Kaya, M., Aydın-Çine feldspatlarının flotasyon ile zenginleştirilmesi. Endüstriyel Hammaddeler Sempozyumu, 1995, s.59.
14. Çakıcı R.İ., Seramik üretiminde alternatif hammaddelerin kullanılma olanaklarının araştırılması ve maliyet azaltma çalışmalarının yapılması. Yüksek Lisans Tezi, İstanbul Üniversitesi Fen Bilimleri Enstitüsü, 2014, (İstanbul).
15. Stockly D. , Fine fireclay- an overview of raw materials and body formulations. 2008, **85**(3), 19-22.
16. Kunduracı N. , Aydın T. , FFC seramik sağlık gereçlerinin yarı mamul ve pişmiş mamul mukavemetlerini arttırarak ultra ince FFC lavaboların üretimi. 2015.

ADVANCED CERAMICS

IMPROVING THE PROPERTIES OF Al_2O_3 - TiC CUTTING TOOLS
BY USING GAS PRESSURE SINTERING TECHNIQUETuğçe Önal¹, Sinem Başkut¹, Ufuk Akkaşoğlu², Servet Turan¹¹Eskişehir Technical University, Faculty of Engineering,
Department of Materials Science and Engineering, Eskişehir, Turkey
²MDA Advanced Ceramics Ltd., 26110, Eskişehir, Turkey**Keywords:** Al_2O_3 , TiC, Mechanical Properties, GPS

ABSTRACT

Al_2O_3 -TiC composites are favorable materials for cutting tool applications due to their superior mechanical properties. In this study, Al_2O_3 - 22.5 wt % TiC, Al_2O_3 - 25 wt % TiC, Al_2O_3 - 27.5 wt % TiC and Al_2O_3 - 30 wt % TiC composites were produced by using gas pressure sintering (GPS) technique. Graphene, titanium diboride (TiB_2) and silicon carbide (SiC) were used to increase the fracture toughness of the Al_2O_3 -TiC composite. In addition, the effects of different sintering temperatures such as 1850 and 1900 °C on the mechanical properties were investigated. The best hardness value was achieved at Al_2O_3 - 27.5 wt % TiC among the produced Al_2O_3 -TiC composites. The fracture toughness of the Al_2O_3 - 27.5 wt % TiC increased by ~ 3, 7 and 0.3 % with the addition of graphene, TiB_2 and SiC, respectively. It was determined that the hardness and toughness values obtained at 1900 °C were higher than those at 1850 °C.

1. INTRODUCTION

Al_2O_3 based ceramics display outstanding properties such as high wear resistance, good chemical stability and excellent thermal resistance that required for materials used in modern cutting tools [1-5]. These properties resulted the Al_2O_3 based cutting tools more preferable than traditional cutting tools such as high-speed steel and cemented carbide for cutting materials that are very difficult to machined. Furthermore, improving their mechanical properties increases the service life and application areas of these cutting tools. In recent years, in order to improve the mechanical properties of ceramics, many techniques such as different particle dispersion in matrix material and addition of second phases such as graphene/carbon nanotube/whisker are used [6,7].

TiC reinforced Al_2O_3 matrix ceramics considered for cutting tools applications for a long time [1-5]. In one of these studies [1], 3, 6 and 9 vol. % TiC were added to the Al_2O_3 matrix and the composites were sintered by using hot pressing. In that study, the highest flexural strength (~ 950 MPa) and hardness (~ 18 GPa) values were obtained in Al_2O_3 containing 6 vol. % TiC, while the highest fracture toughness (~ 8.9 $\text{MPa m}^{1/2}$) was observed in the composite containing 9 vol. % TiC. In addition, Wang et al. [4] measured the hardness, flexural strength, and fracture toughness of $\text{Al}_2\text{O}_3/\text{TiC}/\text{TiN}$ ceramic tool material as 20.8 GPa, 881.4 MPa, and 7.8 $\text{MPa.m}^{1/2}$, respectively. Yang et al. [5] investigated the effects of different sintering temperatures such as 1700, 1750, 1800, and 1850 °C on the densification behavior and mechanical properties of gas pressured sintered Al_2O_3 containing TiCN. They reported that the Al_2O_3 -30 wt % TiCN composite had a relative density of 99.5%, a bending strength of 772 MPa, a hardness of 19.6 GPa and a fracture toughness of 5.82 $\text{MPa.m}^{1/2}$ at 1800 °C.

Considering that information, the main motivation of this study was to find the optimum compositions of GPSed Al_2O_3 -TiC for better performance and longer service life during machining process by improving mechanical properties. Another purpose was to determine the optimum sintering temperature, which provide the highest density and mechanical properties to Al_2O_3 -TiC cutting tool. Another subject that was focused on was to determine the reinforcement material that exhibited the highest performance in improving the fracture toughness of the Al_2O_3 -TiC composite. For this purpose, graphene, TiB_2 and SiC were used as a reinforced material.

2. MATERIALS AND METHODS

2.1. Production of the Materials

Different composites slurries were prepared by adding TiC powder to Al_2O_3 powder in the amount of 22.5, 25, 27.5 and 30 wt. %. Table 1 shows the details of the compositions

Table 1. Composition details of the Al₂O₃-TiC composites.

Materials	Al ₂ O ₃ (g)	TiC (g)
77.5 % Al ₂ O ₃ +22.5 % TiC	31	9
75 % Al ₂ O ₃ +25 % TiC	30	10
72.5 % Al ₂ O ₃ +27.5 % TiC	29	11
70 % Al ₂ O ₃ +30 % TiC	28	12

The Al₂O₃-TiC powder mixtures were prepared by using two different methods. In the first method, the Al₂O₃ and TiC powders were blended in a planetary ball mill (Fritsch, Pulverisette) with isopropanol medium by using zirconia balls at the speed of 300 rpm for 2 h. In the second method, the Al₂O₃ and TiC powders were milled for 2 and 4 h, respectively and then mixed in the planetary ball mill by using zirconia balls for 2 h. In addition, graphene, TiB₂ and SiC powders were added to the Al₂O₃-TiC compositions in different amounts. After mixing of these three reinforced materials with pre-milled TiC for 2 hours, the pre-milled Al₂O₃ powder were added to powder mixture and blended for 2 h by using the planetary ball mill. Table 2 shows the composition components and their amounts.

To evaporate alcohol from the slurries, the mixed powders were dried in a rotary evaporator (Heidolph) at the temperature of 55 °C for 50 min. To obtain green body, dried powders were pressed at 150 MPa (Gabbrielli). The isostatic cold pressing were applied to all green bodies. The composites were sintered at two different temperatures as 1850 °C and 1950 °C by using gas pressure sintering furnace (FCT, Anlagenbau GmbH). A two-stage sintering schedule was utilized in the present study, which included a first stage at a sintering temperature of 1850 °C-1900 °C for 30 min. under a low argon gas pressure of 5 bar and a second stage at the same temperature for 60 min under a high pressure of 95 bar.

Table 2. Compositions details of the Al₂O₃-TiC composites containing graphene, TiB₂ and SiC powders.

Materials	Al ₂ O ₃ (g)	TiC (g)	Al ₂ O ₃ +27.5%TiC (g)	Graphene (g)	TiB ₂ (g)	SiC (g)
Al ₂ O ₃ + 27.5 % TiC	29	11	-	-	-	-
Al ₂ O ₃ + 0.5% graphene + 27.5 % TiC	-	-	19.5	0.5	-	-
Al ₂ O ₃ + 2.5 % TiB ₂ + 25 % TiC	29	10	-	-	1	-
Al ₂ O ₃ + 7.5 % SiC + 20 % TiC	29	8	-	-	-	3

2.2. Characterisation of the Materials

The bulk densities of the GPSed composites were calculated based on the Archimedes method by using deionized water as the immersion medium. To determine the relative density values, all the theoretical values for composites were calculated from volume based rule of mixtures. XRD (Rigaku, RINT-2000) analyses were carried out to sintered samples between 20 and 60° (2 θ) under the conditions of 40 kV accelerating voltage, 30 mA current, 1°/min scan speed and 0.02 step size. Microstructure investigations including backscatter electron (BSE-SEM) images and energy dispersive x-ray spectroscopy (EDS) analyses were performed in the scanning electron microscope (SEM, Zeiss-SUPRA 50 VP).

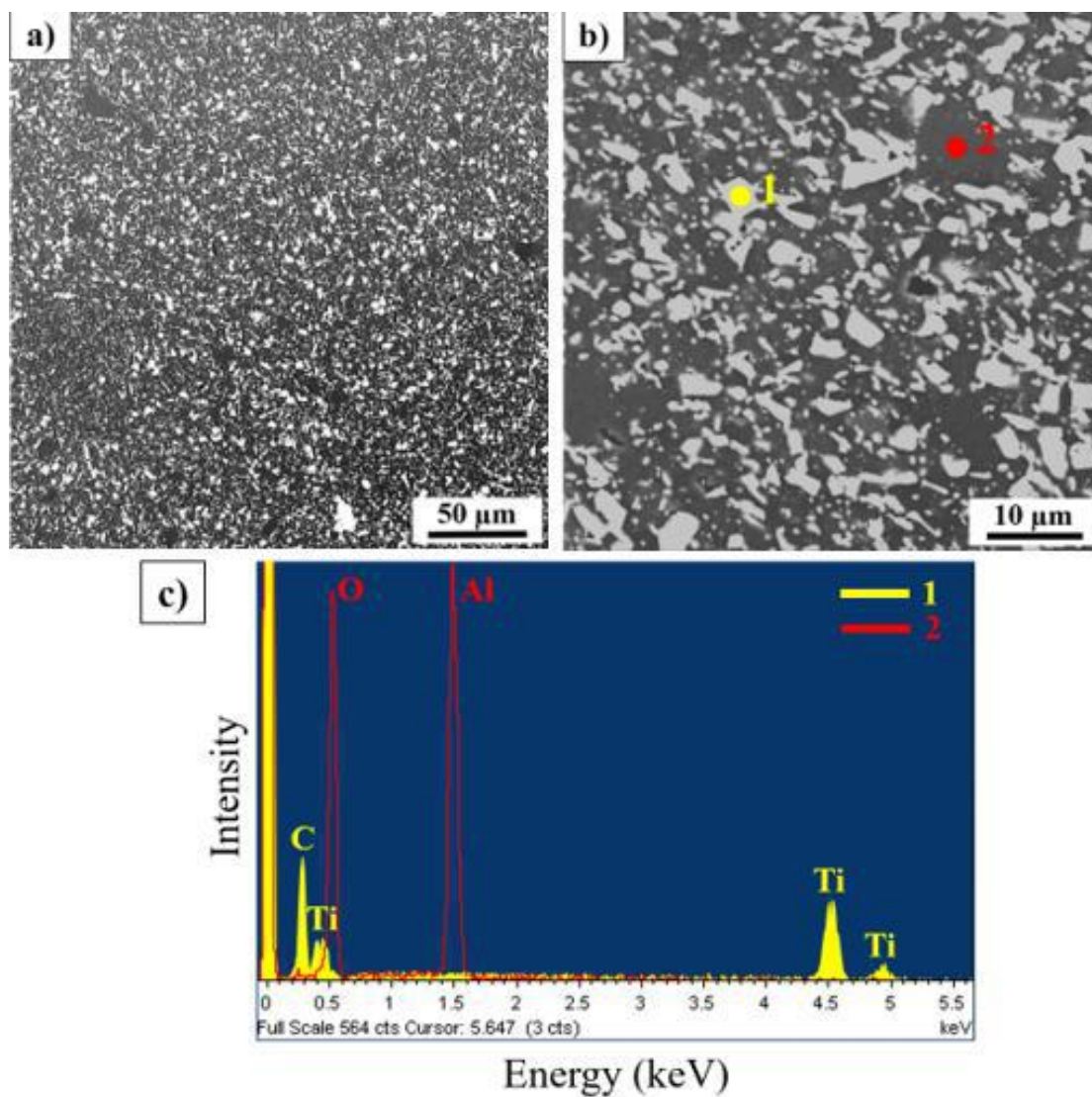
In order to evaluate the mechanical properties of composites, hardness values were measured by applying 5 kg load for 10 s with Vickers indenter (Emco-Test). After Vickers indentations, crack lengths were measured and fracture toughness values were calculated according to the Niihara model [8].

3. RESULTS AND DISCUSSION

Relative densities values, which were higher than 99.5% of all Al₂O₃-TiC composites sintered at 1850 and 1900 °C showed that dense samples were produced at both sintering temperatures. Figure 1 a and b shows the BSE-SEM images of Al₂O₃-27.5 % TiC obtained by mixing Al₂O₃ and TiC powders in the planetary ball mill for 2 hours without pre-milling processes. The fact that there was no porosity in the microstructures showed that the composites were 100 % dense within themselves. Figure 1 c and d illustrate the EDX-SEM analysis results of the different regions in the BSE-SEM images.

Table 3. Relative density values of the Al_2O_3 -TiC composites

Materials	Relative Density Values (%)	
	1850 °C	1900 °C
Al_2O_3 - 22.5 % TiC	99.6	99.5
Al_2O_3 - 25 % TiC	99.6	99.5
Al_2O_3 - 27.5 % TiC	99.5	99.8
Al_2O_3 - 30 % TiC	99.6	99.5



Regions	Phases	Weight (%)				Atomic (%)			
		Al	O	Ti	C	Al	O	Ti	C
1	TiC	-	-	76.00	24.00	-	-	44.3	55.7
2	Al_2O_3	43.6	56.4	-	-	31.45	68.5	-	-

Figure 1. (a) Low and (b) high magnifications BSE-SEM images obtained from the Al_2O_3 -27.5 TiC composites containing Al_2O_3 and TiC powders, which were mixed without pre-milling. (c) EDX results of light gray and dark grey regions.

According to the results, the light gray and dark grey regions represent the TiC and Al_2O_3 , respectively. Considering the images (Fig. 1 a, b), it was noticed that the Al_2O_3 and TiC grains were not distributed homogeneously in the composites microstructures.

As a solution, Al_2O_3 and TiC powders were exposed to 2 and 4 h pre-milling, respectively before blending. The BSE-SEM images taken from the Al_2O_3 - 27.5 % TiC composites prepared in this way are given in Figure 2. Al_2O_3 and TiC grains were more homogeneously dispersed in the sintered composite microstructures compared to the composites produced without pre-milling processes. Therefore, these powder production stages were determined as the optimum conditions for powder preparation.

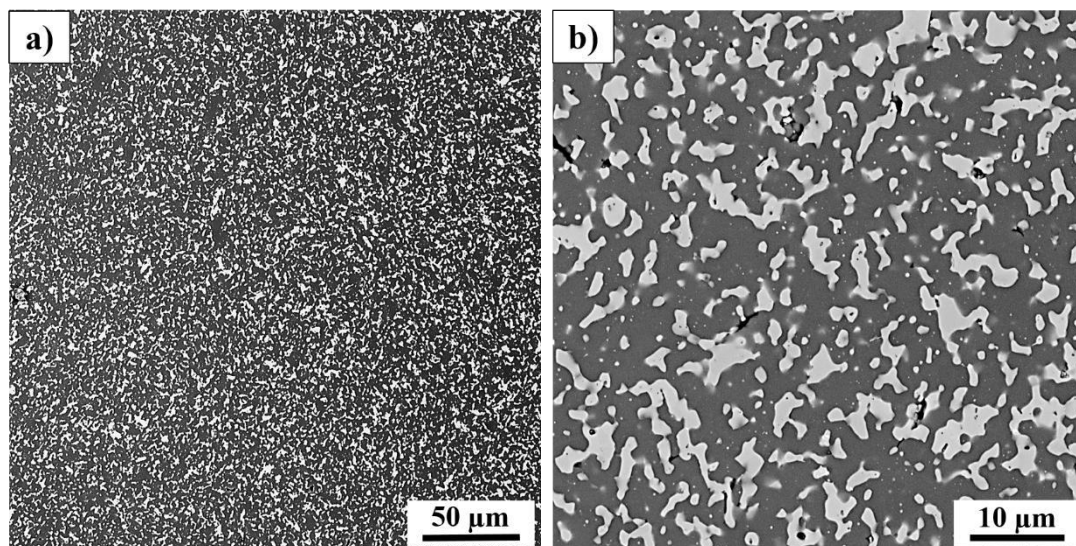


Figure 2. (a) Low and (b) high magnifications BSE-SEM images obtained from the Al_2O_3 -27.5 TiC composites containing Al_2O_3 and TiC powders, which were pre-milled 2 and 4 h., respectively.

Fig. 3 shows the XRD pattern obtained from the grinded form of sintered Al_2O_3 -30 % TiC as representative from all Al_2O_3 -TiC composites. The results indicated that Al_2O_3 and TiC exist as a main crystal phases in the composites. WC phase were formed because of pollution that is mixed into sample from grinding media.

The hardness values of the all Al_2O_3 - TiC composites sintered at both 1850 and 1900 °C were given in Table 4 and plotted in Fig. 4. It was observed that hardness values obtained at 1900 °C were higher than those taken at 1850 °C in the composites containing same amounts of Al_2O_3 and TiC. Therefore, the optimum sintering temperature of Al_2O_3 -TiC composites was determined as 1900 °C. In addition, the highest hardness value was reached at Al_2O_3 -27.5% TiC sintered at 1900 °C (Table 4 and Fig. 4).

On the other hand, different reinforced materials such as graphene, TiB_2 and SiC were used to improve the service life of the Al_2O_3 -TiC composite by increasing their fracture toughness values. The hardness and fracture toughness values of the Al_2O_3 -27.5 % TiC and also Al_2O_3 -TiC matrix composites containing graphene, TiB_2 and SiC sintered at 1900 °C were given in Table 5 and Fig. 5.

Table 4. Hardness values of the Al_2O_3 -TiC composites sintered at 1850 °C and 1900 °C.

Temperature (°C)	Hardness (GPa)			
	Al_2O_3 -22.5 % TiC	Al_2O_3 -25 % TiC	Al_2O_3 -27.5 % TiC	Al_2O_3 -30 % TiC
1850 °C	17.92	17.81	18.80	17.67
1900 °C	20.3	19.71	21.54	20.33

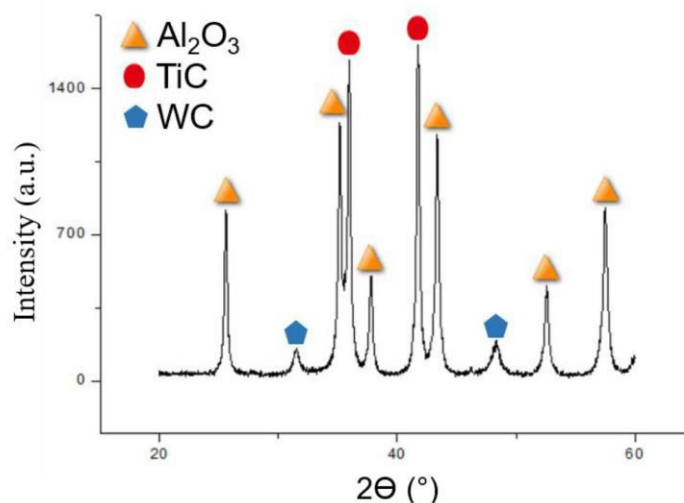


Figure 3. XRD pattern of Al_2O_3 – 30 wt. % TiC

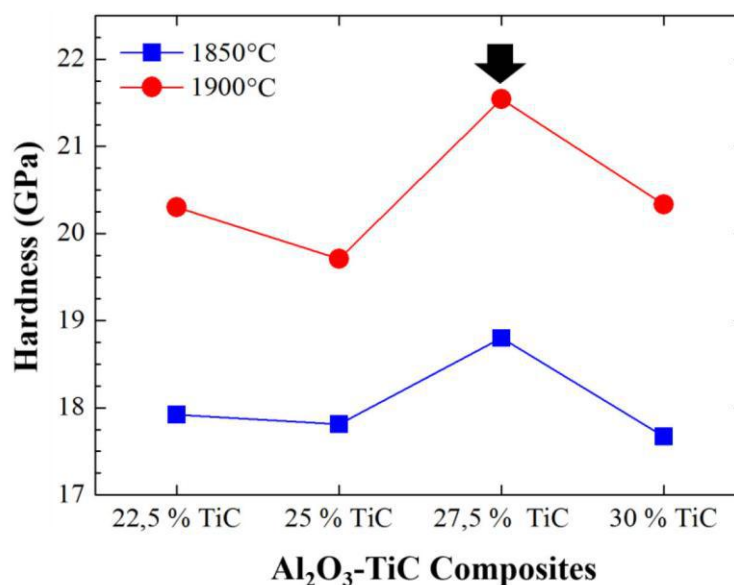


Figure 4. Hardness values of the Al_2O_3 -TiC composites sintered at 1850 °C and 1900 °C

Table 5. The hardness and fracture toughness values of the Al_2O_3 - 27.5 % TiC and graphene, TiB_2 , SiC added Al_2O_3 - TiC composites sintered at 1900 °C

	27.5%TiC - Al_2O_3	0.5% graphene + 27.5%TiC- Al_2O_3	2.5% TiB_2 + 25 %TiC- Al_2O_3	7.5 % SiC + 20%TiC- Al_2O_3
Hardness (GPa)	21.54	19.89	20.15	19.96
Fracture Toughness ($\text{MPa}\cdot\text{m}^{1/2}$)	8.74	9.02	9.39	8.77

It was observed that the hardness values of composites containing graphene, TiB_2 and SiC were lower than Al_2O_3 -27.5 % TiC cutting tool. However, highest hardness value obtained in the TiB_2 added Al_2O_3 -TiC among the composites containing reinforced materials. The fracture toughness of the composite increased by ~ 3, 7 and

0.3 % with the addition of graphene, TiB_2 and SiC , respectively. The lowest fracture toughness was obtained in 7.5 % SiC + 20 % TiC - Al_2O_3 composite while the highest toughness value was achieved in the 25 % TiC - Al_2O_3 composite containing 2.5 wt. % TiB_2 . Therefore, it was decided to use TiB_2 as reinforced materials to increase fracture toughness of Al_2O_3 - TiC composites.

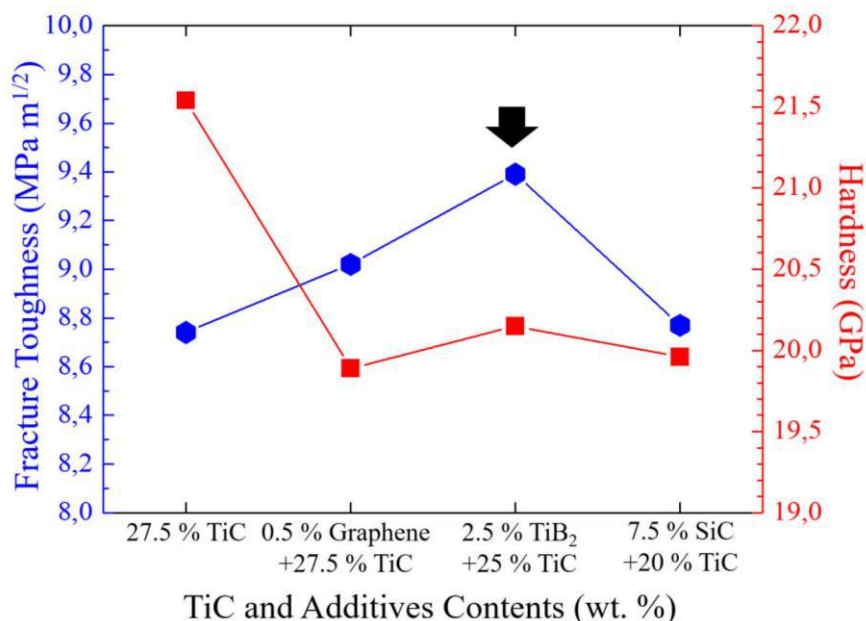


Figure 5. The hardness and fracture toughness values of the Al_2O_3 -27.5 % TiC and also Al_2O_3 - TiC matrix composites containing graphene, TiB_2 and SiC .

4. CONCLUSIONS

Dense Al_2O_3 - TiC composites were produced at both 1850 and 1900 °C sintering temperatures. However, the hardness values were higher at the 1900 °C than 1850 °C. For this reason, the optimum sintering temperature of Al_2O_3 - TiC composites was determined as 1900 °C. The highest hardness value was obtained at Al_2O_3 - 27.5 wt. % TiC among the produced Al_2O_3 - TiC composites. In order to increase the fracture toughness of the Al_2O_3 - 27.5 wt. % TiC graphene, TiB_2 and SiC could be used as reinforcing materials. The fracture toughness of the composite increased by ~ 3, 7 and 0.3 % with the addition of graphene, TiB_2 and SiC , respectively.

REFERENCES

- [1] Z. Yin, C. Huang, B. Zoua, H. Liua, H. Zhua, J. Wang, Preparation and characterization of $\text{Al}_2\text{O}_3/\text{TiC}$ micro-nano-composite ceramic tool materials, *Ceramics International* 39 (2013) 4253–4262.
- [2] M. Masuda, T. Sato, T. Kori, Y. Chujo, Cutting performance and wear mechanism of alumina-based ceramic tools when machining austempered ductile iron, *Wear* 174 (1992) 147–153.
- [3] T. Takahashi, Development of fine and high-strength Al_2O_3 based ceramics, *J. Jpn. Soc. Powder and Powder Metall.* 45 (1998) 496–506.
- [4] D.Wang, C. Xue, Y. Cao, J. Zhao, Fabrication and cutting performance of an $\text{Al}_2\text{O}_3/\text{TiC}/\text{TiN}$ ceramic cutting tool in turning of an ultra-high-strength steel, *Int J Adv Manuf Technol* (2017) 91:1967–1976
- [5] H. Yang, S. Roberts, Gas pressure Sintering of $\text{Al}_2\text{O}_3/\text{TiCN}$ composite, 31 (2005) 1073-1076.
- [6] W. Acchar, Y.B.F. Silva, C.A. Cairo, Mechanical properties of hot pressed ZrO_2 reinforced with (W, Ti)C and Al_2O_3 additions, *Materials Science and Engineering A* 527 (2010) 480–484.
- [7] B. Zou, C.Z. Huang, H.L. Liu, Study of the mechanical properties, toughening and strengthening mechanisms of $\text{Si}_3\text{N}_4/\text{Si}_3\text{N}_4/\text{TiN}$ nanocomposite ceramic tool materials, *Acta Materialia* 55 (2007) 4193–4202.
- [8] Rangel E. R., Fracture Toughness Determinations by Means of Indentation Fracture, *Nanocomposites with Unique Properties and Applications in Medicine and Industry*, InTech, 2011

GENERAL

EFFECT OF DIFFERENT SINTERING SPEEDS ON GRAIN SIZE OF ZIRCONIA CERAMICS

Gürel Pekkan¹, Keriman Pekkan², Eda Taşçı³, Menderes Boz³

¹Dumlupınar University, Department of Prosthodontics, Turkey

²Dumlupınar University, Department of Ceramic and Glass, Turkey

³Dumlupınar University, Department of Materials and Ceramic Engineering, Turkey

Key words: Zirconia ceramic, sintering speed, grain size, characterization

Abstract

Zirconia ceramics are widely used as dental materials because of their high biocompatibility, excellent mechanical and aesthetic properties. In recent years, the fabrication zirconia materials for fixed dental prostheses are conducted by computer-aided design and computer-aided manufacturing (CAD-CAM) systems by usage of yttria-stabilized tetragonal zirconia polycrystalline (Y-TZP) ceramics. 3 mol % stabilized tetragonal zirconia polycrystalline (3Y-TZP) ceramics are generally preferred as restorative materials because of their excellent mechanical properties such as high strength and toughness, good biocompatibility and relatively good aesthetic properties in terms of colour and translucency. Translucency of zirconia is one of the most important aesthetic parameter and it is directly affected by sintering conditions. Translucency is closely related to grain size of the material. The aim of the study is to determine the effect of sintering speeds on grain sizes of zirconia ceramics. Speed, normal and slow type of sintering speeds are used in sintering of pre-sinterized zirconia block pieces. After sintering, characterization of zirconia ceramics are done with scanning electron microscopy (SEM) and the grain sizes of the specimens were evaluated using the SEM machine at 9 kV with a working distance of 6.0 mm. The line segments of 50 randomly selected grains from each representative specimen are used to calculate the mean grain sizes.

1. Introduction

The most known compounds of zirconium, which is usually found in the form of a compound in nature, are zirconium silicate (Zirconium) (ZrSiO_4) and zirconium oxide (Zirconia) (ZrO_2). The use of zirconia as biomaterial started with the hip prosthesis production of Hellmer and Driskell in 1969 [1,2,3]. Zirconia is a material which has been frequently used in dentistry applications for the past 20 years due to its properties such as strength, resistance to pressure, resistance to corrosion, biocompatibility as well as heat and electrical insulation. Zirconia's luminous transmittance and its appearance, which is close to the natural appearance of teeth due to its white colour and transparency, are its other advantages.

Zirconia used in the field of dentistry are separated into three groups as "zirconia toughened alumina" (ZTA), "partial stabilized zirconia" (PSZ), "single-phase polycrystalline tetragonal zirconia" (TZP).

The advancement of technology has made the computer aided design (CAD) and computer aided manufacturing (CAM) techniques to become widespread in dentistry and enabled the use of full ceramic restorations produced with this method. In dentistry, CAD/CAM is a shaping method in which the missing tooth tissue is completed via design and manufactured by means of computer-aided mills using pre-sinterized blocks [5].

The material with the most-widespread area of use in dentistry is 3% mole yttria-doped (Y_2O_3) single-phase tetragonal polycrystalline zirconia (Y-TZP). Zirconium is preferred in dentistry as it is physically more strong and durable thanks to the addition of yttria [6,7].

With regard to the factors affecting the mechanical properties of Y-TZP, the best mechanical properties are achieved with the addition of stabilizer at a rate of 2% with a lesser amount of oxide being added to the zirconia and the homogenous distribution of the same. The increase in the rate of yttria accelerates the phase change. For ideal fracture strength, the grain size of the material should be around 0.3 μm . Grain size negatively affects the mechanical properties of sinterized zirconia [8]. The increase in temperature also negatively affects the mechanical properties of Y-TZP. This is because the transition from the tetragonal phase to the monoclinic phase is spontaneous and that the material loses its semi-stabilized properties due to phase transformation. Tetragonal Y-TZP being exposed to a temperature exceeding 200-300 °C during applications degrades the mechanical properties of the material by excessively increasing the amount transition to monoclinic phase. This is referred to as low temperature degradation [1,9,10,11]. It has been reported that the phase change rate increases when high temperature is accompanied by moisture. It is reported by studies carried out in an experimental environment that the zirconia is more prone to aging with the presence of the water in the environment. In ceramics containing Y-TZP, time-dependent aging occurs due uncontrolled increase in the transition of tetragonal phase to the monoclinic phase. A decrease in strength, hardness and density occurs along with this aging phenomenon [9,10,11]. It has been reported that the uncontrolled increase in the macro and micro cracks inside the Y-TZP reduces the mechanical resistance of the material [12,13].

In this study, the effect of the fast-, normal-, and slow-mode sinterization of Y-TZP ceramics (used in dentistry) on the grain size was examined.

2. Experimental Procedure

Rectangular-shaped samples with a thickness of 1.30 mm were achieved by cutting the pre-sinterized zirconia block (InCoris ZI F2 40/19, Sirona, Bensheim, Germany) in a “low speed diamond saw”. Samples were sinterized in a zirconia sinterization furnace (InFire HTC speed, Sirona). 3 different sinterization regimes were used as follows: 30 min., 1510 °C, fast; 90 min., 1510 °C, normal; 120 min., 1510 °C, slow. Grain size analysis of fast-, normal-, and slow-sinterized samples were characterized using scanning electron microscopy (SEM) (Nova NanoSem 650). With SEM, the image that appears at 9 kV with an operation distance of 6.0 mm and a magnification of 20000X was achieved. 50 images were selected randomly from these images. The diameter of these 50 grains was measured and the results are statistically analysed.

3. Results and Discussion

After Y-TZP samples are sinterized, they were exposed to shrinkage at a rate of approx. 20%. This shrinkage is expected in such types of pre-sinterized blocks. SEM images of the sinterized samples are given in Figure 1-3.

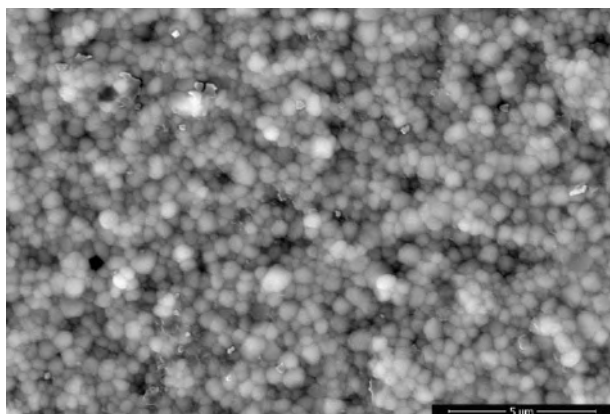


Figure 1. SEM image (20000X) of Y-TZP sample sinterized at 1510 °C for 30 minutes in fast mode.

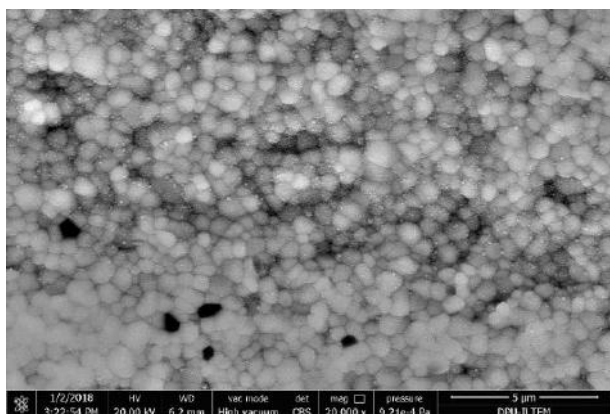


Figure 2. SEM image (20000X) of Y-TZP sample sinterized at 1510 °C for 90 minutes in normal mode.

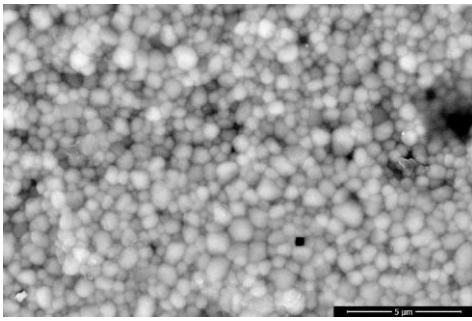


Figure 3. SEM image (20000X) of Y-TZP sample sinterized at 1510 °C for 120 minutes in slow mode

The diameter of 50 different grains randomly selected from the SEM image of the sample sinterized in 3 different modes was measured. The measurements of the 50 grains selected from the SEM image of the sample sinterized in the fast mode are shown in Figure 4. In this image, the mean diameter and standard deviation (mean and SD) of the 50 grains selected were calculated as 547.6 ± 146.7 nm.

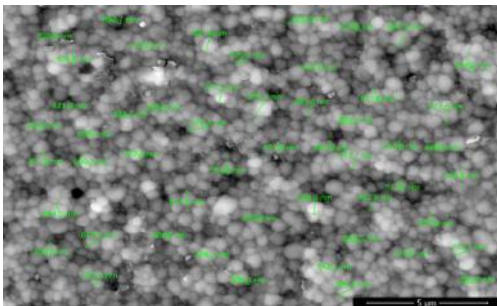


Figure 4. Diameter measurement of 50 randomly selected grains from the SEM images of the Y-TZP sample sinterized in fast mode.

The measurements of 50 different grains selected from the SEM image of the Y-TZP sample sinterized in normal mode are shown in Figure 5. In this image, the measurement values of 50 grains selected were calculated as 629 ± 204.8 nm.

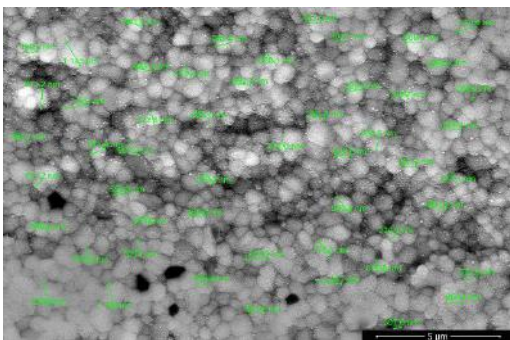


Figure 5. Diameter measurement of 50 randomly selected grains from the SEM images of the Y-TZP sample sinterized in normal mode.

The measurements of 50 grains of Y-TZP sample sinterized in slow mode in the SEM image is shown in Figure 6. In this image, the average size of 50 grains selected was calculated as 655.67 ± 199.83 nm.

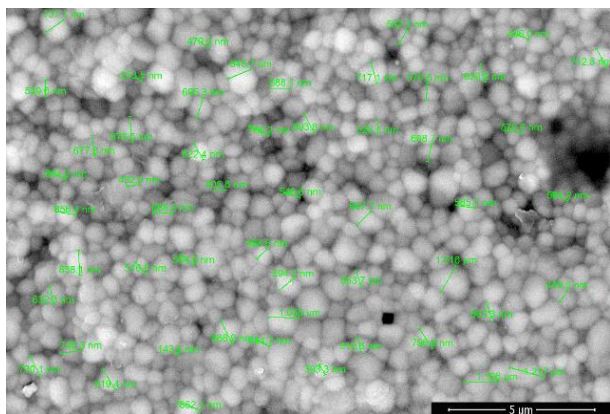


Figure 6. Diameter measurement of 50 randomly selected grains from the SEM images of the Y-TZP sample sinterized in slow mode.

The statistical analysis of the results in the measurements performed was examined in the GraphPad Instadt analysis program. After the mean and standard deviations were calculated, Kolmogorov Smirnov test was performed and it was determined that the groups showed a normal distribution. As a result of the one-way analysis of variance, it was determined that there was a significant difference between the groups ($P = 0.0116$). Comparisons of dual groups were performed using the student-Newman-Keuls test. For example, the grain sizes sinterized in fast mode are found to be significantly smaller than the normal- and slow-sinterized group ($P < 0.05$).

4. Conclusion

In this study, it was determined that the grain size in Y-TZP samples statistically increased significantly as the sinterization time increases. The variation in grain size may provide information on the durability, luminous transmittance and degradation of the ceramics. In this regard, it is important to foresee the variation of grain size depending on the temperature.

Acknowledgments

The authors would like to thank the ILTEM (Advanced Technology Centre) officials of Dumlupınar University and Musa Akman, graduate student in Materials Science and Engineering, for allowing us to carry out the XRD SEM / EDS studies.

References

- [1] Piconi C, Maccauro G. Zirconia as a ceramic biomaterial, a review. *Biomaterials* 1999;29:1-25.
- [2] Vagkopoulou T, Koutayas SO, Koidis P, Strub JR. Zirconia in dentistry: Part 1. Discovering the nature of an upcoming bioceramic. *Eur J Esthet Dent* 2009;4:130-51.
- [3] Hisbergues M, Vendeville S, Vendeville P. Zirconia: Established facts and perspectives for a biomaterial in dental implantology. *J Biomed Mater Res B Appl Biomater* 2009;88:519-29.

- [4] Conrad HJ, Seong WJ, Pesun IJ. Current ceramic materials and systems with clinical recommendations: a systematic review. *J Prosthet Dent* 2007;98:389-404.
- [5] F. Tan Bilgisayar ile tasarlanarak üretilen translüsent monolitik zirkonya ve çift tabakalı zirkonya restorasyonların klinik başarılarının değerlendirilmesi, Ege Üniversitesi, 2016, İzmir, Turkey.
- [6] Manicone PF, Iommetti PR, Raffaelli L. An overview of zirconia ceramics: Basic properties and clinical applications. *J Dent* 2007;35:819-26.
- [7] Denry I, Kelly JR. State of the art of zirconia for dental applications. *Dent Mat* 2008;24:299-307.
- [8] Piwowarczyk A, Lauer HC, Sorensen JA. The shear bond strength between luting cements and zirconia ceramics after two pre-treatments. *Oper Dent*, 2005; 30: 382-8.
- [9] Sato T, Shimada M. Transformation of yttria doped tetragonal ZrO₂ polycrystals by annealing in water. *J Amer Ceram Soc* 1985;68:356-9.
- [10] Luthardt et al. Reliability and properties of ground Y-TZP zirconia ceramics. *J Dent Res* 2002;81:487-91.
- [11] Swabb JJ, Low J. Low temperature degradation of Y-TZP materials. *J Mater Science* 1991;26:6706- 17.
- [12] Triwatana P, Nagaviroj N, Tulapornchai C. Clinical performance and failures of zirconia-based fixed partial dentures: a review literature. *J Adv Prosthodont* 2012;4:76-83.
- [13] Kelly JR, Denry I. Stabilized zirconia as a structural ceramic: an overview. *Dent Mater* 2008;24:289-98.

GENERAL

PRELIMINARY STUDIES ON THE ENRICHMENT OF THE CORUNDUM (RUBY)

¹A. Uçar, ¹S. Karaca, ²V. Uz, ³N. D. Coşkun, ²A. İssi, ⁴B. Uz

¹Dumlupınar University, Mining Engineering Department, Kütahya, Turkey

²Dumlupınar University, Materials Science and Engineering Department, Kütahya, Turkey

³Ordu University, Faculty of Fine Arts, Ceramic and Glass Department, Ordu/Turkey

⁴Istanbul Technical University, Jeoloji Mühendisliği Bölümü, İstanbul, Türkiye

ABSTRACT

Ruby formation and production in the world are found in very few countries. In our country, ruby occurrences have been detected in the Malatya Region in recent years. But production haven't done. For this reason, it is necessary to carry out studies on the enrichability of ruby production. For this purpose, preliminary investigations have been carried out on the ruby samples from Malatya region enriched by magnetic separation method with XRF, XRD, SEM characterization studies.

Key words: Malatya Region Ruby, enrichment, characterization

1. INTRODUCTION

The best rubies are found in the countries of Afghanistan, Pakistan, Tajikistan, Nepal, Burma and Vietnam. Simonet et.al. carried out a study in which it was put forth that the most important corundum (ruby) sources are in Europe and Eastern Africa [1-2]. Rakotondrazafy et.al. carried out another study on corundum beds as a result of which it was put forth that Madagascar is another significant source of ruby ores [2].

Simonet et.al. indicates that mineralization in rubies occurs in two types as primary and secondary [3]. Primary ores are magmatic and metamorphic. Magmatic classification is observed in syenite and monzonites and the syenites in Kenya are examples of this. Metamorphic beds are those in meta limestone, mafic granulite and aluminum gneiss. Whereas secondary beds are magmatic and sedimentary. Bedding in alkali basalts and lamprophyres is in the form of magmatic alluvial whereas bedding in placer is in the shape of sedimentary corundum [4]. Corundum crystallization in metamorphic beds is the result of metamorphism of rocks that are poor in silica or rich in aluminum. These beds develop in aluminum rich gneiss, granulites, meta limestones and mafic granulites. Sri Lanka may be given as an example for ruby mineralization in aluminum rich gneiss and granulites.

Rubies that form in meta limestones are blood red in color with high quality and high chromium ratio. Sapphire has been detected in beds formed as a result of the intrusion of lamprophyres to limestones. Sapphire results in low iron content in addition purple color formation with low amount of chromium [1-5].

Ruby and sapphire have significant importance in precious stone sector after diamond. In addition, these minerals are also used in many technological devices in addition to being used as a precious stone. Ruby is used for red corundum ($\alpha\text{-Al}_2\text{O}_3$), whereas sapphire is used for corundum in blue and other colors. The value of precious stones increase due to colors that developed as a result of element content such as Cr, Fe, Ti and rare V, Mn. The ratio of chromophore elements in the structure is related with the geological environment they are formed in. While the red color is formed due to Cr^{+3} especially in ruby, blue color in sapphire generally differs according to the charge transfer of the Ti^{4+} - Fe^{2+} and Fe^{2+} - Fe^{3+} pairs. Yellow color is formed due to Fe^{3+} or Mg [6-7].

The typical spectrum of ruby is in the red region of the electromagnetic spectrum with 694nm. Single crystal ruby has been used as the first solid laser crystal due to this feature [8]. Ruby is also used in materials that emit red light in addition to laser [3]. It can be observed that ruby will continue to have a significance in the future. Large, dark red colored free particles are observed in the ruby beds located at the Doğanşehir district of the city of Malatya in our country as well as lower quality rubies in hornblendes. In this scope, the purpose of this study was to carry out preliminary studies on the enrichment of bound and low quality rubies in the bed. Thus, the quality of ruby will have been increased and preliminary work will have been carried out for its use [8-9].

2. EXPERIMENTAL STUDIES

2.1. Materials and Method

The samples used in the study have been obtained from low quality ruby raw material at the Doğanşehir District of the city of Malatya. Chemical analyses of the representative samples transformed into powder form have been carried out via Rigaku ZSX X-Ray Fluorescence device. Rigaku, Rint 2000, Japan X-Rays Diffractometer and Bruker D8 XRD devices have been used for the XRD analyses of the same samples and diffractograms were obtained for $2\theta=2\text{-}70^\circ$ via Cu $K\alpha$ radiation at a rate of $0.006^\circ/16\text{ s}$ the results of which were evaluated via MDI Jade6.0 data processing software. In addition, the micro structure images of the sample were obtained using Nova nano SEM 650 model and FEI brand scanning electron microscope. High intensity roller dry magnetic separator was used in magnetic separation experiments.

2.2. Experimental Results and Discussion

There is no study on the evaluation of the ruby beds at the Doğanşehir district. The existence of precious stones such as ruby and sapphire in Turkey was not known until this field was discovered. The existence of ruby was first discovered by Prof. Dr. Bektaş Uz and his team [9].

The study area was comprised of metamorphic and non-metamorphic peridotites, marble and cover units. The peridotite rocks at the foundation indicate unmetamorphised harzburgite lithologies, schist which have been subject to metamorphism at the amphibolite facies under highly metamorphic conditions. These have been covered in marble. Metamorphites represent the base rocks at the region and are comprised of granitic gneiss, Eugen gneiss-mica schists, meta-tuff and schists [10].

Ruby appearance (circled) that is formed inside the amphibolytes on the ruby bed have been shown in Picture 1.



Picture 1. The form that the ruby was found in

While Al_2O_3 content of high quality rubies is 99%, this ratio decreases down to 95% for low quality rubies. Whereas the fundamental ion that gives ruby its natural red color is Cr^{+3} , impurities such as Fe, V, Ti, Ga, Ni, Mn, Mg, Ca are effective on the color of ruby. Oxides such as CaO, MgO, Fe_2O_3 , SiO_2 also affect the color of low quality rubies [11-12].

Table 1 shows the average chemical analyses of gang minerals and ruby samples. The chemical analyses of gang minerals indicate ultra-basic rock group. According to petrographic analyses, mineral composition and textural characteristics are in accordance. The gang bonded with the ruby is rich in aluminum and calcium and contains significant amount of chromium (up to 0.3%). It has been determined that while ruby contains 90-99% Al_2O_3 , 0.1-0.9% Fe_2O_3 , 0.2-0.3% Cr_2O_3 , the gang contains 19-26 % Al_2O_3 , 10-13% MgO, 12-15 % CaO, 2.76-4.49 % Fe_2O_3 and 0.1-0.3 % Cr_2O_3 .

According to the chemical analysis of the sample, the iron content of gang minerals has resulted in magnetic characteristics.

Table 1. Ruby and wall rock average chemical analysis

Component	Gang	Ruby
Na ₂ O	0.96-2.17	0.02
K ₂ O	0.03-0.22	<0.01
CaO	12.50-15.00	0.20
MgO	10.65-13.45	0.20
Al ₂ O ₃	18.45-26.20	95.40
Fe ₂ O ₃	2.76-4.49	0.85
SiO ₂	42.4-43.80	0.62
TiO ₂	0.04-0.08	0.01
Cr ₂ O ₃	0.11-0.29	0.24
P ₂ O ₅	0.01-0.03	<0.01
MnO	0.04-0.07	<0.01
LOI	2.00-2.60	1.09

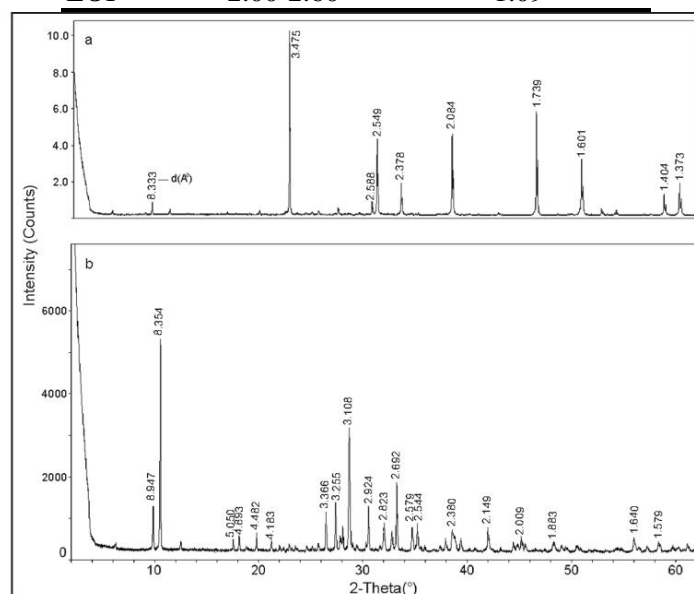


Figure 1. X-Ray dif. for ruby-gang minerals

Hornblende is the primary mineral that the ruby is bonded to. Garnet, feldspar, epidote chlorite, cordierite, Cr-spinel and corundum are the other minerals that are included in the composition. Corundum is a semi-precious mineral that can be found in both high amphibolite as well as garnet amphibolite. Figure 1 shows the X-ray diffractograms of the ruby and gang minerals obtained from the region. Hornblende is the dominant mineral phase at the formation region of ruby at about 65-70%. Meta-amphibolite/hornblende has been determined as a result of petrographic examinations. There are also albite-plagioclase (%20-25 plagioclase) green garnet (%4-5), ruby (%2-3) minerals.

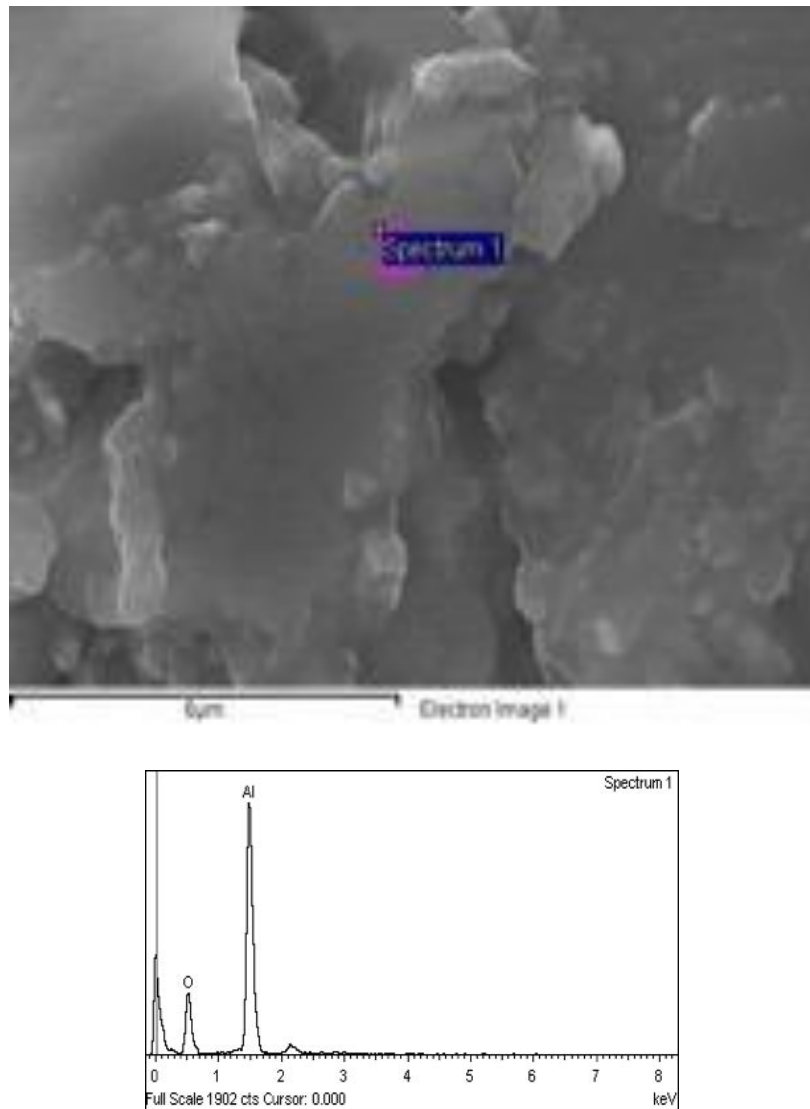
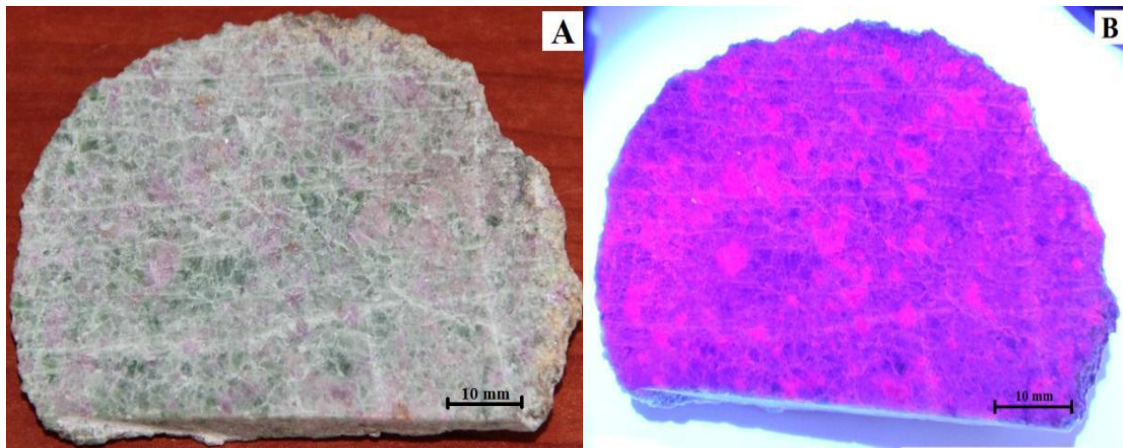


Figure 2. Ruby microstructure (A) and EDX analysis (B)

It was determined during color measurements of natural ruby that L^* : 51.12, a^* : 3.26 and b^* : 0.43. The microstructure appearance of ruby has been given in Figure 2A. Ruby has a dense microstructure appearance. However, the gaps at the interphases indicate that there may be problems in the color quality and cut of ruby. It is thought that such problems will not be observed in rubies sampled from deeper regions and that the ruby quality will increase. It has been determined according to the EDS spectrum obtained from the ruby surface that it only contains aluminum and oxygen (Figure 2B).

Images taken from the surface of ruby formed in amphibolites cut and polished in its natural state under taken under normal light (Picture 2A) and UV light (Picture 2B) have been given in Picture 2. Rubies can be clearly distinguished under white light. However, ruby is more distinct on red color under UV light.

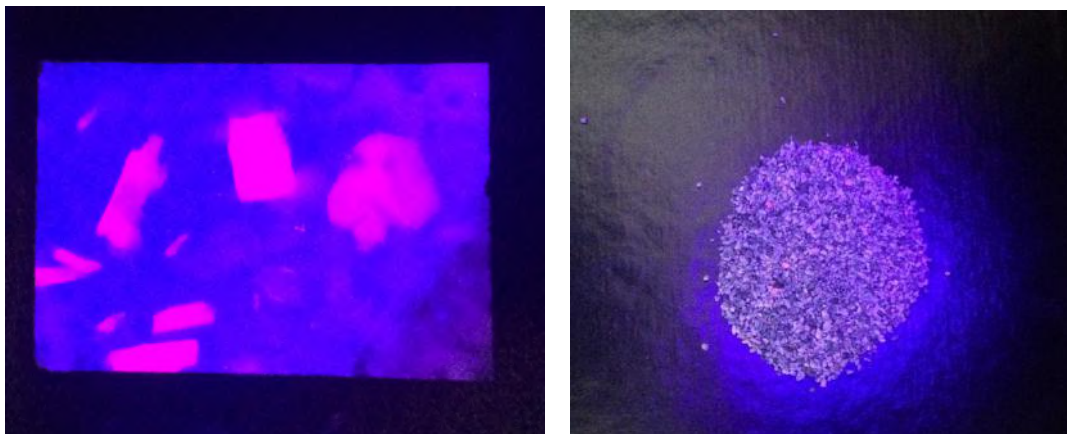


Picture 2. Appearance of ruby and wall rock under normal light (A) and UV (B)

Experiments were carried out under the following conditions using the sample prepared at particle size of -2+1 in high intensity roller dry magnetic separator for determining the separability of ruby and gang.

- Magnetic field intensity: 10 000 Gauss
- Roller speed: 60 rev/min
- Knife angle: 90°

The waste, intermediary product, concentrate and feed obtained as a result of cleaning the concentrate acquired at a knife angle of 110° following the experiments carried out under these conditions were examined with the eye under UV light which were then photographed (Photos A, B). It can be seen from the photos that magnetic separation has been completed distinctively in comparison with the feed. Whereas the number of ruby particles is very low in the waste, it has been observed that the number of ruby particles has increased slightly in the intermediary product and that the real intensity is in the concentrate. However, the gang mineral content in the concentrate is an indication that they do not have any magnetic characteristic.



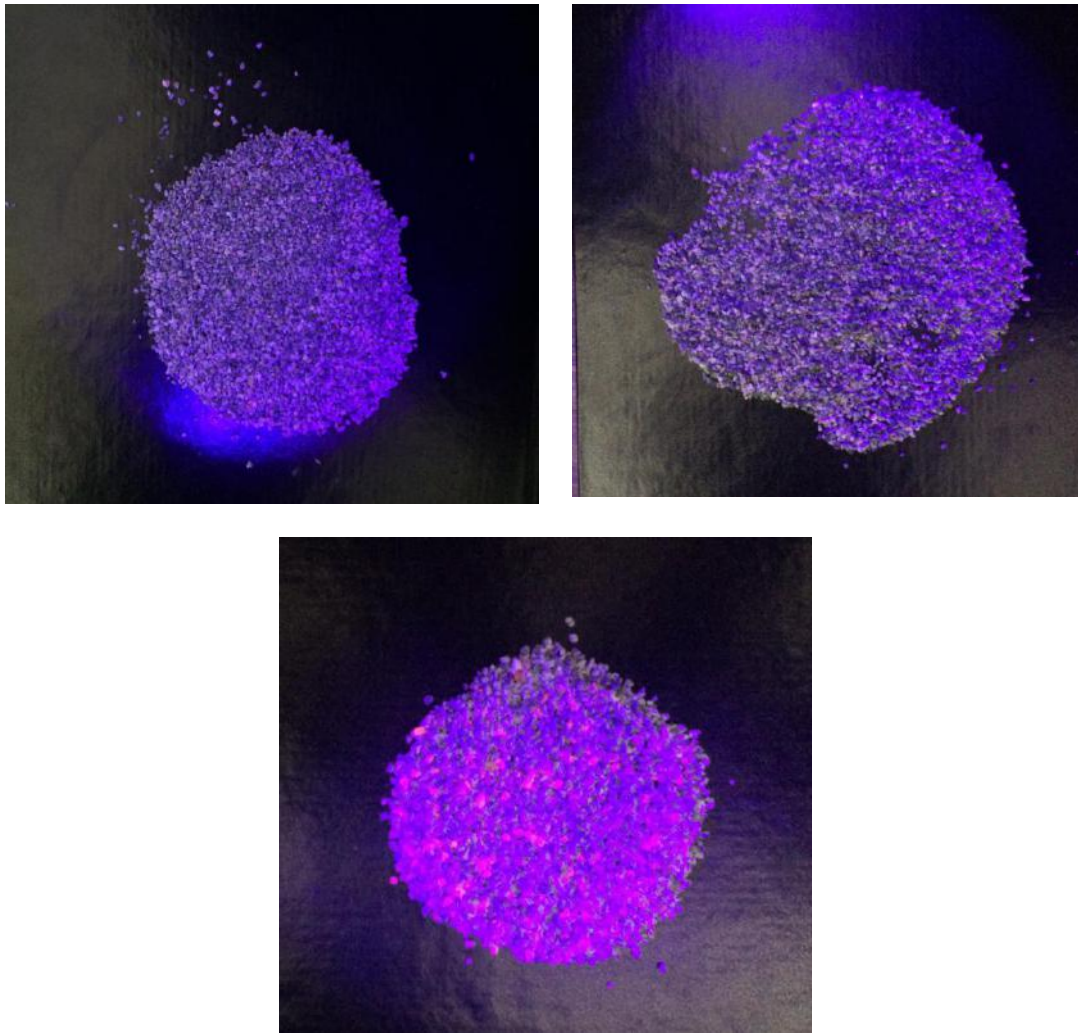


Figure 5. Appearance of the samples before (A) and after (B) magnetic separation

It has been put forth as a result of this study that ruby and gang may be separated under magnetic field and that an efficient separation process can be carried out by determining the required parameters as a result of carrying out separation at different field intensities and particle sizes.

It can easily be determined by examining the products before and after enrichment under blue light (UV) whether the separation has been successful or not due to the luminescent property of rubies. For this reason, monitoring the separation of the particles under blue light during enrichment will ensure that separation can be followed with the eye and that it will also be more economic as a result of less chemical analyses performed thereby resulting in a shorter amount of process time. It has been determined that rubies in hornblendes may be separated via magnetic separation method but that detailed studies should be carried out for determining the parameters which are effective in enrichment. Contributions will have been made to the country economy by providing an important raw material to the precious stone sector as a result of improving the quality of natural rubies as well as developing for their technological use.

3. CONCLUSIONS

- ✓ There are ruby formations from low to high quality in the bed. It has been determined that chromium is the impurity that determines color in ruby but that iron content also results in a change in color.
- ✓ It has been determined that majority of the gang minerals have gained magnetic property due to the 2.76-4.49 % Fe_2O_3 content.
- ✓ Mineral is the primary hornblende that ruby is bound to. Garnets, feldspars, epidotchlorite, cordierite, Cr-spinel and corundum are other minerals that are included in the composition.
- ✓ It has been determined according to the EDS spectrum acquired from the ruby surface that there is only aluminum and oxygen content and that there are also color differences.
- ✓ The magnetic mineral content of gang minerals in the raw material has indicated that they may be separated via high intensity magnetic separators.
- ✓ It has been determined thanks to the luminescence property of ruby that the content of the acquired products may be easily determined under UV light.

ACKNOWLEDGMENTS

This study has been supported by the Dumlupınar University Scientific Studies Projects fund with the project number of DPU BAP 2015-113. We would like to acknowledge field owner Bekir Yıldırım for his support to our field studies and for allowing us to collect ruby samples.

REFERENCES

1. Chapin M., Pardieu V., and Lucas A., Mozambique: A ruby discovery for the 21st century. *Gems&Gemology*, 2015, 44-54.
2. Gubelin E.J., Gemstones of Pakistan: Emerald, ruby, and spinel. *Gems&Gemol.*, 1982, 123-139.
3. Simonet C., Fritsch E., and Lasnier B., A classification of gem corundum deposits aimed towards gem exploration. *Ore Geology Revi.*, 2008, 34,127-133.
4. Kane R.E., and Kammerling R.C., Status of ruby and sapphire mining in the Mokoko Stone tract. *Gems&Gemology*, 1992, 152-174.
5. Hanni H.A., and Schmetzer K., New rubies from the Morogoro area, Tanzania. *Gems&Gem*, 1991, 156-167.
6. Boulon G., Fifty years of advances in solid-state laser materials. *Optical Materials*, 2012, 34, 499-512.
7. Bowersox G.W., Foord E.E., Laurs B.M., Shigley J.E., and Smith C.P., Ruby and sapphire from Jegdalek, Afghanistan. *Gems&Gemology*, 2000, 110-126.
8. Parlak O., Rizaoglu T., Bagcı U., Karaoglan F., Höck V., Tectonic significance of the geochemistry and petrology of ophiolites in South east Anatolia, Turkey. *Tectonophysics*, 2009, 473, 173-187.
9. Özdamar Ş., Çiftçi E., Uz B., Esenli F., and Kırkoğlu S., Ruby occurrences in Turkey: Principle characteristics (Abstract). *Acta Mineralogical Sinica*, 2013, Vol. 33-1, pp. 79.

10. Yılmaz H., Doğu Toroslar'da Sürgü (Doğanşehir-Malatya) Çevresinin Jeolojisi. Cumhuriyet Üniv. Dergisi, 1999, Seri A-Yerbil., 16-1,95-10.
11. Breeding C.M. and Shigley J.E., The 'Type' Classification System of Diamonds and Its importance in Gemology. Gems and Gemology, 2009.
12. Proctor K., GEM Pegmatites of Minas Gerais, Brazil: The Tourmalines of the Araquai Districts. Gems&Gemology, 1985.

GENERAL

DISSOLUTION BEHAVIOR OF SILVER ION DOPED HYDROXYAPATITE COATING ON METAL IMPLANT IN BLOOD PLASMA

Ayşe Gül Toktaş¹, Enes İbrahim Düden¹, Yiğitalp Okumuş¹, Mert Gül², Nusret Köse³, Aydın Doğan¹

¹ Eskişehir Technical University, Department of Materials Science and Engineering, 26555, Eskişehir, Turkey

² Ayfon Kocatepe University, Department of Materials Science and Engineering, Afyonkarahisar, Turkey

³ Osman Gazi University, Department of Orthopedy and Travmatology, Faculty of Medicine, Eskişehir, Turkey

ABSTRACT

In order to prevent infections during and after surgery and due to environmental factors, the surfaces of metal implants were coated with silver doped hydroxyapatite by electro-spray coating method. After that, dissolution of silver ion doped hydroxyapatite coated metal implants was investigated in blood plasma. Silver doped CaP powder was prepared via wet chemical synthesis technique, based on the precipitation of HA precursors from aqueous solutions using calcium hydroxide (CaOH_2) and ortho phosphoric acid (H_3PO_4). Colloidal solution prepared in methanol in a concentration of 1: 1 was coated with metal surfaces with equal geometry by electrospray method. 15 kV electric field was applied on the metal substrate during coating process. Surface area of coated metal implants was calculated that is 184 mm^2 . Blood plasma that is up to ten percent of surface area was added into plastic tube. Coated metals were put into those tubes. Coated metals were held in plasma during 12hour, 24hour, 1week, 2week, 3week, 4week, 6week, 8week and 10week, 16week at 37°C , 100 rpm. The blood plasma in the plastic tube was renewed in 84 hours. Precision scale (Ohaus, advantage) was used to measured changing of weight of metal implants. The scanning electron microscopy (SEM, Zeiss Supra 50VP and Zeiss Evo 50EP) and stereo microscope (Zeiss Axiocam Stemi 2000-C) were used to characterized microstructure and thickness of coated surface. Energy dispersive X-ray Spectroscopy was used characterized of chemical composition of coating. Changing of pH value of plasma was measured by pH meter (Hanna HI83414).

1. INTRODUCTION

Ti alloys and 316 L stainless steel metal implants are generally used in the healing of fractured bones. Metal implants are used with CaP based coatings instead of direct contact with the body due to their low corrosion resistance. HAp is used very often in bone related applications because it has almost the same chemical component as the bone. These HAp-containing applications have 2 different advantages; i) Faster fixation and stronger bonding with host bone ii) Increased healing of bone implant interface and internal structure of bone [1].

HAp is a biocompatible and bioactive material in the human body. HAp is compatible with various tissue types and can be used directly with soft tissue, muscle tissue and bone without any modified layer ie [2-5]. HAp also shows osteoconductive properties. HAp has poor mechanical properties (ductility, tensile strength and impact resistance) despite its excellent bio properties. Consequently, the use of HAP is limited in high load body applications [6]. HAP coatings were developed to the surface of metallic implants and combined with excellent strength and ductility of metal and excellent bio properties of HAP [7,8].

Various technologies are used for coating HAP on the metal surface; for example; dip coating-sintering, electrophoretic coating, hot isostatic pressing, solution deposition, ion beam spray coating In addition to these techniques, thermal spray techniques such as plasma spraying, flame spraying, high

speed oxy-fuel (HVOF) combustion spraying are among the techniques used for coating the metal surface of HAP [8, 9].

Today thousands of implants are using for orthopaedical application because of accident. The major problem with these implants is the lack of osseointegration and occurring infection. [10]. Silver-doped hydroxyapatite is used to increase osseointegration and reduce infection [11].

The synthetic calcium phosphate bioceramic on the implant surface can be transformed into biological apatite by a series of reactions such as plasma dissolution, precipitation and ion exchange. It is important to determine the parametric velocity effects due to the reactions depends on the material [12]. It is important that HA coatings are absorbable and degradable in a biological environment, which can lead to fragmentation of the coatings, leading to the loss of both coating-substrate bond strength and implant fixation [13, 14]. The quality of the HA coating is the main factor for bone fixation and long-term stability. The quality of the coating is important, for example in the dissolution of the coating, bone healing and mechanical fixation [15]. Composition differences, physical and mechanical conditions are the factors that affect the performance of HAP coating [16]. In this study, the coating process steps of the antibacterial HAP to the metal implant surface and the behavior of the coating in human blood plasma were investigated.

2. EXPERIMENTAL

2.1. Synthesis of Ag doped HAP and 6P57 Bioglass

Ag ion doped hydroxyapatite powder was synthesized by wet chemical method [17]. Chemicals used in powder synthesis, respectively; calcium hydroxide ($\text{Ca}(\text{OH})_2$) (Merck), orthophosphoric acid (H_3PO_4) (Sigma Aldrich), and silver nitrate (AgNO_3). First, the calcium hydroxide is added to the pure water and stirred for about 45 minutes. After calcium hydroxide is dispersed homogeneously in water, AgNO_3 (Merck) is added dropwise under continuous stirring. Finally, orthophosphoric acid is added drop by drop and the pH changes of the mixture are controlled simultaneously until the mixture has a pH value of 7. The prepared mixture is filtered with the and dried at 80 degrees for 24 hours. The dried powder is calcined for 1 hour at 1000°C. XRD (Rigaku Ring 2200) was used for pre-calcination and post-calcination phase analysis. For the microstructure and Ca / P ratio of the synthesized powder, SEM / EDX (ZEISS Supra 50 VP) was used with a 20 kV of acceleration voltage.

The ratios of Hench for the 6P57 bioglass were used and weight ratio of precursors are shown in Table 1. The chemicals used are respectively; SiO_2 (Sigma Aldrich), Na_2CO_3 (Carlo Erba), CaCO_3 (Merck), MgCO_3 (Abcr), P_2O_5 (Sigma Aldrich), K_2CO_3 (Sigma Aldrich). After the oxides were precisely weighed and homogeneously mixed, the mixture was melted in platinum crucible at 1350°C in the oven and poured into the water bath. The obtained frit was milled in the planetary mill for 1 hour in aqueous medium. The phase analysis of the bioglass was made by XRD and the thermal analysis was made by TGA.

2.2. Preparation of coating solutions and coating process

On the metal implant, Ag-HAP and 6P57 bioglass are coated with electro-spray method. Figure 1 shows a schematic view of the electro-spray coating method. As a result of the experimental studies and according to the previous study of Gürbüz and Doğan, the optimum electro spray coating parameters acceleration voltage: 14 kV, flow rate: 5ml / s, the distance between the substrate and the sample: 4 cm. In accordance with these parameters, 6P57 and Ag-HAP were coated onto metal implant surfaces respectively for 8 minutes for each [18].

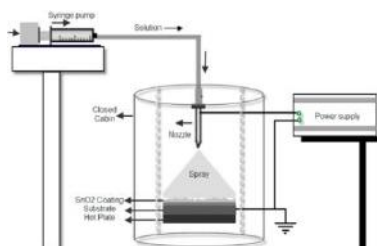


Figure 1. Schematic diagram of Ag-HAP powder

Coating suspensions were prepared in methanol medium at a concentration of 1% from the 6P57 bioglass and Ag-HAP powder separately. The particle size and zeta potential values of the 15 hours of grinded-suspensions were analyzed with Malvern Nano ZS device.

2.3. Sintering Process of Coated Metal Implants

The coated metal implant was put into the quartz tube. The sintering process was carried out under vacuum and implants were cooled under the atmosphere of argon gas. Sintering temperature and time were designated as 4 minutes at 750°C. Figure 2 shows an image of sintered metal implants.

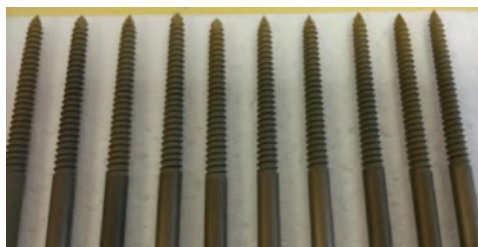


Figure 2. Sintered metal implants

2.4. Preparation of coated metal implants for dissolution test

For the dissolution test, the flat regions of the coated metal implants were cut by a diamond wire with a length of 1 cm using a wire cutting line and the photo of the cutting process is given in the Figure 3. The cut samples were then sterilized and placed in centrifuge tubes. The amount of the added human blood plasma into the tubes was calculated as 1/10 of the surface area of the metal implant. The tubes were incubated at 20 RPM at 37°C for 12 hours, 24 hours, 1 weeks, 2 weeks, 3 weeks, 4 weeks, 6 weeks, 8 weeks, 10 weeks and 16 weeks. In addition, plasma fluids inserted into the tubes were changed every 3.5 days considering that there was a continuous flow in the human body.



Figure 3. Sample preparation for dissolution test

3.RESULTS AND DISCUSSION

3.1. Phase analysis and microstructure of synthesized powder

The pre- and post-calcined phase analysis of synthesized Ag-HAP powder was obtained using the XRD (Rigaku) device. The diffractogram is shown in Figure 4. The XRD scan was from 2 Theta = 10.000 to 70.000 in 0.020 steps with a step time of 2.0 s using Cu-K α radiation.

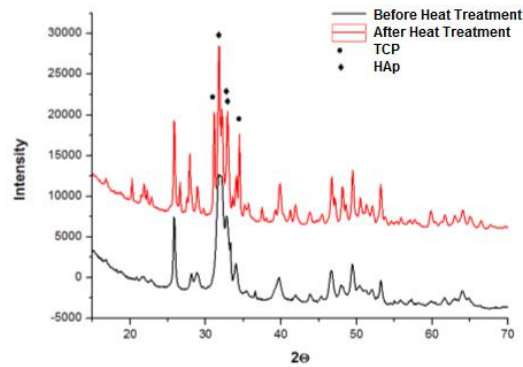


Figure 4. Phase analysis of powder, pre and post calcination

When the phase of powder before calcination was examined, the formed phase was HAp in structure but after the heat treatment HAp phase was observed accompanied by TCP phase. Figure 5 shows the microstructure of the Ag-HAP powder before and after calcination.

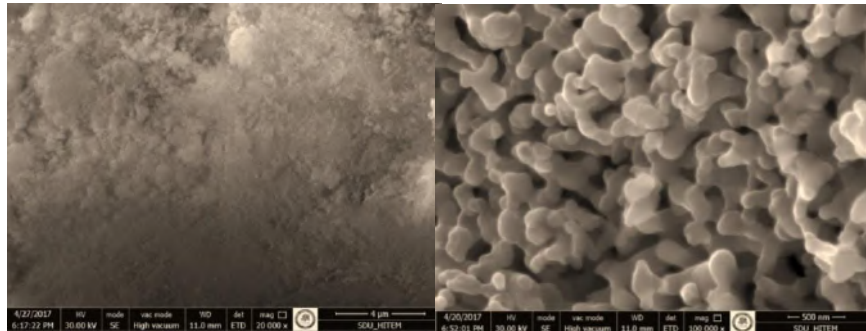


Figure 5. Ag-HAP microstructure before and after calcination

When the microstructures of the synthesized powders are examined, it is seen that the grains got closer and grew together with the heat treatment where the particle sizes of the calcined powders are approximately 40-50 nm. It was also observed that the grains were coaxial in a round shape and tended to clump due to the small size of the grain. The crystal structure analysis of 6P57 synthesized according to Larry Hench (Table 1) was performed with XRD and given in Figure 6.

Table 1. Amount of metal oxides used for 6P57 bioglass production

Compound	SiO ₂	Na ₂ O	CaO	MgO	P ₂ O ₅	K ₂ O
Amount (g)	56,5	11	15	8,5	6	3

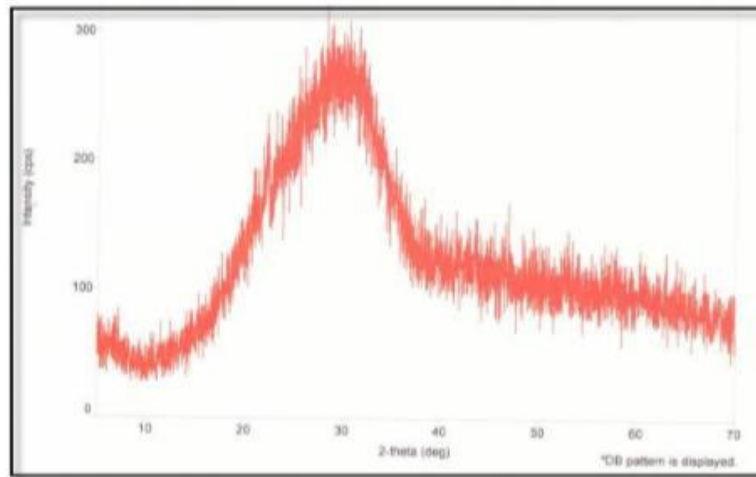


Figure 6. XRD pattern of 6P57 bioglass

In the XRD pattern of the bioglass synthesized in Figure 6, there is a single wide peak instead of unrelated and distinct peaks, indicating that the structure is amorphous. In order to increase the bond strength between the HAP and the metal surface, the 6P57 bioglass was coated onto the metal surface as the first layer. The important point here is to know the softening point of the used bioglass. The sintering temperature is determined according to this temperature. Figure 7 shows the thermal analysis of bioglass.

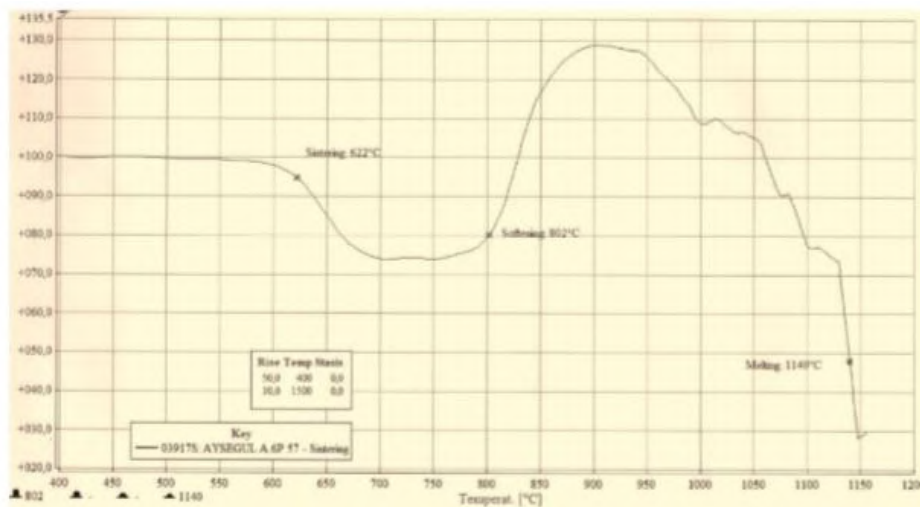


Figure 7. Thermal analysis of 6P57 bioglass

Referring to Figure 7, the bioglass is shown to have a softening temperature of about 800 °C. It is understood from this temperature that bioglass can adhere to the metal surface up to 1140 degrees, which is the melting point.

3.2. Changes in time-dependent plasma and HAP coating

3.2.1. Weight changes of the plasma and pH of the coating

Prior to the dissolution test, the pH of the plasma liquid was measured by Hanna pH meter and the initial pH value was read as 7.24. The time-dependent pH values of the HAP coated metal implant containing plasma liquids were measured. The weight of the HAP coated metal implants, which were subjected to the dissolution test, was measured on the precision scale simultaneously. In order to control the changes in the weight of the coating, the metal implants taken from the plasma liquid were

first cleaned with purified water and dried, then the weights were measured. Table 2 and Figure 8 show the changes in the pH values of liquids and the weights of the coatings.

Table 2. Changes in weight values of dissolution test samples and pH values of plasma liquid

Dinamic Plasma Experiment																									
Sample Name	Time	pH	pH Values																			Weight Changes (g)			
		First	1.	2.	3.	4.	5.	6.	7.	8.	9.	10.	11.	12.	13.	14.	15.	16.	17.	18.	19.	First	End	Difference	% Changes
1. Sample	12 h	7,47	7,64																			2,2883	2,2877	0,0006	0,02622034
2. Sample	24 h	7,47	7,65																			2,3888	2,3884	0,0004	0,01674481
3. Sample	1 week	7,47		6,2																		2,3418	2,341	0,0008	0,03416176
4. Sample	2 week	7,47	7,14	7,42	6,63	5,99																2,2444	2,2435	0,0009	0,0400998
5. Sample	3 week	7,47	6,55	6,19	6,2	6,16	6,17	6,45														2,1949	2,1944	0,0005	0,02278008
6. Sample	4 week	7,47	6,9	6,96	6,15	6,46	6,31	6,25	6,35	6,30												2,1378	2,1369	0,0009	0,04209935
7. Sample	6 week	7,47	6,46	6,05	5,87	6,07	5,98	6,20	5,92	6,09	6,56	5,81		5,72								2,337	2,336	0,001	0,0427899
8. Sample	8 week	7,47	7,51	7,08	6,58	6,66	6,38	6,17	6,36	7,43	6,05	6,30	5,88	5,54				5,46				2,2044	2,2037	0,0007	0,03175467
9. Sample	10 week	7,47	7,16	6,25	6,36	5,96	6,09	5,89	6,13	6,00	5,98	6,09	5,98	5,90	6,00	6,04	5,88	6,15	6,26			2,1881	2,1875	0,0006	0,02742105
10. Sample	16 week	7,47	7,94	6,42	6,1	5,8	6,24	6,14	6,62	6,61	5,80	6,07	6,00	5,74	5,86	6,25	5,78	6,37	5,82	6,20	7,41	2,0974	2,096	0,0014	0,06674931

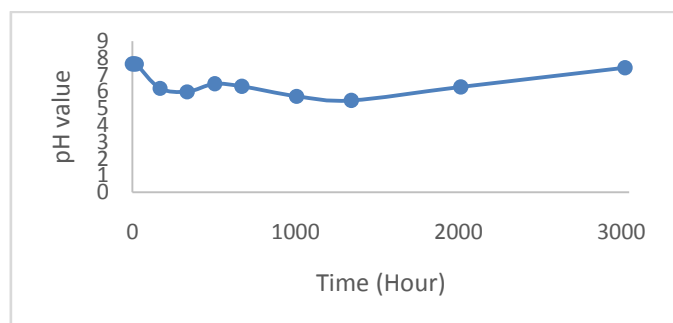


Figure 8. Time-dependent changes on pH values of plasma

There are differences in the pH values of the plasma liquids that were changed every 3.5 days were observed due to the ion exchange between the plasma and the coated sample. However, when each time interval is evaluated in itself, it is seen that there is an increase in pH after 12 hours and it is observed that the coating starts to dissolve in a short time. When a general evaluation is made according to time, it is also found that there is a decrease in pH values, but after a certain time, the saturation point of dissolution is reached and there is not much change. When a general evaluation is made based on time, it is also found that there is a decrease in the pH values but after a certain time the dissolution reaches the saturation point and there is not much change in pH anymore. When the weight changes of coatings were examined depending on time, a gradual increase is observed. 0,0006 grams of the coating have dissolved after 12 hours and at the end of the 6 weeks the amount of the dissolved coating has increased up to 0,001 grams. The weight change of the coating after about 2 months is 0.042%.

3.2.2. Changes in the Surface of Ag-HAP Coated Metal Implants

3.2.1. Investigation of surface changes by optical microscopy

The surfaces of the Ag-HAP coated metal implants were examined by an optical Stereo microscope prior to the dissolution experiment and are given in Figure 9.

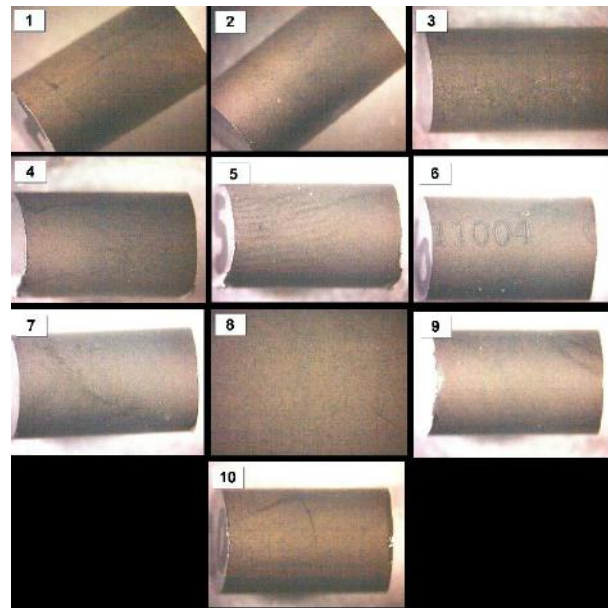


Figure 9. Optical microscope images of samples before dissolution test

The optical images shown in Figure 9 show that there is a complete coating on the metal surface. The surface of the metal substrate does not appear due to the approximately 10 mm thick coating on the surface. The optical images of the coatings that are kept in time-dependent plasma liquid are given in Figure 10.

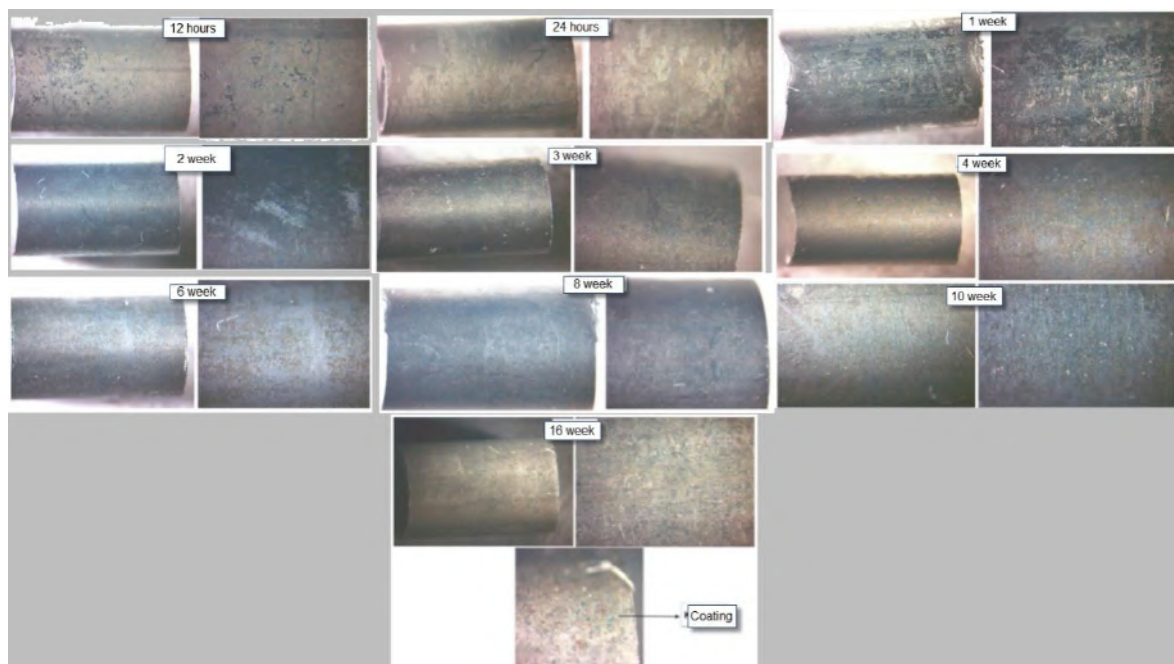


Figure 10. Optical images of changes in time-dependent surfacing of Ag-HAP coatings

When the coated samples were kept in plasma fluid at different time intervals, it was seen that gaps were formed on the surface of the coating at the end of 12 hours. The coating with the plasma fluid interacted in the first 12 hours. When the images were examined individually, the density of the coating on the surface decreased as the soak time increased. After about 8 weeks, the major amount of the coating was dissolved. The metal implant has become clearly recognizable by the optical microscope. However, even at the end of the 16th week, the coating still appears on the metal surface.

Therefore, either the coating was not completely dissolved, or HAP precipitations occurred on the metal surface [20].

3.2.2. Investigation of changes on coating surface by SEM

Variations in the time-dependent microstructures of the coating on the surfaces of the samples subjected to the dissolution test are given in Figure 11.

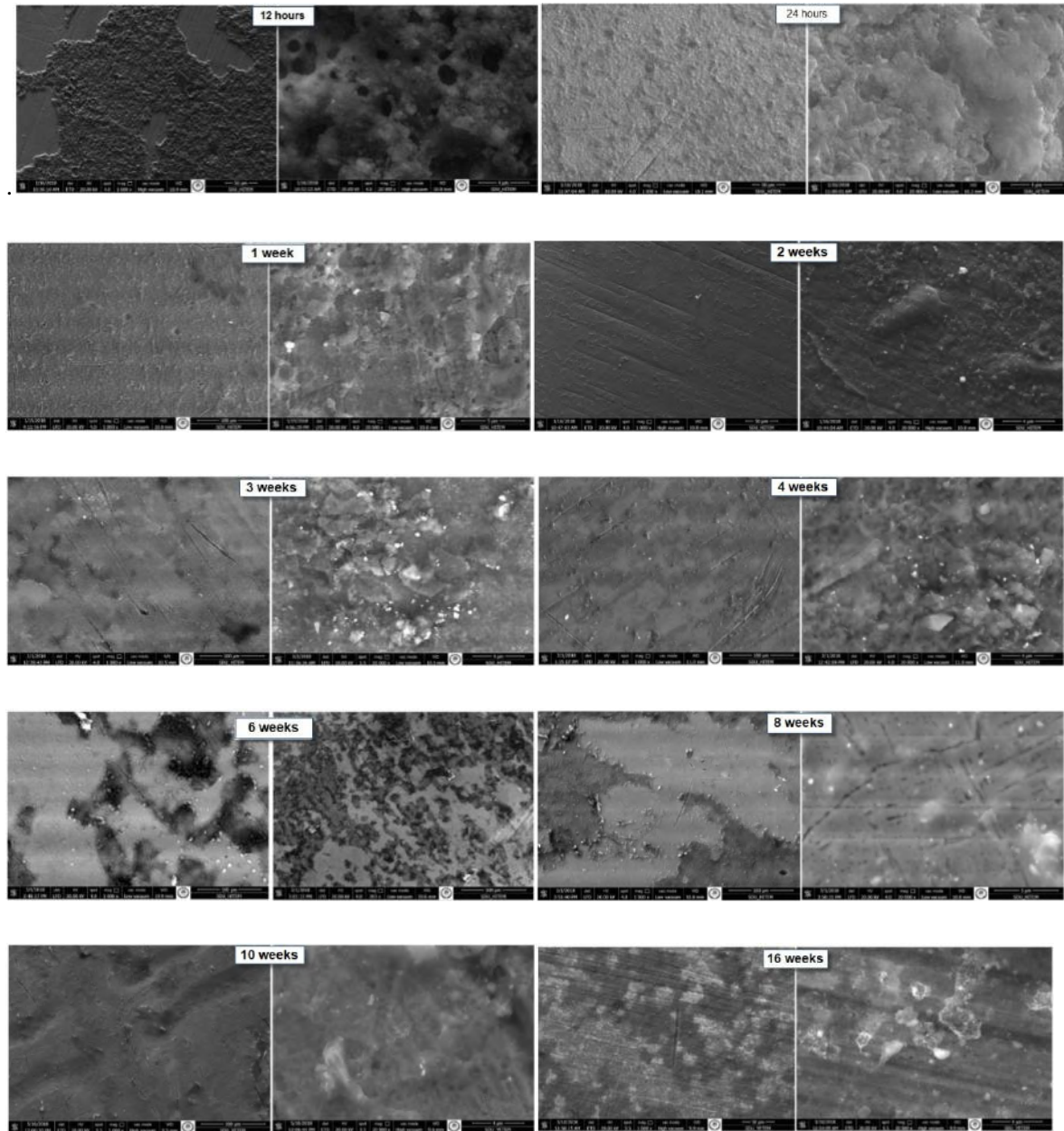


Figure 11. SEM images of samples after dissolution tests

Referring to Fig. 11, there are significant changes in the coating depending on time. At the end of 12 hours, as seen in the optical microscope and SEM, there is an interaction between the plasma and the coating. When the ceramic powder is observed very densely in the coating which is not kept in the plasma liquid, it is observed that the coating subjected to the dissolution test has decreased in time. However, the coating is not completely dissolved. Because even at the end of 2.5 months, it is seen that there is coating on the metal surface.

3.2.3. Chemical analysis of the elements on the coating surface

The variation of the elements in which the Ag-HAP coating was present in the plasma liquid at different times was determined by EDX analysis. In order to make a comparison, chemical analysis was performed from metal base and Ag-HAP coating which were not included in the deposition test. Table 1 shows the results of chemical analysis.

Table 3. Variations of time-dependent elements

	O	Na	Mg	Si	P	Ag	Ca	K	Mo	Cr	Fe	Ni
Metal Substrate									2,11	18,7 5	65,2 2	13,9 2
Ag-HAP Coating Surface	56,1 9	7,77	3,09	13,7	9,17	2,6	7,48					
12 h	51,4 7	8,65	4,92	18,3 4	6,34	1,94	8,34					
24 h	61,2 1	6,09	1,96	13,7 1	6,72	1,82	8,49					
1 w	65,7 9	5,33	2,55	13,6 4	5,25	3,49	3,94					
2 w	74,3 7	5,04	0,74	8,91	6,12	3,93	0,88					
3 w	75,7 8	4,95	0,01	4,07	5,88	1,24	8,05					
4 w	80,1 2	5,26	0,27	8,32	3,07	0,23	2,16	0,57				
6 w	76,6 3	4,57	0,1	6,74	4,11	3,98	2,3	1,56				
8 w	63,6 4	7,91	0,5	3	9,34	4,57	10,7 3					
10 w	73,3 3	8,95	1	6,75	5,82	1,87	2,28					
16 w	69,9 4	12,9 5	2,49	6,42	2,6	3,15	2,45					

At the end of 12 hours, only the antibacterial powder and the elements in the bioglass showed a peak in the graph. However, as the soak time increased, the intensities of Fe, Cr and Ni peaks from the metal undercoat increased. In this case it is concluded that at the end of 24 hours, the coating interacts with the plasma fluid. The peaks from the metal underlay were ignored to make the comparison easier. In this case, the coating was almost completely dissolved between 4-6 weeks. because a large decrease in the percentage of elements took place within this time interval. However, it is understood from the increase of the percentages of the elements, apatite layers originating from plasma were occurred on the metal surface after 6 weeks.

4. CONCLUSION

In this study, Ag-HAP bio ceramic powder was coated with electro spray coating method on metal implant surface. Optimum coating parameters are voltage as 14 kV, distance between the base and the nozzle as 4 cm and flow rate as 5ml / h. The dissolution behavior of the coating under suitable conditions in the body fluid was investigated. The physical and chemical properties of the coated samples which were kept in plasma liquid at different times and under optimum conditions were determined. The dissolution of the Ag-HAP bioglass has started at the end of 12 hours. The complete dissolution of the coating was carried out 4-6 weeks later. On the surface of metal implants which are still kept in plasma fluid, after these weeks, apatite phases were determined by chemical analysis.

REFERENCES

- [1] Sun L., Berndt C.C., Gross K.L., Kucuk A., Material Fundamentals and Clinical Performance of PlasmaSprayed Hydroxyapatite Coatings: A Received, J. Biomedical Research, 2001, 58/5, 570- 592
- [2] De Lange G, De Putter C. Structure of the bone interface to dental implants *in vivo*. J Oral Implantol 1993, 19, 123–135.,
- [3] Jasen J.A., van der Waerden J.P., de Groot K. Development of a new percutaneous access device for implantation in soft tissue. J Biomed Mater Res, 1991, 25, 1535–1545.,
- [4] Denissen H.W., de Groot K., Makkes P.C., van den Hooff A., Kloppe P.J., Tissue response to sense apatite implants in rats. J Biomed Mater Res, 1980, 14, 713–721.,
- [5] Black J., Biological performance of materials (3rd ed.). New York: Marcel Dekker, 1999, 444.
- [6] Jarcho M., Calcium phosphate ceramics as hard tissue prosthetics, Clin Orthop., 1981, 157, 259 – 278.
- [7] Tsui Y.C., Doyle C., Clyne T.W., Plasma sprayed hydroxyapatite coatings on titanium substrates. Part 1: Mechanical properties and residual stress levels, Biomaterials, 1998, 19, 2015–2029.,
- [8] Berndt C.C., Haddad G.N., Farmer A.J.D., Gross K.A.. Thermal spraying for bioceramic applications. Mater Forum 1990, 14, 161–173.
- [9] Lacefield W.R., Hydroxyapatite coatings. In: Ducheyne P, Lemons JE, editors. Bioceramics: Material characteristics versus *in vivo* behaviour, Ann NY Acad Sci 1988, 523, 72– 80.)
- [10] Köse N., Otuzbir A., Pekşen C., Pekşen A., Kiremitçi A., Doğan A., A silver ion-doped calcium phosphate-based ceramic nanopowder-coated prosthesis increased infection resistance, Clinical Orthopaedics and Related Research, 2013, 471/8, 2532-2539
- [11] Köse N., Çaylak R., Pekşen C., Kiremitçi A., Burukoğlu D., Koparal A.s., Doğan A., Silver ion doped ceramic nano-powder coated nails prevent infection in open fractures: *in vivo* study, Injury, 2016, 47/2, 320-324
- [12] Ducheyne P., Radin S., King L., The effect of calcium phosphate ceramic composition and structure on *in vitro* behavior. I. Dissolution, J. Biomedical Materials Research, 1993, 27-1, 25-34
- [13] Bauer T.W., Geesink R.C.T., Zimmerman R., McMahon J.T., Hydroxyapatite- coated femoral stems. Histological analysis of components retrieved at autopsy, J Bone Joint Surg 1991, 73A, 1439– 1452.,
- [14] Collier J.P., Surprenant V.A., Mayor M.B., Wrona M., Jensen R.E., Surprenant H.P., Loss of hydroxyapatite coating on retrieved, total hip components. J Arthroplasty, 1993, 8, 389 –393.
- [15] Dalton J.E., Cook S.D., *In vivo* mechanical and histological characteristics of HA-coated implants vary with coating vendor. J Biomed Mater Res, 1995, 29, 239 –245.
- [16] Soballe K, Overgaard S. The current status of hydroxyapatite coating of prostheses. J Bone Joint Surg., 1996, 78B, 689–690.
- [17] Hench L.L., And introduction to bioceramics, second edition, 2013
- [18] Koparal A.S., Doğan A., Bayrakçı Karel F., Gümüş iyon katkılı antibakteriyel malzeme, patent no: 2011-G-95491, 2011
- [19] Gürbüz M., Günkaya G. and Doğan A., Electrospray deposition of SnO₂ films from precursor solution, Surface Engineering, 2016, 32, 8-10
- [20] Priya A., Nath S., Biswas K., Basu B., *In vitro* dissolution of calcium phosphate-mullite composite in simulated body fluid, J. Mater. Sci: Matter, 2010, 21, 1897-1829

FUEL CELLS AND POWDERS

MODIFICATION OF PECHINI METHOD FOR OBTAINING (Yb₂O₃)_{0.2}(Y₂O₃)_{0.2}(ZrO₂)_{0.6} SOLID ELECTROLYTE

Aynur GURBUZ¹, Serdar YILMAZ²

¹ Mersin University, Advanced Technology Education Research and Application Center,
Ciftlikkoy Campus, 33343, Yenisehir/Mersin/Turkey

² Mersin University, Department of Physics, Ciftlikköy Campus, 33343,
Yenisehir/Mersin/Turkey

ABSTRACT

In this study, solid electrolyte production method was optimized. Firstly (Yb₂O₃)_{0.2}(Y₂O₃)_{0.2}(ZrO₂)_{0.6} electrolyte powder was synthesized by the modified sol-gel Pechini method. In order to determine the optimum amount of citric acid to be used in the synthesis, three molar ratios; CA/MC:C_M were studied by adding the moles of citric acid (CA) and metal cations (MC). The TG/DTA analysis was carried out to determine the mass loss of the binders used during synthesis process and the thermal stability of the sample. As seen in TG analysis results that a large amount of the binder burned out at 550 °C and continued to 750 °C. For this reason, the samples were calcined at 550 °C for 2 hours to completely remove the binders in the sample. However, looking at the samples after calcination, it is seen that the binder has not completely disappeared, and the cavity still continues. It is considered that the sample mass used for calcination is too much and that 550 °C is not enough. For this reason, the samples were calcined again at 600 °C and 750 °C for 2 hours to completely remove the binders in the sample. These temperature values are in agreement with the values seen in TG. The particle size and morphology of the samples were determined by FE-SEM analysis. Also the surface area of powder samples analysed by BET. Nanoparticles in the 30–60 nm range were obtained for the optimum molar ratios of C_M=2.

Key Words: Electroceramic, Solid Electrolyte, Pechini, ZrO₂

Acknowledgement: This study is supported by the Mersin University (project no: 2018-1-TP3-2795).

Aynur Gurbuz E-mail Address: aynurgurbuz@mersin.edu.tr

INTRODUCTION

The high oxygen ion conductivity over wide ranges of temperature and oxygen pressures in stabilized zirconia has led to its use as a solid oxide electrolyte in a variety of electrochemical applications. These include high temperature solid oxide fuel cells (SOFCs) which offer a clean, pollution-free technology to electrochemically generate electricity at high efficiencies. These fuel cells provide many advantages over traditional energy conversion systems including high efficiency, reliability, modularity, fuel adaptability, and very low levels of NO and SO emissions. Quiet, vibration-free operation of solid oxide fuel cells also eliminates noise usually associated with conventional power generation systems [1]. It is well known that high oxygen ion conductivity of doped zirconia results from the formation of oxygen ion vacancies as charge-compensating lattice defects. For example, Y³⁺, Yb³⁺, Sc³⁺ and Dy³⁺, whose ionic radius are near to that of Zr⁴⁺, can dissolve into ZrO₂ easily, thus both stabilizing

the cubic structure of zirconia and producing more structural defects, which can act as ionic charge carrier [2]. Fluorite-structured oxide materials such as yttria stabilized zirconia (YSZ), rare earth doped ceria, and rare earth doped bismuth oxide have been widely investigated as electrolytes for a fuel cell. Of these materials, YSZ has been most successfully employed [3].

The sol-gel technique offers a low-temperature method for synthesizing amorphous materials which are either totally inorganic in nature or composed of inorganics and organics. The process is based on hydrolysis and condensation reactions of organometallic compounds in alcoholic solutions [4]. Sol-gel methods enable homogenous samples to be obtained at low temperatures and the starting cationic composition to be maintained by using metal salts as raw materials and mixing them in a liquid solution. The most obvious advantage of this Sol-Gel method is that reagents are mostly mixed in atomic level, which may increase the reaction rate and decrease the synthesis temperature [7]. In 1967, Pechini developed a process for the preparation of the precursor polymeric resin [5]. First, a mixture of cations is formed in an organic complexing agent, CA, (citric acid or ethylenediaminetetraacetic acid, EDTA) and ethylene glycol solution. Second, the cations become a chelate and the polymeric resin forms. Finally, this polymer decomposes at 573 K. Two reactions are involved—a complex formation between citric acid or EDTA and metals, and a sterification between citric acid or EDTA and ethylene glycol (EG). The background of the proposed approach is esterification reaction between glycol and multifunctional carboxylic acid. For continuous growth of the polymer chain the existence of at least two functional groups in a monomer is important. The viscosity of the solution drastically increases during the polymer chain augmentation [6].

Galceran et al, using modified Sol-Jel Pechini method, synthesized $KRE(VO_4)_2$ ($RE = Gd$ and Yb) nanocrystalline powder. They used two different molar ratios $[Citric\ Acid\ (CA)] / [metal] = CM$ and $[Citric\ Acid\ (CA)] / [Ethylene\ Glycol\ (EG)] = CE$ in the synthesis. The SEM images of the samples they synthesized at these ratios are given in Figure 1.

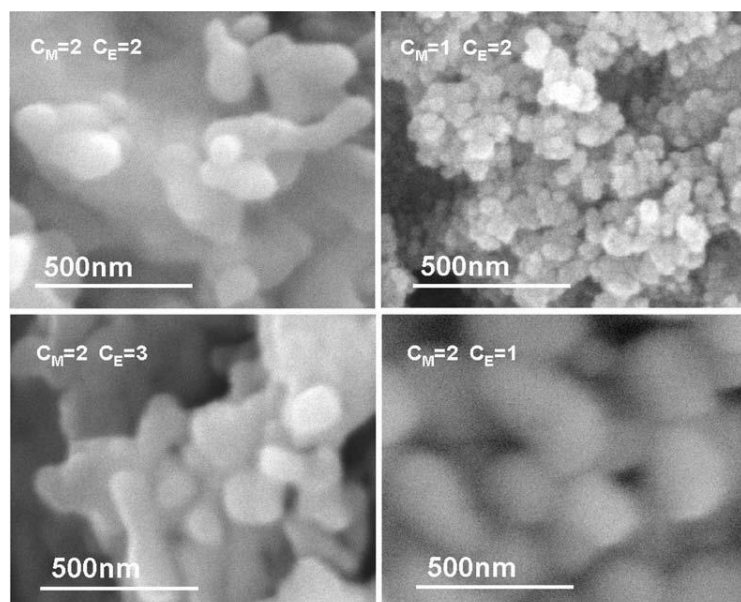


Figure 1. SEM images of KYbW nanoparticles at different CM and CE ratios. The calcination temperature was 973 K for 3 hours [7]

SEM images and other analyzes showed that the most suitable CM and CE ratios were 2 [7].

RESULT and DISCUSSION

Determination of Total Metal / Citric Acid Ratio

ZrCl₄ (Alpha Aesar, 99.5+%, 10026-11-6), Y(NO₃)₃.6H₂O (Alpha Aesar, 99.9% (reo), 13494-98-9) and Yb(NO₃)₃.xH₂O (Alfa Aesar, 99.9% (reo), 237-384-6) was used as starting raw materials. In order to determine the ratio of [Citric Acid (CA)] / [Total metal] = CM, the sample with x+y=4 was determined from the (Yb₂O₃)_x(Y₂O₃)_y(ZrO₂)_{1-x-y} ternary system. In this study, powders were synthesized such that the ratio of [Citric Acid (CA)] / [Ethylene Glycol (EG)] = CE was 2, at 3 different CM ratios of 0.5, 1 and 2. The chemicals used in the synthesis of powders and their amounts are given in Table 1.

Table 1. The chemicals used in the synthesis and amounts.

	Yb(NO ₃) ₃ .xH ₂ O (g)	Y(NO ₃) ₃ .6H ₂ O (g)	ZrCl ₄ (g)	Citric Acid (g)	Ethylene Glycol (g)	Ethylene Glycol (ml)
2Yb2YSZ (C _M =0.5)	0.588	0.628	8.784	3.936	1.968	1.768
2Yb2YSZ (C _M =1)	0.588	0.628	8.784	7.872	3.936	3.536
2Yb2YSZ (C _M =2)	0.588	0.628	8.784	15.743	7.872	7.071

ZrCl₄ weighed in the beaker on the magnetic stirrer inside the fume hood. 32 ml of pure water was slowly added over ZrCl₄ in the fume hood and ZrCl₄ was dissolved. Y(NO₃)₃.6H₂O and Yb(NO₃)₃.xH₂O were weighed into the beaker each with 2 mL of water. The mixture was started by placing magnetic fish in the beaker. After starting the mixture, the citric acid was weighed in the determined ratios. The temperature of the magnetic stirrer was then increased to 100 °C by adding ethylene glycol to the micropipette. Gel formation was observed after approximately 3 hours.

The gels formed were allowed to dry at 120 °C for 24 hours. TG / DTA analysis was carried out to determine the dissolution temperatures of the binders used during the synthesis and the thermal stability of the sample. The TG / DTA curves of the samples are given in Figure 2.

When the TGA curves of the samples were examined, it was seen that the weight loss was as fast as 550 °C and the loss was slowed down from this temperature. It was thought that the temperature of 550 °C would be sufficient for calcination to remove the binders in the samples. The samples are calcined in the Protherm marked oven at 550 °C for 2 hours. It was determined that the binders within the samples are not completely removed. The samples were calcined at 600 °C for 2 hours but the binders did not removed again. Finally, the samples were calcined at 750 °C for 2 hours and the binders in the sample were completely removed.

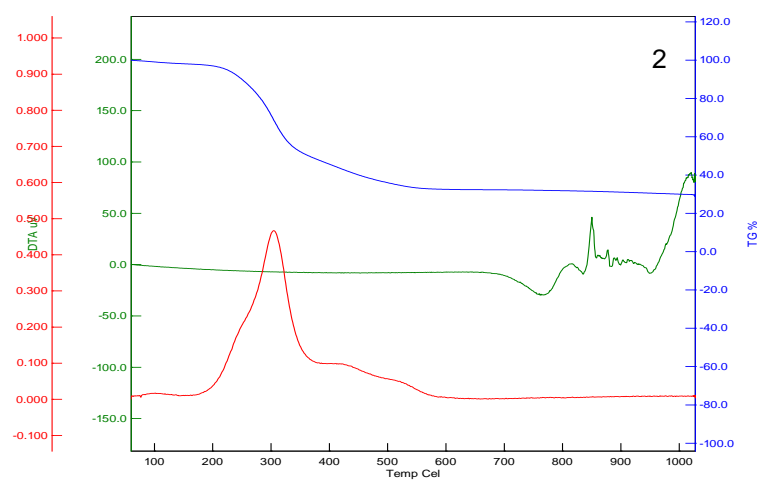
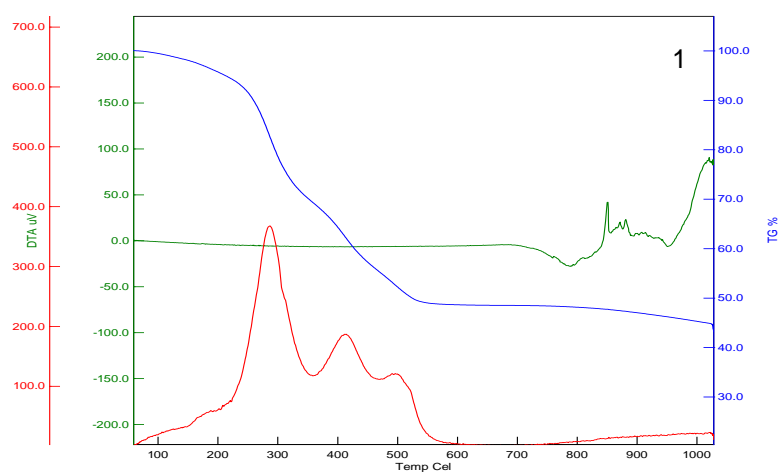
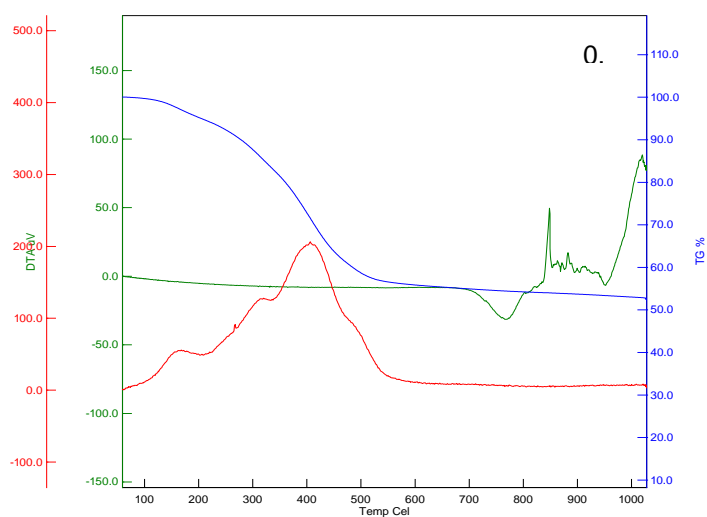


Figure 2. TG / DTA curves of 0.5, 1 and 2 coded samples.

The grain structure and morphology of the samples were determined by FE-SEM analysis and the surface area was determined by BET analysis. SEM images of the samples are given in Figure 3. When we look at the images of samples 0.5 and 1, it is seen that the nanoparticle is not formed and the samples are in macro structure. The sample number 2 was found to have a nanoparticle size of 30-60 nm.

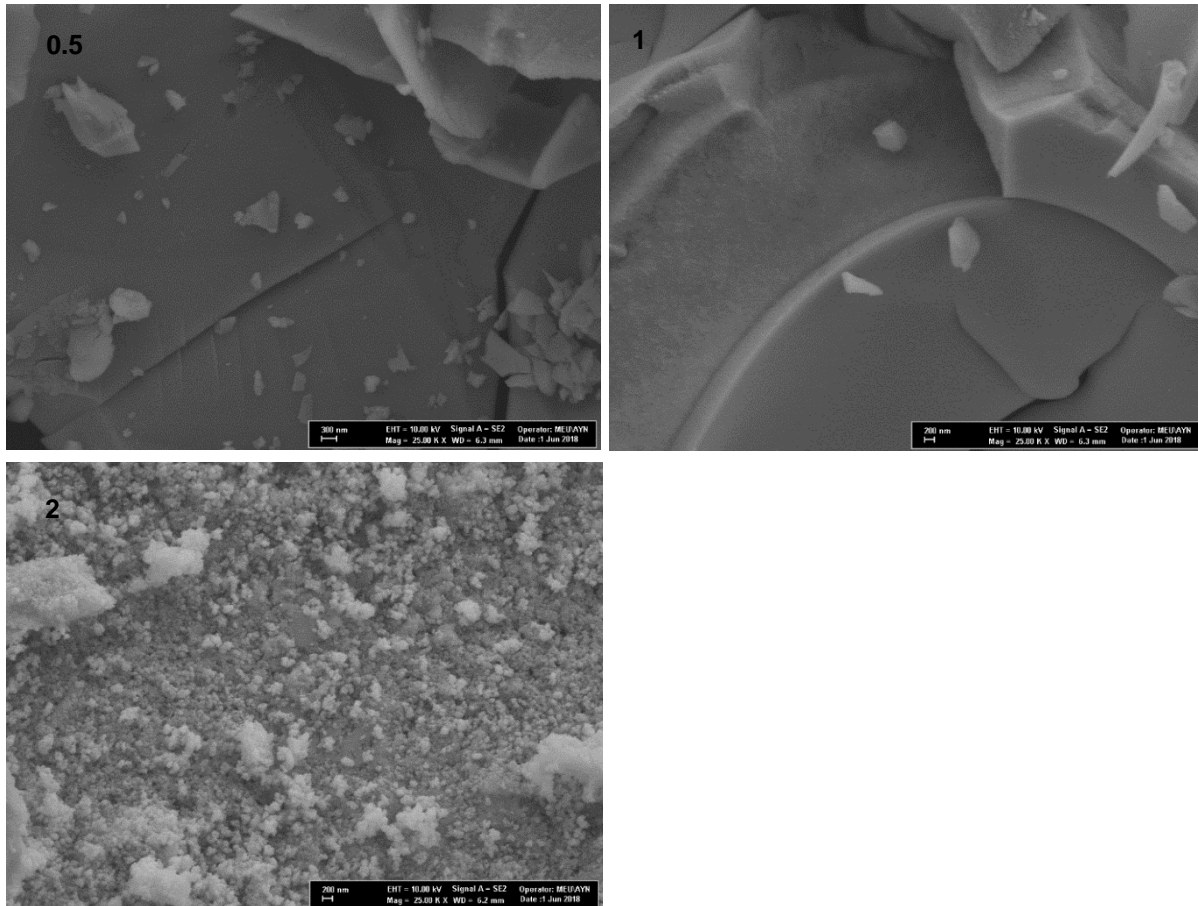


Figure 3. FE-SEM images of 0.5, 1 and 2 coded samples at 10 kV, 25.00KX.

Table 2 shows the BET Surface Area values of the samples. There is a decrease in surface areas of the samples due to increase in CM ratio. Since the sample 2 is of the nanoparticle size, the surface area value is expected to be high. However, BET surface area measurements are a method used for porous samples and the similarity of the results due to the fact that our samples are not porous shows that the particle surfaces of the macro-sized samples are similar. Sol-gel produced by the method of Samarium, Gadolinium, Prosedium and Terbium-doped Cerium-based electrolyte, the BET surface area value of $17 \text{ m}^2/\text{g}$ being the synthesis of BET surface area values of the samples according to the method indicate that, consistent with literature [8].

Table 2. BET surface area values of 0.5, 1 and 2 coded samples.

	Surface Area (m ² /g)
2Yb2YSZ (C _M =0.5)	20.0932
2Yb2YSZ (CM=1)	17.9722
2Yb2YSZ (CM=2)	12.6094

REFERENCES

1. Singhal, S. C., Advances in Solid Oxide Fuel Cell, Solid State Ionics, 135, 2000, 305–313.
2. Ridder, M., Welzenis, R.G., Brongersma, H. H., Kreissig, U, Oxygen exchange and diffusion in the near surface of pure and modified yttria-stabilised zirconia, Solid State Ionics, 158, 2003, 67 – 77.
3. Dell, R. M., Hooper, A., Hagenmuller, P., Gool, W. van, (Eds.), Solid Electrolytes, Academic Press, New York, 1978, 291.
4. Reisfeld R., Jorgensen CK., Optical properties of colorants or luminescent species in sol-gel glasses, structure and bonding. Springer-Verlag, Heidelberg, 1992, 208.
5. Pechini, M. ‘Method of preparing lead and alkaline earth titanates and niobates and coating method using the same to form a capacitor’, United States Patent, 1967, No: 3330697A.
6. Sakka, S., ‘Handbook of solgel science and technology: processing, characterization and applications’, Kluwer Academic Publishers, 2005, 22.
7. Galceran M., Pujol M. C., Aguil’o M., Diaz F., ‘Sol-gel modified Pechini method for obtaining nanocrystalline KRE(WO₄)₂ (RE = Gd and Yb)’, Sol-Gel Sci Techn., 2007, 42, 79–88.
8. Guo M., Lu J., Wu Y., Wang Y., Luo M., “UV and Visible Raman Studies of Oxygen Vacancies in Rare-Earth-Doped Ceria”, 2011, pp. 3872–3877.

CERAMIC SANITARYWARE AND TABLEWARE

CHARACTERIZATION OF COMMERCIAL CLAYS USED IN CERAMIC SANITARY WARE SECTOR

Veli Uz¹, İskender Işık¹, Nihal Derin Coşkun², Serkan Yener³, Eray Çaşın³, Ali İssi¹

¹ Dumlupınar University, Faculty of Engineering, Metallurgy and Materials Engineering Department,
Kütahya/Turkey

² Ordu University, Faculty of Fine Arts, Ceramic and Glass Department, Ordu/Turkey

³ECE Banyo Gereçleri San.ve Tic. A.Ş., Çorum/Turkey

ABSTRACT

In the ceramics industry, the clays are the main raw material with important features in terms of both shaping and strength of the final product. Increasing of the production cause the reduced quality of clay reserves. This provides the basis for the supply of quality materials in these materials. Nowadays, many companies prefer these type of clays which is commercially available. Clays are more important in ceramic sanitary ware than other areas due to their plasticity. However, there are not many detailed studies in the literature other than ready-made data and general physical tests from companies. For this reason, we have investigated five different sample usage characteristics of the clays belonging to different firms which have intensive use in ceramic sanitary ware sector. In this direction, physicommechanical properties, chemical constituents, dilatometer behaviors, crystal structures and mineralogical structures of clays have been determined and their advantages and disadvantages have been revealed.

Keywords: Commercial Clays, Sanitary ware, Characterization.

1. INTRODUCTION

The raw materials used in ceramic sanitary ware are defined as plastic and non-plastic. Plastic raw materials are comprised of clay group with plasticity while quartz and feldspar group raw materials make up the non-plastic raw materials. The mixing ratios of these raw materials in ceramic products are 20-25 % for clay, 25-30 % for kaolin, 30-35 % for feldspar and 15-20 % for quartz [1]. Clays are used in many areas ranging from paper, drilling, refractory to petroleum and they are also used as basic raw material in the ceramic sector [2]. However, the mineralogical content of the clays used may vary due to their particle size distribution and the ratio at which they are found with fluxing agent minerals [3]. Clays contain many minerals, however they are having fine particles and have a plasticity feature when mixed with water. Clays lose their water molecule content with

temperature and display refractory characteristic at increasing temperatures [4]. Clays are among indispensable raw materials for sanitary ware production due to their many characteristics such as plasticity, pre-firing strength, vitrification during firing [5]. The fact that meta kaolin content of clays transform into needle-shaped mullite crystals and silica glass at certain temperature intervals plays a role on its sintering behavior [6].

The properties of the clay to be used are effective for the selection of the other raw materials and production costs. Therefore, selection of clays suited for ceramic products is an important factor for the product characteristics gained during production after drying, shaping and firing. Even though the search for alternative raw materials in the ceramic sector is still ongoing, studies are also carried out for new clay beds and their usability [6-7]. Mullite which is among the most important phases of ceramics forms when the kaolinitic minerals in the structure are treated at high temperature. Mullite is defined as crystal structures that are rarely formed in nature but which develop when the alumina silicate structures in the ceramic transform into needle shaped, rod-like crystals with increasing temperature [8]. Clays and kaolin as sources of SiO_2 and Al_2O_3 are thin minerals which are included among starting raw materials with significant impact on the formation of mullite. The increase of initial clay-kaolin amount in the structure increases mullite formation [9]. The formation of tertiary, secondary and primary mullite crystals affect the characteristics of the sanitary ware produced [10]. The purpose of this study was to determine the properties of various clays used in vitrified products and compare them to put forth their impacts on the production processes as well as on the final product.

2. MATERIALS AND METHOD

Five different clays used in sanitary ware production have been used in this study. Chemical and mineralogical analyses were applied on the clays used for determining their rheological characteristics, thermal behavior and physico-mechanical properties. Chemical analyses were performed via Spectro X-Lab 2000 model XRF device. Seger ratios of clays were calculated according to the acquired results. Rigaku, Rint 2000, Japan X-Ray Diffractometer device was used for the mineralogical analyses of raw clay samples ($\text{Cu-K}\alpha$, 20 5-70°, 2°/min). The X-Ray diffractograms of the clays were used for determining their mineral and phase ratios while the crystal structure parameters were determined using the MAUD 2.8 software. The crystal structures of the mineral content of the clays were drawn using Crystal Maker 9.2 crystal software. Sanitary ware products are shaped via casting. The rheological properties of clay should be determined and considered attentively in order to be able to produce products without any deformations in the casting method. For this purpose, the casting characteristics of the clays used in the studies were determined. Dilatometer analyses were carried out using 402 CL model Netzsch Brand device for determining the thermal behavior of clays. The clays were shaped and fired in kilns at the plant where sanitary ware production is carried out. The color values of the fired samples were measured. Physico-mechanical properties were determined for at least four of the fired and shaped

clays after which their average was calculated to obtain the results. The strength values were determined using a Shimadzu brand three-point bending device, whereas the $L^*a^*b^*$ values in color measurements were determined using a Konica - Minolta Cm-23-00-B Spectrophotometer.

3. RESULTS

3.1. Chemical analyses and Seger Values

Chemical analyses results indicating the oxide ratios of the clays used have been given in Table 1. Fe_2O_3 content in clay decreases the refractory characteristic and causes colorings to occur. The lowest Fe_2O_3 ratio was determined in K5 clay with 0.92 %, while the highest ratio was determined in the K3 sample with 2.27 %.

Table 1. Chemical analyses results

Oxide	K1	K2	K3	K4	K5
SiO_2	56,18	54,43	56,73	58,46	56,18
Al_2O_3	27,67	28,31	27,44	26,30	27,91
Fe_2O_3	1,96	2,07	1,78	2,27	0,92
CaO	0,26	0,43	0,21	0,28	0,14
MgO	0,58	0,83	0,38	0,59	0,58
Na_2O	0,23	0,30	0,32	0,20	0,31
K_2O	1,85	1,84	1,38	2,12	2,07
TiO_2	1,08	1,15	1,20	1,03	1,03
P_2O_5	0,05	0,07	-	0,10	0,06
A.Z.	10,14	10,57	10,56	8,65	10,80

The Seger values for the clays calculated using the chemical analysis results have been given in Table 2. The highest Na_2O content according to the Seger values has been determined in K3 and K5 clays. Lowest Al_2O_3 and SiO_2 values were determined in the K2 sample and highest in the K3 clay sample. The K_2O values as fluxing oxide content were higher in comparison with the Na_2O ratios.

Table 2. Seger Calculations for Clays

Sample	Acidic				Amphoteric		Basics	
	Na_2O	K_2O	CaO	MgO	Al_2O_3	Fe_2O_3	SiO_2	TiO_2
K1	0,087	0,463	0,109	0,341	6,378	0,288	22,014	0,317
K2	0,092	0,370	0,145	0,393	5,252	0,245	17,168	0,272
K3	0,156	0,444	0,113	0,287	8,129	0,336	28,572	0,453
K4	0,071	0,495	0,109	0,324	5,663	0,312	21,400	0,283
K5	0,114	0,500	0,057	0,329	6,216	0,131	21,270	0,292

3.2. Mineralogical characteristics

Determining the impact of the mineral content of clays on the properties of clay and on the ceramic structure is an important factor in ceramic production. The X-ray diffraction patterns for the mineral content of the five types of clays used in the study have been given in Figure 1. It was determined that the general mineral content of clays is comprised of kaolinite, quartz and muscovite.

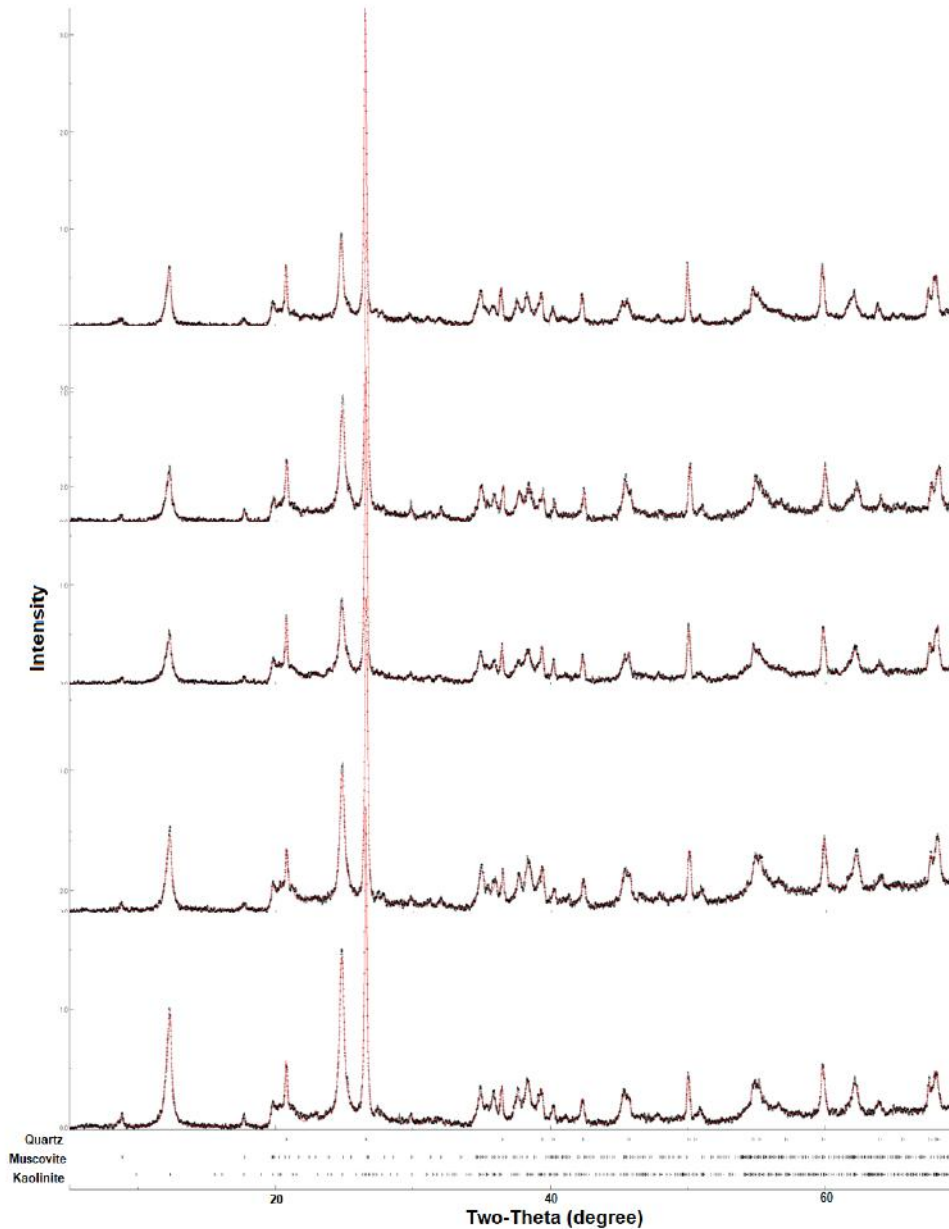


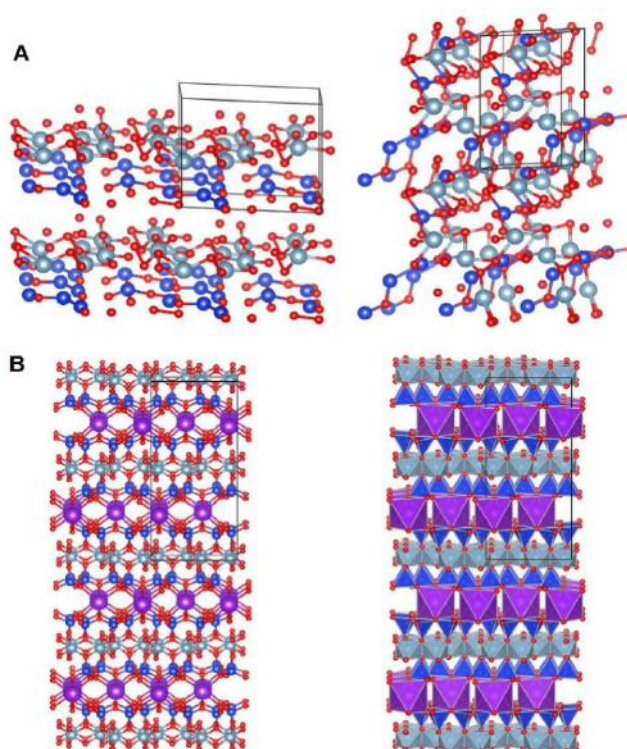
Figure 1. X-Ray Diffraction Patterns of Clays

The mineral ratios of the clays calculated using the patterns obtained via X-Ray analyses have been given in Table 3. Highest kaolinite content was determined in K1 and K2 samples while the lowest kaolinite content was determined in K5 samples. Muscovite content was about 26 % in K4 clay. Lowest muscovite content is about 10 % in K2 sample.

Table 3. Mineral ratios of clays

Mineral	K1	K2	K3	K4	K5
Kaolinite	61.153	63.752	59.875	55.051	49.097
Muscovite	16.895	9.8159	14.761	25.708	23.903
Quartz	21.952	26.432	25.364	19.242	27.000

The crystal structure appearance for the kaolinite (Figure 2A) and muscovite (Figure 2B) content of clays calculated using the Rietveld method according to the XRD analysis results have been given in Figure 2.

**Figure 2.** Crystal structure appearances of the mineral content of clays

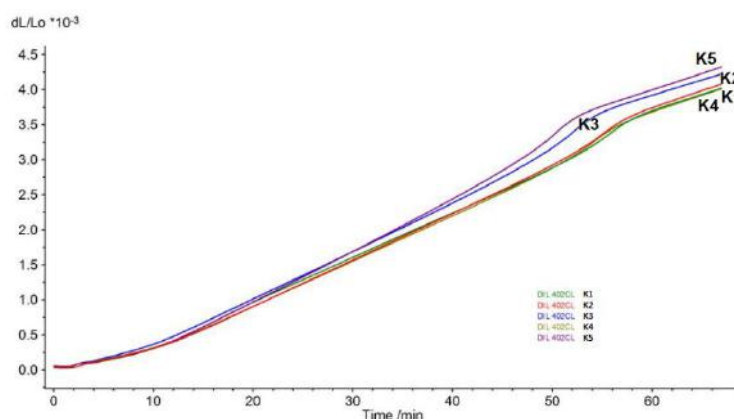
3.3. Rheological properties

The electrolyte amount used in adjusting the rheological properties and viscosity of clays was highest in K3 clay (Table 4). High amounts of electrolyte use may lead to unstable mud in production. In addition, defects and silicate traces may also develop in the product due to excessive electrolyte use. The casting rate of K5 clay with the highest thixotropy value was the lowest in comparison with other clays. K1 and K2 clays had the highest casting rate values. However, high casting rate value does not indicate that it can be used in any casting. Because it should also be suited to the production process. Accordingly, the clay with a high performance thanks to its workable structure especially in pressure casting during production was the K5 raw material.

Table 4. Casting properties of clays

	K1	K2	K3	K4	K5
Electrolyte amt. (5 poise) (%/gr)	0.53	0.56	0.74	0.61	0.65
Electrolyte amt. (5 poise) (%/cc)	0.38	0.39	0.53	0.44	0.47
Liter weight (gr/lt)	1655	1645	1646	1654	1645
Dry Matter, %	62.62	63	63	63	63
Gallenkamp, V' (°G)	324	320	323	334	322
Gallenkamp 6V' (°G)	281	262	270	283	262
Thixotrophy	43	58	53	51	60
Silicate value (%/gr)	0.64	0.72	0.96	0.8	1.05
Silicate amt. (%/cc)	0.45	0.51	0.69	0.57	0.76
60' Casting Rate (mm)	6.5	6.8	4.8	5.78	4.50
Casting rate (mm ² /min.)	0.70	0.77	0.38	0.56	0.34

The mineral content of the raw materials is effective in firing rapidly and without any deformation in the firing of the ceramic products and sintering of the particles. The dilatometer curves of the clays used have been given in Figure 3. Temperature values that are critical for firing can be determined in the dilatometer curves by taking into consideration the points where glassy phase forms and shrinkage starts as well as the points where fluxing ends and shrinkage stops. In addition, deformations in the products due to expansion during firing up to a certain temperature may also be prevented according to dilatometer curves by determining the expansion behaviors of the mineral content of the raw materials prior to fluxing. The temperature values of the pre-heating region in the kilns may be determined according to these expansion behaviors. Thus, it is possible to shorten the kiln pre-heating region or decrease firing times by increasing temperature. Highest expansion values in the dilatometer curves were observed at a temperature of 700°C for the K3 and K5 samples. The expansion ratios of the other clays were about 4 %.

**Figure 3.** Dilatometer results of the clays used

The curves for the first derivative values of the dilatometer values indicating the time dependent elongation (expansion) values for the clays have been given in Figure 4. It was determined that the K3 and K5 clay samples continued to display higher expansion values with increasing temperature values above 200°C in comparison with other clays. Similarly, the curves of both clay samples above 700°C move down rapidly indicating a slowing down in the expansion and shrinkage behavior at an earlier time in comparison with the other clays.

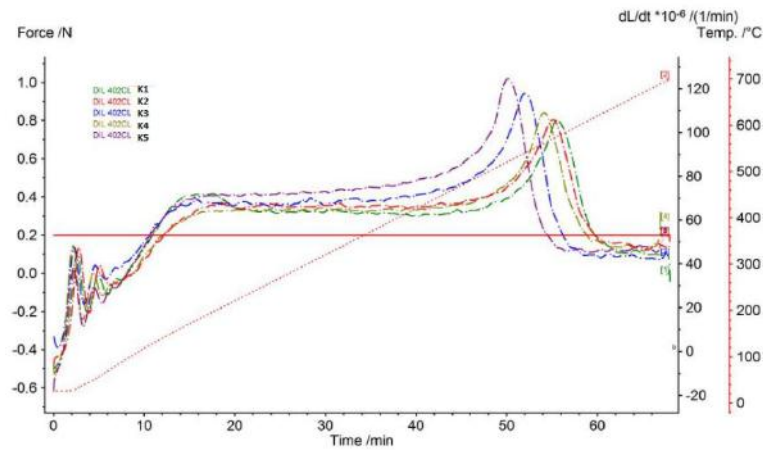


Figure 4. Dilatometer results of the clays used

Thermal expansion behaviors and volumetric bulk density values for the clays determined according to the dilatometer analyses have been given in Table 5. Highest thermal expansion values were determined at a temperature of 300°C for the K3 clay and the lowest expansion value was that of the K4 clay. Whereas at high temperature, highest expansion was for the K5 sample with a value of 66.74 at a temperature of 600°C, whereas the lowest value was determined as 60.82 for K4 clay. According to the bulk density values calculated based on the weight losses obtained from dilatometer analyses and the sample volume, the lowest value was obtained as $1.667 \times 10^{-3} \text{ gr/mm}^3$ for the K3 sample, whereas the highest density was obtained as $2.043 \times 10^{-3} \text{ gr/mm}^3$ for the K2 sample.

Table 5. Comparative thermal expansion and density values

Value	K1	K2	K3	K4	K5
α 300	52.98	51.15	54.05	48.51	52.43
α 400	55.87	55.33	58.05	52.91	58.22
α 500	57.47	57.94	61.52	55.7	63.13
α 600	61.98	62.71	65.84	60.82	66.74
Density, $\times 10^{-3} \text{ gr/mm}^3$	2.008	2.043	1.667	1.965	1.943

3.5. Physico-mechanical properties

The lowest shrinkage based on the shrinkage values obtained after drying the clays following the shaping procedure was determined in the K2 clay while the highest value was 5.5 % for the K3 clay. The highest dry strength value was 60.42 kg/cm² for the K4 sample. Lowest water absorption value was obtained for the clays fired in the sanitary ware kiln as 1.40 % for the K4 sample, whereas the highest water absorption value was about 4.31 % for the K3 sample (Table 6).

Table 6. Physico-mechanical analyses result for the clays

	K1	K2	K3	K4	K5
Firing loss (%)	9.72	9.95	10.69	8.91	10.35
Dry Shrinkage (%)	5.00	4.30	5.50	4.60	4.70
Total Shrinkage (%)	12.30	12.40	12.10	11.60	12.20
Deformation 20 cm.	6.0	7.5	5	10	7.0
Water Absorption (%)	3.95	3.98	4.31	1.40	2.12
Dry Strength (kg/cm ²)	39.39	44.75	49.85	60.43	54.28
Ccs Ring (°C)	1215	1211	1217	1212	1217

3.6. Color measurement results

The maximum L* value indicating the whiteness value for the raw clay samples was obtained as 72 for the K2 sample. The whiteness values increased significantly in fired samples (Table 7). Whereas the highest whiteness value was obtained as about 86 for K1 and K2 clays, the whiteness values decreased to about 71-73 in K3, K4 and K5 clays. The K1 and K2 clays with higher kaolinite content are whiter according to the L* values which vary between ~86-87 for the fired product and between ~65-71 for the raw product. While the highest redness value +a* was obtained in the fired K4 sample, K5 clay had the highest redness value among the raw products. Yellowness value +b* provides a better color scale for sanitary ware products with a value of 8.83 in fired and raw K1 sample [11].

Table 7. Color values for raw and fired clays

Sample	Chromatic coordinates					
	L*		a*		b*	
	Raw	Fired	Raw	Fired	Raw	Fired
K1	65,81	86,9	0,77	-0,15	8,83	8,83
K2	71,96	87,23	0,81	-0,43	9,45	14,27
K3	64,47	73,93	1,36	-0,36	8,27	14,31
K4	70,41	71,47	0,65	-0,15	10,38	16,5
K5	64,59	72,79	1,57	1,24	6,32	13,88

According to the obtained results;

- The Al_2O_3 content of clays was determined between 26-29%. Lowest Fe_2O_3 ratio that causes coloring after firing in clay samples was 0.92 % in K5 clay, while the highest ratio was 2.27 % in K3 clay.
- Clay samples contain kaolinite, quartz and muscovite minerals. Highest kaolinite content was determined in K1 and K2 clays with values ranging between 61-64 %. While the lowest kaolinite content was 49 % in K5 sample. Highest muscovite ratio was determined as 26 % in K4 clay and the lowest ratio was 10 % in K2 clay sample.
- Highest thixotrophy value among the clay samples in rheological properties and the lowest casting rate were determined in K5 clay.
- Highest time dependent casting rate was determined in K1 and K2 samples. However, K5 clay samples had the highest performance in operating conditions with their workable structure in pressure casting.
- Highest expansion was observed in K3 and K5 samples with 4.5 % at 700°C. Whereas the expansion ratios of the other clays were at 4 %.
- Highest and lowest thermal expansion values at 300°C were determined in K3 and K4 samples respectively. Highest expansion at a high temperature of 600°C was observed in the K5 sample with a value of 66.74.
- Lowest and highest bulk densities were determined as $1.667 \times 10^{-3} \text{ gr/mm}^3$ and $2.043 \times 10^{-3} \text{ gr/mm}^3$ for K3 and K2 clay samples according to the weight loss values obtained from dilatometer analyses and the sample volume.
- Dry shrinkage values of shaped clay samples were determined as lowest in K2 and highest in K3 clay with 5.5 %. Highest dry strength value was obtained as 60.42 kg/cm^2 for the K4 sample.
- Lowest water absorption value for the clay samples fired in kilns was determined as 1.40 % for K4 and the highest value was determined as 4.31 % for the K3 clay sample.
- Whiteness value (L^*) of raw clays was highest for the K2 sample with a value of 72. The highest whiteness value in fired samples was determined as 86 for the K1 and K2 clay samples. The L^* values after firing increased by 20 % in comparison with the raw clay samples. It was determined that the K1 and K2 clay samples had higher whiteness values due to high kaolinite content.
- It was determined that using only laboratory scale measurements for deciding on the raw materials to be used in products shaped via casting would be difficult. It was determined that pilot trials should be carried out at plant scale as well.

REFERENCES

1. Kingery W.D., Bowen H.K., Uhlmann D.R., Developments of microstructure in ceramics. Introduction to Ceramic John Wiley & Sons. Inc, 1976, Canada.
2. Karakaya M.Ç., Karakaya N., Systematic mineralogy. Selçuk University Faculty of Engineering-Architecture, 2007, Konya, 454.
3. Stathis G., Ekonomakou A., Stournaras C.J., Ftikos, C., “Effect of firing conditions, filler grain size and quartz content on bending strength and physical properties of sanitaryware porcelain”. Journal of the European Ceramic Society, 2004, 24, 2357-2366.
4. Kumbasar I., and Akyol A., Mineraloji, İtü Yayınları, 1993, İstanbul.
5. Fortuna, D., Ceramic technology sanitaryware. Graphic Line, Faenza, 2000, Italy.
6. Taşçı E. H., UZ V., Sintering Behavior of Muttalip Region Clay. 4th Int. Eskişehir Terra Cotta Sym., 2010, Eskişehir Tepebaşı Belediyesi. 619-634.
7. Monteiro S. N., Vieira C. M. F., Influence of Firing Temperature on The Ceramic Properties of Clays from Campos dos Goytacazes. Applied Clay Science, 2004, Brazil, 27, 229-234.
8. Schneider H., et. al., Structure and Properties of Mullite-A Review. J. Eur. Ceram. Soc., 28, 2008, 329-344.
9. Becker, C. R., Mixture, S.T., Carty, W.M., The role of flux choice in triaxial whiteware bodies. Ceramic Engineering and Science Proceedings, 2000, 21-2, 45-51.
10. İssi A., Derin Coşkun N., Tiryaki V., Uz V., Casting and Sintering of Sanitary ware Body Containing Fine Fire Clay (FFC). J. Aust. Ceram. Soc., 2017, 53:157-162 DOI 10.1007/s41779-016-0020-8.
11. Eppler R.A., Glazes and glass coatings. A.m. Ceram. Soc., 2000, Westerville, 130-135.

CERAMIC SANITARYWARE AND TABLEWARE

BEHAVIOR OF COBALT SPINEL PIGMENT IN TRANSPARENT GLAZE

Kemal Karadal¹, Müzeyyen Şirin¹, Hanife Kadioğlu¹, Veli Uz²

¹Kütahya Porcelain Research & Development Department, Kütahya

²Kütahya Dumlupınar University, Metallurgy and Material Engineering, Kütahya

Abstract: Spinel structures favor in ceramic materials having stability at high temperatures. In this study, the crystal structure changing of cobalt aluminates pigment in spinel structure was researched in transparent glaze into added different at percent ratios. In addition, phase analyses were carried out after the pigment was fired at 1140°C which was then added at different ratios into transparent glaze. It was determined that color of glaze and lattice parameter of cobalt spinel changed by addition ratio. Pigment addition into the transparent glaze at increasing ratios resulted in color change. The spinel pigment includes 3% unstable phase after firing at 1140°C. Amorphous phase ratio decreases with increasing pigment ratios added to transparent glaze while quartz and spinel phases increase. It has been determined that the desired color values can be attained by determining the pigment ratio according to furnace temperature and that color change problems may be resolved by way of phase analysis.

1. Introduction

Majority of the colors used as under glaze, in glaze, slip and over glaze are obtained from oxides or carbonates. Cobalt oxide is a strong colorant oxide for obtaining blue color [1-3]. While 0.2% cobalt oxide addition to the glaze results in navy blue color, different color tones ranging all the way to sky blue are obtained when the amount of fluxing agent in the glaze is decreased [4]. Spinel structure CoAl_2O_4 is generally produced via different methods with the reaction between two oxides [5-10]. It is used frequently in semi-conductors, sensors, colored plastic, paint, fiber, rubber, glass, cement and ceramic bodies due to its strength against acids and bases as well as against atmospheric conditions [11-13]. The color of blue pigments may vary from blue to blue-turquoise colors with decreasing particle size [2,3,6].

In general, two and three valence metal ions may be found in the spinel structure according to oxidation. Metal ions take place in two different coordination in the spinel structure. While the oxygen ions are coordinated in octahedral shape in the first section, they are coordinated in tetrahedral shape in the second region. While only two valence metal ions are present in tetrahedral regions in the normal spinel structure, only two valence metal ions are present in the octahedral region [14]. This is effective in ensuring that the pigment is stable since dissociations take place when stoichiometric ratios are not proper [13,15,16]. It has been used in recent years in stoneware and earthenware

products [9]. The purpose of this study was to determine the impacts on color formation of phases that develop in the glaze due to the addition of the blue color pigment to the glaze at different ratios as well as the changes in spinel structure.

2. Experiments

The spinel structure pigment samples used in the study are used in ceramic products. Pigmented glazes were prepared by adding 1%, 5%, 10% of spinel structure pigments into the transparent glaze. The pigmented glazes prepared were coated onto a 10x10 cm flat tile surface via pistol method. The glazed tiles and the pigment were baked as powder in plant ovens at a temperature of 1140°C. The chemical analyses of the pigment were carried out using the Spektro x-lab 2000 XRF device at the Kütahya Porcelain R&D labs. Mineralogical and phase analyses were carried out using the Rigaku Miniflex brand XRD device at the Kütahya Dumlupınar University Metallurgy and Material Engineering Department. Phase analyses of the samples were carried out using the Rigaku X-ray Diffractometer model Rint 2000 device. Phase analyses were carried out under conditions of 30 kV and 15mA (Cu-K α , $\lambda=1,541 \text{ \AA}$, 2θ 5-70°, 2°/min.). MDI Jade6.00 software was used for determining the phases and crystal calculations were carried out using the MAUD 2.80 crystal analysis software. glassmeter device was used for color measurements.

3. Results

3.1. Chemical Analysis Results

The chemical analysis results for the pigment used in the study have been given in Table 1. Blue color pigment primarily contains about 28% Co₃O₄ and 42 % Al₂O₃ with 5 % MgO and 19 % SiO₂.

Table 1. Chemical analysis of blue color pigment

Oxides	Ratio (%)
Na ₂ O	0.50
K ₂ O	0.02
Al ₂ O ₃	41.67
SiO ₂	19.43
Cr ₂ O ₃	0.24
ZnO	0.35
CaO	0.15
TiO ₂	0.02
Fe ₂ O ₃	0.29
MgO	4.77
ZrO ₂	0.72

Co ₃ O ₄	28.44
LOI	0.12

3.2. Color values

The color values for the pigmented glaze added to raw, baked pigment and transparent glaze have been given in Table 2. While the whiteness value of pigment that was not subject to heat treatment was 39, it was determined that the L* value decreased to about 36 and that the a* value was 1.89 after baking at 1140°C. The fact that a* value decreased as the pigment color started to darken after heat treatment meaning that there was a tendency in L* to decrease is an indication that the color shifted towards the green region. However, the color shifts towards the blue region with increasing b* resulting in a color at the green-blue interval. The L* value, meaning the whiteness decreases with increasing pigment ratios added to the transparent glaze. While the color values of the pigment added to the glaze shift towards the red and blue regions up to 5% addition ratio, a* and b* values decrease after this addition ratio thereby resulting in a shift towards the green-yellow region. The -b* value close to the blue region is -43.21 for pigment with 5% additive. It has been determined that using pigment ratios of above 1% and below 5% may be suited for obtaining color appearance in the region with the color value of blue.

Table 2. Color values for the pigment and glazes with additive

Sample	Color Values					
	L*	Changing ratio, %	a*	Changing ratio, %	b*	Changing ratio, %
Raw	39.22	-	2.72	-	-46.76	-
Fired	35.59	-9.26	1.89	-30.51	-47.90	2.44
% 1	46.69	19.05	5.34	96.32	-27.58	-41.02
% 5	17.99	-54.13	22.54	728.68	-43.21	-7.59
% 10	3.87	-90.13	14.31	426.10	-24.93	-46.69

3.3. Phase analyses

It was determined during the phase analyses of the raw (Figure 1A) and heat treated (Figure 1B) forms of the blue pigment that there was very little change in the peak intensities of the samples. It has been determined based on the pigment ratios added to transparent glaze that the hump which shows the amorphous phase in Figure 1C for the 1% additive ratio is taller, that the peak intensities increase with increasing additive ratios at 5 % addition (Figure 1D) for the spinel phase and at 10 % addition (Figure 1E) for the spinel and quartz phases, that the hump intensity which is an indication of amorphous phase decreases and that the quartz and spinel phase peaks are observed distinctively.

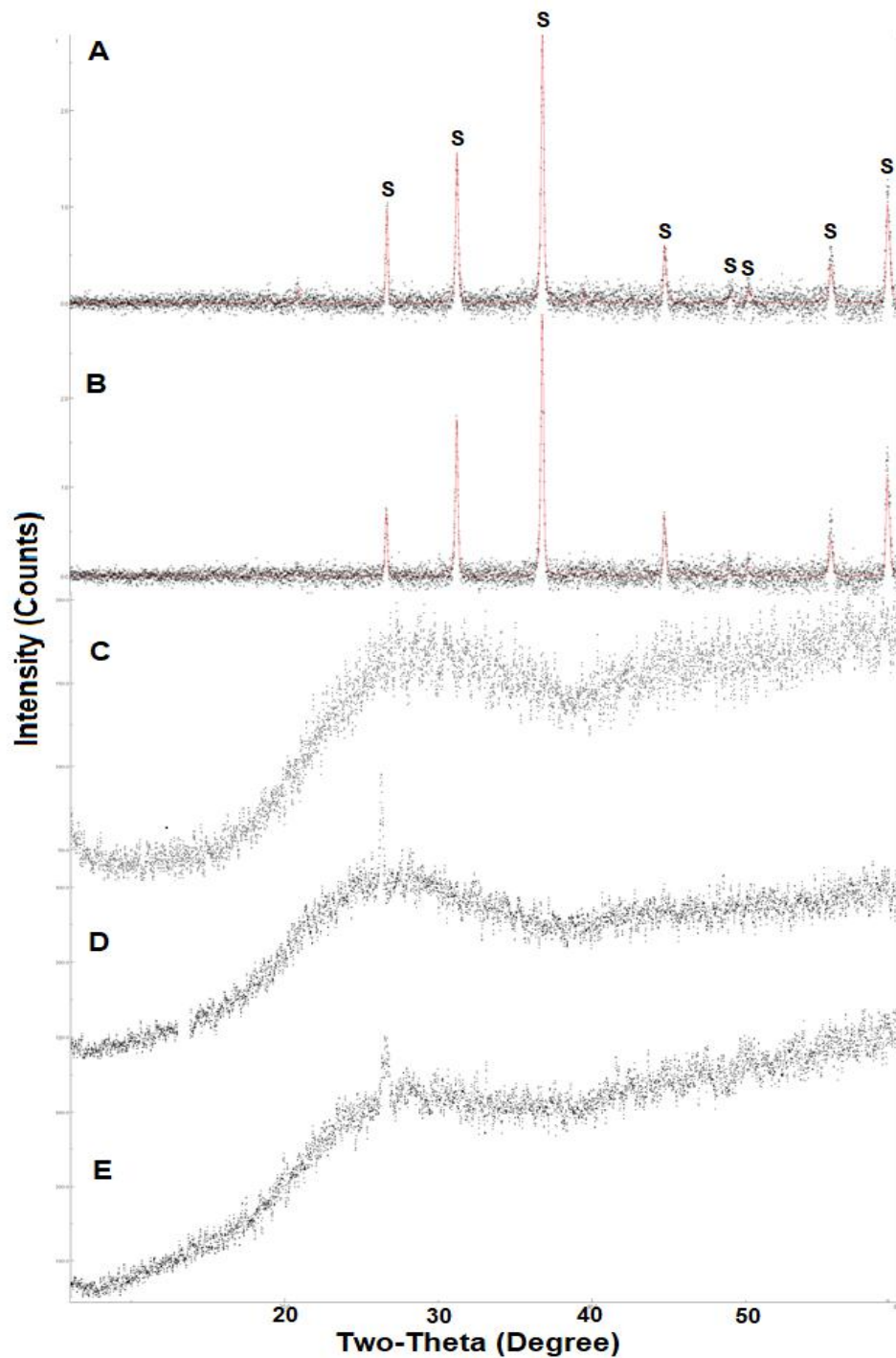


Figure 1. X-Ray patterns of pigments

The phase ratios for pigments as raw, after heat treatment and after addition to transparent glaze calculated according to the X-ray patterns have been given in Table 3. It was determined that spinel phase decreased by about 6.4% in the spinel structure following the baking of the pigment at 1140°C and that the quartz ratio increased. It was determined that the spinel pigment contained 6.4% unstable phase at 1140°C temperature. It was determined based on the increasing pigment addition rates to

transparent glaze that the amorphous phase ratio decreased while the spinel and quartz phases increased. Quartz ratio increased further with increasing pigment addition ratio. It was determined that the amorphous phase ratio decreased with increased addition of a spinel pigment to transparent glaze. Quartz and spinel also increase with the addition of transparent glaze at increasing ratios.

Table3. Phase analyses of pigments

Sample	Phases		
	Spinel	Quartz	Amorphous phase
Raw	87.82	12.18	-
Fired	81.45	18.55	-
% 1	0.59	0.94	98.47
% 5	1.44	1.33	97.23
% 10	3.65	2.76	93.59

The lattice parameter of the spinel phase increased by 0.09 % after heat treatment (Table 4). Similarly, it was determined that the lattice parameters of quartz increased after heat treatment, but that the change in the a-axis direction was higher in comparison with that of the c-axis. It has been determined that the lattice parameter of the spinel phase increases with pigment addition to the glaze, that quartz decreased at both the a-axis and c-axis directions at 1 % and 10 addition ratios, while the a-axis and c-axis increased with the other 5 % addition.

Table 4. Lattice parameters of the phases of the pigment

Sample	Spinel		Quartz			
	a-axis, Å	Changing ratio, %	a-axis, Å	Changing ratio, %	c-axis, Å	Changing ratio, %
Raw	8.1006	-	4.9108	-	5.4042	-
Fired	8.1076	0.09	4.9238	0.26	5.4043	0.002
% 1	8.1361	0.44	4.5344	-7.66	5.3995	-0.09
% 5	8.1312	0.38	4.9115	0.01	5.4363	0.59
% 10	8.1597	0.73	4.4400	-9.59	5.3060	-1.82

According to the obtained results;

- It has been determined that the blue color cobalt spinel pigment provides color formation in the red-blue region above 1 % and up to 5 % addition ratio to transparent glaze and that color formation occurred at the green-yellow region with increasing addition at 10 % addition ratio in comparison with 5 %.
- It is thought that 6.4 % unstable phase forms as a result of cooking the spinel pigment at 1140°C and that the unstable phase should also be taken into consideration while adjusting the pigment amount for use in glaze applications.
- It was determined that the pigment spread out inside the glaze with the addition of pigment below 1 % to transparent glaze and that the spinel phase in the amorphous phase is not very distinct.
- It was determined that the peaks of spinel and quartz phases were determined together with the hump indicating the amorphous phase for pigment ratios added to transparent glaze above 1%. However, it was also determined that the quartz peaks were more intensive at 10% addition ratio.
- It was determined that the highest lattice parameter was obtained after the spinel pigment was added to the transparent glaze at a ratio of 10 %.
- Quartz a-axis parameter decreased the most at a pigment addition of 1% and 10% to transparent glaze, while the c-axis decreased at both ratios, the c-axis decreased more at 10% pigment addition in comparison with 1%.

Kaynaklar

1. M.Gaudonn, L.C. Robertson, E. Lataste, M. Duttine, M. Ménétrier, A. Demourgues, Cobalt and nickel aluminate spinels: Blue and cyan pigments, *Ceramics Int.* 40 (2014) 5201-5207
2. M. Llusar, A. Fores, J.A. Bedenes, J. Calbo, M.A. Tena, G. Monros, Colour analysis of some cobalt-based blue pigments, *European Ceram. Soc.* 21, (2001) 1121-1130.
3. Y. Tang, C. Wu, Y. Song, Y. Zheng, K. Zhao, Effects of colouration mechanism and stability of CoAl_2O_4 ceramic pigments sintered on substrates, *Ceramics Int.* 44 (2018) 1019-1025
4. S. A. Eliziário, J. M. Andrade, S. J.G. Lima, C.A. Paskocimas, L. E.B. Soledade, P. Hammer, E. Longo, A. G. Souza, I. M.G. Santos, Black and green pigments based on chromium–cobalt spinels, *Mater. Chem. and Phy.* 129 (2011) 619-624
5. Salavati M.N., Farhadi M.K., Davar F., Bright blue pigment CoAl_2O_4 nanocrystals prepared by modified sol-gel method, *Sol-Gel Sci. and Tech.*, 52:321-327, (2009).
6. J. Merikhi, O.H. Jungk, C. Feldmann, Sub-micrometer CoAl_2O_4 pigment particles-synthesis and preparation of coatings, *Materials Chemistry*, 10-6, 1311-1314, 2000.

7. R. Ianos, R. Lazau, P. Barvinschi, Synthesis of $Mg_{1-x}Co_xAl_2O_4$ blue pigments via combustion route, *Advanced Powder Tech.* 22 (2011) 396-400
8. K. Mokhtari, Sh. Salem, A novel method for the clean synthesis of nanosized cobalt based blue pigments, *The Royal Society of Chemistry* 2017, *RSC Adv.*, 2017, 7, 29899-29908
9. A.A. Elguezabal, M.R. Aguirre, L.T. Saenz, P.P. Ruiz, M.B. Bernal, Synthesis of $CoAl_2O_4/Al_2O_3$ nanoparticles for ceramic blue pigments, *Ceramics Int.* 43 (2017) 15254-15257
10. M.C.G. Merino, A.L. Estrella, M.E. Rodriguez, L. Acuna, M.S. Lassa, G.E. Lascalea, P. Vazquez, Combustion Syntheses of $CoAl_2O_4$ Powders Using Different Fuels, *Proc. Mater. Sci.* 8 (2015) 519-525
11. I. Mindru, G. Marinescu, D. Gingasu, L. Patron, C. Ghica, M. Giurginca, Blue $CoAl_2O_4$ spinel via complexation method, *Mater. Chem. and Phy.* 122 (2010) 491-497
12. A.A. Ali, E. El Fadaly, I.S. Ahmed, Near-infrared reflecting blue inorganic nano-pigment based on cobalt aluminate spinel via combustion synthesis method, *Dyes and Pigments* 158 (2018) 451-462
13. Taylor N., Pottebaum A.J., Uz V., Laine R.M., Phase Evolution in The Transformation of Atomically Mixed Versus Ball-Milled Mixtures of Nanopowders in The Formation of Composite $MO_3Al_2O_3$ Spinels: Bottom-up Processing is Not Always Optimal, *American Ceramic Society* 97-11, 3442-3451, 2014.
14. sistematik miner
15. Taylor N., Pottebaum A.J., Uz V., Laine R.M., The Bottom Up Approach is Not Always The Best Processing Method. Dense $\alpha-Al_2O_3/NiAl_2O_4$ Composites, *Advanced Functional Materials*, 24, 3392-3398, 2014.
16. M. Yoneda, K. Gotoh, M. Nakanishi, T. Fujii, T. Nomura, Influence of aluminum source on the color tone of cobalt blue pigment, *Powder Tech.* 323 (2018) 574-580

CERAMIC SANITARYWARE AND TABLEWARE

THE EFFECT OF ZIRCON SILICATE PIGMENT ON AMORPHOUS PHASE OF TRANSPARENT GLAZE

Harun Taşdemir¹, Müzeyyen Şirin¹, Hanife Kadioğlu¹, Veli Uz²

¹Kütahya Porcelain Research & Development Department, Kütahya

²Kütahya Dumlupınar University, Metallurgy and Material Engineering, Kütahya

Abstract

Pigments and pigment structures affect ceramic quality. In this study, it was investigated in study the effect of pigment based on zircon in transparent glaze on the changing of crystal and amorphous phase ratios. It was determined that the zircon amount in the zircon based pigment is about 4% of unstable zircon after heat treatment at 1140°C. Amorphous phase and brightness decreased with increasing addition of zircon based glaze to transparent glaze. It has been determined that issues may arise in brightness when high ratios of zircon based pigment are used and that the color values may change.

Keywords: Porcelain, Pigment, Glaze, Amorphous Phase

1. Introduction

Zircon based pigments are generally used in many fields due to their stability [1]. It is desired for pigments used in ceramic products that the products do not lose their color characteristics based on firing temperature [2]. However, the heat resistance of the pigment used in addition to whether it dissolves completely inside the amorphous phase or remains undissolved may have an impact on color quality [3, 4]. Zircon based pigments are prepared in ceramic pigment production due to their high resistance against high temperature [3, 5, 6]. Different pigment oxides may be added during zircon based pigment production to obtain pigments with different color tones [7-9]. In this study, it was examined whether the zircon based yellow pigment was stable or not after firing at 1140°C along with its impacts on amorphous phase ratios and color values when added to transparent glaze at different ratios.

2. Material and method

The zircon based pigment samples used in the studies are used in ceramic product. Pigmented glazes were prepared by adding zircon based pigment to transparent glaze at ratios of 1%, 5%, 10%. The prepared pigmented glazes were coated on flat tile surface with dimensions of 10x10cm via pistole method. The glazed tiles and pigment were fired in plant kilns at 1140°C. The chemical analyses of

the pigments were made using the Spectro x-lab 2000 XRF, device at Kütahya Porcelain R&D labs. The mineralogical and phase analyses were carried out using the Rigaku Miniflex Brand XRD device at Kütahya Dumlupınar University Metallurgy and Material Engineering department laboratories. The phase analyses of the samples were carried out using the Rigaku X-ray Diffractometer model Rint 2000 device. Phase analyses were carried out under conditions of 30 kV and 15mA (Cu-K α , $\lambda=1,541$ Å, 2θ 5-70°, 2°/min.). MDI Jade 6.00 software was used for phase determination and MAUD 2.80 crystal analysis software was used for crystal calculations.

3. Results

3.1. Chemical analysis results

The chemical analyses for the pigment used in the studies have been given in Table 1. It was determined that the pigments mostly contain zircon silicate and low ratios of colorant manganese, iron and oxides of chrome element.

Table 1. Chemical analysis of pigments

Oxides	Ratio at weight (%)
Na ₂ O	0.60
K ₂ O	0.04
Al ₂ O ₃	0.11
SiO ₂	48.14
Cr ₂ O ₃	0.79
MnO	0.15
CaO	0.01
TiO ₂	0.01
Fe ₂ O ₃	0.18
MgO	0.35
ZrO ₂	45.46
LOI	0.75

3.2. Color Values

The color values obtained by adding yellow colored zircon based pigment to raw, heat treated and transparent glaze at certain ratios have been given in Table 2. It was determined upon firing the pigment at 1140°C for determining whether the pigment is stable or not that the L* value of the pigment increased at about 4.4%, the a* value decreased at about 30.6% while the b* value increased at about 2%. It was determined that the L* value decreases with increasing pigment ratio in pigmented glaze added to transparent glaze. It was determined that the a* value decreased with increasing pigment ratio in transparent glaze and that there was a change from the green region to the red color region. No linear change was observed with increasing pigment ratio in the b* values indicating yellow and blue

color regions. While the b^* was 35 for the pigment addition ratio of 1%, a shift towards the yellow color region at 70,27 was observed at 5% addition. The b^* value was 85 after adding 10% pigment again and the color was in the yellow region.

Table 2. Color values of pigment and pigmented samples

Sample	Color values					
	L^*	Changing Ratio, %	a^*	Changing Ratio, %	b^*	Changing Ratio, %
Raw	85.90	-	6.80	-	71.55	-
Fired	82.09	-4.44	4.72	-30.59	72.92	1.91
%1	84.93	-1.13	-4.53	-166.62	35.33	-50.62
%5	83.27	-3.06	-3.62	-153.24	70.27	100.38
%10	81.65	-4.95	-0.27	-103.97	85.26	19.16

3.3. Phase analyses

The phases that the pigment contains as raw were determined as zircon, baddeleyite and quartz (Figure 1A). A decrease in the intensity of the zircon peaks was determined after firing the pigment at 1140°C for determining whether it is stable or not (Figure 1B). A hump which is an indication of amorphous phase along with peaks for certain amounts of zircon and quartz were determined in samples with 1% zircon based pigment added to transparent glaze (Figure 1C). In addition, it was determined that the zircon and quartz peaks shifted to the right. The tensions in the crystal and changes in the crystal lattice parameters are effective in the peaks shifting to the right or left. It was observed at a pigment addition of 5% that the hump intensity was lower in comparison with the 1% addition ratio and that the zircon and quartz peak intensities increased along with an increase in FWHM peak width (Figure 1 D). It was determined that the amorphous phase hump intensity decreased at a 10% addition to transparent glaze and that the intensity of the zircon peaks increased (Figure 1 E).

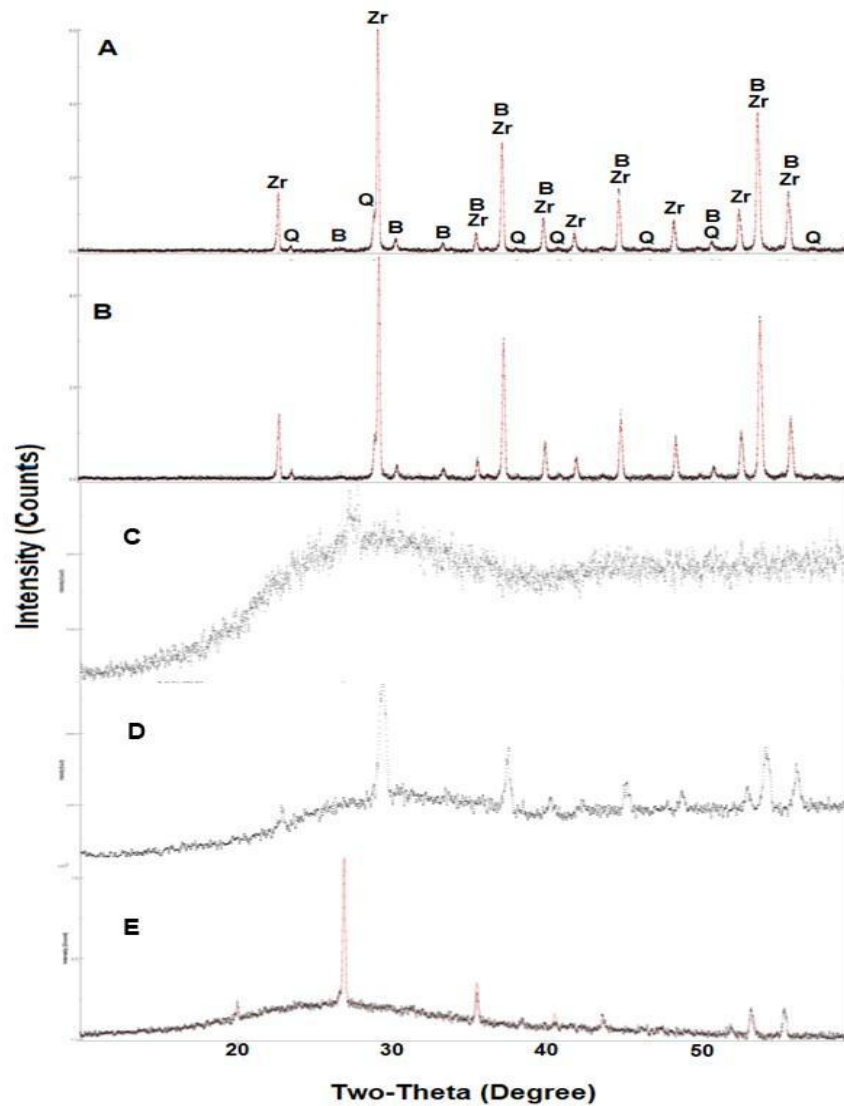


Figure 1. X-Ray diffraction patterns for Pigment samples (Z: Zircon, B: Baddeleyite, Q: Quartz)

The phase ratios calculated from the X-ray diffraction diffractograms of pigment samples have been given in Table 3. It was determined that the raw pigment contains about 82% zircon, 5% baddeleyite and 13 % quartz. It was determined that the zircon amount decreased by about 4%, whereas baddeleyite and quartz increased by 1.6% and 2.5% respectively after firing the pigment at 1140°C. It was determined that the zircon based pigment contains about 4% unstable zircon. Zircon and quartz peaks may be observed in the amorphous phase in samples for which zircon based glaze has been added to transparent glaze at a ratio of 1%. In addition to the difficulty of calculating these phases accurately in the amorphous phase, the fact that these phases are visible and that they remain in the amorphous phase without melting indicate its stability. It has been determined that the amorphous phase decreases and that the quartz phase increases with increasing pigment addition ratios to transparent glaze.

Table 3. The phases in pigment samples and their ratios

Sample	Phases			
	Zircon	Baddeleyite	Quartz	Amorphous Phase
Raw	81.57	4.99	13.44	-
Fired	77.42	6.63	15.95	-
%1	0.81	0.13	1.98	97.08
%5	3.36	1.63	1.48	93.53
%10	5.53	2.61	2.55	89.31

The lattice parameters calculated for the phases in the pigments added to raw, after firing and transparent glaze have been given in Table 4. The a-axis and c-axis of the zircon based pigment increased slightly after heat treatment. While the a-axis and b-axis decreased after heat treatment in the baddeleyite structure, an increase was observed in the c-axis. The lattice parameters of quartz had a tendency to increase with heat treatment. While the a-axis and c-axis of the zircon contained by the pigments added to transparent glaze increased at 1% addition, the values decreased at 5% addition and both axes increased for the sample with 10% addition. However, the beta angle of baddeleyite samples with 10% addition decreased. This indicates the formation of structural deformities and tensions.

Table 4. Lattice parameters of the phases in pigment samples

Phases	Lattice Values, Å	Raw	Fired	%1	% 5	% 10
Zircon	a-axis,	6.6233	6.6272	7.1103	6.6084	6.6580
	Change ratio, %	-	0.06	7.35	-0.22	0.52
	c-axis	5.9939	5.9969	6.2655	5.9912	6.0317
	Change ratio, %	-	0.05	4.53	-0.05	0.63
Baddeleyite	a-axis	5.1571	5.1556	5.2569	5.1462	4.7219
	Change ratio, %	-	-0.03	1.94	-0.21	-8.44
	b-axis	5.2009	5.1981	5.3657	5.2088	5.5661
	Change ratio, %	-	-0.05	3.17	0.15	7.02
	c-axis	5.3380	5.3597	5.3790	5.3098	5.3816
	Change ratio, %	-	0.41	0.77	-0.53	0.82
	Beta angle	99.17	99.07	97.56	99.22	96.65
	Change ratio, %	-	-0.10	-1.62	0.05	-2.54
Quartz	a-axis	4.9168	4.9209	5.3554	4.9131	4.7870
	Change ratio, %	-	0.08	8.92	-0.08	-2.64
	c-axis	5.4090	5.4160	5.8171	5.4037	5.6393
	Change ratio, %	-	0.13	7.54	-0.09	4.26

According to acquired data;

- It was determined that there was unstable zircon content at 1140°C after the zircon content of the zircon based pigment decreased by about 4% after heat treatment.
- Decrease in the a-axis of zircon and increase in the c-axis was observed after heat treatment. It was also determined that there was a decrease in the a-axis and b-axis of baddeleyite and an increase in the c-axis.
- It was determined that the amorphous phase decreased resulting in decreased brightness with zircon based pigment addition to the glaze at increasing ratios.
- The decrease of L^* and a^* values after heat treatment indicate that the color appearance shifted towards the darker region and red color region.

References

1. E. Özel, S. Turan, Production of coloured zircon pigments from zircon, European Ceramic Society 27 (2007)1751-1757.
2. L.M. Schabbach, F. Bondioli, M.C. Fredel, Colouring of opaque ceramic glaze with zircon pigments: Formulation with simplified Kubelka–Munk model, European Ceramic Soc. 31 (2011) 659–664.
3. Y. Sun, Q. Yang, H. Wang, Q. Zhang, Depression of synthesis temperature and structure characterization of $ZrSiO_4$ used in ceramic pigments, Mater. Chem. and Phy. 205 (2018) 97-101.
4. D.A. Earl, D.E. Clark, Effects of Glass Frit Oxides on Crystallization and Zircon Pigment Dissolution in Whiteware Coatings, J. Am. Ceram. Soc., 83 [9] 2170–76 (2000).
5. E. Zumaquero, M. J. Orts, V. Sanz, S. Mestre, Iron zircon pigment synthesis: Proposal of a mixing index for the raw materials mixtures, Boletín Sociedad Española Cerámica, 56 (2017) 177-185.
6. A. Assifaoui, W. Atmani, A. Daoudi, R. Moussa, P. Blanchart, Grain growth of zircon pigment in tile glaze, British Ceramic Transactions 2003 Vol. 102 No. 2, 57-60.
7. M. Cannio, F. Bondioli, Mechanical activation of raw materials in the synthesis of Fe_2O_3 – $ZrSiO_4$ inclusion pigment, European Ceramic Soc. 32 (2012) 643–647.
8. T. I. Dimitrov, Synthesis and Structure of Zircon-Based Ceramic Pigments Containing Mn, Co, and Ni as Chromophoric Elements, Glass and Ceramics, Vol. 67, No. 11-12, March, 2011, 383-385.
9. F. Zhao, W. Li, H. Luo, Sol-gel modified method for obtention of gray and pink ceramic pigments in zircon matrix, Sol-Gel Sci. Tech. (2009) 49:247–252.

GLASS AND GLASS CERAMICS

AN INVESTIGATION OF RAW MATERIAL EFFECTS ON NANO SiC BASED FOAM GLASS PRODUCTION

Aylin Şahin¹, Yasemin Kılıç¹, Mustafa Kara¹, Abdulkadir Sarı², Burcu Duymaz²¹TUBITAK Marmara Research Centre, Materials Institute, Kocaeli, Turkey²VEFA Prefabricated Structures Industry Trade and Inc., Kocaeli, Turkey**Keywords:** Foam glass, insulation, silicon carbide, thermal conductivity, waste glass

ABSTRACT

Foam glass is an innovative material which is composed of glass and carbon/carbonate based minerals; and has incomparable properties like lightweight, high thermal insulation and high porosity with sufficient mechanical strength. In the present study, the effects of the glass type and mineral addition on the foam glass properties were investigated. Nano sized SiC was fixed as foaming agent at the whole of the samples, mixed glass waste and sheet glass were selectively used as glass sources; finally, Al₂O₃ was used as mineral additive. These raw material powders were mixed homogeneously with different proportions, and then prepared mixtures were pressed and sintered optimum foaming conditions. Finally, obtained samples were characterized based on the required properties of foam glass material and optimum results were determined. At the end of the study, 0.049 W/mK thermal conductivity, 72 % porosity, 0.20 g/cm³ apparent density and 3.38 MPa compressive strength values were determined as optimum results. It can be said that the foam glass materials can be preferred as an alternative insulation material rather than polymeric based conventional insulation materials because of supplying high thermal insulation properties without containing unhealthy chemicals and burning risks.

1. INTRODUCTION AND PURPOSE

In the last years, energy efficiency has been quite considered and insulation materials have become more necessary. According to the market researches, 30 % of the energy is consumed at the buildings and 85 % of this energy is used for heating purposes. However, about 50-60 % of the consumed energy may be saved with a proper thermal insulation [1]. Besides of the energy saving and energy efficiency, thermal insulation provides an advantage about economical, safety and health issues with a clear reduction on environmental problems.

Coefficient of the thermal conductivity (λ) value is very important when a material is considered as thermal insulation material. According to ISO and CEN standards, to classify a material as a thermal insulation material, its thermal conductivity coefficient (W/mK, λ) must be lower than 0.065 W/mK [2]. On the other hand, applicators should seriously consider fire resistance, mechanical strength and environment-friendly features. In our country, thermal insulation materials like XPS, EPS, fiberglass, stone wool etc. are frequently preferred in construction sector; however, these insulation materials could not supply both of that high thermal insulation, high compressive strength, fire resistance and eco-friendly properties because of their raw material content and application processes.

Foam glass is unique material, which has lightweight, low thermal conductivity, cellular and rigid structure with moderate compressive strength, non-flammability, chemically inert and nontoxic, rodent and insect-resistant, bacteria-resistant, water/steam resistant and freeze-resistance [3]. One of the basic advantages of foam glass is giving reliance on health and safety due to the main raw material is glass. Equivalent polymer based insulation materials, which are frequently used in the construction sector, are composed of mostly cancerogen and easily flammable materials.

Foam glass is generally composed of glass, gas-generating agent (foaming agent) and mineral additive. Glass powder, foaming agent and optionally mineral additives are mixed in a specific composition ratio. This mixture is granulated and shaped (pressed with a hydraulic press or filled in a mold); after then, sintered at elevated temperatures. During heating process, glass particles soften and some gas bubbles (CO/CO_2) evolve from the foaming agent due foaming reactions. The preliminarily obtained gas bubbles are small and spherical; moreover, they continue to grow and transform polyhedral shape during heating schedule and cause an increase on gas pressure and expansion of glass. At the final stage of the process, foam glass material, which has homogeneous porous and cellular structure, is achieved [3, 4].

Scarinci et al. (2005) specified that any glass (favorably in powder form) could be transformed into foam by addition of proper foaming agents. Based on the gas generation mechanism, foaming agents are divided into two groups: reducing and decomposable agents. At the temperatures above glass softening temperature, gas generation occurs from reaction (from reducing agent) or decomposition (from decomposable agent). If gas evolution occurs at temperatures below the softening point of glass, gaseous products cannot be held by the mass because of the glass powder is not sintered yet to form closed porosity. Moreover, if the gases arise when the glass viscosity is too low, evolved gases escape from the melted body and cause a non-porous glassy product. It was indicated that the most suitable viscosity of standard sheet soda-lime glass composition is between 800-1000°C to obtain maximum porosity and minimum apparent density from foam glass [3].

Reducing agents, also known as redox agents are usually carbon-based materials like carbon (C), coke, anthracite, soot, graphite and silicon carbide (SiC) which react with glass and provide occurring of some gaseous products like CO or CO_2 [5]. Within the reducing agent types, silicon carbide (SiC) is referred as very effective to gain homogeneous cellular structure and to control of the microstructure [6, 4]. Tulyaganov et al. (2006) reported that even very small additions of SiC can influence the foaming process by oxidation and releasing CO_2 gas during sintering [7].

The important inferences from the literature were briefly represented as follow:

Mear et al. (2007) developed a foam glass material with using waste cathode ray tube (CRT) glass and foaming agent (SiC and TiN). In addition, sintering was applied at 750-850°C for 60-120 minute. Obtained foam glasses provide 4 MPa – 68 MPa bending strength and 0.08 – 0.43 W/mK thermal conductivity coefficient [8]. Attila et al. (2013) investigated of foaming behavior of soda-lime window glass polishing wastes at 700-950°C. The density was calculated between 0.206 – 0.378 g/cm³ and thermal conductivity coefficient was measured between 0.048 – 0.079 W/mK from the obtained foam glasses [9]. In the experiments of Francis et al. (2013), granulated blast furnace slag and glass cullet (70 wt. %) were used as main raw material and glass source, while SiC (1-10 wt. %) was used as foaming agent. Optimum results were determined as 1.18 – 1.8 MPa from compressive strength and 0.61 g/cm³ when foaming at 998°C for 33 minute with addition of 1.73 wt. % SiC foaming agent [10].

In the present study, two different types of glass sources (mixed glass waste and sheet glass) were investigated at foam glass production process. Nano SiC was chosen as foaming (reducing) agent because of high purity and high foaming ability. In addition, Al_2O_3 effect was researched as mineral additive. At the end of the study, it is aimed to have low density and low thermal conductivity, but mechanical strength properties of foam glass samples to be obtained.

2. LABORATORY SCALED STUDIES

2.1. RAW MATERIALS

Laboratory scaled experimental studies were conducted in TUBITAK MRC Materials Institute. *The primary raw materials* used in the studies were mixed glass waste and sheet glass; while nano sized SiC powder was used as *foaming agent*. Also, Al_2O_3 was added as *mineral additive* and CMC was used as *binder*.

In experimental studies, nano sized SiC powder was fixed as foaming agent; while, the effects of two different glass sources (mixed glass waste and sheet glass) were examined. It is thought that the use of waste glass and the utilization of a waste material in a new product will benefit from both economic and environmental aspects. However, because the composition of the waste glass is not stable, it has been decided to alternatively use sheet glass which can be produced in the same composition by Şişecam Inc. in the production of foam glass. In addition, Al_2O_3 was added to the mixture to accelerate the foaming reaction by increasing the viscosity of the glass and to prevent agglomeration between the grains during the glass melting. The effect of Al_2O_3 on the physical, chemical and mechanical properties of the glass foam material produced in this way has been also investigated.

2.2. CHARACTERIZATION OF RAW MATERIALS

The raw materials were characterized by particle size distribution, DTA/TG analysis, mineralogical and elemental analysis. At the beginning of the study, waste and sheet glasses were supplied as glass cullet. To obtain the micron sized glass powder, mixed glass waste and sheet glass samples were separately milled and ground at 72 rpm by applying wet and dry milling. Al_2O_3 and SiC was used with their original particle sizes. Nano scale SiC particle size distribution was determined with Malvern Zetasizer Nano ZS, also micro scale glass and Al_2O_3 powders particle size distribution were measured with Mastersizer-2000. DTA/TG results of raw materials were determined by SEIKO ExStar 6300 DTA/TG thermal analysis device (Table 1).

Table 1. DTA/TG Results and Particle Size Distribution of Raw Materials

	Mixed Glass Waste(μm)	Sheet Glass (μm)	SiC (nm)	Al_2O_3 (μm)
Weight loss (%) (30-1000°C)	1.3	1.2	0.4	1.0
T_g (°C) (Transition Temp.)	595	576	-	-
T_c (°C) (Crystallization Temp.)	703	710	-	-
T_s (°C) (Softening Temp.)	744	735	-	-
Size d_{10}	2.71	2.57	-	0.47
Distribution d_{50}	14.98	14.08	202.1	1.44
d_{90}	36.88	38.10	-	44.86

The chemical analysis of glasses was made by Philips PW 2404 X-ray fluorescence and results are shown in Table 2.

Table 2. Chemical Analysis Results of Glasses

Compound	Mixed Glass Waste (%)	Sheet Glass (%)
SiO ₂	72,387	70,904
Al ₂ O ₃	2,217	3,080
CaO	9,928	9,358
Cl	0,032	0,024
Cr ₂ O ₃	-	-
Fe ₂ O ₃	0,154	1,266
Ga ₂ O ₃	-	-
K ₂ O	0,190	0,054
MgO	5,977	6,226
MoO ₃	-	-
Na ₂ O	8,768	8,833
NiO	-	-
SO ₃	0,270	0,179
SrO	0,006	-
TiO ₂	0,061	0,066
V ₂ O ₅	-	-
WO ₂	-	-
ZrO ₂	0,009	0,010

Mineralogical analyses of raw materials were made by using SHIMADZU XRD-6000 Diffractometer device (Table 3). In addition to moissanite and silicon carbide phases, SiC, Si, C and SiO₂ phases were determined in SiC raw materials. In glass raw materials, as expected, the amorphous SiO₂ phase is proven by XRD analysis.

Table 3. XRD Analysis Results of Raw Materials

Mineralogical Phase	SiC	Al ₂ O ₃	Mixed Glass Waste	Sheet Glass
Moissanite, SiC	*			
Silicon Carbide, SiC	*			
Silicon, Si	*			
Graphite, C	*			
Ferrihydrite, FeO(OH)	*			
Silicon Oxide, SiO ₂	*			
Aluminum Silicate, Al ₂ Si ₄ O ₁₀	*			
Corundum, Al ₂ O ₃		*		

2.3. EXPERIMENTAL STUDIES

In the experimental studies, various compositions were prepared with mixing of glass waste, sheet glass, SiC and Al₂O₃ at different ratios. These compositions were mixed within the ball mill for 3 hours at 155 rpm to achieve homogenous compositions. The optimum compositions (Table 4) were analyzed in this paper.

Table 4. Composition Ratios of Raw Materials

Foam Glass Sample Name	Mixed Glass Waste (wt. %)	Sheet Glass (wt. %)	SiC (wt. %)	Al ₂ O ₃ (wt. %)
A	97	-	3	-
B	96	-	3	1
C	-	97	3	-
D	-	96	3	1

After mixing process, these different compositions were granulated with adding CMC binder (7 wt. %), and then, they were pressed under 500 kg/cm² with using cylindrical mold (Ø: 23 mm) by using hydraulic press. These pressed samples were sintered at for 2 hours at 850°C sintering schedule. Images of the obtained samples before sintering and after sintering process and internal views of fired samples were shown at Figure 1.

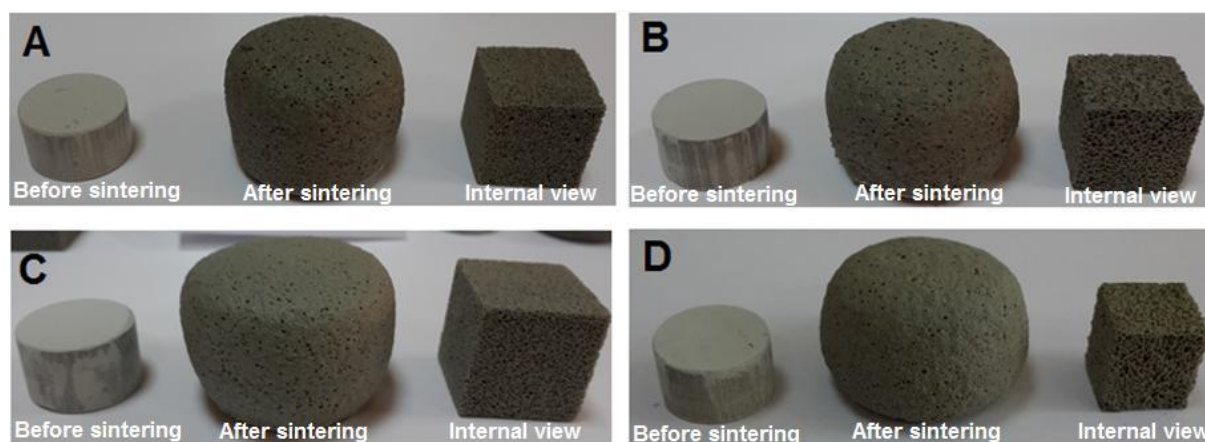


Figure 1. Photos of obtained samples (Before sintering, after sintering and internal views, respectively)

Foam glass samples were characterized by measuring volume expansion ratio, Zwick Z250 Universal test device (compressive strength), TS EN 1602:2013-06 (apparent density), C-Therm Technologies TH89-05-00400 (thermal conductivity), FEG- SEM JEOL JSM-6335 F device (microstructural examination) and Quantachrome Corporation-Poremaster 60 device (total porosity).

3. RESULTS AND DISCUSSION

As a nature of foam glass production process at high temperatures, some gases (CO, CO₂) evolve from the foaming agent and these gases result in a pressure within the viscous glass, and then large number of porous cells occur and lead to expansion of glass. Thus, cellular and macro porous foam glass material arises because of volumetrically expansion of glass. Volume expansion is a preferred situation because it supplies cellular and lightweight structures, which lead high thermal insulation property. To determine the volume change of the samples, their bulk volume were measured before and after sintering process; then volume expansion ratio (%) of all samples were calculated. Apparent density values of foam glass samples were measured according to the TS EN 1602:2013 standard [11]. The other technical properties of foam glass material are measured according to the standard TS EN 13167:2013-04 (Thermal Insulation Products for Buildings - Factory Made Cellular Glass (CG) Products-Specification) [12]. Characterization results like volume expansion ratio, apparent density, thermal conductivity, compressive strength and total porosity of foam glass samples were given in Table 5. The identified values for foam glass materials at the standard TS EN 13167:2013-04 were illustrated in Table 5, also.

Table 5. Characterization Results of Foam Glass Samples

Sample Name	Volume Expansion Ratio (%)	Apparent Density (g/cm ³)	Thermal Conductivity (W/mK)	Compressive Strength (MPa)	Total Porosity (%)
A	550	0.221	0.064	3.64	50.86
B	649	0.200	0.053	2.44	37.93
C	615	0.202	0.057	3.38	58.05
D	590	0.213	0.049	2.41	72.43
TS EN 13167:2013-04		0.090 – 0.180	0.045 – 0.060	0.4 - 3	

Mineralogical (XRD) analysis results of foam glass samples were shown in Table 6. Cristobalite (SiO₂), Moissanite (SiC), Sodium Calcium Silicate (Na₂Ca₃Si₆O₁₆) and Calcium Magnesium Silicate (Ca₃Mg (SiO₄)₂) were observed by XRD analysis at all of the foam glass samples. According to the literature, releasing of silicon oxides from the foaming agents may cause partial crystallization of glass with precipitation of cristobalite phase [3].

Table 6. Foam Glass Samples XRD Analysis Results

Mineralogical Phases	Sample Name				PDF Card Number (JCPDS #)
	A	B	C	D	
Cristobalite, SiO₂	*	*	*	*	4-8-7642
Moissanite, SiC	*	*	*	*	29-1129
Sodium Calcium Silicate, Na₂Ca₃Si₆O₁₆	*	*	*	*	23-671
Calcium Magnesium Silicate, Ca₃Mg(SiO₄)₂	*	*	*	*	4-11-6738
Amorphous Structure	*	*	*	*	-

Microstructural examination shows that all of the foam glass samples have homogeneous cellular and porous structure (Figure 2). It can be said that these cells at the microstructure resulted from evolving of CO/CO₂ gases during foaming reactions. According to the microstructural images, spherical closed cells were observed at homogenous distribution. At the beginning of the foaming process, small and spherical cells occur, and then these cells transform into polyhedral shape during foaming reaction. Sample D revealed tiny pores throughout the grain line that is resulted low compressive strength according the other samples as shown in Table 5. It is also clear that Al₂O₃ containing samples (B and D) pore size is higher than the samples (A and C).

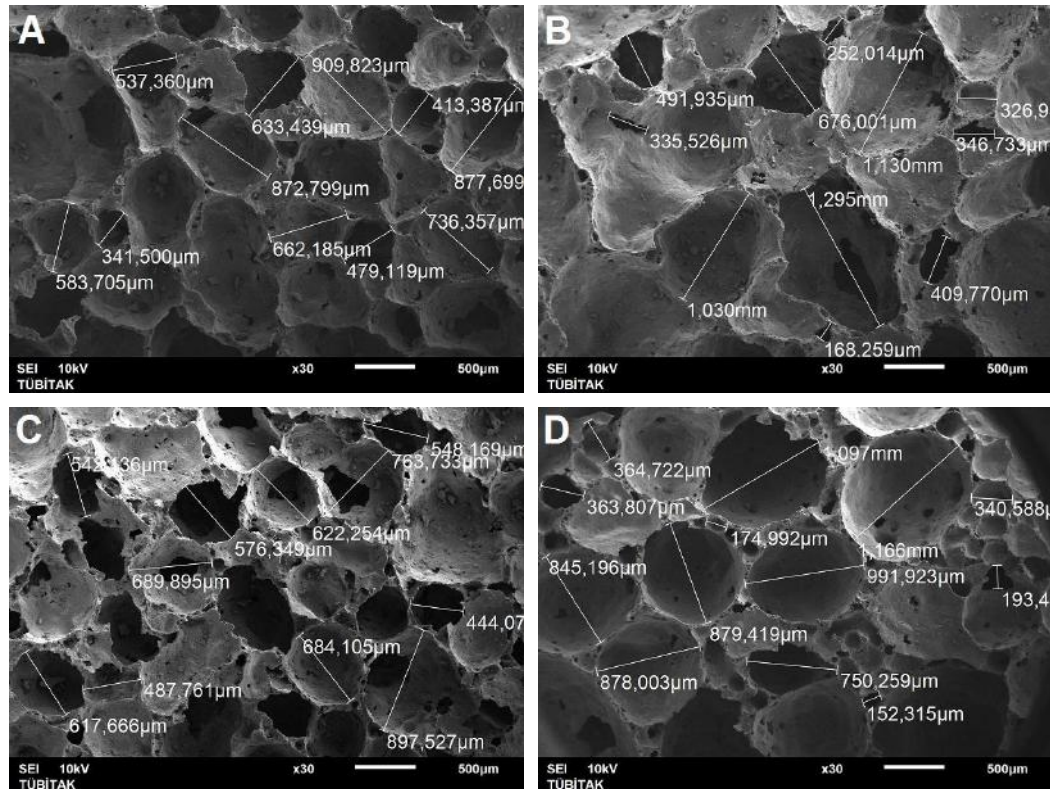


Figure 2. SEM images of foam glass samples

In the experimental studies; two different glass sources were used and effect of glass type on the foam glass were investigated. When the foaming agent (nano SiC) and sintering schedule was fixed but the glass sources (mixed glass waste or sheet glass) were alternated, the following results were achieved:

Glass Type Effects on Foam Glass Samples

- Comparison of Sample C (sheet glass + nano SiC) and Sample A (mixed glass waste + nano SiC) was showed that using of sheet glass provided higher foaming, higher porosity, lower density and lower thermal conductivity. This situation is thought to be caused by the difference in elemental analysis of glasses. There is more Fe_2O_3 in sheet glass than mixed glass waste. Fe_2O_3 is the main source of oxygen for silicate glasses. Fe_2O_3 can be used as a potential oxidizing agent because it increases the speed of the gas releasing at foam glass sintering process.
- It is also seen that glass type is highly effective on porosity. The samples produced with sheet glass have less but larger cells; however, the samples produced with mixed glass waste more but smaller cells. The highest porosity value was observed at Sample C (sheet glass + nano SiC) and Sample D (sheet glass + nano SiC + Al_2O_3).
- The thermal conductivity of a material is directly proportional to its porosity. In general, the samples produced with sheet glass supplied higher porosity. It was seen that the sample D had the highest porosity and lowest thermal conductivity. However, the compressive strength values decreased according to increasing porous structure, also.

Al_2O_3 Addition Effects on Foam Glass Samples

- Comparison of Sample A (mixed glass waste + nano SiC) and Sample B (mixed glass waste + nano SiC + Al_2O_3) was indicated that Al_2O_3 addition has positive effect on foaming process

and volumetric increasing. Thus, Sample B could have lower density and lower thermal conductivity values rather than Sample A.

- Because of the Al_2O_3 addition provided lower density, compressive strength of these samples decreased as expected. However, the compressive strength results of foam glass samples were at the requested limit values.

4. CONCLUSION

In the present study, foam glass material production was aimed with using different types of glass sources. Also, nano sized SiC was preferred because of its high purity and foaming ability. Moreover, Al_2O_3 was evaluated as a suitable additive to accelerate the foaming process. The highest porosity and the lowest thermal conductivity value was achieved from the Sample D (Sheet glass + Nano SiC + Al_2O_3). It can be said that using sheet glass and adding Al_2O_3 in foam glass production supplied higher porosity, lower density and lower thermal conductivity, which are the desired properties from insulation materials.

ACKNOWLEDGEMENTS

This study was a part of the project which name is “Investigation of Production Method of a Novel Nano Structured Foam Glass with Low Thermal Conductivity” and funded by the VEFA Prefabricated Structures Industry Trade and Inc. and the authors are grateful to VEFA and TUBITAK TEYDEB for the financial support.

REFERENCES

- [1] Özutku, O., Karakuş, C. (2011). Binalarda Isı Yalıtımı Yoluyla Enerji Tasarrufu ve Örnek Bir Uygulama: MKÜ Mühendislik Fakültesi Binasının Enerji Performans Değerleri ve Maliyetleri. X. Ulusal Tesisat Mühendisliği Kongresi, 13-16 Nisan, İzmir, Türkiye.
- [2] Yaman, Ö., Şengül, Ö., Selçuk, H., Çalikuş, O., Kara, İ., Erdem, Ş., Özgür, D. (2015). Binalarda Isı Yalıtımı ve Isı Yalıtım Malzemeleri. Türkiye Mühendislik Haberleri (TMH), 487(4), 62-75.
- [3] Scarinci, G., Brusatin, G., Bernardo, E. (2005). Glass Foams, Cellular Ceramics: Structure, Manufacturing, Properties and Applications, Editors; Scheffler, M., Colombo, P., 158-176, WILEY-VCH Verlag GmbH & Co. KGaA, Weinheim, Germany.
- [4] Hurley, J. (2003). A UK Market Survey for Foam Glass. Glass Development and Research Final Report, WRAP Creating Markets for Recycled Resources, GLA-0015, Published by: The Waste and Resources Action Programme, Oxon, England.
- [5] Spiridonov, Y.A., Orlova, L.A. (2003). Problems of Foam Glass Production. Glass and Ceramics, Vol.60, No.10, 313-314.
- [6] Brusatin, G., Bernardo, E., Scarinci, G. (2004). Production of Foam Glass from Glass Waste, Sustainable Waste Management and Recycling: Glass Waste, Editors; Limbachiya, M.C, Roberts, J.J., 67-82, London, UK.
- [7] Tulyaganov, D.U., Fernandes, H.R., Agathopoulos, S., Ferreira, J.M.F. (2006). Preparation and Characterization of High Compressive Strength Foams from Sheet Glass. J Porous Mater, Vol. 13, 133–139.
- [8] Méar, F., Yot, P., Viennois, R., Ribes, M. (2007). Mechanical Behaviour and Thermal and Electrical Properties of Foam Glass. Ceramics International, 33, 543–550.
- [9] Attila, Y., Güden, M., Taşdemirci, A. (2013). Foam Glass Processing Using a Polishing Glass Powder Residue, Ceramics International, Vol. 39, pp. 5869-5877.
- [10] Francis, A.A., Rahman, M.K.A. (2013). Experimental Design for Optimisation of Density and Water Absorption Capacity of Glass–Ceramic Foams Prepared from Silica Rich Wastes. Powder Metallurgy, Vol. 56, No. 4, 295-303.
- [11] TS EN 1602:2013-06 (2013). Thermal Insulating Products for Building Applications-Determination of Apparent Density. Turkish Standards Institute, Ankara, Turkey.
- [12] TS EN 13167:2013-04 (2013). Thermal Insulation Products for Buildings - Factory Made Cellular Glass (CG) Products-Specification. Turkish Standards Institutes, Ankara, Turkey.

GLASS AND GLASS CERAMICS

MARBLE LOOK QUARTZ SURFACES WITH CRISTOBALITE

Esra ARICI¹, Duygu ÖLMEZ¹, Gökhan DENİZ¹, Nurcan TOPÇU¹, Bekir KARASU²¹Belenco Quartz Surfaces, Research and Development Centre, Manisa/Turkey² Eskişehir Technical University, Department of Materials Science and Engineering, İki Eylül Campus
Eskişehir/Turkey

ABSTRACT

Products with marble appearance are formed by mixing natural quartz minerals from underground with specially developed polyester resin and then by designing with different colour pigments and quartz granules of different sizes, shaping in the form of plates and firing them afterwards. Due to the opaque and dark appearance of the quartz, cristobalite raw material was used to design the plate in the natural stone view. Cristobalite is a chemical inert product in high purity and whiteness, formed by calcining silica at high temperature. Excellent optical properties are widely used in various applications as filler and raw material due to chemical inertness, absorption properties and controlled particle size distribution. Since quartz inhibits different properties, all the parameters used in the production formula for quartz have been redeveloped for cristobalite. As a result, instead of the dark and opaque quartz, a white Carrara marble look with a very white and transparent appearance, rare in nature, was designed by Belenco Firm for the first time in the world.

Keywords: Quartz, Composite stone, Cristobalite, Carrara marble look.

1. INTRODUCTION

Turkey is not very rich country in terms of quartz deposits and so far identified reserves is only 4–5 million tons. However, especially the transmission of transparent quartz is very limited. The Mohs hardness grade of quartz is 7 and the specific weight is 2,65. It is colourless, white or coloured with the presence of foreign materials it contains. The composition is 46.7 % Si, 53.3 % O [1–2].

The most important quartz deposits are in Çanakkale (Ezine, Bayramiç and Biga); Aydın (Çine), Muğla, İzmir, Ankara, Kütahya and Bitlis. In the world, major quartz producers are Spain, Norway, Chile, India, Brazil, Italy, Australia and Belgium [1].

Quartz crystals have three distinct polymorphs in nature: quartz, tridymite, cristobalite. The most common naturally occurring polymorph is quartz, which accounts for about 12 wt. % of the Earth's crust. During heating, these three crystal forms turn into crystal structures which are different from each other. The polymorphic transformations are indicated in Fig. 1. Cristobalite is a high temperature silica polymorph being stable in the temperature (T) range of 1470–1705 °C, but that also occurs out of its field of stability as a metastable phase. The theoretical sequence of the silica transformations upon heating involves α quartz, β quartz (573 °C), β tridymite (870 °C) and β cristobalite, which has a cubic structure (1470 °C). Given that the formation of β tridymite requires particular impurities to be present, β cristobalite can even appear at lower temperature [1–3].

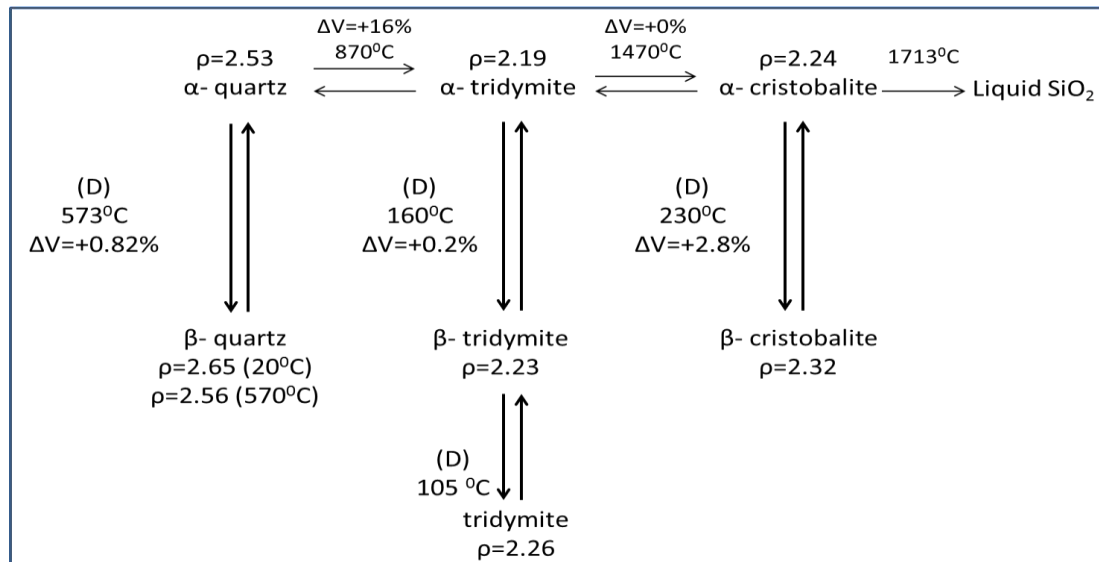


Figure 1. Polymorphs of quartz crystals [1].

Although α -quartz is the stable form at normal atmospheric temperatures and pressures, β -quartz, tridymite and cristobalite do metastably exist and are not uncommon minerals. They occur if the polymorph inversion on cooling has been inhibited by a rapid drop in temperature, for example during volcanic eruptions. Cristobalite formation is kinetically favoured on devitrification of amorphous silica and volcanic glasses and on heating quartz and some silicates above about 900°C . The cristobalite so formed does not invert to quartz on cooling [4].

In this study, cristobalite raw material was used in different granule sizes to obtain a very white and transparent appearance.

2. MATERIALS AND METHODS

Production process of quartz surfaces are presented in Fig. 2.

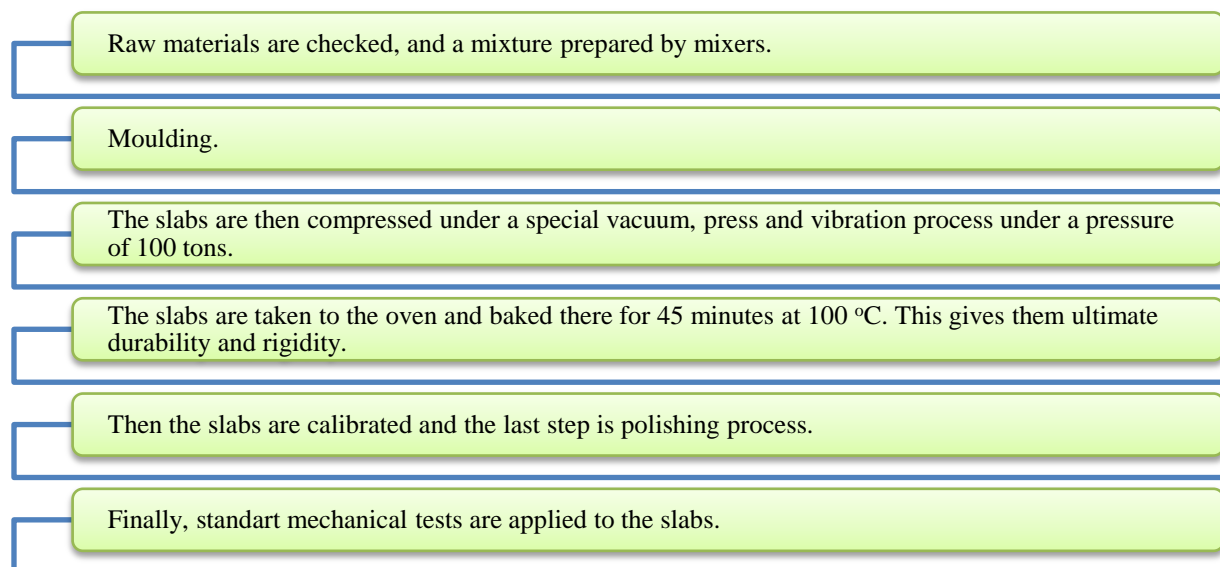


Figure 2. Production process of quartz surfaces.

In the current study, cristobalite raw material of Sibelco Company with different grain sizes M72T, M3000, M4000 and M6000 was used. These are high-purity silica produced by thermal treatment at high temperature of selected and treated quartz grains. The modified crystal structure “cristobalite” is afterwards stabilised by fast cooling down. M72T is sieved in a special way to limit coarse particles. The results of the chemical analysis carried out by Sibelco related to different grain size raw material with XRF device are listed in Table 1.

The granulometric data and physical characteristics of samples (Sibelite M72T, M3000, M4000 and M6000) are also represented in Table 2.

Table 1. Chemical analyses of the samples

	M72T	M3000	M4000	M6000
SiO₂	99.5	99.5	99.5	99.5
Fe₂O₃	0.03	0.03	0.03	0.03
Al₂O₃	0.20	0.20	0.20	0.20
TiO₂	0.02	0.02	0.02	0.02
K₂O	0.05	0.05	0.05	0.05
CaO	0.01	0.01	0.01	0.01

Table 2. The granulometric data and physical characteristics of the samples

	M72T	M3000	M4000	M6000
D50 (µm)	300	14	5	3
Density (kgdm⁻³)	2.3	2.3	2.3	2.3
Bulk density (kgdm⁻³)	1.1	0.7	0.46	0.42
Hardness (Mohs)	6.5	6.5	6.5	6.5
pH	9	9	9	9
Colour	L:97 a:-0.15 b:0.60	L:98 a:0.03 b:0.57	L:98 a:0.02 b:0.33	L:98 a:0.01 b:0.27

Firstly, d10, d50, d90 values were determined with the Malvern particle size analyser to checked the cristobalite grain size (Fig. 3). The Retch vibratory sieve shaker depicted in Figure 4 was employed for bigger grain sizes of cristobalite. The Denver Moisture Analyser was used to determine the moisture of cristobalite raw materials (Fig. 5). Colour analysis was performed with Konica & Minolta spectrophotometer presented in Figure 6.



Figure 3. Malvern particle size analyser.

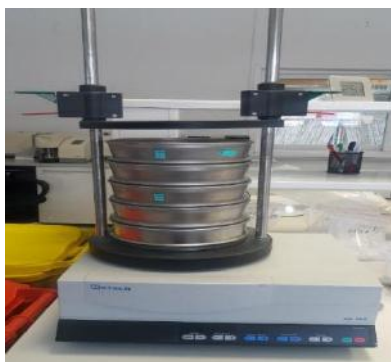


Figure 4. Vibratory sieve shaker.



Figure 5. Moisture analyser.



Figure 6. Spectrophotometer.

Secondly, standard control tests were carried out for the resin. With the exothermal test applied to the resin, the gelling, peak-temperature and reached times to the max temperature were determined. The viscosity of the resin was evaluated by Haake type viscometer. The Barcol hardness of the resin was determined by Barcol hardness tester and the colour of the resin was determined by Gardner colour scale.

After the control tests were finished for resin and different granule sizes of cristobalite, the most appropriate formulation was tried to be formed. Tests have been carried out with different proportions of resin and cristobalite. It was decided to use cristobalite raw materials granule sizes of which are M72T and M3000. Two formulations were designed which were named as “Kashmera White” and “Perla White”. Standard mechanical tests were applied to these slabs.

As a result, a white Carrara marble look with a very white and transparent appearance, rare in nature, was designed successfully.

3- RESULTS AND DISCUSSIONS

In this research, experiments were carried out using cristobalite instead of quartz. Two formulations were designed as “Kashmera White” and “Perla White”. The photographs of these composite stones are presented in Figs. 7 and 8.



Figure 7. Perla White.

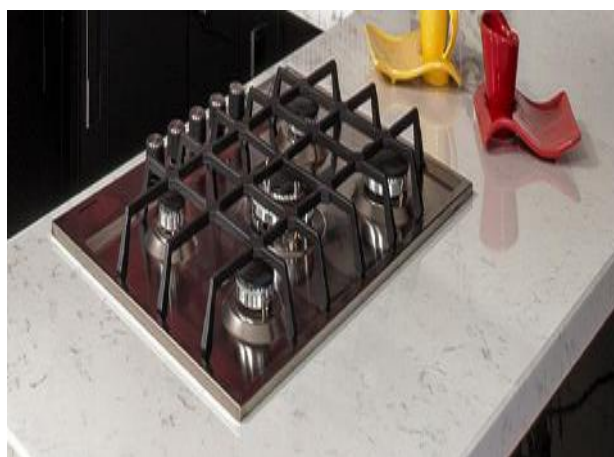
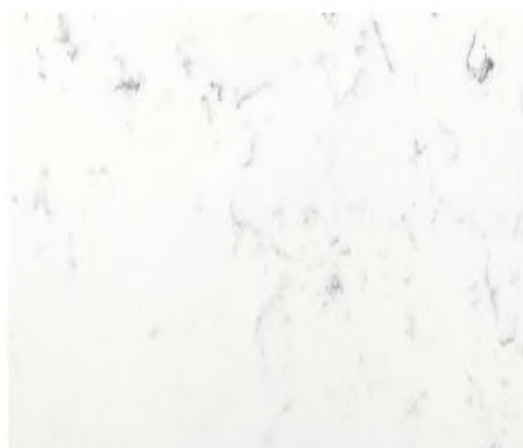


Figure 8. Kashmera White.

Mechanical tests (impact and abrasion resistance, flexural strength and water absorption) were applied to these samples (Table 3).

Table 3. The results of the mechanical tests

Samples	Impact Resistance (joule)	Abrasion Resistance (mm)	Flexural Strength (N/mm²=MPa)	Water Absorption (%)
Kashmera White-1	8.63	28.35	94.28	0.012
Kashmera White-2	8.63	28.34	93.62	0.012
Kashmera White-3	8.63	28.16	99.62	0.012
Kashmera White-4	8.63	28.25	84.25	0.012
Kashmera White-5	8.63	27.97	92.87	0.012
Kashmera White-6	8.63	28.70	99.79	0.011
Perla White-1	8.63	27.12	68.13	0.014
Perla White-2	8.63	27.38	73.01	0.014
Perla White-3	8.63	27.14	72.33	0.014
Perla White-4	8.63	28.54	78.13	0.014
Perla White-5	8.63	28.46	70.35	0.013
Perla White-6	8.63	27.84	83.62	0.013

According to the mechanical test results of final products given in Table 3, It can be said that successful results were reached.

Table 4. Mechanical test criteria of Belenco Quartz Surfaces

Property	Criteria
Flexural Strength	> 35 MPa / F4 (EN 14617-2)
Abrasion Resistance	≤ 29 mm / A4 (EN 14617-4)
Impact Resistance	> 3,36 joule (EN 14617-9)
Water absorption	< 0,07 % / W4 (EN 14617-1)

Colour analysis of the slabs were also performed with Konica & Minolta spectrophotometer presented in Figure 6, and the results were presented in Table 5.

Table 5. The colour analysis of slabs

	L	a	b
Perla White-1	89.86	-0.68	2.49
Perla White-2	89.94	-0.65	2.44
Perla White-3	89.88	-0.63	2.47
Perla White-4	89.92	-0.67	2.45
Perla White-5	89.96	-0.68	2.48
Perla White-6	89.89	-0.65	2.42
Kashmera White-1	88.53	-0.53	2.50
Kashmera White-2	88.52	-0.53	2,44
Kashmera White-3	88.50	-0.57	2.51
Kashmera White-4	88.61	-0.52	2.49
Kashmera White-5	88.58	-0.54	2.47
Kashmera White-6	88.54	-0.56	2.45

Consequently, instead of the dark and opaque quartz, a white Carrara marble look with a very white and transparent appearance, rare in nature, was designed by Belenco for the first time in the world.

REFERENCES

- [1] Kayacı K., “Karaköy (Bilecik) yöresi mikrogranitinin jeolojisi ve seramik bünyelerde kullanım olanaklarının araştırılması”, Doktora Tezi, İstanbul Teknik Üniversitesi, Fen Bilimleri Enstitüsü, Jeoloji Mühendisliği 2007, s. 201.
- [2] Sacmi I., “Applied Ceramic Technology”, Vol. 1, 318,1124, 2002.
- [3] Pagliari L., Dapiaggi M., Pavese A., Francescon F., “A kinetic study of the quartz–cristobalite phase transition”, Journal of the European Ceramic Society, 33, 3403–3410, 2013.
- [4] Moore M., “Crystalline silica: Occurrence and use”, Indoor Built Environment, 8, 82–88, 1999.

GLASS AND GLASS CERAMICS

EFFECT OF TiO_2 AND B_2O_3 ADDITION ON CRYSTALLIZATION BEHAVIOR OF $\text{K}_2\text{O-MgO-Fe}_2\text{O}_3\text{-Al}_2\text{O}_3\text{-SiO}_2\text{-F}$ SYSTEM GLASS-CERAMICS

Umut ÖNEN¹, Ediz ERCENK², Şenol YILMAZ²

¹Cumhuriyet University, Engineering Faculty, Department of Metallurgical and Materials Engineering, Campus, 58140 Sivas, Türkiye.

²Sakarya University, Engineering Faculty, Department of Metallurgical and Materials Engineering, Esentepe Campus, 54187 Sakarya, Türkiye.

ABSTRACT

Glass-ceramics are polycrystalline materials of fine microstructure that are produced by the controlled crystallisation (devitrification) of a glass. Glass-ceramics can be obtained from various sources, such as pure oxides, natural rocks, and industrial wastes (blast furnace, arc furnace, cupola furnace, flying ashes etc.). $\text{K}_2\text{O-MgO-Fe}_2\text{O}_3\text{-Al}_2\text{O}_3\text{-SiO}_2\text{-F}$ system glass-ceramics are described in machinable glass-ceramic group. In this study, the glass produced by melt-quench technique. The recipe prepared by calcined vermiculite mineral and pure oxides such as K_2CO_3 , SiO_2 , Al_2O_3 , B_2O_3 , TiO_2 and MgF_2 . The starting raw materials were mixed together and milled in a mill with alumina ball at 250 rpm for 2 h. The mixed powders were melted by aluminium crucible at 1500 °C. The melted glass was cast into graphite mould (approximately 5 mm high, 10 mm wide and 10 mm long). The glass-ceramics characterized by differential thermal analysis (DTA), X-ray Diffraction (XRD) and scanning electron microscopy (SEM) techniques. The results indicate that the crystalline phases in the glass-ceramic system.

Keywords: Vermiculite, glass, crystallization, glass-ceramic

INTRODUCTION

Glass-ceramics were discovered accidentally in 1953. Since that time, many papers published by universities and research institutes. They were defined a material which contain amorphous and polycrystalline phases. Glass-ceramics are produced by controlled crystallization of certain glasses induced by nucleating additives. They always contain a residual glassy phase and one or more embedded crystalline phases. The crystallinity differs mostly between 30 to 70 percent [1-3].

Several researches have been published on glass-ceramics, particularly in the areas of interest the effects of different nucleating agents, such as TiO_2 , B_2O_3 , ZrO_2 , CeO_2 , WO_3 , Cr_2O_3 , NiO , CaF_2 , V_2O_5 , P_2O_5 , and alkali oxides. And they also reported the effects of these agents after the heat treatment of glass samples on the mechanical, thermal, and electrical properties [4-10].

The aim of this study is to investigate the effect of B_2O_3 and TiO_2 addition as a nucleating agent on crystallization behaviour on $\text{K}_2\text{O-MgO-Fe}_2\text{O}_3\text{-Al}_2\text{O}_3\text{-SiO}_2\text{-F}$ system.

EXPERIMENTAL

The chemical composition of calcined vermiculite and glass-ceramics were given Table 1 and Table 2 respectively. The starting powder prepared from K_2CO_3 , MgF_2 , SiO_2 , Al_2O_3 and calcined vermiculite as a recipe then TiO_2 and B_2O_3 used for additives. They were mixed by using an alumina ball mill at

250 rpm for 60 min in an alumina media. The mixture was sieved to a particle size fraction of 75 μm and then melted in the alumina crucible at 1500 $^{\circ}\text{C}$ for 1 h, and cast into the graphite mold. The bulk glass sample obtained from casting process were exposed to differential thermal analysis (DTA-TA Instrument Q600) for 1 h at heating rate of 10 $^{\circ}\text{C}/\text{min}$ for crystallization temperatures determination. Table 3 shows heat treatments of glass-ceramic samples. The samples were heat treated at different glass transition temperatures (T_g) between 600 $^{\circ}$ - 660 $^{\circ}$ for 1 h, then at 860 $^{\circ}\text{C}$ crystallization temperature (T_c) for 2 h. Rigaku D-max 2200-type diffractometer with Cu $K\alpha$ radiation was used to analyze X-ray diffraction (XRD). Hardness values were performed with a Future-Tech FM 700 micro indentation hardness tester. Glass-ceramics micrographs analysed by SEM-Jeol 6060 scanning electron microscope device.

Table 1. Chemical composition of calcined vermiculite.

	SiO₂	Al₂O₃	TiO₂	Fe₂O₃	CaO	MgO	K₂O	L.O.I
wt. %	39.49	17.06	2.78	11.98	2.58	18.91	5.67	1.53

Table 2. Chemical composition of glass-ceramics (wt. %)

	B₂O₃	K₂O	SiO₂	MgF₂	Al₂O₃	vermiculite	TiO₂
B0Ti3	-	9.00	23.00	11.00	7.0	50.00	1.66
B0Ti7	-	9.00	23.00	11.00	7.00	50.00	6.03
B3Ti3	3.00	9.00	22.00	10.00	6.00	50.00	1.66
B3Ti7	3.00	9.00	22.00	10.00	6.00	50.00	6.03

Table 3. Heat treatments of glass-ceramic samples.

	T_g	Time (hour)	T_c	Time (hour)
B0Ti3	660	1	860	2
B0Ti7	610	1	860	2
B3Ti3	660	1	860	2
B3Ti7	600	1	860	2

RESULTS AND DISCUSSION

In the results of the thermal analysis, the glass transition temperature as endothermic peaks, and the crystallization temperatures as exothermic peaks are as seen in Table 3 and Fig. 1. The TiO₂ addition caused decreasing in the glass transition temperature and it has no effect on the crystallization temperature [11].

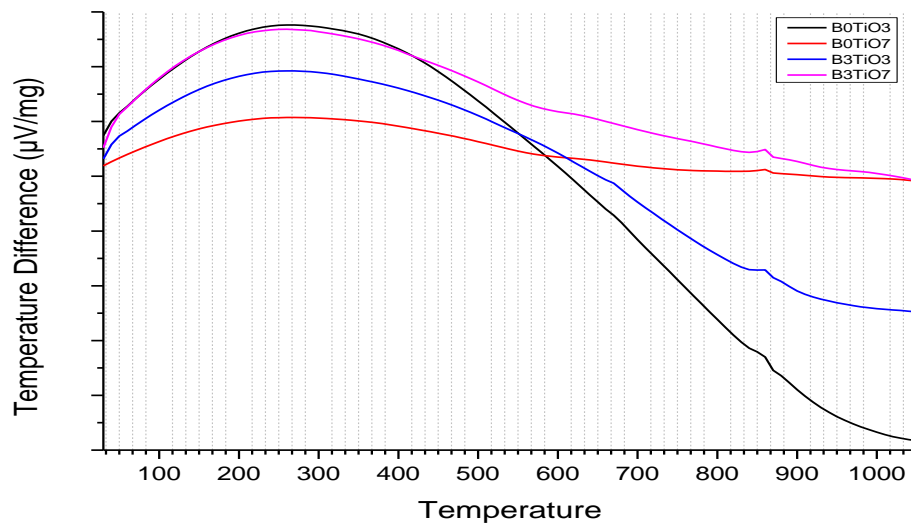


Figure 1. Differential Thermal Analysis curves of glass samples.

XRD analysis of the samples before and after crystallization heat treatment given in Figure 2 and 3. Analysis on the samples before crystallization shows intense amorphous phases along with several peaks denote partial crystallization. This is thought to be due to nucleation agent effect of TiO_2 on glass-ceramics [12]. Phases formed on the glass-ceramics after heat treatment were found to be Phlogopite ($\text{K}_3\text{Mg}_9\text{Si}_9\text{Al}_3\text{O}_{33}\text{F}_3$) Forsterite ($\text{Si}_4\text{Mg}_{6.89}\text{Fe}_{1.11}\text{O}_{16}$) and Perovskite ($\text{Ca}_8\text{Ti}_4\text{Si}_4\text{O}_{24}$) (Table 4). Phlogopite is the main phase in machinable glass ceramic systems and an important element of mica groups [13]. Forsterite phase is mainly composed of silicon-magnesium oxide structures and frequently observed in machinable glass ceramic systems [13].

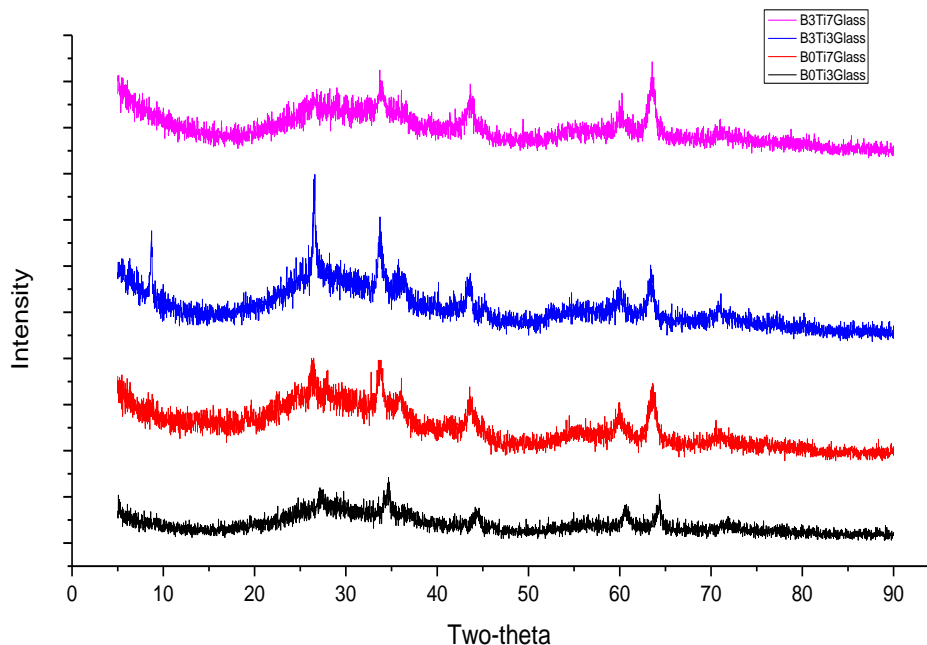


Figure 2. XRD patterns of glass samples.

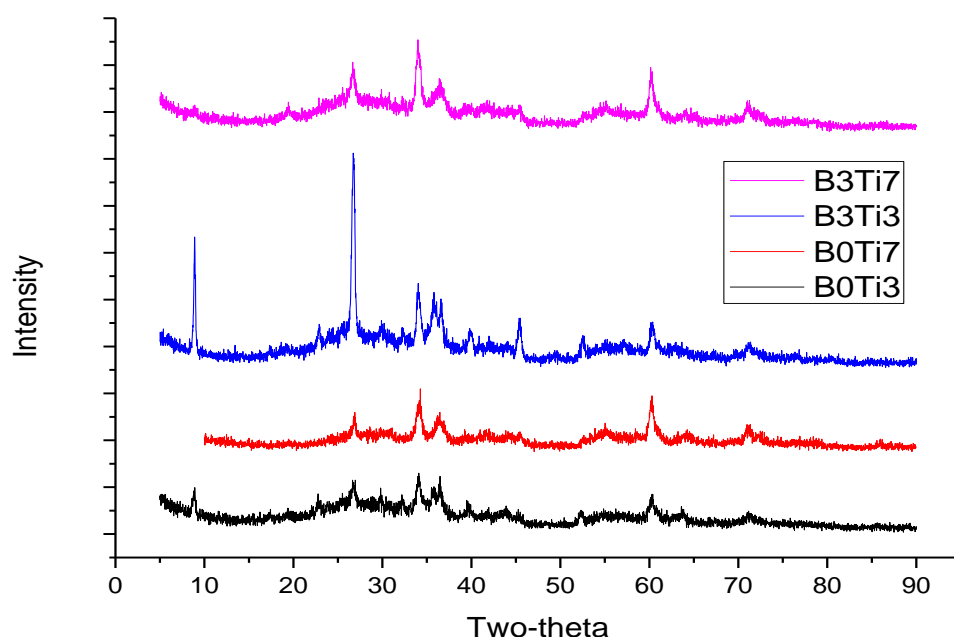


Figure 3. XRD patterns of glass-ceramic samples.

Table 4. Crystalline phases after heat treatment

Sample Code	Crystalline Phases
B0Ti3	Phlogopite, Forsterite
B0Ti7	Phlogopite, Perovskite
B3Ti3	Phlogopite, Forsterite
B3Ti7	Phlogopite, Perovskite

In this study, XRD pattern of iron containing relevant phase was detected. Perovskite phase is a member of a large calcium titanate phase group and rarely observed in machinable glass-ceramic studies due to less TiO_2 component. We observed phlogopite and forsterite phases on low TiO_2 including samples titled B0Ti3 and B3Ti3, whereas on high titanium including samples titled B0Ti7 and B3Ti7 we observed phlogopite and perovskite phases. Rietveld analysis showed that the sample titled B0Ti3 crystallized in the form of 85 % phlogopite 15 % Forsterite, B3Ti3 84 % phlogopite and 16 % forsterite. On high TiO_2 including samples, both on B0Ti7 and B3Ti7, 70 % phlogopite and 30 % perovskite phases crystallized. In accordance with the literature we observed that on less TiO_2 including samples forsterite phase crystallized and upon increasing TiO_2 the crystallized phase converted into perovskite structure.

Hardness analysis results carried out on glass and glass ceramic samples were given in Figure 4. Analysis on the results revealed that in all sample groups hardness values increased from glass to glass ceramics as a result of crystallization. In general, hardness values are lower on low TiO_2 including samples (titled B0Ti3 and B3Ti3) compared to higher TiO_2 including samples (titled B0Ti7 and B3Ti7). Forsterite phase observed in low TiO_2 including samples has the hardness of 6-7 on Mohs scale whereas Perovskite phase observed in high TiO_2 including samples has the hardness of 5-5.5 on Mohs scale. Perovskite phase observed in high TiO_2 doped system is different than classical calcium titanate phase and known as double perovskite on literature. This phase is a cubic structure consisting of one alkaline or alkaline-earth element, several transition metal and oxygen [14]. Increasing hardness observed in high titanium including samples are thought to be due to double perovskite structure.

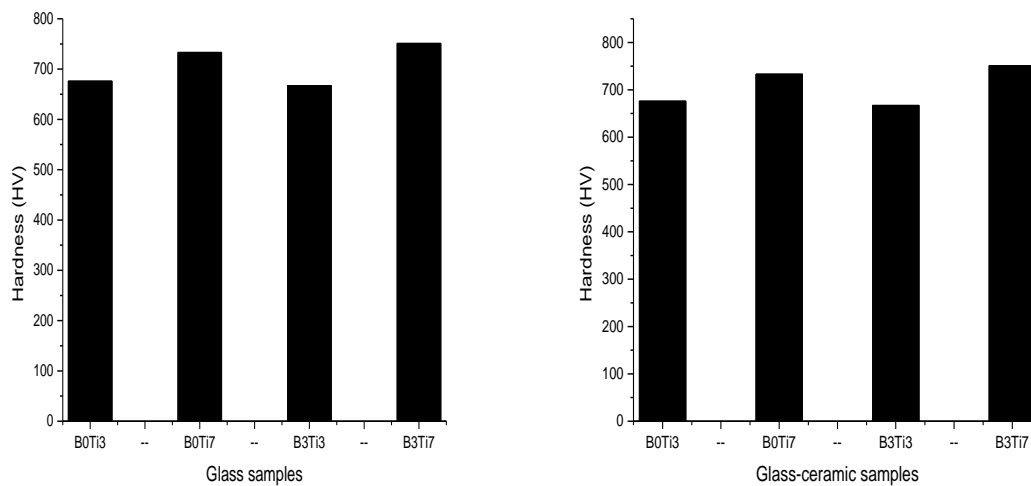


Figure 4. Hardness test results of glass and glass-ceramic samples (HV).

Machinability test results of glass ceramic samples were given in Figure 5. Analysis on the results show that machinability is higher on low TiO_2 including samples compared to high TiO_2 including samples. Hardness test results are in accordance with these results where hardness obtained in B0Ti7 and B3Ti7 are higher than that of obtained in B0Ti3 and B3Ti3. Rietveld analysis showed that the amount of phlogopite phase observed in low TiO_2 including samples are higher than high TiO_2 including samples. Therefore with the increase of TiO_2 content, perovskite phase crystallized and phlogopite crystal density decreased which results in less machinability.

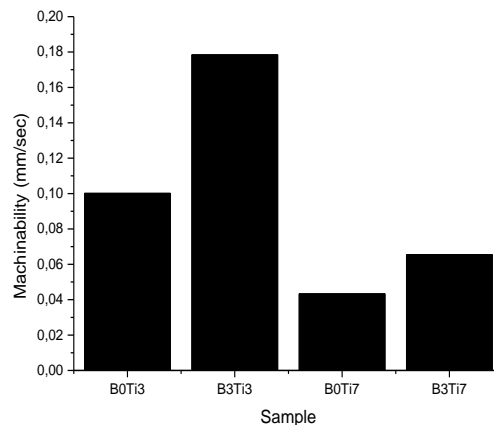


Figure 5. Machinability test results of glass-ceramic samples (mm/second).

Figure 6. shows the SEM microstructures of glass ceramics. Analysis literature reveals that mica phases display needle-like or cabbage structure morphologies. In this study we observed that instead of needle-like structures machinability is originated from cabbage like structures. In alignment with XRD results cabbage structure representing phlogopite phase is denser on low TiO_2 including samples as observed in SEM analysis.

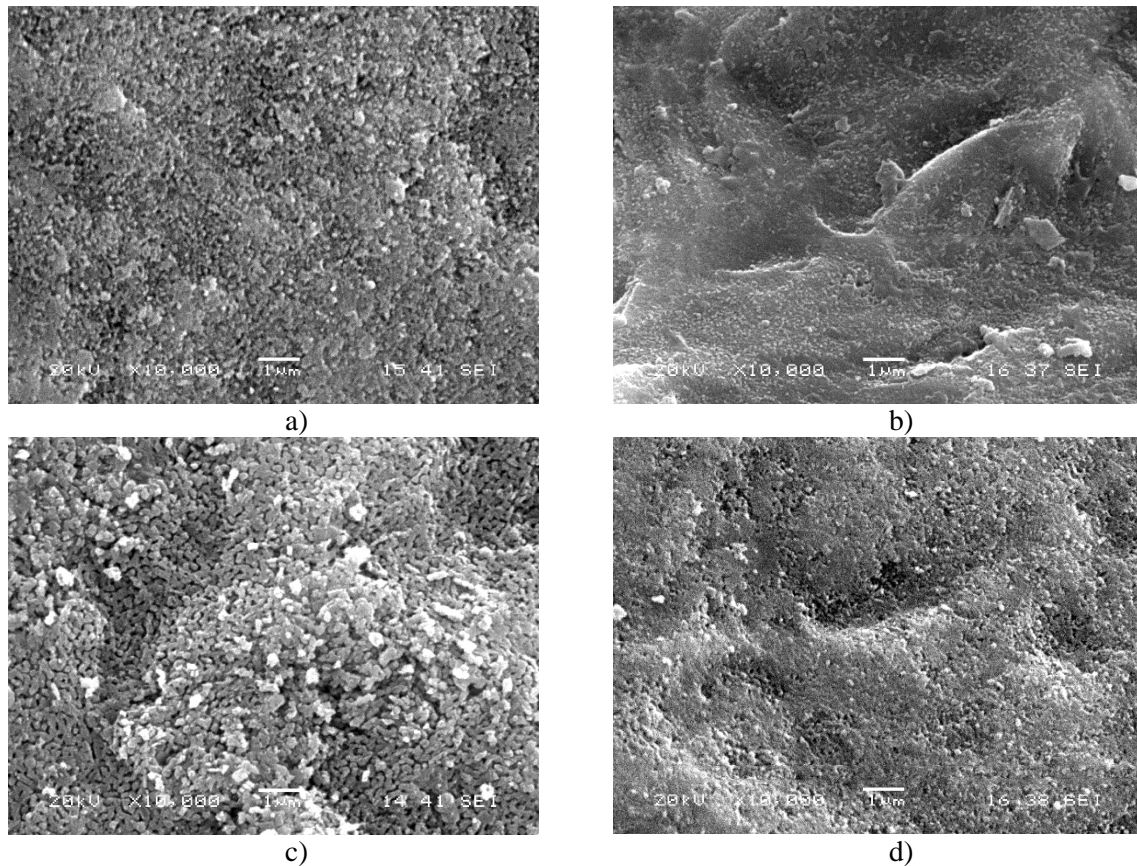


Figure 6. SEM micrographs of glass-ceramic samples. a) B0Ti3, b) B0Ti7, c) B3Ti3, d) B3Ti7.

CONCLUSION

In the current study, effect of TiO_2 and B_2O_3 additions on vermiculite based machinable glass-ceramic system was investigated. TiO_2 addition provides decreasing in glass transition temperatures and it has no effect on crystallization temperatures. B_2O_3 addition has a similar effect on glass transition and crystallization temperatures. In the samples having lower TiO_2 content, phlogopite and forsterite phases were determined by XRD. In the samples having higher TiO_2 content, phlogopite and perovskite phases were observed. Changing forsterite to perovskite relates to increasing in TiO_2 content, possibly. The hardness of the samples including lower TiO_2 content was lower than the others, and machinability test results have good agreement with these results. The samples including lower TiO_2 content showed better machinability. In the SEM microstructures, nano-crystalline structures were observed in all samples. Cabbage structures indicating mica crystals are more intense according to the samples including higher TiO_2 content.

REFERENCES

1. Zanotto, E.D., A bright future for glass-ceramics. American Ceramic Society Bulletin, 2010., 89 (8), 19-27.
2. Yılmaz Ş., PhD. Thesis, Istanbul Technical University, 1997.
3. Ercenk E., Yılmaz Ş., Sintering Behavior and Machinability in Mica Glass-Ceramic of the System $\text{SiO}_2\text{-Al}_2\text{O}_3\text{-MgO-K}_2\text{O-B}_2\text{O}_3\text{-F}$. Acta Physica Polonica A., 2014, 125, 629-631.
4. W. Vogel and W. Holand, "Nucleation and Crystallization Kinetics of an $\text{MgO-Al}_2\text{O}_3\text{-SiO}_2$ Base Glass with Various Dopants"; in Advances in Ceramics, Vol. 4, Nucleation and Crystallization in Glass. Edited by I. H. Simmons, D. R. Uhlmann, and G. H. Beal. American Ceramic Society, Columbus, OH, 1982, 125-45
5. Zdaniewski W. A., Crystallization and Structure of an $\text{MgO-Al}_2\text{O}_3\text{-SiO}_2\text{-TiO}_2$ Glass-Ceramic. J. Mater. Sci., 1973, 8, 192-202.
6. Barry T. I., Cox J. M., Morrell R., Cordierite Glass-Ceramic—Effect of TiO_2 and ZrO_2 Content on Phase Sequence during Heat Treatment. J. Mater. Sci., 1978, 13, 594-610.
7. Zdaniewski W. A., DTA and X-ray Analysis Study of Nucleation and Crystallization of $\text{MgO-Al}_2\text{O}_3\text{-SiO}_2$ Glasses Containing ZrO_2 , TiO_2 , and CeO_2 . J. Am. Ceram. Soc., 1975, 58 5-6, 163-69.
8. Gregory A. G., Veasey T. J., The Crystallization of Cordierite Glass. J. Mater. Sci., 1973, 8, 333-39.
9. Zdaniewski W. A., Microstructure and Kinetics of Crystallization of $\text{MgO-Al}_2\text{O}_3\text{-SiO}_2$ Glass-Ceramics. J. Am. Ceram. Soc., 1978., 61 5-6, 199-204.
10. Bridge D. R., Holland D., McMillan P. W., Development of the Alpha-Cordierite Phase in Glass-Ceramics for Use in Electronic Devices. Glass Technol., 1985, 26 (6), 286-92.
11. Akin I., Goller G., Effect of TiO_2 addition on crystallization and machinability of potassium mica and fluorapatite glass ceramics. J Mater Sci., 2007, 42, 883-888.
12. Mukherjee D. P., Influence of TiO_2 content on the crystallization and microstructure of machinable glass-ceramics. J. Asian Ceramic Soc., 2016, 4, 55-60.
13. Maiti P. K., Mallik A., Basumajumdar A., Kundu P., Influence of fluorine content on the crystallization and microstructure of barium fluorophlogopite glass-ceramics. Ceramics International, 2010, 36 (1), 115-120.
14. Androulakis J., Katsarakis N., Giapintzakis J., Vouroutzis N., Pavlidou E., Chrissafis K., Polychroniadis E.K., Perdikatsis V., LaSrMnCoO_6 : a new cubic double perovskite oxide. Journal of Solid-State Chemistry. 2003, 173 (2), 350-354.

ADVANCED CERAMICS

SYNTHESES OF AlN NANOPOWDER

Hamza Boussebha¹, Emre Akcan, Ali Osman Kurt

Sakarya University, Engineering Faculty, Department of Metallurgy and Materials Engineering,
54187, Sakarya, Turkey.

Abstract:

Aluminium Nitride (AlN), proved itself as a promoting ceramic for electric and electronic uses. Because of the advantages of having fine powders, in matters of energy and structure characteristics, many researches focused on reducing the particle size to a nanoscale. There are many processes to obtain AlN nano-powders, however, direct nitridation (DN) and carbothermal reduction nitridation (CRN) are considered as the preferable methods to be commercially used. Each one of these methods has its advantages and disadvantages, which mainly, has an important impact on the as-synthesized product and its price. However, none of these methods gives nano-scale AlN powders. Therefore, engineers are always trying to achieve their desired properties using the most practical and cost-effective process. In our work, AlN nanopowders were successfully synthesized for the first time via thermo-mechano-chemical (TMC) process using carbothermal – reduction – nitridation (CRN) method. Furthermore, in this paper other AlN nanopowder synthesis roots are discussed.

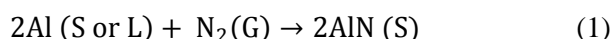
Keywords: AlN, Aluminium Nitride, CRN, Nanopowder Synthesis

1. Introduction:

In the last years, Aluminium Nitride (AlN) has attracted much of attention as a ceramic with good thermal and electrical properties, due to its excellent characteristic. Aluminium Nitride is a ceramic with a covalent bond, it has a hexagonal crystal of the Wurtzite type,^[1] Because of its low atomic mass, strong interatomic bonding, simple structure and low anharmonicity, AlN is a phonon heat conductor with a high thermal conductivity (320 - 330 W/mK)^[1,2]. The high electric insulation ($>10^{14} \Omega \cdot \text{cm}$)^[2], makes of AlN one of few ceramics that possess both high thermal conductivity and excellent electrical insulation^[3]. Moreover, AlN has a low thermal expansion coefficient ($3.2 - 4.6 \times 10^{-6} \text{ K}^{-1}$) close to that of Si^[4,5], low dielectric constant, non-toxicity, high mechanical resistance and high temperature resistance^[3,4]. All these properties make of AlN the best choice for substrates. AlN, can also be used for many high brightness LED and power electronics applications,^[3] microwave packages, hybrid power-switching packages, optoelectronic parts, heat sinks, cutting tools, laser diode, heat spreaders, and fillers for polymer and glass compound.^[1] Unlike Alumina, that is formed naturally, which makes it cheaper, AlN can only be obtained via synthesis. Many studies have been conducted over the production of AlN powders. Syntheses were performed via various techniques, like carbothermal reduction and nitridation (CRN),^[3,5-8] direct nitridation (DN),^[9,10] processing of $\gamma\text{-Al}_2\text{O}_3$ by gas nitridation,^[2,11] chemical synthesis methods and chemical vapor deposition CVD technic^[2]. A reduced powder size gives big advantages in sinterability which can be performed at a lower temperature, and fine grain size giving better characteristics. All the recent studies aimed to reduce the size of AlN powders to a nanoscale, using a cheap and easy root. Although, aluminium nitride can be synthesized via various methods, yet carbothermal reduction nitridation and direct nitridation are the techniques mostly used to produce tonnage scale quantities^[3], and each one of these roots, has its advantages and disadvantages. In what follows, these techniques are briefly explained.

1.1. Direct Nitridation:

Aluminum nitride can be obtained directly from aluminum metal and nitrogen gas using the direct nitridation process, this method is an exothermic reaction which is known as self-propagating synthesis (SPS).^[3] Direct nitridation, consists on ignition of aluminum powders in an atmosphere of nitrogen at a temperature above 1200°C^[1] following reaction (1). The exothermic reaction generates an energy of 328 kJ/mol at 1527°C, aluminium begins to melt at 660° C, then starts a self-sustaining process by reacting with nitrogen at 800°C^[3]. These make of the direct nitriding, an economical, energy efficient and environmental friendly process, seeing as the energy generated from the ignition, plays the role of assistant in the process.



The disadvantage of this method is that the reaction products need further processing either by milling or classification to obtain a final powder. Furthermore, a nitride film forms on the surface of particles which causes a restriction of penetration for nitrogen atoms, restricting the continuous reaction^[4]. Moreover, there is a possibility to obtain an impure powder due to the multiple size reduction processes required to achieve the needed particle size. This size reduction is consequence of an uncontrollable reaction sequence and exothermic temperature that result a considerable necking between aluminum nitride particles.^[3] The ball milling is a mechanical technique used in the production of nanopowder, which has been in development over the last years to reduce its long milling time and increase the low production efficiency, by introducing physical energy fields, such as ultrasonic, magnetic field and electric discharge. Sen Wang et al^[4] were able to obtain AlN nano powders from a mixture of Al and LiOH-H₂O powders in the atmospheric N₂ by combining the ball milling and electrical discharge to enhance the chemical reactions. A new synthetic and processing way was achieved resulting a nanopowder of 40nm after 6h milling. Mikimasa et al^[9], in an earlier study, synthesized AlN nanopowders by transferred type arc plasma using ammonia NH₃ as a reacting/quenching gas blown into aluminium gas at a temperature between 2000° and 2400°K, passing the synthesized powder through ethanol traps the unreacted Al particles and by that, increased the content of AlN by 99%. A powder of an average diameter of 20nm was obtained using this method. The use of ammonia in AlN syntheses, was earlier reported by Hotta et al^[1], who stated that using a mixture of ammonia and nitrogen gas gives the possibility of obtaining AlN powder at lower temperature for a reason that ammonia is more reactive than nitrogen.

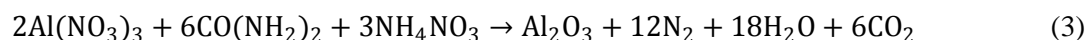
1.2. Carbothermal Reduction Nitridation:

This method consists on heating a mixture of alumina or aluminium based precursor and carbon source to a high temperature (1100°C – 1600°C)^[1] in a flowing nitrogen or ammonia. The Alumina is reduced by carbon, then nitrogen comes into action reacting with the aluminium to produce AlN. The general reaction is given with equation (2):



From the reaction, we can see that for each mole of alumina we need 3 moles of carbon. As a result, to achieve completion of the reaction and enhance its kinetics, we need extra carbon^[1] ($\approx 15\% - 30\%$ to achieve full conversion to AlN)^[3]. By consequence of this excess, unreacted carbon remains in the product, and a further burning in air is needed to eliminate it. This elevate the risk of oxidation of the AlN surface. The raw oxide for CRN process includes α -Al₂O₃, γ - Al₂O₃, AlOOH and materials that can convert to aluminium oxides. The carbon source can be of carbon black, graphite or materials with the possibility of producing carbon after pyrolysis like sugars and polymers^[1]. Mahua^[8], was able to obtain a 20 to 50 nm powder after a nitridation of alumina gel in nitrogen for 3h at 1350°C. The alumina gel was obtained by carbothermal reduction of aluminium isopropoxide C₉H₂₁O₃Al, with dextrose as source of carbon. Earlier studies^[1,2,11] suggested that among the various alumina forms, γ -Al₂O₃ possesses the best reactivity to produce AlN at a lower temperature and with less unreacted alumina. Some studies^[6,7,12], showed that AlN can be obtained from combustion synthesis precursor based on urea, glucose/sucrose and Al(NO₃)₃·9H₂O following reactions (3) and (4). Kuang et. al.^[7] synthesized nano-scaled AlN from a precursor obtained by dissolving urea, glucose/sucrose and

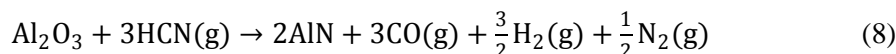
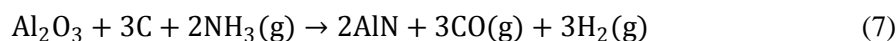
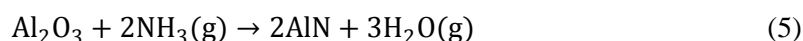
$\text{Al}(\text{NO}_3)_3 \cdot 9\text{H}_2\text{O}$ in distilled water then ammonium nitrate, added as combustion assistant. A black foam was obtained after heating the mixture to a temperature of 300°C to 500°C. Calcination between 1200°C and 1500°C for 2 to 3h under flowing N_2 followed by carbon removal at 700°C for 2h in air gave nano-scaled AlN powders.



CRN method allows the production of a higher quality powders. The final particle size and purity can be determined by precursor size and synthesis temperature. Thus, excessive milling can be avoided because of the availability of fine precursor powders. Nevertheless, it can be used in order to homogenize the powder and reduce the size ^[1,3]. The cost of carbothermal reduction nitridation, however, is high. intensive energy is needed, and non-reacted carbon causes a bad impact ^[3].

1.3. Processing of aluminium oxide by gas nitridation:

Gas nitridation is a technique that is efficient in the syntheses of nitrides. It is a CRN generally, with the difference of using a gas mixture to both reduce and nitride the alumina. This technique was mainly developed for synthesizing oxynitride powders. ^[12] From the different allotropic forms of alumina, various studies showed that AlN can be best obtained from the conversion of $\gamma\text{-Al}_2\text{O}_3$. ^[1,2,11,14] The general reaction of this process is given by equation (5), while equations [(6) – (8)] represent the equilibrium states where gas mixtures are used. Propane (C_3H_8) is used due to its positive effect on nitridation. Suehero et. al. ^[15] showed that an addition of Propane mixed with ammonia (NH_3) in AlN synthesis, accelerates the rate of nitride formation. 94% conversion to AlN was achieved in 0,5h at 1500°C. This acceleration is explained thermodynamically as the reaction represented by equation (6) has the lowest Gibbs free energy (ΔG°). Fig. 1 shows ΔG° change as function of temperature.



Because of its fine particle size, high surface area and good reactivity, $\gamma\text{-Al}_2\text{O}_3$ can be treated with ammonia or nitrogen to produce AlN nanopowders at a lower temperature than the classic carbothermal reduction nitridation process. Yamakawa et al ^[2], explained the better reactivity of $\gamma\text{-Al}_2\text{O}_3$ as its tetrahedral AlO_4 sites are preferentially nitrated than the octahedral AlO_6 sites of the $\alpha\text{-Al}_2\text{O}_3$. The synthesis behavior of $\gamma\text{-Al}_2\text{O}_3$ is better than $\alpha\text{-Al}_2\text{O}_3$, for a reason that $\gamma\text{-Al}_2\text{O}_3$ contains both AlO_4 and AlO_6 , when $\alpha\text{-Al}_2\text{O}_3$ only contains the stable AlO_6 . They were able to obtain 100% nitridation of $\gamma\text{-Al}_2\text{O}_3$ in a mixture of $\text{NH}_3/\text{C}_3\text{H}_8$ for 2h at 1400°C, with an average particle size of 76nm.

Many aluminium oxide precursors can be used as a starting material to give $\gamma\text{-Al}_2\text{O}_3$ which can be nitrated to AlN. $\text{Al}(\text{OH})_3$ was found to be good reactive starting material ^[3]. Kroke et al ^[14], tried using many aluminium oxides precursors such as $\text{Al}(\text{NO}_3)_3$, $\text{Al}(\text{OH})_3$, $\text{Al}(\text{OH})(\text{O}_2\text{CH}(\text{C}_2\text{H}_5)(\text{C}_4\text{H}_9))_2$ and $\text{Al}(\text{OCH}(\text{CH}_3)_2)_3$ in order to obtain AlN nanopowders. It was found that in a NH_3 atmosphere at temperature range of 1000 to 1400°C, the precursors starts transforming to either γ or α alumina at 1000-1200°C (for $\text{Al}(\text{NO}_3)_3$ α alumina at 1200°C, while for other precursors γ alumina at 1000°C) then convert to AlN with a small amount of $\alpha\text{-Al}_2\text{O}_3$ at 1400°C. The formed product was a single phase AlN with crystallites of 5-60nm. The biggest challenge for the processing of $\gamma\text{-Al}_2\text{O}_3$ is maintaining the unstable γ phase and stopping it from forming the stable α alumina, when the temperature of transformation is reached. Another problem is the high surface energy of the nano-sized powders, which form agglomerates in order to decrease that energy, making it hard to keep the powders at a nano scale ^[5].

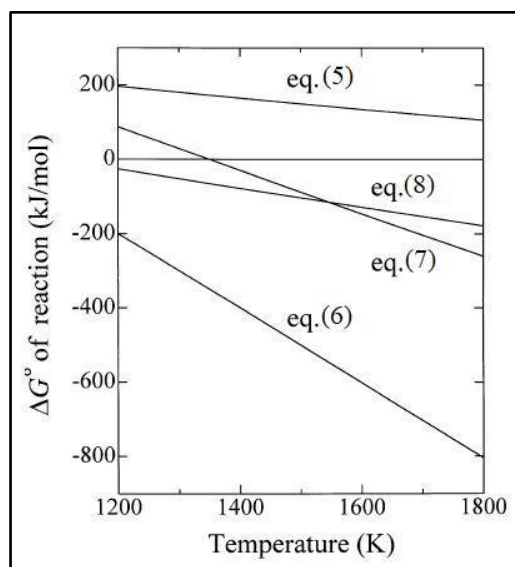
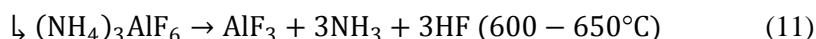
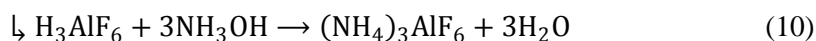
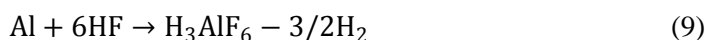


Fig. 1: ΔG° changes of equations [(5) – (8)] as function of temperature change ^[15]

1.4. Other synthesis methods:

1.4.1. Chemical synthesis:

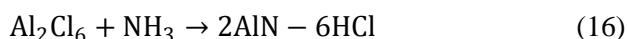
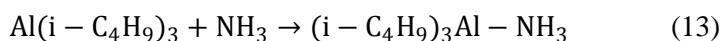
Chemical synthesis can give powders with very good quality. Precursors, which can be both organic and inorganic compounds are used, such as AlX_3 , $(\text{NH}_4)_3\text{AlF}_6$, $\text{Al}(\text{NH}_2)_3$, $\text{Al}(\text{NHR})_3$, AlH_3 , $\text{AlR}_n\text{X}_{3-n}$ and $\text{AlH}_{3-n}(\text{NR}_2)_n$, where X is a halogen atom, R is an alkyl group, and n is 1 or 2. ^[1] In order to obtain the powder, the precursor must first be prepared then put under reaction with nitridation gas such as ammonia. Some example equations for the obtention of a precursor and its nitridation are given below:



Although the powders synthesized by this method have high purity and a controlled particle shape and distribution, yet a commercial use is far undesired for a reason of high cost, being non-practical and hard to control.

1.4.2. Chemical vapor deposition:

CVD method can produce powders with better quality than the other described methods. Its advantage over other the previously described processes are the possibility to control both the chemical homogeneity and purity, and the ability to produce a powder with high surface area. The main precursors for this process are AlCl_3 and AlR_3 , where R is either methyl, ethyl or butyl, and ammonia is used as reactant and carrier gas. ^[1] some of example equations are given below:



The main disadvantages of this method are its raw material's high costs, the agglomeration of powder, and the difficulty to handle a large quantity and to separate fine powders from the gas steam.

In our work, we used a novel technique to synthesize AlN nanopowders which is a kind of Dynamic Carbothermal Reduction Nitridation (DCRN), where the powder is synthesized in moving system, allowing the CRN to take a place with less consumed energy. DCRN was experimentally proved to be successful in achieving fine technical ceramic powders at both reduced temperatures and time. [16-18] In this work, we modified the DCRN by introducing alumina balls into the system, to be alongside with the powder inside the alumina tube. Thus, the previously explained AlN synthesis techniques are compared with our root.

2. Experimental procedure:

In order to synthesize aluminum nitride powders, aluminium hydroxide $\text{Al}(\text{OH})_3$ (Merck Group, Turkey; reference 101091.1000), was used. Tab. 1 states the composition of $\text{Al}(\text{OH})_3$. Alumina balls made of Al_2O_3 with a purity of 99,9% purity (Alfa Aesar) were used inside the DCRN rotating system. High purity and low-sized ISAF-220 carbon black (Körfez Petrochemical Refinery, Koceali Izmit, Turkey) was used as a reducing agent. Nitriding source was 99,99% pure nitrogen N_2 gas (ARTOK, Adapazarı, Sakarya, Turkey). SEM (JEOL 6060 LV) micrograph of both $\text{Al}(\text{OH})_3$ and Al_2O_3 are given in Fig. 2.

Material	Size	Elements					
		Al	Fe	Na	Cl	SO_4	Other
$\text{Al}(\text{OH})_3^*$	<150 μm	Balance	0,01	0,30	0,01	0,05	-

Tab. 1: Composition of the $\text{Al}(\text{OH})_3$ starting powder obtained from producing company

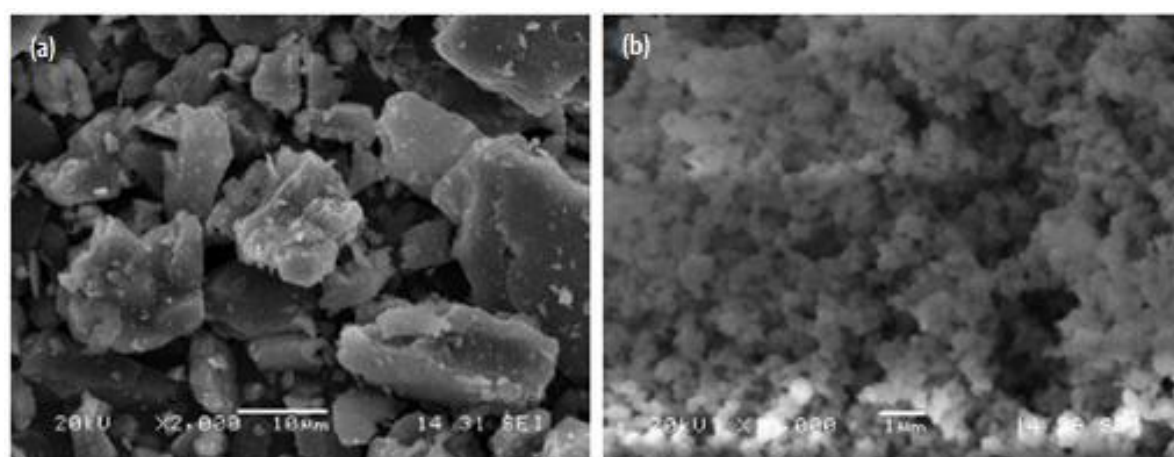


Fig. 2: SEM micrographs of: (a) $\text{Al}(\text{OH})_3$ starting powder (b) Al_2O_3 powder of alumina balls

Heating was carried out in Protherm 1600°C type tube furnace with heating rate control capability. The furnace was modified in order to introduce a rotating system into it by installing a 3v DC servomotor externally on the alumina tube using pinion gears, in a way to control the desired rotation speed. A schematic representation of the DCRN system is given in Fig. 3.

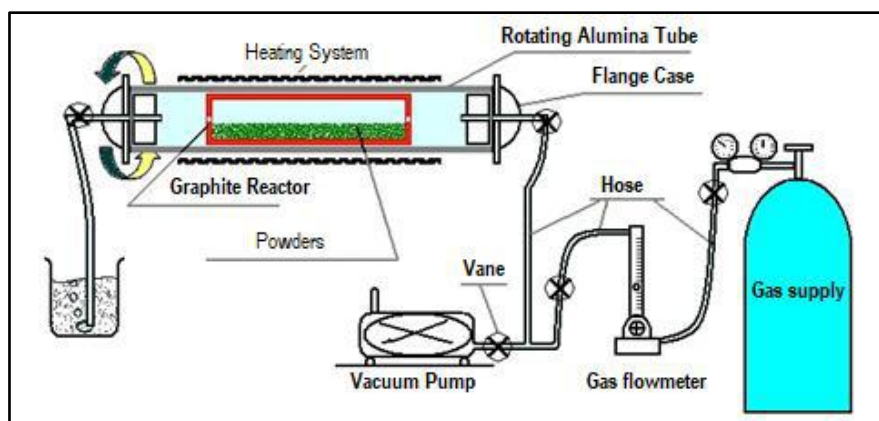


Fig. 3: Schematic representation of the DCRN system

Powders were mixed in an alumina mortar with stoichiometric ratio of $C/Al(OH)_3=21$. The mixture contained $Al(OH)_3$ and C as 4,44 and 1,37 times the stoichiometric ratio respectively. In order to obtain a better homogeneity, the powder mixture was placed in a planet mixer for 30mn in presence of steel balls, as 5 times the weight of the powder. The obtained mixture was placed in a graphite reactor with a weight of 5mm diameter alumina balls, and 4g powder. 3 samples were tested by varying the Balls/Powder (B:P) weight ratio as 5, 20 and 30. Powder mixture and alumina balls were then introduced into the alumina tube of the DCRN furnace for heat treating, under nitrogen atmosphere. Gas flow was set as 75lt/mn for the first 30mn of heating to remove the oxygen inside, then set down to 60lt/mn. Rotation speed of the alumina tube was set to 1rpm from until 700°C, then doubled to 2rpm until 1450°C where the mixture was maintained for 2h. In the cooling process, the gas flow was set to a minimum. The rotation speed was set down to 1rpm at 700°C then stopped at 500°C, then, the temperature was brought to room temperature with a controlled cooling. The obtained powder was fired in a Protherm (model PLF 130/18 1300°C capacity) furnace in atmospheric conditions, with a heating rate of 10°/mn then maintained at 680°C for 1,5h. Temperature was selected according to results of AlN and carbon black DTA/TG (Netzsch, STA 449) analyses. DTA/TG curves of both AlN and carbon black samples are given in Fig 4. After burning in open air, the obtained powder was characterized using XRD (Rigaku D/Max-2200/PC) and FESEM (FEI model Quanta FEG 450).

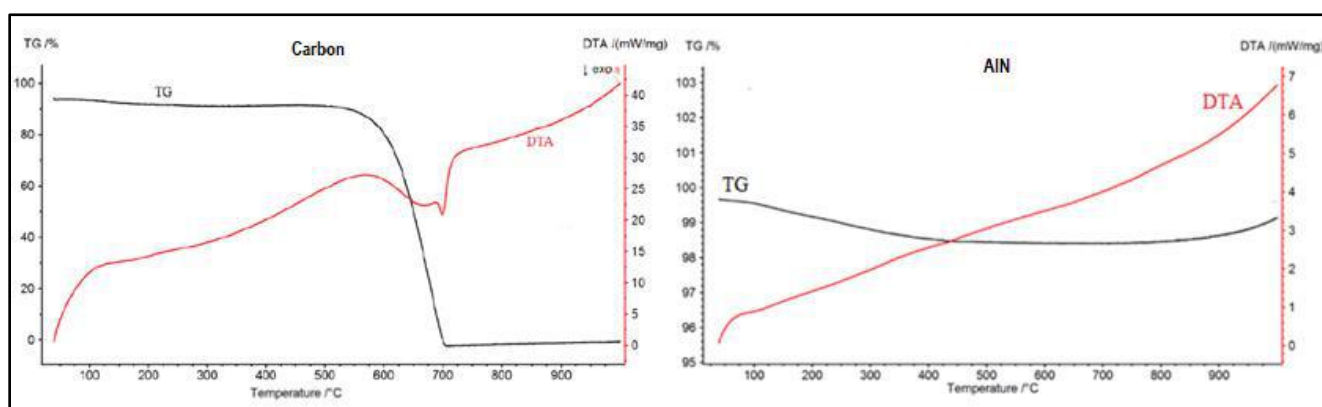


Fig. 4: DTA/TG curves of carbon black and AlN

3. Results and Discussion:

The powder obtained after cooling to room temperature had black color due to the carbon black excess. Burning was necessary to eliminate the residual carbon. Consequently to burning, the final powder colors changed gradually from light grey for B:P=5 (close to white) to grey for other samples. XRD was performed later to determine the crystalline nature of the obtained powders. XRD patterns of the B/P=5, B:P=20, and B:P=30 samples are given in Fig. 5, 6 and 7 respectively. For B:P=5

sample (Fig. 5), high intensity peaks corresponding to AlN crystallites were observed. This is a good result in matter of powder purity. By raising the B:P ratio to 20 (Fig. 6), AlN is still observed at same angles, the intensity of the peaks, however, falls down to almost half the previous one. For B:P=30 (Fig. 7) AlN peaks intensity, again falls down slightly. To observe the morphology of the produced powders FESEM analysis was performed for the 3 samples. Micrographs corresponding to B:P=5, B:P=20, and B:P=30 samples are given in Fig. 8, 9 and 10 respectively. For B:P=5 sample (Fig. 8), irregular AlN blocks of about $10\mu\text{m}$ size, are recorded at a magnification of $\times 10000$, zooming into the blocks, AlN nano-crystallites were observed. The average size of these crystallites was 85nm. For B:P=20 sample (Fig. 9), smaller blocks were observed at $\times 5000$. Then at magnification of $\times 200000$, irregularly shaped crystallites were observed, with average size of 75nm. The best result in matter of morphology was obtained from B:P=30 sample (Fig. 10). FESEM micrographs showed round crystallites of 35nm average size regularly shaped. These crystallites were also in form of blocks which seemed like agglomerates.

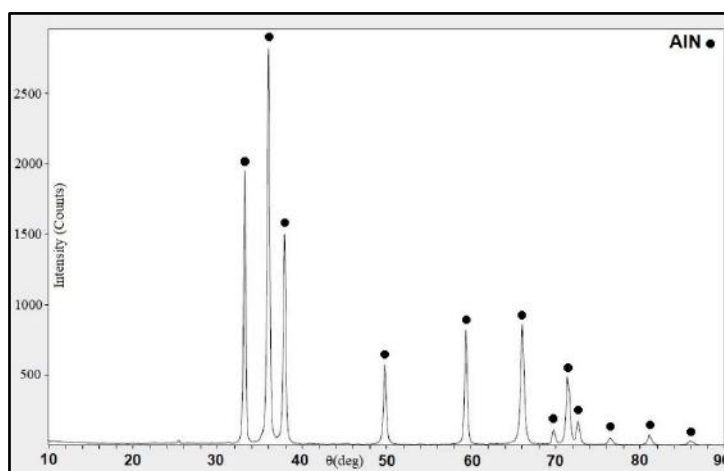


Fig. 5: XRD pattern of the B:P=5 sample

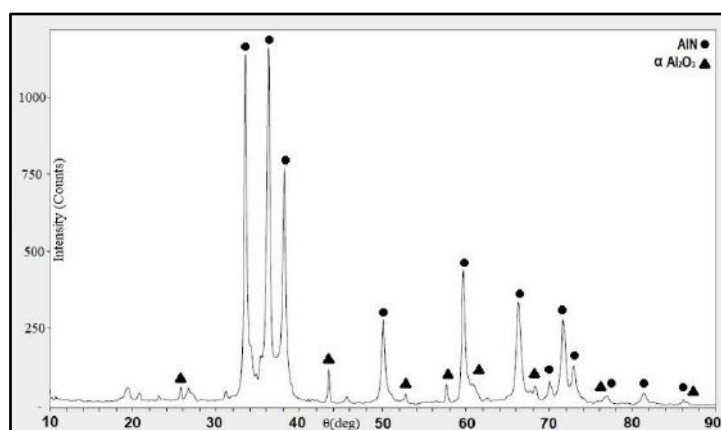


Fig. 6: XRD pattern of the B:P=20 sample

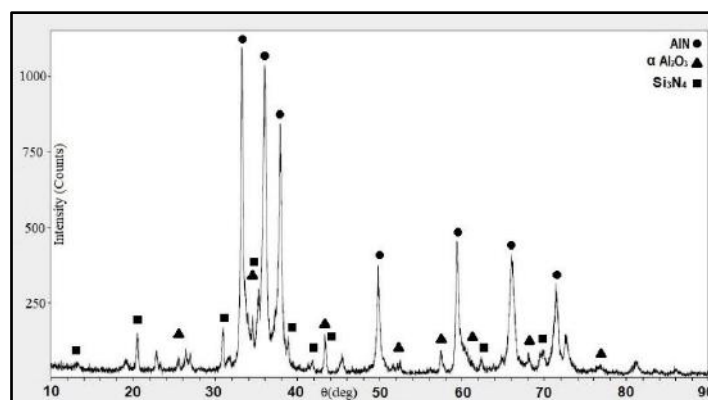


Fig. 7: XRD pattern of the B:P=30 sample

Alumina balls had different effects on the powder. The morphology of powder was better for bigger balls to powder ratio, suggesting that smaller and better powder shape, can be obtained for a big B:P ratio such as 30. This is due to the activating effect of the balls in the system. During heating inside the DCRN furnace, alumina balls help activating the reaction during the rotation of the tube. When more balls are present in the system, reaction can take place at a lower temperature. Furthermore, bonds are easily broken and smaller crystallites are formed. The intensity, however, was recorded to be falling down with B:P ratio raise, with some amount of unreacted alumina. This can be explained with balls activating the reaction in a way that α - Al_2O_3 phase is formed. Kroke et. al.^[14] reported that before conversion to AlN, $\text{Al}(\text{OH})_3$ converts first to the unstable γ - Al_2O_3 phase. If the reaction isn't well controlled, γ - Al_2O_3 transform to the stable α phase, which is more likely to result an uncomplete conversion to AlN, leaving some amount of unreacted alumina. In an attempt to completely eliminate the residual unreacted alumina, a different heating was performed. The conditions were the same with the difference of raising the temperature to 1475°C and stopping the rotation at the beginning of the cooling process. AlN was successfully obtained. The amount of unreacted alumina was reduced; however, a complete elimination was not possible. This confirms that once transformed to α phase, alumina cannot be easily nitrided. Another possibility of unreacted alumina may be from the alumina balls. Being present in the rotating system at elevated temperature, the possibility of alumina balls to be in reaction with the powder is not excluded.

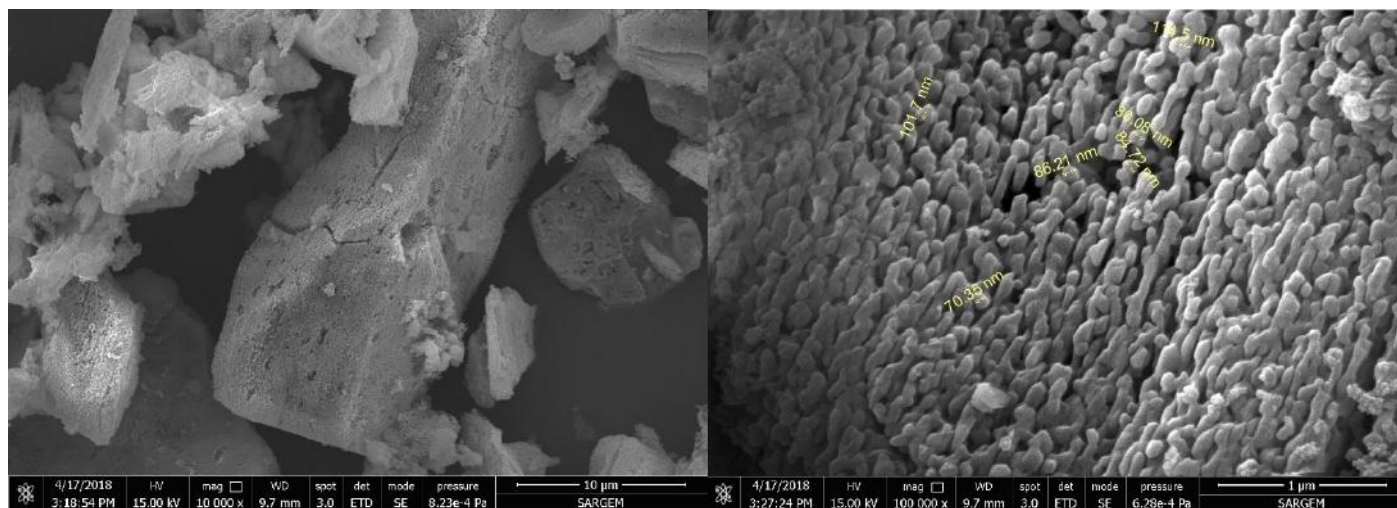


Fig. 8: FESEM micrographs of the B:P=5 sample

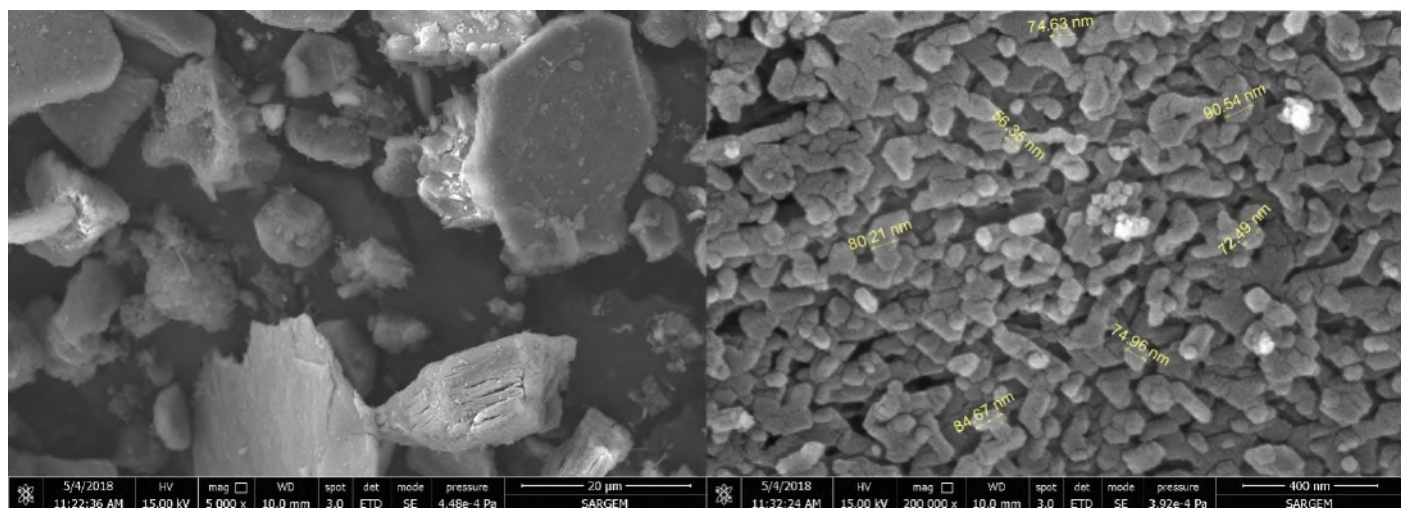


Fig. 9: FESEM micrographs of the B:P=20 sample

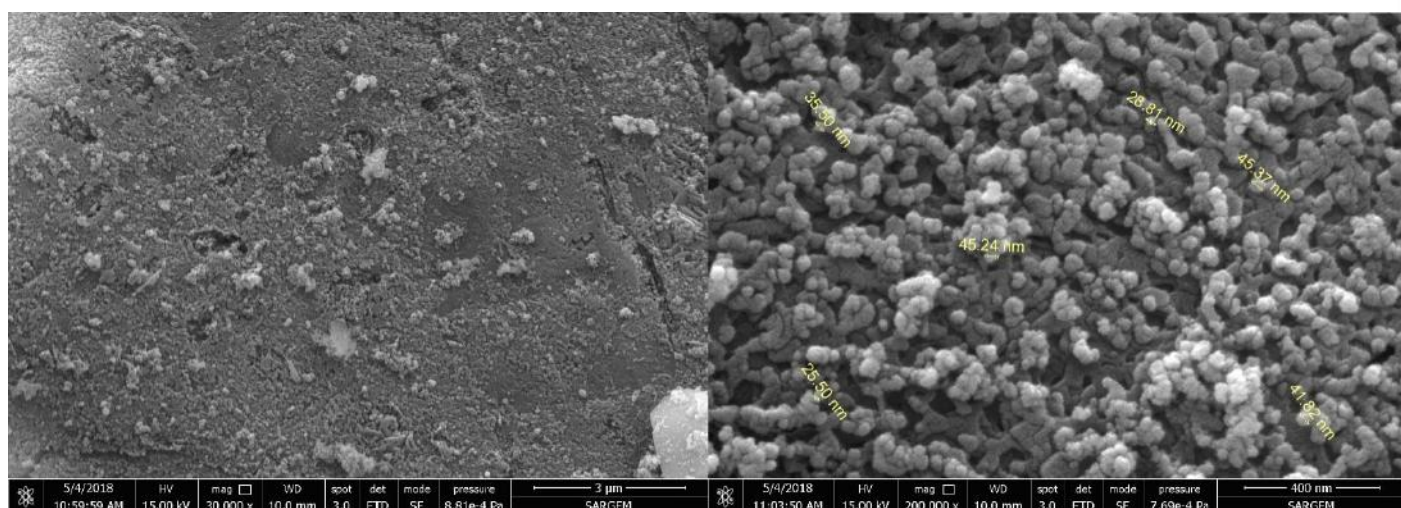


Fig. 10: FESEM micrographs of the B:P=30 sample

The nano crystallites were in form of blocks which seemed the same as the raw $\text{Al}(\text{OH})_3$ powder. This is due to the fact that reduction nitridation occurs with a removal of oxygen and hydrogen, then nitridation leaving the powder in an agglomerate-like form. Another explanation of having blocks is the agglomeration of nano crystallites. This is due to the high surface energy of the nanopowders, which can agglomerate in order to reduce the energy. The size of the blocks decreased with B:P ratio increase. Nevertheless, it was difficult to keep the powder separated to room temperature. In an attempt to separate the nanopowders, an ultrasonic shaking was performed for 1, 2, 4 and 6 hours. The obtained results are given in Fig.11. For 1h shaking (Fig. 11a), a partial separation of some of the big blocks was observed. When the shaking time was extended to 2h (Fig. 11b), the blocks started taking a rounder shape. Extending the time of shaking to 4h (Fig. 11c), resulted a partial spherization of the powders. When the time of shaking was 6h (Fig. 11d), the spherization process continue with the separated nano crystallites joining the spherical granulates. The result was powder granulates of 40µm average size sphere-like shape. From this we can conclude that the ultrasonic shaking can help give a sphere-like shape but not separate the nano crystallites.

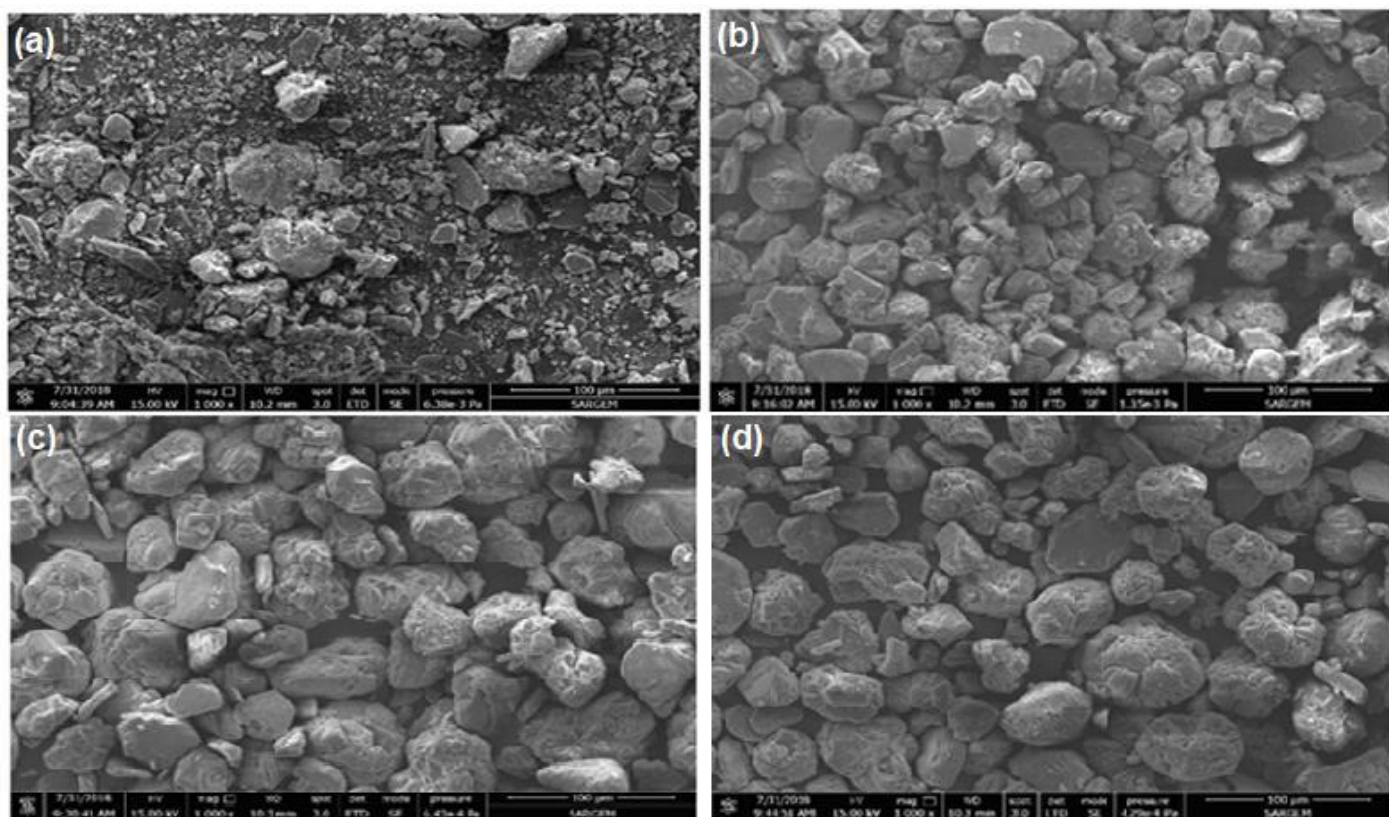


Fig. 11: FESEM micrograph of the AlN powder after ultrasonic agitation for: (a) 1h, (b) 2h, (c) 4h and (d) 6h.

In comparison with the previously explained AlN syntheses, our approach comes with the advantage of lower size than the classic CRN. The nanopowders in our results were less than what it had been reported for classic CRN (our average size was between 35 and 85nm comparing to 80 to 150nm average for classic CRN). The problems of unreacted alumina and nano crystallites in form of blacks, however, are still present and couldn't be eliminated. The obtention of AlN via DCRN is still being explored and developed to control the reactions inside the moving system. Perhaps, a use of gas processing, can help preventing the transformation to the stable α alumina phase, with the advantage of reducing the excessive energy, with the use of gas mixtures. This will eliminate the carbon excess, and the necessity of its burning.

4. Conclusion:

Aluminium Nitride nanopowders were successfully synthesized from $\text{Al}(\text{OH})_3$ via DCRN. Other synthesis methods were presented and discussed. Among all the processes, CRN is still the preferable method for the synthesis of AlN nanopowders due to its simplicity and the availability of cheap precursors. DCRN is an optimization of the classic root with the advantage of giving fine particle size. The resulted nanopowders comes in the form of blocks which needs to be separated. Nevertheless, these blocks still can be used in that form with the advantages of nanopowders in processing. Controlling the reaction is also a big challenge of this method. A good control of the transformation of aluminium oxide precursors to $\gamma\text{-Al}_2\text{O}_3$, and maintaining it from transforming to α phase will result a full conversion to AlN with no residual unreacted alumina. Long ultrasonic shaking time can help give the powder a sphere-like shape. However, it is not a good choice to separate the agglomerates.

5. References:

1. Chiang, Chunyen, Ph.D Thesis. Synthesis of ultrafine aluminum nitride powder using a new carbothermal reduction process. Rutgers The State University of NJ - New Brunswick. (1993)
2. T. Yamakawa, J. Tatami, T. Wakihara, K. Komeya, and T. Meguro. Synthesis of AlN Nano-powder from γ -Al₂O₃ by Reduction–Nitridation in a Mixture of NH₃–C₃H₈. J. Am. Ceram. Soc., 89 [1] 171–175 (2006)
3. Matthew Albert Duarte. Synthesis and Processing of Nanocrystalline Aluminum Nitride. Ph.D Thesis. California University Riverside. (2016)
4. Sen Wang, Wen-Chun Wang, De-Zheng Yang, Zhi-Jie Liu. Direct synthesis of AlN nano powder by dielectric barrier discharge plasma assisted high-energy ball milling. J Mater Sci: Mater Electron 27:8518–8523(2016)
5. Mingli Qin, Xueli Du, Zixi Li, Islam S. Humail, Xuanhui Qu. Synthesis of aluminum nitride powder by carbothermal reduction of a combustion synthesis precursor. Mat Resch Bulletin 43 2954–2960 (2008)
6. JiaCai Kuang, ChangRui Zhang, XinGui Zhou, QiCheng Liu, Chang Ye. Formation and characterization of cubic AlN crystalline in a carbothermal reduction reaction. Materials Letters 59 2006– 2010 (2005)
7. JiaCai Kuang, ChangRui Zhang, XinGui Zhou, SiQing Wang. Synthesis of high thermal conductivity nano-scale aluminum nitride by a new carbothermal reduction method from combustion precursor. J. of Crystal Growth 256 288–291 (2003)
8. Mahua Ghosh Chaudhuri. Feasibility Study of Synthesis of Nanostructured Aluminum Nitride Through Sol-Gel Route. Int. Journal of Engineering Research and Applications. Vol. 6, Issue 4 (2016)
9. Mikimasa Iwata, Kazuo Adachi, Shizue Furukawa, Tadashi Amakawa. Synthesis of purified AlN nano powder by transferred type arc plasma. J. Phys. D: Appl. Phys. 37 1041–1047 (2004)
10. Lei Jia, Katsuyoshi Kondoh, Hisashi Imai, Motohiro Onishi, Biao Chen, Shu-feng Li. Nano-scale AlN powders and AlN/Al composites by full and partial direct nitridation of aluminum in solid-state. J. of Alloys and Compounds 629 184–187(2015)
11. Takayuki Suehiro, Naoto Hirosaki. Synthesis of Aluminum Nitride Nano-powder by Gas-Reduction–Nitridation Method. J. Am. Ceram. Soc., 86 [6] 1046–48 (2003)
12. JiaCai Kuang, ChangRui Zhang, XinGui Zhou, SiQing Wang. Influence of processing parameters on synthesis of nano-sized AlN powders. J. of Crystal Growth 263 12–20 (2004)
13. Li Zhang, L. Zhang, Z. Lin, Y. Jiang, J. He, W. Cai, S. Li, Synthesis of β -SiAlON Nanopowder by Ammonolysis of Alumina–Silica Gel, J. Am. Ceram. Soc., 97 [1] 40–43 2014
14. Edwin Kroke, Lars Loeffler, Fred F. Lange, Ralf Riedel. Aluminum Nitride Prepared by Nitridation of Aluminum Oxide Precursors. California. J. Am. Ceram. Soc., 85 [12] 3117–19 (2002)
15. T. Suehiro, J. Tatami, T. Meguro, S. Matsuo, K. Komeya, Synthesis of spherical AlN particles by gas-reduction nitridation method, J. of the Eur. Cer. Society 22, 2002, 521–526
16. Nuray Canikoğlu, B. Özdemir, Y. Y. Özbek, Ali O. Kurt, Synthesis of TiN Powders Using Dynamic CRN Method, SAU JOURNAL OF SCIENCE, e-ISSN: 2147-835X 2017
17. Ali O. Kurt, Yusuf G.Vardar, DİNAMİK KARBOTERMAL YÖNTEM İLE α -Si₃N₄ SERAMİK TOZU ÜRETİMİ, Afyon Kocatepe University JOURNAL OF SCIENCE, 125-130 2003
18. Engin B. Türker, Ali O. Kurt, Dinamik Karbotermal İndirgeme–Nitrürleme Yöntemiyle TiN Seramik Tozu Üretimi, AKÜ FEMÜBİD 14, 2014, OZ5789 (565-569)

ADVANCED CERAMICS

FABRICATION AND CHARACTERIZATION OF $\text{Al}_2\text{O}_3\text{-Cr}_2\text{O}_3$ CERAMICS BY USING 5 VOL. % Cr_3C_2 AS PRECURSOR

Betül Kafkaslıoğlu Yıldız¹, Yahya Kemal Tür¹

¹ Gebze Technical University, Department of Materials Science and Engineering, Gebze/Kocaeli

ABSTRACT

The purpose of the study was enhancing the hardness of pure alumina by adding chromium oxide via the formation of a solid solution. In the present study, chromium carbide powder was used as a precursor for obtaining chromium oxide while preparing the powder mixtures. The prepared powders were subjected to different heat treatments at 500° C and 700° C in both air and H_2/Ar atmosphere. The powders were uniaxially pressed in disc form and then cold isostatic pressed. The specimens were pressureless sintered at 1550° C for 2 h in both air and H_2/Ar atmosphere once again. Phase analyses were performed by X-ray diffractometry and the density was determined by the Archimedes' water replacement method. The microstructure was studied by scanning electron microscopy. For hardness measurement, the Vickers indentation technique was used. After sintering at 1550° C, only alumina peaks could be identified because chromium oxide forms a solid solution with alumina. The densification was higher in H_2/Ar atmosphere compared to the air atmosphere. Vickers hardness values were measured as 21 GPa in spite of low relative densities.

Keywords: Alumina, Chromium Oxide, Sintering, Hardness

1. INTRODUCTION

Alumina (Al_2O_3) ceramics are among the most used advanced ceramics due to its attractive properties like high compressive strength, high corrosion and wear resistance [1]. However, the hardness of pure alumina ceramics is generally between 15-19 GPa and it is lower when compared to the carbide ceramics with high hardness values as 20-30 GPa [2]. This becomes crucial especially for the applications that require to be hard such as armor ceramics, cutting tools. It has been reported that chromium oxide (Cr_2O_3) produces a solid solution with Al_2O_3 over the full range of compositions and it improves the mechanical properties [3,4,5]. The increase in mechanical properties (hardness, tensile strength, and thermal shock resistance) was mainly attributed to the changes in the microstructure [5]. However, Cr_2O_3 is not stable due to the evaporation of Cr_2O_3 as CrO_3 especially in the air with high oxygen partial pressure. So, the densification of the ceramic body with Cr_2O_3 becomes critical.

There are several studies in the literature that chromium carbide (Cr_3C_2) has been successfully added Al_2O_3 to increase its mechanical properties especially fracture toughness [6]. However, as other carbides and nitrates, chromium carbides tend to oxidize at elevated temperatures [7]. It was established that chromium carbides begin to oxidize at 700° C [8]. Therefore, sintering of Al_2O_3 - Cr_3C_2 ceramics is usually carried out in an oxygen-free atmosphere like purified argon or vacuum [7]. In this study, the Cr_3C_2 powder was added to Al_2O_3 to obtain Cr_2O_3 after the heat treatments. 90% $\text{Ar}+10\% \text{H}_2$ and air atmosphere were chosen to evaluate the densification and the hardness of Al_2O_3 ceramic.

2. EXPERIMENTAL PROCEDURE

$\text{Al}_2\text{O}_3/\text{Cr}_3\text{C}_2$ ceramic powder mixture with 5 vol. % Cr_3C_2 was prepared by using an alfa alumina powder (Alfa Aesar, 99.95 %, 0.25-0.45 μm , Germany), Cr_3C_2 powder (Atlantic Equipment Engineers, 99.8%, 1-5 μm , USA), (Sigma Aldrich, % 99 purity), polyacrylic acid as a dispersant (Darvan 821A from MSE Tech Co. Ltd., Turkey) and polypropylene carbonate (PPC) (QPAC 40, Empower Materials, USA) as a binder. Al_2O_3 , 5 vol. % Cr_3C_2 and 0.5 wt.% (equivalent to total powder weight) polyacrylic acid were first mixed in distilled water and ball milled for 24 hours with alumina

balls. After ball milling, the powder mixture was dried and pulverized in an agate mortar. Then the powder mixture was exposed to different heat treatments. Table 1 shows the heat treatment procedure for the prepared powder mixture. ACC and cross express $\text{Al}_2\text{O}_3/\text{Cr}_3\text{C}_2$ and applied heat treatment for each powder group with same carbide volume ratio, respectively.

Table 1. The heat treatment procedures for the prepared $\text{Al}_2\text{O}_3/\text{Cr}_3\text{C}_2$ powder mixture with 5 vol. % Cr_3C_2

	500°C 2h air	700°C 4h air	700°C 4h H_2/Ar	1550°C 2h H_2/Ar	1550°C 2h air
ACC 1	X	X			X
ACC 2	X				X
ACC 3	X		X		X
ACC 4	X	X		X	
ACC 5	X		X	X	
ACC 6	X			X	

All the powder groups were heated at 500° C/2h in the air to remove the polyacrylic acid. Then, in either H_2/Ar or air atmosphere, the powder mixtures (ACC 1, ACC 3, ACC 4, ACC 5) were heated at 700° C for 4h. 3 wt. % PPC binder was added to the powder mixtures to increase the green strength. The stock solution of PPC was prepared by dissolving it in acetone before addition. Acetone could evaporate from the powder mixture before sieving for pressing. The powder mixtures were sieved down to 90 μm and uniaxially pressed under 40 MPa into a disc form by using a steel mold with 16 mm diameter. The uniaxially pressed specimens were cold isostatically pressed under 200 MPa. All the specimens were pressureless sintered at 1550° C/2h in H_2/Ar and air atmosphere separately. For comparison, the pure Al_2O_3 powder was prepared under the same conditions.

The phase composition was determined by X-ray diffraction (XRD) and the bulk densities of the sintered specimens were measured using Archimedes' method. Particle sizes were measured by a Malvern Hydaro 2000 particle size analyzer before and after the heat treatments. The microstructure of the specimens was characterized by using scanning electron microscopy (SEM) and the alumina grain size was measured by using SEM micrographs with the linear intercept method where more than 100 intercepts were counted. The Vickers hardness was measured by using an Instron® tester (Wolpert Testor 2100) under 5 kg load for 10 s. Thermal etching was carried out for only the specimens sintered in an air atmosphere at 1400° C for 90 min.

3. RESULTS AND DISCUSSION

Particle sizes of the starting powders and particle sizes of the prepared powders with the heat treatments were given in Table 2. After the ball milling process, the particle sizes of Al_2O_3 and Cr_3C_2 were reduced. The difference in particle sizes of 700° C can be attributed to the oxidation of Cr_3C_2 . For H_2/Ar atmosphere, the presence of both Cr_3C_2 and Cr_2O_3 particles can be considered. Figure 1 shows the XRD pattern of ACC 1 sintered specimen. Al_2O_3 was present as corundum and the XRD result did not detect the presence of Cr_2O_3 due to the same corundum crystal structure. The new compound was not formed by the addition of Cr_3C_2 after sintering. For all the prepared sintered specimens, XRD patterns showed the same corundum structure. So, only the ACC 1 pattern was given in the figure. Figure 2 shows the XRD patterns of all the specimens after sintering with a slow scan from 34° to 36°. Zhao et al. showed in their study that changes in the Cr_2O_3 content have a strong effect on (104) peak with high intensity [9]. Doping of the Cr^{+3} ions cause lattice strain in the c-axis direction on the hexagonal close-packed structure, so it would increase the lattice dimensions of Al_2O_3 . This will reflect to the XRD patterns by shifting towards low 2θ angles compared to the pure Al_2O_3 peak. The shifting of (104) peak shows the presence of a solid solution between Al_2O_3 and Cr_2O_3 for all the specimens with different heat treatments.

Table 2. Particle sizes of the starting and prepared powders

Particle Size (μm)	D 0.1	D 0.5	D 0.9
Pure Al_2O_3	0.168	0.306	1.711
Pure Cr_3C_2	0.993	3.935	8.247
Al_2O_3 - Cr_3C_2 powder mixture after ball milling	0.156	0.230	0.443
Al_2O_3 - Cr_3C_2 (500 air)	0.167	0.263	0.515
Al_2O_3 - Cr_3C_2 (700 H_2/Ar)	0.169	0.342	5.312
Al_2O_3 - Cr_3C_2 (700 air)	0.164	0.280	2.232

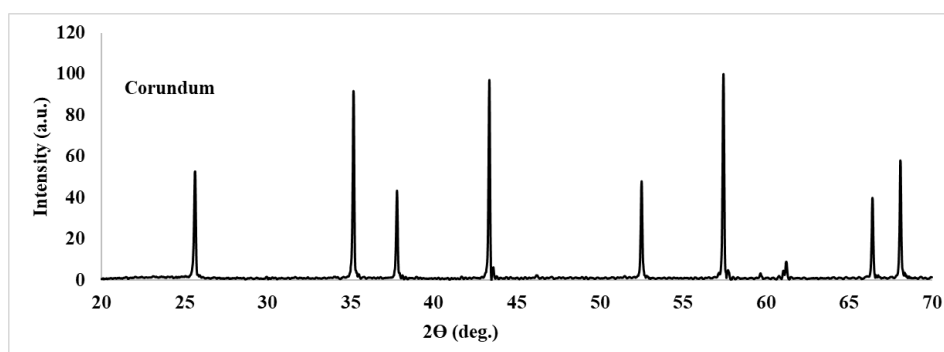


Figure 1. XRD pattern of ACC 1 sintered specimen in air

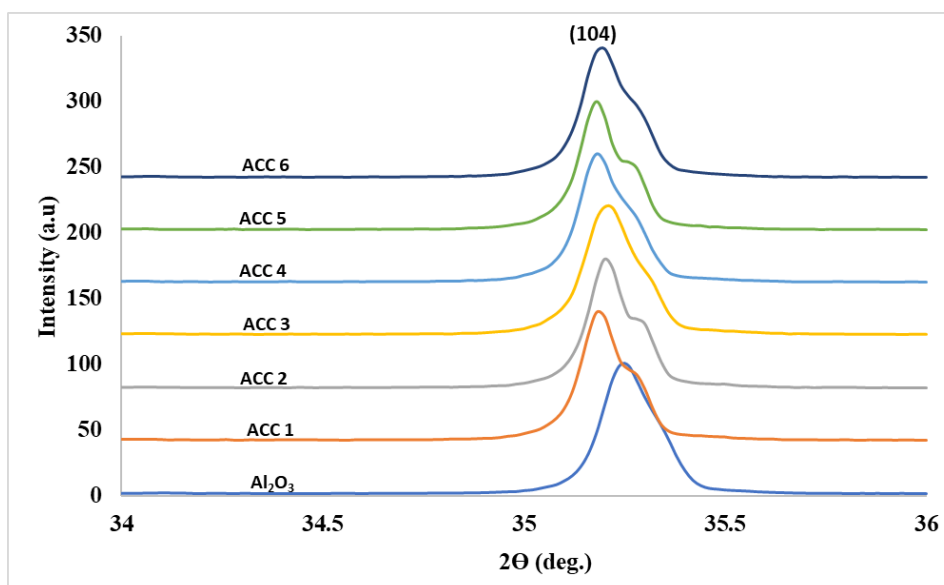


Figure 2. The XRD patterns of all the specimens after sintering

Figure 3 shows the green bodies that were pressed with the powders exposed to the different heat treatments and discs after sintering. After the heat treatment at 500° C/2h in the air and at 700° C/4h in H_2/Ar , the color of the powder was dark gray but after the heat treatment at 700° C/4h in the air, the color of the powder was green. The color change indicates that after 700° C/4h in the air, oxidation of Cr_3C_2 is apparent and in the H_2/Ar atmosphere, there is still a mixture of $\text{Cr}_3\text{C}_2 + \text{Cr}_2\text{O}_3$. It can be

verified by the green color of Cr_2O_3 and black color of Cr_3C_2 . After sintering in both air and H_2/Ar atmosphere, the color of the specimens was burnt rose.

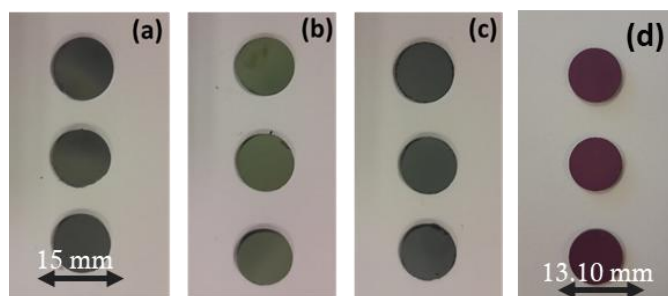


Figure 3. The specimens after the pressing a) 500°C in the air, b) 500°C in air- 700°C in the air, c) 500°C in air- 700°C in H_2/Ar , and d) after sintering

Figure 4 shows SEM-backscattered electron mode micrographs of the specimens (ACC 1, ACC 2, ACC 3) sintered at $1550^\circ\text{C}/2\text{h}$ in air and thermally etched at $1400^\circ\text{C}/90\text{ min}$ in air. For all ceramics, most of the Al_2O_3 grains have an angular shape and abnormal grain growth is no apparent. The average Al_2O_3 grain sizes of ACC 1, ACC 2, ACC 3 are $1.94\ \mu\text{m}$, $1.95\ \mu\text{m}$, $2.12\ \mu\text{m}$, respectively. It seems that different heat treatments did not affect the particle sizes. As seen in Table 3, the relative densities that estimated by using theoretical density though evaporating of Cr_2O_3 were nearly same and used for comparison.

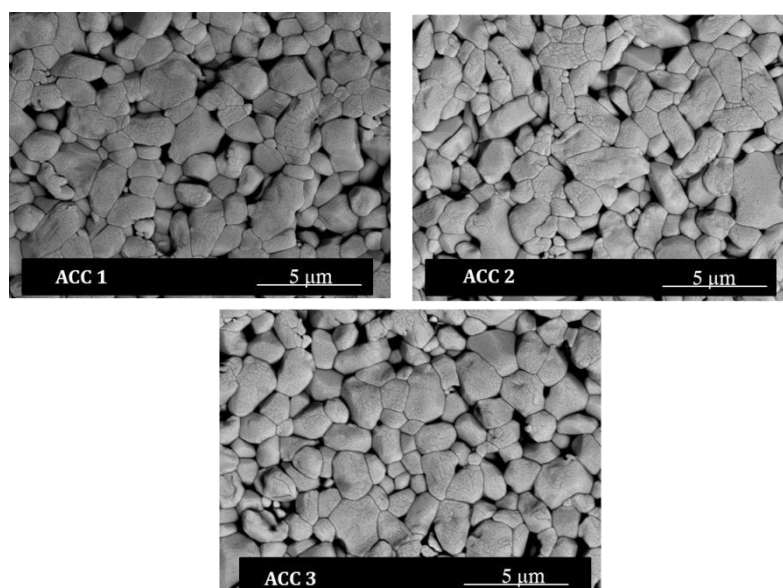


Figure 4. SEM-backscattered electron mode micrographs of ACC 1, ACC 2, ACC 3 specimens

Vickers hardness measurements show that similar relative densities give similar hardness values for these ceramics. The hardness value of the ceramics sintered in air $\sim 16\text{ GPa}$ for 90 % relative density. The relative density of pure Al_2O_3 that was prepared under the same conditions (sintered in air) was (3.95 g/cm^3) 99 %, and the hardness value was $\sim 22\text{ GPa}$. The average grain size of pure Al_2O_3 was $2.38\ \mu\text{m}$. Addition of Cr_2O_3 to pure Al_2O_3 hindered the densification and reduced the hardness. However, for the specimens sintered in the H_2/Ar atmosphere, the relative density values increased, and the hardness values reached to 21 GPa. Compared to the density and hardness values with pure Al_2O_3 , these values are nearly same. So, in the H_2/Ar atmosphere, denser and harder Al_2O_3 .

Cr_2O_3 ceramics can be produced in contrast with the sintering in air. Additionally, Cr_3C_2 can be used as a precursor to prepare Al_2O_3 - Cr_2O_3 ceramics.

Table 3. Properties of the prepared specimens after sintering

	Al_2O_3	ACC 1	ACC 2	ACC 3	ACC 4	ACC 5	ACC 6
Theoretical Density (g/cm^3)	3.98	4.042	4.042	4.042	4.042	4.042	4.042
Bulk density (g/cm^3)	3.95	3.66	3.67	3.66	3.77	3.78	3.80
Relative density (%)	99.2	90.6	90.8	90.6	93.3	93.5	94.0
Al_2O_3 grain size (μm)	2.38	1.94	1.95	2.12	-	-	-
Vickers Hardness (GPa)	23.17 ± 1.36	16 ± 1.06	15.73 ± 1.68	16.54 ± 0.78	21.91 ± 1.60	21.15 ± 0.94	21.30 ± 0.61

4. CONCLUSIONS

In the present study, 5 vol. % Cr_3C_2 was added to the pure Al_2O_3 as Cr_2O_3 precursor to enhance the hardness. The powders were prepared with different heat treatments at 500°C and 700°C in both air and H_2/Ar atmosphere. Sintering was also carried out in both air and H_2/Ar atmosphere. In air atmosphere at 700°C , Cr_3C_2 oxidized and the color of the powder was belonging to self-color of Cr_2O_3 , green. However, in the H_2/Ar atmosphere, there was still a mixture of $\text{Cr}_3\text{C}_2 + \text{Cr}_2\text{O}_3$ with its gray color. After sintering, all the specimens were in same color. Similar relative densities were obtained for the specimens sintered in air, so their hardness values were almost same. Sintering in the H_2/Ar atmosphere reduced the evaporation of Cr_2O_3 as CrO_3 and increased the relative density of ceramic up to 94 % and the hardness value up to nearly 22 GPa. So, even in low density, hardness values as high as pure Al_2O_3 could be obtained with the addition of Cr_2O_3 by sintering in the H_2/Ar atmosphere.

ACKNOWLEDGEMENTS

The support of G.T.U Scientific Research Council 2017-A105-48 project is greatly appreciated.

REFERENCES

1. Zhang X.F., Li Y.C., On the comparison of the ballistic performance of 10 % zirconia toughened alumina and 95 % alumina ceramic target, Mater. Des., 2010, 1945.
2. Karandikar P.G., Evans G., Wong S., Aghajanian M.K., Sennett M., A review of ceramics for armor applications, Ceram. Eng. Sci. Proc., 2009, 163.
3. Arahori T., Dow Whitney E., Microstructure and mechanical properties of composites Al_2O_3 - Cr_2O_3 - ZrO_2 , J. Mater. Sci., 1988, 1605-1609.
4. Zhang H., Xu Y., Jin H., Qiao G., Effects of Cr_2O_3 addition on mechanical and electrical properties of alumina ceramic, Adv. Mater. Res. Vols., 2014, 513-516.

5. Riu D.H., Kong Y.M., Kim H.E., Effect of Cr_2O_3 addition on microstructural evolution and mechanical properties of Al_2O_3 , J. Eur. Ceram. Soc., 2000, 1475-1481.
6. Huang J.L., Twu K.C., Lii D.F., Li A.K., Investigation of $\text{Al}_2\text{O}_3/\text{Cr}_3\text{C}_2$ composites prepared by pressureless sintering (Part 2), Mater. Chem. Phys., 1997, 211-215
7. Fu C.T., Li A.K., Lin J.T., Wub J.M., The mechanical properties of $\text{Al}_2\text{O}_3\text{-Cr}_3\text{C}_2$ composites after high temperature annealing in air, Mater. Chem. Phys., 1994, 362-369.
8. Voitovich R.F, Pugach É.A., High-temperature oxidation characteristics of the carbides of the Group VI transition metals, Powder Metall Met Ceram., 1973, 314–318.
9. Zhao P., Zhao H., Yu J., Zhang H., Gao H., Chen Q, Crystal structure and properties of $\text{Al}_2\text{O}_3\text{-Cr}_2\text{O}_3$ solid solutions with different Cr_2O_3 contents, Ceram. Int., 2018, 1356–1361.

CEMENT, CONCRETE AND GEOPOLYMERS

AN EXPERIMENTAL STUDY ON LIGHTWEIGHT GEOPOLYMER SYNTHESIS

Rana Selin İp¹, Evren Arıöz¹

¹ Eskişehir Technical University, İki Eylül Campus, Faculty of Engineering, Department of Chemical Engineering, 26555/Eskişehir/Turkey

ABSTRACT

Concrete is most widely used construction material. Lightweight concrete is a type of concrete which has low thermal conductivity, high fire resistance and sound insulation. It has a lower unit weight compared to normal weight concrete; therefore, it is thought that it will reduce the dead load and provide flexibility in buildings resulting in lower costs. Geopolymers are new construction materials which can be alternative to concrete. They are environmentally friendly materials and can be produced by utilizing waste or by-products such as fly ash and blast furnace slag. Fly ash is generated in thermal power plants in millions tones and consumed in low quantities, hence it causes landfill problems. In this experimental study, lightweight geopolymer was produced by utilizing fly ash as raw material. The unit weight and the flexural strength of the samples were determined. The results revealed that the lightweight geopolymers can be synthesized by fly ash.

Keywords: Fly ash, geopolymer, air-entraining admixture, lightweight concrete

1. INTRODUCTION

In concrete structures, higher specific gravity and the heavier materials used causes the increase in dead load and the forces on soil. Therefore the building can be more affected by the earthquakes [1]. Lightweight concrete has some advantages on structural load-bearing and thermal insulation. Lightweight concrete can be produced by using lightweight aggregates or by creating air voids [2]. The density of concrete ranges between 2200-2600 kg/m³ where the density of lightweight varies in the range of 300-1800 kg/m³ [2,3].

The cost of lightweight concrete can be reduced by using fly ash [3]. Geopolymers are environmentally sustainable construction materials. They have very low emissions contributing greenhouse gas and can be produced by waste materials such as fly ash and blast furnace slag [4]. Geopolymerization occurs by dissolution of silica and alumina species in the raw material and polycondensation reactions between reactive species and an alkaline solution [5].

Million tons of fly ash is generated in power plants. Most of the fly ash is disposed of as landfill, but it will soon be cost too high in the future [6]. In this experimental study, fly ash was used as raw material for geopolymerization reactions to offer solutions for landfill problems and to convert waste material to a valuable material.

2. MATERIALS AND METHOD

In this experimental study, fly ash, sodium hydroxide, sodium silicate and air-entraining admixture were used to produce lightweight geopolymer. Sodium hydroxide solution (6M) was prepared 24 hours before the experiment and mixed before the preparation of alkali activator solution. Sodium silicate and sodium hydroxide were mixed with mechanical stirrer for 15 minutes to get alkali activator solution. Alkali activator was added to the fly ash and mixed until a homogeneous mixture was obtained. Air-entraining admixture was added to geopolymer paste at varying ratios as 0.5, 1 and 2% (w/w). The geopolymer paste was poured into 40 mm x 40mm x 160 mm steel molds. The pastes were cured at 60°C and 100°C for 24 hours. After curing, the geopolymer samples were demolded and aged for 3 and 7 days in the laboratory. The flexural strength, porosity and the density of all the samples were determined. The porosity and density of the samples were determined according to Equation 1 and 2 [9] given below:

$$\rho_d = \frac{M_{dry}}{V} \quad (\text{Eq. 1})$$

$$\varepsilon = \frac{M_{sat} - M_{dry}}{V} \quad (\text{Eq. 2})$$

3. RESULTS

The flexural strengths of geopolymer samples cured at the temperatures of 60°C and 100°C for 24 hours are given in Figure 3.1.

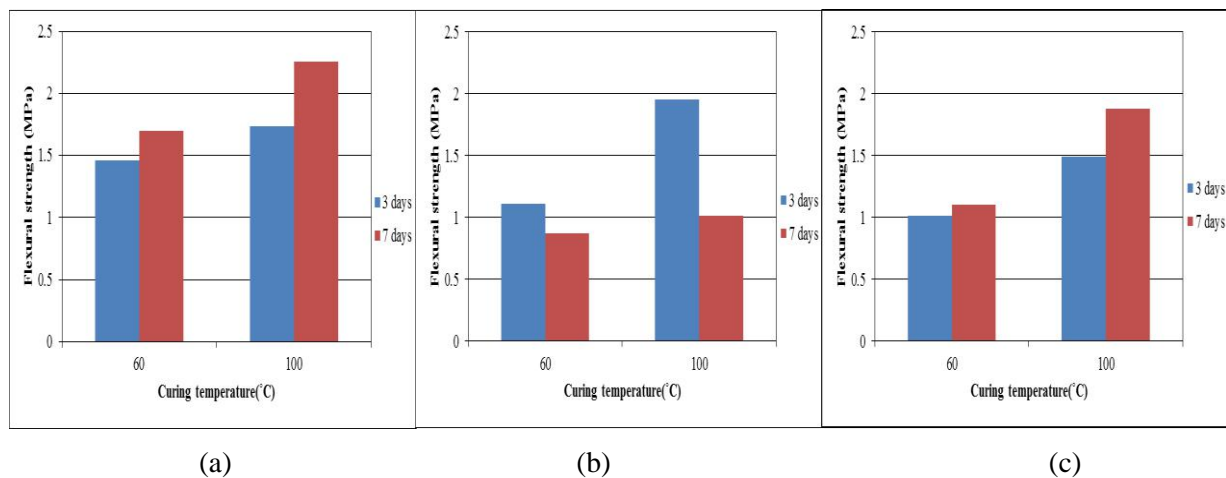


Figure 3.1: The flexural strength of geopolymer samples with varying admixture ratios a) 0.5% b) 1% c) 2%

As it can be seen from the figure, the flexural strength of the geopolymer samples increased with increasing temperature. For the 3 days aged samples, the highest flexural strength was found as 1.95 MPa for sample containing 1% air-entraining admixture. For the samples aged for 7 days the highest flexural strength was determined as 2.26 MPa for the sample containing 0.5% admixture. The flexural strength values increased with increase in age of the samples prepared with %0.5 and %2 admixture ratio. The strength of the geopolymer samples prepared with the admixture ratio of 1% decreased with increase in aging. The flexural strengths of geopolymer samples generally decreased with increasing admixture ratio.

The porosity of geopolymer samples cured at the 60°C and 100°C for 24 hours are given in Figure 3.2.

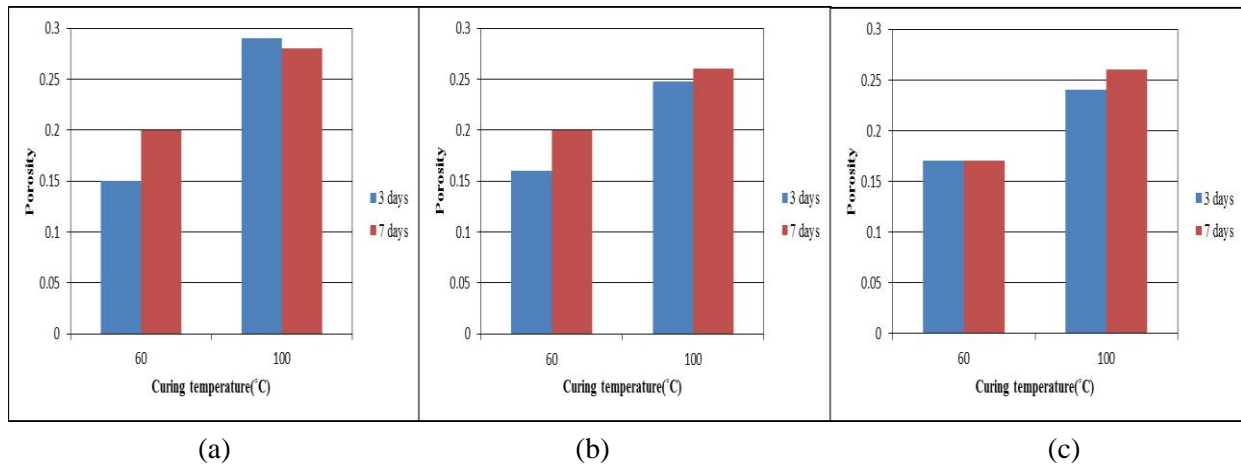


Figure 3.2: The porosity of geopolymer samples with varying admixture ratios a) 0.5% b) 1% c) 2%

Test results revealed that the porosity of geopolymer samples increased with increasing temperature for all the samples. The maximum porosity was determined as 0.29 and 0.28 aged for 3 and 7 days respectively for the samples containing 0.5% air-entraining admixture and cured at 100°C. The porosity of all geopolymer samples also increased with aging. The porosity of geopolymer samples generally increased or did not change with increasing admixture ratio.

The density of geopolymer samples are given in Figure 3.3.

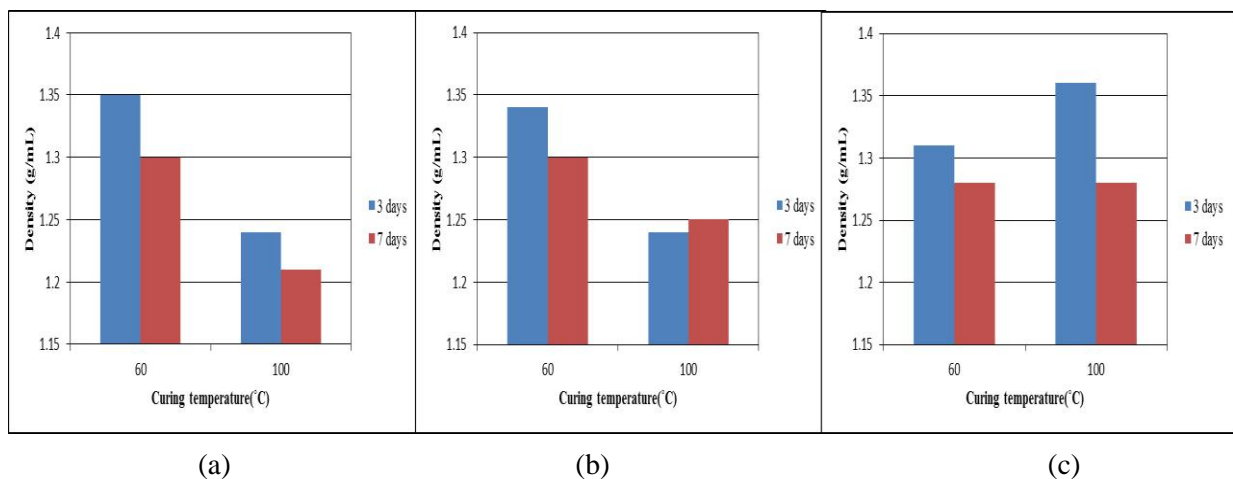


Figure 3.3: The density of geopolymer samples with varying admixture ratios a) 0.5% b) 1% c) 2%.

The density of geopolymer samples generally decreased with increasing temperature from 60°C to 100°C. The density decreased as the aging increased but only for the sample containing 1% admixture and cured at 100°C decrement was observed.

4. CONCLUSION

The production of lightweight geopolymer production was the aim of this experimental study. The geopolymer samples were prepared with air-entraining admixture at varying ratios and at varying curing temperatures. The flexural strength of the samples generally decreased with increase in admixture ratio but increased with curing temperature. The voids in the samples increased with increasing air entraining admixture ratio, so the flexural strength values decreased. As the curing temperature increased, the strength of the geopolymeric gel binder increased and positively affected

the flexural strength. The flexural strength values decreased by aging for the samples prepared with the admixture ratio of 1%. This can be originated from the fly ash used in the experiments because the composition of fly ash can be different because of the variable composition of each loading in the thermal power plant.

The porosity of the samples generally increased or did not change with admixture ratio but decreased for certain samples. It was clear that the air bubbles were loosed when the geopolymer pastes were poured into the steel molds. The density of the lightweight geopolymer samples were compatible with the porosity values. The density of the samples varied between 1.21 g/mL and 1.36 g/mL. The results revealed that all the samples classified as lightweight.

References:

1. Ariöz, Ö., Karasu B., Tuncan A., Tuncan M., Arslan G., Kaya G., Kılınç K., Kıvrak S., Kale B., Production of expanded clay aggregates and light weight insulation wall materials. VII. Ceramic Congress With International Participation, 2008, Sakarya (Turkey), 699-715.
2. Arellano Aguilar R., Burciaga Díaz O., Escalante García J.I., Lightweight concretes of activated metakaolin-fly ash binders, with blast furnace slag aggregates. *Construction and Building Materials*, 2010, 24, 1166–1175.
3. Abdullah M. M. .B., Hussin K., Bnhussain M., Ismail K. N., Yahya Z., Razak R. A., Fly Ash-based Geopolymer Lightweight Concrete Using Foaming Agent. *International Journal of Molecular Sciences*, 2012, 13, 7186-7198.
4. Duxson P., Provis J.L., Lukey G.C., van Deventer J.S.J., The role of inorganic polymer technology in the development of 'green concrete'. *Cement and Concrete Research*, 2007, 37, 1590–1597.
5. Karthik A., Sudalaimani K., Kumar C.T.V., Investigation on mechanical properties of fly ash-ground granulated blast furnace slag based self curing bio-geopolymer concrete. *Construction and Building Materials*, 2017, 149, 338–349.
6. Ahmaruzzaman M., A review on the utilization of fly ash. *Progress in Energy and Combustion Science*, 2010, 36, 327–363.

CEMENT, CONCRETE AND JEOPOLYMERS**ASSESSMENT OF MECHANICAL PROPERTIES IN PORTLAND CEMENT BY OPTICAL MICROSCOPY AND NUMERICAL COLOR ANALYSIS**

Taner Kavas^{1*}, Recep Kurtuluş¹, Melis Er¹

¹Afyon Kocatepe University, ANS Campus Gazlıgöl Yolu, 03200/Afyonkarahisar/Turkey

Cement industry has an production output of clinker which directly affects the quality of cement. Different raw materials preferred and furnace conditions followed have an essential impact on clinker and cement characteristics. Therefore, determination of phase occurrences, sintering behavior and porosity aspects are sensitively followed so as to achieve high quality clinker as well as cement. However, controlling and confirmation of final product parameters take very long times. In this study, it is aimed to assess the mechanical properties of ordinary Portland cement (OPC) by performing optical microscopy measurement and numerical color analysis. For that purpose, two types of cement samples (CEM I 42,5R and CEM I 52,5N) were taken from a company in Afyonkarahisar/Turkey. Uniaxially pressing was performed to moisturised cement samples in order to have flat surface, and then pressed samples were stucked to lamelleas and made thin sections to get visible and smooth surface for optical microscopy measurement. The images taken from optical microscopy were analyzed via MATLAB software to obtain color distributions in terms of RGB (red-green-blue) values. It was observed that consistent results regarding cement type was determined and these consequences were also verified with production datas, particularly mechanical properties. It was found that as blue color value increase the mechanical properties of cement is improved.

Key words: cement, clinker, color, numerical analysis

1. Introduction

Cement production, as one of the most energy consuming industry, takes great importance for building, construction and transportation [1]. Among the cement classes produced including aluminate cement, white cement, etc., ordinary Portland cement is commonly preferred class reaching up to 90% among others around the world. Portland cement is mainly composed of clinker, gypsum and/or fly ashes which depends on the target application area in terms of constituents and amounts [2]. The clinker is produced by mixing clay and lime stone raw materials in the appropriate amounts and fired up to nearly 1500 °C so as to achieve compositionally stable clinker phases and morphologically homogeneous powder at the end of the process [3]. Since the clinker has a significant role on the characteristics of cement as well as concrete it is so crucial to control the properties of clinker during process conditions. Therefore, phase occurrences, sintering behavior and porosity aspects are sensitively followed in order to obtain high quality clinker as well as cement [4].

In the clinker, it has been identified more than thirty phases occurred, however just four phases, that are listed in Table.1 are carefully focused on [3]. All these phases have different crystal structures, meaning that different properties can be encountered. That is to say, alite ensures short term resistance whereas belite provides long term resistance to the end product. On the other hand, aluminate and ferrite have a reasonable impacts on resistance of cement [5].

Table 1. Main phases, chemical formulas and abbreviation of clinker phases.

Name	Chemical Formula	Abbreviation
Tricalcium silicate (alite)	$3\text{CaO} \cdot \text{SiO}_2$	C_3S
Dicalcium silicate (belite)	$2\text{CaO} \cdot \text{SiO}_2$	C_2S
Tricalcium aluminate (aluminate)	$3\text{CaO} \cdot \text{Al}_2\text{O}_3$	C_3A
Tetracalcium ferroaluminate (ferrite)	$4\text{CaO} \cdot \text{Al}_2\text{O}_3 \cdot \text{Fe}_2\text{O}_3$	C_4AF

From the viewpoint of production plants, controlling and confirmation of all these different process parameters during production stage take very long times. To support with an example, preparation of samples for variety of measurements in accordance with TS EN 197-1, TS En 196 series and so on are so cumbersome that both number of samples prepared periodically and person in charge in every working shifts are extra cost for production plants. To overcome timing trouble as well as cost aspects, faster and reliable methodologies would be preferred and numerical color analysis is one of those, especially digital image processing has increasingly been performed in many areas including aerospace, defence, medical diagnosis, etc [6]. Not only fast response can be taken but also non-destructive experiments can be carried out along with process conditions in production plants.

In the field of image based analysis, color concentrations and their distributions in the intended region of samples are of interest. Color is defined as an interaction between matter and light. The physics of light, the chemistry of matter and object geometry as well as visual perception of human are the primary parameters of color occurred. For determination of color assortment, several models

including RGB, HSV, L*a*b' can be utilized [7]. In this study, Matlab software is preferred for numerical color analysis and RGB values are found out thanks to the digital image processing calculations. It is observed that consistent results regarding cement classes can be assigned and these consequences can also be verified with production experiment results, particularly mechanical properties.

2. Experimental Data

Two different classes of ordinary Portland cement were obtained from Afyon Cimento Inc. located near to Afyonkarahisar province. The cement classes and related chemical compositions are listed in Table 2. The obtained CEM I 42,5R and CEM I 52,5N types of OPCs were firstly uniaxially pressed using vacuum pressing machine by applying 2000 kg/cm² pressure, and thus two samples for each classes, totally four circular shaped samples with flat surfaces, were achieved. The pressed samples were then stuck onto lamealleas and grinding operation with sandpapers were carried out until light transmission from samples was apparent. In addition to sandpaper grinding, silicon carbide abrasive powders was used so as to obtain smoother surface, as well. The prepared samples can be seen in Fig.1. Sample numbers of 1 and 2 relates to the class of CEM I 42,5R while 3 and 4 numbers refers to CEM I 52,5N class.

Table 2. Chemical compositions of OPC samples.

Constituent	CEM I 42,5R	CEM I 52,5N
LOI	3,78	2,15
SiO ₂	18,83	19,85
Al ₂ O ₃	5,14	5,07
Fe ₂ O ₃	2,65	3,02
CaO	63,01	64,65
MgO	2,05	1,79
SO ₃	2,91	2,95
Na ₂ O	0,34	0,12
K ₂ O	0,88	0,38
Cl ⁻	0,0099	0,0071
Insoluble HCl	0,38	0,19

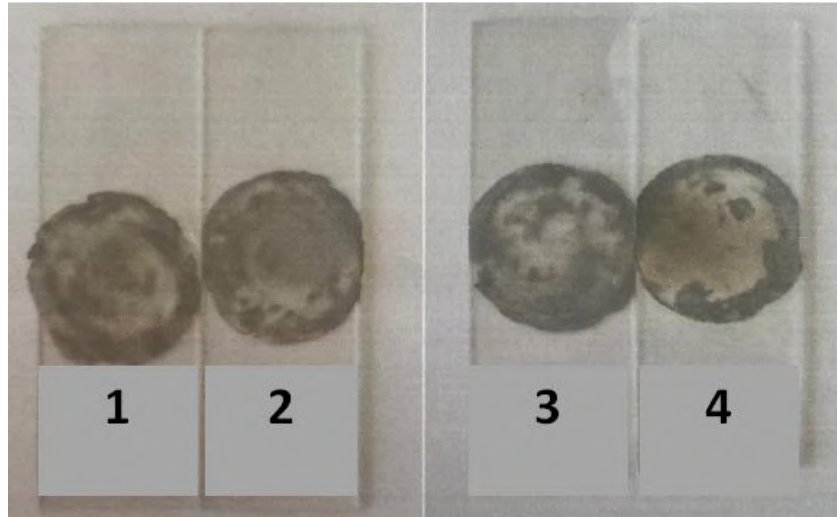


Fig.1 Grinded cement samples (1, 2 : CEMI 42,5R and 3,4 : CEMI 52,5N).

As flat and smooth sample surfaces were obvious optical microscopy measurement with Olympus BX51M was performed in order to take surface images. The optical microscopy images are revealed in Fig.2. The magnification of 50x was applied for each samples independently. The images taken from optical microscopy were analyzed via Matlab software to obtain color calculations in terms of RGB (red-green-blue) values. The results of image processing and mechanical properties of OPC classes are presented in the upcoming section.

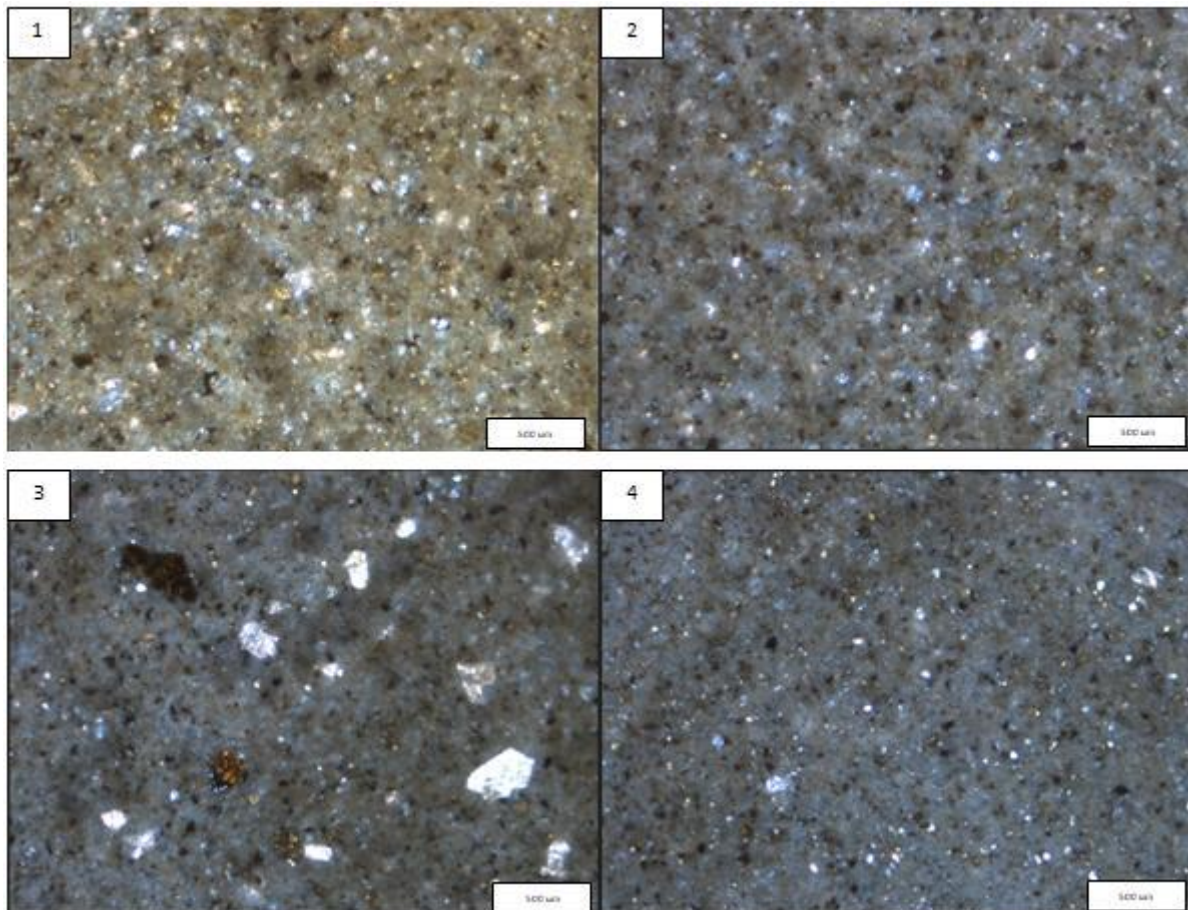


Fig. 2 Optical microscopy images of cement samples (1, 2 : CEMI 42,5R and 3,4 : CEMI 52,5N).

3. Results and Discussion

Two different classes of cement samples were analyzed via Matlab software in order to calculate RGB values after sample preparation and taking optical microscopy images and the results are given in Table.3. As can be seen from B-values in Table.3, it begins to increase as cement class changes, particularly it is important to focus on 1 and 4. Sample number of 1 describes CEM I 42,5R cement classes whereas number 2 states CEM I 52,5N.

Table 3. RGB values related to the cement samples.

Sample No.	R	G	B
1	24,9	4,7	5,4
2	13,0	8,3	46,3
3	8,5	9,4	51,7
4	2,8	6,4	78,0

Further, illustration of the values given in Table.2 can be seen in Fig.3. Thanks to the RGB color space illustration, it can be obviously observed that the coordinates of color shifts to dark blue

region, especially it is very sharp between 1 and 4. It is essential to emphasize that there are small differences in blue values between 1 and 2, and 3 and 4 although they represent the same cement class. This small changes can be assumed as tolerance values, in any way.

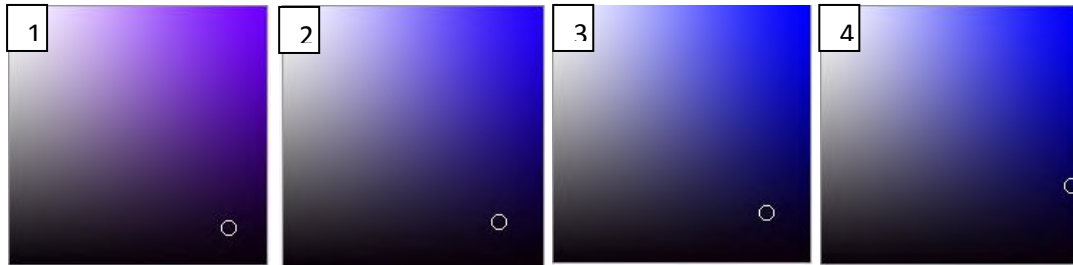


Fig. 3 Illustration of RGB values in RGB color space [8].

When it comes to analyze the production experiment results of cement classes, it is clearly revealed in Table 4. Compressive strength values upon 2, 7 and 28 days waiting periods for cement classes can be seen. As the waiting period increases, compressive strength values increase for both classes of cement materials. However, CEM I 52,5N class of cement has higher compressive strength values compared to CEM I 42,5R in different days.

Table 4 Production datas for compressive strength of cement classes.

Cement Type	Compressive Strength (2 days)	Compressive Strength (7 days)	Compressive Strength (28 days)
	N/mm ²	N/mm ²	N/mm ²
CEM I 42,5R	31,6	44,6	55,4
CEM I 52,5N	35,6	51,0	65,3

4. Conclusions

In this study, we propose a faster and reliable methodology by using optical microscopy imaging followed by numerical color analysis for assessment of mechanical properties in ordinary Portland cement rather than performing time consuming measurements. It was observed that consistent results regarding cement class can be assessed and these consequences were also verified with production datas, particularly mechanical properties. It was found that as blue color value increase in RGB calculations the compressive strength of cement will increase. In this sense, this study is just for the beginnng to assess the mechanical properties without experimental efforts and these assessments can be improved by increasing the number of samples analyzed. Besides that, a database

can be created by accumulating the assessment results which can later on allows to create a software capable of soft computation.

5. Acknowledgments

The authors would like to kindly thank to Mr. Naim Karasekreter for numerical color analysis.

6. References

- [1] Zhang H., Building materials in civil engineering, Ch. 4 Cement, 2011, 46-423
- [2] Aitcin P.-C., Science and technology of concrete admixtures, Ch. 3 Portland cement, 2016, 27-51
- [3] Benmohamed M., Alouani R., Jmayai A., Amara A.B.H., Rhaïem H.B., Morphological analysis of white cement clinker minerals: Discussion on the crystallization-related defects. Int.'l Journal of Analytical Chemistry, 2016, Vol. 2016.
- [4] Felekoglu B., Gullu D., Klinker incelemelerinde optik mikroskop ve görüntü işleme tekniklerinin kullanılması. IMO Teknik Dergisi, 2006, 3761-3770.
- [5] Çimento kalite kontrol parametreleri ve beton üzerindeki etkileri. Çimsa Çimento Araştırma ve Uygulama Merkezi, 2017.
- [6] Comak B., Beycioğlu A., Basyigit C., Kılınçarslan S., Beton teknolojisinde görüntü işleme tekniklerinin kullanımı. 6th Int'l Advanced Technologies Symposium, 2011, 220-227.
- [7] Mujawar S. M., A study on testing cement concrete quality for curing process by image processing techniques. Int'l J. of Latest Trends in Engineering and Technology, Special Issue IDEAS, 2013.
- [8] <https://www.colorsfire.com/rgb-color-wheel/>

CEMENT, CONCRETE AND JEOPOLYMERS**MECHANICAL AND PHYSICAL PROPERTIES OF CARBON BLACK BLENDED CONCRETE**Tayfun UYGUNOĞLU¹, Emriye ÇINAR², Barış ŞİMŞEK³, İlker Bekir TOPÇU⁴^{1,2}Afyon Kocatepe University, Engineering Faculty, Civil Engineering Department, 03200, Afyonkarahisar, Turkey³Çankırı University, Engineering Faculty, Chemical Engineering Department, Çankırı, Turkey⁴Eskişehir Osmangazi University, Engineering Faculty, Civil Engineering Department, 26480 Eskişehir, Turkey**Abstract**

Most of the materials that are considered as waste in the world are made up of recyclable materials. The recycling of these materials, the protection of the balance of nature and the environment, the minimization of damage to nature, and the economy of the country are very important. Carbon black is a material obtained from waste car tires with recycling material. As a result of the recovery process, 25-30% of the tire amount is recovered as carbon black. Carbon black is now used as a basic raw material or additive in many industries. Carbon black, with 95% carbon element content, contains small amounts of oxygen, hydrogen and nitrogen. The high electrical conductivity of the material due to the high amount of carbon is a high material. In this study, the effect of carbon black concrete, which is a waste product, on the mechanical, physical and electrical conductivity properties of concrete was investigated by adding different ratios. With increasing carbon black ratio, water absorption, unit volume weight, strength, electrical resistivity decreased and porosity ratio increased.

Keywords: Concrete, Carbon Black, Waste Product, Electrical resistivity

1. Introduction

Concrete is basically made of aggregates glued by a cementitious materials paste, which is made of cementitious materials and water. Each one of these concrete primary constituents, to a different extent, has an environmental impact and gives rise to different sustainability issues [1,2]. The current concrete construction practice is thought unsustainable because, not only it is consuming enormous quantities of stone, sand, and drinking water, but also two billion tons a year of portland cement, which is not an environmentfriendly material from the standpoint of energy consumption and release of green-house gases (GHG) leading to global warming[3]. Furthermore, the resource productivity of portland-cement concrete products is much lower than expected because they crack readily and deteriorate fast. Since global warming has emerged as the most serious environmental issue of our time and since sustainability is becoming an important issue of economic and political debates, the next developments to watch in the concrete industry will not be the new types of concrete, manufactured with expensive materials and special methods, but low cost and highly durable concrete mixtures containing largest possible amounts of industrial and urban byproducts that are suitable for partial replacement of portland cement, virgin aggregate, and drinking water [4,5]. According to this new vision, notwithstanding the energy consumption of cement production and the related carbon dioxide emissions, concrete can “adsorb” these negative effects and become an environmentally sustainable material. This outstanding effect is mainly attributable to the opportunity of easily incorporating mineral additions in concrete. Such mineral additions are quite different in nature, composition, and origin. Thanks to concrete technology developments, particularly connected to advances in concrete admixtures, mineral additions are used quite frequently in concrete today. In fact, many by-products and solid recyclable materials can be used in concrete mixtures as aggregates or cement replacement, depending on their chemical and physical characterization [6]. Carbon black is a

material obtained from waste car tires with recycling material. Carbon Black is used in a diverse group of materials in order to enhance their physical, electrical and optical properties. Its largest volume use is as a reinforcement and performance additive in rubber products. In rubber compounding, natural and synthetic elastomers are blended with Carbon Black, elemental sulfur, processing oils and various organic processing chemicals, and then heated to produce a wide range of vulcanized rubber products. In these applications, Carbon Black provides reinforcement and improves resilience, tear-strength, conductivity and other physical properties [7]. Carbon Black is the most widely used and cost-effective rubber reinforcing agent (typically called Rubber Carbon Black) in tire components (such as treads, sidewalls and inner liners), in mechanical rubber goods, including industrial rubber goods, membrane roofing, automotive rubber parts (such as sealing systems, hoses and anti-vibration parts) and in general rubber goods (such as hoses, belts, gaskets and seals) [8]. Besides rubber reinforcement, Carbon Black is used as black pigment and as an additive to enhance material performance, including conductivity, viscosity, static charge control and UV protection. This type of Carbon Black (typically called Specialty Carbon Black) is used in a variety of applications in the coatings, polymers and printing industries, as well as in various other special applications [9]. In this study, the effect of carbon black (CB) concrete, which is a waste product, on the mechanical, physical and electrical conductivity properties of concrete was investigated by adding different ratios (0%, 1%, 2% and 3%). With increasing carbon black ratio, unit volume weight, strength, electrical resistivity decreased, porosity ratio and water absorption increased.

2. Experimental works

In the experimental study, crushed sand and aggregate have been used. Specific gravity of crushed sand and aggregate are 2.67 and 2.70, the maximum grain sizes are 4 mm and 11.2 mm. In the experiments, CEM I 42.5 R cement which is suitable to TS EN 197-I [10] standards have been used.

2.1. Materials

Cement: CEM I 42.5 N cement which is suitable to TS EN 197-I standards have been used as binder. Chemical components of cement are given in Table 1.

Table 1. Component of cement

Oxide	CaO	SiO ₂	CaO/ SiO ₂	Al ₂ O ₃	Fe ₂ O ₃	MgO	Na ₂ O	K ₂ O	SO ₃	K.K.
Component, %	63,6	16,6	3,83	4,72	3,27	1,91	0,34	1,06	4,72	2,69

Aggregate: In the experimental study, crushed sand and aggregate have been used. Specific gravity of crushed sand and aggregate are 2.67 and 2.70, the maximum grain sizes are 4 mm and 11.2 mm.

Carbon Black: Carbon black is a material obtained from waste car tires with recycling material. Carbon black with a particle size of 30 µm was used in the concrete.

Mixing Water: Drinking water was used for mixing.

2.2. Production of specimen

Concretes with a water / cement ratio of 0.65 and carbon black (CB) content of 0%, 1%, 2% and 3% were produced. Initially for the mixture of concrete, crushed sand, aggregate and cement were mixed for 1 minute in order to have dry mixture. Then almost 2/3 of mixture water was added to the dry mixture. Finally the rest 1/3 of water were put into the mixture and the process of mixing was continued for 5 min. The 25 L capacity mixer is used. Then they are put in plastic moulds whose sizes are 10 cm x 10 cm x 10cm. Unit volume components of %0, %1, %2 and %3 rate carbon black substituted concrete have been shown in Table 2. After 24 hours, the samples were taken from the molds and cured in 20 ± 2 °C lime saturated water for 28 days.

Table 2. Component of concrete per cubic meter

Carbon black ration	Cement, kg/m ³	Water, lt/m ³	Carbon black kg/m ³	Crushed sand kg/m ³	Aggregate kg/m ³
%0	300	211	0	865	882
%1	297	211	3	865	882
%2	294	211	6	865	882
%3	291	211	9	865	882

3. Concrete Test

3.1. Porosity Ratio, Water Absorption and Unit Volume Weight

Porosity ratio, water absorption and unit volume weight, which are the basic physical properties of the samples, were determined by using standard TS EN 480-11 [11] test methods. The specific weight of the charges is determined by the Archimedes principle. The sample was allowed to stand at a temperature of 105 ± 5 ° C until it reached a constant weight (approx 24 h), after which the dry weights of the samples were determined. Subsequently, the specimens soaked in water for 24 h were saturated and their weights in water were determined and the apparent specific gravity, water absorption capacity and porosity values were calculated.

3.2. Compressive Strength

The compressive strength is most important characteristic of hardened concrete and normally for the purposes of the specification. Concrete cube test is the test the most knowledgeable, and is used as a method to measure the strength of the standard pressure for quality control purposes. The compressive strength of the concrete cubes was tested according to TS EN 13791 [12] for 1 and 28 days.

3.3. Electrical Resistivity

Electrical resistivity measurement of carbon black reinforced concrete in accordance with ASTM C 1760 [13] and resistance values (ohm-meter) were measured by two plate method. The resistivity values (R) were also determined by the following equation (1).

$$\rho = R \frac{A}{L} \quad (1)$$

Where, ρ is resistivity ($\Omega \cdot m$), R is resistance (Ω), A is sample area (cm^2) and l is sample length (m).

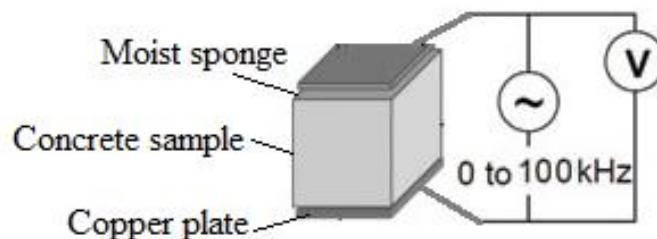


Figure 1. Electrical resistivity measurement on concrete

4. Results and Discussions

4.1. Porosity Ratio, Water Absorption and Unit Volume Weight

The porosity values of carbon black (CB) added concrete are given in Figure 2. It has been observed that the ratio of porosity slightly increases with increasing carbon black ratio. As the amount of carbon black increases, the amount of cement decreases. As the amount of cement decreases, the porosity rate increases. As the amount of cement decreases, the binding ratio decreases, so porosity increases. Porosity 13,77 was determined in unused concrete with carbon black. Porosity 14,97 of concrete containing 3% ration carbon black.

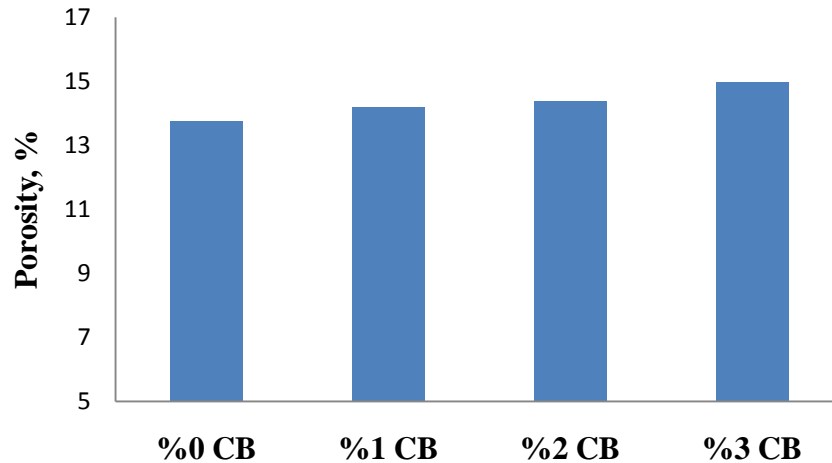


Figure 2. Porosity values of carbon black added concrete

The water absorption values of carbon black added concrete are given in Figure 3. It has been observed that the ratio of water absorption increases with increasing carbon black ratio. For instance, water absorption was increased from 6.16% to 6.83% when 3 wt.% CB was added into the concrete. It demonstrated that CB had adverse effect on the water absorption of concrete. This was mainly due to the very high surface area of CB particles.

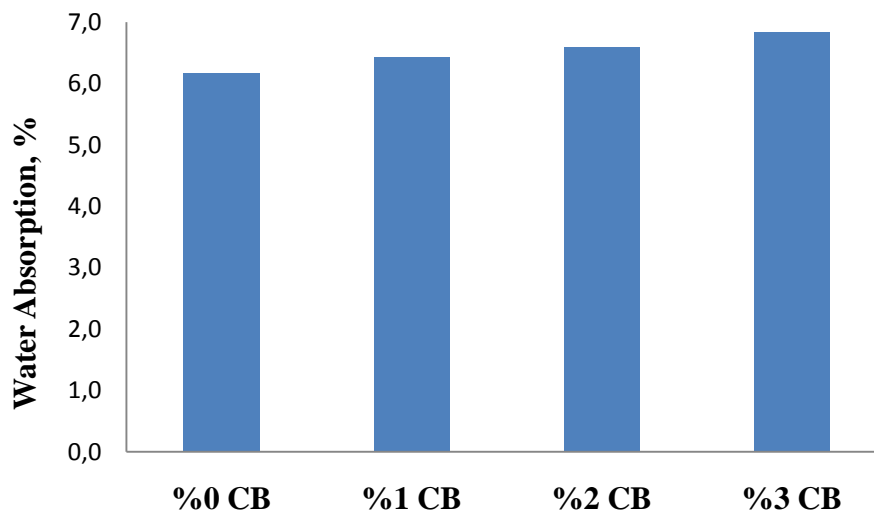


Figure 3. Water absorption values of carbon black added concrete

Unit volume weight values of carbon black added concrete are given in Figure 4. The unit weight slightly decreased with increasing carbon black ratio. When the unit weight of plain concrete is 2.24 kg/dm³, it is 2.15 kg/dm³ for 3% of CB blended concrete.

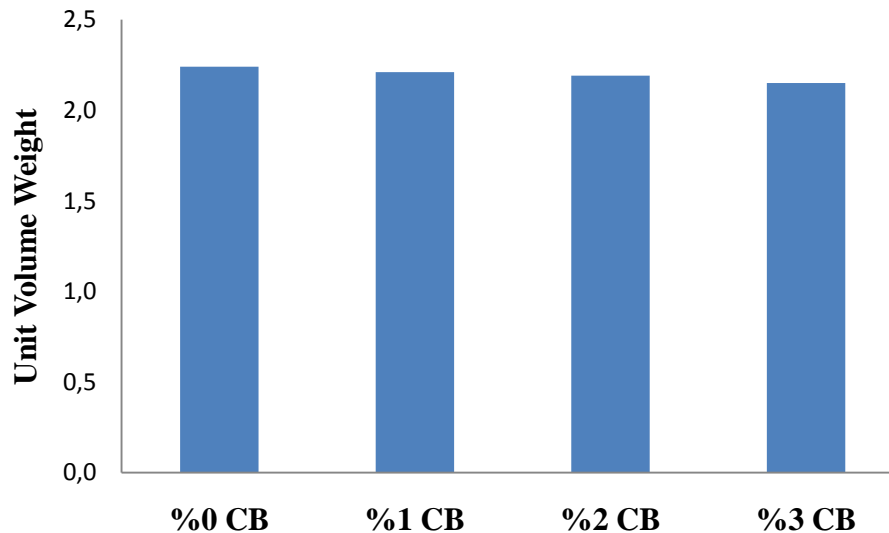


Figure 4. Unit volume weight values of carbon black added concrete

4.2. Compressive Strength

Compressive strength values of carbon black added concrete are given in Figure 5 for 1 and 28 days. With the increase of the ratio of carbon black, the compressive strength of 1 day decreased. With the increase of the ratio of carbon black, the compressive strength of 28 day decreased. As the amount of carbon black increases, the binder requirement also increases due to filling effect of very fine particles of carbon black. Therefore the compressive strength decreases.

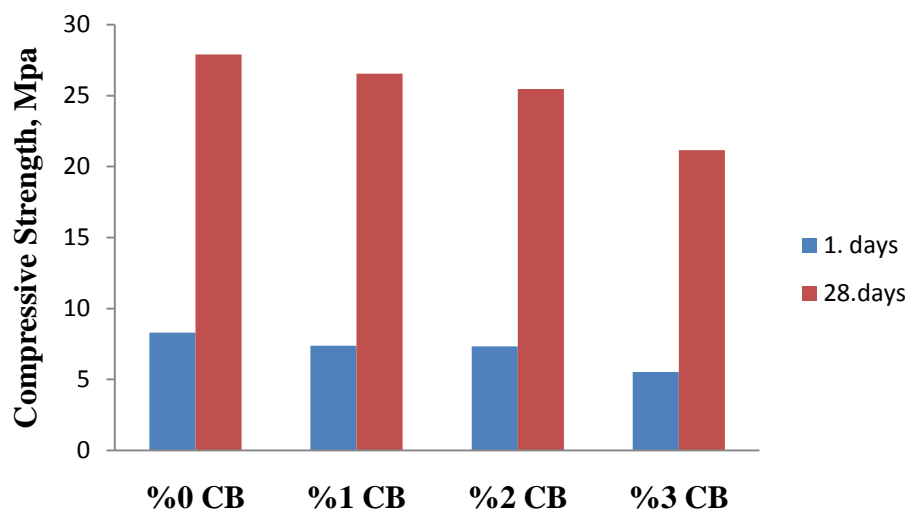


Figure 5. Compressive strength values of carbon black added concrete

4.3. Electrical Resistivity

The electrical resistance values of carbon black concrete with different ratios depending on the frequency are given in Figure 6. As is known, frequency is the number of cycles per second of an AC signal. In cement-based systems, electrical conductivity occurs due to ion transfer in cavity solutions and ion transfer is accelerated with increasing frequency. Therefore, resistance decreases. With the increase of carbon black ratio, electrical resistivity decreased. The electrical conductivity of carbon black has brought the concrete to the conductive structure, thus reducing the resistance.

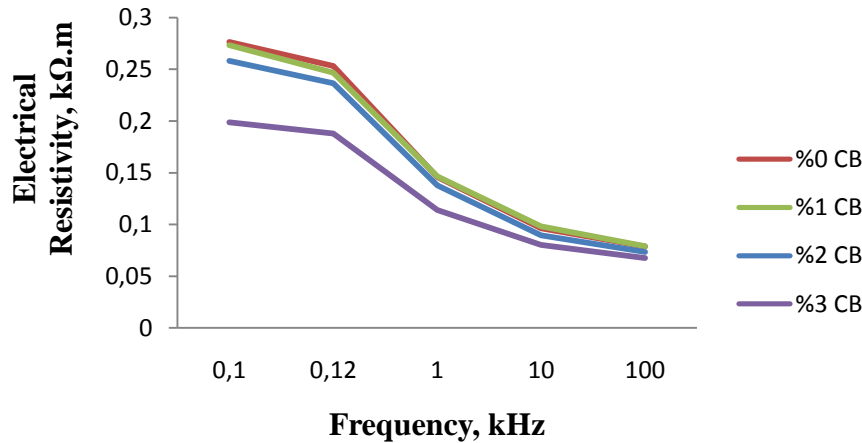


Figure 6. Electrical resistivity according to different frequency values

5. Conclusions

In this study, physical, mechanical and electrical properties of the concrete produced by adding carbon black in different ratios were investigated and the results obtained are given below.

- It has been observed that the ratio of porosity increases with increasing carbon black ratio.
- It has been observed that the ratio of water absorption increases with increasing carbon black ratio.
- The unit weight decreased with increasing carbon black ratio.
- With the increase of the ratio of carbon black, the compressive strength of 1 day decreased.
- With the increase of the ratio of carbon black, the compressive strength of 28 day decreased.
- With the increase of carbon black ratio, electrical resistivity decreased.

Acknowledgement

Authors thank to Afyon Kocatepe University for supporting the study with 17.FEN.BIL.40 Scientific Project.

REFERENCES

- [1] Mehta, P.K. 1999. Concrete technology for sustainable development, Concrete International, 21(11): 47-53.
- [2] Mehta, P.K. 2001. Reducing the environmental impact of concrete, Concrete International, 23(10): 61-66.
- [3] Mehta, P.K. 2002. Greening of the concrete industry for sustainable development, Concrete International, 24(7): 23-28.
- [4] Holland, T.C. 2002. Sustainability of the concrete industry – What should be ACI's role?, Concrete International, 24(7): 35-40.
- [5] Corinaldesi, V. & Moriconi, G. 2006. Behavior of beam-column joints made of sustainable concrete under cyclic loading, Journal of Materials in Civil Engineering, 18(5): 650-658.

- [6] Malhotra, V.M. 2003. Concrete technology for sustainable development, In Sustainable development in cement and concrete industries, Proc. two-day intern. seminar, Milan, Italy, 17-18 October 2003, 11-18.
- [7] Monteiro, A.O., Cachim, P.B., Costa, P.M.F.J., Electrical properties of cement-based composites containing carbon black particles, 5th International conference on Advanced Nano Materials, 2015, 193-199.
- [8] Mahoutian, M., Lubell, A.S., Bindiganavile, V.S., Effect of powdered activated carbon on the air void characteristics of concrete containing fly ash, Construction and Building Materials, 2015, 80, 84-91.
- [9] Gonga, H., Li, Z., Zhang, Y., Fan, R., Piezoelectric and dielectric behavior of 0-3 cement-based composites mixed with carbon black, Journal of the European Ceramic Society, 2009, 29, 2013-2019.
- [10] TS EN 197-1, Cement- Stage 1: General cements – component, TSE, Ankara (2010) Turkey.
- [11] TS EN 480-11, Admixtures for concrete, mortar and grout - Test methods - Part 11: Determination of air void characteristics in hardened concrete, Turkish Standard Institute, Ankara, Turkey, 2008.
- [12] TS EN 13791, Assessment of in-situ compressive strength in structures and precast concrete components, TSE, Ankara (2010) Turkey.
- [13] ASTM C 1760. Standard test method for bulk electrical conductivity of hardened concrete. West Conshohocken (PA): ASTM; 2012.
- [14] B. Chen, B. Li, Y. Gao, T.C. Ling, Z. Lu, Z. Li, Investigation on electrically conductive aggregates produced by incorporating carbon fiber and carbon black, Construction and Building Materials 144 (2017) 106–114.

CEMENT, CONCRETE AND JEOPOLYMERS

MECHANICAL AND FREEZE-THAW RESISTANCE PROPERTIES OF C30 CLASS CONCRETE: THE EFFECT OF FINELLY MILLED WIRE AND RUBBER OBTAINED FROM WASTE TIRE

Tuba BAHTLI^{1,*}, Nesibe Sevde ULVAN²

¹ Necmettin Erbakan University, Faculty of Engineering and Architecture, Department of Metallurgy and Materials Engineering, 42090, Meram, Konya, Turkey

² Necmettin Erbakan University, Institute of Science and Technology, Department of Mechanical Engineering, Konya

ABSTRACT

In this study the effects of finelly milled wire and rubber, that were obtained from waste tire, on the mechanical properties and freze-thaw resistance of C30 class concrete were investigated. Wire obtained from waste tire was added to C30 class dry concrete mortar by 5% by weight. Then: i) rubber and wire (2,5% for each) produced from waste tire were added to dry concrete mortar ii) rubber and wire (5% for each) produced from waste tire were added to dry concrete mortar. Samples were cured for 28 day. The open porosity, density, cold crushing strength values and freeze-thaw resistances of cured concrete were determined. Microstructure and fracture surfaces of those materials were characterized by scanning electron microscopy. It was obsorved that the strength and freze-thaw strength of of concretes containing rubber and wire produced from waste tire were decreased.

Keywords: waste tire, recycling, concrete, mechanical properties, freze-thaw

INTRODUCTION

A tire is a composite of complex elastomers, fibers and steel/fiber cord [1]. Because of the environmental threat of waste tires, that need a larger storage space than other waste due to their large volume and fixed shape, there has been an increased interest in using the recycled waste tire products [2, 3]. There are a number of applications of waste tires, including use in reefs and breakwaters, playground equipment, erosion control, highway crash barriers, guard rail posts, noise barriers, asphalt pavement mixtures and as fuel in cement kilns. In addition, waste tires have been used as as feedstock for making carbon black, and as artificial reefs in marine environment [1, 4]. Rubber from waste tires is one of the waste materials investigated for its potential use in the construction field [4]. The brittle nature of concrete and its low loading toughness compared to other materials, has prompted the use of

waste tire particles as a concrete aggregate to possibly remedy or reduce these negative attributes. Elastic and deformable tire–rubber particles could improve concrete properties. Waste tire rubber modified concrete is characterized as having high toughness and low strength and stiffness [5, 6].

Also, the steel beads contain a significant volumetric percentage of steel wires (30–70%), the recycled steel bead concrete (RSBC) could be considered as a relative material to steel fiber reinforced concrete (FRC). The authors believe that the RSBC will exhibit better mechanical properties compared to concrete made with the addition of other recycled tire products such as crumb rubber or tire chips [2].

In this study, the uses of wire and rubber obtained from waste tire in C30 class concrete and then the changes of mechanical and freeze-thaw resistance properties of this concrete were investigated.

MATERIALS AND METHODS

In this study, Baunit trademark and C 30 class dry concrete mortar was used. The wires that come out of waste tire were milled in the ring mill approximately 5 minutes, and made ready for use. Sieve analysis were carried out to determine grain size distributions of this mortar and wire from waste tire.

Table 1. Sieve analysis of dry concrete mortar

Sieve opening (mm)	% wt.
+4	3,178
+2	26,97
+1	23,31
+0,5	8,418
+0,250	9,898
+0,150	3,618
+0,063	3,108
Powder	21,50
Total	100

Table 2. Sieve analysis of waste tire wire.

Sieve opening (mm)	% wt.
+0,5	6,99
+0,250	72,86
+0,150	17,38
+0,100	1,29
+0,08	0,53
+0,063	0,25
+0,05	0,70
Total	100

Compounds: i) Pure C30 class concrete, ii) C30 concrete incorporating 5 % wire obtained from waste tire, iii) C30 concrete incorporating 2,5 % wire and 2,5% rubber obtained from waste tire, iv) C30 concrete incorporating 5 % wire and 5% rubber obtained from waste tire, were produced by using 5*5*5 cm³ chill moulds. All produced concrete samples were cured for 28 day.

Received parts for each samples were boiled for 2 hours in order to determine densities and open porosities by Archimedes.

Cold crushing strenght (CCS) of samples examined by Liya mark cold crushing test machine with 200 kN load.

With the Impact branded tester called Schmidt attractor, the hammer was pressed into 3 different regions of the concrete samples and the values were read. By taking the average of these values, the approximate compressive strength values of the samples were determined. Also, impact brand ultrasonic inspection device was used to determine the speed of the sound waves sent from one end of the concrete sample to other end, and deductions were made about the space in the sample.

Freeze-Thaw resistances of concrete samples were determined by freeze-thaw test machine according to ASTM C666. For this test, respectively 10, 25 and 50 freeze-thaw cycles between $\pm 20^{\circ}\text{C}$ were actualized for 150 minutes.

Microstructures of concrete samples were characterized by scanning electron microscopy (SEM) with backscattered electron detector at Dumlupınar University Advanced Technology Center. Fracture surfaces of samples were examined by SEM with secondary electron detector at Necmettin Erbakan University Science and Technology Research and Application Center.

RESULTS AND DISCUSSIONS

Physical and Mechanical Properties

Density, open porosity and CCS values of pure concrete and concretes incorporating wire and rubber obtained from waste tire were given in Figure 1.

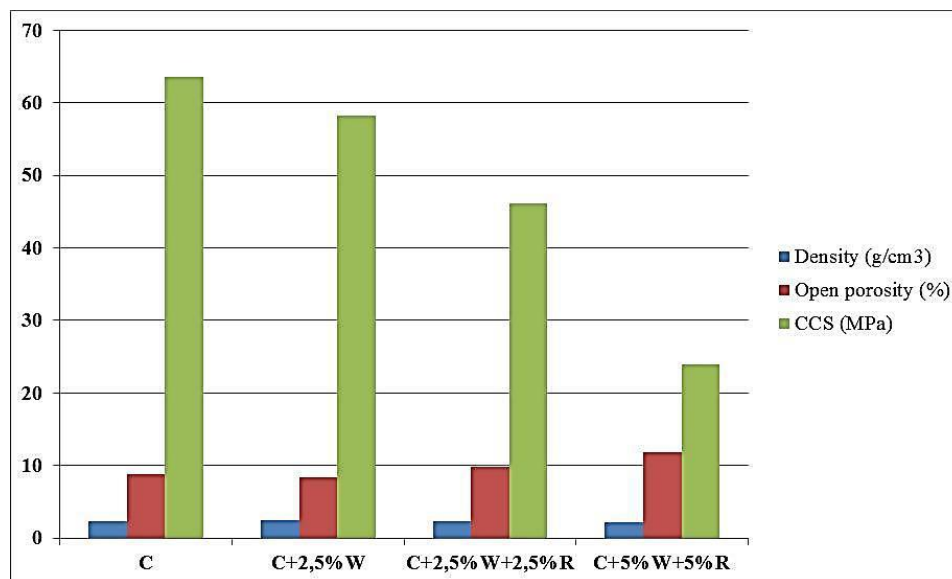


Figure 1. Density, open porosity and CCS values of concrete materials (C: concrete, W: wire, R: rubber)

According to Figure 1, incorporation of wire produced from waste tire to concrete had no distinct effect on physical and mechanical properties of C30 class concrete. However, the density values

decreased, the amount of open porosities increased, and thus the CCS values decreased with waste tire rubber addition due to the fact that a weak bond between the rubber, concrete and wire.

Strength and the speed of the sound waves results obtained from Schmidt method (Table 3) indicated that the increase in the amount of waste tire rubber and the decrease in strength was more significant, and also the speed of sound decreased due to the greater amount of porosity.

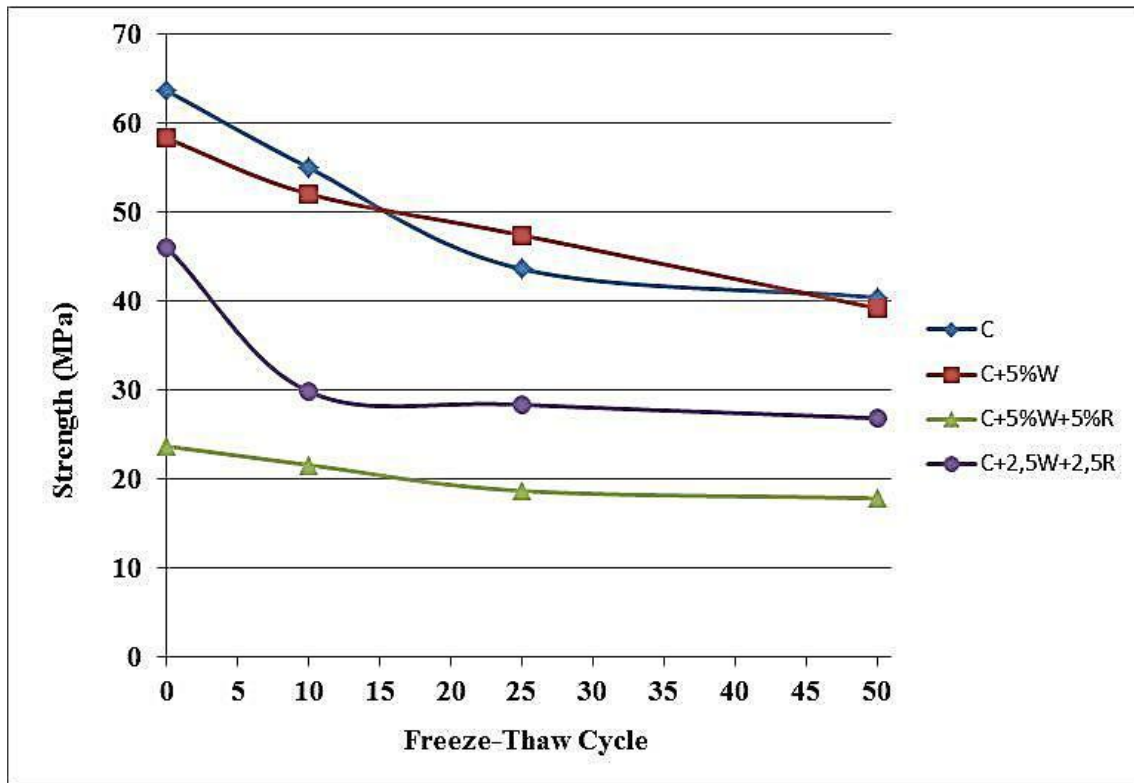
Table 3. Results of strength and the speed of the sound waves according to Schmidt test

Material	Average strength (Mpa)	The speed of sound along the specimen (m/s)
C	53,57	4567
C+5% W	45,87	4529
C+2,5%W+2,5R	31,43	4286
C+5% W+5%R	27,02	3927

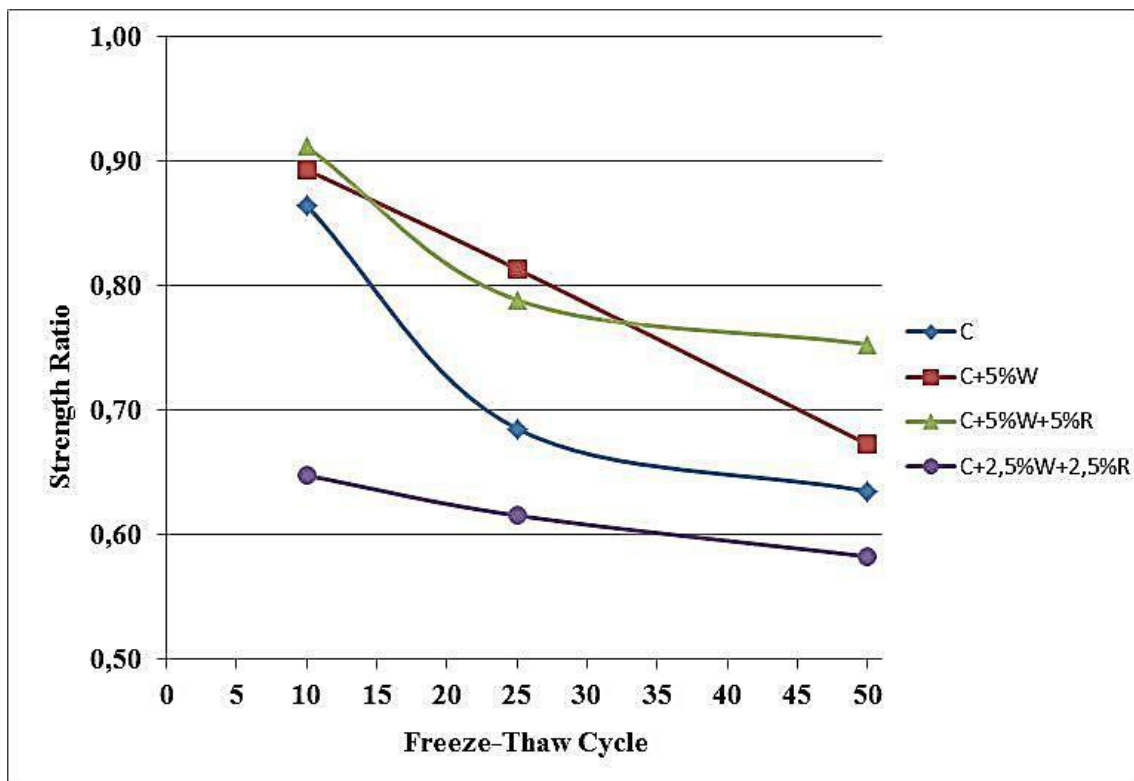
Freeze-Thaw Results

The strength (CCS) and strength ratio of concrete materials after 10, 25 and 50 freeze-thaw cycles were given in Figure 2. Generally, strength values decreased as the number of cycles increased. It's thought that the amounts of structural defects as porosity and cracks increased with the number of freeze-thaw cycles, then CCS values decreased.

Similarly, strength ratio values decreased and concrete materials could not retain their strength values anymore with the number of freeze-thaw cycles. Eventhough the strength of concretes incorporating waste tire rubber were at minimum level, decreases in strength ratios were not sharp as those of pure concrete and concrete containing wire produced from waste tire.



(a)



(b)

Figure 2. Strength and strength ratio values of concrete samples after freeze-thaw cycles.

Microstructural Analysis Results by SEM

SEM images of concrete samples produced as unreinforced and with waste additives were given in 3-10.

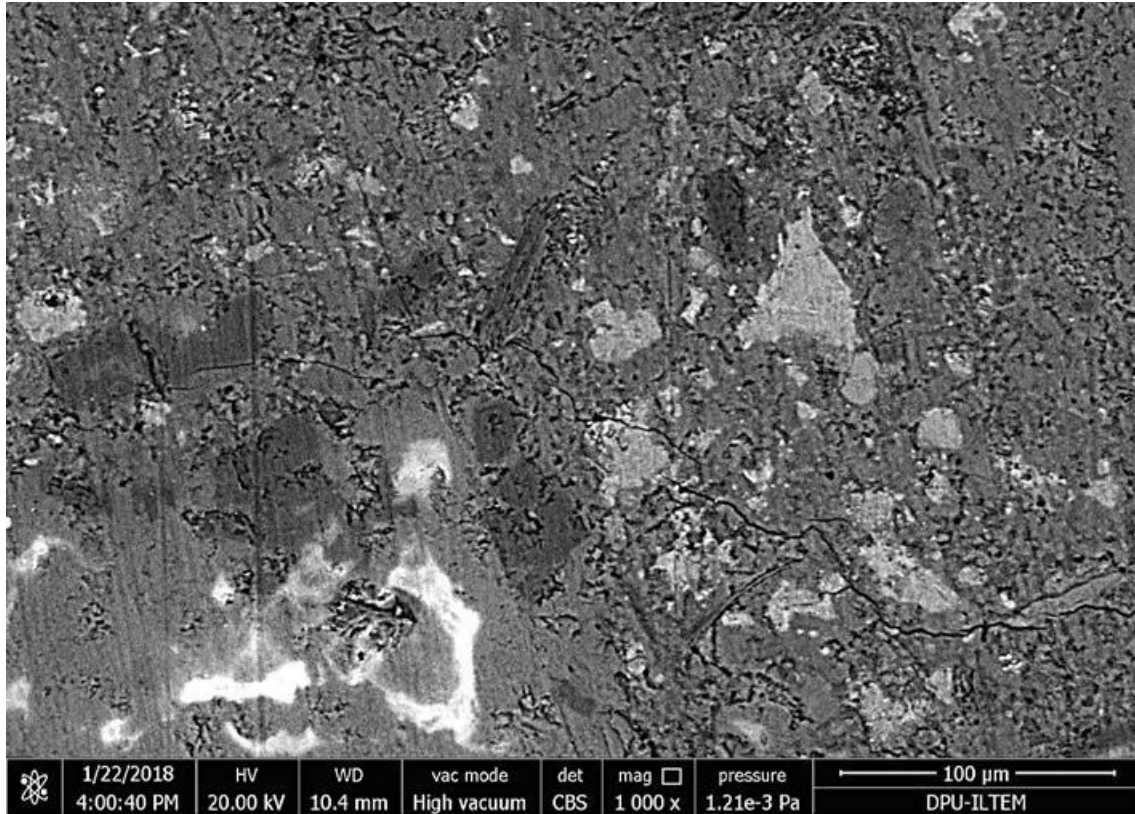


Figure 3. SEM backscattered electron image of of pure concrete (C)microstructure (1000X).

Mainly Ca, Si and Al elements, that were contained in cement phase, porosities and microcracks, however generally the dense structure of concrete were seen in pure concrete microstructure (Figure 3 and 4).

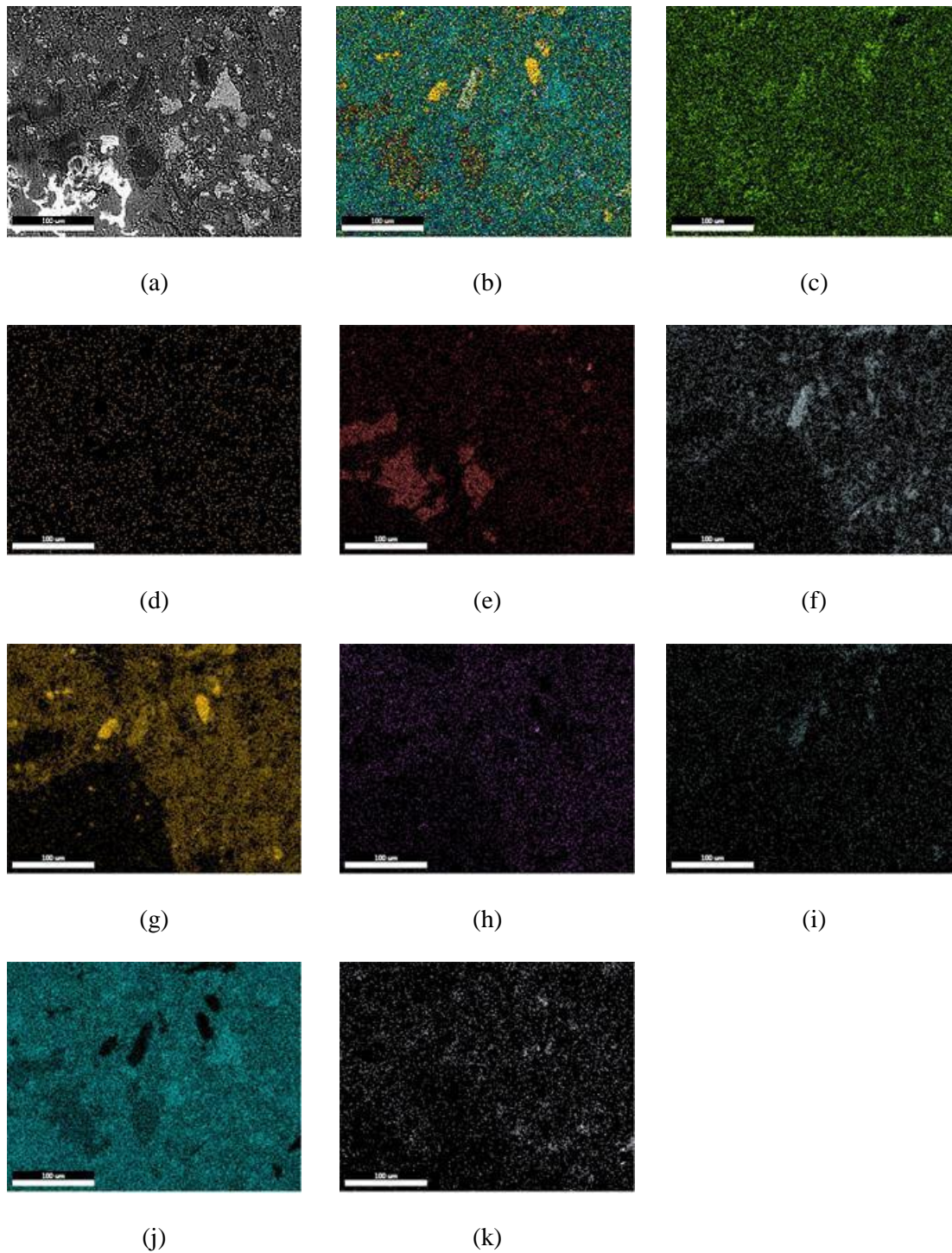


Figure 4. a) Microstructural image recorded with backscattered electrons (1000x), b) colorized BSE image of C concrete material and its element distributions: c) O, d) Na, e) Mg, f) Al, g) Si, h) S, i) K, j) Ca, k) Fe

According to SEM backscattered electron image of C+5%W concrete material incorporating 5% wire obtained from waste tire, there were microcracks and also lower strong bonding at interfaces between

wires and concrete matrix microstructure that caused lower strength value than that of pure concrete (Figure 5 and 6). Differently from pure concrete, C element that came from wire was seen in Figure 6.

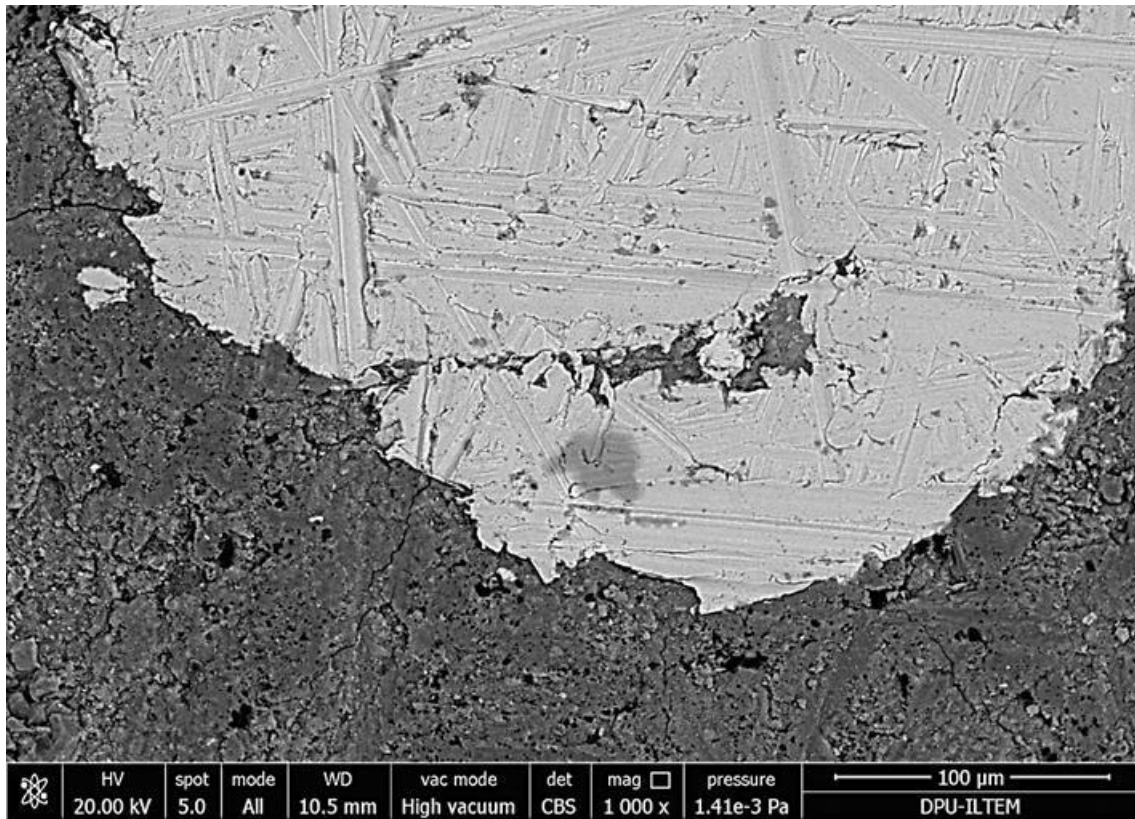


Figure 5. SEM backscattered electron image of concrete microstructure incorporating 5% wire obtained from waste tire (C+5% W) (1000X).

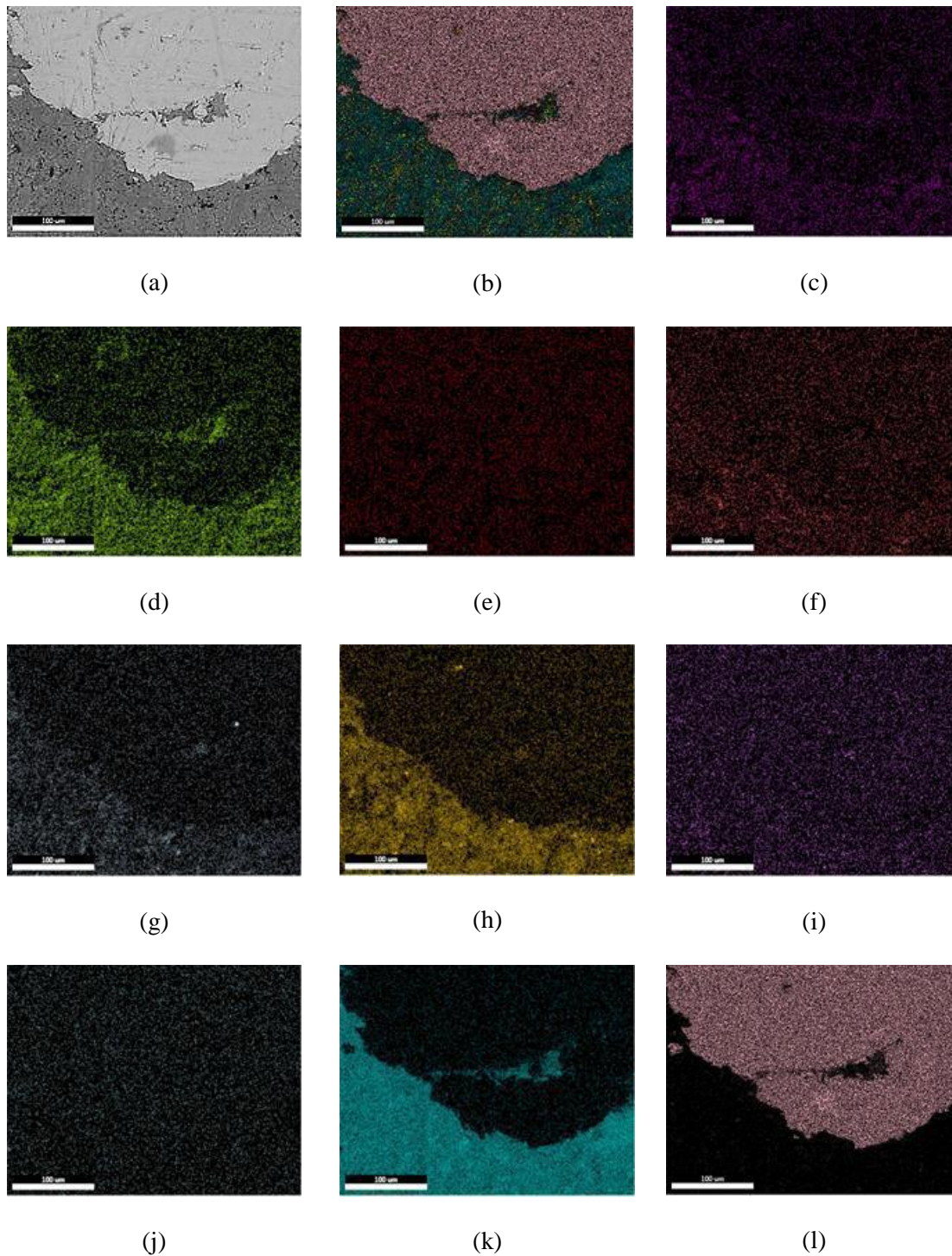


Figure 6. a) Microstructural image recorded with backscattered electrons (1000x), b) colorized BSE image of C+5%W material and its element distributions: c) C, d) O, e) Na, f) Mg, g) Al, h) Si, i) S, j) K, k) Ca, l) Fe

Microstructures and elemental distributions of concretes incorporating 2,5% wire+2,5% rubber (C+2,5%W+2,5R) and 5% wire+5% rubber (C+5%W+5R) obtained from waste tire were given in Figures 7, 8 and Figure 9, 10 respectively.

Bonding at interfaces between all phases became weaker due to addition of rubber which was obtained from waste tire. Also there were more porosities, microcracks and deep cracks appeared. Due to these affects, density and CCS values of those concrete samples.

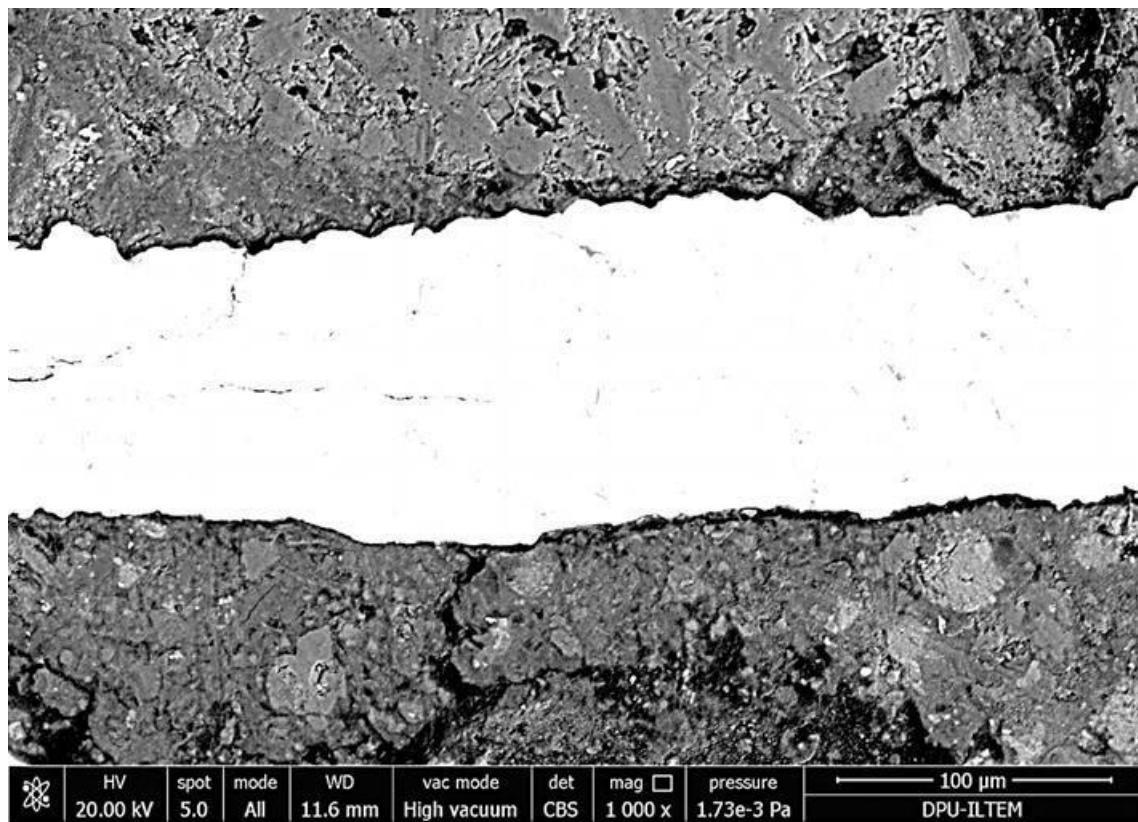


Figure 7. SEM backscattered electron image of concrete microstructure incorporating 2,5% wire and 2,5% rubber obtained from waste tire (C+2,5%W+2,5R) (1000X).

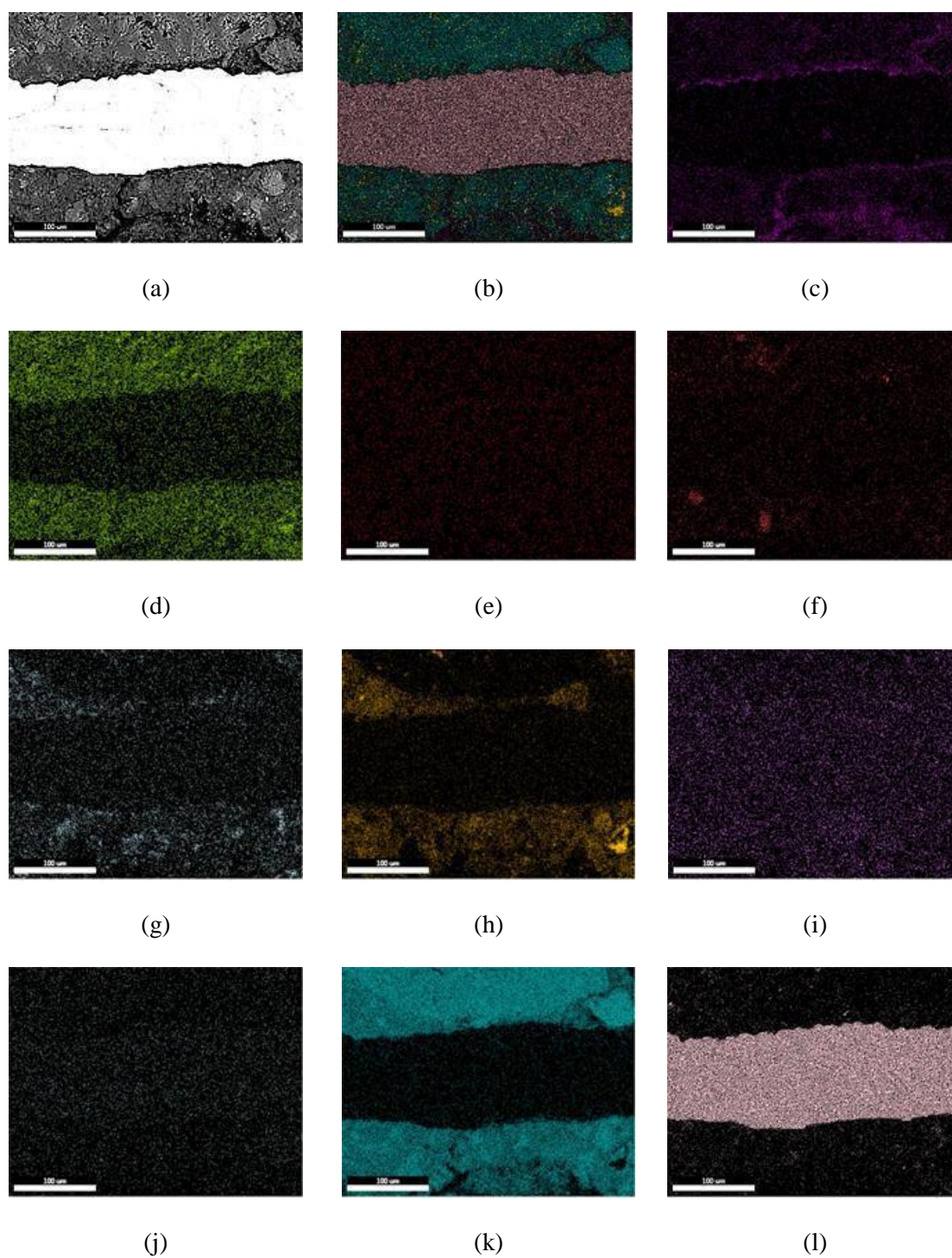


Figure 8. a) Microstructural image recorded with backscattered electrons (1000x), b) colorized BSE image of C+2,5%W+2,5R and its element distributions: c) C, d) O, e) Na, f) Mg, g) Al, h) Si, i) S, j) K, k) Ca, l) Fe

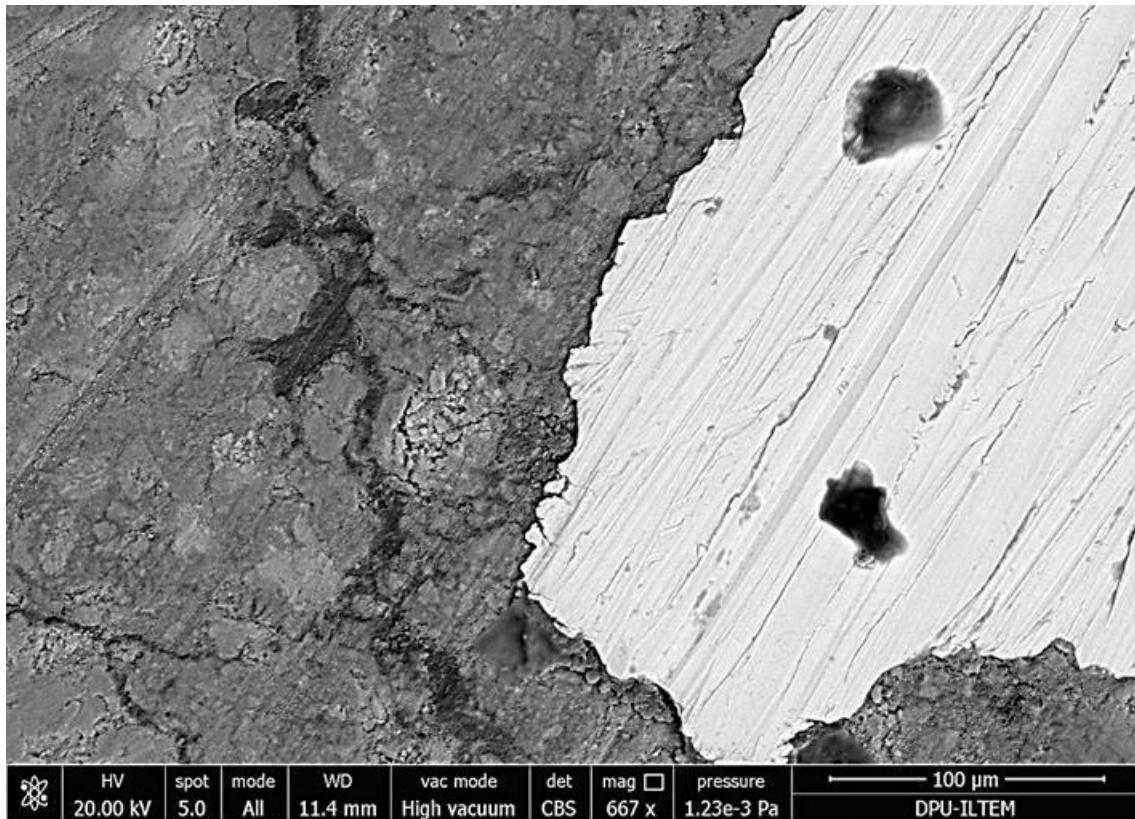


Figure 9. SEM backscattered electron image of concrete microstructure incorporating 5% wire and 5% rubber obtained from waste tire (C+5% W+5R) (1000X).

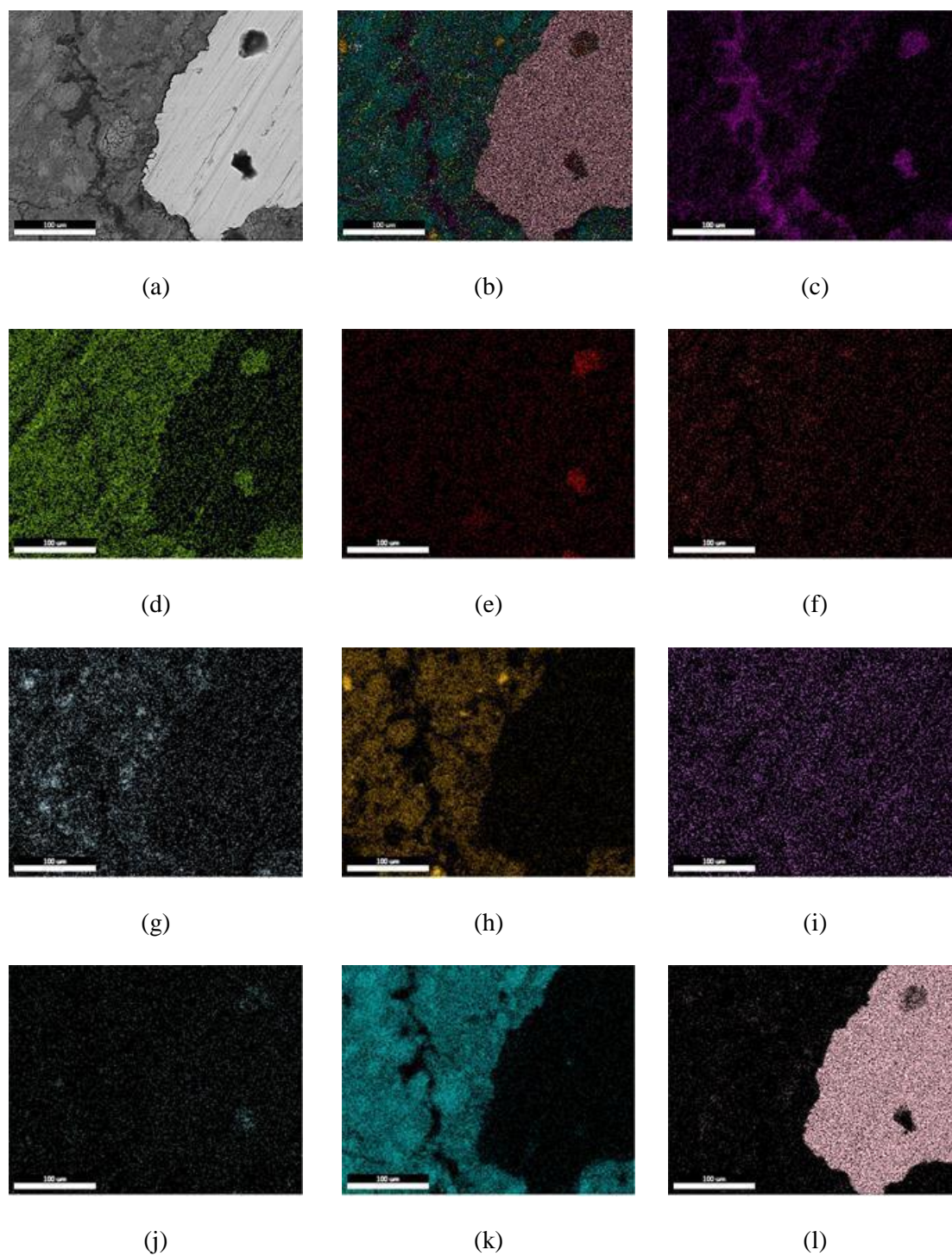


Figure 10. a) Microstructural image recorded with backscattered electrons (1000x), b) colorized BSE image of C+2,5%W+2,5R and its element distributions: c) C, d) O, e) Na, f) Mg, g) Al, h) Si, i) S, j) K, k) Ca, l) Fe

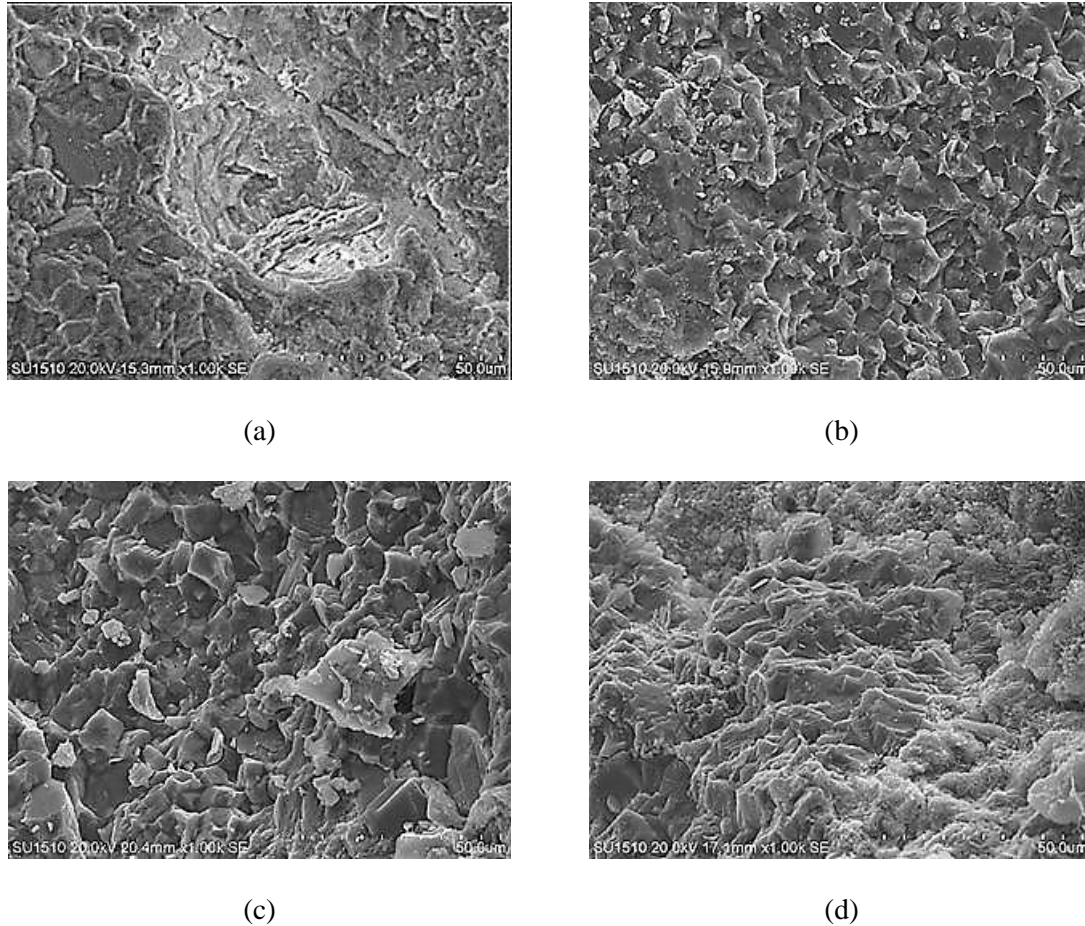
Table 4. EDX analysis of concrete samples

Elements (%)	Material			
	C	C+5%W	C+2,5%W+2,5R	C+5%W+5%R
C	0	2	5	5
O	9	4	5	5
Na	1	2	1	2
Mg	3	2	2	2
Al	4	3	4	4
Si	12	8	8	11
S	3	3	4	5
K	2	2	2	2
Ca	64	24	35	31
Fe	2	50	34	33

According to EDX analysis of concrete samples, Ca content that comes from cement was maximum in pure concrete and its amount decreased as the amounts of additives increased. All concretes incorporating wire had C and Fe elements and also C+5%W material that contained only wire additive had maximum Fe element. By adding rubber obtained from waste tire, amounts of C and S elements increased while the amount of Fe decreased.

Fracture Surfaces Characterizations of Concretes by SEM

Before and after freeze-thaw test, fracture surfaces images of concrete samples either pure or produced with waste additives were given in Figure 11, 12.



Şekil 3.5. Before freeze-thaw test, fracture surface images (secondary electron images) of a) Pure concrete, b) concrete incorporating 5% wire obtained from waste tire c) concrete incorporating 2,5% wire and 2,5% rubber obtained from waste tire, and d) concrete incorporating 5% wire and 5% rubber obtained from waste tire (magnification: 1000X).

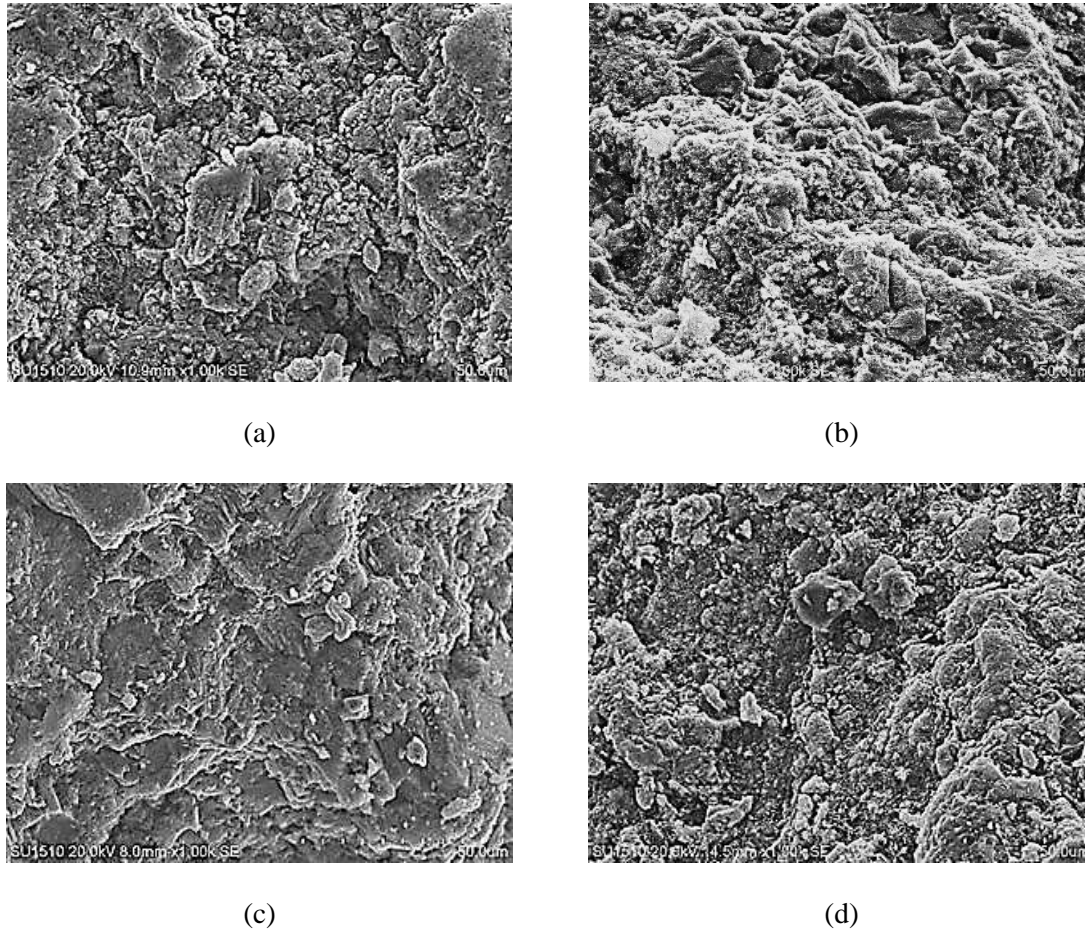


Figure 12. After freeze-thaw test, fracture surface images (secondary electron images) of a) Pure concrete, b) concrete incorporating 5% wire obtained from waste tire c) concrete incorporating 2,5% wire and 2,5% rubber obtained from waste tire, and d) concrete incorporating 5% wire and 5% rubber obtained from waste tire (magnification: 1000X).

Before and after freeze-thaw test, generally pure concrete sample had either transgranular or intergranular fracture.

For other concrete samples, transgranular fracture type became more dominant as the amount of additives increased before freeze-thaw test. However both type of fracture were observed after freeze-thaw test. Though, strength values of concretes incorporating wire and rubber additives, that were produced from waste tire, were smaller than pure concrete, strength ratio values of those concretes were higher. This means that decrease in strength values for those concretes were not sharp as pure concrete.

Especially C+5%W+5R material had the highest strength value after 50 freeze-thaw cycle. This concrete retained seventy-five percent of its initial strength value. Intergranular type fracture became more dominant for this concrete after freeze-thaw test. This transition from transgranular fracture type to intergranular fracture type was effective in mechanical properties.

CONCLUSIONS

Concretes incorporating wire and especially rubber that were obtained from waste tire had lower density and CCS values than pure concrete due to the fact that a weak bond between the rubber, concrete and wire.

However those concretes had higher strength ratio values after freeze and thaw test. Transition from transgranular fracture type to intergranular fracture type was effective in increase of mechanical properties.

ACKNOWLEDGE

This study was supported by Necmettin Erbakan University Scientific Research Projects under project no: 171351001.

REFERENCES

1. H. A. Toutanji, The Use of Rubber Tire Particles in Concrete to Replace Mineral Aggregates, *Cement & Concrete Composkes* 18 (1996) 135-139
2. Rafat Siddique, Tarun R. Naik, Properties of concrete containing scrap-tire rubber – an overview, *Waste Management* 24 (2004) 563–569
3. Ali R. Khaloo *, M. Dehestani, P. Rahmatabadi, Mechanical properties of concrete containing a high volume of tire–rubber particles, *Waste Management* 28 (2008) 2472–2482
4. Guoqiang Lia, Michael A. Stubblefield, Gregory Garrick, John Eggers, Christopher Abadie, Baoshan Huang, Development of waste tire modified concrete, *Cement and Concrete Research* 34 (2004) 2283–2289
5. C. G. Papakonstantinou, M. J. Tobolski, Use of waste tire steel beads in Portland cement concrete, *Cement and Concrete Research* 36 (2006) 1686–1691
6. Wang Her Yung, Lin Chin Yung, Lee Hsien Hua, A study of the durability properties of waste tire rubber applied to self-compacting concrete, *Construction and Building Materials* 41 (2013) 665–672

CEMENT, CONCRETE AND JEOPOLYMERS

THE EFFECT OF WATER/CEMENT RATIO ON THE COMPRESSIVE STRENGTH OF THE CEMENT MORTARS PRODUCED BY POLYCARBOXYLATE BASED PLASTICIZING CHEMICAL ADMIXTURE

Deniz Tuğçe Algan¹, Evren Arıöz¹, Ömer Arıöz², Ömer Mete Koçkar¹

¹ Eskişehir Technical University, İki Eylül Campus, Faculty of Engineering, Department of Chemical Engineering, 26555/Eskişehir/Turkey

² Hasan Kalyoncu University, Department of Civil Engineering, Gaziantep/Turkey

ABSTRACT

Concrete is one of the most widely used construction material all over the world. Concrete consists of cement, aggregate, water and if necessary chemical admixtures depending on the desired property. The water/cement ratio is one of the important parameters in concrete mix design since the strength is influenced directly by water/cement (w/c) ratio. When w/c ratio reduces the compressive strength increases. Plasticizing admixtures are used to improve workability of freshly mixed concrete. Plasticizing admixtures are also called water reducers and therefore it is also possible to achieve high strength values by using plasticizers. In this experimental study, the effect of water/cement ratio on the compressive strength of the cement mortars was investigated. Cement, sand, water and commercial polycarboxylate based plasticizer were used to produce mortars. The w/c values varied between 0.4 and 0.55 while the plasticizer dosage was kept constant as 1 % of cement. The flow and compressive strength values of the mortars were determined. The highest compressive strength was achieved as 47.14 MPa for mixtures produced by w/c ratio of 0.475.

Keywords: Plasticizing admixtures, water/cement ratio, cement, compressive strength

1. INTRODUCTION

Concrete, is a homogeneous mixture of cement, water, aggregate (sand, crushed stone, etc.), and if required chemical admixture (plasticizer, retarder, accelerator, air entraining, antifreeze, etc.), and mineral admixtures (blast furnace slag, fly ash, silica fume, etc.). Concrete is initially in the plastic form which can be shaped and hardened over time gaining strength and then in the elastic form which can gain strength and bear structural loads [1].

High strength concrete is of interest nowadays. In order to produce high strength concrete, a low water/cement ratio is required [2,3]. Low water/cement ratio decreases the workability of the concrete while increasing the strength. Superplasticizers (melamine or naphthalene based and polycarboxylate-based) increase the workability and compressive strength at low water/cement ratios [2].

Superplasticizers disperse agglomerates of cement particles with electrostatic charge and enhance the characteristic properties of concrete such as fluidity and durability [4]. The chemical structure of polycarboxylate-based superplasticizers can be designed due to the components of the admixture [5]. Polycarboxylate-based superplasticizers are generally consisted of a polymer backbone and grafted charge-neutral side chains [6]. On the other hand, increasing superplasticizer ratio may cause segregation of concrete mixes therefore it should be used at limited ratio [7]. Superplasticizers may also cause other problems including varying flow properties and uncontrolled setting [8].

In order to determine the flow properties and the compressive strength, different cement mortars were prepared with different water/cement ratios while the superplasticizer ratio was constant in all mixes. The effect of water/cement ratio on the compressive strength and the crystalline structure of the cement mortars were investigated.

2. EXPERIMENTAL METHODS

In this experimental study, cement, sand, water and commercial polycarboxylate based superplasticizer were used. Experiments were carried out with varying water / cement ratios between 0.4-0.55 while the superplasticizer ratio was constant at 1%. Cement mortars were prepared according to TS EN 196-1. The superplasticizer was firstly mixed with water and then added to cement and sand mixture. The flow values of each mortar were measured in flow table. The mortars were cast into 4x4x16 cm steel moulds and vibrated to avoid air bubbles. Samples were cured in water bath for 7 and 28 days. The compressive strengths were performed on specimens. The crystalline structures of samples cured for 28 days were determined by X-ray diffractometry (XRD).

3. RESULTS AND DISCUSSION

The flow ratio of the cement mortars for different water/cement ratios are given in Table 1.

Table 1: Flow ratios of cement mortars

Water/cement Ratio	Flow Ratio (%)
0.400	20
0.450	55
0.475	60
0.500	70
0.525	140
0.550	-

Test results revealed that the flow ratio of the mortars increased with increase in water/cement ratio and could not be measured of the mortar prepared with the water ratio of 0.550. Figure 1 presents the compressive strength values of the mortars.

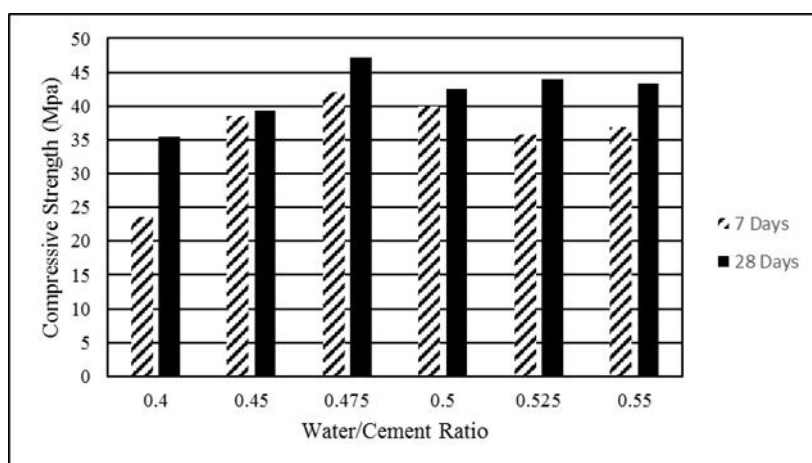


Figure 1. The compressive strength values of cement mortars

Test results indicated that the compressive strength of the mortars increased when the water/cement ratio increased to 0.475. However, the strength values slightly decreased with increasing w/c ratio. The compressive strength values of all samples increased with age of sample. The highest compressive strength value was obtained as 47.14 MPa for 7 days cured samples and 41.96 MPa for 28 days cured samples. When the water/cement ratio increased to 0.550, the compressive strength values decreased to 36.93 MPa for 7 days cured specimens and 43.3 for 28 days cured specimens. The crystal phases

existing in the cement mortars were investigated by X-ray diffractometry between $10 - 70^\circ 2\theta$ and given in Figure 2.

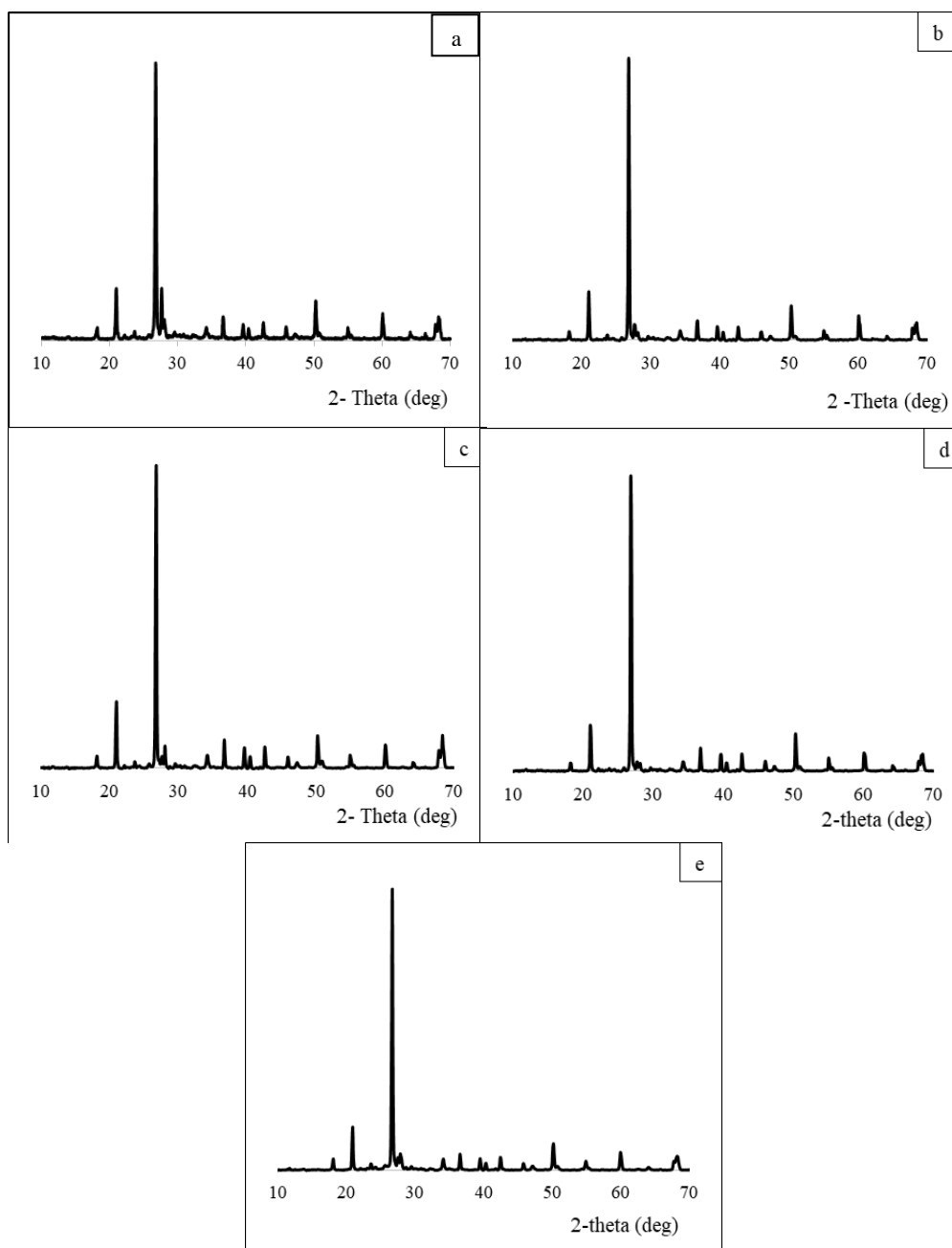


Figure 2. XRD spectrum of the cement mortars cured for 28 days with water/cement ratio a) 0.40 b) 0.45 c) 0.475 d) 0.5 e) 0.55

The quartz peaks were observed strongly at $\sim 28^\circ 2\theta$ and $\sim 50^\circ 2\theta$ in the spectrum of all the mortars. Portlandite was seen at $\sim 18^\circ 2\theta$ and the peak at $\sim 20^\circ 2\theta$ was assigned to alite. The peaks indicating belite were observed at $\sim 35^\circ$, 55° and $70^\circ 2\theta$. Tobermorite crystals were seen at $\sim 40^\circ 2\theta$ and $\sim 45^\circ 2\theta$. The intensity of alite and belite observed at $\sim 70^\circ 2\theta$ increased when the water/cement ratio increased to 0.475, and then decreased with water/cement ratio.

References

1. Ekinici, C.E., Ay, S., Baykuş, N., Ay, A., Lignin sülfonat esaslı yapı kimyasalların taze ve sertleşmiş betona olan etkilerinin incelenmesi. Pamukkale Üniversitesi Mühendislik Bilimleri Dergisi, 2016, 22(6), 478-485.
2. Antoni, Halim, J. G., Kusuma, O.C., Hardjito, D, Optimizing polycarboxylate based superplasticizer dosage with different cement type. Procedia Engineering, 2017, 171, 752-759.
3. Feng, J., Li, J., Chen, L., Li, P., Wang, Z., The Polycarboxylate-based superplasticizers modified with thickening agents: the performance and influence on cement hydration. 5th International Conference on Advanced Design and Manufacturing Engineering, 2015, China, 1995-1999.
4. Collepardi, M., Admixtures used to enhance placing characteristics of concrete. Cement and Concrete Composites, 1998, 20, 103-112.
5. Yamada, K., Takahashi, T., Hanehara, S., Matsuhisa, M., Effects of the chemical structure on the properties of polycarboxylate-type superplasticizer. Cement and Concrete Research, 2000, 30, 197-207.
6. Zhao, H, Wang, Y., Yang, Y., Shu, X., Yan, H., Ran, Q., Effect of hydrophobic groups on the adsorption conformation of modified polycarboxylate superplasticizer investigated by molecular dynamics simulation. Applied Surface Science, 2017, 407, 8-15.
7. Kwan, A.K.H., Fung, W.W.S., Roles of water film thickness and SP dosage in rheology and cohesiveness of mortar. Cement & Concrete Composites, 2012, 34, 121-130.
8. Alonso, M. M., Palacios, M., Puertas, F., Compatibility between polycarboxylate-based admixtures and blended-cement paste. Cement & Concrete Composites, 2013, 35, 151-162.

CEMENT, CONCRETE AND GEOPOLYMERS

AN INVESTIGATION ON THE PRODUCTION POTENTIAL OF GEOPOLYMER MORTAR WITH TUNÇBİLEK FLY ASH

Serhat Çelikten¹, Mustafa Sarıdemir²

¹ Eskişehir Technical University, Vocational School of Transportation, 26470, Eskişehir, Turkey

² Niğde Ömer Halisdemir University, Faculty of Engineering, 51240, Niğde, Turkey

Abstract

Fly ash (FA) is a waste material of thermal power plants. The utilization of FA in concrete technology is important for the reduction of the storage and environmental problems. For this purpose, FA has been used as a mineral admixture in mortar and concrete mixtures for several years. In addition, the activation of FA with alkalis to produce a new generation binder material called as geopolymer is a new topic for the utilization of FA. In this study, mortar mixtures were prepared for the activation of Tunçbilek FA with the sodium silicate and sodium hydroxide. The mixtures were made with 4%, 6% and 8% Na content of FA weight. 4x4x16 cm prism mortar specimens taken from the mixtures. The unit weights of FA mortars were determined after demoulding the mortars. And also, the flexural and compressive strength tests were performed on the mortar specimens after the production of 7 days. The flexural and compressive strength values of the Tunçbilek FA mortars reached to 8.4 and 41.2 MPa at 7 days, respectively. As a result of this study, Tunçbilek FA has a high potential for the production of geopolymer and investigation of the durability properties of Tunçbilek FA geopolymer mortars is recommended for further studies.

Keywords: Fly ash, geopolymer, mortar, mechanical properties

Introduction

The production of each ton cement clinker cause to discharge same amount of CO₂ to the environment (Pacheco-Torgal et al. 2008). In order to reduce the CO₂ emissions, the researchers have been studying on the obtaining of cement-free binders by activating mineral admixtures, for recent years (Hossain et al. 2015). Fly ash, ground-granulated blast furnace slag, metakaolin and rice-husk ash are the most commonly precursors used to manufacture the alkali activated binders. The precursors activated with the alkalis of sodium hydroxide (NaOH) and sodium silicate (Na₂SiO₃) solutions in different proportions, in generally (Sarker et al. 2013; Phoo-ngernkham et al. 2016).

Geopolymers are determined a subset of alkali-activated binders by researchers. The binding phase of the geopolymers is mainly composed of alumino silicates. The chemical structure of the geopolymers are similar with the natural zeolites except of the amorphous microstructure (Davidovits, 1994). In addition, fly ashes have low calcium content and calcined clays are the most commonly used precursors for the geopolymer production (Rahier vd., 1997; Duxson vd., 2007).

Fly ash based geopolymers have high potential to be used as a construction material due to its comparable mechanical properties with ordinary Portland cement concrete. Due to this potential, the studies on the physical, mechanical and durability properties of geopolymers have been going on to reveal its suitability for using in the construction applications (Rangan, 2006; Hardjito et. al., 2004). Some researchers concluded that the fly ash based geopolymer cured at 60-80 °C show low drying shrinkage, high early compressive and flexural strength, high durability to chemical attacks and good fire resistance (Fernandez-Jimenez et al. 2006, Zhao and Sanjayan 2011, Sarker et al. 2014, Olivia and Nikraz, 2012, Hardjito et al. 2004). These characteristics clarify the geopolymers have a promising future for utilization in structural applications as a “green” material (Fan et. al., 2018). In addition, the parameters effecting the properties of fly ash based geopolymers such as; physical properties and chemical composition of fly ash, dosage of activator proportions and cure conditions etc. have been

investigated by many researchers to enhance the performance of geopolymer composites (Al Bakri et. al. 2011, Palomo et. al. 1999, Andini et. al. 2008, Provis et. al. 2010).

In this study, the potentials of fly ash supplied from Tunçbilek thermal power plant in Kütahya Turkey to manufacture geopolymer mortars has been investigated. For this purpose, mortar mixtures prepared with different sodium concentrations and Ms modulus. Thus, the changes on the mechanical properties of the geopolymer mortars according to these parameters were observed.

Materials and Methods

The precursor used to manufacture geopolymer mortars was supplied from Tunçbilek thermal power plant in Kütahya, Turkey. The properties of the fly ash were given in the Table 1.

TABLE 1. PROPERTIES OF THE FLY ASH

SiO ₂	Al ₂ O ₃	Fe ₂ O ₃	CaO	MgO	SO ₃	Spec. Gravity	Fineness, m ² /g
59.4%	20.6%	9.47%	2.12%	8.94%	0.79%	2.4	0.36

The fly ash was activated with the two activators named as sodium hydroxide (NaOH) and sodium silicate (Na₂SiO₃). The activators (Na₂SiO₃ and NaOH) were supplied from local resources. The NaOH used in the mixtures was in solid form and the Na₂SiO₃ was in liquid form. While the mortar mixtures were preparing, the solid alkali-activator NaOH was dissolved in some of the mix water. The Eskişehir tap water was used in the mortar mixtures. And also, the standard Rilem Cembureau sand was utilized to form mortar mixtures of geopolymers.

The mortar specimens were manufactured with a mortar mixture that composed of 450 g fly ash, 1350 g standard sand and 225 g water. The Na₂SiO₃ and NaOH were used in the mortar mixture as to the mixture consist 4%, 6% and 8% Na of fly ash content by weight. In addition, the Ms modulus (the total Na₂O/SiO₂ ratio of activators) of the activators was adjusted as 0.75, 1 and 1.25 in the mixtures. The 225 g water content was composed of the tap water and the water in the Na₂SiO₃.

The, fly ash, water, alkali activator and standard sand were placed into the mortar mixer, respectively. After placing the fly ash, water, and alkali activator, mortar mixer was adjusted to slow gauge and run for 30 seconds. While the mixer was running at slow gauge, sand was added to the mixture. After that, the mixer was run at fast gauge for 30 seconds. Finally, after waiting for 15 seconds, the mixer was run with fast gauge for 60 seconds and mixing process was ended. Then, the mixtures were compacted on vibrator table and placed in the prismatic moulds with the dimensions of 40×40×160 mm. In addition, the mortar mixtures were coded according to Na concentration and Ms modulus, respectively. For example, 6/1.25 mixture was composed of %6 Na content and made with 1.25 Ms modulus of alkali activators. The mix proportions of the fly ash based geopolymer mortars were shown in Table 2.

Table 2. mix proportions of THE geopolymer mortars

Mixture Code	Na (%)	Ms	Fly Ash (g)	Na ₂ SiO ₃ (g)	NaOH (g)	Sand (g)	Water (g)
4/1.25	4	1.25	450	106	19	1350	159
4/1	4	1	450	85	22	1350	172
4/0.75	4	0.75	450	64	24	1350	185
6/1.25	6	1.25	450	159	29	1350	126
6/1	6	1	450	127	32	1350	146
6/0.75	6	0.75	450	95	36	1350	165
8/1.25	8	1.25	450	212	38	1350	93
8/1	8	1	450	170	44	1350	119
8/0.75	8	0.75	450	128	48	1350	146

In this study, the unit weight values of the specimens were calculated before the flexural and compressive strength tests performed. The flexural strength tests performed on the 40×40×160 mm prismatic specimens whose unit weight values were measured. The compressive strength measurements were obtained by placing 40×40 mm plates to top and bottom of the specimens which were broken into two pieces during the flexural strength test. Strength measurements were performed according to the TS EN 1015-11/A1 2013 standard.

Results and Discussion

The unit weight values of hardened mortar mixtures were obtained according to the procedure as follows. Firstly, each specimen was weighed separately. Secondly, the means of weight values of three specimens were calculated to determine weight value of each mixture. Finally, unit weight value of each hardened mortar mixture was calculated with dividing the mean weight by the specimen volume. Hardened unit weight values of hardened mortar mixtures at the age of 7 days are given in Fig. 1. When this figure is examined, it can be seen that the unit weight values of geopolymer mortars are between 2.12 and 2.14 gr/cm³. While the unit weight values did not show a significant change with Ms modulus and Na concentration.

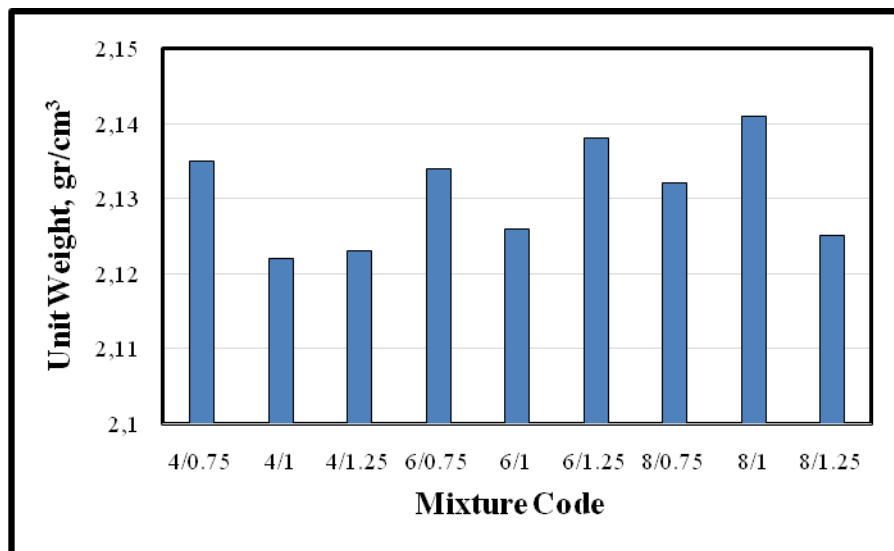


Figure 1. The unit weight values of fly ash based geopolymer mortars

The flexural strength values of the mortar specimens are given in the Figure 2. The values obtained by subjecting to three specimens belong to each mixture to the three-point flexural test. The flexural strength values of each mixture were calculated by the mean breaking load values of these three specimens. The flexural strength values of geopolymer mortars were between 1.1 and 8.4 MPa at the age of 7 days. According to the Figure 2, the values were increased with the Na content. And also, the values were raised with the increase in Ms modulus. So, the maximum flexural strength value was observed on the mortar mixtures have 8% Na content and made with the Ms modulus of 1.25. In addition, the flexural strength values of the mortar mixtures have 1.25 and 1 Ms modulus were increased sharply with increasing the Na content from 4 to 8. And also, the flexural values of the specimens composed of 6% and 8% Na were increased up to 80% and 100% with the increasing of Ms modulus from 0.75 to 1.25, respectively.

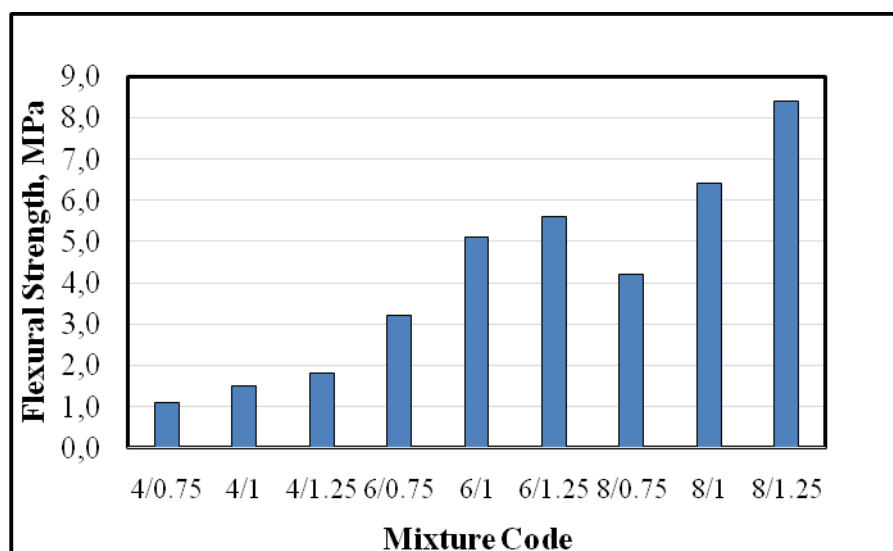


Figure 2. The flexural strength values of the mortars at the age of 7 days

The compressive strength values of each mixture were given in Fig. 3. According to the Fig. 3, the compressive strength values of the fly ash based geopolymer mortars increased with the Na content in the mixture. The values increased up to 260% with the increase of Na concentration from 4% to 8% in the mixtures composed of Ms 1.25. And also, compressive strength values increased with the raise of the Ms modulus. In the mixtures consist of 6% and 8% Na, the compressive strength of mortars increased with Ms up to 50% and 190%, respectively.

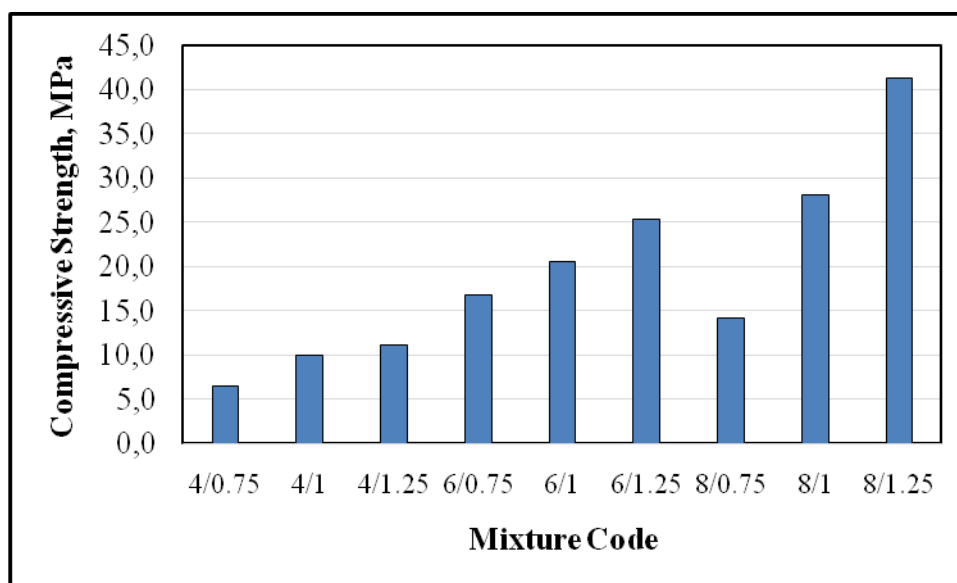


Figure 3. The compressive strength values of the mortars at the age of 7 days

Conclusion

In this study, an experimental research as to the mechanical properties of geopolymer manufactured using the class F fly ash and NaOH and Na_2SiO_3 alkaline activators under different Na concentrations and Ms modulus is performed. Based on the experimental results, the following conclusions can be drawn.

- The unit weight values of fly ash based geopolymer mortars changed between 2.12 and 2.14 gr/cm³ and the changes in these values were independent from the Ms modulus and Na concentration.
- The flexural strength of mortars increased with Na content and Ms modulus. The flexural strength of the mixture made with 8% Na and Ms modulus of 1.25 was reached to 8.4 MPa, at the ages of 7 days.
- While the maximum compressive strength value of mortar specimens made with 4% Na was 11.2 MPa, the value of mortar specimens composed of 8% Na was reached to 41.2 MPa in a short time of 7 days.
- The compressive strength of the fly ash based geopolymer mortars increased with the Ms modulus raise.

As a result of this study, it can be concluded that the Tunçbilek fly ash is suitable for to be a precursor for geopolymer production. Thus, the 8.4 MPa of flexural strength and 41.4 MPa of compressive strength obtained by activating of the fly ash in a short time of 7 days. In addition, investigation of the development of mechanical properties of the Tunçbilek fly ash based geopolymers with time and its durability performance can be proposed.

References

1. Pacheco-Torgal, Fernando, Joao Castro-Gomes, and Said Jalali. "Alkali-activated binders: A review: Part 1. Historical background, terminology, reaction mechanisms and hydration products." *Construction and Building Materials* 22.7, 2008, 1305-1314.
2. Hossain, M. M., et al. "Durability of mortar and concrete containing alkali-activated binder with pozzolans: A review." *Construction and Building Materials* 93, 2015, 95-109.
3. Sarker, Prabir K., Rashedul Haque, and Karamchand V. Ramgolam. "Fracture behaviour of heat cured fly ash based geopolymer concrete." *Materials & Design* 44, 2013, 580-586.
4. Phoo-ngernkham, Tanakorn, et al. "Compressive strength, bending and fracture characteristics of high calcium fly ash geopolymer mortar containing portland cement cured at ambient temperature." *Arabian Journal for Science and Engineering* 41.4, 2016, 1263-1271.
5. Davidovits, J. "High-alkali cements for 21st century concretes." *Special Publication* 144, 1994, 383-398.
6. Rahier, H., et al. "Low-temperature synthesized aluminosilicate glasses." *Journal of Materials Science* 32.9 1997, 2237-2247.
7. Duxson, Peter, et al. "Geopolymer technology: the current state of the art." *Journal of materials science* 42.9 2007, 2917-2933.
8. Rangan BV. Studies on low-calcium fly ash-based geopolymer concrete. *Indian Concr J* 2006, 80:9-17.
9. Hardjito D, Wallah SE, Sumajouw DMJ, Rangan BV. On the development of fly ash-based geopolymer concrete. *ACI Mater J* 2004;101(6):467-72.

10. A.M. Fernandez-Jimenez, A. Palomo, C. Lopez-Hombrados, Engineering properties of alkali-activated fly ash concrete, *ACI Mater. J.* 103 (2), 2006, 106–112.
11. R. Zhao, J.G. Sanjayan, Geopolymer and Portland cement concretes in simulated fire, *Mag. Concr. Res.* 63 (3), 2011, 163–173.
12. Prabir Kumar Sarker, Sean Kelly, Zhitong Yao, Effect of fire exposure on cracking, spalling and residual strength of fly ash geopolymer concrete, *Mater. Des.* 63, 2014, 584–592.
13. M. Olivia, H. Nikraz, Properties of fly ash geopolymer concrete designed by Taguchi method, *Mater. Des.* 36, 2012, 191–198.
14. D. Hardjito, S.E. Wallah, D.M.J. Sumajouw, B.V. Rangan, On the development of fly ash-based geopolymer concrete, *ACI Mater. J.* 101 (6), 2004, 467–472.
15. Fan, Fenghong, et al. "Mechanical and thermal properties of fly ash based geopolymers." *Construction and Building Materials* 160, 2018, 66-81.
16. Al Bakri A.M.M, Kamarudin H., Bnhussain M., Khairul N. I., Rafiza A.R., Zarina Y., *Journal of Engineering and Technology Research.* 3 (2), 2011, 44.
17. Palomo A., Grutzeck M.W., Blanco M.T. *Cem. Concrete Res.* 29 (8), 1999, 1323.
- 18 Andini S., Cioffi R., Colangelo F., Grieco T., Montagnaro F., Santoro L., *Waste Manage.* 28(2), 2008, 416.
19. Provis J.L., Duxon P., van Deventer J.S.J., *Adv. Powder Technol.* 21(1), 2010, 2.

CEMENT, CONCRETE AND JEOPOLYMERS

INVESTIGATION OF HYDRATION PROPERTIES OF SLAG-BLENDED CEMENTS

Abdullah Demir¹, M.Uğur Toprak², EdaTaşçı³

¹Kütahya Dumlupınar University, Faculty of Engineering, Department of Civil Engineering, Center
Campus, Kütahya/ Turkey

²Kütahya Dumlupınar University, Faculty of Engineering, Department of Civil Engineering, Center
Campus, Kütahya/ Turkey

³Kütahya Dumlupınar University , Department of Metallurgy and Materials Engineering, Kütahya/
Turkey

Due to the complex interactions between clinker and slag; the addition of slag affects the hydration process and so the amount, composition and physico-chemical properties of the hydrated phases. In this paper, hydration properties of slag blended cements were investigated through XRD and FT-IR analysis at 3, 7 and 28 days. Three substitution rates of cement by slag were used (10, 20 and 30%). Furthermore by SEM, 28-days microstructure were determined and evaluated together with compressive strength results. It is observed that the substitution of slag has increased the setting time, necessitated smaller amount of water demand and consumed Ca(OH)_2 during the hydration.

Keywords: Slag, Cement, Hydration, Microstructure, FT-IR.

1. INTRODUCTION

The improvement of the cement industry came with a couple problems, whereby the production of a ton of Portland cement clinker oscillates at around 0.97 tons of CO_2 . This makes the cement industry responsible for 7% of CO_2 emissions [1]. Energy efficient way for reducing environmental problems and also gaining technological and economic advantages is the increasing usage of industrial by products and wastes in cement and concrete industry. Slag cements results in resource conservation, reducing energy consumption and minimizing emission of green house gases, especially CO_2 [2-7]. Blast furnace slag (BFS), a solid waste material, is a co product in iron making and is composed primarily of CaO , SiO_2 , Al_2O_3 and MgO . Molten slag, which is discharged from the blast furnace, is cooled highly rapid by water quenching. BFS solidifies into a glassy and granular form to produce a sand-like product [8]. BFS is said to undergo both a pozzolanic reaction and a latent hydraulic reaction. [9-11]. The partial replacement of cement by BFS reduced the electrical charge passing

through the concrete (during the rapid chloride penetration test) and the water permeability of concrete. This was the result of BFS reacting with water and Portlandite to form extra calcium silicate hydrate (C-S-H) gel and more refined microstructure [12, 13].

Toyoharu [14] claimed that the hydration of C_3S in blended cement accelerated by the presence of BFS. This implies that BFS play the role of precipitation site of C-S-H which is the hydrate of C_3S . The capillary porosity of BFS blended cement pastes is larger at lower hydration degree, and remarkably decreases as its hydration progresses. Gel water in BFS paste increase nonlinearly with the hydration degree of BSF. This implies that C-S-H produced from BFS hydration at later age has larger amount of gel water and becomes lower density, can fills in large pores more efficiently. In the present study, optimum usage of slag in cement was evaluated considering early and later age SEM, XRD and FTIR analysis and compressive strength tests.

2. MATERIALS AND METHOD

Portland cement CEM I 42.5 (OPC) from Çimsa Cement Factory/ESKİŞEHİR and blast furnace slag (BFS) from Ereğli Iron and Steel Plant/ZONGULDAK were used in this study. Separate grinding has the advantage of grinding BFS and clinker on their optimum fineness. Blaine fineness of OPC was $3378 \text{ cm}^2/\text{g}$. BFS was ground up to $3412 \text{ cm}^2/\text{g}$ (fineness close to OPC) in order to compensate the effects of fineness on specimens. OPC consist of 63.58% CaO, 21.30% SiO_2 while BFS comprises 34.68% SiO_2 , 14.19% Al_2O_3 , 39.58% CaO ve 7.48% MgO. BFS has 24.27% amorf SiO_2 . Amorf/total SiO_2 ratio is 69.98%. According to Bogue formulations OPC consist of C_3S 58.09%, C_2S 17.24%, C_3A 4.88% and C_4AF 8.18%.

To determine the compressive strength, mortar series were prepared in a mortar mixer, with a water/cement ratio of 2:1 and cement/aggregate ratio of 1:3. Mortars were water-cured till the experiment day. Microstructure versus mechanical properties of slag substituted cement is investigated through unit weight, ultrasound velocity and uniaxial compressive strength (TS-EN 196-1), SEM, XRD, FTIR (on fractured paste parts of comp. strength specimens, at 3, 7 and 28 days. Three substitution rates of OPC by BFS were used (10, 20 and 30%) and these series are labeled as BFS10, BFS20 and BFS 30 respectively.

3. RESULTS AND DISCUSSION

SEM images of different (0, 10, 20 and 30%) BFS substituted specimens at 28 d are given in Fig. 1 a,b,c and d respectively. Ca(OH)_2 crystals embedded in C-S-H gel can be observed in SEM images of BFS10, which confirm the results of XRD.

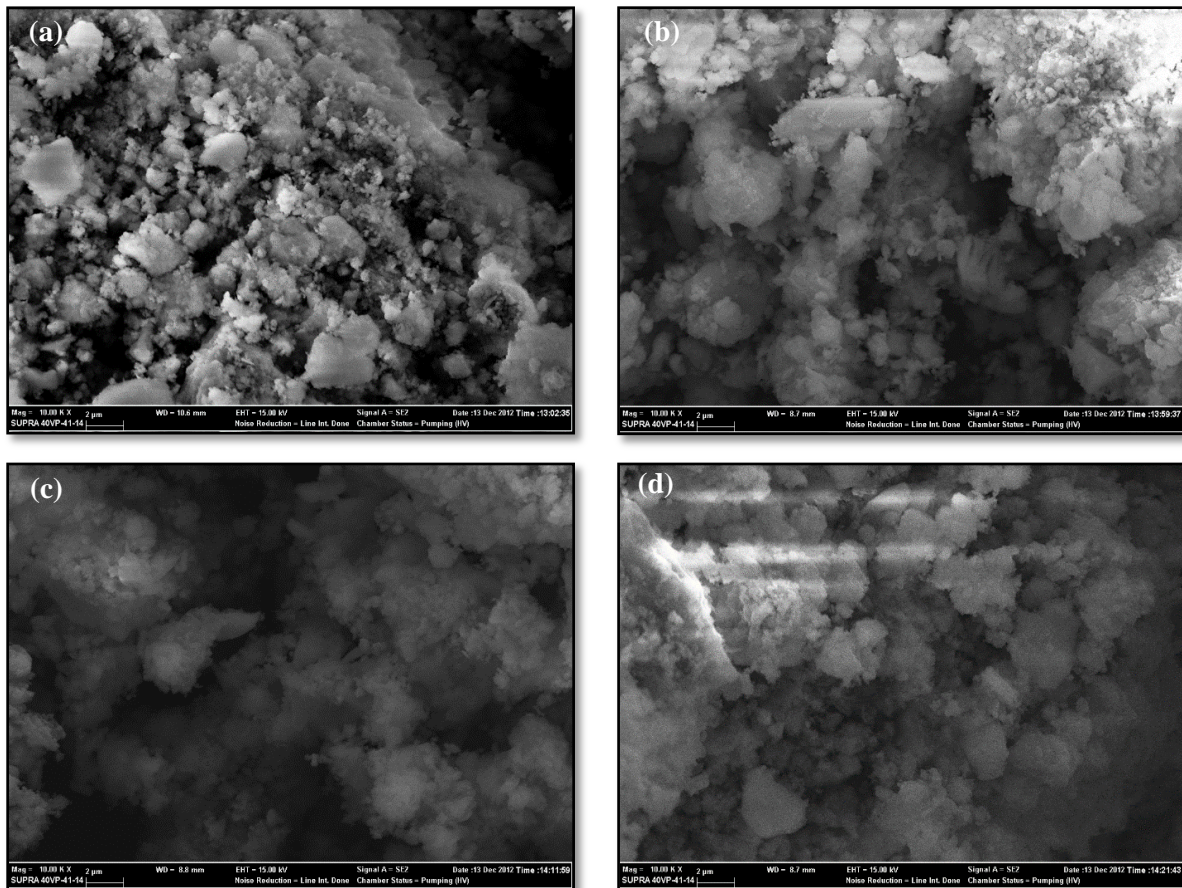


Fig. 1 SEM images of OPC (a) , BFS10 (b), BFS20 (c) and BFS30 (d)

It's clearly seen that BFS plays the role of precipitation site of C-S-H (BFS20 and BFS30). Besides, $\text{Ca}(\text{OH})_2$ seems to be consumed in BFS20 and BFS30 series. Thus, the microstructure of BFS series seems much denser than that of OPC. However, significant amounts of unreacted slag is also noticeable in Fig 1.d, which can explain the lower compressive strength of BFS30 series. Verification by comp. strength experiment showed good agreement with SEM observations.

Compared with cement, the hydration rate of slag cement is slightly slow at room temperature, resulting in low early strength but high strength development at later age. This is primary attributed to the small mass fraction of clinkers thereby the content of C_3A and C_3S are reduced, which feature by faster hydration rate and higher hydration heat [15]. Besides, The hydration of BFS, in the presence of Portland cement, depends greatly upon the breakdown and dissolution of glassy slag structures by hydroxide anions generated by the cement clinkers hydration [16].

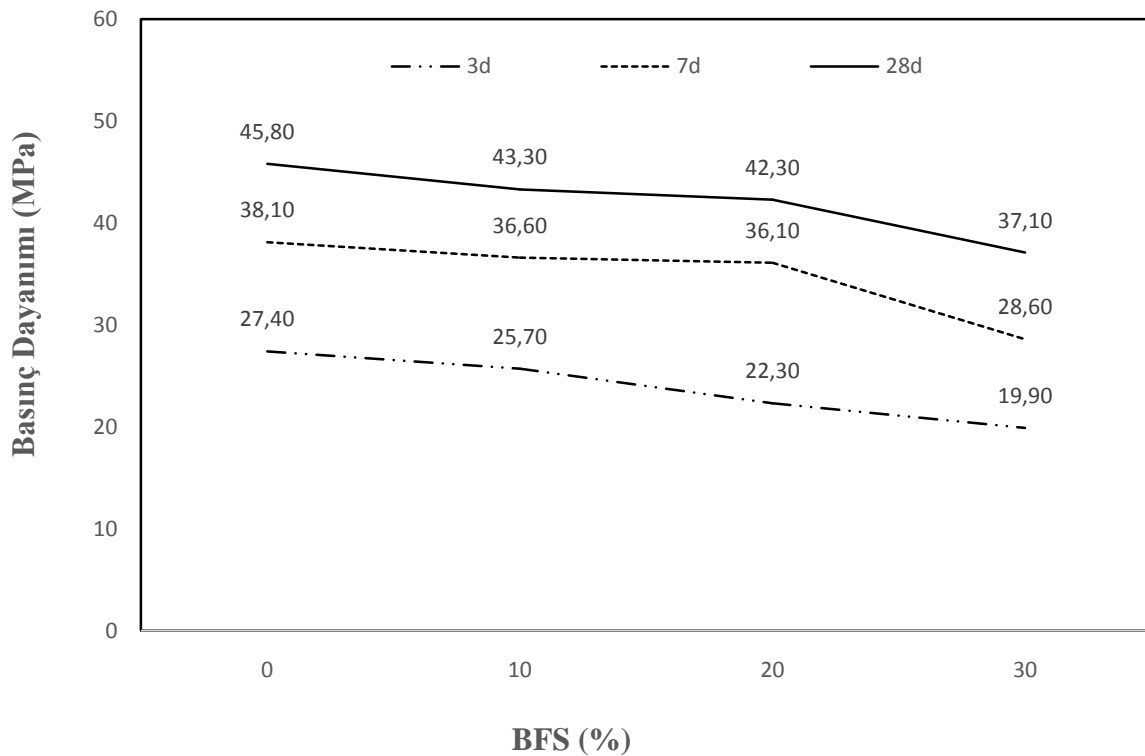


Fig. 2 Effect of BFS (%) on Compressive strength

High (30%) replacement of OPC by BFS causes a notable deterioration (25 and 19%) of the compressive strength at 7 and 28 d. This also proves that comp. strength development enhances at later ages of hydration. For 10 and 20% BFS substitution, comp. strength values were close to OPC comp. strength at 7 and 28 d.

Figure 3, 4, 5 shows the XRD patterns of the blended cements. Hydrated cement paste includes: hydration products Portlandite (CH), calcium silicate hydrate (C-S-H) and unhydrated clinker minerals (C_3S and C_2S). The OPC paste has CH peak with a higher value than the others. The hydration products of BFS substituted cements were similar to those of OPC at the age of 28 days except for the differences in their intensity of diffraction peaks. The comparison of the integrated intensities belonging to the CH phase ($17-19^\circ 2\theta$ to $45-50^\circ 2\theta$) indicates that the content of CH decreases with time. For all hydration times, the CH content is highest in the OPC samples, which leads to the conclusion that the addition of pozzolans reduces the content of free CH. The results of the FTIR analysis confirm the XRD measurements. In addition, characteristic peaks for calcite was also detected in OPC and BFS. At the age of 7 and 28 d, the main products were almost the same except the characteristic peak intensity of $Ca(OH)_2$ labeled as (CH) in XRD patterns. During the hydration; CH was enhanced in OPC while it was weakened in BFS substituted samples. Because production of CH increased in OPC samples while the production rate of CH by clinker was much slower than its consumption rate by BFS. C_3S and C_2S (labeled as A and B) were consumed during the hydration reaction, which resulted in the formation of C-S-H and CH phases. In BFS10, BFS20 and BFS30 there

was a significant decrease in the peaks of A and B with the progress of hydration. In BSF 20, the level of the CH was very high on 3 hydration day, and indicating that the BFS has not consumed CH. Therefore the BFS contributed little to the early strength.

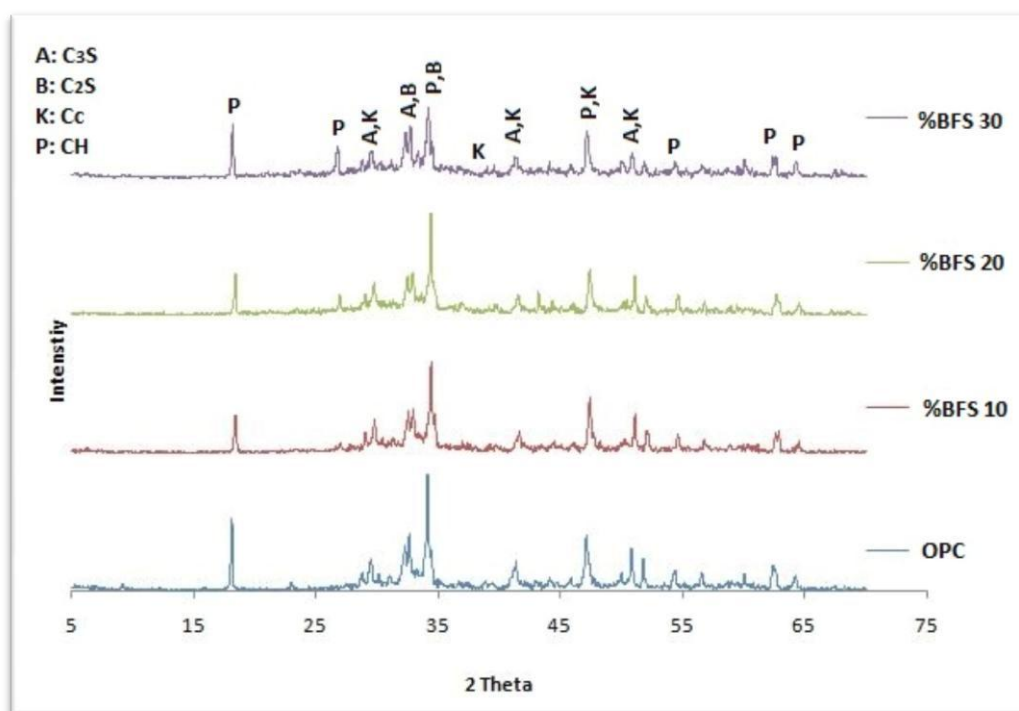


Figure 3. X-ray diffraction patterns (3 d)

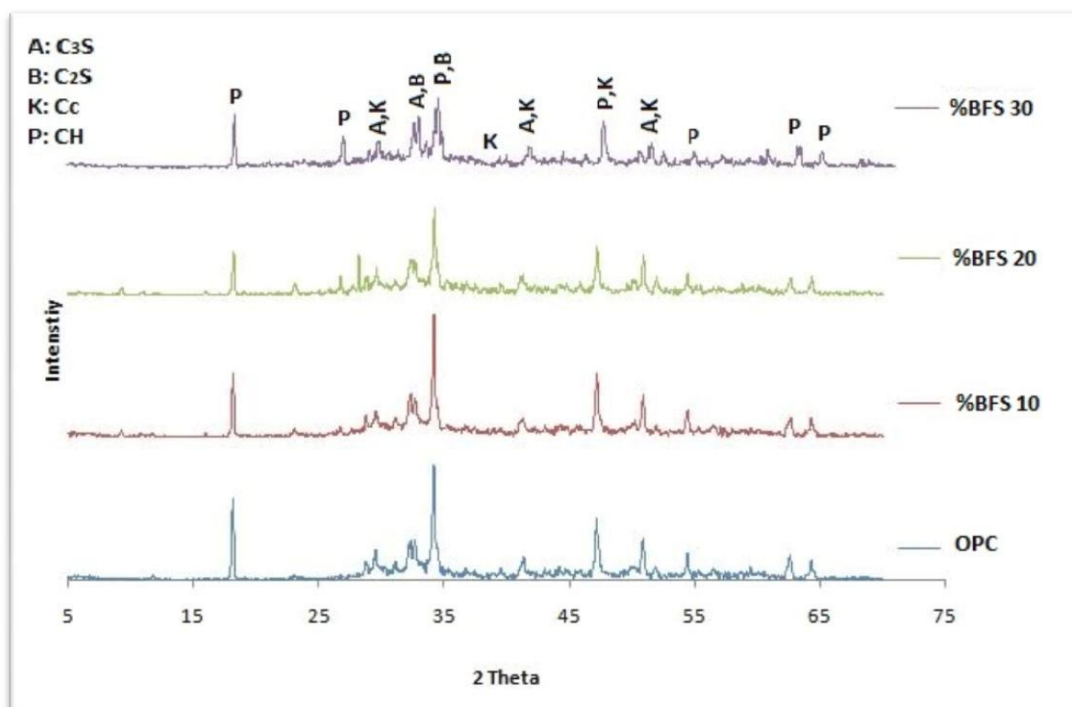


Figure 4. X-ray diffraction patterns (7 d)

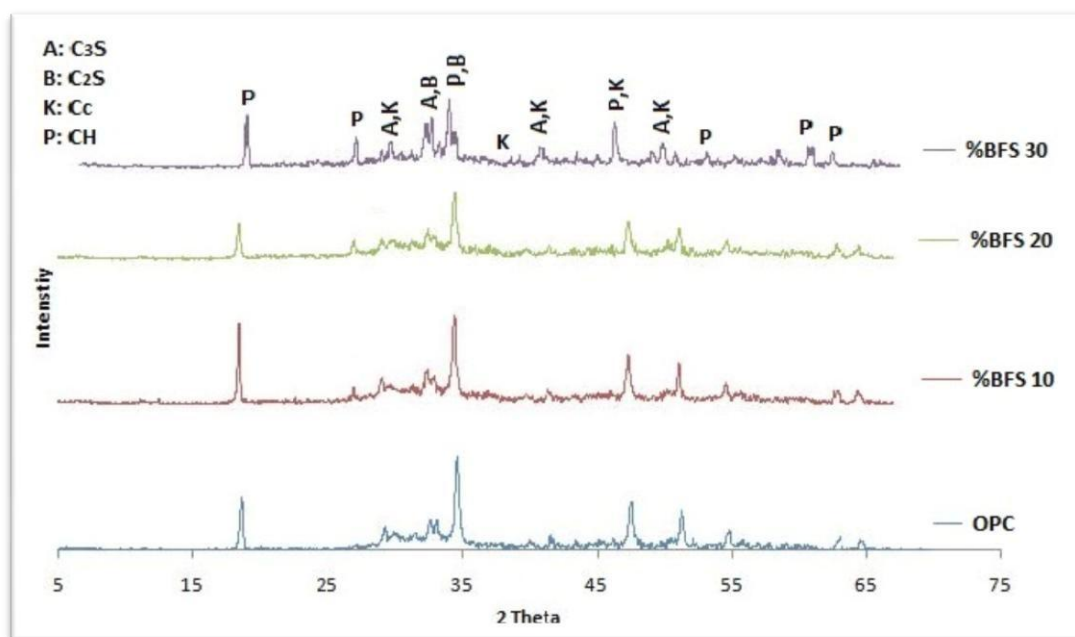


Figure 5. X-ray diffraction patterns (28 d)

FT-IR analyses can be used to define molecule groups in particle. In the FT-IR studies related to cement and pozzolan, the infrared spectrum is considered in mainly 4 wide band region. They are composed of peaks corresponding to the deviation in Si-Al, S, C and OH bonds. [17,18]. Besides, the differences in the number of vibrations in this wave length can be evaluated locally. Surface structures of the molecules for different ratios of BFS blended cement were determined from the FT-IR results (Figure 6, 7 and 8). The unhydrated calcium silicates peak intensity at $\sim 465 \text{ cm}^{-1}$ in OPC was higher than BFS10 and BFS20 and it gets lower by time for all series. This indicates that hydration promotes with time. The structure of C-S-H gel is very complex with a variable Ca/Si ratio corresponding to different molecular structures. In hydrated cement pastes, the main mid FT-IR bands for C-S-H gels appear at $\sim 975 \text{ cm}^{-1}$ (Si-O stretching vibrations), $675\text{-}680 \text{ cm}^{-1}$ (Si-O-Si bending vibration) and $457\text{-}468 \text{ cm}^{-1}$. These mid FT-IR bands change systematically in frequency and/or intensity with Ca/Si ratio in C-S-H. The C-O stretching at around 1430 cm^{-1} is characteristic band of CO_3^{2-} . The wide absorption band at wave number $2800\text{-}3700 \text{ cm}^{-1}$ represents existence of CaCO_3 , which shows the trend of weakening with the progress of hydration.

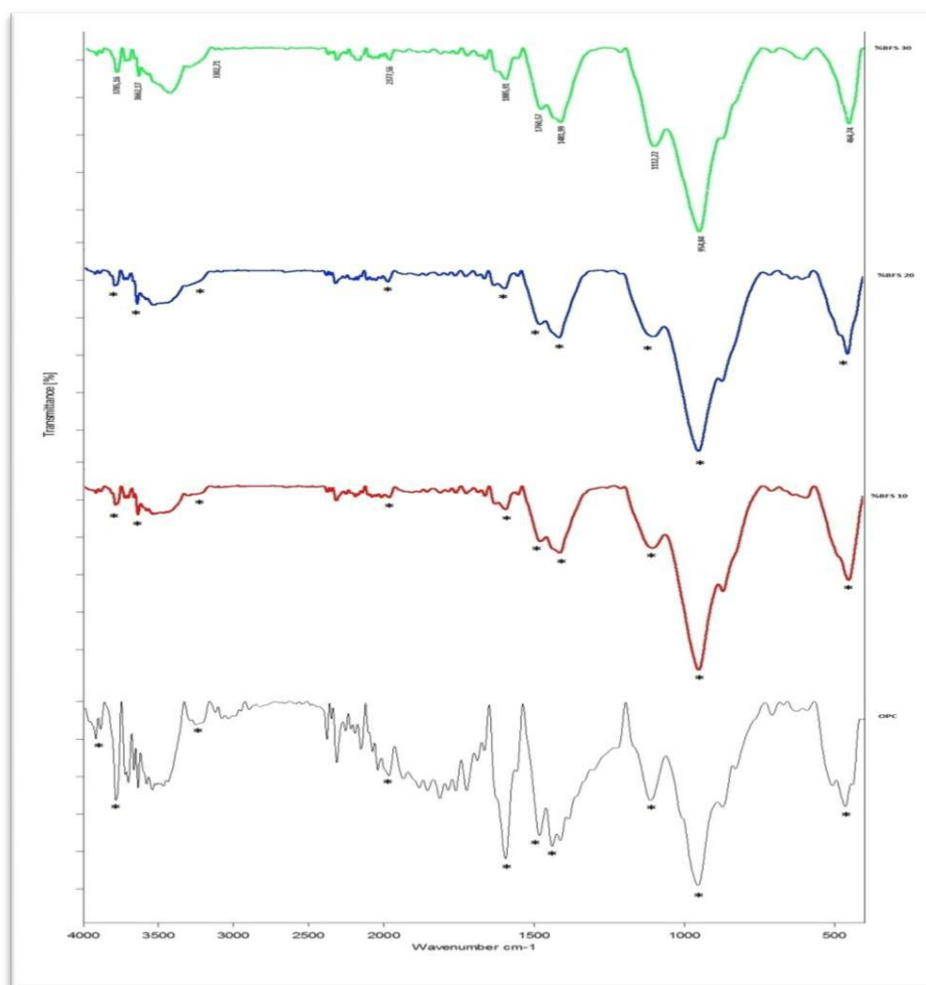


Figure 6. FT-IR spectrum analysis (3 d)

A broad band centered at $\sim 3400\text{ cm}^{-1}$ is due to symmetric and antisymmetric stretching vibration of water bound in hydrations products. With the progression of hydration these peaks decreased. A small but defined peak appeared at $3600\text{--}3647\text{ cm}^{-1}$ in 28 day samples can be attributed to the OH band from calcium hydroxide [19-21]. The max peak of $\text{Ca}(\text{OH})_2$ was seen at 3 day OPC sample. We also observed that it has decreased considerably with time. Calcium carbonate (CaCO_3) were detected by XRD. The presence of calcium carbonate is attributed to both the carbonate in the cement blend fraction (because the addition of limestone to the cement) as well as the potential carbonation of samples by the environment.

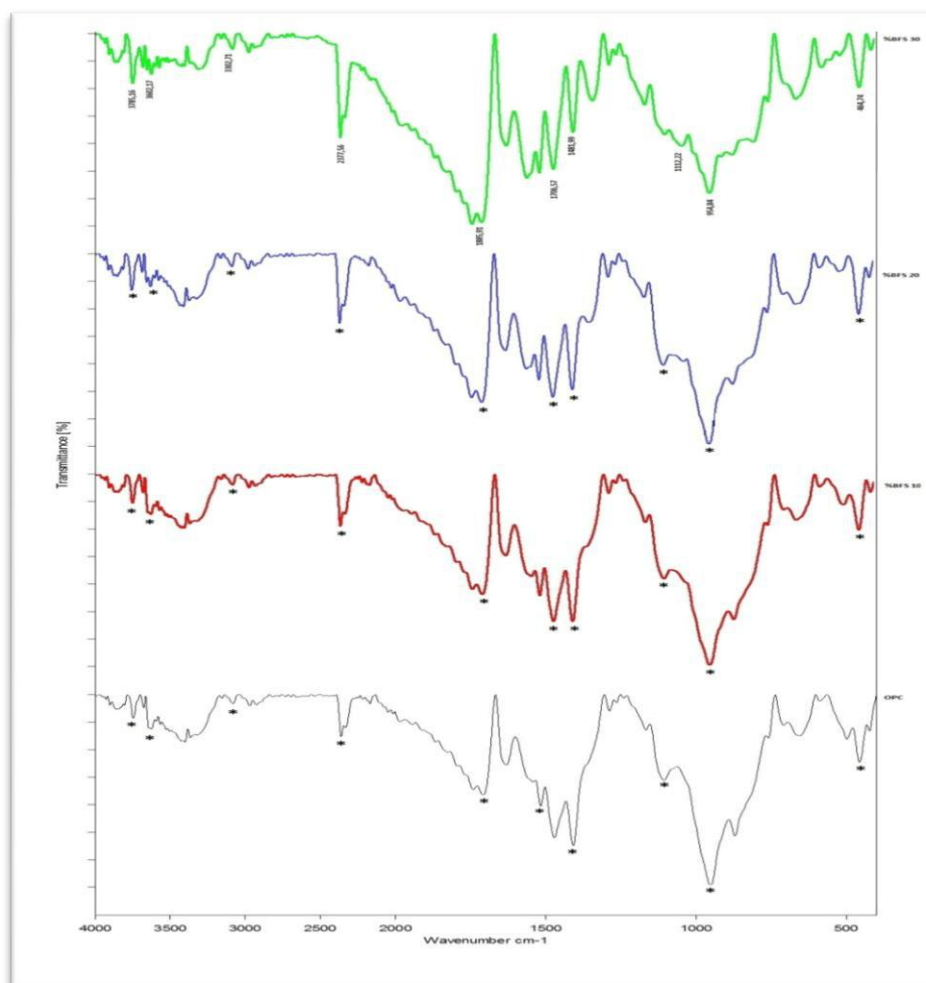


Figure 7. FT-IR spectrum analysis (7 d)

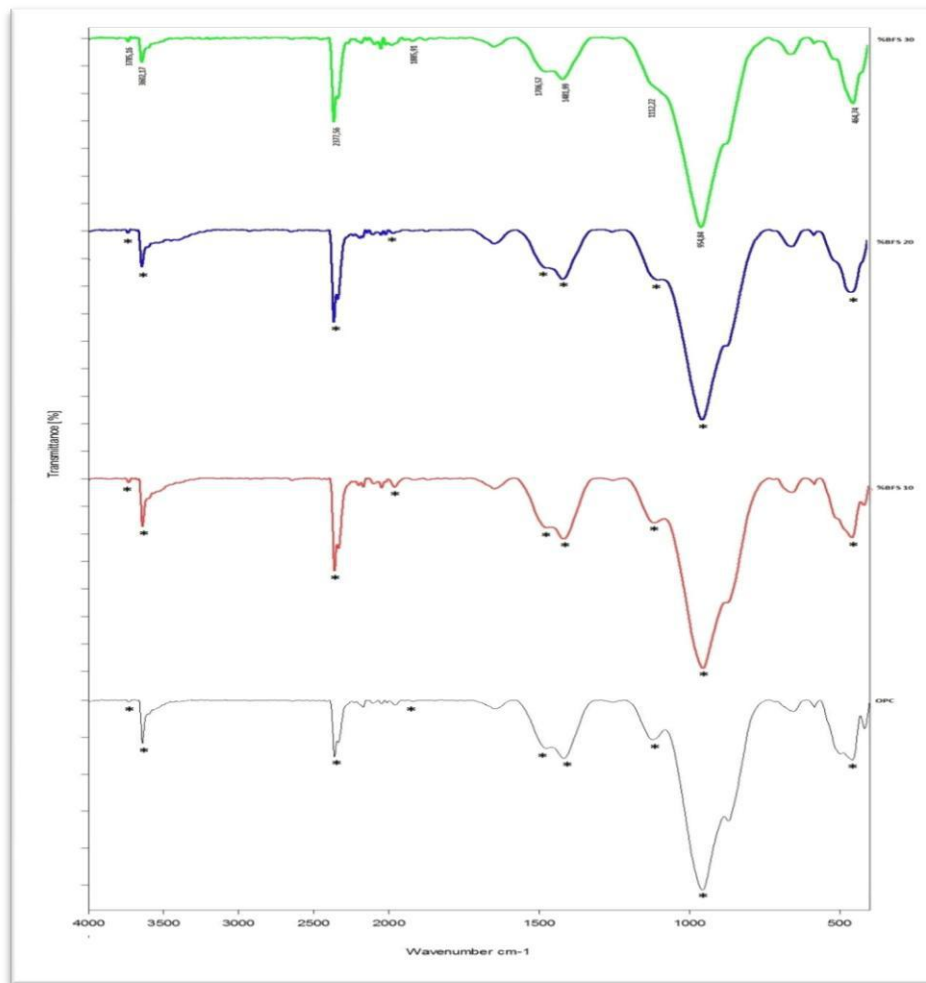


Figure 8. FT-IR spectrum analysis (28 d)

4. CONCLUSION

The results indicate that the substitution of BSF can lead to an increase C-S-H structure. In SEM observations, unreacted grains, C-S-H, CH structure and the porosity of the samples were evaluated. Microstructure of BFS10 and BFS20 were much denser than that of OPC at 28d. For 10 and 20% BFS substitution, comp. strength values were close to that of OPC series at 7 and 28 d. During the hydration; CH was enhanced in OPC while it was weakened in BFS substituted samples. It was revealed that the unhydrated calcium silicate peaks can be followed by FT-IR for evaluating the hydration degree of cement based binders.

Acknowledgements

We acknowledge the BAP Proje no. 2012-5 for measurements. We owe our special thanks to Buğra Asıltaş and Musa Akman for kind support during analyses.

REFERENCES

- [1] Mehta, P.K., Reducing the Environmental Impact of Concrete, Concrete International, Vol. [23], 10, (2001), 61-65.
- [2] L. Dongxu, W. Xuenquan, S. Jinlin, W. Yujiang The influence of compound admixtures on the properties of high-content slag cement Cem. Concr. Res., 30 (2000), pp. 45-50
- [3] E.E. Hekal, S.A. Abo-El-Enein, S.A. El-Korashy, G.M. Megahed, T.M. El-Sayed Hydration characteristics of Portland cement–electric arc furnace slag blends HBRC J., 9 (2013), pp. 118-124
- [4] S. Kumar, R. Kumar, A. Bandopadhyay Innovative methodologies for the utilization of wastes from metallurgical and allied industries Resour. Conserv. Recycl., 48 (2006), pp. 301-314
- [5] S. Kumar, R. Kumar, A. Bandopadhyay, T.C. Alex, B. Ravi Kumar, S.K. Das, S.P. Mehrotra Mechanical activation of granulated blast furnace slag and its effect on the properties and structure of portland slag cement Cem. Concr. Compos., 30 (2008), pp. 679-685
- [6] J.L. Marriaga, P. Claisse, E. Ganjian Effect of steel slag and Portland cement in the rate of hydration and strength of Blast furnace slag pastes J. Mater. Civ. Eng., 23 (2) (2011), pp. 153-160
- [7] F. Bellmann, J. Stark Activation of blast furnace slag by a new method Cem. Concr. Res., 39 (2009), pp. 644-650
- [8] D.M. Sadek, Effect of cooling technique of blast furnace slag on the thermal behavior of solid cement bricks, J. Cleaner Prod. 79 (2014) 134–141.
- [9] Abdelkader Bougara, Cyril Lynsdale, Neil B.Milestone, The influence of slag properties, mix parameters and curing temperature on hydration and strength development of slag/cement blends Construction and Building Materials Volume 187, 30 October 2018, Pages 339-347
- [10] Xiang Ming Zhou, Joel R. Slater, E. Stuart Wavell and olayinka oladiran, effects of PFA AND GGBS on early-ages engineering properties of Portland cement systems J. Adv. Concr. Tech., 10 (2012), pp. 74-85
- [11] J.I. Escalante-Garcia, J.H. Sharp Effect of temperature on the hydration of the main clinker phases in Portland cement: part II, blended cements Cem. Concr. Res., 28 (1998), pp. 1259-1274
- [12] AliAllahverdi AfsanehMaleki MostafaMahinroosta Chemical activation of slag-blended Portland cement Journal of Building Engineering Volume 18, July 2018, Pages 76-83
- [13] M.D.A. Thomas, A. Scott, T. Bremner, A. Bilodeau, D. Day Performance of slag concrete in marine environment Acids Mater. J., 105 (6) (2008), pp. 628-638

- [14] Toyoharu Nawa, Characterization and Modeling of Hydration and Microstructure Formation for Blast Furnace Slag Cement, Fourth International Conference on Sustainable Construction Materials and Technologies, Las Vegas, USA, August 7-11, (2016)
- [15] Bellmann, F., Stark, J. Activation of Blast Furnace Slag by A New Method Cement and Concrete Research 39 2009: pp. 644 – 650. Shuhua LIU , Weiwei HAN, Qiaoling LI , Hydration Properties of Ground Granulated Blast-Furnace Slag (GGBS) Under Different Hydration Environments ISSN 1392–1320 MATERIALS SCIENCE . Vol. 23, No. 1. 2017]
- [16] Toutanji, H., Delatte, N., Aggoun, S. Effect of Supplementary Cementitious Materials on the Compressive Strength and Durability of Short-Term Cured Concrete Cement and Concrete Research 34 2004: pp. 311 – 319. So the strength development enhances at later ages.
- [17] Varast MJ, De Buergo MA, Fort R. Natural cement as the precursor of Portland cement: methodology for its identification. Cement and Concrete Research 2005;35;2055-65.
- [18] Puertas F, Fernandez-Jimenez A. Mineralogical and microstructural characterisation of alkali-activated fly ash/slag pastes. Cement and concrete Composition 2003;25;287-92.
- [19] Mozgawa W. The relation between structure and vibration spectra of natural zeolites J. Mol Structure 2001;599;129-37.
- [20] Hidalgo A, Petit S, Domingo C, Alonso C, Andrade C, Microstructural characterization of leaching effects in cement pastes due to neutralisation of their alkaline nature Part 1: Portland cement pastes. Cement Concrete Research 2007;37;63-70
- [21] Yılmaz B, Ertün T, Uçar A, Öteyaka B, Önce G, A study on the effect of zeolites (clinoptilolite) on volcanic tuff blended cement paste and mortars. Mag concrete Reseach 2009; 61(2):133-42.

CEMENT, CONCRETE AND JEOPOLYMERS

THE ROLE OF CHEMICAL ADMIXTURES IN READY MIXED CONCRETE MIXTURES

Ömer Arıöz¹, Evren Arıöz²

¹ Hasan Kalyoncu University, Faculty of Engineering, Department of Civil Engineering/Gaziantep/Turkey

² Eskişehir Technical University, İki Eylül Campus, Faculty of Engineering, Department of Chemical Engineering, 26555/Eskişehir/Turkey

ABSTRACT

Ready mixed concrete (RMC) is a composite material consists of cement, water, aggregate and if required chemical admixtures, mineral admixtures, and fibers. RMC is the most widely consumed construction material all over the World. The increasing population of the World causes the need of living and industrial areas hence concrete. Increasing demand of concrete requires enhanced performance related to workability, strength, and durability. In many projects, value added products of RMC are demanded recently. Since the research and investigations on the chemical admixtures may give many important properties to RMC, chemical admixtures have been used in almost every RMC mixture in recent years. Most widely used chemical admixtures for RMC solutions are generally classified as dispersing admixtures, retarding admixtures, accelerating admixtures, and air entraining admixtures. There are also some other chemical admixtures for different solutions such as waterproofing and inhibiting corrosion. In this paper, most widely used chemical admixtures in RMC operations were evaluated and the answers to the questions how they work and what they are able to do were given.

Keywords: Ready mixed concrete, chemical admixtures, workability, strength, durability.

1. INTRODUCTION

Ready mixed concrete (RMC) is a composite material produced by mixing together cement, water, fine and coarse aggregate and if required chemical admixtures, mineral admixtures, and in some cases fibers in an automated mixers, and then delivered to the customer in fresh state [1]. RMC is most widely used construction material all over the world [2]. RMC is a different construction material which is plastic normally 2-3 hours and after setting-hardening it is elastic. In other words, it is in a fresh state in a few hours, then hardened state. Therefore in both states, RMC should satisfy demanded properties. This is the answer for the question “what is good RMC?” The stages and relevant properties of RMC are summarized in Figure 1.

Fresh State	Hardened State
Workability	Strength
Consistency	Durability
Setting time	Volume stability
Unit weight	
Bleeding	
Segregation	
Uniformity	

Figure 1. Stages and relevant properties of RMC

The requirements of RMC are somewhat complex, however the aim is to produce the most economical combinations of raw materials of RMC that will satisfy the performance requirements and specifications [3]. A properly designed RMC mixture should be adequately workable when it is still in fresh state and it should have an appropriate setting time to allow a proper consolidation and finishing. Moreover, a properly designed RMC should also fulfill the required strength parameters and possess good durability.

Workability is defined as the effort required to place a RMC mixture and it is determined largely by the overall work needed to initiate and maintain flow. The flowability of fresh RMC affects the effort required to pump, to place and to compact RMC. In other words, the easier the flow, the less work is required to pump, place and compact concrete. The initiation and continuation of the flow depends on the rheological properties of the cement paste, internal friction between the aggregate particles, and external friction between RMC and formwork. Workability of RMC includes two parameters consistency and cohesiveness. Consistency describes how easily concrete flows while cohesiveness reflects the ability of fresh ready mixed concrete to hold all the ingredients together uniformly. A cohesive fresh RMC should have two important capacities; the water-holding capacity which is the opposite of bleeding and the coarse aggregate-holding capacity which is the opposite of segregation [4]. Therefore, workability of freshly ready mixed concrete can be defined as the property which determines the ease of mixing, transporting, pumping, placing, compacting, and finishing of RMC without segregation and excess bleeding, and excessive amount of effort.

Strength, durability and volume stability are the hardened RMC properties which should satisfy the demands. The compressive strength is the maximum resistance to axial loads applied on a hardened RMC sample. For a normal strength RMC mixture, compressive strength is inversely related to the water/cement ratio of the mixture. For fully compacted RMC mixtures, strength and other desirable properties are governed by amount of mixing water per cement. The relationship between the compressive strength of RMC and water/cement ratio of the mixture is shown in Figure 2. Other than water/cement ratio, compressive strength of RMC depends on some factors such as the properties of cement and cementitious materials, level of hydration reactions between water and cement, curing and ambient conditions, and the age of the sample [5]. However, these factors will also produce similar relationships with similar shapes which can be shown in Figure 2.

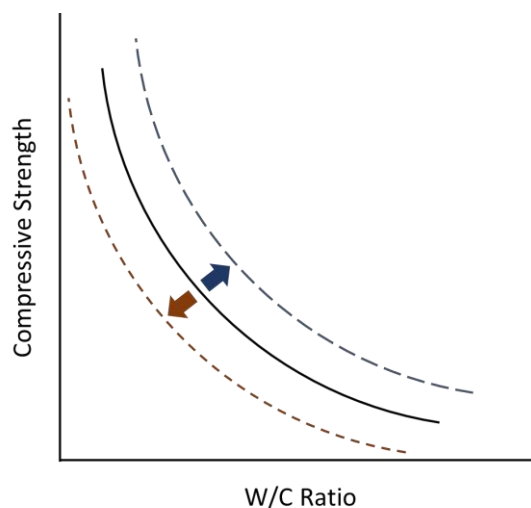


Figure 2. The relationship between the compressive strength and water/cement ratio of RMC

Compressive strength is the most commonly used test to measure the quality of RMC. Although this is an important characteristic, durability, permeability and resistance to weather conditions are often equally prevalent, especially in the life-cycle design of structures. Durability is the resistance of RMC

against to environmental and aggressive effects [6]. In other words, RMC should possess demanded behavior for a long time with requiring little or no maintenance. Durable RMC will retain its original form, quality, and serviceability when exposed to aggressive environments. Although the compressive strength is a measure of durability, stronger concrete may not be more durable in each cases. Therefore, in addition to strength of RMC, environmental and exposure conditions become an important consideration for durability. Generally cracks are formed by volume changes and they are responsible for disintegration of RMC. It should be marked that permeability is the contributory factor for volume change of RMC and higher water/cement ratio is the most important cause of permeability. Therefore, water/cement ratio is the fundamental parameter for the durability of RMC. High water/cement ratio, permeability, volume change, cracks, disintegration, and failure are the points of cyclic process of RMC [7]. Figure 3 indicates this cyclic process for durability of RMC.

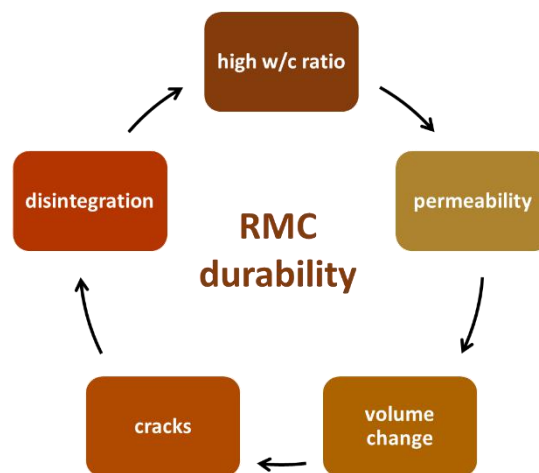


Figure 3. Cyclic process for durability of RMC

Finally, Figure 4 indicates factors related to workability, strength, and durability of RMC which are considered to produce “good RMC”.

Workability	transportation type and duration characteristics and quantity of binder quantity of mixing water ambient temperature ready mixed concrete temperature gradation of aggregate shape and surface texture of aggregate chemical admixtures
Strength	water/cement ratio compaction level of concrete
Durability	permeability material selection proper compaction adequate curing

Figure 4. Factors related to workability, strength, and durability of RMC

2. CHEMICAL ADMIXTURES FOR RMC

Chemical admixtures for RMC are defined as the materials other than cement, water, and aggregates added to batch immediately before or during mixing operation in order to develop or modify the properties of fresh and hardened properties of RMC. The main reasons to use chemical admixture in the production of RMC are reducing the costs of concrete structures, providing some properties effectively, retaining RMC quality during mixing, transporting, placing, and curing operations especially in extreme weather conditions, and overcoming some difficult problems faced during concreting operations [5]. Although the chemical admixtures affect the fresh properties, the benefits of using chemicals are often in hardened state. Chemicals change the fresh RMC properties in ways of changing water demand, hydration rate, air content, or plastic viscosity. One of these effects is the main effect for which the admixture is being used. However, the admixture may influence other fresh properties and these are called secondary effects [8]. Then, chemical admixtures can be divided into following groups; plasticizers, retarders and accelerators, air entraining admixtures, and others for special purposes such as corrosion inhibitors, coloring admixtures, alkali-silica reactivity inhibitors, etc. Plasticizers are the most widely used chemical admixtures used in RMC production. Placing properties of RMC can be improved by using plasticizing admixtures without changing the water/cement ratio of the mixture [9]. Figure 5 indicates the reasons for the use of plasticizers in RMC production.

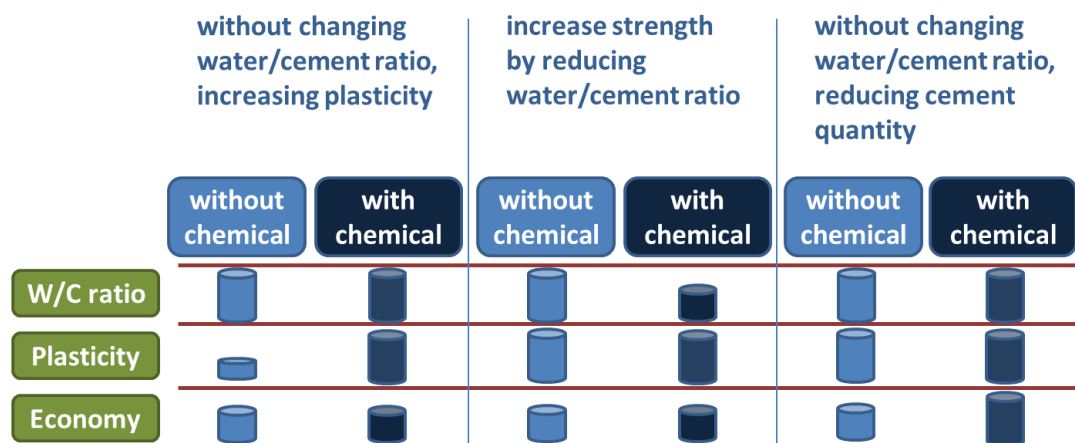


Figure 5. Reasons for the use of plasticizers in RMC production

The effectiveness of the chemical admixtures are dependent on the type and amount of cement and binding materials, the quantity of mixing water, shape and gradation of aggregate, mix proportions, temperature, slump value, and mixing duration of RMC [10]. The purpose of use of water in RMC mixture is two folds; to make reaction with cement giving binding property and to give workability to the mixture. Table 1 summarizes basic ingredients of RMC and their quantities [8].

Table 1. RMC ingredients and their quantities

Ingredients	By weights (%)	By volume (%)
Cement	15	11
Water – required for hydration	3	8
Water – additional – to give workability	5	11
Aggregate	77	70

It should be marked that the additional water to give workability is 11 % by volume. This additional water will not react with the cement but remains free in the concrete after hardening. This forms capillaries that reduce strength, increase permeability and allow diffusion of aggressive chemicals reducing the durability of RMC. Therefore, use of water-reducing admixtures can significantly reduce the volume of this free water leading to stronger and more durable concrete [8].

Chemical admixtures also make enable to produce value added products (VAPs) in RMC industry. Self-compacted concrete (SCC), lightweight concrete (LWC), heavy weight concrete (HWC), high performance concrete (HPC), fiber-reinforced concrete (FRC), mass concrete (MC) are some examples of VAPs in RMC industry. VAPs are the products possessing some different properties compared to ordinary RMC products and add value to the product and this added value is generally demanded by customer. Table 2 summarizes the general criteria for VAPs in RMC industry [1,11,12].

Table 2. Criteria for VAPs in RMC industry

	Criterion
1	Different from ordinary products by means of using different materials or different methods in the production
2	Different from ordinary products by means of technical support and marketing process
3	Add value to the customer
4	Customer is willing to pay

3. RHEOLOGY OF RMC AND EFFECTS OF CHEMICAL ADMIXTURES

Freshly ready mixed concrete behaves as yield stress fluids [13]. Rheology of RMC can be defined as the plastic deformation and flow of RMC. The rheology of a RMC mixture is determined by concrete making materials and the mix design. Therefore, it should be noted that only after the mix design and material selection are optimized should admixtures be used to modify the rheology of RMC. Figure 6 illustrates the effects of mixing materials on the rheology of RMC [8].

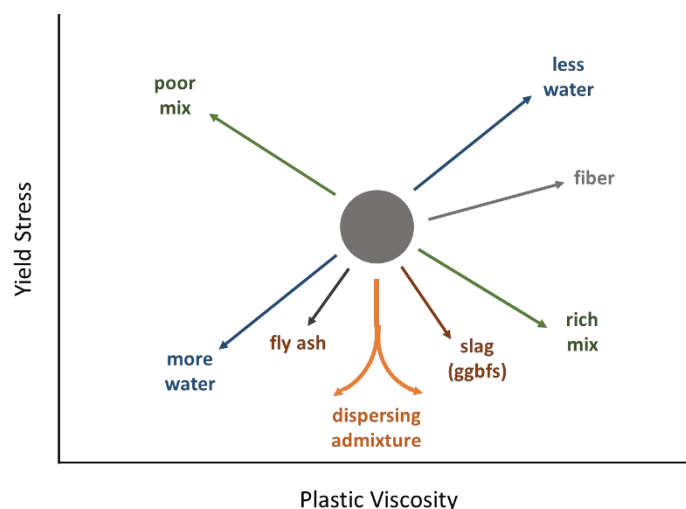


Figure 6. Effects of mixing materials on the rheology of RMC

Rheology of RMC has two parameters; yield stress related to slump value and plastic viscosity related to cohesion of the mixture. When water content of the mixture is increased, both yield stress and plastic viscosity reduce and this increases the slump but the mixture is more prone to bleeding and segregation. Dispersing admixtures which are the plasticizers reduce the yield however they may increase or decrease plastic viscosity of the mixture depending on the secondary effects of the admixture. The mix design of RMC is optimized and the mixture can then be modified by using proper admixture for the required and demanded fresh and hardened properties of RMC [8]. Table 3 indicates different RMCs and the chemical admixtures to be used for demanded properties [1].

Table 3. Different RMCs and chemical admixtures to be used for demanded properties

RMC	Admixture	Property
Normal concrete	Plasticizers Air entraining admixtures	Strength Workability Economy Durability
Extreme weather concreting	Retarders Accelerators	Overcoming possible problems
VAPs	Plasticizers Retarders Accelerators Special admixtures	Strength Durability Special properties

4. CONCLUSION

RMC is the most widely used construction material produced by mixing together cement, aggregate, water, and if required chemical admixtures, mineral admixtures, and in some cases fibers. Although RMC market in the world consists of mostly normal concrete, value added products (VAPs) of RMC are also hopefully demanded recently. It should be marked that extreme weather concreting is also continuously increasing due to the limited times for the constructions. RMC should satisfy minimum requirements and also demanded properties in its fresh and hardened states. As it was discussed in detail above, chemical admixtures are not optional and mostly used in the production of normal RMC, VAPs, and also extreme weather concreting operations. However, it should be marked that first of all material selection should be properly done and mix design should be optimized, proper chemical admixtures can be used to modify the properties of RMC.

References

1. Arioğlu, Ö. Ready Mixed Concrete. Class Notes, 2017, Hasan Kalyoncu University, Gaziantep.
2. Flatt, R.J., Roussel, N., and Cheeseman, C.R. Concrete: an eco material that needs to be improved. *Journal of the European Ceramic Society*, 2016, Vol. 32, pp. 2787-2798.
3. Kett, I. (2009). *Engineered Concrete: Mix Design and Test Methods*. Taylor&Francis Group, London. Arioğlu, Ö. (2017b).
4. Zongjin, L. (2011). *Advanced Concrete Technology*. John Wiley and Sons Inc., New Jersey.
5. Kosmatka, S.H., Kerkhoff, B., and Panarese, W.C. (2003). *Design and Control of Concrete Mixtures*. Portland Cement Association, Illinois.

6. Matarul, J., Mannan, M.A., Mohammad Ibrahim Safawi, M.Z., Ibrahim, A., Jaunudin, N.A., and Yusuh, N.A. (2016). Performance-based durability indicators of different concrete grades made by the local ready mixed company: preliminary results. *Procedia*, Vol. 224, pp. 620-625.
7. Shetty, M.S. (2003). *Concrete Technology: Theory and Practice*. Ram Nagar, New Delhi.
8. Newman, J. and Choo, B.S. (2003). *Advanced Concrete Technology: Constituent Materials*. Elsevier, Burlington.
9. Collepardi, M. (1998). Admixtures used to enhance placing characteristics of concrete. *Cement and Concrete Composites*, Vol. 20, pp. 103-112.
10. Golaszewski, J. (2012). Influence of cement properties on new generation superplasticizers performance. *Construction and Building Materials*, Vol. 35, pp. 586-596.
11. Value Added Products in Ready Mixed Concrete Industry. Class Notes, 2017, Hasan Kalyoncu University, Gaziantep.
12. Arioğlu, Ö. (2018). Roller Compacted Concrete Pavements and Applications. Class Notes, 2018, Hasan Kalyoncu University, Gaziantep.
13. Kovler, K. and Roussel, N. (2011). Properties of fresh and hardened concrete. *Cement and Concrete Research*, Vol. 41, pp. 775-792.

GENERAL

INVESTIGATION OF THE PROPERTIES OF POROUS STAINLESS STEELS COATED WITH BOEHMITIC ALUMINA VIA DIP COATING METHOD

Yasemin KENAR*, Azade YELTEN YILMAZ**, Suat YILMAZ***

*Istanbul University, Department of Metallurgical and Materials Engineering

**Istanbul University, Department of Metallurgical and Materials Engineering

***Istanbul University, Department of Metallurgical and Materials Engineering

ABSTRACT

In the present study, highly porous 17-4 PH stainless steel foam for biomedical applications was manufactured by space holder technique. Metal release and weight loss from the foams was investigated in simulated body fluid solution by static immersion tests. Electrochemical corrosion properties of foams were examined by electrochemical techniques, such as open circuit potential and Tafel extrapolation measurement in simulated body fluid environment. Second part of study, boehmit sole (AlOOH) was obtained via sol-gel process. Highly porous 17-4 PH stainless steel foams were left in boehmit sole via dip-coating method at 7, 14 and 21 days. Studies in progress. In later times dip coated steel foams will be implemented heat treatment. As a result boehmit sole will be converted γ -alumina (γ -Al₂O₃). Finally corrosion tests and immersion tests will be implemented to dip coated steel foams.

Keywords: Sol-gel method, Dip-coating method, Steel foams

1. INTRODUCTION

Metal foams can be used in the fields such as energy absorbers, heat exchangers and biomedical implants. Space holder technique has been used to produce porous foams from steels and titanium alloys which have high melting temperatures. Space holder process produces open-cell structure with suitable for biomedical implant applications. Sol-gel method is a wet chemical method in which inorganic compounds such as metal alkoxide or metal powders, hydroxides, nitrates and oxides are selected as starting material.[1] Sol-gel dip process is applied for the fabrication of transparent layers, for the deposition of oxide films on float glass as a transparent substrate with a high degree of planarity and surface quality [2]. Dip coating techniques can be described as a process where the substrate to be coated is immersed in a liquid and then withdrawn with a well-defined withdrawal speed under controlled temperature. In this study have been used manuel dip-coating method.[3]

1.1. Metal Foams

1.1.1. Specimen Preparation

Starting material for the foam was 17-4 PH stainless steel powder (Carpenter, Sweden). As a space holder, carbamide (Merck, Germany), in the fractions of 710-1000 was used. To enhance the sintering, 0.5 wt.% boron (Merck, Germany) was added to create a liquid phase during sintering. The mixture was compacted at 200 MPa into cylindrical specimens with a diameter of 12 mm and 17 mm heights. Green specimens were immersed in water and carbamide was leached out. The sintering process was consisted of heating at rate of 6 °C/minutes to 390 °C (debinding), followed by heating at rate of 11 °C/minutes to the sintering temperatures. The foams were sintered at 1260 °C for 40 minutes in the hydrogen.

1.1.2. Simulated Body Fluid Preparation

Simulated body fluid (SBF) solution was prepared from calculated amounts of chemicals (Merck, Germany) according to procedure described in the literature. Amounts of the reagents for the preparation of 1L SBF were 8.0 g/L NaCl, 0.15 g/L CaCl₂, 0.4 g/L KCl, 0.1 g/L MgCl₂, 0.06 g/L Na₂HPO₄, 0.6 g/L NaH₂PO₄, 0.35 g/L NaHCO₃, 1.0 g/L glucose. pH was adjusted by using lactic acid.

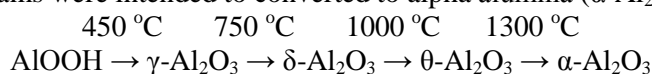
1.1.3. Corrosion Tests

Electrochemical corrosion studies were carried out in simulated body fluid (SBF) by using a potentiostat (Interface 1000, Gamry). High-density graphite was used as a counter electrode, saturated

calomel electrode (SCE) was used as a reference, and sample was used as a working electrode. The open circuit potential (OCP) was measured before the experiments. Tafel curves were obtained by polarizing the specimens from -250 to 250 mV (vs SCE), with respect to the OCP. The specimens were exposed to solution for 14 days. ICP-MS (Thermo Scientific) was employed to measure the release of metal ions. Weight loss was determined by gravimetric method.

1.2. Sol-gel Dip-Coating Method

Sol-gel method consists of 4 steps: hydrolysis, peptization, gelling / drying and heat treatment. In the preparation of boehmitic sol, firstly 40 moles of water (720 ml) was heated to 90°C with a magnetic stirrer in a four necked glass reactor. Hydrolysis process was started by adding 0.4 mol (81.6 g) of AIP alkoxide raw material to pure water heated to 90°C and mixed for 1 hour to complete the reactions. After this time was diluted to %10 HCl (Merck, %37) was added to realize the peptization reaction[1]. When hydrolysis and peptization were terminated, a semi-fluid boehmitic sol (AlOOH) was obtained. The foams were obtained by space holder method dipped in boehmitic sol by manual method. Samples were left for 7, 14 and 21 days. After this time the samples will implement heat treatment. In this way boehmitic sol on the foams were intended to be converted to alpha alumina ($\alpha\text{-Al}_2\text{O}_3$) at 1300°C .



2. RESULTS

2.1. The Results of None Dip Coated Metal Foams

The final pore size values of the foams was about $600\text{--}800\ \mu\text{m}$. Final pore size is associated to the carbamide size. Pore shape (morphology) was also similar to the original carbamide particle shape. Average size of the carbamide particles was slightly higher than the pores in the sintered specimens. The difference was attributed to crushing of carbamide particles during compaction.

2.1.1. Electrochemical Corrosion Tests

In corrosion studies, open circuit potential (OCP) can be employed for evaluation of the stability of an alloy. Figure 1 illustrates the variation of the a) OCP curves and b) Tafel curves of the alloys.

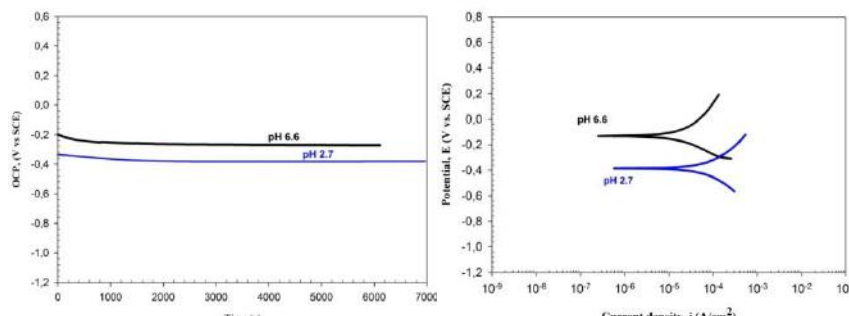


Figure 1. a) OCP curves and b) Tafel curves of the alloys

Figure 2 illustrates the a) metal ion release and b) weight loss (values of the specimens. Metal ion release values of the alloys are not higher than the reference toxic levels of the metal ions in the human body.

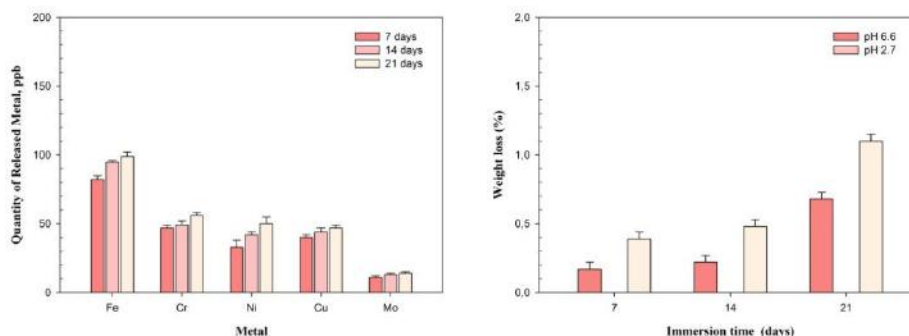


Figure 2. a) Metal ion release and b) weight loss values of the specimens

ACKNOWLEDGEMENT

This work was financially supported by the Research Fund of Istanbul University-Cerrahpaşa as 29820 project ID number.

REFERENCES

- [1] Yelten, A., 2010, Sol-Jel Yöntemi ile Üretilmiş Alümina-Bovine Hidroksiapatit Kompozitlerinin Özellikleri ve Karakterizasyonu, Yüksek Lisans Tezi, İstanbul Üniversitesi.
- [2] T. J. Kang, Jang-Won Yoon, D.-Iel Kim, S. Seop Kum, YongHak Huh, Jun-Hee Hahn, Sang Heup Moon, Ho-Young Lee,n and Yong Hyup Kim, 2006, Sandwich-Type Laminated Nanocomposites Developed by Selective Dip-Coating of Carbon Nanotubes, *Advanced Materials*, 19, 427-432
- [3] H. Schmidt, M. Mennig, 2000. *Wet Coating Technologies for Glass*, INM, Institut für Neue Materialien, Saarbrücken, Germany, November

CERAMICS AND ENERGY: LUMINESCENCE PHOSPHORESCENCE

SYNTHESIS AND OPTICAL PROPERTIES OF Eu^{3+} -DOPED NATURAL FLUORAPATITE

Burak Demir¹, Veli Uz², Erkul Karacaoğlu³, Erhan Ayas¹

¹ Eskişehir Technical University, Turkey

² Kütahya Dumlupınar University, Turkey

³ Karamanoğlu Mehmetbey University, Turkey

Key Words: Fluorapatite, Luminescence, REE, Optical

It is known that fluorapatites (FAP) have suitable host lattice structures for luminescence and laser materials due to their good chemical and thermal stability. Especially in the last decade great efforts have been made to investigate the luminescence properties of FAP equipped with rare earth (RE) ions and many RE-doped FAP with interesting spectroscopic properties have been found. The main objective of this work is to convert the natural FAP powder into a product that can be used in advanced technology products by doping with Eu^{3+} . In order to obtain the optimal results, the samples were conventionally sintered at different temperatures (1100°C, 1150°C and 1200°C) and different Eu^{3+} concentrations (between 0.1 to 1% mole of Eu) to control the microstructure and diffusion. It is observed that when the concentration of Eu and/or the sintering temperature are increased, the diffusion and hence the luminescence property are also increased. Phase and luminescence analyzes were performed by XRD and PL, respectively. The results showed that Eu^{3+} ions entered the FAP lattice and occupied Ca^{2+} sites, which resulted in a decrease in the values of the lattice parameters. Upon excitation by UV radiation, the Eu^{3+} -doped FAP samples demonstrate the characteristic $^5\text{D}_0$ - $^7\text{F}_2$ and $^5\text{D}_0$ - $^7\text{F}_4$ emission lines of Eu^{3+} .

1. INTRODUCTION

Calcium apatites are the main source of inorganic phosphorus in nature. The general structure of apatite is $\text{Ca}_5(\text{PO}_4)_3\text{X}$ ($\text{X} = \text{OH}, \text{F}, \text{Cl}$) and takes the name of hydroxyapatite (HAP), fluorapatite (FAP) or chlorapatite (CLAP) according to the density of the OH, F and Cl anions found in its crystal. Calcium apatites, which are inorganic components of bones and teeth, have a significant interest in biomedical, dental implants, catalysis and environmental engineering due to their bioactive, biocompatible and osteoconductive properties [1-5]. In addition, calcium apatites can be used in other areas because apatites can be very different in structure and property due to their substitution of different groups of anions and cations. The substitutions change the structure and exhibit significant changes in properties such as crystallinity, solubility, mechanical, thermal stability, optics and bioactivities, and this provides them to use in a wide range of applications from biomaterials to optical materials [6-9]. Furthermore, hexagonal apatite allows the substitutions of many rare earth ions without changing the crystal structure and additional rare earth ions are stably located in the crystal lattice [10-13].

Fluorapatite crystallizes in a hexagonal system with $\text{P6}_3/\text{m}$ space symmetry [14]. There are four nonequivalent ions such as F^- , $(\text{PO}_4)^{3-}$, Ca^{2+} (I) and Ca^{2+} (II) in the fluorapatite structure and all these ions can be substituted with various ions [15-17]. Recently, researchers have shown great interest to fluorapatites since their potential use as biomedical materials, including dental implants, drug delivery and deep tissue bioimaging because of excellent biocompatibility and similarity to human bones component of fluorapatites [18-23]. Trivalent rare-earth-ion doped calcium apatites are used as biological fluorescent probes due to their good luminescence properties [24]. The emitted

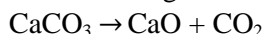
luminescence characteristics of rare earth ions show narrow emission bandwidth, high photochemical stability and long fluorescence life [25,26]. Among the rare earth elements from La to Lu, being an important emitter in the red region of the visible spectrum, Eu^{3+} ions have a $4f^6$ configuration that causes orange-red emission around 610–625 nm, due to various $^5\text{D}_0 \rightarrow ^7\text{F}_{0,4}$, especially $^5\text{D}_0 \rightarrow ^7\text{F}_1$ and $^5\text{D}_0 \rightarrow ^7\text{F}_2$ transitions [27]. Therefore, fluorapatites are good hosts for Eu^{3+} doping because Eu^{3+} has an anion radius approximate to the anion radius of Ca^{2+} in the calcium apatite lattice. The rare earth ions doped calcium apatite nanoparticles have attracted a great deal of attention on the application as cell labeling material [13,28] since their strong luminescence under visible-light excitation. Moreover, there are many studies focused on the synthesis of Eu^{3+} -doped fluorapatite [29-34]. As it is known, the method of Eu-FAP synthesis and Eu^{3+} concentration affect the site occupation [35]. Also, the previous results showed that the luminescent properties of rare earth doped apatite nanoparticles were much related to the thermal diffusion of rare earth ions to the Ca^{2+} sites in crystal lattice [36]. The rising temperature could enhance the crystallinity of apatite and accelerate the diffusion of rare earth ions to the Ca^{2+} sites, resulting in the enhancement of luminescence [29].

In this work, natural fluorapatite was successfully doped with trivalent europium. The effects of concentrations and temperature of thermal treatments on luminescent properties and crystallite size of Eu^{3+} -doped fluorapatite were analyzed. X-ray diffraction (XRD) and photoluminescence spectra (PL) were utilized to characterize the doped samples.

2. MATERIALS AND METHODS

2.1. Preparation of Eu-FAP

In this study, a natural waste was used as a fluorapatite source. XRD pattern in Fig 1. indicated that natural waste powder contains fluorapatite ($\text{Ca}_{10}(\text{PO}_4)_6\text{F}_2$) as a major phase, calcium carbonate (CaCO_3) and quartz (SiO_2) as minor phases. Eu_2O_3 was used as europium source. Europium oxide (Eu_2O_3) was added to natural fluorapatite and series of powder samples of $\text{Ca}_{10}(\text{PO}_4)_6\text{F}_2:\text{xEu}^{3+}$ ($\text{x} = 0, 0.1, 0.3, 0.5$ and 1) were prepared by the wet grinding method. After mixing, the dried Eu-FAP powder was calcined at 850°C for 3 hours under atmospheric conditions. With this process, the impurities in the mixture were removed. The following reactions occurred during calcination.



Calcium carbonate decomposed and formed calcium oxide after calcination. Then calcium oxide and quartz in the structure reacted to form larnite by heating.

2.2. Sintering of Eu-FAP

The sintering process involves calcination, compression at room temperature and heating at elevated temperatures. The prepared powders were molded by hand press after calcination and then compressed under 250 MPa by cold isostatic pressing (CIP). The samples were conventionally sintered at 1100°C , 1150°C and 1200°C with the $5^\circ\text{C}/\text{min}$ heating rate and 60 minutes dwell time.

2.3. Characterization

After sintering, phase and luminescence analyzes were performed by XRD and PL, respectively.

2.3.1. X-ray Diffraction

In order to perform a phase analysis of the final products, the samples were milled to make powder. Samples were characterized by X-ray diffraction (XRD, Rigaku Miniflex, Japan), using $\text{CuK}\alpha$ radiation ($\lambda=0.15418$ nm) with a tube voltage of 40 kV and a tube current of 30 mA. The XRD pattern was recorded with a step size of 0.02° and step duration 2 s in the 2θ range of 20° - 60° . The crystallite sizes of Eu-FAP were determined by using the Scherrer equation.

$$D_{hkl} = \frac{k\lambda}{\beta \cos \theta}$$

where D_{hkl} is the crystallite size (nm); λ the wavelength of monochromatic X-ray beam (nm) ($\lambda=0.15418$ nm for CuK_α radiation); β is the full width at half maximum for the diffraction peak under consideration (rad); θ the diffraction angle ($^\circ$); and k is a constant depending to crystal habit and chosen to be 0.89 [37]. The (002) diffraction peak was chosen to calculate the crystallite size.

2.3.2. Photoluminescence

The photoluminescence spectra of the samples were recorded using a Phosphorescence/fluorescence spectrofluorometer (Photon Technology International, QuantaMaster 30). The excitation spectrum between 400 nm and 900 nm was recorded with an emission wavelength at 618 nm. The emission spectrum between 400 nm and 900 nm was recorded with an excitation wavelength at 280 nm.

3. RESULTS AND DISCUSSION

The results obtained in this study were analyzed in two categories: sintering temperature and doping content that affects the phase composition, crystallite size and luminescent properties of the Eu-FAP. $\text{Ca}_{10}(\text{PO}_4)_6\text{F}_2:0.5\text{Eu}^{3+}$ samples were sintered at different temperatures (1100 $^\circ\text{C}$, 1150 $^\circ\text{C}$ and 1200 $^\circ\text{C}$) to see the effect of sintering temperature. Also $\text{Ca}_{10}(\text{PO}_4)_6\text{F}_2:x\text{Eu}^{3+}$ ($x=0, 0.1, 0.3, 0.5$ and 1) samples were sintered at 1150 $^\circ\text{C}$ to see the effect of concentration.

3.1. Effect of Sintering Temperature

The XRD patterns of Eu-FAP ($x=0.5$) sintered at different temperatures (1100 $^\circ\text{C}$, 1150 $^\circ\text{C}$ and 1200 $^\circ\text{C}$) were shown in Figure 1. There was no significant difference between the XRD patterns of samples sintered at different temperatures. In XRD patterns, three different phases were found as fluorapatite, larnite and europium oxide. The crystallite sizes were calculated by using the Sherrer equation for the plane (002) which had the most significant reflection for fluorapatite in XRD patterns. The crystalline phase compositions of Eu-FAP was not altered along with the increase of sintering temperature.

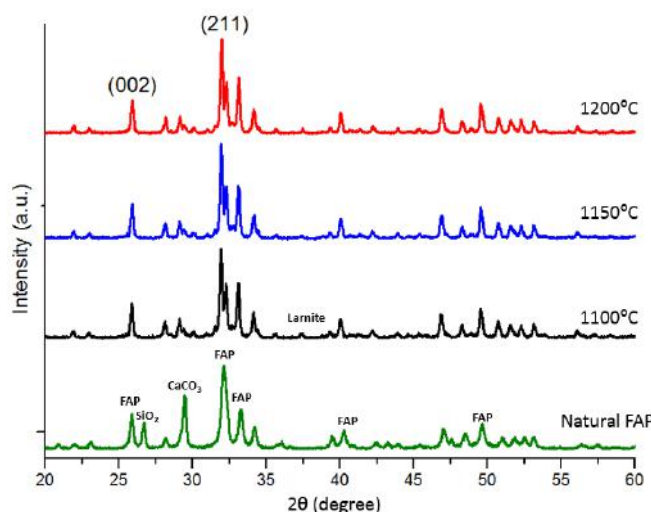


Figure 1. The XRD patterns of natural waste powder and Eu-FAP ($x=0.5$) sintered at 1100 $^\circ\text{C}$, 1150 $^\circ\text{C}$ and 1200 $^\circ\text{C}$

Nevertheless, X-ray diffraction peaks became narrower with the rising of sintering temperature due to crystallite growth. Crystallite size of natural waste powder was 32.2 nm at the beginning. In Figure 2, it was seen that the size of the crystallite rises with the increasing of sintering temperature. Crystallite size was 37.75 nm after sintering at 1100 $^\circ\text{C}$ and rose to 39.20 nm after sintering at 1200 $^\circ\text{C}$. As

known from previous studies, if crystallite size increases, samples show a higher luminescence property [13, 29].

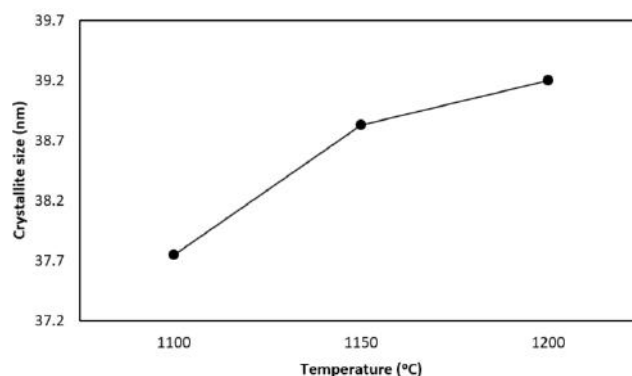


Figure 2. Crystallize size of Eu-FAP ($x=0.5$) sintered at different temperatures

The emission spectrum was recorded with an excitation wavelength at $\lambda=280$ nm. The photoluminescence spectra of Eu-FAP sintered at different temperatures shown in Fig. 3. The luminescence properties of Eu-FAP showed dependences on the sintering temperature. With an increasing of sintering temperature, the photoluminescence spectra of Eu-FAP were enhanced. The highest photoluminescence efficiency was achieved by the sample sintered at 1200 °C. The increasing temperature could enhance the crystallinity of fluorapatite and accelerate the diffusion of europium ions to the Ca^{2+} sites, resulting in the enhancement of luminescence. In all samples, same excitation peaks at 280 nm, 395 nm, 468 nm and 536 nm and two emission peaks at 615 nm and 700 nm were detected. The emission spectra were observed at strong at 615 nm and weak at 700 nm. The characteristic emission spectrum was consistent with europium ion occupying Ca^{2+} (II) site and Ca^{2+} (I) site respectively for 615 nm and 700 nm [38]. For the samples sintered at 1150 °C and 1200 °C, the excitation and emission spectra became narrow and strong. Emission spectrum indicated the strongest emission at 615 nm and small emission at 700nm. These two emissions were dedicated $^5\text{D}_0-^7\text{F}_2$ [39] and $^5\text{D}_0-^7\text{F}_4$ [40] transitions respectively for 615 nm and 700 nm.

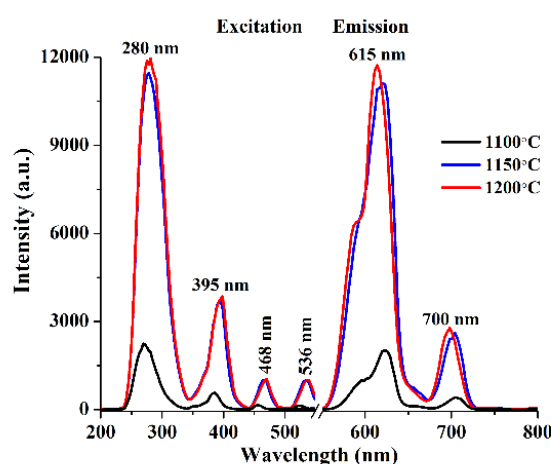


Figure 3. Photoluminescence spectra of Eu-FAP ($x=0.5$) sintered at different temperatures

3.2. Effect of Doping Content

The XRD patterns of $\text{Ca}_{10}(\text{PO}_4)_6\text{F}_2:x\text{Eu}^{3+}$ ($x=0.1, 0.3, 0.5$ and 1) sintered at 1150 °C were shown in Figure 4. There are three different phases as fluorapatite, larnite and europium oxide for all the samples. While the doping content of Eu-FAP rose from 0.1 to 1, the relative intensities of diffraction peaks decreased suggesting that the doping inhibits the FAP crystal growth. Furthermore, for $x=0.5$

and $x=1$, the europium oxide remained stable in the structure indicating that not all the Eu^{3+} ions entered the crystal lattice. The previous results indicated that the luminescent properties of europium ion doped fluorapatites were much related with the thermal diffusion of Eu^{3+} to the Ca^{2+} sites in a crystal lattice. But after some amount of doping, a quenching effect could occur, and the luminescence begins to decrease [41].

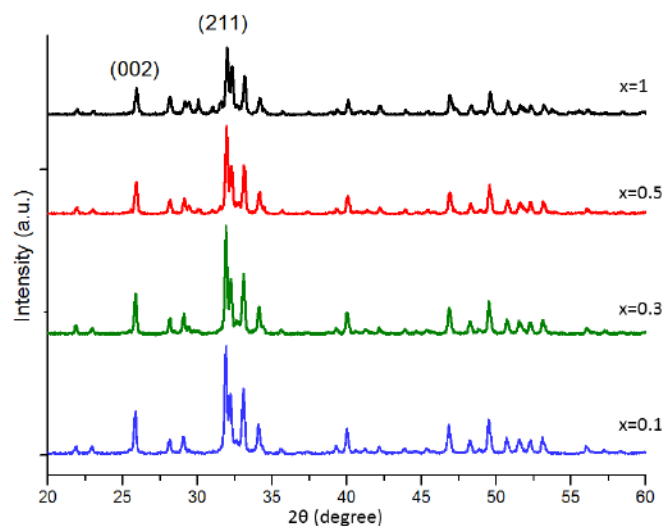


Figure 4. The XRD patterns of Eu-FAP sintered at 1150 °C with concentrations $x=0.1$, 0.3, 0.5 and 1.

The emission spectrum was recorded with an excitation wavelength at $\lambda=280$ nm. The photoluminescence spectra of Eu-FAP sintered at 1150 °C with different concentrations ($x=0.1$, 0.3, 0.5 and 1) shown in Fig. 5. While doping with $x=0.1$ to 1 of Eu, the strong excitation at 280 nm and weak excitations at 395 nm and 465 nm were observed. Emission spectrum indicated the strongest emission at 620 nm and small emission at 703 nm. These two emissions were dedicated $^5\text{D}_0-^7\text{F}_2$ [39] and $^5\text{D}_0-^7\text{F}_4$ [40] transitions respectively for 620 nm and 703 nm. The emission spectra were observed at strong at 620 nm and weak at 703 nm. Characteristic emission spectrum is consistent with europium ion occupying Ca^{2+} (II) at 620 nm site and Ca^{2+} (I) at 703 nm [38]. An enhancement of emission spectrum was monitored with the increase of Eu content up to $x=0.5$. Contrastively, with the increase of Eu doping content up to $x=1$, the relative emission spectra were significantly reduced suggested quenching effect. For the samples sintered at 1150 °C with a different Eu content, the excitation and emission spectra became narrow and strong for $x=0.3$ and $x=0.5$.

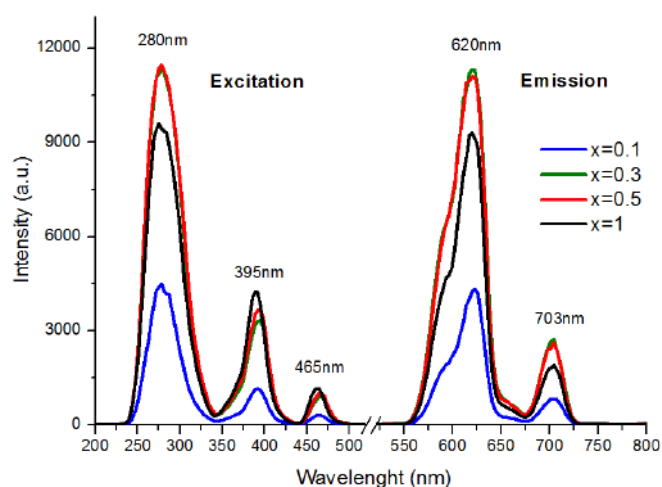


Figure 5. Photoluminescence of Eu-FAP sintered at 1150 °C with concentrations $x=0.1$, 0.3, 0.5 and 1.

4. CONCLUSIONS

In conclusion, Eu-FAP were obtained from natural fluorapatite by doping europium oxide. The integration of Eu^{3+} ions into natural fluorapatite was observed at higher temperatures. Upon excitation by UV radiation, the samples represent the characteristic $^5\text{D}_0\text{--}^7\text{F}_2$ and $^5\text{D}_0\text{--}^7\text{F}_4$ emission lines of Eu^{3+} ion. The luminescence property of Eu-FAP was analyzed for the effect of sintering temperature and doping content. It is observed that luminescence property enhanced with the increasing of sintering temperature from 1100 °C to 1200 °C due to crystallite size growth with increasing sintering temperature. Moreover, the luminescence property was increased with the increase of the doping content from $x=0.1$ to $x=0.5$. However, when there is more than $x=0.5$, the luminescence reduced drastically due to the quenching effect. After all, the sample with the best emission is achieved by Eu-FAP where $x=0.5$ and sintered at 1200°C.

References

- [1] Turkoz M., Atilla A. O., Evis Z., Silver and fluoride doped hydroxyapatites: investigation by microstructure, mechanical and antibacterial properties. *Ceramics International*, 2013, 39(8), 8925-8931.
- [2] Kheradmandfard M., Fathi M.H., Preparation and characterization of Mg-doped fluorapatite nanopowders by sol-gel method, *Journal of Alloys and Compounds*, 2010, 504, 141-145.
- [3] Descamps M., Hornez J.C., Leriche A., Manufacture of hydroxyapatite beads for medical applications, *Journal of the European Ceramic Society*, 2009, 29, 369-375.
- [4] Shanmuga, S., Gopal B., Copper substituted hydroxyapatite and fluorapatite: synthesis, characterization and antimicrobial properties. *Ceramics International*, 2014, 40(10), 15655-15662.
- [5] Bianco A., Cacciotti I., Lombardi M., Montanaro L., Bemporad E., Sebastiani M., F-substituted hydroxyapatite nanopowders: thermal stability, sintering behavior and mechanical properties, *Ceramics International*, 2010, 36, 313-322.
- [6] Gross K.A., Berndt C.C., Biomedical application of apatites, *Reviews in Mineralogy and Geochemistry*, 2002, 48, 631-672.
- [7] Ibrahim M. Z., Sarhan A. A., Yusuf F., Hamdi M., Biomedical materials and techniques to improve the tribological, mechanical and biomedical properties of orthopedic implants—a review article. *Journal of Alloys and Compounds*, 2017, 714, 636-667.
- [8] Elliott J. C., Restricted access, *Reviews in Mineralogy and Geochemistry*, 2002, 48, 427-453.
- [9] Azami M., Jalilifiroozinezhad S., Mozafari M., Rabiee M., Synthesis and solubility of calcium fluoride/hydroxy-fluorapatite nanocrystals for dental applications. *Ceramics international*, 2011, 37(6), 2007-2014.
- [10] Rakovan J., Richard J. R., Intracrystalline rare earth element distributions in apatite: Surface structural influences on incorporation during growth. *Geochimica et Cosmochimica Acta*, 1996, 60(22), 4435-4445.
- [11] Reisfeld R., Gaft M., Boulon G., Panczer C., Jørgensen C.K., Laser-induced luminescence of rare-earth elements in natural fluor-apatites. *Journal of Luminescence*, 1996, 69, 343-353.
- [12] Mayer I., Layani J. D., Givan A., Gaft M., Blanc P., La ions in precipitated hydroxyapatites. *Journal of inorganic biochemistry*, 1999, 73(4), 221-226.

- [13] Han Y., Wang X., Dai H., Li S., Synthesis and luminescence of Eu^{3+} doped hydroxyapatite nanocrystallines: Effects of calcinations and Eu^{3+} content. *Journal of luminescence*, 2013, 135, 281-287.
- [14] Rakovan J., Connoisseur's Choice: Fluorapatite, *Acushnet, Rocks & Minerals*, 2015, 90, 3, 244-269.
- [15] Leroy N., Bres E., Structure and substitutions in fluorapatite, *Eur. Cells Mater* 2, 2001, 36-48.
- [16] Calderin L., Stott M.J., Rubio A., Electronic and crystallographic structure of apatites, *Phys. Rev. B* 67, 2003, 134106.
- [17] Tamm T., Peld M., Computational study of cation substitutions in apatites, *J. Solid State Chem.*, 2006, 179, 1581-1587.
- [18] Xu C.T., Zhan Q., Liu H., Somesfalean G., Qian J., He, S., Engels S.A., Upconverting nanoparticles for pre-clinical diffuse optical imaging, microscopy and sensing: current trends and future challenges, *Laser Photonic Rev.* 7, 2013, 663-697.
- [19] Kheradmandfard M., Fathi M.H., Preparation and characterization of Mg-doped fluorapatite nanopowders by sol-gel method. *Journal of Alloys and Compounds*, 2010, 504(1), 141-145.
- [20] Razavi M., Fathi M.H., Meratian M., Fabrication and characterization of magnesium-fluorapatite nanocomposite for biomedical applications. *Materials characterization*, 2010, 61(12), 1363-1370.
- [21] Wei J., Wang J., Shan W., Liu X., Ma J., Liu C., Wei S., Development of fluorapatite cement for dental enamel defects repair. *Journal of Materials Science: Materials in Medicine*, 2011, 22(6), 1607.
- [22] Kheradmandfard M., Fathi M. H., Fabrication and characterization of nanocrystalline Mg-substituted fluorapatite by high energy ball milling. *Ceramics International*, 2013, 39(2), 1651-1658.
- [23] Cheng L., Yang K., Li Y., Chen J., Wang C., Shao M., Lee S.T., Liu Z., Facile preparation of multifunctional upconversion nanoprobe for multimodal imaging and dual-targeted photothermal therapy, *Angew. Chem*, 2011, 123, 7523-7528.
- [24] Lebugle A., Pelle F., Charvillat C., Rousselot I., Chane-Ching J.Y., Colloidal and monocrystalline Ln^{3+} doped apatite calcium phosphate as biocompatible fluorescent probes, *Chemical Communications*, 2006, 6, 606-608.
- [25] Wang F., Tan W. B., Zhang Y., Fan X., Wang M., Luminescent nanomaterials for biological labelling. *Nanotechnology*, 2005, 17(1), R1.
- [26] Meiser F., Christina C., Frank C., Biofunctionalization of fluorescent rare-earth-doped lanthanum phosphate colloidal nanoparticles, *Angewandte Chemie International*, 2004, 43, 5954-5957.
- [27] Sun Y., Yang H., Tao D., Preparation and characterization of Eu^{3+} -doped fluorapatite nanoparticles by a hydrothermal method. *Ceramics International*, 2012, 38(8), 6937-6941.
- [28] Ciobanu C. S., Iconaru S. L., Massuyeau F., Constantin L. V., Costescu A., Predoi D., Synthesis, structure, and luminescent properties of europium-doped hydroxyapatite nanocrystalline powders. *Journal of Nanomaterials*, 2012, 61.
- [29] Silva F. R., de Lima N. B., Bressiani A. H. A., Courrol L. C., Gomes L., Synthesis, characterization and luminescence properties of Eu^{3+} -doped hydroxyapatite nanocrystal and the thermal treatment effects. *Optical Materials*, 2015, 47, 135-142.
- [30] Zeng H., Li X., Sun M., Wu S., Chen H., Synthesis of Europium-Doped Fluorapatite Nanorods and Their Biomedical Applications in Drug Delivery. *Molecules*, 2017, 22(5), 753.

- [31] Karthi S., Kumar G. S., Kumar G. A., Sardar D. K., Santhosh C., Girija E. K., Microwave assisted synthesis and characterizations of near infrared emitting Yb/Er doped fluorapatite nanoparticles. *Journal of Alloys and Compounds*, 2016, 689, 525-532.
- [32] Karimi M., Ramsheh M. R., Ahmadi S. M., Madani M. R., Shamsi M., Reshadi R., Lotfi F., Reline-assisted green and facile synthesis of fluorapatite nanoparticles. *Materials Science and Engineering: C*, 2017, 77, 121-128.
- [33] Kheradmandfard M., Fathi M. H., Ansari F., Ahmadi T., Effect of Mg content on the bioactivity and biocompatibility of Mg-substituted fluorapatite nanopowders fabricated via mechanical activation. *Materials Science and Engineering: C*, 2016, 68, 136-142.
- [34] Bouslama N., Ayed F. B., Bouaziz J., Sintering and mechanical properties of tricalcium phosphate-fluorapatite composites. *Ceramics International*, 2009, 35(5), 1909-1917.
- [35] Ciobanu C. S., Massuyeau F., Andronescu E., Stan M. S., Dinischiotu A., Predoi D., Biocompatibility study of europium doped crystalline hydroxyapatite bioceramics. *Digest Journal of Nanomaterials & Biostructures (DJNB)*, 2011, 6(4).
- [36] Fleet M. E., Pan Y. Site preference of rare earth elements in fluorapatite. *American Mineralogist*, 1995, 80(3-4), 329-335.
- [37] Cullity B. D., Elements of X-Ray Diffraction, Reading: Addison-Wesley Publishing Company Inc, 1977.
- [38] Gaft M., Reisfeld R., Panczer G., Shoval S., Champagnon B., Boulon G., Eu^{3+} luminescence in high-symmetry sites of natural apatite. *Journal of Luminescence*, 1997, 72, 572-574.
- [39] Li Y. C., Chang Y. H., Lin Y. F., Chang Y. S., Lin Y. J., Synthesis and luminescent properties of Ln^{3+} (Eu^{3+} , Sm^{3+} , Dy^{3+})-doped lanthanum aluminum germanate $\text{LaAlGe}_2\text{O}_7$ phosphors. *Journal of Alloys and Compounds*, 2007, 439(1-2), 367-375.
- [40] Zhang F., Wang Y., Tao Y., VUV spectroscopic properties of $\text{Ba}_2\text{Gd}_2\text{Si}_4\text{O}_{13}:\text{Re}^{3+}$ ($\text{Re}^{3+} = \text{Ce}^{3+}$, Tb^{3+} , Dy^{3+} , Eu^{3+} , Sm^{3+}), *Materials Research Bulletin*, 2013, 48, 1952-1956
- [41] Shinde N. K., Dhoble J. S., Swart, C. H., Park, K., Phosphate Phosphors for Solid-State Lighting, Springer-Verlag Berlin Heidelberg, 2012.

CERAMICS AND ENERGY: LUMINESCENCE PHOSPHORESCENCE

PRODUCTION OF LUMINESCENT Eu^{3+} -DOPED MONTICELLITE BASED CERAMICS OBTAINED FROM BORON DERIVATIVE WASTE

Levent Koroglu^{1,*}, Gozde Cagirman¹, Ece Dagaslan¹, Erkul Karacaoglu², Erhan Ayas¹

¹Eskişehir Technical University, Department of Materials Science and Engineering, İki Eylül Campus, 26555/Eskişehir/Turkey

²Karamanoğlu Mehmetbey University, Department of Metallurgy and Materials Engineering, Yunus Emre Campus, 70100/Karaman/Turkey

Abstract

In the present study, Eu^{3+} -doped monticellite based ceramics were prepared using boron derivative waste and Eu_2O_3 nanopowder. The effects of Eu^{3+} content and sintering temperature on photoluminescent properties of Eu^{3+} -doped monticellite based ceramics were investigated. The qualitative phase analysis and photoluminescence analysis of obtained ceramics carried out in detail. The obtained results showed that all sintered ceramics contain monticellite, akermanite, calcium magnesium borate and quartz crystalline phases. The shifting of monticellite's primary peak indicated Eu^{3+} doping. The increment of Eu content from 5 % to 10 % and of sintering temperature from 900°C to 1000°C determined the formation & decomposition of zeolite LTA and calcium europium oxide silicate phases. Higher dopant content provided higher photoluminescence intensity at 615 nm in the red region ($^5\text{D}_0 \rightarrow ^7\text{F}_2$) under excitation at 267 nm in UV region. The emission intensity for 10 % Eu^{3+} was approximately 3.6 times that for 1 % Eu^{3+} at 615 nm and that kept constant for 10 % Eu^{3+} with the increasing of sintering temperature. Hence, 10 % Eu^{3+} -doped monticellite based ceramics produced in a eco-friendly route (at 900°C for 2 h using boron derivative waste) carry a huge potential to be used as phosphors for white light-emitting diodes (w-LEDs) and as bone graft substitutes for bioimaging applications.

Keywords: Monticellite (CaMgSiO_4), Photoluminescence, Solid-state powder synthesis, Boron derivative waste

1. INTRODUCTION

Rare earth ions-doped silicates have attracted considerable attention due to their high physical-chemical stability, water-resistant properties and good photoluminescence properties. The excitation of Eu^{2+} and Eu^{3+} by the UV and near-UV lights results in strong visible-light emission [1-3]. Moreover, calcium magnesium silicates exhibit various advantages for biomedical applications because of their high biocompatible and bioactive characteristics [4]. For these reasons, Eu-doped calcium magnesium silicates have a potential to be used as phosphors for white light-emitting diodes (w-LEDs) and as bone graft substitutes for bioimaging applications in terms of the monitoring of new bone tissue, tracking the distribution and accumulation of degradation products, chasing the drug delivery, analyzing of bone marrow stromal cells (BMSCs) and bone tumor cells [1,2,5-7].

Turkey has almost 72% of global boron reserves. Throughout production of 1 million tons of borax pentahydrate, 900 thousand tons of solid boron derivative wastes are generated in Eti Mine Works Kirka Plant which causes costly storage problems and serious environmental issues [8]. Hence, monticellite based ceramic powder was synthesized from boron derivative waste before by our research group, however; its photoluminescent properties have not been explored yet. The aim of the study was the investigation of the effects of Eu^{3+} content and sintering temperature on

photoluminescent properties of Eu^{3+} -doped monticellite based ceramics sintered from boron derivative waste and Eu_2O_3 nanopowder.

2. MATERIALS AND METHOD

2.1. Preparation of powder mixture

Boron derivative waste supplied from Kirka Plant of Eti Mine Works General Directorate was used as starting material during the study. Boron derivative waste is composed of dolomite ($\text{CaMg}(\text{CO}_3)_2$), calcite (CaCO_3), quartz (SiO_2), borax pentahydrate (tincalconite, $\text{Na}_2\text{B}_4\text{O}_7 \cdot 5\text{H}_2\text{O}$) and kaolinite ($\text{Al}_2\text{Si}_2\text{O}_5(\text{OH})_4$) crystalline phases. The XRD pattern and chemical composition of waste were given in prior study [9]. Boron derivative waste and Eu_2O_3 nanopowder (99.9 %, Chempur) were mixed using a planetary ball mill (Pulverisette 6, Fritsch, Germany) in a Si_3N_4 media (10 mm ball diameter) with propanol-2 alcohol. The slurry was dried using a rotary evaporator (WB2000, Heidolph) at 50 rpm and 55°C . The obtained powder mixture was sieved under $125\ \mu\text{m}$ to eliminate the agglomerates. Eu_2O_3 nanopowder was weighted at different ratios to keep Eu/Ca ion ratio as 1, 2.5, 5 and 10 mol. % where CaO in boron derivative waste was calcium source.

2.2. Sintering of Eu^{3+} -doped monticellite based ceramics

The powder mixture was calcined at 800°C for 4 h. Following to the crushing and compaction of synthesized powder, Eu^{3+} -doped monticellite based ceramics were sintered at 900°C for 2 hours and at 1000°C for 2 hours in electrically heated furnace (KRC Lab. Eq.) under atmospheric pressure. The heating rate was kept $10^\circ\text{C}/\text{min}$.

2.3. Characterization of Eu^{3+} -doped monticellite based ceramics

Following to two-step thermal process, the qualitative phase analysis of Eu^{3+} -doped monticellite based ceramics carried out using an X-Ray Diffractometer (XRD, Rigaku Rint 2200) with a scan speed of $0.5^\circ/\text{min}$.

3. RESULTS AND DISCUSSION

3.1. Effect of Eu^{3+} content on photoluminescent properties of Eu^{3+} -doped monticellite based ceramics

Table 1. Eu^{3+} content and sintering parameters of all monticellite based ceramics

Sample No	Eu^{3+} Content (mol. %)	Sintering Parameters
S4	1	800°C 4h - 900°C 2h
S5	2.5	800°C 4h - 900°C 2h
S6	5	800°C 4h - 900°C 2h
S7	10	800°C 4h - 900°C 2h
S8	1	800°C 4h - 1000°C 2h
S9	10	800°C 4h - 1000°C 2h

The prior research exhibited that monticellite based ceramic powder synthesized at 800°C for 4 h using boron derivative waste included monticellite, akermanite, diopside, calcium magnesium borate, quartz and zeolite LTA crystalline phases [9]. Comparative XRD patterns of monticellite based ceramics doped with 1, 2.5, 5 and 10 % Eu^{3+} at 800°C 4h- 900°C 2h are given in Fig. 1. A shift in major (120) peak of monticellite occurred at diffraction angle of 24.5° as a sign of Eu^{3+} doping. All ceramics consisted of monticellite

(CaMgSiO_4 ; ICDD 84-1321), akermanite ($\text{Ca}_2\text{MgSi}_2\text{O}_7$; ICDD 76-0841), calcium magnesium borate (kurchatovite, CaMgB_2O_5 ; ICDD 73-0618) and quartz (SiO_2 ; ICDD 46-1045) crystalline phases. Although XRD patterns of sintered monticellite based ceramics after powder synthesis are almost similar, thermal decomposition of zeolite LTA ($\text{Na}_6(\text{AlSiO}_4)_6$; ICDD 42-0217) at sintering temperature was noticed. With the increasing of Eu^{3+} content from 5 % to 10 %, higher degree of crystallinity partially prevented thermal decomposition of zeolite LTA, and calcium europium oxide silicate ($\text{Ca}_2\text{Eu}_8(\text{SiO}_4)_6\text{O}_2$; ICDD 29-0320) was formed.

PL spectra of Eu^{3+} -doped monticellite based ceramics as a function of Eu^{3+} content are given in Fig. 2. The emission spectra monitored under maximum excitation at 267 nm in UV region showed strong bands centered at 615 nm in the red region. The maximum emission band at 615 nm and another band at 700 nm were attributed to $^5\text{D}_0 \rightarrow ^7\text{F}_2$ and $^5\text{D}_0 \rightarrow ^7\text{F}_5$ transitions of Eu^{3+} [10,11]. Higher dopant content provided higher emission intensity and that for 10 % Eu^{3+} was approximately 3.6 times that for 1 % Eu^{3+} at 615 nm. This result indicates that higher dopant content certainly improves photoluminescent properties.

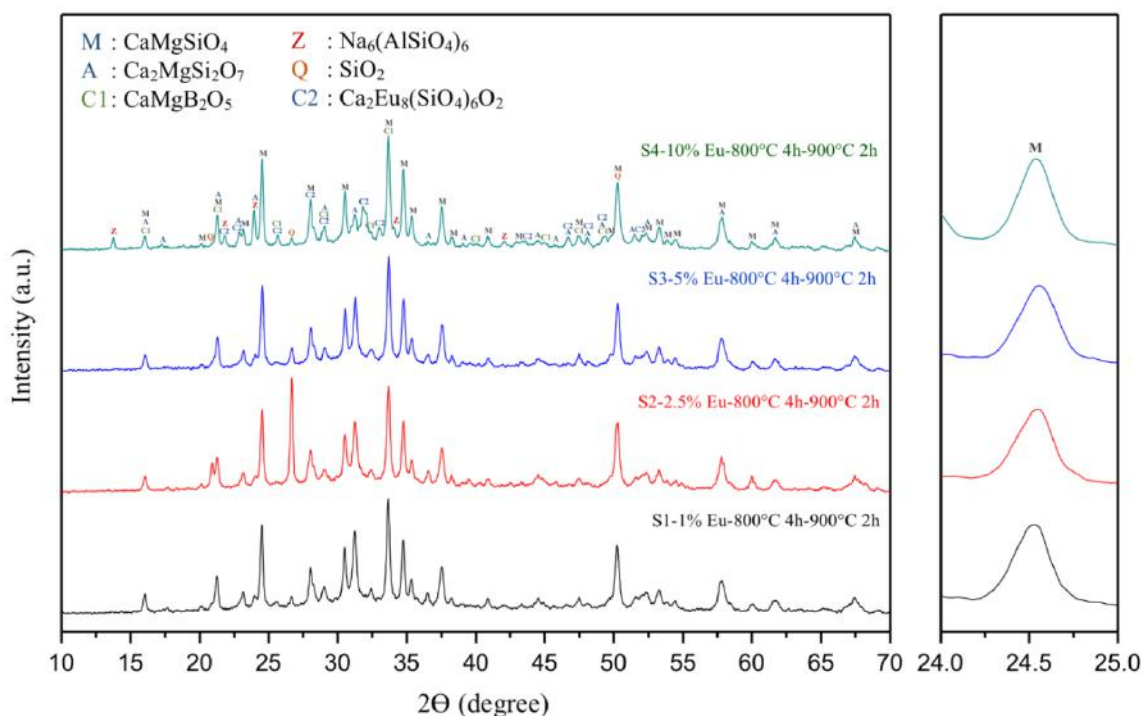


Figure 1. Comparative XRD patterns of Eu^{3+} -doped monticellite based ceramics at 800°C 4h-900°C 2h as a function of Eu^{3+} content

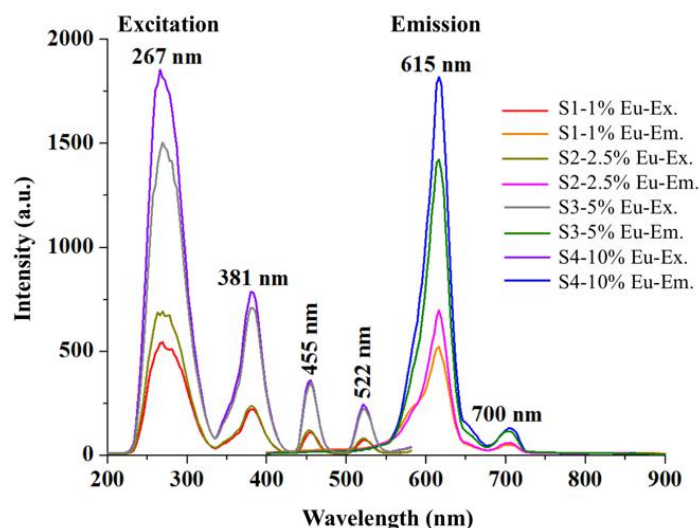


Figure 2. Photoluminescence spectra of monticellite based ceramics as a function of Eu^{3+} content

3.2. Effect of sintering temperature on photoluminescent properties of Eu^{3+} -doped monticellite based ceramics

Comparative XRD patterns of monticellite based ceramics doped with 1 and 10 % Eu^{3+} at 800°C 4h- 900°C 2h and 800°C 4h- 1000°C 2h are given in Fig. 3. A slight peak shifting pointed out Eu^{3+} doping again. Same crystalline phases were detected for ceramics sintered at 1000°C for 2 h. XRD patterns of ceramics doped with 1 % Eu^{3+} at 800°C 4h- 900°C 2h and 800°C 4h- 1000°C 2h were quite similar. They composed of monticellite, akermanite, calcium magnesium borate as major phases, and quartz as a minor phase. While 10 % Eu^{3+} -doped ceramic at 800°C 4h- 900°C 2h contains also zeolite LTA and calcium europium oxide silicate, these phases could not be detected with the increment of sintering temperature from 900°C to 1000°C which means that temperature plays a key role on the amorphization of crystalline phases.

Fig. 4. and Fig. 5 present PL spectra of monticellite based ceramics doped with 1 and 10 % Eu^{3+} as a function of sintering temperature, respectively. The increment of sintering temperature resulted in a slight decrease in the emission intensity at 615 nm for 1 % Eu^{3+} doping. It may be caused by the decreasing of crystallization degree at higher temperature. Unlike, no alteration in emission intensity for 10 % Eu^{3+} doping was observed. It suggests that a comprehensive research is necessary to investigate in detail the effect of crystallinity degree on photoluminescent properties of Eu^{3+} -doped monticellite based ceramics. As a result, 10 mol. % is a fair concentration for Eu^{3+} doping in order to obtain bright emission in the red region.

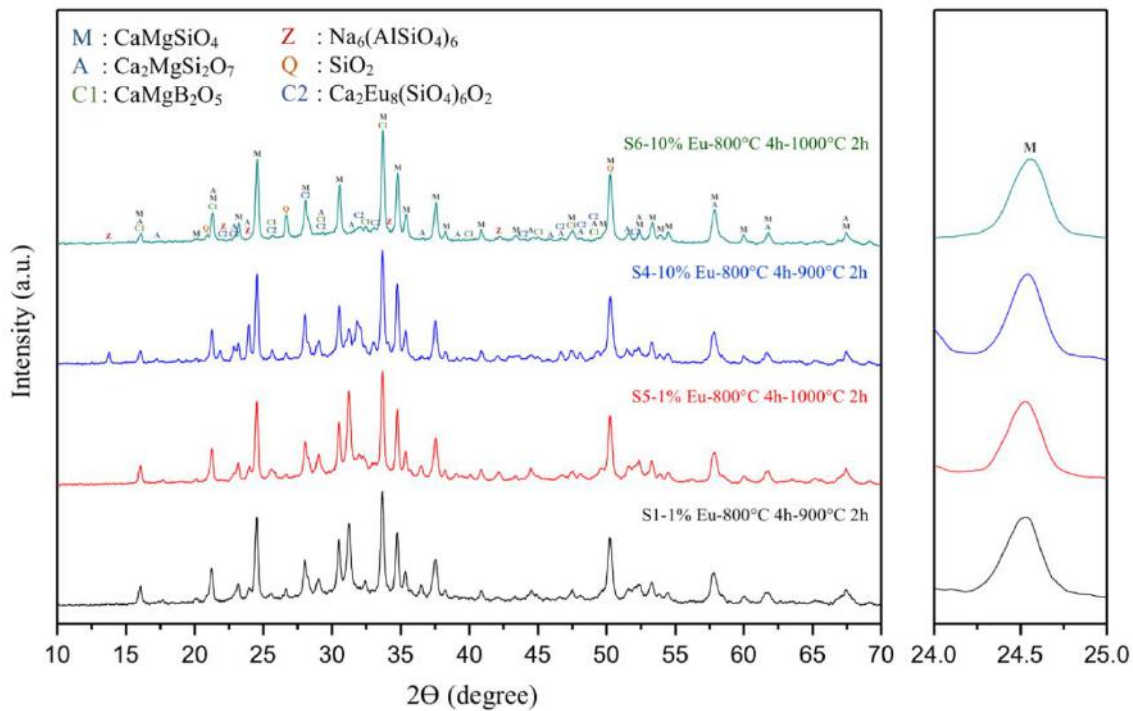


Figure 3. Comparative XRD patterns of monticellite based ceramics doped with 1 and 10 % Eu^{3+} at 800°C 4h-900°C 2h and 800°C 4h-1000°C 2h

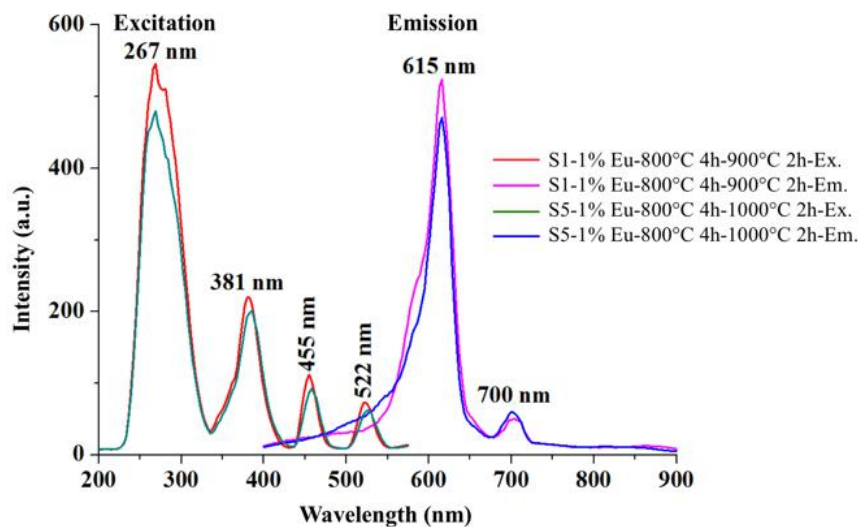


Figure 4. Photoluminescence spectra of monticellite based ceramics doped with 1 % Eu^{3+} as a function of sintering temperature

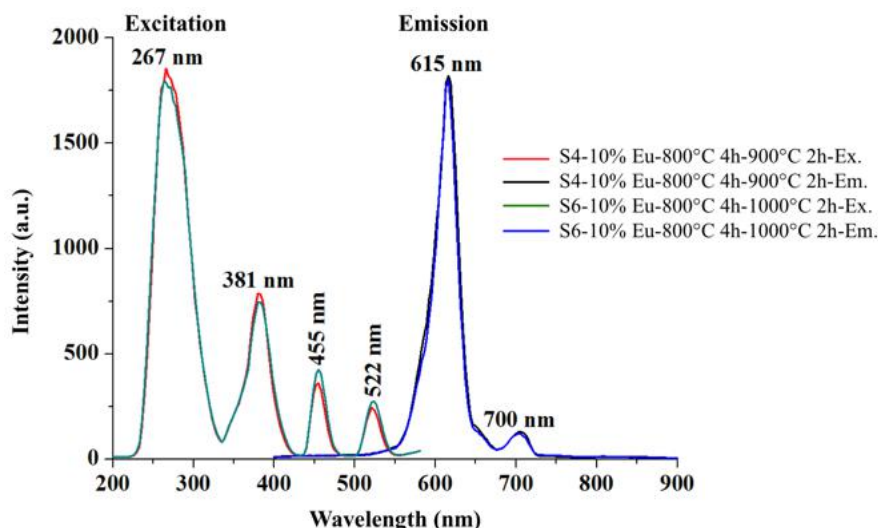


Figure 5. Photoluminescence spectra of monticellite based ceramics doped with 10 % Eu^{3+} as a function of sintering temperature

4. CONCLUSIONS

In the present study, Eu^{3+} -doped monticellite based ceramics were successfully produced from boron derivative waste and Eu_2O_3 nanopowder. The shifting of monticellite's primary peak indicated Eu^{3+} doping. All Eu^{3+} -doped ceramics consisted of same crystalline phases such as monticellite, akermanite, calcium magnesium borate and quartz. With the increasing of Eu^{3+} content to from 5 % to 10 %, thermal decomposition of zeolite LTA was prevented and calcium europium oxide silicate was formed. However, these phases could not be detected with the increment of sintering temperature from 900°C to 1000°C. The photoluminescence intensity obtained at 615 nm in the red region ($^5\text{D}_0 \rightarrow ^7\text{F}_2$) under excitation at 267 nm in UV region for 10 % Eu^{3+} was found roughly 3.6 times that for 1 % Eu^{3+} . The increment of sintering temperature from 900°C to 1000°C resulted in a slight decrease in the emission intensity for 1 % Eu^{3+} while that was constant for 10 % Eu^{3+} . To put in a nutshell, 10 % Eu^{3+} -doped monticellite based ceramics sintered at 900°C for 2h in a eco-friendly way can be used as phosphors for white light-emitting diodes (w-LEDs) and as bone graft substitutes for bioimaging applications.

REFERENCES

- [1] Suresh K., Vijay Babu K., Srinivasa Rao K., Naresh Kumar K., Poornachandra Rao N.V., and Murthy K.V.R., nUV excitable red emitting Eu^{3+} doped alkali earth silicate phosphor for solid state lighting. *International Journal of Luminescence and Applications*, 2015, 5 (2), 229-233.
- [2] Luo X., Cao W.H., Sun F., The development of silicate matrix phosphors with broad excitation band for phosphor-convered white LED. *Chinese Science Bulletin*, 2008, 53 (19), 2923-2930.
- [3] Poort S.H.M., Reijnhoudt H.M., van der Kuip H.G.T., Blasse G., Luminescence of Eu^{2+} in silica host lattices with alkaline earth ions in a row, *Journal of Alloys and Compounds*, 1996, 241, 75-81.
- [4] Diba M., Goudouri O.M., Tapia F., Boccaccini A.R., Magnesium-containing bioactive polycrystalline silicate-based ceramics and glass-ceramics for biomedical applications. *Current Opinion in Solid State and Materials Science*, 2014, 18, 147-167.
- [5] Allu A.R., Das S., Som S., Maraka H.V.R., Balaji S., Santos L.F., Manek-Hönniger I., Jubera V., Ferreira J.M.F., Dependence of Eu^{3+} photoluminescence properties on structural transformations in diopside-based glass-ceramics. *Journal of Alloys and Compounds*, 2017, 699, 856-865.

- [6] Xia Z., Zhang Y., Molokeev M.S., Atuchin V.V., Luo Y., Linear structural evolution induced tunable photoluminescence in clinopyroxene solid-solution phosphors. *Scientific Reports*, 2013, 3 (3310), 1-7.
- [7] Wu C., Xia L., Han P., Mao L., Wang J., Zhai D., Fang B., Chang J., Xiao Y., Europium-containing mesoporous bioactive glass scaffolds for stimulating in vitro and in vivo osteogenesis. *ACS Appl. Mater. Interfaces*, 2016, 8, 11342-11354.
- [8] B. Cicek, Development of glass-ceramics from combination of industrial wastes with boron mining waste (Dissertation thesis), Alma Mater Studiorum, University of Bologna, 2013.
- [9] Koroglu L., Ayas E., A systematic study on solid-state synthesis of monticellite (CaMgSiO_4) based ceramic powders obtained from boron derivative waste. *Advanced Powder Technology*, 2018, In Press.
- [10] Yu-Chun L., Yen-Hwei C., Yu-Feng L., Yee-Shin C., Yi-Jing L., Synthesis and luminescent properties of Ln^{3+} (Eu^{3+} , Sm^{3+} , Dy^{3+})-doped lanthanum aluminum germanate $\text{LaAlGe}_2\text{O}_7$ phosphors. *Journal of Alloys and Compounds*, 2007, 439, 367–375.
- [11] Öztürk E., Karacaoglu E., Luminescence properties of $\text{M}_2\text{TiO}_4:\text{Eu}^{3+}$, Li^+ (M:Mg, Ca) and $\text{MgAl}_2\text{O}_4:\text{RE}^{3+}$ ($\text{RE}^{3+}:\text{Ho}^{3+}$, Sm^{3+} , and Yb^{3+}). *J Therm Anal Calorim*, 2015, 119 (2), 1063-1071.

ENAMELS

INVESTIGATION OF THE LI-FREE ENAMEL FRIT EFFECTS ON SURFACE CHARACTERISTICS OF VITREOUS ENAMEL COATINGS

Ahmet Murat Erayvaz¹, Simone Felloni² Sandra Fazio⁵, Buğra Çiçek^{3,4}, Elisa Rambaldi⁵

¹Gizem Frit Research and Development Center, Sakarya, Turkey

²Gizemfrit Italy Co., Reggio Emilia, Italy

³Department of Metallurgy and Material Science Engineering, Yildiz Technical University, Esenler, Istanbul, Turkey

⁴Boron Based Materials and Advanced Chemicals Research and Application Center, Koc University, Sariyer, Istanbul, Turkey

⁵Centro Ceramico, Bologna, Italy

ABSTRACT

Lithium is an important element that brings technical value and benefits not only to traditional ceramics but also in porcelain, enamel and glass-ceramic technology. Lithium is known as the most active flux and the nucleation agent in glass and ceramics providing unique final characteristics such as high thermal shock resistance and thermal stability in thin coatings. Owing to these properties lithium containing enamel applications can be used in open flame cooking pots as well as oven-to freezer ware products. The research presents an investigation on surface characteristics of vitreous enamel coatings developed using Li-free enamel frits with alternative fluxes and nucleation agents. The frit compositions were prepared with respecting the existing production methods. The particle size, density and chemical characterization of the prepared frit samples were performed in comparison with the commercial compositions. The wet coating of metal sheets and firing of the enameled samples were carried out within the industrial parameters, including the density, viscosity, pH level, substrate material, wet-to dry process and the firing curve values. The surface characteristics of the obtained samples are evaluated in terms of mineralogical composition, microstructural characteristics and surface roughness parameters.

1. INTRODUCTION

It is well known that lithium is an important element that brings real value and benefits not only to traditional ceramic application but also to porcelain and enamel. From the literature review emerged that lithium is not an easy material to work with because it does not follow a straight-line performance but behaves differently in different applications under different environment. It generally requires more than one test to reach the desired objective. Lithium (Li) consumption has grown (grown rate of 20-30%) since the end of 90s due to the production of lithium ion battery.

Lithium is the lightest of all solid elements with a specific gravity of only 0.55334; lithium metal floats on water or gasoline¹⁻². Lithium has the smallest ionic radius and the highest ionic potential of any alkali (Tab. I). It is the highly reactive and does not stay in its elemental form unless protected.

Table I. Relative Ionic Potential of Lithium, Sodium and Potassium

Element	Ionic Radius (Å)	Ionic Potential
Lithium	0,60	1,67
Sodium	0,95	1,05
Potassium	1,33	0,75

It also differs from sodium in that it creates favorable internal nucleation conditions, whereas sodium tends toward internal nucleation. It raises the surface tension of glass and ceramics, whereas sodium and potassium reduce it. Lithium inclusion produce microcrystalline structure³.

Lithium is used extensively in industry. Lithium carbonates, are commonly used in the primary aluminum industry manufacturers and glass and enamel. Lithium stearate is used to make the oil automotive grease. The aerospace industry is hosts Li in its low-density Mg and Al alloys and, increasingly, Li-Si alloys are usable batteries. High Li concentrations in streams in mining regions may represent contamination from mine spoil and colliery wastes⁴.

It is not known that lithium is not necessary for humans; however, it is a biologically active element and Li-based drugs have been used to 225 treat manic-depressive conditions since the 1950s. It is thought to play a role in metabolic pathways and organ functions, although its specific function is unknown. Lithium is possibly toxic to plants at concentrations above 60 µg.⁶⁻⁷

The melting point of lithium carbonate is 720°C and spodumene melts at 1420°C, which means it must be combined with other fluxes to activate the contained lithium and obtain a lower liquid. The temperature composition projection of lithium and sodium oxides demonstrates how the eutectics of lithium and sodium work to lower melting temperatures.⁸⁻⁹

Glaze and enamel are glassy materials and will be handled under a single title. The properties of the application may limit the alumina or ion and may dictate the use of lithium carbonate in place of spodumene which may cause other issues. In both glass and ceramic applications, it has been said that lithium carbonate can cause gas problems because CO₂ is emitted¹⁰. CO₂ in the glass can create more air bubbles, affecting glaze; In ceramics, it may appear as holes in the glaze or body. Mineral sources do not evolve CO₂. Some of the following benefits overlap and may follow from body formula changes that include lithium to lower the firing times and temperatures, absorb free silica, or otherwise require a change in the glaze to much new body properties. General ranges quoted for Lithia to realize fluxing benefits would be as low as 0-10% spodumene or from 0.1% up to 5% LiO₂. As a flux Lithia completely dissolves in the glass phase and reduces expansion as well as firing temperature and/or time. In the glass formulas, it is recommended only 0.05-0,80% LiO₂, to achieve optimal benefits. More does not mean better in the case of lithium, but even though glazes or enamels are glassy materials, the aim of a research could be dictated by other additional levels. The correct source to use, this is usually determined by a combination of chemistry and cost. Generally, lithium for cover coat porcelain enamels tends to come from lithium carbonate because of limits on alumina and other impurities, but in ground applications, spodumene is preferred as lower cost source¹¹.

2. EXPERIMENTAL

2.1 Frit Preparation

The industrial frit named "ABE032" was chosen as reference. Frits were prepared in laboratory by mixing the raw materials (1.5 kg) in a porcelain jar with alumina balls (500 g of balls with diameter 1 cm and 1.5 cm) for 3 hours .. In particular, REFLY7 has modified amounts oxides respecting the industrial frit ABE032 (with about 0-20% of lithium carbonate), while FLY0 frit does not contain

Lithia (Li_2O). Lithium carbonate has been substituted with other carbonates; barium carbonate (BaCO_3), calcium carbonate (CaCO_3) and with sodium-raw materials; soda (NaHCO_3), sodium nitrate (NaNO_3), sodium phosphate (Na_2HPO_4). The frits were melted in a laboratory electric furnace till 1300° for 45 minutes and quenching in water.

2.2 Enamel Preparation and metal coating

Enamels suspensions were prepared by following industrial compositions. Three suspensions were prepared by using the industrial frit ABE032, REFLY7 and FLY0. In Tab. II the SEGER compositions are reported for all the samples named GLFLY7 IND, GLFLY7 LAB and GLFLY0, respectively. Raw materials were weighted and wet milled in a porcelain jar with alumina balls (155 grams of raw materials and 155 grams of alumina media) by using a planetary mill.

The enamel suspensions with the laboratory prepared frits with and without lithium (GLFLY7 LAB and GLFLY7, respectively) required additional water respect to the suspension with the industrial frit (GLFLY7 IND) due to high viscosity. Thus after adding other 30 grams of water over 60 grams, a longer milling time was needed to homogenize the suspensions (25-30 minutes in total).

The characteristics of all the three suspensions are reported in Tab. III in terms of pH, density, residue and particle size. As expected, in the suspensions with the laboratory prepared frits, GLFLY7 LAB and GLFLY7, due to the higher amount of water respect to GLFLY7 IND, pH and density was lower. Moreover, due to the increasing of milling time, resulted lower amount of the residue and particles size.

Metal specimens supplied by the industrial standard of about 1 mm thickness were dip coated on one side and weighted before and after the dipping. Samples were then dried at 110°C before firing.

Table II Seger tables for Enamels composition containing the industrial frit ABE032 (GLFLY7 IND) and the laboratory frits with and without lithium (GLFLY7 LAB and GLFLY0, respectively).

	Oxide	GLFLY7 IND	GLFLY7 LAB	GLFLY0
Seger oxide content (% mole)	R_2O (Na_2O , K_2O)	1,17	1,37	1,23
	RO (CaO , MgO , ZnO)	35,5	35,2	35,7
	R_2O_3 (B_2O_3 , Al_2O_3 , Fe_2O_3)	6,52	6,78	6,74
	RO_2 (SiO_2 , ZrO_2)	56,81	56,65	56,33
	TOTAL	100	100	100
Seger oxide ratio	$\text{SiO}_2/\text{Al}_2\text{O}_3$	45,389	46,448	43,785
	MgO/CaO	0,915	0,898	0,926
Seger molar value	$^a\text{B}_2\text{O}_3$ (BW)	0,144	0,145	0,143
BW content in compositions	BW (wt%)	23,45	24,6	24,3

^a B_2O_3 (BW), boron trioxide derived from boron waste.

Table III - Characteristics of the enamels suspensions

		GLFLY7	GLFLY7	GLFLY0
pH		9.60	8.54	8.67
Density		1.88 g/cm ³	1.67 g/cm ³	1.64 g/cm ³
Particle size	d(10)	6.8 m	3.9 m	2.6 m
	d(50)	46.7 m	35.1 m	22.9 m
	d(90)	115.8 m	85.0 m	58.6 m

2.3 Firing of the samples

The temperature of firing was selected bearing in mind the objective of the project to prepare low melting temperature enamel and by respecting the industrial process. The enamels, after drying in the oven to remove humidity, were transferred into a furnace 840°C. The coated metal samples were fired for 7 minutes in a laboratory electric furnace. Enamel thickness was around 100 -150 μ . The enamels, after drying in the oven to remove humidity, were transferred into a furnace. This slow cooling was done with the aim of establishing some crystalline phases in the resultant coating so as to succeed some good physical properties of the coatings and also to prevent crazing of the coatings. After cooling to room temperature the samples we removed from the furnace and taken for inspection and testing.

3. TESTS

3.1 Citric Acid

Citric acid test was performed following the EN ISO 28706-1 procedure. A fresh solution of citric acid solution was prepared (10 g in 100 ml of bi-distilled water). About 4 ml of this solution was applied in a cleaned area of the sample. This area was then covered (to avoid evaporation) and leaved for 15 minutes. Four areas for each sample were tested. In Fig. 1 some images of the text execution are show. Then, these areas were rinsed with water and dried at room temperature.

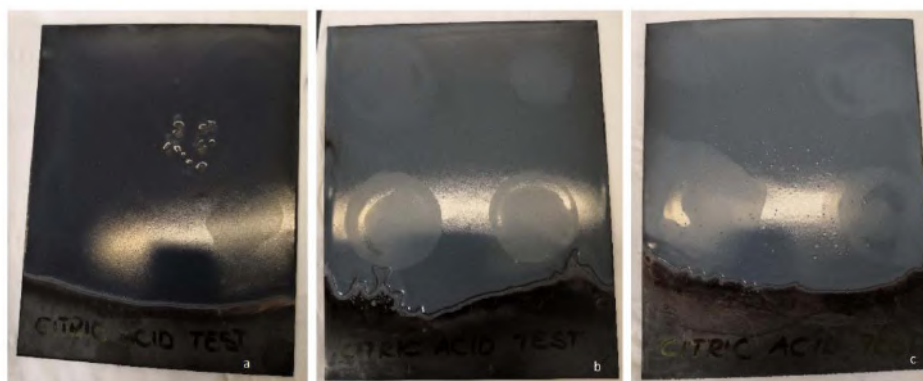


Figure 1. Samples images after the test: GLFLY7 IND (a); GLFLY7 LAB (b); GLFLY0 (c).

3.2 Impact resistance for adhesion evaluation

This test was performed by following the BS EN 10209 procedure. The impact testing machine was supplied by the plot application test. In Fig. 1 the standard classification is shown. The drop height (h) was 300 mm.

The test execution is shown in Fig. 2 and the samples images after the test are shown in Fig. 3. Impact test was repeated twice for all the samples. While the sample with the industrial frit GLFLY7 IND show a good level of adherence, where GLFLY7 LAB and GLFLY0 are both classified in class 5.





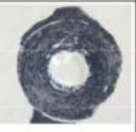




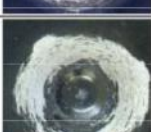
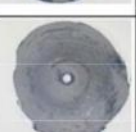

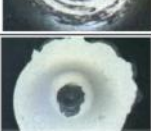


Class	Direct-on enamelling	2 coats/1 fire enamelling	Direct-on over Nickel pre-treatment
1			
2			
3			
4			
5			

Figure 2. Standard classification to evaluate the adherence level on enamels



Figure 3. Samples images after impact test: GLFLY7 IND (a); GLFLY7 LAB (b); GLFLY0 (c).

3.3 Scanning Electron Microscopy (SEM)/EDX Analysis

Scanning electron microscopy (SEM) analysis, an acceleration voltage of 20 kV was used at working distances of 9.5 and 10 mm. The observation of the images related to primary and permanent enamel shows two main morphological characteristics: various degrees of roughness; presence of furrows.

Surface roughness generally improves adherence by creating a greater contact area¹². SEM images of the surface with lithium and without lithium is showed Figure 4,5 and 6. Microscopic images of the representative areas were taken at 150X, 1500X, 10000X magnification on each enamel surface. These micrographs provided the microscopic characteristics of enamel surfaces, and later were used for comparisons between the baseline and follow-up images.

The produced frits do not have highly porous surfaces shown in Fig5. and Fig. 6.

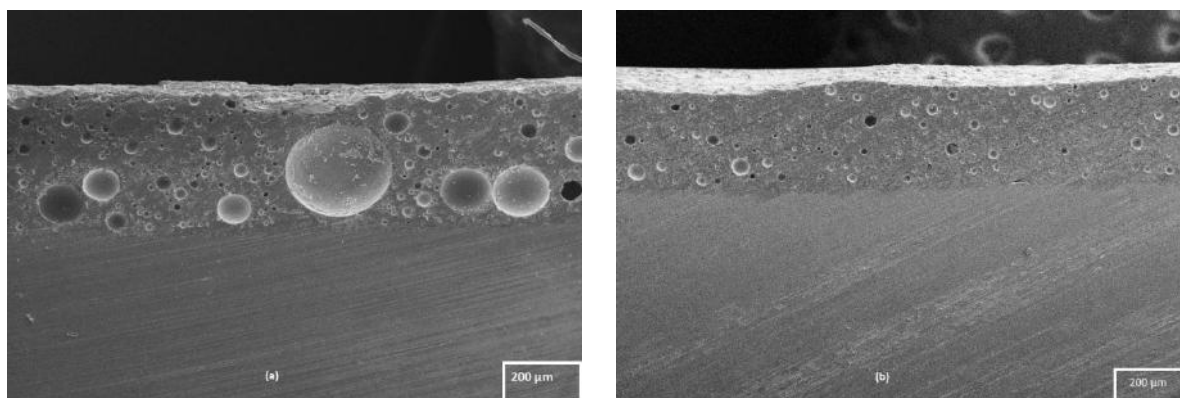


Figure 4. SEM images of surfaces of (a) GLFYLY7 and (b) GLFYLY0

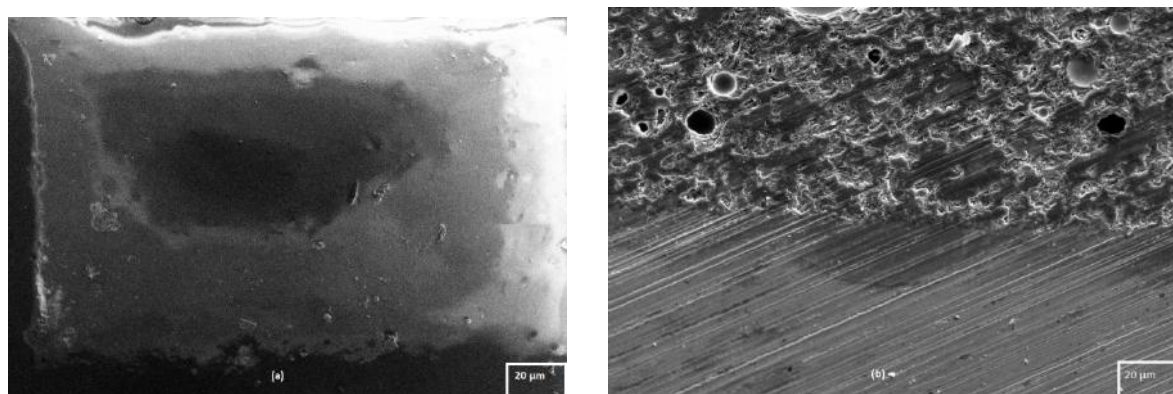


Figure 5. SEM images of surfaces of (a) GLFYLY7 and (b) GLFYLY0

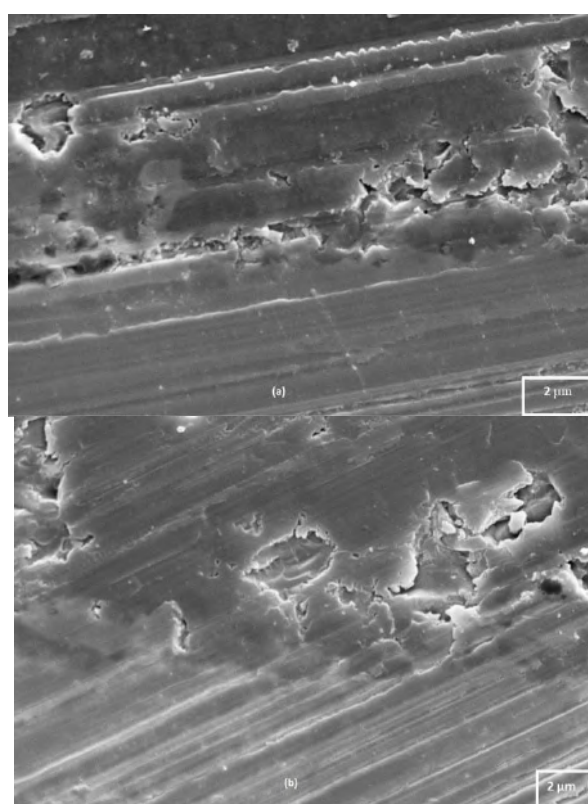


Figure 6. SEM images of surfaces of (a) GLFYLY7 and (b) GLFYLY0

4. CONCLUSION

In this research, novel enamel compositions without Li were studied. The preparation and application of the substrate and the coating enamel were successfully applied respecting the industrial procedure. The enamel coated plate were cooled down to room temperature for complete crystallization and the microstructure was observed with different cooling cycles. Study indicates that GLFLY7 LAB and GLFLY0 prohibits low adherence mechanism as a result of lack of intermetallic bonding. SEM analyses, showed that the developed compositions without Li were meeting the expected microstructure where low porosity vitreous enamel structure was aimed.

The observed amorphous phase was poor compared to that of standard composition due to LiO absence. In following studies, compositions containing different fluxing agents and intermetallic bonding providing metal oxides will be studied. The surface roughness of the obtained samples were within the range of industrial standards, which indicates pre-processed metallic substrate surface can promote expected adhesion mechanism with same composition such as, etched stainless steel.

5. REFERENCES

1. Greenwood, N.N. and Earnshaw, A., Chemistry of the Elements. Pergamon Press, Oxford, 1984
2. R. C. Weast (Ed.), Handbook of Chemistry and Physics, 57th Edition, CRC Press, 1976-77
3. R. Hultgren, et al, Selected Values of Thermodynamic Properties of the Elements, Inorganic Materials Research Division, Lawrence Radiation Laboratory (Berkeley), University of California, January 1973
4. Scrosati B., Lithium batteries: Status, prospects and future, Journal of Power Sources Review, Journal of Power Sources 195, 2010, 2419–2430
5. Chung, D., Elgqvist, E., Santhanagopalan, S., Automotive Lithium-ion Cell Manufacturing: Regional Cost Structures and Supply Chain Considerations, April 2016, Clean Energy Manufacturing Analysis Center (CEMAC)
6. Shorter E. The history of lithium therapy. Bipolar Disord. 2009;11
7. Licht R.W. Lithium: Still a major option in the management of bipolar disorder. CNS Neurosci. Ther. 2012;18:219–226.
8. J. O. Cowles and A. D. Pasternak, Lithium Properties Related to Use as a Nuclear Reactor Coolant, Lawrence Radiation Laboratory, CA, April 18, 1969
9. Gehm M. E., Properties of Li, 2003
10. Chung, D., Elgqvist, E., Automotive Lithium-ion Batteries, in 2015 Research Highlights, C.E.M.A.C. (CEMAC), Editor March 2016
11. US Geological Survey, Minerals Information, Lithium. Statistics and Information, Mineral Commodity Summaries. January 2016
12. Eppler R., et al., Glaze and Glass Coating, Adherence, 2000
13. <https://www.ceramicindustry.com/articles/83296-optimizing-enamel-adhesion>

ENAMELS

DEVELOPMENT OF NEW GENERATION ELECTROSTATIC ENAMEL POWDERS FOR WATER STEAM CLEANABLE FUNCTIONAL COOKING DEVICES

Şemsi Melih GÜLEN¹

¹Gizem Frit Research and Development Center, Sakarya/Turkey

At the present time development of the manufacturing of domestic appliances with high level of performance characteristics, particularly gas and electric, ovens, microwaves, etc. remains relevant. Among various technical solutions that provide high degree of reliability, durability, aesthetic qualities of these products, and simultaneously their competitiveness in different market sections one should distinguish the use of easy-to-clean coatings.

As known; in cooking appliances; an aesthetic appearance; a smooth surface, scratch and abrasion resistance, long-term use, thermal and chemical resistance, strong resistance to thermal shocks; enamel coatings are used because of their user-friendly features. In addition, self-cleaning feature of the cooking devices have been preferred by the customers. A self-cleaning which uses high temperature to burn off leftovers from baking, without the use of any chemical agents. But some self-cleaning features can cause problems such as high energy consumption and damage to systems due to high temperatures.

this study investigates the formation of new generation frit compositions and electrostatic powder enamel that can be worked on the cooking devices which used for self-cleaning feature only water vapor.

Keywords: Frit, Electrostatic Enamel, Coating, Aquatic / Hydroclean

1. INTRODUCTION

Vitreous enamel coatings, well-known since antiquity for use in jewellery, nowadays are widely employed for protection of different metals from corrosion, in particular, at high temperatures and pressure. Multitude of application fields of enamel coatings is motivated by an outstanding combination of wide variety of technical and decorative properties, viz., chemical and thermal durability, water, abrasion and temperature resistance, mechanical strength, hygiene as well as ability to be coloured with nearly perpetual preservation of colour characteristics. Therefore, in spite of wide use of polymer, metal and composite coatings, the vitreous enamel coatings remain highly demanded and even irreplaceable in certain fields.

At the present time development of the manufacturing of domestic appliances with high level of performance characteristics, particularly gas and electric stoves, ovens, microwaves, roasters etc., remains relevant. Among various technical solutions that provide high degree of reliability, durability, aesthetic qualities of these products, and simultaneously their competitiveness in different market sections.

In the domestic appliances, the quality race and competition environment, which started with the aim of raising the awareness of consumers and changing their demands, caused great changes in the sector. Depending on these, firms in the sector are working to increase product quality, diversity and capability for economic competitiveness. One of the most important product items of the sector, the cooker devices also vary in customer demand and market demands, and new device development efforts are accelerating. R & D activities are also inevitable in the chemical coating sector where the sector is in close cooperation with the works and increasing demands. The coatings used in the sector are seen as competitive elements in terms of customer and market expectations. As is known, in cooking devices; aesthetic appearance; smooth surface, scratch and abrasion resistance, long-term use, thermal and chemical resistance to protect, high and thermal shocks; because of its features such as user-friendly enamel coatings are used.

The search for competitiveness in the field of cooking appliances has instigated the development of new materials and new technologies of synthesis of vitreous enamels with special properties.

2. EXPERIMENTAL

2.1 Frit Preparation

Frits were prepared at laboratory and named "FRIT A, FRIT B, FRIT C"

Frit A	
Na ₂ O	6.19 - 10.76
K ₂ O	1.28 - 4.28
Li ₂ O	2.04 - 4.14
CaO	1.62 - 2.33
MgO	0.03 - 1.04
CoO	0.49 - 0.71
Fe ₂ O ₃	1.80 - 3.45
Cr ₂ O ₃	0.00 - 0.05
Sb ₂ O ₃	0.96 - 1.31
P ₂ O ₅	0.68 - 0.97
Al ₂ O ₃	0.31 - 3.78
B ₂ O ₃	13.35 - 19.18
SiO ₂	37.06 - 73.94
TiO ₂	2.46 - 4.97
ZrO ₂	5.04 - 8.85
MoO ₃	0.34 - 1.50

Frit B	
Na ₂ O	5.79 - 14.16
K ₂ O	1.5 - 4.16
Li ₂ O	0.5 - 0.99
CaO	1.0 - 4.40
BaO	1.0 - 1.31
CoO	0.1 - 2.23
MnO	0.4 - 0.69
Fe ₂ O ₃	0.8 - 1.16
Al ₂ O ₃	2.0 - 4.92
B ₂ O ₃	9.2 - 16.01
SiO ₂	54. - 88.41
F	1.2 - 3.81

Frit C	
Na ₂ O	5.09 - 11.25
K ₂ O	2.46 - 3.53
Li ₂ O	1.08 - 4.02
CaO	1.59 - 5.29
CoO	0.59 - 0.85
MnO	0.51 - 0.73
Fe ₂ O ₃	2.90 - 3.78
Al ₂ O ₃	1.28 - 1.67
B ₂ O ₃	10.43 - 19.30
SiO ₂	47.45 - 71.89
TiO ₂	1.79 - 4.58
ZrO ₂	5.03 - 8.56
MoO ₃	0.39 - 2.56
F	1.27 - 4.66

2.2 Preparation of enamel

Ball-mill grinding of the glass is accomplished using porcelain or high alumina balls 1.5–5.0 cm in diameter. Mill size, speed, and charge, and ball size and charge are important parameters for the determination of the milling time required for optimum size distribution in prepared slip. Electrostatic powder enamels are formed by grinding a number of frits together with pigments. Particularly, some silicone based oil addition and particle size are important for the purpose of providing physical characters. Three types of frits were used in this study. One coat one firing technique used for electrostatic application.

2.3. Characterization of enamel coatings

Porcelain enamels are basically alkali borosilicate glasses. These enamels are complex, however, because of the large number and types of oxides that are needed to develop proper adherence and functional properties. Network-forming ingredients and modifiers are used as in normal glass making practice. The principal network formers are SiO_2 , B_2O_3 , and P_2O_5 . Modifiers include the alkali metal oxides (Na_2O , K_2O , and Li_2O) and alkaline-earth metal oxides (CaO , BaO , and SrO). Other common oxides include Al_2O_3 , MgO , ZrO_2 , ZnO , TiO_2 , Sb_2O_3 , and the halide F_2 . Transition-metal oxides such as Fe_2O_3 , CoO , NiO , CuO , and MnO_2 are used for adherence to the sheet-steel substrate and color development in ground coats. Continuous-cleaning (catalytic) oven enamels have high percentages of the transition-metal oxides to achieve cleaning effectiveness. The silica content of a glass has a significant effect on the chemical and mechanical properties of the porcelain enamel. Increasing silica content is generally associated with increasing acid resistance and lowered thermal expansion. Increasing alkali content, particularly Na_2O , reduces acid resistance and increases the thermal expansion. Various modifiers such as Al_2O_3 (minor amounts) and ZrO_2 increase the alkali resistance, whereas TiO_2 , generally an opacifier if in crystal form, improves the acid resistance. Self opacified cover coats usually have titania as the crystalline phase; however, zirconia and antimony oxide are still used for some nonsheet-steel applications.

The composition of the enamel coatings were investigated with X-ray fluorescence.

ENAMEL	
Na_2O	6.27 - 9.48
K_2O	2.05 - 4.95
Li_2O	2.15 - 5.81
CaO	2.09 - 4.00
BaO	0.30 - 2.44
CoO	0.41 - 1.59
MnO	0.35 - 2.51
Fe_2O_3	2.35 - 6.07
Cr_2O_3	0.30 - 2.44
Sb_2O_3	0.26 - 1.34
P_2O_5	0.18 - 2.27
Al_2O_3	1.64 - 4.14
B_2O_3	11.41 - 19.40
SiO_2	52.12 - 77.98
TiO_2	1.61 - 4.31
ZrO_2	3.38 - 7.41
MoO_3	0.24 - 2.34
F	0.97 - 2.27

2.4. Determination of resistance to corrosion by water vapour

This test was performed by following the ISO 28706-2:2017 procedure. In Figure 1 test application and results

Enamelled test specimens is placed in the liquid zone and/or in the vapour zone of the test apparatus, as required, and exposed to attack by its water vapour, under specified conditions. The same design of test apparatus and the same test principle is employed for the different liquids. The loss in mass is determined and used to calculate the rate of loss in mass per unit area.

TESTS	Water Vapor (g/m ²) (24 hours)
Test 1	5,40
Test 2	4,20
Test 3	4,00

Total loss in mass per unit area;

For each test, calculate the total loss in mass per unit area, $\Delta\rho_A$, in g/m², for the total duration of the test using.

Figure 1

$$\Delta\rho_A = \frac{(m_s - m_f)}{A}$$

where

m_s is the starting mass, in g;

m_f is the final mass, in g;

A is the area exposed to attack, in m².

2.5 Impact resistance for adhesion evaluation

This test was performed by following the BS EN 10209 procedure. The impact testing machine was supplied by the plot application test. The drop height (h) was 300 mm. The test result was shown Figure 2.



Figure 2

CONCLUSION

As a results of beginning of these study, different formulations of frits and enamels will be experemented. Resistance to heat, adherence performance, ability to minimize discoloration, resistance to water vapor, color values, 10 % (w/w) citric acid resistance, pyrolytic capability, ETC feature, electrification ability and optimization will be examined.

This study is targeted; products can be used in water vapor cleaning function cooker devices, no discoloration problem, high resistance to acids, minimize the faraday cage error in chassis applications; a successful homogeneous coating thickness and not contain materials that will risk human health.

REFERENCES

1. Pietro Palmisano Murid Hussaina DeboraFinoa Nunzio Russoa, A New Concept For A Self-Cleaning Household Oven, 1 December 2011, Pages 253-259
2. L Bragina, O Shalygina, N Kuryakin, O. V. Shalygina, Powder Electrostatic Enamelling Of Household Appliances December 2011, Pages 25-26
3. L.L. Bragina, O.V. Shalygina, N.A. Kuryakin, N.M. Guzenko, V.I. Hudiakov, V.Z. Annenkov, Vitreous Enamels for Easy-to-Clean and Catalytic Coatings
4. Pat. 3266477 USA Cl. 126 – 19. Self-Cleaning Cooking Apparatus / A.B. Stiles. applicant and assignee E.I. du Pont de Nemours and Company, Wilmington – No 359984; Filed 15.04.1964; Date of Patent 16.08.1966. 4. Pat. 5387475 USA IPC B32B 9/00, B32B 33/00, B01J 21/00. Catalytic Coating for Cooking Surfaces. / D. Baresel, P. Scharner, H. Janku : applicant and assignee BoschSiemens Hausgeraete GmbH, Munich – No 862534; Filed 13.12.1990 ; Date of Patent 07.02.1995

ENAMELS

ENHANCED THERMAL CONDUCTIVITY PERFORMANCE OF BORON-DOPED REFRACTORY PARTICLE COATINGS ON VITREOUS ENAMEL COOKWARES AND INVESTIGATION OF ITS POTENTIAL APPLICATION ON MEAT COOKING AS A NOVEL METHODS

Büşra Mete ^{1,2,4}, Cansu Çeltik ^{1,5}, Salih Karasu ³, Buğra Çiçek ^{1,2 *}

¹ Department of Metallurgy and Material Science Engineering, Yıldız Technical University, Istanbul, Turkey

² Boron-Based Materials and Advanced Chemicals Research and Application Center, Koc University, Istanbul, Turkey

³ Department of Food Engineering, Yıldız Technical University, Istanbul, Turkey

⁴ Koç University, Department of Chemistry, Rumelifeneri Yolu, Istanbul, Turkey

⁵ Gizemfrit Research and Development Center, Sakarya, Turkey

ABSTRACT

Meat and meat product are usually exposed to any heat treatment before their consumption. The cooking methods directly affect some quality parameters of meat and products such as texture, color, and taste. Besides, some undesirable compounds especial polyaromatic hydrocarbons and cooking lose may occur during heat process. Therefore new approach should be improved to increase the quality of meat product and reduce occurring undesirable compounds and cooking loss. Developed boron doped refractory stable particles possesses high basal plane thermal conductivity compared with other materials (up to 390 W/m.K at room temperature) and almost matching graphite (350-420 W/m.K). In this study, application of boron doped refractory particle coatings on enameled surface promoted homogeneously distributed heat conduction, therefore, provided unique heat dissipation in thermal management configurations. Prevalently used cookware materials has moderate thermal conductivity, such as vitreous enamel (0,9 W/ m.K), PTFE (0,20 W/m.K), stainless steel (16 W/ m.K) and aluminum (205 W/ m.K). These materials lead to non-stable heat dissipation on cookware walls and overheating of sub-regional parts of food. Within the study, developed powders with 11 µm particle size is applied on vitreous enameled cookware surfaces by a spraying method and cured at 760 °C. This material was used to cook meatballs required quality parameters including color, cooking time, shrinkage and cooking loss were measured. The results showed that cooking time, cooking loss, shrinkage value and total color differences were significantly reduced by applying the developed coating as a cooking medium. This study suggested that developed coating material should be successfully used as a cooking material in a meat products.

Keywords: Boron Doped Refractory Particle, Enamel, Thermal Properties, Cookwares

1. Introduction

Cookware material which has high thermal conductivity to heat up faster and provides uniform temperature distribution on food-contacting surfaces should be chosen to improve cookware applications [7]. The majority of cooking devices are composed of metals or ceramics, as it has remarkable ability to endurance against heat. Boron doped refractory particle is a common thermally and chemically resistant refractory compound. The crystalline form has a melting point approximately at 2.400°K [8] and shows excellent thermal conductivity at about 390 W/m.K [1]. Due to the structure similarity, boron doped refractory particle possesses strong mechanical properties similar to graphite, such as thermal shock resistance, easy workability of hot-pressed shapes [9], excellent electrical insulating [10][11] and high chemical inertness (corrosion resistance against acids and molten metals), stability in air up to 1000°C (in argon gas atmosphere up to 2200°C and in nitrogen gas atmosphere up to 2400°C), high temperature stability (melting point approximately 2600°C) with low density ($2,27\text{ gcm}^{-3}$ theoretical density) [12].

Boron doped refractory particle is a naturally lubricious material used to promote thermal and tribological properties, whether used by itself or added into lubricants or appear in as a second phase in the work piece [13]. High thermal conductivity in bulk boron doped refractory particle indicates a potential for efficient heat removal and conduction in further integration and miniaturization of the modern electronics [14]. In order to achieve high thermal conductivity for composites used as a filler [15].

Enamel coating is a healthy alternative to potentially harmful cookware materials, which is comprised vitreous material over metal layer performed with high temperature ($760\text{-}820^{\circ}\text{C}$) reactions. Coating layer firmly bonded with the surface thereby forming a glassy non-toxic inorganic surface on cookware materials that also has mechanical strength and corrosion resistance. In the case of non-direct contact with a heat source, the thermal conductivity of enamel is very low ($0,9\text{ W/m.K}$)[3] compared to other materials (stainless steel, porcelain, aluminum, etc.). However, direct contact provides an ideal thermal distribution on the cooking surface due to silicate structure absorbs heat more efficiently [16]. It is difficult for a single material to meet a wide variety of requirements such outstanding thermal and chemical properties [7]. Therefore, motivated by the superior thermal conductivity of boron doped refractory particle while considering that enamel absorbs the heat productively, better understanding its thermal properties as a component on enamel layer is the main subject of this study. Meat and meat products are usually exposed to any heat treatment before their consumption. The cooking methods directly affect some quality parameters of meat and products such as texture, color, and taste. Besides, some undesirable compounds especial polyaromatic hydrocarbons and cooking lose may occur during heat process. Therefore new approach should be improved to increase the quality of meat product and reduce occurring undesirable compounds and cooking loss.

2. Material and methods

Boron doped refractory particles with 11-micrometer grain size are applied to the enameled surface as a top coat layer.

Cast iron samples with $90 \times 90 \times 3\text{ mm}^3$ dimensions were chosen as the base material. Mechanical cleaning was performed by the abrasive blasting which is an operation to increase the surface area.

Additionally, surfaces were degraded with alcohol and water. Enamel solution was prepared by using a soft frit type which has 760 °C curing temperature, clay, and other additives. Primer enamel coating was selected from low curing temperature frit recipe in an attempt to ensure strong coherency to enamel surface at relatively lower production temperatures. Table 1 indicates to the composition of enamel for primer base applied on each sample.

RTU Frit	
Na ₂ O	9.0 - 11.4
K ₂ O	0.87 - 1.07
Li ₂ O	2.18 - 2.77
CaO	4.32 - 5.33
MgO	0.08 - 0.12
Fe ₂ O ₃	2.12 - 2.70
Al ₂ O ₃	2.48 - 3.16
B ₂ O ₃	12.7 - 15.8
SiO ₂	50.6 - 64.4
TiO ₂	0.84 - 1.04
ZrO ₂	2.24 - 2.85
MoO ₃	0.18 - 0.22
F	1.14 - 1.45

Table 1 Composition of enamel for a primer base

Conventional wet enameling method was chosen in order to coat primer layers of substrates. Raw materials of RTU (ready to use) enamel were mixed and reduced to fine particles by milling process for 15 minutes performed by MMS Ball Miller® with 600 grams of big size alumina ball for 1-liter mill vessel. After water and rheology agents were added to obtain the appropriate viscosity, liquid enamel slurry was fed into the nozzle of a spray gun. The slurry was atomized by compressed air and was ejected from a nozzle onto the metal base surface at 1.5 - 2 bar pressure. The operation was carried out continuously until the desired primer coating thickness (between 150-200 µm) was achieved.

The starting boron doped refractory powders were supplied by H.C.Starck®. High degree of crystallinity boron doped refractory powder with +40 µm grain size was ball milled progressively for 2-3 hours in order to obtain 10-11µm grain size. In the first step, the grain size of the powder was lowered to 16 µm through the wet grinding process (with 150 ml tap water) is performed on MMS Miller® by using large alumina balls. Grinding operation was continued with 200 grams of the smallest size zirconia ball which has high specific weight and Retsch Planetary Mill® (400 rpm, for 30 minutes) for more effective milling operation. It was observed that fine-grained particles ensure better dispersion and abrasion to enamel surface. Laser diffraction method was used for particle size measurement with Malvern Mastersizer 2000 Ver.5.31®. Grain size and curing temperature parameters were evaluated during studies. Ideal grain size was determined to be as 10µm, and suspension of boron doped refractory powder was applied with spraying method over the primer enamel coated surface as a top coat layer. Then the samples were transferred to Protherm® furnace and were cured at 760°C which is below T_g (glass transition temperature) of the primer enamel layer for 15 minutes.

Cooking of meatballs

Two types of heating plate namely enamel and boron-doped refractory particle coatings on vitreous enamel were used to meatballs formulated by chicken meat. The samples were cooked by direct contact heating on a preheated plate surfaces. The cooking process was ended when the central point

temperature of samples reached 75°C. The thermocouple (Digitec, Modena, Italy) recorded the temperature for each 10 second period to determine cooking properties.

Cooking loss, shrinkage and color value

Cooking loss was calculated by measuring weight differences between raw and cooked samples by the following equation;

$$\% \text{ loss} = \left(\frac{\text{Meatball} - \text{Cooked meatball}}{\text{Meatball}} \right) \times 100, \quad \text{Eq(1)}$$

The following equation described the shrinkage value of the meatball samples;

$$\text{Shrinkage (\%)} = \frac{(\text{Raw thickness} - \text{Cooked thickness}) + (\text{Raw length} - \text{Cooked length}) \times 100}{(\text{Raw thickness} + \text{Raw length})} \quad \text{Eq(2)}$$

Surface color change of the samples was determined by a chroma meter (CR-13, KONICA MINOLTA, Tokyo, Japan) at four different edge spots on the surface of each sample before and after the cooking treatment. Total color differences (ΔE) was used to compare the effect of the cooking plate on a surface characteristic of the samples. ΔE was calculated following equation;

$$\Delta E = \sqrt{(\Delta L)^2 + (\Delta a)^2 + (\Delta b)^2} \quad \text{Eq(3)}$$

2. Results

The following outcomes were drawn from this studies are that curing temperature above the T_g leads to surface defects such as gas removal gaps and pin hole over enamel surface. In addition to curing temperature, the viscosity of the boron doped refractory particle suspension, curing time and surface quality of the substrate are important factors about the processability for its application as a developer layer.

Samples	Coating Thickness
Sample 1	171 μm
Sample 2	136 μm
Sample 3	162 μm
Control Group(enamel)	138 μm

Table 2 Coaing thickness of samples

Cooking time and cooking characteristics

Cooking time was determined based on the central temperature (reached 75°C) of the meatball samples. Cooking times were 3.05 and 4.8 minutes for enamel and boron-doped enamel plates. Fig 1 shows the cooking characteristic of two samples. As can bee seen, constant rate cooking behavior was observed for boron-doped enamel, indicating heat transfer rate did not show a declining trend. This can be explained by a low change in physicochemical properties of the food products. For the enamel plate, rapid cooking rate was observed during the initial period of the cooking. However, the cooking rate was reduced with elapsing cooking time. This can be attributed to the formation a crust by fast cooking.

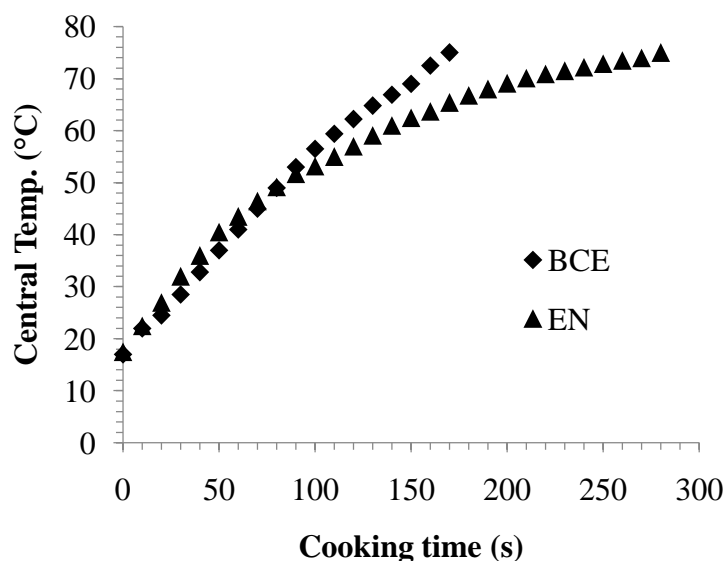


Fig 1 The cooking characteristic of enamel and boron-doped enamel plates

ΔE values were 18.08 and 26.15 for boron-doped enamel and enamel plate. This results showed that boron-doped enamel leads to low color change indicating that low degradation in food material part contacting heating plate was observed. The color quality indicates the formation of some undesirable compounds as well as sensorial quality.

Cooking losses were 8.63 % and 12.5 % for enamel and boron-doped enamel plates. The cooking loss was related to high degradation in protein, removing of fat and stickness of food material to the hot surface. The results showed that boron-doped surface caused low cooking to lose and low degradation. The shrinkage values of the samples were 9.23 % and 6.92 % for enamel and boron-doped enamel plates. Low shrinkage shows the good cooking quality of food materials.

This results suggested that boron-doped surface should be used as a cooking material in a meatball samples due to low cooking loss, color change, and low shrinkage value.

References

- [1] I. Jo, M. T. Pettes, J. Kim, K. Watanabe, T. Taniguchi, Z. Yao, L. Shi, Thermal Conductivity and Phonon Transport in Suspended Few Layer Hexagonal Boron Nitride, *Nano Lett.* (2013), 13; 550–554
- [2] L. Börnstein, Thermal Conductivity of pure Metals and Alloys, Group III Condensed Matter book series Springer, (1991), 15; 426-429
- [3] C. Hull, International Critical Tables of Numerical Data, Physics, Chemistry and Technology, (1929), 5th. Ed. National Academies
- [4] www.engineeringtoolbox.com/thermal-conductivity-d_429.html, accessed at 11.07. 2018
- [5] http://www.farm.net/~mason/materials/thermal_conductivity.html, accessed at 11.07.2018
- [6] <http://hyperphysics.phy-astr.gsu.edu/hbase/Tables/thrcn.html> accessed at 11.07.2018
- [7] M. R.Sedighi, B. N. Dardashti, Heat Transfer Modeling in Multi-Layer Cookware using Finite Element Method, *World Academy of Science, IJMME*,(2012), Vol:6, No:1

- [8] S. Gleiman, Chun-Ku Chen, A. Datye, J. Phillips, Melting and spheroidization of hexagonal boron nitride in a micro wave-powered, atmospheric pressure nitrogen plasma, (2002), J. Mater. Sci. 37;3429–3440
- [9] H.Zhou, J. Zhu, Z. Liu, Z. Yan, X. Fan, J. Lin, G. Wang, Q. Yan, T.Yu, P. M. Ajayan, J. M. Tour High thermal conductivity of suspended few-layer hexagonal boron nitride sheets, J.Nano Research, (2014), 8:1232-1240
- [10] C. Yuan, B. Duan, L. Li, B. Xie, M. Huang, X. Luo, Thermal Conductivity of Polymer-Based Composites with Magnetic Aligned Hexagonal Boron Nitride Platelets, ACS Appl.Mater.Interfaces, (2015), 23: 13000–13006
- [11] C. Sevik, A. Kinaci, J. B. Haskins, C. Tahir, Characterization of thermal transport in low-dimensional boron nitride nanostructures, (2011), Bull.Am. Phy. Soc., Physical Review B, 84
- [12] B. Ertug ,Powder Preparation, Properties and Industrial Applications of Hexagonal Boron Nitride, InTech, (2012)
- [13] N. Ooi, V. Rajan, J. Gottlieb, Y. Catherine and J. B. Adams, Structural properties of hexagonal boron nitride, Model Simul Mater Sc (2006), 3:515-535
- [14] M. J. Meziani, W.L. Song, P. Wang, Y.P. Sun, Boron Nitride Nanomaterials for Thermal Management Applications, ChemPhysChem (2015), 16(7):1339
- [15] Z. Lin, A. Mcnamara, Y. Liu, Exfoliated hexagonal boron nitride based polymer nanocomposite with enhanced thermal conductivity for electronic encapsulation, Compos. Sci. Technol., (2013), 90: 123-128
- [16] edt. A. Çavuşoğlu, SERES 11 II. Int. ceramic, glass, porcelain enamel, glaze and pigment congress, 10 – 12 October 2011

REFRACTORIES

INFLUENCE OF TABULAR ALUMINA ADDITION ON THE PROPERTIES OF SELF-FLOWING MAGNESIA BASED CASTABLE REFRACTORIES

Busra Alpdogan*, Azade Yelten-Yilmaz*, Ferhat Tocan**, Suat Yilmaz*

*Istanbul University- Cerrahpasa, Department of Metallurgical and Materials Engineering, Avcilar Campus, 34320/Istanbul/Turkey

**PiroMET Refractory Plant, Cerkesli OSB Mah. IMES 2. Cad. No.3, Dilovasi, 41455/Kocaeli/Turkey

ABSTRACT

The ever-increasing demand and application of unshaped refractories to replace conventionally shaped refractories due to many major advantages have inspired scientists and manufacturers to continuously investigate these materials in depth and to improve their quality and performance. In the light of these researches studies based on development of self-flowing magnesia (MgO) refractories are becoming gradually widespread. Relatively low hydration resistance of MgO is the main factor that complicates the flowable casting of it. In this study, various properties of the self-flowing MgO based castable refractories were studied for a comparative understanding of the effect of tabular alumina addition in different ratios.

Keywords: Self-flowing castables, magnesia castable, mechanical properties, slag corrosion.

INTRODUCTION

The castable contains wt. 95-99% MgO is generally used for shaped refractories. Many parameters are evaluated to determine which type of magnesia is suitable for the product to be produced for the particular purpose. These magnesia selection criteria determine the physical, thermal, chemical properties of the final product.

Tabular alumina is re-crystalline sintered α -Al₂O₃ with high density and used in refractory industry for shaped and unshaped products. As the material has been sintered it has an especially low porosity, high density, low permeability, good chemical inertness, high refractoriness and is especially suitable for refractory applications.

Industrial applications also demand improved castable properties such as better chemical stability, mechanical strength or abrasion resistance in the intermediate temperature range. [4] In this study, Influence of the chemical composition on the physical and mechanical properties of the MgO based self-flowing refractories containing tabular alumina (α -Al₂O₃) at different ratios was investigated. The obtained samples were dried at 100 °C and fired at 1600 °C. Physical tests such as bulk density, apparent porosity and water absorption determination, mechanical tests such as compression strength test, chemical tests such as slag corrosion test were applied to the fired samples. As the result of these tests, it was aimed to develop the properties of the product further by comparing the mechanical strength and chemical corrosion performances of the MgO based self-flowing refractory samples containing tabular alumina. [1-5]

EXPERIMENTAL

Preparation of samples

The chemical compositions of the castable refractories are given in Table 1.

The steps to be followed in the production stage and the equal conditions have been determined in accordance with the mechanism in which MgO powders are mixed with tabular alumina. MgO powders were obtained by adding α -Al₂O₃ in ratios of wt. 0%, 3%, 6%

and 10% respectively classified as X, Y, Z and T types.

Samples were homogenized by mixing in a 7% aqueous medium, and then formed into small crucibles by shaping through vibration in molds and prepared according to DIN 51069. [3] For mechanical testing, cubic samples with 50x50x50 mm dimensions were prepared by means of vibration. The prepared mud mass is provided of filling the steel mold secured on vibrator. The mass is placed in the mold properly and the air remaining inside it is removed as bubbles with the help of vibrator. The refractory samples were sintered at 1600°C with the heating speed of 10°C/min to achieve hardness. The self-flowing magnesia refractories containing tabular alumina were stored at room temperature for 30 minutes.

Table 1 Chemical composition of castables (wt-%)

MgO	SiO ₂	CaO	Fe ₂ O ₃	Al ₂ O ₃
95,50	1,50	2,10	0,80	0,10

Mechanical properties

Water absorption, apparent porosity and bulk density tests according to Archimedes' principle and compressive strength tests were applied to the samples that had been prepared for mechanical testing.

Test results for samples of the castable refractories are given in Table 2 and Table 3.

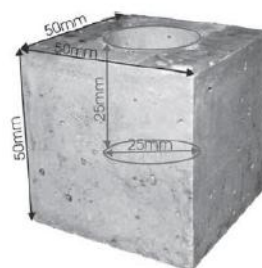


Figure 1 Geometry of refractory crucible

Table 2 Physical properties of castables

	Apparent porosity, %	Water absorption, %	Bulk density, g cm ⁻³
X	11,22	3,81	2,95
Y	9,60	3,37	2,84
Z	13,41	4,61	2,92
T	14,47	5,10	2,83

Table 3 Compressive strength of castables

Specimen	X	Y	Z	T
Compressive strength (MPa)	36,18	21,32	30,54	34,40

Slag corrosion test for castables

The chemical composition of the slag is given in Table 4. Slag charges were applied to the inside of the castable crucible pot samples prepared according to DIN 51069. Slag powder and crucibles were heated up to 1600°C for 1 hour with the heating speed of 10°C/min. After reaction with the slag, corrosion surfaces of castable samples were examined by using a hard diamond cutter in an axial form [1], [2]

Table 4 Chemical composition of ladle slag (wt-%)

MgO	3,40	MnO	4,8
			9
			0,2
Al ₂ O ₃	5,57	SO ₃	8
			0,1
SiO ₂	18,96	K ₂ O	2
			0,5
P ₂ O ₅	0,45	TiO ₂	6
			1,2
Fe ₂ O ₃	29,90	Cr ₂ O ₃	9
CaO	32,78	AZ	1,8

For the quantitative analysis of the slag penetration area, slag-refractory corrosion interface of samples has transferred into computer by using a high resolution (600 dpi) in the Samsung Xpress M2070W model scanner. The obtained data was processed in Adobe PhotoShop-CS6 in order to examine penetration area of the slag. [2]



Figure 2 Slag penetration areas of castables

MATLAB software was used for image analysis after slag-refractory contact surface was uncovered as shown in Fig 2.

CONCLUSION

According to the results obtained from the study on MgO self-flow refractories containing tabular alumina, physical, mechanical properties and slag corrosion resistance characteristics showed that the best result was achieved on specimen "Y" which contains wt. 3% tabular alumina. All the castable samples show relatively close but negative performance. It can be concluded that, a low tabular alumina content of wt. 3% provides a higher granulation effect between MgO grains and increases sintering, which reduces porosity and provides high slag corrosion resistance.

ACKNOWLEDGEMENT

This work was supported by Research Fund of Istanbul University (Grant number 27125) and PiroMET Refractory Plant.

REFERENCES

1. Yilmaz S., "Corrosion Of High Alumina Spinel Castables By Steel Ladle Slag", IRONMAKING, 2006, vol.33, pp.151-156.
2. Kurban C.E., Erzi E., Yilmaz S., "A Novel Approach For Quantitative Measurement Of The Slag Penetration Area In Refractories By Using Computer Aided Image Analysis", Material Prüfung - Materials & Testing, 2011, vol.53, pp.629-633.
3. DIN 51069 Blatt 2: 'Prüfung keramischer Roh- und Werkstoffe; Vergleichende Prüfung des Verhaltens feuerfester Werkstoffe gegen den

Angriff fester und flüssiger Stoffe bei hoher Temperatur, Tiegelverfahren (TV)', Berlin, Nov.1972.

4. Schnabel M., Schmidtmeier D., Rainer K., "Castables for industrial applications – Still room for improvement" Eurogress, Aachen, Germany, Sep.2013, pp.13-19.

GLAZES and PIGMENTS

**SYNTHESIS AND CHARACTERIZATION OF MICRONIZED CoAl_2O_4 SPINEL CRYSTALS
AS CERAMIC PIGMENTS
BASED ON INK-JET PRINTING**

Seçil Aydın¹, Büşra Mete², Oğuzhan Çimen¹, Hilal Nur Güçlü¹, Buğra Çiçek^{3,4}

¹Gizem Frit Research and Development Center, Sakarya, Turkey

²Koç University, Graduate School of Sciences and Engineering, Department of Materials Science and Engineering, Istanbul, Turkey

³Yıldız Technical University, Department of Metallurgical and Materials Engineering, Istanbul, Turkey

⁴Boron Based Materials and Advanced Chemicals Research and Application Center, Koc University, Sarıyer, Istanbul, Turkey

ABSTRACT

The ink-jet printing technology has been an increasingly preferred technology in ceramic tile industry since it has the ability to provide higher resolution with numerous pattern options. It is a well-known fact that, by virtue of ink-jet technology, the time and cost of tile production can be kept under expected levels with containable production.

The micronizing of ceramic pigments still remains as a first step for ceramic ink manufacturing.

The present study represents, micronized CoAl_2O_4 spinel crystals synthesized from a homogeneous mixture of cobalt oxide (CoO) as the source of cobalt (Co) and hydrated alumina ($\text{Al}(\text{OH})_3$) as the source of aluminium (Al) at a ratio of 1:8 (Co:Al) via solid state reaction method.

The samples were calcined at different temperatures ranging between 500°C to 1250°C for one hour in order to determine the effect of the calcination temperature on the properties of CoAl_2O_4 .

The characterization of the samples were assigned based on thermogravimetric and differential thermogravimetric analysis (TG-DTA), X-Ray diffractions (XRD) and Brunauer, Emmett and Teller (BET) surface area analysis.

Results investigate the varying colors and particle sizes as a result of different calcination temperatures. The increase at the calcination temperature resulted in the brighter blue particles as greater particle aggregation of the final product. 1250°C calcination temperature is the optimized heat treatment to obtain ceramic pigment with the highest colorant efficiency. The obtained results are applicable in industrial production.

Key Words: Ceramic pigment; spinel structure; calcination; solid state reaction

1. INTRODUCTION

The ink-jet printing technology has been an increasingly preferred technology in ceramic tile industry since it has the ability to provide higher resolution with numerous pattern options. It is a well-known fact that, by virtue of ink-jet technology, the time and cost of tile production can be kept under expected levels with containable production. [1]

Inorganic ceramic inks which are synthesized from highly dispersed and fluidized inorganic ceramic pigments are required in order to apply the ink-jet printing technology to ceramic products. Ceramic pigments are used in ceramic industry to color the ceramic glazes need to be thermally stable at glaze firing temperatures, have minimal reaction with the molten glaze, and also have good color performance. [2]

Most of the ceramic colouring materials used in pigment industries are of transition metal oxides with the spinel structure having high surface area, thermal stability and chemical resistance [3] The main aspect of spinels is the presence of metal oxides of general formula AB_2O_4 , of which $CoAl_2O_4$ is one. They consist of a cubic close-packed array of oxide ions called as spinel structure with A^{2+} ions and B^{3+} , in tetrahedral and octahedral positions, respectively. $CoAl_2O_4$ is a double oxide with a normal spinel structure. [4]

The color of the pigment is thus related to its crystallinity. Crystallinity changes with the reaction conditions such as temperature. [2] The spinel-type $CoAl_2O_4$ compound can be synthesized by a variety of methods such as the sol-gel, hydrothermal, co-precipitation and thermal decomposition of organic or inorganic precursors. [5] $CoAl_2O_4$ and other oxide spinels for coloring ceramic products are generally produced conventionally via solid-state reaction method. In this study, $CoAl_2O_4$ powder was obtained from a mixture of Co and Al oxalates at a ratio of 1:8 (Co:Al). The material was calcined at different temperatures to obtain thermally stable compound which is useful to ceramic ink-jet printing.

2. MATERIALS AND METHODS

Blue ceramic pigment $CoAl_2O_4$ is produced as a solid solution from cobalt oxide and hydrated alumina. These raw materials were mixed at a molar ratio of 1:8 (Co:Al). The mixtures were milled by water to obtain a very homogenous mixture. The slurries were then dried at 180°C. The materials were calcined in Nabertherm LH 60/14 with Controller B400 Professional Chamber Furnace between 500°C and 1250°C temperatures for one hour by applying a heating rate of 10°C/min. The calcination temperatures were determined from thermogravimetric analysis (TGA; TA Instruments, SDT2960) carried out at a heating rate of 10°C/min in static air with a Perkin Elmer thermal balance. The surface area of the calcined material was determined by using a NOVA 4200e equipment in accordance with the theory of BET (Braunauer-Emmett-Teller). The crystallographic structures present were determined from a Shimadzu diffraction equipment, model XRD-6000, using Cu K α radiation.

3. RESULTS AND DISCUSSION

The thermogravimetric plot of the mixture between cobalt oxide and hydrated alumina mixture (Fig. 1) was used to select the calcining temperatures to obtain $CoAl_2O_4$. Thermal analysis has been carried out on precursor, shows that the compound became thermally stable above 950°C. weight loss percentages were 0,17% at 30–200°C, this can be attributed to elimination of the water in sample. The weight loss of 20,46%, at the temperature 200–400°C, represents the removal of the ligand molecule. The masses remaining at 600-1000°C were % corresponding to the removal of CO, CO_x, and NO_x gases from the sample then the solid solution of cobalt aluminate spinel structure began to form approximately at 1100°C.

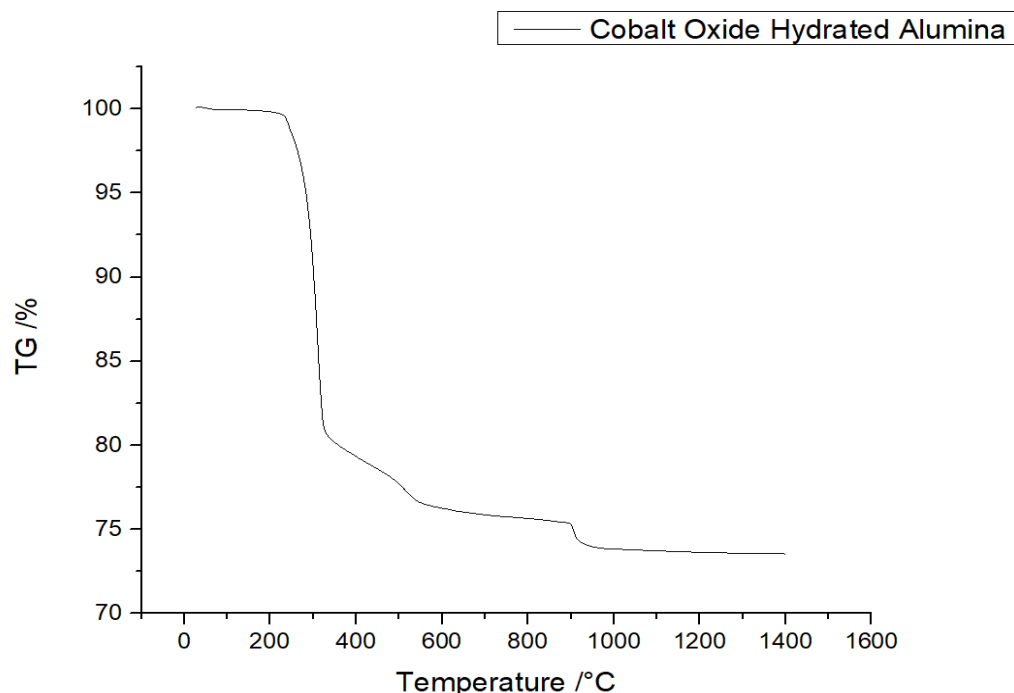


Fig. 1 Thermogravimetric curve of mixture between cobalt oxide and hydrated alumina

Table 1

Effect of the temperature on the surface area of pigments calcinated at 500, 700, 900, 1100 and 1250°C

Sample °C	Co:Al (ratio)	S _{BET} (m ² /g)
CoAl ₂ O ₄ (500)	1:8	119,392
CoAl ₂ O ₄ (700)	1:8	77,057
CoAl ₂ O ₄ (900)	1:8	49,956
CoAl ₂ O ₄ (1100)	1:8	15,475
CoAl ₂ O ₄ (1250)	1:8	7,685

BET data (Table 1) suggested that the surface area of the material decreased with increasing calcining temperature. This affects the milling conditions to micronize the pigments. The X-ray diffraction for calcinated powders at different firing temperatures showed the formation of the spinel phase in Fig. 3. At 1100°C the calcinated powders begin to appear as the spinel of crystalline form producing from amorphous phase. By increasing temperature above 1100°C, intensities of peaks increase gradually until sharpened peaks are observed at 1100°C and 1250°C. The crystalline spinel phase content and also the particles' size increase with increasing calcination temperature that is shown in Table 1.

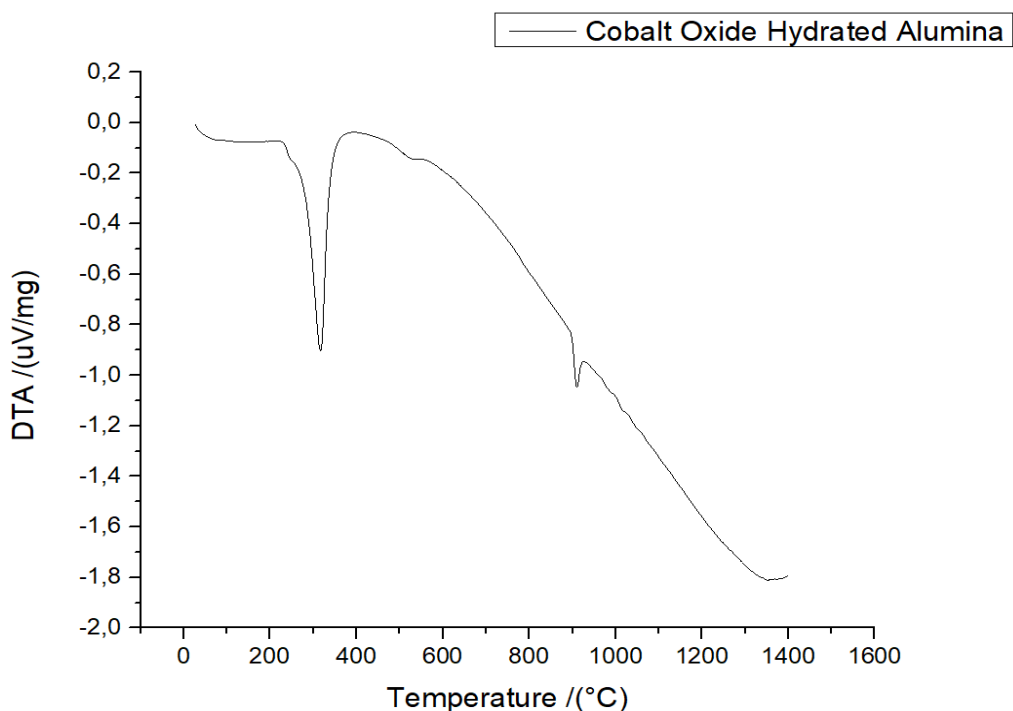


Fig. 2 DTA of mixture between cobalt oxide and hydrated alumina

Decomposition and formation of an oxide occurred at 950°C. Endothermic event that took places at 316,9 C and 910,7°C. Calcination was then carried out 500°C, 700°C, 900°C, 1100°C and 1250°C to promote the spinel crystalline structure. The calcination at 1100°C also aimed at evaluating the thermal stability of the compound at ceramic firing temperatures.

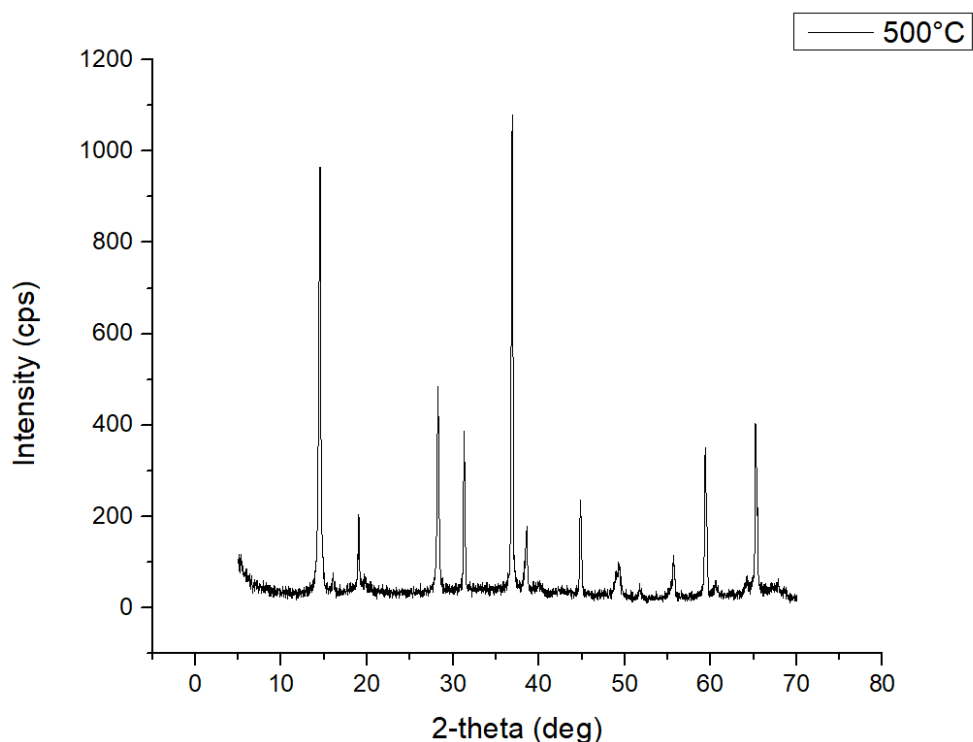


Fig. 3 X-ray diffraction pattern of powder calcinated at 500°C

The X-ray diffraction for calcinated powders at 500°C shows the Cobalt Oxide crystalline structure, Co_3O_4 , according to the ICDD Card No. 00-043-1003 and also Boehmite, (AlOOH) , according to the ICDD Card No. 01-072-0359.

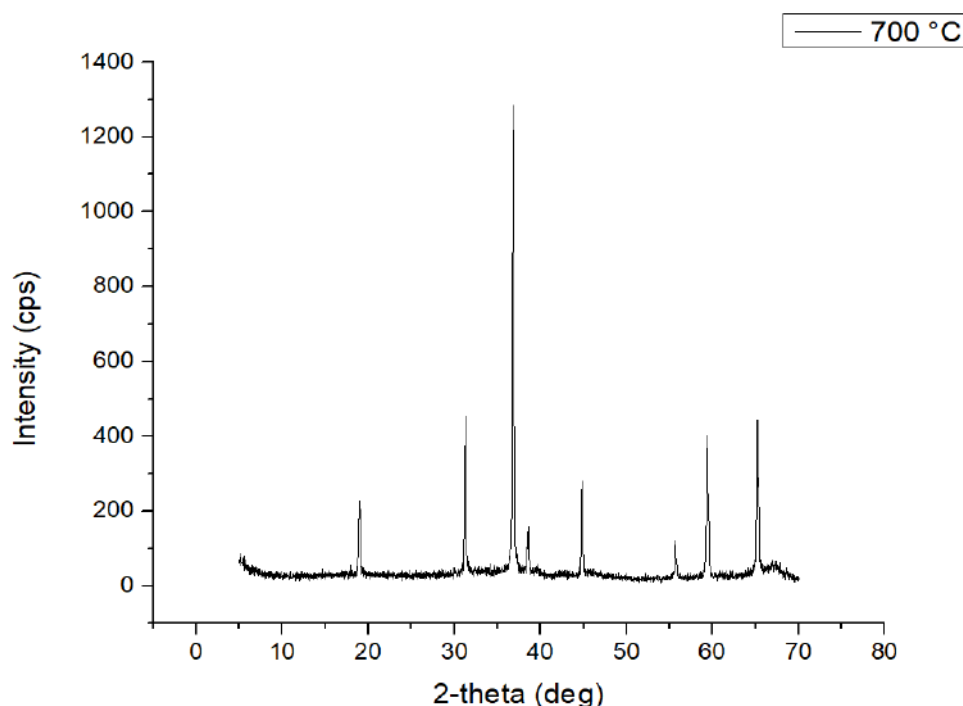


Fig. 4 X-ray diffraction pattern of powder calcinated at 700°C

The only Cobalt Oxide, Co_3O_4 , crystalline structure can be seen from the X-ray diffraction according to the ICDD Card No. 00-043-1003.

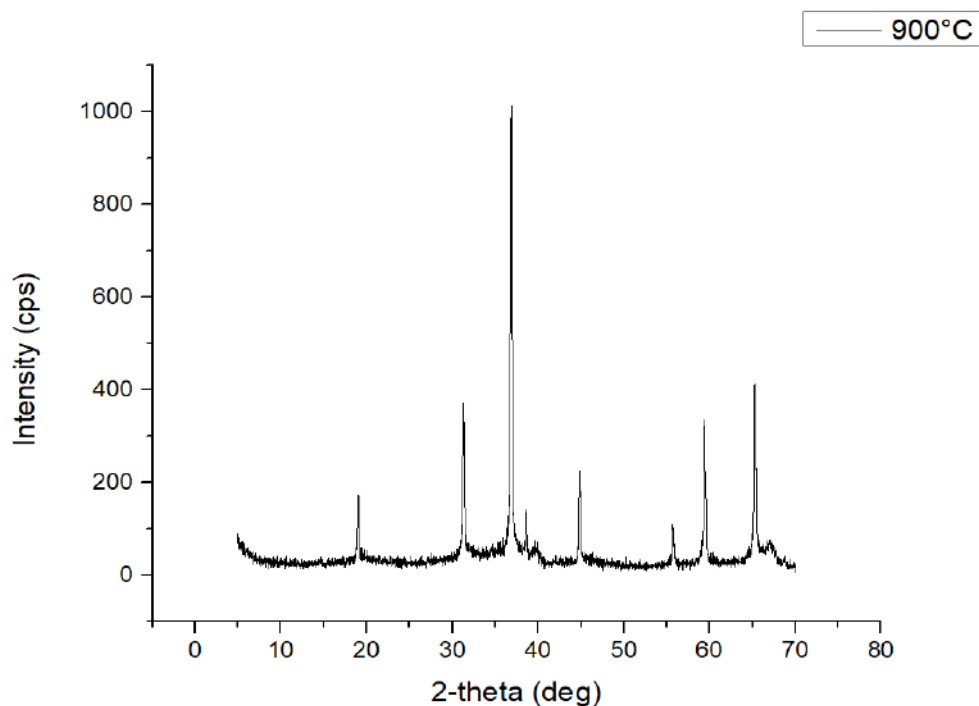


Fig. 5 X-ray diffraction pattern of powder calcinated at 900°C

The X-ray diffraction for calcinated powders at 900°C shows the same results with the material calcined at 700°C.

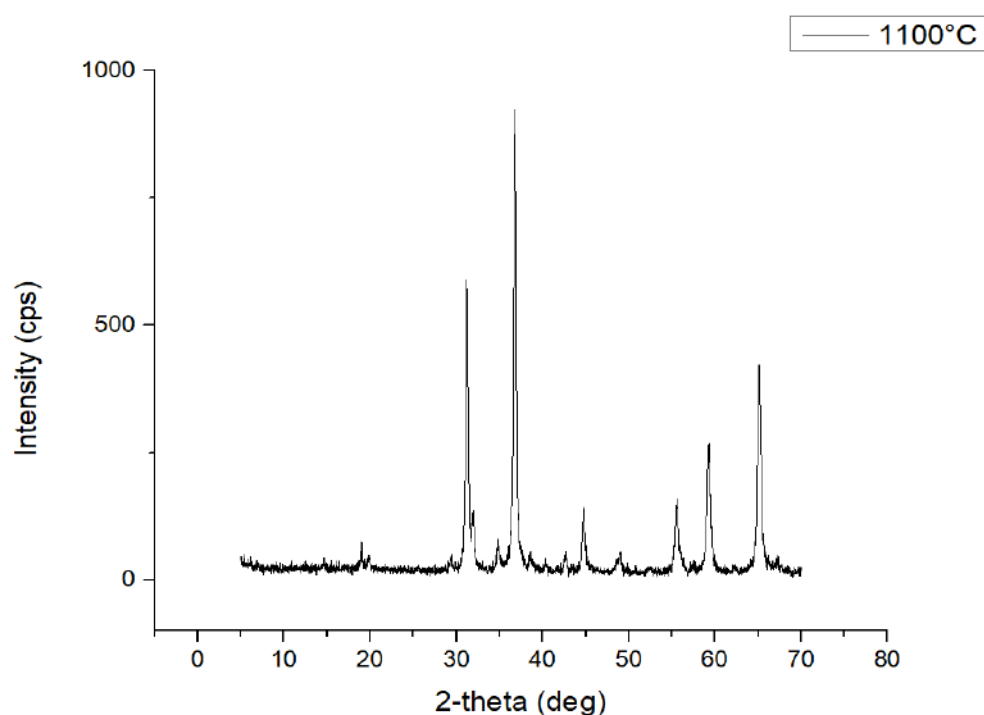


Fig. 6 X-ray diffraction pattern of powder calcinated at 1100°C

The X-ray diffraction for calcinated powders at 1100°C shows the spinel cobalt dialuminium oxide, CoAl_2O_4 according to the ICDD Card No. 01-082-2242, Cobalt Oxide crystalline structure, Co_3O_4 , according to the ICDD Card No. 01-070-2855, Corundum, Al_2O_3 , according to the ICDD Card No. 01-076-7774, Aluminum Oxide, Al_2O_3 , according to the ICDD Card No. 01-076-8188.

1

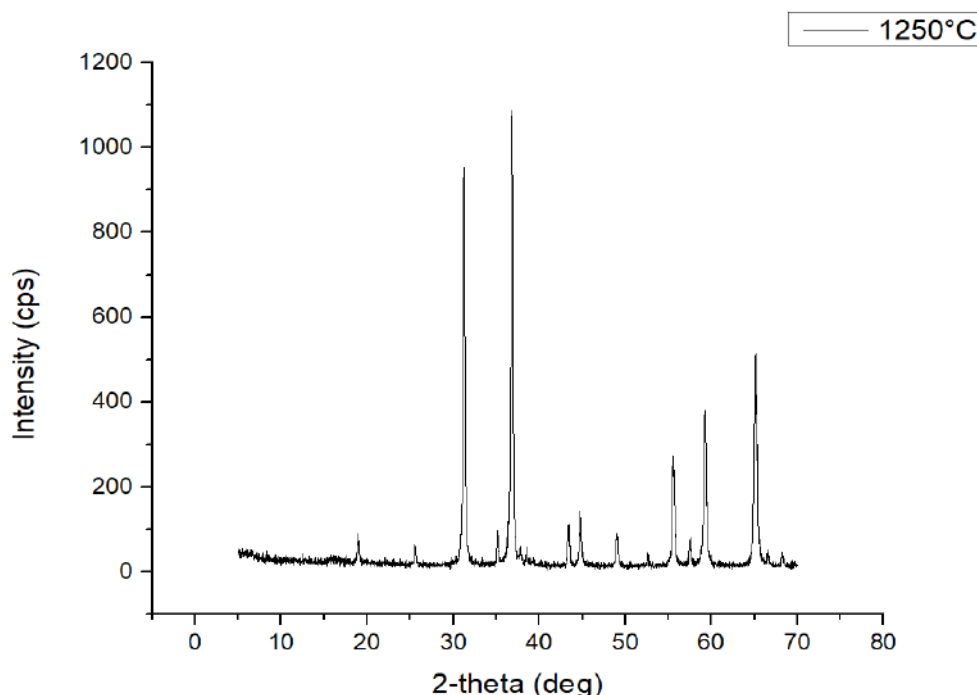


Fig. 7 X-ray diffraction pattern of powder calcinated at 1250°C

The X-ray diffraction for calcinated powders at 1250°C shows the spinel Cobalt Dialuminium Oxide, CoAl_2O_4 , according to the ICDD Card No. 01-082-2241 which has more intensity than the calcined material at 1100°C. Corundum, Al_2O_3 , according to the ICDD Card No. 01-076-7774.

4. CONCLUSION

Blue ceramic pigment CoAl_2O_4 is produced as a solid solution from metallic oxides. This powder prepared by solid-state reaction method. Powders are crystallized by calcining at different temperatures and characterized by different tools. The different calcining temperatures provide different degrees of blue colors. Different temperatures also resulted in the formation of crystalline phases. The best results were obtained calcining the spinel CoAl_2O_4 phase at 1250°C.

References

- [1] Dondi M., Industrial Ink-Jet Application of Nano-Sized Ceramic Inks, *Advances in Science and Technology*, 2006, 174-180
- [2] Cavalcante P.M.T., Dondi M., Guarini G., Raimondo M., Baldi G., Colour performance of ceramic nano-pigments. *Dyes and Pigments*, 2009, 80, 226-232.
- [3] Deraz N. M., Moustafa M.G., Synthesis, Structural, Morphological Properties of Cobalt-Aluminum Nanocomposite, 2013, 2756-2767
- [4] Melo D.M.A., Cunha J.D., Fernandes J.D.G., Bernardi M.I., Melo M.A.F., Martinelli A.E., Evaluation of CoAl_2O_4 as ceramic pigments, *Materials Research Bulletin*, 2003, 38, 1559-1564
- [5] Obata S., Kato M., Yokoyama H., Iwata Y., Kikumoto M., Sakurada O., Synthesis of nano CoAl_2O_4 pigment for ink-jet printing to decorate porcelain, 2011, 119, 208-213

GLAZES and PIGMENTS

FULL LAPPATO GLAZE

Hüseyin Köken

Akgün Group, Research and Development Center, Eskişehir/Turkey

ABSTRACT

Glaze compositions for the production of high-quality full lappato tiles were studied. Perfections have been aimed at in transparency, gloss, internal porosity, mechanical strength, and thermal shock resistance properties of the glaze, in keeping with the actual productivity standards and the real porcelain tile's water absorption (less than 0.1%) besides using current and common tools, equipment, and materials. The roles of each process in the manufacturing of full lappato tiles have been discussed regarding operational excellence.

The achieved impressive results will be shown in this paper, with microscopic images. The effect of mullite on edge chipping and crazing issues will also be mentioned.

INTRODUCTION

Full lappato tiles are polished glazed porcelain tiles. The term *lappato* refers to the semi-polished finish that is attained by polishing only the top of the texture of the glaze for the two depth effects (one level is matte, whereas the other is glossy). In the case of the full lappato finish, the glaze is fully polished by using flexible abrasives that are capable of polishing the surface topography by coping with it.

Full lappato finishes cannot be as straight as levigato finishes (polished unglazed porcelain tile or polished natural stone surfaces) in spite of being fully polished, since the glaze thickness (0.2–0.3 mm) cannot allow required surface calibration, which is applied by grinding up to 0.5 mm with diamond rollers, for the leveling of the surface waviness and thickness variations before polishing. Therefore, on a full lappato tile's surface, the deep bumps may stay as matte zones, or the high ridges may become bald (white) after polishing. In addition, the darker areas may appear milky from porosity or lack of transparency, even though the polished surface has a uniform gloss.

The human eye perceives 12 million colors and 300 dpi resolution from a distance of 30 cm [1-2]. With the ability to print up to 1516 colors at 360 dpi resolution on ceramic tiles, digital printers offer the opportunity to imitate polished marbles by full lappato porcelain tiles. However, a perfect imitation can only be achieved when they are produced with an unwavy and nonporous finish with high and uniform gloss and transparency.

MATERIALS AND METHODS

Milling, glazing, firing and polishing processes were carried out at industrial level in one of the AKGÜN plants. Table 1 displays the most relevant conditions.

Determination of resistance to thermal shock was carried out by Ceramic Research Center (SAM) according to TS EN ISO 10545-9 and also by subjecting tiles to 200°C due to our demand; and both tests were reported as “Not damaged” (R 0394, R 0395).

Information about the engobe and the successful glaze composition is presented in Table 2. The influences of each material on the performance of the glaze will be explained and discussed further in

the Results and Discussion section. However, the other components that were found to either fail or be ineffective during the study are not indicated in this paper.

ENGOBE	
Slip density and quantity / Slip dry content	1450 g/l – 460 g/m ² / 49%
Slip residue (+ 0.045 mm) / Sieve	2-3% / 150 mesh
Application type	Airless pistol
GLAZE	
Slip density and quantity / Slip dry content	1830 g/l – 550 g/m ² / 72%
Slip residue (+ 0.045 mm) / Sieve	2-3% / 150 mesh
Application type	Bell
KILN	
Reference fired size and thickness	600 x 1200 x 10 mm
Cycle / Maximum temperature	60 min / 1210 °C
LAPPATO	
Abrasive type and sequence	Resin bond, 180-5000 Grit
Gloss after polishing	80-85 GU/60°
Nano A / Final gloss	50 g/m ² / 100 GU/60°

Table 1- The most relevant conditions and parameters for the industrial production.

ENGOBE	
Frit type / sphere, half sphere, melting temperatures	Opaque / 1050 °C, 1220 °C, 1250 °C
Clay	over 65% illite
Other raw materials and ingredients	Albite, Quartz, Zircon
GLAZE	
Frit type / sphere, half sphere, melting temperatures	Transparent / 1050 °C, 1180 °C, 1200 °C
Kaolin	over 85% kaolinite
Other raw materials and ingredients	Nepheline syenite, Wollastonite, Barium Carbonate, Zinc Oxide
Seeger formula	Na ₂ O-0.16, K ₂ O-0.03, CaO-0.57, MgO-0.03, BaO-0.06, ZnO-0.15, Al ₂ O ₃ -0.30, SiO ₂ -2.31, B ₂ O ₃ -0.11

Table 2- The information about the engobe and the successful glaze composition.

RESULTS AND DISCUSSION

To have a better understanding by ruling out the operational errors that can eventually cause surface defects, the influences of some production steps on the fired finish need to be discussed before the findings about the glaze composition.

The body: Raw materials containing alkaline earth fluxes such as CaO and MgO can be avoided in body recipes to prevent pyroplastic deformation (warping, roller effect) resulting from a low melting viscosity, which can be caused by the formation of diopside (CaMgSi₂O₆) between 800 °C and 900 °C [3]. Also, kaolin should be free from alunite [KAl₃(SO₄)₂(OH)₆] lest the glaze be ruined by blisters due to the decomposition of K₂SO₄ (K₂O + SO₃) at 1200 °C [4]. In fact, the less the kaolin content of

the body, the better its plastic deformation (cold working, delayed curvature) because of the high cooling contraction of free quartz [5].

Pressing: To avoid bumps in the shaping step, the isostatic punches with plates seem to help for better finishes, especially when the distance between channels is wide enough and the oil-less frame of the punch is as narrow as possible. Also, the size adjustment method of putting paper or metal sheets under the upper punch is never recommended, for the same reason.

Glazing: The thickness of the glaze should not vary throughout the tile surface when it comes to the glazing line, and measuring the amount difference by placing little cups on the center and the edges can be suggested. Furthermore, the engobe and the glaze must both be sieved to eliminate coarse particles that might end up as blisters after firing, as shown in Figure 1.

Firing: High temperature in the firing zone is helpful in blister recovery. By adjusting the flatness of the tiles also at the entrance of the firing zone, warpages in the midsection of the tiles can be reduced, hence the reason for the rise in polished surface quality.

The Glaze Composition

The following figures illustrate the results of the tests conducted by European composed glaze suppliers that aimed to develop their own alternatives to this study in our facility:

- Figure 2 represents this study as the standard glaze.
- Figure 3 and Figure 4 exemplify the glazes composed by the supplier companies.

Of these glazes, which were prepared in the laboratory and applied on the same dark design, it can easily be observed that the standard glaze has much better transparency and porosity.

As the products of this study, the glaze performances of the full lappato tiles resulting from the industrial production are shown in Figure 5 and Figure 6; as seen, the surface pores that are filled with nano coating appear to be white, the deep pores look dull and the near-surface pores seem to be bright.

Wollastonite, nepheline and transparent frit were used in the glaze composition for vitrification. Nepheline, as the main feldspathoid ($\text{Na}_3\text{K}[\text{AlSiO}_4]_4$), was preferred for its 3/1 sodium-potassium eutectic, which makes it a more powerful flux than feldspars, and silica deficiency so that more free quartz is not introduced into the glaze, since partially dissolved quartz grains increase viscosity and favor porosity. Nevertheless, due to its higher alumina and lower silica content, nepheline decreases thermal shock resistance of the glaze by increasing the thermal expansion. Wollastonite (CaSiO_3) was chosen specifically because of its autocatalytic behavior; once dissolved, it makes the glassy phase more aggressive in dissolving other ingredients [6]. In addition, it acts like a natural frit in the composition, with the fluxing ability of CaO , with the contribution of SiO_2 as the major glass former, and without the volatile decompositions. Thus, it was used along with the transparent frit in which the quartz is already dissolved and converted to its amorphous glassy form.

The air inside the interparticle spaces, which amounts to around 50% of the glaze volume, is transformed into gas bubbles when the glaze melts. This is why glazes may have a perfect surface without any bubble defects (dimples, pinholes or blisters), and yet they still have plenty of internal pores. Thus, the only way to clear the bubbles is by diffusing them to the surface, where they may collapse and be partially healed over; afterward, the traces left (pinholes) on the glaze can be completely cleaned by polishing. Degassing the glaze melt and removing all the bubbles requires a low level of viscosity and surface tension. Moreover, a high temperature is needed, especially above the rollers in the firing zone of the kiln, to accelerate the gas release by convection, and to ensure that the quartz grains are melted so they cannot serve as an anchor for the gasses and support their retention in the glaze. Since BaCO_3 and ZnO are active fluxes in lowering the viscosity and surface tension only when they are used in small amounts, they were used together as additives in the glaze composition. The addition of BaCO_3 , as the main source of BaO , was also found to help clear the bubbles in the glaze. This is thought to be associated with the fast decomposition of BaCO_3 ($\text{BaO} + \text{CO}_2$) at 1030°C [7], which may promote the removal of bubbles by increasing their ascension rate to the surface. In this situation, bubbles moving upwards may create extensional flows pulling up the static bubbles from below; and the bubble chaining effect thus generated accelerates the bubble agglomeration that will support the ascension by decreasing the gas-liquid interface area [8]. In our

study, the anticipated color change caused by ZnO was not considered to be an issue because some redness was already needed for our black ink.

Transparent and bubble-free full lappato glazes may become susceptible to crazing even when the thermal expansion of the glaze is less than that of the engobe, which is less than that of the body. These glazes do not have enough barriers, such as pores or crystals, to block the diffusion of the subsurface damages generated by polishing, such as scratches and micro cracks. Therefore, apart from the purpose of keeping other materials in suspension, the amount of kaolin was increased to encourage the formation of needle-like secondary mullite crystals until that amount was proven to be enough to secure the thermal shock resistance and the mechanical strength of the polished glaze, as determined by the results of the tests and observations. These crystals are produced from the amorphous aluminosilicate phase above 1200°C; and they only arise in the presences of a liquid phase (low-viscosity glassy phase) and the amorphous aluminosilicate such as metakaolinite (dehydroxylated kaolinite at 550°C) [9]. Presumably, the crystals are not desirable for transparency because the light passing through the glaze can be refracted or reflected by them. Hence, this subsequent reinforcement of the glaze is most likely to support the idea that a transparent glaze containing acicular mullite crystals can be developed if high flux content is included in the composition [10].

Finally, the nano coating, which is considerably more effective on less porous glazes, is also necessary in order to make the glaze stain-proof after polishing and as glossy as the polished black glass standard with a reflectometer value of 100 GU at 60°.

CONCLUSION

The present study revealed that it is possible to produce a high-quality transparent glaze that is nearly nonporous inside, at the industrial level and under the fast-firing conditions of porcelain tiles. Moreover, using the process presented in this study it is also possible to preserve other important full lappato porcelain tile product features, such as straightness, gloss, mechanical strength and thermal shock resistance, and to ensure that the tiles have less than 0.1% water absorption.

REFERENCES

- [1] R. Hirsch, *Light and Lens: Photography in the Digital Age*, Routledge, NY, 2018.
- [2] L. Alsheimer, B. O. Hughes, *Black and White in Photoshop CS4 and Photoshop Lightroom*, Focal Press, Burlington, MA, 2009, p. 4.
- [3] M. J. Trindade, M. I. Dias, J. Coroado, F. Rocha, Mineralogical transformations of calcareous rich clays with firing, *Applied Clay Science*, 42 (2009), 345–355.
- [4] H. Gülensoy, Türk alünitlerinin termogravimetrik ve mikrokaleorimetrik metotlarla etüdü ve piroliz ürünlerinin suda ve sülfat asidindeki çözünürlüklerinin tespiti, *Maden Tetkik ve Arama Dergisi*, 71 (2015), 93-128.
- [5] H. Köken, Improving the Strength and Stain Resistance of the Body for Polished Porcelain, *Ceramics Technical*, 36 (2013), 113-117.
- [6] W. M. Carty, *Materials & Equipment and Whitewares*, vol. 20, The American Ceramic Society, Westerville, OH, 2008, 10-14.
- [7] I. Arvanitidis, D. Sichen, S. Seetharaman, A Study of the Thermal Decomposition of BaCO₃, *Metallurgical and Materials Transactions B*, 27B (1996), 409-416
- [8] H. Suzuki, Y. Furukawa, R. Hidema, Y. Komoda, Flow and Oxygen-Dissolution Characteristics of Microbubbles in a Viscoelastic Fluid, *Journal of Chemical Engineering of Japan*, 47-2 (2014), 201–206.
- [9] J. B. Wachtman, *Materials and Equipment - Whitewares Manufacturing*, vol. 14, The American Ceramic Society, Westerville, OH, 1993, 117-119.
- [10] F. J. Torres, E. R. Sola, J. Alarcon, Mechanism of Crystallization of Fast Fired Mullite-Based Glass-Ceramic Glazes for Floor-Tiles, *Journal of Non-Crystalline Solids*, 352 (2006), 2159-2165.

GLAZES and PIGMENTS

IMPROVEMENT OF MECHANICAL PROPERTIES OF TRANSPARENT POTTERY GLAZES BY USING BASALT

Elif Eren Gültekin¹

¹Selçuk University, Department of Airframe and Powerplant Maintenance,
Alaeddin Keykubat Campus, 42130/ Selçuklu-Konya/Turkey

ABSTRACT

Basalt is a magmatic rock that preferred due to against wear and climatic conditions. The aim of this study, improve mechanical properties of transparent pottery glazes by using basalt in glaze compositions. For this purpose the basalt of Nevşehir region (Acıgöl-Tatlarin) from Turkey was selected. The experimental studies were carried out under laboratory conditions. Hardness and bending strength values of glazed samples increased with basalt addition.

Keywords: Basalt, glaze, strength, hardness

INTRODUCTION

The application of glaze layer following sintering of ceramic had significantly improved surface hardness of ceramic material [1]. Baharav et al. studied glaze thickness' effect on the fracture toughness and hardness of alumina-reinforced porcelain. Disks of feldspathic porcelain reinforced with 2% aluminum oxide were prepared and glazed for 0, 30, 60, 90, and 120 seconds. Fracture toughness (K_{IC}) and Vickers hardness number (VHN) were determined with a micro indentation technique. Glazed layer increased linearly with an increase in glazing time. At 0 seconds, the minimal glazed layer was so thin that the K_{IC} and VHN values measured were that of the underlying alumina reinforced porcelain. At 30 seconds, glazing time a thin 2 μ m layer of glazed porcelain was formed with a lower K_{IC} . At 60 seconds, the 4 μ m glazing layer exhibited the lowest K_{IC} and VHN values. From 60 seconds, a progressive increase in K_{IC} and VHN was observed. At 90 seconds, the glaze was thicker (6 μ m) and started to show higher K_{IC} and VHN values for the new glaze layer. When the glazed layer was thick enough (8 μ m, 120 seconds), K_{IC} and VHN values surpassed those of unglazed porcelain [2]. In order to improve the hardness of commercial bone china, Kim et al. attempted to control the glaze firing temperature and apply a chemical strengthening process. When the glaze firing time was longer or its temperature was higher than normal conditions, the hardness was improved by approximately 5%. The chemical strengthening process also enhanced the hardness of the glaze by more than 13% compared with bone china [3]. Some additives also enhance the hardness of glazes. Venkatesh et al. used nano zirconia to increase abrasion resistance of ceramic glazes. Abrasion resistance for nano zirconia over 1500 revolutions it is inferred that very less surface erosion and thereby increases surface hardness compared with the standard composition. Surface hardness is less also surface is eroded slightly. It is also can be said as that increasing the percentage 0.5-13.6% of nano zirconia directly increases the abrasion resistance of material [4]. Zhang et al. added Ag/ZnO nanocomposite to achieve improvement of mechanical properties, microscopic structures, and antibacterial activity of glazes. The Ag/ZnO nanocomposite powder significantly affects the performance of glaze. Glaze hardness reached the highest value (96.6 HV) at the low sintering temperature of 1130 °C with the addition of 10% Ag/ZnO nanocomposite powder [5]. Pekkan and Gün investigated different metal oxides' effect on vickers hardness of the frit based crystalline glazes. The metal oxide contribution into the glaze recipe increased the hardness values of the glazes generally. MnO increased the hardness of the glaze much higher than Fe₂O₃, NiO, CoO, Cr₂O₃[6]. Yekta et al. prepared glass-ceramic glaze to improve glaze surface properties of floor tile. With increasing amounts of calcium and magnesium oxides to base glass, the optimum glass-ceramic glaze was obtained. The comparison of micro hardness for the optimum glass ceramic glaze derived in this work with a traditional one used in floor tile industries indicates an improvement of 21%. It was found that

the glaze hardness not only depend on the amount and type of crystalline phases, but also on the residual glass composition [7].

Benson investigated glaze variables' effect on the mechanical strength of whitewares in her thesis. Through the use of flexure testing and fractographic analysis, the effect of multiple glaze variables on the mechanical strength of two commercial porcelain bodies was characterized. Glaze composition was systematically altered through varying the SiO_2 level in the glaze. This in turn, caused a change in the thermal expansion of the glaze. As the amount of thermal expansion mismatch between the glaze and the body was increased, the strength of the samples increased. For the silica body, it appears that a maximum value in strength, of 97 MPa, has been reached. Once the level of mismatch between the body and glaze reached $0.93 \times 10^{-6}/\text{K}$, further mismatch caused no statistically significant increase in strength. The alumina body reached a maximum in strength, of 161 MPa, when a mismatch between body and glaze reached a level of $1.13 \times 10^{-6}/\text{K}$ [8]. Longhini et al. investigated effect of glaze cooling rate on mechanical properties of conventional and pressed porcelain on zirconia. The porcelain can be applied by the conventional handlayer technique onto the zirconia (VM) or by the press technique (PM). The two-way ANOVA was performed for the biaxial flexural strength (MPa) of the bilayered specimens for the porcelain material and the cooling method variables. Fast cooling: immediate removal of the specimens after the end of firing (900°C), leaving them on the bench until they achieve the room temperature and slow cooling: after the end of firing, the oven was switched off and kept closed with the specimens inside, until dropping to room temperature. The means of the flexural strength (σ , MPa) and standard deviations (SD) of the bilayers biaxial flexural strength, cooled at slow or fast rate were: VM9/Slow= 167.15 ± 30.53 ; VM9/Fast= 186.83 ± 51.45 ; PM9/Slow= 234.89 ± 49.19 ; PM9/Fast= 232.24 ± 40.55 . This analysis indicated significance only for the porcelain material variable [9].

Basalt is a magmatic rock which has high chemical durability, high resistance to abrasion and corrosion [10-11]. Dvorkin and Galushko were added 45.5-77.2 wt. % basalt to the glaze composition and they have applied the glazes to pressed clay bodies. They obtained the glaze-body compatibility in the products which they sintered at $1170\text{-}1200^\circ\text{C}$. The basalt containing glazes had high elastic modulus, dynamic strength, acid and alkali resistance [12]. In this study, 20, 60, 100 wt. % basalt of Nevşehir region (Acıgöl-Tatlarin) from Turkey was added to transparent pottery glaze. Hardness and bending strength values of glazed samples were measured.

EXPERIMENTAL STUDIES

Basalt from Nev Beton Basalt Plant (Nevşehir, Acıgöl-Tatlarin) was ground to smaller particle size with ring crusher (Ünal Engineering) in dry basis. The particle size distribution of the basalt was measured using a Malvern Mastersizer 2000 G particle size device (Fig. 1). The mean particle size of basalt is $30.056 \mu\text{m}$. The ground basalt was added to the transparent base glaze at the ratios 20, 60, 100 wt. %. The solid concentrations of the glaze recipes was held constant at 50 % by mass. Glazes were applied on slip cast and semi-wet shaped plates with a dipping method. Firing of the glazed plates was performed at 1000°C in a Protherm PLF 130/25 furnace.

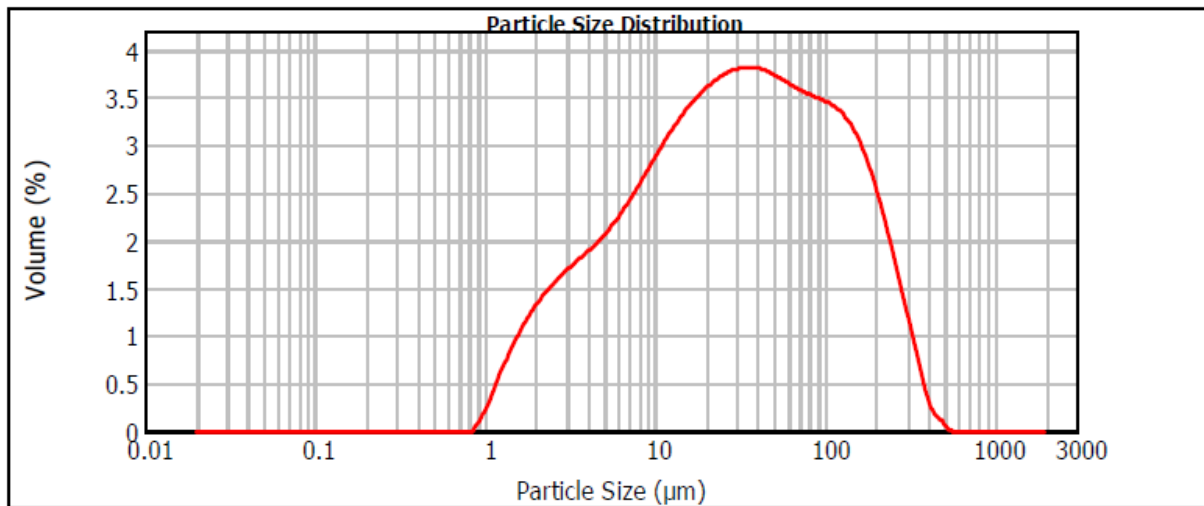


Figure 1. Particle size distribution of ground basalt

CSM nano-indentation testing device was used to measure hardness of glazes. Diamond Berkovich type tip was used for measurements. The tip moves with 3000 nm/min speed and applies a linear force (max: 500 mN) to sample.

The term strength (the stress required to cause fracture) is normally taken (if not specified) to mean bend strength. Bend strength, in three- or four-point loading, is easy to measure, once test bars have been machined to the requisite size and surface finish. The three-point bend strength (σ_{\max}) for a rectangular cross-section bar is obtained from the load (F) required to cause failure using the standard expression

$$\sigma_{\max} = \frac{3Fl}{2bd^2} \quad (1)$$

where l is the distance between the two outer knife-edges, and b is the breadth, and d the thickness, of the bar. The value of σ_{\max} is the maximum stress experienced by the bar, along a line on the bar face, opposite the central knife-edge, and which is where failure should occur [13]. The bend strength of glazed samples was measured by three-point bending test (Gabbrielli CR5) at a loading rate of 1 mm/min (ISO-EN 10545-4).

RESULTS AND DISCUSSIONS

Hardness and strength values of glazed samples were given in Table 1. Hardness of samples increased from 7075.655 MPa to 8530.303 MPa with 100 wt. % basalt addition compared to standard transparent glaze. There was an increment at strength values with basalt addition to the standard transparent glaze.

Table 1. Hardness and strength values

Sample	Hardness (MPa)	Hardness (Vickers)	Strength (kg/cm ²)
Standard	7075.655	655.283	205.1±6.08
20 wt. % basalt	7374.465	682.956	224.0±4.24
60 wt. % basalt	8011.769	741.977	230.0±2.97
100 wt. % basalt	8530.303	789.999	235.8±1.70

CONCLUSIONS

The hardness and strength values increased with the increasing amount of basalt. The experiment revealed that with 100 wt. % basalt addition results in 20.56% increment of hardness value by comparison standard transparent glaze. Nevşehir region (Acıgöl-Tatlarin) basalt can be used to improve mechanical properties of transparent pottery glazes.

ACKNOWLEDGMENT

The author would like to thank TUBITAK (Science, Technology and Research Association of Turkey) and Supporting Programme of Initial Research and Development Projects for the support to the project numbered 217M092. Special thanks to Nevşehir Hacı Bektaş Veli University, Ceramic and Glass Department (Nevşehir-Turkey), Eskişehir Technical University, Materials Science and Engineering Department (Eskişehir-Turkey) and the Ceramic Research Center (Eskişehir-Turkey) for facilitate the study to be conducted satisfactorily.

REFERENCES

1. Mohammed B., Afram B., Nazar Z., An evaluation of the effect of different surface treatment on hardness and smoothness of pressable ceramic (in vitro study). *IOSR Journal of Dental and Medical Sciences*, 2015, 14(2), 84-89.
2. Baharav H., Laufer B.-Z., Pilo R., Cardash H.S., Effect of glaze thickness on the fracture toughness and hardness of alumina-reinforced porcelain. *The Journal of Prosthetic Dentistry*, 1999, May, 515-519.
3. Kim H.-J., Han Y.S., Kim D.-H., Kim D.-M., Choi J.-H., Lee S.-M., Kim Y., Kim H.-T., Improvement of glaze hardness in commercial bone China. *Journal of the Korean Ceramic Society*, 2015, 52(6), 508-513.
4. Venkatesh G., Thenmuhil D., Vidyavathy S.M., Vinothan R., Effect of addition of nano zirconia in ceramic glazes. *Advanced Materials Research*, 2014, 984-985, 488-494.
5. Zhang Q., Xu L.S., Guo X., Improvement of mechanical properties, microscopic structures, and antibacterial activity by Ag/ZnO nanocomposite powder for glaze-decorated ceramic. *Journal of Advanced Ceramics*, 2017, 6(3), 269-278.
6. Pekkan K., Gün Y., Effect of different metal oxides on vickers hardness of the frit based crystalline glazes. *Nevşehir Journal of Science and Technology*, 2018, 7(1), 32-40.
7. Yekta B.E., Alizadeh P., Rezazadeh L., Floor tile glass-ceramic glaze for improvement of glaze surface properties. *Journal of the European Ceramic Society*, 2006, 26(16), 3809-3812.
8. Benson J.L., Effect of glaze variables on the mechanical strength of whitewares. M.Sc. Thesis, Alfred University, Ceramic Engineering, Alfred, New York, 2003.
9. Longhini D., Rocha C.O.de M., Medeiros I.S., Fonseca R.G., Adabo G.L., Effect of glaze cooling rate on mechanical properties of conventional and pressed porcelain on zirconia. *Brazilian Dental Journal*, 2016, 27(5), 524-531.
10. Fomichev S.V., Dergacheva N.P., Steblevskii A.V., Krenev V.A., Production of ceramic materials by the sintering of ground basalt. *Theoretical Foundations of Chemical Engineering*, 2010, 45, 526-529.

11. Cocić M., Logar M., Matović B., Poharc-Logar V., Glass-ceramics obtained by the crystallization of basalt. *Science of Sintering*, 2010, 42, 383-388.
12. Dvorkin L.I., Galushko I.K., Glazes based on basalts. *Glass and Ceramics*, 1969, 11, 36-38.
13. Riley F.L., *Structural ceramics, fundamentals and case studies*, Cambridge University Press, Cambridge, 2009.

seres'18

IV. INTERNATIONAL CERAMIC GLASS PORCELAIN
ENAMEL GLAZE AND PIGMENT CONGRESS
October 10-12, 2018, Eskişehir, Turkey

**Full Text of
POSTER
PRESENTATIONS**

THE EFFECTS OF BLAST FURNACE SLAG ON THERMAL PROPERTIES OF CERAMIC SANITARYWARE BODIES

Tuna Aydın¹

¹Kirikkale University, Engineering Faculty, Metallurgy and Material Engineering Department,
Kirikkale, Turkey

Abstract

In this study, blast furnace slag (YFC) was used as an alternative source of raw materials in vitreous china structures in the production of ceramic sanitary ware. A maximum of 10% of the blast furnace slag was used instead of sodium feldspar. All compositions were prepared under the industrial conditions at Ece Bath factory. Samples were fired at 1220 °C for 15 hour. In this study, both technological properties of the prepared slips and thermal properties such as sintering and pyroplastic deformation of the samples were also investigated. As a result, in this study, the blast furnace slag containing bodies were superior to the standard body in terms of technological properties. The bodies containing YFC did not differ in terms of thermal properties compared to the standard one. This findings shown that blast furnace slag can be used as an alternative raw material in the production of ceramic sanitaryware.

Keywords: recycling, sintering, pyroplastic deformation, sanitaryware

1. Introduction

Sanitaryware bodies are composed of clay, sodium feldspar, kaolin and quartz. They produced from vitreous china body have a water absorption ratio not exceeding 0.5% after sintering process [1]. Sanitaryware bodies are fired between 1200 to 1300 °C. Sodium feldspar provides low-temperature densification of sanitaryware body [1]. The microstructural, physical and mechanical properties of sanitaryware bodies are related with the degree of densification in sintering process. Therefore, knowing the thermal properties of these materials is very important in developing their properties. Sanitaryware production requires further studies on their structures and properties [2-6]. In this study, blast furnace slag (YFC) was used as an alternative raw materials in vitreous china body in the production of ceramic sanitaryware. A maximum of 10% of the blast furnace slag was used instead of sodium feldspar. Within the scope of this study; In addition to physical properties such as water absorption, shrinkage and strength, thermal properties such as sintering and pyroplastic deformation behaviours were investigated using non-contact optical dilatometer and fleximeter.

2. Experimental studies

In this study, sanitaryware body compositions were prepared using industrial raw materials under the industrial conditions at Ece Banyo Co. The chemical compositions of these raw materials were determined by X-ray fluorescence (XRF) analyzer (Rigaku, ZSX Primus). A formulation used for industrial production was selected as the standard body (ST) composition. The composition consisting of blast furnace slag was named as (BFS). The mixture of raw materials was ground in a ball mill with alumina balls for 7 h. The liter weights of the slips were measured using a pycnometer. The viscosity

of slips were measured by using Fordcup. The thixotropy values were measured using Torsion viscometer (Gallenkamp type). The samples were prepared using the slip casting method in plaster mould in order to measure deformation, strength, firing shrinkage, water absorption and Harcourt analysis. After shaping samples were dried at 110 °C for 1 hour. All samples were fired under the industrial conditions at 1220°C for 15 hours. Sintering behaviours were conducted using non-contact optical dilatometer (Misura, ODHT Expert System, Ceramic Research Center, Eskişehir). Pyroplastic deformation behaviours were conducted using fleximeter (Misura Flex, Ceramic Research Center, Eskişehir). Microstructure images were carried out at Eskişehir Technical University (SAM) using SEM, Zeiss EVO 50EP .model SEM device.

3. Result and discussion

3.1. Chemical analyses (XRF) of the raw materials, body compositions and TG-DTA analysis of blast furnace slag

The chemical analyses are given in Table 1. In this study, 2 types of clay and 2 types of kaolin was used. Clay 1 contains a high amount of Al_2O_3 . Kaolin 1 contains a high amount of SiO_2 . Blast furnace slag contains high amount of CaO and MgO.

Table 1. Chemical analyses (XRF) of the raw materials (wt. %)

	Lol.	SiO_2	Al_2O_3	Fe_2O_3	TiO_2	CaO	MgO	Na_2O	K_2O	SO_3	Others
Quartz	2.00	89.9	5.6	0.62	1.00	-	-	0.25	0.12	-	
Clay 1	8.55	56.20	30.00	1.85	1.13	0.29	0.50	0.21	1.6		
Clay 2	10.05	56.75	27.14	1.92	1.01	0.19	0.57	0.19	1.61	0.06	
Kaolin 1	9.02	64.71	24.21	0.64	0.34	0.09	0.05	0.08	0.21	0.47	
Kaolin 2	11.40	48.02	36.01	1.02	0.06	0.07	0.40	0.13	2.73	-	
Sodium feldspar	0.39	69.96	17.84	0.16	0.19	0.57	0.26	9.92	0.41	-	
Blast furnace slag	2.54	40.14	8.97	1.06	1.14	36.68	4.52	0.24	0.67	1.08	5.36

Lol: loss of ignition

TG and DTA analysis of blast furnace slag was shown in Figure 1. DTA of blast furnace slag is shown in Figure 1; three endothermic peaks were observed in this curve at the temperatures of 61.9 and 451.4 °C, respectively. These peaks might be due to the release of physically and chemically combined water, respectively, from BFS particles. In addition to the above reasons, at 451.4 °C glassy phase which was associated in BFS experienced glass transition. Interestingly, an exothermic peak was noticed at 891 °C, which might be due to the crystallization of a new phase named as gehlenite and diopside [2]. The endothermic peak observed at about 1150 °C may be due to the melting of both diopside and gehlenite [2].

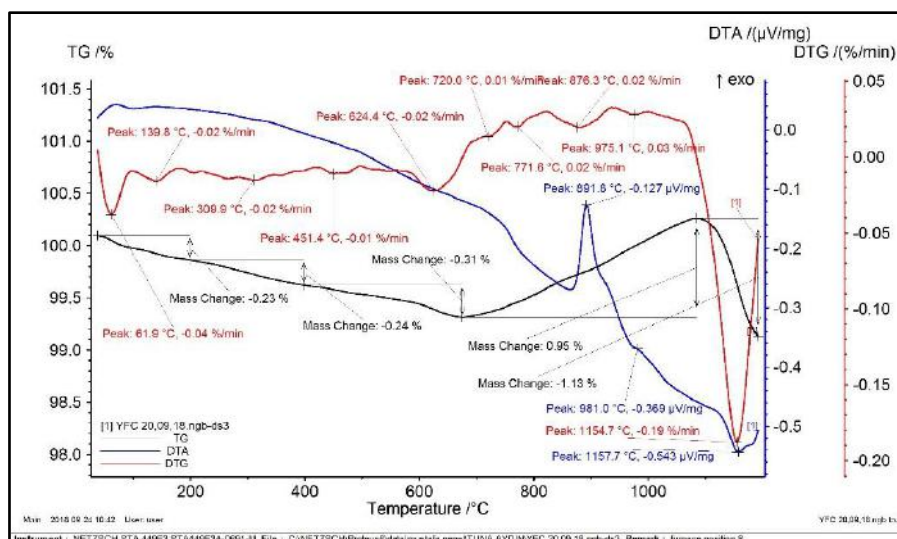


Figure 1. TG and DTA analysis of blast furnace slag

Body compositions are given in Table 2. Blast furnace slag (BFS) was used instead of sodium feldspar in a standard vitreous china sanitaryware composition.

Table 2. Body compositions

	STD	YFWC1	YFWC2	YFWC3
Quartz	17.5	17.5	17.5	17.5
Clay 1	18.41	18.41	18.41	18.41
Clay 2	11.66	11.66	11.66	11.66
Kaolin 1	12.75	12.75	12.75	12.75
Kaolin 2	13.66	13.66	13.66	13.66
Sodium feldspar	26	25	21	16
Blast furnace slag	-	1	5	10

3.2. Rheological properties of slip

Slip liter weight, silicate amount, thickness rate, slurry thixotropy and viscosity results are presented in Table 3. With the addition of blast furnace slag, the thicknesses rate and thixotropy values were increased compared with the standard body. The increase in thickness rate values is an important result. This data is particularly important in reducing the mold stay time of the product. In this way, much more products can be taken in a shorter time from mold. However, with the addition of BFS, high solid rates could not be reached. Slurry viscosity decreased with addition of BFS

Table 3. Rheological properties

Samples	Liter weight g/cm ³	Silicate (%)	Thixotropy (G ⁿ)	Viscosity (G ⁿ)	Thickness rate (60 min)
STD	1859	0.23	69	315	7.3
BFS1	1821	0.22	70	312	7.92
BFS2	1817	0.23	72	309	8.88
BFS3	1815	0.23	80	306	10.2

3.3. Technological Properties

Technological properties of samples are shown in Table 4. As seen on Table 4, with the addition of blast furnace slag the values of shrinkage and water absorption decreased. Bending strength values

increased by approximately 15 %. It is thought that the high percentage of CaO content in BFS plays an important role in this increase. The high CaO content leads to form anorthite phases in the body, resulting in an increase in strength by addition of a second crystalline phase together with the mullite crystals.

Table 4. Technological Properties

Samples	Dry Shrinkage (%)	Firing Shrinkage (%)	Total Shrinkage (%)	Water absorption (%)	Deformation (cm)	Bending strength (kg/cm ²)
STD	2.2	8.4	10.6	0.07	2.4	270
BFS1	2.3	8.6	10.9	0.07	2.6	270
BFS2	2	7.5	9.5	0.02	3.0	280
BFS3	1.8	6.8	8.6	0.01	3.0	310

3.4. Phase analysis (XRD)

Phase analyses of the samples are shown in Figure 2. As can be seen in Figure 2, Quartz and mullite crystals and glassy phase were determined for standard body. The mullite, quartz and anorthite phases together with glassy phase were also observed in the investigated bodies.

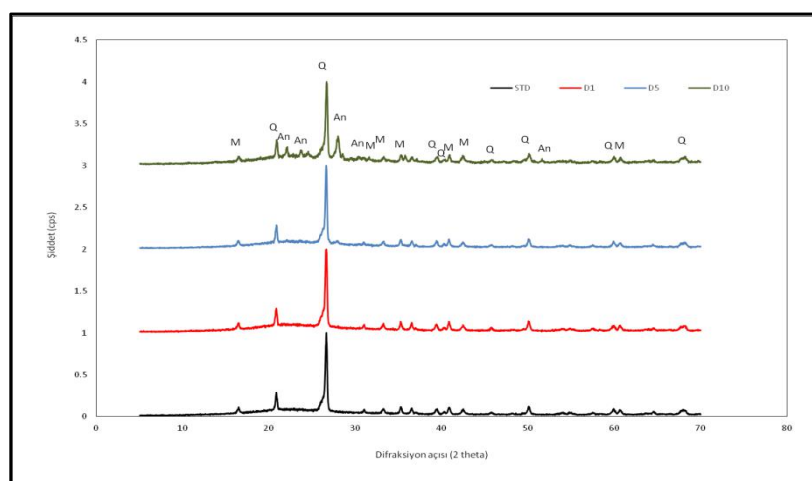


Figure 2. XRD graph of samples

3.5. Sintering behaviour

Sintering behaviours of all samples are shown in Figure 3. As seen on Figure 3, the sintering curves of bodies exhibited expansion up to 900 °C. The increase between 550 °C and 600 °C was because of quartz inversion, and the expansion. After quartz inversion, sintering began between 900 °C and 1000 °C. STD body shows expansion at 918 °C, and BFS1, BFS2 and BFS3 showed expansions at 916 °C, 927 °C and 898 °C respectively. The density increased above 900 °C for all bodies [7]. The shrinkage value reached a maximum at 1310 °C for STD, indicating the completion of the sintering process [7]. The shrinkage value reached a maximum at 1295 °C, 1260 °C and 1245 for BFS1, BFS2 and BFS3 respectively.

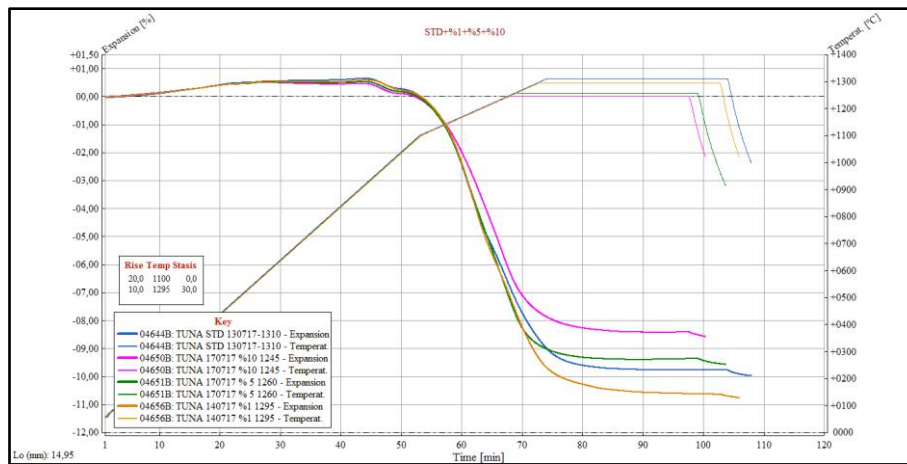
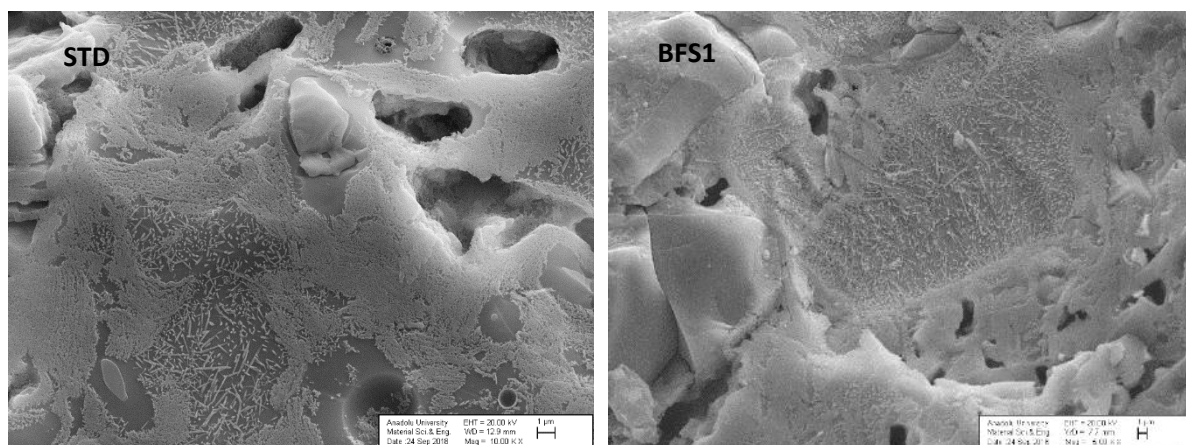


Figure 3. Sintering analyses of samples using Non-contact optical dilatometer

3.6. Microstructural Analysis (SEM)

Figure 4 shows the typical secondary electron (SE) images of fractured and etched surfaces of the STD and bodies containing blast furnace slag. Etching with 5 % HF solution for 2 minutes revealed the constituent crystalline phases embedded in the glassy phase. These crystals are quartz and mullite crystals. Two types of mullite forms in vitreous systems. The first type mullite forms during firing is primary mullite crystals (PM) which is from the decomposition of clay. This type of mullite crystals have a cuboidal or scaly morphology [1]. The second type of mullite crystals is secondary mullite forming from decomposition of the flux and its reaction with clay. They have a granular or acicular morphology [1, 8]. At higher temperatures, the secondary mullite crystals grows as alkali diffuses out of feldspar [9]. As seen on SEM images of BFS2 and BFS3 small spheroidal crystals were also observed. According to the XRD analysis (Figure 2), they are anorthite crystals.



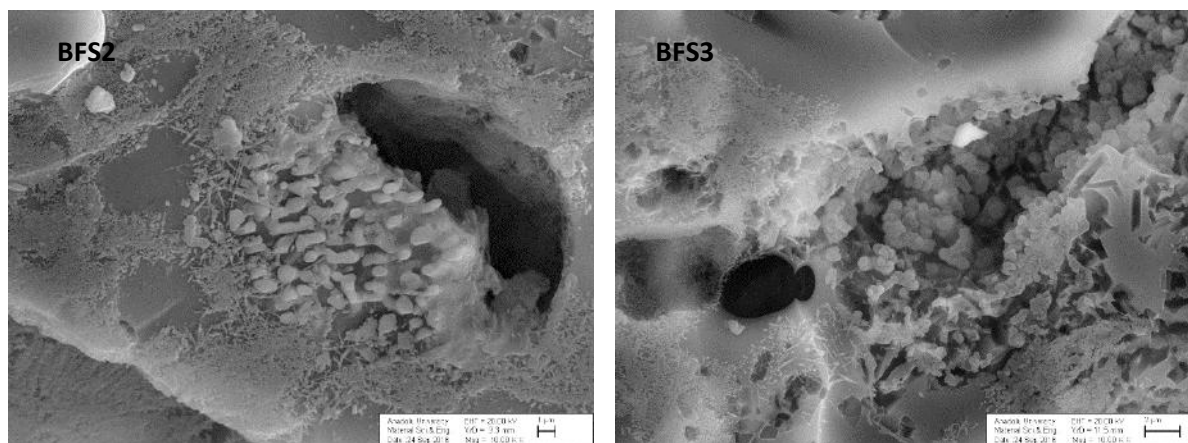


Figure 4. Micrographs of samples

4. Conclusions

Zonguldak Ereğli Iron and Steel factory's blast furnace slag was used in this study. The blast furnace slag was used instead of sodium feldspar in a standard vitreous china composition in a maximum 10 % by weight. It was investigated the effect of the blast furnace slag on the rheological properties and the technological properties of the fired samples. As a result of this study, it has been determined that the use of blast furnace slag increased the thickness of the slip compared to the standard body. This result shows that more product will be removed from the same mold. Deformation values increased. Although the increase in the deformation values seems to be negative, that can be solved by firing at lower temperatures. The sintering analysis results showed already this situation. This findings shown that blast furnace slag can be used as an alternative raw material in the production of ceramic sanitaryware

Reference

- [1] Derya YeşimTunçel, EmelÖzel, Evaluation of pyroplastic deformation in sanitaryware porcelain bodies, *Ceramics International*, Volume 38, Issue 2, March 2012, Pages 1399-1407
- [2] A.A.Francis, Conversion of blast furnace slag into new glass-ceramic material, *Journal of the European Ceramic Society*, Volume 24, Issue 9, August 2004, Pages 2819-2824
- [3] T. Aydın, Investigation of stain resistance of porcelain tiles doped by spodumene, PhD. Thesis, Anadolu University, Eskişehir, (2012).
- [4] N. Kunduraci, T. Aydın, A. Akbay, The Effect of Nepheline Syenite Addition on the Sintering behaviour of Sanitaryware Bodies, *J. Aust. Ceram. Soc.*, 52 (2) (2016) 82-86.
- [5] A. Salem, S.H. Jazayeri, E. Rastelli and G. Timellni, Effect of nepheline syenite on the colorant behavior of porcelain stoneware body, *Journal of Ceramic Processing Research*, Vol.6 , No. 5, (2009), 621~627.
- [6] Y. Iqbal, E. J. Lee, Microstructural evolution in triaxial porcelain, *J. Am. Ceram. Soc.*, Vol [83], (2000), 3121-27.
- [7] Baran Tarhan, Muge Tarhan, Tuna Aydın, Reusing sanitaryware waste products in glazed porcelain tile production, *Ceramics International* 43 (2017) 3107–3112

- [8] W.M. Lee, D.D. Jayaseelan, S. Zhang, Solid–liquid interactions: the key to microstructural evolution in ceramics *Journal of the European Ceramic Society*, 28 (2008), pp. 1517-1525
- [9] W.M. Carty, U. Senapati, Porcelain-raw materials, processing, phase evolution and mechanical behaviour *Journal of American Ceramic Society*, 81 (1) (1998), pp.

THE INVESTIGATION OF BUILDING MATERIAL PRODUCTION CONDITIONS AND ITS PROPERTIES BY USING BLAST FURNACE SLAG AND MAGNESITE WASTE

Gözde Yılmaz Aygün, Şenol Yılmaz

Sakarya University, Engineering Faculty, Department of Metallurgical and Materials Engineering,
Esentepe Campus, 54187 Sakarya, Turkey

ABSTRACT

In this study, the effect of clay addition on building materials from blast furnace slag and magnesite waste has been investigated. Clay in the range of 0–100 wt.% has been added into blast furnace slag and magnesite waste mixture. Cylindrical specimens shaped by pressing and were sintered at 1100, 1150 and 1200 °C for 2 h. The firing shrinkage, bulk density, apparent porosity and water absorption of sintered specimens are explained on the basis of scanning electron microscopy (SEM) analysis. The results showed that clay addition enhance building materials properties. Building materials from blast furnace slag and magnesite waste including clay can be used as wall tile.

Keywords: Wall tiles, blast furnace slag, clay, sintering

1. INTRODUCTION

Blast furnace slag is an industrial by-product obtained from the iron and steel industry. Blast furnace slag is used to improve durability, to produce high-strength and high-performance concrete, and to combine environmental and economic benefits such as resource savings and energy savings[1].

Blast furnace slag is produced in the blast furnace simultaneously with iron. Iron oxides are reduced to molten iron in the furnace by adding a flux such as limestone, dolomite, and a reductant such as coke. The molten slag can be quenched by atmospheric conditions, by slow cooling (air cooled), by cooling (expanded or foamed) with controlled amounts of water or by cooling (by pelleting) with high volume and pressure water sprays (granulated)[2].

Generally, the use of slag; in cement industry, building materials like floor tiles, outside and inside facing of walls, concrete and asphalt aggregate, in briquette and brick making, in glass manufacturing industry, in agriculture and environment applications[3].

Magnesite waste powder is the most important waste collected during the magnesite process. Waste storage is difficult and inevitably damages the environment. It is known that waste magnesite is used in ceramic, wall and floor tiles and glass ceramics industries [4].

In the present study, the effect of clay addition on building materials from blast furnace slag (BFS) and magnesite waste (MW) were investigated. Sintered products were characterized to obtain optimum conditions such as composition, sintering temperature and some properties.

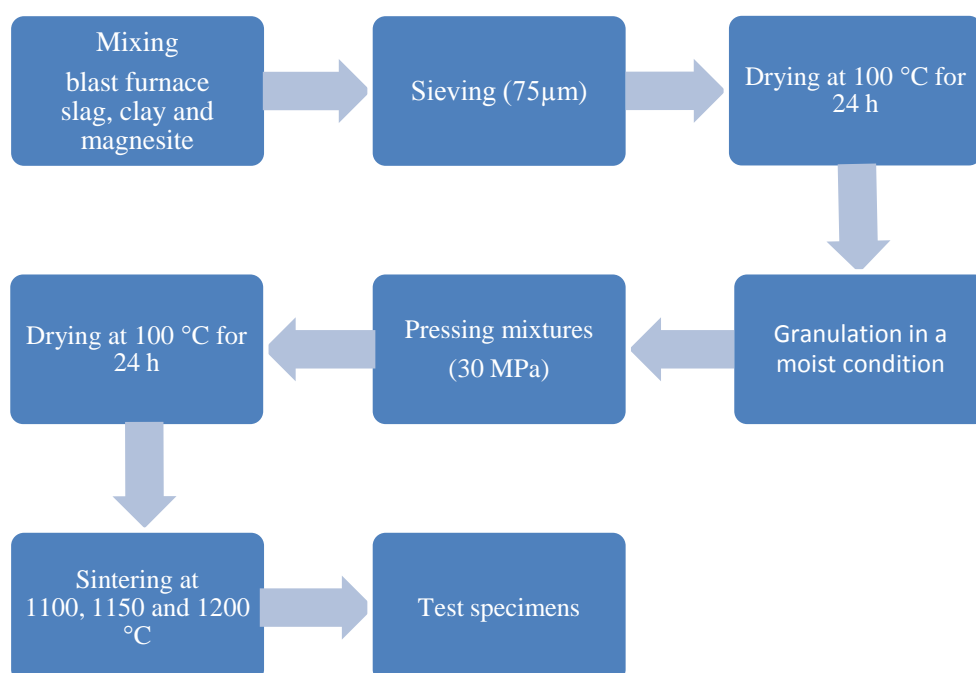
2. EXPERIMENTAL PROCEDURE

Granulated BFS used in this study was obtained from the Erdemir steel plant (Ereğli, Turkey). Magnesite was also supplied from Kümaş refractory (Kütahya). BFS, MW and Clay were mixed in the proportion as shown in Table 1.

Table 1. Batch compositions (wt.%)

Sample No	1	2	3	4	5	6
Clay	-	20	40	60	80	100
Slag	50	40	30	20	10	-
Magnesite	50	40	30	20	10	-

The batch compositions were mixture in a ball mill for 2 h and sieved to pass through 75 μ m. The mixtures were granulated in a moist condition and then semi-dry pressed at 30 MPa to prepare cylindrical specimens with 20mm diameter, 5mm height. After drying at 100°C for 24 h, the specimens were sintered at 1100, 1150 and 1200°C for 2 h in an electric furnace and the specimens were cooled naturally in the furnace. Flow chart of processing route of sample preparation is given in Fig.1.

**Fig. 1.** Schematic details of processing route for test specimens

The linear shrinkage, bulk density, apparent porosity and water absorption of the sintered specimens were calculated from their weights and dimensions. For the microstructural observations scanning electron microscopy (SEM) was used.

3. RESULTS AND DISCUSSION

Fig. 2 shows firing shrinkage of sintered samples. The values of firing shrinkage decreased with the increase in BFS and MW addition. As expected, firing shrinkage values increased with higher sintering temperatures due to the densification of samples as a result of sintering. When the BFS content is low in the specimens, these values are high because of alkali content of clay that gives rise to liquid sintering at these temperatures. By the addition of the wastes, some samples showed growth compared to shrinkage. This situation, which is clearly seen after 40% waste, is probably due to the fact that the gas caused by waste in the body.

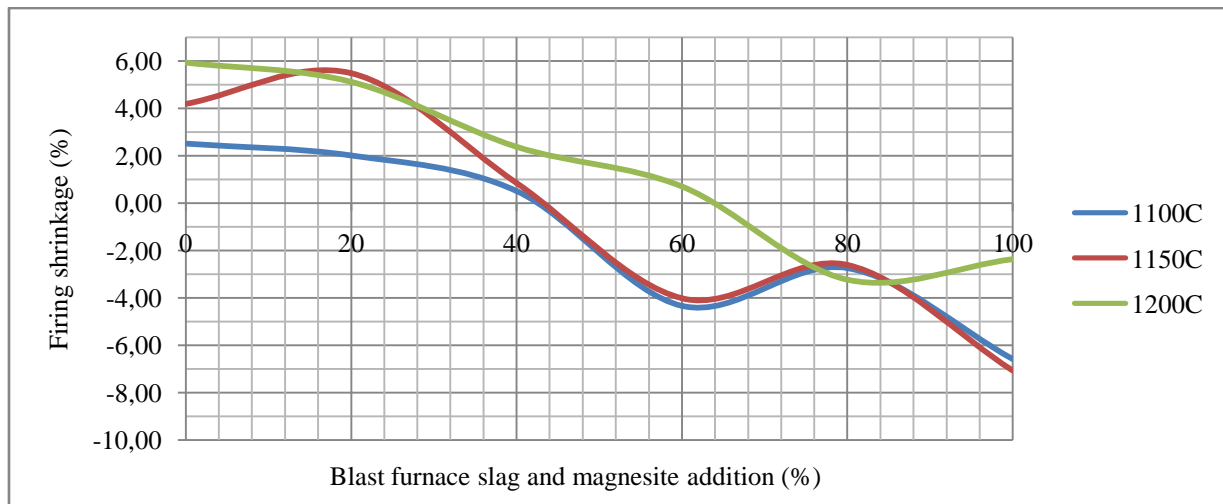


Fig. 2. Firing shrinkage vs. blast furnace slag and magnesite waste addition for different sintering temperature.

The results of apparent porosity versus waste addition shown in Fig. 3 indicates that by increasing waste from 0 to 100 wt.%, the apparent porosity increased due to decreasing alkali content and gas outlet in the body. The values of bulk density decreased with the increase in waste content in Fig. 4 supporting the apparent porosity results. According to the water absorption versus waste addition shown in Fig. 5 indicates that by increasing waste from 0 to 100 wt.%, the water absorption increased supporting firing shrinkage, apparent porosity and bulk density results.

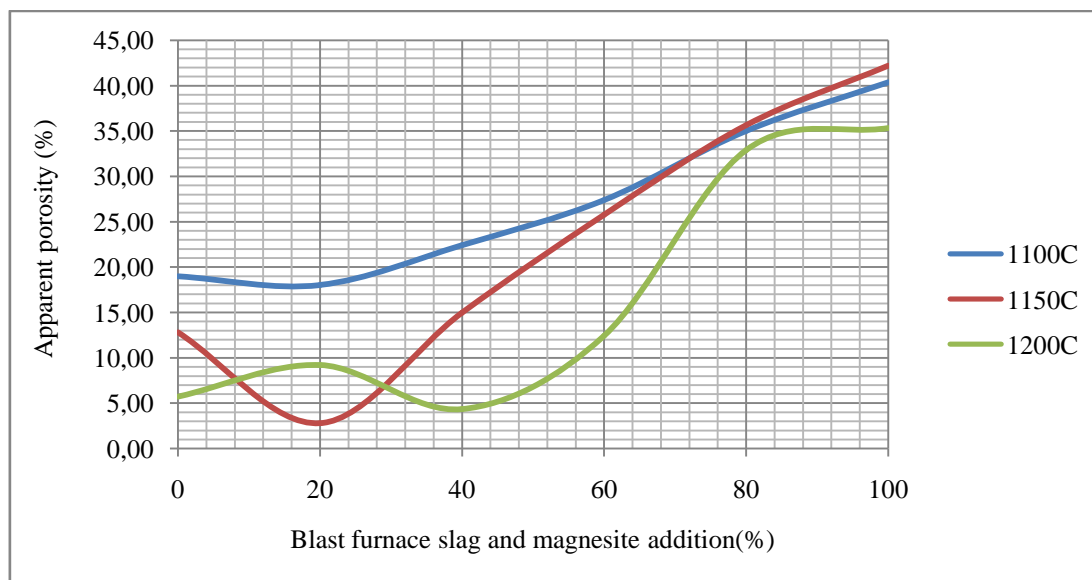


Fig. 3. Apparent porosity vs. blast furnace slag and magnesite addition for different sintering temperature

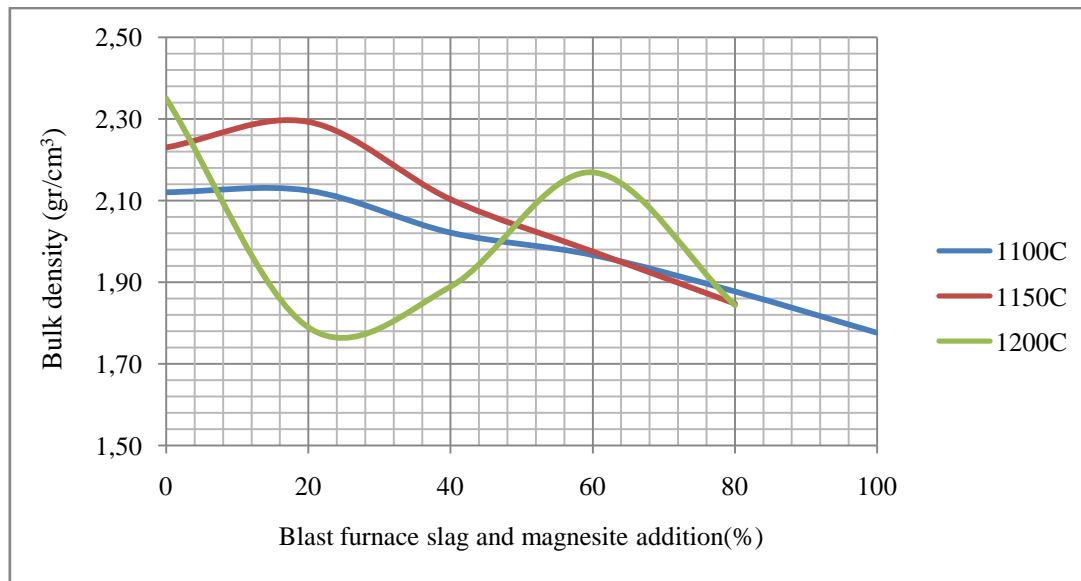


Fig. 4. Bulk density vs. blast furnace slag and magnesite addition for different sintering temperature

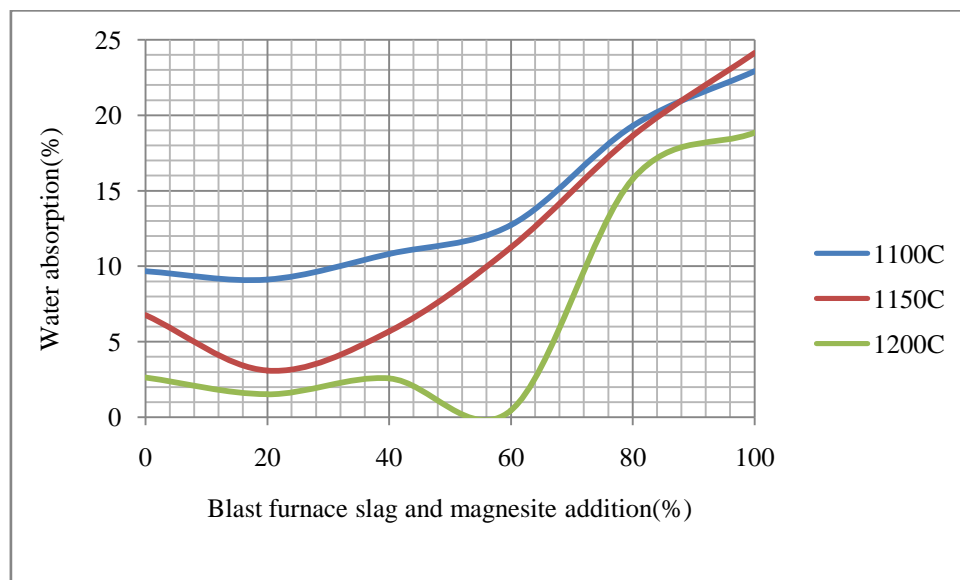
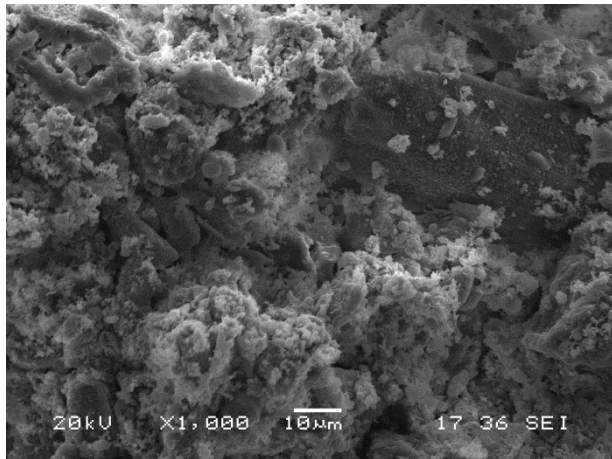
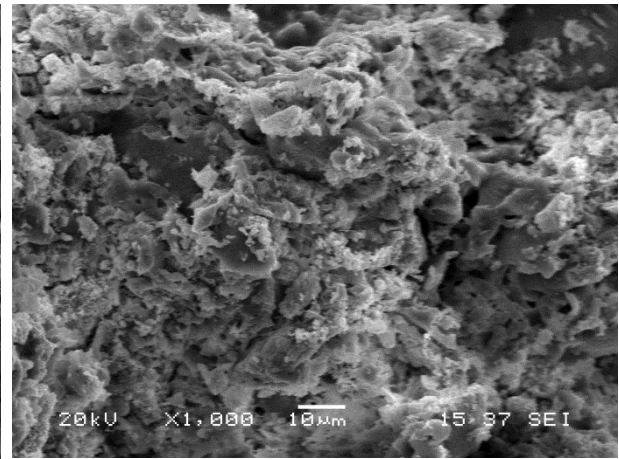


Fig. 5. Water absorption vs. blast furnace slag and magnesite addition for different sintering temperature

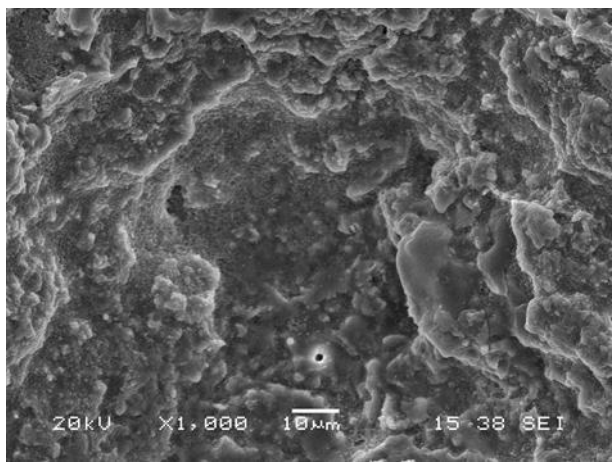
SEM analysis is shown in Fig.6. When the waste content in the body increase porosity is more and glassy phase is lesser. Crystals were embedded in the glassy phase.



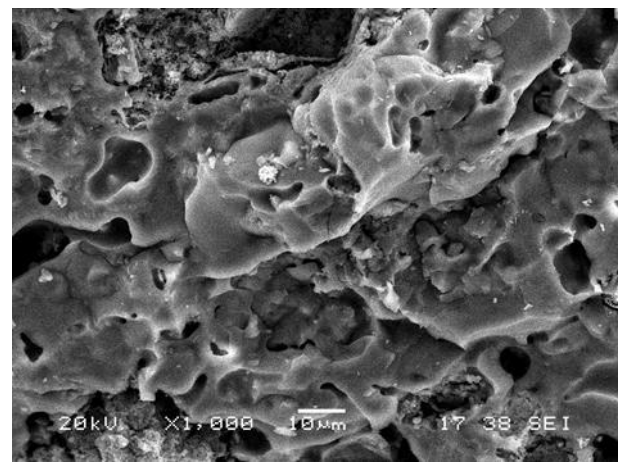
a) Sample 1



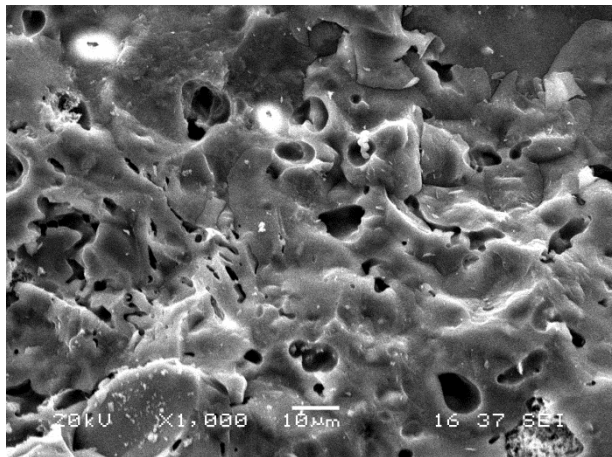
b) Sample 2



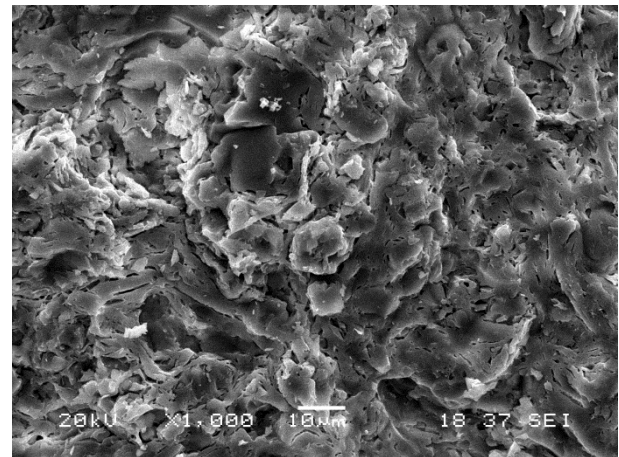
c) Sample 3



d) Sample 4



e) Sample 5



f) Sample 6

Fig. 6. SEM image of samples sintered at 1150°C

4.CONCLUSIONS

- 1)The values of firing shrinkage decreased with the increase in BFS and MW addition. After 40 % waste, samples showed growth compared to shrinkage.
- 2) The water absorption and apparent porosity values of specimens increased with the rise of waste addition.
- 3) Crystals were embedded in the glassy phase in SEM microstructures.
- 4) The mixture of BFS, MW and clay could be used inthe wall tiles fabrication for insulation purposes.

REFERENCES

1. Ulubeyli G.C., Artır R., Sustainabilityfor blast furnace slag: use of some construction wastes.Procedia - Social and Behavioral Sciences, 2015, 195, 2191-2198.
2. Yasipourtehrani S., Strezov V., Bliznyukov S., Evans T., Investigation of thermal properties of blast furnace slag to improve process energy efficiency. Journal of Cleaner Production, 2017, 149, 137-145.
3. Ozturk Z.B., Gultekin E.E., Preparation of ceramic wall tiling derived from blast furnace slag. Ceramic International, 2015, 41 (9), 12020-12026.
4. Erdoğan N.,Enrichment of waste magnesite ore: characterization, properties and magnetic separatorapplication. Selcuk Univ. J. Eng. Sci. Tech., 2015, 3 (4), 58-69.

PRE-TREATMENT TO ESTIMATE THE GLAZE COMPOSITIONS IN CERAMIC GLAZE APPLICATIONS USING ARTIFICIAL NEURAL NETWORKS

Uğur Kut^{1*}, İskender Işık²

¹Kütahya Dumlupınar University, Faculty of Architecture, Evliya Celebi Campus, Kutahya, Turkey

²Kütahya Dumlupınar University, Engineering Faculty, Metallurgy and Materials Engineering Department, Evliya Celebi Campus, Kutahya, Turkey

ABSTRACT

Material preference and deciding the right ratio are crucial in preparing ceramic glazes to obtain the desired characteristics in the glaze. Up to now, mostly Seger formula has been used and many trials have been made to obtain ceramic glazes. There are many materials to be used in glazes with various negative and positive characteristics; therefore, time lost and cost lost have been experienced.

In this study, it was aimed to decrease such lost using artificial neural network model. In the study, formulas were prepared using ternary phase diagram of washed Uşak kaolin, minium and quartz and the specimens were fired at 950 °C and 1150 °C. Toolbox of MatLab 2009 package program was used in the study. Temperature, surface tension and expansion coefficient were chosen as input variables while glaze composition values and glassing values were chosen as output variables.

Training results and test results were compared with actual values to determine the network performance. As a result of training, high performance was obtained between regression for glassing $R^2=0.78$ and regressions for glaze components $R^2=0.85$ and $R^2=0.98$. Likewise, according to test results, high performance was obtained between regression for glassing $R^2=0.81$ and regressions for glaze components $R^2=0.99$ and 0.99 .

Key words: ceramic, glaze component, chemical properties, artificial neuronal network.

1. INTRODUCTION

In order to obtain maximum performance from ceramic glazes, specific characteristics of the materials and their ratios are crucial for designers. In terms of providing the desired physical, chemical, electrical, mechanical and magnetic characteristics, the materials used in the production of ceramic glazes are very important. Other parameters besides these in choosing materials are usability in glaze production, cost, environmental impact, availability and market trends. Considering the great number of materials and rich variety of production processes, multiple preference parameters cause complexity and challenge for designers in choosing the right material [1].

There are methods developed by using artificial neural networks (ANN) to systematically evaluate and analyze the quantitative values of specific characteristics of ceramic materials. For example, Huang et al. [2] thought that the suitability of compositions and components of ceramic set materials are designable and simulateable according to their mechanical characteristics. They also proposed ANN characteristics and using ANN in the design of ceramic materials. Köker et al. [3] aimed in their study to reveal the effect of various training algorithms in the learning performance of neural networks in estimating bending strength and hardness behaviour of particles reinforced with Al-Si-Mg metal matrix composites (MMCs). In their study, Lucon and Donovan [4] used ANN instead of a traditional micro-mechanical approach to determine microscopic and macroscopic elastic characteristics of composite materials whose microscopic geometry was given. Fernández and Zaera [5] developed a new device based on ANN to design light ceramic-metal armours for high-speed crash of solids. Kappatos et al. [6] planned a concept to determine the effect of corrosion damage on the increasing strain characteristics of structural alloys for magnesium alloy AZ31. The concept was based

on using a neural network with radial basic function. Malinov et al. [7] developed a model to analyze and estimate the correlation between process parameters and mechanical characteristics in titanium alloys using ANN application. In their study, Moreschi et al. [8] modelled the relative density of five inorganic particles using ANN. In their study, Gill and Singh [9] emphasized that ultrasonic drilling of hard and brittle ceramic materials is a complex mechanical material removal process which is characterised by relatively slow material removal rates. They used Adaptive Neuro-Fuzzy Inference Systems (ANFIS) to model and simulate the material removal rate in stable ultrasonic drilling of sillimanite ceramics. Usha A. Kumar [10] comparing regression and artificial neural networks on actual data and two simulated specimens, stated that regression was better than artificial neural networks in intricate data and suggested general rules to increase the performance of neural networks for intricate data.

In order to obtain the desired success in the design of ceramic glazes, as a result of physical and chemical interaction between the glaze and the surface, the surface-glaze harmony must be stable, for which surface tensile coefficients and expansion coefficients should be coherent. Also, it is a problem if the glaze doesn't have the desired luminosity.

It is aimed in this study to estimate the luminosity and the appropriate glaze components with ANN using certain data taken from the production process in order to minimize such problems as rise in cost due to labour-lost and time-lost during research and development process. In the following section, applicability of this approach is discussed.

2. MATERIAL AND METHOD

In this study, ESC1 (Eczacıbaşı granule casting mud) was used in the production of ceramic specimens to be glazed. Formulas were prepared in ternary phase diagram using washed Uşak kaolin, minium and quartz compound as initial raw material (Table 1).

Table 1. Chemical composition of initial raw materials (% by weight).

	PbO	Na ₂ O	K ₂ O	CaO	MgO	Fe ₂ O ₃	TiO ₂	Al ₂ O ₃	SiO ₂	LOI
Washed Uşak kaolin	-	0.12	4.34	1.75	1.14	0.94	0.1	14.81	71.6	4.73
Minium	97.66	-	-	-	-	-	-	-	-	2.33
Quartz	-	-	-	-	-	-	-	-	100	-

The raw materials to be used in the glaze trials were obtained as ground material and were filtered dry from the steel sieve whose aperture opening was 355 µm (ASTM-45 mesh). The filtered specimens were weighed as 100 gr specimens on Shimadzu scales with 0.01 sensitivity. The sample blends whose weighing and branding were completed were then mixed with water in a porcelain mortar to homogenize the suspension. After this operation, glaze application was done on the specimens using pouring method. During every glaze application trial, the glaze layer was assured to be 1 mm. After completing the series comprising of 171 trials, following the same steps, the second series was prepared. The firing temperature for the first series was 950 °C, while it was 1150 °C for the second series.

After completing the drying process, firing was carried out designing the spaces between the trial specimens and the heat circulation inside the kiln. The firing program was conducted as seen in Figure 1 and the cooling process occurred on its own accord without any additional operation within its own cooling capacity.

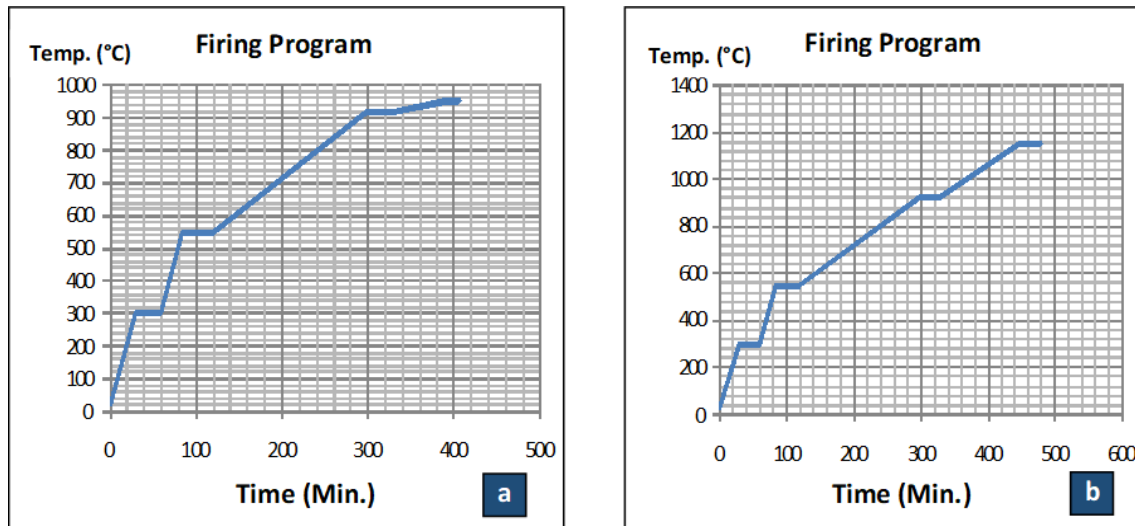


Figure 1. (a) Glazed firing program at 950 °C, (b) glazed firing program at 1150 °C.

Temperature, surface tension and expansion coefficient were used as ANN input variables. ANN output variables were composition values of the glaze and glassing value. The ANN model was formed using Toolbox of MatLab 2009 package program.

3. ARTIFICIAL NEURAL NETWORK MODEL

ANN input variables were determined as temperature, surface tension and expansion coefficient. ANN output variables were the composition values of the glaze (PbO, Na₂O, K₂O, CaO, MgO, Al₂O₃, SiO₂, Fe₂O₃, TiO₂) and glassing value. Total 342 data sets of the study were used as follows: 228 for ANN training and 114 for testing. The block diagram of ANN can be seen in Figure 2.

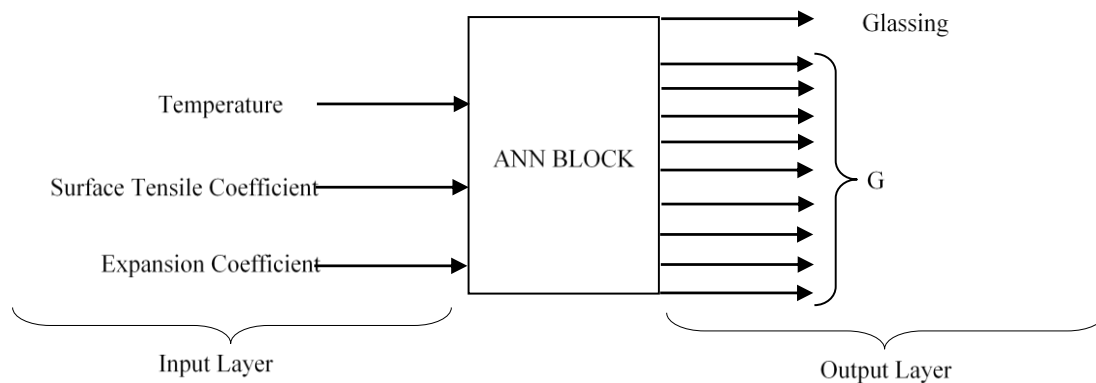


Figure 2. ANN data input and output scheme.

Input and output values were normalized between 0.1-0.9 range using Equation (1) and then transferred to neural networks.

$$NV = 0.8 * \left(\frac{AV - SNV}{BNV - SNV} \right) + 0.1 \quad (1)$$

where *NV* is normalized value, *AV* is actual value, *BNV* is the biggest numeric value in the data set and *SNV* is the smallest numeric value in the data set. The normalized data are given to the neural networks as the input and output information. During ANN training, numerous methods were tried with different activation functions on different neuron numbers. Table 2 shows the neural network models used in the study.

Table 2. Composition of ANN structures.

Neural Type	Training Function	Learning Function	Activation Function	Number of Neurons	Number of Secret Layers
Feed-forwards Back-propagation	TRAINLM	LEARNGDM	Tansig Logsig	3, 3+3, 5, 7, 9, 9+9, 12, 12+12, 15, 15+15, 18, 5+8	1, 2

As a result of the trials, the predictive and actual values for 950 °C and 1150 °C temperatures were compared. The performance of the network during training stage and R^2 value were calculated using

$$R^2 = 1 - \left(\frac{\sum_{i=1}^N (PV_i - AV_i)^2}{\sum_{i=1}^N (AV_i)^2} \right) \quad (2)$$

Also, the mean error rates of the test results for 950 °C and 1150 °C temperatures were calculated using

$$\begin{aligned} & \text{ERROR}\% \\ &= \left(\frac{AV - PV}{AV} \right) \\ & * 100 \end{aligned} \quad (3)$$

where PV is the predictive value and AV is the actual value.

For prediction, ANN should be trained first. The network was trained with surface expansion coefficient and expansion coefficient for 950 °C and 1150 °C temperatures. In the trained network, glaze composition values named as the target file and glassing value existed for input variables. After completing the training of the network, prediction was done for glaze composition and glassing between 950 °C and 1150 °C. Among the trial models, logsig activation function model was chosen the most appropriate for application. This model has one secret layer and 20 neurons.

Figure 3 shows the ANN model with 20 neurons designed as 3 input and 10 output. The training file containing the data between 950 °C and 1150 °C was taught to the ANN model. Training of the ANN model was achieved in 1000 iterations (Figure 3).

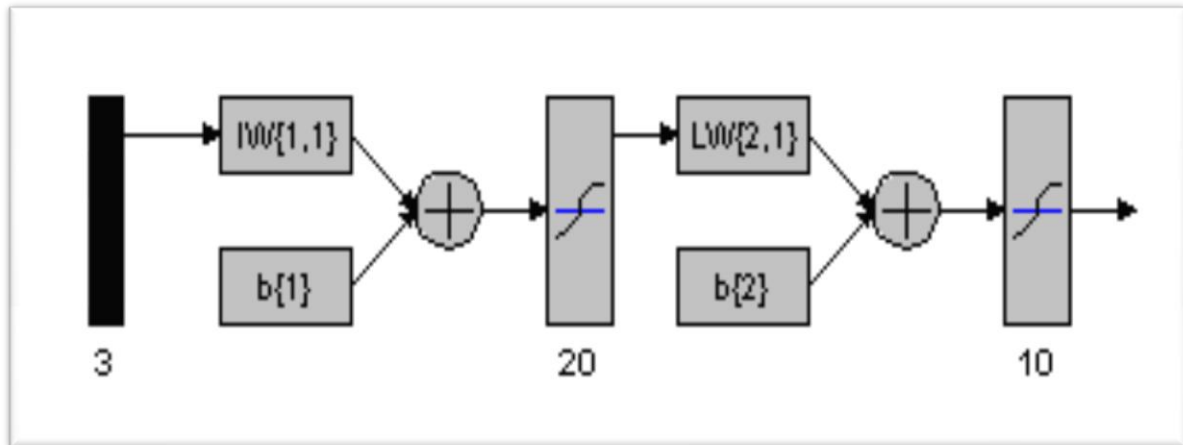


Figure 3. Structure of ANN model.

4. CONCLUSION

How much the training data of the 20-neuron model of logsig activation function converge to the actual values was checked. The coherence of ANN training with actual values was checked with R^2 . R^2 value was computed using Equation (2) where R^2 value denotes Regression analysis. Regression is an analysis method used to find the relation between two or more variables. Using Regression analysis, information can be gained about whether there is a relation between variables and, if any, how significant this relation is [11]. The coherence in distribution for glazing can be seen in Figure 4a, for PbO in Figure 5a, for Na₂O in Figure 6a, for K₂O in Figure 7a, for CaO in Figure 8a, for MgO in Figure 9a, for Al₂O₃ in Figure 10a, for SiO₂ in Figure 11a, for Fe₂O₃ in Figure 12a and for TiO₂ in Figure 13a.

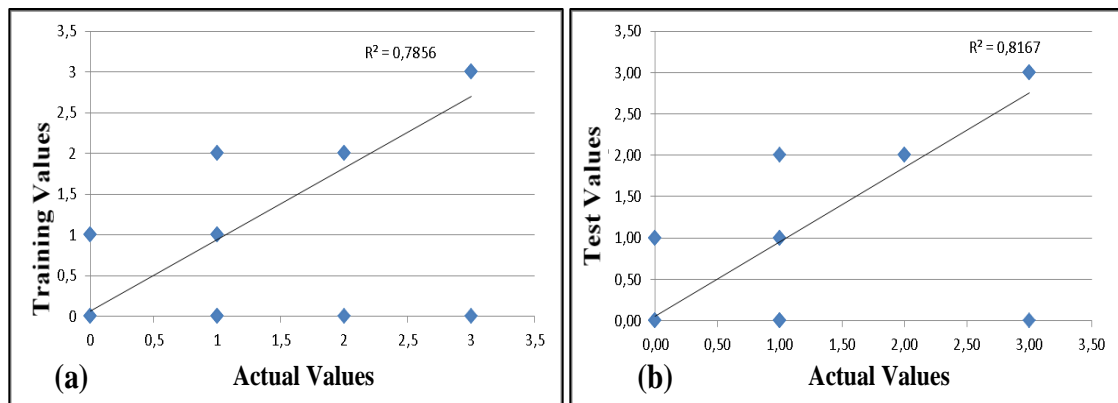


Figure 4. R^2 distribution of glassing output variable between training (a) and test (b) values of ANN model and actual values.

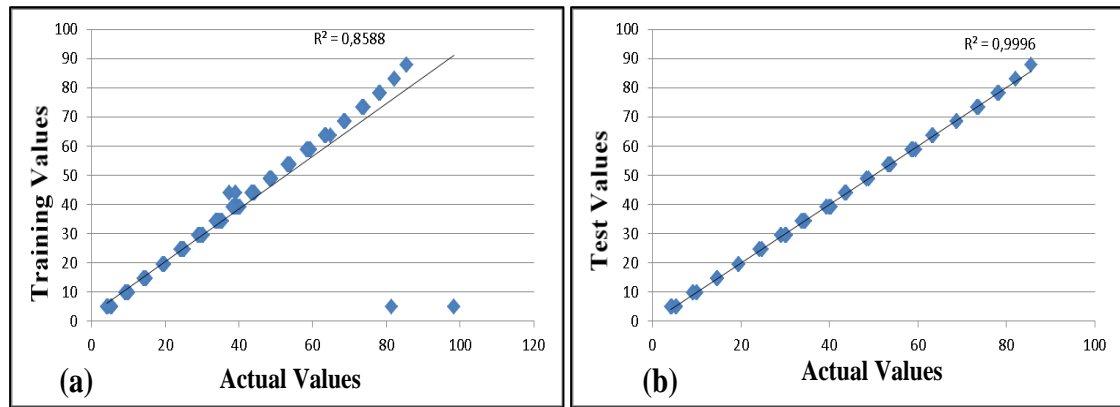


Figure 5. R^2 distribution of lead (PbO) output variable between training (a) and test (b) values of ANN model and actual values.

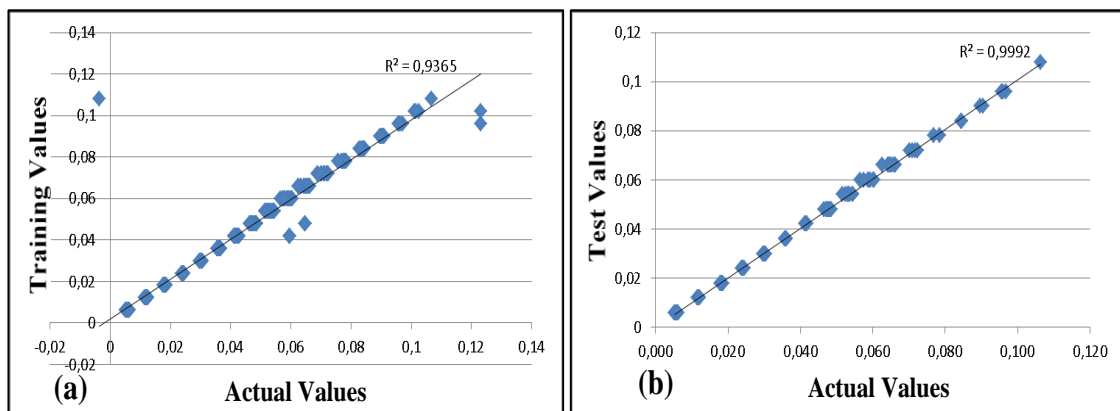


Figure 6. R^2 distribution of sodium (Na_2O) output variable between training (a) and test (b) values of ANN model and actual values.

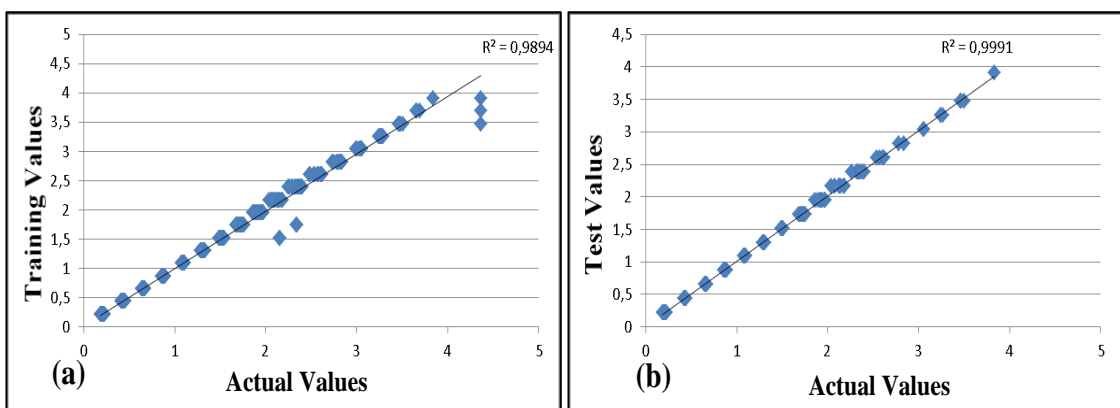


Figure 7. R^2 distribution of potassium (K_2O) output variable between training (a) and test (b) values of ANN model and actual values.

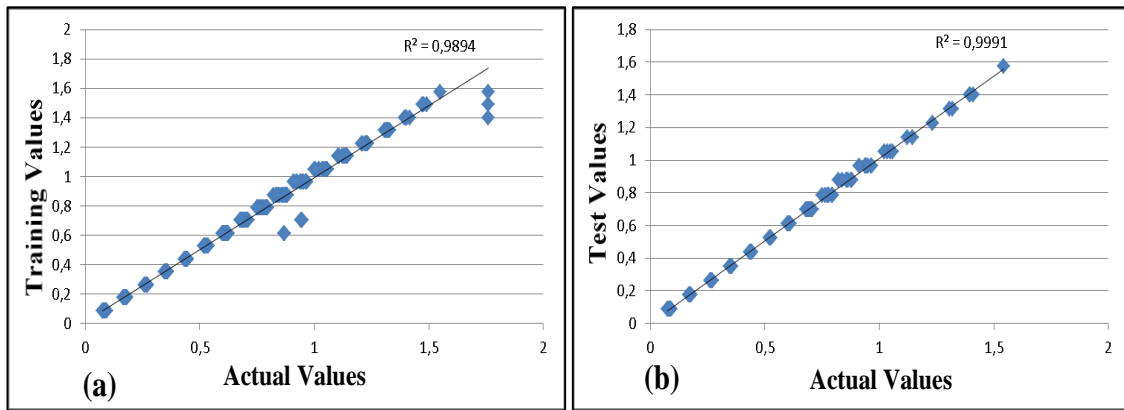


Figure 8. R^2 distribution of calcium (CaO) output variable between training (a) and test (b) values of ANN model and actual values.

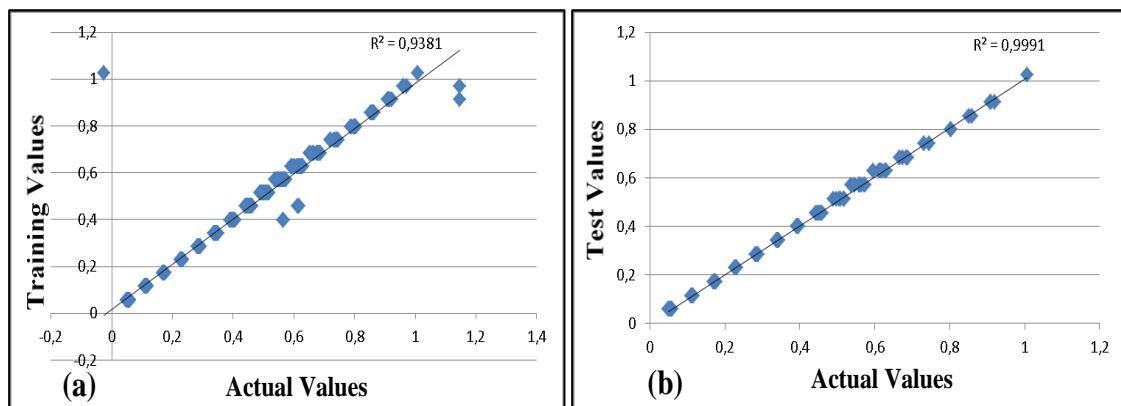


Figure 9. R^2 distribution of magnesium (MgO) output variable between training (a) and test (b) values of ANN model and actual values.

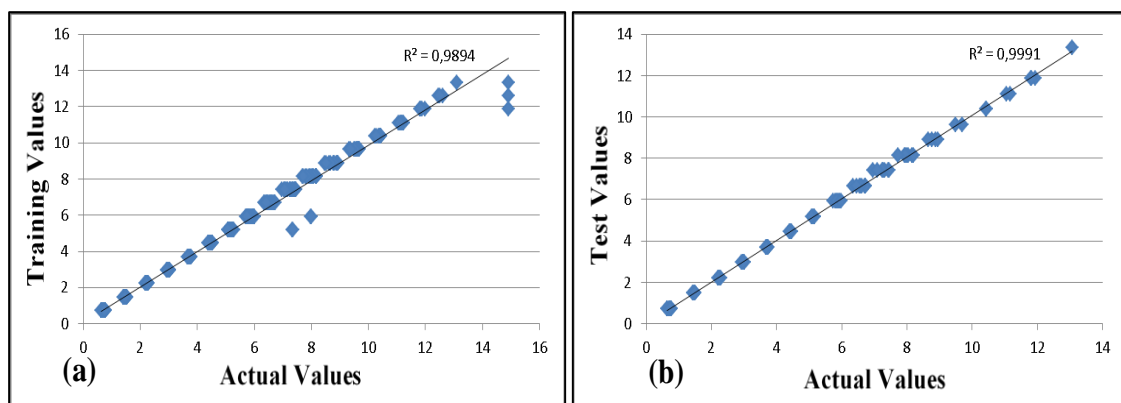


Figure 10. R^2 distribution of aluminium (Al_2O_3) output variable between training (a) and test (b) values of ANN model and actual values.

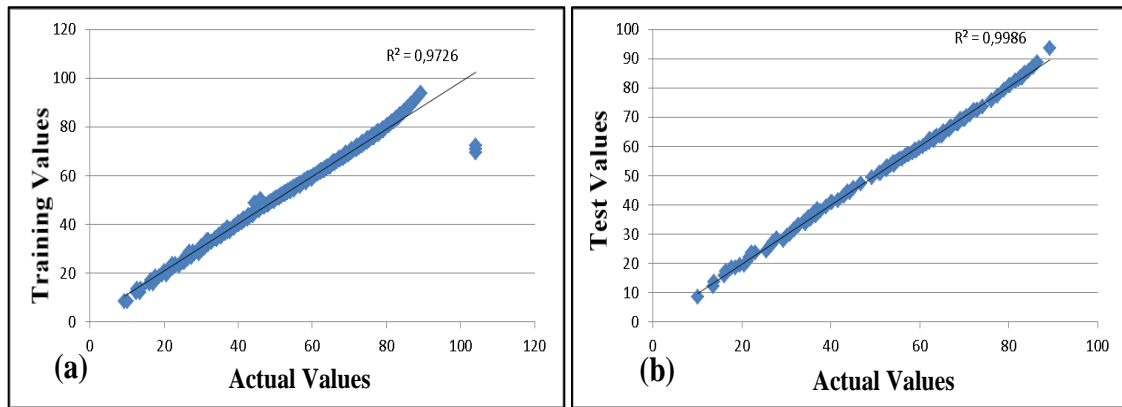


Figure 11. R^2 distribution of silicon (SiO_2) output variable between training (a) and test (b) values of ANN model and actual values.

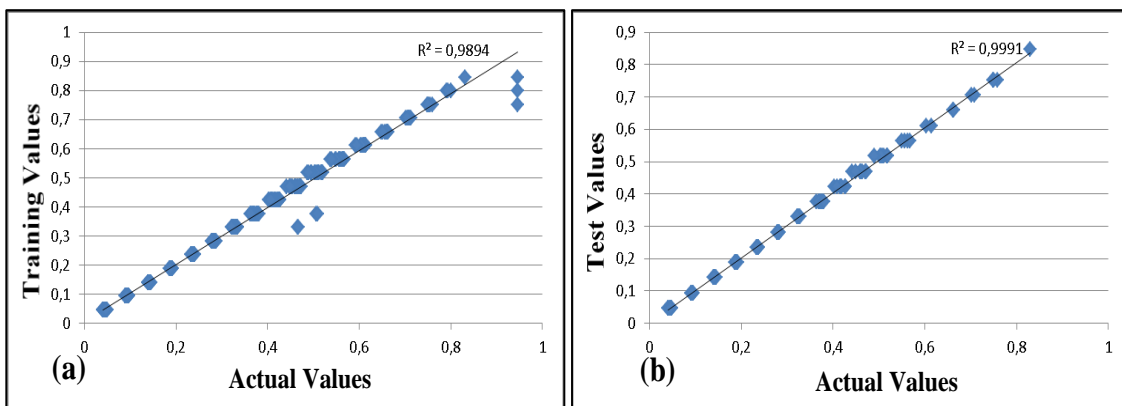


Figure 12. R^2 distribution of iron (Fe_2O_3) output variable between training (a) and test (b) values of ANN model and actual values.

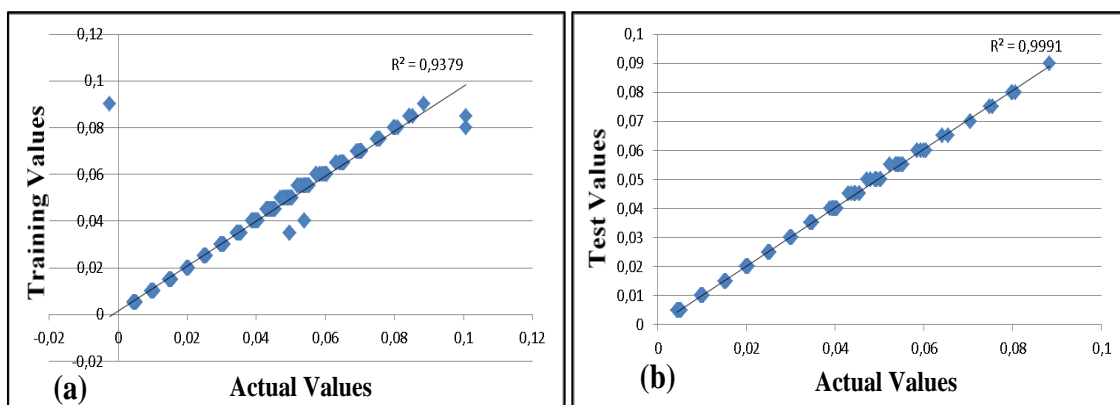


Figure 13. R^2 distribution of titan (TiO_2) output variable between training (a) and test (b) values of ANN model and actual values.

R^2 values showing the coherence between ANN output values and real values were computed using Equation (2). The coherence in distribution for glazing can be seen in Figure 4b, for PbO in Figure 5b, for Na_2O in Figure 6b, for K_2O in Figure 7b, for CaO in Figure 8b, for MgO in Figure 9b, for Al_2O_3 in Figure 10b, for SiO_2 in Figure 11b, for Fe_2O_3 in Figure 12b and for TiO_2 in Figure 13b.

The mean error values of test data were computed using Equation (3) as 7.02 for glassing, 8.63×10^{-3} for PbO, 0.65 for Na₂O, 0.63 for K₂O, 0.63 for CaO, 0.63 for MgO, 0.63 for Al₂O₃, 0.29 for SiO₂, 0.63 for Fe₂O₃ and 0.63 for TiO₂.

5. DISCUSSION

In this study, 171 glaze specimens prepared using washed Uşak kaolin, minium and quartz ternary phase diagram were fired at 950 °C. The same operation was repeated at 1150 °C. ANN was then trained using randomly chosen 228 of 342 specimens acquired after firing, their expansion and surface expansion coefficients and their firing temperature values as input data. At the end of training, ANN showed such a high performance in regression and mean error for glassing $R^2=0.78$ and 7.02%, for PbO $R^2=0.85$ and $8.63 \times 10^{-3}\%$, for SiO₂ $R^2=0.97$ and 0.29% and for Na₂O, K₂O, CaO, MgO, Al₂O₃, Fe₂O₃ and $R^2=0.98$ and 0.63% for TiO₂. The remaining 114 test specimens were tested with ANN. According to the test results, ANN showed such a high performance in regression and mean error for glassing $R^2=0.99$ and 7.02%, for PbO $R^2=0.99$ and $8.63 \times 10^{-3}\%$, for SiO₂ $R^2=0.99$ and 0.29% and for Na₂O, K₂O, CaO, MgO, Al₂O₃, Fe₂O₃ and TiO₂ $R^2=0.99$ and 0.63%.

Although the model was a success, statistical data showed that it didn't performed well in determining glassing; however, in reality, it is not so because discrete values were used for glassing. Glassing was categorized as undeveloped, opaque, luminous and very luminous. Therefore, even the slightest variations between the actual results and tests results of the model lead to enormous statistical numeric changes. These findings indicated that the ANN model can be used successively in decreasing the cost-lost during prototype production in ceramic sector in terms of glaze and structure harmony. Also, it enabled reaching for results more quickly by lessening the time during glaze trials.

6. SUGGESTIONS

The model is a preliminary study in which

- The temperature range can be extended,
- The data set can be enriched by trying different glaze compositions,
- Cost-loss in ceramic sector can be tried to be decreased by using different intelligent systems.

REFERENCES

1. Sarfaraz, K.R., et al., *A simplified fuzzy logic approach for materials selection in mechanical engineering design*. Materials & Design, 2009. **30**(3): p. 687-697.
2. Huang, C.Z., et al., *A study on the prediction of the mechanical properties of a ceramic tool based on an artificial neural network*. Journal of Materials Processing Technology, 2002. **129**(1): p. 399-402.
3. Koker, R., N. Altinkok, and A. Demir, *Neural network based prediction of mechanical properties of particulate reinforced metal matrix composites using various training algorithms*. Materials & Design, 2007. **28**(2): p. 616-627.
4. Lucon, P.A. and R.P. Donovan, *An artificial neural network approach to multiphase continua constitutive modeling*. Composites Part B: Engineering, 2007. **38**(7): p. 817-823.
5. Fernández-Fdz, D. and R. Zaera, *A new tool based on artificial neural networks for the design of lightweight ceramic-metal armour against high-velocity impact of solids*. International Journal of Solids and Structures, 2008. **45**(25): p. 6369-6383.
6. Kappatos, V., A.N. Chamos, and S.G. Pantelakis, *Assessment of the effect of existing corrosion on the tensile behaviour of magnesium alloy AZ31 using neural networks*. Materials & Design, 2010. **31**(1): p. 336-342.
7. Malinov, S., W. Sha, and J.J. McKeown, *Modelling the correlation between processing parameters and properties in titanium alloys using artificial neural network*. Computational Materials Science, 2001. **21**(3): p. 375-394.
8. Moreschi, V., et al., *Modelling the tap density of inorganic powders using neural networks*. Journal of the European Ceramic Society, 2009. **29**(15): p. 3105-3111.

9. Gill, S.S. and J. Singh, *An Adaptive Neuro-Fuzzy Inference System modeling for material removal rate in stationary ultrasonic drilling of sillimanite ceramic*. Expert Systems with Applications, 2010. **37**(8): p. 5590-5598.
10. Kumar, U.A., *Comparison of neural networks and regression analysis: A new insight*. Expert Systems with Applications, 2005. **29**(2): p. 424-430.
11. wikipedia. *Regresyon*. 2018; Available from: <http://www.wikizero.co/index.php?q=aHR0cHM6Ly90ci53aWtpcGVkaWEub3JnL3dpa2kvUmVncmVzeW9u>.

THE EFFECT OF STRONTIUM ADDITIVE ON THE BIOACTIVITY PROPERTIES OF BIOACTIVE GLASS

Cansu Karakaya, Esra Tavukçuoğlu, Ediz Ercenk, Şenol Yılmaz

Sakarya University, Engineering Faculty, Department of Metallurgical and Materials Engineering,
Esentepe Campus, 54187 Sakarya, Turkey

ABSTRACT

In this study, the effect of strontium on the bioactivity properties of bioactive glass system consisting of $\text{SiO}_2\text{-Na}_2\text{O-P}_2\text{O}_5\text{-B}_2\text{O}_3\text{-CaO}$ was investigated. Bioactive glass compositions containing strontium in four different proportions (0, 0.5, 1, 2 wt.%) were produced by the melting method. Bioactivity analyzes of the obtained bioactive glasses were carried out in the artificial body fluid for various periods (1, 7, 14 and 28 days), surface characterizations and bioactivity analyzes were performed using XRD, SEM and EDS analysis. The results showed that the strontium addition has a positive effect on the bioactivity properties.

Keywords: Bioactive glass, strontium, bioactivity, hydroxyapatite

1. INTRODUCTION

The key component in the construction of bioactive glasses is SiO_2 , which constitutes 45-52 % by weight. This silicate ratio is the most important feature that separates the bioactive glasses from conventional soda lime-silica glass. Another feature of the bioactive glasses is high Na_2O , CaO content and high $\text{CaO/P}_2\text{O}_5$ ratio. Thanks to these properties, bioactive glass can be exposed to body fluids, resulting in strong binding between the host tissue or bone. This binding is due to the accumulation of silica ions and the formation of hydroxyapatite coating on the surface of the bioactive glass. The hydroxyapatite layer attracts osteoprogenitor cells, allowing the formation of bone by absorbing proteins [1,2].

Recently, the effects of ionic products dissolved from bioactive glasses on osteogenic and angiogenic processes have been investigated [3]. Research has shown that ions released from bioactive glasses; revealed that proliferation of bone-forming cells increases the production of insulin-like growth factor II, regulates the levels of protein production of cell-cycle regulators and countless genes [4]. Therefore, to improve bone production properties, ions may be added to the chemical compounds of bioactive glasses to stimulate bone cells. It is known that strontium accelerates the bone healing process and has a positive effect on bone tissue repair [5-9]. However, strontium has various effects on bone metabolism depending on the dose used. At low dose levels, stable strontium is of great benefit in bone formation as mentioned above. In contrast, a high dose of strontium reduces defective bone mineralization and inhibits the formation of hydroxyapatite [10].

In this study the effect of strontium addition on the bioactivity properties of $\text{SiO}_2\text{-Na}_2\text{O-P}_2\text{O}_5\text{-B}_2\text{O}_3\text{-CaO}$ bioactive glass system that has not been investigated before was investigated. Bioactive glasses were produced by using melting method and kept in various conditions in artificial body fluid (SBF) produced under laboratory conditions and bioactivity analyzes were performed.

2. EXPERIMENTAL

Bioactive glass compositions containing four different percentages of SrO with a composition comprising 47 % SiO_2 , 7 % Na_2O , 13% P_2O_5 , 2 % B_2O_3 , x % SrO and (31-x) CaO (x = 0, 0.5, 1, 2) was milled at 250 rpm for one hour in a ball mill with a grain size of - 45 μm . The ratio of SrO ratio is

limited to a maximum of 2 %, as the high strontium oxide content in the composition adversely affects bioactivity and biocompatibility [11]. The milled biomass powders were melted in alumina crucibles at 1500 °C for 1 h using an electric furnace. The molten glasses were cast into a graphite mold. To remove thermal residual stress from the glass sample, it was annealed in a regulated muffle furnace at approximately 600 °C for 1 h, followed by slow cooling to room temperature. Sample code system according to SrO Content (wt.) was given in Table 1.

Table 1. Sample code system according to SrO Content

Sample code	SrO Content (wt. %)
Sr00	-
Sr05	0.5
Sr10	1
Sr20	2

X-ray diffractometry (XRD) was performed to determine the crystal phases formed on their surfaces as a result of bioactivity tests carried out with SBF and determination of their post-cast structures to the bioactive glass samples produced. Differential thermal analysis (DTA) was performed to determine the glass transition temperatures (T_g) and crystallization temperatures (T_c) of the produced bioactive glass samples. In the experiments, the reference material was α - Al_2O_3 and the glass samples were heated to 1200 °C with a heating rate of 10 °C / min. In addition, 1, 7, 14 and 28 days in SBF were kept to observe the bioactivity of the glass produced (Fig. 1). During the waiting periods, the SBF solutions in which the samples were placed were placed in the oven and the temperature was kept constant at 37 °C. In order to observe the hydroxyapatite layer formed on the bioactive glass samples, a scanning electron microscope (SEM) with energy distribution x-ray spectroscopy (EDS) was used.

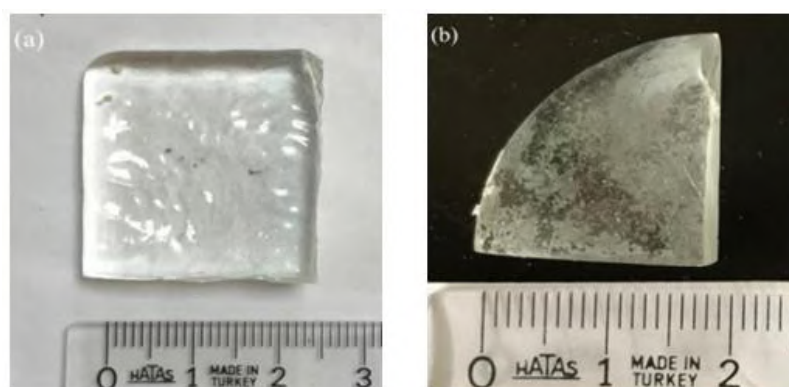


Figure 1. (a) Bioactive glass produced by melting process, (b) bioactive glass after 28 days in SBF

3. RESULTS

All of the graphs obtained after the analyzes were made with some abbreviations to avoid confusion. The graphs of the XRD analyzes applied to bioactive glasses containing four different ratios (0 %, 0.5 %, 1 %, 2 %) SrO are given in Figure 2a. As a result of the analysis, no crystalline phase was observed and the samples were found to be amorphous [12]. This result showed that the strontium additive did not have a tendency to crystallize during cooling and did not affect the glass structure.

DTA analysis of bioactive glass samples is shown in Figure 2b. When the DTA curves are examined, it is observed that the endothermic peak indicating the glass transition temperature of the samples is in the range of 780-825 °C and the exothermic peaks indicating the crystallization temperature in the 805-920 °C range and the temperature of the T_g and T_c decreases with the strontium admixtures.

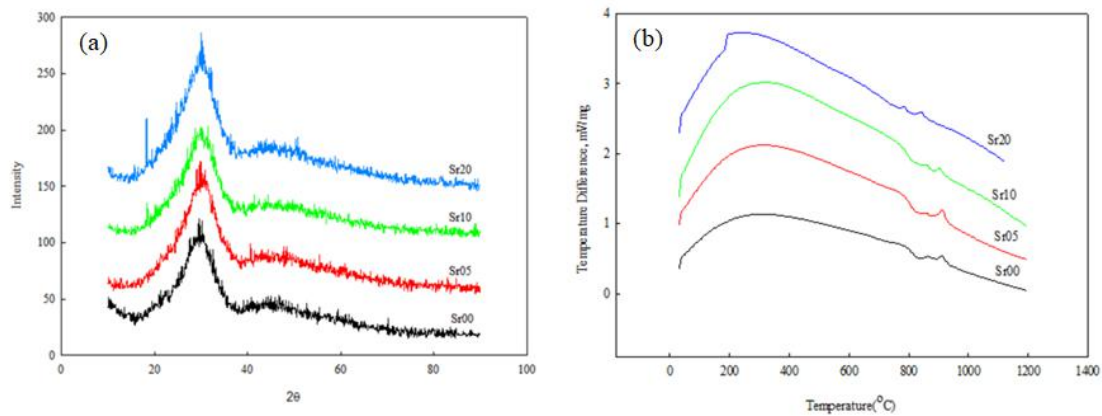


Figure 2. a) XRD graph of bioactive glasses, b) DTA graph of bioactive glasses.

The XRD graphs of bioactive glass samples containing four different amounts of SrO additive were kept in the SBF for 1, 7, 14, and 28 days (Fig. 3). When the graphs are examined, it was determined that the amorphous structures of the original bioactive glass samples determined were lost and a crystalline peak was formed at $2\theta = 33^\circ$. It was determined that this peak belongs to the hydroxyapatite- $\text{Ca}_{10}(\text{PO}_4)_6(\text{OH})_2$ phase. However, it was observed that hydroxyapatite peak was formed in all samples starting from the first day and increased in proportion to the waiting times in artificial body fluid.

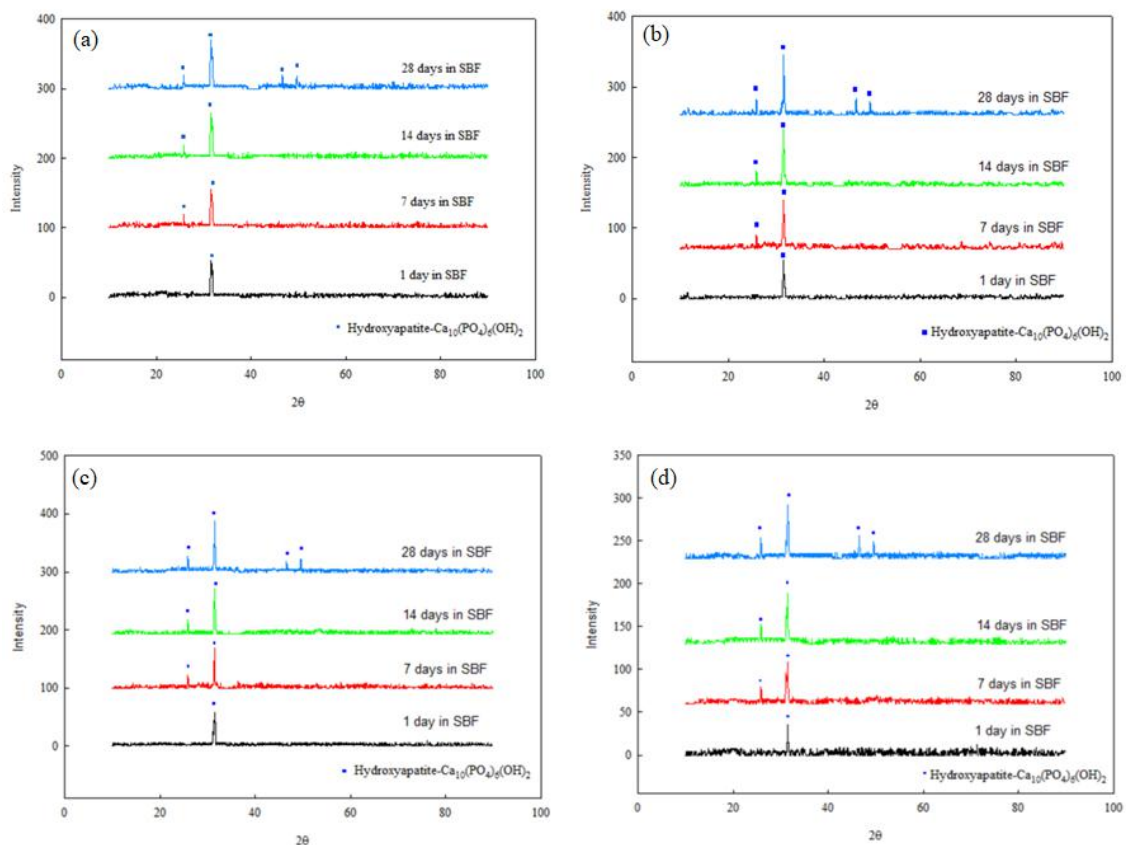


Figure 3. Bioactive glass samples kept in SBF for various periods XRD graphics; (a) Sr00, (b) Sr05, (c) Sr10, (d) Sr20

The samples of the bioactive glass produced were examined by the scanning electron microscope (SEM) before and after the rest in the SBF, and their images are given in Figure 4. When the images are examined, it is seen that all samples have an amorphous structure and do not contain any crystalline phase before being kept in SBF. However, the samples were kept in SBF for 28 days and

their surfaces were covered with a homogenous layer of hydroxyapatite which was white. It is observed that the HA crystals in the varn form are more intense in the glass samples containing SrO.

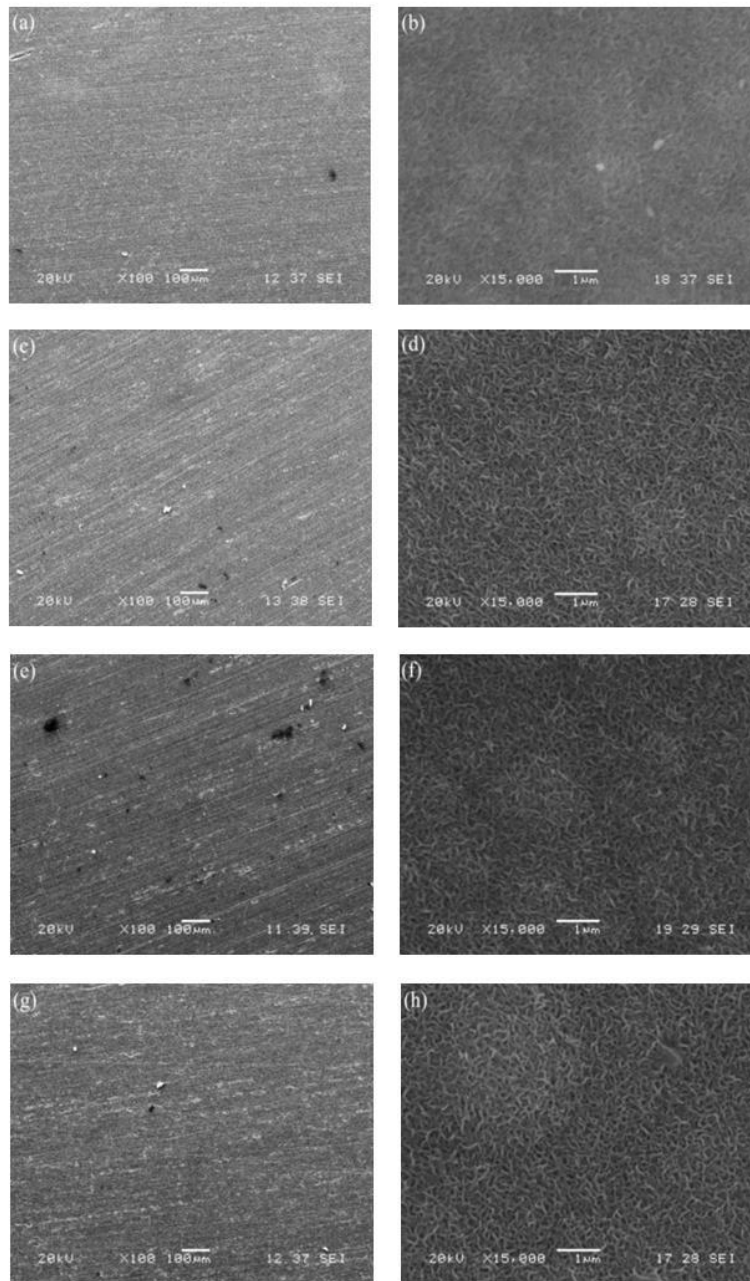


Figure 4. SEM images of bioactive glasses before and after waiting in SBF. a) Sr00 before SBF, b) Sr0 after waiting SBF for 28 days, c) Sr05 before SBF, d) Sr05 after waiting SBF for 28 days, e) Sr10 before SBF, f) Sr10 after waiting SBF for 28 days, g) Sr20 before SBF, h) Sr20 after waiting SBF for 28 days.

EDS measurements of all bioactive glass samples were also performed with SEM analysis (Figure 5.). The percentages of calcium and phosphorus determined with EDS on the surfaces of the sample obtained from SEM photographs are given in Table 2. When the values in Table 2 are examined, it is seen that the Ca/P values of all the samples are higher than the $\text{Ca/P} = 1.65$ required for HA formation. This confirms the presence of the HA structure observed in the SEM images. It was also found that the additive of strontium increased the Ca/P value.

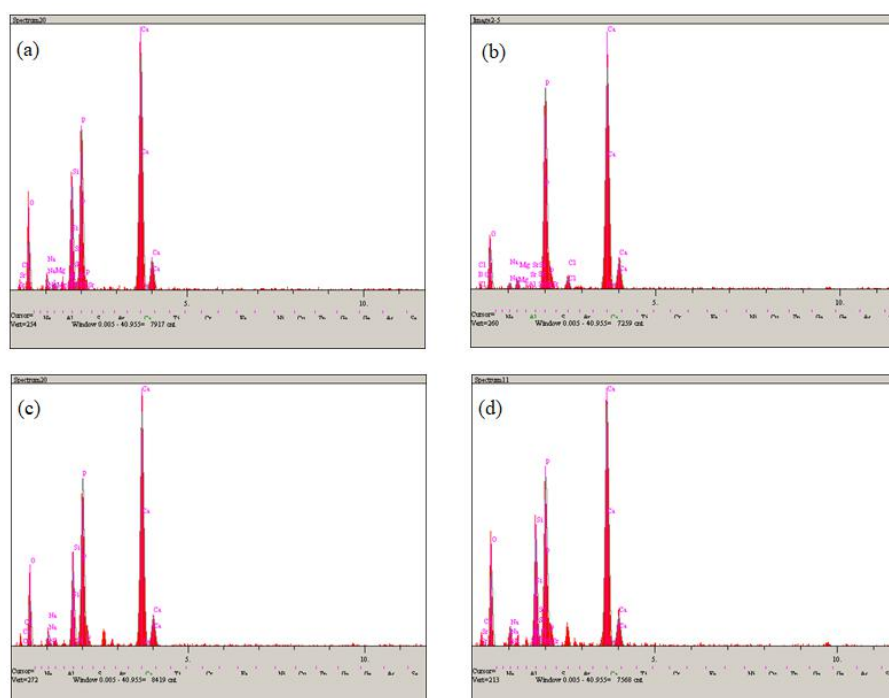


Figure 5. EDS analysis of bioactive glass samples; (a) Sr00, (b) Sr05, (c) Sr10, (d) Sr20

Table 1. Ca / P ratios of biomass samples kept in SBF for 28 days

Material	Ca/P ratio
0% SrO doped bioactive glass	1,67
0.5% SrO doped bioactive glass	1,73
1% SrO doped bioactive glass	1,83
2% SrO doped bioactive glass	1,82

4. CONCLUSIONS

1. Four different proportions (0 %, 0.5 %, 1 % and 2 %) of the strontium oxide additive (wt.%) containing the samples were produced by smelting method and XRD analysis revealed that amorphous glassy structures were formed.
2. As a result of the DTA applied to the bioactive glass samples produced, glass transition temperatures (780-825 °C) and crystallization temperatures (805-920 °C) were determined.
3. Produced bioactive glass samples in SBF for various periods (1, 7, 14, 28 days) after the application of XRD, SEM and EDS applications on the surfaces of all samples from the first day of hydroxyapatite layer was observed and the samples were determined to have bioactivity properties. It has also been observed that the contribution of strontium increases the bioactivity of bioactive glass samples.
4. After all the analysis, bioactive glasses with $\text{SiO}_2\text{-Na}_2\text{O-P}_2\text{O}_5\text{-B}_2\text{O}_3\text{-CaO-SrO}$ system are thought to be potential materials for the production of tissue scaffolds in bone tissue engineering.

REFERENCES

1. Välimäki V.V., Aro H.T., Molecular basis for action of bioactive glasses as bone graft substitute. *Scand. J. Surg.* 2006, 95-102.
2. Neo M., Nakamura T., Ohtsuki C., Kasai R., Kokubo T., Yamamuro T., Ultrastructural study of the A-W GC-bone interface after long-term implantation in rat and human bone. *J. Biomed. Mater. Res.* 1994, 28, 365-372.
3. Wu C., Zhou Y., Lin C., Chang J., Xiao Y., Strontium-containing mesoporous bioactive glass scaffolds with improved osteogenic/cementogenic differentiation of periodontal ligament cells for periodontal tissue engineering. *Acta Biomater.* 2012, 8, 3805-3815.
4. <http://www.biltek.tubitak.gov.tr/bdergi/yeniufuk/icerik/biyomalzemeler.pdf> Date of access: 03.12.2008.
5. Canalis E., Hott M., Deloffre P., Tsouderos Y., Marie P.J., The divalent strontium salt S12911 enhances bone cell replication and bone formation in vitro. *Bone*, 1996, 18 (6), 517-523.
6. Gentleman E., Fredholm Y.C., Jell G., Lotfibakhshaiesh N., O'Donnell M.D., Hill R.G., Stevens M.M., The effects of strontium substituted bioactive glasses on osteoblasts and osteoclasts in vitro. *Biomaterials*, 2010, 31, 3949-3956.
7. Zhang W., Shen Y., Pan H., Lin K., Liu X., Darvell B.W., Effects of strontium in modified biomaterials. *Acta Biomater.* 2011, 800-808.
8. Wu C., Zhou Y., Lin C., Chang J., Xiao Y., Strontium-containing mesoporous bioactive glass scaffolds with improved osteogenic/cementogenic differentiation of periodontal ligament cells for periodontal tissue engineering. *Acta Biomater.* 2012, 8, 3805-3815.
9. Wu C.T., Fan W., Gelinsky M., Xiao Y., Simon P., Schulze R., Bioactive SrO-SiO₂ glass with well-ordered mesopores: characterization, physiochemistry and biological properties. *Acta Biomater.* 2011, 7, 1797-1805.
10. Verberckmoes S.C., De Broe M.E., D'Haese P.C., Dose-dependent effects of strontium on osteoblast function and mineralization. *Kidney Int.* 2003, 64, 534-543.
11. Wang W., Yeung W.K., Bone grafts and biomaterials substitutes for bone defect repair: A review. 2017, 2 (4), 224-247.
12. Fu H., Fu Q., Zhou N., Huang W., Rahaman M.N., Wang D., Liu X., In vitro evaluation of borate-based bioactive glass scaffolds prepared by a polymer foam replication method. *Materials Science and Engineering C*, 2009, 29 (7), 2275-2281.

THE EFFECT OF ZnO ADDITION ON THE PROCESSING OF CERAMIC TILES FROM WASTE GLASS AND FLY ASH

Mustafa Çetin, Ediz Ercenk, Şenol Yılmaz

Sakarya University, Engineering Faculty, Department of Metallurgical and Materials Engineering,
Esentepe Campus, 54187 Sakarya, Turkey

ABSTRACT

In this study, the effect of ZnO addition on ceramic tiles from waste glass and fly ash has been investigated. ZnO in the range of 0–20 wt. % have been added into waste glass and fly ash mixture. Cylindrical specimens, shaped by pressing and were sintered at 900, 950, 1000 and 1050 °C for 2 h. The firing shrinkage, bulk density, apparent porosity and water absorption of sintered specimens are explained on the basis of X-ray diffraction (XRD) and scanning electron microscopy (SEM) analysis. The results showed that ZnO addition enhance ceramic tiles properties. Ceramic tiles from waste glass and fly ash including ZnO can be used as wall tile.

Keywords : Fly ash, waste glass, ZnO, tile

1. INTRODUCTION

Fly ashes are waste generated from coal-fired thermal power plants. As industrial ash fly ash will adversely affect the environment, it is prevented from getting out of the chimneys of the production plants to the air. With the use of such wastes, environmental problems are reduced and economic contributions are provided and higher quality products can be produced [1,2].

75-85% of the fly ash resulting from combustion in thermal power plants is extracted from the boiler by flue gases and generally high efficiency electro filters are used to keep the fly ash. The most common feature of fly ash is its physical, chemical, mineralogical and pozzalonic properties that vary from locality to locality, even in the same region. The type of coal that forms the source of a fly ash, the degree of crushing of the coal prior to burning, the type of boiler used, the combustion temperature and other operating parameters, the characteristics of the ash collection and removal systems, and the additives added to the coal affect the properties of the fly ash [3].

A large part of working with coal or lignite and production of energy from thermal power plants in Turkey are provided. Most of the fly ash grains are composed of alumina and siliceous compounds [4]. It is possible to produce high strength mortar as a result of activation of fly ash with various alkalis. Therefore, it is also considered as building material [5].

Fly ash, which is an important by-product, is the conversion of the molten material which occurs as a result of the coal burning at high temperatures to the partially or completely spherical shaped ash particles by gas flow. The ash particles are very thin (0.5 - 150 µm) and are called fly ash because they are drained by the flue gases [6]. Due to the chemical composition of fly ash, it can be used in many fields such as construction sector, ceramic, plastic, wastewater treatment, cement, concrete, brick, light aggregate, gas concrete and highways [7,8].

A large part of the structure of fly ash (60% -90%) is in amorphous condition. At the same time, some fly ash can contain crystals such as mullite, quartz, magnetite and hematite. Areas of use according to the properties of the particles are different [9]. In parallel with the development of the construction sector in Turkey is trying to show that the production of more and better quality building materials [10].

There are over 200 million tons of coal reserves at the mining sites in Seyitömer Lignite Enterprises. The average calorific value of the coal burned in the power plant is 1700 Cal / kg and approximately 6.000.000 tons of coal is consumed annually in response to the normal production of the power plant [11].

The aim of this study was to investigate the effect of ZnO addition in the amount of 0 to 20% by wt. of waste glass and fly ash on ceramic tiles. Experimental tests and analyzes were determined by the addition of different ratios of ZnO to the mixture of waste glass and fly ash.

2. EXPERIMENTAL

At the beginning, the window glass waste which will be used in experimental studies was milled in the dry mill for 2 hours. After this milling process, waste glass powder was obtained below $-75\mu\text{m}$. A main mixture was obtained by adding 50% by wt. of Seyitömer Thermal Power Plant fly ash to the obtained glass powder. Then 4 different compositions were prepared by adding 0, 5, 10 and 20% ZnO by wt. to fly ash and waste glass mixture. The chemical composition of Seyitömer fly ash and waste glass used in the study are given in Table 1. Sample code system according to ZnO content (wt. %) was given also in Table 2.

Table 1. The chemical composition of Seyitömer fly ash and waste glass (wt. %)

Chemical Compound	Fly ash	Waste glass
SiO ₂	56.90	72.00
Al ₂ O ₃	17.25	2.00
TiO ₂	0.70	-
Fe ₂ O ₃	10.63	-
CaO	4.32	12.00
MgO	5.14	-
Na ₂ O	0.31	14.00
K ₂ O	1.55	-
MnO	0.23	-
P ₂ O ₅	0.12	-
L.O.I	2.85	-

Table 2. Sample code system according to ZnO Content

Sample code	ZnO Content (wt. %)
Zn00	-
Zn05	5
Zn10	10
Zn20	20

The mixture was stirred for 2 hours at 250 rpm for homogeneous mixing of mixtures containing ZnO in different ratios. Cylindrical samples were produced by pressing the obtained powders. Samples produced by pressing method were sintered at 900, 950, 1000 and 1050 °C for 2 hours. The flow chart of the experimental studies is given in Figure 1.

The linear shrinkage, bulk density, apparent porosity and water absorption of the sintered specimens were calculated from their weights and dimensions. Characterization of the phases in the selected sintered specimens was carried out by XRD analysis. For the microstructural observations SEM was used.

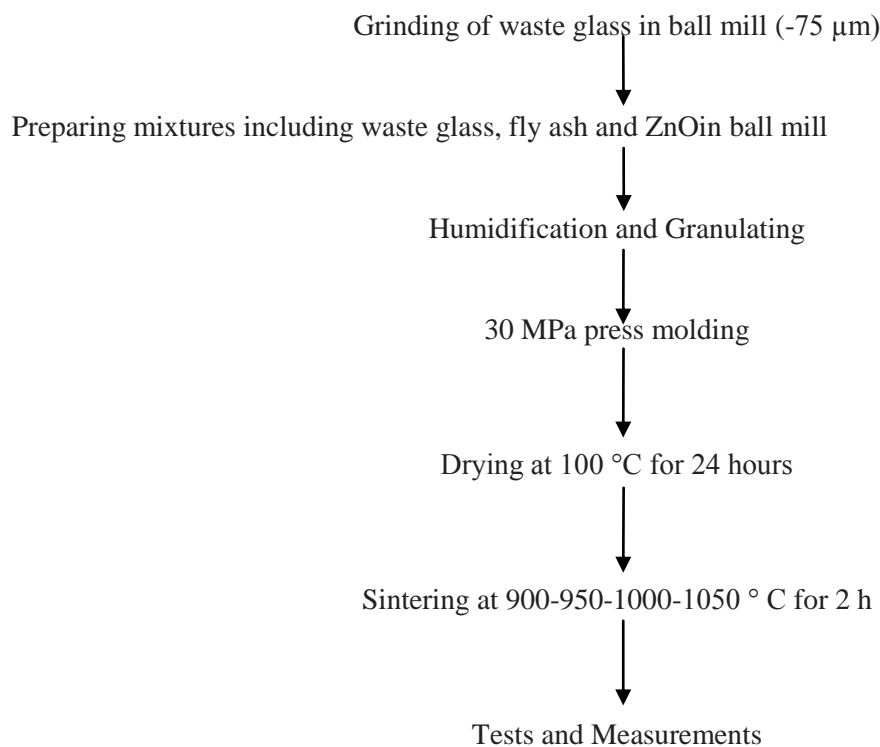


Figure 1. Flow chart of experimental studies.

3. RESULTS AND DISCUSSION

The firing shrinkage of sintered samples with the addition of different ratios of ZnO is shown in Figure 2. The amount of firing shrinkage occurring in the sintered samples decreased with ZnO addition. The fewer firing shrinkage values were observed at the highest sintering temperature. In general, the rate of firing shrinkage decreased with the addition of ZnO.

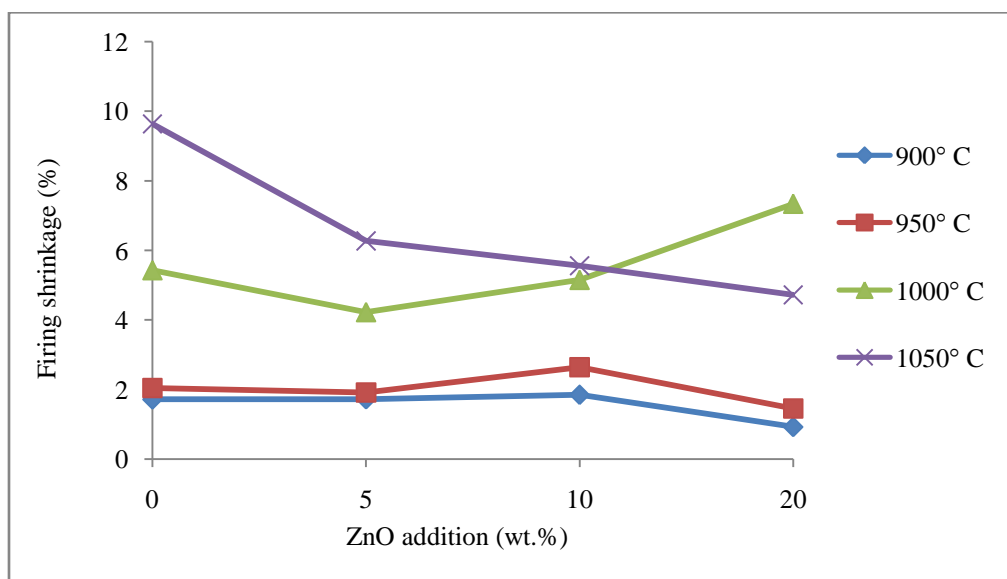


Figure 2. Firing shrinkage vs. ZnO addition for different sintering temperatures.

The results of apparent porosity versus ZnO addition shown in Fig. 3 indicates that by increasing ZnO from 0 to 20 wt.%, the apparent porosity decreased by increasing in sintering temperature due to increasing in glassy phase. The values of bulk density increased with the increase in sintering temperature and ZnO content in Fig. 4 supporting the apparent porosity results. According to the water absorption versus ZnO addition shown in Fig. 5 indicates that by increasing ZnO from 0 to 20 wt.% and sintering temperature, the water absorption decreased.

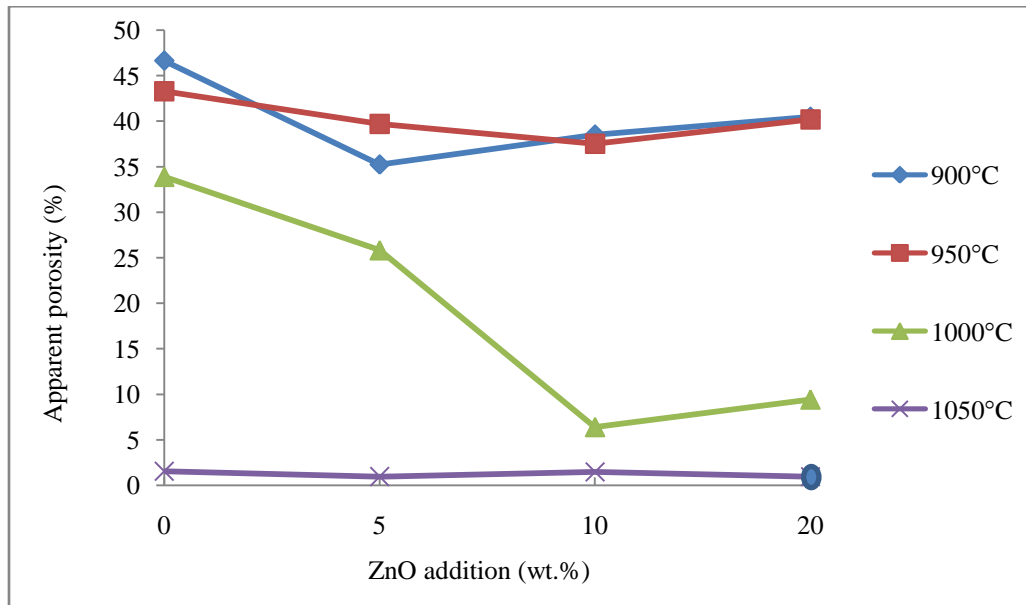


Figure 3. Apparent porosity vs. ZnO addition for different sintering temperature.

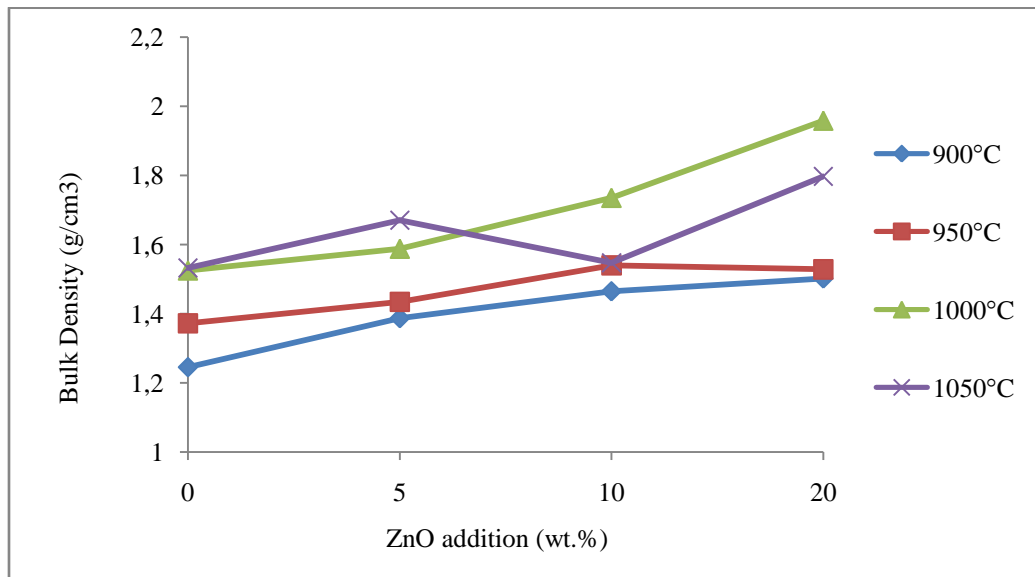


Figure 4. Bulk density vs. ZnO addition for different sintering temperature.

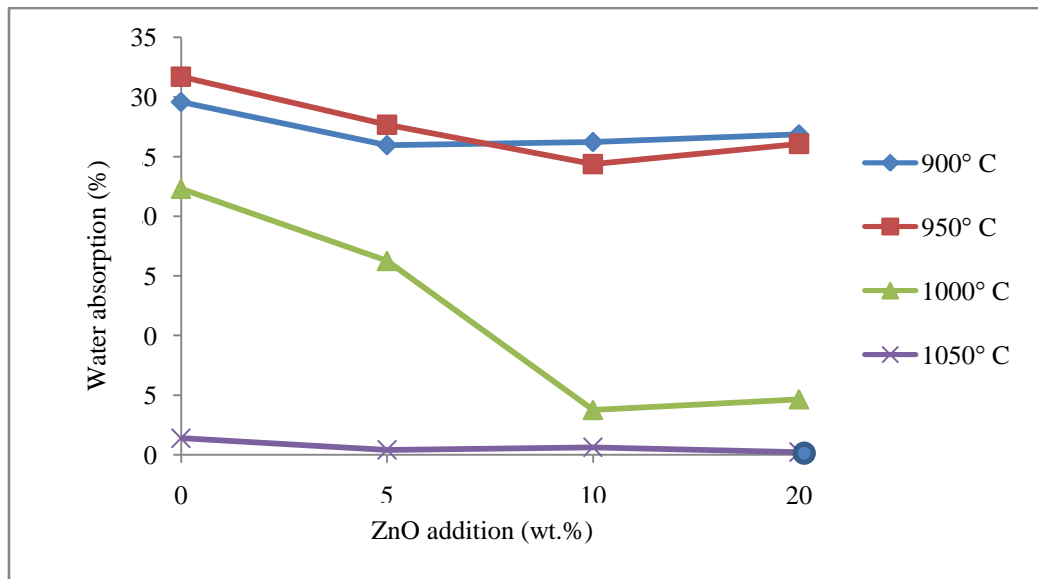


Figure 5. Water absorption vs. ZnO addition for different sintering temperature.

XRD analysis of samples sintered at 1050 °C for 2 h is given in Figure 6. Presence of Diopside ($\text{CaMgSi}_2\text{O}_6$), Augite ($\text{Ca(Fe,Mg)Si}_2\text{O}_6$), Willemite (Zn_2SiO_4), Tridymite (SiO_2) and Nepheline ($\text{Na}_{6.65}\text{Al}_{6.24}\text{Si}_{9.76}\text{O}_{32}$) phases has been detected. Willemite (Zn_2SiO_4) phase was identified by ZnO addition and its phase intensity increased by ZnO additions.

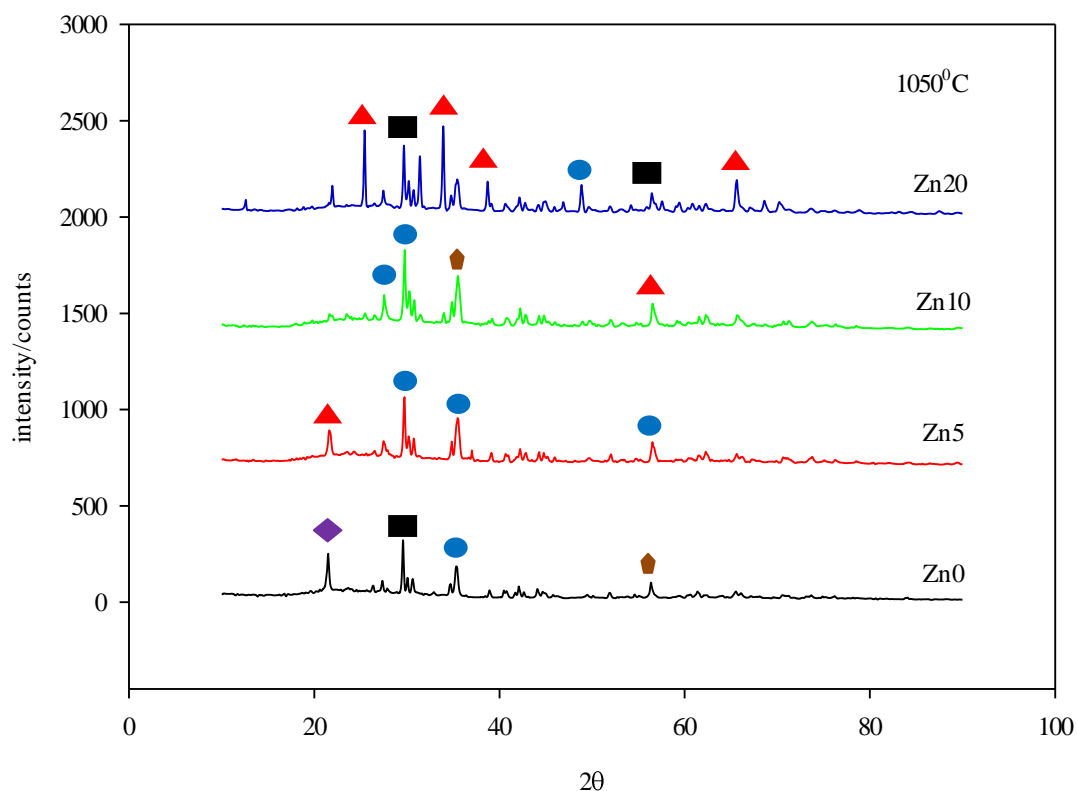


Figure 6. XRD pattern of samples sintered at 1050 °C for 2 h. (Diopside - $\text{CaMgSi}_2\text{O}_6$, Augite - $\text{Ca(Fe,Mg)Si}_2\text{O}_6$, Willemite - Zn_2SiO_4 , Tridymite - SiO_2 , Nepheline - $\text{Na}_{6.65}\text{Al}_{6.24}\text{Si}_{9.76}\text{O}_{32}$) SEM images of samples are shown in Figure 7. In the SEM images, scattered small crystals and pores in glassy structure were observed.

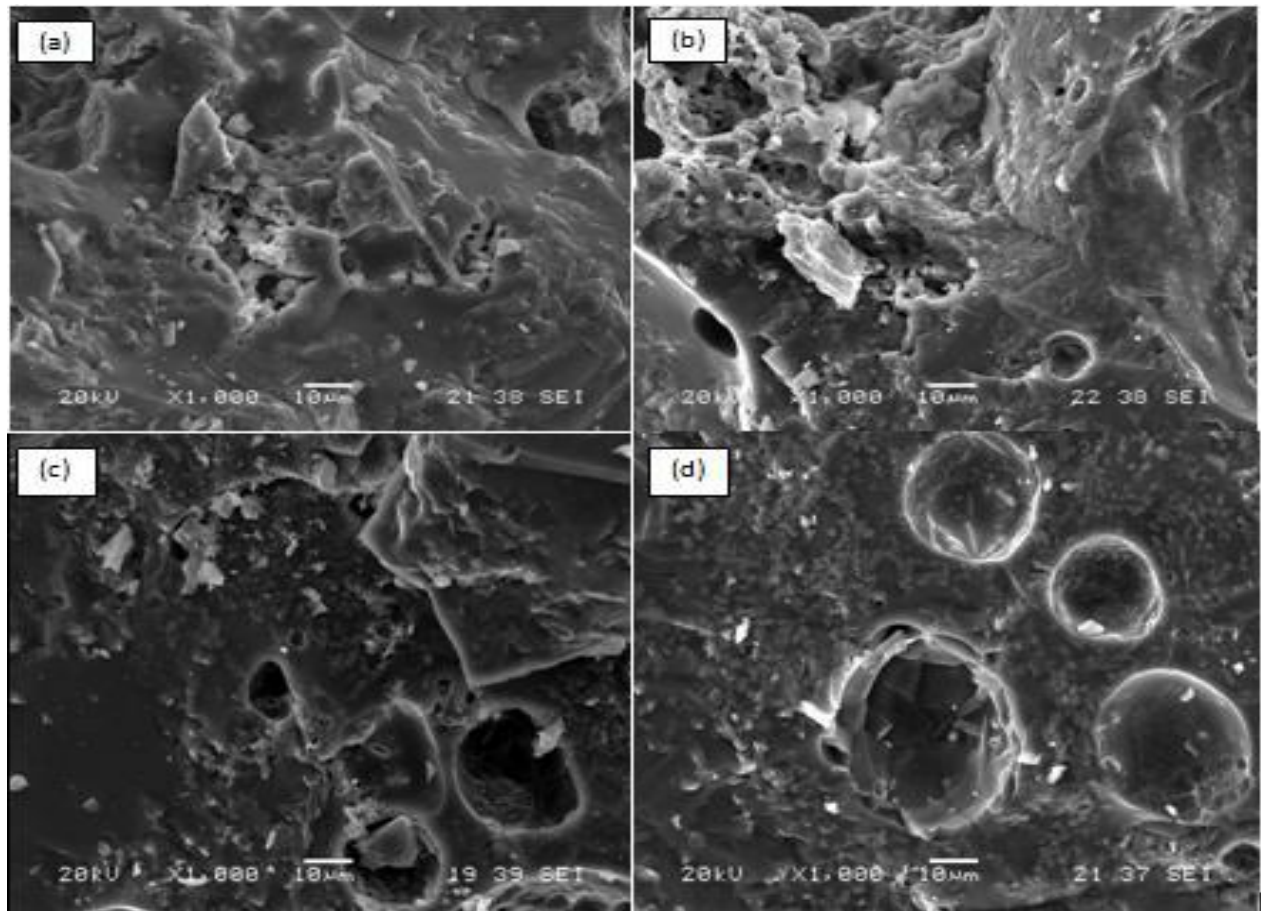


Figure 7. SEM images of samples sintered at 1050 °C for 2h. a) Zn00, b) Zn05, c) Zn10, d) Zn20

5. CONCLUSIONS

- 1) The values of firing shrinkage decreased with ZnO addition. The fewer firing shrinkage values were observed the highest sintering temperature.
- 2) The water absorption and apparent porosity values of specimens decreased with increasing in sintering temperature and ZnO content.
- 3) The bulk density of sintered samples increased with the increase in sintering temperature and ZnO content.
- 4) Small crystals were embedded in the glassy phase and some pores are shown in SEM microstructures.
- 5) Mixtures of fly ash, waste glass and ZnO could be used in the wall tiles fabrication on the basis of physical properties and phases formed after firing.

REFERENCES

1. Turker P., , Erdogan B., Katnas F., Yeğınobalı A., Classification and properties of Fly Ash in Turkey. TÇMB/R & D/Y03.03, July 2009, Ankara (Turkey), 5-9.
2. Haluk M., Baran Y., The Effect Of Seyitomer And Cayirhan Thermal Power Plant Fly Ashes to Initial And Final Setting Time Of PC-FA Pastes. Journal of Polytechnic, 2003, 6 (1), 397-409.
3. Güler G., Güler E., İpekoğlu Ü., Mordoğan H., Properties and Uses of Fly Ashes. Proceedings of 19th International Mining Congress and Expo, IMCET2005, 09-12 June 2005, Dokuz Eylül University, Izmir (Turkey), 419-423.
4. Ozdemir O., Characterization of Tuncbilek Thermal Power Plant Fly Ash and Elimination of By-Products. M.Sc. Thesis, February 2001, Istanbul Technical University.
5. Kaya M., Investigation of the mechanical and durability properties of alkaline activated mortars produced by using different types of fly ash. PhD Thesis, June 2016, Sakarya University.
6. Cıncın Y., Investigation of Light Brick Production with Lime Additive from Lignite Burning Thermal Power Plant Ashes. M.Sc. Thesis, August 2015, Dokuz Eylül University.
7. Bentli İ., Uyanık A.O., Demir U., Şahbaz O., Çelik M.S., Usage of Seyitömer Thermal Power Plant Fly Ash as Brick Additive Raw Material, Proceedings of 19th International Mining Congress and Expo, IMCET2005, 09-12 June 2005, Dokuz Eylül University, Izmir (Turkey), 385-389.
8. Yılmaz Ş., The Utilization of Seyitömer Thermal Power Plant Waste Fly Ash as Building Material, M.Sc. Thesis, 1992, Istanbul Technical University.
9. Demir İ., Baspınar M.S., Görhan G., Kahraman E., Preliminary Investigation of Seyitomer Fly Ash For Use In Building Brick Manufacturing, Afyon Kocatepe University Journal Of Science, 2010, 131-137.
10. Ozdemir İ., The investigation of production conditions and properties of building materials obtained from blast furnace slag, M.Sc. Thesis, 2003, Sakarya University.
11. http://celiklerholding.net/grup-sirketleri_2/celikler-seyitomer Date of access: 14.09.2018.

CHARACTERIZATION AND INVESTIGATION OF CORROSION PREVENTION PERFORMANCE OF METAL INDUSTRIAL COATINGS CONTAINING DIFFERENT TYPES OF RESIN

İrem Toprakçı¹, Nil Acaralı¹

¹Yildiz Technical University, Department of Chemical Engineering, Davutpasa St., N.127, Esenler, Istanbul, Turkey

Corrosion, an important concept for coatings, is a major cause for limited metal resources in the world and an event that threatens human life and health. Unprotected metals can be converted to oxides at various ratios of corrosion. One of the most effective methods of counteracting corrosion is the application of a suitable and effective coating method. Another important issue is the increase in the amount of damage caused by rapid population growth, uneven urbanization and the number of fires caused by rapid industrialization. One of the measures to be taken is the use of non-combustible or flame retardant materials. Boron is one of the indispensable sources of mineral which are the main inputs of the developing industry and technological progress with strategic precaution that can meet all these needs. The advantages of boron chemistry and boron end products are their ability to reduce gaseous emissions and increase the adhesion of metals to plastics. Since they do not have toxic properties, they do not require special tools to be added to resins.

In this study, an optimization method was carried out by applying Design Expert which is an experimental design program for different parameters and levels (0-6%, w/w) of prepared organic coating materials containing additives to improve material properties. As a result, it was observed that the addition of different materials to the surface of the coating improved the properties of flame retardancy, hydrophobicity, corrosion, adhesion resistance, and had superior properties.

Keywords: corrosion, boron, coating, resin

Introduction

Organic coatings is a very important protective layer and it is also possible to define it as "a material that forms a decorative and protective film layer when applied to a surface [1]. Solvent, binder, pigment, filler and additives are the main components of the organic coatings. The main difference between the organic coatings is the resin or polymers used as binders [2].

Corrosion is, as a general definition, the breakdown of the metallic properties as a result of reactions of metals and alloys with their environment. In other words, corrosion can be defined as "destruction of metal-structure alloys due to their electrochemical properties and the effect of the environment [3].

Metals are used in industrial application areas widely because of their extraordinary mechanical properties and their high strength. But there is one thing that is dangerous about metals, when they are exposed to a corrosive effect, their service life can get shorter and they can lose their protective properties. This particular status can cause important economic effects for all countries [4]. To reduce corrosion losses as much as possible, many methods have been developed. The most common ones used are stainless steel production method, inhibitor uses, anodic protection method, cathodic protection method and surface coating method. The cheapest and the easiest one is the surface coating method [5].

Organic coatings are the most common method for corrosion protection of metallic materials, common examples can be seen in aircrafts, automobiles, ships, pipelines, buildings, bridges, etc. Protective organic coatings includes various discontinuous solid functional additives that can be named as "pigments" that are contained within a continuous polymeric phase known as the "binder". Pigments

contribute functionality in the coating and polymeric binder is assumed to contribute adhesion of the coating to the substrate. Organic coatings can isolate the metal surface and prevent water and oxygen from reaching the metal surface [6].

Normally, solvent-based system often selected for application of industry coating for protecting the metal against corrosion. Although, some factors about environmental regulations and cost factors introduce water-based system in the industrial application. Water borne systems have a need for improvements per contra steady progress of this systems. Right polymer selection must be achieved for the corrosion protection [7].

Another important issue is to increase the fire resistance of the materials to minimize the damage that may occur in the event of an accident or fire [8]. Boron compounds don't cause toxic gas release when used as flame retardants, so they are environmentally friendly. They cover the burnt material and that cuts off the oxygen contact and it leads to suppressing the burn. Studies on the use of boron end products as flame retardants are increasing day by day. Sadowska et al. (2015) used boron in order to prepare polyurethane and polyisocyanurate foams and they observed that the boron has flame retardant effect on these foams [9]. Akarslan (2015) reviewed the flame retardant property of boric acid in cotton fabrics and he observed that boric acid reduced the tensile strength in the cotton fabrics and increased its flame retardancy [10].

In one study, some boron compounds were added to the styrene acrylic coating at different concentrations. The effects of flame retarding, smoke suppression and antimicrobial activities against two bacterial strains were investigated. While experiments and analyzes indicated that zinc borate would be a reagent against *S. aureus* bacteria, sodium tetraborate could have a flame retardant and smoke suppressant effect, even though there was no antibacterial activity [11].

In another study, corrosion performance of concrete samples coated with basaltic pumice, barite, colemanite and high furnace slag added coatings were investigated separately. Coatings have been produced with various combinations of these four materials. The samples were kept in 3.5% NaCl solution for a year. At the end of this period corrosion strengths and wear losses of the concretes were measured. The results show that colemanite and barite are usable additive materials for corrosion resistant coatings production [12].

It is now possible for the painted surfaces to self-clean thanks to newly developed coating technologies [13]. As an important feature of the chemistry, the wettability of a surface have great importance in basic and industrial applications [14]. We can give the lotus seeds of nature as an example of hydrophobic surfaces. When the smallest piece of dust comes onto this plant, the dust pushes towards the other part. Besides, when it starts raining, it is self-cleaned using rain drops [13]. Control of surface wettability is very important for many applications such as self-cleaning glasses for the aerospace and automotive industry, non-abrasive structures for the construction industry, waterproof textiles, optical instruments and non-contaminated surfaces for mobile phones, membrane applications, cell and antibacterial adhesion [14].

In this study, an optimization method was applied for different parameters and levels of prepared organic coating materials to enhance material properties. The results showed that the usage of coatings containing different types of resin and additives improved flame retardancy, hydrophobicity, corrosion, adhesion resistance on metal surfaces.

2. Experimental

2.1. Materials

Boron chemical (B1) was supplied by Çolakoğlu A.Ş. in Turkey. Additive-methacrylate based (MB1), a powdery-non-metallic mineral (P1) were provided from DuPont and a mining company, respectively.

2.2. Methods

Additives (B1, MB1, P1) were used in range of 0-6% (in terms of organic coatings, w/w). The additives (B1, P1) were homogenized by using mechanical stirrer (Fig. 1). The coating was stirred at 500 rpm for 5 minutes. The applicator film thickness was used with 150 μm (Fig. 2). Opacity charts (the surface chequered with black and white colours) were used for the visual test. Hydrophobicity, corrosion and adhesion tests were performed to surfaces. Design Expert method was used to determine the plan of experiments (Table 1).



Fig. 1. Mechanical stirrer

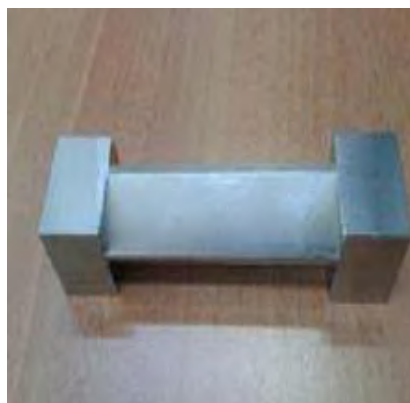


Fig. 2. Applicator

Table 1. Design Expert Method

Parameters	Level 1 (%)	Level 2 (%)	Level 3 (%)
B1	0	3	6
MB1	0	3	6
P1	0	3	6

3. Results and Discussion

3.1. Design Expert method

Experimental researches require a long time, attention and dedication, so nowadays raw materials, labor and time consumptions are minimized by using experimental design techniques. Design Expert software is the most known and used in scientific studies because it gives easily applicable and also true

results with high correlations [15]. With this program, the experiments can set up quickly and when the data is analyzed the results can be seen in graphical form.

Design Expert's powerful optimization features can maximize or minimize concurrent outputs. In order to optimize the process or product with this program, many experimental design methods such as factorial design, response surface methods (RSM), mixed design techniques, combined designs can be applied [16]. One of the Design Expert software's aim is helping the user with the design and interpretation of multi-factor experiments. In polymer processing, we can build an experiment with this software to see how a property like tensile strength varies with changes in the processing conditions [17].

In this study, the effect of parameters on viscosity was investigated, comparatively. As a result, it was observed that the parameters could interact binary and influenced viscosity.

3.2. Visual test

A sample of visual test result was shown in Fig. 3 for organic coatings containing additives at different concentrations. It was observed that hiding power of organic coatings was high for industrial applications.



Fig. 3. A sample of visual test

3.3. Hydrophobicity test

Wettability is an important property of solid surfaces from both fundamental and practical aspects. However, various industrial products require not only hydrophilicity but also hydrophobicity. Water as a volume of 0,1 ml pipette was dropped on the dry coating film a period of time. As a result, it was observed that surface was hydrophobic in the dry coatings film. (Fig.4).

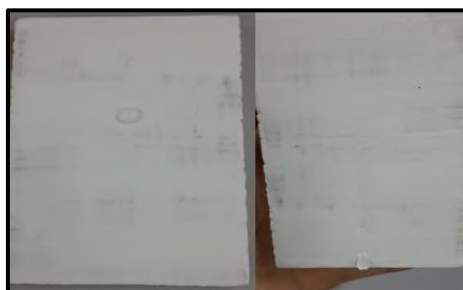


Fig. 4. A sample of hydrophobicity test

3.4. Corrosion test

Firstly the samples were kept in 5% NaCl solution for 2 hours. Then the metal plates were kept in a water vapor containing 98% moisture for 24 hours. It was observed that the prepared additives coatings were resistant to corrosion (Fig. 5).



Fig. 5. Corrosion test result for a sample

3.5. Adhesion test

In the adhesion test, the dry coating film of 1.5 -2 cm long 45° angle on the two diagonals and the line was drawn on the side edges 135° angle in facing relation of adhesive tape. Air bubbles between the fingers panel rubbing was resolved. Releasing a tip end of the adhesive tape held by the tape was drawn perpendicular to the surface with a jerk. As a result of the adhesion tests, scratches edges fully uniform, none of the square formed by combing shedding was observed (Fig.6).

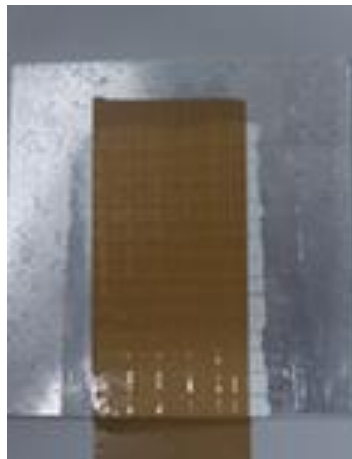


Fig. 6. A sample of adhesion test

4. Conclusion

Consequently, the number of experiments was minimized by using Design Expert Method for 3 parameters and 3 levels. Visual, hydrophobicity, corrosion and adhesion test results showed that the usage of additives affected the improvement of coating properties, positively.

KAYNAKLAR

1. Paksoy A.S., Boya el kitabı. Kimya Mühendisleri Odası, 1999, 1-281.
2. Lambourne R., Paints and surface coatings theory and practice. Ellis Horwood Limited, 1987.
3. Eriç M., Yapı Fiziği ve Malzemesi. Literatür Yayıncılık, 1994.
4. Betremieux I., Boone A., Chambat C., Delmas G., A new way to ensure metal protection with waterborne dispersion. Arkema Coating Resin, 2013.
5. Biçer A., Koç T., Alıcılar A., Arslan A., Ceyhan Bölge, Dörtöl işletme müdürlüğü tesislerindeki beton korozyonu raporu. Boru Hatları ile Petrol Taşıma A.Ş. Genel Müdürlüğü, Gazi Üniversitesi Mühendislik Mimarlık Fakültesi, 1997.

6. Kinsella E.M., Mayne J.E.O., Ionic conduction in polymer films-I: Influence of electrolyte on resistance. *Br. Polym. J.*, 1969, 1, 173–176.
7. Orozco R., The effects and economic impact of corrosion. *Universidad Veracruzana*, 2011.
8. Aydın D.Y., Gürü M., Ayar B., Çakanyıldırım Ç., Bor bileşiklerinin alev geciktirici ve yüksek sıcaklığa dayanıklı pigment olarak uygulanabilirliği. *Bor Dergisi*, 2016,1, 33-39.
9. Sadowska J.P., Czupryn'ski B., Liszkowska J., Boron-containing fire retardant rigid polyurethane– polyisocyanurate foams part II-preparation and evaluation. *Journal of Fire Sciences*, 2015, 33(1), 48–68.
10. Akarslan F., Investigation on fire retardancy properties of boric acid doped textile materials. *Acta Physica Polonica A*, 2015, 128, 403-404.
11. Alıcılar A., Ökenek F., Kayran B., Tutak M., Bor katkılı stiren akrilik boyaların alev geciktirme, duman bastırma ve antibakteriyel etkinlikleri. *Gazi Üniversitesi Mühendislik-Mimarlık Fakültesi Dergisi*, 2015, 30(4), 701-709.
12. Binici H., Durgun M. Y., Katkılı boyalarla kaplanan betonarme donatılarının korozyon performansı. *Teknik Dergi*, 2012, 388, 6141-6162.
13. Gür M., Nanomimarlık bağlamında nanomalzemeler. *Uludağ University Journal of The Faculty of Engineering*, 2010,15(2), 81-90.
14. Zhi J.H., Zhang L.Z., Yan Y., Zhu J., Mechanical durability of superhydrophobic surfaces. *The Role of Surface Modification Technologies Applied Surface Science*, 2016, 392, 286-296.
15. Mete M., Design expert. *Türkiye Kimya Derneği Dergisi*, 2015,1(3), 1-60.
16. Eğri N., Deney tasarım tekniği uygulanmamış optimizasyon çalışmalarının irdelenmesi. *Gazi Üniversitesi Fen Bilimleri Enstitüsü Yüksek Lisans Tezi*, Ankara, 2008, 1-56.
17. Buxton R., Software for design of experiments. *Mathematics Learning Support Centre*, 2007.

THE INVESTIGATION OF THE EFFECTS OF GLAZE COMPONENTS CHANGES TO CERAMIC DIGITAL INK PERFORMANCE ON FLOOR TILE MAT GLAZES

Süleyman Önder VARIŞLI^{1,2}, Bünyamin ÖZTÜRK¹, Şenol YILMAZ², Soner ÖZTÜRK¹

¹ Gizemfrit A.Ş Ceramic Research and Development Center, Sakarya\Turkey

² Sakarya University, Department of Material Science and Engineering, Sakarya\Turkey

ABSTRACT

Inks are the most expensive part of ceramic tile production. Due to high cost of ceramic digital inks, nowadays it is very important to use less amount of ink and getting the tonality required. The goal of the study to understand which oxides will effect on the colour performance.

The aim of the study is to investigate colour performance of ceramic inks with adding different raw materials into floor tile mat ceramic glaze formulation and to understand what will be the effects of raw materials to digital colour performance. In order to observe the changes on glazes and colour performance, glaze formulations will be checked spectrophotometric tools. After these analyses colour gamut comparisons of glaze formulations will be analysed with profiling tools.

Keywords: Glaze, Inkjet, Colour Gamut, Floor Tile

1. INTRODUCTION

Being one of the main reasons for the choice of ceramic materials, its physical and chemical advantages as well as its aesthetics are a sought after feature. Firstly, the production method with inkjet, which is used in textile sector, has been started to be applied on ceramic tiles with the development of technology. In inkjet technology, ink particles are transferred directly onto the printing surface by spraying. In this technology, the imaging system, image carrier and ink unit are combined in a single unit. For this reason, the electronic data is sent to the printing head and the ink is transferred directly to the printing surface [1]. With this method of production, it is easier and faster to switch to different products according to other decoration methods, it is possible to obtain all colours with only CMYK inks, less ink waste is formed, the transition time from design to design is much shorter and the need for less variety of ink is preferred because of its advantages [2]. Inks used in inkjet decoration are mostly pigment suspensions consisting of inorganic and complex metal oxides [3]. The desired properties of floor tiles; strength, abrasion resistance, low level of water absorption and anti-slip properties. The colour properties are also very important as physical properties. The expectation from ink colours is to become more intense tonality. In order to reducing the cost of the tile, the glaze compositions can be changed due to raw materials changes on glaze formulations. The changes on glaze compositions can make the printed design duller and fainter. Therefore the adjusting glaze recipes are getting more importance in order to get better colour performance on colours. Usually barium oxide, zinc oxide, wollastonite, dolomite, potassium feldspar, albite, nepheline raw materials are used in floor tile mat recipes. Depending on the increment or decrement of these raw materials used, the colour perception and gamut volume change. It is possible to obtain optimum glaze recipes using raw materials thus stronger colour perception and decrement of ink consumption can be obtained.

2. EXPERIMENTAL PROCEDURE

A usual floor tile matte recipe was accepted as the standard recipe and new recipe constructs were created by changing the proportions of the raw materials. The total weight of the recipes prepared was weighed as 300 grams. The recipes milled on ceramic jars and residue has been measured for each recipes. The residue of the recipes are %1-1,3 grs (45 micron or 325 mesh sieves. Residue over sieve) The densities of the recipes were adjusted to 1650 g/cm³, and the tiles were applied to the floor tiles of 45x45 cm with a spray gun of 160 grams. A tile was prepared for each recipe. The gamut scale was printed on the tiles dried in the oven and placed in the furnace. The tiles were fired in a furnace regime of 1190 °C 45 minutes. The colour values of the tiles, which have become the final product, were read by i1 profiles device and the data was transferred to the computer. From the obtained data, gamut volumes and L-a-b colour values were determined. The gamut volumes were determined by using Color Think Pro 3.0.3 program in order to analyse the obtained data. The obtained profiles were also converted the profile in a design determined by the Photoshop program, modelling was done to give insights on how the recipes would show. Gamut and colour scale printed on tile surfaces and Seger ratio of recipes are given in Fig.1, and Table 1., respectively.

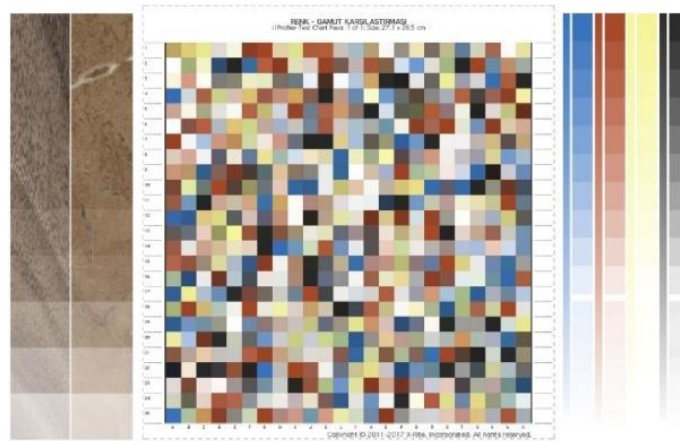


Fig-1. Gamut and colour scale printed on tile surfaces

Table-1. Seger ratio of recipes

	STANDART	A	B	C	D	E	F	G	H	J	K	L
SiO₂	2.044	1.98	2	2.109	2.088	2.023	2.064	2.226	1.732	2.04	1.708	1.855
Al₂O₃	0.412	0.417	0.414	0.407	0.411	0.415	0.409	0.43	0.405	0.419	0.359	0.39
K₂O	0.094	0.113	0.085	0.074	0.103	0.122	0.065	0.079	0.074	0.075	0.065	0.07
Na₂O	0.091	0.074	0.101	0.109	0.081	0.063	0.119	0.128	0.121	0.129	0.111	0.123
CaO	0.547	0.542	0.544	0.552	0.549	0.545	0.549	0.612	0.466	0.544	0.47	0.511
MgO	0.116	0.12	0.118	0.111	0.113	0.117	0.114	0.026	0.193	0.117	0.101	0.011
B₂O₃	0.012	0.012	0.012	0.013	0.013	0.012	0.012	0.013	0.012	0.011	0.01	0.01
ZrO₂	-	-	-	-	-	-	-	-	-	0.065	-	-
ZnO	0.121	0.119	0.119	0.122	0.122	0.121	0.121	0.122	0.115	0.107	0.228	0.1
BaO	0.032	0.032	0.032	0.032	0.032	0.032	0.032	0.032	0.03	0.028	0.024	0.085

The rates of the recipes according to the Seger Theory were modified. In the A Recipe, the rate of potassium oxide increased from nepheline while the rate of sodium oxide is decreased from albite. In the B Recipe, the rate of potassium oxide was decreased from potassium feldspar while the rate of sodium oxide is increased from nepheline. In the C Recipe, the rate of potassium oxide was decreased

from nepheline while the rate of sodium oxide is increased from albite. In the D Recipe, the rate of potassium oxide was increased from potassium feldspar while the rate of sodium oxide is decreased from nepheline. In the E Recipe, the rate of potassium oxide was increased from potassium feldspar while the rate of sodium oxide is decreased from albite. In the F Recipe, the rate of potassium oxide was decreased from potassium feldspar while the rate of sodium oxide is increased from albite. In the G Recipe, The rate of calcium oxide and quartz was increased from wollastonite while the rate of magnesium oxide was decreased from dolomite. In the H Recipe, The rate of calcium oxide and quartz was decreased from wollastonite while the rate of magnesium oxide was increased from dolomite. In the J Recipe, The rate of zirkonium oxide was increased while the rate of frit was decreased. In the K Recipe, The rate of zinc oxide was increased while the rate of frit was decreased. In the L Recipe, The rate of barium oxide was increased while the rate of frit was decreased.

3. RESULT AND DISCUSSION

Color, brightness and gamut volume data read from the tile surface is given in Table 2. Colour values according to the measurement results are shown in Figs. 2 and 3. The colour gamut volumes of the G and J recipes are larger than the other recipes. The Gamut volume recipe G; The yellow field also shows more expansion. The colour quality of the designs in yellow tones seems to be more intense than recipe G, and also according to L-a-b values recipe G is more intense than standard recipe on black colour gamut. Gamut volume of J recipe increases on yellow and blue area. The colour perception of the recipes B and H was much lower than the standard recipe.

Table-2. Color, brightness and gamut volume data read from the tile surface

		BLUE	BROWN	YELLOW	BLACK	GROUND-COLOR	GLOSSY	GAMUT VOLUME
STD	L	47.21	45.12	81.6	29.33	82.26	23.2	9749
	a	9.09	21.7	-6.44	-0.56	-0.23		
	b	-29.51	31.76	19.78	3.58	3.75		
A	L	46.96	44.84	81.61	30.22	81.49	18.3	8022
	a	9.12	21.62	-5.5	-0.3	-0.07		
	b	-29.47	30.56	17.41	3.19	3.62		
B	L	48.36	45.56	80.69	30.77	80.53	14.5	6644
	a	8.31	20.9	-4.92	-0.15	0.07		
	b	-28.13	29.44	15.8	3.33	3.56		
C	L	47.16	43.57	82.47	29.14	82.76	20.4	9759
	a	7.45	22.35	-7.4	-0.47	-0.32		
	b	-28.37	30.24	22.77	3.55	4.08		
D	L	47.71	44.77	82.1	28.28	82.01	25.9	8865
	a	9.15	22.13	-6.03	-0.22	0.03		
	b	-29.49	31.08	18.94	3.54	3.5		
E	L	47.08	44.49	81.83	29.03	82.18	22.7	9598
	a	9.2	22.11	-6.07	-0.22	-0.11		
	b	-29.84	31.89	18.82	3.36	3.45		
F	L	50.87	46.11	83.53	32.78	83.19	18	8737
	a	7.36	20.74	-6.41	-0.24	-0.23		
	b	-26.35	27.27	20.31	2.86	4.05		
G	L	47.68	48.05	81.38	25.83	81.11	37.8	11262
	a	7.96	23.7	-7.36	-0.96	-0.26		
	b	-29.13	36.08	23.39	3.69	4.32		
H	L	52.72	45.83	85.82	34.02	86.36	13.8	6475
	a	7.19	19.48	-4.28	0.28	-0.19		
	b	-26.69	24.87	13.16	4.67	3.58		
J	L	48.01	44.07	84.46	27.96	84.76	23.9	12123
	a	9.4	22.55	-7.3	-0.6	-0.18		
	b	-30.72	31.05	22.63	3.23	3.79		
K	L	45.25	43.14	81.11	22.47	81.74	21.7	9451
	a	7.94	22.51	-6.13	0.97	-0.14		
	b	-28.77	31.19	19.76	3.76	3.87		
L	L	48.5	44.33	82.23	28.12	81.76	19.1	9038
	a	8.77	21.9	-5.56	-0.16	0.03		
	b	-28.45	30.82	17.81	3.86	3.71		

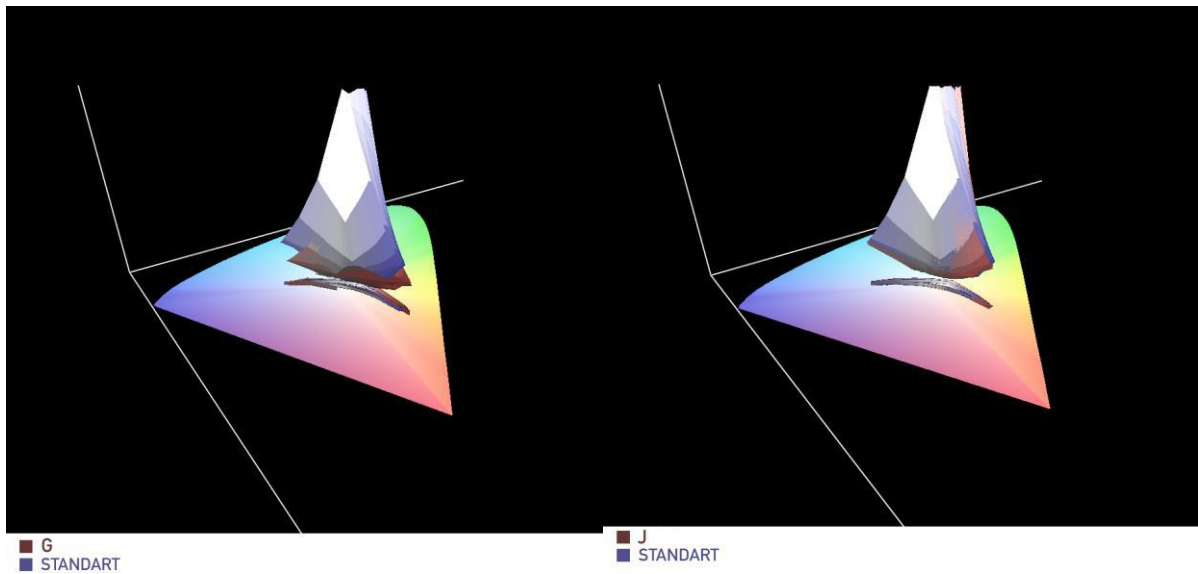


Fig-2. Gamut volume comparison of G and J secrets according to standard

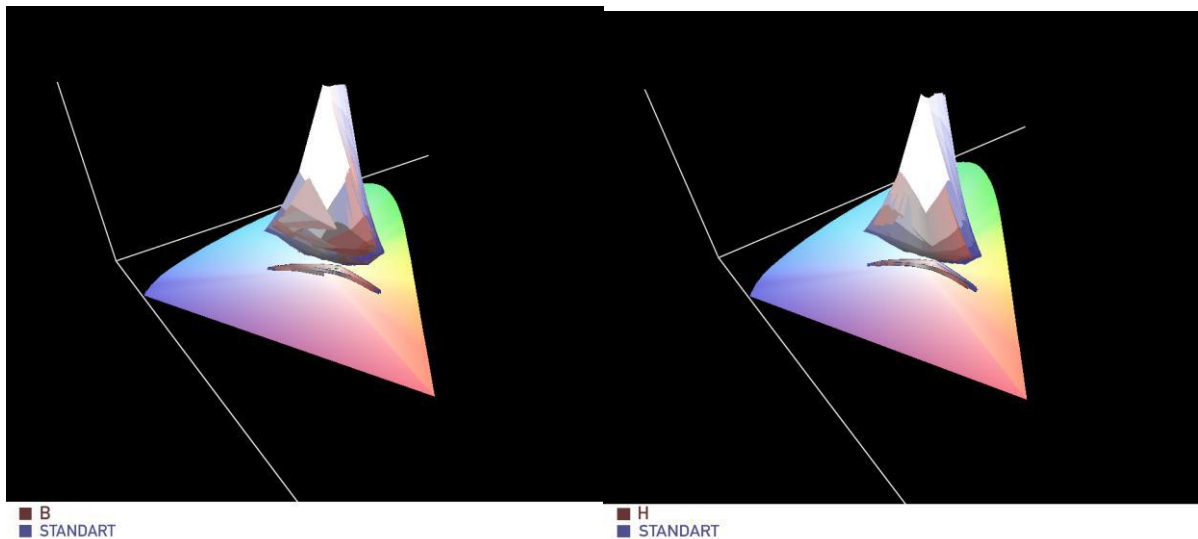


Fig-3. Gamut volume comparison of B and H secrets according to standard

The same image converted with icc profiles which were made with i1 profiler from the recipe G and recipe B (Fig. 4). The image appearance on recipe is deeper, clearer and sharper.

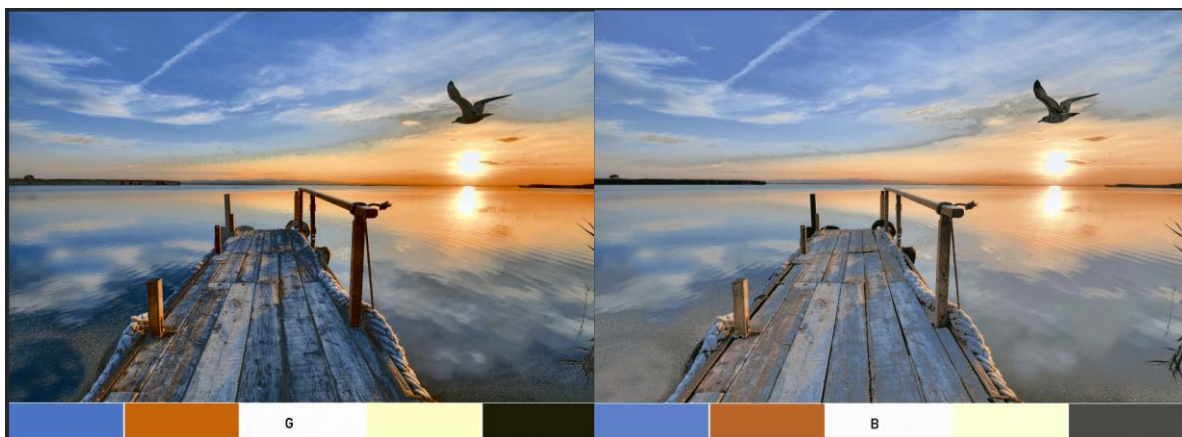


Fig-4. G and B recipe, convert the profile design images

4. CONCLUSSION

It was observed that raw material changes in glaze recipes affected the colour values on the printing surface. In the studies, it was seen that the gamut volume of the standard recipe decreased and increased according to the raw material changes. In general, studies on feldspar group showed that when potassium feldspar was used in recipes of potassium oxide, colour perception was increased. In the recipes where sodium oxide was increased, the amount of sodium oxide in the glaze was increased from albite, and when we supported the system with nepheline instead of potassium feldspar, our colour perception decreased and when we supported with feldspar instead of nepheline, our colour perception increased. When we look the difference between dolomite and wollastonite from calcium oxide sources, it was observed that wollastonite increased its colour perception much more and dolomite decreased the colour perception of the standard recipe. It was observed that the colour volume of the recipe made with zircon oxide was wider. Thanks to the improvements in floor tile mat glaze recipes, it was learned that glazes with better colour perception can be made.

REFERENCES

1. Altay, B.N., Determining of Sunstrate Materials Effects on Colour Gamut Used in Digital Printing System. April 2010, Marmara University.
2. Glaze and Decoration Application Techniques. Sacmi Applied Ceramic Technology, Editrice La Mandragora, Bologna; Italy, 2005, 175-207.
3. Küçükoğlu, E., Characterisation of Nano Pigments Used in Inkjet Inks and Production by Grinding. 2014, Anadolu University Graduate School of Sciences Advanced Technologies Program.

GLASS-CERAMIC COATED STAINLESS STEEL AS SOLID OXIDE FUEL CELL SEALANT

Hasan Tavil, Ahmet Çapoğlu

Gebze Technical University, Department of Materials Science and Engineering, Gebze/Kocaeli, Turkey

ABSTRACT

In this study, glass-ceramic coatings in $\text{BaO-SiO}_2\text{-B}_2\text{O}_3\text{-Al}_2\text{O}_3$ glass system for stainless-steel surfaces were investigated for its suitability to be used as a sealant for solid oxide fuel cell (SOFC) purposes. The sealant is the key parameter in the success of planar SOFC fabrication. Glass-ceramics can be used as a sealant because they can be tailored to have the required physical properties like coefficient of thermal expansion (TEC). In order to determine the applicability of coating; crystallization characteristics, wetting behavior, TEC values, densities, firing shrinkages and microscopic investigation of interface regions between metal and glass-ceramic coatings were studied in detail. Melted glass was poured into cold water in order to obtain the glass in the form of frit and then wet ball milled to produce powders with the appropriate grain size. Slips with various solid contents were prepared by distributing powders in either distilled water or organic solvent media. The prepared slips were applied onto AISI 304 and 430 type stainless-steel surfaces and dried under ambient conditions. Heat treatment was performed by holding the coated substrates at 860°C for 2 hours and cooled down to room temperature with a $3^\circ\text{C}/\text{min}$ rate. By using the XRD method, it was determined that heat treated glass coating was crystallized sufficiently enough to create the glass-ceramic structure. The formed barium disilicate crystals were observed at the interface regions between stainless steel and glass-ceramic coatings by SEM analysis. As a result of good wetting behavior and acceptably low thermal expansion differences between the coating and metal substrate ($\Delta\alpha=1,92\times 10^{-6} \text{ } 1/^\circ\text{C}$) well adhered coatings onto 430 type stainless steel surfaces were achieved.

Keywords: Glass-ceramic, SOFC, Sealant, $\text{BaO-SiO}_2\text{-B}_2\text{O}_3\text{-Al}_2\text{O}_3$ system

1. INTRODUCTION

Glass-ceramics allow combining the properties of the conventional sintered ceramics with the distinctive characteristics of glasses. This is an opportunity to produce a material with extraordinary properties. It is even possible to create a material with behaviours completely different than both glass and ceramic. Basically, a glass-ceramic is formed with precipitating crystal phases in the precursor glass. From there, any glass shaping method could be used to shape the precursor glass then by applying a special heat treatment the glass-ceramic could be produced. Powder glass-ceramic method is also one of the options for forming the body. Glasses obtained in fritted form can be processed to be a powder like a ceramic raw material. This glass powder can be shaped by consolidation methods and after that, it can be produced in glass-ceramic form with the proper heat treatment. The key factor in this method is controlling the rate of crystallization and densification to achieve the desired properties. If the densification completes at very early stages, it can hinder the crystallization. Increased crystallization will result in a material much like having the properties of the main crystal [1,3,4].

In solid oxide fuel cells (SOFC), the sealant is one of the most important component due to its ability to seal the cell which will predict the performance. If a material is used as a sealant with the thermal expansion coefficient (TEC) closer to cell components and showing a good bonding

with components, the SOFC cell's output could be maximized. So, the glass-ceramic is the perfect candidate for such an application due to the possibility of tailoring its properties like TEC, wetting behaviour and softening temperatures. Also, they show a good bonding character between both metal and ceramic surfaces as well as they can be chemically inert for the cell environment [1,2].

E-mail: hasantavil@outlook.com

2. EXPERIMENTAL

2.1 Glass preparation

In this project, for the glass-ceramic coatings production powdered glass method was preferred. The glass batch was prepared by using raw materials of BaCO_3 , SiO_2 , H_3BO_3 , $\text{Al}(\text{OH})_3$ with lab grade purity. The prepared batch to obtain 400g melted glass was placed in an Alumina crucible and melted at 1400°C in an electrically heated furnace. The melt was poured into cold water to obtain frits for easy milling.

Frits were crushed to be able to pass through a sieve with 500-micrometer mesh size. Then, crushed frits were placed in an alumina milling pot with alumina balls and distilled water. Mastersizer 2000 instrument was used to determine particle size distribution of milled powders. Powders having different particle size distributions ranging from $10\mu\text{m}$ to $2\mu\text{m}$ were produced by controlling the milling time. Table 1 shows the average particle sizes of milled powders.

Powder	d(0.5) μm average particle size
GC-K	10,862
GC-I	6,616
GC-II	4,512
GC-II2	2,426

Table 1. Average particle sizes of powders

2.2 Characterization Methods

NETZCH STA 449F3 Differential thermal analysis instrument was used to determine glass transition and crystallization temperatures. DTA analyses were performed by heating the powders up to 1100°C with a rate of 5°C/min.

In order to determine the softening and wetting behavior of glass, the heating microscope was used. The glass powders were pressed into a cylindrically shaped samples and placed on alumina and steel plates, individually. The changes in shapes of samples were monitored up to 1150°C with a heating rate of 10°C/min.

In order to carry out sintering study, some of glass powders were granulated and pressed into pellets form with 13mm diameter. In total 160 pellets, 40 for each of GC-K, GC-I, GC-II, GCII2 group powders were pressed separately. These pellets were heat-treated at 775°C - 800°C - 825°C - 850°C temperatures for 5-10-15-30-60 minutes. For each heat treatment cycle two pellets were used. After heat treatments, the diameters, heights of pellets were measured with the caliper, micrometer and and weights were determined with precision scale then density values were calculated according to equations 1 and 2.

$$V = \pi \cdot (D/2)^2 \cdot h \quad (1)$$

$$d = m/V \quad (2)$$

D: diameter, h: height, V: volume, d: density, m: weight

To obtain the crystallization degree, one of the pellets from each treatment were ground and analyzed by XRD with CuK α radiation. Figure 1 shows the images of the heat-treated pellets from GC-I

powder.

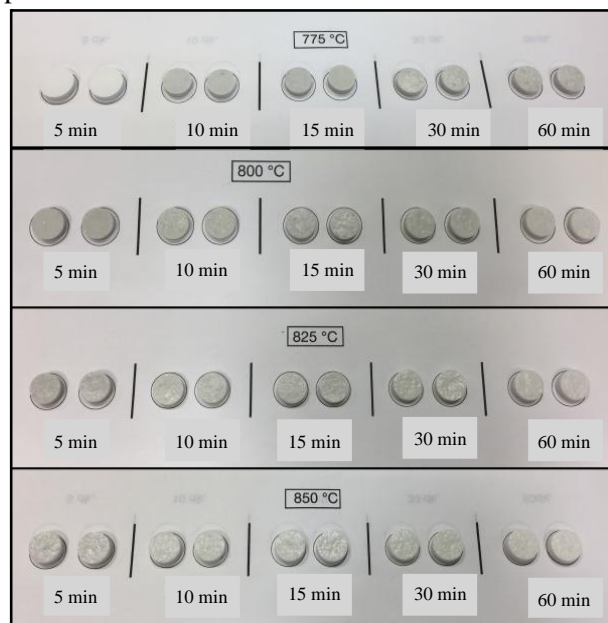


Fig. 1. Image of the crystallized pellets

Cylindrical rod-shaped thermal expansion specimens (5.5 x 25.5 mm) were formed by pressing 8 grams of GC-K and GC-I powders and heat treated at 850°C for 1 hour. NETZSCH DIL 420EP dilatometer instrument was used to determine to TEC values of glass-ceramic bodies.

2.3 Coating

AISI 304 and 430 stainless steel plates were selected to use in experiments. Steel substrates were prepared by cutting metal plates into square shape (2 x 2 mm) and ultrasonically cleaned in ethyl alcohol. TEC values of the plates were determined with the dilatometer.

In coating application, slip method was used. This method consists of slip preparation, application on a surface, drying and heat treatment stages. Various slips with distilled water and organic solvent media were prepared to optimize the coating quality. Electrolyte and glycerine additives were used to improve the viscosity of slips. Combinations of ingredients were studied with each powder as well as mixtures of the powders. Coated sample's drying behaviors were observed under ambient and controlled atmosphere conditions.

Samples which were placed on alumina boats heat-treated in a tubular heat treatment furnace. Table 2 shows the applied heat treatment schedules for coatings.

Heat treatment	
1	850 °C - 60 min
2	850 °C - 30 min
3	900 °C -120min + 860°C - 60min + 850 °C - 60min
4	1120 °C - 60min + 860 °C - 60min
5	1125 °C - 15min + 860 °C - 90min
6	1075 °C - 30min + 850 °C - 90min
7	860 °C - 300min
8	860 °C - 120min

Table 2. Heat treatment schedules

2.4 Coating Investigation

Successfully coated specimens were investigated to observe crystallization in coatings on the steel surface with XRD method. Samples were cut into half to investigate to interface regions in scanning electron microscope (SEM). They were placed in epoxy resin and hardener mixture and surfaces of specimens were prepared with a grinding method. After polishing specimens were chemically etched for 70 seconds

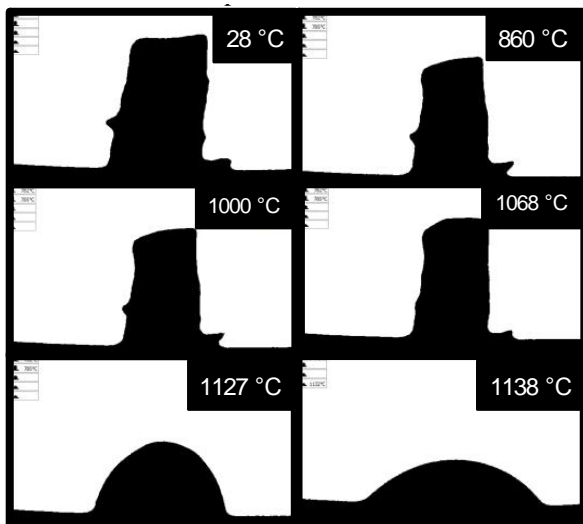


Fig. 2. Wetting Observations

with hydrofluoric acid and cleaned with water and alcohol. After that SEM images were obtained.

3. Results and Discussion

DTA analysis shows that the glass transition T_g and crystallization temperatures (T_c) of the glasses. They were determined as 650°C for T_g and 750°C for T_c . Two more crystallization peaks were also observed at 808°C and 875°C temperatures.

Figure 2 shows the wetting behavior of glass on the steel surface. Bulk shrinkages observed by

increasing temperature up to 860°C and after that specimen expanded up to 1068°C. At higher temperatures, it couldn't maintain its shape. It shows a good wetting both on steel and alumina surfaces with a wetting angle lower than 45°.

It can be seen from Fig. 3 that powder particle size affects the consolidation behaviour of the bodies. The coarsely milled powder coded as GC-K showed higher densification degree with increasing temperature than the smaller particle sized powders. Similar results in density values against particle size were obtained by either increasing temperature or time. Particle size must be optimized to produce a dense body without hindering the crystallization.

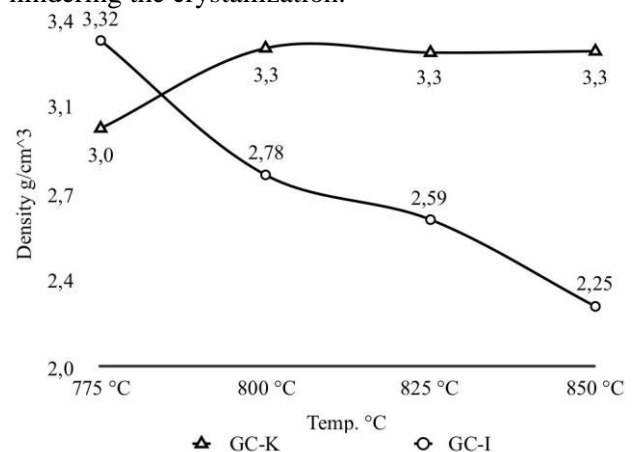


Fig. 3. Densities of the pellets

Fig. 4 shows the XRD patterns obtained from pellets that were heat treated on various temperatures for 1 hour. Increase in the heat treatment temperature results in a higher degree of crystallization in samples. Also, the time has the similar impact on crystallization degree. Crystallization rate increases with both time and temperature. XRD investigations with the different particle sized powders showed that smaller particle size increases the degree of crystallization. Finely powdered samples can be crystallized shorter times than the coarse particle sized ones on same temperatures. Main crystal was encountered in samples was BaSi_2O_5 . In addition, small amounts of BaO and $\text{Ba}_3\text{Si}_5\text{O}_{13}$ crystals were also detected.

TEC investigations of the two glass-ceramic rods showed similar values ranging from $11.42 \times 10^{-6} \text{ 1/}^\circ\text{C}$ to $11.59 \times 10^{-6} \text{ 1/}^\circ\text{C}$. TEC curves of the 304, 430 steel and the glass-ceramic were shown in Fig. 5. In order to achieve good bonding between materials, their TEC values have to be same or similar. It's shown that TEC difference between glass-ceramic and AISI 304 steel is tremendous. This has a catastrophic impact on heat treatment stage and restricts to obtain

successful coating. With AISI 430 steel, the difference in TEC values was comparable so, coatings were successfully bonded to surfaces. TEC difference of $1,92 \times 10^{-6} \text{ } 1/^{\circ}\text{C}$ is in the acceptable region for the application.

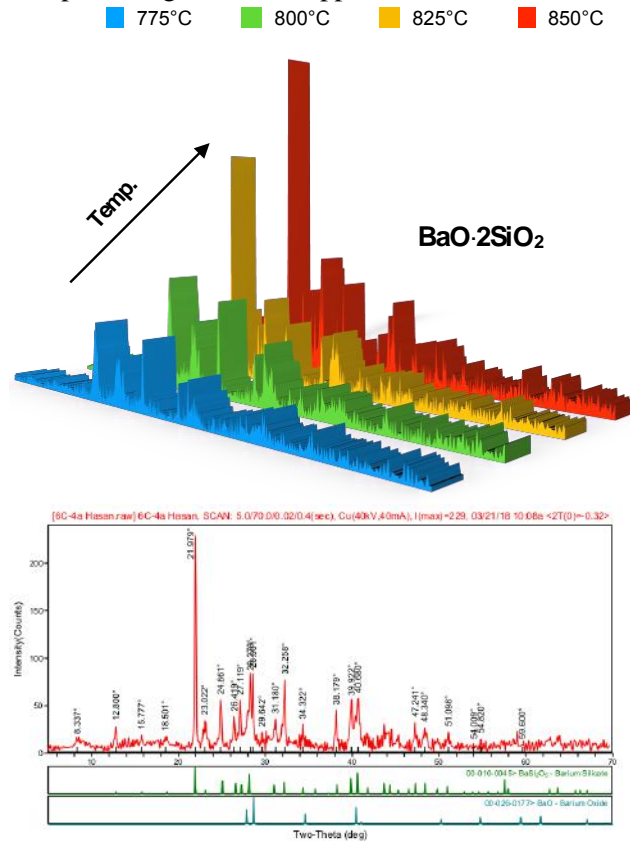


Fig. 4. XRD investigation of the pellets

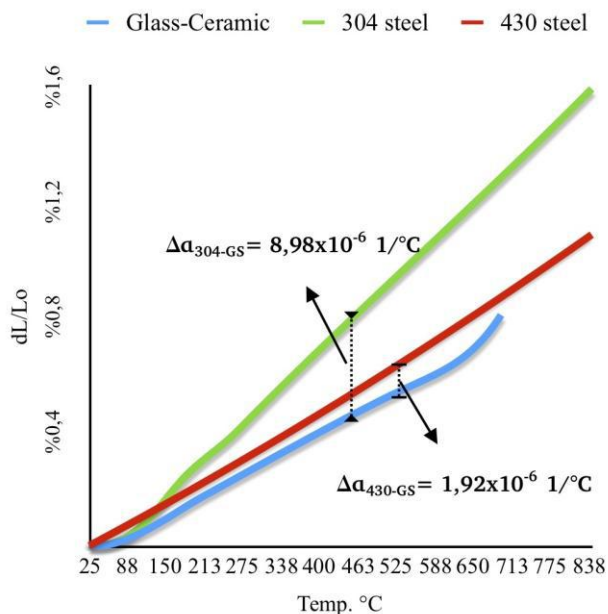


Fig. 5. TEC values of steels and glass-ceramic

An extensive study on slip preparation and drying properties showed that fine particle size inhibits the coating to be applied on a surface. Particle sizes lower than 10 microns produces drying cracks. In order to obtain the coatings with GC-I, GC-II and GC-II2 powders, various studies were conducted. Altering the type of media which was varied from water to organic solvents didn't solve the cracking problem. Electrolyte and glycerine additions also did not fix the problem. Controlling the drying environment's humidity and temperature couldn't make much differences. It can be concluded that slurries made by using GC-K powder with organic solvents under ambient drying condition is the best and easiest choice.

By combining all the data, the powders with GC-K code was selected to be used in coating applications on steel surfaces. Powders with specific particle size distributions was chosen in order to obtain a balanced crystallization and consolidation behaviour. These two processes compete with each other throughout the heat treatment.

Fig. 8. Image of the C-4 Sampled coating

Coated samples were heat treated with the treatment schedules shown in Table 2.

Sample	Steel	Powder	H. Treatment
C-2	430	GC-K	8
C-3	430	GC-K	5
C-4	430	GC-I	5

Table 3. Heat treatment schedules for coatings

Table 3 shows the coated samples and their heat treatment details. In Fig. 6 it can be seen that coating coded as C-2 successfully coated on steel surfaces and it's rather a dense and well-adhered layer of coating.



Fig. 6. Image of the C-2 coded coating

Fig. 7 shows the image belongs to coating coded as C-3 and the coating stays on the steel surface however it is rather a porous layer. Higher temperature treatments caused this porous structure but this layer also showed some degree of crystallization. Modifications in heat treatment processes allowed to observe this distinct behaviour.

The image seen in Fig. 8 belongs the coating in

Fig. 9. SEM images of the coating

C-4 groups of coatings. The coating layer cracked during drying and it was observed that those drying cracks were not healed during heat treatment. As a result, cracked parts were shrunken towards its centers but it's well bonded to surface of steel and well crystallized. High temperature heat treatments caused the glass powders to viscous flow and it acted like a self-healing mechanism for coating layer.

All of the coatings were tested with XRD to observe their crystallization behavior. All of them crystallized and they consist of mainly BaSi_2O_5 crystals. Increase in heat treatment time as compared to pellets, allowed sufficient time to achieve a body with full of Barium Silicate crystals. The coating coded as C-4 has the highest rate of crystallization but it's fine particle size distributions resulted with drying crack problems. C-2 and C-3 coded coatings were well also adhered to surfaces and crystallized successfully.

C-2, C-3 and C-4 coatings were used to analyze their interface regions. In order to do that the SEM and EDS investigations were conducted. Fig. 9 shows cross section SEM images of the coatings. There are two different morphologies present at the glass-ceramic regions and they stuck together. On the surface region (2), it can be seen that there is a porous morphology which can be as a result of the atmospheric interaction. At the bottom of the surface (3), crystals were grown like



a

Fig. 7. Image of the C-3 Sampled coating



colony and created a network structure. Crystals were grown from many centers and showed a bulk crystallization behavior. This is done without the use of any nucleating agents. There are glassy phases around the crystals and they have some microcracks. It could be the impact of the acid in the etching process causing cracks due to TEC difference between glass and glass-ceramic.

In the 4th image, barium silicate crystals is shown. It has a succulent like structure which is cuboids grown from the common centers.

Interface region has a glassy form and crystallization were hindered there, it can be seen in Fig. 10 which is also bearing a TEC difference problem between the glass-ceramic and the interface. Due to steel's and glass-ceramic's close average TEC values, coatings still successfully bonded to surfaces. EDS analysis showed that there is an iron atom diffusion through the glass-ceramic body. Fe atoms diffusion might be the reason for the hindered crystallization at the interface region. EDS analysis shows that Barium atoms were present throughout the glass-ceramic body. Crystals were detected at the intersection of Barium and Silicone atoms.

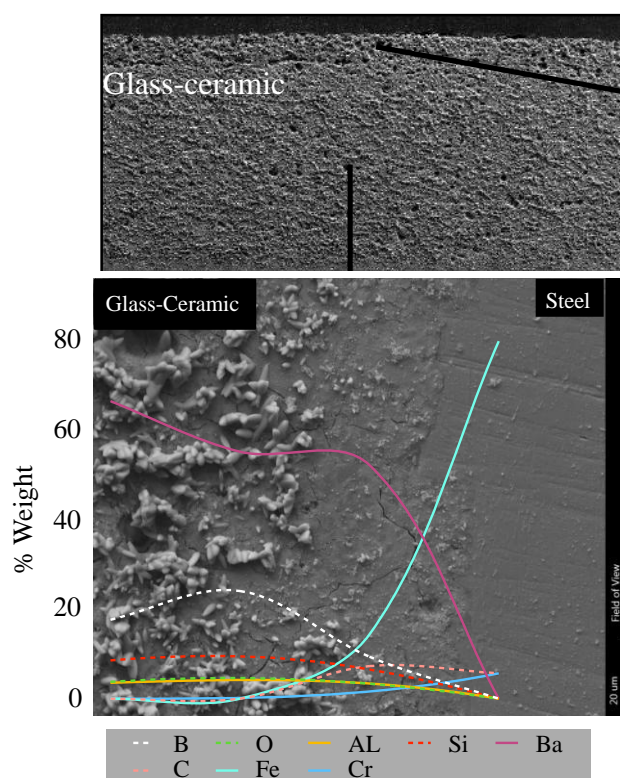


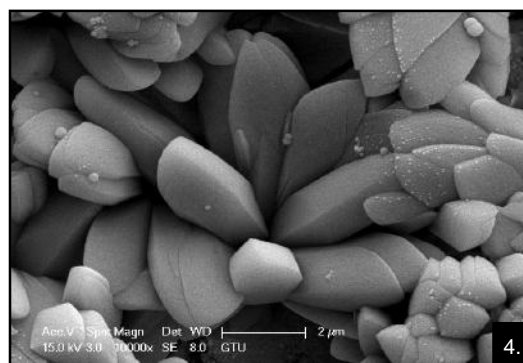
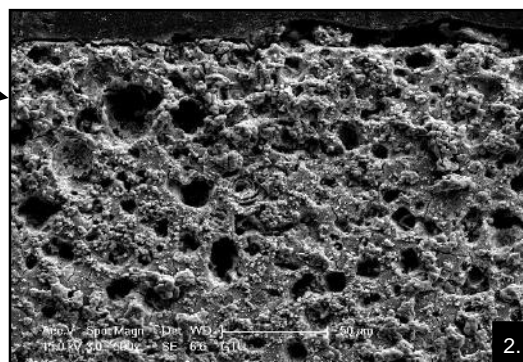
Fig. 10. SEM-EDS analysis of the coating

4. Conclusion

A glass-ceramic based on $\text{BaO-SiO}_2\text{-B}_2\text{O}_3\text{-Al}_2\text{O}_3$ glass system were investigated for properties and possible applications. The glass-ceramic were successfully crystallized without the use of any nucleating agent. The glass was showing a good wetting behavior and close TEC value with the AISI 430 steel. It's also be noted that the particle size of the precursor glass has a major impact on the final glass-ceramic body's characteristics. With all of the data present, it can be concluded that the coating is an appropriate candidate for SOFC sealant applications. During the study also the porous body formation was discovered which wasn't be able to encounter in literature but it might be an advantage for a diversified applications.

References

- 1) Wolfram Höland, George H. Beall, "Glass-Ceramic Technology" 2nd edition, Pages 1-72, Wiley.
- 2) Sea-Fue Wang, Yuh-Ruey Wang, Yung-Fu Hsu, Ching-Chin Chuang, "Effect of additives on the thermal properties and sealing characteristic of $\text{BaO-Al}_2\text{O}_3\text{-B}_2\text{O}_3\text{-SiO}_2$ glass-ceramic for solid oxide fuel cell application", International Journal of



Hydrogen Energy, Volume 34, Issue 19, 2009, Pages 8235-8244.

- 3) Höland, Wolfram & Rheinberger, Volker & Schweiger, Marcel. (2003). "Control of Nucleation in Glass Ceramics", Philosophical Transactions of The Royal Society A: Mathematical, Physical and Engineering Sciences. 361. 575-589.
- 4) G. H. Beall, "Design and properties of glass-ceramics", Annual Review of Materials Science 1992 22:1, 91-119 .

ENGOGLAZE DEVELOPMENT FOR THE PRODUCTION OF GLAZED PORCELAIN TILES

Sule Kanca Eryilmaz, Sezgi Isik , Yasin Ufersoy

Gizem Ustunel, Ilkyaz Yalcin

NG Kutahya Ceramic Research and Development Center, Kutahya/Turkey

ABSTRACT

Improvement of the digital tile application, lots of process revolutions have occurred in the tile production. In order to create unique and inimitable designs, all the competitors start to try different applications. Both European and domestic ceramic producers focus on the deep and realistic surfaces. In this study, trend of engoglaze, which is becoming wide spread in glaze porcelain tile designs to create the more intensive colours, were investigated. The aim of the study is to develop engoglaze formulation that support to digital ink activation. Thermal expansion coefficient values of engoglazes were determined by a dilatometer. Chemical analyses of engoglazes were made by XRF. Sintering behaviours of engoglazes were tested by heat microscopy. According to these glaze formulation studies, it has been reported that using engoglaze could easily reduce to the digital ink consumption of the design. On the other hand, both advantage of the production cost is gained and deepness of the design is provided.

Keywords: Engoglaze, Digital ink, Digital ink activation, Glazed porcelain tile

INTRODUCTION

Ceramic tiles industry has undergone significant changes in recent years to meet the latest market demands [1–3]. This trend has highlighted the need to control the entire production process to ensure an effective reproducibility of the final material in addition to maintaining high standards of quality. It is known that the production of ceramic tiles is a complex process influenced by many variables ranging from those directly related to the technology to those linked to the environmental conditions during production [4,5]. These variables directly affect the final product in terms of color, dimension and presence of defects on the surface [6].

One of the more recent innovations in the production of ceramic tiles regards the decorating technique, and in particular the introduction of inkjet printing technology that enables high quality printing on ceramic support and a wide range of aesthetics properties [7]. Its advantages compared to the conventional methods [8] are mainly related to the fact that it is a digital process and a non-contact method therefore fragile substrates and non-flat substrates, which are difficult to be treated in the conventional printing methods, can be processed and a wide range of materials can be deposited on the substrate (pigments, dyes, glass frits and metallic particles).

Moreover the digital image definition and the flexibility of the process allow a more realistic representation of natural materials that is one of the main interesting effects in the tiles market.

Despite the advantages of this printing technique, its performance in ceramic production strongly depends on how well the printer is integrated in the production line. Different process variables can directly affect the final properties in terms of presence of defects, accuracy and reliability of color intensities over the whole decorated surface. The knowledge of the correlations existing between

process variables and final aesthetic properties allows to control and therefore to improve both efficiency and quality of the manufacturing process. This skill represents an extremely powerful tool to design and optimize tiles with specific features countering the market demands [9].

Catching to the deeper and realistic ceramic surfaces, to make designs with high ink usage could cause line effect, longer drying time and some surface defects (hole, bubble..). In this study, developing to engoglaze formulation provides to reduce ink consumption with gaining to digital ink activation.

EXPERIMENTAL

In experimental studies, melting behaviors of the engobes and engoglaze were measuremented by Misura ODHT HSM 1600-80 heat microscope at SAM laboratories. Heat microscope analyses cycle of a temperature is 10 °C/min.

Sample	Sintering Temperature (° C)	Softing Temperature (° C)	Sphere Temperature (° C)	½ Sphere Temperature (° C)	Melting Temperature (° C)
Engobe-1	1144	1292	-	-	1392
Engobe-2	1158	1298	1374	1422	1466
Engoglaze	1148	1358	-	-	1438

Table 1: Results of the engobes and engoglaze samples Misura ODHT HSM 1600-80 heat microscope.

Chemical analyses were measurement by XRF instrument Rigaku ZSX Primus at SAM laboratories.

	A.Z	Na ₂ O	MgO	Al ₂ O ₃	SiO ₂	ZnO	K ₂ O	CaO	TiO ₂	Fe ₂ O ₃	ZrO ₂	BaO	Hf
Engobe-1	1,85	3,24	0,51	14,95	60,89	0,38	2,91	2,04	0,63	0,22	11,08	0,4	0,2
Engobe-2	1,9	3,56	0,33	14,17	61,58	0,37	3,23	2,29	0,65	0,24	11,09	0,35	0,2
Engoglaze	3,61	2,11	1,19	15,57	62,72		2,03	2,06	0,31	0,54	8,8	0	0,19

Table 2: Rigaku ZSX Primus XRF instrument

In the coefficient of expansion measurements were made with the Netzch DIL 402 PC dilatometer at NG Kutahya Ceramic R&D Center laboratory, Generally, expansion coefficient of engobes is 65-70 exp 10⁻⁷/C at 400 °C. Engoglaze that was developed at NG Kutahya Ceramic laboratories coefficient of expansion was measurement 66,94 exp 10⁻⁷/C at 400 °C.

Standard application steps for glaze porcelain tile is given at Figure 1.

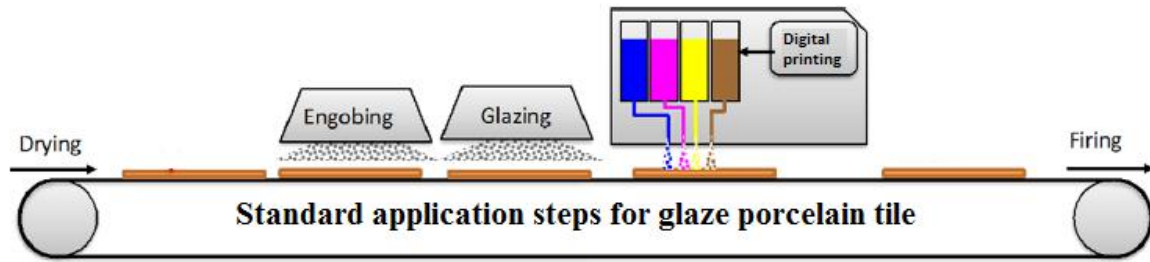


Figure 1. Standard application steps for glaze porcelain tile

The glaze application steps have been changed with the developed engoglaze. In this way, digital printing is applied between the engoglaze and top glaze at Figure 2.

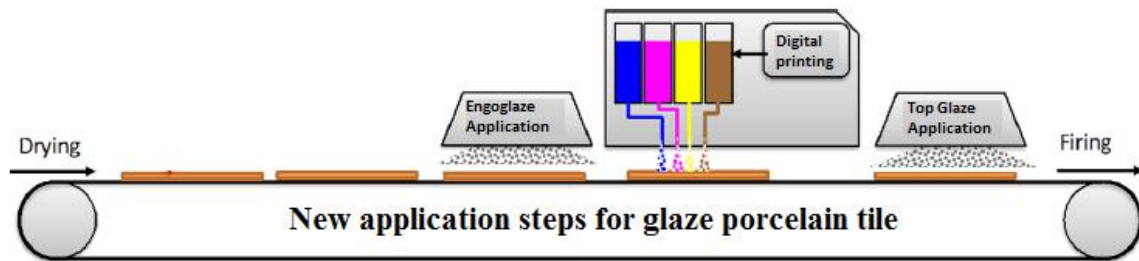


Figure 2. New application steps for glaze porcelain tile

After the production tests the digital effects and results were discussed. For the dark design; standard product digital ink consumption is also between 9-10 gr/m². For the light design; standard product digital ink consumption is also between 2-3 gr/m². They're given picture with standard application at Figure 3 and Figure 5, next picture with new application at Figure 4 and Figure 6.

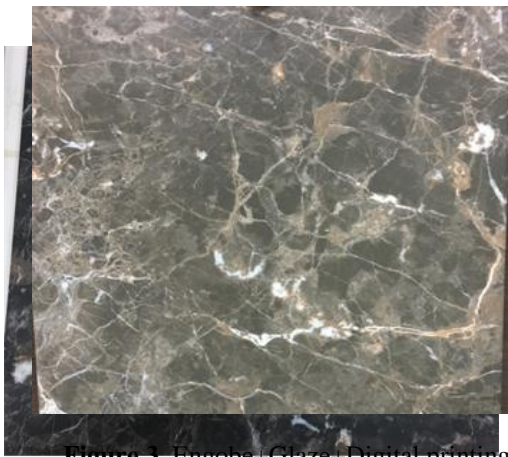


Figure 3. Engobe + Glaze + Digital printing with dark colored image

Figure 4. Engoglaze + Digital printing + Top Glaze with dark colored image



Figure 5. Engobe+Glaze+Digital printing with light colored image

Figure 6. Engoglaze +Digital printing + Top Glaze with light colored image

The CIE Color Systems use three coordinates (L^* , a^* and b^*) to place a color in a tridimensional space. Specifically, while L^* defines the lightness, a^* denotes the red/green value (negative values indicate green while positive values indicate red) and b^* the yellow/blue one (negative values indicate blue and positive values indicate yellow). Variations of these three parameters ΔL^* , Δa^* , Δb^* can be used to compare two colors: the total difference (distances in the CIELAB space diagram) can be stated as a single value, known as ΔE^* (Equilibrium 1) [10]. Graphic of LAB coordinates is given Figure 7.

$$\Delta E_{ab} = [(\Delta L^2) + (\Delta a^2) + (\Delta b^2)]^{1/2}$$

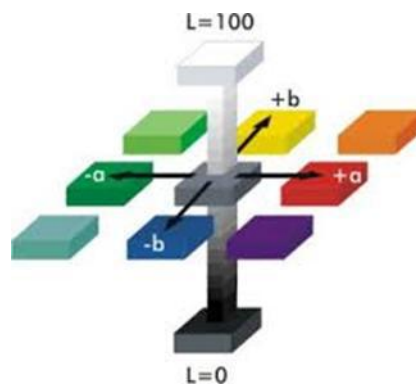


Figure 7. Lab coordinates

Color scales were obtained by both application methods for L a b comparison. Color scales samples were fired two different firing cycles. First cycle is 1190/1190 °C 38 minutes, the second cycle is 1200/1200 °C 54 minutes.

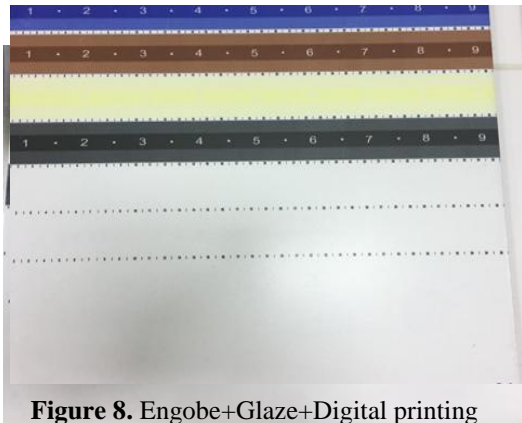


Figure 8. Engobe+Glaze+Digital printing with color scale (1190/1190 38' minutes)

Figure 9. Engoglaze+Digital printing + Top Glaze with color scale (1190/1190 38' minutes)

	Color of ink	L	a	b	Firing temperature and cycle
Engobe+Glaze+Digital Printing Application	Blue	47,18	9,89	-32,76	1190/1190°C 38 minutes
	Brown	50,91	10,84	10,39	
	Yellow	87,88	-7,14	23,59	
	Black	35,97	-0,52	1,2	
	Color of ink	L	a	b	Firing temperature and cycle
Engoglaze+Digital printing+Topglaze Application	Blue	41,24	7,93	-30,99	1190/1190°C 38 minutes
	Brown	39,07	16,72	15,39	
	Yellow	86,3	-8,79	35,47	
	Black	31,51	-0,23	-1,53	

Table 3: L,A,B results of color scale at 1190/1190°C 38 minutes firing cycle.

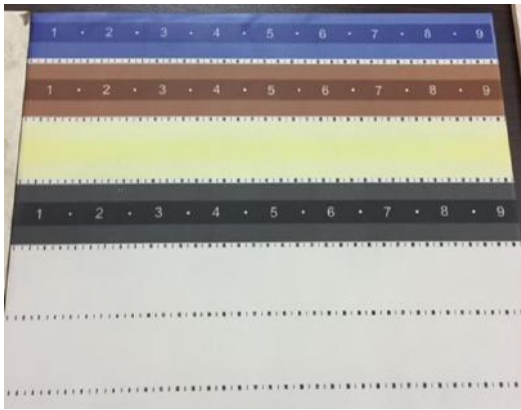


Figure 10. Engobe+Glaze+Digital printing with color scale (1200/1200 °C 54 minutes)

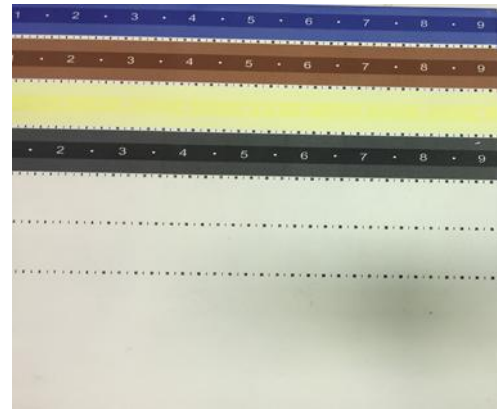


Figure 11. Engoglaze+Digital printing + Top Glaze with color scale (1200/1200 °C 54 minutes)

	Color of ink	L	a	b	Firing temperature and cycle
Engobe+Glaze+Digital Printing Application	Blue	46,83	7,24	-27,28	1200/1200°C 54 '
	Brown	41,51	16,08	15,02	
	Yellow	93,7	-8,56	28,5	
	Black	31,2	-0,5	-1,14	
	Color of ink	L	a	b	Firing temperature and cycle
Engoglaze+Digital printing+Topglaze Application	Blue	49,22	8,12	-28,76	1200/1200°C 54 '
	Brown	51,75	12,57	13,78	
	Yellow	85,45	-7,19	21,4	
	Black	37,02	-1,04	0,97	

Table 4: L,A,B results of color scale at 1200/1200°C 54 minutes firing cycle

CONCLUSION

As a result of technical tests, the new application method (engoglaze+digital printing+ topglaze) provides higher color intensity than standard application method (engobe+glaze+digital printing). Namely, this way has different advantages that top glaze protects the digital printing and gives higher deepness to the design. When L.a.b. color scales are compared; both yellow and brown color intensity is higher than the standard application method (Table 5.)

Firing Cyle	1190/1190 °C 38 minutes	1200/1200 °C 54 minutes
Blue	-5%	-5%
Brown	40%	15,60%
Yellow	50%	33%
Black	12%	15%

Table 5. Increasing Rate of Color Intensities

Finally, using this new application method in the production could give possibility to obtain nearly %30 high colour intensity with low digital ink consumption.

REFERENCES

- [1] A.M. Berto, Ceramic tiles: above and beyond traditional applications, *J. Eur. Ceram. Soc.* 27 (2–3) (2007) 1607–1613.
- [2] C. Ferrari, A. Libbra, A. Muscio, C. Siligardi, Design of ceramic tiles with high solar reflectance through the development of a functional engobe, *Ceram. Int.* 39 (8) (2013) 9583–9590.
- [3] E. Sánchez, J. García-Ten, V. Sanz, a Moreno, Porcelain tile: almost 30 years of steady scientific-technological evolution, *Ceram. Int.* 36 (3) (. 2010) 831–845.
- [4] R. Casasola, J.M. Rincón, M. Romero, Glass–ceramic glazes for ceramic tiles: a review, *J. Mater. Sci.* 47 (2) (2011) 553–582.
- [5] Digital decoration of ceramic tiles, Acimac Notebooks, 2009.
- [6] H. Elbehery, A. Hefnawy, M. Elewa, Surface Defects Detection for Ceramic Tiles Using Image Processing and Morphological Techniques, 2005.
- [7] V. Sanz, Y. Reig, C. Feliu, Y. Bautista, C. Ribes, M. Edwards, Technical evolution of ceramic tile printing, *J. Imaging Sci. Technol.* 56 (5) (2012) 1–7.
- [8] O. Watanabe, T. Hibino, M. Sakakibara, Development of an ink-Jet printing, *Qualicer* (2012) 1–10.
- [9] G. Peris-Fajarnés, P. Latorre, B. Defez, I. Tortajada, F. Brusola, Evaluation of color prediction models in the decoration of ceramic tiles, *J. Ceram. Soc. Jpn.* 116 (1349) (2008) 146–152.
- [10] M. Montorsia,n,, C. Mugonia, A.Passalacquab, A.Annovic, F.Maranic, L.Fossac, R.Capitanid, T.Manfredinib Improvement of color quality and reduction of defects in the ink jet-printing technology for ceramic tiles production: A Design of Experiments study. 1461, 2015.

EFFECT OF COMPOSITION ON FLY ASH GEOPOLYMERS

¹Cansu Kurtuluş*, ²M. Serhat Başpınar

¹Afyon Kocatepe University, Engineering Faculty, Materials Science and Engineering Dept., Turkey

²Afyon Kocatepe University, Faculty of Technology, Metallurgy and Materials Science Engineering Dept., Turkey

ABSTARCT

The geopolymer technology provides a new good and green solution to the utilization of fly ash, avoiding its negative impact on environment and ecology. The aluminasilicate minerals in fly ash can be activated with alkali silicate solution to form geopolymer. In this study highly porous fly ash based geopolymer foams (GFs) were fabricated by a gelcasting technique using hydrogen peroxide as a pore former in combination with stearate based surfactant at different compositions. Moreover, factors that the influence amount of porosity and cell size distribution were investigated. We found that porous geopolymers with density values 620kg/m^3 by this method. Interesting results will be reported.

Key words: Geopolymer, Fly Ash, Peroxide, Foam

1.INTRODUCTION

Fly ash is one of the solid residues composed of the fine particles that are driven out of the boiler with flue gases in coal-fired power plants. It is generally captured from flue gases by electrostatic precipitators or other particle filtration equipment before the flue gases reach the chimneys [1]. Depending upon the source of the coal being burned, the components of fly ash vary considerably. In general, the components of fly ash typically include SiO_2 , Al_2O_3 , CaO and Fe_2O_3 , which exists in the form of amorphous and crystalline oxides or various minerals. In addition to Si, Al, Fe, and Ca, usually fly ash also contains many other trace metal elements, such as Ti, V, Cr, Mn, Co, As, Sr, Mo, Pb and Hg. The concentrations of the toxic trace elements in fly ash could be 4-10 times higher than those in coal [2]. Thus, fly ash is considered as a hazardous material, and the improper disposal of fly ash will not only increase the occupation of land but also deteriorate the environment and ecology [3].

Fly ash (FA) is the most used and suitable waste material in geopolymerization due to the huge amount produced worldwide, estimated to be around 780 million tons annually and its great workability [4]. The geopolymer technology provides a new good and green solution to the utilization of fly ash, avoiding its negative impact on environment and ecology. The alumina and silica in fly ash can be activated with alkali to form geopolymer. Moreover, the toxic trace metal elements can be trapped and fixed in the geopolymer structure [5].

Geopolymer is a synthetic material produced from the reaction of aluminosilicates with an alkaline hydroxide or silicate solution, rendering amorphous polymeric structures with interconnected $-\text{Si}-\text{O}-\text{Al}-\text{O}-\text{Si}-$ bonds. The aluminosilicates can be obtained from natural sources such as kaolin and volcanic ash or from industrial wastes such as fly ash and blast furnace slags [6]. Among many products that are based on geopolymer precursors, geopolymer foams appear to be a very promising material since they are formed at temperatures below 100°C and possess properties similar to foamed

glass or foamed ceramics, both of which are produced at highly elevated temperatures, above 900 °C [7].

There are two main constituents of geopolymers, namely the source materials and the alkaline liquids. The source materials for geopolymers based on alumina-silicate should be rich in silicon (Si) and aluminium (Al). These could be natural minerals such as kaolinite, clays, etc. Alternatively, by-product materials such as fly ash, silica fume, slag, rice-husk ash, red mud, etc could be used as source materials. The alkaline liquids are from soluble alkali metals that are usually sodium or potassium based. The most common alkaline liquid used in geopolymerisation is a combination of sodium hydroxide (NaOH) or potassium hydroxide (KOH) and sodium silicate or potassium silicate [8]. Research studies carried out on the development of porous geopolymer were mainly oriented for the development of insulating materials for potential building applications and, some of the foamed agents used included air foaming generator, sodium perborate, hydrogen peroxide, aluminum powder, and biomass materials [9]. Hydrogen peroxide is a well-known blowing agent while the redox reaction of Al in alkaline solution induces porosity by H₂ evolution [10].

Shrinkage of concrete at early age is generally considered as a critical parameter for durability design of concrete structures [11]. Drying shrinkage is a time-dependent deformation due to loss of water by hydrostatic tension from the small capillary pores of the hydrated concrete specimens and may cause severe cracking in concrete that eventually allow the ingress of aggressive agents inside the concrete [12]. Several factors such as aggregate properties, alkaline liquid and water content, binder materials and the curing environment are considered to affect shrinkage behavior of geopolymer concrete [13].

Efflorescence is the formation of white salt deposits on or near the surface of concrete. For geopolymers, as they contain much higher soluble alkali content than conventional cement, efflorescence can be a significant issue when the products are exposed to humid air or in contact with water [14]. Although geopolymer foam concretes are not predominantly intended for structural applications exposed to the weather, efflorescence is still a potential problem. Further investigations to prevent efflorescence, or at least to reduce its rate, are required [15].

The aim of this study was to develop geopolymer by preventing drying shrinkage and also efflorescence in view of potential applications in the field of thermal insulation. The geopolymeric matrices were prepared using different proportions of fly ash and blast furnace slag as the aluminosilicate raw powder and also fiber and perlite as a healing element. To prepare alkali aqueous solutions NaOH and Na₂SiO₃ were preferred.

2. EXPERIMENTAL PROGRAM

2.1. Materials

In the present study, class F fly ash and blast furnace slag were used as binder materials and chemical compositions are listed in Table 1. Sodium silicate solution and 6M NaOH solution was used as an alkali activator. H₂O₂ (50% concentration) was used in experiments as foaming agent. Foam stabilizer (FS) was used in order to obtain foam stabilization. Chopped short polypropylen fiber and expanded perlite were used also.

Table 1. Chemical Composition of Binder Materials (%)

	Fly Ash (FA)	Blast Furnace Slag (BFS)
SiO₂	50,3	35
Al₂O₃	19,1	12
Fe₂O₃	12,4	1
CaO	4,55	40
MgO	4,67	1,5
SO₃	1,8	9,8
K₂O	2,16	0,4
Na₂O	0,786	0,3

2.2. Mixture and Specimen Preparation

The sodium hydroxide flakes were dissolved in water to make a solution. The sodium hydroxide and the sodium silicate solutions were mixed together and then added to dry materials and mixed for about five minutes. After mixing in shear type mixer, samples were casted into the 100x100x100 mm plastic moulds. Samples were cured at 60 °C for 24 hour to obtain faster geopolymerization. Four types of samples were produced based on low and high FA content. Mix design of the samples are given at Table 2. Additive amounts were given as percent weight of total weight of FA+BFS. In this study, BFS is incorporated at %0, %10, %30, %50 level to the total binders and the codes were given B0, B10, B30, B50 respectively. In addition B30 and B50 mixtures were prepared without superplasticizer also. The codes were given BS30 and BS 50. Bulk density of the samples was calculated by simply dividing weight of the samples to volume.

Table 2. Mix design of the samples and measured properties.

Main Components	% wt
FA	50-100
BFS	0-50
Total	100
Additives	Wt % of Main Components
FS	0,75
Sodium silicate sol.	50
6 M NaOH	63
Polypropylene fiber	0,2
Perlite (expanded)	0-2,5
Super plasticizer	5,5
H ₂ O ₂	0,85
Bulk density Kg/m ³	620-710

3. RESULTS AND DISCUSSION

It has been observed from this experimental investigation that fluidity of geopolymer paste increased significantly with the increment of the BFS in the mixes. For that reason, O₂ gas which is produced by decomposition of H₂O₂, escaped from the slurry. The pore amount in the fresh geopolymer paste strongly depends on the fluidity of the mixture. The cells are closed and almost spherical.

Bulk density of the samples depends on type of aluminosilicate raw material. Bulk density increased with the increment of BFS content. Porosity nature is also affected from composition. Increment of BFS distort the homogeneity of pore structure and also main structure. In the samples B30 and BS30 separation started approximately 1-2mm from bottom (Figure 1a) and the samples of B50 and BS50 foams separated into two parts (Figure 1(b)). Bottom parts of them has non-porous and dense structure and the top part is porous. The only difference between mixtures was superplasticizer. However, noticeable difference was not observed other than dense part volume decrease.

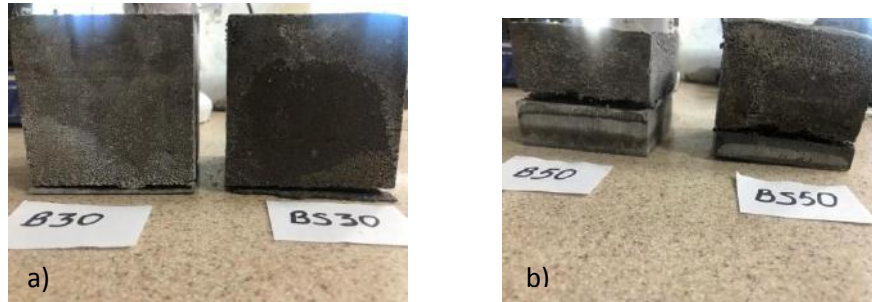


Figure 1. (a) Sample B30 contains %30 BFS and Sample BS30 contains %30 BFS without superplasticizer (b) Sample B50 contains %50 BFS and Sample BS50 contains %50 BFS without superplasticizer

Geopolymerization temperature was also important factor for the production of defect free geopolymer foam samples. Geopolymerization temperature higher than 60 °C increased the risk of drying crack formation and resulted in higher shrinkage. On the other hand lower geopolymerization temperatures decreased the foaming ability of the mixtures and lower geopolymerization rate. It is well known that the foam generation ability of the H_2O_2 increases with increased temperature.

Shrinkage of concrete is a critical parameter for durability of concrete structures. Drying cracks can occur inside geopolymer foam and decrease mechanical properties. By using large aggregate and fiber, drying shrinkage was prevented. BS30 and BS50 samples shrank more as per B30 and B50. In addition that increment of BFS increased drying shrinkage of samples.

Efflorescence is a problem for fly ash geopolymers. Efflorescence potential of samples in different compositions were investigated. Although they contains different amounts of FA and BFS, meaningful results could not achieved. Temperature increase was effective to eliminate efflorescence. It was tried with sample B10. High temperature eliminate the production of white particulates on the samples noticeably (Figure 2).

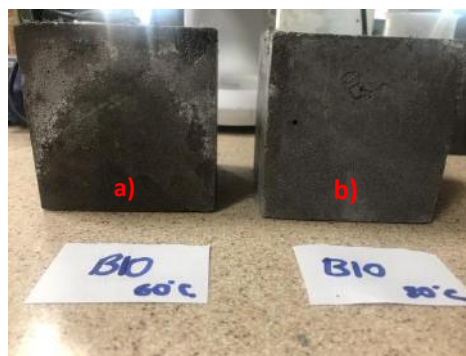


Figure 2. Sample a) was cured at 60°C and sample b was cured at 80°C

All samples were dried at the laboratory conditions. Every day weight of the samples was measured. All samples showed similar drying curve. Calculated density vs. time graphic was drawn (Figure 3).

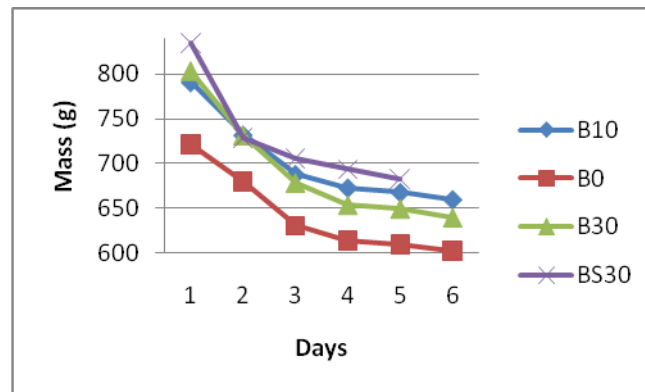


Figure 3. Drying rate of samples

4. CONCLUSION

Based on the above study the following conclusions can be drawn:

- The foam ability was significantly affected by the mix fluidity.
- In the case of high fluidity of the mixture (high BFS) the foam ability is lower. Additionally the increment of BFS causes separation.
- Specimens with lower FA content result in lower strength and higher density.
- Increasing the content of BFS increases fluidity and the fibers uniformly distributed inside the geopolymer paste.
- Efflorescence problem can be overcome with temperature increase.
- All samples showed similar drying curve.
- Addition of higher amount of fly ash resulted in the reduction of drying shrinkage. It can also be observed that addition of higher amount of fly ash reduced mass change as well as drying shrinkage. Any sample not showed drying cracks. This result was achieved by the agency of perlite and fibers inside geopolymer paste.
- The blast furnace slag substitution upto 10% had shown a good fluidity and the samples were in good shape at the end of the process. Higher than %10 of BFS content causes separation.
- Compressive strength was adversely affected by increment of BFS. Max strength was achieved with the sample of B0 and the lowest one with B30 as 1,80MPa and 1,06MPa, respectively

5. REFERENCES

- [1] Ahmaruzzaman M., "A review on the utilization of fly ash," *Prog. Energy Combust. Sci.*, vol. 36, no. 3, pp. 327–363, Jun. 2010.
- [2] Neupane G. and Donahoe R. J., "Leachability of elements in alkaline and acidic coal fly ash samples during batch and column leaching tests," *Fuel*, vol. 104, pp. 758–770, Feb. 2013.
- [3] Zhuang X. Y. *et al.*, "Fly ash-based geopolymer: Clean production, properties and applications," *J. Clean. Prod.*, vol. 125, pp. 253–267, 2016.
- [4] Duan P., Yan C., and Zhou W., "Influence of partial replacement of fly ash by metakaolin on mechanical properties and microstructure of fly ash geopolymer paste exposed to sulfate

- attack,” *Ceram. Int.*, vol. 42, no. 2, pp. 3504–3517, Feb. 2016.
- [5] Li Q. *et al.*, “Immobilization of simulated radionuclide $^{133}\text{Cs}^+$ by fly ash-based geopolymer,” *J. Hazard. Mater.*, vol. 262, pp. 325–331, Nov. 2013.
 - [6] Duxson P., Fernández-Jiménez A., Provis J. L., Lukey G. C., Palomo A., and Van Deventer J. S. J., “Geopolymer technology: The current state of the art,” *J. Mater. Sci.*, vol. 42, no. 9, pp. 2917–2933, 2007.
 - [7] Srinivasan K. and Sivakumar A., “Geopolymer Binders: A Need for Future Concrete Construction,” *ISRN Polym. Sci.*, vol. 2013, pp. 1–8, 2013.
 - [8] June J. *et al.*, “Geopolymer Concrete with Fly Ash,” *Second Int. Conf. Sustain. Constr. Mater. Technol.*, vol. 7, no. 6, pp. 1493–1504, 2010.
 - [9] Novais R. M., Buruberri L. H., Ascensão G., Seabra M. P., and Labrincha J. A., “Porous biomass fly ash-based geopolymers with tailored thermal conductivity,” *J. Clean. Prod.*, vol. 119, pp. 99–107, 2016.
 - [10] E. Landi *et al.*, “Alkali-bonded ceramics with hierarchical tailored porosity,” *Appl. Clay Sci.*, vol. 73, no. 1, pp. 56–64, 2013.
 - [11] Bakharev T., Sanjayan J. G., and Cheng Y.-B., “Alkali activation of Australian slag cements,” *Cem. Concr. Res.*, vol. 29, no. 1, pp. 113–120, Jan. 1999.
 - [12] Deb P. S., Nath P., and Sarker P. K., “Drying shrinkage of slag blended fly ash geopolymer concrete cured at room temperature,” *Procedia Eng.*, vol. 125, pp. 594–600, 2015.
 - [13] Kong D. L. Y. and Sanjayan J. G., “Effect of elevated temperatures on geopolymer paste, mortar and concrete,” *Cem. Concr. Res.*, vol. 40, no. 2, pp. 334–339, Feb. 2010.
 - [14] Škvára F., Kopecký L., Myšková L., Šmilauer V., Alberovská L., and Vinšová L., “ALUMINOSILICATE POLYMERS-INFLUENCE OF ELEVATED TEMPERATURES, EFFLORESCENCE,” 2009.
 - [15] Zhang Z., Provis L., Reid A., and Wang H., “Geopolymer foam concrete: An emerging material for sustainable construction,” *Constr. Build. Mater.*, vol. 56, pp. 113–127, 2014.

EVALUATION OF PHOSPHORESCENT PIGMENTS PREPARED BY SOL–GEL METHOD ON EARTHENWARE SURFACES

Bekir Karasu¹, Muhammed Said Özer², Münevver Çakı³

¹Eskişehir Technical University, Materials Science and Engineering Department, Eskişehir/TÜRKİYE

²Osmangazi University, Eskişehir Vocational School, Eskişehir/TÜRKİYE

³Anadolu University, Faculty of Fine Arts, Eskişehir/TÜRKİYE

ABSTRACT

Glazed and unglazed earthenware artefacts were used for phosphorescent pigment applications. Pigments are based on $\text{SrAl}_2\text{O}_4\text{:Eu}^{2+}$, Dy^{3+} system produced by sol–gel method. A low–temperature frit suitable for such an application was employed. After grinding it down to desired particle size pigments were added to frit and applied on pre–fired earthenware surfaces. All the samples were decor–fired at 800 °C. Emission intensity and time–drive emission capacity of pigment was compared with the glazed surfaces.

1. INTRODUCTION

Long afterglow phosphorescence is becoming more and more popular research subject since last decades [1–3]. Especially rare earth doped $\text{SrO–Al}_2\text{O}_3$ type pigments come forward among the long afterglow photoluminescents [4–6]. These materials are known to be used in several technologies such as LEDs, energy systems and decorative applications like those on glass and glassy surfaces [7–11]. However, there are very limited study found in the literature about the application of phosphorescent pigments onto glazed bodies.

Earthenware is a common material for artistic and decorative applications. The raw materials of these products are typically a clay or combination of clay mixtures which gives the conventional red colour [12]. To form a strong solid body, the mud should be fired at a certain temperature and for required duration according to composition and type of clay [13]. The earthenware also called as terra–cotta can be sintered as both glazed and non-glazed products at moderately low temperatures. The final product can be defined as a soft and porous (not dense) ceramic. Iron–oxide ingredient gives the alluring red colour and also provides a good sintering at lower temperatures [14–15].

Sol–gel method has several advantages against conventional solid–state sintering like better cohesion, uniform mixing of components, obtaining certain crystal structures at lower temperatures etc. [16–17]. For the case of photo luminescent pigments, sol–gel driven powders exhibit very tiny particle size and higher luminescence [4, 18–21]. Previously, solid–state sintering driven pigments were applied onto red mud surfaces [12]. In this work, glazed and unglazed earthenware bodies were used for decorative phosphorescent applications. This is a preliminary report of an ongoing study which aims increasing phosphorescence efficiency and performance of sol–gel driven pigments in ceramic glazes. Later on, further findings will be published.

2. EXPERIMENTAL

Earthenware artefacts are prepared by mould pressing and bisque–firing at 900 °C in an electric furnace. Chemical analyses of the mud are given in Table 1. Bisque–fired plates are glazed with transparent glaze which is then fired at 1000 °C. Glaze recipe is given in Table 2.

Table 1. Chemical analyses of red mud (weight %)

SiO ₂	Al ₂ O ₃	Fe ₂ O ₃	CaO	MgO	Na ₂ O	K ₂ O	TiO ₂	*I.L.
58.27	18.09	7.98	1.88	2.10	1.17	2.50	1.29	6.72

*I.L.: Ignition loss

Table 2. Recipe of transparent glaze applied onto earthenware (weight %)

Na-Feldspar	K-Feldspar	Ulexite	Red Lead	Quartz	Clay
15	15	40	10	10	10

SrAl₂O₄:Eu²⁺, Dy³⁺ phosphorescent pigment powder was produced with sol-gel method. Raw materials were composed of nitrate salts of main crystal formers, rare-earth dopants and boric acid as fluxing agent. First, dopants Eu₂O₃ and Dy₂O₃ are dissolved in dilute nitric acid with a little amount of ammonia addition. In second step, Sr(NO₃)₂, Al(NO₃)₃.9H₂O and H₃BO₃ were added and stirred at room temperature until a clear solution is obtained. Citric acid and PEG (poly-ethylene glycol) were incorporated for polymerization and gel formation. After gelation occurred the xerogel was not dried at low temperature but heated to 300 °C instead in order to burn out most of the organic binders (first step of binder removal). A highly voluminous black cake was obtained. Second binder removal step was carried out at 1000 °C which resulted a shrinkage in volume and whiten the porous cake. In order to activate dopants to excited state the white cake was sintered at 1350 °C in a mildly reducing atmosphere of H₂-N₂ mixture. Final product was gently ground in an agate mortar and sieved to 75 micrometres. For the application of phosphorescent pigments, a secondary fritted glaze recipe was prepared and applied onto earthenware surfaces by screen printing method and fired at 800 °C.

3. RESULTS AND DISCUSSION

The XRD graph of phosphorescent pigment shows the main crystal phase after sintering is SrAl₂O₄ with europium dopant and a minor phase also exists as (SrO)₄.(Al₂O₃)₇ again with europium dopant (Figure 1).

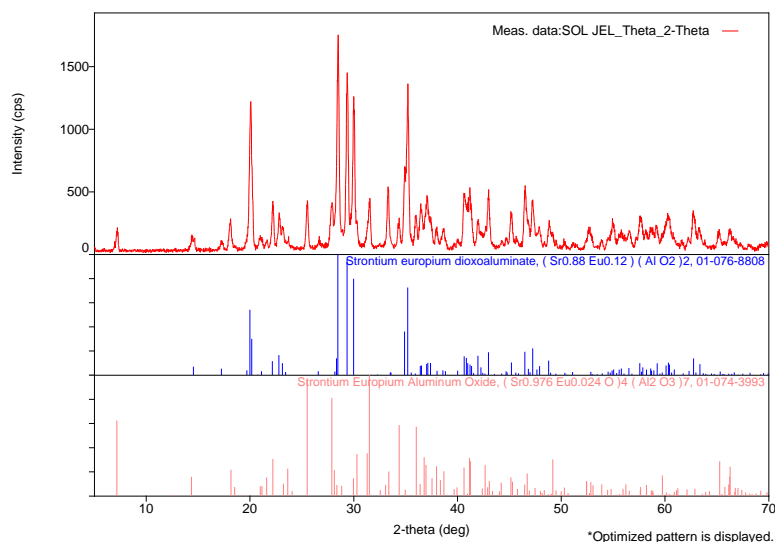


Figure 1. XRD patterns of phosphorescent pigment powder after sintering at 1350 °C.

Decorative pigment application onto glazed surface was successfully achieved after decor-firing at 800 °C. In Figure 2, earthenware plate was shown both in (a) daylight and (b) in the dark.

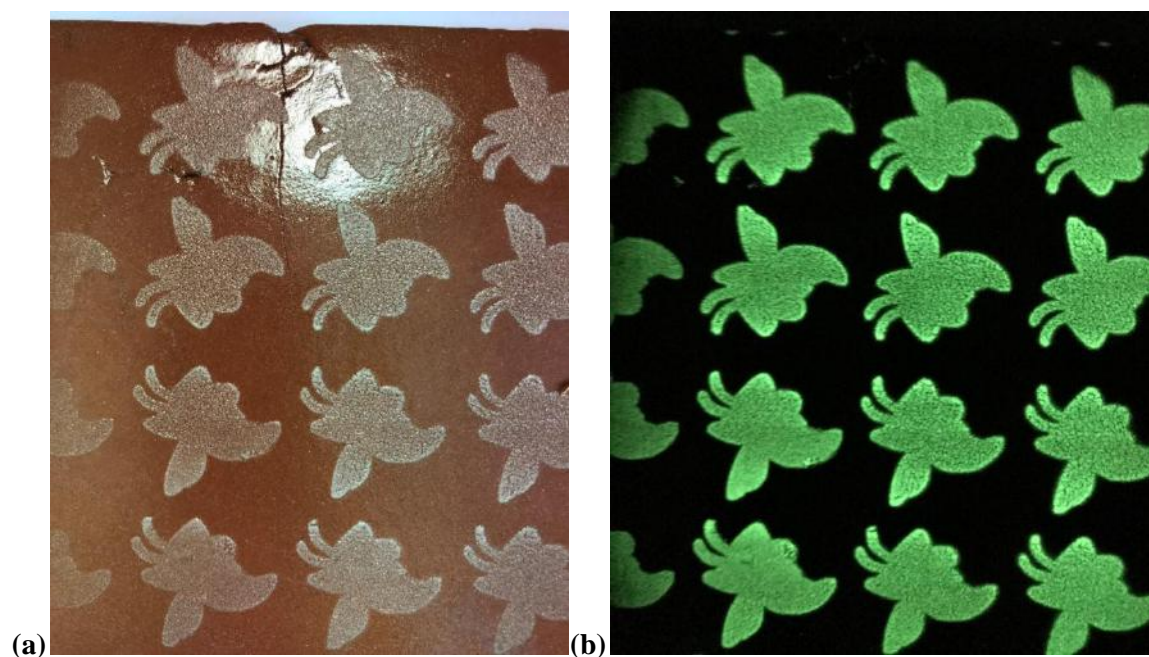


Figure 2. Decorative glazed earthenware plate, daylight view (a) and appearance in the dark (b).

In order to identify the performance of phosphorescent pigment in glazed surface, luminescence emissions of neat pigment powder and glazed surface were measured. Pigment powders were sieved with 75 microns for measurement. A small piece of earthenware plate appropriate to device holder was cut with diamond disc. Emission intensity and long-term emissions were measured by Perkin Elmer LS55. Figure 3 compares the emission intensities of pigment in powder form and decorative glaze.

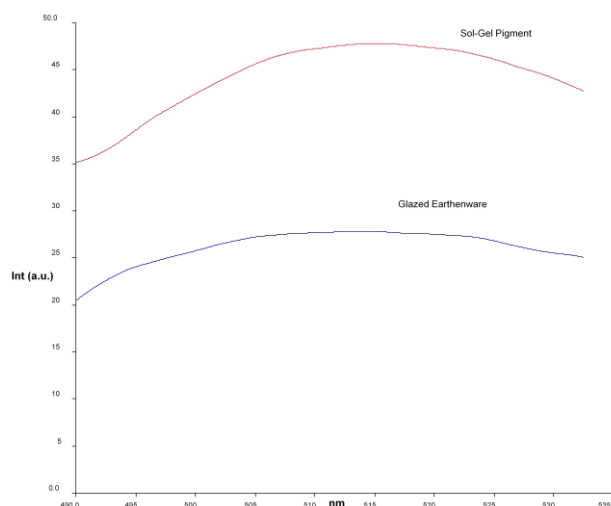


Figure 3. Comparison of emission intensities of pigment and decorative glaze.

Emission intensity of phosphorescent glaze is lower than that of pigment itself as expected since the additional heat treatment at 800 °C and the glaze environment damage the photoluminescence mechanism of dopants and also crystal structure of pigments [7, 11, 22–24]. However, peak intensity of glaze is at almost 515 nm which is very similar to pigments emission wavelength. This is a good indication for SrAl_2O_4 structure not transforming into a different crystal but probably getting smaller in size in the liquid glaze. Long-term photoluminescence emissions of pigment and glaze were measured for 5 minutes' duration. Figure 4 indicates that the emission performance of decorative glaze is however more than two times lower than that of pigment powder.

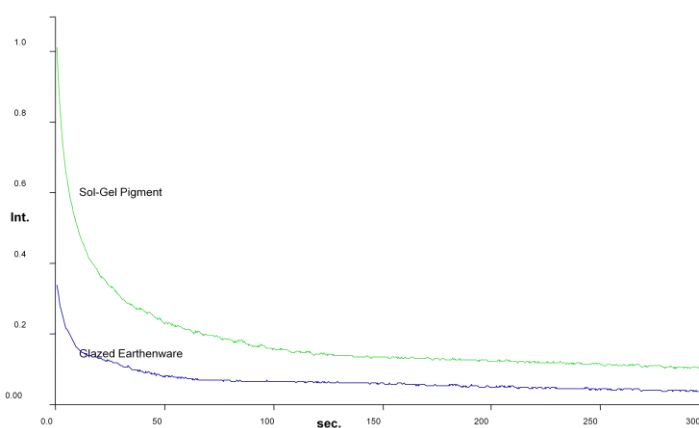


Figure 4. Long-term emission of pigment and glaze.

Comparing Figures 3 and 4 we can deduce that the possible damage of heat and liquid environment of glazing affected the Dy^{3+} sites more. Because, Eu^{2+} dopants are known to be the emission centres and Dy^{3+} ions are referred as retarding agent for long-term emission [3, 5, 11, 22, 25–26]. Depending on this phenomenon, retarding mechanism should be improved and protected during high temperature liquid glaze environment in order to obtain persistent luminescence. Basically, for a decorative glazing pigment apart from decomposition (or melting) temperature, powder size distribution, surface area and particle shape of the pigment particles are critical physical parameters [23–24, 27–30]. Specifically, for phosphorescent pigments, the more the excited dopant ions (Eu^{2+} , Dy^{3+} etc.) protected the better luminescence performance would be achieved in glazes. To understand and visualise the effect of

primary glazing, the phosphorescent pigments are also applied onto non-glazed bisque-fired bodies. Daylight view of plates (a) and appearances in the dark (b) can be seen in Figure 5.

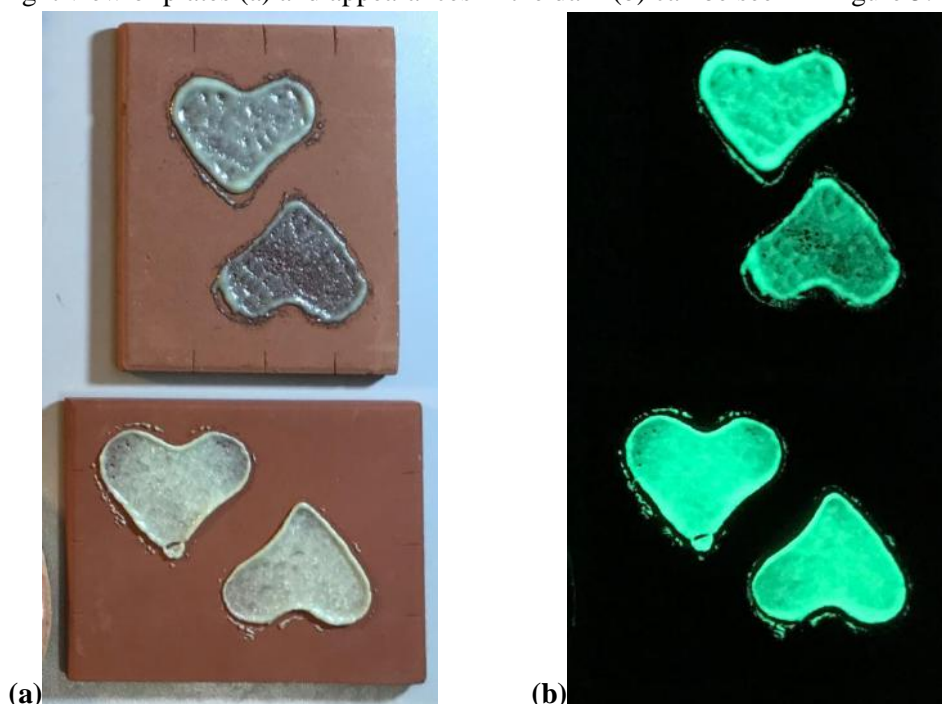


Figure 5. Decorative application on non-glazed earthenware plate, daylight view (a) and appearances in the dark (b).

At first, firing conditions in terms of heating/cooling rate and holding duration were adjusted same as the glazed tile. This slow firing operation resulted in a highly vitreous structure [Figure 5 (a)–up side image]. During vitrification of frit composition most of the pigments are sunk into the porous surface of non-glazed tile body and luminescence emission of this tile was diminished [Figure 5 (b)–up side image].

Secondly, ten times faster heating/cooling rate and shorter firing duration was applied to prevent sinking of pigments into tile body. Consequently, frit composition did not vitrify much [Figure 5 (a)–down side image] and did not spread into the tile surface. Emission intensity of fast fired [Figure 5 (b)–down side image] decorative application is comparably higher than the slower fired one [Figure 5 (b)–up side image].

For non-glazed tiles decorative phosphorescent glaze applications, both slow and fast-firings resulted in aesthetical and technical drawbacks. They cannot be a valid procedure for an industrial production. However, these findings are some keystones for further studies to improve the photoluminescence ability of pigments in glazes.

(The tile surface may be treated with a thin layer of solid-oxide powder instead of glazing which may reinforce the photoluminescence activity rather than deactivating the excited $\text{Eu}^{2+}/\text{Dy}^{3+}$ ions. Another possible improvement would be controlling the furnace atmosphere during glazing.)

4. CONCLUSION

Europium and dysprosium-doped SrAl_2O_4 phosphorescent pigments were employed for decorative glazing applications on earthenware tiles. Pigments were prepared with sol-gel method and sintered under reducing atmosphere to obtain persistent luminescence. X-ray diffraction analyses confirmed that the main phase is SrAl_2O_4 crystals with dopants. Glazing is resulted in reducing the afterglow performance of pigments as it is an additional heat treatment and also a vitreous environment which

destroys the crystal structure of pigment powders. However, there are still possibilities to improve luminescence properties of glaze applications with adjusting process parameters such as heating rate, glazing temperature/duration, glazing furnace environment, surface treatment of tiles prior to decorative operation and strengthening pigments by compositional variations against heat deformation or using more stable crystals as phosphorescence pigments.

REFERENCES

- [1] Jpoort, S., H., M., Blockpoel, W., P. and Blasse, G., Luminescence of Eu^{2+} in barium and strontium aluminate and gallate, *Chemical Materials*, 7, 1995, 1547–1551.
- [2] Jia, W., Y., Yuan, H., B., Lu, L., Z., Liu, H., M. and Yen, W., M., Phosphorescent dynamics in $\text{SrAl}_2\text{O}_4:\text{Eu}^{2+}$, Dy^{3+} single crystal fibers, *Journal of Luminescence*, 1998, 76:424.
- [3] Lin, Y., Zang, Z., Tang, Z., Zhang, J., Zheng, Z. and Lu, X., The characterization and mechanism of long afterglow in alkaline earth aluminates phosphors co-doped by Eu_2O_3 and Dy_2O_3 , *Materials Chemistry and Physics* 70, 2001, 156–159.
- [4] Zhang, P., Li, L., Xu, M. and Liu, L., The new red luminescent $\text{Sr}_3\text{Al}_2\text{O}_6:\text{Eu}^{2+}$ phosphor powders synthesized via sol-gel route by microwave-assisted, *Journal of Alloys and Compounds*, 456, 2008, 216–219.
- [5] Sanchez-Benitez, J., Andres, A., Marchal, M., Cordoncillo, E., Regi, V., M. and Escribano, P., Optical study of $\text{SrAl}_{1.7}\text{B}_{0.3}\text{O}_4:\text{Eu}$, R (R=Nd, Dy) pigments with long lasting phosphorescence for industrial uses, *Journal of Solid State Chemistry*, 171, 2003, 273–277.
- [6] Shafia, E., Bodaghi, M., Esposito, S. and Aghaei, A., A critical role of pH in the combustion synthesis of nano-sized $\text{SrAl}_2\text{O}_4:\text{Eu}^{2+}$, Dy^{3+} phosphor, *Ceramics International*, 40, 2014, 4697–4706.
- [7] Wu, S., Zhang, S. and Yang, J., Influence of microwave process on photoluminescence of europium-doped strontium aluminate phosphor prepared by a novel sol-gel microwave process, *Materials Chemistry and Physics*, 102, 2007, 80–85.
- [8] Li, Q., Zhao, J. and Sun, F., Energy transfer mechanism of $\text{Sr}_4\text{Al}_{14}\text{O}_{25}:\text{Eu}^{2+}$ phosphor, *Journal of Rare Earths*, 28, 1, 2010, 26–29.
- [9] Nisimama, P., D., Ntwaeaborwa, O., M., Coetsee, E. and Swart, H., C., The influence of the number of pulses on the morphological and photoluminescence properties of $\text{SrAl}_2\text{O}_4:\text{Eu}^{2+}$, Dy^{3+} thin films prepared by pulsed laser deposition, *Physica B*, 404, 2009, 4489–4492.
- [10] Georgobiani, A., N., Gutan, V., B., Demin, V., I. and Semendyaev, S., V., Luminescence and optical-memory model of $\text{SrAl}_2\text{O}_4:\text{Eu}^{2+}$, Dy^{3+} and $\text{Sr}_4\text{Al}_{14}\text{O}_{25}:\text{Eu}^{2+}$, Dy^{3+} , *Inorganic Materials*, 45, 2009, 1289–1294.
- [11] Karacaoğlu, E., Karasu, B., General review on the persistent luminescence phosphors in Türkiye and the World, *Abstract Book of Paint İstanbul Fair and Congress*, p. 93, 2012.
- [12] Karasu, B., Özer, M. S., Çakı, M., Gür, M. E., Kuru karıştırmalı geleneksel yöntemle hazırlanmış fosforiştirilmiş pigmentlerin kırmızı çamur yüzeyinde değerlendirilmesi, XII. Ulusal Eskişehir Pişmiş Toprak Sempozyumu Bildiriler Kitabı, 2018.
- [13] Speight, C. F., Toki, J., *Hands in Clays*, The McGraw-Hill Companies, Chris Freitag, 5–6, 2004.
- [14] Conrad, J. W., *Advanced Ceramic Manual Technical Data for the Studio Potter*, Falcon Company, San Diego, 47, 2007.
- [15] Mattison, S., *The Complete Potter—The Complete Reference to Tools, Materials, and Techniques for all Potters and Ceramicists*, Barron's Educational Series, 20, 2003.
- [16] Pechini, M., P., US Patent No. 3330697, 1967.

- [17] Ion, E., D., Malic, B. and Kosec, M., Characterization of PbZrO_3 prepared using an alkoxide-based sol-gel synthesis route with different hydrolyses conditions, *Journal of the European Ceramic Society*, 27, 2007, 4349–4354.
- [18] Tang, Z., Zhang, F., Zhang, Z., Huang, C. and Lin, Y., Luminescent properties of $\text{SrAl}_2\text{O}_4\text{:Eu, Dy}$ material prepared by the gel method, *Journal of the European Ceramic Society*, 20, 2000, 2129–2132.
- [19] Escribano, P., Marchal, M., Sanjuan, M., L., Alonso-Gutierrez, P., Beatriz, J. and Cordocillo, E., Low-temperature synthesis of SrAl_2O_4 by a modified sol-gel route: XRD and Raman characterization, *Journal of Solid State Chemistry*, 178, 2005, 1978–1987.
- [20] Dos Santos Jr, B., F., dos Santos Rezende, M., V., Montes, P., J., R., Araujo, R., M., dos Santos, M., A., C. and Valerio, M., E., G., Spectroscopy study of $\text{SrAl}_2\text{O}_4\text{:Eu}^{3+}$, *Journal of Luminescence*, 132, 2012, 1015–1020.
- [21] Chen, T., M. and Chen, C., Effect of host compositions on the afterglow properties of phosphorescent strontium aluminate phosphors derived from the sol-gel method, *Journal of Materials Research Society*, 16, 5, 2001, 1293–1300.
- [22] Kshatri, D., S. and Khare, A., Comparative study of optical and structural properties of micro- and nanocrystalline $\text{SrAl}_2\text{O}_4\text{:Eu}^{2+}$, Dy^{3+} phosphors, *Journal of Luminescence*, 155, 2014, 257–268.
- [23] Kaya, S., Y., PhD thesis, Anadolu University, Institute of Science, 2008 (in Turkish).
- [24] Nag, A. and Kutty, T., R., N., Role of B_2O_3 on the phase stability and long phosphorescence of $\text{SrAl}_2\text{O}_4\text{:Eu, Dy}$, *Journal of Alloys and Compounds*, 354, 2003, 221–231.
- [25] Kaya, S., Y., Karacaoğlu, E. and Karasu, B., Effect of Al/Sr ratio on the luminescence properties of $\text{SrAl}_2\text{O}_4\text{:Eu}^{2+}$, Dy^{3+} phosphors, *Ceramics International*, 38, 2012, 3701–3706.
- [26] Peng, T., Huajun L., Yang, H. and Yan, C., Synthesis of $\text{SrAl}_2\text{O}_4\text{:Eu, Dy}$ phosphor nanometer powders by sol-gel processes and its optical properties, *Materials Chemistry and Physics*, 85, 2004, 68–72.
- [27] Karasu, B., Kaya, G. and Ozkara, O., Application of phosphorescence glazes on bricks and roof tiles, 2nd International Terra Cotta Symposium Proceedings Book, Eskişehir, 108–13, 2002.
- [28] Fu, J., Ochi, Y. and Uehara, S., Long-lasting phosphorescent glasses and glass-ceramics, United States Patent, US 6.287.993 B1, 2001.
- [29] Pekkan, K., Taşçı, E., Gün, Y., Kaymak, K., Acer, O., Karasu, B., Fosforesans pigmentler için çini siri geliştirilmesi, üretimi ve ilgili bünyeler üzerine uygulanması, TÜBİTAK 3001 Projesi, 114M135, Proje Son Raporu, 2017.
- [30] Pekkan, K., Gün, Y., Taşçı, E., Karasu B., Effects of the physical properties of phosphorescent glazes on luminescence, *Proceeding Book of the X. International Eskişehir Terracotta Symposium*, 633–639, 2016.

PRODUCTION AND CHARACTERISATION OF Al_2O_3/Si CERAMIC-METAL COMPOSITE ARMORS

Dilan Yıldız¹, Gürsoy Arslan¹

¹ Eskişehir Technical University, Department of Material Science and Engineering,
İki Eylül Campus, 26480/Eskişehir/Turkey

In every period of the world, the greatest problem is the people's efforts to harm people are increasing rapidly. As new threats are developed, new protection systems are being developed. In the last period, composite materials that can resist the higher threat levels (NIJ standards of thread level) are used to meet this need. Within the scope of this project, ceramic-metal composite material which has been successfully used and widely used in the production of armor and ballistic plates is produced. As ceramic matrix, alumina (Al_2O_3) material, which is available, low cost, easy to produce by sintering and has desired hardness, strength, elastic modulus values, has been chosen. As a metal reinforcement, not only does it not reduce the mechanical properties of the matrix but also the silicon (Si) material which enhances the toughness of the matrix with the advantage of being metal and supporting them. Alumina has been successful for armor and ballistic systems, but its properties remain low compared to other ceramics used in this area (boron carbide- B_4C , silicon carbide-SiC, titanium diboride- TiB_2). For this reason, in the project, the mechanical properties of alumina are being tried to be increased by the effect of grain size. The 90% Al_2O_3 - 10% Si materials used as powder are mixed by dry mixing to promote homogeneity. Alumina with three different grain sizes is used in the mixture (210 nm, 2 μm , 120 μm). Spark Plasma Sintering (SPS) method is used as the production method. The advantages of the SPS method used for this system for the first time are investigated. The high density (> 99.72%) was achieved by high heating rate (100 °C / min), mechanical pressure applied to the material during sintering (16 kN) and sintering at lower temperatures (~ 1450 °C – 1500 °C). In order to characterization, X-ray Diffraction and Scanning Electron Microscopy were used. Also, samples were evaluated with hardness test by mechanically. All composite were obtained and characterized. Sintered composites exceeded to 99.7% in bulk densities. Hardness values of composites were found in the range of 1514 ± 13.01 Hv. Results show that the decreasing of particle size of Al_2O_3 increases the densification for both green body and sintered body, and also,. Significant differences were seen on the structure images with changing particle size.

Keywords: Al_2O_3 , Si, Composites, Spark Plasma Sintering

1. INTRODUCTION

Experiments were executed using three different size of alumina (Al_2O_3) and a silicon (Si) via spark plasma sintering (SPS) that was specifically selected for three reasons.

First, Al_2O_3 possesses some superior properties such as low density (3.9 g/cm^3), high strength (2100 MPa), high elastic modulus (380 GPa), high hardness (1370 Hv – for 99.7% Al_2O_3 at Hv5, 1 kg load), excellent chemical and thermal stability, excellent oxidation/corrosion resistance and excellent high temperature creep resistance which these make significant material used in many desired applications [1].

Second, silicon provides the mechanical properties of the system with their elastic modulus (150 GPa) and strength (120 MPa) which are high in contrast to other metals [2].

Third, spark plasma sintering (SPS) method leads the near-fully dense compact structure. SPS is a comparatively new sintering process relatively other conventional methods that provides compaction of ceramic and metal powders at low temperature with short holding time and high heating rate. Heating rate prevents the abnormal grain growth in the structure. Three parameters contribute the densification of powders which can be noticed: (i) the applying of a mechanical pressure; (ii) the using of rapid heating rates; and (iii) the using of direct current, the samples are also subjected to an electrical field. Applying of mechanical pressure contribute to remove pores from compacts and enhancing diffusion. The heat transfer from the graphite mould to the sample is very significant situation in this process, because the graphite mould acts as a heating element. During the process, pulses generate spark discharges and plasma between the powder particles that is why is named spark plasma sintering [3].

2. EXPERIMENTAL PROCEDURES

Three different sized commercially available Al_2O_3 (Alpha Aesar, MERCK) and Si (Alpha Aesar) was mixed with TURBULA Shaker-Mixer through 3-dimension. The average particle sizes of Al_2O_3 were measured as 210 nm, 2 μm and 122 μm via MasterSizer and ZetaSizer.

The mixtures were sintered by spark plasma sintering method with the identical sintering regimes. The mixtures were heated from 450°C to 1500°C with heating rate of 100°C/min., sintered at 1500°C during 5 minutes and cooled from 1500°C to 25°C with cooling rate of 150°C/min. under 50 MPa mechanical pressure.

In order to calculate the densification and relative density percentage, Archimedes Principle was used. Structural analysis of composites were done by scanning electron microscopy (Phenom-Pro). Before the SEM, samples must be prepared. First, samples were moulded (with resin, hardener). Polishing was applied with Piano (10 min), Largo (10 min), NAP (5 min), DAC (5 min) polishers. Then, Gold-Palladium (Au-Pd) coating was made on the samples.

In order to compare the mechanical properties of composites, hardness values were done by using Vickers hardness test (emco TEST-M1C 010). More than five indents were made at the middle of each sample (to minimize near-surface effects) for average hardness values.

X-ray Diffraction (Miniflex-Rigaku) was used for phase analysis of composites which determines the reaction products formed as in-situ. For the analysis, the half of the products were grinded via grinder and they were converted into the powder. Analysis is done between 20° - 50° with $1^\circ/\text{min}$ and 0.02 step interval.

3.RESULTS

Chemical composition and measured particle size of the prepared powder mixtures is given in Table 1.

Table 1. Particle size of prepared powders

Composition	Particle Size of Al_2O_3	Al_2O_3 (wt%)	Si (wt%)
90A10S-1	210 nm	90	10
90A10S-2	2 μm	90	10
90A10S-3	122 μm	90	10

Relative and bulk densities of $\text{Al}_2\text{O}_3/\text{Si}$ composites are given in Table 2. The relative densities of produced $\text{Al}_2\text{O}_3/\text{Si}$ composites were above 99.7%. The amount of open porosity content in composites was measured to be less than 1.0%. Density of Al_2O_3 is 3.95 g/cm^3 and bulk density of produced composites ranged from 3.82 to 3.84 g/cm^3 .

Table 2. Relative and bulk density of $\text{Al}_2\text{O}_3/\text{Si}$ composites

Composition	Green Density (%)	Relative Density (%)	X-ray Density (g/cm^3)
90A10S-1	54.1	99.7	3.84
90A10S-2	58.8	99.8	3.83
90A10S-3	35	99.8	3.82

Besides, Si addition contributes to the reduction of the weight of composites.

Although melting temperature of Si is 1410°C , Si starts to melt at above 1000°C during sintering under the influence of applied pressure (50 MPa)(Fig 1). The shiny region on the Fig. 2 indicates the Si phase, while the dark region indicates the Al_2O_3 phase.

Figure 1. includes time-temperature and time-piston travel curves. From the graphes, we see that the sintering temperature is sufficient, because samples start to sinter at beginning from 1450°C .

The sintering process causes the crystallographic reorganization mechanism which makes more shrinkage in the $122 \mu\text{m}$ -sized $\text{Al}_2\text{O}_3/\text{Si}$ mixtures [4]. Densification can be explained according to the this reason and also, diffusion which is increased with decreasing particle size.

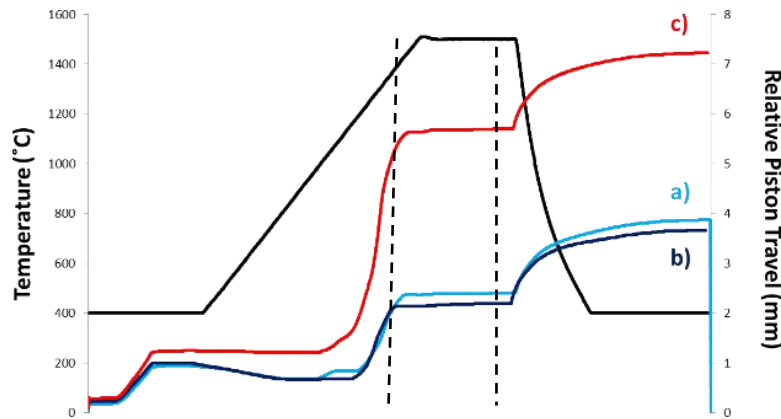
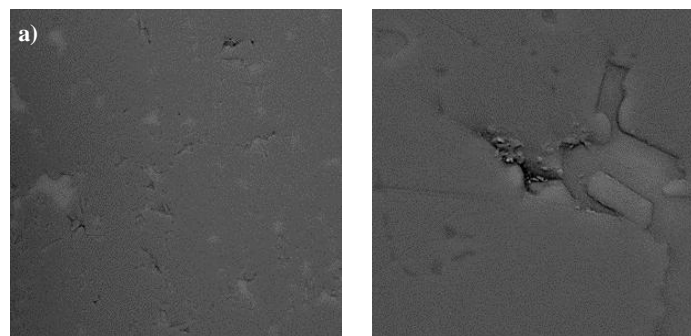


Figure 1. Sintering graph of a)90A10S-1, b)90A10S-2, c)90A10S-3

In Figure 2.a, there is almost no porosity and relatively more homogeneous dispersion than the other samples is seen. The grain boundaries of Al_2O_3 is almost never seen in SEM images. Although this sample have lower bulk density, its hardness value is higher. Because there is much more grain boundaries in unit volume. The grain boundaries act as a barrier to prevent the dislocation motion. This behavior increases the mechanical preoperties.

In Figure 2.b, homogeneous dispersion and small amount of porosity is seen and some particles rupture from grain boundaries. When the particle size distributions of the powders are similar, densification occurs more. That is why the bulk density is relatively higher than other samples.

In Figure 2.c, there are almost no porosity and there is agglomeration of Si particles are seen. Also, we can see the elongated Al_2O_3 particles. The tips of the elongated particles are not wanted because, they are potentially crack especially in ceramic base systems. On this surface which is polished, during the polishing, some particles that are more than $2\text{ }\mu\text{m}$ -sized Al_2O_3 mixture break away from the grain boundaries. This means that the interfaces of these particles which are grain boundaries are not strong. This effects the mechanical properties badly.



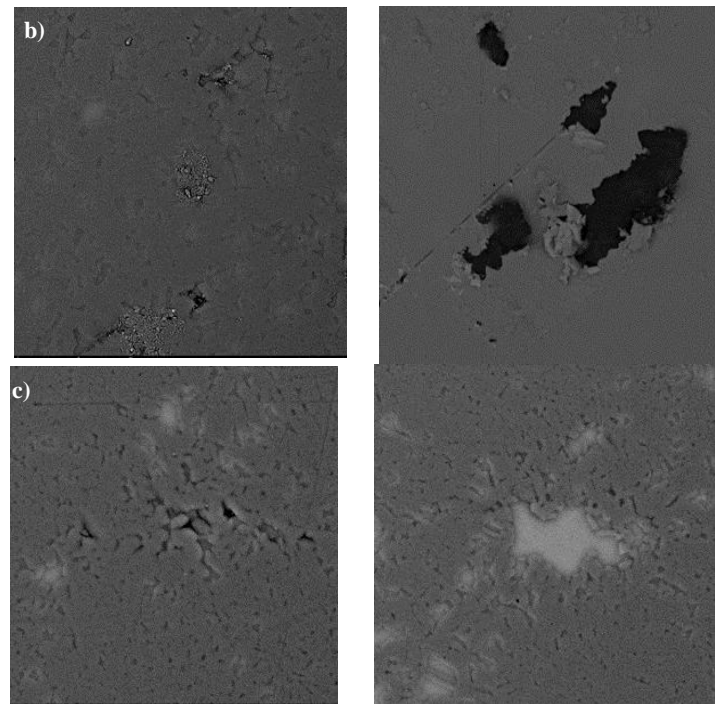


Figure 2. SEM microstructure (Phenom-Pro) images of $\text{Al}_2\text{O}_3/\text{Si}$ composites, a)90A10S-1 (15000x), b)90A10S-2, c)90A10S-3 (at 5000x)

Figure 3 shows the hardness of produced $\text{Al}_2\text{O}_3/\text{Si}$ composites. The hardness of composites were measured as 1528, 1502 and 1514 Hv5. According to the hardness values were examined, the mean is 1514.67. Although all of them are acceptable for the application due to the no significant difference in hardness, nm-sized $\text{Al}_2\text{O}_3/\text{Si}$ sample has better hardness than others.

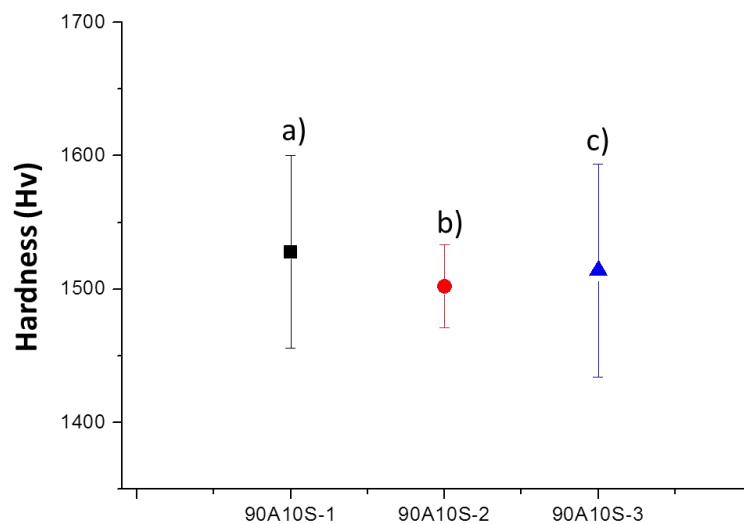


Figure 3. Hardness of produced composites a)90A10S-1, b)90A10S-2, c)90A10S-3

X-ray diffraction patterns of starting powder mixtures are given in Figure 5. and sintered composites are given in Figure 6. In diffraction patterns of starting powder of 122 μm -sized Al_2O_3 gives the peaks from the different Bragg's angles due to the $\gamma\text{-Al}_2\text{O}_3$ phase. These phases are converted into the α -

Al_2O_3 at the temperature above 1200°C [4]. Corundum has hexagonal crystal structure and $\gamma\text{-Al}_2\text{O}_3$ has cubic crystal structure [5,6]. After the sintering process, qualitative x-ray diffraction revealed that all produced composites contained the phases corundum and Si. In other words, the existence of reaction products could not be verified within the detector limits of the XRD method.

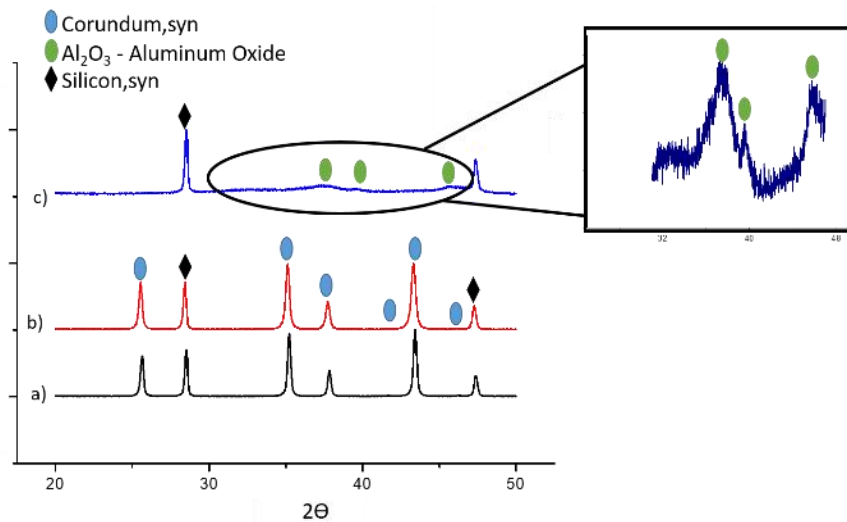


Figure 4. XRD patterns of starting powder of $\text{Al}_2\text{O}_3/\text{Si}$ mixtures a)90A10S-1, b)90A10S-2, c)90A10S-3

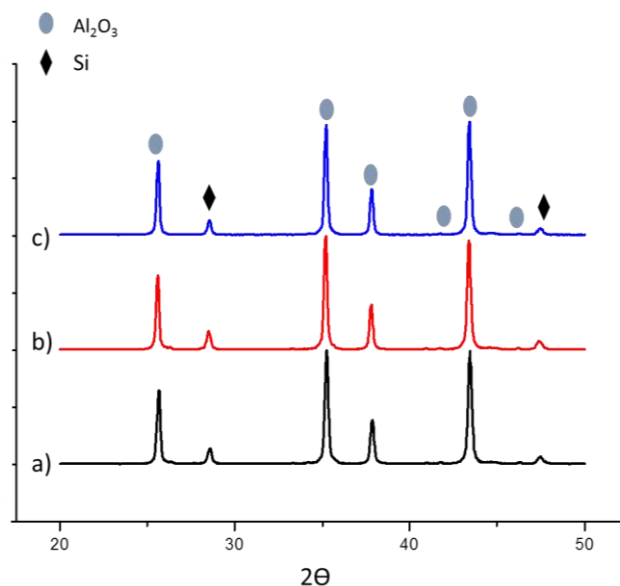


Figure 5. XRD patterns of $\text{Al}_2\text{O}_3/\text{Si}$ composites a)90A10S-1, b)90A10S-2, c)90A10S-3

4.CONCLUSIONS

At the beginning of the comparison of the results, it is necessary to draw attention not only to the grain sizes of the alumina but also to the differences between the grain sizes of alumina and silicon. Differences between the particle sizes in the 90A10S-1 and 90A10S-3 samples are more than 90A10S-

2 sample that has almost same particle sizes. The packing abilities of the sample 1 and 3 are better than the sample 2 due to this differences.

As seen in Fig 1., piston travel is further on the curves of a and c. Although the 90A10S-1 is expected to densified more, the densification of 90A10S-3 is better. This unexpected result is explained with the XRD graphes of the starting powder mixtures. Al_2O_3 component of the sample 3 has γ -phase unlike from the sample 1 and 2 that have α -phase as seen in Fig 4. When the XRD graphes of the sintered powders are interested on the Fig 5, γ -phase is invisible in the structure. In short, only reorganization of particles takes place in the sample 1 and 2, while either reorganization or phase transformation takes place in the sample 3. This transformation contributes the sintering ability a little. Despite of this, the hardness values in Fig 3 and XRD density values of the samples in Table 2 show that the mechanical properties of 90A10S-1 are better than other samples.

As the SEM images in Fig 2, there is almost no porosity in the samples. 90A10S-3 is unwanted structure for armor production. In the Fig 2.c, it is seen the agglomeration of Al_2O_3 particles. Also, the particles are elongated and the tips of its are sharp. During the fracture, these tips are seen as potentially mistakes and they tend to propagate the cracks. In Fig 2.b, it is seen that the some particles of Al_2O_3 rupture from grain boundaries. This situation is also unwanted for armor production. It is expected that the grain boundaries are strengthened, the crack is lose some of its energy as it moves through the grain and slower. In Fig 2.a, there is no agglomeration and it has more homogeneous structure. The grain boundaries are stronger.

In conclusion, the properties of $\text{Al}_2\text{O}_3/\text{Si}$ composites are enhanced by decreasing of Al_2O_3 particle size.

REFERENCES

1. C. J. Roberson, P. J. Hazell, P. L. Gotts, IM Pickup, R. Morrell, "The Effective Hardness of Hot Pressed Boron Carbide with Increasing Shock Stress
2. Moskovskikh, D., O., Lin, Y.-C., Rogachev, A.,S., McGinn, P.,J., Mukasyan, A., S., "Spark plasma sintering of SiC powders produced by different combustion synthesis routes", Journal of the European Ceramic Society 35, 477-486, 2015
3. M. Tokita, "Trends in Advanced SPS Spark Plasma Sintering System and Technology," J. Soc. Powder Technol., Jpn., 30 [11] 790–804 (1993).
4. Samir Lamouri , Mohamed Hamidouche, Nouredine Bouaouadjaa, Houcine Belhouchet, Vincent Garnier, Gilbert Fantozzi, Jean Francois Trelkat, "Control of the γ -alumina to α -alumina phase transformation for an optimized alumina densification"
5. Wiberg, E.; Holleman, A. F. (2001). Inorganic Chemistry. Elsevier. ISBN 0-12-352651-5.
6. ASM Engineered Materials Reference Book, Second Edition, Michael Baucchio, Ed. ASM International, Materials Park, OH, 1994.

seres'18

IV. INTERNATIONAL CERAMIC GLASS PORCELAIN
ENAMEL GLAZE AND PIGMENT CONGRESS
October 10-12, 2018, Eskişehir, Turkey

Abstract of INVITED SPEAKERS

KEYNOTE SPEAKERS**LITHIUM-ION BATTERIES AND ELECTRIC VEHICLES: POTENTIAL OF TURKEY****Davut UZUN, Osman OKUR**

TÜBİTAK Marmara Research Center Energy Institute

Barış Mah. Dr. Zeki Acar Cad. No:1 41470, Gebze-Kocaeli/Türkiye

The importance of energy storage systems increases with increasing the share of renewable energy resources in total energy production and the need for portable energy. In particular, the need for portable stored energy has created a pressure on the rapid development of battery technologies. The importance of electrochemical battery technology which has become critical especially for electric vehicle applications increases day by day. Nowadays, the increase in demand for portable electronic systems and electric vehicles causes the increase in importance of electrochemical energy storage. Lithium ion battery technology is preferred because of the high energy density for storage of portable energy needed both in electronic systems and in electric vehicles worldwide. It is predicted that lithium ion battery technology will be the most preferred battery technology for portable applications in the next 30-40 years period. As of today, it is known that only alternative to lithium ion batteries is again lithium battery technology (lithium sulfur, lithium air, all solid-state lithium batteries, etc.).

In our country, lithium ion battery production is not available in commercial size as of today. When market reports are examined, the installed capacity in the world as of 2017 is about 120 GWh. Serious investments are planned and implemented especially within the boundaries of the European Union. It is predicted that lithium-ion battery production will reach 210 GWh levels by 2025. When examining HS6 foreign trade reports, our country's annual import of batteries is about 400 million dollars. The share of lithium batteries among imported batteries is in the order of \$ 80 million. Vision 2023 Technology Foresight Project clearly emphasizes that it is important for our country to have claims in the area of advanced energy technologies and to increase supply security. Vision 2023 Energy and Natural Resources Panel "The development of lithium ion battery technologies with a specific energy of 350 Wh / kg and above" was defined as the target. When technological forecasting and technological goals of different countries are examined, the existence of a similarities can be found. When the target of our country's 2023 year is examined, the ratio of renewable energy sources in electricity generation is determined as 30%. By 2023, 3 GW for solar energy and 20 GW for wind power are targeted. These targets clearly demonstrate the importance of energy storage.

In this study, the technological developments since 1990 by the year of commercialization of lithium ion batteries, and the contributions of these developments to the market and to the technological developments have also been evaluated. The development of electric vehicles which has the largest market share in portable applications, and the current state of battery technology considering as forming the barrier to this development have also been evaluated. Additionally, information is given about the Li-ion battery studies done in our country. Effort has been spent to estimate the requirements related to the subject by evaluating lithium ion battery development and battery production activities in our country. As a result, it is estimated that we need to develop our original technology for lithium ion batteries which have many applications in constant and mobile fields and it is also estimated that the original developed technology should be producible in our country.

KEYNOTE SPEAKERS

GLOBAL CROSSOVERS

Professor Neville Assad-Salha

Australia

The Seres '18 Exhibitions are a role model for the world. They comprise of an extreme diversity of different professional approaches through the material, Clay. It is wonderful to see these exhibitions broken up into 3 major themes: - "Fantastic Teapot", "Ceramic Jewelry" and "Old & New" which includes glass artists.

These exhibitions give ceramic and glass artists an opportunity to explore different areas and perceptions through their medium.

The Turkish educational and wider ceramic community is rapidly becoming a leading role- model as it incorporates many different approaches and theories behind the education of ceramics.

The Symposiums have given the opportunity to many international artists to come to Turkey and absorb the rich culture that it has to offer, in turn creating influence throughout the world. We can see wonderful crossovers and inspirations happening through many different cultures. Since the 8th Century, Turkey has been a leading force in paving the way in ceramics and adapting ceramics into functionality and aesthetic form which has given a great deal of influence to contemporary ceramics throughout the world.

We have seen clay going from a strong position in the Arts in the 1960's and '70's to a lesser position in later decades, and now has returned to a major platform which is currently in a very strong position in the art world. This is wonderful to see as it is now giving many of the younger members of the community the opportunity to express themselves through a malleable material. It also allows established clay workers to reposition themselves in the art world and re- explore a range of approaches which feeds back into the educational departments in Ceramics etc.

Ceramics currently has gone into many different areas from the most simplistic and minimal forms to the more rugged, organic and robust artworks. It has also allowed the artist to move into the most decorative forms, along with conceptualizing through the material, Clay.

The Macsabal Symposiums which have taken place over the past 20 years in Korea, Turkey and China, have proved to be extremely successful in bringing international artists together from many different countries and influences within the medium of ceramics.

Finally, exhibitions of this kind advance the global field as to how we see and move forward with contemporary ceramics. Thanks to the Turkish Ceramic Society and Anadolu University for organizing these 3 major international Seres 18 Exhibitions. Thanks to the International Macsabal Symposium organized in 3 countries, including Ankara, Turkey; China and Korea. Also thanks to the International Terracotta Symposium in Eskişehir, the Mayor of Eskişehir Municipality and his council members for their continued support.

These symposiums are the intersection point for the meeting of the artists in the world. Finally, a special thanks to Lecturer Mutlu Baskaya and her committee.

INVITED SPEAKERS

CERAMIC NANOCOMPOSITE NEGATIVE ELECTRODES FOR LI-ION BATTERIES

Hatem Akbulut*, Mahmud TOKUR, Tuğrul Çetinkaya, Mehmet Uysal, Hasan Algül,
Mehmet Oguz Güler
Sakarya University, Engineering Faculty, Department of Metallurgical & Materials Engineering,
Esentepe Campus, 54187, Sakarya/TURKEY

ABSTRACT

Electrochemical energy storage has become a critical technology for a variety of applications, including grid storage, electric vehicles, and portable electronic devices. Ceramic based anodes (SiO_x, GeO, SnO₂, ZnO, Fe₂O₃ or more complex stoichiometry, etc.) have much higher Li storage capacity than the intercalation-type graphite anode that is currently used in Li-ion batteries (LIBs). Almost all the ceramic based or ceramic supported negative electrodes are considered as a promising anode material for rechargeable LIB, owing to their high theoretical specific capacity. Despite the low capacity, graphite anodes still dominate the marketplace due to the fact that alloy anodes have two major challenges that have prevented their widespread use. However, the practical implementation of metal (M) and metal oxide (MO) anodes is still blocked due to three major problems [1]: poor cycle-life results from pulverization during the huge volumetric fluctuations (>300 %), drastic irreversible capacity loss and low coulombic efficiency, the solid electrolyte interphase (SEI) breaks as the nanostructure shrinks during delithiation. This results in the exposure of the fresh MO or similar active material surfaces to the electrolyte and the reformation of the SEI, resulting in the SEI growing thicker with each charge/discharge cycle and highly possible particle aggregation [2]. The critical issue of fabricating high specific capacity, high rate capability, and long cycle life LIB device is the advanced nano architected design and flexible electrode materials with good mechanical deformations. Nanocomposite structures are pivotal for the progresses in electrode materials due to their manageable surface-area, stunted mass and charge- diffusion span, and volume change acclimatization during charging/discharging. CNTs, CNFs and Graphene with their special structures provide excellent conductivity, mechanical flexibility and significantly large surface-area, are considered ideal additives to enrich chemistry of electrodes [3].

In order to prevent these challenges, most common and effective strategy to adopt nanoscale materials with various morphologies, including nanoparticles and, nanowires, nanotubes and hollow spheres. Compared to bulk active materials, such nanostructured ceramic based oxides, nitrides and carbides are able to accommodate elevated mechanical stress, resulting in prolonged cycling stability. Optimization of ceramic based electrodes can be achieved by incorporating nano structures with various conductive matrixes, such as graphene and, carbon nanotubes, and carbon and to form core-shell and yolk-shell nanocomposites. The introduction of such a carbon architectures with ceramic phases play a key role in alleviating the agglomeration of nano structured active materials [4]. In this review, we summarized the recent progresses on developments of ceramic based nanocarbon supported (CNT, CNF, Graphene etc.) negative electrodes for high performance Li-ion batteries. The synthesis techniques of the 1-D, 2-D and 3-D electrodes has been discussed for special hierarchical structures and free standing electrodes. The main research activities of Sakarya University electrochemical energy storage group has also summarized. The electrochemical performances of the ceramic based active materials and their nanocomposite structures were reviewed.

References

- [1] Kang, Meng, Breger, Grey and Ceder, Science 311, 977 (2006).
- [2] Wu and Cui, Nano Today 7, 414 (2012).
- [3] Tokur, Algul, Ozcan, Cetinkaya, Uysal, Akbulut, Electrochimica Acta 216, 312 (2016).
- [4] Li, Tang, Kang, Zhang, Yang, Zhu, Zhang and Lee, Small 11, 1345 (2014)

INVITED SPEAKERS**CERAMICS AND LITHIUM ION BATTERIES: SOLID ELECTROLYTES**

Servet Turan¹, Kamil Burak Dermenci¹, Musah Abdulai¹, Cem Eren Özbilgin¹

¹ Eskişehir Technical University, Department of Material Science and Engineering,
İki Eylül Campus, 26480/Eskişehir/Turkey

Electrolytes in Li-ion batteries provide the ionic conductivity between anode and cathode. Organic electrolytes are the most common electrolyte found in Li-ion battery market. They show satisfactorily high ionic conductivity but their easily flammable nature concerns to meet the regulations regarding safety. They also form a Solid-Electrolyte Interphase (SEI) which block chemical reactions and ion transportation between electrode material and electrolyte.

Solid-state electrolytes offer a new sight in the Li-ion battery field because of their enhanced safety. SEI could not be formed when solid electrolytes used. They consist of polymeric gels, inorganic solid compounds and inorganic glasses. Among them, inorganic solid electrolytes show relatively high ionic conductivity and relatively low electronic conductivity, a wide electrochemical stability window. The widely known examples of the inorganic solid electrolytes are Perovskite, Na-SuperIonic CONductor (NASICON), Lithium SuperIonic CONductors (LISICON) and Garnet type electrolytes. Perovskite structure of AB_3 general formula has excellent tolerance for ion substitution on both A and B sites resulting with large vacancy concentrations. Lithium conductivity depends on Lithium and vacancy concentrations. Even if NASICON and LISICON show good ionic conductivity; they are both highly unstable with Lithium metal. Garnet type electrolytes stand out with their excellent stability with Lithium, air and CO_2 . They also have high decomposition potential of 6V against Li along with considerably high ionic conductivity.

In this study, the state-of-the-art inorganic solid electrolytes that show Li^+ ion conductivity will be summarized and then, studies in our group and in Turkey on these types of electrolytes will be discussed.

INVITED SPEAKERS

NANOCOMPOSITE CERAMIC BASED POSITIVE ELECTRODES FOR LI-ION BATTERIES

Mehmet Oguz Guler*, Aslihan Guler, Seyma Duman, Hatem Akbulut

*Sakarya University, Engineering Faculty,

Department of Metallurgical & Materials Engineering, Esentepe Campus, 54187,
Sakarya/TURKEY

Today, the importance of energy storage in telecommunication, automotive, energy and satellite technologies gradually increased. Lithium ion technology are lately extensively employed energy storage device for electric vehicles and all portable electronics. High gravimetric energy densities (up to 150 Wh/kg), cost friendly and enhanced safety with performance make Li-ion batteries suitable candidates for these applications. However, development of new cathode electrodes with higher energy densities with improved stability is still needed for enhanced devices. An intercalation cathode is a solid host network, which can store guest ions. The guest ions can be inserted into and be removed from the host network reversibly. In a Li-ion battery, Li^+ is the guest ion and the host network compounds are metal chalcogenides, transition metal oxides, and polyanion compounds. These intercalation compounds can be divided into several crystal structures, such as layered, spinel, olivine, and tavorite.

This review covers key technological developments and scientific challenges for a broad range of Li-ion battery electrodes. Periodic table and potential/capacity plots are used to compare many families of suitable materials. Performance characteristics, current limitations, and recent breakthroughs in the development of commercial intercalation materials such as lithium cobalt oxide (LCO), lithium nickel cobalt manganese oxide (NCM), lithium nickel cobalt aluminum oxide (NCA) and lithium iron phosphate (LFP). New polyanion cathode materials are also discussed. The cost, abundance, safety, Li and electron transport, volumetric expansion, material dissolution, and surface reactions for each type of electrode materials are described. Both general and specific strategies to overcome the current challenges as in the form of composites are covered and categorized.

INVITED SPEAKERS**CERAMICS AND SODIUM ION BATTERIES**Şaban Patat^{1,2}¹Erciyes University, Faculty of Science, Department of Chemistry, Kayseri/Turkey²ENDAM, Middle East Technical University, Ankara/Turkey

Lithium-ion batteries have been extensively used as power sources for portable electronics and electric vehicles due to the high energy density and long cycle life. The large-scale applications of lithium ion batteries in portable electronics and electric vehicles will increase the price of Li resources due to its low abundance in the Earth's crust and its non-uniform geographic distribution. The increasing price of Li resources will result in the application of lithium ion batteries in stationary energy storage uneconomical in the near future. Therefore, the development of low cost, highly-safe and cycling stable rechargeable batteries based on abundant resources is becoming important and highly desirable. Sodium ion batteries have attracted great interest in portable electronics, electric vehicles and grid energy storage because of the cheap and abundant of sodium resources and using low cost Al current collectors for both cathode and anode electrodes.

The major challenge for sodium ion batteries is to find suitable electrode materials with excellent sodium storage performance. Transition-metal layered oxides, polyanion compounds and other compounds are used as cathode materials for sodium ion batteries while carbonaceous materials and oxides are used as anode materials.

In this presentation, cathode and anode materials for sodium ion batteries are reviewed, focusing on the latest research progress. Advantages and disadvantages of the currently available electrode materials will be discussed based on our experience and the literature.

INVITED SPEAKERS

HOW TO SATISFY THE EU DEMAND FOR A SLIP RESISTANCE TEST THAT ENABLES LONG TERM SAFETY

Richard Bowman

Intertile Research, Melbourne, Australia

European Directive 89/106/EEC required construction products remain safe during their entire life cycle. EU Regulation 305/2011 requires floors remain slip resistant throughout economically reasonable life cycles. The CEN/TC 339 slip resistance standards committee was obliged to establish a single slip resistance test method. The European Commission has funded the SlipSTD, Ultragrip and Slipsafe slip resistance research projects.

The SlipSTD project found the German ramp tests were generally applicable except on smooth surfaces (at the slippery end of the spectrum). The BOT 3000 and GMG 200 tribometers overestimated the wet slip resistance of very smooth floors due to slip-stick effects, while measurements on structured and textured surfaces were impaired by loss of contact. The pendulum was well suited to smooth, structured and textured surfaces. Measurements on profiled surfaces were considered to be impaired by impact variations, but specimen orientation can overcome this issue. The pendulum has the widest operating range. It also only requires a small test area.

The Ultragrip project used an industrial tile polishing machine to provide a sufficiently large worn area for slip resistance testing: there was good correlation between the slip resistance of accelerated conditioned tiles and those that wore in service. The Slipsafe project used a washability tester for accelerated conditioning and the pendulum for slip resistance testing of resilient flooring.

In Australia, accelerated conditioning is routinely used to assure long-term slip resistance. Satisfying the EU sustainable slip resistance mandate requires testing products after appropriate accelerated conditioning. When will CEN/TC 339 take the lead?

INVITED SPEAKERS

EFFICIENT USE OF NEPHELINE SYENITE AS A FLUXING AGENT IN INDUSTRIAL CERAMIC FORMULATIONS

Onur Emre Sağlam^{1,2}, Pervin Gençoğlu¹, Tümay Çalbaş², Alpagut Kara^{1,3}, [Claudio](#)

Cataldi² ¹Ceramic Research Centre, Anadolu University, Yunusemre Campus ETGB

Anadolu Technology Park, Eskişehir/Turkey

² Nefelin Madencilik ve Endüstri Hammaddeleri San.Tic. A.Ş.,Bozüyük/ Bilecik/Turkey

³ Eskişehir Technical University, Department of Material Science and Engineering,

İki Eylül Campus, 26480/Eskişehir/Turkey

Feldspar and clay minerals are employed in ceramics industry as a raw material. Apart from these, feldspathoid (especially nepheline syenite) group minerals are commonly preferred in formulations. Nepheline syenite is a quartz-free aluminum silicate complex rock consisting of different mineral phases such as nepheline, alkali feldspar, and biotite. Because of its extremely low melting point and high alumina content, nepheline syenite is used as a glass phase promoter, a ceramic flux and also as a functional filler in paint, plastics etc. Like Feldspar, nepheline syenite is used as a flux in tile, sanitaryware, porcelain, vitreous and semi-vitreous bodies. It contributes high alumina without associated free silica in its raw form and fluxes to form silicates with free silica in bodies. This stabilizes the expansion curve of the fired body. It is an excellent filler and flux, especially for fast firing conditions. Nepheline syenite is valuable in glass batches to achieve the lowest melting temperature while acting as a source of Alumina. Kırşehir Buzlukdağ nepheline syenite represents one of the largest and unaltered alkaline intrusive body in Central Anatolia region of Turkey. Main mineral composition is nepheline (15-35 wt. %), K-feldspar (orthoclase) (41-69 wt. %), albite (25-37w. %), biotite (0.3-2.5 wt. %). Buzlukdağ nepheline syenites have K₂O/Na₂O and Na₂O/K₂O ratios between 0.44-1.5 wt. % (mean 0.60 wt. %) and 0.89-2.66 wt. % (1.53 wt. % on average) respectively, thus they are very suitable for ceramic and glass industries.

In this study, Usability of Buzlukdağ nepheline syenite was examined as fluxing in place of albite in ceramic tile and ceramic sanitaryware bodies. The rheological behavior, energy efficiency and its effect on technical properties of the representative bodies were examined.

INVITED SPEAKERS**OPTIMIZATION OF FIRING PROCESSES OF CERAMICS USING THERMAL ANALYSIS METHODS AND KINETIC MODELLING**

J. Janoschek, J. Blumm, E. Moukhina,
K. NETZSCH-Gerätebau GmbH, D-95100 Selb, Germany

In the production of ceramics, a green body is frequently manufactured of ceramic powder and additives (binder, sintering aids). This material is then shaped into a green body. The green body is converted into the final product through thermal treatment at high temperatures. The temperature program during the firing process, especially during the binder burnout and in the sintering phase, has a lasting effect on the subsequent characteristics of the product. Optimization of the temperature program during firing and to shorten the duration in the kiln will increase productivity and reduce production costs. Thermophysical properties like density change, specific heat and heat transfer have to be known. Pushrod dilatometers have been used for decades to investigate length changes of ceramics during sintering. Thermogravimetric measurements can be used to analyze the binder burnout and decomposition reactions. Differential Scanning Calorimetry (DSC) can be used to measure the specific heat and enthalpy changes. Laser flash method is well- established for determination of the thermal diffusivity. By combining the results of all measurement methods, it is possible to determine the thermal conductivity of the material and to predict the temperature gradients in ceramic parts by employing finite element simulations. Measurements on Zirconia with the different methods will be shown as example.

Using measurement results achieved at different heating rates and an applying advanced thermokinetic analysis software (NETZSCH KineticsNeo), one can analyze the kinetics of the binder burnout and sintering processes. Understanding the reaction processes allow modelling of the temperature profile for various scenarios. Examples will be presented showing optimized temperature programs shortening the firing time.

INVITED SPEAKERS**EVOLUTION OF SPANISH TILE MANUFACTURING INDUSTRY.
SUSTAINABILITY MARKS THE FUTURE****Vicente Sanz***Instituto Universitario de Tecnología Cerámica. Universitat Jaume I. Castellón*

The manufacture of ceramic tiles in Spain has a long tradition. Spain is one of the main world producers, with a product of excellent quality endorsed by the great penetration in a large number of world markets. It is a sector in constant technological evolution that has led to the transformation of a productive process derived from the purest artisanal tradition, to a highly technified process in line with the digital era.

However, the production of ceramic tiles still presents important challenges derived, fundamentally, from the need to harmonize their evolution with an increasingly sustainable development. The large consumption of material resources (raw materials and water), energy, as well as greenhouse gas emissions are the great future challenges of this industry.

This paper describes, in a first part, the main milestones of the Spanish ceramic tile industry in the last 40 years, including the role that the Institute of Ceramic Technology of the Universitat Jaume I of Castellón has developed during all these years.

Based on this evolution, the ongoing and future developments necessary to achieve an increasingly sustainable industry are described. The full development of water-based digital decoration, the use of energy and its exploitation for water recovery, the reduction of the carbon footprint and the incorporation of renewable energies in an efficient way in the process are some of the aspects that, without any doubt, will be part of this sector in the near future.

INVITED SPEAKERS

DIGITAL “KNOW-HOW”

Giorgia Ferrari

Smaltochimica SpA offers to its customers a wide range of possibilities in the digital ceramic world. These opportunities include finished digital products (inks, effects, and glues), mediums for milling directly in customers' plants and the whole milling and quality control system.

Regarding digital products, Smaltochimica portfolio includes:

Inks: “NIK” series

Effects: “SDM” series

Glues: “DIGICOL” series

In the last 2 years, Smaltochimica has gained a high expertise in digital glues formulation, production and application. Digital glues have born as an answer to the fast and deep technological digital revolution of the last few years, substituting the traditional sbobba thanks to many pros, in terms of application and yield.

Smaltochimica has developed different classes of DIGICOL, from total liquid glues to product containing an inorganic phase, to respond to a highly demanding market.

In parallel, customers can build their own milling plant and become independent, with the constant support from Smaltochimica, which includes installation and continuing assistance. Production plants consist of mills, storage tanks, automatic or manual filtering and bottling system, lab supplies for quality control.

Smaltochimica can also offer different proposals of milling and dilution mediums, which allow our customers to create their own system of production, depending on their necessities. Among this portfolio, MCF series is surely the most versatile.

Last but not least, our specialized department, Colour Service, is able to support costumers in the colour management world, with specific software (Colour Profiler) and instruments (spectral scanners).

INVITED SPEAKERS

SLABS PRODUCTION AND FULL DIGITAL DECORATION CONTINUA+ AND TRADITIONAL PRESSING NEW PLANT PROPOSALS

Benedetto Spinelli

SACMI

In order to compete in the global market of ceramic tiles it is necessary to propose a wide range of products and different size and decoration possibilities.

In parallel it is also important to limit production costs.

Each new logic of production must foresee a high flexibility and to this purpose Sacmi proposes plant solutions based on the new available technologies.

One is surely represented by Digital Decoration, which allows easy realisation of a great number of products having excellent aesthetical quality with competitive costs.

A second opportunity is represented by plants for Large Sizes, which considerably simplify the production flow and allow to produce a great variety of modular sub-sizes.

Digital Decoration

The Digital Decoration has already widely established thanks to its unquestionable advantages, which hugely overcome the initial problems.

High graphic resolution, easy realization of prototypes and product changes, decoration without contact even on structured surfaces, little production lots,, limited production costs.

So far the introduction of Digital Decoration occurred with two main aims:

- simplify the decoration lines and realise products of good quality with a lower number of applications
- implement the digital machines on the existing lines, by integrating traditional applications

On the contrary, the real revolution in glazing will be possible thanks to the introduction of full digital decoration, with effective reduction of lines length, greater automation, opportunity of connecting the effects deriving from both dry and wet decoration and easier running.

Therefore, the digital decoration aims at the application of traditional glazes and engobes but above all at the realisation of ceramic surfaces having new chromatic/optical (glossy/matt, iridescent effects, ...) and tridimensional (relief structure) effects.

Lines for Large Sizes

Sacmi plant proposal, with the aim of achieving the highest production flexibility, is represented by recent introduction of lines for large size porcelain slabs.

The advantages of a plant for large sizes are: easy running, higher quality of achievable products, possibility of producing modular sub-sizes by cutting without any die change, reduction of the number of stored finished products.

The most typical large size is 1200x1200 without doubt, which is multiple of standard 600 and 300-sizes.

The size 900x1800 is also interesting for exploiting the space between press columns.

Anyhow the large size par excellence is 3000x1500, with several combinations of interesting submultiples.

On the contrary, the production of only one size at kiln outlet hugely reduces warehouse cost (an intermediate warehouse is enough) but then the cutting costs are higher.

Sacmi proposals for the production of large sizes are:

- traditional line with PH10000 and fast die change, in case
- Continua+

Traditional line with PH10000 and fast die change

It allows the realisation of 1200x1800-max. size and any thickness (3÷30 mm) with output up to
m²/day.

Continua+

It is the NEWEST compacting technology by roller from Sacmi, which allows to produce very large sizes (up to 1600x"unlimited"). It is suitable for thickness ranging from 3 to 20 mm, in function of which it is possible to achieve very high output (12.000 m²/day).

In particular, the new Continua+ technology shows a simple, linear and automated working flow and perfectly integrating with Digital Decoration technologies, such as Dry Digital Decoration, Digital Glazing and Inkjet Decoration.

As a consequence, Sacmi believes the production lines for Large Sizes integrated with digital technologies represent a valid solution for the development requests of the ceramic market because it deals with highly flexible solutions, able to realise products with high added value and with limited costs.

INVITED SPEAKERS

INKJET INKS FOR CERAMIC

Carlos David Diez

Many customers tell us: “I’m using ceramic inkjet inks but I’m only know that is a coloured liquid”

The main issue in this conference is to give a simple tour around an inkjet ink and a ceramic inkjet ink:

What’s an inkjet ink?

What’s a colouring matter?

What’s a medium?

How to make a ceramic inkjet ink?

What parameters do we need to control?

What we need to avoid in any ceramic inkjet ink?

What kind of inkjet inks MEGACOLOR others?

INVITED SPEAKERS

COLOROBIA: ON THE VERGE OF SOMETHING BIG

Miguel Angel JOVANI Colorobia

Colorobia has focused on the latest technological innovations to offer, to the worldwide producers of large format tiles, a top level of expertise not only in Manufacturing, Engineering and Design but also in novel application techniques.

Innovation means that Colorobia's wide portfolio of product series, comprising frits, pigments, compounds, hardened spray dried glazes, digital inks, granular frits, protections etc... provides an infinite number of combinations to obtain enhanced performance and aesthetics and thus high added value large format tiles. Actually, Colorobia series of special frits for porcelain body have become a market standard for top quality porcelain tiles.

Another clear example of technological progress is that the production lines of large and extra large formats have become more simple thanks to extensive industrial experience with the use of spray-dried glazes in the pre-press stage, and consequently less energy consuming. Going several steps further, Colorobia has developed the AIR (Air-friendly Inks Range) concept to minimise the levels of both atmospheric emissions and unpleasant smell at the exit of kiln chimneys, which occur due to incomplete combustion of organics when high laydowns of oil based inkjet inks are applied. Today, the AIR concept, which is based on a Full Digital process, is the best rated environmental solution in the Ceramics market.

Finally, Colorobia has been fully committed to the development of the Industry 4.0 Evolution, having several open collaboration projects with the leading producers of large format lines to analyse and evaluate different continuous monitoring systems.

As always, Colorobia develops and studies continuously all the products from the source, paying maximum attention to environmental and safety aspects which are related with the manufacturing processes, a strong policy and commitment established since the day that the company was born almost one hundred years ago. The proof is our strong knowledge of international regulations and requirements from the markets and local authorities but also from our customers, because our highest commitment with them is to be a trustful partner.

INVITED SPEAKERS**RECENT STUDIES ON REFRACTORY MATERIALS AND NEW MARKETS IN
MAGNESIA PRODUCTS**

Dr. Özkan KURUKAVAK,
KÜMAŞ Manyezit Sanayi A.Ş., Kütahya/Turkey

KÜMAŞ produces and supplies sintered magnesia, fused magnesia, fused oxychrom and calcined magnesia. These products are derived from high quality microcrystalline natural magnesite ore for supply into the industrial minerals market. In addition KÜMAŞ produces basic refractory materials such as magnesia, dolomite and alumina based refractory brick and mortars in its integrated refractory plant. KÜMAŞ has raw material mines, thereby gaining advantage of continuity in production, consistently high quality products and cost control which is reflected in the commerciality to its customers. From raw materials to refractory products and up to complex refractory concepts – our successful basic research is based on in- depth knowledge of the relevant process technologies of the user industries especially iron- steel, cement, lime, glass and non-ferrous metal industry. In recent times, KÜMAŞ is focused on projects related with magnesium chemicals to produce value added products from its own magnesite raw material. Magnesium chemicals are used in waste water treatment, hydrometallurgy, fertilizer, heating elements, animal nutrition, flame retardant and construction panel industry.

INVITED SPEAKERS**FROM LAB TO MARKET: STORY OF A NEW GENERATION PARTICLE TECHNOLOGY: MICNO®**

Ender Suvacı

Department of Materials Science and Engineering, Eskişehir Technical University,
Eskişehir, Turkey Entekno Materials Ltd. Co., 26470, Eskişehir, Turkey

Nanomaterials play critical roles in today's world. Among them, nanoparticles are the most widely utilized group and they have been successfully utilized in many technological applications from electronics to medical industry. Fine size of nanoparticles (typically <100 nm) brings unique properties that can not be achieved at larger sizes (i.e., in submicron or micron form). Although nanoparticles possess unique properties, their fine size may cause processing difficulties such as uncontrolled agglomeration, health and environmental problems. Consequently, when scientists deal with nanoparticles, they should not only focus on advantages of them and produce more and more of those particles but also be aware of the potential problems associated with such fine particles and develop new solutions to overcome such potential problems while maintaining unique properties of nanoparticles. Accordingly, our research group with the sponsorship of Entekno Materials, Ltd. (www.enteknomaterials.com) developed innovative MicNo® Particle Technology, provides both safe and environmentally benign nanoparticle solutions. MicNo particles are designed, platelet shaped micron particles which are composed of nano primary particles. In this presentation, application of the MicNo particle technology to ZnO system and subsequently both optical and biological properties of MicNo®-ZnO particles will be discussed in detail. In addition, transition of MicNo®-ZnO particles to commercial applications will be presented.

INVITED SPEAKERS**SERAMİK PROTOTİP ÜRETİM METOTLARI**

Doç. Dr. Yüksel PALACI

Yıldız Teknik Üniversitesi, Gemi İnşaatı ve Denizcilik Fakültesi. Beşiktaş-İstanbul

Prototip üretimi seri üretime geçmeden önce, ARGE amaçlı sınırlı üretim ve yedek parça üretimi için önemli rol oynamaktadır. Seri üretime geçmek zaman ve maliyet gerektirmektedir. Ürünlerin, seri üretim öncesi performanslarını ölçmek ve bir bütün olarak, diğer ürünlerle etkileşimini inceleme fırsatı sunmaktadır. Ayrıca seri üretim öncesi müşteri onayı ve gerekli kalite belgeleri ve sertifikaların alınması aşamasında zaman kazanılmasını da sağlamaktadır.

Seramik prototipleri de, çeşitli metotlarla üretmek mümkündür. Bu metotları, plastik şekillendirme, eklemeli üretim ve eksiltmeli üretim olarak sıralayabiliriz. Plastik şekillendirme metotları olarak, Düşük basınç enjeksiyon kalıplama, ekstrüzyon, presleme, şerit döküm, asıntı döküm, ve benzeri verilebilir. Eklemeli üretimlerde, eritme/katılaştırma, ısı ile sertleştirme, yapıştırma, lazer sinterleme, ve eritme biriktirme olarak sıralayabiliriz. Eksiltmeli üretimi de, lazer veya iyon demeti buharlaştırma, yaş işleme, beyaz işleme ve sinter sonrası işleme olarak sıralayabiliriz.

Bu sunumda, farklı metotlarla üretilmiş prototiplerden örnekler verilecek ve metotların ürün özelliklerine, üretim süresine ve maliyete etkileri tartışılacaktır.

INVITED SPEAKERS**CERAMIC PROTOTYPE MANUFACTURING METHODS**

Assoc.Prof. Dr. Yüksel PALACI

Yıldız Technical University, Faculty of Naval Architecture and Maritime, Beşiktaş-İstanbul.

Prototype production plays an important role for limited production, spare parts production and for R&D before serial production. Passing serial production requires time and cost. Prototype production offers the opportunity to measure products' pre-production performance and, as a whole, to explore interaction with other products. It also provides pre-production customer approval and time-saving of obtaining required quality documents and certificates.

Ceramic prototypes can be produced by various methods. We can list these methods as plastic forming, additive manufacturing, and subtraction manufacturing methods. Examples of plastic forming methods are low pressure injection molding, extrusion, pressing, type casting, extrusion, slip casting, and etc. In additive manufacturing, we can list as melting/freezing, UV light hardening, glue bonding, Selective laser sintering, and melting accumulation like ion beam melting. We can rank subtractive production as, laser or ion beam evaporation, green machining, white machining, and machining after sintering.

In this presentation, examples of prototypes produced with different methods will be given. Prototype ceramic part characteristics depending on the manufacturing methods, production time, and financial effects will be discussed.

INVITED SPEAKERS

PRIME

Massimo PRODI

The demand for product personalization and the reduction of lots, the complete digitalization of processes, the use of shared resources and the efficient management of data, are new challenges with modern manufacturing industries. These are fundamental elements for the sustainable development of the new paradigm based on:

- Intercommunicating Technologies “Industrial Internet of Things”;
- Perimeter of action “from Customer to sensor”
- Improvement of the concept of “Lean Manufacturing”
- Implementation of “Make to Order”;

PRIME is the answer of System: a software services platform developed internally, interface natural 3D real time, integrated with Enterprise Resource Planning (ERP), direct connected with machines, designed to be predictive, incorporates analysis tools, covers the 5 levels of stack ISA 95.

The system, highly integrated and connected, makes it possible to organize the information flows of entire plants, and is designed to meet the following requirements:

- control entire plants and more factories;
- standardize data management;
- provide simple information to guide decisions;
- reduce product change times;
- optimize production lot;
- obtain the actual production cost;
- move towards the «zero defects» target;

INVITED SPEAKERS

NEOS AWARE

Ximo PIQUER
Neos Ceramics

NEOS AWARE proposes modeling, simulation and mathematical optimization as an alternative to trial-error procedure. NEOS AWARE computer engineering combines a self-awareness concept with the ceramic know-how, suitable to find solutions in complex and heterogeneous systems in our industry.

This artificial intelligence technology provides quick by evaluating millions of formulas to achieve maximum cost reduction and increased quality

INVITED SPEAKERS

LAMGEA TECHNOLOGY FOR PRODUCTION OF BIG TILES & SLAB

Enrico QUARTIERI

System Ceramics

This is a presentation of System's technology Lamgea for the production of ceramic big tiles and slab surfaces. System Spa introduces this technology in the market 13 years ago, and specially in the last 3 years we made relevant numbers of installations and this technology is spreading well all over the world.

Thanks to Lamgea technology is possible to produce big size ceramic slabs, in variable thickness from 3 to 30 mm, and with dimension up to maximum size 1600x4800mm, with very high production capacity.

After the press, the slab can be handled and produced in its big entire dimension, or green cut in subsizes, according to the necessity of the customer and the final destination of use, allowing the customer to be free to decide whatever thickness he needs to produce irrelevant by the size.

The main technical characteristics and advantages of the ceramic product realized with our technology are:

- No residual tension inside the body after the press
- Limited caliber variation at kiln exit: ± 2 mm (optimization in rectifying process)
- Great planarity of the product (optimization in polishing/full lap top process)
- Possibility of structured relief surfaces, with structures up to 2 mm depth, in high resolution
- Possibility of production big size in lower thickness, with great saving of raw material, great saving of energy (electrical and gas), transport cost (lighter material)

Moreover, here below the main advantages and plus point of our Lamgea technology:

- Press functionality easy to learn
- Simple process to manage and very stable over the time
- Use of standard body: no additive nor specific composition
- Standard body humidity 4 – 6%
- No foundations requested
- 100% waste recovery
- Reduction of greenhouse emissions
-

The products realized with our technology can have several different destination of use, such as wall and floor application, outside façade, countertop for bathrooms and kitchens, interior furnishing and complements.

INVITED SPEAKERS**CERAMICS AND ARMOURS: THE STATE OF THE ART IN CERAMIC ARMOURS
AND FUTURE POTENTIALS IN TURKEY**

Gökçe DARA

Roketsan

Ceramics with their intrinsic properties became material of choice for ballistic protection against armor piercing rounds in body armour and aircraft platforms. With increasing asymmetric warfare situation armies increasingly looking for better armor protection, thus survivability and ballistic protection became the main factor for land vehicle designers.

The lighter and higher protection capability composite armors increasingly relied on ballistic ceramics and polymeric composites for protection against light to medium caliber direct fire threats and improvised explosive device (IED) threats in the last 20 years. With the wide spread use of anti-armor shape charge threats ballistic ceramics found a new application field in passive armors providing better performance in some aspects accordingly becoming an alternative to reactive armor for armored vehicles.

Turkey with significant number of armored vehicle manufacturers has great requirement and potential for armor development and production. Al_2O_3 , SiC and B_4C constitutes the bulk of the ballistic ceramic market with significant research going into reducing price and increasing performance of these materials. On the other hand so called nano-ceramics and novel ceramic composites and 3D printing techniques allowing bio-mimicking structures combining two or more materials requires special attention for future armor applications.

In this review a brief summary of ballistic ceramic evolution will be given followed by current market shares and future trends will be explored.

INVITED SPEAKERS**PROCESSING AND PERFORMANCE OF α/β -SIALON CERAMICS**

Ferhat KARA
Eskişehir Teknik Üniversitesi

Ferhat Kara¹, Servet Turan¹, Alpagut Kara¹, Ufuk Akkasoglu^{1,2}, Ali Celik³,
Hande Marulcuoğlu¹, Hasan Mandal⁴

¹Department of Materials Science and Engineering, Anadolu University, 26555 Eskişehir, Turkey

²MDA Advanced Ceramics Ltd., Teknoloji Gelistirme Bolgesi, Organize Sanayi, 26140 Eskişehir, Turkey

³Department of Metallurgy and Materials Science Engineering, Bilecik Seyh Edebali University, 11230 Bilecik, Turkey

⁴Faculty of Engineering and Natural Sciences, Sabanci University, 34956 Tuzla, Istanbul, Turkey

SiAlONs are ceramic materials with a range of technically important applications, from cutting tools to wear parts and the properties of SiAlONs can be tailored for specific applications.

α/β -SiAlONs have been widely used for machining of cast irons and superalloys where the performance of the material is governed by intergranular phase chemistry.

With this respect, types and amount of liquid phase sintering additives, which affect the distribution and crystallinity of intergranular phase and remnant of the additives after sintering, play an important role.

This presentation will address the effect of various types of sintering additives on the intergranular phase chemistry and microstructures of α/β -SiAlONs and their subsequent performance in cast iron turning and in high speed superalloy milling. Some processing issues related to SiAlON ceramics including pressureless sinterability as well as shaping of complex parts by coagulation casting will also be mentioned.

INVITED SPEAKERS

PIEZOELECTRIC CERAMIC FIBERS AND FIBER-BASED PIEZOCOMPOSITES

Sedat ALKOY
Gebze Technical University

INVITED SPEAKERS**EMERGING APPLICATIONS OF HALLOYSITE-POLYMER NANOCOMPOSITES**

Yusuf Ziya Menciloglu

Sabanci University, Faculty of Engineering and Natural Sciences, 34956, Istanbul, Turkey

Halloysite is a clay material with hollow nanotube structure. As a naturally occurring nanotube with aluminosilicate chemistry, nano-sized radius, high length-to-diameter ratio and contrast chemical properties between inner and outer lumina, Halloysite Nanotubes (HNTs) have been intriguing templates to immobilize nanoparticles. In addition, HNTs are very convenient materials for nanocomposite applications due to their cost-efficient mass-production. Therefore, these natural nanotubes have been promising materials in many research fields, particularly in industrial research applications.

A remarkable application of HNTs is the loading of inner lumene with various active agents, including macromolecules, followed by extended/delayed release of the active agent. Incorporating with industrial polymers, this method offers a wide variety of substantial applications ranging from chemical carriers to controlled release agents. Preparation and applications of nanocomposite films, in which the active agent-filled HNTs are incorporated into polyolefin matrices, will be discussed in two case studies. The applications of such films in the area of active food packaging and controlled release of pesticides will be explained in detail. Process details along with mechanical and thermal traits of nanocomposite films will be explained. Activity tests of the nanocomposites and the observed advances with respect to application area will be presented.

INVITED SPEAKERS**POWDER SYNTHESSES OF ADVANCED CERAMICS USING NOVEL APPROACH – DCR PROCESS**

Ali Osman KURT

Sakarya University, Research-Development and Application Centre (SARGEM), 54187, Sakarya, Turkey.

Advanced ceramics are critical material in many industries, such as health, electronics, military, high temperature and many other area of applications. They are in general costly products due to the nature of their production methods that initially rely on high quality synthetic powders. Good quality powders, i.e., high purity, very fine and uniax grains are very expensive and could be obtained with complicated and costly processes. Therefore, it is important developing new and competitive powder production techniques to enabling easy access to cheap ceramic powder raw material supply. In this concept, recently the dynamic / carbothermal reduction (DCR) process was developed and successfully applied in synthesizing some advanced ceramics powder, namely silicon nitride (both α or β form of Si_3N_4), aluminium nitride (AlN), boron nitride (BN), boron carbide (B_4C), titanium nitride (TiN), zirconium nitride (ZrN) and titanium diboride (TiB_2). DCR is the high temperature process taken place between 1300 – 1500 °C under controlled atmosphere in rotary furnace. Although DCR technique was successful in synthesizing such important advanced ceramic powders in required quality, it was only applied in laboratory scale (i.e. on the order of a few grams per day). Further work for prototype scale (a few kilograms per day) synthesis of such powders are planned before moving to the industrial scale (a few hundred or tons per day) production.

INVITED SPEAKERS**LOW TEMPERATURE SYNTHESIS AND CHARACTERIZATION OF HIGH PURITY NANO BORON CARBIDE (B₄C) STRUCTURES**

Cengiz Kaya^{1,2*}, Suna Avcioglu^{3,4}, Figen Kaya⁴

¹Materials Science and Nano Engineering, Faculty of Engineering and Natural Sciences, Sabanci University, Istanbul, Turkey

²Nanotechnology Research and Application Centre (SUNUM), Sabanci University, Istanbul, Turkey

³Department of Materials Science and Engineering, Faculty of Engineering, Ondokuz Mayıs University, Samsun, Turkey

⁴Department of Metallurgical and Materials Engineering, Faculty of Chemistry and Metallurgy, Yildiz Technical University, Istanbul, Turkey

Abstract

Boron carbide (B₄C) is accepted as an important engineering material due to its high melting point, high hardness, high Young's modulus, excellent radiation (neutron) absorption properties and low thermal conductivity. Although different methods, such as high temperature carbothermic reduction and chemical vapor decomposition, have been used to synthesize boron carbide, a low cost technique that provides high purity B₄C with no residual carbon, is required by industry. Therefore, in the present study, synthesis of high purity, high crystallinity nanostructured boron carbide particles with various morphologies, is proposed using a modified low-temperature sol gel process. The effects of starting chemicals, calcination and sintering temperature/time on the formation of B₄C structures, morphology and stoichiometry were reported. Detail characterization studies including TEM, XRD, NMR and DTA were used to support the results on the formation of stoichiometric boron carbide with high crystallinity at low temperatures.

Acknowledgements

The authors are grateful for the financial support from the The Scientific and Technological Research Council of Turkey (TUBITAK) under the contract numbers of 216M140 and 216M145.

INVITED SPEAKERS**SYNTHESIS OF ENVIRONMENTALLY FRIENDLY (H00) ORIENTED PLATE-LIKE
LEAD FREE CERAMIC POWDERS FOR HIGH PERFORMANCE PIEZOELECTRIC
CERAMIC DEVELOPMENT**

Murat Avcı¹ and Ender Suvacı^{1,2} ¹ENTEKNO, Corp. Eskişehir/Turkey

² Department of Material Science and Engineering, Eskişehir Technical University, İki Eylül Campus,
26480/Eskişehir/Turkey

It is estimated that global market for piezoelectric actuators alone to be approximately \$ 7 billion with a steady 13% growth rate annually. Most of the products in the market have > 60 wt.% lead oxide within their compositions which is very toxic for environment and human health. With the increase of environmental awareness, most developed countries have regulations which restrict the use of toxic materials and encourage the development of lead-free materials for electronic applications. There are two approaches to develop lead-free ceramics with high and applicable performances: (i)- designing chemical composition and (ii)- texturing microstructure with desired crystallographic direction. Very high piezoelectric responses and strains can be obtained by texturing. (h00) oriented anisometric particles (templates) are basic components for textured ceramics. In recent technology some transition temperature variations could be occurred in textured ceramics produced via Templated Grain Growth (TGG) or Reactive TGG methods. It is postulated that lattice mismatch between the templates and oriented grains could cause interfacial stress and polar nanoregions and thus the phase transition temperature variations. According to synthesis techniques, templates could have some impurities which affect crystal structure beside chemical composition. The findings in this work facilitates to design chemical and physical properties of templates for textured lead free piezoelectric ceramics with high temperature stability and piezoelectric performance. In this presentation, effects of processing conditions on particle chemistry, size and shape during plate- like particle synthesis will be discussed in detail.

INVITED SPEAKERS

RECENT DEVELOPMENTS IN THE FIELD OF EPITAXIAL FERROELECTRICS

Lucian Pintilie

National Institute of Materials Physics, Atomistilor 405A, Magurele, Romania

Ferroelectrics are multifunctional materials with a broad range of applications, many of them based on two very important material quantities: the spontaneous polarization and dielectric constant. Here we discuss a few aspects regarding the two quantities, namely:

- Complex relation between electrode interfaces, polarization and leakage current, based on experimental results showing that the properties of the electrode interface (especially the magnitude of the barrier height) are largely controlled by the spontaneous polarization. Examples will be given for several materials including two PZT compositions, BaTiO₃ and BiFeO₃.
- Possible self-doping effects in epitaxial ferroelectric films, suggested by the results obtained on PZT layers grown on SrRuO₃ electrodes. The microscopic analysis underlines that vacancies are involved, being generated during the growth of the films with dominantly upward polarization. The results also suggest that compensation mechanisms are different in very thin films and bulk.
- Uncertainty on the values of material constants, especially dielectric constant, as the reported numbers spread over order(s) of magnitude. Examples are given, in relation to microstructure, interfaces and measurement conditions. All the results strongly suggest that extremely high precautions should be taken when selecting experimental values for simulations or theoretical modeling. A few comments are made on this problem of “material constants”.

At the end, some new developments towards applications in high-tech domains will be presented (e.g. non-volatile memories, pyroelectric IR detectors).

INVITED SPEAKERS**SHAPEABLE MAGNETOELECTRONICS AND MAGNETORESISTIVE BIOSENSORS**H. Pişkin^a, B. Özer^a, N. Akdoğan^{a,b}^aDepartment of Physics, Gebze Technical University, 41400 Gebze, Kocaeli, Turkey ^bInstitute of Nanotechnology, Gebze Technical University, 41400 Gebze, Kocaeli,

Shapeable (flexible, printable, and even stretchable) magnetoelectronics became one of the most important technological research fields of the last years. Foreseeable applications of highly sensitive, cost effective and re-shapeable magnetoelectronics also include magnetic particle detection in microfluidics and lab-on-a-chip platforms. Magnetoresistive-based biochips, detect magnetic labels instead of fluorescent labels, have been extensively investigated for sensitive measurement of low bio-target concentration in body fluids. The main aim of these investigations is development of high sensitive magnetic field sensors that are optimized for magnetic label detection. All magnetic biosensors detect the stray field of magnetic particles that are bound to biological molecules. Since the biological environment is normally non-magnetic, the possibility of false signals being detected is negligible. In this talk, I will give a brief information about shapeable magnetoelectronics and explain the principles of magnetoresistive biosensors. I will also talk about our ongoing research on planar Hall effect-based biosensor applications.

This work was supported by TÜBİTAK (The Scientific and Technological Research Council of Turkey) through project number 116F083.

INVITED SPEAKERS**DISPLAY TECHNOLOGIES AND THIN FILM DEPOSITION TECHNIQUES**Emine Tekin ^a^aMaterials Institute, Marmara Research Center, TUBITAK, 41470 Gebze,

Kocaeli, TURKEY

OLED is a new technology, which can be applied for Displays and Lightings. OLEDs have many advantages over the alternative technologies: They are thinner, lighter and more flexible. OLED devices require low voltage and low power. Since OLEDs can be flexible, they have robust design facilities in terms of geometry, size etc. In a typical OLED device: there are substrate, anode, hole transport layer (HTL), emissive layer (EML), electron transport layer (ETL), and cathode. OLED substrates should have good H₂O and O₂ barrier properties besides transparency. OLED active layer materials are generally two types: polymers and small molecules. Small molecules have limited solubility therefore they are processed by vacuum deposition method to produce thin films. Polymers are soluble and can be processed by solution based methods spin coating, inkjet etc. Inkjet printing is used to deposit exact amount of material on an addressable places. Therefore one can print RGB materials in different pixels in very defined way. For this method almost there is no material waste. On the other hand small molecule fabrication requires high vacuum, shadow mask and mask aligning for RGB pixels. Material waste is very high, so it is expensive method.

INVITED SPEAKERS

SMART STRUCTURES: METAL OXIDE NANOSCALE MATERIALS

Ramis Mustafa Öksüzoğlu *

Department of Materials Science and Engineering, Faculty of Engineering, Technical University of Eskişehir 26555, Turkey

The metal oxide materials (VO_x, WO, V-WO, Y-Ba-Cu-O, TaO_x, BaSrTiO₃ and La-Sr-Mn-O) compared with metallic and semiconductor resistor materials (Pt, Si-Ge, amorphous Si) became importance due to their high and widespread application potentials in optoelectronic devices and systems. Among these materials, vanadium oxide has gained great importance due to its superior electrical and optical properties. Several efforts were made to produce vanadium oxide (VO_x) ceramics in nanoscale due to their outstanding physical and chemical properties applicable in many technologies such as smart windows, thermochromics, energy-harvesting, batteries, thermal cameras, night seeing, security issues etc. [1,2]. In form of nanoscale thin films, VO_x ceramics indicates low electrical resistivity, adequate temperature coefficient of resistance (TCR), low electronic noise and capability to integrate into the CMOS devices, which make these thin films essential for uncooled IR-detectors, i.e. microbolometers [3]. Between different phases (VO, V₂O₃, VO₂, V₆O₁₃, V₃O₇ and V₂O₅), V₂O₅ phase indicate high TCR, but high electronic noise [3-5]. VO₂ is desired due to its extended optical properties [6,7], adequate TCR and low electronic noise; however, high deposition or post-annealing temperatures (>400°C) are crucial in production of the films with VO₂ phase. Recent works reveal that the post-annealing processes open more possibilities to optimize properties of vanadium oxide thin films for detector applications [8,9]. However, the post-annealing conditions must be applicable to the CMOS production, especially annealing temperatures (<400°C) are necessary to protect the CMOS structure [1]. The present work focuses on the influence of post-annealing process on the structural properties. The correlation between structural and electrical properties including electrical noise is going to be discussed.

*This research is supported by the Scientific and Technological Research Council of Turkey (TUBITAK) and Aselsan - MGEO A.Ş with different projects (Project numbers: 109M025, 213M494, 111T351).

- [1] Bin Wang *et al*, Infrared Physics & Technology, 57, 8-13, 2013.
- [2] V. Y. Zerov *et al*, Technical Phys. Letters, 27, 5, 378–380, 2001.
- [3] R.T. Rajendra Kumar *et al*, Materials Research Bulletin, 38, 1235–1240, 2003.
- [4] Szabolcs Beke, Thin Solid Films, 519, 1761–1771, 2011.
- [5] R. M. Öksüzoğlu *et al*, Optics & Laser Tech. 48, 102, 2013.
- [6] Ulas Kürüm, R. M. Öksüzoğlu *et al*, Optics Communications 333, 109–114, 2014.
- [7] Ulas Kürüm, R. M. Öksüzoğlu *et al*, Journal of Optics 17(1):015503, 2015.
- [8] Nicholas Fieldhouse *et al*, J. Phys. D: Appl. Phys., 42, 055408, 2009.
- [9] Rong-Hong Chen *et al*, IEEE Electron Device Letters, 35, 7, 2014.

INVITED SPEAKERS

SPINTRONICS AT NANOSCALE METAL/CERAMIC INTERFACES

Ramis Mustafa Öksüzoğlu*

Department of Materials Science and Engineering, Faculty of Engineering, Technical University of Eskişehir 26555, Turkey

Magnetic sensors using different effects based on the spin of electron are now being used in automobile and mobile systems as well as in DNA or protein detection [1, 2], under the name "spintronic devices (spintronics)". In parallel, the "Industry-4.0 revolution" – digitalization and intelligent systems – has further increased the potential of spintronic devices to be used in the "intelligent materials" category [3]. Design of the spintronic devices are based on Spin Hall (SHE) [4] and Tunnel Magneto Resistance effects (TMR) [5]. The disadvantages of spintronic devices using SHE and TMR effects can be listed as complex and costly production processes, the high energy consumption and necessity to use of an external magnetic field.

The recently developed spin Hall magnetoresistance (SMR) effect based on the SHE has drawn increasing interest. SHE effect is closely related to the spin-torque effect [6], which enables to design spintronic devices with low energy consumption and without an external magnetic field. In this context, different materials have been studied: YIG, CoFe_2O_4 , NiFe_2O_4 , Fe_3O_4 , LaCoO_3 , CeFeB , Pt, Pd [7, 8, 9]. Based on current research results, it is stated that the ratio of SMR effect at the extruded metal/ceramic interfaces such as W/ CoFeB / MgO /Pt can be increased up to 70%, based on the comparison between nanoscale metal/ceramic binary and triple thin film systems [6]. Material systems with higher SMR effects can be more easily utilized in spintronic devices with lower production cost and low energy consumption [7, 8].

In the present work, the potential spintronic device structures and nanoscale metal/ceramic material systems are going to be discussed.

*This research is supported by the Scientific and Technological Research Council of Turkey (TUBITAK) and Anadolu University with different projects (Project numbers: 106M517, 1001F98, 1006F138).

- [1] S. G. Grancharov, H. Zeng, S. Sun et al., *Journal of Physical Chemistry B*, vol. 109, no. 26, pp. 13030–13035, (2005).
- [2] J. M. Daughton, *IEEE Transactions on Magnetics*, vol. 36, no. 5, pp. 2773–2778, (2000).
- [3] Robert Bogue, *Assembly Automation* Vol. 34 Issue: 1, pp.16-22, (2014).
- [4] Kato, Y. K., Myers, R. C., Gossard, A. C. & Awschalom, D. D. *Science* **306**, 1910–1913 (2004).
- [5] M. Yıldırım, R. M. Öksüzoğlu, *Journal of Magnetism and Magnetic Materials* 379, 280–287 (2015).
- [6] Guang Yang, Yongye Li, Xi Chen, Jingyan Zhang, and Guanghua Yu, *Advances in Condensed Matter Physics*, Article ID 9734610, (2016). <http://dx.doi.org/10.1155/2016/9734610>.
- [7] S. Cho, S. H. Baek, K. D. Lee, Y. Jo, and B. G. Park, *Sci. Rep.* 5, 14668 (2015).
- [8] M. Isasa, A. Bedoya-Pinto, S. Vélez, F. Golmar, F. Sánchez, L. E. Hueso, J. Fontcuberta, and F. Casanova, *Appl. Phys. Lett.* 105, 142402 (2014).
- [9] T. Lin, C. Tang, H. M. Alyahyaei, and J. Shi, *Phys. Rev. Lett.* 113, 037203 (2014).

INVITED SPEAKERS**CERAMICS AND ENERGY: INTERMEDIATE TEMPERATURE SOLID OXIDE FUEL CELLS**

Tayfur Öztürk

ENDAM, Center for Energy Materials and Storage Devices, Middle East Technical University ,
06800 Ankara Dept. of Metallurgical and Materials Engineering, Middle East Technical
University, 06800 Ankara

Dept. of Metallurgical and Materials Engineering, Middle East Technical University, 06800
Ankara

Recent developments in renewable energy is likely to transform the current energy system into a new form. Solar and wind energy with a cost less than those produced by fossil fuels would be the dominant mode of energy production. Intermittent nature of these energy pose a number of problems that need to be solved in coming years. Intense research efforts are currently underway to develop low-cost batteries to be able to store these energies and release it when needed. The overall energy system involves not only electricity but also natural gas. These two grids need to be considered together in the coming era. To switch energy from one grid to the other is essential for the proper integration of these energy system. Currently it is possible to convert the energy of natural gas to electricity via thermal power plants. The reverse is also possible in theory, i.e. power to gas conversion, but currently there are a very few examples of it. This switch from conversion of power to gas is important not only for the proper integration of the energy system, but also because it is much easier to store gas than it is to store electricity.

Fuel cells as a energy conversion devices have been in the center of much research efforts over a number of decades. Solid oxide fuel cell(SOFC) with its versatile use of fuels has attracted much attention. This was also the case for SOEC, i.e. solid oxide electrolyser cell, which can convert electricity to gas. Although the operational SOFCs were developed in 1980's in the temperature range of 850–1000 °C, they have not penetrated into the market because of the high operating temperatures. Although there are suitable materials that can function at these temperatures, it is very problematic to sustain the required durability and to afford high material cost. Thus, in order to decrease the material cost and to increase the life time of the cell, it is necessary to reduce the operating temperature of SOFC. Therefore, efforts concentrated towards the so-called intermediate temperature solid oxide fuel cells (IT-SOFC), i.e. cell that have acceptable performance at temperatures between 700-500 °C. Electrolyte and anode materials are already available that would function at these reduced temperature, but the main problem is sluggish ORR in the cathode materials. Therefore, efforts to develop IT-fuel-cells amounts to finding cathode materials that would have sufficiently fast ORR.

In this work, we report results from an extensive research program that we have undertaken at ENDAM, METU to develop LSC based cathode materials with an acceptable ORR kinetics [1,2]. The material under study was LSC113-LSC214 composites fabricated via sputter deposition in a wide range of compositions, i.e. 0.10:0.90< LSC113/LSC214<0.90:0.10 using combinatorial approach. The study has shown that the mid- compositions were particularly favorable yielding acceptable ORR kinetics at temperatures as low as 575oC. Cathodes at mid-compositions were either amorphous or nanocrystalline with a very stable performance over extended use.

- [1] Z. Ç. Torunoğlu, D. Sarı, O. Demircan, Y. E. Kalay, T. Öztürk, Y. Kuru “One pot synthesis of (La,Sr)CoO₃/(La,Sr)₂CoO₄ for IT-SOFCs cathodes” International Journal of Hydrogen Energy, 2018, DOI: 10.1016/j.ijhydene.2018.04.238
- [2] D. Sari, F. Piskin, Z. C. Torunoglu, B. Yasar, Y. E. Kalay, T. Öztürk “Combinatorial development of nanocrystalline/amorphous (La,Sr)CoO₃-(La,Sr)₂CoO₄ composite cathodes for IT-SOFCs”, Solid State Ionics (in press)
- [3] D. Sarı, B. Yasar, F. Piskin, Y. E. Kalay and T. Öztürk “Segregation resistant co-sputtered LSC-113/LSC-214 composite cathodes for It-SOFCs” (in preparation)

INVITED SPEAKERS**CERAMICS AND ENERGY: STATE OF THE ART IN CATHODE MATERIALS FOR SOFC**Aligül Büyükaksoy¹¹Department of Materials Science and Engineering, Gebze Technical University,
Kocaeli/Turkey

The growing world population and the widespread use of personal technological devices cause an increase in the world's energy demand. This demand has been met by the combustion of fossil fuels, which result in the fast depletion of limited fuel resources and enhanced carbonaceous gas emissions that are harmful for human health. Solid oxide fuel cells (SOFCs) are ceramic membrane-based energy conversion devices that can operate either on hydrogen or hydrocarbon fuel gases with efficiencies reaching 80%. This renders them promising alternatives to the conventional energy conversion routes. However, SOFCs are yet to become a commercial success, due to the high cost per power they offer and the long-term instability they exhibit at the operating temperatures of 800 – 1000 °C. These issues can be resolved by obtaining high specific powder density from SOFCs and, if possible, achieving this goal at low operating temperatures (e.g., ≤ 700 °C).

To develop SOFC cathodes that can exhibit high ORR activity, three different approaches of research have been adopted; pursuit of *i*) mechanistic understanding that would later allow the development of new strategies for cathode development, *ii*) novel cathode material chemistries that exhibit high electrocatalytic activity or *iii*) new fabrication methods that would yield desirable microstructures and thus, high electrochemical performance. In this talk, along with a brief literature review, the research of our group at Gebze Technical University on the development of novel SOFC cathode fabrication methods and the microstructure- electrochemical performance relationship they yield will be presented. More specifically, fabrication of single-phase mixed ionic electronic conductor (MIEC) perovskite and perovskite- ionic conductor composite thin film cathodes by polymeric precursor-based methods and the resulting properties will be the focus.

INVITED SPEAKERS

ELUCIDATING MICROSTRUCTURAL EVOLUTION IN SOFC CATHODE PROCESSING BY TRANSMISSION ELECTRON MICROSCOPY

Cleva W. OW-YANG^{1,2}, Aligül BÜYÜKAKSOY^{3,4}, E. Aycan EKSIOGLU⁵, Meltem
SEZEN²

¹Materials Science and Nano-engineering Program, Sabancı University, Orhanlı, 34956
Tuzla/İstanbul, Turkey

²SUNUM Nanotechnology Research Center, Sabancı University, Orhanlı, 34956
Tuzla/İstanbul, Turkey

³Department of Materials Science and Engineering, Gebze Technical University, 41400
Gebze/Kocaeli, Turkey

⁴Institute of Nanotechnology, Gebze Technical University, 41400 Gebze/Kocaeli, Turkey

⁵Department of Physics, Gebze Technical University, 41400 Gebze/Kocaeli, Turkey

When it comes to portable, off-grid power, fuel cells are a compelling technology. With an infinite supply of oxygen from ambient air, they will convert chemical potential energy from a fuel, *i.e.* some form of hydrogen, to generate electricity. Despite subverting the need for expensive metal catalysts, solid oxide electrolyte fuel cells (SOFCs) require high operating temperatures to offer impressively high efficiencies. Improving SOFC performance at lower temperatures, while preserving the high energy conversion efficiency, has motivated numerous innovative engineering design solutions for SOFC materials, such as the development of nanocomposite electrodes. One example is a cathode that allows the gas phase to directly contact 2 nano-sized solid phases, La_{0.8}Sr_{0.2}MnO₃ (LSM) and Sm-doped CeO₂ (SDC), simultaneously. Oxygen is reduced at this 3-phase junction, where it forms oxygen ions with electrons supplied from LSM, and these ions are transported through the SDC percolation path to the electrolyte. Because a longer 3-phase contact line would increase the reaction density, we sought to produce cathodes composed of LSM and SDC nanoparticles. Our hypothesis was that the optimal system could be produced by a Pechini-based approach, by annealing an amorphous, homogeneous gel coating. Our goal was to understand the processing parameters to control the induced crystallization of nanoparticles of 2 phases simultaneously. Thus, for feedback on the microstructural evolution of such a morphologically and chemically complex system, we performed high resolution imaging and spectroscopy analyses on FIB-milled lamellae in a spherical aberration-corrected scanning transmission electron microscope (STEM). Spectrum imaging using characteristic x-ray and primary electron energy loss signals allowed us to evaluate local variations in stoichiometry and segregation due to differences in ionic diffusivity.

INVITED SPEAKERS**PHASE TRANSFORMATIONS OF MINERALS DURING CALCINATION OF
BULGARIAN KAOLIN AND OBTAINING PRODUCTS WITH A COMMERCIAL
APPLICATION**

Kremena Mincheva¹, Erdem Kurt², Aylin Dzhelyaydinova³,

^{1,3}Kaolin EAD, Senovo/Bulgaria

² KAOLIN Endustriyel Mineraller San. ve Tic. A.S. Istanbul/Turkey

Phase transformations in the calcination of Kaolin EAD's Bulgarian enriched kaolin, mined from Vetovo area, Ruse region, are examined. For this purpose, kaolin is heated to 1350°C and at certain points of the temperature interval (850°C, 1100°C and 1350°C) characteristics of the products obtained – chemical content (RFA), mineralogical composition (XRD), specific density, water absorption, color etc. are determined. The results show that at 850°C the kaolinitic lattice is completely decomposed which results in the formation of a maximum amorphous phase amount without thermal changes in the structure of the quartz. At 1100°C mullite formation starts and at 1350°C mullite, cristobalite, quartz and amorphous phase are registered at the same time. Water absorption, a criterion for the degree of kaolin sintering, logically decreases with increase in temperature, while the specific density slightly rises, and then lowers because of cristobalite phase formation.

The products obtained at these temperatures – metakaolin, calcined kaolin and chamotte, respectively, have specific properties and find application in a number of areas (ceramics, plastics, rubber, paints, coatings, concrete etc).

INVITED SPEAKERS**FIRING BEHAVIOR OF THE CLAYS USED IN THE CLAY-BASED CERAMIC PRODUCTION**

Aydın Aras

Van Yüzüncü Yıl University, Geological Engineering Department Van /Turkey 65080

The most common type of clay used in clay-based ceramic production e.g., tile, sanitary ware, and tableware is sedimentary origin i.e., “ball clay” that is composed primarily kaolinite accompanied by one or more of the mica-minerals such as illite, chlorite, and montmorillonite. The common clays used in pottery and brick production contains a large amount of illite and little amount of kaolinite. The ball clay and common clay may also contain varying amounts of smectite. The residual kaolin i.e. china clay used in the production of sanitary ware and tableware is well dressed and may contain very low amounts of illite-mica and other oxide impurities and has high crystallinities degree. The natural and industrial mixes of these three main clay classes; i.e., kaolinite, illite, and smectite groups are used together with feldspar and quartz minerals in clay-based ceramic production. The high-temperature phases of relatively pure clays of these three classes have been studied extensively and documented in the literature. The natural and industrial mixtures. i.e., the complex mineralogical composition of the green body makes the high-temperature phases and related physical properties of the fired body complicated and poorly reliable predicting. This work aims to summarize our knowledge about the high-temperature phases and formation sequence in clay-based ceramic bodies derived from the main three classes; i.e., kaolinite, illite and smectite and provides a reliable predicting model for the mineralizing processes taking into account results natural and industrial of mixture of these clay classes used in production . The main intrinsic characteristics e.g., crystallinity degree of kaolinite minerals in kaolinitic clays and the chemical composition of octahedral layer and interlayered cations of illite and smectite minerals have major importance in high-temperature phase formation and formation sequence. The different phases and formation sequences are observed between the ball clay and china clay, between cheto and wyoming type of smectite, between biotite with muscovite type of illite. Besides , the alkaline and earth alkaline elements contents and their concentration gradients and diffusion rates are also major importance newly-formed phases of clay based ceramic bodies.

INVITED SPEAKERS

MODERN MATERIAL PREPARATION FOR THE CERAMIC INDUSTRY: TRIED AND TESTED SOLUTIONS SUITABLE FOR PROCESSING SLURRIES AND SUSPENSIONS

Alban BUNJAKU

EIRICH

Various techniques are available for the production of suspensions and emulsions. The machines used for these mechanical dispersing techniques are generally only designed for a certain dispersion viscosity range, and the processing times are long. EIRICH dispersing technology is different. It can be used to process a free choice of viscosity ranges (and consistencies), and this within processing times of just minutes. EIRICH dispersing mixers, which are now also known as MixSolvers[®], have been in use for decades in many industries. They are used to process e.g. coating pigments for paper manufacturing, microsilica or pigment suspensions, road marking compounds, printer toner, lithium-ion compounds for rechargeable batteries and spray slip/casting slip e.g. for tiles, sanitary ceramics and technical ceramics, such as dispersions for film casting processes.

For manufacturers of technical ceramics, a special property of the MixSolver[®] is of particular interest: By virtue of the system, upscaling is very straightforward. This is important because the production process is normally preceded by the development of the formulation in the laboratory. Thus, MixSolvers[®] are in use in many research institutions and universities, taking advantage of the fact that a process developed for new products can be easily upscaled from a laboratory mixer to a production mixer.

In addition, both intrinsically viscous (shear-thinning) and dilatant (shear-thickening) suspensions can be reproducibly manufactured. Here, the purity of the material is preserved, as contamination with abrasion from the parts that come into contact with product is prevented through the use of corresponding linings and armor coating.

INVITED SPEAKERS

**MECHANOCHEMICAL SYNTHESIS AND CHARACTERIZATION INVESTIGATIONS OF
RARE-
EARTH BORIDES AND TUNGSTEN BORIDE AND TUNGSTEN SILICIDE POWDERS
FABRICATED FROM LOW COST OXIDE POWDERS**

Prof. Dr. M. Lütfi Öveçoğlu

Particulate Materials Laboratories(PML), Dept. of Metallurgical & Materials Engineering, Istanbul
Technical University, Maslak 34489, Istanbul, TURKEY

Room temperature mechanochemical routes were carried out in the syntheses of nano-sized rare-earth boride (MB_6 , $M = La, Sm, Ce$) powders from M_2O_3 - B_2O_3 -Mg blends, tungsten boride powders from WO_3 - B_2O_3 -Mg blends and tungsten silicides from WO_3 - SiO_2 -Mg powder blends. All synthesis reactions were driven by high-energy ball milling and were gradually examined in terms of milling duration and process control agent. Following the mechanochemical synthesis, unwanted MgO phase and Fe contamination worn off from the milling vial/balls were removed with HCl acid leaching under the effect of ultrasonics stirring. Pure rare-earth boride, tungsten boride and tungsten silicide powders were obtained after repeated centrifuging, repeated washing and drying. Subsequent annealing was performed in a tube furnace under Ar atmosphere in order to reveal residual elements. Phase and microstructural characterizations of the milled, leached and annealed powders were performed using X-ray diffractometry (XRD), differential scanning calorimetry (DSC), scanning electron microscopy (SEM) and transmission electron microscopy (TEM) techniques. High-purity (> 99.99 %) LaB_6 , CeB_6 and SmB_6 powders were successfully synthesized having average particle sizes of 80 nm, 86 nm and 81 nm, respectively.

Using stoichiometrically excess amounts of B_2O_3 , pure W_2B_5 powders with an average particle size of 226 nm and an average grain size of 55.3 nm were successfully synthesized. Likewise, TEM analysis revealed that pure W silicide nanoparticles with an average size of 97 nm were encapsulated by SiO_2 layers with an average thickness of 15 nm.

INVITED SPEAKERS**INORGANIC HOLE TRANSPORTING MATERIALS FOR STABLE AND HIGH EFFICIENCY PEROVSKITE SOLAR CELLS**Savas Sonmezoglu^{a,b}^aNanotechnology R&D Laboratory, Karamanoglu Mehmetbey University, Karaman, Turkey^bDepartment of Metallurgical and Materials Engineering, Karamanoglu Mehmetbey University, Karaman, Turkey

Nowadays, perovskite solar cells (PSCs) employing organo-lead halide perovskite absorber materials have attracted substantial attention because of their excellent qualities, such as large absorption coefficient, direct band-gap, high charge carrier mobility, and long diffusion lengths. On the basis of its superior advantages, certified power conversion efficiency (PCE) of 22.7% was achieved. Despite the success in high PCE of perovskite solar cells, there are certain concerns about the poor stability (thermal, moisture and light stability) of perovskite devices that can potentially hinder their commercialization.

Since inorganic materials are expected to be more stable than organic ones in terms of high temperature and moisture, a variety of inorganic HTMs. Therefore, instead of organic materials, PSCs to surmount the drawbacks of organic HTMs. In this review, we have investigated in detail the progress of inorganic HTM-based PSCs and discussed the effect of inorganic HTM on PCE and stability.

Keywords: Inorganic hole transporting layer, Stability, Perovskite Solar Cells

INVITED SPEAKERS

THE PRODUCTION AND CHARACTERIZATION OF LOW LEAD CONTENTING ORGANIC- INORGANIC PEROVSKITE SOLAR CELLS

Hasan Göçmez¹, Seher Çetin¹, Mustafa Tuncer¹, Cengiz Soykan², Cihangir Duran³, Hilmi Yurdakul⁴,

¹Kütahya Dumlupınar University, Faculty of Engineering, Metallurgical and Materials Engineering Department, Kutahya/Turkey

²Ahi Evran University, Vocational School of Health Service, Kırşehir/Turkey

³Ankara Yıldırım Beyazıt University, Faculty of Engineering, Metallurgical and Materials Engineering Department, Ankara/Turkey

⁴Alanya Alaaddin Keykubat University, Faculty of Engineering, Metallurgical and Materials Engineering Department, Alanya/Turkey

The main purpose of this study is to prepare low lead content organic-inorganic perovskite solar cell by controlling power conversion efficiency of cell. It proposes the reduction of lead content of organic-inorganic perovskite solar cell. Perovskite is a flexible material that is possible to add many elements in the periodic system (Co^{+2} , Fe^{+2} , Mn^{+2} , Pd^{+2} and Ge^{+2} etc.). Goldschmidt's tolerance factor ($t=1$) is used to determine which element can be formed stable perovskite structure. The stability and decomposition of perovskite depends on tolerance factor. In the cubic form, the ideal tolerance factor is unity. Therefore, Co^{+2} is selected due the unity of Goldschmidt's tolerance factors, Sr^{+2} is recommended due to similar ionic Radius to Pb, Ca^{+2} that has tolerance factor near to lead based perovskite solar cell, and also the addition of Bi^{+3} is proposed that it is successfully used in the lead free composition of piezoelectric materials. First time in the literature, cobalt ($\text{CH}_3\text{NH}_3\text{Pb}_{1-x}\text{Co}_x\text{I}_3$) and bismuth ($\text{CH}_3\text{NH}_3\text{Pb}_{1-x}\text{Bi}_x\text{I}_3$) based organic-inorganic perovskite solar cell will be obtained and their efficiency will be measured. Cell components, photoanodes prepared by spin coated and tape casting, then perovskite structure obtained with adding hole transporting materials and electrodes covered on top of it finally cell is assembled. Electronic properties, band gap and phases of selected composition of targeted cell components will be calculated theoretical first time in the literature. Photovoltaic properties will be measured with standard characterization methods.

***This work was supported by TÜBİTAK (The Scientific and Technological Research Council of Turkey) through project number 116F073.**

INVITED SPEAKERS**CERAMIC APPLICATIONS IN TÜPRAŞ REFINERIES FOR ENERGY SAVINGS**

Cem Açıksarı¹, Yeşim Teke¹, Serdar Çelebi¹

¹TÜPRAŞ-Turkish Petroleum Refineries Corporation, R&D Center, Kocaeli, TURKEY

Tüpraş is Turkey's largest industrial enterprise and seventh biggest refining company in Europe, with 28.1 million tones crude oil processing capacity and operating four refineries with more than 5000 employees. Tüpraş R&D Center certified by Turkish Law "Supporting Research and Development Activities" was established in 2010. Tüpraş carries out R&D projects in line with the objective of developing sustainable production strategies alternative fuels, fuel production and energy minimization technologies. A refinery infrastructure mainly is made out of metals however; ceramics also have key roles in daily operation. Ceramic materials such as refractory bricks, thermally stable oxide compounds, catalyst carriers and supports with controlled shape and geometry, coatings and thermal insulation materials are widely used in refineries. Ceramic materials are used in nozzle, seal, valve and membrane components and the places where thermal insulation and corrosion resistance are strictly required. Ceramic based thermal insulation for energy savings is one of a significant application not only for energy dense-industries but also for petroleum refineries. These materials are mainly classified into two parts: traditional (mineral, rock wool etc.) and new generation (aerogel, porous powder etc.). In this talk, refinery ceramics used for energy savings will be shortly discussed and new opportunities for collaboration with universities and companies will be addressed.

INVITED SPEAKERS

SACMI TECHNOLOGY APPLIED TO HIGH-PRESSURE CASTING CELLS

Simone SILOCCHI
SACMI

Going through crucial steps from casting to pre-drying and final drying regardless of whether traditional low-pressure casting or high-pressure casting is used: finished product quality is preserved anyway.

Over the years Sacmi has developed an integrated system which applies various aspects of ceramic technology to high-pressure casting and introduces advanced technology to its installations.

These include: Structural verification of ceramic bodies, Modelling, Mould management, Feedback product control, Control of pre-drying phase.

INVITED SPEAKERS

SINTERING BEHAVIOURS AND MICROSTRUCTURAL DEVELOPMENTS IN OXIDE AND NON-OXIDE CERAMICS

Prof. Dr. Volkan GÜNAY

Yeditepe Üniversitesi, Mühendislik Fakültesi,
Malzeme Bilimi ve Nanoteknoloji Mühendisliği Bölümü 34755, Ataşehir, İSTANBUL

In this presentations, first basic understanding of sintering mechanisms in ceramic materials will be discussed and sintering behaviours of ceramics will be presented by choosing some examples such as Al_2O_3 , ZrO_2 , PSZ, AlN , Si_3N_4 and $\text{SiC-Si}_3\text{N}_4$ systems. Microstructural development will be given by considering the sintering temperatures, powder characteristics (powder size, composition, amount of additives).

Special attention will be given to Al_2O_3 -based and B_4C armour ceramics and their fracture behaviours in real testing conditions.

INVITED SPEAKERS

HIGH TEMPERATURE PROCESSING AND SINTERING

Fatih Üstel

Sakarya Üniversitesi, Mühendislik Fakültesi, Metalurji ve Malzeme Mühendislik Bölümü,
54187, Sakarya

Yüksek teknolojik uygulamaların esasını teşkil eden uzay ve havacılık sektörü katma değeri en yüksek uygulamalı bilim alanını oluşturmaktadır. Metalik ve seramik malzemelerin yüksek sıcaklık dayanımının sonuna kadar zorlandığı günümüzde; uzay ve havacılık uygulamalarına yönelik yeni malzeme arayışları devam etmektedir. Sunulan çalışmada; yüksek sıcaklık uygulamalarına yönelik olarak yeni sentez seramik malzemeleri uzay ve havacılık sektöründe kullanılan ısı bariyer kaplamalarına odaklanılmıştır. Termal ve çevresel bariyer kaplamaları konusunda genel bilgi paylaşımı, ilgili üretimlerin gerçekleştirildiği Sakarya Üniversitesi Kaplama Laboratuvarlarının tanıtımı ve imkanları katılımcılarla paylaşılacaktır.

INVITED SPEAKERS**INJECTABLE BIOCERAMICS IN ORTHOPAEDIC AND DERMAL APPLICATIONS**

Levent Mete ÖZGÜRBÜZ

BMT Calsis A.Ş., Ankara/Turkey

ABSTRACT

Bioceramics can be defined as a group of customized forms of ceramic products that are used in medicine to be able to fix and/or reconstruct the body parts that are damaged or diseased. Injectable bone substitutes (IBS) have been widely used in the last three decades. are mostly preferred for an important advantage: the better ability to integrate and assimilate forming a bond with the bone when compared with the other bioinert or nearly inert compositions. Recent research in the last years have focused on how to take out the regenerative potential and bring out alternative injectable bone substitutes (IBS) constituents that are made of beta-tricalcium phosphate (β -TCP) and hyaluronan for alveolar bone regeneration. In order to correct facial lines (from moderate to severe) and regain the lost volume a type of bioceramics, calcium hydroxyapatite is used as dermal filler worldwide. This talk will be focused on the use of bioceramics in these two different indications.

INVITED SPEAKERS

NEWLY DEVELOPED LITHIUM DISILICATE BASED GLASS-CERAMICS FOR 3D PRINTABLE ARTIFICIAL BONES

Emrah Dölekçekiç

Eskişehir Technical University, Department of Material Science and Engineering, İki Eylül Campus, 26480/Eskişehir/Turkey

In recent years, there has been an increasing interest in porous fabricated biomaterials that can be fabricated in three dimensions in order to remove hard tissue damage and strengthen tissues¹. Designed for this purpose, bioactive glass-ceramics are specialized biomaterials, which form strong bonds by reacting with tissues and / or bones². Glass-ceramics containing lithium disilicate are an important milestone in the use of bioactive glass-ceramics as an implant. Lithium disilicate (Li₂Si₂O₇) glass-ceramics have superior aesthetic and optical properties, high bending strength (300-400 MPa) and high fracture toughness (2.8-3.5 MPa.m^{1/2})³. These properties, which are superior to other bioactive glass-ceramics, are thought to serve as a skeleton for the formation of new bone tissue and can be used instead of damaged bone tissue.

There are various methods for the production of Li₂Si₂O₇ glass ceramics. Commonly used are classical melting method and sol-gel method. In classical melting process, the formation of a fine-grained microstructure is accompanied by an increase in strength and wear resistance⁴. However, there are limitations to the use of this method due to the evaporation of volatile oxides at high temperatures. In sol-gel method, glass porosity can be controlled at low temperatures and glass materials having a much more homogeneous structure than glass produced by the conventional method can be produced. In recent years, with the development of technology, bioactive glass-ceramics production is being done by using 3D printer which is computer aided design and production method. The purpose of the present study is to develop a Li₂Si₂O₇ glass- ceramic based system for 3D printing applications of artificial bones.

References

1. Mallick K., 2009. "Freeze Casting of Porous Bioactive Glass and Bioceramics", J. Am. Ceram. Soc., 92 [S1] S85–S94.
2. Kükürtçü B., "Biyoaktif Cam ve Cam-Seramik Malzemelerin Üretimi ve Yapay Vücut Sıvısı İçerisindeki Davranışlarının İncelenmesi", Yüksek Lisans Tezi, İstanbul Teknik Üniversitesi, Fen Bilimleri Enstitüsü, İstanbul.
3. El-Meliegy E., van Noort R., 2012 "Glasses and Glass Ceramics for Medical Applications", Springer Science Business Media, LLC.
4. McMillan, P.W., 1979. "Glass-Ceramics", Second Edition, Academic Press, London.

INVITED SPEAKERS

HIGH TEMPERATURE PROPERTIES OF SIALON

Dilek Turan², Alper Uludag² Yağmur Deniz³, Sinem Baskut, Serkan Ulukut⁴, Ferhat Kara¹ and
Servet Turan¹

¹Department of Materials Science and Engineering, Eskişehir Technical University, 26480, Eskişehir,
Turkey

²Department of Airframe and Powerplant Maintenance, Eskişehir Technical University, 26480,
Eskişehir, Turkey

³Department of Metallurgical and Materials Engineering, Pamukkale University 20160,
Denizli, Turkey

⁴TEI-TUSAŞ Engine Industries Inc, 26210, Eskişehir, Turkey

Silicon nitride (Si_3N_4) and its solid solutions (SiAlONs) are widely used ceramics for structural applications due to their exceptionally good physical and mechanical properties, such as high wear, hardness and creep resistance. The service life of Si_3N_4 and SiAlON materials at a high temperature under stress is limited by deformation over time, which is termed creep. Because of their highly covalent Si-N bonds and low diffusion coefficients, sintered silicon nitrides are usually densified with the aid of additives which form a liquid phase at the sintering temperature promoting solid transport by the liquid phase sintering mechanism. Unfortunately, on cooling, the liquid generally transforms into a residual intergranular amorphous phase whose quantity, distribution and chemical composition control the mechanical properties at high temperature. In order to minimize the amount of vitreous phase, several techniques have been tested such as crystallization heat treatments which improve the creep resistance by limiting the viscous flow in the recrystallized phases. In this study, different heat treatments (AET, BET), different second phase additions (SiC), different additives (Er, Yb and Lu oxides) were used to improve creep properties of SiAlON ceramics. The creep results will be explained in terms of microstructure.

INVITED SPEAKERS**TÜRK SERAMİK SANAYİNİ BEKLEYEN TEHLİKE KARBON EMİSYON TİCARETİ**

Germiyan SAATÇİOĞLU

- Emisyon Ticareti Sisteminin (EUETS) Avrupa’da doğuşu ve bugüne kadar geldiği safhaları.
- Avrupa’da EU ETS’e tabi olan sanayiler, tabi olma kriterleri.
- Türkiye’nin emisyon azaltımı için taraf olduğu anlaşmalar.
- Türkiye’de emisyon azaltımı için çıkartılmış yasalar, yönetmelikler.
- Türkiye’de karbon emisyonlarının azaltımı için yapılan modelleme çalışmaları.
- Danışmanlar tarafından tavsiye edilen Emisyon azaltım araçları.
- Karbon vergisi, Emisyon Ticareti Sistemi, Yenilenebilir enerji.
- Türkiye’de emisyon azaltımı için yasal ve kurumsal altyapı.
- Emisyon Ticaretinin uygulanması halinde örnek seramik tesislerine getireceği mali yük.
- Seramik Kaplama Malzemeleri Sanayi Seramik Sağlık Gereçleri Sanayi
- Emisyon tahsisleri, bedelsiz emisyonlar,
- Emisyon Ticareti Sisteminin getirdiği tehlikeler ve korunma önlemleri, Karbon Kaçağı uygulaması.
- Avrupa’da Karbon Kaçağı kriterleri ve uygulama safhaları

INVITED SPEAKERS**SUSTAINABILITY AND BENCH-MARKING ENVIRONMENTAL IMPACTS IN
TURKISH CERAMIC TILES AND SANITARYWARE**

Hüdaî KARA

Metsims Sustainability Consulting, Istanbul, Turkey

ABSTRACT:

Environmental impacts of construction materials have recently been attracting attention due to fast developments in green building assessment schemes across the world. Measuring environmental impacts such as climate change across the life cycle of a building is becoming an essential part of these assessment schemes. The EU's new Level(s) framework aims to on measure sustainability in buildings and communicate to the end users and to facilitate circular economy thinking in construction. Availability of environmental impacts based on life cycle approach of construction materials is an important aspect of these developments.

Turkish Ceramic sector has been very responsive to these developments with product level disclosures using Environmental Product Declarations (EPD). Driven by Construction Products Europe, EPDs are harmonised by EN 15804 norm, and thought to become the foundation of Product Environmental Footprint (PEF) for construction products, a newly developing policy option by the EU Commission. This presentation will bench-mark and show the environmental impacts of Turkish ceramic tiles and sanitaryware per a functional unit and compares against their competitors and draw attention to potential climate change reduction and resource efficiency savings.

Keywords: life cycle, construction materials, environmental product declarations, green building assessment, climate change, environmental impacts, ceramic tiles, ceramic sanitaryware

INVITED SPEAKERS

UNIMAK SHUTTLEKILNS

Jerome MEAKIN
Unimak Makina San. Tic. A.Ş.

Unimak Shuttle kilns are unique to the market and provide industry leading fuel efficiency. Our temperature control system is based on the venturi principle.

Fuel efficiency is achieved thanks to a combination of design features that Unimak has developed to give maximum benefit to our objectives and targets:

Burner design is specially selected to give the optimum velocity and power for our heating objectives.

Combustion air supply dynamics are calculated to accentuate the burner venturi effect.

Combustion control equipment is selected to provide the maximum flexibility to reach our goals of homogeneous temperature control.

A waste gas and pressure control system is utilised that compliments the venturi effect created from the combustion system.

Refractory and insulation features of the kiln and the kiln cars provide further enhancement of the circulation of a homogenous atmosphere around the product.

Dedicated software programming has been developed to provide precise control of the equipment.

A SCADA system is used to monitor and record all critical data during each firing cycle, this provides the opportunity to analyse the complete control system and make adjustments to achieve optimum performance and efficiency of the kiln.

INVITED SPEAKERS

CERAMICS AND ENERGY: THERMOELECTRIC MATERIALS

S. Altın¹, S. Avci², A. Bayri¹

Inonu University, Physics Department, 44280, Malatya, Turkey

Istanbul Medeniyet University, Dept. of Engineering Physics, Istanbul

In this century, humanity faces the challenge of limited energy sources due to increased energy consumption. Energy problem can be divided into three categories, production, efficient consumption and storage of the energy. Thermoelectric materials is one of the components of the devices which produce electrical energy from the waste heat. The first discovery of the thermoelectricity in the material science has started with metals and alloys such as Te, Sb, PbTe... However, performance of the thermoelectric modules fabricated by alloys decreases with time due to oxidation of the components.

Ceramic thermoelectric materials have better stability in oxidizing environments. Their use enables the fabrication of more durable devices. Therefore, the thermoelectric research has focused on the oxide materials such as p-type NaCo₂O₄, p-type Ca₃Co₄O₉ and n-type ZnO, SrTiO₃, and CaMnO₃.etc.

After discovery of the large Seebeck coefficient for the ceramic material of NaCo₂O₄, the scientists have been studying to find new materials. Thermoelectric performance of the ceramics will be reviewed and the future of the ceramics as thermoelectric materials will be discussed.

References

1. Oxide Thermoelectric Materials for Heat-to-Electricity Direct Energy Conversion (2009)
by Michitaka Ohtaki
2. ABANTI NAG and V.SHUBHA, Oxide Thermoelectric Materials: A Structure– Property Relationship, Journal of ELECTRONIC MATERIALS, Vol. 43, No. 4, 2014

INVITED SPEAKERS

THERMOELECTRIC MATERIALS MODELLING

Cem Sevik

Department of Mechanical Engineering, Eskişehir Technical University

Recent developments in hardware and software computer technologies together with the development of accurate materials modeling techniques enable researchers to accurately model various phenomena observed in materials, prediction of their behavior under different conditions and the development/ design of cost-effective materials with improved or desired properties. Nowadays, it is possible to perform such simulations even for a large number of materials using the advantages of new neural network and big-data algorithms.

Efficient thermoelectric materials research, as a topical materials science and condensed matter physics problem, has been a good candidate to be investigated with state-of-the-art materials simulation techniques due to the complexity of the experimental procedure and large number of possible candidate materials. Highly accurate predictions, in particular regarding the effect of defects, grain boundaries, and dimension reduction on both electronic and thermal transport properties have led to discovery of novel thermoelectric materials and new directions to experimental studies on already known thermoelectric materials.

Within the past 10 years, we also have investigated thermoelectric properties of both bulk and nano materials by means of density functional theory and molecular dynamics simulations. Our systematic studies on the in particular controlling the thermal transport properties of the novel nano materials, in order to enhance thermoelectric figure of merit of the materials, have been also one of the pioneering studies in the literature and inspired many new studies. The model interatomic potentials developed within the scope of our TE research effort have been still extensively used in the literature.

INVITED SPEAKERS**NANOSCALED BIOACTIVE GLASSES**

Melek Erol Taygun

Department of Chemical Engineering, Istanbul Technical University,
Maslak 34469 Istanbul, Turkey

Nanotechnology approaches are being proposed for biomedical applications. Nanoscale bioactive glasses are gaining increasing attention due to their superior bioactivity, enhanced osteoconductivity and antibacterial properties in biomedical applications. The use of nanosized bioactive glasses has advantages in biomedical applications comparing with conventional micron-sized particles. A range of techniques has been using to fabricate nanoscale bioactive glasses including sol-gel, laser spinning, microemulsion and gas-phase synthesis. The produced nanoscale bioactive glasses are being proposed for the design of numerous nanomaterials for biomedical applications, including: combination of nanofibers or nanoparticles with polymeric matrices to produce nanocomposites, incorporation of nanoparticles or nanofibers into porous 3D scaffolds, nanoparticle coatings on implant surfaces and production of non-porous materials containing nanoparticles in the form of gels, injectable materials or hard devices. This presentation covers key technological developments and scientific challenges for nanoparticle and nanofibrous bioactive silicate glasses.

INVITED SPEAKERS
DEVELOPMENTS IN TURKISH REFRACTORY
INDUSTRY

Assoc. Prof. Dr. Ziya Aslanoğlu, RD Director Konya Selçuklu

Chrome Magnesite Brick Co.

Turkey has growing economy. Construction is one of the largest sectors in Turkey. The increase in infrastructure construction activities is the primary driver for the Turkish economy. Refractory material is a key material for the production of steel, cement, lime and glass which is used for construction sector. The refractories industry largely follows trends set by its main driver, steel and cements industries. The steel, cement and lime industries are estimated to account for about 85% of the total refractory market. There is an increase in steel and cement production capacity of Turkey in 2017. Therefore, the demand for refractories is expected to rise from the cement and iron-steel industries. The Turkish refractories market is growing at a moderate pace. The refractory companies are extensively working on enhancing their production capacity, product portfolio and bringing out new, customized products. Despite their crucial role, manufacturers of these products are facing significant challenges from changing global trends. The situation of Turkish refractory industry, effects on the economy and new trends were summarized in this work.

Keywords: Turkish refractory, Refractory materials, development trends,

seres'18

IV. INTERNATIONAL CERAMIC GLASS PORCELAIN
ENAMEL GLAZE AND PIGMENT CONGRESS
October 10-12, 2018, Eskişehir, Turkey

Abstract of ORAL PRESENTATIONS

LITHIUM ION BATTERIES POTENTIAL IN TURKEY

ECO-FRIENDLY SYNTHESIS OF LITHIUM IRON SILICATE BASED CATHODE MATERIAL FOR LI-ION BATTERIES

Yiğit Akbaş¹, Kamil Burak Dermenci¹, Servet Turan¹

¹ Eskişehir Technical University, Department of Material Science and Engineering,
İki Eylül Campus, 26480/Eskişehir/Turkey

Nowadays, increasing energy demand is met by fossil fuels. This cause tremendously high carbon emission. Air pollution by carbon emission has been forced us to use renewable energy sources. Transferring to the renewable energy sources is vital for the sustainable future. However, the limited availability of renewable energy triggered scientists to search for energy storage systems that has high capacity and energy density. Li-ion batteries (LIB's) are good candidates for those applications. Typical LIB consists of anode, electrolyte and cathode. Cathode materials attract much interest since their capacity is required to be improved for the purpose of reaching high energy density. $\text{Li}_2\text{FeSiO}_4$ (LFS) based cathode material promise high theoretical capacity. Moreover, it has the most abundant element on earth which makes it cheapest cathode candidate. In this study, eco-friendly synthesis of LFS is covered by using limonite as Fe source with different amount of excess silica and reducing agent (Carbon). Effect of solid-state synthesis parameters (temperature, time, heating rate) on impurity phases is investigated by XRD phase analysis. As a result, monoclinic LFS is synthesized. Electrochemical tests made for half-cell of LFS. The discharge capacity at first cycle found as 12 mAh/g (C/50) at room temperature while, 60 mAh/g (C/17) at 60°C.

BATTERIES AND SUPERCAPACITORS

A NOVEL DENSIFICATION MODEL FOR $\text{Li}_7\text{La}_3\text{Zr}_2\text{O}_{12}$ SINTERING

Kamil Burak Dermenci¹, Servet Turan¹

¹ Eskişehir Technical University, Department of Material Science and Engineering,
İki Eylül Campus, 26480/Eskişehir/Turkey

Inorganic solid ion conductors are considered as one of the crucial member for safety concerns in Li-ion batteries. Among them, garnet type $\text{Li}_7\text{La}_3\text{Zr}_2\text{O}_{12}$ (LLZO) stands forward as an important solid ion conductor with their outstanding performance on safety, stability and ionic conductivity. The typical microstructure of LLZO contains a significant number of closed porosities. Even though, Archimedes Method is the unique technique used for density evaluation in the field of LLZO synthesis, it's insufficient in the presence of closed porosities. The use of relative density for the purpose of indicating closed porosity changes is questionable for two main reasons that directly affects the theoretical density calculations:

- i) Dopant incorporation within garnet LLZO structure and atomic replacements changes the theoretical density and calculations are experimentally challenging
- ii) The actual composition of Lithium in the garnet LLZO structure could vary due to high temperature Lithium losses and accordingly, it changes the theoretical density.

Radial shrinkage has not been used in the field of LLZO synthesis and believed that would increase the reliability on the density of sintered samples. For better assessment of densification behavior of LLZO, a combination of both Archimedes (True) density and radial shrinkage measurements should be considered. Therefore, this work aims to reveal the role of radial shrinkage on LLZO densification. By combining Archimedes density, optical dilatometer measurements, radial shrinkage and fractured surface images, a densification model as a function of temperature is also introduced within the present study.

BATTERIES AND SUPERCAPACITORS

COMPARISON OF SPARK PLASMA AND PRESSURELESS SINTERING TECHNIQUES ON THE STRUCTURE AND IONIC CONDUCTIVITY OF CUBIC LLZO SOLID ELECTROLYTE

Musah Abdulai¹, Kamil Burak Dermenci¹ and Servet Turan¹

¹ Eskişehir Technical University, Department of Materials Science and Engineering, 26555, Eskişehir-Turkey

Over the years, the solid-state electrolytes such as LLZO ($\text{Li}_7\text{La}_3\text{Zr}_2\text{O}_{12}$) have been sintered through the conventional pressureless sintering method. The method which is usually time-consuming as it requires higher sintering temperature (1200°C) for a longer period (about 18-36H) and therefore, it is cost ineffective process. During this process, the evaporation of lithium increases and the oxide grains become larger which adversely affect the performance of LLZO solid-state electrolyte. It is on this ground that this study intends to use SPS as an alternative sintering technique and compare the result with the pressureless sintering method. The synthesis of LLZO solid electrolyte has been carried out by using the conventional solid-state method. High-quality powders of Li_2CO_3 , La_2O_3 and ZrO_2 were used. Al_2O_3 is used as Al source for the stabilization of the cubic phase. A stoichiometric weighed quantity of the starting powders was ground and calcined at 1000°C for 10 hours. The calcined powder was pressed into a pellet and cold isostatically pressed at 265 MPa. It is sintered in air at 1200°C for 12-18 hours. For the SPS process, the powder is sintered at the temperature range of 750°C to 1050°C . The phase identification was carried out with X-ray powder diffractometer. A Scanning electron microscopy was used to study the morphology of the grains and the microstructure in general. The densities of the samples were determined using the Archimedes principles with 2-propanol as immersion medium. In characterizing electrical properties, a thin film of gold-palladium is sputtered on the samples. High temperature ionic conductivity measurements for the activation energy calculation was carried out over the temperature range of 70°C to 150°C . An AC electrochemical impedance method was used in the frequency range from 1Hz to 1MHz, AC voltage of 30 volts at room temperature. The work has recorded ionic conductivity as high as $1.2 \times 10^{-4} \text{ S/cm}$ at a lower temperature of 950°C , which is among the highest values reported in the literature by the pressureless method. Optimization of sintering temperature is needed to reduce the existing pyrochlore phases in order to further improve the ionic conductivity.

BATTERIES AND SUPERCAPACITORS**CUBIC PHASE STABILIZATION OF $\text{Li}_7\text{La}_3\text{Zr}_2\text{O}_{12}$ BY USING MULTI-ELEMENT CONTAINING NATURAL RAW MATERIAL: LIMONITE ORE**

Ahmet Furkan BULUC¹, Kamil Burak DERMENCI¹, Servet TURAN¹

¹Eskişehir Technical University, Department of Material Science and Engineering,

İki Eylül Campus 26480/Eskişehir/Turkey

Recently, global energy consumption is increasing due to the increasing electrical energy demand. Non-renewable energy sources would be finished in the near future. Renewable energy sources offer a solution for this problem, but the energy from renewable sources need to be stored. Lithium-ion batteries (LIBs) are one of the candidate energy storage devices due to their high energy density, cycle life and high peak load current. LIBs consist of 3 parts; anode, cathode and electrolyte. Despite its widespread usage in the field of LIBs, organic based liquid electrolytes show high toxicity, flammability and explosiveness. Solid electrolytes bring a new insight in the field of LIBs with their outstanding electrochemical stability, high temperature performance and improved mechanical properties. The more recently developed solid electrolyte is $\text{Li}_7\text{La}_3\text{Zr}_2\text{O}_{12}$. However, high ionically conductive cubic LLZO phase needs to be stabilized at room temperature. The research so far conducted on the purpose of cubic phase stabilization is either increasing sintering temperature or incorporating of elements such as Al, Si, Ga and Fe. In this regard, the utilization of ores with their multi-element content as potential stabilizer is still not to be addressed. Therefore, the aim of the study is to stabilize the cubic LLZO phase by using multi-element doping approach. For this purpose, Limonite ore (common Fe source used in the ceramic industry) was used. It's found that, limonite participation could not only lower the stabilization temperature but also it increases the ionic conductivity. The impurities in the limonite ore act as dopant elements. Also, dopants cause nano-defects which increases the ionic conductivity.

ADVANCED CERAMICS**SPS OF CBN INCORPORATED CERAMIC MATRIX COMPOSITES**

Ufuk AKKASOGLU^{1,2}, Ferhat KARA³, Servet TURAN³, Umut SAVACI³, Alpagut KARA³, Hasan MANDAL⁴

¹MDA Advanced Ceramics, Eskişehir, 26110, Turkey

²Anadolu University, Faculty of Engineering, Department of Materials Science and Engineering, Eskişehir, 26555, Turkey

³Eskişehir Technical University, Faculty of Engineering, Department of Materials Science and Engineering, Eskişehir, 26555, Turkey

⁴Sabancı University, Faculty of Engineering and Natural Sciences, Department of Materials Science and Engineering, İstanbul, 34956, Turkey

cBN has been widely used as cutting tools for high speed machining of cast iron, due to its high hardness and low reactivity with iron. Dense cBN and cBN based materials are produced by high pressure high temperature process due to its strong covalent nature and phase transformation to hBN, which degrades mechanical properties, at moderate temperatures. The addition of cBN particles to a ceramic matrix could increase the hardness, flexural strength and fracture toughness of the composites. However, it diminishes the densification.

In this study, cBN up to 50 vol% was added into ceramic matrix including SiAlON and the composites were fabricated by Spark Plasma Sintering. Densification, microstructure and mechanical properties of the composites and the phase transformation of cBN to hBN were investigated. Densities of the composites were depended on the sintering temperature which was chosen to be between 1200°C – 1650°C. cBN to hBN transformation was followed with associated properties.

PIEZOELECTRICS / FERROELECTRICS**SYNTHESIS OF SR-DOPED PMN-PT PIEZOELECTRIC CERAMICS BY A SOLUTION COATING METHOD**Volkan Kalem^{1,2}, Wan Y. Shih³, Wei-Heng Shih²¹Department of Metallurgical and Materials Engineering, Konya Technical University, 42130, Konya /Turkey²Department of Materials Science and Engineering, Drexel University, Philadelphia, PA 19104, USA³School of Biomedical Engineering, Science and Health Systems, Drexel University, Philadelphia, PA 19104, USA

Effects of Sr addition and PMN/PT ratio on the structural, dielectric, and piezoelectric properties of PMN-PT ($\text{Pb}(\text{Mg,Nb})\text{O}_3\text{-PbTiO}_3$) ceramics were investigated. In order to distribute Sr uniformly in PMN and PT, and to lower the sintering temperature, double precursor solution coating (PSC) method was used to synthesize the $(1-x)[(\text{Pb}_{1-y}\text{Sr}_y)(\text{Mg}_{1/3}\text{Nb}_{2/3})\text{O}_3]\text{-x}[\text{Pb}_{1-y}\text{Sr}_y\text{TiO}_3]$ (PsMN-PsT) (y : 0-0.10, x : 0.35-0.40) ceramics. PSC method has been shown previously to provide an improved densification rate than that of the well-known columbite approach. Microstructural and compositional analyses of the synthesized samples have been carried out using scanning electron microscope (SEM) and X-ray diffraction (XRD). It has been found that the PSC method can lead to pyrochlore-free and highly dense PMN-PT based ceramics. Effect of composition on the dielectric and piezoelectric properties was also investigated. When $x=0.35$, the ceramic composition with $y=0.02$ exhibited the highest apparent density of ~97% and highest d_{33} value of 420 pC/N. Furthermore, when $y=0.02$ and by varying PMN/PT ratio, it was found that $x=0.37$ led to even better dielectric and piezoelectric properties with the optimal dielectric constant ϵ_r (4000), piezoelectric strain coefficient d_{33} (630 pC/N), electromechanical planar coupling factor k_p (0.52), and Curie temperature T_C (210 °C).

PIEZOELECTRICS / FERROELECTRICS**FINITE ELEMENT MODELING, ANALYSIS AND FABRICATION OF CLASS V FLEXTENSIONAL TRANSDUCERS**

Mustafa Yunus Kaya, Sedat Alkoy

Gebze Technical University, Department of Materials Science and Engineering,
41400 Gebze-Kocaeli /Turkey

Lead based piezoceramic ceramic compositions have been widely used for decades for actuator, sensor and transducer applications. Transducers were aimed mainly to operate in underwater applications such as SONARs. However, using a single transducer design at the frequency range from 1 kHz to 1MHz is not possible because of acoustic impedance matching problems and resonance frequency requirements. Therefore, numerous transducer designs have been developed to adjust the operating frequency and impedance. Flextensional Transducers-FT is one of these designs and it consists of a piezoelectric ceramic and a metal shell. Seven classes of flextensional transducer designs have been developed since 1950's to operate at lower frequencies. In this study, a novel and unique Class V flextensional transducer device design was developed using ATILA finite element analysis (FEA) software. Ceramic parts of transducers were fabricated from high performance piezoceramic compositions with convex shape. Metal shells were formed using press molds to be symmetrical with ceramic shells. Sintering of green ceramic bodies were done at a range from 1100 to 1260°C temperatures depending on compositions. Poling process were done under 20kV/cm DC field. The metal and ceramic shells were fixed together using adhesive element. In air admittance spectrums were taken frequency at a range from 1kHz to 300kHz for ceramic shells and devices. Comparison of FEA and experimental results were reported and discussed.

POLIMER-CERAMIC COMPOSITES

COMPRESSION BEHAVIOR OF FILAMENT WOUND GLASS FIBER REINFORCED EPOXY COMPOSITES AS A PROMISING CANDIDATE MATERIAL FOR CRASH BOX APPLICATIONS

Nur Üret, Selim Durunay, Uğur Korkmaz, Ahmet Eren Çimen, İlhan Kahraman, Abdullah Tuğrul Seyhan

Department of Engineering, Materials Science and Engineering, Eskişehir Technical University

Automotive manufacturing companies are interested in developing an energy impact attenuator component called crash box in order to improve crashworthiness and energy absorption in the event of a frontal impact. Crash box is known as one of the most important energy absorption components and typically mounted at the front end of an automobile. Crash box, as a deformable element, collapses with absorbed crash energy to protect passengers and other automobile parts. Conventionally, thin-walled aluminium and steel structures in varying shapes are used massively as impact attenuator components. Due to their lightweight, aluminium tubes with different cross-sections, aluminium sandwich panels and aluminium honeycomb structures are frequently employed as a crash box, too. Filament winding is an economic and preferred method for mass-produced composite structures. In this study, filament wound tubular glass fiber reinforced polymeric (GFRP) structures are investigated as a potential alternative to substitute conventional crash box materials, particularly aluminium. Energy absorption performances of the composites that were produced with different pretension and winding angle values were evaluated by means of quasi static tests under compression. Their microscale failure modes were then examined through SEM investigation. The results obtained were then briefly discussed.

POLIMER-CERAMIC COMPOSITES**PRODUCTION OF EXPANDED GRAPHITE WITH A CONTROLLED PORE STRUCTURE
AS A CARBON SUPPORT MATERIAL**

Özgü ÇALIN¹, Ayşe KURT² and Yasemin ÇELİK¹

Eskişehir Technical University, Department of Materials Science and Engineering, İki Eylül Campus,
Eskişehir, Turkey

Eskişehir Technical University, Graduate School of Sciences, Nanotechnology Program, Eskişehir,
Turkey

Expanded graphite, which has a highly porous worm-like structure, is a promising material as a carbon support for catalyst and battery applications due to its high surface area, resistance to both acidic and basic environments and easy production route with a relatively low cost. However, it is crucial to control the pore structure of this material in order to obtain a uniform distribution of particles throughout it. In this study, the relationship between expansion degree and pore structure of expanded graphite was investigated by altering the expansion temperature of expandable graphite materials with different flake sizes (*10 mesh, 50 mesh and 325 mesh*). Expandable graphite was produced from natural flake graphite materials and then subjected to an abrupt heating at high temperatures to form expanded graphite. The expansion degree and the morphology of the produced expanded graphite materials was then characterized and compared by XRD, Raman and SEM analyses.

CERAMIC TILE

RESIDUAL STRESSES IN PORCELAIN TILES. MEASUREMENT AND PROCESS VARIABLES ASSESSMENT

E. Sánchez^{(1)*}, V. Sanz⁽¹⁾, J. Castellano⁽¹⁾, K. Kayacı⁽³⁾, M.U. Taşkıran⁽³⁾, Ü.E. Anıl⁽³⁾

⁽¹⁾ Instituto de Tecnología Cerámica (ITC). Universitat Jaume I. Castellón (Spain)

⁽²⁾ GEA CERAMICA S.L, Castellón (Spain)

⁽³⁾ Kaleseramik Canakkale Kalebodur, Çan (Turkey)

Porcelain tile manufacturing has undergone a spectacular growth in the last years, as a result of the good technical and functional performance associated to the impervious feature of the sintered product, together with great advances of the process. As a consequence, larger and larger sizes are being engineered which can reach higher than one meter length. Larger sizes dramatically increase the risk for residual stresses to appear during fast firing cycles.

This research addresses the residual stresses phenomenon taking place during the manufacture of porcelain tiles. Firstly, a measurement method to quantify residual stresses in a tile piece has been fine-tuned. The method, named strain relaxation slotting method, is based on the fact that the stresses are released when a cut (slot) is made leading to a change of curvature. A strain gauge records the change in tile curvature as progressively deeper slots are provoked in the tile. Then, a simple model turns the deformation values into stress profile.

Once the method was validated, the impact of process variables such as starting body composition, sintering degree (microstructure) and cooling rate of firing cycle were investigated. Findings showed that cooling rate is the most impacting variable in terms of residual stresses. Thus, faster cooling rate results in higher compressive, residual stress. In addition, it was observed that polishing of a stressed tile gives rise to a decreasing of deformation as a consequence of stress release by mechanical grinding.

CERAMIC TILE

CONTROLLED PORE FORMATION IN PORCELAIN STONEWARE FOR INSULATING PURPOSES

Aslı Tuğba İlhanoglu, Ahmet Çapoğlu

Gebze Technical University, Department of Material Science and Engineering,
Çayırova Campus, 41400/Kocaeli/Turkey

Porcelain stoneware, is a highly densified material with a water absorption value of less than 0.5% and a strength value of 37-55 kg / cm² and can be produced without the application of glazing. Generally, this material is used as covering material for either flooring or outside the building surfaces. For flooring, porcelain stoneware is applied directly on to concrete surfaces via chemical bonding materials. Relatively high thermal conductivity of both concrete and stoneware (approximately 2 W/mK) and highly densified body of stoneware impairs the living comfort in the buildings. Materials having porous structure have found applications for thermal or acoustical insulating purposes. In order to improve the insulating properties it was aimed to create some porosities within the highly densified porcelain stoneware body without affecting adversely its defined properties such as low water absorption and strength values. In this work, inorganic based insulating body materials were introduced in different amounts into a porcelain stoneware mix in order to control the total porosity and evaluate the contribution of the closed porosity on the insulating and technological properties. The amount of insulating material addition is varied between 0-12% and these compositions were individually prepared into granulated form. The cylindrical and rectangular bar shaped specimens were produced from granulated powders by using manuel hdyrolic press and stainless steel dies. The specimens were then heat treated at the temperatures between 1200-1250°C. The sintered materials were characterized by measuring densification, firing shrinkage (in this case fire expansion) and water absorption. The mechanical properties such as elastic modulus, flexural and compression strength values were also determined. It was found that the stoneware body containing around 6 or 9% insulating powder produced well controlled porous structure without adversely affecting much of the defined properties of porcelain stoneware material.

CERAMIC TILE

INVESTIGATION OF RELATIONSHIP BETWEEN FIRING TEMPERATURE AND MOISTURE EXPANSION IN DIFFERENT WALL TILE RECIPES

Mustafa Fahri Özer¹, Emre Yalamaç², Rabia Gün^{1,2}

¹ Graniser Granit Ceramic Research and Development Center, Akhisar/Manisa/Turkey

² Faculty of Engineering Metallurgical and Materials Engineering Department,
Manisa Celal Bayar University, Muradiye Campus Manisa/Turkey

In ceramic industry floor and porcelain tiles are more stable than wall tiles because wall tiles have high porosity and high water absorption values ($E > 10$ (EN 14411 Grup BIII)). The main phases of ceramic bodies can absorb water when they contact with water and fired wall tiles' dimensions can increase. Because of moisture expansion, glazed ceramic can craze and ceramic tiles can fail.

The moisture expansion is characterized by increasing in the size of solid materials when in contact with water vapor. Considering the inevitability of the moisture expansion, procedures must be established to prevent their undesirable effects.

Moisture expansion is related to mineralogical composition of the fired body. Especially the body recipe contains calcium carbonate as the driving force of the phenomenon. In the porous ceramic tiles, crystalline phases of gehlenite, anorthite and some mullite have formed after sintering at 1050°C. Anorthite and mullite were better developed and gehlenite was reduced in increasing temperature.

According to the ISO 10545-10 standard, moisture expansion of ceramic tiles, after hydration in boiling water, should be less than 0,06 % (0,6 mm/m). The aim of this study is to decrease the firing temperature by developing new wall tile body recipes in accordance with ISO 10545-10 standard. Therefore, different tile body recipes will be prepared and sintered at different firing temperatures. Their moisture expansion will be investigated and compared according to dilatometer method.

CERAMIC TILE

APPLICATION OF FELDSPATOID BASED RAW MATERIAL IN THE TILE BODY FORMULATIONS

Mustafa Fahri Özer¹, Senem Kerenciler Batar¹, Didem Şahankaya¹, Rabia Gün¹,
Oğuzhan Dayı¹, Emre Yalamaç²

¹ Graniser Granit Ceramic Research and Development Center, Akhisar/Manisa/Turkey

² Faculty of Engineering Metallurgical and Materials Engineering Department,
Manisa Celal Bayar University, Muradiye Campus Manisa/Turkey

In our country for the ceramic tile production, the body preparation raw materials are mostly supplied from domestic quarries. In today's economy, raw material input costs have increased considerably due to high transportation and storage costs. The use of local raw materials in the production of ceramic tiles is important from day to day. Besides, it is also important to know the reserves of the raw material quarries which will be used in ceramic tile industries. In this study, it is aimed to obtain an efficient production process by reducing the input costs and evaluating the feldspatoid quarry in Aydın-Buharkent belonging to Graniser Granit Ceramic A.Ş. In order to decrease the peak temperature and soaking time in firing process, natural flux forming raw materials like feldspatoids are employed to the body recipes. By using Aydın-Buharkent raw material, it is aimed to decrease the kiln temperature and cycle. The samples taken from the quarry will be tested for their chemical, mineralogical, thermal and physical properties (XRF, XRD, water absorption, expansion coefficient, modulus of rupture test etc.). After analysis to be applied to the raw material, with the help of Neos Aware Masse Simulation Program, Floor, Wall and Porcelain tile recipes will be worked in laboratory conditions. The results of recipes will be compared in accordance with TS-EN 14411 Group BIII standards.

TEXTURED & EPITAXIAL PIEZOELECTRICS / FERROELECTRICS**ELECTRICAL AND STRUCTURAL PROPERTIES OF 0.9PMN-0.1PT RELAXOR CERAMICS**Yusuf Kılıç¹, Ayşe Berksoy Yavuz¹ and Ebru Menşur-Alkoy¹¹Department of Materials Science and Engineering, Gebze Technical University,
41400, Gebze, Kocaeli, Turkey

Lead magnesium niobate (PMN)-lead titanate (PT) $[\text{Pb}(\text{Mg}_{1/3}\text{Nb}_{2/3})\text{O}_3\text{-PbTiO}_3]$ piezoelectric ceramics of 0.9PMN-0.1PT was specifically chosen for this study because of relaxor ferroelectric properties of this composition. Piezoelectric ceramics were synthesized by modified solid-state reaction route. The source powders were stoichiometrically mixed and 2% excess PbO was added to compensate lead loss during calcination and sintering processes. The powders were ball-milled and then calcined at 800 °C for 4 h to obtain PMN-PT. Disc-shaped samples were prepared and these samples were also sintered at 1150 °C for 2 h, 4 h and 6 h. Microstructural and compositional analyses have been carried out using scanning electron microscope (SEM) and X-ray diffraction (XRD), respectively. A pure perovskite structure was obtained as desired. Temperature-depended measurement of dielectric constant was carried out. Piezoelectric coefficient (d_{33}) was measured as 52 pC/N. Electric field induced strain was measured as ~0.13% at 30 kV/cm. The Curie temperatures were measured at 1 kHz, 10 kHz and 100 kHz as 41°C, 43°C and 47°C, respectively.

In addition, some samples were produced with tape casting and their electrical measurements and structural examinations were also performed for tape-casted PMN-PT samples. The dielectric, ferroelectric and piezoelectric properties of the PMN-PT system were studied in detail.

Acknowledgement

The financial support provided by Air Force Office of Scientific Research (AFOSR) Grant #FA9550-18-1-0450 is gratefully acknowledged.

TEXTURED & EPITAXIAL PIEZOELECTRICS / FERROELECTRICS**ELECTRICAL AND OPTICAL PROPERTIES OF SOL-GEL DERIVED PZT AND PLZT THIN FILMS ON DIFFERENT SUBSTRATES**

Mustafa Çağrı Bayır¹, Ebru Menşur-Alkoy¹

¹Department of Materials Science and Engineering, Gebze Technical University,
41400, Gebze, Kocaeli, Turkey

In this study, lead zirconate titanate (PZT) and lead lanthanum zirconate titanate (PLZT) thin films were prepared by sol-gel method. The films were coated on two different substrates: platinum coated silicon substrate ($\text{Pt}_{(111)}/\text{Ti}/\text{SiO}_2/\text{Si}_{(100)}$) and gallium doped zinc oxide (GZO). PZT and PLZT sol-gel precursor solutions were prepared as 0.4 and 0.5M. The films were annealed at 600°C and 700°C for 1 hour called as rapid thermal annealing (RTA). The processing conditions of these films with pure perovskite phase were produced from stoichiometric and %2-mole lead excess sol-gel precursor solutions, and they were annealed at 600°C for 1 hour. Thickness of the films was measured as ~530 nm with scanning electron microscope (SEM). The aim of this study was to discuss substrate and lanthanum doping effects on electrical properties of the films. Also, it was desired to report how optical properties can be improved and which parameters are effective for PLZT as transparent ferroelectric material. The UV-Vis measurements were done in 200-1000 nm range. The experimental results were discussed on the way of these aims.

Acknowledgement

The financial support provided by Gebze Technical University for the Scientific Research Project (BAP #2018-A101-08) is gratefully acknowledged.

TEXTURED & EPITAXIAL PIEZOELECTRICS / FERROELECTRICS**FABRICATION OF ANTIFERROELECTRIC PZSNT BULK CERAMICS**

Hüseyin Alptekin Sarı, Ebru Menşur-Alkoy, Sedat Alkoy

Gebze Technical University, Department of Materials Science and Engineering., 41400 Gebze,
Kocaeli, Turkey

Antiferroelectric ceramics can be used in many areas today such as high energy density capacitors, electromechanical systems. Although they have spontaneous polarization, the dipoles are aligned antiparallel to each other, thus they do not exhibit permanent polarization; however, they can switch between ferroelectric and antiferroelectric states by application and removal of electric field. PZSnT ceramics are widely well-known antiferroelectric ones. Generally antiferroelectric ceramics are fabricated by thin film or Sol-Gel methods. In this work, antiferroelectric PZSnT ceramics were produced by utilizing the traditional solid state calcination method using oxide powders. Intrinsic and doped PZSnT powders have been synthesized and ceramic samples were fabricated by dry pressing and sintering. Polarization electric field hysteresis loops and field induced strain behavior of the samples have been measured, reported and discussed.

Keywords: Antiferroelectric; Bulk; PZSnT, High Energy Density Capacitor,

TEXTURED & EPITAXIAL PIEZOELECTRICS / FERROELECTRICS**TEXTURED 0.675 [PB(MG_{1/3}NB_{2/3})O₃] - 0.325 [PBTiO₃] SYSTEMS FOR ENERGY HARVESTING APPLICATIONS**

Ayse Berksoy-Yavuz, Ebru Mensur-Alkoy

Gebze Technical University, Department of Materials Science and Engineering,
41400/ Kocaeli/Turkey

Even though the energy harvesting (EH) applications have been studied for a long time in history, how to design for smart systems is a relatively new technology. In recent years, EH device have become a popular field of research area particularly in wireless sensor networks, wearable products, military or civil mobile and wireless electronic device applications. For EH design, the parameters such as the coupling mode, electrode pattern, parallel or series connection of all plates, the type of supporting platform, stress application and selection of piezoelectric materials properties are very important. In this study, 0.675[Pb(Mg_{1/3}Nb_{2/3})O₃]-0.325[PbTiO₃] (abbreviated as PMN-PT) ceramics have been developed and produced in textured form for enhanced electrical properties, instead of commercial Pb(Zr,Ti)O₃ (PZT). In addition Mn doping ratios (0.2, 0.4, 0.6 and 0.7 mol%) to enhance soft properties and the figure of merit (FOM ($d_{33} \cdot g_{33}$)) for EH were investigated. The FOM value of textured PMN-PT, was found to be as high as $\sim 25999 \times 10^{-15} \text{ m}^2/\text{N}$ and increased to $\sim 30690 \times 10^{-15} \text{ m}^2/\text{N}$ for 0.7 mol% Mn-doped textured PMN-PT. As a final result, the textured ceramics with 0.7 mol% MnO₂ added have a higher energy density and would be more suitable for EH applications.

TEXTURED & EPITAXIAL PIEZOELECTRICS / FERROELECTRICS**DENSIFICATION OF UNDOPED SnO_2 CERAMIC TARGET VIA SPARK PLASMA SINTERING**

Cem Aciksari, Levent Koroglu*, Erhan Ayas, Emel Ozel, Ender Suvaci
Eskişehir Technical University, Department of Materials Science and Engineering, İki Eylül Campus,
26555/Eskişehir/Turkey

Tin oxide (SnO_2) is an important electronic material which has been widely used in an extensive range of applications such as gas sensor, catalyst, heat mirror, varistor, transparent thin film electrode, optoelectronic device etc. In gas sensor application, thin film based SnO_2 has unique properties such as high sensitivity, selectivity and fast response. One of the well-known and promising technique is the sputtering from high pure ($> 99.9\%$) and dense ($>95\%$ TD) oxide ceramic target. However, undoped SnO_2 bulk ceramics cannot be densified by pressureless sintering because of the evaporation & condensation process. For this reason, densification of undoped SnO_2 nanopowder was performed using Spark Plasma Sintering (SPS) furnace (HPD-50, FCT GmbH) under a vacuum atmosphere. The process parameters such as sintering temperature, holding time, sintering pressure and heating & cooling rate were optimized to reach highest bulk density. The qualitative phase analysis, microstructural analysis, Vickers hardness test and fracture toughness measurement of sintered ceramics carried out in detail. Monolithic SnO_2 ceramic sintered under optimal conditions (at 950°C for 10 min under 30 MPa) possessed 94.52 % relative density which is consistent with literature. The obtained results showed that limited grain growth improved mechanical properties.

DEVELOPMENT IN CERAMIC POWDER SYNTHESIS AND BORON BASED CERAMICS**SYNTHESIS OF HfB_2 -HfC NANOCOMPOSITE POWDERS VIA BALL-MILLING ASSISTED ANNEALING**

Emre Tekoğlu¹, Duygu Ağaoğulları¹, Siddika Mertdinç¹, M. Lütfi Öveçoğlu¹

Istanbul Technical University, Faculty of Chemical and Metallurgical Engineering, Metallurgical and Materials Engineering Department, Particulate Materials Laboratories (PML), 34469 Maslak, Istanbul, Turkey

In this study, $\text{Hf-B}_2\text{O}_3\text{-Mg-C}$ powder blends were subjected to high-energy ball milling at various durations (0, 2, 3, 4 and 8 h). The milled powders were then annealed at 1400 °C for 12 h under Ar atmosphere in order to obtain HfB_2 and HfC phases as reaction products. X-ray diffractometry (XRD) and scanning electron microscopy/energy dispersive spectrometry (SEM/EDS) techniques were utilized due to perform microstructural characterization of the powders. The analysis results showed that HfB_2 and HfC phases existed in the annealed powders which were exposed to ball milling for 8 h. MgO phase was removed after HCl leaching process. 8 h of milled and annealed powders did not exhibit any undesired phases, and pure nanocrystalline HfB_2 -HfC composite powders were successfully obtained after leaching step.

DEVELOPMENT IN CERAMIC POWDER SYNTHESIS AND BORON BASED CERAMICS**TAILORING THE MORPHOLOGY AND COMPOSITION OF SOL GEL SYNTHESIZED BORON CARBIDE (B₄C) POWDERS BY CONTROLLING THE GEL NETWORK**Figen Kaya^{1*}, Suna Avcioglu^{1,2}, Cengiz Kaya^{3,4}

¹Department of Metallurgical and Materials Engineering, Faculty of Chemistry and Metallurgy, Yildiz Technical University, Istanbul, Turkey

²Department of Materials Science and Engineering, Faculty of Engineering, Ondokuz Mayıs University, Samsun, Turkey

³Materials Science and Nano Engineering, Faculty of Engineering and Natural Sciences, Sabanci University, Istanbul, Turkey

⁴Nanotechnology Research and Application Centre (SUNUM), Sabanci University, Istanbul, Turkey

In the last decade, significant scientific attention is observed in the area of synthesis of carbide based engineering ceramics via sol gel process in order to reduce production cost. As very well established, in sol gel technique, a homogenized mixture of precursors at molecular level decreases subsequent heat treatment temperature. Furthermore, better control over the purity, morphology and particle size of powders could be achieved. However, the relationships between gel network and powder characteristics, such as composition, crystallinity, particle size, and morphology are still not clearly understood.

In the present work, high purity B₄C powders were synthesized by a modified sol gel technique in an attempt to lower the formation temperature of pure stoichiometric boron carbide. Polymeric gel products were prepared by condensation reaction of glycerin and boric acid. For understanding the effects of gel network on phase content and morphology of B₄C, different carboxylic acids were used as stabilizer. Thermal behavior of gels was analyzed by using DTA/TG. Fourier transform infrared (FT-IR) spectra of the gels were inspected. Nuclear magnetic resonance (NMR) measurements were also carried out to gain better understanding on gel network. After the calcination of gels in atmospheric conditions, the precursors were consolidated at temperatures ranging from 1300 to 1500 °C. Microstructural and phase characterizations of both gels and powders were also carried out by using TEM, SEM and XRD techniques. The results indicate that borate ester bonds (B-O-C) were successfully achieved during condensation reaction. The yield strongly depends on the amount and the type of carboxylic acids, therefore the molecular structure of condensed gel. Carboxylic acid promotes the formation of rod and plate-like B₄C particles. Results shown that achieving high quality B₄C powders could be possible by tailoring the molecular structure of the gel.

Acknowledgement: The authors are grateful for the financial support from the The Scientific and Technological Research Council of Turkey (TUBITAK) and Yildiz Technical University under the contract numbers of 216M140, 216M145 and FDK-2017-3138, respectively.

DEVELOPMENT IN CERAMIC POWDER SYNTHESIS AND BORON BASED CERAMICS

TiB₂ POWDER SYNTHESIS VIA DCR METHOD

Zeynep Yıldızlı, Mustafa Özçiftçi, Ali Osman Kurt¹

Sakarya University, Engineering Faculty, Department of Metallurgy and Materials Engineering,
54187, Sakarya, Turkey

Titanium diboride (TiB₂) is a titanium boron compound containing 31.1% boron by weight of the Ti-B system. TiB₂ has been one of the important engineering materials due to its superior mechanical properties, high hardness, high thermal and electrical conductivity, good wear, thermal shock and corrosion resistance, chemical stability and high melting point. As a result, TiB₂ is increasingly used day by day. Commercial production of TiB₂ powder is carried out using carbothermic methods using TiO₂, B₄C and carbon at temperatures of 2000°C or above. In this study, a new ceramic powder production method called dynamic / carbothermal reduction (DCR) was applied and the effects of different test parameters on TiB₂ production were investigated. In this new technique, the granules are prepared from B₂O₃, TiO₂ and C mixture. Then granules were charged in a graphite reactor placed in an atmospheric controlled alumina tube furnace where heating rate was controlled during reaction with continues flow of argon gas having some propane. Reactor rotating speed, temperature, gas mixture and amount of B₂O₃ additions all affected on the TiB₂ formation. According to XRD and FESEM analyses, the rotational speed of 2 rpm and the temperature of 1500°C for 1 hour reaction were the ideal in obtaining TiB₂ powders. These parameters are very advantageous over the systems reported in literature for producing TiB₂ powders.

DEVELOPMENT IN CERAMIC POWDER SYNTHESIS AND BORON BASED CERAMICS**SYNTHESIS OF B₄C POWDERS VIA DIFFERENT CARBOTHERMAL REDUCTION METHODS**

Kamil Kiraz^{1*}, Özge Balcı^{1,2*}, Özge Çoşut¹, Tuğhan Akbaşak³, Buğra Çiçek^{1,4},
Mehmet Somer^{1,2}

¹Koç University Akkim Boron-Based Materials and High Technology Chemicals Research and
Application Center, Rumelifeneri Yolu, Sarıyer, İstanbul, Turkey

²Koç University, Department of Chemistry, Rumelifeneri Yolu, Sarıyer, İstanbul, Turkey

³Ak-Kim Kimya San. ve Tic. A.Ş., Çiftlikköy, Yalova, Turkey

⁴Yıldız Technical University, Department of Metallurgy and Material Science Engineering, Esenler,
İstanbul, Turkey

Boron carbide powders and their composites have been attracting great interest for years due to their excellent properties such as extreme hardness, high strength, low density and good neutron absorption ability. They have been used as precursors of abrasive materials in polishing and grinding media, lightweight armor ceramic composites and shielding materials in nuclear industry. In this study, the synthesis of micro-scale B₄C powders was carried out via different carbothermal reduction methods by using native boron sources of Turkey from Eti Maden. Various powder preparation processes such as tumbler mixing or mechanical milling were employed prior to the synthesis experiments. The synthesis was carried out in a tube or induction furnace by using the raw materials of B₂O₃ and different carbon sources that were heated up to maximum 1750°C under Ar gas. The effects of reaction conditions (e.g. temperature, duration) and the ratio of starting materials on the properties of the final powders were investigated. The variation of unreacted C content with changing reaction conditions was reported. Phase, microstructural and thermal characterizations were performed by X-ray diffractometer (XRD), scanning electron microscope (SEM) coupled with an energy dispersive X-Ray spectrometer (EDS) and differential scanning calorimeter (DSC). Particle size distributions were determined by using laser diffraction particle size analyzer. B₄C powders having an average particle size of 30-40 µm and a minimum purity of 95 % were obtained after the reaction at 1700°C for 3 h.

DEVELOPMENT IN CERAMIC POWDER SYNTHESIS AND BORON BASED CERAMICS**PRODUCTION OF FUNCTIONALLY GRADED SiC-TiB₂-Al COMPOSITES BY SPARK PLASMA SINTERING TECHNIQUE AND THEIR CHARACTERIZATION**

Merve Taner¹, Gürsoy Arslan¹

¹ Anadolu University, Department of Material Science and Engineering,
İki Eylül Campus, 26480/Eskişehir/Turkey

In this study, production of functionally graded silicon carbide-titanium diboride-aluminium composites by spark plasma sintering technique was investigated. Silicon carbide-titanium diboride-aluminium powder mixtures containing 70-90 weight % silicon carbide-titanium diboride and 10-30 weight % aluminium were sintered at 1800°C for 5 minutes by spark plasma sintering.

SiC-TiB₂-Al composites were sintered in a single step by using the spark plasma sintering method. Furthermore, the produced SiC-TiB₂-Al composites were designed as functionally graded composite material (FGM) layers having different compositions.

Results obtained show that produced composite FGM's have a microstructure characterized by a co-continuous ceramic-metal network. Furthermore, it was determined that the bulk density of the produced functionally graded composite layers was always above 99,5 %, the hardness gradually decreased from the front layer to the back layer, while the compressive strength decreased in just the opposite manner.

LEAD-FREE, TEXTURED & EPITAXIAL PIEZOELECTRICS / FERROELECTRICS & OTHER ELECTROCERAMICS

THE EFFECT OF DOPING AND SINTERING ATMOSPHERE ON ENVIRONMENT FRIENDLY KNN PIEZOCERAMICS

Murat Murutoglu¹, Erdem Akca², Huseyin Yilmaz¹

¹Technical University of Gebze, Department of Materials Science and Engineering, Kocaeli/Turkey

²Cumhuriyet University, Department of Metallurgy and Materials Engineering,
Sivas/Turkey

Although lead-based piezoceramics exhibit high electrical and electromechanical properties, environmentally friendly KNN based ceramics have been studied intensively in recent years due to the damages of lead to the environment and human health. In this study, environmentally friendly KNN-KCN ceramics, which are being developed as alternatives to lead based piezoceramics, were studied as a function of doping, sintering atmosphere and time to improve their electrical properties. KNN-KCN ceramics were doped with 3 % Sb, 1 % Sn or 0,8 % ZnSn. Doped and undoped ceramics were sintered for 2, 4, or 6 h in air or oxygen atmosphere. The problem of internal heating during service due to dielectric losses especially for high power applications (like ultrasonic drilling, cutting, motors) was studied. The Cole-Cole analysis were done using impedance phase spectroscopy, from which activation energies were calculated.

LEAD-FREE, TEXTURED & EPITAXIAL PIEZOELECTRICS / FERROELECTRICS & OTHER ELECTROCERAMICS

FABRICATION AND ELECTRICAL PROPERTIES OF $0.5[(\text{Ba}_{0.85}\text{Ca}_{0.15})\text{TiO}_3]-0.5[\text{Ba}(\text{Zr}_{0.1}\text{Ti}_{0.9})\text{O}_3]$ LEAD-FREE PIEZOELECTRIC CERAMICS

Ömer Çakmak¹, Önder Tuna¹, Ebru Menşur Alkoy¹, Sedat Alkoy¹

¹Gebze Technical University, Faculty of Engineering, Department of Materials Science and Engineering, 41400/Kocaeli/Turkey

The processing conditions and properties of lead-free piezoelectric barium calcium titanate-barium zirconate titanate (BCT-BZT) have been reported in this study. This material has been attracting much attention as potential replacements for lead-based commercially available piezoceramics. In this work, lead free $0.5[(\text{Ba}_{0.85}\text{Ca}_{0.15})\text{TiO}_3]-0.5[\text{Ba}(\text{Zr}_{0.1}\text{Ti}_{0.9})\text{O}_3]$ piezoelectric ceramics were prepared at temperatures in the range of 1360°C-1480°C by conventional solid-state sintering process. The structural and electrical properties of 0.5BCT-0.5BZT ceramics were measured and reported as a function of temperature. X-ray diffraction (XRD) results were taken at room temperature and obtained the formation of single perovskite phase for all sintering temperatures. Scanning electron microscopy (SEM) analysis of sintered 0.5BCT-0.5BZT ceramics confirmed dense and homogeneous microstructure with increasing temperature. Polarization-electric field (P-E) and strain-electric field (S-E) measurements of the 0.5BCT-0.5BZT samples showed an enhancement in polarization and strain levels with the increase of sintering temperature.

LEAD-FREE, TEXTURED & EPITAXIAL PIEZOELECTRICS / FERROELECTRICS & OTHER ELECTROCERAMICS

INVESTIGATION OF BORON DOPING IN LEAD-FREE PIEZOELECTRICS

Samet Abbak¹, Mahmud C. Yalcin¹, Metin Özgül^{1,2}

¹ Department of Materials Science and Engineering, Afyon Kocatepe University,
Afyonkarahisar/Turkey

² Technology Application and Research Centre (TUAM), Afyon Kocatepe University,
Afyonkarahisar/Turkey

Boron (B_2O_3) is added to various perovskite type piezoelectric ceramics and substantial property improvements were reported. However the stability of piezoelectric properties is usually overlooked. The main goal in this study is systematically track the changes in properties after poling in various compositions as a function of differing conditions such as electric field, time and temperature. In this perspective, $0.94(Bi_{0.5}Na_{0.5}TiO_3)-0.06BaTiO_3$ (BNT-6BT) ceramics were synthesized as undoped, B^{3+} doped, and B^{3+} co-doped with several other cations possibly acting as donors or acceptors. Sintered samples were characterized by X-ray diffraction (XRD) and fracture surfaces of the specimens were imaged by scanning electron microscope (SEM). Dielectric and piezoelectric properties were measured at room temperature for all the samples following a DC poling. Measurements were repeated for all the samples after holding at various temperatures (RT, 40, 60, 80 and 100°C) as a function of time up to 10^5 s to determine the influence of doping on depolarization behavior of BNT-6BT ceramics. The results of the study will be discussed in light of various crystalline defect formations due to different dopants to understand their role on the stability of electrical properties after poling.

LEAD-FREE, TEXTURED & EPITAXIAL PIEZOELECTRICS / FERROELECTRICS & OTHER ELECTROCERAMICS

INVESTIGATION OF FERROELECTRIC PROPERTIES OF LITHIUM AND MANGANESE DOPED NBT-6BT CERAMICS

Mert GÜL^{1,2}, A.Baturay GÖKÇEYREK³, Mevlüt GÜRBÜZ⁴, Ayşe Gül TOKTAŞ³,
Taner KAVAS¹, Aydın DOĞAN^{2,3}

¹ Afyon Kocatepe University, Department of Materials Science and Engineering, Afyonkarahisar, Turkey

² Nanotech High Tech Ceramics Company, Eskişehir, Turkey

³ Eskişehir Technical University, Department of Materials Science and Engineering, Eskişehir, Turkey

⁴ Ondokuz Mayıs University, Department of Mechanical Engineering, Samsun, Turkey

Lead-free NBT-BT ceramics are alternative composition of PZT for its electrical properties due to environmental RoHS standards. Multilayer forms of lead free compositions were studying to use in the applications requiring precise control and fast response [1]. Although multilayer ceramics have high reliability, costs are high due to their manufacturing method and precious metal content such as palladium. In inner electrodes containing silver and palladium, palladium content is wanted to be decreased. So sintering temperatures must to be decreased to have good electrical properties. For this reason lithium is used for lowering sintering temperatures [2]. Besides this piezoelectric properties are affecting by doping some elements such as Manganese. In this work NBT-6BT composition is modified by using lithium and lithium-manganese. Then sintered for 2 hours at varying sintering temperatures lower than the 1100°C. Surfaces of the pellets were electroded with silver paste and polarized at 60°C oil bath under voltage 3kV/mm for 15 minutes. Piezoelectric properties were measured on the pellets and ferroelectric behaviour was determined at the frequency of 1 Hz.

Keywords: Lead-Free, Low Sintering, manganese, lithium

References

- [1] Sapper E., Gassmann A., Gjodvad L., Jo W., Granzow T., Rödel J.(2014) "Cycling stability of lead-free BNT-8BT and BNT-6BT-3KNN multilayeractuators and bulk ceramics" Journal of the European Ceramic Society 34; 653-661
- [2] Yoo J., Lee C., Jeong Y., Chung K., Lee D., Paik D.(2005) "Microstructural and piezoelectric properties of low temperature sintering PMN-PZT ceramics with the amount of Li₂CO₃ addition" Materials Chemistry and Physics [90] 386-390.

LEAD-FREE, TEXTURED & EPITAXIAL PIEZOELECTRICS / FERROELECTRICS & OTHER ELECTROCERAMICS

EFFECTS OF LANTHANUM DOPING ON DIELECTRIC AND FERROELECTRIC PROPERTIES OF $PB(Zr_{0.70}, Ti_{0.30})O_3$ CERAMICS

Namık Kemal Gözüaık¹, Ebru Menşur Alkoy¹, Sedat Alkoy¹

¹Gebze Technical University, Faculty of Engineering, Department of Materials Science and Engineering, 41400/Kocaeli/Turkey

Lanthanum doped lead zirconate titanate (PLZT) ceramics are very promising materials with their great functional properties such as piezoelectricity, ferroelectricity, antiferroelectricity, electrostrictive effect, and electrooptic effect. PLZT ceramics are widely used in smart sensors and optical processing devices thanks to their unique characteristics. PLZT ceramics have been synthesized with lanthanum content changing from 8.0 to 9.0 at. % La and a Zr/Ti ratio of 70/30, via conventional solid-state reaction method. The effect of La content on the structural and electrical properties of PLZT (Zr/Ti=70/30) ceramics has been investigated. The studies about the ferroelectric and dielectric properties of PLZT ceramics were conducted. Hysteresis loops and strain curves were shown and discussed. The results indicated that antiferroelectricity stability was improved while the lanthanum content was increased. With the increasing La content, polarization and strain values of ceramics decreased. All the PLZT ceramic samples exhibited a dispersive dielectric behavior. The maximum dielectric constants and the Curie temperatures were also decreased with increasing La content.

LEAD-FREE, TEXTURED & EPITAXIAL PIEZOELECTRICS / FERROELECTRICS & OTHER ELECTROCERAMICS

COMPARISON OF ELECTRICAL PROPERTIES OF ZNO-BI₂O₃ BASED CERAMICS PREPARED BY CONVENTIONAL AND SPARK PLASMA SINTERING (SPS) METHOD

Fatih Apaydın 1, Ali Çelik 1, Ferhat Kara 2

¹Bilecik Şeyh Edebali University, Department of Metallurgy and Material Engineering, Bilecik /Turkey

²Anadolu University, Department of Material Science and Engineering, İki Eylül Campus, 26480/Eskişehir/Turkey

Zinc oxide based varistors protect electronic circuits and circuit components against voltage fluctuations due to their nonlinear current-voltage (I-V) characteristics. The nonlinear I-V characteristic is that the varistor exhibits different resistances at different voltage values and, if the critical voltage value is exceeded, protects the circuit by ensuring that the high current generated by losing the majority of the varistor resistor passes on itself.

The electrical characteristics of varistors depend directly on the microstructure of the material. During the production process, various chemical elements are dispersed into the microstructure and high resistance occurs in the grain boundaries while high conductivity occurs in a grain.

The Spark plasma sintering (SPS) has been developed since the 90's with the introduction of pulsed direct current by developing the hot press method. SPS allows dust particles to be attached at low temperatures and in a short period of time by charging the powder particles with electrical energy. While SPS is a suitable technique to sinter difficult to sinter materials such as structural nitride and carbide ceramics, it can also be utilized to obtain a fine grain microstructure which is critically important for ZnO based varistors in order to obtain high electrical conductivity.

In this study, 1% -3% CuO was added to ZnO-6% Bi₂O₃ binary ceramic system. The compositions were sintered by using both traditional and SPS methods. The microstructural, chemical and electrical properties of the ZnO based varistors were investigated comparatively.

LEAD-FREE, TEXTURED & EPITAXIAL PIEZOELECTRICS / FERROELECTRICS & OTHER ELECTROCERAMICS**SYNTHESIS AND UTILIZATION OF ZINC TIN OXIDE (Zn_2SnO_4) PARTICLES IN ELECTRONIC DEVICES**

Cem Aciksari^{1,2}, I. Gozde Tuncolu³, S. Pelin Erden¹, Umut Savaci¹,

Servet Turan¹, Emel Ozel¹, Ender Suvaci¹

¹Department of Materials Science and Engineering, Eskişehir Technical University, Eskişehir/Turkey

²TUPRAS Research and Development Center, Kocaeli/Turkey

³Fematek Uluslararası Ticaret AŞ, İzmir/Turkey

Zinc Tin Oxide is an important electronic material which has been widely used in an extensive range of applications such as gas sensors, transparent and amorphous thin film transistors (TFTs), transparent conductive electrodes (TCOs) and anode material in Li-ion batteries. ZnO-SnO_2 system has two ternary compounds, zinc orthostannate- Zn_2SnO_4 and zinc metastannate- ZnSnO_3 , are n-type intrinsic semiconductor that have recently received attention because of its high electron mobility, high electrical conductivity, low visible absorption, and the better environmental stability compared with its binary compounds (ZnO and nO_2). Zinc Stannate (ZTO) is one of the significant alternative compositions to replace Indium-Tin-Oxide (ITO) which is currently used material for electronic application such as TFTs and TCOs because of its high abundancy in Earth's crust, relatively low cost, non-toxic nature. TFTs and TCOs are composed of thin films generally prepared via sputtering technique. To produce high quality thin film, the oxide target material used in the sputtering technique should be high purity (≥ 99.9 wt%), almost dense ($\geq 95\%$ Theoretical Density) and having homogeneous microstructure. Desired target properties are controlled by the quality of as-synthesized oxide powder. In the present study, the critical powder characteristics on the electrical and optical properties of sputtered film will be discussed and the particle characteristics of ZTO will be evaluated as a function of different synthesis procedures such as solid state and liquid phase synthesis.

SANITARYWARE**THE EFFECTS OF DIFFERENT TYPES OF FLY ASH ON THE PROPERTIES OF
SANITARYWARE CERAMICS**

İbrahim ERDOĞAN¹, Hülya KURŞUN¹, Umut ÖNEN¹, Tahsin BOYRAZ¹,
Turhan KURŞUN²

¹Cumhuriyet University, Department of Metallurgical and Materials Engineering, TURKEY

²Cumhuriyet University, Department of Manufacturing Engineering, TURKEY

Coal burning products are a waste derived from the burning of coal in in large power plants, and bottom ash, include fly ash, boiler slag and flue gas desulfurization materials. Fly ash usually recovered by mechanical filtration or electrostatic precipitation methods. It is valuable waste and can be used in the production of value added products. Fly ashes are appropriate for industrial recycling and have a wide range of uses in many industrial areas. In this study, the use of fly ash wastes obtained from some thermal power plants in Turkey (Çatalağzı-Zonguldak, Çayırhan-Ankara, Kangal-Sivas ve Afşin/Elbistan-Kahramanmaraş) in sanitaryware ceramics have been examined. Sanitaryware body mixes are prepared with 0-30% fly ash by weight. Then, mixtures (fly ash and fly ash-sanitaryware) were shaped with uniaxial pressing and sintered at different temperature. These ceramic materials were subjected to physical and mechanical tests such as dried strength, dried shrinkage, bend strength, fired shrinkage and water absorption. As a result, mechanical, thermal and microstructural properties of sintered samples were characterized and the effects of different fly ash additives on the sanitaryware properties were determined.

SANITARYWARE**PREPARATION AND INVESTIGATION OF MULTIFUNCTIONAL CERAMIC
PRODUCTS FOR SANITARYWARE**

Demet Topaloğlu Yazıcı, Meltem Ayrancı, Orkun Söylemezoğlu, Selin Uzun,
İrem Öztürk

Eskişehir Osmangazi University, Department of Chemical Engineering, Meşelik Campus,
26480/Eskişehir/Turkey

Nowadays according to the changing living conditions, people spending most of their time outside the home. Especially in crowded areas, microorganisms can spread easily and therefore infectious diseases also increase. Epidemics occur in areas where there are too many microorganisms. The importance of sterile environments for a healthier life is increasing day by day. In this study, preparation of ceramics with two recipes, coating by using different solutions and investigation of them to evaluate in building materials and to adapt in sterile environments were aimed. Dip coating method was used. Polymer solutions with different including were prepared for coating. Ceramic products prepared in this study will be presented for the use in areas where hygiene is important such as hospitals, operating theaters, intensive care units. Experimental studies have been carried out to observe the resistance of the prepared products to water, acidic and basic solvents, moisture retention capacity, surface contact angle and antibacterial properties. So, the prepared products may be presented to the ceramic sector. Beside these experimental investigations, surface morphologies of the coated products and the thickness of the coating were also examined by scanning electron microscope and optic microscope, respectively. After the experiments, some of the coated ceramic products showed well resistance to chemicals. It was also found that contact angle values of the products increased after coating.

SANITARYWARE**THE POTENTIAL EFFECTS OF ALBITE AND ORTHOCLASE ON SANITARYWARE COMPOSITION**

Selçuk Özkan¹, Emin Karabay¹ and Hasan Göçmez²

¹Güral Porcelain and Sanitaryware Research and Development Center, Kütahya/Turkey

²Kütahya Dumlupınar University, Faculty of Engineering, Metallurgical and Materials Engineering Department, Kutahya/Turkey

Sanitaryware products, the one of main group of traditional ceramic, contain mainly clay, kaolin, quartz and feldspar. They are slightly different than regular ceramic products because of their size and complex shape. During the manufacturing of sanitaryware products, it is critical to control rheology, casting thickness, deformation and sintering behavior of body. In this study, albite ($\text{NaAlSi}_3\text{O}_8$) and orthoclase (KAlSi_3O_8) were added into sanitaryware or vitreous china slip composition to determine the effect of rheology, casting and engineering properties on slip composition. Three different slips were prepared by adding albite, orthoclase and albite/orthoclase (50/50) replacing with regular feldspar into vitreous china compositions. Then, viscosity, casting thickness, green strength, deformation, water absorption of samples were measured by standard test methods. In addition, the characterization of samples were determined by X-ray Fluorescence, Thermogravimetric and differential thermal analyzers.

ADVANCED CERAMICS**EFFECT OF LiF ADDITION TO EAG- Al_2O_3 EUTECTIC CERAMICS FOR DENSIFICATION, MICROSTRUCTURAL AND MECHANICAL PROPERTIES**

Ece ÖZERDEM, Kübra GÜRCAN^{1*}, Erhan AYAS¹

¹Eskişehir Technical University, Department of Material Science & Engineering
İki Eylül Campus, 26555, Eskişehir/TURKEY

Al_2O_3 -based eutectic ceramics are well known polycrystalline oxide ceramics which present superior creep and oxidation resistance, high temperature strength retention up to their eutectic temperature makes them an important candidate for high-temperature applications above 1500°C. Al_2O_3 -EAG eutectics exhibiting comparable densification levels, microstructural features and mechanical properties have been investigated for the development of structural materials, which withstand high temperatures under decent loading conditions on energy generated fields. For this purpose, $\text{Al}_2\text{O}_3/\text{Er}_3\text{Al}_5\text{O}_{12}$ (EAG) eutectic was prepared by an arc melting process under Argon atmosphere. Obtained eutectic fine powders were then consolidated by the spark plasma sintering (SPS) technique with the addition of % 0.25, % 0.5 and % 1 LiF addition applying 2 min. dwell times at 1530°C and 1700°C under 15-50 MPa uniaxial pressure. Systematic investigations on the effect of LiF addition on densification behavior, microstructure and its stability properties and mechanical properties of the eutectics were investigated intensively.

BIOCERAMICS**CURRENT IMPROVEMENTS OF THE MECHANICAL PROPERTIES ON LITHIUM DISILICATE DENTAL RESTORATIONS**Burcu Ertuğ¹¹ Department of Mechatronics Engineering, Nişantaşı University, Maslak Mahallesi 1453 Söğütözü Sokak, No: 20 Ağaoğlu Maslak 1453 Sarıyer/İstanbul

The ceramic materials can mimic the natural appearance of a tooth very well. However, characteristic brittleness of the ceramics leads to mechanical unreliability. Thus it is of great importance to analyze the mechanical properties of dental ceramics. IPS Empress1 is the hot-pressed ceramic as the first generation. 65 vol % lithium disilicate is present as the main crystalline phase in IPS Empress2. Before lithium disilicate ($\text{Li}_2\text{Si}_2\text{O}_5$) crystals grow during the crystallization stage, lithium metasilicate (Li_2SiO_3) and cristobalite (SiO_2) phases form as revealed by several studies. The lithium disilicate crystals are randomly oriented, fine-grained and highly interlocked, which leads to an increase in the strength. Later on, Ivoclar Vivadent company developed IPS e.max Press, which is a lithium disilicate glass-ceramic ingot produced by the pressing. In comparison to IPS Empress, IPS e.max press has higher flexural strength. The fracture toughness has been measured by three-point bending and biaxial testing methods to be $3.1 \text{ MPa}\cdot\text{m}^{1/2}$ and $2.5 \text{ MPa}\cdot\text{m}^{1/2}$, respectively. The hardness values have been measured to be 6.6 GPa and 5.3 GPa for IPS-Empress and Empress 2, respectively. Using biaxial testing, the strength has been measured to be 265 MPa and by the three-point bending method, the strength has been determined to be 280 MPa. The fracture toughness by the indentation has been measured to be $1.26 \text{ MPa}\cdot\text{m}^{1/2}$ for IPS-Empress and $1.67 \text{ MPa}\cdot\text{m}^{1/2}$ for Empress 2, respectively.

Keywords: Ceramics, Dental, Lithium disilicate, Restoration.

BIOCERAMICS**3D-PRINTED HYDROXYAPATITE STRUCTURES BY USING WET CHEMICALLY PRECIPITATED POWDERS**Azade Yelten-Yilmaz¹, Suat Yilmaz¹¹ Istanbul University-Cerrahpaşa, Department of Metallurgical and Materials Engineering, Avcılar Campus, 34320/Istanbul/Turkey

Hydroxyapatite ($\text{Ca}_{10}(\text{PO}_4)_6(\text{OH})_2$, HA) is the mineral constituent of bone and teeth. Production of HA in different forms like powders, fibers, granules etc. is important for curing or renovating operations of the damaged or lost hard tissues. At this point, preparation of patient-specific parts attracts attention in terms of not only reducing the healing duration but also improving the recovery process of the tissue. Rapid prototyping (RP) techniques present the chance of achieving parts with the required geometrical properties by using different precursors like metals, polymers and so on for several fields such as architecture, aviation, automotive, etc. Biomedical market also take place among these application areas and researches on obtaining implants, prostheses and artificial organs through the RP approach are daily increasing. Three dimensional (3d) printing is one type of RP systems and can be utilized for producing parts from powder form materials. In this work, HA powders were synthesized considering the wet chemical precipitation principle which can be described as an ideal way to attain HA powders in large amounts economically. Process parameters are pretty essential on the features of the obtained particles and therefore, present work focused on the acid-alkaline (for this research calcium hydroxide-phosphoric acid) reaction temperature, acid addition rate and heat treatment temperature. HA structures were 3d-printed by using the mentioned HA powders and the optimum process parameters that are proper for the powders which can be employed in 3d printing devices were investigated.

Acknowledgement: This work was supported by Scientific Research Project Coordination Unit of Istanbul University [grant numbers 37881 and 28135]. The authors also would like to thank the Teaching Staff Training Program Office (ÖYP) of Istanbul University for providing financial support to this project.

GENERAL

THE ASSESSMENT OF PORCELAIN WASTES FROM PRESS AND BISCUIT FIRING IN THE PRODUCTION OF CREAM WHITE PORCELAIN

Musa Hilal Gürbüz¹, Ramazan Dutar¹, Metin Yüce¹, Ahmet Kahya¹ and Hasan Göçmez²

¹Güral Porcelain and Sanitaryware Research and Development Center, Kütahya/Turkey

²Kütahya Dumlupınar University, Faculty of Engineering, Metallurgical and Materials Engineering Department, Kutahya/Turkey

Isostatic press is commonly used forming technique in the porcelain production. During this process, significant amount (up to 20%) of production may be waste, which is derived from turnings and finishing operations. In the meantime, biscuit waste (up to 5%) also occurred during the firing. It is crucial to regain this waste and used again in the production without changing composition as well as quality of porcelain.

The waste slurry has similar composition with cream white porcelain. In addition, the characterization of samples showed that the current composition of cream white masse and broken biscuit were similar. In this study, the waste from isostatic press and biscuit can be reused in the production by controlling processing steps. Especially, grinding conditions of waste was optimized by controlling parameters such grinding time and loading order of powder and ball/powder ratio.

GENERAL**INVESTIGATION OF USAGE OF Na-HUMATES IN CERAMIC PRODUCTION**

Eda ATAN¹, Pervin GENÇOĞLU¹, Alpagut KARA^{1,2}, Nesli KÜÇÜKTEPE³, Ayhan SEZGİN³,
Zeki OLGUN³

¹ Seramik Araştırma Merkezi A.Ş., Eskişehir

² Anadolu Üniversitesi, Mühendislik Fakültesi, Malzeme Bilimi ve Mühendisliği Bölümü, Eskişehir

³ Türkiye Kömür İşletmeleri Kurumu Genel Müdürlüğü, Ankara, Türkiye

Our country is one of the leading countries in the world in terms of industrial ceramics production and, production quantities increase every year. Because of high production quantity, researchers and manufacturers cooperate to develop new technologies. During forming process, slip stability is particularly critical point. Slip stability is provided by determining and controlling rheology of slip like viscosity, thixotropy, density, yield point. Silicates (Na-Silicates), carbonates (Na-Carbonate) and organic compounds are added to control rheological properties in ceramic manufactories. In order to prevent agglomeration, i.e., to stabilize the slip, it is necessary to arrange for optimal repulsive forces to act between the solids particles. Here, the addition of suitable deflocculants and dispersants makes it possible to exert a controlled influence. In this study, Na-humate effect on rheological properties will be examined the ceramic sanitaryware part and ceramic tile production.

FUEL CELLS AND POWDERS

LA_{0.6}SR_{0.4}COO₃ THIN FILM CATHODES PREPARED BY POLYMERIC PRECURSORS FOR SOLID OXIDE FUEL CELLS

Sevim ERDÖL¹, Cleva OW-YANG^{2,3}, Meltem SEZEN³, Aligül BÜYÜKAKSOY¹

¹*Material Science and Engineering, Gebze Technical University, Gebze, Kocaeli 41700, TR*

²*Sabancı University, Faculty of Engineering and Naturel Sciences 34956, Tuzla, Istanbul*

³*Sabancı University, SUNUM Nanotechnology Research Center 34956, Tuzla, Istanbul*

La_{0.6}Sr_{0.4}CoO₃ (LSC) is a very attractive solid oxide fuel cell (SOFC) cathode material owing to its high activity for oxygen reduction. Until now, it has generally been fabricated in the form of thin films by pulsed laser deposition, which requires very high costs and thereby is not suitable for industrial production. In this project, we aim to fabricate LSC thin films with high surface area and chemical homogeneity using spin-coating deposition, an easy-to-apply and cost-effective method, of cation-loaded polymeric solutions and followed by heat treatment at low temperatures ($\leq 800^\circ\text{C}$).

X-ray diffraction analyses revealed that the deposited thin films had a nearly amorphous structure upon annealing at 600°C , while increasing the annealing temperature resulted in the formation of tetragonal SrLaCoO₄ and rhombohedral La_{0.6}Sr_{0.4}CoO₃ perovskite phases. Focused ion beam milling in an SEM was used to prepare electron-transparent lamella of these specimens. Energy dispersive x-ray spectroscopy performed in a scanning TEM showed that while the La, Sr and Co were somewhat homogeneously distributed when the films were annealed at 600°C , Co-rich regions formed when the annealing temperature was increased to 800°C . Electrochemical impedance spectroscopy (EIS) measurements of symmetrical half-cells in air showed that the minimum cathode polarization resistance obtained was $1.08\ \Omega\cdot\text{cm}^2$ at 600°C .

FUEL CELLS AND POWDERS

DEVELOPMENT OF YTTRIA STABILIZED BISMUTH OXIDE (YSB) CERAMICS FOR SOFC ELECTROLYTE APPLICATIONS

Gebze Technical University, Department of Materials Science and Engineering

**Yavuz Selim Ayhan *Aligul Buyukaksoy*

In order to contribute to the efforts to solve the inefficient energy production problem, solid oxide fuel cell (SOFC) technology has been widely investigated. SOFCs allow the use of hydrogen or hydrocarbon gases with high efficiency (>80%) to produce electricity. However, the observation of performance loss during long-term operation at high temperatures (700-900 °C) yet remains the barrier preventing the commercialization of these devices.

Development of electrolyte membranes exhibiting high ionic conductivity and long-term stability at low temperatures (≤ 650 °C) seems to be the simple approach to address this problem. Therefore, we focus our efforts on YSB ceramics with a proven ionic conductivity that is two orders of magnitude higher than that of the generic electrolyte material, yttria stabilized zirconia at 650 °C.

In this work, a detailed study on the fabrication of YSB electrolyte ceramics, their electrical conductivity and their long-term stability at 650 °C, in air is presented. Synthesis of the fluorite phase YSB powders with fine particle size (200 nm) was realized by using the Pechini method. The consolidation of these powders via die pressing or tape casting resulted in dense ceramics (ca. 93% of the theoretical density) upon sintering at 1000 °C for 6 hours.

An electrical conductivity of 1.7×10^{-2} S/cm at 650 °C in air was obtained after our initial electrochemical impedance spectroscopy results. After being exposed to 650 °C for 100 hours in stagnant air, ca. 33% electrical conductivity loss is observed. Possible sources of this degradation are currently being investigated.

FUEL CELLS AND POWDERS

DEVELOPMENT of $\text{La}_{0.8}\text{Sr}_{0.2}\text{MnO}_3\text{-Ce}_{0.8}\text{Sm}_{0.2}\text{O}_2$ NANOCOMPOSITE CATHODES for SOLID OXIDE FUEL CELLS

E. Ayca EKSIOGLU¹, Cleve OW-YANG², Meltem SEZEN³, Aliğul BUYUKAKSOY⁴

¹ *Gebze Technical University, Department of Physics 41400, Gebze, Kocaeli*

² *Sabancı University, Faculty of Engineering and Natural Sciences 34956, Tuzla, Istanbul*

³ *Sabancı University, SUNUM Nanotechnology Research Center 34956, Tuzla, Istanbul*

⁴ *Gebze Technical University, Department of Material Science and Engineering 41400, Gebze, Kocaeli*

Solid oxide fuel cell (SOFC) electrodes are fabricated in form of composites consisting of electrocatalyst, ionic conductor and gas (pore) phases. The electrochemical reactions take place at the intersection of these three phases, that is at “triple-phase boundaries”. At elevated operating temperatures (800-1000°C) a shortening of the triple phase boundary (TPB) length, and hence a drop in the electrode performance, is observed, caused by microstructural coarsening. Therefore, we aimed to reduce the operating temperature of these devices down to ≤ 650 °C. To make up for the electrode performance loss that the slower electrode reaction kinetics would cause, we sought to develop electrode materials with long TPB lengths by a novel method.

In this study, we investigated the fabrication of $\text{La}_{0.8}\text{Sr}_{0.2}\text{MnO}_3\text{-Ce}_{0.8}\text{Sm}_{0.2}\text{O}_2$ (LSM-SDC) composite cathode thin films by a polymeric precursor solution method. Here, the mixture of separately prepared polymeric LSM and SDC precursors are co-deposited onto dense electrolyte substrates by spin-coating. The molecular level mixing of the ionic conductor and electrocatalyst cations and the mutual insolubility of the two phases allow the formation of the nanocomposite structure upon heat treatment at the relatively low temperatures of 600-800°C. X-ray diffraction studies revealed that the crystallization of both LSM and SDC phases could be observed at 700°C. The transmission electron microscopy-energy dispersive x-ray spectroscopy analyses were in agreement with this result and revealed a microstructure with an average particle size of *ca.* 100 nm. Electrochemical impedance spectroscopy measurements suggested that the cathode polarization resistance decreases significantly when both phases are crystallized.

FUEL CELLS AND POWDERS

$\text{La}_{0.8}\text{Sr}_{0.2}\text{MnO}_3 - \text{Bi}_{1.44}\text{Y}_{0.56}\text{O}_3$ Thin Film Cathodes for Solid Oxide Fuel Cells

Busra AKTAS¹, Cleva OW-YANG^{2,3}, Meltem SEZEN³, Aligul BUYUKAKSOY⁴

¹Gebze Technical University, Department of Physics, 41400, Gebze, Kocaeli

²Sabancı University, Materials Science and Nano-engineering Program, 34956, Tuzla, Istanbul

³Sabancı University, SUNUM Nanotechnology Research Center, 34956, Tuzla, Istanbul

⁴Gebze Technical University, Department of Material Science and Engineering, 41400, Gebze, Kocaeli

To avoid degradation at high operating temperatures of 800-900 °C, we propose developing cathode materials that have a long triple-phase boundary—boundaries where the electrochemical reactions take place (TPB)—lengths and therefore exhibit high performance even at low temperatures ($\leq 600^\circ\text{C}$). In this study, the widely used electrocatalytic cathode material, $\text{La}_{0.8}\text{Sr}_{0.2}\text{MnO}_3$ (LSM), was used in the form of a composite blended with Y_2O_3 -stabilized- Bi_2O_3 (YSB), due to its extremely high oxygen ion conductivity and more recently discovered activity, for oxygen reduction. To achieve our goal of enhanced electrochemical performance at low temperatures, LSM-YSB cathodes were fabricated as nano-composite thin films by a cost effective and facile polymeric precursor solution method. In this case, the polymeric precursors of LSM and YSB were prepared separately, then mixed together to obtain a clear solution mixture and finally deposited onto a dense YSB electrolyte by spin-coating. Upon heat treatment at 600-800 °C, this approach produced a thin film microstructure with nanoscale diameter particles, and consequently a long TPB length.

X-ray diffraction experiments showed that heat treatment at 600 °C results in crystallization of the rhombohedral LSM phase alone, leaving the rest of the film amorphous. Electrochemical impedance spectroscopy measurements of symmetrical half-cells in air showed that the LSM-YSB cathodes exhibited cathode polarization resistances as low as $0.55 \Omega\cdot\text{cm}^2$ at 600 °C. The LSM-YSB thin film microstructure and the elemental distribution within the film were investigated by SEM and transmission electron microscopy (TEM) coupled with energy dispersive x-ray spectroscopy. TEM lamella were prepared by FIB milling.

FUEL CELLS AND POWDERS

DEVELOPMENT OF NiO-YSZ PRECURSORS FOR SOLID OXIDE FUEL CELL ANODE FABRICATION

B. Bilbey¹, A. Buyukaksoy¹

¹ Department of Materials Science and Engineering, Gebze Technical University, 41400 Gebze, Kocaeli, Türkiye

For high performance Solid Oxide Fuel Cell (SOFC) operation, it is imperative that the fuel electrode (anode) allows fast electrochemical reactions. The most widely preferred anode material is a porous composite called cermet, composed of an electro-catalytic metal (Ni) and an ion-conducting ceramic (Yttria stabilized zirconia-YSZ). The electro-oxidation of fuel takes place at the intersection of the Ni-YSZ and gas phases (i.e., triple phase boundary).

The conventional method to fabricate Ni-YSZ anodes involve the sintering of NiO-YSZ powder mixtures at high temperature (i.e., 1200-1450°C), followed by the in-situ reduction of NiO to Ni. High sintering temperatures results in coarse microstructures, thus short TPB length and consequently poor electrochemical performance. Therefore, in the present study, we attempt to use the versatile polymeric precursor fabrication approach for the synthesis of powders as well as the deposition of thin films by spin coating method, Ni and YSZ phases being distributed very homogeneously in both cases. Polymeric precursor method does not require high temperature calcination for phase formation, while allowing molecular level mixing and fine particle sizes. Therefore, the achievement of long triple phase boundary length and consequently high electrochemical performance is enabled with this method.

X-ray diffraction studies revealed the crystallization of cubic YSZ and cubic NiO phases upon calcination of the dried NiO-YSZ polymeric gels at temperatures above 600°C. The composite powder particle size laid at ca. 1 µm. The scanning electron microscopy analysis showed that a very conformal and homogeneous NiO-YSZ thin film was formed by the spin-on deposition of polymeric precursors.

FUEL CELLS AND POWDERS

Electrochemical Performance of $\text{La}_{0.6}\text{Sr}_{0.4}\text{O}_3$ Thin Film Cathodes with Porous Ag Current Collectors

E. Demirkal^a, A. Büyükaksoy^a

^aMaterial Science and Engineering, Gebze Technical University, Gebze, Kocaeli 41700, TR

It is the common opinion in the solid oxide fuel cell (SOFC) community that, to obtain high power densities, the oxygen reduction reaction (ORR) activity in the cathode side must be enhanced. To achieve this goal, there are two problems that need to be addressed. First, a cathode consisting of an effective electrocatalyst with a microstructure enabling high surface area must be developed. Second, to effectively deliver the electrons to the cathode for the ORR to take place, an electronically conductive current collector layer must be formed on top of the cathode.

In this study, $\text{La}_{0.6}\text{Sr}_{0.4}\text{O}_3$ (L6S4F) thin film cathodes were fabricated by spin-on deposition of polymeric precursors onto dense electrolyte substrates. The relatively low heat treatment temperatures required in this fabrication technique resulted in microstructures with nanoscale particle and pore sizes. In addition, an investigation to develop effective current collectors was carried out by comparing the electrochemical performance measurements of the L6S4F thin film cathodes using commercial and in-house Ag current collector inks. The use of commercial Ag current collector yielded very high polarization resistance values. This was related to the frit content in the ink (intended to enhance adhesion) resulting in a dense Ag microstructure which prevented the oxygen gas from reaching the cathode surface. The in-house Ag current collector ink contained no frit, thus produced a porous microstructure allowing the oxygen to pass through to the cathode surface. Consequently, a more accurate measurement yielded a very promising cathode polarization resistance of $0.5 \Omega \cdot \text{cm}^2$ at 700°C , in air.

CERAMIC SANITARYWARE AND TABLEWARE**INVESTIGATION OF THE EFFECTS OF RED/CORAL PIGMENTS
ON THE GLOSSY OPAQUE SANITARYWARE GLAZE**

Hakan KIRAN¹, Ebru AKDOĞANOĞLU^{1*}, Kaan DEMİR¹

¹ Ege Vitrifiye Sağlık Gereçleri San. ve Tic. A. Ş.,

İzmir / TÜRKİYE

Abstract

In this study, the surface effects of different inorganic pigments in reddish tones are investigated. The final colors of fired glaze samples are aimed to have same values according to CIELAB color scale, by proportioning and mixing pigments that have different tones and chemical compositions.

It was known that the pigment dissolution in ceramic firing was affected by the firing cycle and governed by amount and chemical composition of the liquid phase. In this study, these parameters and other dissolution rate manipulating industrial variables are kept constant and the effect of chemical content of pigments are investigated on surface quality of the final product.

During the study, ceramic sanitaryware glaze is used as the matrice for colorants and applied onto vitreous china slip and all glazed bodies are fired according to European NF EN 997+A1:2015 and NF EN 14688:2015 vitreous china standards.

In conclusion it is identified that iron oxide containing coral pigments could create problems in the finished glaze quality during firing like pinholes and small craters while selenium and cadmium based pigments have no such negative effect.

Keywords: Red pigments, iron oxide, sanitaryware, ceramic

CERAMIC SANITARYWARE AND TABLEWARE**THE EFFECT OF BORON CONTAINING FRIT ON THE ANORTHITE FORMATION AND SINTERING BEHAVIOUR OF WHITEWARE BODIES**Fazilet GUNGOR¹, Berda ALTUN¹¹Kutahya Porselen Ar-Ge Merkezi, Kutahya Porselen, Eskisehir Yolu, 8. km. KUTAHYA/ TURKEY

In order to investigate the effect of boron containing frit on anorthite formation and sintering behaviour of whiteware bodies, wollastonite and bone ash based body recipes were prepared. Frit containing 20 % B_2O_3 was commercially provided. Compositions were designed in fixed ratios of SiO_2 , Al_2O_3 , CaO and MgO whereas B_2O_3 was used instead of Na_2O and K_2O . Slips were granulated and cylindrical pellets prepared from each of the batches by uni-axial press and fired at 1200, 1250 and 1300 °C. The variation of the bulk densities of the products as a function of temperature were examined. The phase content of the fired compositions were determined by XRD. The polished surfaces of the selected fired samples were examined using SEM. Physico- mechanical properties of the fired samples were also determined and compared with each other.

Key Words: B_2O_3 , Whiteware, Porcelain, Anorthite, Sintering Behaviour.

CERAMIC SANITARYWARE AND TABLEWARE**PARTICLE SIZE DISTRIBUTION MAPPING ON CERAMIC PRODUCTS AFTER DRY PRESS**

Enver Tarım¹, Müzeyyen Şirin¹, Hanife Kadioğlu¹, Fazilet Güngör¹, Dilek Birben Şen¹, Berda Altun¹,
Handan Çatır¹, Kemal Kardal¹, Harun Taşdemir¹, Veli Uz²

¹Kütahya Porcelain Research & Development Department, Kütahya

²Kütahya Dumlupınar University, Metallurgy and Material Engineering, Kütahya

Abstract

Recently, dry production of ceramic materials favor because of lower production cost and production time instead slurry production. In this study, it was investigated the particle size distribution of particles in porcelain product after dry pressing. As a result, it was determined that the particle size distribution change according to product size and shape.

Keywords: Porcelain, Dry Press, Particle Size, Ceramic

GLASS AND GLASS CERAMICS

EFFECT OF SECOND STEP IN ION EXCHANGE PROCESS ON MECHANICAL BEHAVIOR OF SODA LIME SILICATE GLASS

İpek ERDEM, Süheyla AYDIN

Istanbul Technical University, Turkey

Conventional chemical tempering involves a one step ion exchange where the hardness, cracking behavior, bending strength are enhanced by the compressive stress generation on glass surface by the incorporation of larger ions. A different ion exchange method to generate compressive stress is known as Engineering Stress Profile (ESP), which involves a controlled outer diffusion of potassium ions from the surface using a second ion exchange step that Na^+ and K^+ counter exchange at the very surface. So compression stress is relaxed to an extent at the surface and gradually increases through the thickness aggravating the propagation of cracks. Multiple cracking is seen in these type of glasses, as the glass is not fractured until all the flaws reach a crack size limit

In the present study, Corning® 2947 soda-lime glass slides with two air sides were submitted to two step ion exchange process using KNO_3 containing salt bath in the first step and $\text{KNO}_3\text{-NaNO}_3$ salt bath in the second step. Prior to ion exchange process, grinding was applied to a party of the samples to see the effect of cutting on mechanical behavior. Varying temperatures below the glass transition temperature and varying durations were applied in stainless steel tanks. Four point bending test was used to characterize the mechanical properties of the two step ion exchanged glasses. Concentration profile of Potassium and Sodium ions incorporated into surface of the ion exchanged glasses were investigated by using energy dispersive X-ray spectroscopy (EDS) and Linescan EDS techniques.

Keywords: Two step ion exchange, chemical strengthening, soda-lime glass, mechanical properties

GLASS AND GLASS CERAMICS

ANNEALING OF GLASS AND GLASS FIRING SCHEDULES

Ecem Yılmaz¹, Göktuğ Günkaya¹

¹ Anadolu University, Department of Glass, Yunus Emre Campus, 26480/Eskişehir/Turkey

Studies on annealing, which is an important step for glass since the discovery of glass, is still in progress. It is one of the most difficult heat treatment stages in glass production process, especially in artistic glass production. The reason why it is important for artistic glass production is because of unique glass production. Especially in artistic glass production, since limited number of glass piece production, different annealing and furnace diagrams have to be written for each kind of glass piece. For the annealing process, after the glass was taken from the melting furnace and shaped, it should be kept at the annealing temperature for a suitable period of time and then cooled to room temperature in a controlled manner. In order to remove the stress or most of the stress in the glass, it is necessary to anneal according to the properties of the glass. Therefore, according to the glass type, the thickness of the glass and the shape of the glass, the glass product must be kept in the furnace for a certain period of time. If proper annealing is not carried out at this stage, various sizes of stresses occur in the glass. And then these stresses turn to cracks because of thermal expansion-shrinkage and impact. There are different types of furnace and annealing diagrams, such as Libensky annealing diagram, Ornella annealing diagram, Effetre glass annealing diagram and so on. In this study, it has been examined that how the annealing diagram parameters were determined and how the annealing diagrams were constructed.

ADVANCED CERAMICS**EFFECTS OF GAS MIXTURES ON THE SYNTHESIS OF ALN POWDERS**

İbrahim Gelen¹, Ali Osman Kurt

Sakarya University, Engineering Faculty, Department of Metallurgy and Materials Engineering,
54187, Sakarya, Turkey.

Aluminium nitride (AlN) ceramics are stable at very high temperatures in inert atmospheres and melts around 2200°C. Among the applications of AlN are opto-electronics, dielectric layers in optical storage media, military applications, as a crucible to grow crystals of gallium arsenide, semiconductor manufacturing, electronic substrates and chip carriers where high thermal conductivity is essential. It is critical to have very fine, uniax and high purity powders to start with. In this study, very fine high quality homogeneous AlN powders from readily available cheap $\text{Al}(\text{OH})_3$ raw materials were produced using the dynamic / carbothermal reduction-nitridation (DCRN) method. Based on this new powder production technique, conditions of the manufacturing process and new design parameters for AlN powder production have been determined. Instead of using solid carbon as a reducing agent, gases of C_3H_8 and NH_3 or their mixtures were used with N_2 . According to XRD and FESEM analyses, the rotational speed of 2 rpm and the temperature of 1400 °C for 2 hour reaction using approximately 50% NH_3 - 50% N_2 gas mixture with little amount of C_3H_8 were the ideal in obtaining AlN powders.

ADVANCED CERAMICS**THERMAL PROPERTIES AND MICROSTRUCTURAL CHARACTERIZATION OF
MULLITE ($3\text{Al}_2\text{O}_3 \cdot 2\text{SiO}_2$) / Y_2O_3 -STABILIZED ZIRCONIA (ZrO_2) CERAMICS**

Mehmet Akif Hafizoğlu¹, Ahmet Akkuş¹, Umut Önen², Tahsin Boyraz²

¹Cumhuriyet University, Mechanical Engineering, Sivas, Turkey

²Cumhuriyet University, Metallurgical and Materials Engineering, Sivas, Turkey

Yttrium-stabilized zirconia (YSZ, with mol 3% Y_2O_3) has superior high temperature properties such as high tolerance for thermal shock, low thermal conductivity, mechanical properties, elevated melting point, good phase stability and excellent oxidation resistance. Mullite is a good, low cost refractory ceramic with a nominal composition of $3\text{Al}_2\text{O}_3 \cdot 2\text{SiO}_2$. It has excellent high temperature properties with improved thermal shock and thermal stress resistance owing to the low thermal expansion, good strength and interlocking grain structure. In this study, YSZ and mullite powders were prepared at different temperatures at the first stoichiometric ratios. Then Mullite / YSZ ceramics with different percentages of mullite (%w. 0,5,10) was prepared using powder metallurgy techniques. The microstructural, mechanical and thermal properties were characterized using XRD, SEM and hardness. Thermal shock resistance behaviour under water quenching of the as-prepared ceramics was also evaluated. Results, revealed that the addition of mullite to YSZ matrix improves the properties of the mullite / YSZ ceramics.

ADVANCED CERAMICS

APPLICATION OF RAMAN & FTIR SPECTROSCOPY FOR ANALYZING POLYCRYSTALLINE CERAMIC $\text{SrO-AL}_2\text{O}_3$ COMPOUNDS

Arzu COŞGUN¹, Sirous KHABBAZ ABKENAR¹, Ece DENİZ¹, Elif Nur DAYI¹,
Cleva W. OW-YANG^{1,2}

¹Materials Science & Nano-engineering Program, Sabanci University, Orhanli, Tuzla-Istanbul 34956, Turkey

²SUNUM Nanotechnology Research Center, Sabanci University, Orhanli, Tuzla-Istanbul 34956, Turkey

Eu^{2+} , Dy^{3+} , and B co-activated strontium aluminate ceramics are attractive candidates for zero energy consumption lighting, due to their potential for extremely long afterglow. Because the mechanism by which B extends afterglow remains not well understood, we seek to elucidate this mechanism by understanding the dopant-induced structural changes via Raman and FTIR spectroscopy. Rietveld phase analysis of XRD data reveals that multiple competing phases are forming during our usual preparation of long afterglow, doped $\text{Sr}_4\text{Al}_{14}\text{O}_{25}$ by the Pechini method. Because multiple phases are being interrogated simultaneously, it is challenging to determine the atomic structure and subtle changes to atomic position due to incorporated dopants. Moreover, while EDX analysis in an electron microscope is useful for mapping elemental distribution, such methods will not provide information on the actual atomic arrangements of atoms in a crystalline solid. Instead, micro-Raman spectroscopy offers spatial resolution on the size scale of our ceramic powders, as well as the potential for phase identification, and FTIR spectroscopy complementarily reveals the presence of non-active Raman vibration modes.

In this talk, we present our work in fingerprint analysis of grains in Pechini-processed, undoped $\text{Sr}_4\text{Al}_{14}\text{O}_{25}$. By using solid-state reaction and Pechini methods (Dutczak, 2015), we prepared pure, single-phase reference powders of monoclinic SrAl_2O_4 , orthorhombic and monoclinic SrAl_4O_7 , hexagonal SrAl_2O_9 and orthorhombic $\text{Sr}_4\text{Al}_{14}\text{O}_{25}$. We generated reference sets of vibration spectra, *i.e.*, their fingerprints, using micro-Raman and FTIR spectroscopy. These fingerprints were then applied to determine the phase of each grain evaluated in the undoped version of our long afterglow $\text{Sr}_4\text{Al}_{14}\text{O}_{25}$.

ADVANCED CERAMICS

MICROSTRUCTURAL CHARACTERIZATION OF GRADED POROUS ALUMINA CERAMICS

Gülsüm Topates

Ankara Yıldırım Beyazıt University, Department of Metallurgical and Material Engineering, Keçiören,
Ankara/ Turkey

Pore characteristics (pore volume, size and/or morphology) have been varied along the cross section in graded porous ceramics. This special, graded pore properties enable property enhancement for ceramics (i.e. dense base material with higher strength and porous layer with improved surface area). Graded porosity can be used for filters, biomaterials to mimick the bone structure and functionally graded materials as preforms. Several techniques have been applied during the fabrication graded porous ceramics. Pressing, tape casting, slip casting, centrifugal sintering and freeze casting are some of the examples. In this study, alumina ceramics were produced in graded structure via dry pressing technique by using several pore formers. After burn-out at 600°C and sintering at 1540°C steps, final ceramics were produced. By using ImageJ, thresholding and segmentation processes of the SEM images of the samples were carried out to evaluate the graded structure. Also, 3D images of the graded ceramics were generated. Results showed that according to pore former type, the final porosity of graded ceramics produced from starch and PMMA were obtained as 12 and 16%, median pore size were 3 and 11 μm , respectively.

CERAMICS AND ENERGY: THERMOELECTRIC MATERIALS**CERAMIC AND ENERGY: THERMALLY CONDUCTIVE CERAMICS**

Pınar Uyan ^{1*}, Pınar Kaya², Servet Turan²

¹ Vocational School, Metallurgy Program, Bilecik Seyh Edebali. University, Gülümbe Kampüsü,
11210/ Bilecik/Turkey

²⁻³ Anadolu University, Department of Material Science and Engineering, İki Eylül Campus,
26480/Eskişehir/Turkey

Abstract

Si₃N₄ ceramics are commonly used in industrial applications where thermal conductivity is important. Type, amount, and distribution of phases in microstructure affect thermal conductivity. In this study, the effect of microstructure on thermal diffusivity has been studied by examining in detail with TEM techniques. Phase analysis has been performed on each surface of the samples by XRD method. The intensity of pyroxene and melilite phases on outer surface is high, the reason for the occurrence is related to inward diffusion of nitrogen from the surface and to clearly unveil the effect of crystallization. The thermal diffusivity of the outer surface with crystallization has been discovered as 15.475 mm²/sec, for the inner section, on the other hand, the value was 17.391 mm²/sec. Crystallization has reduced thermal diffusivity by ~11%.

Keywords: Thermal Diffusivity, Ceramics, Energy

CERAMICS AND ENERGY: THERMOELECTRIC MATERIALS

PHASE EVOLUTION DURING CRYSTALLIZATION FROM AN AMORPHOUS PRECURSOR OF LONG AFTERGLOW STRONTIUM ALUMINATE COMPOUNDS

Sirous KHABBAZ ABKENAR¹, Clewa W. OW-YANG^{1,2}

¹. Materials Science & Nano-engineering Program, Sabanci University, Orhanli, Tuzla-Istanbul 34956, Turkey

². SUNUM Nanotechnology Research and Application Center, Sabanci University, Orhanli, Tuzla-Istanbul 34956, Turkey

The presence of B dramatically extends afterglow to >8 hours in Eu and Dy co-doped strontium aluminate ceramics, making such pigments very attractive for zero-energy consumption lighting. While B clearly modifies the crystallization kinetics, due its well-known role as a sintering flux agent, exactly how it modifies the energy transfer between Eu and Dy in these long afterglow ceramics is still not as clearly understood. We believe that B also plays a role in the evolution of microstructural features that support long afterglow. Because thermal analysis offers insight into structural transformations and chemical reactions, we have applied differential thermal analysis (TG-DTA) to investigate the microstructure evolving in stoichiometric $\text{Sr}_4\text{Al}_{14}\text{O}_{25}$ during Pechini processing, *i.e.*, from the amorphous gel formed by polymerization of ethylene glycol and citric acid-chelated cations. In this talk, we present a detailed TG-DTA study to determine the actual sequence of phase formation during crystallization. By following a stepwise strategy of adding precursor components to evaluate their influence on crystallization, our results reveal the occurrence of 2 phase transformations. Metastable SrAl_2O_4 and SrAl_4O_7 phases start to form simultaneously from the amorphous precursor, after organic burn-off, between 700-800°C. At the first phase transition exotherm, with onset at 925°C, the amount of SrAl_2O_7 phase increases, while SrAl_2O_4 starts to disappear. The target phase $\text{Sr}_4\text{Al}_{14}\text{O}_{25}$ evolves from SrAl_2O_7 beyond the second phase transition temperature at 1150°C.

GLASS AND GLASS CERAMICS

RESEARCH AND TECHNOLOGICAL DEVELOPMENT IN ŞİŞECAM

Duygu GÜLDİREN

Şişecam Science, Technology and Design Center, Gebze/Turkey

Today, new glass-based products and applications are used in architecture, construction, automotive, transportation, informatics, data storage, electronics industries, and in imaging technologies and optics, energy generation, distribution and storage, passive and active coatings, smart/hygienic glass packaging, interactive glass household appliances, medicine, biology, pharmaceuticals, agriculture, and anti-radiation products, and anywhere else our imagination takes us. The global competition for adding value to the comforts and aesthetics in life through innovation, is guiding remarkable research and technological development efforts in the science and technology of glass.

The first priority of Şişecam is ensuring “sustainable future” which is imprinted on each link of its value chain from the first blend to the end user on a very wide spectrum ranging from flat glass, glassware, and glass packaging to chemicals needed by the industry and mining operations. Thus, it has dedicated its Research and Technological Development (R&TD) efforts and production operations to have highly innovative, environment-friendly, competitive products and production technologies, which are free of harmful compounds threatening our future.

Şişecam is strengthening its open innovation and pre-competition cooperation approach on a corporate scale, through joint studies and projects it is conducting with a growing number of universities and research centers. The organizations it is in collaboration with reached 21 domestic universities and public and private research institutes and 9 foreign universities and 6 research centers as of the end of 2017.

Şişecam is conducting its corporate R&TD efforts together with regional laboratories and production groups located near the Şişecam Science, Technology and Design Center. The Center, operating in 9400 square meters closed area with 27 specialization laboratories has international LEED GOLD Certificate and a state-of-the-art infrastructure, allowing performance of various activities ranging from fundamental research to pilot production on lab scale.

Prominent RTD studies are related to integrated furnace models to ensure efficiency of energy, which is one of the largest inputs in production; improvement of heat transfer efficiency; new refractory materials and new glass melting technologies; new glass production technologies; paradigm shifting new raw materials, new products and new applications; advanced operation control systems; measurements techniques based on advanced technologies, and new high temperature materials, as well as modeling and simulation works in these areas.

GLASS AND GLASS CERAMICS
DEVELOPMENT OF GLASS CERAMICS WITH LOW THERMAL EXPANSION
COEFFICIENT

Merve Akdemir Kutluğ¹, Banu Arslan¹, Cevher Tol¹, Barış Demirel¹, Melek Erol Taygun²

¹Şişecam Science, Technology and Design Center, Gebze/Turkey

²Department of Chemical Engineering, Istanbul Technical University,

Maslak 34469 Istanbul, Turkey

Glass ceramics have been investigated for more than three decades are polycrystalline solids produced by controlled crystallization of glasses. Glass ceramics with low- or zero thermal expansion can be obtained from $\text{Li}_2\text{O}-\text{Al}_2\text{O}_3-\text{SiO}_2$ (LAS) system. Due to their very low thermal expansion coefficient (CTE), good resistance to thermal shock and high transparency, glass ceramics are of highest economic interest and are widely used for manifold commercial products, such as cooktop panels or large telescope mirrors.

It is important to design the composition and control the crystallization of the glass to obtain desired properties. Controlled crystallization usually involves a two-stage heat treatment, respectively nucleation and crystallization stages. In the nucleation stage, small nuclei are formed after this nuclei formation, crystallization proceeds by growth of a new crystalline phase. Therefore, the amount of species and nucleating agents are important to control the nucleation and crystallization processes of LAS glasses.

In this study, LAS glass ceramic system was obtained for cooktop panels. In the first part of the study, glass composition with the optimized amount of nucleating agents were developed to gain LAS-glass ceramic in amber color with low thermal expansion coefficient and high thermal shock resistance. In the second part, the optimum heat treatment conditions (controlled crystallization) was examined by DTA analysis to obtain a homogeneous crystal phase and high mechanical properties of glass ceramics. By controlled crystallization, optimum temperature and time for nucleation and crystallization were detected. Glass ceramics formed based on optimized composition and heat treatment were characterized by using techniques such as differential thermal analysis (DTA), X-ray diffraction analysis (XRD), dilatometric analysis.

GLASS AND GLASS CERAMICS

APPLIED PERFORMANCE TESTS OF VARIOUS REFRACTORY TYPES FOR ACCURATE SELECTION IN DESIGNING GLASS FURNACES

A. Melih Üstün¹, E. Burak İzmirlioğlu¹,

¹Şişecam Science Technology and Design Center,

Analysis & Support Services/ Material Analysis and Characterization Management,

Gebze, Kocaeli/Turkey

Establishment of a glass furnace is a very complicated business, in which refractories cost around millions of dollars. That is why glass companies are always in search of supplying cheaper refractories for saving currency. However, preferring cheaper refractories might have sometimes catastrophic results when a furnace which is constructed half price by using cheaper refractories causing a decrease in both campaign life and production yield. Because of this critical issue, the main question to be asked is “does the cheaper refractory meet our expectations?”. Therefore, the first step should be to define the right criteria for refractories.

In this study, the expectations are defined simply as a comparison of performance tests between the alternative cheaper refractories and actual refractories in use. Considering the place of use of the refractories there are several kinds of performance tests conducted. For the glass contact refractories (AZS and Alumina) corrosion, stone tendency, exudation and bubble tendency tests have been performed. Besides, for the crown (silica) refractories alkaline penetration and sulfate attack tests have been performed. According to the results of the performance tests, alternative refractories have been compared with the refractories in use and it has been detected that some of the cheaper alternative refractories can be used by considering the cost-performance balance.

GLASS AND GLASS CERAMICS

MELTING PROPERTIES OF FIBER GLASS BATCH WITH LOW GAS CONTENT

Gülin Demirok*, Mustafa Oran, Hande Sesigür

Glass making as a high temperature, energy intensive process produces a huge amount of fuel related CO₂. The process itself liberates additional CO₂ from the decomposition of carbonates such as limestone and soda ash during its melting stage. The use of raw materials containing low CO₂ during their decomposition is supposed to improve the melting conditions reducing not only CO₂ emissions, also energy consumption which needs for melting and fining.

This article highlights the results of experimental study regarding the influence of pure and preprocessed raw materials on melting process. Two different industrial E-glass batches with pure limestone and calcined one were treated with a given temperature profile using High Temperature Melting Observation System including evolved gas analysis. It is shown that the type of limestone has an impact on the melting kinetics resulting the melting/fining behavior.

GLASS AND GLASS CERAMICS

DEVELOPMENT OF GLASS FIBER COMPOSITION WITH HIGH ELASTIC MODULUS

Ceren Ocak¹, Mustafa Oran², Arca İyiel², Gülin Demirok², Duygu Güldiren², Ebru Menşur Alkoy¹

¹Gebze Technical University, Department of Material Science and Engineering,
41400/Gebze/Kocaeli/Turkey

²Şişecam Science Technology and Design Center, Çayırova/Kocaeli/Turkey

Rapid technological developments and difficulties in competition at industries such as automotive, aerospace and defence have required the design of products with high performance. This demand from industries has prompted the manufacturers to develop materials which provide higher strength with lower weight. High modulus glass fiber is one of these materials and superior properties such as lack of flammability, low toxicity when heated and low cost compared to alternatives make it attractive. In this study, several glass fiber compositions which present high Elastic (E) - modulus and low density have been developed to make enable the design of longer wind turbine blades. Accordingly various combinations were experimented by varying the proportions of the components and adding new oxides and the effect of each component on the E - modulus was examined. In the measurement of the E - modulus, different measurement and calculation methods were studied and in consequence of literature research, Resonance - Frequency Method which is conventional and gives most accurate results has been used. In addition to the effect on the E - modulus, melting performances and physical properties such as density and viscosity are experimentally investigated.

GENERAL

APPLICATION AND IMPORTANCE OF TECHNOLOGY READINESS LEVEL FOR INDUSTRIAL CERAMIC SECTOR

Betül Yıldız¹

¹Eczacıbaşı Building Product Co. VitroA Innovation Centre, Bilecik/Turkey

Technology Readiness Levels (TRLs) are a systematic metric/measurement system that supports assessments of the maturity of a particular technology and the consistent comparison of maturity between different types of technology. It is increasingly used for benchmarking, risk management, and funding decisions in all over the world. So that decision-makers are able to figure out whether and when to integrate (launch) a technology (product) into larger systems (markets). First TRL methodology (with 7 levels) was developed by Stan Sadin with NASA in 1974. Among the countries adopted this TRL scale are Canada, United Kingdom, Australia, and European countries. The scale is increasingly being embraced by many organizations including but not limited to OECD, EU, NATO, and NAMSA.

Since 2000s, the process has evolved and is used across a wide range of different areas. However, this methodology is not a panacea that will work for every firm or every industry in its original form. Consequently, for the scale to be truly useful, it has to be adapted to fit the unique features of different firms and industries. Although there are different studies adopting TRL scales for different disciplineries there isn't any study concerning ceramic sector. Therefore this study aims to propose a revised and domain-specific TRL scale for evaluating technology maturity in ceramic industry. The revised TRL scale help to assess technology maturity and reduce risk by delivering better project and technology evaluations and providing a 'common language for ceramic industry.

GENERAL

UTILIZATION OF SUGAR BEET PRESS FILTER CAKE IN DIFFERENT RATIOS FOR PRODUCTION OF CALCIUM ALUMINA SILICATE (CAS) CERAMIC BODIES

Vacide Selin Kaya^{1,2}, Mücahit Sütçü³

¹İzmir Katip Çelebi University, Graduate School of Natural and Applied Sciences, Department of Materials Science and Engineering, İzmir, Turkey

²Ege University, Aliğa Vocational Training School, Metallurgy Program, İzmir, Turkey

³İzmir Katip Çelebi University, Department of Materials Science and Engineering, İzmir, Turkey

In this study the properties of CAS ceramic bodies produced using of sugar beet press filter cake as CaO resource in different ratios (between 20% and 80%) and chamotte as alumina silicate oxides source. The press filter cake (PFC) is a solid waste, which is a by-product in the production of sugar from sugar beet. This solid waste occurs about 500.000 tons per year in Turkey. The aim of this study is to examine the utility of PFC as alternative raw material in the preparation of CAS ceramic bodies. The raw materials were characterized for particle size, chemical composition (XRF), phase content (XRD) and thermal behaviors (TGA). The composition of samples comprised of between 20% and 80% PFC and chamotte by weight. The pressed samples were fired from 1100°C up to 1300°C for 2 hours. Fired samples were characterized for physical properties (bulk density, apparent porosity), occurring crystalline phases (XRD), mechanical properties, thermal conductivity and microstructural properties. Between 20% and 50% PFC compositions, anorthite phase was major phase in ceramic bodies. The highest mechanical strength value was observed in 20% PFC composition because of presence of mullite phase.

GENERAL

THERMODYNAMIC ANALYSIS AND REACTION BEHAVIOR OF MoO_3 UNDER ETHANOL FLOW

Melek Cumbul Altay¹, Şerafettin Eroğlu¹,

¹ Istanbul University - Cerrahpasa, Faculty of Engineering, Avcılar, 34315/Istanbul/Turkey

The present study aimed to investigate reduction and carburization behavior of MoO_3 under $\text{C}_2\text{H}_5\text{OH}$ (Ethanol) atmosphere in a tubular furnace. Prior to the experiments, thermodynamic calculations were performed by a Gibbs' free energy minimization method to predict gaseous species and solid phases likely to be present in the Mo-O-C-H-Ar system. Based on the thermodynamic analysis, it was proposed that Mo_2C was obtained at high temperatures as a result of the reactions between MoO_3 and the pyrolytic gas species derived from the ethanol pyrolysis process. For example, the thermodynamic analysis carried out at 1000 K predicted single Mo_2C formation in the ethanol mole fraction range of 0.53–0.75. The experiments were carried out during heating to 800-1100 K and also under isothermal conditions in the temperature range of 1000-1100 K. Mass measurement, X-ray diffraction, scanning electron microscopy techniques were used to characterize the products. It was determined that the extent of MoO_3 reaction with ethanol increased as the isothermal reaction time was raised to about 60 min, 30 min, and 15 min at 1000 K, 1050 K and 1100 K, respectively. The reaction mechanisms were discussed in terms of thermodynamic results and open tube flow. The present study demonstrated that ethanol might be used for the reduction and carburization of MoO_3 .

CERAMICS AND ENERGY: LUMINESCENCE PHOSPHORESCENCE**INVESTIGATION OF LUMINESCENCE PROPERTIES OF Eu^{2+} , Dy^{3+} DOPED YAlO_3 PHOSPHORS SYNTHESIZED THROUGH COMBUSTION METHOD**Yusuf Ziya Halefoglu¹¹*Cukurova University, Ceramic Department, 01330 Balcali, Adana, Turkey,*

$\text{YAlO}_3:\text{Eu}^{2+},\text{Dy}^{3+}$ phosphor has been synthesized by the combustion reaction method with boric acid used as a flux. The resulting $\text{YAlO}_3:\text{Eu}^{2+},\text{Dy}^{3+}$ phosphor was characterized by XRD and Scanning Electron microscope (SEM/EDAX). The results of XRD patterns indicate that the prepared sample contain crystalline phases and has a orthorhombic structure with size in range of 50–60 nm. Synthesis of phosphors, the effect of lanthanide concentrations on light emission intensity and duration investigated by using photoluminescence (PL) measurements. Thermoluminescence (TL) glow curves were recorded from room temperature to 400°C at a constant heating rate of 1°C/s after preheat process at 130°C for 10 second using lexsys smart TL/OSL reader. As a result, all the luminescence properties of phosphors $\text{YAlO}_3:\text{Eu}^{2+},\text{Dy}^{3+}$ structure have been tried and discussed.

CERAMICS AND ENERGY: LUMINESCENCE PHOSPHORESCENCE**DEPOSITION AND CHARACTERIZATION OF EUROPIUM ACTIVATED Gd_2O_3
LUMINESCENT THIN FILMS**Berk Alkan¹, Kürşat Kazmanlı¹, Mustafa Ürgen¹¹Istanbul Technical University, Istanbul, Turkey

Red emission mechanism of europium-activated phosphors have been known for a long time and $Gd_2O_3:Eu(+3)$ is a well-known red emitting ceramic scintillator. Thin film oxide scintillators represents promising properties for high-energy particle and radiation imaging, detectors, plasma displays, microelectronics, and solar energy harvesting. $Gd_2O_3:Eu$ thin films in different Eu concentrations (atomic %1, %3, %5, and %7) were grown on platinized Si(111) surfaces using RF magnetron deposition technique. $Gd_2O_3:Eu$ powders were compacted and sintered under O_2 atmosphere for target preparation purpose. Stoichiometric powders were synthesized from gadolinium nitride and europium nitride using modified Pechini based sol-gel method. High temperature heat treatment process at open atmosphere was applied to the deposited thin films. Emission characteristics of the thin films were investigated under X-ray excitation. Deposited $Gd_2O_3:Eu$ thin films were characterized using X-ray diffraction, RAMAN and electron microscopy techniques. Laser induced photoluminescence effect observed at RAMAN spectrums. RAMAN analysis result correlated with XRD and luminescent characteristics.

ENAMELS

THE USE OF ENAMELS IN DAILY LIFE

Selime Öztürk¹

¹Gizem Frit A.Ş. Sakarya 2.Osb,1.st,No:18,54300/Sakarya/Turkey

The history of enamel starts in the old centuries but it was always come to contact with human needs as a best solution preferred. Because of vitreous containment, it is always healthy, durable and aesthetical solution compared to the alternative materials.

Mostly borax, quartz, soda and calcite in the recipe melts at high temperature to create a miracle flake type frits.

The surface appearance can be colorful, super opaque, semi opaque and matte.

Depending on the usage field, the content can be different causing a different color, fluidity and test results of XRF, bayer, etc.

By increasing the popularity in its sector, enamels have been used in whitegoods, ovens, high temperature applications (hot water tanks, heat exchangers etc.) BBQs, cookware, sanitaryware and etc.

Direct use as ground coat, acid durable applications, easy to clean, pyrolytic and high temperature applications are possible beverages. It can be applied as cover coat colorful , self cleaning and to occur shiny surfaces and it can be used as third coating like stove and stove pipe coating called majolica.

REFRACTORIES

UNDERSTANDING THE ROLES OF COMPOSITION AND MICROSTRUCTURE ON PROPERTIES AND PERFORMANCE OF MAGNESIA-ZIRCON REGENERATOR BRICKS

Abdullah Elbeyoğlu¹, Murat Avcı¹, Merve Uçak², Oktay Uysal¹, Özkan Kurukavak², Ender Suvacı^{1,3}

¹ Entekno Industrial, Technological and Nano Materials Corp., Anadolu University, Yunusemre Campus ETGB Anadolu Teknoparkı, Eskişehir/Turkey

²KÜMAŞ Magnesite Inc., Eskişehir Karayolu 9 Km. Merkez – Kütahya/Turkey

³Anadolu University, Department of Material Science and Engineering, İki Eylül Campus, 26480/Eskişehir/Turkey

Magnesia-zircon bricks provide regeneration of the heat energy by absorbing the waste gas produced in the combustion in glass furnaces. These regenerator bricks can recover the enthalpy value of 50-75% of the waste gas. In the same capacity, a furnace without regenerator blocks has a production capacity of 35-40% less than a regenerative furnace. One of the main problems in regenerator refractories is that the refractory used (mostly magnesia-based bricks) is corroded because of the chemical penetration. Formation of forsterite-zirconia ($\text{Mg}_2\text{SiO}_4\text{-ZrO}_2$) composite structure by increasing the sintering temperature in the magnesia-zircon bricks prevents this corrosion by surrounding the magnesia granules. Therefore, the formation of this microstructure is highly critical. In this study, the microstructural evolution of magnesia-zircon refractories and the effects of microstructure development on properties and performance were investigated. Phase transformations and microstructural development in the magnesia-zircon system were also investigated. The expansion and shrinkage associated with these phase transformations were determined. Particle packing studies were carried out to achieve optimum porosity required for heat absorption and to obtain the proper pressure value for the pressing process. Measurements of apparent porosity, bulk density, cold crushing strength (CCS), hot modulus of rupture (HMOR), permanent linear change (PLC) and refractoriness under load (RUL) were performed. In addition, to monitor phase development, microstructure evolution and distribution of the elements throughout the microstructure, quantitative analysis by XRD, scanning electron microscope (SEM) and energy-dispersive spectroscopy (EDS) characterization methods were used, respectively.

REFRACTORIES

INNOVATIVE SPINEL MATERIAL HAVING ENHANCED CORROSION RESISTANCE

Özkan Kurukavak¹, Ersan Pütün², Muharrem Timuçin³

¹KÜMAŞ Manyezit Sanayi A.Ş., Kütahya/Turkey

²Anadolu University, Faculty of Engineering, /Eskişehir/Turkey

³Middle East Technical University, Faculty of Engineering, Ankara/Turkey

Magnesite-spinel bricks have the characteristics of composite materials which consist of spinel and sinter magnesite particles spreading into the magnesite matrix as structural design. Magnesite component of the composite is called as resistor since it is resistance to corrosive effects of the clinker liquids. As for the spinel component, it is bring capability of elastic deformation to the brick to some extent. Although a very high spinel amount is desired to enhance the thermal shock resistance of refractory brick, the spinel amount must be minimum due to the formation of liquid phases of calcium-aluminum oxide that has low melting temperature and occurring with calcium oxide attacks. To this end, instead of $MgAl_2O_4$ spinel, the design and synthesis of new generation spinel (innovative) material having higher corrosion resistance was performed in our study. Corrosion tests of synthesized spinel and the spinel which is still in use was done. In the study done with scanning electron microscope, it was identified that by formation of a boundary between the corroded surface and the non-corroded surface of the innovative spinel material, infiltration of impurities from this boundary to clean area is prevented. As for the existing spinel material, the infiltration of CaO at the clean non-corroded area was detected. In the next step of the study, MgO-spinel refractory brick was produced and the physical properties, mechanical properties, effects to the thermal shock behaviors and corrosion behavior of MgO-spinel refractory brick produced using the innovative spinel material was investigated. It was determined that the physical properties, mechanical properties and thermal shock behaviors of these bricks are similar to existing products and also the innovative spinel material used as elasticizer is effective to enhance the corrosion resistance.

REFRACTORIES**INFLUENCE OF THE MAGNESITE GRAIN TYPE ON DECARBONIZATION BEHAVIOR
OF MgO-C BRICKS**

Özkan Kurukavak¹, Nafiz Özdemir¹, Muharrem Timuçin²

¹KÜMAŞ Manyezit Sanayi A.Ş., Kütahya/Turkey

²Middle East Technical University, Faculty of Engineering, Ankara/Turkey

MgO-C refractory bricks having different kinds of magnesia grains were prepared for the determination of the effect of magnesia grain type on oxidation resistance of the refractory composite. In manufacturing the bricks, the magnesite fraction was introduced as grains of high and low quality fused magnesite, grains of sea water magnesite or as those of natural dead burned magnesite. Also dead burned magnesite resources are classified according to production method; single fired in rotary kiln, single fired in shaft kiln, double fired in shaft kiln. The crystallite sizes ranged as 750 µm, 250 µm, 80 µm, and 110 µm, 75 µm, 90 µm respectively. Data on the rate of decarbonization in air were obtained by performing static weight loss measurements at temperatures ranging from 1200 to 1600 °C.

The data obtained in weight loss determinations revealed that rate of decarbonization in MgO-carbon bricks manufactured by using high quality fused magnesite grains was lowest at all temperatures. The decarbonization behavior of MgO-C bricks having natural magnesite grains were quite comparable except single fired DBM in rotary kiln, it has the lowest decarbonization behavior among dead burnt magnesite grains. It was shown that the oxidation resistance of MgO-C bricks made with natural grains of magnesite could be enhanced with proper additions of antioxidants leading to a cost-effective brick with considerable improvement in performance.

GLAZES and PIGMENTS**SYNTHESIS OF VANADIUM-DOPED ZIRCON PIGMENT BY SOLID-STATE REACTION
AT LOW TEMPERATURE**

Belgin Tanışan

Eskişehir Osmangazi University, Department of Metallurgical and Materials Engineering,
Batı Meşelik Campus, 26480/Eskişehir/Turkey

In this study, vanadium-doped zircon ($V-ZrSiO_4$) blue ceramic pigments were synthesized by the conventional ceramic route from a mixture of monoclinic zirconia, amorphous silica (both rice husk ash and precipitated silica) with NH_4VO_3 as colouring agent as well as NaF as mineralizer. Effect of the calcination temperature on the crystalline phase formation was followed by X-ray diffraction while the morphology of the synthesized pigments was characterized by scanning electron microscopy. Furthermore, colour properties of the prepared pigments were evaluated in comparison with commercially blue $V-ZrSiO_4$ pigment by using an UV-Vis spectrophotometer. While zircon formation started even at 750 °C, strong blue colour formation was obtained for the pigments calcined at 950 °C for both silica sources. Lower calcination temperatures of zircon formation were due to the fine particle size of the reactants, particularly silica sources.

GLAZES and PIGMENTS**CERAMIC PROPERTIES OF CLAY FROM ASLANTAS DAM LAKE BED,
OSMANIYE IN TURKEY**

Mustafa Daday¹, Nergis Kılınç Mirdalı², Mine Taykurt Daday³

¹Anadolu University, Department of Material Science and Engineering,
İki Eylül Campus, 26480/Eskişehir/Turkey

²Cukurova University, Department of Ceramic, Balcali Campus, 01330/Saricam/Adana/Turkey

³Adana Science and Technology University, Department of Materials Engineering,
01250/Saricam/Adana/Turkey

The historical past of the Karatepe Aslantas area in Osmaniye dates back to the 8th century BC. The Aslantas Dam built in this historical region has located Karatepe Open-Air Museum which has been very important archaeological exhibition and its excavation areas. Based upon the historic past of the region, clay taken from the dam bed was investigated in terms of usage in the production of ceramic art works. Particle size and distribution was defined with laser particle sizer. The chemical and mineralogical composition of clay was determined by X-ray fluorescence (XRF) and X-ray diffraction (XRD) methods. Thermal behaviour of sample was studied by Optical Dilatometer (ODHTM). Test samples were prepared by semi-dry (plastic shaping) and fired at 900, 1000, 1100 and 1200 °C. Shrinkages during drying and firing were measured for each sample. The color properties obtained after firing was defined as CIE-L*a*b* parameters. In the light of such results, the examined clay from Aslantas Dam Lake Bed could be used as raw material in ceramic production.

seres'18

IV. INTERNATIONAL CERAMIC GLASS PORCELAIN
ENAMEL GLAZE AND PIGMENT CONGRESS
October 10-12, 2018, Eskişehir, Turkey

Abstract of POSTER PRESENTATIONS

EFFECT OF THE AQUEOUS ENVIRONMENTAL CONDITIONS ON THE ZINC STANNATE PROPERTIES

Sadiye Pelin Erden, Emel Özel, Ender Suvacı

Anadolu University, Department of Materials Science and Engineering, İki Eylül Campus,
26480/Eskişehir/Turkey

Recently, synthesis and properties of Zn_2SnO_4 (ZTO) have been investigated for various applications such as gas sensors, electrode materials for dye sensitized solar cells (DSSC) and catalyst for photo-degradation of dyes because of having unique properties such as high electron mobility, high electrical conductivity and novel optical properties. To achieve maximum performance in such applications, chemical stability of ZTO materials in aqueous environments must be well known. Therefore, the research objective of this study was to investigate the effect of the aqueous environmental conditions on the properties of the ZTO materials. Accordingly, ZTO powders were synthesized by solid-state method at 1200°C for 4 h. Then these powders were aged for 30 days in 24 h intervals in aqueous media with pH 3, pH 7 and pH 9 that were prepared by adding HCl acid and NaOH base solutions to the water. In addition, the chemical stability of ZTO powder was also studied in KI/I_2 electrolyte solution which is commonly used in DSSCs. After aging, dissolution amount of the Sn^{+4} and Zn^{+2} ions from ZTO powders were determined with ICP-OES and aged powders were characterised with XRD, FTIR, UV-Vis. ZTO powders were found to be chemically more stable at pH 9 (~ 0.008 mmol/L of total ion concentration) than acidic conditions (~ 0.4 mmol/L). In aged ZTO powders, any phase transformation or new bond formation was not observed comparing to the starting powders. Consequently, these materials can be used safely for several applications in aggressive chemical environments.

INVESTIGATION OF CORDIERITE MULLITE & MULLITE CERAMIC FOAM FILTERS FROM SANITARY WARE KILN WASTES

Eray Çaşın, İskender Işık

¹Ece Banyo Gereçleri San. ve Tic. A.Ş., Çorum/Turkey

²Dumlupınar University, Engineering Faculty, Metallurgy & Materials Engineering, Kütahya/Turkey

The metallic melts shaped with casting method include unwanted impurities within the product. The ceramic foam filters are using for removing these impurities. Proverbially, the mullite based filters are suitable for high temperature applications as its technical features such as low coefficient of thermal expansion, chemical and mechanical stability at higher temperature and thermal shock resistance. Due to these properties, mullite is the potential matrix material for relatively higher temperature applications.

In this study, the wasted sanitary ware kiln materials will be reused to investigate as the source of material for mullite and cordierite mullite ceramic filter. In this context, Ece Banyo Sanitary Ware Plant's kiln roller materials and kiln plates will be used (both of which are cordierite and mullite and alumina mullite) to utilized in the manufacturing ceramic foam filter.

This work is a preliminary study about how to reuse waste kiln materials in order to manufacture value added materials. Physical, chemical, mineralogical, thermo gravimetric, micro structure and sintering behavior tests will be made over these prescription samples. Also these tests will be made for nowadays marketing filters-mullite and cordierite mullite-for benchmarking. According to the results of these tests, the right and suitable prescription sample will be selected and shaped with foaming process. Furthermore, the shaped filters will be tested in casting process.

INFLUENCE OF ALUMINA RICH SPINEL ADDITION ON THE PROPERTIES OF SELF-FLOWING MAGNESIA BASED CASTABLE REFRACTORIES

Büşra Alpdoğan*, Azade Yelten-Yilmaz*, Ferhat Tocan**, Suat Yilmaz*

*Istanbul University-Cerrahpaşa, Department of Metallurgical and Materials Engineering, Avcılar Campus, 34320/Istanbul/Turkey

**PiroMET Refractory Plant, Çerkeşli OSB Mah. İMES 2.Cad. No.3, Dilovası, 41455/Kocaeli/Turkey

Castable refractory materials are produced by mixing the aggregate with water and casting it into a mold to create a concrete. Magnesia (MgO) based refractories draw attention due to their high refractoriness, reasonable hydration resistance and chemical stability at high temperatures and in alkaline environments. In this study, influence of the chemical composition on the physical and mechanical properties of the MgO based self-flowing refractories containing alumina rich spinel at different ratios was investigated. The prepared flowing slurry mixtures were cast in vibrating molds and cubic samples with 50x50x50 mm dimensions were produced for the slag corrosion test. The obtained samples were dried at 100 °C and fired at 1600 °C. Physical tests such as bulk density, apparent porosity and water absorption determination, mechanical tests such as compression strength test, chemical tests such as slag corrosion test and other characterization analyses like XRD and SEM/EDS were applied to the fired samples. As a result of these tests, it was aimed to develop the properties of the product further by comparing the mechanical strength and chemical corrosion performances of the MgO based self-flowing refractory samples containing alumina rich spinel.

Acknowledgement: This work was supported by Scientific Research Project Coordination Unit of Istanbul University [grant number 27125].

ECO-FRIENDLY CERAMIC MEMBRANE BIO REACTOR (MBR) BASED ON RECYCLED AGRICULTURAL AND INDUSTRIAL WASTES FOR WASTE WATER REUSE

Alpagut KARA¹, Pervin GENÇOĞLU², M.Fahri ÖZER²

¹ Eskişehir Teknik Üniversitesi, Mühendislik Fakültesi, Malzeme Bilimi ve Mühendisliği Bölümü, Eskişehir

² Seramik Araştırma Merkezi A.Ş., Eskişehir

REMEB (Recycled Membrane Bioreactor) is a Research and Development project funded by the European Commission under grant agreement No. 641998, in the framework of the call H2020-WATER-2014. It has a duration of three years, starting in September 2015 and concluding in August 2018. REMEB project is integrated by a total of 11 partners from seven different countries. The main objective of the REMEB project is the implementation and validation of a low cost recycled ceramic membrane bioreactor (MBR) for water reuse in a Wastewater Treatment Plant (WWTP). In this sense, REMEB project will develop a ceramic, ecological and competitive MBR for municipal and industrial wastewater treatment plants (WWTP), from ceramic raw materials and by-products and agro-industrial wastes. In REMEB project, Ceramic Research Center (SAM) is working on traditional ceramics topics with the partners with a great experience in this field SAM will be working in WP1, WP2, WP3, WP5 and WP7; especially on replicability. The principal aim of work package 3 is the manufacturing of the low cost recycled membrane for the REMEB MBR. At WP5 the replication of the ceramic membrane manufacture (at pilot scale) will be undertaken by SAM (Turkish raw materials and wastes). Turkish fired tile scraps, olive stones and marble dust were chemically and mineralogically analysed and compared with other research center results. A support recipe was studied by using local raw materials and wastes. The recipe was well extruded at laboratory scale dried and fired. The physical, mineralogical and permeability properties of the fired bodies were measured. Scanning electron microscopy (SEM) and energy dispersive X-ray spectroscopy (EDX) were further employed in order to observe the microstructural and microchemical characteristics of the fired bodies.

PRODUCTION AND CHARACTERIZATION OF C-BN AND B₄C REINFORCED COCRFENI HIGH ENTROPY ALLOY MATRIX COMPOSITES

Burak YALMAN^{1*}, Kübra GÜRCAN¹, Erhan AYAS¹

¹Eskişehir Technical University, Department of Material Science & Engineering

İki Eylül Campus, 26555, Eskişehir/TURKEY

As a different from conventionally alloys, high entropy alloys are at least comprise five or more principal elements. Each principal element should have a concentration between 5 and 35 at. %. It is seen that such alloys are formed simple solid solutions instead of forming complex microstructure with many elements. Experimental results showed that the higher mixing entropy in this alloys facilitates the formation of solid solution phase with simple structures and thus reduces the number of phases. High entropy alloys have outstanding properties such as excellent wear resistant, good high temperature strength, high hardness, good oxidation and corrosion strength. In order to enhance its high temperature strength, evaluation of high entropy alloys as matrix material for composite approach were extensively investigated.

For this purpose, boron carbide (B₄C) and cubic boron nitride (c-BN) reinforced CoCrFeNi high entropy alloy composites was prepared. CoCrFeNi high entropy alloys was prepared by mechanically alloying process under argon atmosphere. The prepared powders were consolidated using Spark Plasma Sintering (SPS) with the addition of 3, 5 and 10 vol% B₄C and c-BN at 1000 °C for 8 min under 30 MPa uniaxial pressures in vacuum atmosphere. Effect of particle size of reinforced materials on microstructure, wear resistant and mechanical properties were investigated intensively.

EXAMINATED OF DEFORMATION OF THE CERAMIC OBJECT USING ANFIS

Uğur Kut¹, Eyyüp Gülbandılar²

¹ Kütahya Dumlupınar University, Faculty of Architecture, Germiyan Campus, Evliya Celebi Campus, Kutahya, Turkey

²Eskişehir Osmangazi University, Faculty of Engineering&Architecture, Department of Computer Engineering, Meselik Campus 26480, Eskişehir/Turkey

In the development and design of new products in ceramic industry need to be prepare a large number of prototypes to obtain the appropriate form. These trials lead to increased costs and loss of labor in the production stage, due to the deformation. In this study, it is aimed to develop computer software to reduce these losses in the ceramic industry.

Cylindrical specimens were produced using the different ceramic masse, sintering temperature, and sintering period. These specimens, after the drying process have been scanned with the 3D scanner, and at the same time measured using classical methods. Later, these samples are fired at different sintering times and temperatures in ceramic kiln and measured using the same methods. Subsequently the deformations in the base, side and mouth regions of the cylindrical samples are identified. In the light of this experimental data, were developed the ANFIS model by used MatLab Toolbox. In the ANFIS model, the temperature, sintering time and composition of ceramic samples have been used as the input data while the amount of deformation is used as the output data. 58 of the experimental specimens were used for the training, and used 22 of experimental specimens for testing of MLPNN model (Multilayer perceptron neural network). We founded a significant correlation between ANFIS and experimental data with X^2 test ($p < 0.001$ and for base, mouth and side $\kappa = 0.3, 0.06, 0.3$, respectively). But it is not significant relationship between ANFIS and experimental data for mouth deformation ($\kappa = 0.06$).

EFFECT OF MILLING ON MICROSTRUCTURAL EVOLUTION DURING FIRING OF NEPHELINE SYENITE CONTAINING BONE CHINA BODY

Elif Kabakcı, Ahmet Çapoğlu

Gebze Technical University, Department of Materials Science and Engineering, 41400,
Gebze/Kocaeli, Turkey

Typical bone china contains bone ash, fluxing material and kaolin. In this study, nepheline syenite was added into the bone china composition as a flux. This reformulated body composition was wet milled for five different times in order to investigate the effect of milling on the microstructural evolution in detail. Bar shaped samples were produced from granulated composition by uniaxial dry pressing under the load of 40 MPa. The samples were sintered for 2 hours at a rate of 3 °C/min at 1200, 1225 and 1250 °C. After sintering, the samples were prepared to SEM analysis. For this purpose, the samples were molded in epoxy resins. After the resins cured, surface of the samples were grinded with SiC abrasive papers and polished. This steps were followed by chemical etching using 3% HF solution with 2.5 min dwelling time then, the specimens were coated with gold. Microstructures of the prepared samples were investigated by scanning electron microscopy (SEM) analysis. The results showed that shorter milling time produced microstructure containing large porosities and high amount of huge residual quartz. However, longer milling periods caused less amount of residual quartz with smaller size and eliminated the large pore formation. This result showed that the milling time hence the amount and particle size of residual quartz plays an important role for formation and elimination of porosities in the microstructure.

SELF-CLEANING ORGANIC COATINGS CONTAINING BORON/BORATE ADDITIVES

Gizem Toprakçı¹, Nil Acaralı¹

¹Yildiz Technical University, Department of Chemical Engineering, Davutpasa St., N.127, Esenler, Istanbul, Turkey

Along with the developing technology, the demand is increasing rapidly for the usage of paintings with superior properties like high impact resistance, flame retardancy, corrosion resistance and hydrophobicity in the metal industry such as automotive, shipbuilding, aircraft industry in recent years. When the liquid painting or powder coating materials as an organic coating is applied on a surface, they are not used only decorative purposes, but also forms a protective layer on the various surfaces. Taking all technological improvements, customer-oriented approach, long-term usage of products, and consumer's demands into consideration, expectations about improvements in relation to material properties are inevitable. For this reason, on the surfaces which can be coated with painting, desired properties can be provided by improving the painting prescription.

In this study, the aim is to acquire paint with enhanced features, especially by utilizing the features of minerals found in abundance in our country. In accordance with zinc borate and boron oxide composites, two sets of experimental sets were created. With the Taguchi Optimization method taking the paint viscosity as the response, paint mixtures with optimum qualities were determined for both experimental sets, and the application of the prepared paint to various metal surfaces was executed. Aside from boron oxide, with the addition of mineral additives and fluorine-based surfactant, when the surfaces the prepared paint were applied are subjected to various tests in accordance with TSI and DIN requirements; progress in fire resistance, corrosion resistance and hydrophobicity was observed.

CHARACTERIZATION INVESTIGATIONS OF SEQUENTIALLY MILLED AND SINTERED AL-7 WT.% SI-2 WT.% LaB_6 COMPOSITES

Siddika Mertdinç¹, Emre Tekoğlu¹, Duygu Ağaoğulları¹, M. Lütfi Öveçoğlu¹

¹Istanbul Technical University, Faculty of Chemical and Metallurgical Engineering, Department of Metallurgical and Materials Engineering, Particulate Materials Laboratories (PML), Ayazağa Campus, 34469 Maslak, Istanbul, Turkey

This study reports on the physical, microstructural and mechanical properties of the Al-7 wt.% Si and Al-7 wt.% Si-2 wt.% LaB_6 composites produced by sequential milling (mechanical alloying and cryogenic milling) and pressureless sintering. Firstly, powders were mechanically alloyed (MA'd) for 4 h in a Spex 8000D Mixer/Mill (1200 rpm). After that, MA'd powders were cryomilled in the presence of liquid nitrogen for 5, 10 and 15 min in a Spex 6870 Freezer/Mill to optimize the cryogenic milling time. 10 min was determined as an ideal cryomilling time due to microstructural investigations, particle size and surface area measurements. Then, 2 wt.% LaB_6 particles incorporated into Al-7 wt.% Si matrix and they were mechanically alloyed for 4 h, cryomilled for 10 min and then MA'd for 1 h again. After that, sequentially milled powders were compacted and sintered at 570°C for 5 h under Ar gas flow. X-ray diffractometer (XRD) and scanning electron microscope (SEM) were used for microstructural characterizations of the powders and sintered composites. Besides, densities of the sintered compacts were measured using the Archimedes method. Vickers microhardness measurement and sliding wear test of the sintered compacts were conducted to determine the mechanical properties of the composites. Produced LaB_6 reinforced composite a microhardness value of 1.51 GPa and wear volume loss of 0.128 mm³.

CONTEMPORARY ART CERAMIC: DIALOGUES BETWEEN TECHNIQUES AND CULTURE OF THE BRAZILIAN NATIVE PEOPLE 1

1 This study is linked to the project "Aspects of the Guarani culture in RS for a contemporary artistic production". Support by Pro-Rectorate of Research, innovation and Post-Graduation (PROPPI) – Federal Institute of Education, Science and Technology of Rio Grande do Sul (IFRS), Brazil.
Silvia Regina Grando¹, Emanuelle Bottega Ramos², Milene Back Juwer³, Heloísa Tenroller Viviane Diehl^{1,5}

1 Federal Institute of Education, Science and Technology of Rio Grande do Sul (IFRS), *Campus Viamão/Brazil*

2 Federal Institute of Education, Science and Technology of Rio Grande do Sul (IFRS), *Campus Feliz/Brazil*

3 Federal Institute of Education, Science and Technology of Rio Grande do Sul (IFRS), *Campus Feliz/Brazil*

4 Federal Institute of Education, Science and Technology of Rio Grande do Sul (IFRS), *Campus Feliz/Brazil*

5 Federal Institute of Education, Science and Technology of Rio Grande do Sul (IFRS), *Campus Feliz/Brazil*

The materiality, the creative process, the technical developments, bring visibility to the artistic ceramics in Vale do Caí, in the south of Brazil. This region stands out for the production of structural ceramics, especially bricks and roof tiles, with opportunities for work and income for the community. In this context, research on artistic ceramics is now unfolding in projects that bring challenges to think about the condition of the Brazilian native people. The recognition of the Guarani people, among the native groups that inhabit the south of Brazil, stands out for the production of ancestral ceramics. It is from this universe that the proposal of the artistic production for an intercultural education that allows to extend the aesthetic experience arises. The objective in this study is to problematize and move reflections that reverberate in the production and poetic presentation of artistic work in ceramics, constituted from the study and recognition of the Guarani culture contribution for the Brazilian people formation. The dialogue of the creative process in the plastic production is made with experimentations in an alternative silkscreen print process and alternative kilns to fire techniques. The Guarani culture influence in the artistic production in contemporary ceramic, move the aesthetic education that is an educative possibility of contribution to the culture. Ceramic art work contributes to breaking with segmentation, and by instigating curiosity, showing the correlations between knowledge, the complexity of life, and relationships of affection, is capable of problematizing what is lived in a shared culture.

KEY WORDS: Guarani culture, ceramic art, alternative process, interculturality.

¹ This study is linked to the project "Aspects of the Guarani culture in RS for a contemporary artistic production". Support by Pro-Rectorate of Research, innovation and Post-Graduation (PROPPI) – Federal Institute of Education, Science and Technology of Rio Grande do Sul (IFRS), Brazil.

ETİ ALÜMİNYUM NEWLY DEVELOPED SPECIALTY ALUMINA PRODUCTS

Seyit Avcu¹, Gökhan Kürşat Demir¹, Meral Baygül¹, Mustafa Server¹,

¹ ETİ Alüminyum Inc, Konya/Turkey

ETİ Alüminyum Inc. is the only producer of aluminium hydroxide, alumina and primary aluminium from its own raw bauxite ore in Turkey. The alumina refinery commenced mass production by 1973 and the smelter unit started to work in 1974 utilizing Söderberg cell technology (SCT). After it was privatized by Cengiz Holding in 2005, heavy modernization efforts have been taken place. Especially the significant investment is the modernization of smelter unit, ETİ Alüminyum changed SCT to Pre-baked technology and installed a stationary alumina calciner with high thermal efficiency to replace the existing conventional rotary kilns. ETİ Alüminyum didn't leave these rotary kilns as idle equipment and started producing specialty alumina products especially for ceramic, refractory and glass industry. These products have been classified according to specific surface area, alpha content, primary crystal size and specific density in order to meet market demand. These products are coded as EtiALU375, EtiALU345, EtiALU313, EtiALU305 and EtiALU301, currently available on the market. During the production of these products, ETİ Alüminyum has improved rotary kiln itself in terms of mechanical, electrical and refractory especially utilization of high temperature resistance refractory bricks, application of wet refractory mortars to required points for sustaining stable production and ensuring always same product quality. ETİ Alüminyum constantly strives for the best specialty alumina product quality and enhancing innovative R&D capabilities to meet the customers' highest expectations. ETİ Alüminyum commitment is to provide full technical support from the first call to delivery of the relevant products.

PERLITIC REDUCTION GLAZES: A PRELIMINARY STUDY

İstem Şencan Tosun¹, Zeliha Yayla², İlker Özkan²

¹Qua Granite, Aydın, Turkey

²Dokuz Eylül University, Torbalı Vocational School of Higher Education, Industrial Glass and Ceramics Department, Izmir, TURKEY

This study aims to use expanded perlite as a raw material reduction glazes. In this research, an amorphous volcanic glass named perlite was used. Perlite can easily be supplied commercially. It includes mainly SiO₂ and other oxides which can be used in ceramic glazes.

Perlite has some physical and chemical advantages. It can easily be grinded when it is expanded and used for production of ceramic glazes and bodies. Also expanded perlite has low density and is a thermally resistant material. For this reason it is used as an additional raw material for preparing light weighted sculpture bodies and also for preparing raku body.

The expanded perlite used in this study was obtained commercially from Etibank with a brand of “Etiper Super Fine”. The physical and chemical properties of perlite were determined. Different glaze recipes were prepared by using (Perlite-Ulexite and Orthoclase). 1 and 3 % (by weight) copper (II) oxide was used as a coloring agent. The batches were prepared by using wet grinding technique. The prepared glazes were applied to test plates by pouring method. Samples were fired at 910°C in oxidation atmosphere. Reduction firing is performed in the same kiln at 730°C. Results were discussed and the selected glazes were applied to different forms.

MULTI-PHASE ARMOR PRODUCTION AND CHARACTERISATION INVOLVING B₄C – SiC – TiC WITH SPARK PLASMA SINTERING TECHNIQUE

Gamze U. SAPANCI^(a), Gökçe DARA^(b), Derya A. KÜRÜM^(c), Servet TURAN^(d), Alpagut KARA^(e), Ferhat KARA^(f)

^(a) Mühendis, Roketsan, Kemalpaşa Mah. Adem Kutlu Sok. No: 21, Elmadağ, Ankara,

^(b) Dr., Roketsan, Kemalpaşa Mah. Adem Kutlu Sok. No: 21, Elmadağ, Ankara,

^(c) Mühendis, Roketsan, Kemalpaşa Mah. Adem Kutlu Sok. No: 21, Elmadağ, Ankara,

^(d) Prof.Dr., Anadolu Üniversitesi, Malzeme Bilimi ve Mühendisliği, Eskişehir

^(e) Prof.Dr., Anadolu Üniversitesi, Malzeme Bilimi ve Mühendisliği, Eskişehir

^(f) Prof.Dr., Anadolu Üniversitesi, Malzeme Bilimi ve Mühendisliği, Eskişehir

Boron carbide (B₄C) is the most commonly used material for armor applications due to its light and high hardness. However, the high cost is one of the most important obstacles in the front. On the other hand, sintering is very difficult and requires sintering with a hot press (HP) at temperatures around 2200 °C to bring it to the theoretical density. However, the mechanical properties of monolithic B₄C are not good enough to be used in industrial applications. For this reason, numerous studies have been carried out on the production of B₄C -containing composite materials by the addition of different compounds such as silicon carbide (SiC) and titanium carbide (TiC). The addition of these compounds improves both the properties and reduces the sintering temperature.

In this study, optimum B₄C-SiC-TiC multi-phase ceramic composite compositions were designed and produced by spark plasma technique bearing in mind the hardness – toughness – cost – lightness - performance relationship. In addition, the effect of these carbides was also investigated by adding only TiC or SiC powders into pure boron carbide powder. The addition of SiC did not affect the hardness and toughness, but the addition of TiC resulted in increased toughness in spite of decreased hardness. When microstructure analyzes and x-ray diffraction patterns were evaluated together, residual graphite and SiC were found to exist in pure B₄C, and when TiC was added, residual graphite and small amounts of SiC, as well as TiC and B₄C, reacted to form titanium diboride (TiB₂). When SiC and TiC were added together, hardness decreased whereas fracture toughness increased. Because of the fact that boron carbide is a light material, all the additives added increase the weight, while the costs were reduced because all the additives are cheaper than B₄C.

DEVELOPMENT OF HIGH ALUMINA ADDITIVE PORCELAIN PRODUCTS WITH HIGH TRANSLUCENCY AND GLAZE RESISTANCE IN SOFT PORCELAIN CLASS

Zuhal KARAAĞAÇ¹, Gonca DURNA², Zehra Emel OYTAÇ³

^{1,2}Porland Porselen Research and Develop Center, Bilecik/Turkey

³Ceramic Research Center, Anadolu University, Eskişehir/Turkey

Nowadays, as the standard of living increases, porcelain tableware expectation is increased. Recently, more aesthetic, healthy, hygienic and ergonomic products are being requested by the customers on the market. Most of tableware products which are produced in Turkey are hard porcelain. On the other hand, most of the imported tableware products are composed of soft porcelain products. The bone china products in the soft porcelain group are known as the most attractive and expensive tableware with their aesthetic properties. However, the glaze resistance of bone china is lower than hard porcelain products. Therefore, market share is limited in gastronomy market. In this project, it is aimed to develop new products by combining the properties of bone china such as cream color, high translucency and the properties of hard porcelain such as glaze resistance. By using a new composition with alternative raw materials and adapted firing curve, a new product which has high technological properties such as cream color, high translucency, glaze resistance and impact resistance, have been developed by using existing hard porcelain technology and it can compete with bone china as a low cost product. In recently developed body recipe studies, calcine alumina and MgO source raw materials were added to the system at different ratios and analysed mineralogically, microchemically and microstructurally. For glaze composition that provides the requested standards, glaze recipes with suitable thermal expansion coefficient and high scratch resistance have been studied in terms of glaze-body compatibility. The sintering of the developed glaze was carried out by adapting the firing curve in the oxidative atmosphere.

INVESTIGATION OF GLAZE OF LOWER THERMAL EXPANSION FOR SANITARYWARE THINNER BODY

Hasan Sarı¹, Zehra Emel Oytaç²

¹Kale Seramik Research and Development Center, Can/Canakkale/Turkey

²Ceramic Research Center, Anadolu University, Eskişehir/Turkey

Ceramic sanitaryware is the leading and rapidly growing industry in Turkey. Turkey is among the top manufacturing country of ceramic sanitaryware products in the world and a major market driver. Increasing in population, changing lifestyle and growth of real estate market has driven demand for the sector. Product demand is expected to be high in consumer sectors such as hospitals, hotels, educational institutes, industries and other public places. Most ceramic sanitaryware products perform almost the same functionality but the design is one of the most effective parameter that can easily change end user preferences. Thin wall products especially in washbasins is the latest trend that demonstrate the good combination of innovation and design. It is not possible to get a thinner ceramic body with a traditional sanitaryware compositions. So Kaleseramik carried out a project that was based on designing a new sanitaryware composition that is strong, malleable and can provide a thinner ceramic body without changing the traditional production process. This project is directly related to the glaze that is fitted perfectly with the new ceramic body. The new ceramic body has a lower thermal expansion coefficient ($55,2 \times 10^{-7} \text{ }^{\circ}\text{C}^{-1}$) according to the traditional one. Thus exists a thermal shock crack in the products. To prevent this fault and satisfy the need a glaze that has a lower thermal expansion coefficient ($< 55 \times 10^{-7} \text{ }^{\circ}\text{C}^{-1}$) was studied.

INVESTIGATION OF TECHNICAL PROPERTIES IN BRICKS BY USING COLOR IMAGE ANALYSIS

Taner Kavas^{1*}, Recep Kurtuluş¹, Emel Coşkun¹

^{1*} Afyon Kocatepe University, ANS Campus Gazlıgöl Yolu, 03200/Afyonkarahisar/Turkey

Bricks, as one of terra cotta based construction materials have a large production capacities in Afyonkarahisar/Turkey industry. Continuous improvements either in raw materials or manufacturing conditions take great importance for mass production. In this sense, color image analysis was studied in order to assess the technical properties consistently in the earliest time possible. For this purpose, three different brick samples, having different kinds of raw material compositions and firing temperatures, were supplied from different companies located near to Afyonkarahisar city. These samples were initially cutted in thin sections and dry grinding operation was carried out so as to achieve smooth surfaces. The samples were placed on lamellae and once again sensitively grinded, and afterwards optical microscopy images were obtained. The obtained images were then processed by numerically via MATLAB software and RGB (red-green-blue) values were found out. The assessment of technical test results of company samples and RGB values were figured out, and it was concluded that color image analysis is satisfactorily consistent with technical test results of companies and can be utilised in place of time consuming analysis efforts during production in companies.

Key words: bricks, color, image analysis

**MATRIX POWDER AND TEMPLATE SYNTHESIS FOR LEAD-FREE, GRAIN ORIENTED
 $K_{0.5}Bi_{0.5}TiO_3$ - $BaTiO_3$ - $Na_{0.5}Bi_{0.5}TiO_3$ CERAMICS WITH HIGH PIEZOELECTRIC
 PERFORMANCE AND
 HIGH TEMPERATURE STABILITY**

Ozan Şükrü ATEŞ^{1,2}, A. Murat AVCI² and Ender SUVACI^{1,2}

¹Eskişehir Technical University, Department of Materials Science and Engineering, İki Eylül Campus,
 26480/Eskişehir/Turkey,

² ENTEKNO Corp. Eskişehir/Turkey

Piezoelectric materials is growing very fast due to their diversified potential applications, such as actuators and sensors. Commonly used lead-based piezoelectric ceramics are very toxic for natural life. It is necessary to develop environment-friendly lead-free piezoelectrics. Recently, lead-free NBT based piezoelectric materials are good candidates to replace for lead-based piezoelectric materials. NBT-based lead free systems can exhibit high piezoelectric performance if their grains are oriented. However, textured ceramics may exhibit less depoling temperature which may be caused by lattice mismatch between matrix grains and templates that are used for inducing grain orientation. Therefore, the research objective of this study was to synthesize and characterize KBT-BT-NBT matrix powder and KBT-BT-NBT and KBT-BT-NBT plate-like templates that can be later used for producing textured ceramics with high piezoelectric response and high temperature stability. Synthesis of the templates with various chemistries enable one to design experiments to investigate the relationship between degree of lattice mismatch between matrix powder and templates and high temperature stability and piezoelectric performance. In this study, KBT-BT-NBT matrix powder was synthesized by mixed-oxide technique. The templates with controlled properties were synthesized by molten salt method. In this presentation, effect of processing parameters on particle characteristics will be discussed.

ESKİŞEHİR İLİ MİHALIÇIK İLÇESİ SORKUN VILLAGE POTTERY

Nurcan TURAN CANDAN¹, Mert ALBAYRAK², Ayşegül EVREN³, İrem DESTİCİ⁴, Ferhat
SUNGUR⁵

1.Eskişehir Emine Şahbaz Bilim ve Sanat Merkezi Odunpazarı/ESKİŞEHİR

2. Eskişehir Emine Şahbaz Bilim ve Sanat Merkezi Odunpazarı/ESKİŞEHİR

3.Eskişehir Emine Şahbaz Bilim ve Sanat Merkezi Odunpazarı/ESKİŞEHİR

4. Eskişehir Emine Şahbaz Bilim ve Sanat Merkezi Odunpazarı/ESKİŞEHİR

5.Eskişehir Emine Şahbaz Bilim ve Sanat Merkezi Odunpazarı/ESKİŞEHİR

Ever since the Neolithic era, pottery art is still living in Anatolia with all the historical stages. The most primitive art of pottery or the most advanced methods with Turkey "are also applied with great comfort and a high level of handicraft, there has been a certain extent on estimates. Numerous researches have been carried out on the centers that have traditionally produced in Neolithic period in Anatolia.

These traditional production centers have been uncovered in terms of historical development, raw materials used, production stages and product types. These researches are of great importance in terms of survival and development of pottery centers whose numbers are gradually decreasing.

350 people living in Sorkun village of Mihaliçık district of Eskişehir work in the production of hand-made eye nuru pots until they are baked from the extraction of the soil. It is not known how old the history of the construction of the horror pod is based. There are rumors that it is 700-800 years old. Sorkun villagers produce and sell over 200,000 pottery in a year.

60 per cent of this number is pottery, 30 percents is fish frying pan, and 10 per cent is frying pan. However, Eskişehir and our country do not know much about Sorkun pottery, which is both publicity and economic importance. It was also the goal of our work to study the clay types used in the construction of the scarecrow pots and to study the process of pottery making in the village.

This made the work Bilecik Kinik, İzmir-Menemen, Aydın-Karacasu, Nevşehir-Avanos, Mihaliçık'a-Sorkin, Konya Doganhisar Turkey "And when traditional pottery called has detailed research on mind from the most important properties of clay also used in the construction of merkezlerdendir.çömlek but pots construction stage and presentation is also important for our country and our city.

THE POWDERY BEAUTY; Korean Buncheong Ware

Leman KALAY

Kyung Hee University, Global Campus College of Art & Design, Department of Ceramic Art, 1732
Deokyoungdaero, Giheung-gu, Yongin-si, Gyeonggi-do, 17104, Republic of Korea

The concept of fast firing is now the dominating technology in the ceramic tile sector and the time available to reach an optimal stabilization of the ceramic body is reduced to few minutes. Ceramics have been closely connected with a nation's lifestyle as a commodity. Pottery is an aesthetically unique invention and a piece of life that reflects culture and society. In particular, Buncheong ware in the early Joseon Dynasty reveals its unique style. Buncheong together with white porcelain became mainstream in the early Dynasty. During the Joseon Dynasty, main production was centered on Buncheong ware and white porcelain. Unlike white porcelain, buncheong was produced only during the first 150 years of the Dynasty. "Buncheong", meaning "powdery blue", was actually named by Ko Yoo-Sup who was the first Korean art historian. It represents a distinctive style of ceramics, more rustic and dynamic than the celadon that represented the refined aristocratic taste of the Goryeo. This is visible in both its form and decoration. Buncheong has provided new beauty through folksy expression, contrary to the delicate high-class Goryeo celadon. Buncheong showed interesting aesthetic styles with various views of texture, atmosphere, and patterns based on its free and experimental intention. It contained the lives of ordinary people makes daily life and art encounter each other. It has also been widely applied with modern expressionism in the present time.

THE CHANGING OF LATTICE PARAMETERS OF ALBITE AND ORTHOCLASE FIRED IN TWO DIFFERENT BISCUIT FURNACES

Handan Çatır¹, Müzeyyen Şirin¹, Hanife Kadioğlu¹, Fazilet Güngör¹, Dilek Şen¹, Enver Tarım¹,
Berda Altun¹, Harun Taşdemir¹, Kemal Karadal¹, Veli Uz²

¹*Kütahya Porcelain Research & Development Department, Kütahya*

²*Kütahya Dumlupınar University, Metallurgy and Material Engineering, Kütahya*

Albite and orthoclase minerals are important for ceramic materials. In this study, it was determined the changing of lattice parameters of albite and orthoclase fired in two different biscuit furnaces. It was found that lattice parameters of albite and orthoclase changed according to the firing furnace.

Keywords: Porcelain, Feldspar, Albite, Orthoclase, Firing

HYDRATION, STRENGTH AND SURFACE PROPERTIES OF PORTLAND CEMENT-SILICA FUME BLENDS

Abdullah Demir¹, M.Uğur Toprak², EdaTaşçı³, Musa Akman⁴

¹Kütahya Dumlupınar University, Faculty of Engineering, Department of Civil Engineering, Center Campus, Kütahya/ Turkey

²Kütahya Dumlupınar University, Faculty of Engineering, Department of Civil Engineering, Center Campus, Kütahya/ Turkey

³Kütahya Dumlupınar University, Department of Metallurgy and Materials Engineering, Kütahya/ Turkey

⁴Kütahya Dumlupınar University, Department of Metallurgy and Materials Engineering, Kütahya/ Turkey

Silica Fume reacts with lime during cement hydration to form additional calcium silicate hydrates (C-S-H gel) which bonds the components together creating a dense matrix. In addition to its pozzolanic properties it is also a very good filler due to its particle size. In this paper, hydration and surface properties, physical and mechanical properties of silica fume added cements is investigated through XRD, SEM and contact angle analysis at 3, 7 and 28 days. Three substitution rates of cement by silica fume are used (5%, 15% and 25%). Silica fume seriously effected the 28th day specimen properties, specimen properties were similar at all silica fume ratios for 56th day specimen properties. Substitution of silica fume (5%) considerably (36%) increased the 28th day mortar compressive strength. Compact structure obtained in SEM photos supported this. High percentage (15%) silica fume substitution adversely effected the workability of mortars.

Keywords: Silica fume, Cement, Hydration, Surface Properties, Microstructure

EFFECT OF SINTERING ADDITIVES ON THE TYPE AND MORPHOLOGY OF Si_3N_4 PRODUCED VIA CARBOTHERMAL REDUCTION AND NITRIDATION OF SiO_2

Mert Yüksel, Burak Alici, Gülsüm Topates

Ankara Yıldırım Beyazıt University, Department of Metallurgical and Material Engineering, Keçiören,
Ankara/ Turkey

The study investigated the effect of sintering additive types on the final morphology of Si_3N_4 via carbothermal reduction and nitridation (CRN) technique of SiO_2 . The CRN is one of the techniques preferred for the Si_3N_4 powder production. C black and quartz powder were preferred as starting materials with the molar ratio of 2.2. Three types of sintering additives Y_2O_3 , CeO_2 and Yb_2O_3 were used in the study. Four different compositions were prepared using these additives and CRN process was done at 1500°C for 3 h. The results showed that the increased amount of eutectic phase prevented $\alpha\text{-Si}_3\text{N}_4$ formation and favored $\beta\text{-Si}_3\text{N}_4$ precipitation and growth. Depending on the sintering additive type, the morphology of Si_3N_4 grains changed to hexagonal-columnar from fiber-like structure and ratio of α/β varied. The lowest ratio was obtained as 15% for the addition of Y_2O_3 and Yb_2O_3 . The highest ratio around 40% was achieved by using CeO_2 as sintering additive by higher amount of fiber-like Si_3N_4 grains.

ANTIBACTERIAL APPLICATION OF NOVEL MICNO® PARTICLES FOR CERAMIC SANITARY WARE AND TILES

İsmail Şahin¹, Pervin Gençoğlu², Ender Suvacı^{1,3} and Alpagut Kara^{1,2}

¹ Department of Materials Science and Engineering, Eskişehir Technical University,

İki Eylül Campus, 26480/Eskişehir/Turkey

² Ceramic Research Centre Corp., Eskişehir Technical University,

İki Eylül Campus, 26480/Eskişehir/Turkey

³ ENTEKNO, Corp. Eskişehir/Turkey

Ceramic sanitary ware and tiles, which are widely used today, are in the most critical places of our lives. These regions, which are ideal living areas for microorganisms, are very dangerous in terms of human health. It is possible to reach healthy environments by preventing reproduction of bacteria and/or by killing bacteria such as *Escherichia coli* (ATCC 8739) and *Staphylococcus aureus* (ATCC 6538), which threaten human health by causing various diseases. Hygienic surfaces can be obtained by adding antibacterial agents such as Cu or Ag, as well as inorganic compounds such as Ag_2CO_3 , Bi_2O_3 , CuO , SnO_2 , TiO_2 , ZnO to the sanitary ware and tiles during production of glazes or with antibacterial surface coatings. The antibacterial effect of nano Ag, which is higher than the others, is used in large quantities to be effective in the glaze composition. It is known that the cost of nano Ag is high and the whiteness of the glazes is sacrificed. As an alternative to the widely used nano Ag, in this study it has been examined the effect of designed ZnO-based particles, called as MicNo® on microorganisms when they are used on sanitary ware and tile applications without breaking the glaze surface properties. Accordingly, the MicNo® powders have been added to ceramic sanitary ware and tile standard glaze recipes at different fractions to examine the sintering behaviors, production parameters, colors, surface properties and antibacterial properties.

APPLICATION OF AL-DOPED MICNO®-ZINC OXIDE PARTICLES AS CONDUCTIVE FILLERS IN POLYMER MATRIX COMPOSITES

Pinar Sengun¹, M. Tumerkan Kesim², Mujdat Caglar³, Umut Savaci¹, Servet Turan¹,
Ismail Sahin¹, Ender Suvaci^{1,2}

¹Department of Materials Science and Engineering, Eskişehir Technical University, 26555 Eskişehir,
Turkey

²Entekno Materials Corp., Eskişehir, Turkey

³Department of Physics, Eskişehir Technical University, 26470 Eskişehir, Turkey

Conductive fillers are mostly used in conductive polymer composites (CPCs) materials to build up conductive path into the polymer matrix phase. CPCs are utilized for protecting sensitive electronic components by preventing electrostatic discharge events. Generally, carbon-based materials and metal nanoparticles used as conductive fillers in CPCs. However, these materials have some disadvantages such as aesthetically dark color of carbon-based fillers, easy surface oxidation of metal nanoparticles, difficulties in production processes and toxicity. In addition, zinc oxide (ZnO) can be used for this purpose. Pure ZnO has relatively high electrical resistivity ($\approx 10^4$ ohm) and doping is one of the widely applied methods to enhance the electrical conductivity. To date, Al doped ZnO nanoparticles have been used in CPCs as conductive fillers, because of their low electrical resistivity. However, agglomeration of nano filler particles in polymer matrix is a critical problem which may lead to isolation of fillers. Therefore, there is a need for new alternative materials with better percolation behavior and low electrical resistivities. MicNo® particles which are platelet shaped micron particles, composed of strong chemically bonded nano-sized primary particles exhibit both micron and nano size characteristics. Accordingly, we developed micron sized platelets of Al-doped ZnO particles (MicNo®-AZO) that exhibits ≈ 40 K Ω .cm bulk resistivity and addition of 10 wt% (2 vol%) MicNo®-AZO into epoxy resin reduces the resistivity from ≈ 6 M Ω .cm to $\approx 1,7$ M Ω .cm. The results show that MicNo®-AZO are suitable for utilization in CPCs.

TEXTURED LEAD FREE $\text{Na}_{0.5}\text{Bi}_{0.5}\text{TiO}_3\text{-K}_{0.5}\text{Bi}_{0.5}\text{TiO}_3\text{-BaTiO}_3$ CERAMICS WITH HIGH PIEZOELECTRIC PERFORMANCE AND HIGH TEMPERATURE STABILITY

Ceren AŞKIN¹, H.Şule TETİK¹, Ozan ATEŞ^{1,2}, Murat AVCI² and Ender SUVACI^{1,2}

¹Eskişehir Technical University, Department of Materials Science and Engineering,

İki Eylül Campus, 26480/Eskişehir/Turkey

²ENTEKNO Corp. Eskişehir/Turkey

In today's technology, most of piezoelectric ceramics are lead-based. Lead-based piezoceramics (LBPs) are very dangerous for natural life. $\text{Na}_{0.5}\text{Bi}_{0.5}\text{TiO}_3$ (NBT) based ceramics are important alternatives for toxic LBPs due to their high piezoelectric performances and high reproducibility. $\text{K}_{0.5}\text{Bi}_{0.5}\text{TiO}_3$ (KBT) and BaTiO_3 (BT) modification of NBT ceramics results in superior electrical properties with relatively high phase transformation temperatures. In addition, texturing ceramics with desired crystallographic orientation is another approach to obtain considerably high piezoelectric responses from NBT based ceramics. Texturing ceramics with Templated Grain Growth (TGG) technique is commonly used to produce grain oriented ceramics via the orientation of anisotropically shaped templates in equiaxed matrix particles. In this process, evolution of lattice mismatches between templates and oriented grains may decrease the depoling temperatures. The research objective of this studies, synthesis of plate-like NBT, KBT, BT and NBT-BT-KBT templates and using such templates for texturing NBT-BT-KBT ceramics via TGG route. The textured ceramics were then characterized by X-ray Diffraction and Scanning Electron Microscopy techniques. Here, Microstructure and texture development of KBT-BT-NBT ceramics were investigated as a function of temperature, time and platelet type.

FABRICATION AND CHARACTERIZATION OF LOW COST CERAMIC MEMBRANES FOR WASTE WATER OF TREATMENT

İsmail Kırdı¹, Gülşin Arslan²

¹Selcuk University, Faculty of Science, Department of Chemistry, Alaaddin Keykubat Campus,
Konya/Turkey

²Selcuk University, Faculty of Science, Department of Biochemistry Alaaddin Keykubat Campus,
Konya/Turkey

Ceramic materials have been applied in many fields from health sector to space vehicle sector, from engine piston production to energy transmission material. One of these industries is membrane technology. Ceramic membranes, which are an important method especially for wastewater treatment, have a wide application area because they are resistant to high temperature and high pressure. The structure of ceramic membranes is usually composed of commercially available metal oxides such as Al, Zr, Si and Ti. The cost of ceramic membranes obtained from these metal oxides is high. Therefore, natural clay and waste materials with similar contents are emerging as an alternative in the production of ceramic membranes. In this study, it was aimed to produce low cost ceramic membranes from natural clay (attapulgate) and waste material such as red mud, which a waste product of bauxite processed in the aluminum production industry in Seydisehir, Konya. Characterization studies such as porosity, average pore size, water permeability and strength have been carried out to determine the usability of the produced ceramic membranes for wastewater treatment. Besides, SEM (scanning electron microscopy) was applied to examine the surface of the membranes. This study demonstrated that natural and local clay minerals and industrial waste containing metal oxides can be used in production ceramic membranes.

AN INVESTIGATION OF TECHNICAL FEATURES OF CASTABLE REFRACTORIES

Taner Kavas^{1*}, Abdullatif Durğun¹

¹ Afyon Kocatepe University, Department of Material Science and Engineering,
A.N.S Campus, 03200/Afyonkarahisar/Turkey

In this study, the performance characteristics of castable refractory samples obtained with 4 different cement mortars were compared with the shaped basic refractory bricks. For this, the cement mortars named as S1, S2 S3 and S4 were mixed with water ratio of 5.4%, 5.4%, 17% and 18.5% wt., by a mechanical mixing device until a homogenous mixing was achieved and plastic flowability was obtain. The castable refractory samples were prepared by pouring the cement mortars to moulds in dimensions appropriate to TS EN test standards. The prepared samples were sintered at 1200°C by applying the specified heat treatment regime. After heat treatment, mechanical abrasion resistance, corrosion resistance, compressive strength, density analysis, thermal shock resistance, thermal conductivity, thermal analysis (TG-DTA), mineral phase (XRD) and microstructure (SEM) analyzes were carried out. Finally, the analysis results of castable refractories are compared with the shaped basic refractory samples and the acquired performance characteristics and losing performance characteristics of castable refractories are discussed in detail.

Key words: Refractory mortar, shaped refractory product, technical properties, mechanical abrasion.

EVALUATION OF PHOSPHORESCENT PIGMENTS PREPARED BY DRY MIXING CONVENTIONAL METHOD ON SCHAMOT SURFACES

Bekir KARASU¹, Muhammed Sait ÖZER², Münevver ÇAKI³, Mehmet Eren GÜR¹

¹Eskişehir Technical University, Faculty of Engineering, Department of Materials Science and
Engineering, Eskişehir/ Türkiye

²Osmangazi University, Eskişehir Vocational School, Eskişehir/ Türkiye

³Anadolu University, Faculty of Art, Department of Ceramics, Eskişehir/Türkiye

Abstract

Schamot mud is a well-known mud type preferred by ceramic artists using it in their indoor and outdoor artefacts. It is pleasurably employed especially in ceramic sculpture, plate, city furniture or garden ceramics designs. Although it is not suitable for plastic forming it has certain advantages such as high temperature firing, low deformation, durability against outdoor atmospherically conditions and chemical composition in which iron oxide content varies giving very large colour spectrum.

In the current study schamot substrates were bisque-fired at 1000 °C, then surfaces covered with transparent glaze were gloss-fired at 1160 °C and finally decoration glaze containing phosphorescent pigment prepared by dry mixing conventional firing were applied and fired at 800 °C. Final products were characterized.

Keywords: Schamot mud, Phosphorescent pigment, Dry mixing, Solid state sintering method, Evaluation, Characterization.

PRODUCTION OF CEMENT AND CONCRETE PHASES (C4AF) BY USING ALTERNATIVE RAW MATERIALS AND METHODS

Mert Gül¹ Taner Kavas¹,

¹ Afyon Kocatepe University, Materials Science and Eng. Dep. Afyonkarahisar, Türkiye

Hydration of cement is the most important and misunderstandable part of the reaction of the cementitious materials [1]. There are some methods has been used changing hydration behaviour of the cementitious materials. Magnetic field also used to vary sensitivity of water and improve the properties [2]. Also crystallisation time of calcium carbonate can be accelerating by changing magnetic field [3]. This paper presents the results of experimental study on the microstructural and dielectric properties of C₄AF clinker phase with static magnetic field exposed to while hydrating. Pore size determining, specific surface area and density measurements of cement samples subjected to standard hydration under magnetic field at the ratio of water / cement (w/c) ratio of 0.3 were made. Surface area of the magnetic field holded sample is higher than non-magnetic sample. This can be due to crystallites observed by using SEM. Phase analysis was performed as a result of hydration. After these analyzes, the samples were gold plated and dielectric measurements were made at frequencies of 0.1 kHz and 1 kHz. In addition cement samples were hydrated under magnetic field with different water cement ratio 0.5 w/c for dielectric measurements. It was determined that the dielectric properties of the modified w/c ratio and the samples hydrated under the magnetic field had lower dielectric constant [4].

[1] Bullard J.W., Jennings H.M., Livingston R.A., NonatA., Scherer G.W., Schweitzer J.S., Scrivener K.L., Thomas J.J.,(2011), "Mechanisms of cement hydration" Cement and Concrete Research 41; 1208–1223.

[2] Gopalakrishnan R., Barathan S., Govindarajan D., "Magnetic Susceptibility Measurements on Fly Ash Admixture Cement Hydrated with Groundwater and Seawater", American Journal of Materials Science, 2012, 2(1): 32-36

[3] Lundager Madsen H.E.(2004) "Crystallization of Calcium Carbonate in Magnetic Field in Ordinary and Heavy Water" Journal of Crystal Growth 267, 251-255.

[4]Gu P., Beaudoin J.J., (1997),"Dielectric behaviour of hardened cementitious materials" Advances in Cement Research, 9, No. 33, January, 1-8

Note: Thanks to Rifat İşler for his experimental support.

PRODUCTION OF GEOPOLYMER-BASED POROUS THERMAL INSULATION CERAMIC

Taner Kavas^{1,*}, Emel Cengiz¹

¹Afyon Kocatepe Üniversitesi, Malzeme Bilimi ve Mühendisliği Bölümü, 03200, Afyonkarahisar

Geopolymer concrete (GPC) which emits least green-house gas to the atmosphere is an innovative construction material synthesized from alumina silicate material activated by alkaline solution. In generally, kaolinite was preferred as alumina silicate material but nowadays industrial wastes are increasingly being reported in the literature as they have been shown to be advantage in terms of monetary and environmental. Recent innovations in geopolymer technology have kept light to the development of various different types of geopolymeric products, like highly porous geopolymer-based foams. This study focuses on the preparation of geopolymer-based porous thermal insulation ceramic by using various proportions of silica sand (SS) and bottom ash taken from brick (BAB) production process. The effects of BAB mass ratio on compressive strength, density and thermal insulation were investigated. Several geopolymer-based porous samples were formed and cured at 60°C, 70°C, 80°C for 24 hours, 12 hours and 6 hours to observe the effects of temperature on those sample properties. Water-insoluble stabilized geopolymer ceramics were obtained in all group of samples. The results of the laboratory analyses indicate that low density, reasonable compressive strength and good thermal insulation properties can be achieved by using both BAB and SS raw materials to produce geopolymer-based porous ceramic materials.

Key Word: brick bottom ash, geopolymer-based insulation materials, silica sand, low density

CHARACTERIZATION OF PORTUGUESE CLAY

Rasim Ceylanteğin¹

Münire Cebeci¹

Murat Kaya²

¹ Kütahya Dumlupınar University Dep. of Metal. and Mater. Eng. Kütahya, Turkey

² KRM Seramik San. ve Tic. Ltd. Şti. Kayseri, Turkey

This study focuses on the chemical, mineralogical, thermal and ceramic properties of the clays from Portuguese. Clay samples were characterized by XRD, XRF, DTA, TMA and grain size measurements. Results show that clay samples have major amount of kaolinite, medium content of illite/muscovite and quartz with smaller amount of orthoclase. They consist of fine particles with medium to high plasticity. Thermal behavior shows two endothermic and two exothermic reactions, indicating physical and crystal water removal, and mullite/spinel formation, respectively.

With increasing the firing temperature, water absorption and porosity decreases and density increases. In the view of the analytical and physical results, the studied samples can be considered as to have potential in number of areas.

PRESSURELESS SINTERING BEHAVIOR OF TiO₂ NANOPOWDERS

Uğur Can Özöğüt¹, Ashı Çakır¹, Tolga Tavşanoğlu¹

¹ Muğla Sıtkı Koçman University, Faculty of Engineering, Department of Metallurgical and Materials Engineering, 48000/Muğla/Turkey

In this study, pressureless sintering behavior of TiO₂ nanopowders with particle size under 25 nm was investigated. Before sintering, the powders were uniaxially compacted by cold pressing into pellets of 2 cm diameters. Sintering temperatures between 600 and 1000 °C were selected. Conventional sintering processes were realized in air with a heating rate of 5 °C/min. Microstructural and chemical properties of the nanopowders and sintered bodies were investigated by SEM and EDS analyses respectively. XRD was used to determine the crystallinity. Relative densities of the sintered bodies were obtained by using Archimedes' principle, the volume shrinkage with the increase in the temperature were also investigated.

DETERMINATION OF EFFECT OF YTTRIUM DOPANT ON CUBIC PHASE STABILIZATION AND IONIC CONDUCTIVITY OF SOLID STATE LITHIUM LANTANUM ZIRKONATE ELECTROLYTE

Esra ŞAHİN¹, Alparslan Ali BALTA¹, Servet TURAN¹

¹Anadolu University, Department of Material Science and Engineering,
İki Eylül Campus, 26480/Eskişehir/Turkey

With rapidly growing energy demands, there is a large increase in demand for more efficient and renewable energy resources. Today, we rely on fossil fuels for most of our energy needs. Combustion of fossil fuels leads to the emission of greenhouse gases into the atmosphere. Global warming is a direct consequence of the accumulation of greenhouse gases. Internal combustion engines are a major source of CO₂ emission and hence alternative energy sources for automotive propulsion applications is one of the prime focuses of research throughout the world. The renewable sources such as solar energy and wind energy are “green” sources of energy but these are intermittent sources. For a continuous use, storage of energy is necessary. Batteries are electrochemical storage devices with which we can store energy in the form of chemical potential difference and use it whenever and wherever it is needed.

The energy demands of the countries changes in parallel with the development of industrialization and technology. In addition to economic development, it is also important that energy can be produced continuously, safely and at low cost so that contemporary living standards can be achieved. The adverse impacts on the environment as well as the limited availability of fossil fuels have directed the scientific world to alternative energy sources. Lithium ion batteries are also used as one of the alternative energy sources and have many advantages over other energy sources. These pills, mobile phones, laptop computers, such as many electric vehicles have a wide range of uses.

Existing commercially available ion batteries use volatile, organic liquid electrolyte. But; liquid electrolyte systems can degrade above 80 ° C, even though they are satisfactory at ambient temperatures, causing breakdowns and explosions. This is not particularly suitable for electric vehicles, and can put human life and driving safety at risk. With today's increasing demand for electric vehicles, battery systems that can operate at high temperatures have been needed to overcome safety problems caused by liquid electrolyte. Although solid electrolytic batteries are safe, their use is limited due to their low ionic conductivity.

Li₇La₃Zr₂O₁₂ (LLZO) is a promising solid electrolyte to be an alternative to liquid electrolytes in lithium-based batteries due to its high Li-ion conductivity and chemical stability. In addition, LLZO has a physical barrier property to prevent lithium dendrite progression and is a suitable combination to improve the performance and safety of lithium ion batteries.

On this project, solid state garnet type Li₇La₃Zr₂O₁₂ (LLZO) electrolytes have been produced. The problem with Li₇La₃Zr₂O₁₂ (LLZO) is tetragonal phase is stable instead of cubic phase which has higher ionic conductivity. Y doping will stabilize the LLZO at room temperature to cubic structure which shows the higher ionic conductivity rather than tetragonal form. With this project LiNO₃, La(NO₃)₃, ZrOCl₂ and Y(NO₃)₃ powders with sol-gel method were mixed with water by stoichiometric mole ratios and with 15 % excess LiNO₃. Different Y contents are used 0.10 mole %, 0.20 mole %, 0.30 mole %, 0.60 mole % and 0.90 mole %. And also different sintering temperatures (1150°C-1200°C) and sintering times (9-12-24 hours) have been tried to obtain desired cubic phase. Later phase analyze has been carried out by XRD and density measurements of pellets were done and by using Archimedes method and measurement of ionic conductivity of the samples were performed. As a result, cubic phase was stabilized at 1200 °C at 12 hours and also 1200 °C at 24 hours by different amount of Y.

A STUDY ON α - Al_2O_3 SEEDED SOL-GEL DERIVED ALUMINA POWDERS

Bediha Orbay¹, Azade Yelten-Yilmaz¹, Suat Yilmaz¹

¹ Istanbul University-Cerrahpaşa, Department of Metallurgical and Materials Engineering, Avcılar Campus, 34320/Istanbul/Turkey

Alumina (Al_2O_3) is famous for superior mechanical, optical, etc. properties and can be functioned in various areas such as biomedical, refractory, etc. Pure Al_2O_3 powders can be successfully synthesized through the sol-gel technique. This work examines the effects of seeding on the properties of the sol-gel derived α - Al_2O_3 powders. Aluminium isopropoxide (AIP, $\text{Al}(\text{OC}_3\text{H}_7)_3$), the starting material, was hydrolyzed at 90 °C and α - Al_2O_3 (0.063-0.2 mm), the seeding agent, was mixed with AIP and added together to the distilled water. Hereby, potential nucleation areas were formed in the boehmite (AlOOH) sol owing to the seeding agent surfaces. Un-seeded and wt. 3, 6 and 10% of AIP seeded samples were compared to analyze the seeding influence. AlOOH solutions were gelled at 110 °C for 6 h. Heat treatments of the gel samples were done at 1300, 1450 and 1600 °C for 2 h and α - Al_2O_3 powders were produced. After grinding, pellets were prepared and sintered at 1600 °C for 1 h. X-ray diffraction (XRD), apparent porosity (%) and compression strength tests were performed. XRD results showed that “Corundum” powders were synthesized in all samples. Apparent porosity decreased as the seeding ratio increased especially for the samples heat treated at 1300 and 1450 °C. Samples heat treated at 1600 °C displayed the lowest mechanical strength due to heterogeneous grain coarsening. Seeded α - Al_2O_3 powders which were heat treated at 1300 °C presented better mechanical properties than the ones heat treated at 1450 and 1600 °C depending on the uniform morphology and smaller grain sizes.

Acknowledgement: This work was supported by Scientific Research Project Coordination Unit of Istanbul University [grant numbers 21009 and 28135].

CALCIUM ION-EXCHANGE BEHAVIOR OF GEOPOLYMERS

Berk USTA¹, Burak AFŞAR¹, Berkay YAZIRLI^{1,2}, Ferhat KARA¹

¹Anadolu University, Department of Material Science and Engineering,
İki Eylül Campus, 26480/Eskişehir/Turkey

²Kale Seramik Research and Development Center, Çan/Çanakkale/Turkey

Geopolymers are amorphous inorganic materials which consist tetrahedral silicate and aluminate network. Each tetrahedral aluminum balanced by Na^+ or K^+ ions. These cations can be exchanged by other cations which modifies the composition of geopolymer. In this study Ca^{2+} ion was attempted to be exchanged by Na^+ in a sodium geopolymer which had a composition of $\text{SiO}_2/\text{Al}_2\text{O}_3=2.86$, $\text{Na}_2\text{O}/\text{Al}_2\text{O}_3=1.27$ and $\text{H}_2\text{O}/\text{Na}_2\text{O}=11.9$ molar ratios. Temperature, time and cation concentration with various process parameters on exchange behavior were investigated. After ion-exchange process geopolymers which has different $\text{Na}_2\text{O}/\text{CaO}$ ratios were obtained. Samples thermally treated at fast firing cycle 1200°C for 5 minutes. XRD results shows that ion-exchanged compositions mainly composed of solid solutions of plagioclase and amorphous phase while pristine geopolymer was amorphous. It can be concluded that ion-exchange process could be a viable method for obtaining various crystalline materials from geopolymers.

COCHLEA SHAPED ENERGY HARVESTING DEVICE

Hakan Güleç¹, Mert Gül², Ayşe Gül Toktaş³, Mevlüt Gürbüz⁴, Aydın Doğan³

¹ Nanotech High Tech Materials and Electrical-Electrical Systems Corporation,
Eskişehir/Turkey

² Ayfon Kocatepe University, Department of Materials Science and Engineering,
Afyonkarahisar/Turkey

³ Eskişehir Technical University, Department of Materials Science and Engineering, 26555,
Eskişehir/Turkey

⁴ Ondokuz Mayıs University, Department of Mechanical Engineering, 55139, Samsun/Turkey

Some of the piezoelectric devices work more efficiently around the resonance frequencies. Piezoelectric structures have the highest displacement and charge generation closer to the resonance conditions. In this study, we purposed a new wide band energy harvester with a spiral metal plate design for energy harvesters which have the potential to harvest vibrational energy over a broad range of ambient frequencies. In this design, metal shim with various leaf lengths were integrated with piezo ceramic rings in a spiral form like inner cochlea. Each metal shim has its own resonance frequency. Neighboring metal shim has also its own resonance frequency. Intriguingly, resonance frequency of each shim is close to trigger each other vibration. With such a structure it will be possible to scavenge energy in vibrating structure with a wider frequency range. In this study, resonance frequency of piezoelectric ceramic is optimized by clamped metal shim geometry. Parametric studies were performed to investigate the optimal condition of such a structure.

ANTIBACTERIAL EFFECT OF SILVER IN SANITARY WARES

Ayşe Gül Toktaş¹, Enes İbrahim Düden¹, Yiğitalp Okumuş¹, Aslan Gencer², Mert Gül³, Fadime Karaer⁴, Göktuğ Günkaya⁵, Taner Kavas³, Savaş Koporal⁴, Aydın Doğan¹

¹ Eskişehir Technical University, Department of Materials Science and Engineeri,
26555,Eskişehir,Turkey

² Color Prisma San.Tic. Ltd.Şti

³ Ayfon Kocatepe University, Department of Materials Science and Engineering, Afyonkarahisar,
Turkey

⁴ Eskişehir Technical University, Department of Environmental Engineering, 26555/Eskişehir/Turkey

⁵ Anadolu University, Faculty of Fine Arts, Department of Glass, Eskişehir, Turkey

The ceramics have a wide range of applications from the beginning of history until today. Sanitary ware products are today's unrivaled products. The fundamental properties expected from these products are bright and nonporous surface, prevention to bacteria, microbes and dirt, resistance to chemicals and abrasion. The addition of silver ions into the glaze increases antibacterial and self-cleaning properties significantly. Silver ions interfere with bacterial DNA and inhibit the cellular proliferation, breathing of bacterial cells and passing of important substances from the cell membranes. In this study, silver ion doped calcium phosphate based antibacterial powder was developed for use in the glaze of sanitary ware. The silver doped antibacterial powder was synthesized by the wet chemical method. In the scope of the study, the antibacterial powder with three silver ion ratios was synthesized. These synthesized powders were added into the glaze composition used in the vitrified products at different concentrations to investigate the antibacterial effect of the amount of silver. The antibacterial tests were performed in accordance with ASTM E3031 - 15 standard by using reference samples in the department of environmental engineering. Structural, morphological and chemical characterizations of the synthesized powders were carried out by XRD, SEM, XRF and EDX. The silver amount in the wastewater of synthesis was determined by ICP analysis. As a result of this work, the optimum amount of silver to obtain antibacterial effect was determined for using in glaze compositions of vitrified products.

CHARACTERIZATION OF COLORING AND OPAQUENING AGENTS IN ROMAN MOSAIC GLASS TESSERAE FROM SINOP BALATLAR CHURCH, TURKEY

Özden Ormancı Öztürk^{1,2}, Meriç Bakiler^{1,2}, Gülgün Koroğlu^{1,3}

¹ Mimar Sinan Fine Arts University, Material Research Center for Cultural Property and Artworks, Cumhuriyet Mahallesi Silahşör Caddesi 34380 Şişli İstanbul, Turkey

² Mimar Sinan Fine Arts University, The School of Conservation and Restoration of Movable Cultural Property, İstanbul, Turkey

³ Mimar Sinan Fine Arts University, Vocational School, Cumhuriyet Mahallesi Silahşör Caddesi 34380 Şişli İstanbul, Turkey

Glass tesserae is usually opacified by micro crystalline particles dispersed in a vitreous matrix and different types of opacifier have been used throughout history. Due to the addition of a range of elements as opacifier/colourant, the compositions of glass tesserae are complex. The main objective of this study is to provide a compositional characterisation of Roman glass tesserae from the Sinop Balatlar Church and special emphasis was put on the identification of these agents.

The glass tesserae samples investigated in this study consist of a selection of the detached tesserae found on the excavation area. Scanning electron microscopy were used to give information about the porosity of glass pastes and alteration layers at the surface. The opacifiers and their distribution in the glassy matrix were also observed using SEM-EDS. The attribution of the Raman signatures was made by comparison with data present in the literature and XRD analysis were also performed to identify the crystalline phases. The preliminary characterization studies by SEM-EDS and Raman ascertained the presence of Ca-antimonates in green, blue and turquoise tesserae. Bindheimite is also detected in green tesserae together with Ca-antimonates, while chromophore ions found out are Cu (II) (green, turquoise) Cu (O) (brown sample), Co (II) (deep blue sample) and Mn as a decolourant. Black, yellow and white glasses will also be investigated.

DEVELOPMENT OF THERMAL COMFORTABLE CERAMIC FLOOR TILES

Safa Korkmaz¹, Alpagut Kara^{1,2}

¹Eskişehir Technic University, Faculty of Engineering, Department of Material Science and Engineering, İki Eylül Campus, 26480/Eskişehir/Turkey

²Ceramic Research Center, Anadolu University, Eskişehir/Turkey

In addition to the decorative and structural properties of ceramic floor tiles, additional functions such as thermal insulation and thermal comfort are added. All of the specified functions depend on careful control of the total pore quantity, size and morphology of the structure. By reducing the thermal conductivity, it will be possible to produce alternative tiles for wood materials, especially for indoor applications. In this context, porcelain tile bodies were prepared using different ratios of silicon carbide (SiC) powder and sintered at different temperatures under industrial fast firing conditions. In this study, the effect of additive amount, particle size, composition and temperature of sintering on pore formation process were investigated. In this study, 0.1%, 0.2%, 0.3% SiC powder with a surface area of 25m² / g was used. Within the scope of this project, it is aimed to develop lighter floor tiles with low density in pores (SiC). The water absorption value of less than 3% and the average standard floor tile strength values (150-300kg / cm²), but the thermal conductivity of the value of wood products thermal conductivity values (0.3-0.4W / mK) is aimed to develop close to the body.

THE EFFECT OF MULTI-ELEMENT DOPING ON NANO-DEFECT STRUCTURE IN $\text{Li}_7\text{La}_3\text{Zr}_2\text{O}_{12}$ BY USING NATURAL RAW MATERIAL

Emine ERSEZER, Kübra ACER, Mustafa YILDIZLI, Tuğçegül İDİNAK,

Ahmet Furkan BULUÇ, Kamil Burak DERMENCİ and Servet TURAN

¹Eskişehir Technical University, Department of Material Science and Engineering,

İki Eylül Campus 26480/Eskişehir/Turkey

Recently, most of the electrical devices become mobile devices. Therefore, a need for rechargeable energy systems have been increasing. Lithium Ion Batteries (LIBs) are one of the best solution for electrochemical energy storage systems. LIB's have high energy density, long discharge times and long cycle life. LIB's are assembled in 3 parts: anode, cathode and electrolyte. However, there are some problems about liquid electrolytes which can easily explode at minor temperature changes. Solution of this problem looks to be solid state electrolytes, but solid electrolytes have less ionic conductivity compared to liquid electrolytes. Additionally, their production cost is very high. $\text{Li}_{10}\text{GeP}_2\text{S}_{12}$, Li- β -Alumina and $\text{Li}_7\text{La}_3\text{Zr}_2\text{O}_{12}$ (LLZO) can be given as examples of solid electrolytes. Among them, LLZO is the most promising electrolyte with its comparable but still low enough ionic conductivity. Si is recently used in order to improve ionic conductivity of LLZO as a single-ion dopant and it was shown that by creating nano-defects, ionic conductivity can be tuned. As a common Si source and due to its multi element content, sepiolite would be an option to incorporate into LLZO structure. Therefore, the goal of the present study is to discuss electrolytic performance of LLZO produced by using sepiolite addition. Varying amounts of Sepiolites were sintered via solid-state method and the effect of sintering temperature and time on the ionic conductivity was evaluated via XRD, SEM and EIS.

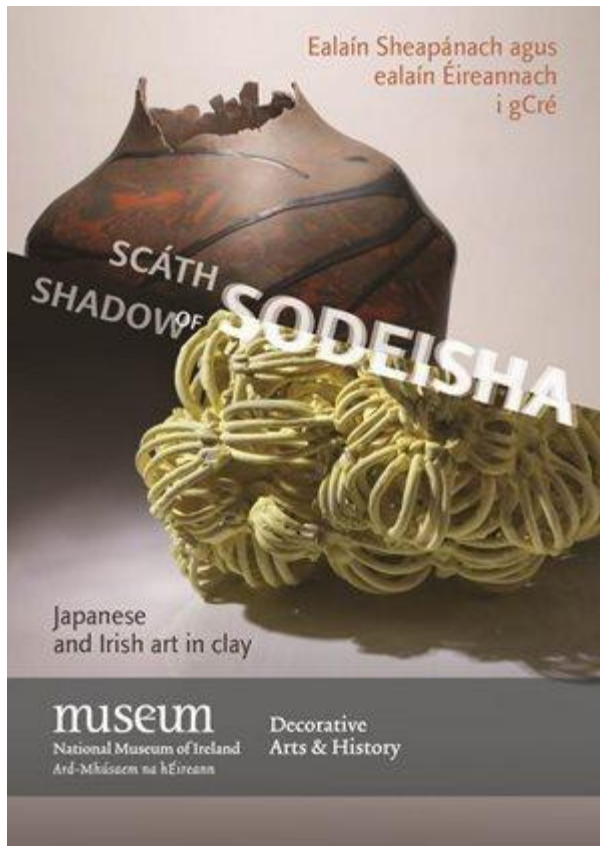
seres'18

IV. INTERNATIONAL CERAMIC GLASS PORCELAIN
ENAMEL GLAZE AND PIGMENT CONGRESS
October 10-12, 2018, Eskişehir, Turkey

ARTISTIC INVITED SPEAKERS

THE SODEISHA JOURNEY

Michael Moore
Ulster University, Belfast School of Art, Ireland



a. The National Museum of Ireland, Collins Barracks, Dublin 8, Ireland.

This paper describes the evolution of 3-year project that examines the creative links between Ireland and Japan through Ceramics. It describes the organisations and artists involved in the project that led to a year long exhibition at the National Museum of Ireland, Dublin. The exhibition programme also included curator's talks, artists workshops guided tours, all with the intention of celebrating ceramics in the museum context.

'The Shadow of Sodeisha, Japanese and Irish Art in Clay' exhibition explored a themed collaboration between artists from Ireland and Japan. The exhibition occurred in the year (2017) both countries celebrate their 60th anniversary of Diplomatic relations.

The concept began in 2015 when Michael Moore of Ulster University visited the Lafcadio Hearn Japanese Gardens, in Tramore, Co. Waterford, Ireland and initiated a discussion with the Gardens Director, Ms. Agnes Aylward. Lafcadio Hearn, the writer and poet, 1850- 1904 was the son of an Irish born Military Surgeon in the British Army. Hearn spent much of his time from 1857 travelling between Dublin, Tramore and Bangor in Wales. After periods in England and the USA, Hearn went to Japan in 1890 to work both as a journalist and as a teacher. Over the period of 14 years he extensively wrote about his experiences of Japan and Japanese culture. (1)

The discussion between Moore and Ms. Aylewood focussed on creative connections, both historical and contemporary between Ireland and Japan. Pivotal to this research was the Cultural Secretary of the Japanese Embassy in Ireland, Mr. Yuichi Yamada, who guided Moore through the (successful) Japan Foundation Grant application in 2016. (2).



b. Lafcadio Hearn Japanese Gardens. Photograph by Michael Moore.

Considering the role of Hearn as both a poet and writer based in Ireland and Japan, Moore then began to research further creative links between Ireland and Japan closer to Ceramics. This led to an examination of the post WW2 artists Group 'The Sodeisha' which was founded in Japan 1948. Rejecting traditional and functional pottery as the only way to create in clay, the Sodeisha Group were the first group of Japanese artists to consider clay as a material to make abstract art. Such was their influence in general in ceramics and in particular in Ireland, Irish Artist Deidre McLoughlin spent three years in Japan to learn more about the Sodeisha Group. The long established traditional ceramic practice, primarily functional, often decorative was now being challenged. Objects, sculptures were now being built, indeed hand built, without spouts, handles or lids, some were hollow and open, others hollow and entirely closed. This was in defined contrast to the long-established craft of traditional pottery from Japan.

In 1948 the Sodeisha artists mailed out postcards with their 'motto' or artistic credo: "The post-war art world needed the expediency of creating associations in order to escape from personal confusion, but today, finally, that provisional role appears to have ended. The birds of dawn taking flight out of the forest of falsehood now discover their reflections only in the spring of truth. We are united not to provide a 'warm bed of dreams', but to come to terms with our existence in broad daylight". (3).

This may seem uncontroversial in 2018, but imagine taking this step seventy years ago. And to do so in a country steeped in traditional material culture only two years after the ravages of the Second World War. Research establishes that three young artists are credited with the foundation of the Kyoto based Sodeisha Group: Yagi Kazou, Yamada Hikaru and Suzuki Osama. All were born in the 1920's. While some Sodeisha Ceramics were vessel based and hollow, others were enclosed forms more akin to modernist abstract sculpture than functional pottery.

We must consider the enormous presence of traditional functional pottery in the broader landscape of Ceramics as a material culture to understand the ambitious nature of this contrary, arguably rebellious evolution of another role and philosophy for ceramics. One can also argue that in 1948 in Japan, it was simply sensational.

This research lay the foundation for the theme of 'The Shadow of Sodeisha, Japanese and Irish Art in Clay'. It also opened the question of what to do next? The ambition was always to create a visual intellectual exchange between Ireland and Japan. Moore contacted one of the leading contemporary ceramics maker and educators, in Japan, Mr. Hiroaki Morino. Mr. Morino is one of Japan's most influential ceramicists, and represented Japan on the Council of the International Academy of Ceramics for many, many years.

The idea of the *Shadow* of Sodeisha was not to imply something ominous or dark. It was intended to focus the theme on something moving, shifting and evolving over time. This tied in well with the 18-month period of reflection artists which will be discussed later in this paper.

Discussions followed with Mr. Morino and Mr. Mitsuo Shoji to develop a selection of six artists from Japan to be involved in the exhibition. What began to establish itself was remarkable and as the creator of the concept and collaborative exhibition, Moore had no role in this. As the discussion evolved it

began to appear that the only Japanese artists involved in the Shadow of Sodeisha were those who had some link to the actual Sodeisha Group. The artists were either directly taught by members of the Group or were taught by those who were previously taught by Sodeisha artists. Therefore, some kind of legacy or lineage, linking back to Sodeisha came to be. By March 2016 the Japanese exhibitors (and one from Taiwan) were now selected: Mitsuo Shoji, Hidemi Tokutake, Jia Har Liang, Akito Morino, Satoru Hoshino and Kazou Takiguchi.



c. Akito Morino Vessel. Photograph by Michael Moore 2017. d. K. West Form (l), D. McLoughlin Form (r). Photograph by M. Moore 2017.

Mitsuo Shoji is known for his finely finished ring forms and contorted twisting sculptures, often with treatments of fine gold or slip decoration. Hidemi Tokutake, taught by Shoji, created clusters of vessel forms united by flanges and rings of clay in a very organic leaf like construction with dry dark blue and black glazes. Other forms are dry glazed in warmer ochre colours. Jia Har Liang created a 'Space and Transformation Series' of wall mounted, stemmed geometric vessel like forms. Satoru Hoshino created two immense hillside inspired forms in dark clay and heavy show like glazes, describing the destruction of landscape following earthquakes and landslides in Japan. Kazou Takiguchi presented two blended clay vessels that should never exist. These blends of clay rarely survive the kiln firing process as the clays want to pull away from each other and crack. However, these two magnificent forms have been fired with mastery with perfect structure and surface.



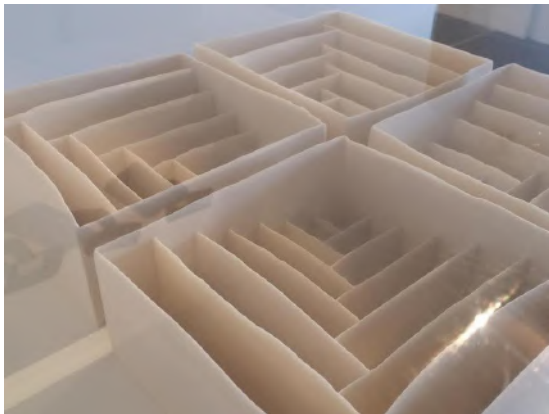
e. Kazou Takiguchi, Form. Photograph by Michael Moore. 2017. f. Jia Huar Liang, Wall Forms. Photograph by Michael Moore. 2017.

The selection of six Irish artists was made by Dr Audrey Whitty, Keeper, Art & Industry (Head of Decorative Arts, Design & History) at the National Museum of Ireland. While Moore created the project from the beginning, he did not select himself for the exhibition. All invited Irish artists had to submit work for independent adjudication by Dr. Whitty.

Rather than simply submitting work, the Irish Artists were invited to respond to a piece of text. This was circulated to the artists eighteen months before opening of the exhibition in March 2017. Artists were invited by Moore to read the text and live with the concepts of Sodeisha, for over a year. This allowed for an extended period of reflection to allow the philosophies of Sodeisha to truly emerge in the work submitted to the exhibition. All works made by the Irish artists were a direct response to the text. No works were submitted which were created prior to the circulation of the text. The circulated text was Louise Allison Court's (4) article 'Crawling Through the Mud: Avant-Garde Ceramics in Post War Japan' (5). Moore informed Ms Court of the intention of referencing her essay as a source of inspiration for the Shadow of Sodeisha. The response to this communication is as follows:

What a wonderful way to begin the day, with your message about the exhibition at the National Museum of Ireland bringing together Irish and Japanese (and one Taiwanese) potters! Thank you for alerting me. I'm glad to know my writing was of use..... I'd love to see some images of the installation and the individual works, and to know more about how you chose the Japanese artists. (6).

Louise Allison Court was then advised of the selection procedure which was in place with Mr. Morino making the recommendations for the selection of Japanese artists for the exhibition.



g. Isobel Egan Forms, Photograph by Michael Moore 2017.
Form, Photograph by Michael Moore 2017.



h. Frances Lambe

For the Shadow of Sodeisha Isobel Egan presented 4 intricately constructed forms in Porcelain Paper Clay. The gradual reduction in the scale of each slab of porcelain in each Isobel quadrant of the grid form, intensified the depth of tone and shadow, making these four fine porcelain forms ideally appropriate for the theme of the exhibition.

Frances Lambe submitted a series of hand-built clay forms. These are intricately pierced oriole forms with hours of painstaking surface work to create these pieces. In one the surface is entirely neutral, in another small pools of gold leaf populate the forms surface.

Deidre McLoughlin explored a range of scales in the 3 highly polished with minute application of glazed forms. One stand-out piece illustrated earlier in this text is actually the smallest piece in the exhibition. A smooth polished white bone like form contracting in scale very well to the large Katharine West form decorated in blue engobe. West also submitted a large swooping funnel form in white clay with implications of transition from one phase or state to another, also reflecting the Sodeisha belief of evolution and change.

Nuala O' Donovan created two forms which examine irregular patterns in nature. These are highly fragmented forms, built around chaotic wire constructions, perhaps testing our presumed associations of the material characteristics of clay and its potential. O' Donovan also makes some quite remarkable constructed forms (7) which have a more defined stature compared to these more fragile forms exhibited in this exhibition.



i. Nuala O'Donovan. Photograph by Michael Moore 2017.

The two pieces made by Michael Moore have direct links back to Laffadio Hearn and Tramore Co. Waterford. Both are hand built hollow clay forms, undecorated to allow the light and shade to work in harmony with the polished clay surfaces of each piece. 'After Laffadio' is a direct reference to the tiered and ridged layout of the Laffadio Hearn Gardens in Tramore with three distinct horizontal clay ridges in the form.



j. After Laffadio.

l. The Guillamene.

Photographs by Michael Moore 2017.

k. The Guillamene and After Laffadio Works in progress.

'The Guillamene' sculpture is a direct reference to a place in Tramore, Ireland. For generations people have dived, jumped and plunged into the Atlantic Ocean of the beaches and diving pools around Tramore. It takes courage to go to the highest of three diving points off the rocks of the Guillamene. The Guillamene in ceramic reflects on the courage taken to climb to the highest diving point off the cliffs, perhaps as Laffadio Hearn once did.



m. Tramore, Co. Waterford, Ireland. Photograph by Michael Moore.



n. The Guillamene Co. Waterford, Ireland.

All artists submitted non-functional forms for this exhibition, in line with the themes and ethos of Sodeisha. While some referred to the vessel, all were hollow forms, none had any utilitarian application. The Exhibition was opened by Her Excellency Ms. Miyoshi, Ambassador of Japan in Ireland on March 30th 2017.

A seminar series was programmed for October 2017, the Curators Tour occurred in May 2017 and the Dublin Culture Connects 'Culture Club' were hosted at the Sodeisha Exhibition by Dr. Whitty and M. Moore June 30th 2017. The 'Shadow of Sodeisha, Japanese and Irish Art in Clay' received external research funding from The Japan Foundation and The Design and Crafts Council of Ireland. The Shadow of Sodeisha was the only themed exhibition to open at the National Museum of Ireland, Collins Barracks throughout 2017.



o. The Shadow of Sodeisha opening, March 2017. Ambassador of Japan in Ireland. 2017.



p. Her Excellency Ms. Miyoshi,



q. Culture Club Curators talk at the National Museum of Ireland. 2017
Museum of Ireland. Photo. by M. Moore.



r. The National

Foot Notes:

1. <https://lafcadiohearngardens.com>
2. The Shadow of Sodeisha received funding support from The Japan Foundation and The Design and Crafts Council of Ireland.
3. <https://en.wikipedia.org/wiki/S%C5%8Ddeisha>
4. Louise Allison Court is Curator for Ceramics at the Freer Gallery of Art and Arthur M. Sackler Gallery, at the Smithsonian Institution USA. <https://studiopotter.org/crawling-through-mud-avant-garde-ceramics-postwar-japan>
5. The Sodeisha Group. <https://studiopotter.org/crawling-through-mud-avant-garde-ceramics-postwar-japan>
6. Email exchange between Moore and L. A. Court, March 2017.
7. <http://nualaodonovan.com/gallery>

Illustrations.

- a. The National Museum of Ireland, Dublin 8, Ireland. Photograph by Michael Moore 2017.
- b. Lafcadio Hearn Japanese Gardens. Photograph by Michael Moore 2017.
- c. Akito Morino Vessel. Photograph by Michael Moore 2017.
- d. Photograph by Michael Moore 2017.
- e. Photograph by Michael Moore 2017.
- g. Isobel Egan Forms (4) Photograph by Michael Moore 2017.
- h. Frances Lambe Pierced form. Photograph by Michael Moore 2017.
- i. Nuala O'Donovan. Photograph by Michael Moore 2017.
- j. Michael Moore. After Lafcadio. Photograph by Michael Moore 2017.

- k. Michael Moore. After Lafcadio and The Guillamene Work in progress. Photograph by Michael Moore 2017.
- l. Michael Moore. The Guillamene. Photograph by Michael Moore 2017.
- m. Tramore, Co. Waterford. Photograph by Michael Moore 2017.
- n. The Guillamene Co. Waterford, Ireland.
https://images.search.yahoo.com/search/images;_ylt=A0PDsBwbpo9bfiwATvZXNyoA;_ylu=X3oDMTB0N2Noc2l1BGNvbG8DYmYxBHBvcwMxBHZ0aWQDBHNiYwNwaXZz?p=the+guillamene+co.+waterford&fr2=piv-web&fr=mcafee#id=15&iurl=https%3A%2F%2Ffloneswimmer.files.wordpress.com%2F2013%2F02%2Foverall-1_mg_1217-resized.jpg&action=click
- o. The Shadow of Sodeisha opening, March 2017.
- p. Her Excellency Ms. Miyoshi, Ambassador of Japan in Ireland, opening the Shadow of Sodeisha exhibition. 2017. National Museum of Ireland.
- q. Culture Club Curators talk at the National Museum of Ireland. 2017.
- r. The National Museum of Ireland. Photo. by M. Moore.

STOP MOTION USING CLAY

Mogharbel Samar
Lebanon American University (LAU), Lebanon

DEFINITION

Stop motion is an animation technique using objects, or series of photos that can produce motion.

In 1932 a pioneer called Lew Cook made a film called the “Little Baker” using plasticine.

The principle is placing an object in front of the camera, take a picture, move it slightly, take another picture. Doing this many times will create a movement illusion; the object will appear to move; typically, 12 frames create one second of animation.

In movies, animators use articulate dolls, with a metal skeleton that could be quite sophisticated, it is called armature, with joints on all the movable parts. Most puppets cannot stand by themselves they have to be screwed to the set, usually they have a series of replaceable body parts, or the entire head can be replaced. Nowadays 3D printing will produce accurate replicas of parts of the face.

Some stop motions could be constructed entirely using still photos like the film of Chris Marker, “La Jetée” (1962) tells the story of post-nuclear war experiment in time travel, shot in black and white.

Another technique is plasticine figures technique called “clay-mation” also known as model animation.

The primary material used to cover the armature, is a synthetic malleable one, these characters created could move their whole body, and even walk with ease with incredible details.

Some examples of these clay-mation feature films are Shaun the Sheep, Coraline, Wallace and Gromit etc.

MY OWN EXPERIMENTS

I studied at the very university where I teach in at the moment, “the Lebanese American University” LAU, Business/Computer major where I learnt to write programs in complicated computer languages. This gave me a predisposition and patience to tackle the editing of computer programs. It was only later that I went to Goldsmith’s University in London to earn a Postgraduate degree in Ceramics.

I believe that this background that I have in computer programming and editing is what gives me the patience for the technicalities of the work required for my stop motion projects and films.

This type of expression gives me an additional tool on top of my regular expressions in high fired ceramics.

Using the same medium and treating it differently.

Stop motion animation offers a bit more freedom with clay work, it has the freedom of expression and the freedom of the making as opposed to my usual high fired ceramics. For example the distorted faces of the figures, due to the manipulation of the clay are done on purpose to create a direct almost childlike figure.

Stop motion offers the same pleasures of clay work but with fewer constraints, and less considerations, however it has to be a quick process, and done in one day usually due to the fast drying nature of clay.

In 2005 a friend of mine Greta Naufal, a committed visual artist of the war generation, an educationalist who teaches Art in a French School (College Protestant Français) and a colleague at LAU asked her 14-year-old students to illustrate two poems of a French popular poet “Jacques Prevert” (1977-1990), his poems are taught widely in French schools. Prevert’s poetry is surrealistic,

being closely related to the communist party, he denounces social oppression.

Greta asked me to animate those drawings, which were my first attempts in animation and I did with them great pleasure.

The first animation is “at the florist” where a man enters to the florist shop to buy flowers, then suddenly he puts his hand on his heart and falls, his money rolls on the floor and does not stop rolling....

The second poem “The funeral of a dead leaf” of the same author it is the story of two snails going in the autumn to bury a dead leaf, when they arrive it is spring the leaves are all resurrected ... “yes” the author says, live, love, sing “the song of summer”, “it is a pretty evening, a pretty summer evening...”



At the time, I used a program called “After Effect” to animate those different drawings.

(See film “at the florist”)

<https://www.youtube.com/watch?v=V9pCMWXSPfE>

(See film “The funeral of a dead leaf”)

<https://www.youtube.com/watch?v=2sIanl3hlIE>

On the 12th of July 2006, Israel launched a massive war on Lebanon, where the southern part of Lebanon had been bombed extensively and invaded. People fled from the south (border with Palestine), and came to Beirut.

The displaced population stayed in schools and theatres.

The displaced population stayed in schools and theatres and naturally kids needed some sort of entertainment, so the civil society organization mobilized educators to be with them, Greta and I were called upon to do something with the kids at “al Madina” theatre, one of the theatres that hosted many families.

The war was raging, all the bridges connecting the south to Beirut, most of the houses in the South and many hospitals underwent massive destructions, and many Lebanese died...

We encouraged the children to express themselves, to draw these atrocities to help them heal their wounds... they made several drawings.



I took those drawings and made an animation called “the war on Lebanon through the eyes of the kids”. This film was shown in our local cinemas and in many countries around the world.

It was a documentation of this war, and the feelings and expressions of these who suffered because of it, it was the only way to retaliate, to give the children hope for the future and to let our sufferings be shown to the world. At the end we did win the war and at the end of this film a man comes out of his peaceful house playing the oud. Israel left Lebanon, and will eventually leave our neighborhood.

(See film “the war on Lebanon through the eyes of the kids”)

<https://www.youtube.com/watch?v=CZk6F4P11YQ&t=101s>

Through my career as an artist who lives in a country that has been ravaged by wars, my works in general express those hard moments. It is my way to mark the time, to write the history of Lebanon.

Greta Naufal and I had a major show in the peaceful Sweden, in Milles Garden museum where we exhibited our works and the dominating theme was wartimes. In this exhibition I had an installation of battered empty oil barrels that were used as shields against snipers, dismembered human parts, and broken archaeological Phoenician replicas.



In 2009, An actress who did not have the necessary connections to pursue a career in acting in Lebanon, posed as a model for drawing classes at many different universities, including the Lebanese American University where I teach Ceramic courses .

She was passing through a difficult phase at that time, which led her greedy brother to commit her to a hospital for mental illness in order to take her savings.

This incident inspired my next film.

The film is called “Deir el Salib” the Covent of the Cross in English, which is also the name of the mental health institution in Lebanon where she was unjustly locked in.

And so, it is based on a true story...

Here I also tackle the relation of the artist /sculptor with his model...

What if the clay, this living material can talk to you while you are modeling it?

In my ceramic teachings, I highly encourage students be attentive to the clay, to listen with all their senses, and notice the reactions of the clay.

Forms can develop in an intuitive way rather than with cerebral considerations.

In this animation, many steps and modelling processes are shown.

The film in itself could be a lesson in sculpting a human head.

(See film “Deir el Salib”)

<https://www.youtube.com/watch?v=bwn-DAsCKrY>

In 2003 a young man, Ibrahim Rizkallah came to ask me to animate a story he has written. His first scene was about a man walking in a city; but I could not go beyond that...It was not feasible to create the whole city.

This led me to create a whole series of Lebanese houses that were threatened to be demolished. Memory of the places and the people was my initial idea, where I was also longing for my childhood house which was also destroyed to erect a new building in its place.



This idea of the old Lebanese houses, was later used in my next stop motion animation “black white”.

In “Black White” the scene is set to an old house and two children, twins, coming out of the door one after the other. The latter was indoors playing with her older brother, when called to come out to play with her twin. They then stop to pose for a photo that their father is taking on the terrace. This was done as an homage to my late father who was passionate about photos all his life.



(See film “black white”)

<https://www.youtube.com/watch?v=8C8oR3MAjJc>

In 2009, I made a stop motion of a potter making pots on the wheel; we see the process of the making, and failures. It is called "Clay from Clay".

The "creation of man from clay" is a [miraculous birth theme](#) that recurs throughout world religions and mythologies.

- According to [Sumerian mythology](#) the gods [Enki](#) or [Enlil](#) create a servant to the gods, humankind, out of clay and blood.
- According to [Egyptian mythology](#) the god [Khnum](#) creates human children from clay before placing them into their mother's womb.
- According to [Chinese mythology](#); [Nüwa](#) molded figures from the yellow earth, giving them life and the ability to bear children.
- In the Babylonian creation epic [Enuma Elish](#), the goddess [Ninhursag](#) created humans from clay.
- In [Greek mythology](#), according to Pseudo-Apollodorus Prometheus molded men out of water and earth.
- According to [Hindu mythology](#) the mother of Ganesh, Parvati, made Ganesh from clay and turned the clay into flesh and blood.
- According to [Genesis](#) "And the Lord God formed man of the dust of the ground, and breathed into his nostrils the breath of life; and man became a living soul".
- According to the [Qur'an](#)^[23:12-15], God created man from clay.
- According to [Inca mythology](#) the creator god [Viracocha](#) formed humans from clay on his second attempt at creating living creatures.
- According to some [Native American](#) beliefs, the [Earth-maker](#) formed the figure of many men and women, which he dried in the sun and into which he breathed life^[1]

(See film "Clay from Clay")

<https://www.youtube.com/watch?v=P7JfcYrugPs>

Later in 2011, I made another film related to my childhood memories. From 1924 until the independence in 1943, we had the French mandate in Lebanon. Therefore French started being taught in schools and became mandatory. This film is a reading of a poem by Jean de La Fontaine (1621-1695) a French poet and fabulist, one of the most widely read French poets of the 17th century who is known above all for his [Fables](#). This film shows a clay child figure reading the poem in French with an Arabic accent, "la laitière et le pot au lait" The Milkmaid and the Pot of Milk. It criticizes the French schooling of young Lebanese children who were expected to memorize long verses of these fables in old French, with obsolete vocabulary.

(See film "leçon de français")

<https://www.youtube.com/watch?v=70XQUjTVGCw>

Most recently in August 2018, for the SERES'18 "IV. International Ceramic, Glass, Porcelain Enamel, Glaze and Pigment Congress" that is organized from 10 to 12 October 2018 in Anadolu University, Yunusemre Campus, Congress Centre, Eskişehir/Turkey. I made 2 new stop motions, the first one is called "nowhere and everywhere" in collaboration with a young Lebanese writer Ibrahim Rizkallah born 1981; his stories are very profound and absurd. He has participated in several writing workshops in Lebanon and France.

"Nowhere and Everywhere" is about our present Middle Eastern political situation, based on the Greek mythology, "the myth of Sisyphus". Sisyphus, the king of Corinth defied the Gods by escaping death on two occasions; he was therefore punished by having to repeatedly roll a huge stone up a hill only to have it roll down again as soon as he had brought it to the summit.

The French philosopher Albert Camus wrote a book of the same title, Sisyphus is the absurd hero who lives life to the fullest, hates death, and is condemned to a meaningless task.

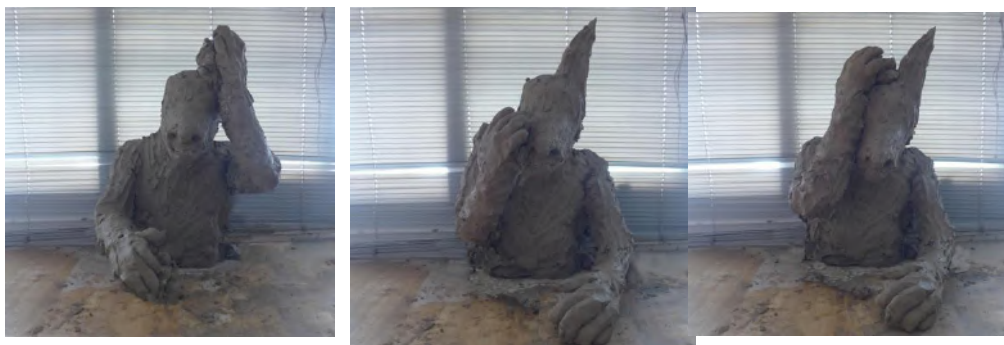
“Camus is interested in Sisyphus’s’ thoughts when marching down the mountain, to start anew. After the stone falls back down the mountain Camus states that “It is during that return, that pause, that Sisyphus interests me. A face that toils so close to stones is already stone itself! I see that man going back down with a heavy yet measured step toward the torment of which he will never know the end.” This is the truly tragic moment, when the hero becomes conscious of his wretched condition. He does not have hope, but “there is no fate that cannot be surmounted by scorn.” Acknowledging the truth will conquer it; Sisyphus, just like the absurd man, keeps pushing. Camus claims that when Sisyphus acknowledges the futility of his task and the certainty of his fate, he is freed to realize the absurdity of his situation and to reach a state of contented acceptance. With a nod to the similarly cursed Greek hero Oedipus, Camus concludes that “all is well,” indeed, that one must imagine Sisyphus happy”^[2]

Ibrahim Rizkallah’s text is about a white envelop that will never be opened; this action is postponed day after day until death comes to relieve him from this ordeal. In the film, we see a huge clay mountain where a rock rolls upwards, alone, and when it reaches the summit, it rolls back down, then a small figure rolls it back up to the summit and follows it back downhill, this is repeated 3 times while listening to the text.



The second stop motion I made, called “nightmare stories” is about the corruption in our country. Here a human clay figure with no features, is modeling his head while describing himself as a faceless, soulless, country less creature, a piece of clay, attaching long ears to his head to become a donkey. A short dialogue starts where he wonders why the basic necessities do not exist in our lives, he blames himself for bringing back the same people to the parliament under the pressures of sectorial divisions.

Corruption and divisions in Lebanon are deep-rooted in our society, where simple daily issues of garbage removal, water, and electricity are not yet resolved, leaving us with daily electrical cuts of several hours and garbage on the streets, beaches, mountain and valleys....



TECHNICAL NOTES

First consideration when making a film, is to choose the theme, mine are actual and relatable topics, tackling our socio-political situation in the Middle East. Going from the personal to reach the global is my way to be true to my subject. In the beginning the script usually follows my instinct, and later I develop it and amend it appropriately.

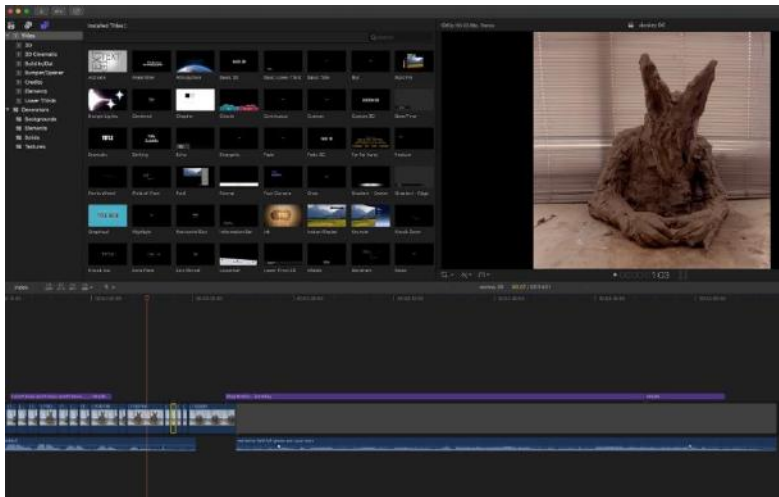
On some occasions, I make the stop motion animation, make notes on the theme and then ask a script writer to write the dialogue or text.

Once the theme is set I start building my clay form on a simple armature using perforated metal while respecting the proportions of my character.

As I mentioned in the introduction, the process is about taking many, many photos where the subject should be moved very slightly, and each time, a photo is shot, therefore creating the animation. As I am using natural clay and handling it, the clay will naturally start drying, giving me a deadline to finish the work, the whole work should be made and shot in one day. It is worth noting that many trials are made and destroyed in the process of reaching the final outcome.

Once the main character is built and the dialogue is almost set I gesticulate my character to follow the lip synchronization. All the frames are digital photos which I can edit using Photoshop, I can change the background, edit the colors, or clean the surfaces. In the next step, which is the final one, the photos are imported into an editing program; the one I use is called Final Cut pro. The dialogue should be digitally recorded and also imported to the Timeline. Now all the photos and dialogue are set on the Timeline I start editing to match lip synchronization.

The frames durations and timings are changed to match the photos. Any additions to the editing, like music, sounds effect, subtitles and credits should be done once the film is finished.



This elaborate work is done with patience and resilience.

I hope I was able to convey to you the work, process and the hidden meanings behind my 3 minutes films.

REFERENCES

- 1 - Wikipedia contributors. (2018, September 10). Creation of man from clay. In *Wikipedia, The Free Encyclopedia*. Retrieved 18:59, September 10, 2018, from https://en.wikipedia.org/w/index.php?title=Creation_of_man_from_clay&oldid=858906708
- 2 - Wikipedia contributors. (2018, September 4). The Myth of Sisyphus. In *Wikipedia, The Free Encyclopedia*. Retrieved 19:02, September 10, 2018, from https://en.wikipedia.org/w/index.php?title=The_Myth_of_Sisyphus&oldid=857973342

IN MEMORY OF HAMIYE ÇOLAKOĞLU

Candan Dizdar Terwiel

Hacettepe University Faculty of Fine Arts, Department of Ceramics, Ankara

Abstract

Hamiye Çolakoglu is one of the leading artists in our country, who skillfully achieved the goal of developing ceramics from traditional culture to the level of universal art. She also leded Hacettepe University Fine Arts Faculty Department of Ceramics, of which she is the founder, to be a worldwide education center. She will always be present with her contributions to art throughout her life, her exemplary and positive character, students she educated and art works she left behind.

Key Words: Ceramics, Art, Hamiye Çolakoglu.

Building a life in art, spending this life on producing original works of art, serving as a model and leading the way, Hamiye Colakoglu passed away on December 31 2014, in the apartment she had been living in Ankara.



Image 1: Prof. Hamiye Çolakoglu, Sen Petersburg, 2006. (Personal Archive)

Hamiye Colakoglu, who has a privileged place in Turkish arts, left her mark to the national history in 60 years by firing ceramic pulp over a high heat, a material of Plastic Arts which is equivalent to the human history. Her life story which begun in Sürmene/Trabzon in 1933, still remains in Ankara since 1945. Her first gallery on ceramic was hold at Tuna Street in 1957. When her own works on behalf of the ceramics are evaluated by considering its own era, traces of courage and a perspective ahead of her time would be clearly seen as surfaces, forms and monumental ceramics at global line.



Image 2: “Bilim Ağacı” (“Science Tree”), Porcelain Sculpture, Bilkent University, 1997. (Department of Ceramics Archive)

She is the first female ceramic artist in Turkey who applied firing over a high heat at 1280⁰C as a work of art and hold exhibitions. Surfaces of her ceramics exist with abstract lines of humanity, unique ceramic shaping compositions and porcelain sculpts. It can be considered that she is inspired by Anatolia’s incomparable beauty for each of her piece.



Image 3: Hamiye Çolakoğlu in her studio. (Department of Ceramics Archive)

From 1950s, she has attached great importance to the developments on Turkish Handicrafts and become a leading artist in this field. She has visited most of the countries in the world and served her accumulation through the arts to her students in an unselfishly way.



Image 4: International Ceramics Academy Meeting, with Hamiye Çolakoğlu , Güngör Güner (middle) and Bingül Başarır (from left to right last) in Riga, 2006. (Personal Archive)

Mrs. Çolakoğlu is an artist of many parts who has several national and international awards, jury memberships, numerous pieces that have place in museums and collections, a biography by M. Sıtkı Erinç (1998), hundreds of articles, encyclopaedical information and documents, national and international exhibitions. She is a founder of Hacettepe University Faculty of Fine Arts, Ceramic Department in 1983 and worked as a long-termed chief of the department.



Image 5: II. International Macsabal Wood Firing Symposium Honourable Artist Hamiye Çolakoğlu. (Department of Ceramics Archive)

She has felt a sense of belonging which composes her artistic stance and identity, in Ankara where she mostly lived in and turned her house in Beysukent near to the university, into a unique Culture House by a will of converting it to a Ceramic Museum in the future.



Image 6: Hamiye Çolakoğlu Culture House downstairs studio. (Department of Ceramics Archive)

She presented her most fascinating pieces among the others that she made during her artistic life to Ankara and enriched the city. By her indoor and outdoor ceramic works that enrich the architecture, the building of Hacettepe University, Bilkent University and Land Forces Command lost their simplicities and gained a model structure to be protect in the future. In addition to her contribution to the ceramic arts, she is a leading artist in Turkey, who could bring a culture and perspective to the people and her neighborhood, by the beginning from Yenimahalle where she was born to the whole city.



Image 7: From the opening of “Derman Çeşmesi” (“Cure Fountain”), Hamiye Çolakoğlu with her family.



Image 8: “Derman Çeşmesi” (“Cure Fountain”) after years, Beytepe Campus, Ankara, 2017. (Personal Archive)

It was impossible for her to stay without changing and beautifying the places around her. Her mentioned characteristics serve as a model by the students that she trained. She is an artist who spreads the art to her whole life and look to the world from this perspective.



Image 9: Hamiye Çolakoğlu, while working for Füreya Koral Kuş Evi (Birdhouse) Exhibition in the Department of Ceramics. (Personal Archive)

She is an idol not only because of her ceramic pieces, but also her poems, patriotism, arias, that she sing, friendship with men of culture, family bonds and love. Hamiye Çolakoğlu is one of the most important cultural worker in Turkey. She chose one of the most difficult way in fields of art, cultivating the clay by the fire to make ceramics that she still exists with. She will maintain her presence with it. In an interview, her answer to the question of “Could you please share the importance and meaning of ceramics for your life, with us?” also reflects the core of her existence;

“Ceramics is a way of life for me. I fell into clay and I cannot get out of it. I am one with clay. I speak and sometimes argue with it. I work sometimes by beating it and sometimes by being gentle to it. I glaze it through my special methods and fire it with different fuels and in different temperatures. I am a slightly crazy person who is building her dreams. There is nothing missing in my philosophy. I am never afraid of or I never avoid the effort of reaching the point I aim to reach. The passion I have to see the result, accelerates my energy and research.”

References :

1. Erinc, Sıtkı M., ”Toprağın Erki Hamiye Çolakoğlu / The Power of Earth Hamiye Çolakoğlu”, Çanakkale Seramik Sanat Yayınları, 1998.
2. Terwiel, C. (2015) Hamiye Çolakoğlu Hacettepe Yılları ve Sonrası , *Seramik Türkiye* Türkiye Seramik Federasyonu Yayını, Mart-Ağustos, s : 98-103, İstanbul.
3. Ulueren, Ş.D.(2006) Seramiğin Toprak Anası...Hamiye Çolakoğlu; “Ben Ana Tanrıçayım” Röportaj, *Türk Seramik Federasyonu Dergisi*, Sayı:14, Mart/Nisan, s.103.
4. Tunçalp. M.(2015) Kadim Dostum Hamiye Çolakoğlu'na , *Seramik Türkiye* Türkiye Seramik Federasyonu Yayını, Mart-Ağustos, s : 94-96, İstanbul.

IN MEMORY OF İBRAHİM BODUR

Mustafa Tunçalp
Efes Ceramics, İzmir (his own studio)

I want to Welcome all of you. Today I want to talk about Mr. İbrahim BODUR which is founder and honorary chairman of Kale Group. He is one of the entrepreneurs and exchange pioneers in Turkey. The first factory of ceramic was established by him in Çan/Çanakkale. Also he is a real visioner. It's been 3 years since he passed away. But still we are so thankful and respectful to him. Also I am pleased, honored and thankful to be here and talking about him too.

I worked with him for 45 years in Kale Group. And it was the golden time of my art career. Because I felt the power of Mr. Bodur and Kale group behind myself every day.

He never accepted ceramic as only art material also he was believing its soul and connection between both. That's why he always supported to art and artists in his whole life. And the important one of these things for us is the ceramic factory which established by Mr. Bodur in 1997 in Çan as I told you before. Over the years many exhibitions have been organized in this museum. And it still continues to be regulated.

İbrahim Bodur wasn't caring only artistic activities, he also was caring many publications. Lots of ceramic artists and painters found a chance of working and researching in this factory and also they have been guest and it made them feel like home. I want to give name some of them; Painter (artist) Bedri Rahmi EYÜBOĞLU, my dear teacher Jale YILMABAŞAR, my friend Birgül BAŞARIR, Ceramic artist and my best friend Hamiye ÇOLAKOĞLU. Hamiye always says here is my World and I share it with you and you already inside of my World. Also she made lots of artwork with supported by This factory for 45 years.

Still lots of ceramic artists, especially young artists get supported by this factory. Still the chairman of Kale group Zeynep Bodur OKYAY supports to artworks and artists. That's why we are still so thankful to Kale Group and Miss Zeynep Bodur OKYAY.

He was gifting many artworks to vip and special guests in every year. Also he was taking some artworks to gifting when he was going to abroad. And I was making these artworks for him. He always was caring to artist and artworks as I told you. And it makes us feel better and motivated us.

Today we are here for thanks and showing your respect to him for everything he's done for us. And again I want to say to him thanks for everything you done for development of industry.

IN MEMORY OF SADİ DİREN

Süleyman Belen

Mimar Sinan Fine Arts University, Faculty of Fine Arts, Department of Ceramics

Sadi Diren 1927 yılında İstanbul'da doğdu, 1949 yılında da Güzel Sanatlar Akademisi'ne girdi. Akademiden önce iki yıl kadar Hukuk Fakültesine devam etmiş ve hoşlanmadığı için bırakmış, askere gitmiş ve akademiye girmiştir. Önce iç mimarlık bölümü en sonundadır seramik bölümüne gelerek bu alanda eğitim almaya başlamış Or. Geldiğinde tek öğrencidir, bozuk bir Prın, çalışmayan bir çömlekçi tornası ile başlayan mesleği yıllar sonra onu bugün tanıdığımız Sadi Diren olarak konuşmamıza vesile olmuştur.

Ben öğrencisi, asistanı ve en son halefi olarak sizlere kendi gözümden ve zihnimdeki Sadi Diren olarak size aktarmak istiyorum. Bundan sonra doğa olarak kendisinden Sadi Hoca olarak bahsedeceğim.

Kendisi 88 yılı geride bırakmış olan Seramik Bölümünün en önemli kişidir. Özellikle 1977 yılında Bölüm Başkanı olmasıyla, Sanayii ile olan yakın ilişkisi, tecrübesi ve sevgisi ile bölümü gerçek anlamda gel iştirmiş ve gerçek bir eğitim ortamına dönüştürmüştür.

Sadi Hoca arkeoloji ve Anadolu Medeniyetleri çok fazla ilgisini çekerdi bellide bu ilgide yakın arkadaşları Prof. Dr. Ufuk Esin'in büyük etkisi ve katkısı olmuştur. Yapı Oğısı sanat çalışmalarını büyük ölçüde arkeoloji referansları taşıymaktaydı.

Sadi Hoca sanat ifadesinde kullandığı malzemenin dilini en iyi anlamış ve kullanan bir sanatçıydı. Ya pıtlarında yara lığı formlar, ancak seramikten yapılırsa anlam kazanabilecek forumlardı. Bu gün Beni de en çok rahatsız eden hususlardan biri sanat ifadesinin, seramik malzemesini kullanarak farklı bir d ille ifade edilmesidir. Hoca da bu durumdan çok rahatsız olduğunu ifade ederdi.

Sonuç olarak ya şan Omin 40 yılını aşkın bir süresini birlikte geçirdiğim hocamı saygı ve sevgi ile anarak, konuşmamı bitirmek istiyorum. Huzur içinde Yatsın

BLACK POTTERY FIRING SINCE PREHISTORIC TIMES TO THE PRESENT

Sevim Çizer

9 Eylül University, Faculty of Fine Arts, Department of Ceramics, İzmir

This is one of the most common production way of traditional pottery, where the pots are turned black color by stopping combustion at the end of firing period. This could be in different ways, for example, by smothering the fire with fine dunk, damp grass or branches of trees, sticks of pine trees etc. and then covering all of apertures of kiln.

Sometimes the pots are taken out of the fire and plunged into grass, sawdust, dunk or straw... There are two main black firing methods:

Bonfire in 500°- 600°C carbonization – filling into the pores of the clay body.

Reduction after firing above 800°C and modification of red iron oxide to black iron oxide.

This firing method is still using by the potters in many countries over the world...

ARTISTIC APPROACH WITH ZISHA CLAY IN YIXING

Wu Ming

Art Vocational and Technical College of Wuxi, Yixing / China

Wu Ming has been engaged in the creation of Zisha clay for more than 40 years, and the poetry and painting as well, setting design, manufacture and carvings in one. He is the earliest person in researching the creation of modern Zisha clay. There are hundreds of articles published and dozens of papers, and more than 20 provincial and national professional awards. His works have been selected into the international ceramics art exhibition of Mino Japan and got the special awards of judges. Many times he has been invited to go abroad to do exhibitions, lectures, and publishing personal monographs. His works are collected by many galleries and museums. His creation inherits tradition, deduces the modern and pays attention to the future, which forms his own style. He has a positive influence on the creation of modern Zisha, and be praised as establishing a precedent and new style in modern ceramics art.

Yixing, the capital of pottery in China, has a history of more than seven thousand years of making pottery. Yixing Zisha was flourishing in the Ming Dynasty. Zisha clay has strong plasticity, it adopts mud insert and flapping molding, the process is unique, the product is rich in shape, and the pot is the main type.

CULTURAL INTERACTION BETWEEN EAST-WEST AND ITS REFLECTIONS ON CERAMICS

Fatma Batukan Belge
Fatih Sultan Mehmet Vakıf University, İstanbul & Turkish Ceramic Society

ABSTRACT

Ceramic holds a very important place in the history of humanity and culture. The process of spreading Homo sapiens to the world began in the Neolithic Age. During "aceramic" period of this age food production is known but terracotta pots have not yet been built. Ethnological researches suggest that there is a connection between the sedentary society and ceramics. Ceramic products shed light on the past as cultural indicators that reflect every era. The first documents of humanity are written on ceramic.

In the past thousands of years people have been affected by each other's cultures. Ceramics was an object bought and sold in commercial events that provided this interaction. It is therefore an indication of the cultural stages of mankind. The cultural interaction between East and West could have turned into a Eurocentric style as Europe began to colonize much of the world.

However, European civilization has been enriched by the contributions and influences of the cultures that preceded it. Today, war and conflicts, reactionary ideologies, and an outdated geography of Eastern geography, had the most developed cultures that influenced Europe. "All cultures have their own achievements, their own art and music, philosophy and sciences, literature and lifestyles, and other contributions to the advancement of humanity. There is no doubt that their knowledge will benefit us and enrich our lives" says Bernard Lewis.

KEYWORDS: Civilisation, culture, cultural interaction, ceramic, trade.

Ceramic holds a very important place in the history of humanity and culture. The process of spreading Homo sapiens to the world began in the Neolithic Age. During "aceramic" period of this age food production is known but terracotta pots have not yet been built. Ethnological researches suggest that there is a connection between the sedentary society and ceramics.

Pottery found in Çatalhöyük, Hacılar, Göbeklitepe settlements in the territory of our country is one of the examples of this relation. The ceramic products, whose production began in the Neolithic period, shed light on the past as cultural indicators reflecting each period. The clay tablets written by the Sumerians 5000 years ago, the hieroglyphics of the ancient Egyptians, the Mayans, the Mexicans, and the writings of the Central Americans have enabled us to have knowledge of the already abandoned civilizations.

The first documents of humanity were written on ceramics. So much so that scientists have developed a project shortly before the ceramics could survive for thousands of years. The "Memory of Mankind"

project aims to protect the humanity's most important documents from the catastrophes by embedding them in ceramic tablets and burying them in the salt. Another project called "Human Document Project" which aims to transfer the knowledge of humanity to a million years later, started to work together with the Memory of Mankind". Since there is little chance of future generations finding tablets hidden in a cavity, some small tokens showing the location of the tablets will be prepared and distributed to the strategic points of the world.

I would like to briefly present some examples of how cultural interactions are reflected in a phenomenon that is of great importance for human history. In the meantime, I would like to emphasize the past accumulation of the East, which is positioned against the Western-European systems, which are regarded as the symbol of civilization. But first I should briefly touch on the concept of cultural interaction.

Crosscultural Interaction

In the simplest sense, interaction is the mutually influence one another of people, objects or events. It is a process, a resource can change its message based on the response from the receiver and mutually construct a new message. When explaining the concept of crosscultural interaction, the relations between cultures should be considered.

"From the most primitive to the most advanced, the social / cultural system does not exist in a single individual. There is a cultural environment, far and close neighbors. There are frequent and strict cultural relations with the environment of the system. There are diffusion waves spreading environmentally as well as diffuse waves reaching near and far away from the system. The cultural system is an open system that is in contact with the far-near societies around it."

Prof. Bozkurt Güvenç

In cultural interaction, the source of the message is culture, and communication between different cultures creates this interaction. For thousands of years, people have been influenced by each other's cultures. This interaction turned into a Eurocentric form when Europe began to colonize much of the world. World was under political, economic and cultural dominance of Europe. Today, we can say that Western-European systems affect the world.

Multiversum (Multi-universe)

In this context, it is useful to remember the multiversum, the multi-universe concept, which Ernst Bloch first introduced in 1956. Heinz Kimmerle borrowed this concept from Ernst Bloch in his article: *"We place the concept of a multi-universe (Multiversum) of cultures, which are emphasized by the political, economic and religious structures of cultures, as opposed to the Western- European universe. It is remarkable that this statement is not only a geographical but also a temporal dimension*

in Bloch."

In the multi-universe of cultures, one culture can take something as long as there is consensus. Culture has the property of change and this change takes place through harmony. Cultures; they are similar to their neighbors through spreading, borrowing, emulation. Especially, in the light of commercial, economic and political relations, we can define the mutual cultural effect on societies as crosscultural interaction.

Today, globalization dissolves borders between countries and cultures. But on the other hand, the world's dominant powers create cultures that are moving away from each other in the name of civilizations in conflict.

Crosscultural interaction can be transformed into a Eurocentric form when Europe's large central colonization begins. But let us not forget that European civilization is enriched by the contributions and influences of the cultures that preceded it.

"European civilization is not unique to Europe. Like all other cultures known in history, it has been enriched by the contributions and influences of the cultures that preceded it, especially those that emerged in Egypt and the Fertile Crescent countries." (Cultures in Conflict: Christians, Muslims, and Jews in the Age of Discovery)

Bernard Lewis

West Europe; through the Phoenicians, Greeks and Romans, always had the cultural mark of the Orient. The subsequent invasion of Islam also had a huge impact on Europe as a whole. Today, East is synonyms war and conflict, reactionary ideologies, outdated societies. But it once contained the most advanced cultures that influenced Europe. One of the biggest factors that enabled this interaction was **commercial activities**. Ceramic was an object that was bought and sold in every period. Therefore, it is an indication of the cultural phases that human beings have.

According to Karl Marx, *"The history of mankind must always be examined and asked in terms of industry and trade."* Trade is a phenomenon that affects world history as much as war. The major trade routes in the past have made important contributions in shaping world history and spreading cultures by connecting distant countries and peoples. Through trade, societies have enriched, dialogue with different societies and crosscultural interaction has taken place.

In the 7th and 6th centuries BC the Phoenicians; in the 8th and 12th centuries, Islamic societies; in the 15th and 16th centuries, Venetians; in the 17th century, Genoese and Ottomans; In the 18th and 19th centuries the British were ahead in trade. This influenced their arts, scientific studies and technologies; transformed the societies. Trade relations have led to the emergence and spread of new cultures by stimulating intercultural influence.

Based on the importance of the Silk Road over the centuries, China has now taken steps to revitalize it under the name of “One Belt One Road” project. The project, which includes 65 countries, can shape the next 50 years in terms of China's rising role in the world.

CULTURAL INTERACTION EXAMPLES REFLECT ON CERAMICS

Facing and Deal With Unfamiliar Objects

Dr. Philipp W. Stockhammer , an archaeologist from the Institute of Pre-Protohistory at Heidelberg University says that he was seeking an answer to following question with his research titled *Asia and*

Europe in a Global Context :

“Why the people of Eastern Mediterranean (today Israel-Lebanon) did buy Aegean pottery in 1400-1100 B.C. My questions are about adaptation, the way of using pottery, how people integrate them in their practise. We are talking about a transcultural context. The people has been facing and dealing with unfamiliar and strange objects and deciding to accept or not. The following is an example for the creative use of these unfamiliar objects under such transcultural conditions. In Greece water and vine were traditionaly mixed together in large vases, so-called Kraters. These Kraters also arrived in the Levant. After eximining visual images and other archeological finds, I found out that the Kraters at the Southern Levant were not use for mixing water and vine as was the case in Greece but were probably used for drinking beer through straws. This example shows the creative process of adaptation. It demonstrates how people in such contexts deal with unfamiliar objects and how they integrate them as their own.”

“Culture is not a plant that grows from the core, isolated from its environment; it is a continuous learning process driven by curiosity, needs and attention. In particular, it grows through the learning request from the “other”, the “strange” and the “unfamiliar”. The timeframe of the Eastern influence provided such an opportunity for cultural development.”(Near Eastern Effects in Greek Culture)

Walter Burkert

REFLECTIONS...

The effects of different cultures on ceramics are manifested in the fields of **raw materials**, **techniques** and **decor**. Like...

Raw materials:

- Kaolin samples brought from China by travelers provide the production of ceramic and porcelain products in Europe;
- The Chinese called the blue as Muhammad blue because they brought the cobalt from Iran...

Techniques:

- In the 10th-14th century, the Egyptian craftsmen imitated the Chinese porcelain and the gray-green

celadon which were very popular in the Middle Ages in the palaces

- Covering ceramic vessels with a mineral oxide by Sasanis to extend the luster technique to Rome, Western Europe, Africa, China and India.

Decor:

- Blue-white Chinese porcelain influences Ottoman tiles;
- Chinese imitation patterns in European porcelain ...

We all know that in the history of ancient Greece the **Orientalizing period** is the cultural and art historical period informed by the art of Anatolia, Syria, Assyria, Phoenicia and Egypt. It started during the later part of the 8th century BCE. It encompasses a new, Orientalizing style, spurred by a period of increased cultural interchange in the Aegean world. The period is characterized by a shift from the prevailing Geometric style with different sensibilities, which were inspired by the East.

One example is the Assyrian winged genie which took the form of winged beasts such as the Griffin and the Chimera in Greek art.

The story begins in seventh-century China, during the Tang dynasty (618–907), when *sancai* (three color) funerary wares were popular productions. Making their way across the Silk Road, these amber, brown, and green lead-glazed wares served as inspiration in Iran. The artist of the Nishapur bowl has included an innovative *sgraffito* (incised) pattern into the body of the clay using both geometric and floral forms. From 12–13th-century Byzantium illustrates the further spread of this style, some 500 years and thousands of miles from its origin. Evidently this glaze had a timelessness to it!

At the same time, artisans in China were producing porcelain—the most coveted and most technically advanced ceramic in the world. Porcelain was made with kaolin clay, a substance unique to China in this period, which was found near Jingdezhen, a great ceramic-producing city. When fired at an extremely high temperature, kaolin clay transformed into a very fine, hard, semi-translucent white ceramic that local collectors coveted and remained in high demand as a trade object.

Potters in Basra, Iraq, attempted to emulate the beauty of this pure white color, but without access to the naturally occurring kaolin clay, potters had to improvise and instead chose a white slip (liquefied suspension of clay particles in water) to cover the ceramic body. Some objects from this period, as we saw here, were embellished with a cobalt blue design.

Given the back and forth of shape and style across the Silk Road, it is possible these ninth-century cobalt-and-white Basra ceramics inspired the famous blue-and-white wares made in China during the Yuan dynasty. We cannot know for sure, and scholars have varying opinions, but blue-and-white Chinese porcelain was a very popular collector's item in the Islamic world for shahs and sultans, and

served as inspiration for ceramicists working in Iznik, Turkey, as well as various cities in Iran. On these sites, artists made imitation blue-and-white ware of excellent quality, both for the local market as well as for export to other parts of Asia.

A folio from the Palace Album (Akkoyunlu Sultan Yakup Bey), 15th century

The styles and motifs that became popular in Iran during the Mongol Ilkhanid Period (1206–1353). Potters in Iran imitated Chinese glazes, such as the bright-green celadon.

And Chinese decorative motifs, such as the dragon and mythical phoenix bird started appearing on all kinds of Iranian decorative arts, especially ceramics.

DIFFUSION OF MAIOLICA

The most constant relationship with imported Eastern goods in Italian decorative arts is seen in ceramics. In the second half of the 15th century, Italian pottery developed a worldwide pottery together with the Renaissance. On the other hand, continued to collect ideas and patterns from Islamic art, Chinese porcelain and Iznik tiles.

In the first Italian pottery manual (*Il Libro del Arte Vasaio-1557*), Piccolpasso called these ceramic products as "maiolica." The technique had been reached from Spain in Italy; in the Middle Ages, this name was used because the export routes were usually passed through the island of Maiorca. The Italian city of Faenza was a recognized center for earthenware production. The French called the earthenware produced in Faenza "faïence," later referring to their own earthenware products by the same name.

Far Eastern cultures; it is unthinkable that it does not affect its neighbors as it affects cultures at the other end of the world. We can also talk about a technology transfer between China, Korea and Japan.

IMARI FROM JAPAN TO HOLLAND

Imari is a style of porcelain named after the Japanese port from which it was shipped to the West, beginning in the late 17th century. Originally made in the town now known as Arita, which became a center for porcelain thanks to its proximity to kaolin-rich Izumiyama. Imari ware took its design cues from colorful Japanese textiles of the day.

KAKIEMON STYLE (1680-1725)

Kakiemon wares had simple, asymmetrical designs exposing a fine milk-white body. A brilliant palette of cerulean blue, soft-coral red, green, yellow and black enamels was applied onto the glazed surface and fired again at a lower temperature. Several independent enamelling studios were active in

Arita, one was owned by the Kakiemon family from whom the whole category of ware takes its name.

WILLIAM DE MORGAN (1839 –1917) AND IZNIK

De Morgan's work is heavily inspired by the brilliant colours of Islamic pottery, especially the bright turquoise he had first admired on Iznik work of the 16th century which he had studied at the recently opened South Kensington Museum, which is today known as the Victoria and Albert Museum.

HERITAGE / CONTEMPORARY CERAMIC ART

Beril Anılanmert

Işık University, Faculty of Fine Art, Department of Industrial Design, İstanbul

In recent years, the cultural transformation and cultural diffusion within society made me to reevaluate how today's ceramic art is conceived by public.

The question was that "is the rich ceramic heritage create an understanding or is a hindrance to the communication with the contemporary works."

The parameters of traditional values and practices are stated to reveal the underlying aesthetic taste of the viewer. The form and composition methods are bound to strict rules and creativity is expressed through technical perfection and various range of fine decoration which takes the place of content of the work.

The interaction to the ceramic art of today - experimental, without aesthetic concern, rebellious to set rules, critical approach to social and political issues – is analyzed on the light of this heritage on content and on creativity.

COLOUR IN GLASS ART

Mustafa Ağatekin
Anadolu University, Faculty of Fine Arts, Department of Glass

This research traces the possibilities of plastic expression regarding to the color of the glass, while ranking the artists who use it by examining the relationship between color and expression in glass. By assigning the meaning to the color perception take place in the scope of the worldwide artists who uses glass in their works.

In the first part, the possibilities of color in glass are mentioned in technical terms, and technical details are mentioned by giving examples of how artists use glass. The studies related to color hereby the transparent structure of the glass are mentioned and the trace of the combination of light and color is traced. Examples are given through the works of the artists who use these features as a bearer. Artists who use color as a bearer on their compositions, and artists who use color monochrome are also mentioned briefly.

Keywords: Glass, color, contemporary art, glass art.

"MULTIPLE MODERNISMS": A PERSPECTIVE ON CONTEMPORARY ASIAN GLOBALISM

Ray Chen

People say that the Chinese are especially intelligent, I disagree. The Chinese success is not primarily the result of intelligence but rather the result of diligence, self-discipline and regulation with hard work. This lifelong process of applying effective and positive pressure from an early age is what the Chinese refer to as the driving force. Its influences and conditioning is not only affected by particular social, cultural, historical, and family circumstances but also establishes cultural beliefs and values, which in turn, affects those life experiences that shape cultural expectations.

The subject of this talk reflects the critical thinking process, development, and artistic evolution that have opened a vast array of possibilities and challenges worldwide as they break through cultural barriers and confirm their evolutionary path to a more vibrant contemporary ceramic arts expression in the Twenty-First Century. In recent years we have seen a paradigm shift in the way we think about modernity and aesthetic modernism as witnessed in the creation of multiple expressions around the world. The globalization of Asian ceramic art rests upon its discovery of new contexts within the scope of modernism. Globalization remains the most critical channel through which ideological possibilities may adapt and emerge.

Globalization has become a philosophical issue because of its active role and interest in cultural adaptations, integrations and transformations that trigger, in various ways, the development of mass culture changes and a re-structuring of ancient culture templates. The transformation of Asian cultures has drawn much attention, especially since China, joined by other southeastern Asian countries, began opening its doors to the world. More and more people have had a chance to visit, experience and witness the tremendous growth and progress first hand. It did not happen in one day, it took a long time.

Since 1949, China has made great strides upwards, except during some rough times. The Silk Route, the Great Wall, the Terracotta Warriors, The Forbidden City-The Palace Complex in central Beijing, the Temple of Heaven, the Summer Palace, and Tiananmen Square were not created yesterday or "now." Also the invention of paper, the printing press, gunpowder, the compass, and acupuncture; and the list goes on; Taoism, Buddhism and Confucianism (a blend of three teachings) did not evolve overnight.

The development of Asian globalization has powerful ideological underpinnings which still dominate and continue to bewilder our understanding of the processes and forces. New technologies not only facilitate the growth of international interconnectedness but also cross-border exchanges, as well as, trans-cultural phenomena and help foster cultural transactions.

The globalization of cultures in Asia forges multi-layered experiences and stimulates an emerging aesthetic and cultural consciousness. It holds different views which contribute towards new learning experiments, specifically involving Western learning and adaptation to Western cultures. Some positive Western values have been absorbed by Asians in this process. Asia is re-structuring its position on learning with a new mentality, which fosters growth and promotes cultural exchanges.

A few years ago at the NCECA (National Council on Education for the Ceramic Arts) conference, I was talking with Ann Currier, professor of ceramics at Alfred University, New York, The United States, who retired last year. She asked me: "Ray, do you know the term "post studio"? I answered that it may possibly apply to a cross cultural studio experience in the form of a residency. I also returned the question to her: "What is the meaning of 'post studio' from your understanding?" She explained that "post studio" specifically refers to artists in our field who travel to China to work and collaborate with skilled Chinese ceramic laborers in ceramic factories and studios, most commonly in the porcelain capital-Jingdezhen. It is an extension of a work creative and production studio because the work processes and possibilities with the final results can be reached at different levels of

completion in time and technique, as well as, at a saving of labor and expense compared to Western home based studios. When the work is completed, artists ship their artwork back to their own home studio. Since artists produce their artworks from a different location than their personal studio, it is called “post studio.”

Today, we also ask, what impact, or influence, has Western culture or Western ceramic artists brought into China and Asia through this “post studio” experience and cultural exchange process, and 2), how the new oriental culture, specifically in terms of contemporary ceramics perception, has been integrated and/or adapted from this experience?

The ‘post studio’ influence has refashioned the relationships between process and vision, and diverted some attention toward aesthetics and concept, as well as, impacted the way Asian clay artists think and work, and apply language as expression to the material. There is a recognition that when breaking with tradition in technique, process and subject matter, there is a new consciousness brought to light by experimentation and/or changes in the way of traditional ceramics making and processing. And, the influence continues to reach beyond physicality and intellectualism. The new concept helps create a new vocabulary for the Asian’s large artistic ceramic-making population, gives a new meaning to ‘ceramic’ and its old traditions, and offers insight into contemporary, revolutionary, and various culturally and progressive related stages of modern and post-modern perspectives. Furthermore, it inspires and stimulates generations of ceramic artists, even those who may still have traditional Eastern artistic motifs in their work, preserving Asian belief, tradition and value, to express their commentary on contemporary artistic movements. It also challenges young and up-coming artists who have pushed themselves new ways to honor their traditions of the past and, who at the same time, want to explore a more personal and unexpected artistic expression, to freely engage their creativity into exaggerated perspectives and expressive distortions in clay to achieve great artistic effects as a personal language. This ‘post studio’ experience, overall, represents a significant and new Oriental vision, away from its conventional norms.

Traditionally, oriental ceramic art involves a more mental notion of form; one that is leaning more toward an internal rather than external perception. It is not loud. It is not fast. It is not linear in its approach to composition and thought. It does not place a high value on originality and invention. It is against self-consciousness. It is highly theoretical, but then, theory in Eastern training implies getting beyond theory and learning to listen. Its purpose is not to analyze from the outside, but to understand from within.

Today, the creative process and artistic expression must reach beyond the boundaries of human development, time, culture, and history to expand and impact the changing dynamics of the visible and invisible natural forces that allow the questioning and redefining of new possibilities. Twenty-First Century modernism and post-modernism is characterized by pluralism. The critical thinking of artists around the world vary greatly; especially that of Asian artists who have been carrying oriental customs and traditions within their work, and who have profoundly influenced and disseminated their native philosophy, virtue, etiquette and traditions toward a better quality of artistic expression and research, distinguished by value and process. The process in itself embodies historical and cultural merits. It is a testimony of cultural continuity, change, possibility, and potential that elevates motivation and vision.

Innovation and creativity travel the same path. Expanding cultural relations between East and West, in tandem with increasing global communications, will ensure that Contemporary Asian ceramic today galvanizes its position at the intersection of progress and evolution. Artistic shifts ingrained in past traditions will give way to a more global perspective and vibrate new and fresh energy.

Asian modernism has been a cultural language of openness, forwardness, and focused energy toward connecting with the ever changing modern Western world. Recurrent themes of “nature” and “symmetry”, expressed through “balance” and “stability,” adorn the power of life and the Asian tradition. To that end, the Asian post-modernist approach continues to explore, derive inspiration and

engage in a new cultural connection infused with globalized sensibility and understanding.

Asian tradition rests upon the premise that to be capable is to open the restless mind to many wonders. We discuss and challenge our limitations and objectives; we examine our place in time, consider aesthetics viewpoints, and push existing limits to the next stage, we unfold a multitude of opportunities to reach the broadest and most positive definition of visual expression and quality. We overturn, modify and question our way of seeing and comprehending the contexts of visible and invisible connections that symbolize visual languages. We also expose the symbolic, philosophical vision and aesthetic force of our images as we push the artistic tradition far into the future with possibilities and potential. Questioning is the only constant for learning to wonder about life, as well as, to wonder about art.

Contemporary Asian globalism has the boundless power to cross time, connect history and challenge the intellectual process. Reflective of this changing dynamic, contemporary and post-modern ceramics continues to explore its role and to challenge perceived constraints of the media. Its receptivity to the unexpected and its response to the world aesthetically and intellectually attest to the existence and influence of Asian globalism.

Twenty-First Century Asian globalist thinking in ceramics can broadly exist and be cultivated through initiative, critical thinking and efforts that challenge our intellectual and creative processes. Post-Modernism reflects a time of great progress, and “progress” is an important metaphor for change. Change is seen not as a linear progression, but as a series of networks and flows, connections and reconnections that, because they are always forming and reforming, never have time to solidify.

In conclusion, Asian modernism’s favorable reception into the world today is the result of global interaction and globalization. One of the most noteworthy consequences is the extraordinary increase in number and variety of activities at the regional and international levels; it has generated. Emerging artistic initiatives are creating positive dynamics and have taken onboard an international approach. From Asian tradition to modern times, ceramics and its expression of context, permeated with critical thinking, initiative, cultural significance, and emerging technological innovations, fulfill an important role throughout the world. It entices us to explore ceramic arts in a new context, instinctively motivated by its inviting and responsive sensory qualities. Today, Asian modernism and its globalization not only impact diverse areas of ceramic production but also provide a new base for rethinking and modifying the way we imagine, understand, and are more creative as an artist. As we become more involved with the world and others, and connect our response-ability to our responsibility with both the Arts and the world community; we begin to open ourselves to other imaginative endeavors and commitments, and discover how to keep up with the artistic energy.

Metamorphosis is the beginning of a rebirth that allows us to move fluidly across, above and beyond, and in between Traditions and Modernisms. It gives us a new understanding about contemporary, post-modernism, and what is “current,” and challenges our boundaries, creative expressions and processes, and connections within the rich history of ceramics and artistic movements. It gives rise to a new vitality within the broader body of ceramic art and time, paramount as the future begins.

ESKİŞEHİR INTERNATIONAL TERRA COTTA SYMPOSIUM EXEMPLAR: CITY, PUBLIC SPACE AND CERAMIC SCULPTURES

Mutlu Başkaya

Hacettepe University, Faculty of Fine Arts, Department of Ceramics

Abstract

Eskişehir International Terra Cotta Symposium is an exemplar event which creates added value particularly for Eskişehir. This symposium is important in regard to exhibiting the transformative influence of local governance on the city culture and vitalization of the identity based on soil (clay) culture specific to Eskişehir. Besides, the fact that the ceramics industry is developed in the region also contributes to the symposium. In order to organize an event, four important qualities must be found in the organizers: capital, vision, knowledge and experience. Lack of one of them negatively influences the sustainability of the event. It is a precursor in Turkey as an event which comprises these qualities and it brings art to wider masses by making the public spaces gain terra cotta sculptures. The perception of art of the people who see ceramic sculptures in their streets develops. By means of the symposium, it is provided that students, local residents and industrialists get together and be in contact with one another, and the city's level of development increases. In addition to the fact that artists from different countries get to know the city and promote it in their countries, it is also ensured that local people meet different cultures and interact with them. In this context, the article entitled “*Eskişehir International Terracotta Symposium Exemplar: City, Public Space and Ceramic Sculptures*” is approached in the 12th year of the symposium to contribute to making the importance and the value of the subject understood, specifically with respect to the modern ceramic sculptures placed in the public space. The definition and the meaning of public space and the values which make a city exist are discussed and it is aimed to introduce the Symposium by providing information about it and by this means to spread the cooperation among industry, art and science also in different cities and to make a note of the event.

Keywords: Symposium, Sculpture, Local Governance, Art, Ceramics, Municipality, Eskişehir.

City, Public Space and Sculptures

Cities are settlement areas where society's needs such as settling, housing, moving, working, leisure and entertainment are fulfilled. A collective, cultural, artistic, political and social life is necessary in order for the cities to exist. These spheres are called public spaces in the present time. In this respect, public spaces are considered as centres which give the city an identity, create an opportunity of sharing, and enable the individuals with common interests to interact in every respect.

With the book of Habermas entitled *Structural Transformation of the Public Sphere: An Inquiry into the category of Bourgeois Society* published in 1962, the concept of the public sphere and the values it represents started to be discussed. The book was translated into English in 1989 and to Turkish in 1997. These years are significant as they were the years when the concept of public sphere came to the agenda in the West and in Turkey. Habermas, who states “Public sphere is a term used to describe the common activity ground serving the purpose of producing and developing ideas, expressions and actions to determine and realize public interest in modern society doctrine” defines a sphere free from every kind of interest, independent from the pressure of the state authority and commands, and hegemony of the capital. Even though the definition of the concept is still problematic in Turkey, it is accepted in the meaning Habermas defines.

It is known that until the 20th century, private and public spheres were not differentiated and there was not a public sphere tradition. It is a significant development for art and the city that today the transformative and guiding role of art have started to be taken into consideration, even though not fully. By this means, it enables art to reach a socially and culturally diverse audience while urban identity, culture and shared memory are being created and by creating a certain impact an aesthetically

intellectual conscious and quality of life is generated in the perception of the urbanite who establishes a relationship with art. In the public sphere which generates transformative impacts on the ways of behaviour and thinking, relationships and actions of the urbanite the representation of art mostly takes place through the art of sculpture. The reason of this is that the durability of the material used and the possibilities of sizing in the art of sculpture is technically appropriate for open spaces in the public sphere. The technical possibilities of sculpture and its artistic language which leaves emotional, intellectual and ideological traces, creates identity and becomes symbolic by forming a common memory integrates with the public sphere.

Urban culture which is an extension of the modernization process which started with the proclamation of the Turkish Republic and its product, public space and the concept of public space sculpture certainly do not have a rooted history or tradition. Even though in the first years, sculpture examples other than Atatürk sculptures were not seen, the togetherness of public sphere and sculpture was achieved thanks to the republican achievements.

“New city centres and squares which became an indication of Republican ideology, 'modernity, secularism, nation-state understanding' were furnished with monument applications and thus these sculptures as one of the features which 'distinguish Republican cities from Ottoman cities' became important symbols in strengthening the functions of the new public spaces (Yaman, 2011: 52)” (Kedik, 2011)



Today, even though a progress is seen on the subjects such as public sphere and aesthetic values, when compared with the developed countries, it is known that the progress is not at the expected level. This is the case particularly for sculpture and regarding the subject of “ceramic sculpture”, no example of a ceramic sculpture is seen in the public sphere in Turkey. With failing to associate ceramic material with sculpture and with the ideas that it is indurable or cannot be applied in large-scale, the possibility of encountering terra cotta sculptures in the public sphere was even slighter.

Image 1: Joan Miro, Woman and Bird / 1983 / 22 m × 3 m

City, Urban Space and Ceramic Sculpture

Terra cotta (ceramics) which is known in Turkey and specifically in Eskişehir as a roof or wall coating element is a familiar material, traditional product. It is roof tile, brick, bowl but it is ignored that it can also be sculpture. Even for being an answer to the frequently encountered question “city, urban space and ceramic sculpture?” Eskişehir International Terra Cotta Symposium is the only example in its field and takes over an important mission. With their use of unfamiliar Modern terracotta sculptures placed in the public spaces of Eskişehir through the symposiums held until today have enabled the viewer to break down her/his structures of thought, re- explore her/his perception and environment and to observe and the viewer has discovered a completely different field of use of a familiar material. Symposiums have also played a role in improving the level of social development of Eskişehir.



Image 2: Christine Lübge
Photo: Özgür Çamurlu



Image 3: Semih Kaplan
Photo: Özgür Çamurlu



Image 4: Hanefi Yeter
Photo: İbrahim Demirel



Image 5: Özgür Saraçoğlu Kaptan
Photo: Mutlu Başkaya

Eskişehir International Terra Cotta Symposium basically creates three different added values. It contributes both to the visibility of the transformative influence of correct and good cooperation between local governance and the artist on the urban culture and to the revival of the identity based on the undefined earth (clay) culture specific to Eskişehir and to the development of the industry of the city. Besides, by bringing in modern terra cotta sculptures to public spaces for the first time in Turkey, it introduces art to wide masses. By means of the symposium, it is provided that students, local residents and industrialists get together and be in contact with one another, and the city's level of development improves. In addition to the fact that artists from different countries get to know the city and promote it in their countries, it is also ensured that local people meet different cultures and interact with them.



Image 6: Rodney Harris, 2012
Photo: Özgür Çamurlu



Image 7: Charles Pilkey
Photo: İbrahim Demirel

Indicating the importance of this symposium in terms of art and environment interaction, the symposium consultant Prof. Bilgehan Uzuner states “the symposium has been enlarged and improved by the regulation committee formed in 1999 under the leadership of Mayor of Tepebaşı and their primary aim is to emphasize the city’s undefined character of earth, bringing together the knowledge in this context and providing the ground for new expansions”. In the organization and smooth administration of the symposiums, besides the leadership of Bilgehan Uzuner, there is a serious team work such as the funding and labour power support that Eskişehir Tepebaşı Municipality provides and the parks and gardens which it opens to the permanent placement of the artworks produced in the activity, the support of the Ministry of Culture and Tourism, the support of Anadolu University and sponsorships of many private institutions, participation of valuable artists and students” (Yıldırım 2014).

Eskişehir International Terra Cotta Symposium

The earth on which Eskişehir is found is an area of rich clay beds. Kurt Tile and Brick Factory founded in 1927 by Sait and Muhtar Başkurt as well as Arslan Tile Factory built by Bulgarian Çirkof Brothers has been the first tile production enterprises. For enabling the boom and development of the tile-brick industry which makes a great contribution to the economy of the city Eskişehir Tepebaşı Municipality provides support. These enterprises have taken an active role in development of Terra Cotta Symposium as much as in making Eskişehir gain momentum in economic and cultural respects. This symposium has long been held in the location of the currently unused old tile factory named Çift Kurt, built in 1933 by Kurt Sait. The old tunnel kiln and the garden that houses the kiln was accepted as the symposium area. During the symposium, this wide area which was bringing industrialists, artists and students together was almost being turned into a cultural centre. At this wide garden a space which solo exhibitions of artists invited from different countries or cities were opened, group exhibitions which bring different artists together on a common theme were organized. Seminars and workshops in which the invited artists convey their knowledge and share their experiences were held in this area. In the workshops held in 2010, opportunities of sharing were created in alternate firings such as Mürşit Cemal Özcan's raku firing, Mutlu Başkaya's paper kiln firing, Hasan Başkırkan's Sagar firing, Emre Feyzoğlu's coal firing and in various subjects, experiences were shared and applications were made. After the old kiln which was in this space, the roof of which was destructed because of heavy snow in 2014, ETİ Factory started to be used as the new symposium space. The same social and cultural environment was established here this time and the symposium has been held here since the year 2015. During all these activities, the invited artists shape their sculptures in the workshop located at this building and finish the firing process in the kilns located in the same garden.



Image 8: Ulla Vioti
Photo: Özgür Çamurlu



Image 9: Hristo Yankov
Photo: Özgür Çamurlu



Image 10: Oya Turay Uzuner
Photo: Özgür Çamurlu

Different artists from different parts of the world and our country participate in the symposiums and produce original sculptures in this area which is turned into a cultural center for a period of 15 days. Students from ceramics and glass departments and fine arts Faculties of Anadolu University and different universities. By this means, both an opportunity of working together with global artists and benefiting from their experiences is given to the students who are the academics and artists of the future and they are enabled to take this environment of social production and sharing as an example (Yıldırım, 2014).



Res 11: Vilma Villaverde
Photo: Özgür Çamurlu



Res 12: Thatree Muangekaew
Photo: Özgür Çamurlu

Each year many artists from Turkey and the world are invited to the symposium and they are enabled to produce original terra cotta sculptures for the public spaces of Eskişehir. Though the invited artists are dominantly from the field of ceramics, artists from every field of plastic arts are given a place for sure. Thus, it provides that artists from different disciplines gain experience by using a material outside their own materials and gain new experiences in the name of art and have opportunities of sharing with one another. Eskişehir International Terra Cotta Symposium Catalog is designed by İbrahim Demirel and printed by Tepebaşı Municipality. In this catalog, the formation process of the artworks and the pictures of all the works in the area are documented and an important archive is generated, thus a record is made for history. The artworks at the Tepebaşı Municipality Building in Eskişehir are in a number and level enough to form an “Eskişehir Contemporary Ceramics Museum”. I hope that dear **Ahmet Ataç** will exhibit this collection one day at a space called “**Eskişehir Contemporary Ceramics Museum**”. Moreover, especially the Tepebaşı region of Eskişehir is like an open-air museum where one can find ceramic sculptures on its roads.

The 12th of the Eskişehir International Terra Cotta Symposium was held on 1 September-16 September 2018 and the number of the artworks in public spaces reached 170. Up to now, 125 artists produced works for this city in the symposium.



Image 13: Gunter Praschak
Photo: Özgür Çamurlu



Image 14: Kim Yong Moon, Totemler
Photo: Kim Yong Moon

Participating as an invited artist to the terra cotta symposium held in 2010 and making my work entitled “hope” a part of the public space made me gain an important experience as a young artist that time. It is very important for art and the urbanites that such an opportunity is given to the artists and artists share their ideas with people through the works that they bring in to the public spaces.



Image 15: Mutlu Baskaya “detail of work: hope” 2010
Photo: Fatma Kadı



Image 16: Mutlu Baskaya “hope” 2010

Photo: Özgür Çamurlu

I hope that the people who make efforts to hold Eskişehir Terra Cotta Symposium will continue to bring artists together in the connective power of art to shape clay, place sculptures in the public spaces of the city, sculpture parks of the city will be enlarged, the relationship among urbanites, artists, industrialists, universities and local governance will continue resolutely and be an example for other cities.



Image 17: Kamuran Ak, 2017
Photo: Mutlu Başkaya

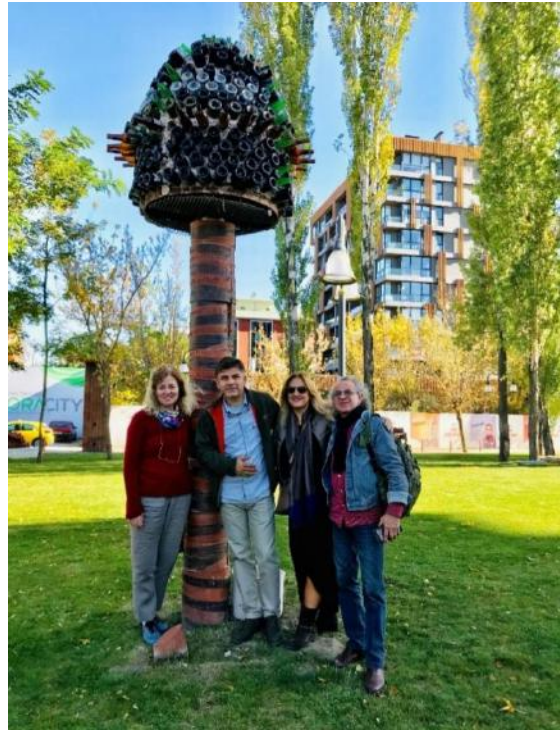


Image 18: Bilgehan Uzuner, “şişe fırından heykel” 2014
Photo: Mutlu Başkaya



Image19: Tuk Sukumural
Photo: Mutlu Başkaya



Image 20: Kaan Canduran
Photo: Mutlu Başkaya



Image 21: Veysel Özel, 2013

Photo: Özgür Çamurlu

References

1. Habermas, J. 2003. 'Kamusallığın Yapısal Dönüşümü', (çev. Tanıl Bora, Mithat Sancar), İletişim Yayınları, İstanbul,
2. Kedik, A.S. 2011. 'Kamusal Alan Ve Türkiye'de Heykelin Kamuya Açık Alanlarda Var Olma Koşulları', <http://dergipark.gov.tr/download/article-file/192449>, E.T.: 12.8.2018; 17:38
3. Yıldırım B. 2014. 'Park-bahçe seramikleri açısından ayrıcalıklı bir kent olarak Eskişehir ve bu bağlamda Prof. Bilgehan Uzuner ile yapılan söyleşi', <http://www.dieweltdertuerken.org/index.php/ZfWT/article/view/611/611>,

Visual References

1. Woman and Bird (Dona I Ocell), John Miro. https://en.wikipedia.org/wiki/Dona_i_Ocell
2. İbrahim Demirel's Photo Archive.
3. Özgür Çamurlu Photo Archive.
4. Mutlu Başkaya photo Archive.

seres'18

IV. INTERNATIONAL CERAMIC GLASS PORCELAIN
ENAMEL GLAZE AND PIGMENT CONGRESS
October 10-12, 2018, Eskişehir, Turkey

**ARTISTIC
ORAL & POSTER
PRESENTATIONS**

TRADITIONAL PORTUGUESE WALL TILES

Assoc. Prof. Deniz ONUR ERMAN

Ankara Hacı Bayram Veli University, Faculty of Fine Arts,
Department of Painting, Block A, Gölbaşı Campus, Ankara, Turkey

The use of clay in architecture as a building material dates back to the early ages when humans have started to live in settlements. Durability of fired clay and its potential as decorative objects have enabled humankind to apply this material for coating of both indoor and outdoor surfaces in various forms.

Among many towns and periods of production, Azulejos ceramics constitute a worthy example for ceramic tiles which have enriched the city characteristics significantly. Originally an Arabic word, the actual meaning of Azulejos is “polished stone”. The first Azulejos ceramics date back to the 13th century, while the most prominent examples have emerged after the 17th century in Portugal, and especially in Lisbon and Porto. This genre of ceramics has initially been used to decorate churches and monasteries in Portugal. Afterwards, they have become an ornamental element of various buildings, thus transforming the identity of towns. Through historical and cultural influences, these ceramics have evolved in time. Blue, green, yellow and white colors are generously employed to produce these ceramics in diverse decors, while blue-white ones remain the most noticeable. Themes that are elaborated in rich colors, forms and textures include, but are not limited to, geometric forms, landscapes, flowers and leaves, figures, ships, religious motifs and icons. These exceptional ceramic tiles that have been used in both interior and exterior surfaces distinguish Portuguese towns from many others. After the 19th century, these have been subject to a modern interpretation and transformation.

This article aims to cover the characteristics, emergence, historical evolution and, production of traditional Portuguese Azulejos wall tiles. Outstanding examples, especially from Porto and Lisbon, will be explored and will be analyzed in comparison to contemporary instances in other locations.

Key words: Azulejo, Portuguese ceramic tiles, Portuguese ceramic art, Ancient ceramic tiles.

INTRODUCTION

"Azulejo" is a word used in Spain and Portugal to designate a glazed tile: a terracotta tile covered with an opaque glazing. In these two countries, azulejos have been frequently used since the 13th century to cover and decorate walls, fountains, pavements, ceilings, vaults, baths, or fireplaces. These tiles and its use in huge decorative panels can be considered a precious, but fragile cultural heritage from Brazil to India, countries influenced by Portuguese culture. Morphologically, these tiles are composed of a porous clay-based ceramic body, the terracotta, covered by a protective glassy phase, the glaze. As artistic paintings, these murals incorporated various kinds of pigments in the glaze layer to create a pictorial impact on the walls of rich palaces or churches, real and durable monumental works of art. (Pereira M., Lacerda de T. and others, 2009, pg.79) The term 'azulejo' comes from the Arabic word az-zulayj, meaning "polished stone." The Moorishes brought this term to the Iberian Peninsula. (<http://www.golisbon.com/culture/azulejos.html>) Azulejos used to denote a square plaque of ceramic material, one side of which is decorated and glazed. Azulejos of this kind are also employed in other countries, such as Spain, Italy, Holland, Turkey, Iran and Morocco. Due to the fact that they have been used for five centuries without interruption, and the way in which they are used as a determining element in Portuguese architecture, as well as the significance that has been attached to them over the centuries, they are not just seen as decorative art, but also as a basis for the display of new tastes and as a record of the images in the lexicon of their users. (<http://cvc.instituto-camoes.pt/azulejos/eng/azulejo.html>)

Of all European countries, Portugal is the one where the glazed tile, or azulejo, showed the greatest development as well as the most original and functional utilization, particularly in architecture. In no other country as in Portugal did the tiles play such a complex part in transforming the closed character of the architectonic spaces. Surfaces were immaterialized and space geometrically reconstructed by oblique lines, prevailing in the abstract coverings. In the figurative compositions, a similar effect was achieved by enlarging the field of vision of the walls, introducing perspectives and a three-dimensional suggestion of the space. At the same time, the tiles played a moderating and regulating role in architecture with the development of the borders and the use of corrective scales, bringing homogeneity in the compositions through variations of the decorative modules. In Portugal, all these characteristics were reinforced because of the great quantities of tiles and their intensive use, often reaching a monumental scale in a many buildings. The use of the tiles spread from the European Continent to the Atlantic Islands and the overseas territories which were Portuguese colonies in the past, mainly Brazil, lasting from the end of 15th century until nowadays. This intensive use also explains why we can find in Portugal some significant examples of foreign production, particularly from Holland or cities like Antwerp, Seville, Talavera de la Reina and Urbino (Meco.1994, p.5). Another glory of the Portuguese tiles lies in the development of a specific ceramic painting, by adopting, during the last third of the 17th century, the basic cobalt blue paint, with its impressionist impact and almost abstract aesthetic value.

Azulejos have outperformed their decorative function in Portugal to become one of the most expressive art forms of Portuguese culture. Although azulejos do not originate from Portugal, their extensive and continuous use for over five centuries, covering large surface areas on both the inside and outside of buildings, mean they have become representative of developments in Portuguese art for the last 500 years. Azulejos exhibit influences from numerous cultures, from the first Moorish style designs to the European plant and animal themes of the Gothic and Renaissance and inspirations from the fabrics of India and the Orient. However, it is the tile production of the 17th century golden period that sees the true development of azulejos in Portugal, a tradition that was reawakened, in a modern manner, in the urban development of the 1950s. (Mitchell. 2016, p.341)

ARCHAIC TILES

Azulejos date as far back as the 13th century, when the Moorishes invaded the land that now belongs to Spain and Portugal, but they secured their foothold in Portuguese culture between the 16th and 17th centuries. Originally they were fairly simple structures cut into geometric shapes in neutral tones. The earliest architectural application of Portuguese ceramics are the medieval pavements formed by plain tile mosaics, in geometric forms, colored with a mixture of metallic pigments and lead-glaze, especially used in the Cistercian abbeys. The entire apse of the Alcobaça Monastery showed pavements of this type, probably from the 13th century, unfortunately torn off during a bad restoration in the present century. Some specimens were left on the spot; others were framed to form panels giving samples of the various decorative schemata, in the Monastery's Museum. (Meco.1994, p.5)

According to Reynaldo dos Santos; the ascent of azulejos in Portugal start with King Manuel 1st, who was dazzled by the Alhambra in Granada (Spain), and decided to have his palace in Sintra decorated with the same rich ceramic tiles. The early ones were imported from Seville, and in accordance to Islamic law, they portrayed no human figures, only geometric patterns. However, it cannot be excluded that some might also have been manufactured within the Portuguese territory. During the first decade of the 16th century, King Manuel 1st put a number of orders with workshops of Andalucía for his Royal Palace in Sintra. These early azulejos still subsist and make up a unique group of great historical importance (Santos, 1957, p.16). Subsequently glazed tiles started to be used to decorate walls and vaults in churches and monasteries, but also on the palaces of nobility who followed the trend set by their king. No tilework from the time of the Moorish occupation survives in Portugal.

TRADITIONS AND INFLUENCES

Azulejos were introduced to Portugal by Spanish Moorish invaders early in the 15th century, who had in turn adopted the craft from the Persians. The majority of tiles from the early centuries have Moorish designs which have interlocking, curvilinear, lace-like and looping designs, or have geometric or floral motifs. Portugal retained a Moorish taste for completely covering wall and floor surfaces with

decorations in the tradition of *horror vacui* (fear of empty spaces). As stated above, the first examples of azulejos in Portugal appear to have been imported from Seville by King Manuel 1st who used the tiles to decorate the floor and walls of the Arab room at his palace at Sintra in 1503. These tiles consisted of the ‘*cuerda seca*’ mentioned above and a Moorish tradition in the form of panel tile mosaic called azulejos alicatados (Mitchell. 2016, p.341). The patterns on the tiles are those of Spanish Muslims called ‘*Mudejar*’ and consist of simple glazed tiles in one color decorated in geometric patterns. The tiles are similar to those found in the 14th Century Alhambra Palace in Granada. Arab Room in National Palace, Sintra (Image 1) shows the geometric tiles covering having a highly dynamic effect, dating from around 1500. (Meco.1994, p.11)



Image 1: View of the Arab Room, Sintra National Palace, C. 1500. Photograph by: Carlos Monteiro
(<http://cvc.instituto-camoes.pt/azulejos/eng/azulejo.html>)

By the 16th century, Portugal was receiving influences from other European tile makers. The Italians had developed the majolica technique which saw paint directly applied on to the tiles, making it possible to depict a more complex range of designs such as figurative themes and historical stories. These techniques had also spread to Flanders where motifs developed in the Flemish Mannerist style. By mid-century the Italian and Flemish potters moved to Portugal to fulfil the demand for tiles. Gradually Portuguese craftsmen adopted the majolica technique and production was established (Mitchell. 2016, p.342). Some of the earliest and most monumental compositions of this period include *Susanna and the Elders* in the National Museum of Azulejos in Lisbon by Marçal de Matos (1565) (image 2,3), altarpiece of *Lady of Life (Virgin Mary)* (1580) in the Church of Santo Andre Lisbon, built in 16th Century.

The National Tile Museum became an independent and national museum in 1980. It was created to preserve and present the history and culture of decorative tiles spanning five centuries. It has an amazing collection of mostly pieces dating before the 19th century (Meco.1994, p.13). Most of the azulejos illustrate allegorical or mythological and biblical scenes, or hunting scenes, and the

workshops accumulated veritable libraries of engravings that they re-used for the different orders. The Church in particular ordered small individual panels depicting saints, religious emblems and narrative scenes.



Image 2: Altarpiece of our Lady of Life (Virgin Mary) 1580, Church of Santo Andre Lisbon, Portugal.

(<https://www.alamy.com/altarpiece-of-our-lady-of-life-virgin-mary-1580-html>)

Image 3: Detail from the Lady of Life

(http://www.museudoazulejo.gov.pt/Data/ContentImages/pecas_destaque/G_138%20-%20Nossa%20Senhora%20da%20Vida.jpg)

Two different tendencies are found in Portuguese tiles of the 17th century, one maintaining naturalism, the other returning to the stylization of the late 15th century. The tiles of the naturalistic tradition made during this century have a wider range of color, adding green, violet, rose and brown to the basic blue, yellow and white. They include not only the devotional panels already mentioned, but also a new series of arabesque tiles in which ferronnerie patterns are replaced by more freely handled acanthus foliage, sculptural masks and Baroquely conceived putti (Smith. 1968, p.231) (image 4). During the 17th century, a large number of framed tile compositions were produced which interwove the Mannerist drawings such as the life of a saint, with representations of roses and camellias or garlands. The second half of the 17th century saw the introduction of blue and white tiles from the Netherlands. The majority of these were the large tile panels displaying historical scenes. These blue and white tiles quickly became the fashion (<https://www.euromkii.com/content/portugal-azulejo-tiles-history>) (image 5). To the second half of the 17th century belong the earliest storytelling and genre tiles, which led to the great preoccupation with these subjects during the 18th century. They seem to have been inspired by Dutch tiles, which were exported to Portugal and Spain after 1650 and also led to the almost exclusive use of blue and white, which lasted until about 1750. The same restricted color scheme, borrowed from Chinese porcelains, is found in both Dutch and Portuguese faience of the 17th century. (Smith. 1968, p.232)



Image 4: Ancient wall panels from 17th century from Portuguese National Tile Museum.

(<https://humidfruit.wordpress.com/page/9/>)

Image 5: Blue white wall tiles from National Palace of Sintra.

(personal photograph archive)

By the 17th century motifs were inspired by works from the Orient and India. This is particularly seen in azulejos used for altar decoration, which became common up until the 18th century, and which imitated oriental fabrics. Between 1650 and 1680 imported Indian printed textiles that displayed Hindu Symbols, flowers, animals and birds became influential, and an azulejo composition, called "aves e ramagens" (birds and branches), became fashionable (Mitchell. 2016, p.348) (image 6). In 1755, a strong earthquake destroyed a sizeable part of Lisbon claiming many victims. The date of this event is often considered a turning point, mostly because it brought to power an enterprising minister, the Marquis de Pombal, who presided over the reconstruction. The whole city center was designed on modern urban conceptions and the stair walls and kitchens of the new multi-storey buildings were often finished with simple patterned azulejos, limited by a linear frame, the so-called 'Pombalino-style' (<http://repositorio.lnec.pt:8080/bitstream/1.pdf>) (image 7)



Image 6: Medici vase azulejo wall panel from 17th century, Museum of Azulejo Lisbon.

(http://www.azulejos.fr/index_en.html)

Image 7: Pombalino style azulejos in Lisbon.

(<https://theculturetrip.com/europe/portugal/articles/a-brief-history-of-portugals-beautiful-azulejo-tiles/>)

GOLDEN AGE AND THE CYCLE OF MASTERS

The late 17th and early 18th centuries became the 'Golden Age of the Azulejo', the so-called Cycle of the Masters. A great demand for Portuguese azulejos had been created both in Portugal and in her colonies, especially Brazil. Churches, monasteries, palaces and even houses were covered inside and outside with azulejos, many with exuberant Baroque elements.

The most prominent master designers in these early years of the 18th century were: artist Antonio Pereira, Manuel dos Santos, the workshop of Antonio de Oliveira Bernardes and his son Policarpo de Oliveira Bernardes; the Master PMP (only known by his monogram) and his collaborators Theotonio dos Santos and Valentim de Almeida; Bartolomeu Antunes and his pupil Nicolau de Freitas. As their production coincided with the reign of King Joao V (1706-1750), the style of this period is also called the Joanine style. In the 1740s the taste of Portuguese society changed from the monumental narrative panels to smaller and more delicately executed panels in Rococo style and these panels depict gallant and pastoral themes. (<https://www.euromkii.com/content/portugal-azulejo-tiles-history>). They realized some of the most famous compositions of Portuguese tile, brilliantly solving the various problems raised by the figurative panels. They managed to find the ideal scale for the figures which are part of the coverings in order that they would not collide, but rather blend, with the total dimension of the composition and that of the individual tiles (Meco.1994, p.49) (image 8,9).



Image 8: Lisbon church of Mercês. Covering of azulejos work by Antonio de Oliveira Bernardes from 1714.

(<http://mariomarzagaoalfacinha.blogspot.com/search?updated-max=2015-11-22T13:00:00Z&max-results=500&start=3&by-date=false>)

Image 9: Neoclassical Historical panel, from 18th.century by Jose Berardo

(photograph: Carlos Monteiro. Mitchell R. Portuguese art: Portuguese azulejos, 2016, 341.

https://michelangelo.pixel-online.org/files/Manual_of_fine_arts/New%20Manual%2012%20portugal.pdf.)

In the 18th century, the frames become more and more invaded by the Baroque style and the entanglements of festoons, angels, and architectural elements. Then appears the Rococo style, again with complex ornamentation. The decors are often inspired by Watteau and his engravings representing gallant, pastoral, and bucolic scenes, and promenades of aristocratic couples. After this extravagance, the 19th century promotes a return to the virtue and simplicity of the antique world. The style is known as "neoclassical". The frames of the panels are simplified. This style marks especially the return to a rich polychromy. The Neoclassicism which grew up in response to this style in Portuguese architecture, was also evident in Portuguese tile production as a reaction, simpler and more delicate. Neoclassical designs started to appear with more subdued colors (http://www.azulejos.fr/index_en.html). (image10, 11)



Image 10: 18th century, Maritime and country scenes Portuguese painted Baroque tiles, 199cmx440cm.

(Levenson.J.A. The age of the Baroque in Portugal, 1994, 212-213)

Image 11: Polychrome tile panel from the 18th century, in rocaille style, 13cmx9cm.

(<https://doreytiles.pt/wp/?p=9364&lang=en>)

The French invasions (1807-1811) and social changes which characterized the first half of the 19th century meant that development of decorative tiles went through a period of stagnation during this time. The second half of the century found a new use for Portuguese tiles as Brazilian immigrants introduced the Brazilian trend of decorating the façades of their houses with azulejos. These generally comprised of the less expensive type of standard-pattern tile produced in Lisbon. Some factories used new semi industrial techniques such as the transfer print method of production onto blue-and-white or polychrome azulejos. Towards the end of the century, this developed into a different type of transfer printing which used cream ware blanks. Stylistic differences occurred in the production of tiles. In the north tiles were characterized by a taste for volume and prominent relief, displaying contrasts between light and shade, while the tiles of the south remained more traditional in their patterns with smooth and flat patterns (Mitchell. 2016, p.354).

One of the most notable creations of azulejos during this century was the monumental decorations, consisting of 20,000 azulejos, in the vestibule of the São Bento railway station in Porto, created by Jorge Colaço. These depict historical themes in the narrative style of a picture Postcard. The transportation hub located in the heart of Porto does more than shuttle people back and forth. The

French Beaux-Arts structure holds within 20,000 magnificent azulejo tin-glazed ceramic tiles depicting Portugal's past - its royalty, its wars, and its transportation history. The blue and white tiles were placed over a period of 11 years (1905–1916) by artist Jorge Colaço. Built in 1900, the beautiful station was named after a Benedictine monastery that once occupied its space back in the 16th century. Destroyed by fire in 1783, the house of worship was rebuilt but by the 19th century was torn down to make way for the expanding railway system. Built by architect José Marques da Silva, the very first stone was laid by King Carlos I himself. Five years after the station was built, the intricate tile work began. Included in the landscapes and ethnographic displays are the Battle of Valdevez (1140) and the Conquest of Ceuta (1415) along with several other important events and places that created the vibrant city that this unusual and beautiful station resides in. There are approximately 20,000 azulejo tiles, dating from 1905–1916, that were composed by Jorge Colaço, an important painter of azulejo of the time (<https://www.atlasobscura.com/places/sao-bento-station>). (image 12)



Image 12: Blue-white tiles from Sao Bento Railway Station in Porto.
(personal photograph archive)

The characteristic of the early 20th century is the lack of the creative homogeneity of the previous century, and the parallel evolution of opposite tendencies: on one hand, the modern expressions of the Modern Style or Art Nouveau and the Art Deco; on the other hand, the traditionalist trend, maintaining the late revivalist and romantic character (Meco.1994, p.83). Some patterns can be distinguished, like the water lilies, frogs, ornamental friezes with grasshoppers and butterflies, often to be found in bakeries. (Image 13)



Image 13: 19th-20th Century Portuguese Art Nouveau Azulejos.
(<https://www.1stdibs.com/19th-20th-century-portuguese-art-nouveau-azulejos/id>)

MODERN TILES AND CONTEMPORARY DESIGNS

The 1950s and its vast urban development brought about a revival in tile design, but on a modern platform and with modern materials. A new generation of architects commissioned young artists to create tile panels for their new urban projects. Artists began exploring the plasticity of clay as well as other new materials. The new Lisbon underground likewise provided space to be filled with compositions on a monumental scale. The majority of these designs are from Maria Keil. Her abstract designs combined the new modern aesthetic with the Portuguese taste for surfaces covered with all-embracing ceramics. In particular her decorations of the station 'Intendente' is considered a masterpiece of contemporary tile art. The use of decorative ceramic and tile wall coverings still remains relevant in Portuguese art and architecture. Some contemporary artist combines traditional standard-pattern with the new technics. For example Ivan Chermayeff's work in the Oceanarium, combines traditional standard-pattern mass-produced tile with new computer technology to portray large marine animals. Manual techniques can still be found in the work of Luís Camacho who draws symbols onto the glazed surface of tiles and the traditional witty and narrative painted tiles of Bela Silva (Mitchell. 2016, p.360) (image 14,15).



Image 14: Experimental ceramic panel by Julio Pomar, dating from 1984 in Lisbon underground station wall.

(<https://www.tumblr.com/search/lisbon%20underground>)

Image 15: Tile panel by Manuel Cargaleiro in the lobby of the Lisbon metro station.

(<https://www.tumblr.com/search/lisbon%20underground>)

CONCLUSION

Today, the azulejo is one of the major symbols of Portugal. The iconic ceramic tiles can be seen everywhere: on the façades of churches, grand old residences, houses, public benches, fountains, modern apartment buildings, universities, even in many of Lisbon and Porto's Metro stations. Many remarkable azulejos dating back to the second half of the 15th century are also on display in the exhibition of the Museu Nacional do Azulejo (National Tile Museum) in Lisbon. This exquisite piece of cultural heritage and ongoing tradition is certainly worth exploring and is definitely a feast for the curious eye.

REFERENCES

- 1- Levenson.J.A.The age of the Baroque in Portugal, 1994, 212-213.
- 2- Meco H., The art of azulejo in Portugal- Portuguese glazed tiles, 1994, 5-89.
- 3- Mitchell R. Portuguese art: Portuguese azulejos, 2016, 341.
- 4- https://michelangelo.pixel-online.org/files/Manual_of_fine_arts/New%20Manual%2012%20portugal.pdf. Access: 10.09.2018
- 5- Pereira M., Lacerda de T., Aroso M.J.M., Gomes A., Mata L.C.Alves., Colomban Ph., Ancient Portuguese ceramic wall tiles (azulejos): characterization of the glaze and ceramic pigments. Journal of Nano Research Vol. 8, 2009, pg 79.
- 6- Santos dos Reynaldo, O azulejo em Portugal, 1957, 16.
- 7- Smith C.Robert., The art of Portugal 1500-1800, 1968, 229-263.
- 8- <http://www.golisbon.com/culture/azulejos.html>. Access: 10.09.2018.
- 9- <http://cvc.instituto-camoes.pt/azulejos/eng/azulejo.html>. Access: 13.09.2018.
- 9- <https://www.euromkii.com/content/portugal-azulejo-tiles-history>. Access: 13.09.2018
- 10- http://repositorio.lnec.pt:8080/bitstream/123456789/1004174/2/MFtesi_DSspace.pdf. Access: 06.09.2018
- 11- http://www.azulejos.fr/index_en.html. Access: 06.09.2018
- 12- <https://www.atlasobscura.com/places/sao-bento-station>. Access: 10.09.2018
- 13- <http://lizbon.be.mfa.gov.tr/Mission/ShowInfoNote/121317> Access: 24.08.2018
- 14- <http://www.tale.company/blog/2014/11/12/dunyanin-en-guzel-cinileri-nerede>. Access: 10.09.2018.
- 15- <https://www.discoverlisbon.org/2017/11/22/azulejo-portugal/> .Access: 10.09.2018.
- 16-<https://theculturetrip.com/europe/portugal/articles/a-brief-history-of-portugals-beautiful-azulejo-tiles/#Access>: 24.08.2018.
- 17- <https://www.lisbonlux.com/culture/azulejos.html>. Access: 24.08.2018
- 18- <https://tr.pinterest.com/pin/338825571949317580/?lp=true>. Access: 24.08.2018
- 19- <https://humidfruit.wordpress.com/page/9/> .Access: 24.08.2018
- 20- <https://www.veniceclayartists.com/portuguese-azulejos-art-grandeur/> Access: 24.08.2018
- 21- https://en.wikipedia.org/wiki/S%C3%A3o_Bento_railway_station Access: 10.09.2018
- 22- http://www.azulejos.fr/index_en.html Access: 10.09.2018

THE USE OF SOUND WAVES IN CERAMIC DESIGN AS A NEW FORMING METHOD

Sanver ÖZGÜVEN

Necmettin Erbakan University Fine Arts Faculty Konya/TURKEY

The increasing number of computer programs in ceramics design have changed the creative process and applications to a significant extent. Despite providing more flexibility and convenience, the innovations in sense of design emergence and formation have remained limited. With the help of computer-aided design software, artists can use various tools instead of pencil and paper, but eventually all visual design can only be created with visual data.

Developments in the field of software has brought innovations to the visual arts. Today, software that transforms visual to audio data and vice versa is becoming more and more widely used and accessible. While these types of design tools can be used to produce an audio output from a visual data entry, a two or three dimensional visual output can be obtained from an audio data entry.

Software with a function to convert sound waves to three-dimensional forms can enable an artist to create a ceramic object without making a visual draft. The artist can use any sounds or music for this purpose instead. The transformation of these designs from digital media into real objects also causes some differences in design, depending on the structure of the ceramic materials used. It is possible to determine how the sound waves will behave, making some changes in the software. These changes are entirely under the control of the artist, but at the same time the structural properties of the ceramic material should also be taken into consideration.

Keywords: Ceramic, Sound, Processing, Computer Aided Design, 3D Printing.

INTRODUCTION

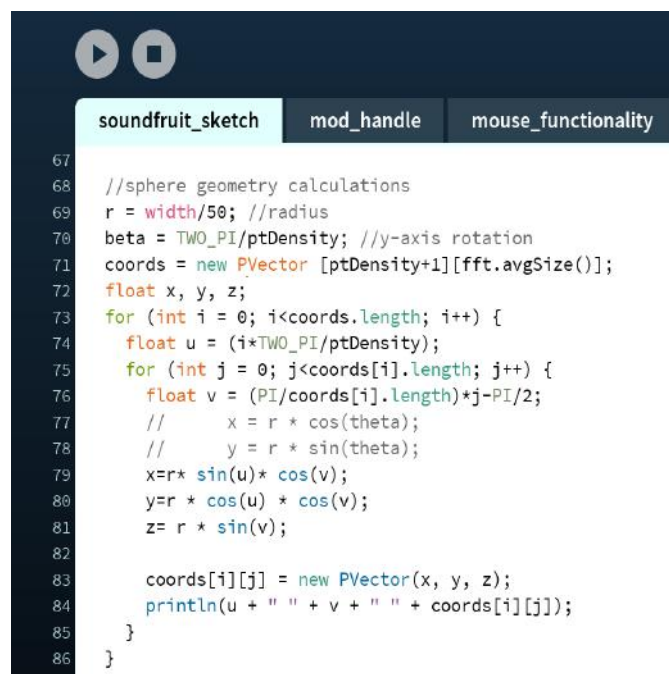
Throughout the ceramics history, different methods of forming have been used. Ceramic objects can be designed and formed with new digital tools that are emerging today. One of these new digital techniques is the processing of sound waves in digital media and the conversion of them into three-dimensional objects. While ceramic objects were designed to make sound in the past, today sound waves are used as a forming method to make ceramic objects.

With help of software, sound waves can be transformed into three-dimensional forms or two-dimensional shapes. The software called Processing (version 3.4, 2018) is used by designers who work in the field of visual design. By using specific codes within the software, a visual object can be designed as desired. The on-screen position, front and rear colors, and different effects of light, especially in three-dimensional forms, can be designed using Processing.

This study includes three dimensional designs that were created using sound waves. It is important for them to be in harmony with ceramic material. Some of these designs may not be produced with three-dimensional ceramic printers. Algorithms that are responsible for converting sound frequency into shape and form of the object, can create a structure that might be incompatible with ceramics. Such problems can be solved by changing the sound frequencies or by rearranging the algorithms in the software.

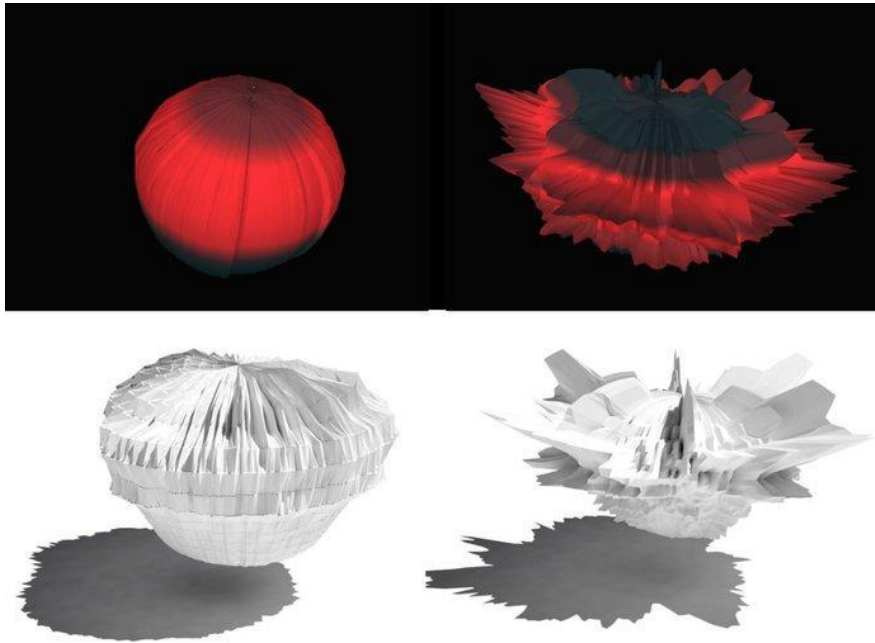
SOUND FRUIT PROJECT

A project named Sound Fruit is an example of a design created in computer environment using sound waves, but incompatible with ceramic materials. On the other hand, this study is important in terms of showing three-dimensional design with sound waves. Processing software allows to create a sphere by simply writing “sphere()” code in a command line. But for this project, the designer created the sphere using mathematical formulations instead. This allowed to transform each point of the sphere surface with sound waves. In Visual 1, mathematical expressions of sphere can be seen.



Visual 1. The sphere code as displayed in Processing software window.

After the sphere was created, the desired sound record played in Processing. This deformed the neat structure of the object. (Visual 2). This deformation was caused by the reaction of each point on the surface of the sphere according to the length and frequencies of the audio file.



Visual 2. Sphere deformation by sound waves.

SOLID VIBRATIONS

The effects of sound waves on ceramic surfaces can also be seen without using any software. During the working of a three-dimensional printer, different surfaces can be obtained by the sound vibrations that are sent to the place where the ceramic form is located. These examples can be seen in the series of Solid Vibrations made by Oliver van Herpt. When printing is in progress, the vibrations of sound waves sent by the speaker from under the three-dimensional printer cause deformation on the ceramic surface. No software is required for such shapes. Sound waves directly give a movement on the bed of three dimensional printer and that allows the deformation of ceramic surfaces.



Visual 3. The effect of sound waves on the ceramic surface.

The regular transmission of sound waves to three-dimensional ceramic printers allows regular shapes to form on the ceramic surface. The continuity of sound waves can easily be seen on the surface of a ceramic form. This helps to create a dynamic effect on usually static ceramic surface.

“Solid Vibrations is a collaboration between Ricky van Broekhoven and Olivier van Herpt. Ricky specializes in sound design. His projects are often landscapes of noise that live briefly in the mind. To combine the temporal sound driven nature of his work with 3D Printing would let noisescapes become things. A moment in time, a song a sound, they can now become objects that encapsulate the moment forever. Vibrations turned into shapes by the 3D Printer. A specially constructed speaker rig mounted below the build platform produces very low sound.

These amplify and create Moiré patterns on the 3D Printer. Olivier had noted previously that the printer produced Moiré patterns naturally. This error was an interesting one. Rather than eliminate it, he turned to sound designer Ricky and teamed up with him to see if they could make objects from sound waves.” (2018, August 26) Retrieved from <http://oliviervanherpt.com/solid-vibrations/>

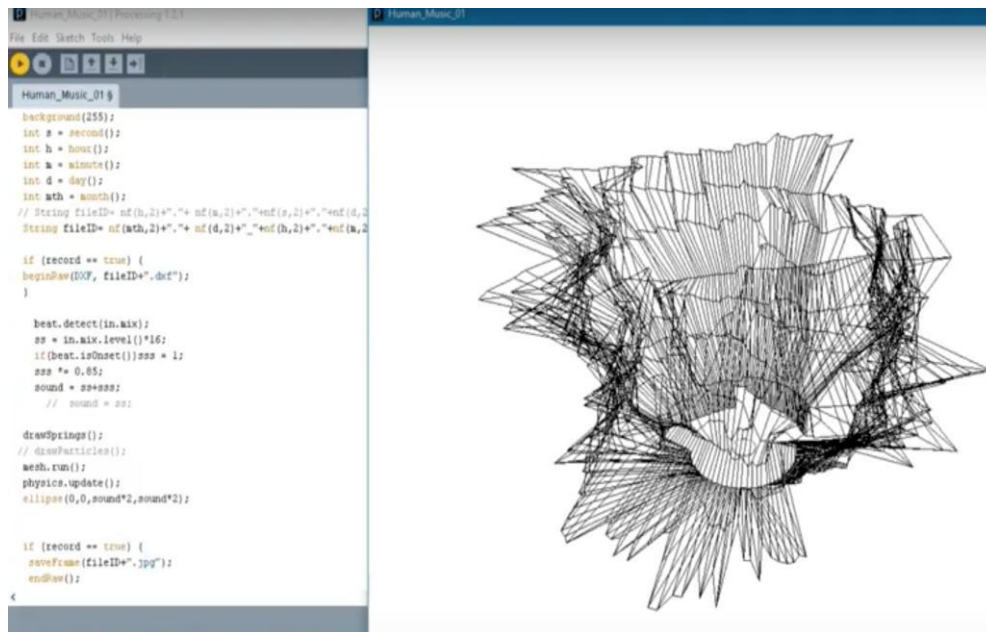


Visual 4. Ricky van Broekhoven and Olivier van Herpt, Sound Vibration Series, 2015.

SOUND SURFACE SERIES

Jonathan Keep's Sound Surface series is one of the first examples of designing a ceramic form using only sound waves in Processing in ceramic art. In the Sound Surface series, it is possible to create a three dimensional structure consisting of points by using the sound vibrations with the algorithm that is written by himself. This structure also moves upwards in a spiral form. As the sound recording continues, the three-dimensional spiral forms continue to move upward. Surfaces that move from the base to the top become a representation of the sound waves. In the Sound Surface series, the artist shows different effects of sound waves on the surface of ceramics that he previously designed in Processing. Once the design of the ceramic form is completed in the Processing, it can be saved as a

“STL” file format and printed with a three-dimensional printer. In Visual-6, ceramic vases that were designed using sound waves and then printed with a three-dimensional ceramic printer can be seen.



Visual 5. A code and visual representation of a vase created with sound waves as seen in Processing software window.

In the ceramic art where the traditional methods such as hand shaping are very common, a ceramic artist Jonathan Keep has used sound waves to create ceramic forms. This is his explanation on how the idea emerged:

“Tradition is not set in time it continues. There was a time when the pottery tradition did not include the pottery wheel because the wheel had not been invented. Now we see the ‘wheel’ as tradition. Plaster of Paris moulds is a newer addition to the tradition of ceramic making. Each time this tradition progresses the relationship of the maker (the human hand) changes so I do not have a hang-up about the ‘hand’ and handmade. What is important to me in my work is to find a ‘visual language’ that reflects the age in which we live, we live in a digital age. So as far as I am concerned the progression of the tradition of ceramics needs to reflect the technologies of our age. There is still a lot of hand work in my work and a lot of craft but I am most interested in form and expression. The craft and my ability with my hands is secondary to the expression and the communication (emotional through vision and tactile quality) that I hope to achieve with the viewer.

So now to answer your question about sound – as you are probably aware I am interested in the natural patterns and processes that govern our world, our environment, that have developed through and are the result of evolutionary progression. We humans are part of this same system. Sound is part of this same system and so why do we find certain sound qualities beautiful. My starting point is to explore the ‘biology of beauty’, if we have evolved out of the same patterns, systems and processes that make up nature out there in the wilderness how does this relate to us who now live in the modern world. Sound is interesting in this relationship in that you can hear the patterns and rhythms so initially I was interested to see if I could translate the audio data to visual data and see what it looks like.

This interest in systems had led me to learning computer coding. I saw how scientist were managing to understand the natural world by using computer coding as a tool to mimic or copy natural patterns and codes. An example is in the flocking of birds, those beautiful clouds of birds you get in flight. A simple computer algorithm explains how it happens but does not explain why we find it beautiful. So the coding becomes a tool set that we can now use to explore beauty, it can be added to the range of craft tools that we have to work with clay – we can sculpt with code.” (J. Keep, Personal Interview, 09.08.2018)



Visual 6. Jonathan Keep, Sound Surface.

Jonathan Keep, one of the pioneering ceramic artists working on this field, has the following statements about three-dimensional ceramic printers, computer technology and the future of ceramic art:

“Computer technology will not go away so I am sure it will continue to slowly more and more effect ways of working in ceramics. If you think about it we have been using digital kiln controllers for years and no one talks about losing the skill of firing a kiln. There are still wood fire kilns and all that tradition and there are digital electric and gas kilns. The future will be like the past; things will slowly change.

There has been a media hype around 3D printing in general that fortunately is dying away as reality of the technology takes a hold. There is a bit of a lag with ceramic 3D printing, we are currently seeing lots of clay extrusion printing but I feel the difficulties and limitations will show up and the trend will calm down. There will always be a hardcore who will keep developing and using it in creative ways. We have yet to see which of the three kind of ceramic 3D printing, powder printing, slip sintering or paste extrusion is going to be best for what sort of production and or requirements. Each of these technologies still need a lot of development. I do not have specific concerns it all just takes time.

With regards using computer technology for design and the creation of ideas and objects this will continue. User friendly software is being developed all the time and as we become more and more computer literate it will become second nature.

As to the use of the hand, this is a whole essay in itself but probably not surprisingly I do not have a hang-up with the hand and ceramics, I see that whole debate as rather romanticised. I have been working with an augmented reality head set and 3D modelling and there are interesting fields of bodily movement and virtual shaping to be explored. There is so much more to the duality of handmade or machine that needs to be considered – the pottery wheel is a machine.” (J. Keep, Personal Interview, 09.08.2018)

BREATH VESSEL PROJECT

Another artist who uses sound waves in combination with Processing and Arduino software, biosensors and three-dimensional ceramic printers is Jenny Filipetti. In her work, Breath Vessels, the audience creates different three-dimensional objects by blowing them into a ceramic shell-like form. With the help of sensor inside of the ceramic shell, sound waves can be transformed into the three dimensional objects. Later these can be 3D printed or slipcast in ceramic.



Visual 7. Design process of Breath Vessel series

“The printer used to create the vessels is based on artist Jonathan Keep’s design, and it’s powered by an Arduino board outfitted with an accelerometer and anemometer – or wind meter – which captures the data. The accelerometer and anemometer readings are transferred to a Processing-based algorithm, which then generates the 3D model in real time as a response to the pattern of the measured breath. That data becomes an “STL” file for printer output, and an image of that virtual model is captured and added to an “archive” of individual breath samples.” (2018, September 15) Retrieved from <https://3dprint.com/68778/clay-3d-printed-breath-vessels/>



Visual 8. Three-dimensional forms created by sound waves in Breath Vessels project.

Filipetti, has given the following statements about this project called Breath Vessels:

“Breath Vessels draws attention to the very physical nature of this life-sustaining ritual. Just as immaterial words can have tangible effects in the world, our breath is deeply tied to both our biological and emotional life, and thus it too has real effects on ourselves and our world.” (2018, August 26) Retrieved from <https://cfileonline.org/art-technology-jenny-filipetti-breath-vessels/>



Visual 9. Jenny Filipetti, Breath Vessels.

CONCLUSION

The adventure of ceramic art, which started with hand shaping methods, continued with the use of different tools within the years. In addition to mass-production techniques and a number of new methods with industrialization, three-dimensional ceramic printers have also been used in recent years in ceramic art. The ongoing relationship between ceramic and sound from past to present, has gained a different dimension with the inclusion of digital technologies. The emergence of different design tools has brought back different forms of expression in ceramic art. These new methods have opened up new frontiers for ceramic artists to express themselves.

Along with the emergence of user-friendly new interfaces, complex software has been widely used among artists. In the future, it is expected that such new shaping techniques will be widely used in ceramic art, besides traditional tools and equipment. In this respect, concepts such as electronic, mechanic, software or artificial intelligence will contribute practically to the ceramic art in the near future.

One of the important points is to adapt to such new shaping methods and to use such tools not only as a technical demonstration, but also as a new form of expression. In the coming years, with the use of different software and electronic devices, it is especially important that different disciplines communicate together. Thus, in addition to the works that will be produced by people from different disciplines, ceramic artwork that will be designed and produced completely by artificial intelligence will also take part in ceramic art.

As a result, it is important to use new software languages and to create original algorithms so that artists can express themselves. In addition to using different design programs, it is necessary to produce an original program for each artist.

References

Chittenden, T. (2018). Printed pots and computerized coils: The place of 3D printing in ceramic practice. *Craft Research*, 9(1), 9-40.

Krasteva, M. The Impact of Technology on the Modern Art, Digital Presentation and Preservation of Cultural and Scientific Heritage International Conference 26-28 September 2016, Bulgaria.

Van der Stelt, G. (2007). Puls Gallery, Barbro Aberg and Jonathan Keep Contemporary Ceramics. *Ceramics Art and Perception*, (67), 91.

<https://3dprint.com/68778/clay-3d-printed-breath-vessels/>

<https://cfileonline.org/art-technology-jenny-filipetti-breath-vessels/>

<https://www.instructables.com/id/Sound-Fruit-How-to-Make-a-Sculptural-Audio-Visuali/>

<http://jennyfilipetti.com/project/breath-vessels/>

http://www.keep-art.co.uk/digital_sound.html

<http://oliviervanherpt.com/solid-vibrations/>

<https://www.thisiscolossal.com/2015/04/turn-songs-into-3d-printed-sculptures-you-can-listen-to-with-reify/>

THE USE OF EGYPTIAN PASTE IN CONTEMPORARY CERAMIC ART

Can Gökçe¹, Ezgi Gökçe²

¹ Uşak University, Banaz Vocational High School Architectural Decorative Arts Department 64100 Usak/Turkey

² Uşak University, Faculty of Arts, Turkish Traditional Art Department, 64100 Usak/Turkey

ABSTRACT

The Egyptian paste, which has around 7000 years of history in Egypt, is especially turquoise (Nile blue) and has the property of being self-glazed in a single firing. The Egyptians gave this material a name means "glamorous, very bright" or "dazzling". The Egyptian paste, also called "Egyptian Tile and Egyptian Clay" is widely used for small objects, especially small sculptures, bead making, Ancient Egyptian jewelry and musical instruments. It is known that larger sizes of cups, bowls and wall tiles produced with Egyptian paste are located in the temples.

The Egyptian Paste contains quartz, soda and feldspar which can be found in the content. Surface-containing and water-soluble melts, such as sodium bicarbonate in the blend, are combined with bristled silica and alumina to form the thin layer of surface glaze. This chemical property is glazed. Despite difficulties, the Egyptian Paste, which is glazed by itself, has attracted interest in this area and become an inspiration to ceramic artists.

Native and foreign artists use this material in their works. In this study, examples of the use of "Egyptian Paste" in modern ceramics art will be presented and evaluated to open new horizons for artists who want to work in this area.

Keywords: Egyptian paste, stonepaste, quartzpaste, contemporary ceramic art

HISTORY OF EGYPTIAN PASTE, RAW MATERIALS AND SHAPING

The first actual glazed surface occurred in Egypt approximately five thousand years ago. The usual theory of the first glaze development comes from the probable use of sandstone containing considerable sodium and potassium, called Natron, which was used to build a fireplace. Natron has a very low melting point and the surface of the rock facing the fire would easily develop to a fused glaze. People started to make small statues from this sandstone and heat them, and this is what most likely led to the first glaze on pottery. When the material dried, soluble sodium materials transferred to the surface, forming a powdery scum. When heated to a low heat, this scum melted-and combined with the clay to form a glaze. This is, in fact, a self-glazing clay called Egyptian Paste. It was often colored natural or produced of metallic compounds of copper, manganese, iron and cobalt (1).

Some of the earliest Egyptian Paste objects made in Egypt were beads, small temple and royal tomb objects. Egyptian Paste was inlaid into furnitures and walls as a tomb and temple decoration (Figure 1). The most recognizable forms of faience are small figures of gods (Figure 2-3), animals, and shabtis (Figure 4), as well as jewelry (Figure 5-6), amulets, scarabs, and vessels (Figure 7).¹

¹ See for further information: Güner G., Bir Nil Mavisinin Öyküsü, Uluslararası Seramik Kongresi Bildiriler Kitabı 1992, s. 619-621., Özen T. A., Alpman G., Mısır Çamuru ve Seramiği, Art Decor Şubat 1998, s.80-85., Kingery D. W., Vandiver P. B., Ceramic Masterpieces Art-Structure-Technology, The Free Press London, 1986., Nicholson P., UCLA Encyclopedia of Egyptology-Faience Technology, California Digital Library, 2009., Tite, M., Ian F., Mavis B., Egyptian faience: An investigation of the methods of production. Archaeometry 25-1983, pp. 17 - 27., Tite M., Panagiotis M., Andrew S., A technological study of ancient faience from Egypt, Journal of



Figure 1: Wall tiles from the funerary apartments of king Djoser, 2630–2611 B.C., Egypt, Accession Number: 48.160.1 (2)



Figure 2: Statuette of Isis and Horus, 332–30 B.C. Egypt, Accession Number: 55.121.5 (3)



Figure 3: Amulet of the God Bes, 1070–712 B.C. Egypt, Accession Number: 26.7.878 (4)

Archaeological Science 34-2007, pp. 1568 - 1583., Noble J. V., The Technique of Egyptian Faience, American Journal of Archaeology, Vol. 73, No. 4 (Oct., 1969), pp. 435-439.,



Figure 4: Shabti of Seti I, 1294–1279 B.C, Egypt, Accession Number: 26.7.919 (5)



Figure 5: Broad Collar of Wah, 1981–1975 B.C. Egypt, Accession Number: 40.3.2 (6)



Figure 6: Openwork faience ring, 1090–900 B.C., Egypt, Accession Number: 74.51.4540 (7)



Figure 7: Lotiform Chalice, 945–664 B.C. Accession Number: 26.7.971 (8)

An important development was the production of moulded glazed objects from a specially prepared quartz body which became vitreous, when fixed with a glaze, developing on the surface. These wares are known as faience or Egyptian paste. They were manufactured in ancient Mediterranean and Near East regions for five thousand years, faience beads found in Egypt and Mesopotamia go back to about 4000 BC (9).

Egyptian Paste is a self glazed ceramic material with quartz body. It contains silica alkaline salts (the source of natron or plant ash), small amounts of lime and a metallic colorant. During the firing process, the alkali (acting as a flux) and lime (acting as a stabilizer) react with silica into a glaze phase on the surface.

The raw materials in Egyptian paste were available in Egyptians' surroundings. Silica was obtained from fine desert sands or quartz rock, quartz pebbles and siliceous limestone which were abundant in Egypt. Some scholars proposed that the raw materials for faience were obtained as a by-product of hard stone drilling. Copper tools were used with abrasive sand to drill or saw granite and hard limestone artifacts. The waste powders remained from this process consisted of quartz and lime from the limestone besides particles of copper from the drill, potentially providing an available source for the materials to make faience. Egyptian soil is rich in saline substances such as niter, natron, alum, rock salt, and sea salts—providing the alkaline component for faience. Niter forms as an efflorescence on the surface of the soil during dry periods. Natron is collected from the saline encrustations of dry lake beds of Wadi Natrun in the West Nile Delta. Rock salt and alum are mined from the ground (10).

Egyptian paste is a body barely or not containing clay, which can be modeled and carved into simple forms or pressed into molds. It has a high silica, soluble salts and low contents of clay. Small figures and objects like amulets and beads could be formed by hand-modeling, common ways to shape clay molds as confirmed by the multitude of faience molds found in the archaeological archives (Figure 8). Although they are uncommon, there are larger objects made of Egyptian paste. The paste can also be put into a slab by shaking and patting to create flat objects such as inlays or tiles. Another technique for working with Egyptian paste is to form the paste around organic materials. A layer of paste is either modeled around the combustible organic materials or dipped into a slurry of faience ingredients (11).



Figure 8: Mold for a Grape Cluster Pendant, 1353–1336 B.C. Egypt, Accession Number: 21.9.23 (12)

MODERN EGYPTIAN PASTE APPLICATIONS, FORMULAS AND EXPERIMENTS

Artists are in constant search; this is sometimes an idea, sometimes a tool or a new material. For some ceramists different bodies like Egyptian paste, quartz body, frit body, stone paste and faience offer a different way to make new artistical ceramics. Recipes for Egyptian Paste chosen from artists and researchers are as follows:

Barbara Kleinman's Egyptian Paste Formula (13)

3 scale ashes (from salt lake plants' in Gum city)

3 scales Calcite

2 scales Quartz

½ scales Wood coal

% 1 Copper slag

Prof. Güngör Güner's Egyptian Paste Formula (14)

20 gr Vine Branch Ash

10 gr Calcine Soda

30 gr Calcite

20 gr Quartz

5 gr Wood Coal Powder

8,5 gr Copper Oxide

Different application attempts and materials were included in this study. The two recipes and applications are as follows:

Formula 1

Quartz 68

Frit 18

Bentonite 8

Sodium bicarbonate 16



Figure 9: Trials from Formula 1, personal archive

Formula 2

Quartz 33,7

Sodium Feldspar 33,7

Kaolin 12

Sodium carbonate 5,4

Sodium bicarbonate 5,4



Figure 10: Trials from Formula 2, personal archive

This mixtures that difficult to form were used in different ways. Applications are usually made by compression of two different clay bodies. In addition, a different approach was maintained by adding openwork plates on Egyptian Paste (Figure 11-13-14-15-16-17).



Figure 11: Can Gökçe, Bordure, Egyptian paste and earthenware, 2008, personal archive

Egyptian paste is also applied on glazed forms like slip, glaze or dye for decorating (Figure 12).



Figure 12: Can Gökçe, Untitled, Egyptian paste and earthenware, 2007, personal archive



Figure 13: Can Gökçe, Stoneware and Egyptian Paste, 2010, personal archive



Figure 14: Can Gökçe, Stoneware and Egyptian Paste, 2013, personal archive



Figure 15: Can Gökçe, Stoneware and Egyptian Paste, 2013, personal archive



Figure 16: Can Gökçe, Stoneware and Egyptian Paste, 2013, personal archive



Figure 17: Can Gökçe, Stoneware and Egyptian Paste, 2013, personal archive

A form created with a mix of “Egyptian Paste” and two types of clay featuring unique textures of quartzpaste (Figure 18)



Figure 18: Ezgi Gökçe, Stonepaste and Egyptian Paste, 2007, personal archive

Egyptian paste is not widely used in modern ceramic art. In this research, it was determined that very few ceramic artists work with this material. Some artists use this material on their ceramic bodies like a glaze, some use for building the main form and some use to combine with different materials (Figure 18-19-20-21-22-23-24-25).



Figure 19: Mutlu Başkaya, “Akıl Süzgeçleri”, Egyptian Paste and Porcelain, 2008 (15)



Figure 20: Mutlu Başkaya, wire mesh and Egyptian paste, raku (16)



Figure 21: Katherine Rhynus Cesark, Untitled, Egyptian paste, 2013 (17)



Figure 22: Carmen Argote, Knee, Terracotta, Egyptian paste, dried moss, wire, epoxy, 2011(18)



Figure 23: Carmen Argote, Penitentiary Capacitor, Ceramic, egyptian paste, steel, 2007 (19)



Figure 24: Bernadette Pratt, Out on a Limb 2016, egyptian paste (20)



Figure 25: Heather Nameth Bren, Tritanopia and Deuteranopia 2016, egyptian paste (21)

CONCLUSION

“Egyptian Paste”, an important technical development for the history of world ceramic art appears as a new material that can be enhanced with experience and further applications. Contemporary ceramic artists working with this material are uncommon. However, “Egyptian Paste” can be preferred in contemporary ceramics as a rewarding material due to its features as vibrant colors, unique texture, self-glazing body and being able to combined with different materials in a single firing. When the works of ceramic artists using Egyptian Paste are examined, it is seen that bright colors and texture of the material are featured. In the literature, “stonepaste, quartzpaste and fritpaste” which are mentioned as quartz bodies have been approached mostly by art historians with their past as a research object, yet there are a few artists work with these materials. It is considered that, researches on quartz bodies used in the past will contribute to today’s art environment, in which artists create their own forms of expression and use different materials as a tool.

In conclusion, it was observed from these recent applications of Egyptian paste that very different effects can be derived upon handling and retesting the ancient techniques under different conditions. Additionally, contemporary forms may be recreated adhering to this technique. Those interested in the subject may produce new objects using the same ancient technique and raw materials, which are easily available today. Experimental style approaches, started with intuitive knowledge in the process of capturing a contemporary language of expression and making use of traditional technique provide artists to discover something new. The acquired experience and knowledge may not be adequate for the same form to come out of the kiln and change beyond the designed form is observed. This coincidental situation is a source of inspiration for new works.

References:

1. Hopper R., The Ceramic Spectrum a Simplified Approach to Glaze & Color Development, Krause Publications, Iola 1984, 8.
2. <https://www.metmuseum.org/toah/works-of-art/48.160.1/> (Accessed: 10.05.2018)
3. <https://www.metmuseum.org/toah/works-of-art/55.121.5/> (Accessed: 10.05.2018)
4. <https://www.metmuseum.org/toah/works-of-art/26.7.878/> (Accessed: 10.05.2018)
5. <https://www.metmuseum.org/toah/works-of-art/26.7.919/> (Accessed: 10.05.2018)
6. <https://www.metmuseum.org/toah/works-of-art/40.3.2/> (Accessed: 10.05.2018)
7. <https://www.metmuseum.org/toah/works-of-art/74.51.4540/> (Accessed: 10.05.2018)
8. <https://www.metmuseum.org/toah/works-of-art/26.7.971/> (Accessed: 10.05.2018)
9. Cooper E., Ten Thousand Years of Pottery, The British Museum Press, London 2002, 29.

10. Riccardelli C., Egyptian Faience: Technology and Production, https://www.metmuseum.org/toah/hd/egfc/hd_egfc.htm, The Metropolitan Museum of Art, December 2017.
11. Riccardelli C., Egyptian Faience: Technology and Production, https://www.metmuseum.org/toah/hd/egfc/hd_egfc.htm, The Metropolitan Museum of Art, December 2017.
12. <https://www.metmuseum.org/toah/works-of-art/21.9.23/> (Accessed: 20.06.2017)
13. Yoleri H., Çizer S., Yarol Y., Kahraman D., Nazar İnancı ve Geleneksel Katır Boncukları, Türk Seramik Federasyonu Dergisi, Mart-Nisan 2006/14, 104-113
14. Hacettepe Üniversitesi, Sanat Müzesi Macsabal Koleksiyon Sergisi 14-30 Mayıs 2013, Kataloğu
15. Başkaya M., Tasarımcıya ve Sanatçıya Esin Veren Malzeme ve Nesneler, Türk Seramik Federasyonu Dergisi, Temmuz-Eylül 2008/26, 130
16. <https://krhynuscesark.com/artwork/3590758-Untitled-egyptian-Paste.html> (Accessed: 30.06.2017)
17. <http://carmenargote.com/work/knee/> (Accessed: 30.07.2018)
18. <http://carmenargote.com/work/penitentiary-capacitor/> (Accessed: 30.07.2018)
19. <https://www.bernadettepratt.com/egyptian-paste#1> (Accessed: 30.07.2018)
20. <https://www.heathernamethbren.com/artwork?lightbox=dataItem-ini8zxqk> (Accessed: 10.08.2018)

RECONSTRUCTION THE ARTISTIC MEANING: DESTROYING AS AN ACTION IN CONTEMPORARY CERAMICS

Assoc. Prof. Safiye Başar
Kocaeli University
Fine Art Faculty of Ceramic Department
41300 Anıtpark Kocaeli/Turkey

Abstract

Ceramic has been known not only as a traditional production material but also art material from the beginning of the 20th century. However, the most important progression and transformation in the field ceramic art are experienced after Second World War. This progression is observed in the artworks created by some important artists such as Hans Coper, Ruth Duckworth. These works, which showed a formalist approach at the beginning, evolves towards critical approaches in the future. Especially this critical approach has been observed in “Pop and Funk” since the late 1960’s and it continues today.

Nowadays, everything can be the material of art. In addition to the traditional materials, today art works are created with a wide variety of material such as inner oil, artist’s blood, glass, ceramic or wheat seed and these materials becomes an instrument for artists to express their feelings and to materialize ideas and meanings. At this point, ceramic material is considered by relating physical characteristics, historical ties, rich layers of meaning comes from tradition of production in the art works belongs to modern artists such as Ai Weiwei, Jeff Koons, Charless Craft.

In these art works, the most remarkable thing is that artists destroy or broke ceramic sculpture or object. Even that this actions may be interpreted as vandalism. Is it possible to consider that the action of destruction is a process for to create the level of meaning, when it has been take into consideration the art theory of Kant that is based on “*aesthetic idea*” and the art theory of Danton based on “*embodied meaning in the object*”?

Key Words: Destruction, Action, Ceramic, Contemporary Art

Introduction

The ceramic, which is pressed in the discussions of art and craft, have succeed to get out of these debates by adding contemporary art in the late 20th century. Today we are going through a period when everything is turned into artistic material. In addition to traditional materials, a wide variety of materials, such as inner oil, artist's blood, glass, ceramics, wheat seeds, serves as a medium for the artist to express his ideas. At this point, ceramic material which is considered by relating physical characteristics, historical ties, rich layers of meaning comes as a principal medium of contemporary art.

From sculptures and installations to actions and performances, many different studies are based on the physical characteristics of the ceramics such as rich historical tradition, fragility and sound. Among these works, the actions that the ceramic works are destroyed and sometimes vandalized are very remarkable. The vandalism history that can be described as a conscious destruction of artworks dates until the ruin of ancient temples at the beginning of the Christian era (Sözen, Tanyeli, 1992:248). Vandalism and destruction are fundamental problem in contemporary art. Today this destructive action can be evaluated in two different approaches. First destruction as a crime and then destruction as an artistic action, artistic anarchism.

This research develops around the following question, moving from the definition of art that Danton refers to as ‘*embodied meaning*’. Can acts of destruction, and sometimes even vandalistic, be regarded as a process of producing meaning? This paper focuses mainly on destructive and vandalizes actions based on the historical contexts and physical characteristics of ceramic in contemporary art.

Action As An Art Form

In the process of autonomy that started with romance in the beginning of the 19th century, art evolved from artistic forms to anti-artistic acts in the early 20th century. Cutting off ties with hundreds of years of tradition based on the representation of nature and object, art has begun to corrode the boundaries between life and itself. The action that we can define as an effort to

change the situation that is consciously and purposefully present, has infiltrated into the art from everyday life. Although the first artistic actions are considered in the Futurist movement, the Dada movement can be regarded as a breaking point. Before Dada, all the interventions were directed to epistemology and phenomenology of art but it intervened in the ontological structure of art. Dada “*destroyed the object of art and took action instead. It did not evaluate what art was. It targeted its presence. (It) denied art as a universal, rational, and positive category in the sense Kant defined.*” (Artun, 2018) It replaced nihilism. In the source of nihilism, there is a rebellion against organizations such as exhibition, museum, and the art market.

The Berlin and Munich-based Dada movement is related to the philosophy of Nietzsche. In the beginning World War I, Dada sprouts up in an environment of international anti-war artistic solidarity with the initiative of a group of young artists who have migrated to the Swiss city of Zurich.

“Dada artists who are in the desire to deny the null values which are accepted without being questioned without being questioned in the social and cultural sense have given importance to methods of randomness and improvisation in order to express these destructive and negating feelings. Dada has given priority to an uncontrollable intellect, just in the face of rational thinking in order to expose the mindlessness of people who are dragged into a ridiculous war, and to express their mindlessness. Dada artists want to show mindlessness of humanity in their absurd actions.” (Antmen, 2008; 123)

Dada is separated from other avant-garde arts by their actions that ranging from to burn down to suicide. Dadaist Raoul Hausmann states that they are aiming to destroy and shatter everything in order to expose the new world within them. (Artun, 2018) At a Dada exhibition in Cologne with the participation of Hans Arp and Marx Ernst that they are thought to have disintegrated the works with hammer. (Antmen, 2008; 126) This vandalistic actions that force the boundaries of life and art. Even it has transformed into the end of life. According to Art historian Gavin Gridon, Dadaists put action into the art and converted art an aesthetic event.



Robert Rauschenberg, “Erased De Kooning Drawing 1953,”
<https://www.sfmoma.org/artwork/98.298/essay/erased-de-kooning-drawing/>
 John Baldessari, ‘Cremation’ 1970 <https://www.tate.org.uk/context-comment/articles/lost-art-john-baldessari>

At the beginning of the 20th century, 'action' as an anti-art form emerges as the production process of the work of art in the middle of the century. In this period of rapid consumption and popularization of cultures, Robert Rauschenberg's vandalistic activity affected the art world. The artist wipes over a pattern of William De Kooning with an eraser and titled 'Erased de Kooning Drawing'. Rauschenberg uses stuffed animals, coca cola bottles, and quilts in their work. Instead of representing that reality, he prefers to include it directly in his works. This action of Robert Rauschenberg which has the permission of De Kooning can be read as an intervention to the representation of reality.

It is an destructive action that discusses what the art object is 'Cremation'. John Baldessari burned all his paintings between 1953-1966 in a crematorium in 1970's. He keeps some of his



Ai Weiwei, *Dropping a Han dynasty urn*, 1995, <http://paul-barford.blogspot.com/2011/06/artist-ai-weiwei-and-damage-caused-by.html>

Ai Weiwei, *Painted Vase*, 2009, <http://paul-barford.blogspot.com/2011/06/artist-ai-weiwei-and-damage-caused-by.html>

ashes in the container. Some of the ash was cooked by putting it in the cookies. Baldessari has given this action as the best piece he has ever made. This vandalistic action contains a sub-text to capture the relationship between artistic practice and the life cycle.

It is possible to increase examples of artistic actions from New Realists to Fluxus in the art of the 20th century. In the next part of this article, it will be carried out through actions involving destructive, occasional vandalistic approaches that have been carried out on the historical contexts and physical characteristics of ceramic ware.

Ceramics and Action in Contemporary Art

In contemporary art ceramics comes out with two different approaches as a subject and object of artistic action. In conceptually based artistic actions, ceramics takes place in the subject position. Historical contexts of material; physical properties such as fragility, insulation, and sound come to the forefront as an element that strengthens the artistic expression. Ai Weiwei's 'Dropping a Han Dynasty Urn', Kris Martin's 'Vase' Lia Bagrationi's 'Vacancy' studies show that the physical characteristics of material, such as fragility. In formalist studies, ceramics is an object that is influenced by the process of action. Fragility has been used only as a feature that is utilized in forming form.

The known province of destructive actions dealt with in the historical context of ceramics comes from the Chinese artist Ai Weiwei. He is known as a activist. Ai produces works in different disciplines such as performance sculpture, video. Focusing on history and memory in his works, he says, "*History is always the missing part of puzzle in everything we do*" (Kataoko, 2012: 17) Each piece is a moment from the millions of years of human history to millions of Chinese. "*Focusing on fragments is, for Ai a manifestation of the objective awareness of history, time and society.*" (Kataoko, 2012: 17)

Weiwei's work, focusing on China's history and culture, begins when he returns to his country in 1993 from the United States where he went to study. In that period also China's political and cultural transformation began. Ai Weiwei performs his first destructive action in those years. (Kataoko, 2012: 17), (Başar, 2012: 43)

Weiwei breaks down a ceramics urn. It is approximately 2000 year-old belonging to the Han Empire period, which ruled between 206 - M.S 220 BC. Ceramic vessel is not only an archaeological data but also it is symbol of Chinese history and cultural so it very important. This action, deliberate breaking of a pot from Han Dynasty period can be read as a vandalistic attempt to break the ties with China's past and destroy its cultural heritage. However, in this action, Ai points out that it is possible rebuild in contrast to destruction. The artist makes a statement as a result of the reaction. He explains that his works bases on a word of Mao Zedong, the leader of the Chinese Cultural Revolution: "we can build a new world only by destroying old ones". This strength of the artist is a powerful irony in itself.



Kris Martin, Vase, 2005 <http://artasiapacific.com/Magazine/71/AHistoryOfViolence>

Lia Bagrationi, Emptiness, 2015, <https://cfileonline.org/lia-bagrationi-contemporary-ceramic-art/>

Cultural heritage of past civilizations destroyed by the state during the Mao era is now considered to be a symbol of cultural heritage and rich Chinese history. The ancient ceramic form, which Weiwei regards as a cultural ready object, is the subject of artistic action. He was specially selected by the artist because of the symbolic values about the history of Chinese and culture. This Urn which is actually a functional container. It concern with the historical and cultural contexts at Ai's work. In another vandalistic action, artist painted fifty-fifty pieces of Neolithic ceramic tiles with colorful industrial paint. This action, which takes place about ten years after the first work, contains references to the policies that the Cultural Revolution calls destructive. In this work, where an ironic approach is followed, Ai closes over historical and cultural data and makes it invisible, hiding under the dyes. But reality continues its existence under the paint. It will continue to exist in the corridors of time and history, despite the fact that it is covered.

Ai Weiwei says that "Regardless of how art represent destruction or negativity, it is a progressive explanation of mankind's understanding of self and of the world." (Brougher, 2012; 42) Thus, the destruction in Ai's action took place in the history of art as an extraordinary method in the reconstruction of the meaning.

Another artist who works with cultural data is Kris Martin from Belgian. In the center of the his action called "Vase" is an ancient ceramics form, which he describes as a 'cultural ready object'. Kris Martin buys an ancient, blue and white porcelain vase of Twenty-five centimeters high in length from Ghent It is from Qing Dynasty (1644-1911) broken before. The value of ancient Chinese vases, which are highly appreciated by European collectors, is quite high. Many broken ancient forms, such as Martin's example, continue to remain in circulation without losing market value. In fact, this has also led to the arrival of well-imitated products on the market over time. (Yan, 2010)

Kris shattered this ancient form in the middle of the art gallery. then he re-creates and displays the form by sticking each broken piece. The porcelain vase was an ancient form of Chinese culture before Martin's intervention and at the same time a commercial product.

This vase, which once came to Belgium through commercial relations between Europe and China, is in fact a functional container, a valuable commodity. With Kris choosing it as a ready object, all the marks and symbols that it is carries on change. Vase is now a new ceramic object as a cultural data, an invaluable antique form. The intervention of Kris does not remove the historical and cultural context of the vase. Ordinary a object, transforms into an artistic work, an intellectual proposal that contains cultural, historical, aesthetic traces in life.

while the context of the porcelain form is unchanged in the first break, when and where it is unclear, after destructive action of artist it include a new context about with. The action that results in the breaking of the ancient porcelain vase, which can be associated with the concepts of wealth, grandeur power and prestige, brings to mind the question of 'what determines the value of an object / artistic work'. Therefore Martin's action is a philosophical proposition to find answers to this question. Will the value of the vase be changed when it is broken and glued

for another exhibition? The repetition of Kris Martin's crushing process is a sense of curiosity about the end Martin defends this destructive feeling as a precondition for creating. "Something else can be pre-conditioned when something goes wrong" (Jongh 2008)



Clara Twomey, *Consciousness/Conscience*, 2001-2004

https://www.google.com.tr/search?q=clare+twomey&safe=active&source=lnms&tbm=isch&sa=X&ved=0ahUKEwi8sM2CirbdAhVQilSKHKBBDIMQ_AUICigB&biw=989&bih=458#imgdii=yMuwtJxBSqWvmM:&imgcr=0n4_GD4DFvEnM

Lia Bagrationi uses the privileged language of action and performance that includes sound, movement, form and anti-form in her artistic work. The artist's 'On Point' exhibition, dated 2015, is the result of the performance. Ceramic is in the center as a material in this action with historical context as well as physical characters.

Bagrationi breaks the pots that it is the most dominant form of ceramics production tradition, with a hammer. Before the action the pots were filled with a completely white solid material. The pots rub off the from the ceramic layer due to the severity of the breakage. It becomes an independent new

form. The pottery which is intended to preserve something in the emptiness. But Bagrationini uses it as a metaphor for a empty.

British artist Clare Twomey deals with concepts such as memory, consumption, change, conservation and desire in ceramic works. In addition to ceramics sculptures, she produces work that runs around the boundaries of installation and performance. (Twomey 2017) The artist's most well-known work is the (2001) 'Consciousness and Conscience'. The artist tries to reveal the relationship between the work of art and the audience at her destructive works. Before the action, Twomey covered the floor of the gallery and the museum, which were functioning to protect the works of art and meet the audience, with about seven thousand ceramic boxes, just like a flooring plaque. The materials of the boxes, the cooking grades, were examined and tried before hand by the artist. (Mark Currah, 2003) While the audience, who came to the gallery to watch the exhibition, was heading towards his artworks, the ceramic boxes were broken under her feet. Thus, Twomey adds the tension due to fragility in her work and uses it as a metaphor of consciousness and conscience. Also, an ordinary movement, 'walking action', from life has gained an artistic identity in the work of Twomey.

In the eighties ceramic material is added to contemporary art in Turkey, two avantgarde action that breaks the bonds of tradition, occurred in Istanbul and Izmir. The first action is realized by Kadir Demir in Taksim Anadolu Bank Art Gallery in 1987. The second action is performed by Aylin Coleri in the American Pavilion of Izmir Cultural Park in 1993.¹

Kadir Demir was graduated Ceramic Department of Academy. When he was a student in the eighties 'It was going on discussions on art and art work, and was being experimental works by some groups and initiatives such as Akademia and Barbart. In installation and actions Kadir Demir has a conceptual approach. He make criticize at his earliest works the art of commodification, arts market and the galleries. (Karavit 2002, p.46) (Zeytinoglu, 1993) Kadir Demir and the Anatolian Bank Art Gallery negotiates for a personal exhibition in 1987. Before the exhibition some problems experienced by the art gallery administration disturbs the artist. For this reason, Demir decides to change the format of the exhibition. He puts ash glazed ceramic pots on a table covered with lace in the gallery.² (Karavit 2002, p.46)

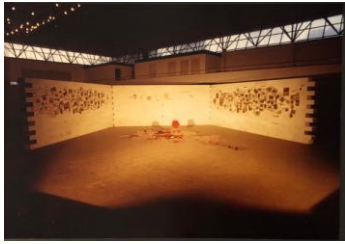
At first, this installation reminds us an invitation with the precious porcelain and ceramics and

¹ Up to this day, two examples could be reached. It is possible to get similar examples

² Safiye Basar, Interview with Kadir Demir, 6.09.2018

underlines the functionality of the ceramics. At the opening of the exhibition, the artist breaks down ceramic pots about twenty-four pieces with a hammer. This destructive action is an anti-art movement that protests the arts market. Demir explains his views on this issue as follows: " ... art has a message. This is my message. Your artist has to act with the competitions and the galleries. Colorlessness of the art scene in Turkey, being forced to take part in gallery, to being convict the sentences that written by critics. Here's to all of these. My exhibition is a reaction to the art in Turkey.'" (Guner, 1987)

In the action of Demir, the historical and functional context of ceramic is shattered. it associated with labor and artistic production processes.



Aylin Coleri, Peace, 1993, Artist's Personal Archive

About six years after the action of Kadir Demir, the artist Aylin Coleri realized an action. The fragility of ceramic material is in the central at this action. Having started her art education at Hacettepe University Ceramics Department, Coleri completed master's degree as a scholarship student at New York University. She returned to Turkey in 1991 and started to work at Dokuz Eylul University.

In 1990s, the peace and prosperity disappeared in the Balkans and the Gulf, the war grew steadily. In an interview with her, Coleri said, "*In those years, there was news*

of war and violence on television every day. Daily newspapers were filled with war photos. I reacted to killing the war."³

She says that she started to cut off news, photos, newspaper clippings. In fact, Coleri saved the history of violent as an archive in the same years. Journalist Ugur Mumcu died at a terrorist attack in 1993. This event deeply affected artist. She was against war, reacted to terrorism and killing. The work of 'peace' is the result of this reaction. It is a memory for Ugur Mumcu.⁴



Safiye Basar, Silent Scream, 2012, Artist's Personal Archive

The artist built three walls into the American Pavilion. In the middle of this space there was an anonymous poem written on the floor and newspaper clippings on the wall. There was two young who were holding black and white ceramic sphere, and standing at the opposite corners of the room. They leaved the spheres by the order of the artist. They collided rapidly, moving towards each other. The red liquid that spilled from the broken spheres jumped onto the audiences. The violence of the explosion caused fear and panic.⁵ Thus artist created an illusion of the violence of war and terror. She underlined the thin line between life and death and also

³ s.i.

⁴ s.i.

⁵ Safiye Basar, Interview with Aylin Coleri, 7.09.2018

peace.

After so many years, following the pioneering work mentioned above, there are examples of enriching the language of artistic expression with by technological possibilities like video. Safiye Basar and Burcak Bingol force the limits of ceramic as a artistic material in their video art works.

Safiye Basar deals with gender, labor and environment issues in his work. In the recent period she takes references to the production of women's tradition at her sculptures produced from porcelain materials. The artist uses marriage packs of Anatolian as a basic form for his works. This marriage package (bohca) holding in the dreams of young girls and their desires about the future. It is dealt with in a metaphoric approach in Basar's work. The artist is seen breaking her own works, (bohca), in the video, 'Silent Scream'(2012). Fragility is the center of the artistic expression in this work. At the first perception, destruction may seem like a negation but, the artist accepts the destruction as a positive attack for a new beginning. It is the rebellion of the woman to all the social and cultural enforcements. (Ağatekin, 2016), (Başar, 2012) Violence against women and girls, women's trade, secondary status of women are universal problems. It requires an international field of struggle. 'Silent Scream' makes visible these unexpressed or half-mouth expressions. (Agro, 2015)



Burcak Bingol, Self-Conscious, 2015
<http://www.brandlifemag.com/burcak-bingol-metropolitan-muzesi-daimi-koleksiyonunda/>

Burcak Bingol deals with issues of identity, alienation and history in her works. In recent works she analyzes the dilemma and tension caused by the fragility of the ceramics that is a hard material. (Ergenç, 2017) (Bingol, 2016) She focuses on the concepts of history, culture and cultural heritage in solo exhibition 'Mitos and Utopia'. The art work, called 'Self-Conscious' (2015) is a 43-second video recording of a conscious breakdown of a vase. This thin necked pitcher, one of the classic ceramic form of the Ottoman period, is pushed suddenly by the artist's enthusiasm from the edge of the table. (Ulya Soley 2016), (Bingol,

2016, 2017), The broken particles are smeared around. The integrity of the form is diffused. Therefore, the work of Burcak Bingol is not a destructive action in which cultural data is destroyed. On the contrary, it is an art form that is built with the consequences of destruction, breaking and violence. The artistic action has fragility just as our personal and social history

Instead Of The Result

Art history is full of many examples of art works being destroyed. But the 20th century artist tried to transform the destruction of borders into an artistic form. In recent years, fragility, the peculiar physical structure of ceramic materials, is central to the creation of the artwork and its meaning of fiction. We often complain that a hard material such as ceramics is cracked. This negative feature has transformed into a medium of expression in studies involving critical approaches to issues such as history, culture, identity, and so on. Fragility is at the center of artistic activities, including vandalism.

While destruction damages the formal integrity of existence, it as an artistic action is defined as a method of producing a new reality, a new form. In fact, it is not the object and the material that is destroyed. Its historical context is fragmented. Therefore, the destruction comes out as an attempt to establish meaning in contemporary art.

Referances

1. Antmen, A., (2008) 20.Yüzyıl Batı Sanatında Akımlar, Sel Yayıncılık, İstanbul
2. Artun, A., (2018a) Dada Hakikati, Erişim: 15.09.2018, <http://www.e-skop.com/skopbulten/dadanin-hakikati/3702>

3. Artun, A., (2018b) Sanatın Sınırları, Erişim 15.09.2018
<http://www.aliartun.com/yazilar/sanatin-sinirlari/>
4. Başar, S. (2012) Çin Çayı Yada Coca Cola, Genç Sanat, Sayı:208, s. 41-43
5. Bingöl, B., (2016) Seramik Yapmak ya da Yapmamak, Pera Müzesi, “Seramik Sanatında Dün ve Bugün”, Söyleşi, 15 Nisan 2016 <https://www.youtube.com/watch?v=W1vaeDWvNIU>
6. Bingöl, B., (2017) ARTtv, Burçak Bingöl, Mitos ve Ütopya | Zilberman Gallery, <https://www.youtube.com/watch?v=m4enC864kDY30> Mar 2017 tarihli söyleşi, Erişim:6 Ağustos 2018
7. Brougher, K., (2012). According What?, Ai Weiwei, Hong Kong, s:38-43
8. Carson, M. (2013), Performans, Dost Kitapevi yayınları, Ankara
10. Currah, M., (2003), ‘Consciousness/Conscience’, Erişim 12.04 2011
http://www.claretwomey.com/projects_-_consciousnessconscience.html
11. Danto, A. (2013) Sanat Nedir, Cev.Zeynep Baransel, Sel Yayıncılık, İstanbul
- Ergenc, E., (2017), Neither Mythos, Nor Utopia Unlited, https://docs.wixstatic.com/ugd/685bc7_275e750da978403cb2cef697c828baed.pdf
12. Germaner, S., (1997), 1960 Sonrası Sanat Akımlar, Eğilimler, Gruplar, Kabalcı Yayınevi, İstanbul
13. Güner, K., (1987), Eylemde Bir Sanattır, 2000’e doğru Dergisi ‘Eylem de Bir Sanattır’ Nisan- Mayıs
14. Jongh, K., (2008) Kris Martin , Erişim: 02.09.2018
<https://files.artbutler.com/file/77/28c2b6dc0aa74635.pdf>
15. Karavit, C., (2002) Akadegilmi: Akademiden Üniversiteye Geçiş Sürecinde 1980-1990 Yılları Arasında Öğrencilerin Deneysel Hareketleri, Stüdyo İmge.
16. Mundy, J., (2012), Lost Art: John Baldessari, <https://www.tate.org.uk/context-comment/articles/lost-art-john-baldessari>
17. Soley, U., (2016), Burçak Bingöl, Pine Magazine Aralık / December 2016 https://docs.wixstatic.com/ugd/685bc7_86ea084a89274eeabf868d31616923e7.pdf
18. Sozen, M., Tanyeli, U., (1992) Sanat Kavram ve Terimleri Sözlüğü, İstanbul
20. Twomey, C., (2017) Why I Create, Erişim:01.09.2018
<http://uk.phaidon.com/agenda/art/articles/2017/september/20/clare-twomey-why-i-create/>
21. Yap, C., (2010). A History Of Violence, Art Asia Pasific magazine, Erişim: 02.09.2018 <http://artasiapacific.com/Magazine/71/AHistoryOfViolence>
22. Zeytinoğlu, E., Leyla İle Mecnun Öyküsünün plastic Yorumu, Hürriyet Gösteri, sayı 155 (Ekim 1993). p.76-77

<https://cfleononline.org/lia-bagrati-oni-contemporary-ceramic-art/>
http://www.claretwomey.com/projects_-_consciousnessconscience.html
<http://safiyebasar.blogspot.com/>

THE USE OF CERAMIC MATERIALS IN ARCHITECTURE AND ITS CURRENT STATE

Melda Genç

¹Ondokuz Mayıs University, Faculty of Architecture, Fine Art Campus, Samsun /Turkey

The ceramics, which are as old as the human history, have been formed by the combination of earth and fire, allowing the nature itself to be transformed into objects which are used for different purposes. Throughout the history, ceramics, which is a part of nature, sometimes have been functional objects that have met people's needs and sometimes have become tools reflecting their own feelings and emotions, their culture and history. Items such as religious idols, ornaments, kitchen tools and utensils have been used as architectural building elements in many areas. Especially today, the position that Ceramics has established in both art and industry, has become very important with the developing and evolving technologies. Being one of the most important employment areas in Turkey, Turkish ceramic industry managed to be among the first 10 countries in the world in global ceramic sector in the fields of the ceramic sanitary stoneware, ceramic floor and wall coverings. Not only in commercial areas, but also with the developing technologies, with the ever developing and evolving ceramic production methods, artists and designers are able to produce different, creative and new alternative works. In this context, the use of ceramics in the historical process of the Architecture will be investigated in order to understand the present state of the Ceramic Materials in Architecture, to investigate the significance, effects and contributions in the Architectural constructions, and to reveal more creative and alternative ideas and solutions. In the scope of this research, the purpose and area of use of the ceramics will be examined by the supporting visuals.

Usage of the Material Ceramic through the Historical Process

We have encountered ceramic in different forms from the past to the present. While ceramic started to appear in meeting the daily needs of people in ancient ages, it has turned into a tool through which people express their thoughts. It has enlightened the way for us to obtain information on the civilization that has been living from the past to the present. In short, ceramic is obtained by mixing clay and water and making the resulting product durable by using fire. In addition to this, ceramic, which is a part of nature, has led to the emergence of products in a very broad range as it is waterproof, durable and suitable for both functional and artistic usage (Table 1). The historical process witnessed various forms of its usage such a production of pots and pans and jars for storage, idols and containers for religious ceremonies, lamps for lighting, tablets for communication and documentation, tiles, drains and pipes as construction materials, and ornamental objects for daily use.

AREAS OF USAGE FOR CERAMIC IN THE HISTORICAL PROCESS

for	storage	symbolic significance and religious ceremonies	provide illumination	to communicate information and keep records	construction materials	Personal adornments	Domestic items	Placing the ashes of the dead and	burial
Clay was shaped into	Pots and jars	Idols	lamps	tablets	Bricks, roof tiles, water pipes and water channels	Jewelry	Pots, bowls, hearths and spindles	urns	sarcophagi

Table 1. Areas of Usage for Ceramic in the Historical Process

In the present era, developments in technologies and the changes in the sociocultural and economic aspects of societies have led to the expansion of the product range of ceramic. It has developed into a sector that ranges from electronics to spacecraft (Table 2).

AREAS OF USAGE FOR CERAMIC TODAY

Building Ceramics	Bricks, Tiles, Wall and Floor Upholstery Plates, Water and Drainage Pipes, Medical Tools
Ceramics as Household Objects	Pots, Pottery, Ornaments, Table Ceramics
Electricity	Breaker and Fuse Parts, Low-High Voltage Isolators
Electronics Ceramics	Magnetic, Dielectric, Piezoelectric Ceramics
Refractory Ceramics	Firebricks, Silica, Basic, Carbon Bricks, Graphite, Fire Cement
Abrasive Ceramics	Grinding Wheels and Sands, Synthetic Diamond
Bio-ceramics	Ceramic Bones, Prosthetics, Teeth
Nuclear Ceramics	Nuclear Fuel System Ceramics, Heavy Concretes against Radiation
Mechanical Ceramics	Pistons, Engine Blocks
Cermets	Ceramic-metal Blend Parts
Spacecraft Ceramics	Coatings That are Resistant to Heat and Friction, Runway Platforms
Superconductor Ceramics	Energy Transmission Systems

Table 2. Areas of Usage for Ceramic Today

Usage of the Material Ceramic in Architectural Structures in the Historical Process

In general, ceramic has a very broad area of usage including building materials, household objects, electronic and refractory ceramics, nuclear, bio-, mechanical and spacecraft ceramics. If we look at the historical process, in usage of ceramics in architecture, the abundance of clay which is the raw material of ceramic has made them easily accessible materials. Its usability in buildings is possible due to its transformation into a hard and durable material when heated, its waterproof nature and fire-resistant properties. In time, adding colorings in addition to the raw materials that form ceramic and then the invention of glazing led it to be used for decorative and ornamental purposes. Its usage for building purposes may include bricks, tiles, wall and floor upholstery plates, water and drainage pipes and ceramic medical tools. Before the utilization of fire, the usage of ceramic in buildings throughout the history may be dated back to the practices of shaping clay in Anatolian and Mesopotamian lands in the Neolithic Period. The usage of ceramic by firing the clay started in the Bronze Age. As a coating material, it was both used to provide protection from external effects and for ornamentation. It was used for both building and ornamentation purposes in the civilizations of the Assyrians, Babylonians, Etruscans, Phrygians and Lydians especially in the Iron Age. Walls were covered with plates that were called Terra Cotta in the Phrygian and Lydian civilizations (Kayserilioğlu, 2010,6-7). The usage of earthenware bricks was dated back to the 4th century BCE. The excavations by Robert Koldwey between the years of 1887 and 1917 reached information on the making of bricks in the city of Babylon. In around the year 2000 BCE, the drainage pipes of the Babylonians were made of ceramic. As the need for roof materials increased with the usage of earthenware bricks, the Corinthians started to build tiles that were called Concave Tiles. The Romans facilitated the formation of the standards in the improvement of tiles and bricks. Archeological excavations revealed that the usage of earthenware bricks in Anatolian lands was started by the Lydians around the 4th century BCE. While the ceramic building materials of bricks and tiles became standards, ceramic coatings also started to change and develop around the same time. In the 6th century BCE, the Phrygians started to embellish the embossed plates they made in a similar way to glazed tiles. The first glazed examples in history were seen in Anatolia in the 10th century. Luster tiles were found in the city of Samarra. In the 8th century BCE, several cultures such as the Egyptians and Tunisians, Karakhanids and Ghaznavids were influenced by glazed tiles. The Anatolian Seljuks and Great Seljuks were highly advanced in using glazed tiles. They gained worldwide fame especially with glazed tiles from İznik that were used in mosques, madrasas, domes and shrines. Developments and changes on floor and wall upholstery plates continued through time. In the 16th century İznik, as one of the centers of tile-making then, lost its influence, but Kütahya have preserved this tradition up to our time. After the establishment of the republic, ceramic has become a sector, and ceramics artists started to contribute to architectural structures. After 1950, usage of artistic ceramic wall plates in the interior and exterior surfaces of modern architectural structures, hotels, government buildings and factories became highly popularized. After 1970, usage of ceramic products and their applications on surfaces increased.

Ceramic is still prevalently used in bricks and tiles. In particular, using bricks not only for building walls but also in floor upholstery, parks and walking paths, and even usage in sculptures, has continued.

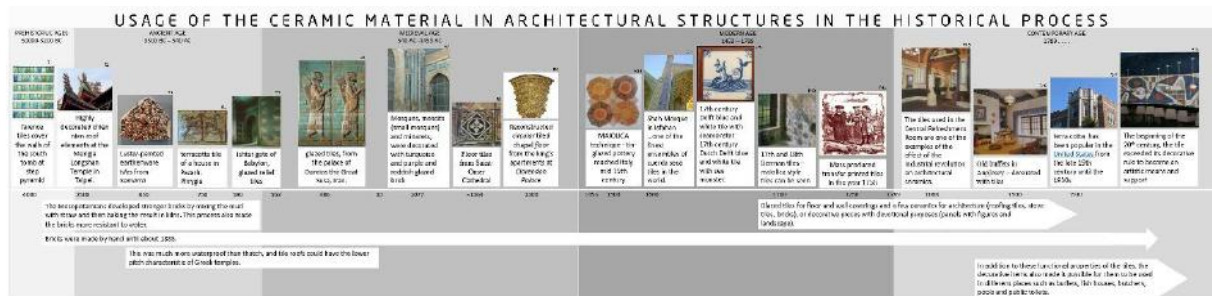


Table 3. Usage of the Material Ceramic in Architectural Structures

Usage of the Material Ceramic in Architectural Structures Today

With the development of ceramics technology today, there has been significant improvements regarding the raw materials of ceramics and formation of glazes. After the developments and diversifications that have been experienced in the raw materials of ceramics and glazing and today's advanced technology were combined, this led to changes and developments in the methods of manufacturing such products. In recent years, even personalized floor and wall upholstery plates started to be produced by reflecting the desired pattern, picture and color on the desired surfaces in architectural structures using ceramic printers that are able to print the desired images on a surface. Different designs could be possible by cutting tiles into a desired shape by the development of water jets. Likewise, the possibility of cutting bricks by equipment such as water jets provided opportunities for different and alternative designs.

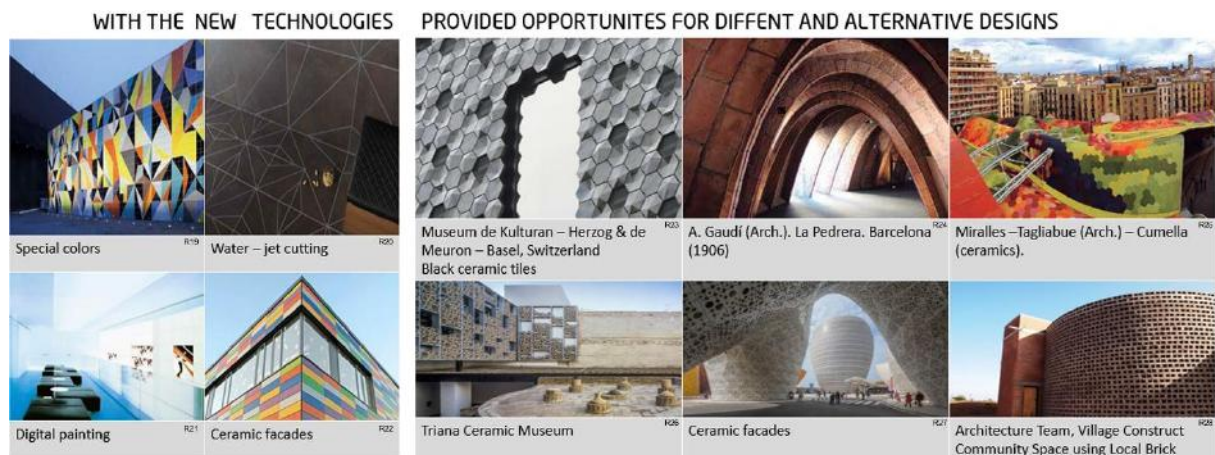


Table 4. Ceramics Practices That are Used in Architectural Structures Today

Conclusion

Usage of ceramic in architecture in the historical process occasionally gave way to the emergence of the floor and wall upholstery, ceramic medical tools and brick and tile sectors. The history of ceramic in Anatolia, which is deep-rooted, brought the ceramics sector in Turkey to a significant position in the World. However, there is a necessity for changes in both production and design with more creative and alternative solutions considering to the changing needs due to sociocultural changes. This study reveals the significance of the material ceramic from the past to the present. This significance has stayed on a level whose influence cannot be neglected in terms of both functional and artistic aspects.

REFERENCES

- Ağatekin, M., *Cumhuriyet Sonrası Çağdaş Türk Seramik Sanatının Gelişimi ve Anlatım Dili Yönünden Değerlendirilmesi*, Yüksek Lisans Tezi, AÜ Sosyal Bilimler Enstitüsü, 1993.
- Özturanlı, G., *Çağdaş Seramik Sanatında Geleneksel İzler*, III. Uluslararası Katılımlı Seramik, Cam, Emaye, Sır ve Boya Semineri, Eskişehir, 17-19 Ekim 2005.
- Görçüz, G., "Tuğla ve Kiremit Endüstrisi Kısa Tarihçesi", *Tuğla ve Kiremit Endüstrisi. Tukder Tuğla ve Kiremit Sanayicileri Derneği*, 1996 1.1: 16-18.
- Era, A. C. Geleneksel Harman Tuğlası ve Üretimi. *Mesleki Bilimler Dergisi (MBD)*, 2(2).
- Kayserilioğlu, S. Selçuklu ve Endülüs Dönemi Kaplama Seramiklerinin Karşılaştırmalı Değerlendirilmesi ve Günümüz Karo Endüstrisine Yansımaları. Yayınlanmamış yüksek lisans tezi. Mimar Sinan Üniversitesi, 2010.
- Tokman, L.Y., *Mekan Psikolojisinde Renk, Doku, Seramik ve İnsan*, III. Uluslararası Katılımlı Seramik, Cam, Emaye, Sır ve Boya Semineri, Eskişehir, 17-19 Ekim 2005.

IMAGE REFERENCES

- R1 https://commons.wikimedia.org/wiki/File:Tile_LACMA_M.80.198.100.jpg
- R2 Betchold, M., Kane, A., King, N. *Ceramic Material Systems in Architecture and Interior Design*. Almanya: Birkhauser ,2015
- R5,, 10,15 Herbert, T., Huggins, K. *The Decorative Tile in Architecture and Interiors*. (reprint 2000). Londra:Phaidon, 1995.
- R4 <https://www.ack-images.co.uk/archive/-2UMDHUHGK9FV.html>
- R8, R9, R13, R16 Lemmen, H. V. *Tiles in Architecture*, Laurence King Publishing, 1993
- R26 <https://www.archdaily.com/571235/triana-ceramic-museum-af6arquitectos/54729a4de58eced61f0000eb-portada-jpg>
- R27 <https://archiobjects.org/archea-associati-liling-ceramic-museum-in-china/>
- R28 <https://cfileonline.org/architecture-cylindrical-contemporary-ceramic-architecture-rural-edition/>

CERAMIC EDUCATION UNDER EVALUATION UNIVERSITY-SECTOR COOPERATION IN TURKEY

Prof.S.Sibel Sevim¹, Fulya Savaş²

¹Anadolu University ,Faculty of Fine Arts, Department of Ceramic ,Yunus Emre Campus, 26470
Eskişehir /Turkey

²¹Anadolu University ,Faculty of Fine Arts, Department of Ceramic ,Yunus Emre Campus, 26470
Eskişehir /Turkey

The transformation of the industry is based on the republican era ceramic art in Anatolia. Provider of the ceramic industry coincides with the planned development period in the 1950s. Being one of the leading Turkish ceramic industry sector of our country with the number of people directly and indirectly employed is over 220 thousand.

Turkey also ceramics education, first in 1929 in the academic sense, began with the establishment of the ‘‘Sanayi-i Nefise’’ school opened up within the Department of Decorative Arts . After that developing when the ceramic training process, where today 21 programs at the undergraduate level in Turkey, but when the training given in these programs is examined it is precisely parallel to the ceramic sector is not observed. The dynamics of the industry disagree with the content of the course leads students graduated in the sector remain inadequate. Despite the rise of universities that growth and education of the ceramics industry ceramics are faced with problems in education. These issues are also slow the effects of the ceramics industry. The reason for this is the university and the dialogue in the ceramic sector is not done sufficiently. Ceramic education in Turkey in this article, ceramic industry and ceramic solutions by examining the relationship between education providers will be universities.

Keywords: ceramics industry, ceramics education, ceramics, ceramic art

1. INTRODUCTION

The industrialization of ceramic art in the Anatolian came across with the development period in 1950's. After World War I, many reforms made about socio-cultural and economics due to extend the lost. With the effect of the Industrial Revolution, it made radical changes in economy with the support of government new business locals came up. The process after the, Industrial Revolution educates art due to had an impact of art education with the new art education the ceramic industry came up with a new period.

Established at the beginning of 1950's developed the ceramic industry after the 1980's and was competitive. After the 1990's the ceramic industry modernized and changed with global technologic systems. Today, Turkish ceramic industry is the most powerful and developed industry on global marketing, thus ceramic materials, ceramic medical materials, ceramic kitchen materials, technical materials and porcelains e.t.c. have a very important role in these industry. Directly and indirectly, the number of persons employed is over 220 thousand.

The formation of ceramics in our country as an art branch and the establishment of education in this context are seen together with the establishment and spread of the industry. The tendency to send education to abroad, which is seen in other art branches within the movement of change with the foundation of the Republic, also lives in ceramic art. In this direction İsmail Oygur and Vedat Ar in France; It is known that İzzeti is the first ceramic education in Germany and ceramic

education with its home country started in our country. This article research, which examined the relationship between university and industry cooperation by considering which university education in Turkey, ceramics and ceramic industry will be solutions.

2. THE HISTORICAL DEVELOPMENT OF CERAMIC EDUCATION IN TURKEY

The education of Turkish ceramics started with the establishment of the Department of Decorative Arts first opened in 1929 in the academic sense of Industry Nefise School. After 1952 in Ankara, Gazi Muallim art and industry school had opened the new ceramic education school. In 1957 in İstanbul fine arts faculty of İstanbul University opened a new department about ceramic art education. With the new schools and departments had an very important role in Turkish Republic and industry.

With the establishment of Turkish Republic it had been many developments and radical changes due to economic life, socio-cultural life and and modernization. with these radical developments, Turkish ceramic art had reached in an important process. After the National establishment, the developing of ceramic industry grew faster with the reforms made about fine arts. Socio-cultural revolution and industry, ceramic locals and business stores factories began to reach because lack of the western education system in turkey education schedules, programs and students went to abroad.

İsmail Hakkı Oygar, Vedat Ar and Hakkı İzzet impressed by the “Arts and Craft” Art Nouveau, Bauhaus school and art Deco Art Crafts. They bring together their education system due to they saw and imprison in Europe and, and academic art works together. They an very important role in ceramic art and education, within the industry. They were a role model to many ceramic artists and academic professors within they succeed their art reforms many years. İsmail Hakkı Oygar, Vedat Ar and Hakkı İzzet believed after the establishment of Republic the ceramic education system and ceramic art must work with together and made studies about that topic Oygar said that “as seen the reason of industrial revolution, the arts and crafts impressed the early republic ages not so well. the industrial stuffs should be designed by arts works. Ceramic industry, ceramic art and ceramic education always support themselves.” (Aslan, 2014:15-17)

Being formal researches about the ceramic industry. In the years of 1950 ceramic industry factories that producing ceramic with traditional methods had gained importance within students who had ceramic education can collaborate with more quality systems and schools. By the way, industrial studies gained speed in Turkey the artists design project became importance. With the developing of university and academic education programs with the industry made up unique art-workers designs in ceramic industry.

The establishing of Eczacıbaşı Art Studio in 1950 was the main support business sector to artists and art-workers. Ceramic artists worked in Eczacıbaşı art studio many years and gained many different experiences about ceramic educations. Melike Kurtiç, Sadi Diren, Atilla Galatalı, Alev Ebuzziya were the main art-workers in Eczacıbaşı art studio Alev Ebuzziya continued her work in Denmark, Melike Kurtiç in Copenhagen kingdom porcelain fabric, Atilla Galatalı continues his work as personal and Sadi Diren continues to be an art-worker in fine arts academy.

By the way at the 1950's in Turkey, a new system came out. Impressed by the Bauhaus school process Prof. Dr. Adolf Schneck (Stuttgart fine arts academy) came up with the idea of opening a governmental support fine arts academy. The main goal is developing turkey's industrial art-workers. There are; graphic design, art, ceramic, textile, architecture etc.. in five stages. There are many foreign educators in school. The governmental support fine arts academy is now as a department in Marmara University. (Aslantürk, 2009:62) Then in 1983 in Hacettepe Anadolu and in 1987-88 in Dokuz Eylül University opened the department of ceramic of ceramic industry

Ceramic education has a very important role in the industry by the last years. We can think that; its an industrial development and impact by the ceramic education today in Turkey 21

programs are available with bachelor degrees in ceramics. (Ağatekin,2017:134) In general education system is applianceful and they still use the Bauhaus method. The education system about ceramic is now modernized and has gained an importance in global.

3.EVOLUATION OF CERAMIC EDUCATION OVER CERAMIC SECTOR IN TURKEY

According to the development of ceramic education, and with common ceramic raw in Turkey. Thus, Anatolian people acquainted with this material for thousand years during the Republican Period in Turkey. ceramic develops both as an art and an important industry material. That way ceramic industry material. That way, ceramic industry development was an important step, in terms of 1. Economics at the Congress in 1923. "The real need of art and the need of art-workers designs" (Oral,2005:2) with the new radical change about ceramic artists in Turkey, the collaboration made a revolution thus ceramic is an art after the establishment of the Republic, development of the ceramic industry has a main role about industrialization in Turkey.

Industry in the process of being established as a result in Turkey after 1950 the development of transport facilities, increase in population from rural areas to cities to begin the migration, factors such as the well to invest in industrial private sector as well as the public sector has led to the development and diversification of the ceramics industry.

The industrialization of ceramic began with the industry revolution in 18. Century. After the industrial revolution serial production of requirement causing the ceramic industry and designing to lack of need.

The Turkish Ceramics Industry has gained an important place in the world with the increase caught in capacities since the beginning of 2000's. Export in Turkey in the ceramic tile industry in the world export ranking 5, 9 in the world production ranks 3rd in Europe. In 2013, an amount of 102 million m2 of exports reached 606 million dollars in the end of the year in coating materials. Ceramic sanitary ware has closed its year-end with sales of approx. 10 million units, with the first in Europe in export and the third in the world in terms of sanitary ware category 203 million dollars. The number of persons employed in direct and indirect employment and in sales, marketing and application is 220.000 persons in assistant industry, design, number of workplaces and employment in industry. In parallel with the development in the construction sector, the number of companies producing free based recertification in the sector and the amount of production increased rapidly in the last 20 years (Ağatekin, 2017: 134)

In parallel with the developments in the ceramic industry in recent years, there is a considerable increase in the number of universities offering ceramics education. We can +think the rates are the impress and reason back to 1980's. Today we can see that it takes 21 programs about ceramic education with bachelor degree. . Also, we can see that, the main role in ceramic education is being creative. Designing materials are also important. Also we can see that, the education is not enough for students. For example: digital machines in ceramic ed systems are extremely expensive, the classes are not available for industrial designs. With these problems students may have problems with adaptation after graduate.

Ceramic education in Turkey, parallel exchange of art and industry / development in unstable conditions and competition in the information age in which we live is very important. Today, important investments are being made by the state and private sector in order to improve the art of ceramics, industry and education, and to train better equipped individuals in the field. The Ceramic Research and Development Centers (SAMs), which are established especially in the structures of the universities, aim to investigate and develop ceramics belonging to the locality they belong to primarily in structural, structural and industrial areas. Such initiatives are very important for sector and university relations.

In the increasing competitive environment in the world, the importance of education is great for companies not to attract qualified personnel due to the rapid change of technology and

knowledge at every stage of production. Young population with ceramic industry in Turkey in sectors such as manufacturing, design stages for the growth of the age of information and personnel with the skills required by industry-university cooperation will take place in the sector by making qualified personnel should be trained. Even if the universities follow the technological developments in the ceramic sector, they can not reach the technology that the sector has because they can not make production. Because the costs of the machines used in the sector are quite high and there is no necessary environment for these machines and devices to be able to implement because they can not be owned in universities. In this process, it is expected that the universities of the sector will open their doors. The industry has to increase the production capacity and add the latest technological devices to make quality products. On the other hand, if we think that the students will take part in the sector after graduation because of the lack of technological devices in terms of education given in universities, there will be a problem in terms of adaptation proces. In this case, the students who will be in important positions in the future by opening their doors to the universities of the industry should not see them as a footstep at the beginning of their business life.

The university industry collaboration was always a topic within years but the industry should work with university talking and mention about it not enough. For example with that topic is; uşak university. Serenova ceramic fabric can do a collaboration due to make students ed system more quality. Part students under this protocol; students have the opportunity to develop their practice by familiarizing themselves with the practical applications of the courses in the curriculum and the production processes. Among the graduates, those who fulfill the criteria of the company are employed. At the 2018 UNICERA ceramics trade fair, Hasan Hilmi Alper, Chairman of UMPAŞ Holding, stated that they will provide all kinds of ease by opening up the young people and they will employ a part of the students who graduated in the forthcoming periods on a regular basis every year. Meanwhile, the firm that supports the academicians, Instructor Şirin Koçak exhibited the works of Özeskici at the ceramics exhibition and showed his support to the academicians.

Another initiative in terms of industry-university cooperation is the exhibition of the designs of the students in the UNICERA Ceramics, Bath and Kitchen exhibition, which are designed by Prof. S.Sibel Sevim in the context of the Industrial Decorations Course.



Visual 1. Ceramic tile designs of Prof.S. Sibel Sevim students

UNICERA Ceramic Fair, 2018



Visual 2. Sefer Can Yilmaz's tile design within the scope of Industrial Decoration Applications course conducted by Prof.S.Sibel Sevim

It is considered that the original designs made during the period are producible in the sector. All students in the ceramics industry to exhibit their designs UNICERA ceramics exhibition, where in Turkey; On the one hand, it is possible to present a unique and different design concept to the firm, while on the other side opportunities to meet and discuss with the most important companies and companies that the students will never see together, and students who are on the eve of graduation are allowed to find work. This initiative; it is a very motivating situation both in terms of sector, student and academicians. Such trends and relationships are important and promising for the development of industry and university cooperation and for shedding light on the future. The other side is the sector; they also need to take advantage of the ideas of highly valued academics. Because it is important to remember how important it is to those who give direction to information when it is taken into consideration today. When these relations are achieved, the following tabloda will be able to invest in the future of the companies with the right supports that will be lucrative on both sides, educated and will play an important role in the development of the economy.

Gains of the ceramic industry	Gains of the university
Access to the facilities of the university	Development of the university curriculum for education and training
Industrial corporations gain positive prestige of working with universities	Access to potential business opportunities for graduates
The knowledge accumulated in the counseling of teaching staff	Becoming an industrial member of the university's advisory committees
Participation of lecturers in conferences organized by industry	Provision of internships and other similar opportunities for students
Solution of problems in industrial projects	To support the knowledge of faculty members, researchers and students with practical applications
Opportunity to work together and gain economic benefit	Government funding for applied research with industry
	Access to the possibilities of the industry

4. CONCLUSION

When the university-industry cooperation is established as required, as mentioned in the above table, significant contributions will be made if the future of the country is opened by benefiting both sides. As long as the university is in good communication, the sector will have access to each other's opportunities. Long-lasting cooperation and technology development between university and industry can be sustained on the basis of mutual trust. The competencies of universities, human resources, technological research infrastructures as well as the industry can be achieved only by combining the right and self-compatible requirements.

Today's students with creative thinking, which is an integral part of the system, can be provided by tomorrow's innovative researchers, but with the right goals. Our universities can decide on what kind of initiatives they should undertake in their own organizations by attaching importance to cooperation with industry and determining their own policies and considering them as a part of their missions. Having industrial members in the council of universities is a prestige in terms of industrialists and an important issue for the development of relations. On the other hand, if the sector opens its doors to universities, the students will be able to see the applications of their designs with developing technology like digital production, as exemplified above, where academicians can follow the technology that is constantly progressing. Students will also be able to apply their skills in the sector and if they graduate they will be ready to work in the sector and will be able to easily adapt their adaptation processes. Together with the support of the university, which is one of the sectors that shape the ceramic industry, Turkey's economy will solve the problem of qualified staff so that graduating students will be able to exercise their profession. In the event that the sector does not miss important details such as business alliance with universities in a competitive environment, more accurate planning about the future will be made. With such initiatives, with both sides benefiting, a significant added value will be achieved by using the employment opportunities in the country correctly.

REFERENCES

- 1.Ağatekin M., "Ceramic Training Programs at the undergraduate level in the Fine Arts Faculty in Turkey About Situation Analysis and Assessment", Seven Art, Design and Science, İzmir Dokuz Eylül University Faculty Publications Fine Arts, Issue 17,2017, 134.
- 2.Aslan E., "Arts and Crafts Movement and Contemporary Turkish Ceramics Manuscripts", Erciyes University Fine Arts Faculty Magazine, Erciyes Sanat,2014,15-17.
- 3.Aslantürk G., "European influences on contemporary Turkish ceramics in the 20th century", Ege University, Institute of Social Sciences, Department of Turkish Islamic Art, Doctorate Thesis, İzmir,2009, 62.
- 4.ORAL M.E.,Development of Contemporary Ceramic Art in Turkey,2005,2.

**A SURVEY ON COMPUTER AIDED DESIGN PROCESS WITH 3D PRINTING
IN CERAMIC EDUCATION
CASE STUDY: A CREATIVE DESIGN EXPERIENCE FROM DIGITAL SPACE TO
PHYSICAL 3D PRINTING**

Assoc.Prof. Ezgi Hakan Verdu Martinez¹, Research Assistant Emre Can¹
¹ Anadolu University, Faculty of Fine Arts, Ceramics Department, Eskişehir

ABSTRACT

Throughout the history of mankind, while the pots, which are one of the most basic needs of man, began to take their place in the history stage, with pots rising by coiling method of the Neolithic Age, ceramics turned into daily use items and became indispensable for mankind by invention of the potter's wheel. This adventure which started in 10.000 B.C., and continued uninterruptedly; in the meantime, ceramics took an important place in human life today in a wide range of products such as tableware, sanitary ware, high technology products as well as artistic sense content.

Along with the developing technology, new shaping methods have begun to be used in ceramics, in addition to traditional shaping methods. Computer-aided design and production technologies, which started to be used in the 20th century, brought a different dimension to industrial design and production, leading to the rapid production of designs in the field of ceramics. Rising the forms with the 3D Printer is also one of the new shaping methods. It is noted that 3D printing is still under development, while it is being used as rapid prototype tool at the beginning of the 21st century, in mass production based systems; besides attracting attention of ceramic artists interested as a supporting shaping tool in their artistic expressions.

While such technological developments are experienced in the ceramics sector, these developments have also become inevitable in ceramic education. It is important for students in ceramics education to gain awareness about the use of technology in the ceramic field.

In this research, a case study is presented which is transformed from 3D printing works carried out using computer aided design and production methods by ceramic students. The aim of this research is to draw attention to the necessity of using the technologies that orient the ceramic sector in computer generated ceramic design courses in the Faculty of Fine Arts Faculty Ceramic Departments. Such trends allow students to see their designs in a computer modelling as a three-dimensional prototype and to develop their creativity in a digital environment. Believing that this would provide an advantage for students to be aware of technology opportunities at the point of developing their career potential after their training.

Keywords: ceramic, education, computer, 3d print

INTRODUCTION

3D printing, the latest point of Rapid Prototyping technology is an additive manufacturing process that has reached to the level to use ceramic materials in the last quarter century, thanks to its pioneers who developed ways to shape ceramics by 3D printers with ceramic powder and clay, besides various plastics and filaments which obtain the textures of wood, metal, paper by using layered manufacturing methods.

Having the roots of invention dating back to 30 years, 3D printing has been introduced to ceramics world after Adrian Bowyer's self-manufactured RepRap 3D printer, which enabled the introduction of 3D printing technology, to the designers and ceramic world around 10-12 years ago from now. Since this FDM (Fused Deposition Modeling) type printer is self-manufactured, it leads artists and designers in their studios who want to make 3D printing and enables studio-type 3D printers set up at low costs.

English Professor Stephen Hoskins and his team at the Print Research Center, affiliated to the University of West England in Bristol, launched the first 3D ceramic printing, binding ceramic powders at Z-corp printer (Powder Binding), with the project that they initiated in 2007 to investigate the usability of 3D printing to produce prototypes in collaboration with the ceramic industry (Hoskins, 2013, 49).

In 2009, the first ceramics forms were printed by Unfold design studios in Belgium by Dreis Verbruggen and Claire Warnier installing a ceramics kit to a FDM type of 3D printer which originally works with melting or paste materials with extrusion method; so that a new technique has been discovered useful for the ceramic artists. This development has been an important step in encouraging the ceramic artists to proceed their own 3D print experiences in their personal studio (Hoskins, 2013, 64).

For the last 10 years, the three-dimensional printing method which is rapidly integrated into ceramic arts by certain leading research and design groups, especially in England and Belgium, attracts attention of many researcher artists. Apart from the teams that have developed projects in Europe, Far East USA in this field, university-sponsored projects stand out in various parts of the world.

STEPS OF CASE STUDY: PRODUCTION WITH 3D PRINTERS

3d printing is a digital layered manufacturing method which resembles hand coiling method used by human being centuries ago to shape the clay. In fact, alike hand skill for lining up the coils successively, the production completed by 3D printing may be defined as a process which requires ability and skill. Computer programming which is inevitable element of 3D printing system shall also be included within designer's point of interest in this process. Designer's dominancy on CAD programs, his ability to solve existing mechanical problems practically, as well as his knowledge about the nature of the ceramic materials enables him to improve fast.

Below the case study, which is practiced during computer aided design course at Anadolu University faculty of fine arts ceramics department has been explained as a process. This study has been led in the spring term of 2018 in the aim of improving computer and design skills, getting involved with modern design issues by increasing technology awareness of ceramic students. The process has been described step by step, starting from research, paper based drawings, Cad modelling to print and firing.

Steps 1: Design: sketch drawing and CAD modelling

In this case study, primarily, the process begins with designer students' sketches and drawings after a period of research. Based on these drawings, firstly the process started on a digital 3D modeling program (NX), using various sections, utilizing CAD software resources. After using solid or surface operations, a form is created on the screen with 3 dimensions with surfaces.

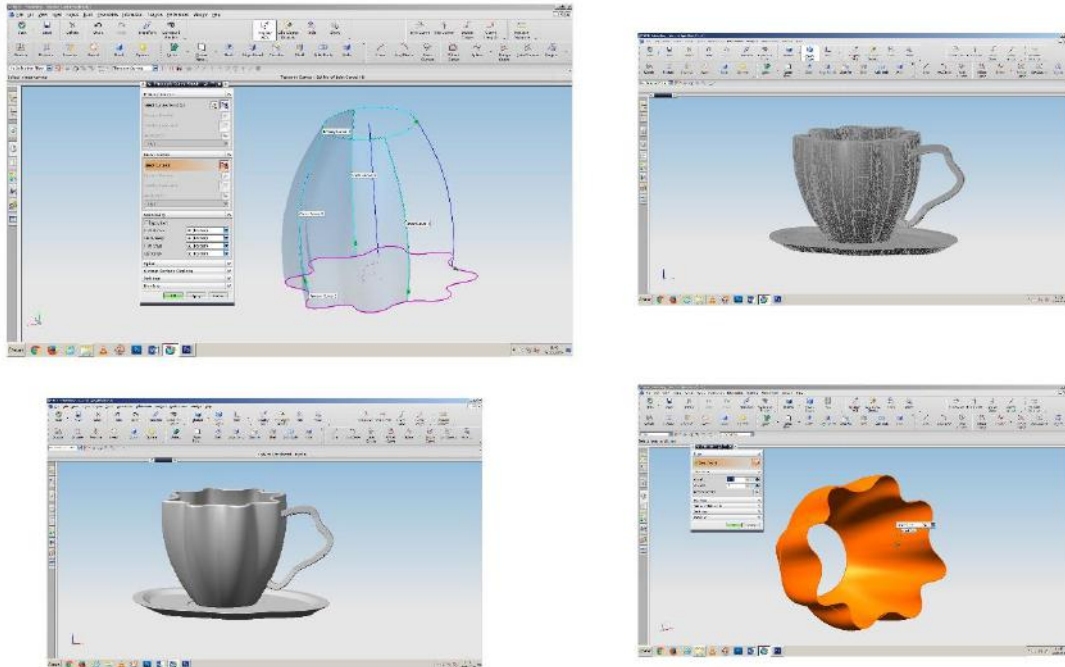


Image 1. CAD Modelling (NX)

Step 2: Layer slicing and converting the model to SLA format

After modelling and deciding the final design in NX program, the computer generated model is recorded in SLA format. Afterwards, part is transmitted to a mediator program such as Cura, and separated into layers in the digital environment, according to wall thickness so as to be produced in 3D printer. The thickness of coils is being determined at this stage. Mediator program slices the form and brings it into a printable manner in the printer. Later the file is sent to 3D printer as G code, thus the process continues upon the creation of digital data therein. While printer is reading the digital file to print, the production period may be calculated approximately.

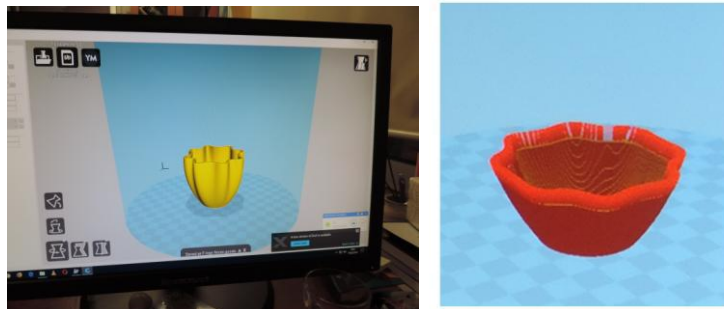


Image 2.3. SLA format of converted digital file, slices of layers to be printed

Step 3: Kneading clay, filling the tube of 3D printer

Later on, the students go ahead to work on the clay in order to transmit the designs from the digital environment into physical environment. It is important to plasticize the clay well and to take air bubbles out, in order to knit the layers firmly during printing stage. After kneading the clay well, the clay has been squeezed and filled inside the tube layer by layer, – which will be subject to injection – with an appropriate plasticizing humidity degree, so that the clay should not dry and stay at proper consistency.



image 4.5. Preparing the clay

Step 4. Controls and starting the print

The tube which is filled with clay shall be combined and placed into the ceramic head of the printer through the air pipe. A plaster slab with perpendicular surface shall be put below the printer before starting, for carrying the form during the printing process. Finally “start” command shall be given to begin printing for the part which has been transmitted from the computer into the printer’s memory by sd card.

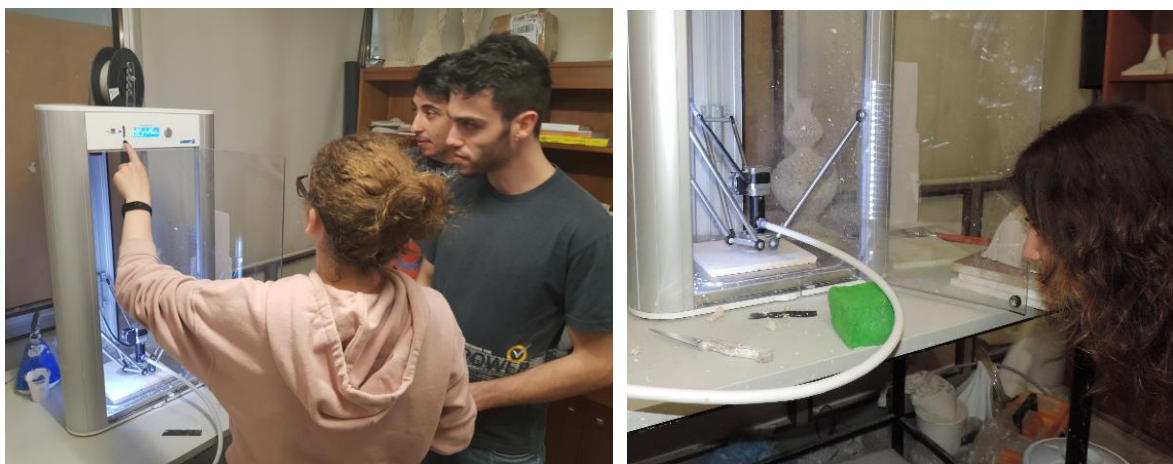


image 6.7. Commanding and checking the printer before process

Step 5. Printing stage

Metal injector (tube) which is connected to the printer through a thin pipe starts to push and squeeze the clay by the air pressure coming from the compressor. As the motor of the printer starts to extrude the clay, the nozzle of ceramic kit begins coiling up the digital file object layer by layer. While the layers are bonding to each other, due to the diameter of the nozzle and the determined layer thickness, the form begins to rise up on the printer. Speed of printing can be determined due to complexity and size of the form.



image 8.9.10.11.12. Printing layer by layer from base to top

At this point, students experience 3D printing as a process which centers the human and which is not far away from craftwork. Processes starting by kneading the clay develops well due to designers work in coordination with the printer. 3D printing; despite being a machine based production method, is such a process where the human approaches towards production.



Image 13.14. Printed plate and cup, left to dry

Step 6. Evaluating, revision

After the printer builds up the form, as it gets to leather hard stage, it can be examined by means of design aesthetics, ergonomics, function and originality. After evaluation, necessary changes can be made on the cad modelling and the file can be sent again to be printed as a revised version. Next to printing all parts of the design such as handle or plate, parts can be attached while the clay is still wet.

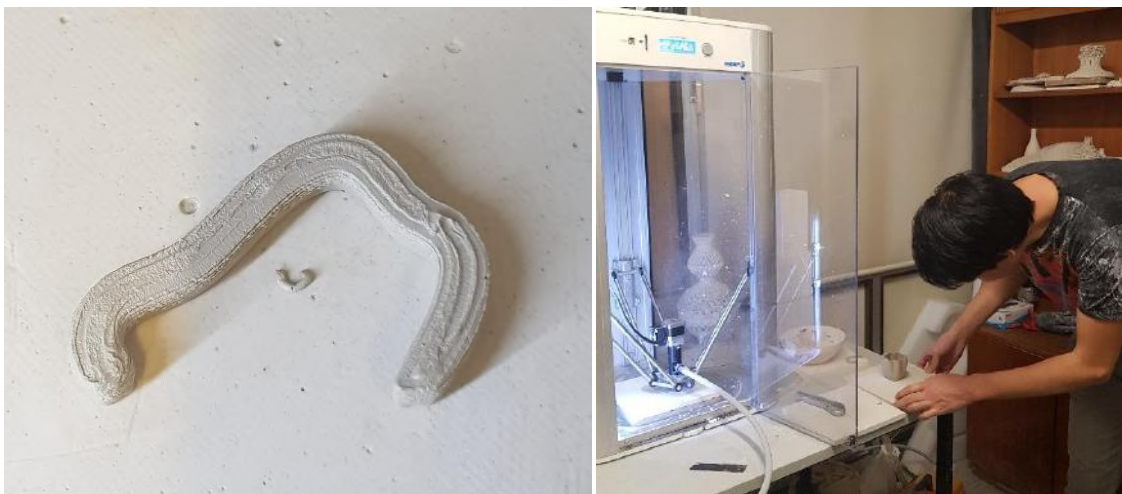


Image 15.16. Hands on learning experience process



image 17.18. Revised piece and detail

Step 7. Finishing touches, drying glazing firing

As the final production is achieved, it can be left to dry, right after retouches it can be sent to firing.



Image 19. 20. Fired piece top and front view

The printer should be viewed during the process to control the movement of the print head to construct a durable form. During printing, the students stay interactive with the printer to stop and make alterations. They make parametric alterations or manual interventions and improvements. In the 3D ceramic works which seriously require attention, patience, elaboration, follow up and control. This helps to improve their communication skill with clay and mechanical dominancy which is a key for the success of the process to cope with today's digital procedures.

ADVANTAGES AND BENEFITS OF USING 3D PRINTERS in CERAMIC EDUCATION

3D print technology gives various opportunities to students from various fields, who are researching material and production techniques. It is a very useful technique for the designers who wish to use various techniques together.

Forms which are unable to be shaped manually or by mold structurally can be produced with 3D printers and give exciting affects while rising on 3D printer. It seems very attractive to students to achieve rapid prototypes and to add their creativity collaborated with artistic touches.

Computer generated design and production has a language and it is reflected to the forms during production. Being a good CAD user provides the capability of using this language in the best manner for students.

In fact, despite being a digital procedure based on computers technically, it is seen that artists can take away their pieces from the mechanic appearance through the artistic sensibility.

Technically, at the final point where RP Technology reached, 3D print system is the final and it enables the trial process by revising the form until it the desired level is achieved. So students can learn to make parametric changes in their designs and broaden their perception.

It helps students to develop different perspectives of thinking and design while expanding horizons. Combining computer technologies with hand-crafting and hand-crafting methods of ceramics art, this offers students the opportunity to develop design and computer skills in a unique and harmonious manner.

CONCLUSION

In this research, a case study has been implemented and presented which is transformed from 3D printing works carried out using computer aided design. The aim of the practice was to work with 3D printers to learn how to manage and rule a digital process from beginning to finish. This has been an experience for students to try an individual design experiment, while having a collaborative work share.

In the last 25 years it is obviously seen that the technologies orient the ceramic sector. The mass production is based on digital systems and it is inevitable to adapt this to ceramic education in the century of high robotic technologies. While working on the programs of ceramic departments, it is necessity to consider the computer aided design as a subject. Computer aided courses in the Faculty of Fine Arts, Ceramic Departments are popular especially for the students who want to develop themselves by means of industrial design. Such trends allow students to develop their creativity in a digital environment and to save time and to see prototypes of their computer generated designs in short time in three-dimension. So improving design skills with computer and 3D printers, students start to lead their design processes to reach the results easier in shorter time and more practical manners. Embracing technological utilities, this would give opportunity to students to face with new generation problems, create solutions and adapt digital implementations to art practices. Pushing the boundaries of imagination, awakening creativity of students, this would help them to widen their perspectives of design and production.

It is also anticipated that integrating training in new technologies and introducing individuals to these technologies during the bachelor degree, will provide an advantage for them at the point of developing their career potential after their training. Awareness of new technologies would support the students to improve computer skills and gain abilities which are demand of design departments at factories based on digital production. Getting involved with industrial production systems and experiencing the

process, the students start to get qualified to work in this field as the companies are looking for employees with digital abilities.

REFERENCES

Hakan, Ezgi. New Technologies of Ceramic Product Design-3D Computer Aided Programs Integrated into Design Practices in The Field of Ceramic Art Education, Journal of Literature and Art Studies, 2012, 329-339

Hoskins, Stephen. 3D printing for Artists Designers and Makers, Bloomsbury, 2013

Makela, Maarit. Ceramics and its dimensions: Shaping the future, 2016

Martinez Hakan Verdu, Ezgi ve Can, Emre. Bilgisayar Destekli Seramik Üretim Yöntemi Olarak Üç Boyutlu Yazıcılar Ve Günümüz Koşullarında Bir Uygulama Örneği, Sanat ve Tasarım Dergisi , Anadolu Üniversitesi, 2016 Haziran

Martinez Hakan Verdu, Ezgi ve Can, Emre. Üç Boyutlu Yazıcı ile Yapılan Farklı Seramik Üretim Yöntemlerinin Karşılaştırılarak Değerlendirilmesi, Pişmiş Toprak Sempozyumu, Eskişehir, 2016

Warnier Claire, Verbruggen Dreis. Printing Things Visions Essentials for 3d Printing, Gestalten, 2014

ÇİN SERAMİK SANATINDA KÜLTÜR, SEMBOLİZM VE ZANAATKÂR

Onur Fındık¹, Sevim Çizer²

¹ Uşak Üniversitesi Güzel Sanatlar Fakültesi Uşak/ Türkiye

² Dokuz Eylül Üniversitesi Güzel Sanatlar Fakültesi, İzmir/ Türkiye

“Doğaya bağımlı kültürlerde, biçim içeriğin aynasıdır”¹

Giriş

Sanat Tarihçisi Jale Nejdert Erzen Çoğul Estetik adlı kitabında, güzel olanın iyi olduğu yargısının doğru olması durumunda, en büyük iyi olan tanrı imgesinin en üstün güzellik kaynağı olabileceğini dile getirmekte ve ardından konuya şu şekilde devam etmektedir.

“Dünyadaki güzellik tanrının bir göstergesi ya da onun eserinin büyüklüğü, muhteşemliğidir. Tanrı ile ya da kutsal olanla ilgili her şey güzelleştirilir, süslenir, tanrıya, kutsala layık kılınır. İnsan değer verdiği şeylere bu değeri öncelikle onları güzelleştirerek, süsleyerek, güzel bir şey vererek gösterir. Demek ki güzel değer verilenin ifadesidir. Bundan ötürü bütün sanatların başlangıcında öncelikle tanrılara layık olanın, onlara şükranın, onlara yaklaşmanın bir göstergesi ve ifadesi olmuştur güzel. Tanrılarla ilgili bütün ifadelerde onları en güzel şekilde temsil etmek o kültürün sanatının da başlıca gayesi olmuştur. Tapınaklar, dini resimler, heykeller öncelikle güzel olmak durumundadırlar, zira tanrının mükemmelliği bu güzellik temsili ile ortaya konulur. Güzel, tanrıya yakın olduğu için de iyidir” (Erzen, 2016: 91).

Bu tanım kültür, nesne ve doğa arasındaki güçlü bağa dair önemli ipuçları sunmaktadır. Tanımda da belirtildiği gibi, güzel olana ulaşma ya da onu kavrayabilme isteği, özellikle antik çağlardan günümüze değin zanaatçılar/sanatçılar tarafından üzerinde durulan bir konu olmuştur. Özellikle Antik Yunan’da “mimetik” kavramı ile ortaya çıkan, Rönesans ile birlikte doruğa ulaşan doğa nesnelerinin taklit edilmesi ve hatta bu eserlerin haddinden fazla Tanrı’nın güzelliğine yaklaşması Michelangelo’da durumu gösterir. Onun bile resimlerinde bu kadar inandırıcı bir görüntü yarattığı için Tanrı ile rekabet ettiği evhamına kapılarak ondan af dilediği rivayet edilmektedir (Erzen, 2016: 22). Güzel olana, doğaya veya tanrıya olan bu yöneliş sonucu zanaatçı/sanatçılar tarafından onun mükemmelliğine yaklaşabilmek adına sayısız eser üretilmiştir. Bu çalışmada batı sanatının aksine, özellikle doğu zanaatı/sanatındaki doğanın, tanrının veya güzelin nasıl tasvir edildiği ve zanaatçı/ustaların bu yaratımları hangi değerler etrafında şekillendirdikleri açıklanmaya çalışılacaktır. Bu bağlamlar kültürel bir nesne olarak Çin seramikleri üzerinde birleştirilecektir. Zanaatın ve sanatın kesiştiği bir nokta

¹ Nejdert Erzen, Çoğul Estetik, Metis Yayınları, 2011, s. 23

olarak Çin porseleni özellikle bu çalışmanın ana materyalidir. Çin porselenini açıklamaya başlamadan önce Doğu sanatında doğanın nasıl soyutlandığı, kültürün doğa ile nasıl bir bağlantıya sahip olduğu, ustaların toplum içindeki konumlarının ne olduğu ve bunlar sonucu ortaya çıkan kültür nesnelerinin neyi ifade ettikleri üzerine bir sorgulamaya girmek mecburiyet gerektirmektedir. Çünkü en basit bir zanaat ürünü veya sanat eseri bağlı olduğu kültüre ait çok karmaşık bağların ipuçlarını verebilmektedir. Bu bakımdan ilk olarak günümüzde sanat denilen eylemin Doğu’da hangi değerler üzerinden kavranarak icra edildiğine dair bilgiler verilmeye çalışılacaktır.

1.1. Geleneksel Çin El Sanatlarının Bilgi Sistemi İçinde Zanaatkâr

Başlangıç olarak, doğu hakkında bilgi temelli örneklerle yer verilirken, batının özellikleri göz ardı edilmemelidir. Ayrıca doğu ve batı kavramları ve içerdikleri anlamlar son derece kaygan bir zemine sahiptir. Bu konuda çok kapsayıcı genellemeler veya tanımlar koymak mümkün olmayabilmektedir. Çünkü çağlar boyu farklı dönemler ve farklı topluluklar arasındaki kültürel alışveriş, herhangi bir karşıtlık ortaya koyma sonucunda yanıltıcı olabilmektedir. Diğer bir husus, doğu ve batı olarak anılan karşıt kültürler, farklı dönemlerde farklı topluluklara ait olmuştur. Örneğin yunanlılar ve persler antik dönemlerde doğu ve batıyı temsil eden iki karşıt uygarlıktır. Ama ortaya çıkan bilgiler ışığında yunan ve pers sanatı kültürel anlamda birbirinden beslenmiştir. Genel bir tanım koymak gerekirse, batı analitik ve eleştirel bir bakış açısına sahipken, doğu daha yaşama temellendirilmiş bir görüşe sahiptir. Bu doğrultudan hareketle Erzen, Doğu’ya özgü durumu şöyle açıklamaktadır;

“Batı-dışı ve yirminci yüzyıla kadar geleneksel kalmış kültürler, sanatları ile daha ziyade geleneksel değerlerini ve yerleşik dünya görüşlerini ifade etmişlerdir. Batı-dışı kültürlerde ve sanat ifadelerinde inanç sorgulanmaz; aklın her zaman daha üstün bir güce bağlılığına inanılır; bilgilerin kesinliğinden emin olunamaz. En önemli ilgi alanı, içinde bulunulan evren ve dünyadır. İnsan onun içinde, ona bağımlı bir ögedir, onun dışında değildir, ona içeriden bakar” (Erzen, 2016: 128).

Bu tanım üzerinden Batı-dışı bir uygarlık olarak Çin’e bakıldığında, doğa ile uyum içinde ve sanatsal olarak bu kaynaktan beslenen bir kültür karşımıza çıkmaktadır. Özellikle resimsel betimlemelerle donatılmış porselen eserlerinde bu etki güçlü bir şekilde kendisini göstermektedir. Bu noktada, bu betimlemelere yalnızca salt birer görüntü olarak bakma dışında, toplumsal bir bilgi kaynağı olduğu gerçeği ile de bakılmalıdır. Konuya böyle yaklaşıldığında primitif veya karmaşık, geleneksel veya endüstriyel herhangi bir teknik nesnenin kaçınılmaz olarak zihinsel bir kullanım planına göre bilgi yüklenerek biçimlendirildiği bir tasarım pratiğinin söz konusu olduğu söylenebilmektedir. Bu durumda tasarım, nesneyi biçimlendirecek bilgiyi nesneye uygulama işidir. Bu nedenle zanaatkar nesnede tanımlanabilir bir değişiklik ortaya koymak için onun materyal özüne bilgi yüklemektedir. Bu bilginin kodları ise zanaatkârın/ ustanın içinde yaşadığı kültürün anlam dünyası ve

estetik kaynağından gelmektedir. Bu ekseninde, özellikle geleneksel zanaatta herhangi bir teknik uygulamanın bir yönü somut bir nesneyi gösterirken, bu nesnenin işlevsel hale gelmesinde kodlayıcı bir zihinsel imgeleme sürecinin sonuçları da cisimleşmektedir. Dolayısıyla kültürel bir birikime sahip zihinsel imgelem (zanaatkâr/ usta), karmaşık gelişigüzeğe eğilimli doğal varlığı insani taleplere uygun bir düzenlemeye sokarak, bu varlığa bilgi kullanımı yoluyla form vermektedir (Baştan, 2017, s. 901).

Baştan'a göre maddi kültür, topluluk yaşamının organize edildiği görülebilir bir insan ortamı oluşturmak üzere insanların çevrelerindeki doğal kaynakları türettiği ve farklılaştırdığı nesnelerden oluşturduğu kültür olarak tanımlamaktadır. Başka bir ifade ile maddi kültür kavramı insanların tekniklerle, teknolojilerle dönüştürdükleri varlık alanı olan fiziksel çevrelerini işaret etmektedir. Bu alanda düşünceler, eylemler ve insan yapımı nesneler iç içe geçmektedir (Baştan, 2017: 899). Bu nedenle zanaatkâr ustalar maddi kültürü ortaya çıkarmada başat bir rol üstlenmektedir. Bu noktada geleneksel Çin zanaatkârının bilgi sistemi üzerinde durmakta fayda bulunmaktadır.

Çin literatüründe el işi sanatkârlığı anlamında kullanılan kavram özel bir değer taşımaktadır. İngilizcedeki “handwork” veya “craft” Çin literatüründeki “Shou-gong-yi” kavramının anlamına yeterince yaklaşmamaktadır. Çünkü Çin kültürünün binlerce yıllık çok katmanlı kültürel ve geleneksel bir alt yapıya ve doğa ile koordineli bir dünya görüşüne sahip olması, kaçınılmaz olarak insan elinden çıkan nesnelere karşı çok daha derin bir duyumsamayı gerektirmektedir. Yaygın kullanım olarak Çin’de iki belirgin bilgi sistemi bulunmaktadır. İlki yazı dilidir. Bu metinsel gelenek uzun bir geçmişe sahiptir ve Konfüçyüs’ün öğretilerinde birleşmektedir. İkinci bilgi sistemi bedensel performans ve diğer metinsel olmayan yollar ile aktarılmıştır. Gündelik yaşamsal faaliyetlerdeki yaygın kanının ve toplumun alt tabakalarının teknik bilgi sisteminin çoğu bu geleneğe aittir. Çin’de bilgi sistemi geleneksel el zanaatlarına bağlıdır. Üretim süreci içinde gerekli olan materyaller ve teknikler hakkında uzmanlık bilgisi bu bilgi sistemine dâhil olmaktadır. Aynı zamanda ortaya çıkarılan ürünlerin formları hakkındaki bilgi de bu sistem içerisinde. Kısacası bu bilgi sistemi Çin kültürüne ait bütün formel biçimlerin hikâyesidir. Çağlar boyunca Çinli ustalar üretim, öğrenme ve uygulamalar üzerinden bilgi edinmeye devam etmişlerdir. Her yeni bilgi eski olan bilgi sisteminin kurduğu temel üzerinde yükselmiştir. Dolayısıyla geleneksel el sanatlarının bilgi sistemi, geçerli olan sistem etrafında sürekli olarak eklektik bir şekilde yeniden üretilmiştir (Xu, 2013: 156-157).

Bu bağlamda, Çin kültüründe bir bütün olarak ele alınan çeşitli zanaatların tarihsel süreci gösteriyor ki, materyalin ve tekniğin doğası hakkında sistematik bir kavrayışın üretime dâhil edilmesi ideal bir sonuç için hayati önem arz etmektedir. Çin’in önemli klasik metinlerinden olan “Spring and Autumn Annal” da materyale dair şu ifade yer almaktadır;

“Tanrı beş element yaratmıştır. İnsanlar bu elementlerin hepsini reddetmeksizin kullanmışlardır”
(Xu, 2013: 157).

Bu beş element metal, odun, su, ateş ve topraktır. Bu elementler eski Çin filozofları için fiziksel ve metafiziksel ilkeler olarak önemli sayılmıştır. Bu doğal malzemelerin hepsi çeşitli formlar içinde Çin’in maddi kültürünü ortaya çıkarmasında kaynak oluşturmuştur. Üretim sürecinde tekniklerin nasıl uygulanacağı ve nasıl kullanılacağı kararı ustanın malzemenin doğasına dair kavrayışına sıkı sıkıya bağlıdır. Özetlenecek olursa, doğal fenomenlerin sistemi hakkındaki bilginin oluşmasındaki temeli şekillendiren olgular, üretim sürecinde zanaatkar/usta tarafından elde edilmektedir. Böylece materyal hakkındaki pratik bilgi ortaya çıkmaktadır. Sonuç olarak hammaddenin kalitesi tamamlanmış ürünün kalitesi için bir anahtardır ve hammaddenin değerlendirilmesi teorik bilginin gelişmesi ile mümkün hale gelmektedir. (Xu, 2013: 158)

Çin’in kültür dünyasındaki felsefi, ruhsal ve estetik değerler, insan üretimi nesnelerin süslemesi, biçimi ve yapısını destekleyen kurallar içinde özünde bulunmaktadır. Bu noktadan bakıldığında, zanaatkar tabiatın işleyiş kurallarına benzer bir şekilde öze bağlı kalarak bir seramik kap formuna biçim vermektedir. Bu durum “Artificer’s Record” adlı eserde şu şekilde ifade edilmiştir;

“ Gökyüzünden zamana dair bilgi, topraktan yeryüzünün bütün imkanları, materyalden ideal olanı ortaya çıkarma ve ustanın becerisi iyi bir eserin oluşması için esastır” (Xu, 2013: 169).

Dolayısıyla bütün bileşenler bir araya geldiğinde anlaşılıyor ki, bir zanaat nesnesinin biçimi ve yapısı direkt olarak zanaatkârın becerisinin ifadesidir. Bu durum maddi kültür açısından Çin’deki belli bir dönem aralığının gerçeklik kazanmasını sağlamaktadır. Çin asıllı Amerikan fizikçi Anthony Zee en basit düzeyde doğanın güzel idesine göre tasarlanmış olduğunu dile getirmektedir. Antik Çin filozoflarından Zhuangzi ise bu ifadeye gökyüzü ve yeryüzünün en takdire şayan şekilde uyum içinde ilerlediğini söyleyerek konunun felsefi boyutunu gözler önüne sermektedir (Xu, 2013: 169).



Resim 1: Ming dönemine ait ejderha figürü bezemeli mavi beyaz porselen, 1426–1435

1.2. Çin Sanatında Doğa Teması ve Sembolik Anlamlar

Bir önceki bölümde Doğu sanatlarının tabiata tevazu ile yaklaşarak onu nasıl bir nesnel dönüşüme uğrattıkları genel bir çerçeveden sunulmuştu. Bu noktada özellikle Çin sanatının içindeki sembolik durumların açıklanması önemlidir. Çünkü Doğu'nun binlerce yıllık kültür birikimi, sembol ve simgeler üzerinden kendisini bugüne taşımıştır. Bu sembollerin en güçlü örneklerini Çin porselenlerinin yüzeylerine işlenmiş olan betimlemelerde görmekteyiz.

İnsan yapımı nesnelerin ve dinin dışında Çin porselenlerinin süslemeleri sürekli bir şekilde tabiat betimlemeleri (hayvanlar, çiçekler, meyveler, böcekler ve kuşlar) ile ilgilidir. Bu resimsel betimlemeler, Sung Hanedanlığı (M.S. 960-1279) dönemindeki Çin resim sanatının kendisine özgü niteliklerinden gelmektedir. Çin sanatındaki doğadan esinlenen bu etkiler, üstün estetik özellikler taşımasının yanında, kullanılan semboller çok katmanlı bir tarihsel altyapının anlamsal boyutunu da gözler önüne sermektedir. Doğaya karşı gerçekleştirilen bu sembolik yaklaşım gerçekte yalnızca Doğu'ya özgü bir durum değildir. Batı sanatı da bu soyutlama yeteneğini ortaya koyan önemli sanatsal bir altyapıya sahiptir. Bu durumda Çin betimlemelerine doğuya özgü simgeleştirme yönüyle bakmakta ve batı sanatına karşıt bir sanat anlayışı olarak konumlandırmamakta fayda bulunmaktadır. Çin sanatının ifade gücü yalnızca kendi içinde incelendiğinde önemi ortaya çıkmaktadır.

Çin porselenlerinin yüzeylerindeki zengin resimsel dokuların içinde bulunan birçok kuş, böcek ve çiçek türü alegori ile güçlendirilmiş bir öneme sahiptir. Avrupalı ve Çinli zanaatkarların eşit

düzydeki betimleme yetenekleri mit ve gerçeklik içinde birbirine karışmaktadır. Bu dokulara yakından bakıldığında, herhangi bir Çin vatandaşı kendisini evindeymiş gibi hissetmektedir. Çünkü bu betimlemelerdeki tek boynuzlu hayvanlar, aslanlar, leoparlar, geyikler, ördekler, çiçekler, meyveler ve böcekler bir bütün olarak bireyin ait olduğu kültürün ve fiziksel çevresinin içeriğinde aşına olduğu sembolik motiflerdir. Tabii ki bu durum Çin insanına ait bir özellik değildir. Her birey ait olduğu toplumun, kültürün ve mekânın bir anlamda simge ve sembollerine kaçınılmaz olarak aitlik hissetmektedir. Bu nedenle Geleneksel Çin el sanatlarında sıkça kullanılan doğa tasvirleri ve mitsel karakterlerin altında yatan anlamları incelemek önemlidir.

Dünyanın her yerinde bilinen en önemli mitsel karakterlerden biri ejderhadır. Örneklerine birçok farklı kültür ve toplulukta rastlanmaktadır. Ama köken olarak doğuya özgü bir karakter olduğu belirtilmektedir. Doğuya özgü ejderha sembolü genellikle ekinler için yağmur getiren kutsal bir yaratık olarak görülmektedir. Bu mitsel karakter ortaçağ yaratık betimlemeleri ile karşılaştırılamayacak bir öneme sahiptir. Çin’de ejderha imparatorun simgesidir. Örneğin ejderha betimlemesi eski bir kıyafetin üzerinde görülüyorsa, bu iyi bir kehanetin veya belirtinin işaretidir. Bu ejderha betimlemeleri işlenirken genellikle yanında kuş formunda başka bir mitsel karakterle yan yana görülmektedir. Bazı betimlemelerde ejderha sembolü nadir görülen üç renkli Ming dönemi vazolarının kulp bölümleri üzerinde kertenkeleye benzer bir biçimde temsil edilmiştir. Bu da Chou hanedanlığının dini kitabına göre, üç bin yıldan eski olduğu belirtilen Gökyüzü Ejderhası (Azure Dragon) gökyüzünün doğu bölümüne hükmederken, Kızıl Kuş (Vermilion Bird) güney bölümüne hükmetmektedir. Bu mitsel motifler dini tören kıyafetlerinde çağlar boyunca kullanılmışlardır. Ayrıca mezar ve tapınak süslemelerinde de sıkça karşılaşılmaktadır. Bir diğer karakter turna en yaygın kullanılan sembollerden biridir. Çin mitolojisine göre turna, altı yüz yaşına ulaştığında artık beslenmeye ihtiyaç duymamaktadır. Yalnızca su içmekte ve böylece bin yaşına kadar yaşamaktadır. Çin’in dini inancının erken dönemlerinde aslan sembolünün olduğuna dair çok fazla bilgi bulunmamakta ve Han Hanedanlığı (M.Ö. 206- M.S. 220) döneminde ortaya çıktığı düşünülmektedir. Buna ek olarak benzer semboller daha sonraları kanatlı aslan biçiminde Yakındoğu’da görülmüştür. Hindistan’da Budist inancının aslan figürü yaşamın ve kutsal mekânların koruyucusu olarak Çin sanatının içinde yerini almıştır. Çin’de bulunan saray ve tapınakların birçok giriş bölümünü koruyan aslan figürü, vahşi bir koruyucudan ziyade, iri yarı olan pekin köpeği ile benzerlik göstermektedir. Hepsinin ötesinde bu mitsel karakter cesaretin ve enerjinin sembolü olarak Çin kültüründe benimsenmiştir. Çin sanatında Chi-lin adlı karakter dört ayaklı hayvanların kralı olarak bilinmektedir. Bazı durumlarda Çin’in unicorn’u olarak kabul görmektedir. Bunun aksine batıdaki benzerine göre farklı özelliklere sahiptir. Chi-lin beş farklı renkte (kırmızı, mavi, sarı, siyah ve beyaz) derisi ile bir aslana benzemektedir. İyi kehanetin habercisi olan bu mitsel yaratığın yalnızca bir bilgenin doğacağı veya cömert bir kralın tahta geçeceği zaman görüldüğü rivayet edilmektedir. Çin inancına göre M.Ö. 600’de Konfüçyüs’ün doğduğu günden itibaren kendisini bir daha gören olmamıştır. Dolayısıyla Chi-

lin soyluluğun ve bilgeliğin sembolüdür ve Konfüçyüs gibi bilgeler ya da iyi kralların sembolü olarak kullanılmaktadır. Çin'de bu tür hayvan sembollerinin en önemli kullanımlarından biri Ming ve Ching hanedanlık dönemlerinde askeri rütbelerde belirleyici olmalarıdır. Chi-lin, aslan, kaplan, leopar gibi karakterler askeri hiyerarşide kullanırken, turna, sülün, tavus kuşu, kaz gibi karakterler sivil hiyerarşide kullanılmıştır (Chow, 1962: 12-24).



Resim 2: 16. yüzyılın ilk yarısı Ming Hanedanlığına ait ejderha ve kızıl kuş bezemeli tabak

Hristiyan sanatında bir kelebeğin yaşamının üç evresi (tırtıl, koza, kelebek) yaşamı, ölümü ve dirilişi temsil etmektedir. Çin inancında ise kelebek yaz mevsimin ve neşenin sembolüdür. Yaz mevsimin bir diğer sembolü yusufoçuk böceğidir. Çinli ustalar bu karakteri sıklıkla betimlemelerinde kullanmışlardır. Çiçekler sembollerin en evrensel olanlarıdır ve Çin sanatında çok sayıda örneği bulunmaktadır. Bahar için şakayık, yaz için lotus, sonbahar için kasımpatı ve kış için karayemiş (halk arasında laz kirazı olarak bilinmektedir) sembol olarak kullanılmıştır. Baharın sembolü olarak şakayık genellikle manolya ile bir arada görünmektedir. Biçiminden ve renk zenginliğinden dolayı çiçeklerin kralı sayılan şakayık, ayrıca aşkın ve kadınsı güzelliğin ifadesi olarak görülmektedir. Lotus, işlevselliği ve görünümünden dolayı hayranlık uyandıran bir bitki türü olarak, Çin kültürünün her döneminde önemini korumuştur. Çin'de neredeyse günlük yaşamın her alanında özelliklerinden faydalanılmıştır. Çin kültüründe bir simge olarak lotusun en önemli özelliği taşıdığı dini yan anlamdır. Bir Budist sembolü olan lotus, Çin süsleme sanatında çok baskın bir şekilde kullanılmıştır. Bunun nedeni bir metafora dayanmaktadır. Bulanık suyun üzerinde yetişen lotus, kusursuz ve estetik

görünümü ile Budist öğretide önemli sayılmaktadır. Bu öğretide “kirli dünyanın üzerinde yükselmek” düşüncesi ile lotusun bulanık su üzerinde yetişmesi arasında bir anlam kurulmuştur. Lotusun formel biçimi yaşamın ya da hakikatin tekerleğine benzetilmiştir. Bu nedenle birçok tasvirde Buda lotus tahtında otururken veya ayakta dururken betimlenmiştir (Chow, 1962: 12-24).

Sonbaharın sembolü kasımpatı, iyi sonuç vermiş bir hasadı ve şenliği işaret etmektedir. Kış mevsiminin sembolü karayemiş ise, Kang-hsi dönemine ait vazolarda sıklıkla kullanılmıştır. Kokulu ve kar beyazı karayemiş (prunus) çiçekleri kışın genellikle yaşlı ağaçların kuru ve yapraksız dalları üzerinde bulunmaktadır. Bu özelliğinden dolayı Çin sanatında bu meyve uzun bir ömrü ve yeniden doğuşu sembolize etmektedir (Chow, 1962: 12-24).

Çin sanatında sıkça görülen diğer bir üslup, çiçeklerin ve meyvelerin bir arada bulunduğu süslemelerdir. Çin süsleme sanatında nar ve şeftali çok fazla karşılaşılan imgelerdendir. Çin’de yerel bir meyve olarak nar, taneli bir yapıya sahip olmasından dolayı doğurganlığı ve verimliliği temsil etmektedir. Bu bilgiye ek olarak nar, bir çok uygarlık ve dini inançta bereketi temsilen kutsal sayılmıştır. Günümüzde halen Anadolu’da evin içinde yere vurularak patlatılan narın etrafa saçılan parçalarının bereket ve bolluk getireceğine inanılmaktadır. Şeftali de süslemelerde çok fazla kullanılmıştır. Çin kültüründe şeftali ölümsüzlük meyvesi olarak anılmaktadır ve ölümlülere ebedi bir yaşam verdiği, sözlü anlatım geleneğinde yerleşen bir kanı olmuştur. Bu inanç daha çok Taoist geleneğinde benimsenmiştir (Chow, 1962: 12-24).

Bu bölümün sonucu olarak, Çin kültürünün doğa ile bağının, çok derinlere uzanan bir geçmiş ve birikime dayandığı görülmektedir. Özellikle porselenlerin yüzeylerinde görülen tabiat betimlemeleri bu durumu açıkça ortaya koymaktadır. Bu betimlemeler konu hakkında yapılan açıklamalardan da anlaşılacağı üzere yalnızca birer imge olmalarının yanında, yaşamın en derinlerine nüfuz etmiş çok katmanlı anlamlara da sahiplerdir. Bu çalışmada üç bin yıldan fazla bir geçmişe sahip olduğu dile getirilen bir coğrafyayı ve kültürü dar bir açıklama ile aktarmak mümkün değildir. Bu kültürün arkeolojik, antropolojik, sosyo-kültürel ve psikolojik birçok bilimsel alan üzerinden incelenerek açıklanması kapsamlı bir çalışmanın ortaya çıkmasında faydalı olacaktır. Fakat bu araştırmada adı geçen alanlar üzerinden çalışmayı ele almak çok güç bir durumdur. Yalnızca genel bir görüntü olarak bir inceleme ortaya koymak adına kısaca hanedanlık dönemleri ve bu dönemler içinde üretilen seramik ve porselen eserlere bakmakta fayda bulunmaktadır. Bu sayede Çin kültürünün en önemli materyali olan porselene ve onun gelişimine dair ipuçlarını görmek mümkün olacaktır.

1.3. Hanedanlık Dönemleri İçinde Çin Seramiğinin Gelişimine Dair Genel Bir Bakış

Çin seramiklerinin gerek biçim gerekse yüzeylerde kullanılan betimlemeler anlamında belli bir gelişim süreci söz konusudur. Bu gelişimin köklerinin izlerini Çin’in Neolitik dönem seramiklerine

kadar temellendirmek mümkündür. Fakat bu derin incelemenin yerine, yaklaşık olarak M.Ö. 500'lerden itibaren Çin'in hanedanlık dönemleri ile sınırlandırmak, seramiklerdeki biçim ve sembol yönü anlamak için tercih edilmektedir. Hanedanlıkların her biri içinde üretilen seramikler, dönemsel olarak toplulukların içinde bulunduğu sosyo-ekonomik ve sosyo-kültürel etkilerle sıkı sıkıya bağlıdır. Bunun yanında Çin kültürünün temelinde bulunan doğa nesnelerine olan ilgi, her dönemde etkisini farklı biçimlerde ortaya koymuştur. Bu dönemlere kısaca bakmak, Çin seramiklerini anlamak için önemlidir.

En eski Çin topluluklarından biri Shang Hanedanlığı'dır (M.Ö. 523-1028). Bu topluluk Neolitik'den gelen kültürel miraslarının üzerine birçok sosyolojik ve teknolojik yenilik ekleyen dinamik bir dönemi oluşturmuştur. Geç Shang döneminde karmaşık bir yazma sistemi geliştirilmiştir. Özellikle fildişi oyması ve yeşim oyma gibi el sanatları bu dönem içinde gelişim göstermiştir. Çin seramiğinin gelişmesinde de bu dönem önemlidir. Shang çömlekçilik zanaatındaki iki önemli yenilik, günümüze kadar uzanan bir seramik mirasını oluşturmuştur. Bunlardan ilki, yüksek sıcaklıkta pişirilen sıvı geçirmeyen zinterleşmiş çömlek; ikincisi, bu seramiklerin yüzeylerine uygulanan yüksek dereceli sırların kullanımıdır. Ancak şehirli Shang topluluğunun öne çıkan en önemli özelliği bronz kullanması ve bunun hakkında bilgi üretmesidir. Ancak en erken Shang bronz eserlerinin birçoğu bilindik çömlek biçimlerini referans olarak almıştır. Ama çok geçmeden, çok sayıda bronz eser yeni form ve süslemeler ile nesnel bir kimlik kazanmıştır (Valenstein, 1975: 116).



Resim 3: Rölyef uygulaması yapılmış olan Geç Shang dönemi kap örneği

Shensi Eyaletinde, Shang hanedanlığının yaşadığı bölgede daha sonra ortaya çıkan Chou Hanedanlığı (M.Ö.256-1027), yaklaşık olarak 1027'de Shang bölgesini fethetmiş ve Çin hanedanlıklarının en uzun süreli olan topluluğunu kurmuştur. Chou Hanedanlığı'nın güçlü olduğu yıllar, M.Ö. 771'de Shensi Eyaleti'ndeki modern Sian'ın başkenti Hao'nun yıkıldığı döneme kadar

sürmüştür. Hanedanlık, Honan Eyaletindeki Lo-yang'ta yeniden kurulmuştur, ancak önceki otoriter yapısı minimuma inmiştir. Chou Hanedanlığı Shang Hanedanlığını fethettikten sonra, temel Shang kültürünü sürdürmüş ve bu geleneği geliştirmiştir. Bu dönemde bronz metalürjisi Sang dönemindeki etkiyi devam ettirmiştir. Yazı sistemi gelişmeye devam etmiştir. Yeşim taşlarının işlenmesi için yeni aletler geliştirilmiştir. Shang döneminde olduğu gibi, birçok Chou çömleğinde, bronz eserlerin ve diğer değerli malzemelerle üretilen nesnelerin izleri bulunmaktadır (Valenstein, 1975: 117).



Resim 4: Chou Hanedanlığı dönemine ait sırlı kap formu

Ch'in devletinin ülkeyi birleşmesiyle ilk Çin imparatorluğu M.Ö. 221'de kurulmuştur. Ch'in imparatorluğu (M.Ö.221-206) kısa ömürlü olmuştur. Sonrasında yeni bir topluluk olan Han Hanedanlığı (M.Ö.206 -M.S.220), Shensi Eyaletindeki Chang'an'da (bugün Xian şehri olarak bilinen) kurulmuştur. Han Hanedanlığı, Çin'in en ihtişamlı dönemlerinden birisi olmuştur. Güçlü ve birleşik bir ülke olarak, muazzam bir dönemi yaşamıştır. Geniş toprak fetihleri gerçekleştirmiştir. Diplomatik ve kültürel alanlarda daha önce görülmemiş bir biçimde gelişim göstermiştir. Özellikle de Sang döneminden itibaren Çin seramikleri üzerinde derin bir baskı yaratmış olan metal eşyaların üstün statüsü, Han çanak çömleğinde gözlemlenmeye devam etmiştir. Bununla birlikte, natüralizme olan iyimser yaklaşım, Han dönemi sanatının tüm aşamalarında hızla yayılmış ve aynı zamanda çömlekçinin zanaatına da etki etmiştir. Bu dönemle birlikte Seramiklerin süslenmesi artık metal işlerinden türetilenlerle sınırlı değildir ve doğal motiflerin yeni kullanım biçimleri ile özgün bir tasarım dili oluşturulmaya başlanmıştır (Valenstein, 1975: 120).



Resim 5: Han dönemine ait rölyef dekorlu ve zeytin yeşili sırlı kap formu

Han Hanedanlığı'nın yıkılışıyla birlikte Çin, M.S. 222 ve 589 yılları arasında başkentleri Nanking olan altı hanedanlık dönemine giriş yapmıştır. Bu dönem 350 yıllık siyasal bir karışıklığın baş gösterdiği bir aralıktır. Siyasi huzursuzluğa rağmen, bu dönemde büyük teknolojik ve kültürel gelişmeler kaydedilmiştir. Bu dönemin Çin yaşamının yapısı üzerindeki en derin etkilerinden biri, muhtemelen Han Hanedanlığı döneminde keşfedilmiş olan Budizm'dir. Altı Hanedanlık dönemine ait mezarlardan çıkarılan hayvan ve insan biçimli sürreal olarak tarif edilebilecek olan sırsız seramik heykeller dönemin sanatsal üslubunu göstermektedir (Valenstein, 1975: 120).

Altı Hanedanlık dönemi sonrası Sui yönetimi (M.S. 581-618) altında güçlü bir merkezi hükümet kurulmuştur. Bu dönem Başkent ve Büyük Duvar yeniden inşa edilmiştir. Bunun yanında buhran dönemi sonrası Çin'in politik ve askeri etkisi sınırlarının ötesinde tekrar hissedilmeye başlamıştır. Sanatsal ve kültürel açıdan Altı Hanedanlığın temelleri üzerine inşa edilen Sui seramikleri önceki dönemin biçimlerine yakınlık göstermiştir. Fakat bu dönemin en önemli özelliği, Sui biçimleri ve üslubunun T'ang hanedanlığının gelişiminin habercisi olmasıdır. Aşağıdaki örnekte de görüldüğü gibi ejderha kulplu zarif amfora biçimi son derece lirik bir üsluba sahiptir. Hepsinin ötesinde Sui Dönemi gerçek porselene doğru önemli bir adımı temsil etmektedir (Valenstein, 1975: 121).

Tang Hanedanlığı (M.S. 618- 906), Çin tarihinin en parlak dönemlerinden biri olarak sayılmaktadır. Hanedanlığın iktidar gücü ülkenin gelişiminde önemli bir rol oynamış ve bunun akabinde Çin kültürü sanatsal ifadenin doruklarına ulaşmıştır. Tang Hanedanlığı'nın Çin üzerinde derin bir etkisi olmuştur ve ülke sınırını Kore'den Orta Asya'ya kadar genişletmiştir. Uzak coğrafyalara uzanan bu egemenlik, ticarete de önemli sıçramalara zemin oluşturmuştur. Ticaret yolu üzerinde temas ettiği bütün kültürlerin sanatsal kaynaklarından esinlenmiş ve bu etkiler Çin sanatında kalıcı kılınmıştır. Tang dönemiyle birlikte yayılan refah ortamı çömlekçilik zanaatında etkisini belirgin bir şekilde göstermiştir. Bu dönem üretilen seramikler, biçim ve süsleme yönünden yoğun bir canlılığı yansıtmaktadır.

M.S. 907'den 960'a kadar olan dönemde Çin toplumu, arka arkaya gelen kısa ömürlü beş hanedanlık süreci yaşamıştır. Bu yıllar Çin tarihinde kargaşalı bir dönem olarak adlandırılmaktadır. Ekonomik ve sosyal açıdan her ne kadar zor bir süreç yaşansa da, seramik endüstrisi varlığını ve gelişimini sürdürmeyi başarmıştır. Bu dönemde en göze çarpan özellik seladon sırlı seramiklerdir.

Song Hanedanlığı (M.S. 960-1279) döneminde kültürel ortam içe dönük bir yapıya sahip olmuştur. Bu dönem aralığı barışın ve huzurun kısmen de olsa hüküm sürdüğü bir zamandır. Ancak Çin sınırlarının çoğunu tehdit eden komşuları, Batı'dan ve kültürel değişimin canlandırıcı etkilerinden yararlanmasına engel oluşturmuştur. Bu nedenle Song dönemi sanatsal ve kültürel faaliyetlerinde ilerleme sağlamak adına kendi içine dönmüştür. Böylece Song dönemi sanatçıları yaratıcılık yönünün kendi özlerinde ve doğada bulunduğunu keşfetmişlerdir. Güney ve Kuzey Song Hanedanlıkları yüksek estetik değerlere sahip seramikler üretmişlerdir. Seramik formlarda son derece sade ve karmaşık olmayan tasarımlar ortaya koymuşlardır (Valenstein, 1975: 123-130).

13. yüzyılla birlikte Moğollar kuzeyden aşağı bölgelere doğru ilerlemişler ve uzun bir süreçte Çin'i fethetmişlerdir. Bu yeni rejim altında Çin, içe dönük Sung döneminden farklı bir döneme giriş yapmıştır. Bu süreçle birlikte Çin, Kore'den Güney Rusya ve İran'a uzanan geniş bir imparatorluk olarak, yabancı milletler ile önemli ticaret kanalları oluşturmuştur. Böylece Çin yaşamına etki eden kültürel etkileşimler ve yenilikçi fikirler sanatsal üretimlerde yansımaları göstermiştir. Song dönemindeki seramiklerde ustalıklı çözümlenmiş ince ayrımlar ve sanatsal kazanım, Moğol etkisi ve himayesi altındaki Yuan Hanedanlığı (M.S.1279-1368) dönemiyle etkisini yitirmiştir. Ayrıca batılı tüccarların da Yuan seramikleri üzerinde etkisi söz konusu olmuştur. Bu nedenle Çinli çömlekçiler Moğolları tatmin etmek zorunda kalmışlardır. Ustalar özellikle porselen eşyalarda ihracata yönelik daha belirgin süslemelere ve kültürel öğeleri ön plana çıkaran bir tarza yönelmişlerdir.



Resim 6: Song Hanedanlığı dönemine ait alçak rölyefli ve seladon sırlı tabaklar

Ming hanedanlığının (1368-1644) kuruluşu ve bunu izleyen süreçte gerçekleşen bir ayaklanma sonucu 1368'de Moğolların Çin üzerindeki iktidarına son verilmiştir. Bu önemli gelişme ile Ming

Hanedanlığının başkenti Nankin olarak belirlenmiştir. Bununla birlikte Ming döneminde sanatsal ve kültürel alanda özgün örnekler ortaya çıkmıştır. Özellikle günümüzde dünya çapında Ming porselenleri, Çin sanatının en tanınan ve özgünlüğü ile ön plana çıkan eserlerdir. Bu noktada Çin sanatının neredeyse belirleyici bir üslubu haline geldiğini dile getirmek yanlış bir tanı sayılmamaktadır.

1644'de Çin topraklarına baskın bir şekilde gerçekleştirilen akınlardan sonra, Güney Mançurya'dan gelen Jurchen topluluğu Ch'ing Hanedanlığı'nı (1644-1912) kurmuştur. Ch'ing dönemi porselenleri, Çin kültürünün binlerce yıllık sanatsal birikiminin en üstün örnekleridir. Bu dönem büyük bir ihracat hareketliliği bulunmaktadır. Özellikle geniş yelpazede üretilmiş olan dekorlu porselenler batı ülkelerine gönderilmiştir. Çin'in Avrupa ile olan alışverişi, Ch'ing dönemi çömlekçiliği üzerinde çok önemli bir etkiye sahiptir. Çünkü 18. yüzyıl ile birlikte doğu ve batı arasındaki kültürel anlamdaki dokunuşlar toplumsal olarak karşılık bulmuş ve bu ortamdan zanaatkârlar da etkilenmiştir. Avrupa'nın Doğu sanatına olan ilgisi Ch'ing dönemi porselenleri ile en üst düzeye ulaşmıştır (Valenstein, 1975: 132-164).



Resim 7: Ming dönemine ait ejderha biçimli kulpları ile mavi-beyaz porselen form



Resim 8: Ming dönemine ait üzerinde doğa betimlemeleri ve içerisinde mitolojik yaratıkları ile mavi-beyaz porselen tabak



Resim 9: Ming dönemine ait üzerinde ejderha ve kıvrıl kuşun betimlendiği mavi-beyaz porselen tabak

Sonuç

Çalışmanın başlığından da anlaşılacağı gibi, Çin seramik sanatına bakıldığında, form yönünün yanında bunun altında yatan etkenler de oldukça önem arz etmektedir. Bir kültüre ait herhangi bir form biçim yönünden izleyici veya tüketicide estetik bir algı yaratabilir. Fakat aynı form ele alınıp irdelendiğinde, o formun her ayrıntısında içinde bulunduğu kültürün izleri ile karşılaşmak mümkündür. Özellikle tarih sahnesinde önemli bir yere sahip Çin gibi bir uygarlığın eserleri incelendiğinde bu durum açıkça ortaya çıkmaktadır. Bu çalışmanın başlıca araştırma alanı, Çin seramiklerinin bezeme ve formlarının altında yatan göstergeler olmuştur. Sonuç olarak incelenen metinlerden elde edilen bilgi, en zor dönemlerde dahi Çin sanatının doğa ve kültür ile olan sıkı bağını koparmadığı ve özgün hikâyelerini semboller üzerinde somut bir hale getirebildikleridir. Bunun yanında zanaatkârlar dünyayı felsefe yönünden kavrayabilmişler ve evrende olup bitenleri bir bütünün parçaları gibi görerek uyguladıkları çalışmalara da aynı düşünceler ışığında yaklaşmışlardır. Günümüz çağdaş sanat alanına baktığımızda, üretimlerde aranan samimi süreç, yüzyıllar önce Çin zanaatkârlarının üretimlerinde gizli durmaya devam etmektedir. Bu önemli bir noktadır. Çünkü bu zanaatkâr ustaların elinden çıkan şeyler, bugün adına sanat eseri denen nesnelerden çok, bir kültürün, bir felsefenin, bir toprağın, en çok da tabiatın biçimleridir. Bu nedenle Çin seramikleri söz konusu olduğunda, tarihi arka planından ustalarına, nesnelerinden doğaya kadar geniş bir yelpazede çok katmanlı bir yapı ortaya çıkmaktadır.

Kaynakça

- Baştan, S. (2017), Tasarım Biçimlerinin Teknik Oluşumuna ve Materyal Kültür Alanının Yapılaşmasına Etki Eden Kültürel Dinamikler, Yönetim ve Ekonomi , 901
- Chow, F. (1962), Symbolism in Chinese Porcelain: The Rockefeller Bequest, The Metropolitan Museum of Art Bulletin, 12-24
- Erzen, J. N. (2016), Çoğul Estetik, İstanbul, Metis Yayınları, 22-23-91-128
- Valenstein, S. G. (1975), Highlights of Chinese Ceramics, The Metropolitan Museum of Art Bulletin, 116
- Xu, Y. (2013), The Knowledge System of the Traditional Chinese Craftsman, West 86th: A Journal of Decorative Arts, Design History and Material Culture, 156-157

TRENDY TRADITION: VIETNAMESE BAT TRANG CERAMICS

Doç. Dr. Funda Altın¹, Prof. Dr. Lale Dilbaş²

¹ Ordu University-Faculty of Fine Arts, Ceramic and Glass Dept., Ordu/Turkey

² ARUCAD Arkin University of Creative Arts and Design-Faculty of Arts, Kyrenia/North Cyprus

Almost 1000 years ago, Vietnam's emperor Lý Thái Tổ, relocated the empire's capital in Hanoi and in order to invigorate the new capital's development, the pioneering merchants and artisans have also been moved there. Back then, 5 prominent potter families settled down at the village called Bat Trang, 16 kilometers far from Hanoi city center, due to the abundant kaolin sources on the banks of Red River. These well-established families maintain their craft and production even today at the same location and created a distinctive Vietnamese ceramic style. They have become the country's largest ceramic exporting potters, sending their products mainly to Japan, Europe, America, Australia and Southeast Asia. Today, Vietnamese pottery, influenced by Chinese, Cambodian and Indian cultures, has created a unique style under the cult of Bat Trang and exports a wide range of products to the whole world.

As well as their minimalist and well balanced patterns, the approach that makes Bat Trang ceramics so popular for over a thousand years, is the originality provided to the material by hand-shaping. The dynamic, flowing and illustrative designs on Bat Trang ceramics recall Hamada's and Leach's ceramic surface interpretations, the two pioneering ceramists who have built a bridge between eastern and western ceramics. Thus Bat Trang ceramics' designs draw attention as features that have a connection with ceramic art's past, yet differentiate from all other examples by baring strong characteristics. In the frame of eastern-western, traditional-contemporary, functional-decorative being, this particular ceramic tradition has an entirely unique identity which refers to the 14th century's elegant forms.

The solidness of the products hidden behind their fragile appearance creates an aesthetical stylistic existence typical for Bat Trang pots. It is essential to examine the Bat Trang potters' mastery in pottery techniques, designs and the approaches developed throughout centuries, especially due to the place they attained in studio-pottery and in global boutique-ceramic market.

Keywords: Traditional Pottery, Vietnamese Pottery, Bat Trang Ceramics, Drawings on Bat Trang Ceramics

BAT TRANG CERAMICS-HISTORY AND FACTS

Vietnamese ceramics, considering the close geographic and historical connections, are under the influence of Chinese, Cambodian and Indian pottery traditions. To allocate a more precise description, it is possible to say that while North Vietnam shows evidence of Chinese influence, in south Vietnam (especially around Ho Chi Minh city), Cambodian and Indian (the use of red clay/earthenware) influences are more evident.

Bat Trang ceramic village, 16 km east of Hanoi, the capital of Vietnam, lies very close to the Red River, which was a region where the first Vietnamese in history, the “*Lac*” people at today’s Hoa Binh city on the northwestern part of present-day Vietnam, appeared around 9.000 BCE. Conquered by the Chinese Han Dynasty on the 1st century, Vietnamese people remained under the Chinese rule for nearly 1.000 years. At 1010, the capital of the country was moved to Hanoi (formerly called Thang Long) by Ly Cong Uan, the emperor of the Vietnamese Ly dynasty. After long years of wars between Chinese, Mongols, Hindu Champas (Muslim and Hindu Champ minorities) and Cambodia, Vietnam had to deal with grand nations like France, Japan, Australia, South Korea and America. (Corfield, 2008; 1-10) Vietnam became an independent country in 1945 under Ho Chi Minh’s leadership.

Before 1896, this region, where Hoa Lo Prison was built, villagers used to produce earthenware home appliances, such as kettles, teapots and portable cooking stoves. In the beginning, the village started by producing bricks for dynasty buildings. As the royals noticed that the quality of the bricks is quite high, the Bat Trang people were asked to use the same material to make table ware for royal gatherings. In 1896 some potter’s villages in Hanoi like Hoa Lo, Phu Khanh, Vinh Xuong and Tho Xuong were transformed by French colonialists into prisons, where they kept revolutionary patriotic soldiers. Many leaders of the Vietnamese government and communist party members were kept there. On 1954, after the North was liberated these prisons were managed and used by the Vietnamese Government to keep law breakers. From 1964 to 1973, especially Hoa Lo Prison, remanded American pilots who were shot down or arrested when bombing the north of Vietnam. (Hoa Lo Prison Museum, 2018)

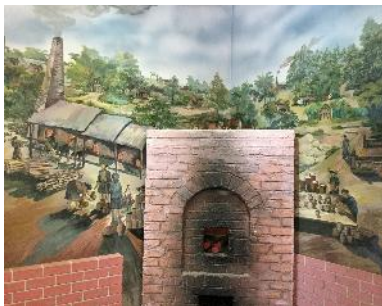


Image 1. Hoa Lo Village before 1896

Due to urbanization, as all villages in Vietnam, also Bat Trang’s identity has started to change but today there are still nearly 400 potters who live and produce in this town since almost 1.000 years. The products in Bat Trang village, showing strong connection with Chinese influence, have some similarities with Chu Dau pots. Chu Dau pottery village, 54 km east of Bat Trang, was formed at the 14th century and after reaching its peak at 15th and 16th centuries the craft vanished due to wars. Roughly a decade ago the government regenerated the pottery tradition in Chu Dau village. A lot of workers, professors and masters of ceramic from Bat Trang and Hai Duong were invited to help resurrect the craft in the village. Now it is a large simulated potter’s village displaying ancient pottery products, calligraphy pottery garden, the house to worship the founder of pottery craft etc. and the village is still on the way to achieve the success in the past. (Giang, Dam, 2018)

While some companies/family run businesses in Bat Trang are focusing on religious items like Buddhist icons (Figures 2-5), some concentrate on tableware, teapots/cups, wine jars and some on vases and lamps or a wide range of souvenirs (Figures 6-13). The expansion of Bat Trang ceramic production helped not only the region but also the surrounding areas to solve the unemployment problem. By attracting nearly 6.000 foreign tourists and local customers per day, Bat Trang potter’s village reached a significant economic status. Thus the economic growth and infrastructure development of the village relies strongly on the ceramic activities. The village dealt with major health, environmental pollution and raw material supplies problems due to high production using old and traditional methods especially during the early 2000’s, where the products were mainly fired by using coal as fuel, though with the introduction of gas kiln and new solutions in technology the quality and quantity of products improved, health issues and production costs decreased. (Tuyen, 2010: 144-147)



Image 2
Bat Trang Ceramics



Image 3
Bat Trang Ceramics



Image 4
Bat Trang Ceramics



Image 5
Bat Trang Ceramics



Image 6
Bat Trang Ceramics



Image 7
Bat Trang Ceramics



Image 8
Bat Trang Ceramics



Image 9
Bat Trang Ceramics



Image 10
Bat Trang Ceramics



Image 11
Bat Trang Ceramics



Image 12
Bat Trang Ceramics



Image 13
Bat Trang Ceramics

Vietnam's ceramic industry is worth around 110 million USD per year and Bat Trang contributes the 40% of it. 83% of Bat Trang inhabitants are potters. Bat Trang's top end ceramic products are considered to be among the best in the world but there is also a significant difference between low and high quality products. Besides, a majority of producers are unaware of the world's new design trends and demands, thus only a few of these potter families/enterprises are able to globalize. (Mc Carty, Record&Riedel, 2005:59)

MINGEI AND BAT TRANG POTTERY

The word *mingei*¹, meaning 'art of the people', was first mentioned by the Japanese philosopher Sōetsu Yanagi (1889-1961) in Japan in the late 1920's. At his young ages, he was living in Korea in the early 1920s and he was taken with the timeless beauty of Yi dynasty (1392-1910) pots which showed a simple and rustic type made in numberless quantities over the centuries and he started to collect old items (not only pots but also woodworks, lacquer ware and textiles). These pots were used for everyday needs from tea cups to *kimchi*² jars, however the pottery was everywhere and taken for granted. Yanagi, however, saw Yi dynasty pottery with fresh eyes, and he considered it among the most beautiful of manmade objects—equal to renowned scroll paintings of the east and paintings and sculptures of the west. Thus *mingei* was a movement, a reaction against the rapid westernization, industrialization and urban growth, which Japan was going through during those years. His writings, lectures and conversations opened the eyes of Koreans to their long-dismissed and anonymous artistic legacy. In 1921, Yanagi opened a folk museum in a small building in the old palace in Seoul, filled with Korean pots and other crafts. It was the first museum of *mingei* in the world. Returning to his homeland, Yanagi began to collect Japanese crafts, believing that his own people, too, needed to discover and preserve anonymous objects of truth and beauty that they had lived with and used over the ages. In 1936, with potters Kanjiro Kawai and Shoji Hamada³, he opened the first Japan Folk Craft Museum (*Nihon Mingei-kan*) and started to publish magazines called *Kogei* (craft). The idea stood for

¹ *Mingei* is an abbreviation of the Japanese words *Minshu-teki* (ordinary people's) and *Kogei* (craft)

² *Kimchi* is a Korean dish of spicy pickled cabbage

³ Shoji Hamada (1894-1978) was born in Tokyo-Japan and after graduating from Tokyo Technical College he founded in 1920 the Leach Pottery in St. Ives-England with the British studio potter Bernard Leach.

‘arts of the people returned to the people’. For these actions he was compared to William Morris and John Ruskin. Yanagi explained the concept of *mingei* in his seminal work, *The Unknown Craftsman* (1989):

“It is my belief that while the high level of culture of any country can be found in its fine arts, it is also vital that we should be able to examine and enjoy the proofs of the culture of the great mass of the people, which we call folk art. The former is made by a few for the few, but the latter, made by the many for many, are a truer test. The quality of the life of the people of that country as a whole can best be judged by the folk crafts.” (Mingei International Museum)

With regard to the bridge that Bat Trang’s contemporary and pacesetter pottery studios built between east and west, it is essential to analyze the concepts of *mingei* and studio pottery⁴ movement. Studio potters have always been attracted to the idea that the pot speaks for itself and furthermore that studio pottery is essentially an independent art form. Thus the self-sufficiency of the maker is reflected in the self-sufficiency of what is made. Autonomous object, a ‘pure aesthetic expression’, self-contained within its own borders and able to speak directly and unambiguously to the receptive spectator. (Murray, 1925: 11) Pottery is admitted medium for the expression of abstractions in form, color and design. Abstract designs, challenged in drawings and paintings, are accepted in Pottery. (Haslam, 1997: 58) Soetsu Yanagi summarized the idea by telling Bernard Leach (1887-1979) as they first met each other in Japan: “Let our work be so great that every man is able to love each other in it”. (Leach, 2012) Bernard Leach’s first travel to Japan was in 1909 and his first impression in eastern style began with the idea that the materials were being allowed to speak for themselves. Leach knew that there was a similarity between Pacific island cultures with Americans, as demographic researches revealed, twenty-five thousand years ago people migrated to the west from Asia. Leach travelled a lot. He was born in Hong Kong and raised at different areas of England. He had met many different friends who were artists to varying extents and who had inspiring approaches towards life and classic art. As the world changed also the understanding of art was different at his time. His parents, relatives and friends were as a whole, what shaped his approach to art. He always painted since his childhood but his encounter with clay changed his perception forever. As he moved to Japan he clearly saw a bridge between the east and west. People were the same indeed regardless of their root. The ancient world was an entirety and the beginning of the twentieth century was the time when this connection needed to re-emerge. This discovery led Leach to produce artworks by using a pure traditional and functional material: the clay and decorating it with his paintings. Thus Leach and Hamada enabled the resurgence of the ‘craft aesthetic’.

A TRADITIONAL POTTERY STUDIO IN BAT TRANG: LC HOME

LC Home Co. Ltd.⁵ -the focus of this paper- is producing clay products since 9 generations in Bat Trang and ranks among the 10-15 largest and strongest pottery companies located in Bat Trang. The company has both a strong and historical pottery background, which makes it a significant example in consideration with studio pottery and its product’s conceptual similarities with Hamada’s and Leach’s approach to contemporary ceramic art. In just the same way as Leach did, this company shows a simple and straightforward approach to east or west to preserve a ceramic culture, it defeats weakened traditions and the violence of modern motivation. Their motifs come from nature, from the soil, the life itself and self-experience, which creates a true balance between east and west, local and universal, regardless of religion, striving after the eye for beauty. (Images 14-16) During ancient times, people moved from one continent to the other. The mobility of people and their cultures started the west and east’s first encounters, then it is radically followed by overseas colonial period, but today the interaction became more universal due to strong digital communication network and people’s mobility. So various people from different cultural backgrounds possess a more or less idea about other cultures.

⁴ Leading studio potters: William Staite Murray, Shoji Hamada, Bernard Leach, Andre Derain, Gordon Baldwin, Norah Braden, Joanna Constantinidis, Hans Coper, Ruth Duckworth, Colin Pearson, Katherine Pleydell Bouverie, Lucie Rie, Gwilym Thomas, Kanjiro Kawai...

⁵ #18, xom 5, Bat Trang, Gia Lam, Hanoi-Vietnam



Image 14. LC Home - 2018



Image 15. Shoji Hamada - 1955



Image 16. Bernard Leach - 1927

The company's products range from plates, bowls, cups, spoons to teapots, jugs and vases. The studio compound consists of 5 floors: underground (molding, hand shaping and wheel throwing), ground (show room and offices), first floor (decoration and painting), second floor (gas kilns and firing), third floor (alternative firing area, such as raku, horse hair and luster). The company uses ancient Vietnamese traditional designs on modern contemporary ceramic products. (Images 17-20) It is currently managed by the 9th generation's grandson Nguyen Van Loi of the legendary Nguyen Thanh Chau, who was designated as a "Living National Treasure" by the late King Le in 1737. The company's main aim is to preserve the local culture by introducing local designs to the world. Their products are 100% handmade, lightweight and do not contain any harmful elements such as lead and cadmium that are detrimental to health and are approved by SGS⁶ and achieved "food safe" certificate. (LC Home) The company takes part in fairs both in Vietnam and abroad every year and introduces its new collections to the domestic ceramic market's leaders.

The current vice director of the company Viet Dam has studied economics in graduate level, however he grew up in a ceramist family, who used to run a simple pottery workshop with relatives for generations and knows the basic pottery techniques, thus is able to produce most of the products himself. The business which kept going on for centuries, though limited with products aimed for the local people, opened up a new phase after 2011. Still producing for the local market at the same time, after that year the company started to export its products to countries like Ukraine, Netherlands, USA, Australia, Japan and South Korea except China which has a long and strong history in pottery making itself. As an identic and contemporary pottery studio, LC Home's products are both traditional and contemporary. In other words, the ancient craft, which also shows evidence of Chinese and Japanese styles, gained a new character under the traditional shelter.



**Image 17
LC Home Production
Studio**



**Image 18
LC Home Decoration
Studio**



**Image 19
LC Home Firing Area**



**Image 20
LC Home Showroom**

They used to buy the clay from Bat Trang village but since 20 years, due to the increasing number of potters and production demands, they started to provide it from Quang Ninh province, 180 km west of Hanoi. The potters are quite satisfied with the quality of the clay, which is even better than the clay of Bat Trang. There are three different natural colors of clay (white, dark white and brown) and all sorts of clays (slip, plastic etc.) come from the supplier as ready to use. However, some workshops in Bat Trang mix their clay with pigments and oxides in order to obtain the desired clay colors. LC Home fires its products at 700°C for biscuit and at 1200°C for glaze firing. (Viet Dam, 2018)

The workers at the company are mainly local people from Bat Trang and some of them come from neighboring villages. Generally, they learn the craft by working in ceramic workshops, which are available all around the area or they may study at the ceramic school in Bat Trang that accepts students after they graduate from the high school. Another opportunity to learn the craft on a more artistic and academic level is the University of Industrial Fine Art (*Trường Đại Học Mỹ Thuật Công Nghiệp*) in Hanoi -built as 'National School of Fine Arts' in 1949- which trains students in higher educational level and aims to preserve and

⁶ SGS (Multinational Testing Laboratories) is an international company which provides inspection, verification, testing and certification for a wide range of products for the health safety of end users.

promote this ancient craft. (UIFA, 2018) The designer of LC Home, Mr. Nguyen Van Loi has also graduated from this university's Ceramic and Glass department.

THE DESIGNS ON LC HOME PRODUCTS

The designs and patterns on LC Home products are significant and prominent motifs on which the company pays utmost attention. Viet Dam's uncle Nguyen Van Loi and his wife Pham Minh Chau are creating the designs for the pots and they renew the designs/the collections every year. As in LC Home products also in Bat Trang the blue color is very popular due to the strong connection with Chinese pottery traditions. Blue is also seen as the basic color for designs along with gray and black, which are very easy to adapt to the surface, hence to create elegant yet modest and pure designs. The European market requirements are also another preference for the selection of blue, gray, black and white combinations. Furthermore, these colors easily match with other decoration and table items, thus it is possible to combine sets with each other. (Images 21-24)



Image 21
LC Home Products



Image 22
LC Home Products



Image 23
LC Home Products



Image 24
LC Home Products

The design process of the products is determined both by the company's own ideas and importing countries requirements. Patterns reflecting the life, habitat, beliefs and philosophy in Vietnam, like lotus, chrysanthemum, taro plant and *Lac Viet* bird (a kind of bird in Vietnamese legendary) are preferred designs on pots. 40-50 % of Vietnamese people are farmers so animals like fish, crabs and dragon flies are very common patterns for them from the past to present. (Figures 1-10) However, one may also see more contemporary and sophisticated ceramic set designs, where only colors (like white-gray-black or red-blue lines on white) are combined and no motifs applied. (Image 21) This is inspired by the fabric, the color combinations and the stitches on the pots reminding of textile surfaces. Besides hand decorations and the abundance of the pattern's combinations, *raku* is also a highly preferred technique at LC Home.



Figure 1

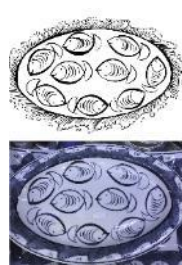


Figure 2



Figure 3



Figure 4



Figure 5



Figure 6



Figure 7



Figure 8



Figure 9



Figure 10



CONCLUSION

Bernard Leach, Shoji Hamada and their common friend Soetsu Yanagi have built a bridge between east and west, they influenced each other and combined the western potter's contemporary form approaches with eastern culture's elegance, fineness, motifs and respect to both form and decoration. Thus almost hundred years ago their casual friendship has been able to establish a perpetual connection between east-west and form-decoration and steered today's studio pottery by laying the foundations of boutique pottery.

Vietnamese Bat Trang pots recall Leach's and Hamada's surface interpretations. Especially LC Home, a prominent studio pottery company located in Bat Trang today, maintains its deep-rooted pottery tradition since 9 generations and still shows evidence of Indian, Vietnamese and Cambodian influence. LC Home generation's priority, to combine eastern-western tendencies with their old family traditions, aims to catch today's trends in studio pottery. However, it is still the west which mainly determines the trends, however this company has been able to protect its conceptual understanding towards western demands yet by preserving their family and cultural traditions.

Leach has traveled a lot in his life and lived both in the west and east. The only cultural exchange chance during his time was based on physical presence. Today it is possible to gain these experiences through innovations which fall under technological/visual communication means. Thus Leach's explorations, regarding the combination of pure tradition with material's functionality according to cultural needs, manifest themselves through the forms, colors, textures and motifs of ceramics produced by main pottery studios based in Bat Trang, regardless of the fact that there will be always an 'east' for the west.

REFERENCES

- Corfield, J., 2008, *The History of Vietnam*, Greenwood Press: USA.
- Dam, V. (2018, September 10). Personal Interview-e-mail.
- Giang, Thu, Vietnam National Administration of Tourism, Chu Dau Pottery Village, Retrieved from <http://www.vietnamtourism.com/en/index.php/tourism/items/2924>, [09.06.2018]
- Haslam, M., 1997, *William Staite Murray*, *Pioneers of Modern Craft* (Margot Goatts, Ed.), Manchester United Press: UK
- Hoa Lo Prison Museum, 2018, *History*, Hanoi, Vietnam.
- LC Home Where the difference is made* [Brochure], n.p., n.d.
- Leach, B., 2012, *Beyond East and West: Memoirs, Portraits and Essays*, Faber & Faber: UK
- Mc Carty A., Record R., Riedel J, 2005, *Competition and Cooperation: Vietnam*, *Industrial Clusters in Asia: Analyses of Their Competition and Cooperation*, Akifumi Kuchiki&Masatsugu Tsuji (Ed.), Palgrave McMillan: New York
- Mingei International Museum, About / History of Mingei, Retrieved from <https://mingei.org/about/history-of-mingei/>, [14.08.2018]
- Murray W. Staite, Pottery and the Essentials in Art, Arts League of Service Bulletin 1923-1924, 1925, s.11.
- Tate Gallery, Art & Artists, Bernard Leach, Retrieved from <https://www.tate.org.uk/art/artists/bernard-leach-1478>, [05.07.2018]
- Tuyen, N. T., 2010, *Knowledge Economy and Sustainable Economic Development-A Critical Review*, Walter de Gruyter GmbH & Co.: Berlin
- UIFA (University of Industrial Fine Art), Hanoi, Vietnam, Retrieved from <http://mythuatcongnghep.edu.vn/>, [17.08.2018]
- Viet Dam, (2018, July 18). Personal Interview. LC Home Co. Ltd., Bat Trang, Hanoi: Vietnam
- Yanagi, S., 1989, *The Unknown Craftsman: A Japanese Insight Into Beauty*, Kodansha Int. Ltd.: Tokyo

IMAGE AND FIGURE REFERENCES

- Figure 1-10 Images by Lale Dilbaş, 2018, Personal Archive, LC Home Co. Ltd., Bat Trang, Hanoi, Vietnam.
- Drawings by Gökçen Dinçer, 2018, Yaşar University, Faculty of Art and Design, Animation Dept., Izmir, Turkey
- Image 1 Funda Altın, 2018, Personal Archive, Hoa Lo Prison Museum, *History*, Bat Trang, Hanoi, Vietnam
- Image 2-13 Funda Altın, 2018, Personal Archive, Bat Trang, Hanoi, Vietnam
- Image 14 Lale Dilbaş, 2018, Personal Archive, Bat Trang, Hanoi, Vietnam.
- Image 15 Tate Online Gallery, 2018, Shoji Hamada Artworks, Retrieved from <https://www.tate.org.uk/search?type=artwork&q=shoji+hamada>, [21.07.2018]
- Image 16 Tate Online Gallery, 2018, Bernard Leach Artworks, Retrieved from <https://www.tate.org.uk/search?q=bernard+leach&type=artwork>, [21.07.2018]
- Image 17-24 Funda Altın, 2018, Personal Archive, LC Home Co. Ltd., Bat Trang, Hanoi, Vietnam

RICE HUSK ASH USAGE AS QUARTZ IN CLAY BODIES

Nagihan Gümüş Akman

Hacettepe University Fine Art Faculty Ceramic Department Beytepe- Çankaya/ANKARA-TURKEY

ABSTRACT

In this study, quartz that one of the ceramic raw materials, has made to be obtained from rice husk ash. Rice husk ash is an organic waste. Quartz, often uses in ceramics and glaze preparations, it is a crystalline form of silicate. Quartz provides easy drying of the interior ceramic body. It controls the shrinking of the globe, increases the resistance to warmth and whiteness.

Rice husks can be converted to silica after being subjected to heat treatment. In the rice husk shell silica has the same essence with the crystalline state of the quartz siliceous material, which is a ceramic raw material.

The rice husk ash is thought to be used as a quartz ceramic body because it contains a high amount of silica. The introduction of the rice husk ash adding into the recipes at various ratios provided an organic waste to the ceramic body as raw material. The results have examined and the availability of rice husk ash as a quartz in the ceramics body has evaluated.

Key Words

Rice Husk Ash, Quartz, Ceramic Body, Organic Waste

INTRODUCTION

The rice husk (glume) used in the ceramic body researches, is a waste material which is obtained by peeling shells of rice plant. The rice husk is very light itself but contrary to its weight, it takes up a lot of space. For this reason, storing rice husk for producers is a big problem and also it ends up as large waste piles.

The glume, mentioned in this research, is the second shell of rice. In all the countries that produce rice, abundant rice husk contains; 40% cellulose, 30% lignin group and 20% hydrated amorphous silica (Görhan, Şimşek, 2011, pp.108). The silica in the rice, forms the inner structure of the shells.

In ceramic body researches, it is necessary to subject the rice husk to calcination process in order to include it in the body recipes. With the calcination process, the organic substances in the material are removed. During the burning of the rice shell, the organic materials are removed in high proportion (60-65%) and the rice husk ash that comes out in the ratio of 20-25%, contains 95-97% SiO₂. (Mansaray, Ghaly, 1997, pp. 9)

Quartz, which is one of the basic raw materials in ceramic art and sector and which is obtained from rocks, is the crystal of pure silicon dioxide (SiO_2). In this study, the silica used in the sintered body recipe will be obtained from the rice husk ash instead of quartz.

CERAMIC BODY TESTS

Calcination Process

To obtain ash, the rice husks were burned at 700 degrees for 3 hours.

Weighing, Grinding and Preparation of Body Recipes

The obtained ash has been ground for 24 hours to make the ash powder, and then the powderized ash has been added to ceramic body recipes in various proportions.

The three recipes which have been used as base are as follows;

Group A contains: 25% clay, 25% kaolin, 25% nepheline syenite, 25% quartz (Altundag, 2008, pp. 10).

Group B contains: 8% potassium feldspar, 18% sodium feldspar, 27% kaolin, 37% clay, 10% quartz (Topateş, Üstündağ, Özay, Yıldız, Baba, 2005, pp. 594).

Group C contains: 35% clay, 15% kaolin, 50% sodium feldspar, 10% quartz (Çiğdemir, Kara, Kara, 2005, page 571).

In these recipes, the quantity of quartz has gradually been reduced and in the final recipes it has completely been removed but the reduced and removed quartz has been replaced by rice husk ash.

The recipes are as shown in the following table;

Recipe	Clay	Kaolin	Na Feld.	K Feld.	Nepheline Syanit	Quartz	Ash	Water
A	25	25	-	-	25	25	-	100
A1	25	25	-	-	25	20	5	100
A2	25	25	-	-	25	15	10	100
A3	25	25	-	-	25	10	15	100
A4	25	25	-	-	25	5	20	100
A5	25	25	-	-	25	-	25	100

B	37	27	18	8	-	10	-	100
B1	37	27	18	8	-	5	5	100
B2	37	27	18	8	-	-	10	100
C	35	15	50	40	-	10	-	100
C1	35	15	50	40	-	5	5	100
C2	35	15	50	40	-	-	10	100

Drying and Firing of the Bodies

The formed test bodies have been left to dry in a moisture free environment. After the drying process, the firing process has started. Bodies were fired in electric kiln at 1050 °C, 1100 °C, 1150 °C, 1200 °C, 1250 °C. The views of the samples are as below.





1050°C

1100°C

1150°C



1200°C



1250°C

A2 PRESCRIPTION

%25 KAOLIN

%25 CLAY

%25 NEPHELINE SYENITE

%15 QUARTZ

%10 RICE HUSK ASH



1050°C

1100°C

1150°C



1200°C



1250°C

A3 PRESCRIPTION

%25 KAOLIN

%25 CLAY

%25 NEPHELINE SYENITE

%10 QUARTZ

%15 RICE HUSK ASH



1050°C

1100°C

1150°C



1200°C



1250°C

A4 PRESCRIPTION

%25 KAOLIN

%25 CLAY

%25 NEPHELINE SYENITE

%5 QUARTZ

%20 RICE HUSK ASH



1050°C

1100°C

1150°C



1200°C



1250°C

A5 PRESCRIPTION

%25 KAOLIN

%25 CLAY

%25 NEPHELINE SYENITE

%0 QUARTZ

%25 RICE HUSK ASH



1050°C



1100°C



1150°C



1200°C



1250°C

B PRESCRIPTION

%8 K FELDSPAR
%18 NA FELDSPAR
%27 KAOLIN
%37 CLAY
%10 QUARTZ



1050°C



1100°C



1150°C



B1 PRESCRIPTION

%8 K FELDSPAR
%18 NA FELDSPAR
%27 KAOLIN
%37 CLAY
%5 QUARTZ
%5 RICE HUSK ASH



1050°C



1100°C



1150°C



1200°C



1250°C

B3 PRESCRIPTION

%8 K FELDSPAR
%18 NA FELDSPAR
%27 KAOLIN
%37 CLAY
%0 QUARTZ
%10 RICE HUSK ASH



1050°C



1100°C



1150°C



C PRESCRIPTION

%35 CLAY
%15 KAOLIN
%50 NA FELDSPAR
%10 QUARTZ



EVALUATION OF SAMPLES

A, B, C recipes have been used as base recipes. The quartz percentages obtained from the rocks in the recipes are 25% for recipe A, 10% for recipe B and 10% for recipe C. These ratios have been reduced by 5% each time, and the reduced amounts have been complemented by quartz obtained from rice husk ash. In the recipes A5, B2, and C2, only rice husk ash has been used as quartz. The resulting clays have been formed by molding. No problem has been encountered during casting, demolding and drying of the samples. Samples have been fired at 1050, 1100, 1150, 1200, 1250 ° C. In the samples, a pinkish beige smooth surface has been observed at 1050 ° C, 1100 ° C, 1150 ° C. There was no discernible difference in the appearance of the samples that have been fired at those temperatures. Samples at 1200 ° C and 1250 ° C have turned grayish white and a slight glare has been observed at 1250 ° C. No light transmission has been observed in any of the experiments. As the rice husk ash content and firing temperature of the recipes were increased, the color obviously lightened and whitened. At the same time, the samples have been observed to get lighter in weight. The samples sintered at 1200 ° C and 1250 ° C. At other temperatures, sintering did not occur as the water absorption percentages were higher than 5%. It has been determined that the grinding process is an important step for the bodies that contain rice husk ash. It has been observed that, besides the quality of the raw material, the grain size of the raw materials must be equal in order to provide a plastic structure.

As the group A recipes have a higher percentage of quartz, the rice husk ash has also reached higher utilization rates. As the ratio of rice husk ash increased in the group A recipes, the colors of the testing bodies have been observed to change from the light pink to the grayish white. All the bodies are durable. The A4, A5, B2, C3 bodies are fine to create thin forms and they are very light. Also in B and

C group recipes, the color lightened as the rice husk ash ratio increased. However, since the quartz ratio in these recipes is less than the group A recipes, it is not possible to see the color change in a wider range. Rice husk ash bodies are thinner, harder and lighter in color than quartz bodies. However, it has been observed that the firing shrinkage rates of rice husk ash bodies are higher than quartz bodies. This situation suggests that the shrinkage rates should be considered even more while working with rice husk ash bodies.

CONCLUSION

In this study, it was experimented to use rice husk ash as quartz in sintered body recipes for the high silica it contains. Samples fired in electric kilns at 5 different temperatures. A total of 60 trials have been evaluated. As a result; rice husk ash has shown the same quality as quartz in ceramic bodies. In fact, due to the light, almost white colored bodies it creates, rice husk ash is thought to be more useful in glaze and decor applications than the bodies that contain quartz. Moreover, the ash bodies are suitable for creating very thin forms. It was already known scientifically that the waste part of a foodstuff that ends up as waste piles in nature can be used as quartz in ceramics, but through this experimentation, it has also been proved to be applicable.

Quartz, which is mined from nature by damaging it, is a mineral with limited resources that can not be replaced or recurred. However, the rice husk is the waste part of a kind of foodstuff which is already being produced and will always be consumed.

As long as the rice is planted, rice husk ash can be used as quartz. As an alternative to the raw material of quartz, the use of rice husk ash in ceramic bodies is also a recycling activity and is expected to make a positive contribution to the environment.

REFERENCES

- Altundağ, Melahat., *1150 C Derecede Gözeneksiz Bünye Araştırması Doğrultusunda Özgün Seramik Uygulamalar*, (Yayınlanmış Sanatta Yeterlik Sanat Eseri Çalışması Raporu) Hacettepe Üniversitesi/ Güzel Sanatlar Enstitüsü, (2008), Ankara.
- Çiğdemir, G., Kara, A., Kara, F., *Porselen Karo Bünyelerinin Kompozisyon Sinterleme kuvars davranışı ilişkilerinin incelenmesi*, Seres III. Uluslararası Katılımlı Seramik, Cam, Emaye, Sır ve Boya Semineri Bildirimler Kitabı, (2005), Eskişehir.
- Gökhan G., Osman Ş., *Betonun Fiziksel ve Mekanik Özelliklerine Pirinç Kabuğz Külünün Etkisi*, Yapı Teknolojileri Elektronik Dergisi Cilt: 7, Sayı: 1, s. 108, (2011).
- Mansaray, K. G., Ghaly, A. E., *Physical and thermochemical properties of rice husk*, Energy Sources, Part A: Recovery Utilization, and Environmental Effects, (1997).
- Topateş, G., Üstündağ, C.B., Özay, Ö., Yıldız, M., Baba, A., *Çan Termik Santral Uçucu Külünün Seramik Sırında Kullanımı*, Seres III. Uluslararası Katılımlı Seramik, Cam, Emaye, Sır ve Boya Semineri Bildirimler Kitabı, (2005), Eskişehir.

CONTEMPORARY ART CERAMIC: DIALOGUES BETWEEN TECHNIQUES AND CULTURE OF THE BRAZILIAN NATIVE PEOPLE

Silvia Regina Grando¹, Emanuelle Bottega Ramos², Milene Back Juwer³, Heloísa Tenroller, Viviane Diehl^{1, 5}

¹ Federal Institute of Education, Science and Technology of Rio Grande do Sul (IFRS), *Campus*
Viamão/Brazil

² Federal Institute of Education, Science and Technology of Rio Grande do Sul (IFRS), *Campus*
Feliz/Brazil

³ Federal Institute of Education, Science and Technology of Rio Grande do Sul (IFRS), *Campus*
Feliz/Brazil

⁴ Federal Institute of Education, Science and Technology of Rio Grande do Sul (IFRS), *Campus*
Feliz/Brazil

⁵ Federal Institute of Education, Science and Technology of Rio Grande do Sul (IFRS), *Campus*
Feliz/Brazil

ABSTRACT

The materiality, the creative process and the technical developments bring visibility to the artistic ceramics in Vale do Caí, in the south of Brazil. This region stands out for the production of structural ceramics, especially bricks and roof tiles, with opportunities for work and income for the community. In this context, research on artistic ceramics is now unfolding in projects that bring challenges to think about the condition of the Brazilian native people. The recognition of the Guarani people, among the native groups that inhabit the south of Brazil, stands out for the production of ancestral ceramics. It is from this universe that the proposal of the artistic production for an intercultural education arises, that allows to extend the aesthetic experience. The objective in this study is to problematize and move reflections that reverberate in the production and poetic presentation of artistic work in ceramics, constituted from the study and recognition of the Guarani culture contribution for the Brazilian people formation. The dialogue of the creative process in the plastic production is made with experimentations in an alternative silkscreen print process and alternative kilns to fire techniques. The Guarani culture influences the artistic production in contemporary ceramic and moves the aesthetic education that is an educative possibility of contribution to the culture. Ceramic art work contributes to breaking with segmentation and instigates curiosity, showing the correlations between knowledge, the complexity of life and relationships of affection, that are capable of problematizing what is lived in a shared culture.

KEY WORDS: Guarani culture, ceramic art, alternative process, interculturality.

1 INTRODUCTION

This study was motivated by the thesis "Educatorartist: meetings of education, visual arts and interculturalism" (DIEHL, 2015), which deals with the relations between poetic production and teaching performance. Thus, the research aims to problematize and to move reflections that reverberate in the production and poetic presentation of artistic works in ceramics, constituted from the

¹ E-mail: viviane.diehl@feliz.ifrs.edu.br

study and recognition of the intercultural relations in the formation of the regional population, potentializing the art as knowledge.

Module notions and repetition always presented in the artistic production are capable of offering operation groups that contribute to render problematics about poetic researches. In these experiments, the visual poetics deal with intercultural relations about studies of the Mbyá Guaraní culture, one of the native groups that contribute significantly to the ceramic production in southern of Brazil.

The abundance of natural raw materials and alternative energy sources enables Vale do Caí, where the Federal Institute of Education, Science and Technology of Rio Grande do Sul - Campus Feliz (IFRS Campus Feliz) is located, to be the main producer of ceramic materials from Rio Grande do Sul. Ceramics have followed the evolution of men and have always been present in daily life since the beginning of history. Firstly, as part of mythical rituals and daily utility objects, pottery has circulated through many spaces and has offered research possibilities.

The project establishes a qualitative research, in which the approach is exploratory and experimental. Initially, an inventoring and descriptive character, evaluates the academic and scientific production in the bibliographic research of primary and secondary sources. The objective was to demarcate the influence of art from Guaraní culture in the people's formation (from Rio Grande do Sul, Brazil), as well as about the ceramic artefacts production.

The theoretical material for the research on primary and secondary sources has been elaborated with regard to the material and immaterial cultural manifestations of the Guaraní people in the southern region of Brazil. These studies expanded the knowledge about the theme, in different levels of depth, contextualizing artistic production in ceramics (AHLERT; GOLIN, 2009; BARDIE, 2015; BRANDÃO, 1990; LA SÁLVIA; BROCHADO, 1989; LIMA COSTA, 2018; POTY; CHRISTIDIS, 2015; RIBEIRO, 2008; SILVA; PENNA; CARNEIRO, 2009).

In ceramic artistic production, the movement between practical aspects and theoretical fields of knowledge is constant. Procedures, techniques, materials, supports, and technologies were experimented, overlapping and recontextualizing the artistic practices. The investigations of ceramic art creation show plastically materialized results, from experimentations in an **alternative silkscreen print process** and **alternative kilns of fire techniques**. The production of artistic pieces using screen printing to transfer the image to a curve surface, as well as surface design by firing techniques, created expressive experimentations with alternative process.

In the artist creative and productive experimental process, the poetic renders problematics and moves the knowledge. These reverberations are materialized in the art ceramic production, leading to critical and aesthetic senses. The public presentation of the artistic work is a possibility of an "encounter", where it is possible to share the ceramic art poetics with people's own life experiences, so an intercultural relation can be established. To Richter (2003, p. 114), "[...] the utilized time into something pleasurable, with a strong symbolic and social sense gives beyond aesthetic satisfaction another socialization through the encounter".

The encounter, the sharing and the intercultural relation provoked by the produced ceramic art in this project are elements which cause interest to foment the aesthetic education. So, the reflexions and dialogues happen attributing meaning to the experienced in life expectations and transform the ways of seeing and being in the world.

2 ABOUT MBYÁ GUARANI CULTURE

Brazil is marked by the miscegenation and diversity of cultures. In relation to this aspect, Richter writes that:

Nowadays, the term "interculturality" has been used, which implies an interrelation of reciprocity between cultures. This term would therefore be the most appropriate for a teaching-learning in the arts that proposes to establish the interrelationship between the cultural codes of different cultural groups. However, we use all these denominations, appearing as synonyms. (RICHTER, 2003, p. 19)

Among so many manifestations, we highlight that ceramic productions of different ethnicities, especially of the original people, has contributed to the formation of Brazilian people. In Brazilian native cultures, we have the production of pottery, that remains present in some people of the national territory, representing aspects of daily life. Commonly, they are utilitarian objects of daily use, like pots and bowls, funeral urns, or sculptural figures with differentiated characteristics.

The exhibition “Indigenous Adornment from Brazil: contemporary resistance” happened in São Paulo and showed elements from material culture to body adornments, created and used by Brazilian ethnicities as a resistance through culture. Today there are about 300 ethnicities and, among of them, the Mbyá Guaraní, that inhabit the south of Brazil (ADORNOS, 2017). Mbyá Guaraní people is scattered in the south of Brazil and live in many cities, from northwest Argentina, Paraguay, Uruguay (SOUZA, 2008). Especially the Mbyá Guaraní culture interests us in this project because they inhabit the south region and produce ceramics; contributing to the creation of the intercultural Brazilian people (POTY; CRHISTIDIS, 2015).

The clay has been used to make utility items as a way of meeting their daily needs. Some examples are pottery, tableware and clay's pipe, used to smoke tobacco. Archaeological studies show that the clay they produced was more anti-plastic and was not found near their village. From the samples collected at the archaeological sites, it is possible to identify the type of the paste (processed clay) and find out where they produced the pieces. In general, most of the pieces were carried out close to the river valleys, considering that in the production process, variables such as environment, technique and time are relevant (LA SÁLVIA; BROCHADO, 1989).

In Guaraní ceramics, the most commonly used shaping technique is coil method, in which they mainly pressed their fingers and nails for detailing and applying for patterns and textures, using tools for finishing the pieces (figure 1). The slip² decoration is used to reduce porosity and increase waterproof in the ceramic body (figure 2).



Figure 1: Archaeological Guaraní ceramics.

Source: <http://museuantropologico.blogspot.com.br/2013/06/tradicao-tupiguarani.html>



Figure 2: Archaeological Guaraní ceramics with slip and graffito design.

Source: <http://museuantropologico.blogspot.com.br/2013/06/tradicao-tupiguarani.html>

The productions of the Guaraní pottery began to be a form of expression and the techniques, little by little, were getting better. The Guaranis started to use tools only for shaping, but the colours and designs are carefully applied to the parts.

² Slip is the suspension of clay in water when in the consistency of thin cream. It is a primary decorating process where slip is placed onto the leather-hard clay body surface before firing, if it is burned, it gives waterproofing condition.

In each culture, ceramic production has specific processes for the development of artefacts with typical characteristics of ethnic group. There is no way to establish a single definition of these traditions because they are elements of different cultures from native people that intertwine one with another. "To deal with ceramics is, in principle, to deal with contrasts: either in the opposition between the mass malleability and the resistance achieved in the burning, or by the recurrent references, though in common sense, from a practice that results both in everyday utilities, as well as splendid examples of plastic sophistication" (GRINBERG, 2008).

Clay, shaping, modelling, handbuilding, surface treatment, materials, firing techniques, surfaces coating and everything else involving this field are researched and selected to suit the proposal for art ceramic design. The handbuilding by coils, by slabs, by insertion and removal clay compose the procedures contemplated with the natural raw clay from the south's region deposits (AMBER, 2012; FRIGOLA, 2006; MILLS, 2011).

The conditions in which the cultural manifestations operate call us for an intercultural dialogue with art, so that they enable them to be historically recognized. The artistic processes can move subjectivities and evoke an understanding constituted of the wisdom of the experience, that bases the knowledge from the relations.

When we share the art ceramic in an intercultural context, we can provide singularities of feeling, thinking and doing in a movement of perceptive, experimental, creative, critical and participative interactions. Thus, we can unlearn the truisms that have been institutionalized in and create reflections about the social responsibilities we can assume.

This project signalizes possibilities to guide the poetic production, rendering problematics and finding ways of expression and ways of operating in the ceramic art with the potential to transform the way to understand the living; the ability to be and live together.

3 EXPERIMENTATIONS BY AN ALTERNATIVE SCREEN PRINTING METHOD

Nowadays, there are numerous options for transferring images to ceramic materials. The techniques are used in different processes to position multiple or repeated images on art work. Materials and equipments are diverse and suitable for each technique.

The ceramic surface with printed images stands out for its versatility and, based on the investigations that have been carried out by the researcher, the results of some experiments with serigraphic impressions arise in the creation of artistic productions in ceramics, as well as the need to broaden and facilitate the technical processes.

Silvia Barrios³ (2009, 2013) studies come to this topic and seek to expand and qualify the development of accessible procedures for the creation in the field of ceramic's silkscreen. Screen printing is a common method for transferring designs. In the project "Study about technical and creative process applied in ceramic's screen printing" (DIEHL, 2017; DIEHL; JUWER, 2017) theoretical-practical approaches were developed based on laboratory experimentation, to identify stages and needs of technical and material processes in ceramic surfaces.

Finally, the silkscreen production was developed from an alternative process with the transference of the image on a curved surface, resulting in artistic works. In this research experimentations, wet green clay, dried clay and sintered surfaces were made to show a variation in printing onto a curve surface.

The methods used to transfer onto a curved piece, made of clay, the final image was printed on plastic film, making the transference process accessible and affordable for everyone. This method simplifies the process and makes use of safe, cheap and accessible materials (BARRIOS 2009, 2013).

Thus, the study collaborated to test and qualify the indicated procedures, which proposes an alternative methodology based on materials of daily use, both for the process of screen's preparation and for the image transference on the curved ceramic surface. These results allowed to expand the expressive possibilities for the artistic production, with different characteristics of graphic printing in ceramics.

³ *Movimiento cerámico-gráfico de Latinoamérica y el Caribe.*

4 ALTERNATIVE FIRING TO LOW-TEMPERATURE TECHNIQUES

A variation of ceramic firing techniques can be done to clay providing resistance, waterproofing and aesthetic character to the ceramics. Alternative kilns, post firing techniques, reduction methods, low-temperature firing processes are possibilities to achieve expressiveness in art work.

Alternative kilns to fire techniques (CHITI, 1980; DIEHL; JUWER, 2018; MILLS, 2011; WATKINS & WANDLESS, 2006; VIDAL; JAMES, 1997) were used in this research to explore chemical components and organic combustion materials. Thus, it provides the development of possibilities to technical props of burning, with the use of accessible materials. The unknown of this process manufacture times imitates experimentation in ceramics, restricting the access of technical possibilities and exercise to inventive creation.

The kiln used to fire the ceramic art with aluminium foil saggars was originally developed to protect ceramics from ash-slagging and flame-flashing in wood firings. Some potters make aluminium foil saggars that used to contain and isolate pots during a sagger firing.

In contemporaneity, this process with aluminium foil is used to contain fumes around a pot, so that the pot picks up colour from the fumes. The aluminium foil is not a material for complete insulation because it partially deteriorates during burning, allowing the effect of the flame and smoke in the reduction atmosphere (WATKINS; WANDLESS, 2006). In this kind of saggars firing, copper sulphate, ferric chloride, fine and coarse sea salt, cottonseed meal, baking soda, copper wire, copper carbonate, titanium dioxide and other materials can be used to pick up different colours and effects.

The alternative kiln was developed in an easy system during the project “Ceramicando”⁴ (DIEHL, 2018) to promote access to interested people in the burning process without complex and expensive equipment. This kiln is made with bricks using a vegetal coal and residual wood by local production arrangement. The material is accessible in the south of Brazil because it is a region that concentrates brick-making companies and furniture companies, whose wood production residues are used as fuel. The kiln is built from a brick base, raising the overlapping walls and the complete process can be known in the video “Alternative kilns to firing techniques” (DIEHL; JUWER, 2018).

Ceramic art production improves relations that inscribe in the clay materiality, in the expressive potentiality of the ceramic language in a continuous flow to be boosted with the poetic production in ceramics, impregnated by the interculturality from the Guarani people. “The artist's practice and his behaviour as a producer determine the relation that is established with his work: in other words, what he produces, in the first place, are relations between people and the world through aesthetic objects” (BOURRIAUD, 2011, p. 59).

Thus, artistic works operate in the theoretical and practical context of interactions with people, collectivity and art, configuring intercultural processes 'in-between' spaces (BHABHA, 2013). Art, therefore, constitutes an ‘in-between’ space of investments, of problematics and of exchanges of aesthetic characteristics, in which collectivises culture from what the artist proposes.

5 METHODOLOGY

Keeping in mind the poetic process that have been developed by the artist in the series “Many Moons”, “Landscapes of the time” and “Encounters”, the ceramic art work made in this study shows elliptical shapes, and it is characterized by circularity. For this purpose, the materiality of the clay and its plasticity provides a diversity of possibilities in the production. In the inventive creation process (DIEHL, 2015), the references built on the intercultural theme with the Mbyá Guarani (LA SALVIA; BROCHADO, 1989; SILVA; PENNA; CARNEIRO, 2009; POTY; CHRISTIDIS, 2015) allowed exploratory and experimental processes for the development of ceramic art pieces.

These pieces were produced with Brazilian commercial white and red ceramic mass, some of them with varied intensities of burnish surface. The shaping was performed using the technique of

⁴ This project has happened annually since 2014 and it aims to disseminate and give visibility to different possibilities of ceramic in the sociocultural context. It consists in a proposal for the development of shared actions with schools in the south of Brazil. Financial Support by Pro-Rector for Extension Programs (PROEX) – Federal Institute of Education, Science and Technology of Rio Grande do Sul (IFRS), Brazil.

plaques and plaster molding (AMBER, 2012; FRIGOLA, 2006), to be burnt between 530 °C and 1000 °C.

In the ceramic art works that are shown in this study, different technique possibilities were used with expressive content for the poetic proposition: screen printing alternative process in curve surface and firing techniques to low-temperature.

5.1 Screen printing alternative process in curve surface

Firstly, the screen printing process was selected for the image transference of the hand-drawn Guarani portraits. The studies related to the drawing were made from a research in the photography book “Mbyá Guarani”, by Poty e Christidis (2005). These drawings are ethnic and expressive references that were printed on green and sintered ceramic surface, based on the alternative process for image's transference by Barrios (2009, 2013, 2017).

On this screen printing alternative process procedures were adapted to make it easier the accomplishment of all the steps in different places; saving money and adapting to spaces, once it does not require specific equipment for this matter. The screen was prepared by using a photosensitive emulsion, and the drying process was performed making use of a hairdryer. For providing a dark place, a cardboard box was used, where the screen could be closed during the corresponding times between drying steps.

The frame with polyester fabric printing of mesh 40 was prepared with a water-based blocking medium and the hand-drawn Guarani portraits on acetate were put on screen, to be printed with oil-based ink (SCOTT, 2013; MILLS, 2011). On the printing step, two kinds of inks were used: One of them was prepared with black pigment and the other one with copper oxide, mixed with twenty percent of flux (low temperature glaze) and pine oil. These prints were transferred to a sintered and green ceramic body (leather hard body) in curve surface. On this process, monoprints were made on stretched plastic film on a tile. After that, carefully by hand, the printed plastic was pressed faced down to the surface, until the image was fixed in the ceramic body. In the end, those pieces were fired in an electric kiln, between 980°C to 1100°C.

5.2 Surface design by firing techniques

Each firing process has a different type of atmosphere, and the appearance of a clay body can be drastically affected by the atmosphere of the kiln. “Many variables can influence the success of a low-temperature reduction-fire piece, including the duration of the burning, the type and size of the wood or other fuel materials used, and the level of reduction atmosphere that is maintained. These firings are suitable for all clay types” (MILLS, 2011). As with forming techniques, one way of firing is not better than another – only different.

Electric kilns do not use oxygen as they create heat, making an oxidized atmosphere. A kiln that heats by burning organic materials as fuel draws oxygen from the atmosphere in the kiln, as well as the clay. This fire creates a reduction atmosphere, in which the “effect in the appearance of a clay caused by reduction is the grey or black colour resulting from the deposited carbon in the pores of the ware during the burning and remaining there in the finished product” (RHODES, 1973, p. 264). More primitive and alternative kilns in construction and potters relied entirely on wood or other solid fuels, so reduction is a natural result; if not of inevitable occurrence, hard to prevent rather than hard to achieve. “Reduction should not be thought of as a difficult process resulting from some involved technique, but rather as the result of a smoke fire, as contrasted with the clean-burning, oxidizing fire which is normal in an efficiently operating kiln” (RHODES, 1973, p. 264).

In low-temperature techniques, the reduction atmosphere enables chemical reactions that yield interesting surfaces and aids in creating a blackened surface from grey to black. The fire and smoke marks that were lively left on the clay from this process, for the most part, are uncontrollable. These characteristics are significant to design surfaces and they can be explored.

In the low-temperature firing category (as in a pit, barrel kiln or brick kiln), the heating reaches 530°C to 750°C (CHITI, 1980; WATKINS; WANDLESS, 2006; MILLES, 2011). Thus, decisions have been taken to fire the ceramic art work keeping in mind the appropriated process by burning surface reaction, in order to create an expressive ceramic art work.

Therefore, two different firing methods were used: **Aluminium foil in an alternative brick kiln** and **high-contrast ceramic surface**. The methodology to make the low-temperature burning that resulted in the ceramic surface was based in Chiti (1980), Watkins and Wandless (2006), Milles (2011), Rhodes (1973) and others.

5.2.1 Aluminium foil saggar in an alternative brick kiln

In this firing method, the alternative brick kiln was used (DIEHL; JUWER, 2018). The ceramics were stacked up in layers, adding sawdust and vegetal coal around them to fill in the kiln. As adding ceramics, organic material was continually being added until the top of the kiln and after, to light the wood. The fire burned from the top to the kiln bottom with the metal lid placed on top of them.

The preparation for the aluminium foil saggar was simple and the works fired this way had a colourful, mottled surface of red, pink, brown, grey and black. (WATKINS; WANDLESS, 2006). For the procedure, two sheets of foil, large enough to cover the ceramic were prepared. One of them had to be crumpled, due its irregular surface, creating small air pockets. Next step was to trace the ceramic body with copper wire and, with safety materials, sprayed ferric chloride (10 to 20g solved in 500 ml water) and copper sulphate solution (10 to 20g solved in 500 ml water); creating accent areas on the surface. Then, coarse salt and copper sulphate were sprinkled in the wet piece and aluminium foil was rolled covering all ceramic body.

These pieces in red and white clay were burned in the alternative brick kiln. The aluminium foil breaks down at 566°C (WATKINS; WANDLESS, 2006). In a direct visual observation, this characteristic was proved in the end of the firing. The expected temperature in this burning cycle is from 530°C to 750°C (CHITI, 1980; WATKINS; WANDLESS, 2006; MILLES, 2011). The burned ceramic has bass and treble characteristic sounds, which confer the quality of clay sintering (ABNT, 2005). After cooling, the pieces could be removed and cleaned.

5.2.2 High-contrast ceramic surface

In this experimentation, an electric kiln was used for heating bisque ceramic body, and red and white clay were used to get quick effects with different materials, for a loose and spontaneous effect on surface. Employing some techniques, using reduction process and ferric chloride in multiple applications result in a rusty red-brown, grey and black effects (WATKINS; WANDLESS, 2006; MILLS, 2011).

Many kinds of organic materials, such as horse hair, feathers, granulated sugar, twigs, soft cotton fabric, Spanish moss, when burned on the hot red and white ceramic creates distinct patterns. The ceramic piece was heated in the electric kiln until 900°C, after that, it was taken out and placed on a refractory material for the bottom to be smoked with a burned paper towel. Then, organic materials were placed into the hot ceramic and the reduction created different effects on its surface, with the carbon producing strong lines and stains in black and grey colours. After that, a ferric chloride solution was sprayed with accent variation, that created tones of rust and amber. When that ceramic was cooled, remaining ashes were removed from the surface.

Each material shows different reactions and the experimentation in this process allows to discover and know what the visual interesting effects are to the poetic artist.

5.3 Results and discussion

The ceramic art work in composition with other materials achieved expressive potential to move ideas and reflections about the Mbyá Guarani related topics; such as rights, colonization, the fight for land, natural resources, religious system and others (BRANDÃO, 1990, LIMA COSTA, 2018; RIBEIRO, 2008), creating associations and intercultural relations as it was observed in some exhibitions presented. These topics and techniques chosen built up the artistic production that was developed in this study.

One of the technical experimentations was performed through screen printing alternative process, bringing ethnical references from young and elder Mbyá Guarani people (figures 2 e 3).

These references put in evidence the Elder, who has the commitment to pass through his knowledge of the “well-being of Guarani life” (BRANDÃO, 1990; CLASTRES, 1990) to the younger generations. The kids are responsible for learning their culture, so it can keep existing in the future as well as being shared to others. (MARQUES *et all*, 2015).

The screen printing alternative process (figures 2 e 3) keep being experimented to qualify this methodology procedures, with alternative possibilities that make the execution of simple equipment easier.

For better results in screen printing alternative process in curve ceramic surface is recommended sintering and wet green body. The sintered ceramic must be heated to about 80°C because, at this temperature, the image transference is fixed on curve surface without losing the design quality. Screen printing was used as a technical resource in the ceramic surface to give visibility to the Guarani's portraits.



Figure 2: “Colonizar”, 20x30x30cm, 2017. With clay, screen printing, black pigment, 1000°C, Guarani basket by nature fiber, pillow, soil. Photo taken by the artist.



Figure 3: “Aquifer Guarani”, 30x30x11cm, 2017. With clay, screen printing, black pigment, 1000°C, fabric pillow, soil. Photo taken by artist.

The surface design by fire burning techniques achieves contrasting results and gives interesting surface effects by chemical and physical reactions. The small air pockets in the aluminium crumpled foil result in random patterns wherever the foil touches the piece according to the added materials. Copper sulphate and ferric chloride solutions can vary depending on how heavily or lightly they were applied. The results had intense and different colours and tones, such as rose, mauve, rust, red, brown; observed in the figure 4. The coarse salt, in contact with the wet ferric chloride, creates intense rust stains, and with the copper sulphate green points can be observed, resulted from the reduction. Copper wire tightly wrapped in the ceramic piece creates irregular line marks from grey and black colours wherever it touches the surface.



Figure 4: “Heads”, 12x80x15cm, 2018. White clay, aluminium foil saggar, reduction firing, 1000°C.
Photo taken by the artist.

In the process of “high-contrast ceramic surface” (figure 5), organic materials create local carbon marks in the immediate area it is in contact with. Horse hair design left strong black lines with ranging trails from grey to black onto the surface, that accent the movements. Granulated sugar must be slightly dropped to result in scattered and light stains. The temperature of the piece must be set at around 600°C, once the organic material carbonizes extremely fast, which can compromise the quality in the design of the patterns when submitted to high temperatures.

For the Mbyá Guarani, land is the origin of all life, and this process has dramatic expression by contrasting strong soil colours.



Figure 5: “Heads”, 12x80x15cm, 2018. White and red clay, high-contrast ceramic surface, 1000°C/600°C. Photo taken by the artist.

In figure 5, it is possible to observe that light ceramic body shows contrasting colours; however, red clay bodies have dark and hot soil shades. The ceramic polished pieces present a satin touch as a surface characteristic result. Furthermore, it is not possible to have fully control of the produced effects by firing techniques methods and materials. These variable results in the art ceramic create relations and senses in the dialog with the Guarani culture.

6 CONCLUSIONS

The presented results in this study for the series “Origins” indicate that a creative expression can be achieved in ceramic art between techniques and cultural studies. The Guarani culture have been experienced through ceramic art, with attention to the singularity of each shape, material and technique.

Ceramics in contemporary art bring it back manual work, materiality, and object shape. The implications of know-how, technical processes, the production routine in art claim and reaffirm by reconfiguring the spaces for another way of doing contemporary art.

In the scientific and poetic fields, documental and experimental, intelligible and sensitive are constituted by 'in-between' spaces where the provocative relations happened in the art production. The process of ceramic art creation is aesthetically understandable and helpful to make connections across cultures, because senses and meanings are singularly produced by each one in relation to this ceramic art work.

The building of theoretical and practical knowledge fomented the creative process to problematize the interculturality by means of aesthetic education; being able to transform the way of seeing and being in the world. The possibility of contemporary ceramic art expression can be a way to bring questions and reflections, sensibility and thoughts to establish connections about the intercultural formation of the Brazilian people and to result in a resonant experience in art exhibition.

7 ACKNOWLEDGMENTS

The authors acknowledge the financial support from the by Pro-Rector of Research, Innovation and Post-Graduation (PROPI) – Federal Institute of Education, Science and Technology of Rio Grande do Sul (IFRS), and National Council for Scientific and Technological Development (CNPq), Brazil.

REFERENCES

1. Adornos do Brasil Indígena: resistências contemporâneas. São Paulo: [s.n.], 2016. 80 p. Exhibition Catalog, 07 sept. 2016-8 jan. 2017. SESC Pinheiros.
2. Ahlert, J., Golin, T., Estatuária missioneira: representações de fronteira. In: Silva, G. F. da, Penna, R., Carneiro, L. (Orgs.). RS Índio: cartografias sobre a produção do conhecimento. Porto Alegre: EDIPUCRS, 2009, 39-70.
3. Amber, S., Hand building. New York: Lark Crafts, 2012.
4. Associação Brasileira de Normas Técnicas, NBR 15310: Componentes cerâmicos - Telhas - Terminologia, Requisitos e Métodos de Ensaio. Rio de Janeiro, RJ, 2009.
5. Bardie, M. C., Rituais de iniciação e relações com a natureza entre os Mbya-guarani. Mana, Rio de Janeiro, v. 21, n. 1, 07-34, Apr. 2015. Available from: <http://www.scielo.br/scielo.php?script=sci_arttext&pid=S0104-93132015000100007&lng=en&nrm=iso>. Access on 08 Sept. 2018. <http://dx.doi.org/10.1590/0104-93132015v21n1p007>.
6. Barrios, S., Serigrafia cerâmica: elaboración de calcomanías, proceso, materiales y armado de un laboratorio. Available from: <<https://silviabarriosplasticaceramista.wordpress.com/2013/01/26/12566/>>. Access on 08 sept. 2018.

7. Barrios, S., Tensado de shablonos y preparado de la emulsión para realizar serigrafía cerámica. Available from: <<https://silviabarriosplasticaceramista.wordpress.com/2009/08/30/serigrafia-tecnica-de-cuerda-seca-elaboracion-de-shablonos-grabado/>>. Access on 08 sept. 2018.
8. Bhabha, H., O local da cultura. Belo Horizonte: UFMG, 2013.
9. Bourriaud, N., Estética relacional. São Paulo: Martins Fontes, 2011.
10. Brandão, C. R., Os Guarani: índios do Sul - religião, resistência e adaptação. Estud. av., São Paulo, v.4, n.10, 53-90, Dec. 1990. Available from: <http://www.scielo.br/scielo.php?script=sci_arttext&pid=S0103-40141990000300004&lng=en&nrm=iso>. Access on 07 sept. 2018. <http://dx.doi.org/10.1590/S0103-40141990000300004>
11. Chiti, J. F., Curso Prático de Cerâmica. Buenos Aires: Ediciones Condorhuasi, 1998, Tomo 3.
12. Clastres, P., A fala sagrada: mitos e cantos sagrados dos índios Guarani; tradução Nícia Adan Bonatti. Campinas, SP: Papirus, 1990.
13. Diehl, V.; Juwer, M. B., Serigrafia na cerâmica. 2017. Available from: <<https://www.youtube.com/watch?v=fSHKOyY1380&t=31s>>. Access on sept. 2018.
14. Diehl, V.; Juwer, M. B., Alternative kilns to firing techniques. Available from: <https://www.youtube.com/channel/UCmXqo15fFsJJ7nFFf5o4WHQ/videos>. Access on sept. 2018.
15. Diehl, V., Estudo sobre os processos técnicos e criativos aplicados à serigrafia em cerâmica. 2017. Available from: <http://sigproj1.mec.gov.br/projetos/imprimir_pdf.php?modalidade=50&projeto_id=244440&temp_id=&original=120:25:46>. Access on 08 sept. 2018.
16. Diehl, V. Ceramicando na escola 2018. Available from: <http://sigproj1.mec.gov.br/projetos/imprimir_pdf.php?modalidade=11&projeto_id=297093&temp_id=&original=120:32:24>. Access on 08 sept. 2018.
17. Diehl, V., Educadorartista: encontros da educação, artes visuais e intercultura. Santa Maria: UFSM, 2015. Tese (Doutorado em Educação), Centro de Educação, Universidade Federal de Santa Maria, 2015.
18. Frigola, D. R., Cerâmica Artística. Lisboa: Estampa, 2006.
19. Grinberg, N., Gestos de contemporaneidade: um recorte sobre a cerâmica ocidental na China. Available from: <<http://normagrimberg.com.br/artista/palestras/palestra/gestos-de-contemporaneidade-um-recorte-sobre-a-ceramica-ocidental-na-china>>. Access on feb. 2014.
20. La Sálvia, F., Brochado, J. P., Cerâmica Guarani. Porto Alegre: Posenato Arte & Cultura, 1989.
21. Marques, F. D., Souza, L. M., Vizzotto, M. M., Bonfim, T. E., A vivência dos mais velhos em uma comunidade indígena Guarani Mbyá. *Psicol. Soc.* [online]. 2015, vol. 27, n.2, 415-427. ISSN 0102-7182. <http://dx.doi.org/10.1590/1807-03102015v27n2p415>.
22. Mills, M. E., Surface design for ceramics. New York: Lark Books, 2011.
23. Museu Antropológico do Rio Grande do Sul. Available from: <<http://museuantropologico.blogspot.com.br/2013/06/tradicao-tupiguarani.html>>. Access on mar. 2016.
24. Poty, V., Christidis, D., Os Guarani-MBYÁ. Porto Alegre: Wences Design Criativo, 2015.
25. Richter, I. M., Interculturalidade e estética do cotidiano no ensino das artes visuais. Campinas: Mercado de Letras, 2003.
26. Rhodes, D., Clay and glazes for the potter. Radnor, Pennsylvania: Chilton Book Company, 1973.
27. Scott, P., Ceramics and print. London: Bloomsbury, 2013.
28. Silva, G. F., Penna, R., Carneiro, L. C. da C. (Org.), RS índio: cartografias sobre a produção do conhecimento. Porto Alegre: DIPUCRS, 2009. Available from: <<http://www.pucrs.br/edipucrs/ahrs/rsindio.pdf>>. Access on mar. 2016.
29. Souza, J. O. C. de., Rios da Bacia do Prata: fronteiras do Mercosul, eixos do horizonte cultural guarani. Anais 26ª Reunião Brasileira de Antropologia – ABA, 01 e 04 de junho, Porto Seguro, Bahia, Brasil. 2008. Available from: <http://www.abant.org.br/conteudo/ANAIS/CD_Virtual_26_RBA/grupos_de_trabalho/trabalhos/GT%2005/jose%20otavio%20catafesto%20de%20souza.pdf>. Access on 08 sept. 2018.
30. Vidal, J., James, P., Ceramicando. São Paulo: Callis, 1997.
31. Watkins, J. C.; Wandless, P. A., Alternative Kilns & Firing Techniques. New York: Lark Ceramics, 2006.

THE POWDERY BEAUTY; KOREAN BUNCHEONG WARE

Leman KALAY

Kyung Hee University, Global Campus College of Art & Design, Department of Ceramic Art, 1732
Deokyoungdaero, Giheung-gu, Yongin-si, Gyeonggi-do, 17104, Republic of Korea

The concept of fast firing is now the dominating technology in the ceramic tile sector and the time available to reach an optimal stabilization of the ceramic body is reduced to few minutes. Ceramics have been closely connected with a nation's lifestyle as a commodity. Pottery is an aesthetically unique invention and a piece of life that reflects culture and society. In particular, Buncheong ware in the early Joseon Dynasty reveals its unique style. Buncheong together with white porcelain became mainstream in the early Dynasty. During the Joseon Dynasty, main production was centered on Buncheong ware and white porcelain. Unlike white porcelain, buncheong was produced only during the first 150 years of the Dynasty. "Buncheong", meaning "powdery blue", was actually named by Ko Yoo-Sup who was the first Korean art historian. It represents a distinctive style of ceramics, more rustic and dynamic than the celadon that represented the refined aristocratic taste of the Goryeo. This is visible in both its form and decoration. Buncheong has provided new beauty through folksy expression, contrary to the delicate high-class Goryeo celadon. Buncheong showed interesting aesthetic styles with various views of texture, atmosphere, and patterns based on its free and experimental intention. It contained the lives of ordinary people makes daily life and art encounter each other. It has also been widely applied with modern expressionism in the present time.

ARTISTIC GLASS APPLICATIONS WITH PATE DE VERRE AND POTTER'S WHEEL TECHNIQUES

Dr. Öğr. Gör. Ergün ARDA
Çanakkale Onsekiz Mart Üniversitesi, GSF, Seramik ve Cam Bölümü

The history of ceramics is ten thousand, the history of glass is five thousand years. Looking at the development of glass, research shows that the source of glass is the Mediterranean environment. It is accepted that the glass is produced first in the regions where the appropriate sand is abundant and the construction of ceramics is developed. From Mesopotamia to Egypt, from Eastern Mediterranean to Anatolia, it is possible to see the first examples of glasswork. Taking advantage of the technical characteristics of the old ceramics, pouring the glass in a mold has been used on a large scale from the first glass samples. The technique was applied using the mold and the French ceramic artist Henry Cros (1840-1907) gave the technique the name Pate de Verre. He searched the art and examples of ancient Egyptian glass, mixed with binding raw materials, milled glass beads in the mold experienced in the body. Today, the mold materials and methods used in the application of this technique vary. Glass forms are obtained by heat treatment with closed or open molds made with heat resistant materials. In this study, the pottery wheel which is the ancestor of all the lathes, the ceramic (open) molds were formed and used to obtain the glass form. For a ceramicist who has not worked the glass before, here the knowledge and experience that can be used to recognize, understand and apply the glass are shared.

Kısa Cam Tarihi

Cam, insanoğlunun hayatına paleolitik dönemde girmiştir. Bu cam malzeme doğanın ürettiği Obsidyen'dir. İnsanoğlu yapay camı 5000 yıl önce yapmayı başarmıştır. Hatta kaynaklar bugün bildiğimiz camın ortaya çıkmasından önce, 6000'lerde camın seramik yüzeylerde sır malzemesi olarak kullanıldığını anlatmaktadır (Ceren Baykan, 2012).



Obsidyen Knife From Çatalhöyük.
<http://www.anadolumedeniyetlerimuzesi.gov.tr>
<https://www.google.com.tr/search?q>



Ancient glass beads

=ancient+glass+beads

İlk yapay cam örnekleri cam boncuk olarak üretilmişlerdir ve çok ilgi çekicidirler. Boncukların ortasında bir delik vardır ve kolye, bileklik gibi aksesuar amaçlı kullanılmışlardır.

Cam tarihinin ilk uygulamalarından bu yana camın temel yapısının elde edilmesi ve bu yapının biçimlendirilmesi iki ayrı uzmanlık alanı olarak gelişmiştir. Camın antik dönem temel hammaddeleri Silis, Soda ve Kireçtir. Bugün soda camı olarak tanımlanmaktadır (Karasu, 2000).

Kalıpla Şekillendirme

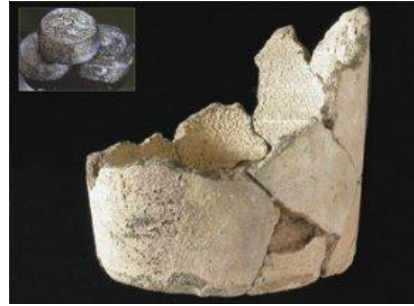
Arkeolojik bulgular, kalıpla şekillendirme yönteminin 6000 yıl öncesinden başlayan bir geçmişi olduğunu göstermektedir. Camın, bir kalıp içine dökülerek biçimlendirilmesi, ilk camcılık örneklerinden bu yana geniş ölçekte kullanılmaktadır. En eski uygulamalarda teknik sınırlılıklar nedeniyle, değişik yöntemler geliştirilmiştir. (Küçükerman, 1985).



Cam külçeler. Bodrum Sualtı Arkeoloji Müzesi.

<https://www.rotasenin.com/bodrum-sualti-arkeoloji-muzesi>

<https://www.sciencenewsforstudents.org/>



Ceramic Mold. 3,250 years ago.

[article/glassworks-ancient-egypt](https://www.sciencenewsforstudents.org/article/glassworks-ancient-egypt)

Archaeologists have found a variety of items used in glassmaking, including this ceramic container, at an ancient Egyptian glass factory. Glass was colored and heated in this vessel, which is about 7 inches across. The inset shows glass ingots from a Bron.



Glass mold, Corning Museum.

<https://www.cmog.org/artwork/mold-7>



Glass mold, Corning Museum.

<https://www.cmog.org/artwork/mold-7>

Romalıların Üfleme tekniğinin geliştirilmesi ile kalıp içine üfleme yaparak çok çeşitli ürün yelpazesine ulaşılmıştır. Bu çalışmada da seramik malzemenin ilk camcılık örneklerinden bu güne kadar bir kalıp nesnesi olarak kullanıldığı bilgisinden hareket edilmiş ve geniş çaplı, yayvan açık seramik tabak kalıplar içinde cam şekillendirilmesi amaçlanmıştır.

Cam Hamuru (Pate de Verre)

Cam hamuru kelimesinin Fransızca karşılığı “pate de verre”, İngilizcede “glass paste”, İtalyancada “pasta vitrea”, Türkçe karşılığı ise “cam hamuru” anlamındadır. Antik Mısır’da kullanılmış bir yöntemdir. Cam hamuru tekniği, Fransız seramik sanatçısı Henry Cros (1840-1907) tarafından gündeme getirilmiştir. Bağlayıcı maddelerle karıştırılmış, öğütülmüş cam tanecikleri ile yaptığı uygulamalarına pate de verre adını vermiştir ve dünyada da bu isimle anılmıştır (Okan, 2008).



Henry Cros (1840-1907), pate de verre rölyef çalışmaları.

<https://www.google.com.tr/search?q=henry+kross+pate+de+verre>

Seramik Kalıp Yapımı

Cam hamuru tekniğini uygulamak için çömlekçi çarkında tek cidarlı kalıplar şekillendirilmiştir. Bu kalıpların en belirgin özelliği kilden yapılmış olmalarıdır. Kalıpların tabanlarında ve kenarlarında hava tahliye delikleri açılmıştır.



Çömlekçi Çarkında Seramik Kalıp Yapımı, 2016, (Fotoğraflar kişisel arşiv)

Tek Cidarlı Açık Seramik Kalıp Yapımı

1- Çömlekçi çarkı üzerine yuvarlak md f yerleştirilir ve tornanın merkezine sabitlenir. 2- Mdf üzerine ve merkezine kil yerleştirilir, elle vurarak yüzeye yayılır. 3- Yayararak, tabanda eşit bir et kalınlığı elde edilir. 4- Torna çalıştırılır ve merkezden dışarı doğru kil yayılarak torna edilir. 5- Kilden bir tabak yapımına başlanır. 6- Öncelikle geniş çaplı bir silindir yapılır.



Çömlekçi Çarkında Seramik Kalıp Yapımı, (Fotoğraflar kişisel arşiv)

7- Silindir dışarı doğru elle bükülür. 8- Merkezden dışarı doğru yüzeye perdah çekilir. 9- Yüzey sistre ile torna edilir. 10- Tabağın kenarları biraz daha bükülür. 11- Kenarlarda 2-3cm genişliğinde düz yüzeli bir bordür yapılır. 12- Kil tabak md f den misine yardımı ile kesilerek ayrılır.

Kurutma Süreci ve Kalıplara Delik Açma İşlemi.

Tabakların ön kurutma süreci. Açık ve kapalı mekânda yavaş yavaş kurutma yapmak uygundur.



Kurutma, dip alma, delik açma süreci, (Fotoğraflar kişisel arşiv)

- 1- Açık veya kapalı mekânda tavlama/kurutma işlemi yapılır. 2- Elle tutulur kıvama gelen tabakların dip alma işlemi gerçekleştirilir. 4- Ağız kenarlarının yamuk olmaması için ters çevrilir. 4- Tabaklara ortasında bir, kenarlarında üç veya dört adet eşit aralıklar ile 2 veya 3mm çapında delik açılır.

Bir kalıbın cam kalıbı olabilmesi için bünyesinde havayı tahliye edebileceği delikler açmak gerekmektedir. Aksi takdirde üzerinde çökertilmek istenen cam plakanın altında kalan hava kendisini dışarı atamayacaktır. Böyle bir durumda camlar kabırır, şişer. Kontrol dışı şekillenmeler meydana gelir. Formun çapına, büyüklüğüne bağlı olarak delik sayısı artabilir. Ortalama 3 ile 5 arasında 2mm çapında delik yeterlidir ve eşit aralıklarla açılmalıdır.

Seramik Kalıpların Astarlanması ve Fırınlanması

Pişmiş toprağa cam yapışmaz. Kırmızı kil veya şamotlu killerden yapılan seramik kalıplara döküm çamuru veya astarı sulu kıvamda sürmek gereklidir, çünkü bu iki kilin bünyesinde bulunan metaller yüzünden kalıp üzerinde kullanılan camın bünyeye yapışmasına sebep olabilmektedir. Bu yüzden kırmızı ve şamotlu kilden yapılan kalıpların yüzeylerine, formlar deri sertliğinde iken astar sürülmelidir. Astar yoksa döküm çamurunun sulu halî fırça ile veya püskürme yöntemi uygulanmalıdır.



Astarlama, (Fotoğraflar kişisel arşiv)

- 1- Çömlekçi çarkında fırça ile astarlama. 2- Büyük çaplı tabakların tornada astarlanması. 3- Astarlanmış tabakların füzyon fırınında pişirimi.

Astarlanmamış ve bisküvi pişirimi olmuş seramik kalıplar astarlandıktan sonra kesinlikle astar pişirimi yapılmalıdır. Aynı zamanda astar pişirimi cama uygulanacak ısı işlem derecesinden yüksek olmalıdır. Örneğin ısı işlem derecesi 800°C - 850°C ise, bisküvi veya astar pişirimi 900°C olmalıdır. Bisküvi pişirim derecesi ısı işlem derecelerinin altına düşerse, seramik kalıplarda cam şekillendirme yapıldığında seramik kalıp pişmeye devam edeceğinden bünyesinden gaz çıkışı yapar, bu da camda habbeciklere dahası kabarmasına ve kontrol dışı şekillenmelere sebep olacaktır.

Tek Cidarlı Kalıplar İle Cam Hamuru (Pate de Verre) Uygulaması.

Paleolitik ve Neolitik dönemde yaşayan insanoğlunun mağara ve kaya yüzeylerine yaptığı el izlerinden feyz alınarak cam hamuru tekniği uygulamalarında insan eli kullanılmıştır.



Tek Cidarlı Yayvan Seramik Tabak Kalıplara Cam Hamuru Uygulaması, Fotoğraflar Kişisel Arşiv

1- Eller seramik kalıp üzerine yerleştirilir. 2- Ellerin etrafına cam tozu dikkatli bir şekilde bir kürek yardımı ile yavaş yavaş dökülür. 3- Eller, cam tanelerinin arasında yavaşça kaldırılır. 4- Sağ ve sol elin boş kalan bölgesine başka bir renk cam yerleştirilir. 5- Cam tabağın et kalınlığı tabağın kendi ağırlığını taşıyacak bir kalınlıkta yapılır, fırına yerleştirilir ve ısı işlem ile cam tanelerinin birbirine tutunması sağlanır.

Füzyon fırınında yapılan ilk tecrübelerde cam hamurunun seramik kalıp içindeki et kalınlığı yetersiz gelmiştir ve kalıp içindeki cam tabak yerinden çıkarılmadan üzerine aynı renklerde ilaveler yapılarak tekrar fırına yerleştirilmiştir.



Tek Cidarlı Seramik Tabak Kalıplara İkinci Kat Cam Hamuru Uygulaması, Fotoğraflar Kişisel Arşiv

- 1- Fırınlanmış cam tabağın fırınlama sonrası et kalınlığı ince kalmıştır ve cam kalınlığı artırılır.
- 2- Tabağın içindeki iki renk için de kalınlık artırılır.
- 3- Kalıbın etrafına cam taneleri dökülmesin diye metal bir sac sarılır ve cam taneleri birbirine tutunsun diye ısıtılır. Fırına girmeden önce seramik kalıp etrafından metal sac alınır, ancak kalıp üzerindeki cam taneleri kalıbı fırına taşıırken ve fırında ısı işlemine maruz kaldığında kalıptan bir miktar dökülmektedir. Bu durum cam formun kenarlarında çok ince tanelerin oluşmasına ve tabağın kenarının girintili çıkıntılı görünmesine sebep olurken, aynı zamanda da narin ve kırılğan olmasına sebep olmaktadır.



Füzyon fırın içi, kalıp kenarına dökülen cam taneleri halkası ve kalıptan çıkarılan tabağın kenarındaki girinti ve çıkıntıların görünümü. Fotoğraflar kişisel arşiv.

Birkaç kez kenarlardaki bu narin girinti çıkıntının önüne geçmek için metal sac kalıpla beraber fırına yerleştirilmiş ve hepsi birden ısı işlemi tabi tutulmuştur. Sac korozyona uğramış ve camın dökülmesini engelleyememiştir. Bu nedenle seramik kalıplarına kenarlık eklenmesi ve çift cidar ile deformasyonların önüne geçmek için yeni kalıp tasarımları düşünülmüş ve imal edilmiştir.

Çift Cidarlı Seramik Kalıp

Tek cidarlı kalıba oranla çift cidarlı kalıbın kuru küçülme sırasında ağız kısmında dönme veya çarpılma olması söz konusu olmamaktadır. Kalıbın ağız kenarına yapılan kenarlık da cam tanelerinin

düşmesini engelleyecek şekilde tasarlanmış ve kalıbın yekpare bir parçası olarak şekillendirilmiştir. Sac gibi başka bir malzeme kullanmaya gerek kalmamıştır.



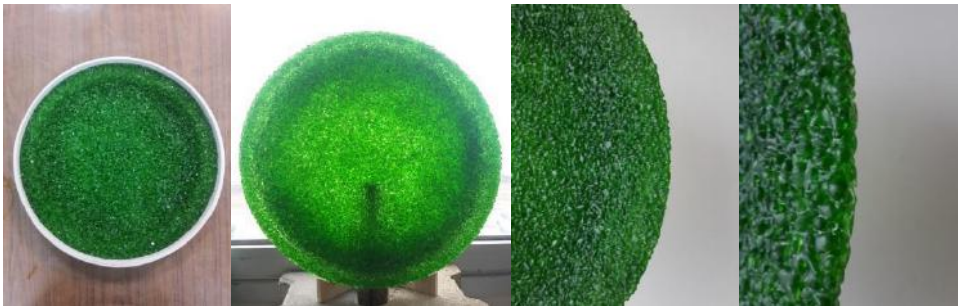
Çömlekçi çarkında çift cidarlı seramik kalıp yapımı. Fotoğraflar kişisel arşiv.

- 1- Çift cidarlı kalıbın ilk cidarı şekillendirilir. 2- İki cidar arasında 3 veya 4 cm boşluk oluşturulur. 3- İki cidar birbirine yaklaştırılarak torna edilir. 4- içteki cidar dışarı doğru yatırılır ve dıştaki cidara yaslanarak iki cidar arasındaki mesafe kapatılarak, iç kısımda yayvan, verevli kenarlığı ve bordürü olan açık seramik bir kalıp şekillendirilmiş olur.



Çift cidarlı kalıpların iç kesiti. Fotoğraflar kişisel arşiv.

Sonuç olarak çift cidarlı pişmiş toprak kalıpta ısıtma işlemiyle şekillendirilmiş 1 ile 4 mm çapındaki cam tanelerinin kalıp içinde ve kenarlarındaki görünümü daha düzgün elde edilmiştir.



Çift cidarlı kalıp ve o kalıptan çıkan cam tabak detayları.

- 1- Çift cidarlı seramik kalıp içinde cam tabak. 2- Kalıptan çıkarılmış cam tabağın görünümü. 3- Çift cidarlı cam tabağın kenar detayı. 4- Daha yakın detay.

Çift cidarlı açık seramik tabak kalıbının dış kenarından yukarı doğru 1-2cm yüksekliğinde bir kenarlık, cam hamuru tekniği uygulamalarında kullanılan kırılmış cam tanelerinin tabağın kenarından düşmesini engellemiş ve kenarların ısıtma işlemi sırasında düzgün şekillenmesine olanak sağlamıştır. Bu kenarlıklar kalıbın içindeki et kalınlığının belirlenmesine de kolaylık sağlamıştır.



Çift cidarlı seramik kalıplar ile şekillendirilmiş cam tabak formları, çap: 45 ile 55cm arasındır, fotoğraflar kişisel arşiv, 2018

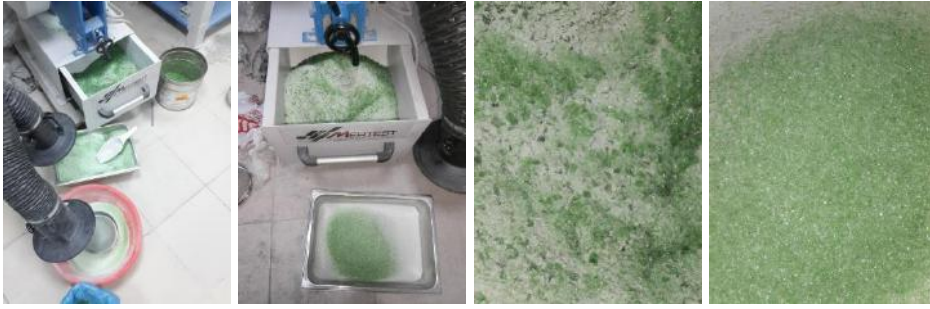
Cam Tozunun Hazırlanması

Cam hamuru yapmak için kullanılan temel malzeme, çeşitli amaçlar için üretilmiş şişe formlarıdır. Günümüzde üretilen bu cam ürünlerin türleri oldukça fazladır. Rapor kapsamında cam hamuru imal etmek için geri dönüşüm mantığıyla, kullanılmış ve çöpe atılmış, soda, bira ve şarap şişesi gibi cam ambalaj malzemeleri toplanmıştır. Cam tozu, kiri sevmez ve doğal olarak kırılacak olan geri dönüşüm şişelerinin önce etiketlerinin çıkarılması ve iyice temizlenmesi işlemi yapılmıştır. Seramikçiler kırma, öğütme işlemlerini genellikle değirmende veya çeneli kırıcılarla yapmaktadırlar. Fakat burada cam hamuru elde etmek için maden mühendislerinin kullandığı ve adına cevher kırma makinesi dedikleri makine kullanılmıştır. Aşağıdaki fotoğraflarda görüldüğü gibi küçük tek motorlu bir makinedir, üstteki konik ağızdan aşağı doğru kırılacak malzeme bırakılır ve iki çelik yivli yüzey arasında sıkıştırılarak kırma işlemi gerçekleşir.



Toplama hazır cam şişler, cevher kırma makinesi ve makinede kırma eylemi.

Kırma işlemi sırasında kesinlikle koruyucu bir gözlük, maske, eldiven ve önlük kullanılmalıdır. Kırılan parçalar basınçtan sıçramaktadırlar, yüze ve en önemlisi göze şiddetli bir şekilde çarpmaları söz konudur. Kırılan cam parçalar makinenin altındaki metal çekmeceli haznede toplanmaktadır. Camların tane irilikleri mikronize boyuttan yarım santime kadar değişmektedir. O yüzden kırma işleminden sonra mikronize metal eleklerle eleme işlemi yapılır. İstenilen tane boyutuna göre elek kullanılarak cam hamuru hazırlanabilmektedir. Elde edilen cam tozlarının çuvallar içinde korunması ve nakliyesinin yapılması uygundur, yırtılmalar söz konusu olacağı için naylon torba gibi ambalaj malzemeleri uygun olmayabilir. Elekten geçirilen camlar 500, 850, 1000 ve 3000 mikron boylarında tane irilikleri ile ayrı ayrı tasnif edilmiş ve kullanım için ambalajlanmıştır.



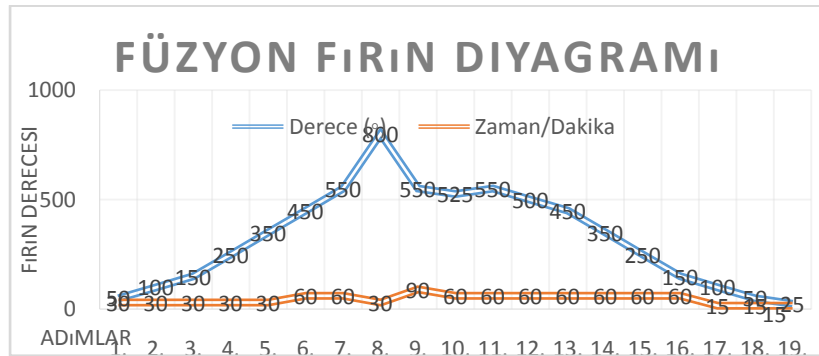
Cevher kırma makinesi, haznesindeki cam taneleri ve elekten geçirilmiş eşit tane boyundaki cam taneleri.

1-Şişelerin kırma işlemi sonrası ve eleme süreci. 2-Makinenin haznesi. 3-Haznedeki farklı tane iriliklerindeki cam taneleri. 7- Elenmiş 850 mikron cam taneleri.

Geri dönüşüm mantığı ile elde edilmiş şişeler ve diğer camlar çeneli kırıcıda kırılmış, her renk cam kırığı birbiri ile karıştırılmadan 3 ayrı boyda tasnif edilerek torbalanmıştır. Renkleri ve tane irilikleri birbiri ile karıştırılmamıştır.

Fırınlama ve Diyagram

Kalıp içindeki cam tozunun fırınlanması füzyon fırınında yapılmıştır. Bir fırın içerisine çapına göre 3 kalıp sığmıştır. Ancak bazen de daha fazla ürün almak için fırın içine raf yerleştirilmiş, kat çıkılmıştır. Ön ısıtma ve soğutma sürelerine dikkat edilmiş ve buna göre fırın dijitaline uygun diyagramlar yazılmıştır. Yapılan cam tabak çalışmaların kalınlığı, çapı ve ağırlığına dikkate alınırsa her fırın için farklı diyagram yazılmıştır.



Gördüğünüz bu diyagram 5 saatte 800°C'ye çıkmış, 30 dakika beklemiş ve 9 saatte de soğutulmuştur. Ön ısıtması ve soğutması hızlı olan bir diyagramdır, kalınlık arttıkça süreler uzatılmaktadır.

Sonuç:

Dünya genelinde Japon Akira Morisitra, Fransız Antoinie Laperlier, Mare Saare Kazimierz Pawlak gibi sanatçılar pate de verre çalışmışlardır.

Türkiye'de cam hamuru tekniğini ilk olarak Güngör Güner 2007 yıllarında uygulamış ve çalışmalarını bir makale ile bizlerle paylaşmıştır. Ayrıca Sema Okan, Necati Şenocak, Naciye Daniş bu konuda yüksek lisans tez çalışması yaparak kendi tasarımlarını pate de verre tekniği ile uygulayanlar arasına girmişlerdir. Ayrıca Ecem Yılmaz kayıp mum yöntemi ile pate de verre tekniğini uygulamaktadır.

Çömlekçi çarkı tekniği kullanılarak yapılacak çift cidarlı açık seramik kalıplar ile birçok tasarım uygulanabilir. En önemli sonuçlar arasında, açık seramik kalıplar ile yapılan pate de verre uygulamalarında %99 oranda başarılı sonuçlar elde edilmiştir.